

LUT Scientific and Expertise Publications

Research Reports – Proceedings, Volume 1 **63**

June 25–30, 2017
Lappeenranta, Finland

**13th International Mine Water
Association Congress
– Mine Water & Circular Economy**



LUT
Lappeenranta
University of Technology

**LAPPEENRANTA
UNIVERSITY OF TECHNOLOGY**

© IMWA – International Mine Water Association 2017

LUT Scientific and Expertise Publications

Name on publication: 13th International Mine Water Association Congress – Mine Water & Circular Economy

Editors: Christian Wolkersdorfer, Lotta Sartz, Mika Sillanpää, Antti Häkkinen

Tutkimusraportit – Research Reports, ISSN-L 2243-3376, ISSN 2243-3376

Serial number: 63

ISBN number, printed publication: 978-952-335-065-6

ISBN number, electronic publication: 978-952-335-066-3

Print and layout: Bookcover Oy, Seinäjoki, Finland

Proceedings 13th International Mine Water Association Congress

Volume 1

**Lappeenranta – Finland
25–30 June 2017**

Table of Content – Volume 1

1 Tekes Projects

Underground Pumped-Storage Hydro Power Plants with Mine Water in Abandoned Coal Mines	6
Compositions of the Microbial Consortia Present in Biological Sulphate Reduction Processes During Mine Effluent Treatment	14
Online Water Flow, Level and Water Quality Monitoring Concept for Mines	22
Development and Application of Series Physical Simulation Test Equipment for Water Inrush in Coal Mine	28
Emergent membrane technologies for mine water purification	36
Synthesis of sorbents from industrial solid wastes by modification with atomic layer deposition (ALD) for mine water treatment	43
Valorisation of Separated Solids from Mine Water Treatment	55
Tailings Seepage Paths Mapped using Electric-Based Technology	64
Operational water balance model for Siilinjärvi mine	73

2 Regional

Assessment of the effects of mine closure activities to waste rock drainage quality at the Hitura Ni-Cu mine, Finland	80
Monitoring of mine water	88
Development and installation of an underground measurement technique at the pilot mine “Auguste Victoria” for a mid- to long-term monitoring of the mine water level rise	94
Mass Flow Reduction in Mining Water: Valuation of Measures with due regard to the requirements of the Water Framework Directive	101
Passive Mine Water Treatment with a full scale, containerized Vertical Flow Reactor at the abandoned Metsämonttu Mine Site, Finland	109
Exploration of Cambrian limestone groundwater runoff zones based on underground tracer tests	117
Similarities in Mine Water Management Challenges in Polar and Desert Climates: Two Case Studies	124
Mine Water Hydrodynamics, Stratification and Geochemistry for Mine Closure – The Metsämonttu Zn-Cu-Pb-Au-Ag-Mine, Finland	132
Leachate generation and nitrogen release from small-scale rock dumps at the Kiruna iron ore mine	140
Evaluation of mine water rebound processes in European Coal Mine Districts to enhance the understanding of hydraulic, hydrochemical and geomechanical processes	147
Pit Lake Modelling at the Aitik Mine (Northern Sweden): Importance of Site-Specific Model Inputs and Implications for Closure Planning	154

Coal mine flooding in the Lorraine-Saar basin: experience from the French mines	161
Sediment And Pore Water Properties Across The Chemocline Of A Mine Water-Impacted Boreal Lake During Winter Stagnation And Autumn Overturn	167
Mine water concept in detail – A case study of closing a German coal mine at Ruhr district	175
Mine Water Management in the Ruhr coalfield	183
Under Ice Treatment and Discharge Of A Tailings Impoundment – A Case Study From The Lupin Mine Nunavut, Canada	189
Large scale grouting to reconstruct groundwater barrier and its geoenvironmental impact	197
Independent investigation of reclamation at exploration drill holes at the remote Pebble copper prospect, Alaska	204
Environmental assessment of closeded coal mine territory using GIS analysis	212
Removal of Metals from Mining Wastewaters by Utilization of Natural and Modified Peat as Sorbent Materials	218
Towards minimum impact copper concentrator – The link between water and tailings	226
Hydrostratigraphy and 3D Modelling of a Bank Storage Affected Aquifer in a mineral exploration area in Sodankylä, Northern Finland	237
Facial and Paleogeografic Understanding of Tertiary Sediments as Basis to Predict their Specific AMD Release	244

3 Physical Water Management

Capão Xavier Mine Water Drainage Management (Minas Gerais, Brazil)	254
Effect of operational parameters on the performance of an integrated semi- passive bioprocess.	262
Break Free from Your Inertia	269
Use of water from the WVII-16 leak in the Wieliczka Salt Mine (Poland)	276
Tailings Water Hydraulics Analyses for Risk Based Design	282
Water management in mining – Measuring and demonstrating value-impact of management strategies	288
Flooding of the uranium mine at Königstein/Saxony – current status and monitoring conducted	296
Integration of Solid Matter Coupled Contaminant Transport into the 3D Reactive Transport Boxmodel by the Example of PCB in German Hard Coal Mining	303
Mercury Accumulation and Bio-transportation in Wetlands Biota Affected by Gold Mining - Modelling and Remediation	312
Utilizing Geophysics As A Delineation Tool for Groundwater Flow Paths And Contaminants Along A Graben	320
Deep mining water control cooperative system based on 3-D directional drilling and controllable grouting techniques	328

Tracing mine water inflows, deriving dewatering measures for an open pit and a first trial to adapt the approach for underground mines	335
Tracer Test in Mine Water of the Abandoned Edendale Lead Mine, South Africa	342
Storage of arsenic-rich gold mine tailings as future resources	350
Integrating Climate Change into Water Management Design	358
Assessing Flood Hydrology in Data Scarce Tropical regions: a Congo (ROC) case study	365
Incorporating Climate Change Scenarios into Mine Design and Permitting Studies	373
Integrated removal of inorganic contaminants from Acid Mine Drainage using BOF Slag, Lime, Soda ash and Reverse Osmosis (RO): Implication for the Production of Drinking Water	381
Aquifer ReInjection Scheme for Excess Mine Water: Design Methodology and Outcomes	389
Important Characteristics of Membranes for Reliable Water and Wastewater Processes for Discharge and Re-use	396
Coal mine pitlakes in South Africa	403
Use of Geothermal Heat of Mine Waters in Upper Silesian Coal Basin, Southern Poland – Possibilities and Impediments	415
Dewatering Impacts of a South African Underground Coal Mine	422
Hydrochemical and isotopegeochemical evaluation of density stratification in mine water bodies of the Ruhr coalfield	430
Biophysical closure criteria without reference sites: Evaluating river diversions around mines	437
Water in Mining – Challenges for Reuse	445
Low-Cost Biological Treatment of Metal- and Sulphate-Contaminated Mine Waters	453
Managed Aquifer Recharge Integration Potentiality In Arid Climate Conditions In The Jordan Rift Valley	461
Mine Water – valued resource or missed opportunity?	469
Integrating water balance modelling in the economic feasibility analysis of metals mining	478

4 Modelling

Simulation of Mine Water Rebound in the Ostrava Basin – Part of the Upper Silesian Coal Basin	488
Waste Disposal In The Open Pits: The Hydrogeological Aspects And The Influence On the Environment (The South Urals, Russia)	489
Novel Approach to Acid Pit Lake Treatment and Management	495
Control of the remediation of anoxic AMD groundwater by sulphate reduction in a subsoil reactor	502
Finely Discretized Numerical Flow Model of Complex Multiple Open Pit Mine For Reliable Inflow and Pore Pressure Simulations – An African Perspective	510
3-dimensional geologic and groundwater flow modelling for coal mining areas as decision support tool - Iterative interaction workflow to establish a reliable groundwater model -	517

Quantitative Evaluation Mining Impact on Unconsolidated Aquifers In Western China's Inner Mongolia-Shaanxi mine Region	524
Reproduction of a Complex Tracer Test through Explicit Simulation of a Heterogeneous Aquifer using Bayesian Markov Chain Monte Carlo	532
Kittilä Gold Mine dewatering assessment: benefits of a new approach	540
The Application of Discrete Fracture Network Models to Mine Groundwater Studies	548
Posiva Flow Log (PFL), Tool for detection of groundwater flows in bedrock	556
Hydrogeological investigation of the Witbank, Ermelo and Highveld Coalfields: Implications for the subsurface transport and attenuation of acid mine drainage	564
Study on Evolution of Mining-induced Crack of Rock Mass Considering Hydromechanical Coupling Effects Based on Stabilized Nano CT Scan	572
Downstream geochemistry and proposed treatment – Bellvue Mine AMD, New Zealand	580
Restoration measures of an AMD polluted watershed based on mixing and geochemical models	588
Gas Flux Rates and the Linkage with Predicting AMD Loads in Waste Rock Dumps, and Designing Practical Engineering Solutions – Field Based Case Studies in Three Distinct Climates	595
Environmental Attributes and Resource Potential of Mill Tailings from Diverse Mineral Deposit Types	603
Progressive Management of AMD Risk During Construction of an Integrated Waste Storage Landform – A Case Study at Martabe Gold Mine, Indonesia	610
Development of a tool for efficient three dimensional reactive multicomponent transport modelling independent from the geohydraulic model system	618
A model-based study on the discharge of iron-rich groundwater into the Lusatian post-mining lake Lohsa, Germany	626
Appropriate Catchment Management can Improve the Profitability of a Mine: A Case Study from Dallol, Ethiopia	633
Geochemical Processes in a Column: Modeling Humidity Cell Test Results	642
Financial Modelling for Mine Discharge Treatment Options	649
Spring Flow Estimation After Mine Flooding in a Dolomitic Compartment	656
Comparison of thermodynamic equilibrium and kinetic approach in the predictive evaluation of waste rock seepage quality in Northern Finland.	664
How geochemical modelling helps understanding processes in mine water treatment plants – examples from former uranium mining sites in Germany	672
The need for improved representation of groundwater-surface water interaction and recharge in cold temperate – subarctic regions	680
Fractional and sequential recovery of inorganic contaminants from acid mine drainage using cryptocrystalline magnesite	689
Risk assessment of acidic drainage from waste rock piles using stochastic multicomponent reactive transport modeling	696
Requirements for numerical hydrogeological model implementation for predicting the environmental impact of the mine closure based on the example of the Zn/Pb mines in the Olkusz area	703

Table of Content – Volume 2

5 Geochemistry

Mineralogical Characterization of Weathered Outcrops as a Tool for Constraining Water Chemistry Predictions during Project Planning	712
Enrichment and Geoaccumulation of Pb, Zn, As, Cd and Cr in soils near New Union Gold Mine, Limpopo Province of South Africa	720
Thallium and other potentially toxic elements in surface waters contaminated by acid mine drainages in southern Apuan Alps (Tuscany)	728
The geochemistry of pore waters in riverbed sediments in a mining-impacted landscape: sources of potentially toxic elements	732
Sulfide Oxidation Kinetics in Low-Sulfide Tailings	737
The Whitehill Formation as a Potential Analogue to the Acid Mine Drainage Issues in the Witwatersrand, South Africa	745
Water quality of the abandoned sulfide mines of the Middle Urals (Russia)	753
Forecasting long term water quality after closure: Boliden Aitik Cu mine	761
Understanding groundwater composition at Kvarntorp, Sweden, from leaching tests and multivariate statistics	770
Water Quality in PGM Ore Flotation: The effect of Ionic Strength and pH	777
Mass transport of hydraulically stowed residues in adjacent aquifers in the Ruhr Area, Germany	785
Comparative Analysis of Waste Material Distribution between Remote Sensing Data and a Geochemical Map	793
Contamination trend at flooded mines: 20 y time-series at Casargiu, Sardinia	801
Delaying flooding of cemented paste backfill mixtures – Effect on the mobility of trace metals	806
Research on transformation characteristics of humic acid based on improved three-dimensional fluorescence regional integral	814
Developing closure plans using performance based closure objectives: Aitik Mine (Northern Sweden)	822
Kinetic Tests of Non-Amended and Cemented Paste Tailings Geochemistry in Subaqueous and Subaerial Settings	830
Behaviour of trace elements during evaporative salt precipitation from acid mine drainage (Agrio River, SW Spain)	836
Investigations on microbial reduction processes in a flooded underground mine	843

6 Valorisation

EU Raw Materials Information System and Raw Materials Scoreboard: addressing the data needs in support of the EU policies – an example for water use in mining	854
--	-----

Green liquor dregs from pulp and paper industry used in mining waste management: a symbiosis project (GLAD) between two Swedish base industries	862
Slag: What is it good for? Utilization of steelmaking slag to remove phosphate and neutralize acid	869
Valorization of pre-oxidized tailings as cover material for the reclamation of an old acid-generating mining site	877
Transformation of Reactive Spoil into Reusable Borrow Materials through Alkaline Waste Valorisation	884
Paperchain Project: Establishing a New Circular Economy Model between the Mining Sector and the Pulp & Paper Industry to Prevent Acid Mine Drainage	892
Ion Exchange by Zeolites and Peat-Based Sorption Media of Chilean Mine Water and their Potential for Secondary Mining	900
Integration of Heat Recovery and Renewables within a Mine Water Treatment Scheme: A UK Case Study	907
Where there's muck there's brass: irrigated agriculture with mine impacted waters	915
Application of alkaline coal seam gas waters to remediate AMD from historical sulfide ore mining operation	923
The KaiHaMe project – increasing raw material value of exploited ores	931
Reduced Inorganic Sulfur Compounds of Simulated Mining Waters Support Bioelectrochemical and Electrochemical Current Generation	939
A Comparative Study on the Rare Earth Elements Recovery of Cross-linked Cellulose Adsorbents and Capacitive Deionization with Cellulose Derived Carbon as Electrode Materials	947
Mine Waste Resource Assessment and Appraisal of Recovery via Mine Water	956
Mining waste as an exploration tool and secondary resource	964
Recovery of copper from low concentration waste waters by electrowinning	972
Hand-held X-ray fluorescence (hXRF) measurements as a useful tool in the environmental and mining sector – Comparative measurements and effects of water content	979

7 Constituents

Recycling bioremediated cyanidation tailings wastewater within the biooxidation circuit for gold recovery: impact on process performance and water management	990
Chemolithotrophic sulfide oxidizers in mine environment	998
Tracking Nitrate Sources at a Platinum Mine – Putting the puzzle together	1006
Quantification of diffuse iron discharge into surface waters in the Lusatian lignite mining district	1014
Characterization of Geo-Hydro-Ecological Factors Affecting the Distribution of Endangered Species in Viiankiaapa Mire, a Mineral Exploration Site	1022

8 Treatment

Iron and Sulfate Removal in Highly Contaminated Acid Mine Drainage Using Passive Multi-Step Systems	1032
Simultaneous Treatment of Thiocyanates and Ammonia Nitrogen in Gold Mine Effluents Using Advanced Oxidation and Nitrification-Denitrification Processes	1039
Performance evaluation of membrane technology for removal of micro pollutants in Hartbeespoort dam water in South Africa	1048
A Novel Sorbents of Metal Ions Based on Thermally Activated, Acidic and Non-acidic Treated Dolomite	1055
Enhanced Mn Treatment in Mine Drainage Using Autocatalysis in a Steel Slag-Limestone Reactor	1063
Electrocoagulation treatment of real mining waters and solid-liquid separation of solids formed	1070
Pilot scale evaluation of the suitability of peat as sorbent filter material for metal removal from mining drainage water	1076
Removal of Dissolved Metals from Acid Wastewater Using Organic Polymer Hydrogels	1080
Field-scale denitrifying woodchip bioreactor treating high nitrate mine water at low temperatures	1087
Investigation of a Pit Lake Acting as a Large-scale Natural Treatment System for Diffuse Acid Mine Drainage	1095
Closed loop for AMD treatment waste	1103
A new approach to recover dissolved metals in AMD by two-step pH control on the neutralization method	1111
Biofouling of reverse osmosis membranes in a process water treatment system in a gold mine	1119
Treatment of historical mining waste using different incineration ashes	1125
Stimulation of Natural Attenuation of Metals in Acid Mine Drainage through Water and Sediment Management at Abandoned Copper Mines	1133
Challenges in Recovering Resources from Acid Mine Drainage	1138
Process development for complex mine water treatment	1147
Electromembrane Processes in Mine Water Treatment	1154
Compact Passive Treatment Process for Acid Mine Drainage, Utilizing Rice Husks and Rice Bran – Process Optimization	1162
Prevention of Sulfide Oxidation in Waste Rock using By-products and Industrial Remnants, a Suitability Study	1170
Assessment of Dewatering Process Using Flocculation and Self-filtration According to the Characteristics of Mine Drainage Sludge	1178
Changes in microbial community structure in response to changing oxygen stress in column tests of denitrification and selenium reduction	1185
Column Tests of Selenium Biomineralization in Support of Saturated Rockfill Design	1191
Enhancing mine drainage treatment by sulfate reducing bacteria using nutrient additives	1196
Are microcosms tiny pit lakes?	1204

Precipitation of metals and sulphate from mining waters: separation and stability analysis of the precipitates	1212
“SPOP”(Specific Product Oriented Precipitation): A new concept to recover metals from mining waste water avoiding hydroxide sludge?	1214
Isolation and application of siderophore producing bacteria from Finnish wetland samples for treatment of mining water effluents	1222
Removal of Iron from Dyffryn Adda, Parys Mountain, N. Wales, UK using Sono-electrochemistry (Electrolysis with assisted Power Ultrasound)	1228

9 Case Studies

Improving Resource Efficiency and Minimize Environmental Footprint – a case study preliminary results	1240
Mapping surface sources of acid mine drainage using remote sensing: case study of the Witbank, Ermelo and Highveld coalfields	1246
Reverse Osmosis Technology to Reduce Fresh Water Consumption – Case Study, Agnico Eagle Finland, Kittilä Mine	1254
Study of Sand Mining and Related Environmental Problems along the Nzhelele River in Limpopo Province of South Africa	1259
Recovery of Uranium using bisphosphonate modified nanoporous silicon	1267
Mining area disturbed by acid mine drainage – Acid Volatile Sulphur and Sequential Extraction studies	1268
Mineralogical and geochemical characteristics of tailings and waste rocks from a gold mine in northeastern Thailand	1277
Heritage of Mining in Sovereign Kyrgyzstan (Kyrgyzstan during the Soviet era and since independence acquisition)	1279
Thermal infrared remote sensing in assessing ground/surface water resources related to the Hannukainen mining development site, Northern Finland	1286
Case Study: Development of an underground depressurisation scheme in an operational mine with reduced pumping capacity	1293

Index

Authors	1302
Key Words	1315

1 Tekes Projects

Underground Pumped-Storage Hydro Power Plants with Mine Water in Abandoned Coal Mines

Javier Menéndez¹, Jorge Loredo², J. Manuel Fernandez³, Mónica Galdo⁴

¹*Mining Engineer. Project Manager at SADIM, S.A.*

Jaime Alberti Street, N° 2, 33900, Ciaño- Langreo, Spain (javier.menendez@sadim.es)

²*Mining Exploitation Department. University of Oviedo. (jloredo@uniovi.es)*

School Of Mines, Independencia Street N°13, 33004, Oviedo, Spain

³*Energy Department. University of Oviedo. (jesusfo@uniovi.es)*

Departmental Building East Zone, University Campus of Viesques, 33271, Gijón, Spain

⁴*Energy Department. University of Oviedo. (galdomonica@uniovi.es)*

Departmental Building East Zone, University Campus of Viesques, 33271, Gijón, Spain

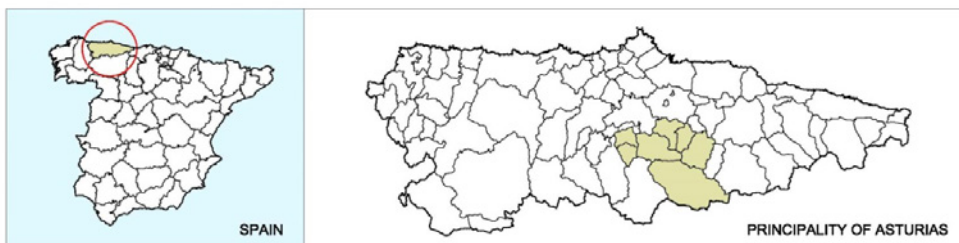
Abstract The Asturian Central Coal Basin in northern Spain has been an exploited coal mining area for many decades and its network of tunnels extends among more than 30 mines. Parts of this infrastructure will soon become available for alternative uses since most of the underground coal mining facilities in Spain will fade out in 2018 (*EU 2010/787/UE*). The network of tunnels in closed-down mines has been suggested as a possible lower storage for the development of an underground pumped-storage project. This infrastructure can hold approximately 200,000 m³ at depths that range between 300-600 m.

Keywords Hydroelectricity, mine water, pumped storage.

Introduction

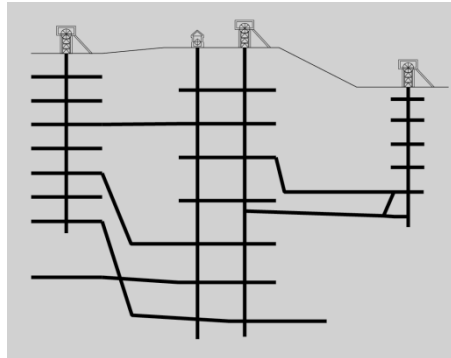
The Asturian Central Coal Basin (ACCB) is located in northern Spain (Figure 1). It has been exploited for more than 200 years through open pit and underground mining, with indoor mining predominating in the last decades. It was one of the most important economic activities in the Principality of Asturias and an outstanding source of employment creation, which therefore contributed to the current development of the surrounding towns.

Figure 1. Asturian Central Coal Basin location



Underground coal mines have a depth of up to 300-600m, with a main infrastructure composed of one or several vertical shafts, used for mineral extraction and for access of personnel and materials. It has a network of horizontal tunnels at different levels, with an average separation between levels of 80-100m (Figure 2).

Figure 2. Typical scheme of shafts and tunnels network in coal mines

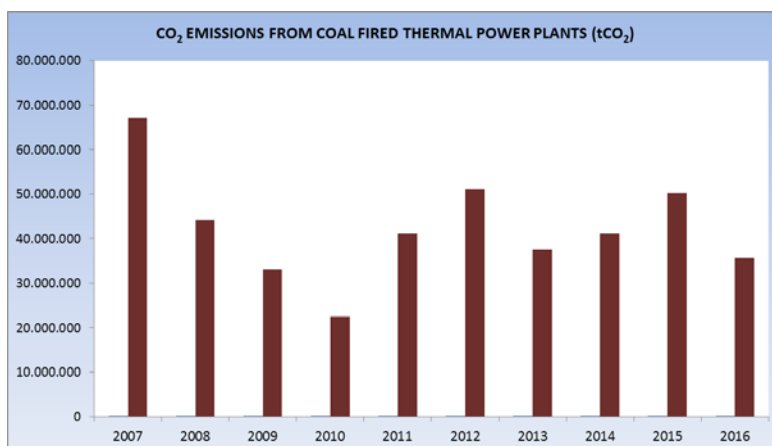


The mineral obtained is used as fuel in thermal plants for the generation of electrical energy. This being one of the most outstanding energy sources within the national energy mix in recent years, with an average participation of 15%. Although on a much smaller scale, the coal produced was also used in the manufacturing of steel.

In recent years there has been a decline in the production of national coal, motivated among other factors by the implementation of European policies focused on the reduction of greenhouse gas (GHG) emissions, as well as on a low competitiveness of national coal marked by a continued decline in the price of international coal, which is also of higher quality than the national coal.

In 2016 coal-fired power generation in Spain accounted for 56% of CO₂ emissions, with more than 35 Million tCO₂, but it only accounted for 13.7% of the electricity demand coverage. The evolution of CO₂ emissions in the generation of electricity with thermal coal since 2007 in Spain, is reflected in Figure 3.

Figure 3. CO₂ Emissions from coal fired thermal power plants (REE)



On the other hand, one of the main conditions of the mining exploitation occurs on the water network. The long history of the Asturian mining has caused a strong alteration in the potentiometric levels and in the natural flow of the aquifers in the affected areas. The exploitations have generated to a triple porosity aquifer (Pendás et al. 2002). Where previously there were small aquifers in sandstone of a small-scale multilayer system, mining tunnels and fractured zones have now been created, that work as aquifers assimilable to the karsts (Pendás and Loredó, 2006). In fact, all the gaps caused by coal mining in the Asturian Central Basin operate as a large underground water reservoir.

Most of the mining work, whether open or underground, intercepts the piezometric level and forces the establishment of a pumping system, which, if interrupted after the closure of the activity, will bring with it a partial or total flood of the mining tunnels.

Presently, the pumping of the infiltrated waters is considered an important cost for the mines, with an average flow of 40 Mm³ per year. Before this, to optimize the use of the economic resources, a first option of cessation of the pumping in the closed shafts was studied, proceeding to the flood of the mining hole. However, this solution is not always applicable due to the uniqueness of the mines, the interconnections created during the exploitation phase and the proximity of the mines to populated areas.

Pumped-Storage Hydroelectricity (PSH)

Pumped hydroelectric energy storage is a large, mature, and commercial utility-scale technology currently used at many locations in the world. Pumped hydro employs off-peak electricity to pump water from a reservoir up to another reservoir at a higher elevation. When electricity is needed, water is released from the upper reservoir through a hydroelectric turbine into the lower reservoir to generate electricity.

Because most low-carbon electricity resources cannot flexibly adjust their output to match fluctuating power demands, there is an increasing need for bulk electricity storage due to increasing adoption of intermittent renewable energy. This technology can be the backbone of a reliable renewable electricity system.

The first idea of exploiting a disused mine as an underground reservoir dated from 1960 (Harza, 1960) and it was developed by several studies and technical reports but not accompanied by functioning pilot projects (Pickard, 2011).

Mount Hope project, located in northern New Jersey was initially proposed in 1975. It intended to use the facilities of an abandoned iron mine as a lower reservoir but it was never developed (Dames and Moore, 1981).

The feasibility of using some of the current coal mining facilities in the Ruhr region as lower reservoir for a pumped storage project has been currently analyzed by a group of five partners in Germany (University Duisburg Essen, Ruhr University Bochum, Rhine Ruhr Institute for Social Research and Political Consultancy RISP, RAG AG and DMT), supported by the European Union.

Madlener and Specht (2013) presented an extremely interesting techno-economical analysis of the possible construction of underground PHES in Abandoned Coal Mines in the Ruhr area (Germany). Also in the Ruhr area, Alvarado et al. (2016) presented a project of the possible construction of underground pumped storage power plant in Prosper Haniel mine in Bottrop (North-Rhine Westphalia), using existing coal mine infrastructure.

This storage concept presents several advantages in comparison with conventional PHES, as for example the higher possibility of social acceptance and the larger number of potential sites. From a technical point of view, even though the construction of an underground storage reservoir is possible, the main limit is the need of competent rock, especially at reservoir depths.

An interesting unconventional pumped hydro project, proposed in Estonia (Project ENE 1001, 2010), is that of Muuga whose completion is expected in 2020. The peculiarity of this project is that it combines two different unconventional reservoirs: the sea as upper reservoir and underground chambers, resulting from granite excavations, as lower reservoir. As regards the worldwide situation, with over 150 GW, pumped hydro storage power plants represent around 99% of the world's electrical energy storage capacity. Currently Japan is the worldwide leader but China expands quickly and is expected to surpass Japan in 2018. Table 1 shows the 10 countries with the most installed capacity.

In the future, as the renewable revolution gains momentum worldwide, hydropower looks to become an even more strategic player. The International Renewable Energy Agency (IRENA) conducted a technology roadmap (Remap) until 2030, and hydro capacity could increase up to 60%, and the pumped hydro capacity could be doubled to 325 GW from the 150 GW installed in 2014.

Table 1. *Installed PHS capacity worldwide (IHA 2015)*

Country	Installed PHS Capacity (MW)
Japan	27438
China	21545
United States of America	20858
Italy	7071
Spain	6889
Germany	6338
France	5894
India	5072
Austria	4808
South Korea	4700

Description

The tunnel network of a mining facility has an unusual geometry for a storage system. Nevertheless, such storage volumes, combined with the depths at which some of these facilities

are located and the high flows of mine water, can be sufficiently appealing to establish a PSH project with a Francis turbine-pump. The most relevant technical aspect is related to the storage structure for the lower reservoir.

In a typical hydropower pumped storage project, the two reservoirs are located on the surface level. In contrast to a conventional PSHP plant, the upper reservoir of an Underground PSH power plant is the smaller problem, as it can basically be established on the surface. If an abandoned coal mine is envisaged, the (potentially large) area of the former mine may be available for use. In the generally densely populated Asturian Central Coal Basin, at least small- and medium-sized storage reservoirs on the surface, may often be done without too much conflict with settlement areas. In the surroundings of the shafts there exist buildings that are protected as industrial heritage, which cannot be demolished.

The lower reservoir inevitably has to be established subsurface and in great depth. An obvious candidate solution is the use of existing cavities. The dominant mining method in the Asturian Central Coal Basin is the long-wall mining technique, which involves a controlled collapse of the sediments. The use of remaining cavities from coal mining must therefore be excluded, leaving us with the following three options: (1) to excavate and secure additional caverns; (2) to make use of existing drifts; or (3) to dig new tunnels (Alvarado et al. 2015). The Figure 4 shows a general scheme of the project with the main components, and the Figure 5 reflects the underground power house with the penstock, the inlet valve, the draft tube, the Francis turbine-pump with vertical axis and the synchronous motor-generator.

Figure 4. Schematic configuration of main components

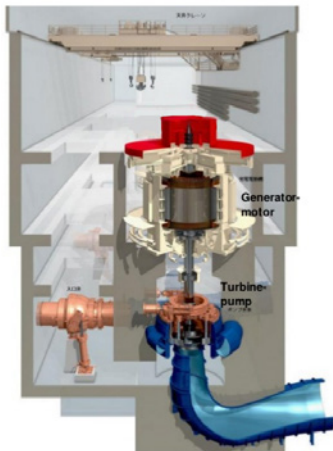
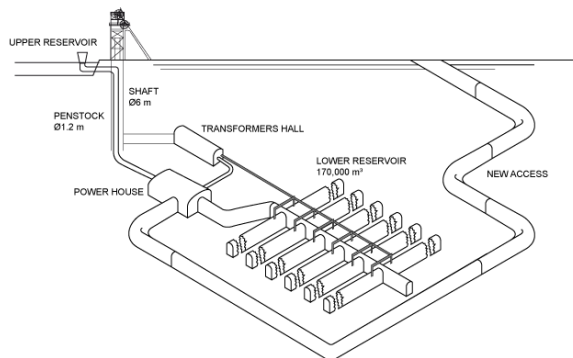


Figure 5. Power house scheme(Alstom)



The conclusion for lower reservoirs is that the use of natural caverns is not possible; the artificial extraction of large cavities is technically demanding and financially expensive and thus does not seem to be very reasonable (Alvarado et al. 2013). In certain cases, existing drifts may at least be partly usable, e.g. after additional extension measures. However, for a

general concept, considerations have to be based on the fact that the drifts for a rib-shaped storage system in the completion stage, would have to be built totally new.

The penstock is located inside the main shaft. It is a vertical pipeline. If the diameter of the penstock is reduced, the load losses increase. If the penstock's diameter is reduced, the head and the output of the turbine are reduced also. The switchyard would be located on the surface, and the rated voltage would be 11,000-30,000 kV.

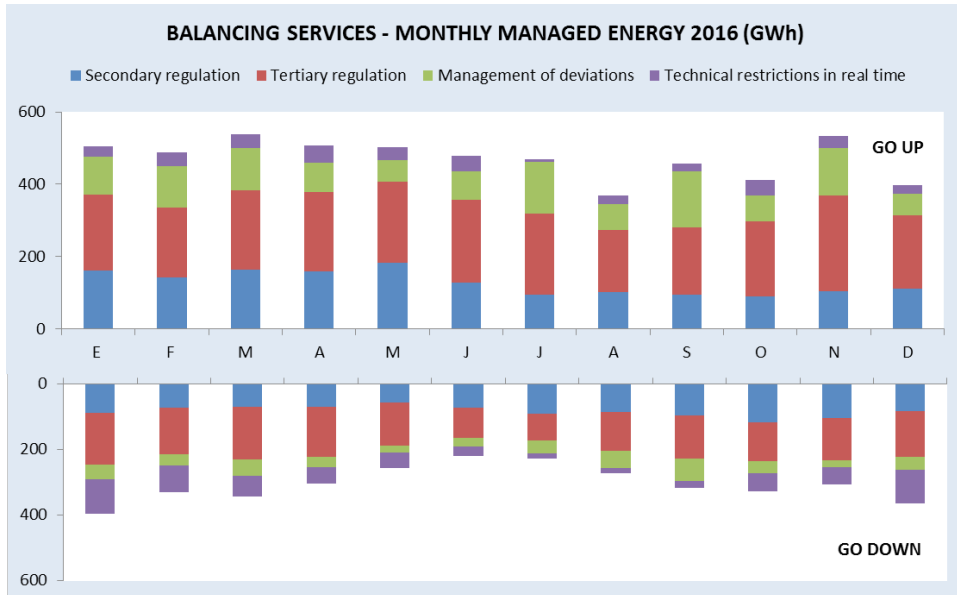
The initial approach is to use the main shaft to introduce the hydraulic and electric equipment and materials. If the dimensions of the shaft are not enough, we can make a new access drift, between the outside and the power house (Figure 4). The dimensions of this drift would be 5 meters wide and 4.5 meters high.

The pumping period takes 9 hours and the turbine period takes 6 hours. Also we can run the turbines at a 50% capacity and produce the same energy in double the amount of time, than if it were to run at 100% capacity. As we want to increase the profitability of the project, we can participate in a secondary electricity market, offering our availability. If we run the turbine during 12 hours at 50% capacity, we can run up and down the turbines output, between the rated output (100%) and the minimum technical output (40% rated output). Nine projects have been studied in mines that are not currently flooded. The main characteristics of a project type, are reflected in the Table 2.

Table 2. Main characteristics and cost assessment

Characteristic	PSH
Total Cost (M€)	40
Cost/kW (€)	1701
Lower Reservoir Length (m)	5700
Cross Section Lower Reservoir (m ²)	30
Net Water Head (m)	300
Reservoir Volume (m ³)	170000
Flow (m ³ /s)	8
Turbine Power (MW)	23,52
Production time 100% Capacity (h)	6
Energy/cycle/MWh	141

The economic feasibility of the project was analyzed taking into account two energy markets in Spain. These markets are the Spot Market (for energy trading) and the secondary control power market (providing electricity balancing services) (Budeux, S. et al. 2016). In Spain the energy managed in the balancing services in 2016 was 21,351 GWh (Figure 6), with a very outstanding participation by the pumped storage plants, due to its dual role of generation and consumption of energy.

Figure 6. Balancing services in electricity markets in Spain 2016 (REE)

Conclusions

The implementation of an underground PSH project using coal mine facilities, is an appealing option for energy storage, particularly in Spain where the underground mining is currently phased out, with an expected closure date at the end of 2018. Also, the significant reduction of the adverse impacts on the landscape and local residents, could be an advantage.

The water necessary for the initial filling of the reservoirs as well as for the replacement of the losses by evaporation, will be taken from the runoff of the mine, so a public water course is not necessary

The most relevant technical aspect is related to the storage structure for the lower reservoir. Based on the techno-economic evaluation, it has been concluded that it is necessary to build a new network of tunnels for the lower reservoir.

PSH can provide many services to the power system, as flexibility of operation and speed to vary the power delivered to the grid. This aspect is fundamental to deal with the variations in production due to fortuitous failures in the thermal power plants and of any significant variations in the production of intermittent renewable power generation.

PSH facilities are the most technologically advanced, widely available resources to provide balancing and integration of variable renewable technologies, such as wind and solar. In addition to the benefits provided by peak power production, pumped storage can generate when the wind is not blowing or the sun is not shining.

References

- Alvarado, R., Niemann, A., Schwanenberg, D. 2013. Concepts for Pumped-Storage Hydroelectricity using Un-derground Coal Mines. Proceedings of 2013 IAHR Con-gress, Tsinghua University Press, Beijing.
- Alvarado, R., Niemann, A., Wortberg, T. (2015). Underground pumped-storage hydroelectricity using existing coal mining infrastructure. In: E-proceedings of the 36th IAHR world congress, 28 June–3 July, 2015. the Netherlands: The Hague.
- Bodeux, S., Pujades, E., Orban, P., Brouyère, S., Dassargues, A. (2016). Interactions between groundwater and the cavity of an old slate mine used as lower reservoir of an UPSH (Underground Pumped Storage Hydroelectricity): a modelling approach. Eng Geol. doi:10.1016/j.enggeo.2016.12.007.
- Dames and Moore. An assessment of hydroelectric pumped storage. 1981. National hydroelectric power resources study. The U.S. Army Engineer Institute for water resources, pp. A-95-96.
- Harza, R.D., 1960. Hydro and pumped storage for peaking, Power Eng., vol. 64(10), pp. 79–82,
- Madlener, R., Specht, J.M., 2013. An Exploratory Economic Analysis of Underground PumpedStorage Hydro Power Plants in Abandoned Coal Mines, FCN Working Paper No. 2/2013.
- Pendas F, Loredo J, Ordonez A., 2002. Revision bibliografica sobre los fundamentos hidrogeologicos de la exploracion y producción de metano de las capas de carbon (CBM). In: Zapatero,MA (ed), Exploracion, evaluacion y explotacion de metano en capas de carbon, Spanish Geological Survey (IGME), pp. 75–103.
- Pendás, F.; Loredo, J.; 2006. El agua en los procesos de cierre de minas en Asturias. Actas de la Reunión Científico-Técnica “Gestión del agua en los procesos de cierre de minas”. E.T.S. Ingenieros de Minas. Universidad de Oviedo.
- Pickard, W. F., 2011. The History, Present State, and Future Prospects of Underground Pumped Hydro for Massive Energy Storage, P IEEE, vol. 100(2), pp. 473-83.

Compositions of the Microbial Consortia Present in Biological Sulphate Reduction Processes During Mine Effluent Treatment

Marja Salo¹, Malin Bomberg¹, Tamsyn Grewar², Lerato Seepei²,
Mariekie Gericke², Mona Arnold¹

¹VTT Technical Research Centre of Finland Ltd, P.O.Box 1000 02044 VTT Finland,
Marja.Salo@vtt.fi, Malin.Bomberg@vtt.fi, Mona.Arnold@vtt.fi

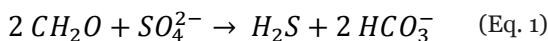
²Mintek, Private Bag X3015, Randburg 2125, South Africa, TamsynG@mintek.co.za,
LeratoS@mintek.co.za, MariekieG@mintek.co.za

Abstract The microbial consortia in sulphate-reducing bioreactors with different operating conditions were studied and compared to the sulphate reduction efficiencies. The results showed vast differences in microbial communities among the reactors. The fraction of sulphate-reducing bacteria correlated with the bioreactor performance. This study sheds new light to the biological sulphate-reducing process applied in bioreactors, which is traditionally seen as a black box.

Key words sulphate-reducing bacteria, bioreactor, sulphate removal, microbial communities, mine water treatment

Introduction

In biological sulphate reduction, sulphate is converted to sulphide in anaerobic conditions by sulphate-reducing bacteria (SRB) that utilize an external carbon source and electron donor. Simultaneously, alkalinity is produced in the form of bicarbonate (Eq. 1) (Vestola and Mroueh 2008).



This process enables the treatment of acidic, sulphate-containing waste water streams. These features are typical to waste waters of the mining industry, and substantial research and development are conducted in the biological treatment of such mining effluents (Bijmans et al. 2011).

Most of the SRB belong to the class Deltaproteobacteria, including genera such as *Desulfovibrio*, *Desulfobulbus* and *Desulfomicrobium*, with some representatives in other groups, e.g. phylum Nitrospirae and the Firmicutes class Clostridia (Muyzer and Alfons 2008). Most known SRB are mesophiles, and the highest sulphate reduction efficiencies in bioreactors are usually obtained in the temperature range of 30 – 45 °C (Bijmans et al. 2011). A pH range of 7.0 – 8.0 in the bioreactor is considered optimal for SRB (Moosa and Harrison 2006), although efficient sulphate removal has also been obtained at lower pH of 4.0 – 5.0 (Santos and Johnson 2017). However, a minimum redox potential of at least -150 mV is required for biological sulphate reduction to occur (Barton 1995).

Substrates used for biological sulphate reduction can be simple compounds, such as hydrogen or lactate, or more complex organic waste materials, such as woodchips or manure. The advantages of simple substrates include wide suitability for SRB, good availability and ease of dosing, whereas organic wastes can be a lower cost and more sustainable option (Bijmans et al. 2011). Full utilization of complex substrates requires co-operation among different microbial groups, and the microbial communities present in bioreactors operated with complex substrates can be expected to be more diverse than in bioreactors operated solely with simple substrates (Hiibel et al. 2011).

In this study, the microbial communities of the effluents of four different laboratory scale sulphate-reducing bioreactors were compared. The substrates used were either complex compounds (woodchips, hay, cow manure) or a combination of complex and simple (lactate, crude glycerol) compounds. Three of the bioreactors were operated in South Africa (SA) and one was operated in Finland (FIN). The effect of reactor configuration and substrate on microbial communities and subsequent sulphate reduction performance is discussed.

Methods

Bioreactors and sampling. The biological systems in this work included two down-flow anaerobic flooded reactors (T1, T2), a continuous stirred-tank reactor (CSTR) (T3) and an up-flow anaerobic sludge blanket (UASB) reactor (T4) (Tab. 1). The bioreactors were operated with either only complex (T1), or a combination of complex and simple substrates (T2, T3, T4). The operating temperatures ranged from 21°C to 30°C while the influent sulphate concentrations ranged from 1.1 g L⁻¹ to 4.5 g L⁻¹. In addition, T2 and T3 received ammonium and phosphate added to the feed. Hydraulic retention times (HRT) varied from one day to 21 days (Tab. 1). Samples for both chemical and microbial analyses were taken from bioreactor effluents after achieving steady operation (after 100 – 300 days of operation). The results of chemical measurements as well as the main microbial findings in the bioreactor effluents are included in Tab. 1.

T1 and T2 were inoculated with cow manure, and T3 with a SRB culture maintained at Mintek, South Africa. Bioreactor T4 was inoculated with the Mintek SRB culture and fresh cow manure, which also served as the sludge blanket for microbes.

T1 simulated a passive system packed with woodchips, wood shavings, hay and manure in a 40/20/20/20 ratio, whereas T2 and T3 contained woodchips and were fed waste glycerol obtained from the biofuel industry (5 ml L⁻¹). T4 was fed with cow manure and lactate in a mass ratio of 75/25 based on the carbon content, with a total substrate excess of 50% for biological sulphate reduction. It was assumed that one mole of sulphate (96 g/mol) requires two moles of carbon (12 g/mol) for biological reduction (Eq. 1), and thus the required organic carbon is one quarter of the sulphate to be reduced. Substrate mixture was added to T4 periodically, with a sufficient substrate dose every 3 – 4 days, as a continuous dosing of manure was not technically possible.

Chemical analyses. Effluent pH and redox potential levels in T1, T2 and T3 were measured with a Metrohm pH sensor and Hamilton redox sensor (mV, vs Ag/AgCl). In T4, pH and

Table 1. The operating conditions, influent specifics, location and results of the effluent analyses of the bioreactors in this work.

	T1	T2	T3	T4
Bioreactor type	Down-flow anaerobic flooded column	Down-flow anaerobic flooded column	CSTR	UASB
Operating T (°C)	23	24	30	21
Substrate	Woodchips, hay, manure	Woodchips, crude glycerol	Woodchips, crude glycerol	Manure, lactate
Added nutrients	None	1.2g/L (NH ₄) ₂ SO ₄ , 0.4g/L H ₃ PO ₄	1.2g/L (NH ₄) ₂ SO ₄ , 0.4g/L H ₃ PO ₄	None
Influent sulphate (g L ⁻¹)	2.7	4.5	4.5	1.1
HRT (d)	21	9	4	1
Location (SA/ FIN)	SA	SA	SA	FIN
pH	8.04	7.05	7.62	7.40
Redox potential (mV)	-236	-399	-396	-176
Relative sulphate removal (%)	95	83	82	59
Total sulphate removal rate (mg L ⁻¹ d ⁻¹)	122	415	923	572
Relative abundance of SRB (%)	1.1	5.4	10.2	8.7

redox potentials were measured with a Consort multi-parameter analyser C3040 equipped with Van London-pHoenix Co. electrodes (Ag/AgCl in 3M KCl). Sulphate concentrations were analysed with the barium sulphate method (Clesceri et al. 1998).

Microbial analyses. The microbial communities in the effluents of the four different bioreactors were characterized with high throughput amplicon sequencing targeting the prokaryotic 16S rRNA gene. The primers used were Bact_0341F/Bact_805R (Herlemann et al. 2011; Klindworth et al. 2013), targeting the variable region V3-V4 of the 16S rRNA gene. For T4, amplicons were prepared for sequencing on the IonTorrent PGM platform from the forward primer, and T1, T2 and T3 were paired-end sequenced on the Illumina MiSeq platform. The IonTorrent sequences were trimmed and quality checked as described in Rajala et al. (2016). The MiSeq sequences were paired using the default quality score values assigned in QIIME version 1.9 (Caporaso et al. 2010).

The sequence data were subsequently analysed with the QIIME software, chimeric sequence reads were removed from the dataset with the USEARCH-algorithm (Edgar 2010) by *de*

novo detection and through similarity searches against the Greengenes reference dataset (Version gg_13_8) (DeSantis et al. 2006). Sequence reads were grouped into Operational Taxonomic Units (OTUs) at minimum 97% sequence homology using the open OTU picking method in QIIME. Taxonomic assignments for the OTUs were based on the Greengenes (gg_13_8) reference database.

Results

Chemistry. The pH of the effluent was similar in all bioreactors, but the redox potentials were significantly lower in T2 and T3 than in T1 and T4 (Tab. 1). T1, T2 and T3 had higher relative sulphate removal efficiencies compared to T4, but according to the total sulphate removal rates, T3 had the highest sulphate removal, followed by T4, T2 and T1 (Tab. 1).

Microbiology. The number of prokaryotic 16S rRNA gene sequences obtained from the different bioreactors varied between 6996 reads for T3 and 39727 reads from T4.

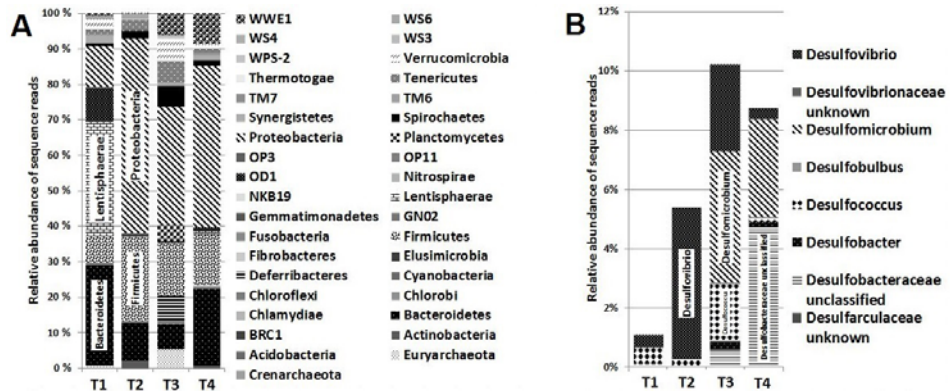


Figure 1 A) The relative abundances of prokaryotic Phyla observed in bioreactor effluents based on the high throughput sequencing, and B) the relative abundances of SRB genera in the bioreactor effluents in detail.

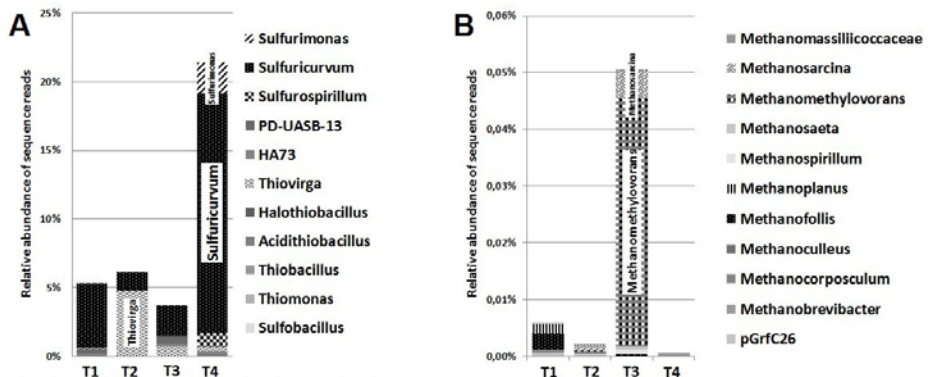


Figure 2 A) The relative abundances of sulfur-oxidizing bacterial genera, and B) the relative abundances of archaeal genera in the bioreactor effluents.

The majority of the microbial community in T1 consisted of Bacteroidetes, Clostridia, Lentisphaera and OD1 bacteria (Fig. 1A). In T2, the most abundant bacteria belonged to Firmicutes and Proteobacteria, and in T3 to Planctomycetes, Proteobacteria, Tenericutes, Verrucomicrobia and WWE1 bacteria. T4 had a high abundance of Proteobacteria, but especially Bacteroidetes, Firmicutes and WWE1 bacteria were abundant. In these samples, the sulphate reducers mostly belonged to the class Deltaproteobacteria (Fig. 1B). Deltaproteobacterial SRB were abundant in T2, T3 and T4. In T2, SRB belonging to the order Desulfovibrionales contributed with 5.1 % of the whole microbial community. In T3, the deltaproteobacterial SRB community consisted of the orders Desulfobacterales, Desulfovibrionales and Desulfuromonadales, contributing with 2.9 %, 7.4 % and 5.5 % of the total number of microbial sequence reads in the sample. In T4, the SRB community mainly consisted of Desulfobacterales and Desulfovibrionales, contributed with 5.1 % and 3.6 % of the microbial community. SRB belonging to the Firmicutes phylum (order Clostridiales) were not detected (Fig. 1B). Instead, T2 had a high abundance of bacteria belonging to the order Syntrophomonadaceae (10.5 % of the total sequence reads). Sulphide-oxidizing Epsilon-proteobacteria were abundant in T4 (*Sulfurospirillum* 1 %, *Sulfuricurvum* 17.4 %, *Sulfurimonas* 2.3 %) in T4 (Fig. 2A). *Sulfuricurvum* was also abundant in T1, T2 and T3 (4.7 %, 1.4 % and 2.2 %, respectively). The archaeal abundance detected with the primers used was generally low, with the exception of T3, for which 5.1% of the obtained sequence reads belonged to methanogenic Archaea of the genera *Methanomethylovorans* (4.5 %) and *Methanosarcina* (0.5 %)(Fig. 2B).

Discussion

All of the tested bioreactors achieved functional sulphate reduction. Although relative sulphate removal was the highest in T1, long HRT caused the total sulphate removal rate to be the lowest of all tested bioreactors. The total sulphate removal rate increased in the experiments as HRT decreased, but in T4 the HRT was most probably too short for efficient sulphate removal. T3 had the best conditions for efficient sulphate removal: sufficient HRT, the highest tested temperature, a suitable mixture of simple and complex substrates and a reactor configuration enabling an effective contact between substrates and bacteria.

The bioreactor effluents contained different microbial consortia. In T1, the most abundant bacteria belonged to the Lentisphaera, Bacteroidetes and OD1 phyla. These bacterial groups are heterotrophic fermenters (Bauer et al. 2006; Choi et al. 2012; Wrighton et al. 2012). In addition, some Bacteroidetes have been shown to have a wide variety of hydrolytic enzymes with which they can degrade high molecular weight organic matter, such as plant polysaccharides, and the OD1 bacteria reduce sulphur. In the other bioreactors, Proteobacteria were the most abundant bacterial groups. SRB did not form the most abundant microbial group in any of the bioreactors. However, in T3 and T4 the relative abundance of SRB reached 10.2 % and 8.7 %, respectively (Tab. 1), whereas in the other bioreactors their relative abundance stayed below 5.5 %. The total sulphate removal rates went according to the order of SRB fractions, as higher SRB fraction resulted in a more removed sulphate. Interestingly, the relative abundance of sulphide-oxidizing bacteria was high, especially in T4, where their relative abundance was over 21 % (Fig. 2A). The abundant sulphur oxidizing

Epsilonproteobacteria in T4 might have oxidized the sulphide produced by the SRB, converting it back to sulphate, and thus decreasing the sulphate removal efficiency. The reason for the abundant sulphide oxidizers is not clear, but it may be an effect of the shorter HRT and lower operating temperature of T4 compared to the other bioreactors.

SRB generally utilize simple substrates more efficiently than complex organic matter, which usually contains slowly degradable compounds that require a long retention time in continuously operated bioreactors for efficient sulphate removal (Gibert et al. 2004). In this study, the effect of substrate on sulphate removal efficiency was difficult to differentiate, as other factors, such as HRT, had a greater influence on the bioreactor performance. T1 received only complex substrates, but the HRT was enough for an efficient relative sulphate removal. However, long HRT may have caused the depletion of sulphate early in the bioreactor, resulting in a decrease in the total fraction of SRB and an increase in the abundance of fermenting bacteria.

T4 had the lowest sulphate load, highest redox potential, lowest operating temperature, shortest HRT and no woodchips as carrier material for biofilm formation and long-term storage of carbon source. The presence of decaying woodchips may provide a steady source of small carbon compounds feeding the microbial consortia in the other bioreactors. Thus intervals of pulses of high concentrations of substrate and times of starvation may be avoided. This may produce a more stable sulphate-reducing consortium than when the bioreactor is fed at intervals of a few days. All SA bioreactors were operated at longer HRT than what was used with T4. The reason for short HRT used in T4 was the effort to optimize an application that would be as efficient as possible, so that the circulation of water in the mine would be swift. A fast turnover would be preferred, because it might not be feasible to store large amounts of water in the mine, although longer HRT could provide a high relative sulphate removal, as seen in T1. Whether the aim is to achieve a certain sulphate concentration in the effluent or a high total sulphate removal rate, the HRT among other parameters can be adjusted accordingly.

Based on these results, the fraction of SRB is a good indicator for sulphate-reducing bioreactor performance. However, the bioreactors of this study were so different that thorough comparison is difficult, as each bioreactor developed a unique microbial consortium over time, and a detailed analysis of the interactions is difficult to conduct. The relationship between microbiology and reactor performance requires more research. For example, experiments on identical bioreactors with varying operation parameters (such as temperature or HRT) should be conducted to suggest appropriate measures, for example, for decreasing the fraction of unwanted microbial groups and increasing the fraction of SRB. In addition, samples from the sludge blanket could help to characterize the microbial population in the bioreactor more accurately.

Conclusions

We found significant differences in the microbial community composition in the different bioreactor effluents based on the high throughput sequence analysis. In the bioreactor with

the highest total sulphate removal rate, the highest relative abundance of SRB was detected. In addition, we showed that the general microbial community composition of the bioreactor with the longest HRT differed significantly from the other bioreactors. Characterizing the microbial communities in detail gives us a tool to follow the development of the microbial consortia in the bioreactors and obtain information about what factors are especially important for the development of a well performing bioreactor. It is a more sophisticated tool than the 'trial and error' approach when altering bioreactor configuration or operation parameters for enhancing the sulphate removal efficiency. With more research, even single methods for removing specific groups and enhancing others could be identified, which would greatly assist in improving sulphate-reducing bioreactor performance universally, regardless of the system configuration in question.

Acknowledgements

This work was funded by the Finnish Funding Agency for Innovation (Tekes, MIWARE project).

References

- Barton L (1995) Sulfate-reducing bacteria. *Biotechnology Handbooks Volume 8*. Springer. 347 pp.
- Bauer M, Kube M, Teeling H, Richter M, Lombardot T, Allers E, et al. (2006) Whole genome analysis of the marine Bacteroidetes 'Gramella forsetii' reveals adaptations to degradation of polymeric organic matter. *Environ. Microbiol.* 8 (12): 2201-2213.
- Bijmans M, Buisman C, Meulepas R, Lens P (2011) 6.34 – Sulfate reduction for inorganic waste and process water treatment. *Comprehensive Biotechnology (2nd Edition)*. Academic Press, pp. 435-446.
- Caporaso JG, Kuczynski J, Stombaugh J, Bittinger K, Bushman FD, Costello EK, Fierer N, Gonzalez Pena A, Goodrich JK, Gordon JI et al. (2010) QIIME allows analysis of high-throughput community sequencing data. *Nat. Methods*, 7:335–336.
- Choi A, Yang SJ, Rhee KH, Cho JC (2013) *Lentisphaera marina* sp. nov., and emended description of the genus *Lentisphaera*. *Int. Jour. Syst. Evol. Microbiol* 63 (4): 1540-1544.
- Clesceri L, Greenberg A, Eaton A (1999) *Standard Methods for the Examination of Water and Wastewater*. American Public Health Association, American Water Works Association, Water Environment Federation. 2671 pp.
- DeSantis TZ, Hugenholtz P, Larsen N, Rojas M, Brodie EL, Keller K, Huber T, Dalevi D, Hu P, Andersen GL (2006) Greengenes, a chimera-checked 16S rRNA gene database and workbench compatible with ARB. *Appl. Environ. Microbiol* 72: 5069–5072.
- Edgar RC (2010) Search and clustering orders of magnitude faster than BLAST. *Bioinformatics*: 26:2460–2461.
- Gibert O, de Pablo J, Cortina J, Ayora C (2004) Chemical characterisation of natural organic substrates for biological mitigation of acid mine drainage. *Water Res.* 38 (19): 4186-4196.
- Herlemann DP, Labrenz M, Jürgens K, Bertilsson S, Waniek JJ, Andersson AF (2011) Transitions in bacterial communities along the 2000 km salinity gradient of the Baltic Sea. *ISME J.* 5:1571–1579. doi:10.1038/ismej.2011.41
- Hiihel S, Pereyra L, Riquelme Breazeal M, Reisman D, Reardon K, Pruden A (2011) Effect of organic substrate on the microbial community structure in pilot-scale sulfate-reducing biochemical reactors treating mine drainage. *Env. Eng. Sci.* 28 (8): 563-572.
- Klindworth A, Pruesse E, Schweer T, Peplies J, Quast C, Horn M, Glöckner FO (2013) Evaluation of general 16S ribosomal RNA gene PCR primers for classical and next-generation sequencing-based diversity studies. *Nucleic Acids Res.* 41:e1–11. doi:10.1093/nar/gks808
- McMurdie PJ, Holmes S (2015) Shiny-phyloseq: Web Application for Interactive Microbiome Analysis with Provenance Tracking. *Bioinformatics* 31: 282–283.

- Moosa S, Harrison S (2006) Product inhibition by sulphide species on biological sulphate reduction for the treatment of acid mine drainage. *Hydrometallurgy* 83 (14): 214-222.
- Muyzer G, Alfons J (2008) The ecology and biotechnology of sulphate-reducing bacteria. *Nature Reviews Microbiology* 6(6): 441-454.
- Oyekola O, van Hille R, Harrison S (2010) Kinetic analysis of biological sulphate reduction using lactate as carbon source and electron donor: Effect of sulphate concentration. *Chem. Eng. Sci.* 65 (16): 4771-4781.
- Santos A, Johnson D (2017) The effects of temperature and pH on the kinetics of an acidophilic sulfidogenic bioreactor and indigenous microbial communities. *Hydrometallurgy* 168: 116-120.
- Vestola E, Mroueh U-M (2008) Sulfaatinpelkistyksen hyödyntäminen happamien kaivosvesien käsittelyssä. VTT Technical Research Centre of Finland Ltd, 58 pp.
- Wrighton KC, Thomas BC, Sharon I, Miller CS, Castelle CJ, VerBerkmoes NC, et al. (2012) Fermentation, hydrogen, and sulfur metabolism in multiple uncultivated bacterial phyla. *Science* 337 (6102): 1661-1665.

Online Water Flow, Level and Water Quality Monitoring Concept for Mines

Jaakko Seppälä, Risto Hiljanen, Lea Nikupeteri

EHP Environment Ltd. Tuotekuja 9 90410 Oulu Finland www.ehpenvironment.com

Abstract Modern technological solutions make it possible to carry out environmental monitoring in real time. By doing so, environmental impact information is available immediately. Early alarm options through automation system ensure minimising environmental hazards and enhance the occupational safety.

Many water-quality parameters, for example: pH, conductivity, turbidity, COD, BOD and up to 5 different metals can be analysed online. Also, online weather and water balance monitoring, which are important to the mine industry, are available.

Online monitoring is also more accurate than traditional manual sampling and in conjunction with laboratory analysis makes the environmental load calculations more reliable.

Background

Water quality can change frequently over time, necessitating frequent, repeated measurements to adequately characterise variations in quality. Modern technologies make it possible to implement environmental monitoring mainly by sensors. Operation of a water-quality monitoring station provides a nearly continuous record of water quality that can be processed and published or distributed directly to the Internet. The water-quality record provides a nearly complete record of changes in water quality that also can serve as the basis for computation of constituent loads at a site. Data from the sensors also can be used to estimate other constituents if a significant correlation can be established, often by regression analyses. The early alarm options as well are important parts of the concept to be presented. The traditional environmental monitoring practices are too slow and not accurate enough for today's industries' needs and for the people and organisations that are connected to them.

The new concept: Environmental Monitoring and Safety Concept, EnMonCon

The environmental monitoring concept where most of the measurements are automated was developed by EHP with its international partners. Mines, as well as other industries; are the core users of the solution. The concept includes online weather (rain, wind, air pressure, temperature and so on), water level, for example in basins or lagoons, and water quality monitoring options, flowing in rivers, ditches and/or in pipelines.

EnMonCon is an answer to a new Environmental Protection law and regulations that require actors and industrial companies to focus on proactive actions to preserve the environment. Implementation of EnMonCon is also the BAT solution for environmental safety monitoring and environmental risk management.

The concept emphasises online measurements instead of manual sampling and laboratory analysis. Almost all the most important parameters can be automated. Through the auto-

mation system, the alarm option minimises the environmental hazards and ensures environmental and occupational safety. The concept also includes laboratory analysis of water samples and field measurements data saved in digital format.

Real-time data from measurements makes load calculations more accurate thus making optimisation of processes easier, ensuring increased productivity and cost savings. Environmental impact reporting can easily be implemented to the authorities through the cloud server, which may speed up the application process for an environment permit. In addition, everyday environmental measurement information can be read from the server by computer or handheld / mobile device. The user-interface for the accessing the data is through an internet browser.

The Environmental Monitoring Concept, EnMonCon, (the full concept is shown in Fig. 1) including all needed environmental monitoring and reporting options and functions is ready to be offered and delivered to industrial clients. This is an optimal solution for mines and industries that have a number of water and weather related measurement requirements to make their operation safe and efficient.

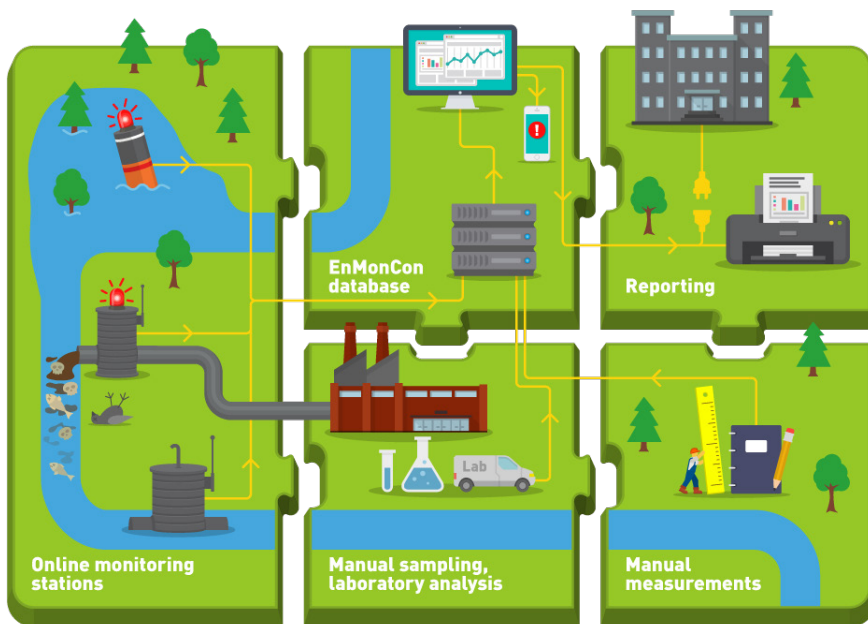


Figure 1. The Environmental Monitoring and Safety Concept, EnMonCon

What parameters can be measured online?

Majority of the water quality parameters can be analysed online as well as the water flow and level in different locations at the mine/industry area and at its environment. Several water quality parameters, for example pH, conductivity, turbidity, COD, BOD and oil-in-

water can be included to the system. Additionally, up to 5 different metals can be continuously monitored by the system. Copper, zinc, nickel and lead are familiar to EHP to be measured online at mine environments, for example. The metal monitoring solution technology is based on a voltammetry principle. Electrochemistry presents good specificity, excellent stability, high sensitivity and low limit of detection for trace metal analysis. The detection limit may be as low as $1 \mu\text{g/L}$ with typical measuring accuracy of $\pm 10 \%$ at level $10 \mu\text{g/L}$, depending on a parameter.

Automated trace metal monitoring systems were tested in-field in an industrial site cooperation with University of Oulu (Mahosenaho et al.) Electrochemical measurement was performed by differential pulse anodic stripping voltammetry (DPASV) for Zn determination. Comparison of online measurement data and reference laboratory analysis results (total trace metal analysis by ICP-MS) for Zn is shown in Fig. 2. According to the results elevated concentrations can be detected using online measurement system. Sudden peaks would have been missed when monitored by laboratory samples. It must though be taken into account that comparing those results is challenging due to the fact that online system detects only electro-labile fraction, not the total concentration of the metal to be measured. Ratio between electro-labile and total concentration of the metal depends on the content of complex-forming compounds present in the sample. Also relatively large measurement uncertainty value ($\pm 20\%$) of ICP technique makes it difficult to compare the results. Despite the mentioned facts, the online metal monitoring system can ideally be used as an early warning system.

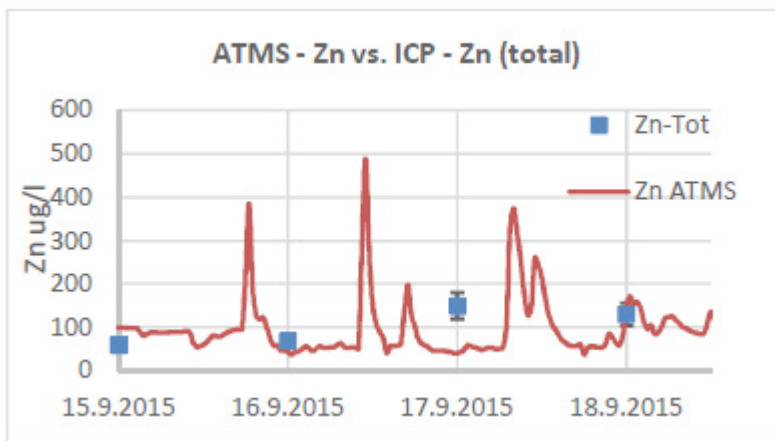


Figure 2. Comparison of online measurement data for Zn with online analyser and reference analysis results for total Zn concentration.

Total measurement uncertainty

Uncertainty of measurement is the most important single parameter that describes the quality of measurements. This is because uncertainty fundamentally affects the decisions

that are based upon the measurement result. Uncertainty that originates in the analytical portion of the measurement is usually known. It has become increasingly apparent that sampling is often the most important contribution to uncertainty and requires equally careful management and control. The uncertainty arising from the sampling process must therefore be evaluated. The total measurement uncertainty of online measurements, manual sampling and laboratory analyses have been studied by VTT Technical Research Centre of Finland Ltd (Ojanen-Saloranta 2016). The measured parameters were pH, turbidity, suspended solids and COD. Simultaneously to online measurements, sampling was carried out by two certified sampling persons representing different organisations. The laboratory analysis were carried out by two accredited laboratories. The results of both monitoring systems are quite equal (even if measurement uncertainties are not taken into account) as can be seen from Figure 3, where pH results of online monitoring and laboratory results are plotted as an example.

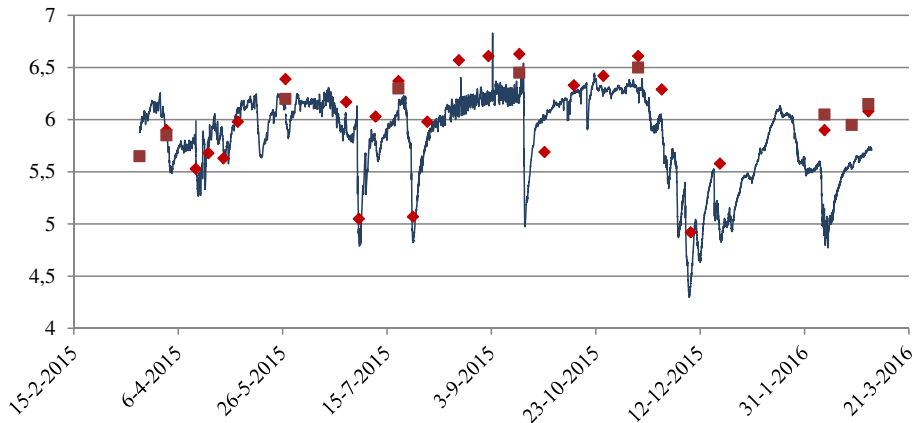


Figure 3. pH results of online measurement (solid line) and laboratory analysis of manual water samples (marked as rhombus and square representing different laboratories)

The main findings of that research were that the manual sampling plays an important role in total measurement uncertainty and online measurements, when properly maintained and calibrated, are more accurate than manual sampling and laboratory analysis.

It can be seen in Figure 4a and Figure 4b that in this study the sampling is more significant uncertainty contribution for the suspended solids measurement than the laboratory analysis. For turbidity and COD measurements, the uncertainties due to sampling and laboratory analyses are of the same order of magnitude. For pH measurement, sampling contributes to the combined uncertainty, but the analysis is the most important contribution.

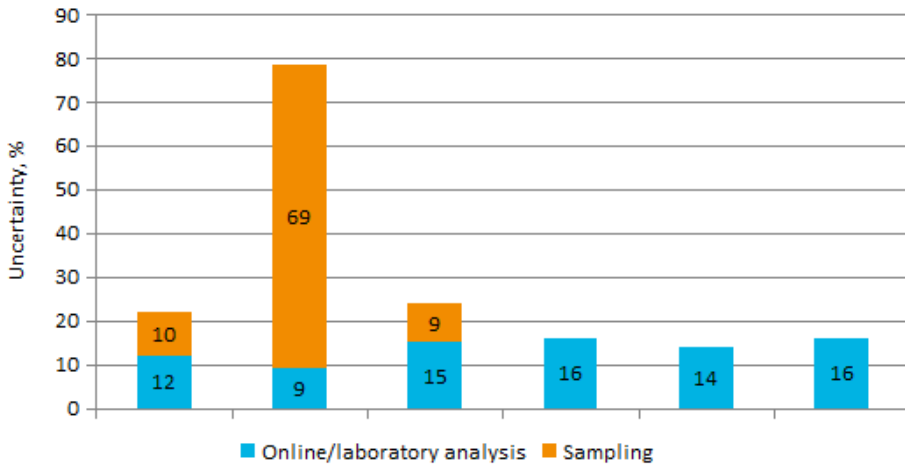


Figure 4a. Uncertainties for turbidity, suspended solids and COD.

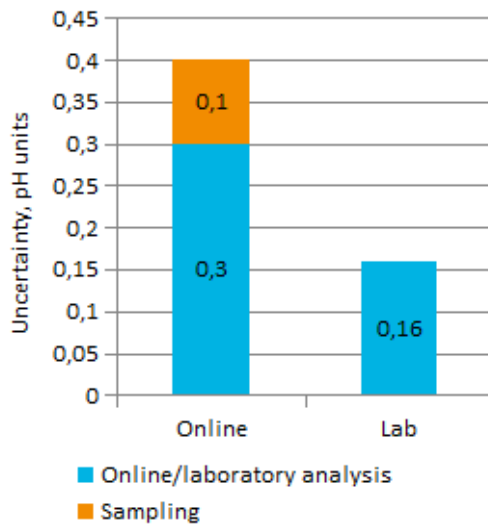


Figure 4b. Uncertainties for pH.

Online Water Balance Management solution for the mine

The online water balance management-function is one essential part of the system. The seepage through dams, that is quantity and quality (e.g. pH, conductivity, turbidity/suspended solids) of the seepage water, can be monitored continuously by the system. Additionally, piezometers for bore water pressure online monitoring and inclinometers for monitoring the earth movements can be included to be part of the system to bring the safety monitoring of the dams in modern online level.

By connecting all essential monitoring devices to the EnMonCon data system, it is possible to automate the water balance monitoring as well as the other monitoring needs, including environmental monitoring data collection and reporting to the authorities.

For predicting and modelling the future situation of the water balance, EHP operates with a partner to provides this information, which is also available online. Water Balance Management at mines has been under careful investigation in Finland during the last years. Online monitoring technology and solutions offers many benefits to follow, report and manage the Water Balance. It also ensures the environmental safety of the mine and prevents environmental hazards.

Conclusions

Online monitoring is an excellent way to know an environmental load in real time. It also significantly reduces costs compared to manual sampling and laboratory analysis, especially when monitoring is required on weekly or even a daily basis. Early warning systems and water balance monitoring enhances environmental and occupational safety. Almost all of the critical parameters can be monitored continuously. By combining all the environmental data to a cloud server, the handling of data is made easier. It also makes the environmental performance more transparent to the stakeholders and authorities and the data is available for key persons globally all the time, where-ever they are located.

References:

- Mahosenaho MJ, Rätty JP, Virtanen V Automated trace metal monitoring systems implemented in field test study in an industrial site, submitted to J Environ Monit
- Ojanen-Saloranta M (2016) Uncertainty estimation of online measurement and manual sampling in water quality measurements, VTT Technology Report 263/2016

Development and Application of Series Physical Simulation Test Equipment for Water Inrush in Coal Mine

Shichuan Zhang¹, Wenbin Sun¹, Weijia Guo¹

State Key Laboratory of Mining Disaster Prevention and Control, Shandong University of Science and Technology, Shandong 266590, China

Abstract With the increase of the depth and intensity of coal mining, the mine has faced a number of challenges such as floor water inrush, roof water inrush and structural water inrush. Different types of water inrush mechanism and disaster mode are difficult to carry out the research by means of the field, so indoor test has become an effective means to solve this problem. The simulation test system for floor water invasion in coal, the simulation test system for water and sand inrush across overburden fissures and the true triaxial rock test system of coupled stress-seepage were developed.

Keywords physical simulation, non-hydrophilic material, water inrush phenomenon, geological structure, data monitoring

Introduction

Mine water-inrush hazards account for the major proportion in the numerous disaster accidents occurred during the mine production and construction. There were 1089 water in-rush accidents with the casualty of 4329 from 2010 to 2011 (James W 2014), while the hydro-geological environments in the mine production will be more complicated along with the continuously deepening mining depth and improving mining intensity in the recent years. Based on the deep mineral resources which account for 27% of the national coal reserve, scholars have to take up various challenges like water-inrushes from mine floors, floors and structures in the fight against water hazards.

Due to the concealment of underground mining engineering, simulation experiment inside the mining laboratory turns to be the effective means to solve such problems for the different types of water-inrush mechanisms and catastrophe modes are difficult to research by means of on-site monitoring etc. Many scholars have made researches on this aspect earlier, Liu (2009) adopted the similar physical model experiment system for water-inrush mechanism in deep mining to research the stresses, deformation (displacements) and failures in surrounding rock influenced by factors i.e. water pressure, mining and complex stress. Li (2010) developed the physical model experimental system for water-inrush (water-inflow) in underground engineering, they adopted the similar materials to simulate the water-inrush supporting during the underground tunnel engineering and successfully explored the catastrophe evolution process for the roadway water-inflow.

Sui (2008) adapted the TST-70 permeameter and conducted simulation test research on the top caving zone of mining working surface for mine production and the seepage deformation failure characteristics of rocks in the fissure zone. Yang (2012) developed

the experimental device for mixed water and sand flow and inrush to reveal the variation characteristics of pore water pressure at the different positions in the fracture channels. Hu (2007) developed the simulation test-bed for 3D solid coupling to simulate the mining above aquifer and provide the theoretical and experimental basis for water-inrush control.

However it can be seen by analyzing the above device that this kind of equipment fails to realize the simulation of the whole process of incubation, development and occurrence for the mine water-inrush hazards; or simulate the complex crustal stress in sealed environment; or directly observe the evolution of the water-inrush channel in the mining process. At the same time, despite the extensive researches (Chang Z 2004, Chen W 2009) the scholars have made focusing on the stress-seepage coupling of the fractured rocks, there is still lack of research on the experimental objects i.e. Large-size test piece (400mm×200mm×200mm) and high seepage pressure etc in addition to the rare researches realizing the tracing monitoring to the expansion and evolution process of the test-piece fractures.

To solve the above problems, Shandong University of Science and Technology has independently researched and developed a series of test equipment such as the similar simulation experiment system for water-inrush from the mining coal seam floor, roof water and sand inrush of mining simulation system as well as the true triaxial rock test system of coupled stress-seepage. It has also established the research lab for water-inrushes and realized the exploration of mine water-inrush by means of lab test; this is of pretty important significance at the same time of providing the multiple means for obtaining the diversified information in the evolution process of mine water-inrush hazards. In this article, it mainly introduces three groups of experiment device, expatiates characteristics of the systems and lists part of the test applications so as to provide the new methods for the researches on the mine water-inrush.

Similar Simulation Experiment System for Water-inrush From the Mining Coal Seam Floor

System Compositions

The similar simulation experiment system for water-inrush from the mining coal seam floor (Sun W 2015 2017, Zhang SC 2017) adopts the 3D solid coupling simulation and computer control technology to obtain the evolution law of the floor mining seepage field under the effects of high water pressure and high confining pressure so as to provide the new research methods for the research on instability and fracture disaster-causing mechanism of seepage channels. The simulation experiment system consists of four subsystems; water pressure control system, servo loading system, test-bed system and intelligent monitoring system as shown in Fig. 1.

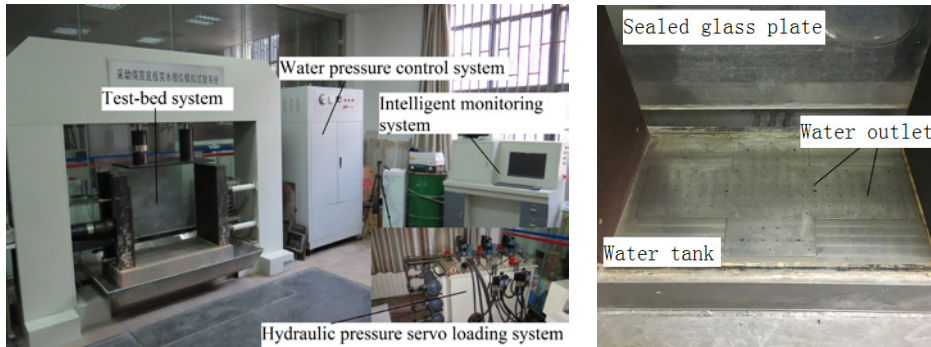


Fig. 1 Similar Simulation Experiment System for Water-inrush From the Mining coal seam floor

Fig. 2 Water-tank Pad

The laying dimension of test-bed model can be as large as 900mm×500mm×800mm (L×W×H). The crustal stress of the simulation mining field during the experiment is realized by the vertical loading system and lateral loading system with the two loading methods of displacement control and load control; the maximum load of the loading unit is 300kN, the displacement sensor range can be 30mm; loading rate of the two subsystem loads shall be 0.01≈100kN/s while the displacement loading rate shall be 0.01≈100mm/min.

The water pressure control system is connected with the test-bed water-tank by the high-pressure hose; the water injection tube and ram-type pump are also connected by the high-pressure hose so as to inject the water into the model from the water-tank through the pad outlet hole (Fig. 2) on top of the water-tank, the maximum water pressure can be 1.5MPa. The front and rear of the test-bed are the new high-strength sealing material--organic glass plate, the adjacent glass plates are closely joined with gasket cement so that the simulation confined water cannot flow out of the model in between the glass plates; in the meanwhile, the whole process of internal water-inrush and fracture evolution can be observed through the organic glasses. 96 fiber optic sensors are equipped on the pad outlet holes on top of the test-bed water-tank in the model to monitor the variations of water pressure and deduce the variation law of the seepage field on the coal seam floor according to the water pressure variation data collected by sensors in combination with the rock fracture positions.

System Characteristics

The similar simulation experiment system for water-inrush from the mining coal seam floor has the following characteristics:

(1) Full process.

The various phenomena during the simulation of water-inrush from the floor i.e.confined water rise, water-resisting floor failure, water-inrush fracture coalescence, formation and evolution as well as formation of structural water-inrush channels etc can be directly observed through the transparent glass plates on both sides of the test system;

(2) Variety.

The diversity of system is seen at the simulation of multiple water-inrush types, multiple-mode control and loading of displacement stress as well as the various ways of data collection. Simulate the different types of water-inrush mode like fracture water hazards, goaf water hazards and surface water hazards by closing the water bags and water manifolds; adopt the different loading modes to simulate the different stress field conditions i.e. submarine tunnel engineering and in-dept exploration etc;

(3) Reliability.

The system is capable of realizing the simulation of water-inrush from the floor under the factors such as different floor structures, mining technologies and water-resisting floor properties etc; through biaxial loading and restraints of organic glass plates, it could realize the simulation of effective crustal stress; by means of water pressure control system, it realizes the pressure preservation of confined water and dynamic water pressure effect in the state of high water pressure; with the help of soil pressure and water flow, the sensor could monitor the variations of stress and seepage field all-around with high precision.

Roof Water and Sand Inrush of Mining Simulation System

System Compositions

Roof water and sand inrush of mining simulation system(Guo W 2016) makes use the closed 3D mining and diversified data acquisition to obtain the overlying strata deformation and failure characteristics, fracture development law, formation of water and sand channels and inrush parameters on the working surface during the mining process, intuitively displays the overlying strata space and the distributional patterns of the water and sand inrush channels after mining the coal, represents the simulation research on the whole process of water and sand inrush hazards on the working surface. This system mainly consists of 7 systems: main bearing support, test chamber, pressure-bearing water tank, mining device, water pressure-water volume dual-control servo system, displacement-stress dual-control servo system and diversified data acquisition system as shown in Fig.3.



Fig.3 Roof water and sand inrush of mining simulation system



Fig. 4 Coal seam drawing board

The effective simulation dimension of the test chamber in the test system is 1200 mm×700mm×400 mm (L×W×H); the water pressure-water volume dual-control servo system could provide the water pressure required by the design as large as 0.8MPa while maximum measuring range of the flow meter is 150L/h and the monitoring precision is ±1.0%; the displacement-stress dual-control servo system could carry out the multiple-mode control of displacement and stress, maximum stroke of the loading device is 400mm, the monitoring precision is 0.01mm and the maximum load is 1000kN; in order to reduce the influences of the non-mining factors on the test, the simulated coal device is designed and made, the coal seam drawing board is as shown in Fig.4; variations of overlying strata stress and water pressure in the overlying strata fractures during simulating the mining process on the working surface are directly monitored by the BX-1 soil pressure sensor with the specification of 0.8MPa and the BS-1 osmometer with the specification of 2.5MPa respectively. To maintain the test conditions of stable water pressure and water flow, energy storage tank is installed in between the water pressure system and test system, the pressure-bearing water tank connected to it is evenly distributed with 28 outlet holes in the bottom with the diameter of 4mm.

System Characteristics

(1) Whole process.

Through the totally-closed and digitized control of this system, the structure, shape and dimension of the water and sand inrush channel under the mining and water pressure effects form spontaneously, conduct the whole-process monitoring on the overlying strata deformation and failure characteristics, fracture development law, formation of water and sand inrush channels as well as the inrush parameters by means of system displacement, mine pressure, water pressure and flow sensor;

(2) Visibility.

The structural configurations formed in the overlying strata space and the distributional patterns of the water and sand inrush channels can be intuitively displayed through the entire piece of transparent glass plate so as to reveal the formation mechanism of the water and sand inrush hazards on the coal working surface and provide the quantitative support for the water and sand inrush hazard evolution mechanism and basic theories estimating the water and sand inrush hazards;

(3) High sealability.

The entire piece of glass plate used in this test, the pressure-bearing water tank and test chamber are sealed by the high-pressure seal ring so that the environment of simulated mining field is fully sealed to realize the flexible loading to the overlying rocks.

True Triaxial Rock Test System of Coupled Stress-seepage

System Compositions

The true triaxial rock test system of coupled stress-seepage(Yin L 2014) makes use of the acoustic emission detection technology to trace and observe the fracture expansion and evo-

lution of the large-size rock test piece in real time under the 3D high-stress and high seepage water pressure effects. The test system consists of 6 major parts: the axial loading subsystem, lateral loading subsystem, high-pressure water flow subsystem, acoustic monitoring subsystem, data acquisition and control subsystem and triaxial test box subsystem(Fig.5)

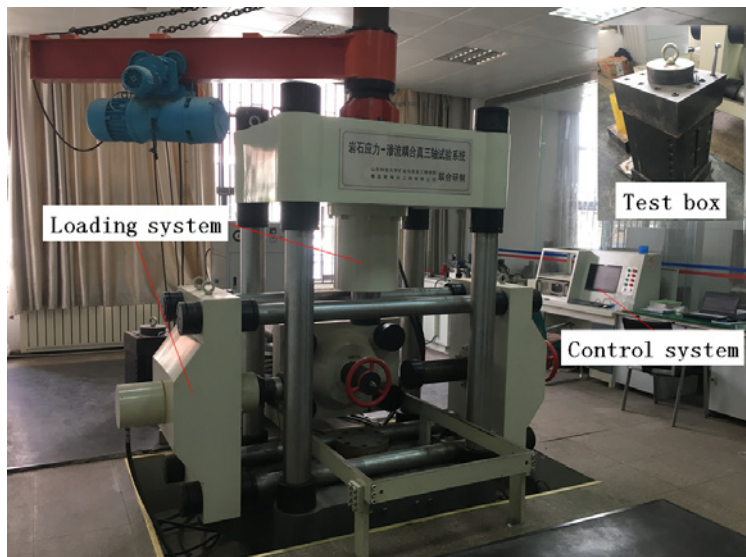


Fig. 5 True Triaxial Rock Test System of Coupled Stress-seepage

The maximum load of the axial loading system can be 1600kN while the two lateral exerted loads can be as large as 1000 and 500kN. The test piece used in this test is rectangular; put the test piece inside the cubic test box made of rigid-flexible hybrid structure, seal the test piece with gasket cement all around evenly; use the high-pressure water seepage subsystem to conduct the water-addition test on the test piece from below. The maximum sealed water pressure can be 5MPa, the stand-up pressure time of the seepage pressure is 10d and the measuring range of water flow is 0.001-2mL/s. Paste 6 sonic probes on the positions of the test piece where the minimum stresses are exerted, arranged in 3D space so as to trace and monitor the acoustic emission events during the test and describe the process of fracture expansion and evolution.

System Characteristics

(1) True triaxial.

It could realize the independent 3D stress loading and deformation displacement measurement on three directions and the true triaxial test is realized by regulating the servo controller so as to change the triaxial principal stress.

(2) Large dimension.

The test system has the test boxes in three different dimensions, the corresponding rock test dimensions are 400mm×200mm×200mm, 300mm×150mm×150mm and 200mm×100mm×100mm;

(3) High seepage water pressure.

The system could provide the maximum sealed water pressure as 5MPa;

(4) Acoustic monitoring and tracing.

During loading and unloading the test piece, the sensor will monitor the micro cracks inside the rocks in real time and transform them into electrical signals to be transmitted to computers and realize the analysis and quantitative description of the fracture expansion process.

Conclusion

(1) The similar simulation experiment system for water-inrush from the mining coal seam floor realizes the simulation of the floor rock failure and evolution under high water pressure and high stress effects, obtains the disaster-causing evolution law and internal mechanism of water-inrush from floor by monitoring the multiple-field information during the evolution of floor water-inrush channels.

(2) Roof water and sand inrush of mining simulation system realizes the research on the catastrophe characteristics of the water and sand inrush on the mining roof under the water-rock coupling effects, through the testing machine, it clearly displays the structural configurations formed in the overlying strata space and the distributional patterns of the water and sand inrush channels after mining the coal.

(3) The true triaxial rock test system of coupled stress-seepage provides the deep loading environment of high stress and high water pressure as well as the 3D stress controlled by the independent servo for the rock test, it realizes the fully-digitized process of data acquisition and obtains the expansion and evolution law of rock fractures as well as the acoustic emissions in the failure process.

Acknowledgments

The research described in this paper was financially supported by the Natural Science Foundation of Shandong Province(No. ZR2016EEB07); Basic Research Project of Qingdao Source Innovation Program(No. 17120111jch); Scientific Research Foundation of Shandong University of Science and Technology Talents (No. 2016RCJJ025); Mining Institute Science and Technology Innovation Foundation of Shandong University of Science and Technology(KYKC17001).

Reference

- Chang Zongxu, ZHAO Yangsheng, HU Yaoqing(2004) Theoretic and experimental studies on seepage law of single fracture under 3d stresses. *Chinese Journal of Geotechnical Engineering*, 23(4): 620-624.
- CHEN Weizhong, TAN Xianjun, LU Senpeng(2009) Research on large-scale triaxial compressive rheological test of soft rock in depth and its constitutive model. *Chinese Journal of Geotechnical Engineering*, 28(9): 1735-1744.
- GUO Weijia, WANG Hailong, CHEN Shaojie(2016) Development and application of simulation test system for water and sand inrush across overburden fissures due to coal mining[J]. *Chinese Journal of Geotechnical Engineering*, 07: 1415-1422.
- HU Yaoqing, ZHAO Yangsheng, YANG Dong(2007) 3D solid-liquid coupling experiment study into deformationdestruction of coal stope. *Journal of Liaoning Technical University*, 26(4): 520-523.
-

- LIU Aihua, PENG Shuquan, LI Xibing (2009) Development and application of similar physical model experiment system for water inrush mechanism in deep mining[J]. Chinese Journal of Rock Mechanics and Engineering, 28(7): 1 335-1 341.
- LI Shucui, LI Liping, LI Shuchen (2010) Development and application of similar physical model test system for water inrush of underground engineering. Journal of Mining and Safety Engineering, 27(3): 299-304.
- James W. LaMoreaux , Qiang Wu, Zhou Wanfang (2014) New development in theory and practice in mine water control in China. Mine Water and the Environment, 29: 141-145.
- Shichuan Zhang, Weijia Guo, Yangyang Li, Wenbin Sun (2017) Experimental Simulation of Fault Water Inrush Channel Evolution in a Coal Mine Floor. Mine Water and the Environment, doi:10.1007/s10230-017-0433-9.
- SUI Wanghua, DONG Qinghong (2008) Variation of pore water pressure and its precursor significance for quicksand disasters due to mining near unconsolidated formations. Chinese Journal of Rock Mechanics and Engineering, 27(9): 1 908-1 916.
- SUN Wenbin, ZHANG Shichuan(2015) Development of floor water nvasion of mining influence simulation testing system and its application. Chinese Journal of Geotechnical Engineering, S1: 3274-3280.
- Wenbin Sun , Shichuan Zhang , Weijia Guo (2017) Physical Simulation of High-Pressure Water Inrush Through the Floor of a Deep Mine. Mine Water and the Environment, doi:10.1007/s10230-017-0443-7
- YANG Weifeng, JI Yubing, ZHAO Guorong (2012) Experimental study on migration characteristics of mixed water and sand flows induced by mining under thin bedrock and thick unconsolidated formations. Chinese Journal of Geotechnical Engineering, 34(4): 686-692.
- YIN Liming, GUO Weijia, CHEN Juntao(2014) Development of true triaxial rock test system of coupled stress-seepage and its application. Chinese Journal of Geotechnical Engineering, S1: 2820-2826.

Emergent membrane technologies for mine water purification

Hanna Kyllönen, Eliisa Järvelä, Juha Heikkinen, Minna Urpanen, Antti Grönroos

VTT Research Centre of Finland Ltd, P.O. Box 1603 FI-40101 Jyväskylä, Finland

Abstract Membrane technologies were studied to purify neutralising pond water for high water recovery and quality. Reverse osmosis produced good flux until it decreased rapidly at a recovery of 60%. Even 80% recovery could be obtained by forward osmosis, except when ammonium carbamate was used as a draw solution and scaling already occurred at the early-stage of filtration. The flux in membrane distillation was good and stable until scaling occurred. If calcium was removed water recovery could be increased to 93%. The order of metal rejection efficiency of the technologies was membrane distillation > reverse osmosis > forward osmosis.

Keywords Mine water, purification, reverse osmosis, forward osmosis, membrane distillation

Introduction

Given the limited availability of water in many countries, water reuse in industry is increasing. On the other hand, the mining industry can have a strong environmental impact. Wastewater from the mining industry needs to be purified before discharging it to surrounding water faces. The limits for metals and sulphate vary from site to site but there is a trend towards tighter limits in the future. The most used practice at mines is to raise the pH to alkaline to precipitate dissolved metals and sulphate before discharging excess acidic water from mine area. This is usually done by lime or limestone in neutralising ponds (Johnson and Hallberg, 2005). Precipitated particles, such as a metal hydroxides and calcium sulphate (gypsum), settle down and the solution, neutralising pond (NP) water, will overflow. The used pH and other present dissolved substances, such as sodium chloride, have an effect on solubility of precipitates (Li and Duan, 2011), thus also on the metal sulphate contents of overflow.

When additional treatment is required for reuse or discharge, either nanofiltration (NF) or reverse osmosis (RO) membranes may be required. Both, NF and RO, produce good water quality, but due to scaling, productivity of the RO process can be quite low, i.e. a water recovery of 50-60% (Shenvi et al. 2015; Kyllönen et al. 2016). When mine waters contain a lot of sulphate and are treated by lime, there is a great risk of gypsum scaling on the membrane. Scaling occurs on the membrane surface when sparingly soluble salts are concentrated beyond their solubility limit, and leads to significant flux reduction and salt rejection impairment, and limits the water recovery of the desalination process (Zhao et al. 2017). In RO, the use of antiscalants is the widely adopted technique to prevent scaling by calcium carbonate and gypsum. Also pre-treatment of the feed by pH adjustment, ion exchange, NF/UF, and precipitation softening may help in reducing scaling (Shenvi et al. 2015). Precipitation softening through the use of a variety of chemicals, such as sodium carbonate or sodium hydroxide and carbon dioxide together, has been utilised for the removal of calcium and magnesium ions from feed water (Zhao et al. 2016).

Due to the very low hydraulic pressure required, forward osmosis (FO) is considered to have a lower fouling tendency than a pressure driving membrane processes (Zhao et al. 2012). The driving force of the FO process is the osmotic pressure created by a salinity difference between a feed water and draw solution which are separated by a FO membrane. Ammonia-carbon dioxide and ammonium bicarbonate (NH_4HCO_3) are considered as promising draw solutions in the FO desalination process, since the fresh water can be recovered from the diluted draw solution by moderate heating (Li et al. 2015). If waste heat is available, the process can be economical. The scaling in the FO process can be induced by both concentration polarization and reversely diffused ions from draw solutions. For example, if NH_4HCO_3 is used as a draw solution and the feed contains calcium-ions, CaCO_3 scaling can be formed when carbonate from the draw solution and calcium from the feed meet in membrane pores (Li et al. 2015).

In thermally driven desalination technology, MD, the increased water vapour pressure from the higher temperature drives vapour through the pores of the hydrophobic membrane, where it is collected on the cooler permeate side. Because only vapour is allowed to cross through the membrane, MD is more fouling resistant than RO and has a potential 100% rejection of ions and macromolecules (Warsinger et al. 2015). In MD, temperature and concentration have a polarisation effect on scale formation. The scaling can cause wetting and thus result in contamination of the permeate by the feed (Warsinger et al. 2015).

Methods

The feed was sand filtered and microfiltered NP from mine water. Feed water and permeate were characterised by pH, conductivity (λ), suspended solids (SS) and element content measurements (Table 1). The pH and the conductivity were measured using standard hand held meters VWR pH 100 for pH and VWR EC 300 for conductivity. SS was determined using a WHATMAN ME25 (0.45 μm) filter drying the solids at 105°C overnight. Chemical elements were analysed by ICP-OES (Inductively Coupled Plasma Optical Emission Spectrometry). The procedure was carried out using a standard SFS-EN ISO 11885. Sulphur, sodium and calcium were the dominating elements in NP water (Table 1).

Table 1 pH, conductivity, osmotic pressure, suspended solids and ICP-OES analysis results of the studied NP water. Variations of the analysed results were within 8 %.

pH	λ mS/cm	π bar	SS mg/L	Ca mg/L	Mg mg/L	Mn mg/L	Na mg/L	K mg/L	S mg/L	Fe mg/L	Al mg/L
9.7	6.9	2.0	<0.3	480	5	<0.05	1400	40	1300	0.39	0.18

Reverse osmosis of NP water was carried out using XFRLE (Dow, USA) at 10 and 15 bar pressure. The fluxes calculated based on the permeate flow measurements were all normalised to a temperature of 25°C. Pure water flux for the XFRLE membrane was 68 ± 5 LMH at 10 bar pressure and 25°C temperature. Magnesium sulphate (MgSO_4) rejection for

the membrane was $99.6 \pm 0.4\%$ and sodium chloride (NaCl) rejection $98.0 \pm 0.4\%$. In FO, a Toray FO (Toray, Korea) membrane and either sodium chloride NaCl, MgSO_4 , or ammonium carbamate ($\text{NH}_2\text{COONH}_4$) were used as draw solutions. FO membrane was characterised with pure water using 1 M NaCl as a draw solution. The average flux was $35 \text{ LMH} \pm 8 \text{ LMH}$ when five pieces of membrane were studied. In direct contact membrane distillation, called MD in this study, a PTFE $0.2\mu\text{m}$ membrane (Sterlitech, USA) was used. Pure water was used at the permeate side so the temperature difference was 60°C feed/ 20°C permeate. Pure water flux for MD membrane was 35 LMH .

Osmotic pressures (Table 2) of the draw solutions were analysed using a Vapro 5600XR osmometer from Wescor, Inc. The calibration was done for the osmolality range $100 - 1000 \text{ mmol/kg}$ ($2.4 - 24 \text{ bar}$). The osmotic pressure of NP water was measured 2.0 bar (Table 1).

Table 2. The properties of draw solutions used in FO process.

	C	pH	Conductivity	Osmotic pressure bar
	g/L		mS/cm	
NaCl (1M)	57	8.0	88	40
MgSO_4	180	7.4	60	43
$\text{NH}_2\text{COONH}_4$	98	10	96	41

In scaling control studies, calcium was precipitated before membrane filtration by increasing the pH of the NP water up to 12.3 using 5M sodium hydroxide (NaOH) and after that by dispersing carbon dioxide (CO_2) through a ceramic microfilter into the NP water when the pH was 10.2. pH was kept above 10 until the precipitate was filtered using a pore size of $10 \mu\text{m}$. Using this procedure, calcium content for the NP water decreased from 430 mg/L down to 6 mg/L . pH was lowered for filtration and kept below 8.0 during filtration by sulphuric acid in order to prevent calcium carbonate scaling.

Results and discussion

The flux in using XFRLE RO membrane decreased at 10 bar pressure from 45 LMH to 28 LMH when water recovery increased to 50%. The decrease was reasonable taking into account the osmotic pressure increase of the NP water. The gypsum precipitates started to be formed in the concentrate and flux started to decrease more rapidly after water recovery (WR) of 65% (Fig. 1). The flux decrease was seen in a significant increase of permeate conductivity. The flux decrease was clearer when a pressure of 15 bar was used. Then the scaling started to form earlier and the flux decreased dramatically at a WR of 57%. RO filtration could not continue after WR.

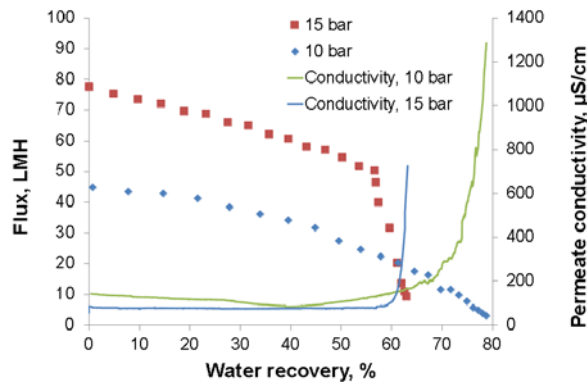


Figure 1. Fluxes and permeate conductivities in RO of NP water at 10 and 15 bar as a function WR.

Good permeate quality and rejections were obtained using a XFRLE membrane for the main components in the NP water, i.e. calcium, sodium, and sulphate. Rejections for them were more than 97% (Table 3).

When the NP water was filtered using ammonium carbonate as a draw solution the flux started to decrease at an early stage of filtration, WR of 10%, due to calcium carbonate scaling. The carbonate ion could transfer from the draw solution side to the feed side. pH adjustment of the feed below 8 did not help in scaling prevention. The flux decrease was not seen when other draw solutions were used or when a pure 1% sodium solution with no calcium was filtered. Similar flux decline was obtained when the NP water was first concentrated up to a WR of 60% using RO and filtered by FO (Fig. 2). The flux started to decrease immediately with ammonium carbamate while other draw solutions, NaCl and MgSO_4 , produced stable flux and good water recoveries, 79% and 83% respectively. FO could be continued, though gypsum started to precipitate. However, FO membranes were also occasionally broken by scaling. The flux with MgSO_4 was very low compared to fluxes in RO and FO using NaCl as a draw solution.

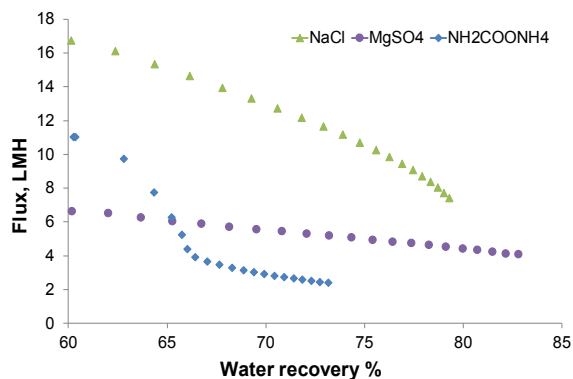


Figure 2. Fluxes of RO concentrate as a function of WR in FO using three different draw solution.

Sulphate rejection for the Toray FO membrane was good, over 97% (Table 3). When the draw solution was MgSO_4 there was back diffusion of salts, $70 \text{ mmol/m}^2\text{h}$, from the draw solution side to the feed side and sulphate rejection was not determined. Back diffusion was clearly seen when using other draw solutions as well. The rejection of calcium was only moderate, 76% or more, for both NP water and RO-concentrate when using the studied draw solutions. In all cases, rejections of monovalents, i.e. sodium and potassium, were very low for the studied membrane.

MD produced very stable flux until at a water recovery of 50% the flux decreased dramatically due to gypsum scaling (Fig. 3). Permeate quality was very good. All the measured components were below detection limit except sodium (Table 3). However, rejection for sodium was also very good, more than 99.9%. The membrane was not wetted during the short lab test and if unbroken it could be used again when rinsing with water.

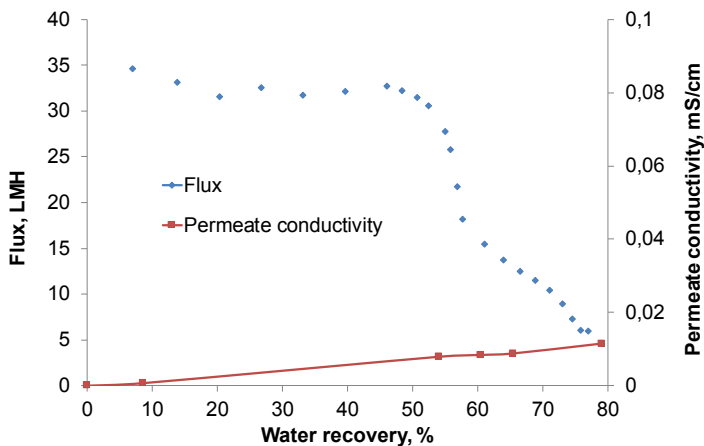


Figure 3. Flux and permeated conductivity in MD of NP water.

Table 3. Measured permeate qualities (mg/L) of NP water in RO and MD. The quality of FO permeates using ammonium carbamate as a draw solution is calculated. <LOD means under limit of detection.

	Ca	Mg	Na	K	S
RO (XFRLE)	1.1	0.2	28	0.3	15
FO (Toray FO)	<LOD	1.8	1400	29	6.8
MD (PTFE $0.2 \mu\text{m}$)	<LOD	<LOD	1.1	<LOD	<LOD

All the filtration methods studied suffered from scaling caused by either gypsum or calcium carbonate. When used sequentially, the highest WR, 93%, was achieved when calcium was removed and the NP water was concentrated first by RO followed by MD. The concentration

factor in this case was 15 (Fig.4). Fluxes were good and scaling was not seen in either of the concentrates. Osmotic pressure of the feed increased and was finally 18 bar in RO. Thus, the hydraulic pressure at the end of filtration was too low and an even higher pressure than 20 bar should have been used. The flux in MD was stable up to a concentration factor of 15 when the hydrate form of sodium sulphate seemed to precipitate and the flux decreased dramatically. In the filtration of calcium removed NP water permeate qualities were very good in both RO and MD concentrations. Rejection of the main components was over 99%.

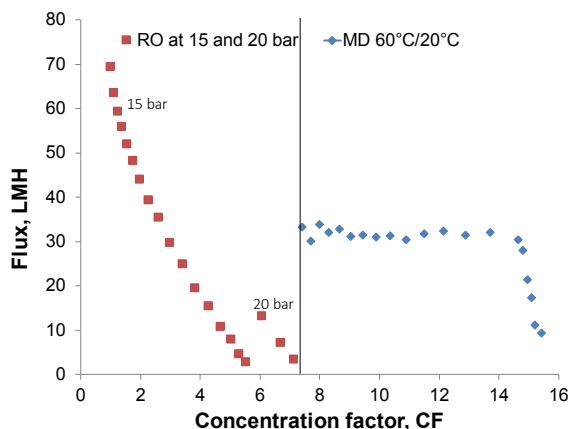


Figure 4. Concentration of calcium removed NP water using RO and MD technologies

Conclusions

Membrane technologies, as well as the emergent technologies of FO and MD, suffer from scaling in mine water purification, which hinders their ability to achieve high WR and concentration factors. The main scalant in NP water is gypsum. FO of NP water also suffers from calcium carbonate scaling when ammonium carbamate is used as a draw solution. High WR and concentration factor can already be obtained by using conventional membrane technology, RO, when the main scalant cause, calcium, is removed. MD produces good fluxes even with a highly concentrated feed. Good quality water can be produced in RO and MD while permeate quality in FO was poor when using the studied membrane.

Acknowledgements

The research was carried out partly in the FO fouling project financed by the Academy of Finland and VTT, and partly in the MinePro project financed by Finnish Funding Agency for Innovation (Tekes), VTT Research Centre of Finland Ltd (VTT) and the companies. The Academy of Finland, Tekes, VTT, Terrafame Group, Aquaminerals, Teollisuuden Vesi, Sansox, Solenis, and Outotec are acknowledged for their support of the MinePro project.

References

Kyllönen H., Grönroos A., Järvelä E., Heikkinen J., Tang C., (2016) Experimental Aspects of Scaling Control in Membrane Filtration of Mine Water, Mine Water and the Environment, September 2016 doi:10.1007/s10230-016-0415-3

- Johnson DB, Hallberg KB (2005) Acid mine drainage remediation options: a review. *Sci Total Environ* 338:3–14
- Li J, Duan Z (2011) A thermodynamic model for the prediction of phase equilibria and speciation in the H₂O–CO₂–NaCl–CaCO₃–CaSO₄ system from 0 to 250 °C, 1 to 1000 bar with NaCl concentrations up to halite saturation. *Geochim Cosmochim Acta* 75:4351–4376
- Li Z., Linares R., Bucs S., Aubry C., Calcium carbonate scaling in sea water desalination by ammonia–carbon dioxide forward osmosis: Mechanism and implications, *Journal of Membrane Science* 481 (2015) 36–43
- Shenvi S., Isloor A., Ismail A., A review on RO membrane technology: Developments and challenges, *Desalination* 368 (2015) 10–26
- Warsinger D.M, Swaminathan J., Guillen-Burrieza E., Arafat H.A., Lienhard V J.H., Scaling and fouling in membrane distillation for desalination applications: A review, *Desalination* 356 (2015) 294–313
- Zhao Y., Cao H., Xie Y., Yuan J., Ji Z., Yan Z., Mechanism studies of a CO₂ participant softening pretreatment process for seawater desalination, *Desalination* 393 (2016) 166–173
- Zhao S., Linda Zou L., Tang C.Y., Mulcahy D., Recent developments in forward osmosis: Opportunities and challenges, *Journal of Membrane Science* 396 (2012) 1– 21
- Zhao Y., Zhang Y., Liu J., Gao J., Ji Z., Xiaofu Guo X., Liu J., Yuan J., Trash to treasure: Seawater pretreatment by CO₂ mineral carbonation using brine pretreatment waste of soda ash plant as alkali source, *Desalination* 407 (2017) 85–92

Synthesis of sorbents from industrial solid wastes by modification with atomic layer deposition (ALD) for mine water treatment

Evgenia Iakovleva¹, Mika Sillanpää^{1,2}, Shoaib Khan¹, Khanita Kamwilaisak³, Shaobin Wang⁴, Walter Z. Tang²

¹Laboratory of Green Chemistry, School of Engineering Science, Lappeenranta University of Technology, Sammonkatu 12, FI-50130, Mikkeli, Finland

²Department of Civil and Environmental Engineering, Florida International University, 10555, West Flagler Street, Miami, Florida 33174, USA

³Department of Chemical Engineering, Khon Kaen University, 40002 Khon Kaen, Thailand

⁴Department of Chemical Engineering, Curtin University, GPO Box U1987, Perth, WA 6845, Australia

Abstract Novel sorbents for acid mine water treatment were developed from industrial solid waste, such as iron sand. The surface of raw materials was modified by atomic layer deposition (ALD) of TiO₂ and Al₂O₃ at the growth rates of approximately 1 Å for each metal oxide. Adsorption properties of synthetic sorbents were studied for the removal of nickel, copper, zinc, iron and sulphate from the synthetic and real acid mine water. It was proved that the deposition of the thin films of metal oxides on the sorbent surfaces increased the removal of ion pollutants compared to original materials. The sorption capacity follows the order of Fe>Cu>SO₄>Zn>Ni for unmodified and both modified sorbents. The maximum adsorption capacities of the modified adsorbents were founded at approximately 650, 220, 200, 150 and 100 mmol g⁻¹ for sulphate, iron, copper, zinc and nickel ions, respectively. In addition, the produced sorbents can be successfully used for the real AMD treatment, achieving removal efficiency of metal ions to 80%.

Keywords Adsorption; metal ions removal; sulphate ions removal; metal oxides coating.

Introduction

Minimisation of water consumption and search for new solutions for effective and low-cost water treatments are challenges for industries and environmental science (Cousin & Taugourdeau, 2016). Mining is one of the largest water consumers for the exploration, extraction and ore processing (Lei et al. 2016; Mudd, 2008) and produces various wastewaters. One of them is acid mine drainage (AMD). Most part of AMD pollutants are iron, copper, zinc and nickel in the sulphates forms (Lei et al. 2016).

Removal of both metal and sulphate ions is the main task for efficient AMD treatment. Such treatment can be active and passive methods (Wolkersdorfer, 2008). Compared to other methods of acid mine drainage treatment, adsorption is one of the cheapest and widely applied for removal of various pollutant compounds (DiLoreto et al. 2016). The choice of sorbents for removing metal ions and sulphates is one of the challenges for purification of AMD. Many methods are based on preliminary neutralization of acid mine water followed by removing of contaminating ions. However, AMD neutralization can lead to precipitation of metals as insoluble salts that increase the amount of solid wastes. A sorbent that will be

able to remove a large amount of ions from wastewater with complex composition without precipitation would be a good solution for this problem.

Modified sorbents based on iron compounds from solid industrial wastes have a good capacity for removal of metal ions and some cations from acid solutions without precipitation (Reddy & Yun, 2016; Theiss et al. 2016; Flores et al. 2012; Iakovleva et al. 2016).

In this study, we employed atomic layer deposition (ALD) to deposit metal oxides on the surface of granulated adsorbents, as modification method of sorbent surfaces. ALD is based on chemical interaction between gaseous reactants and active sites on the substrate surface. The method features a fine control on the film thickness and coating uniformity for the flat surfaces (George, 2010; Puttaswamy et al. 2016), making it ideal for coating complex shape substrate including powders (Iakovleva et al. 2016; Kilbury et al. 2012; Kukli et al. 2016; Tiznado et al. 2014). In this study, deposition of aluminum oxide and titanium dioxides, such as more reactive oxides (Borai et al. 2015), on iron content sorbent surfaces were applied for increasing strength of granules and sorption capacity. The modified sorbents with ALD will be checked for effective capture of ions (Cu, Zn, Fe, Ni and sulphate) from synthetic and real AMDs.

Materials and methods

Solid waste iron sand, named RH, was obtained from Finnish company Ekokem Ltd. The chemical composition and physical properties of raw and modified material are presented in Table 1.

Table 1. Chemical composition of raw and modified RH.

Chemical composition, w%	RH	RH _{Al₂O₃}	RH _{TiO₂}
Si	5.0	5.0	5.0
S	17.6	17.6	17.6
K	0.3	0.3	0.3
Ca	14.4	14.4	14.4
Fe	7.2	7.2	7.2
Al	-	1.5	-
Ti	-	-	2.8

Synthetic AMD solutions of SO₄²⁻, Fe³⁺, Cu²⁺, Zn²⁺ and Ni²⁺, were prepared from analytical grade Fe₂(SO₄)₃·5H₂O, CuSO₄·5H₂O, ZnSO₄·H₂O, and NiSO₄·6H₂O, respectively (obtained from Merck). The concentration of metal ions in stock solutions were 1000 mg L⁻¹ with pH 1.5. All solution were prepared with ultrapure water.

Real mine water were obtained from a sulphide mine in Finland from 700 m depths. The chemical composition of real and synthetic AMD before and after adsorption tests was determined by inductively coupled plasma atomic emission spectroscopy (ICP-OES) and

high-performance liquid chromatography (HPLC) for metal and sulphate ions, respectively. The elemental composition of real mine water is shown in Table 2.

Table 2. Chemical composition of real AMD.

Level m	Cu mg L ⁻¹	Zn mg L ⁻¹	Fe mg L ⁻¹	Ni mg L ⁻¹	Sulfate mg L ⁻¹	Redox E	pH	Cond. ms m ⁻¹
720	4.41	242	52.6	8.1	3470	422	3.2	481

Raw and modified sorbents were characterized with nitrogen sorption at 196 °C using TriStar 3000 (Micromeritics Inc., USA); ZetaSizer Nano ZS, Malvern, UK; XRD, PANanalytical Empyrean powder diffractometer, UK; FTIR, Bruker Vertex 70v spectrometer; SEM, Nova Nano SEM 200, FEI Ltd.

Batch adsorption tests were conducted by mixing RH and modified forms with 45 mL of synthetic and real AMD solutions with known concentrations in a range of 10-300 mg L⁻¹ for all metal ions, according to experiments. All batch experiments was carried out in triplicate. The systematic error of results did not exceed 3%. The mixture was shaken in a mechanical shaker ST5 (CAT M.Zipper GmbH, Staufen, Germany) from 30 min to 72 h, and 10 mL of the solution were taken from the flasks at certain time intervals and then filtered, using 0.20 µm polypropylene syringe filter. The temporal evolution of the solution pH was monitored.

The percentage adsorption (%) was calculated as

$$\% \text{Adsorption} = (C_i - C_f) \times 100 / C_i \quad (1)$$

where, C_i and C_f are the concentrations of the metal ions in the initial and after treatment solutions, respectively.

Sorbents modification

Raw material was granulated before modification by wet-granulation with polyvinyl acetate (PVAc) as a binder. To improve the strength of the granules and their adsorption capacities, modification of their surface with ALD was used. TiO₂ and Al₂O₃ thin films were deposited on the surface of the granules using a TFS500 ALD reactor (Beneq Oy, Finland). For the TiO₂ ALD process, the adsorbent surface was exposed to TiCl₄ and H₂O vapors intermittent with inert gas (N₂) pulses in order to purge the reactor. The pulse time of TiCl₄ and H₂O was 0.6 and 0.25 seconds respectively. In turn, Al₂O₃ film was synthesized by sequential pulses of trimethylaluminium (TMA) and H₂O into the reactor with a pulse time of 1 and 2 seconds respectively. The ALD process was carried out at 350 °C for TiO₂ and 200 °C for Al₂O₃ under pressure of 1 mbar. 300 ALD cycles were used for this material. The silicon substrates <100> (Si-Mat, Germany) were used to control the film thickness of both metal oxides.

Results and discussion

Characterisation of raw and modified adsorbent materials

The adsorbent chemical compositions were obtained with XRD and ED-XRF analyses. The raw RH material contains around 14% of Ca, 7% of Fe and 17% of S. A large amount of sulphur may cause secondary pollution due to desorption during water treatment. However, previous studies have shown (Iakovleva et al. 2016; Iakovleva et al. 2015a), the presence of sulfur is not observed on the surface of the sorbents after modification. FTIR results also confirm the absence of sulphur compounds on the surface of modified sorbents (Table 3). The new bending vibrations corresponding to aluminum oxide at the peak between 980 – 1000 and 610 – 611 cm^{-1} , and titanium oxides with the peak between 450 – 800 cm^{-1} were observed after modification of original RH with TMA and TiCl_4 , respectively. The peak from sulphur compounds (1120 – 1160 cm^{-1}) was observed only from raw RH (Table 3).

Table 3. Band assignment of the FTIR spectra of raw and modified materials.

Adsorbent	Wave number, cm^{-1}						
	O-S-O 1120-1160	Si-O-Si 600-661	O-Si-O 466-473	H-O-H 1620-1690	O-Ti-O 450-800	Al-O 980-1000	O-Al-O 610-611
RH	+	+	+	+			
RH_TiO ₂		+	+	+	+		
RH_Al ₂ O ₃		+	+	+		+	+

The average pore size and specific surface area of unmodified and modified sorbents are presented in Table 4. The pore size of modified sorbents is decreased, however, specific surface area incriscs about twice compared with unmodified one (Table 4).

Table 4. The pore size and specific surface area of unmodified and modified sorbents from this and previous experiments (Iakovleva et al. 2016).

Sorbent	Specific surface area, $\text{m}^2 \text{g}^{-1}$	Pore size, nm	pH
RH	62	180	2.5
RH_TiO ₂	125	3	3
RH_Al ₂ O ₃	115	20	2.8

SEM images showed changes in the surface structure of both modified sorbents (Figure 1b and 1c) compared to raw RH (Figure 1a). The distinctive fine-pored layers of TiO_2 and Al_2O_3 on the surface of RH can be observed (Figures 1b and 1c). Film thickness measurements on reference Si substrate showed that the growth rates were 1.10 $\text{\AA}/\text{cycle}$ and 0.63 \AA for Al_2O_3 and TiO_2 , respectively, and correlated with previous publication (George, 2010).

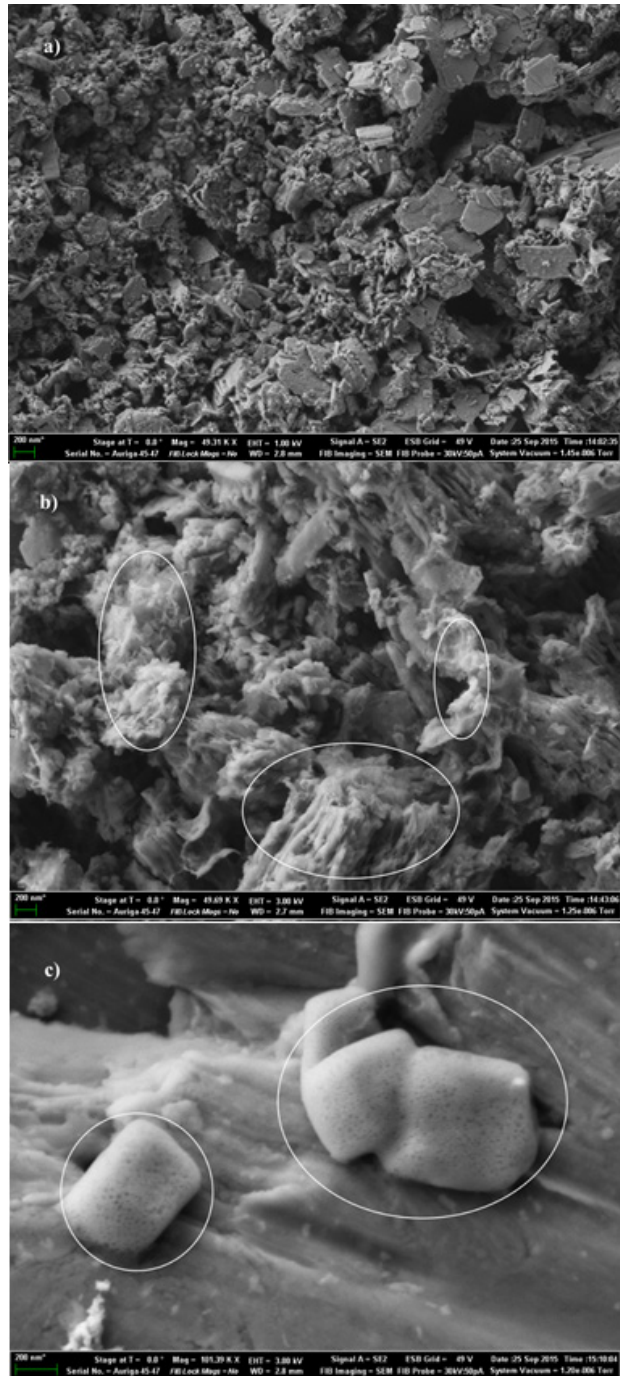


Figure 1. SEM images of a) unmodified RH, b) modified RH with TiO_2 , c) modified RH with Al_2O_3 .

The presence of metal oxides on the surface of the modified sorbents was also confirmed by XRD as well (Figure 2). The peaks (011), (013) and (122) indicate the orthorhombic kappa-Al₂O₃, while the peaks of (011) and (020) correspond to anatase-TiO₂ (Figure 2).

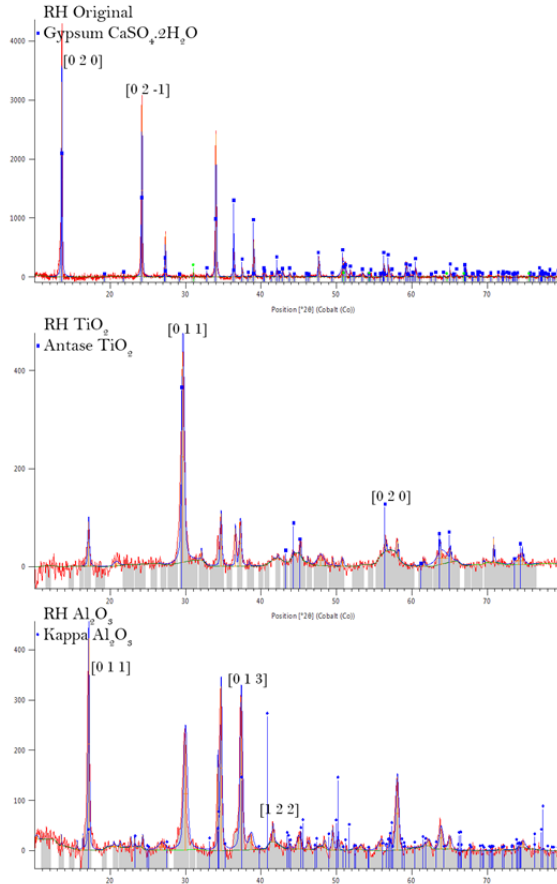


Figure 2. Figure 5. XRD profiles of unmodified and modified RH sorbents.

Optimisation of adsorbent amount for AMD treatment

An optimal mass of modified sorbents for the maximum removal of metal ions and sulphates from synthetic AMD was found at 2 g L⁻¹, 20 times less than that of unmodified RH.

Contact time optimisation

Contact time optimisation of adsorbents and adsorbates was found under the following conditions: the initial concentration of SO₄²⁻ was 3470 mg L⁻¹; Ni²⁺, Zn²⁺, and Cu²⁺ was 100 mg L⁻¹ and 1000 mg L⁻¹ for Fe³⁺. The initial amount of both adsorbents was 10 g L⁻¹. The equi-

librium was reached after 48 h for both sorbents. The pollutants removals were similar for both modified sorbents and amounted around 70% for sulphate cations and 99% for metal ions (Figure 3). The solution pH was found to be changed from 3.5 to 4 slowly (Iakovleva et al. 2016; Silva et al. 2010; Tang et al. 2002).

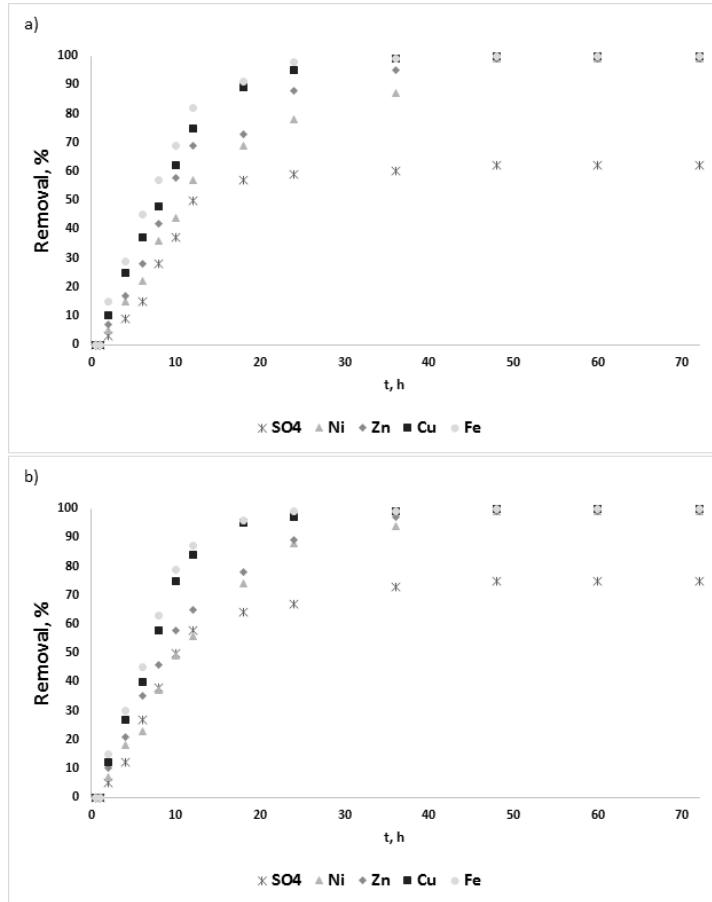


Figure 3. Removal of sulphate and metal ions with modified adsorbents (a) RH_TiO_2 and (b) $RH_Al_2O_3$ (c).

A pH of initial solution was 2.5 and it increased during adsorption process after about 12 h to 5. The maximum adsorption efficiency for all ions was achieved in the same time. The pH affects to ionisation of metals and surface charge. All four metal ions removal increased when the solution pH higher than the pH of sorbents. Because initial sorbents pH is around 3 (Table 4), the pH of treated solution should be higher than this value for better removal of metal ions. However, better sorption capacity for sulphate ions was observed at 5 pH also. The similar effects were observed by many researchers (Bartczak et al. 2015; Boonamnuayvitaya et al. 2004; Genç-Fuhrman et al. 2016). It could be due to the effect of competitions between sulphate and metal ions in complex solution.

Adsorption isotherms

The equilibrium between the adsorption of pollutants on the sorbent surface at a constant temperature was described by Langmuir (Eq. 2) adsorption isotherm.

$$q_e = \frac{q_m K_L C_e}{1 + K_L C_e} \quad (2)$$

where q_e and q_m are sorption capacities (mmol g^{-1}) at equilibrium and maximum, respectively; C_e is concentration of pollutant ions in the solution (mmol L^{-1}) at equilibrium; K_L is Langmuir constant related to the sorption energy.

The parameters were calculated with minimisation of the error distribution between experimental and predicted data by Marquardt's percent standard deviation (MPSD):

$$\sum_{i=1}^n \left(\frac{q_{e,exp} - q_{e,calc}}{q_{e,exp}} \right)_i^2 \quad (3)$$

Langmuir isotherm parameter q_m shows the number of adsorbent site that actively interacts with the pollutant ions (Allen et al. 2004). This parameter increases for all pollutants after modification of raw RH with both methods. The number of sites which participate in the adsorption of ions is much higher for SO_4^{2-} (around 600 mmol g^{-1}). For other ions it is around 200 mmol g^{-1} , expect for nickel ions (around 100 mmol g^{-1}) (Table 5).

The K coefficient is the affinity between sorbate and adsorbent. According to Langmuir theory the affinity between the adsorbents and adsorbates is:



This order is confirmed by many researchers (Alcolea et al. 2012; Aziz et al. 2008; Iakovleva et al. 2015a; Iakovleva et al. 2015b).

The complexation and ion-exchange mechanisms take place during the metal and sulphate ions removal in this experiments. The unmodified and modified RH contain silicate compounds, which can react with ions by following reactions:

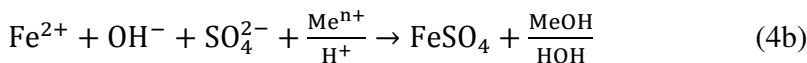


Table 5. Isotherm parameters for unmodified and modified RHs during AMD treatment process.

Langmuir		C_e (mmol L ⁻¹)	$q_{e,exp}$ (mmol g ⁻¹)	$q_{e,model}$ (mmol g ⁻¹)	q_m (mmol g ⁻¹)	K_L (L mmol ⁻¹)	R^2
RH	SO ₄ ²⁻	47.4	11.72	11.24	11.37	18.68	0.74
	Ni ²⁺	1.69	0.11	0.10	0.12	9.01	0.70
	Zn ²⁺	1.54	0.20	0.19	0.17	12.03	0.75
	Cu ²⁺	1.56	0.39	0.40	0.38	21.09	0.82
	Fe ³⁺	1.78	0.75	0.72	0.74	25.12	0.87
RH-Al ₂ O ₃	SO ₄ ²⁻	47.4	650	622	637	20.15	0.82
	Ni ²⁺	1.69	98	100	99	10.17	0.85
	Zn ²⁺	1.54	150	145	152	12.05	0.84
	Cu ²⁺	1.56	201	204	199	20.22	0.87
	Fe ³⁺	1.78	225	215	218	26.30	0.90
RH-TiO ₂	SO ₄ ²⁻	47.4	623	620	625	21.30	0.95
	Ni ²⁺	1.69	85	83	87	9.6	0.85
	Zn ²⁺	1.54	137	136	138	12.5	0.85
	Cu ²⁺	1.56	190	185	187	20.3	0.90
	Fe ³⁺	1.78	215	210	217	25.7	0.93

The addition of aluminium and titanium oxides onto the surface of sorbent allows a significant increase of ion removal. It can be due to the appearance of additional functional groups, which also participate in the removal of ions from solution. As it is known that activated alumina (Al₂O₃) is a highly porous commercial sorbent with a surface area more than 200 m² g⁻¹ used for the removal of various pollutants (Gulshan et al. 2009; Han et al. 2013). Titanium dioxide has a lower chemical reactivity than activated alumina, however, its porosity and big surface area also contribute to application for the removal of various pollutants from water (Borai et al. 2015). Therefore, the increase of pollutant ion removal depends on the increase of the sorbent surface area and the presence of additional functional groups. Modified sorbent with alumina oxide has slightly better adsorption capacity for removal of sulphate and metal ions from synthetic AMD compared to the sorbent modified with titanium dioxide (Table 5). Wettability tests of unmodified and modified granules shows a better strength and stability of the modified granules to the aqueous medium compared to the unmodified ones.

Real AMD treatment with modified RHs

Removal of ions from real AMD was conducted by the batch method at ambient temperature for 720 h with 2 g L⁻¹ of both modified sorbents. Removal efficiencies of sulphate, nickel, zinc, iron and copper ions for both sorbents were 50%, 75%, 80%, 99% and 90%, respectively which are lower compared to adsorption from the synthetic AMD (Fig. 4).

Increasing adsorbents concentration and sorption time did not increase removal efficiency. Equilibrium occurred at the optimal sorption time (48 h) and sorbents concentrations of 2 g L⁻¹. The lower sorption capacity of both sorbents for real AMD compared to synthetic solutions could be due to complex composition of real AMD. Other ions can act as competitors during the adsorption process, such as chloride, ammonium and some trace amount of metal ions.

Conclusions

Novel iron-containing sorbents from an industrial solid waste were produced with ALD technology for TiO₂ and Al₂O₃ coating. The optimal sorption parameters were estimated with synthetic AMD. The optimal time (48 h) and sorbent concentration (2 g L⁻¹) were determined with a batch method. The maximum sorption capacities of RH-Al₂O₃ and RH-TiO₂ were around 600, 200, 200, 150 and 100 mmol g⁻¹ for removal of SO₄²⁻, Fe³⁺, Cu²⁺, Zn²⁺ and Ni²⁺, respectively. The sorption process was carried out using complexation and ion-exchange mechanism. The deposition of TiO₂ and Al₂O₃ on the surface of granules sufficiently increased the sorption capacities of raw material for real AMD treatment. The both produced sorbents could be used for real AMD treatment with a high capacity for some pollutants. The optimisation of modification process with ALD for cost decreasing while maintaining modified sorbents properties could be recommended for the further research. Increasing sulphate ions removal from complex solution should be taken into account also.

Acknowledgements

The authors acknowledge Finnish Funding Agency for Technology and Innovation (TEKES) for financial support.

References

- Alcolea, A., Vazquez, M., Caparros, A., Ibarra, I., Garcia, C., Linares, C., Rodriguez, R. (2012). Heavy metals removal of intermittent acid mine drainage with an open limestone channel. *Minerals Engineering*, 26, 86–98.
- Allen, S.J., McKay, G., Porter, J. F. (2004). Adsorption isotherm models for basic dye adsorption by peat in single and binary component systems. *Journal of Colloid and Interface Science*, 280, 322–333.
- Aziz, H.A., Adlan, M.N., Arffin, K. S. (2008). Heavy metals (Cd, Pb, Zn, Ni, Cu and Cr(III)) removal from water in Malaysia: post treatment by high quality limestone. *Bioresource Technology*, 99, 1578–1583.
- Bartczak, P., Norman, M., Klapiszewski, Ł., Karwańska, N., Kawalec, M., Baczyńska, M., Jesionowski, T. (2015). Removal of nickel(II) and lead(II) ions from aqueous solution using peat as a low-cost adsorbent: A kinetic and equilibrium study. *Arabian Journal of Chemistry*. doi:10.1016/j.arabjc.2015.07.018

- Boonamnuayvitaya, V., Chaiya, C., Tanthapanichakoon, W., & Jarudilokkul, S. (2004). Removal of heavy metals by adsorbent prepared from pyrolyzed coffee residues and clay. *Separation and Purification Technology*, 35(1), 11–22. doi:10.1016/S1383-5866(03)00110-2
- Borai, E. H., Breky, M. M. E., Sayed, M. S., & Abo-Aly, M. M. (2015). Synthesis, characterization and application of titanium oxide nanocomposites for removal of radioactive cesium, cobalt and europium ions. *Journal of Colloid and Interface Science*, 450, 17–25. doi:10.1016/j.jcis.2015.02.062
- Cousin, E., & Taugourdeau, E. (2016). Cost minimizing water main quality index: A static cost minimization approach. *Water Resources and Economics*, 15, 28–42. doi:10.1016/j.wre.2016.06.001
- DiLoreto, Z. A., Weber, P. A., & Weisener, C. G. (2016). Solid phase characterization and metal deportment in a mussel shell bioreactor for the treatment of AMD, Stockton Coal Mine, New Zealand. *Applied Geochemistry*, 67, 133–143. doi:10.1016/j.apgeochem.2016.02.011
- Flores, R. G., Andersen, S. L. F., Maia, L. K. K., José, H. J., & Moreira, R. de F. P. M. (2012). Recovery of iron oxides from acid mine drainage and their application as adsorbent or catalyst. *Journal of Environmental Management*, 111, 53–60. doi:10.1016/j.jenvman.2012.06.017
- Genç-Fuhrman, H., Mikkelsen, P. S., & Ledin, A. (2016). Simultaneous removal of As, Cd, Cr, Cu, Ni and Zn from stormwater using high-efficiency industrial sorbents: Effect of pH, contact time and humic acid. *Science of The Total Environment*, 566, 76–85. doi:10.1016/j.scitotenv.2016.04.210
- George, S. M. (2010). Atomic layer deposition: an overview. *Chemical Reviews*, 110(11-131).
- Gulshan, F., Kameshima, Y., Nakajima, A., & Okada, K. (2009). Preparation of alumina-iron oxide compounds by gel evaporation method and its simultaneous uptake properties for Ni²⁺, NH₄⁺ and H₂PO₄⁻. *Journal of Hazardous Materials*, 169(1-3), 697–702. doi:10.1016/j.jhazmat.2009.04.009
- Han, C., Li, H., Pu, H., Yu, H., Deng, L., Huang, S., & Luo, Y. (2013). Synthesis and characterization of mesoporous alumina and their performances for removing arsenic(V). *Chemical Engineering Journal*, 217, 1–9. doi:10.1016/j.cej.2012.11.087
- Iakovleva, E., Mäkilä, E., Salonen, J., Sitarz, M., Wang, S., & Sillanpää, M. (2015a). Acid mine drainage (AMD) treatment: Neutralization and toxic elements removal with unmodified and modified limestone. *Ecological Engineering*, 81, 30–40. doi:10.1016/j.ecoleng.2015.04.046
- Iakovleva, E., Mäkilä, E., Salonen, J., Sitarz, M., & Sillanpää, M. (2015b). Industrial products and wastes as adsorbents for sulphate and chloride removal from synthetic alkaline solution and mine process water. *Chemical Engineering Journal*, 259, 364–371. doi:10.1016/j.cej.2014.07.091
- Iakovleva, E., Maydannik, P., Ivanova, T. V., Sillanpää, M., Tang, W. Z., Mäkilä, E., Salonen, J., Gubal, A., Ganeev, A.A., Kamwilaisak, K., Wang, S. (2016). Modified and unmodified low-cost iron-containing solid wastes as adsorbents for efficient removal of As(III) and As(V) from mine water. *Journal of Cleaner Production*, 133, 1095–1104. doi:10.1016/j.jclepro.2016.05.147
- Kilbury, O. J., Barrett, K. S., Fu, X., Yin, J., Dinair, D. S., Gump, C. J., King, D. M. (2012). Atomic layer deposition of solid lubricating coatings on particles. *Powder Technology*, 221, 26–35. doi:10.1016/j.powtec.2011.12.021
- Kukli, K., Salmi, E., Jögiaas, T., Zabels, R., Schuisky, M., Westlinder, J., Leskelä, M. (2016). Atomic layer deposition of aluminum oxide on modified steel substrates. *Surface and Coatings Technology*, 304, 1–8. doi:10.1016/j.surfcoat.2016.06.064
- Lei, K., Pan, H., & Lin, C. (2016). A landscape approach towards ecological restoration and sustainable development of mining areas. *Ecological Engineering*, 90, 320–325. doi:10.1016/j.ecoleng.2016.01.080
- Mudd, G. M. (2008). Sustainability Reporting and Water Resources: a Preliminary Assessment of Embodied Water and Sustainable Mining. *Mine Water Environment*, 27, 136–144. doi:10.1007/s10230-008-0037-5

- Puttaswamy, M., Vehkamäki, M., Kukli, K., Dimri, M. C., Kemell, M., Hatanpää, T., Leskelä, M. (2016). Bismuth iron oxide thin films using atomic layer deposition of alternating bismuth oxide and iron oxide layers. *Thin Solid Films*, 611, 78–87. doi:10.1016/j.tsf.2016.05.006
- Reddy, D. H. K., & Yun, Y.-S. (2016). Spinel ferrite magnetic adsorbents: Alternative future materials for water purification? *Coordination Chemistry Reviews*, 315, 90–111. doi:10.1016/j.ccr.2016.01.012
- Silva, R., Cadorin, L., Rubio, J. (2010). Sulphate ions removal from an aqueous solution: I. Co-precipitation with hydrolysed aluminum-bearing salts. *Minerals Engineering*, 23, 1220–1226.
- Tang, D., Wang, H., Gregory, J. (2002). Relative importance of charge neutralization and precipitation on coagulation of Kaolin with PAC:effect of sulphate ion. *Environmental Science and Technology*, 36, 1815–1820.
- Theiss, F. L., Ayoko, G. A., & Frost, R. L. (2016). Synthesis of layered double hydroxides containing Mg_{2+} , Zn_{2+} , Ca_{2+} and Al_{3+} layer cations by co-precipitation methods—A review. *Applied Surface Science*, 383, 200–213. doi:10.1016/j.apsusc.2016.04.150
- Tiznado, H., Domínguez, D., Muñoz-Muñoz, F., Romo-Herrera, J., Machorro, R., Contreras, O. E., & Soto, G. (2014). Pulsed-bed atomic layer deposition setup for powder coating. *Powder Technology*, 267, 201–207. doi:10.1016/j.powtec.2014.07.034
- Wolkersdorfer, C. (2008). *Water Management at Abandoned Flooded Underground Mines. Fundamentals, Tracer Tests, Modelling, Water Treatment*. Springer. doi:10.1007/978-3-540-77331-3

Valorisation of Separated Solids from Mine Water Treatment

Tommi Kaartinen, Petteri Kangas and Mona Arnold

VTT Technical Research Centre of Finland Ltd P. O. Box 1000 02044 VTT Finland

Abstract This paper describes two concepts for simultaneous recovery of magnesium and removal of sulphate from mine effluent. Treatment of mixed gypsum sludge generated in sulphate removal by lime precipitation containing roughly 2/3 of gypsum and 1/3 of magnesium hydroxide was treated with CO₂ to separate Mg from Ca. Another concept utilizes selective precipitation of Mg before any sulphate removal measures to recover as pure magnesium hydroxide as possible. In terms of Mg recovery, the latter concepts seems more promising, but it has impacts on sulphate removal with regards to increased chemical consumption.

Key words sulphate removal, magnesium, valorisation, recovery

Introduction

Solid residues generated in the treatment of mine process waters reflect the quality of the feed to the water treatment as well as chemicals used in the treatment. The most common treatment for sulphate laden water is precipitation with lime. In such case the solids often contain high concentrations of gypsum, but also other minerals that have dissolved in mine processes and precipitate together with gypsum. For instance magnesium, which is present in many metal ores, dissolves into the process water and often precipitates as magnesium hydroxide in the same pH-window with gypsum. Sustainable mining calls for maximal recycling of water and solid materials to be used again in the mine processes. Therefore, it is necessary to search for cost-efficient methodologies to separate solid and liquid streams with different properties from each other to best utilize each of these secondary resources. Moreover, the amount of wet gypsum residuals generated can be substantial and challenging from a disposal point of view. This paper concentrates on magnesium recovery from mine effluent and a mixed sludge of gypsum and magnesium hydroxide. The global market of magnesium has recently seen a rapid increase in demand and production, whereas the production is very heterogeneously distributed (Cipollina et al. 2014). EU has classified Mg among the 14 most critical raw materials.

Recovery of magnesium from mixed gypsum sludge by bubbling with carbon dioxide is described in the literature (Rukuni et al. 2015). Similar technology is also proposed earlier (Bologo et al. 2009). However, these papers do not give clear description whether magnesium is dissolved from gypsum as carbonate or sulphate. If Mg was dissolved as sulphate, it could be crystallized by evaporation and further roasted to form MgO and sulphurous acid gas that could be used in sulphuric acid production (Ozaki et al 2014) Another concept for recovery of magnesium would be selective precipitation of magnesium hydroxide before a mixed gypsum sludge is formed. Cipollina et al. (2014) proposed a reactive crystallization process for concentrated brines, in which magnesium is precipitated with sodium hydroxide to form magnesium hydroxide. They suggested, that the process could be economically viable, if magnesium sulphate with high purity was generated. A drawback in sulphate bearing

water would be the generation of very soluble sodium sulphate, which would not be removable through lime treatment.

This paper describes laboratory scale experimental efforts coupled with thermodynamic multi-phase modelling for recovery of magnesium and removal of sulphate from mine effluent. Two concepts for magnesium recovery are assessed, and a qualitative comparison is made between these concepts together with their possible impacts on sulphate removal, an angle from which the proposed magnesium recovery concepts have not been looked before. The ettringite process, consisting of chemical sulphate precipitation as low-soluble mineral ettringite with the use of lime and aluminium salt, was chosen as the sulphate removal technique in combination with Mg recovery. With the ettringite process very low residual sulphate concentrations are possible to reach, and the process has also been applied in industrial scale (Tolonen et al. 2016).

Materials and methods

Mine effluent

Mine waste water with main characteristics shown in Table 1 was used for the experiments.

Table 1. Major substances in mine effluent

Parameter	Mine effluent
pH	7.0 – 7.5
Sulphate SO_4^{2-} , mg/L	9 200
Calcium Ca, mg/L	450
Magnesium Mg, mg/L	1 900
Potassium K, mg/L	120
Sodium Na, mg/L	220

Studied concepts for magnesium recovery and sulphate removal

Figure 1 shows the flow-sheets of the compared concepts in the study. In concept A a mixed gypsum sludge is formed in the first reactor to remove most of the sulphate. The sludge is then treated with CO_2 for the separation of Ca and Mg. Dissolved Mg is then crystallized by evaporation. In concept B the first step is precipitation of $\text{Mg}(\text{OH})_2$ with NaOH followed by gypsum precipitation in the next phase. Both concepts include the ettringite precipitation (addition of Al-salt and lime) as the last sulphate removal step, after which neutralization of the treated effluent takes place to meet effluent discharge pH-criteria (often pH10 at Finnish mines).

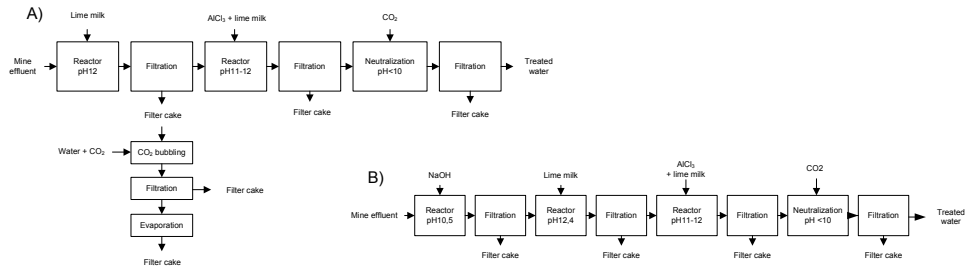


Figure 1. Studied concepts for Mg recovery and sulphate removal.

Computational assessment

Opportunities of recovering magnesium and removing sulphate from mine waters were assessed using thermodynamic multi-phase modelling (Pajarre et al. 2016b) where Pitzer formalisms (Harvie et al. 1984; Holmes and Mesmer 1986) were applied for describing the activities of solute species in the aqueous media. More details of applied database and models are given in the literature where mine water and hydrometallurgical processes are studied (Pajarre et al. 2016a, c; Koukkari et al. 2017).

Multiphase chemical system of Na-K-Ca-Mg-Al-SO₄-CO₃ was utilised for modelling the mine water chemistry. Here ideal mixed gaseous phase, aqueous phase based on Pitzer formalism and pure precipitated phases were included. This thermodynamic database is applicable for elevated temperatures up to 90 °C and up to molality ≈ 10 mol/kg. For modelling purposes following compositions of mine waters and gypsum were applied, Table 2.

Table 2 Composition of treated stream and mixed gypsum sludge (ppm) used for thermodynamic modelling. The elements are converted to respective salts for the thermodynamic multi-phase model (e.g. Na₂SO₄, K₂SO₄, CaSO₄·2H₂O, MgSO₄ and Mg(OH)₂). Note. Slight differences in water composition in comparison to Table 1, because data from different batch of water was used as starting point for modelling.

	Na	K	Ca	Mg	SO ₄
Water before gypsum precipitation	240	130	470	1900	9200
Mixed gypsum sludge	400	200	190000	120000	450000
Water after gypsum precipitation	210	120	850	1,0	1700

Experimental work

All the reactor tests (Figure 1) were performed as batch tests in room temperature in continuously stirred reactors, in which the volume of mine effluent was 10 litres when entering the first stage. In all precipitation steps, water was first added to the reactor, mixing was started,

and the reagents were added as one-time dose into the reactors. In all precipitation tests the duration of experiment was 30 minutes, after which the stirring was ceased and the mixture was filtrated through 0,45 µm membrane filter. CO₂-bubbling of filter cake from lime precipitation step in concept A was performed in 1 litre reactor for 60 minutes, after which the mixture was also filtrated (0,45 µm). The final CO₂ neutralization of ettringite precipitation effluents was monitored with pH meter and ceased when pH was below 10.

Lime was added as 10 % solution (100 g analytical grade Ca(OH)₂ (>96 %) in 1000 mL). Lime dosing was based on pH in steps were only lime was used, and on pH and stoichiometry in ettringite precipitation steps. Extra-pure anhydrous AlCl₃ (>99%) was used as the aluminium source in ettringite precipitation. AlCl₃ was first solubilized, and added as a solution of 25% (25 g in 100 ml). AlCl₃ dosing was based on stoichiometry (molar ratio of sulphate and Al). NaOH was added as 4 M solution, and the dosing was based on pH shown by modelling. CO₂ was added to the treatment step of mixed gypsum sludge as pure CO₂ through a glass sinter, and the dosing was adjusted with a rotameter to 1 litre per minute.

All the filter cakes except for the CO₂-neutralized effluents from ettringite precipitation (small amounts) were characterised for inorganic elemental composition by X-ray fluorescence (XRF). All water samples (mine effluent + samples after filtration) were analysed for sulphate by ion chromatography (IC) and Ca, Mg, K and Na by inductively coupled plasma optical emission spectrometry (ICP-OES). Additionally, for process control purposes sulphate was analysed with Hach Lange DR3900 spectrophotometer and LCK 353 kits. Also pH, conductivity and redox values of all water samples were determined.

Filter cakes from CO₂ treatment of mixed gypsum sludge and NaOH precipitation were washed on the filters in liquid to solid ratio of 5 after collecting the first filtrate. Washing was done to remove dissolved substances from the filter cakes and thus 1) increase the recovery of dissolved Mg in the CO₂ treatment and to 2) purify the Mg(OH)₂ recovered in the selective precipitation. The filtrates from filter cake washing were also analysed for same substances than other water samples.

Effluent from CO₂ treatment from mixed gypsum sludge in concept A was dried overnight at 105 °C in order to evaporate water and crystallize magnesium sulphate. The formed solid was also characterised by XRF.

Results

Computational assessment

Figure 2 shows the results from computational assessment performed in order to suggest the dissolving species of magnesium in CO₂ treatment of mixed gypsum sludge (concept A). The composition of mixed gypsum sludge is given in Table 2 and the amount of gypsum is 100 g per 1000 g of water. Applied temperature is 25 °C and pressure is 1 bar.

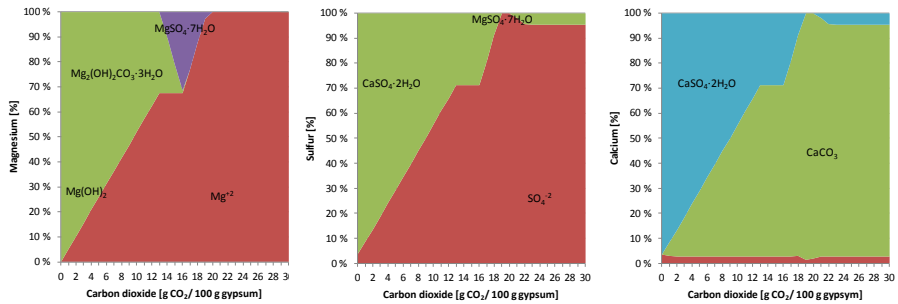


Figure 2 Appearance of magnesium (left), sulphur (centre) and calcium (right) species within the chemical system during the carbon dioxide treatment of mixed gypsum sludge. Here the composition of raw material is 25% of $Mg(OH)_2$ and 75% of gypsum. Amount of water is 1000 g per 100 g of solids.

Based on the thermodynamic analysis, the magnesium is dissolving from the gypsum due to the reaction with carbon dioxide. However, the sulphate ion is dissolving respectively. Thus, the gypsum is transforming to the calcium carbonate and dissolved species is magnesium sulphate. The optimal charge of carbon dioxide is 20 g per 100 gram of treated solids.

Figure 3 shows the results from computational assessment for concept B, where NaOH is used in the first stage to selectively precipitate $Mg(OH)_2$. The composition of treated mine water before precipitation with NaOH is given in Table 2.

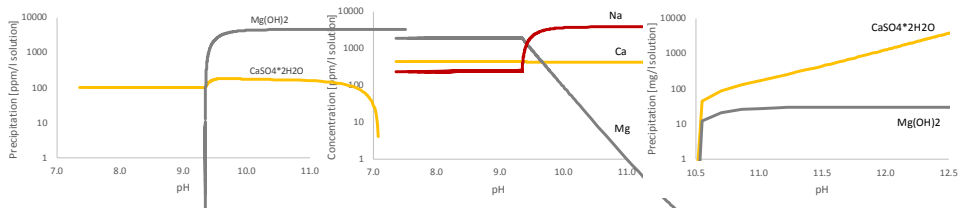


Figure 3 The precipitated phases (left) and dissolved metals (centre) during the neutralisation of mine water by caustic soda. The precipitated phases (right) during the neutralisation of remaining water by lime milk.

Computational assessment, Figure 3, illustrates that $Mg(OH)_2$ could be selectively precipitated at pH level 9.3 – 10.0. Some gypsum precipitates simultaneously. However, the drawback here is the extensive usage of caustic soda resulting in high level of soluble sodium sulphate in treated water. According to the computational assessment, the sulphate level will remain > 6000 ppm even after lime treatment if magnesium is selectively precipitated with caustic soda.

Experimental work

Concept A

Table 3 shows the concentrations of studied substances in liquid fractions collected at different stages of the process in concept A. Table 4 shows the concentrations of same elements

in solid matrices generated in this concept. Sulphate concentrations in lime treatment decreased to below 2 000 mg/L like expected. Subsequent ettringite precipitation further decreased sulphate concentrations to 3.9 mg/L. In CO₂ treatment of mixed gypsum sludge, plenty of sulphate was released to water phase being in accordance with predictions from the modelling work. Magnesium concentrations in the filtrate of CO₂ bubbled sludge were roughly 4.5 times the concentrations in the mine effluent giving justification to this concentration stage. Not much Mg was left in the sludge after CO₂ treatment, whereas Ca retained in solid form in the CO₂ treatment also being in accordance with model prediction. Sulphate ends up mainly in 1) washed sludge after CO₂ bubbling 2) Evaporation residue and 3) ettringite sludge. Some sulphate is also released to the wash water of the CO₂ treated sludge, which would still have to be treated.

Based on Mg concentrations in the mine effluent, amounts of generated solids and Mg concentrations in the solid, some 55 % (w/w) of input Mg was found in crystallized evaporation residue from CO₂ bubbled sludge – filtrate. 9.5 % was retained in the solid form in the CO₂ bubbling, and some Mg (<10 %) was also lost in the washing water of the CO₂ treated sludge. However, mass balance calculations do not reach even close to 100 % in the case of Mg, which most likely is a consequence of the different analytical techniques used for liquid and solid phases and the semi-quantitative nature of the XRF analysis. Based on the concentration of Mg in the evaporation residue from CO₂ bubbled sludge – filtrate, the highest possible purity of the Mg product from concept A, magnesium sulphate, is 84 %.

Overall chemical consumptions for concept A were 10 g Ca(OH)₂ (pure) and 2.7 g AlCl₃ (pure) per litre treated water. CO₂ was dosed in surplus, but modelling work proposed a dose equivalent to 3.4 g CO₂ of one litre treated water. Additional lime and possibly Al-salt would be needed to precipitate sulphate from the filter cake wash water.

Table 3. Water quality in different stages of the concept A.

Parameter	Mine effluent	After lime treatment	Treated water (ettringite precip. + neutralization)	CO ₂ bubbled sludge – filtrate	CO ₂ bubbled sludge – filter cake wash water
pH	7,0	12,2	7,2	7,7	7,8
Sulphate, mg/L	9 200	1 700	3,9	19 000	10 000
Ca, mg/L	450	850	980	83	500
Mg, mg/L	1 900	1,3	0,16	8 900	2 800

Table 4. Characteristics of solids formed in different stages of concept A.

Parameter	Mixed gypsum sludge	Washed sludge after CO ₂ bubbling	Crystallized evaporation residue from CO ₂ bubbled sludge – filtrate	Ettringite sludge
Amount generated (dry), grams per litre treated water	17	9.0	6.2	8.6
S, %	15	11	13	6,9
Ca, %	19	31	2,0	21
Mg, %	13	2.0	17	0.17

Concept B

Table 5 shows the concentrations of studied substances in liquid fractions collected at different stages of the process in concept B. Table 6 shows the concentrations of same elements in solid matrices generated in this concept.

As predicted by modelling, NaOH precipitation removes most of Mg while other major components are passed on to next phases. Lime treatment of NaOH treated water results in slight decrease in sulphate concentrations also in accordance with the model, and ettringite precipitation takes care of the rest of sulphate.

From the input Mg, some 72 % was found in washed precipitate from NaOH precipitation. Sulphate ends up mainly in ettringite sludge. Based on the concentration of Mg in the washed NaOH precipitated sludge, the highest possible purity of the Mg product from concept B, magnesium hydroxide, is 94 %.

Overall chemical consumptions for concept B were 5.3 g NaOH (pure), 20 g Ca(OH)₂ (pure) and 4.5 g AlCl₃ (pure) per litre treated water. Additional lime and possibly Al-salt would be needed to precipitate sulphate from the filter cake wash water.

Table 5. Water quality in different stages of the concept B.

Parameter	Mine effluent	After NaOH treatment	After lime treatment	Treated water (ettringite precip. + neutralization)	NaOH-precipitated sludge, wash water
pH	7.0	10.2	12.6	6.8	8.0
Sulphate, mg/L	9 200	8 200	5 600	4,8	5 600
Ca, mg/L	450	450	630	740	260
Mg, mg/L	1 900	100	<0.15	<0.15	210

Table 6. Characteristics of solids formed in different stages of concept B.

Parameter	Washed NaOH-precipitated sludge	Ca(OH) ₂ precipitated sludge	Ettringite sludge
Amount generated (dry), grams per litre treated water	3,5	11	12
S, %	1,0	0.86	8,4
Ca, %	0,14	47	26
Mg, %	39	1.2	0.16

Conclusions

Based on the computational assessment, it can be concluded that i) magnesium sulphate is dissolved from mixed gypsum waste by carbon dioxide treatment, ii) magnesium can be selectively precipitated by caustic soda but simultaneously the residual sulphate in effluent does not obey lime treatment.

Laboratory scale experimental work was done to validate the findings from computational assessment. The overall conclusion is that modelling and experimental results were in good agreement in this study. Selective precipitation of magnesium with NaOH before any sulphate removal measures led to recovery of quite pure (94 %) magnesium hydroxide and also giving better recovery of Mg (72 %) making this concept more promising for Mg recovery. However, this led to increased chemical consumption in subsequent sulphate removal steps that possibly worsens the economic feasibility of the concept.

References

- Bologo V, Maree JP, Zvinowanda CM (2009) Treatment of Acid Mine Drainage Using Magnesium Hydroxide. In: International Mine Water Conference. Pretoria, South Africa, pp 371–380
- Cipollina A, Bevacqua M, Dolcimascolo P, Tamburini A, Brucato A, Glade H, Buether L, Micale G (2014) Reactive crystallisation process for magnesium recovery from concentrated brines. *Desalination and Water Treatment* 55: 2377–2388
- Harvie C, Møller N, Weare JH (1984) The prediction of mineral solubilities in natural waters: The Na-K-Mg-Ca-H-Cl-{SO₄-OH-HCO₃-CO₃-CO₂-H₂O} system to high ionic strengths at 25 C. *Geochim Cosmochim Acta* 48:723–751.
- Holmes HF, Mesmer RE (1986) Thermodynamics of aqueous solutions of the alkali metal sulphates. *J Solution Chem* 15:495–517. doi: 10.1007/BF00644892
- Koukkari P, Pajarre R, Kangas P, Penttilä K (2017) Multicomponent Solubility Models in Mine Water Management. In: *Mineralteknik 2017*. Luleå, Sweden,
- Ozaki Y, Takahashi J, Yamashita Y, Ohara H (2014) United States Patent Application Publication, Pub. No. US 2014/0348732 A1
- Pajarre R, Kangas P, Penttilä K, Koukkari P (2016a) Multiphase simulation of mine waters and aqueous leaching processes. In: *Mineral Engineering Conference*. Swieradow-Zdroj, Poland,
- Pajarre R, Koukkari P, Kangas P (2016b) Constrained and extended free energy minimisation for

modelling of processes and materials. *Chem Eng Sci* 146:244–258. doi: 10.1016/j.ces.2016.02.033

- Pajarre R, Koukkari P, Kangas P (2016c) Use of kinetically constrained free energy models for concentrated aqueous systems at 25-100 °C. In: *International Symposium on Solubility Phenomena and Related Equilibrium Processes ISSP17*. Geneva, Switzerland,
- Rukuni T, Maree J, Carlsson F (2015) Investigation of carbonate dissolution for the separation of magnesium hydroxide and calcium sulphate in a magnesium hydroxide-calcium sulphate mixed sludge. *Water SA* 41:253. doi: 10.4314/wsa.v41i2.11
- Tolonen E, Hu T, Rämö J and Lassia U (2016) The removal of sulphate from mine water by precipitation as ettringite and the utilisation of the precipitate as a sorbent for arsenate removal. *J of Environ Management* 18: 856–862

Tailings Seepage Paths Mapped using Electric-Based Technology

Cecil Urlich¹, Andy Hughes², Val Gardner³

¹*AECOM, 1111 3rd Avenue, Suite 1600, Seattle, Washington 98101, USA
cecil.urlich@aecom.com*

²*Atkins Global, The Wells, 3 -13 Church Street, Epsom, Surrey, KT17 4PF, UK,
andy.hughes@atkinsglobal.com*

³*Willowstick, 11814 Election Rd, Suite 100, Draper, Utah 84020, USA,
vgardner@willowstick.com*

Abstract Tailings dams have failed at alarming rates compared to water storage dams. Failures are often due to human-controlled design, construction and operation actions which can result in tailings flows, life and property loss, and negatively impact the environmental, social license, company value and industry sustainability. Several technologies are used to help better understand tailings dams, reduce their failure risk, and add value to tailings management. These include the use of electrical current to find seepage paths under a dam. This paper describes this technology by case studies and how it enabled designs to be updated to reduce the failure risk.

Introduction

Tailings dams and storage facilities are unique and are different to water supply dams for many reasons: they store tailings (waste liability) versus water (resource asset); their construction and design evolve as the facility develops and tailings volumes increase while codes, regulations and technologies change; they embrace tailings properties, disposal methods and water management in dam design; and they store tailings in perpetuity.

Properly planned, designed, constructed, operated and maintained tailings dams provide safe and effective tailings storage facility (TSF) structures. Dams are raised by optimizing upstream, centerline and downstream methods to fit site conditions, land constraints and mine operations. TSFs use a host of tailings and water management methods to optimize storage space, reduce operation costs, protect the environment, and maintain indefinite dam stability and safety.

Tailings dams are dynamic structures that grow in size and complexity over their operating life and must be maintained after closure. Their designs evolve with time and not always as originally planned because of global events that mine owners have no control over, to local operation, community, environment, and other challenges.

Evolving designs continue to combine proven existing and new (disrupt mining) technologies to enhance the positive, progressive and collective ability to effectively manage tailings dams and TSFs. For example, several new non-intrusive technologies are now being used to help designers such as a method to identify seepage paths at depth through, under and around tailings dams that helps in the design of TSF and tailings dam stabilizations, expansions, and closures.

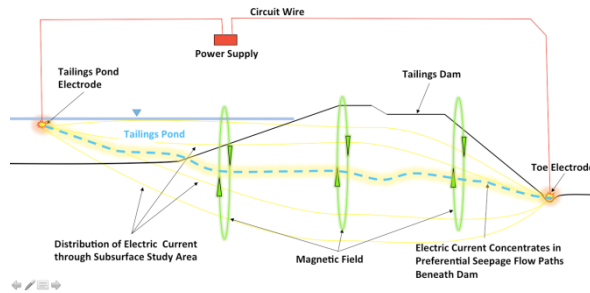


Figure 1. Survey setup

Non-Intrusive Investigative Technology

This paper describes a geophysical technology that uses a low voltage, low amperage, alternating electrical current to energize subsurface water by electrodes placed in tailings water and seepage discharge (Williams et al. 1996 and Kofoed et al. 2011). With one electrode placed in the tailings and the other placed in contact with water below the tailings dam, an electrical circuit is established between the two water bodies (Figure 1).

As with all alternating electrical currents, this circuit generates a magnetic field that is measured and mapped from the surface. This collected data is used to render two- and three-dimensional (2D and 3D) maps and Electric Current Distribution (ECD) models of seepage paths (Figure 2). The technology maps and models preferential groundwater flow paths like an angiogram that lets doctors to “see” blood vessels in a human body.

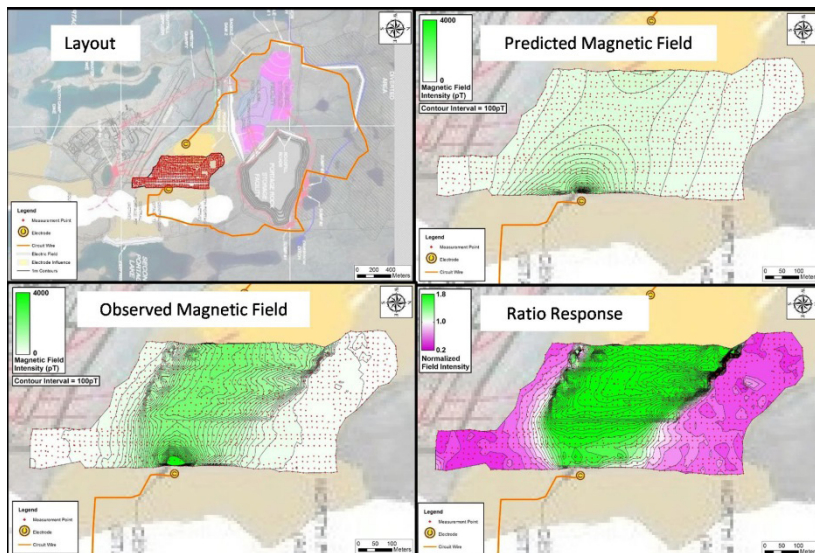


Figure 2 Steps to get data results and two-dimensional maps

The application of the technology to tailings dams is based on the principle that water increases the conductivity of earth materials through which it flows. As the signature electric current travels between electrodes strategically placed upstream and downstream of the tailings dam, it concentrates in the more conductive zones, or highest transport porosity areas, where tailings water preferentially flows out of the TSF as seepage through, under, and around the dam.

An electric circuit is established in the water of interest. Measuring the resultant magnetic field at the surface reveals the electric current flow and distribution. Data is processed and compared to a predicted magnetic field from a theoretical homogenous earth model to highlight deviations from the “uniform” model. 2D maps and 3D models are generated and combined with known sub-surface data to enhance preferential seepage path definitions (Figure 2).

The graphic shading in the following black-and-white figures is shades of gray. Actual survey report graphics range from purple (dark gray) to green (medium gray). Dark gray shows actual flow that is less than flow predicted by the “uniform” model. Medium gray shows actual flow that is more than flow predicted by the “uniform” model, so it likely represents a seepage path.

This paper uses three tailings dam studies to illustrate the procedures, findings and benefits of this technology. Results range from confirming design decisions to identifying new seepage paths. In the latter case, designs were updated based on new data in line with the observational approach (Peck 1969) to provide a more safe and stable tailings dam and reduce risk of failure.

Tailings Dam Study 1

Tailings Dam Study 1 involves a TSF where seepage was suspected in left and right abutments (Figure 3). A dike separates the cells. A settling pond and open pit are near the new dam.



Figure 3 – Valley fill tailings storage facility and dam.

Seepage had been observed at both right and left abutments of the main dam. The seepage flow was not excessive and there was no sign of turbidity. However, the mine decided to investigate further using the electrical-based technology due to its non-intrusive nature and ability to identify the full seepage pathway in plan and elevation.

Six surveys were planned, three each in the left and right abutment areas. Each survey used a slightly different electrode placement on the tailings side of the dam while the electrode downgradient of the crest remained static for each set of three surveys. Each survey covered a different geography with overlap between surveys to confirm any observed anomalies.

No preferential seepage paths were identified in the left abutment area. The electric current through the area was observed to be uniform and evenly distributed in all three surveys. At the right abutment, the electric flow was observed to be more varied. Two seepage paths were observed in each of the three surveys, each providing confirmation of the next (Figure 4).

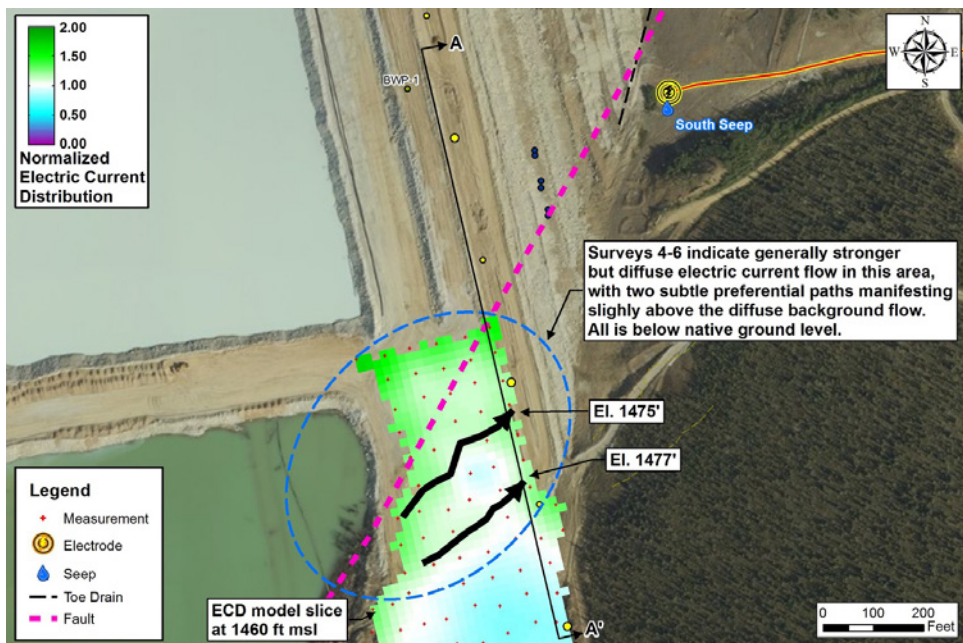


Figure 4 – Identified seepage paths shown in black with elevations posted at dam's crest.

Both seepage paths were found to be located in the native foundation materials beneath the dam (Figure 5). In addition, both of these seepage paths followed the alignment of a fault that had been identified earlier by the mine.

No discrete seepage paths were observed between the TSF and the seepage that had been observed in the left abutment. All three of the south abutment surveys identified the same preferential flow paths in the foundation materials leading to the observed seepage.

Two survey layouts were used with the same upstream electrode in the new tailings pond. For Survey 1, the downstream electrode was in the seepage discharge at the toe of the new dam. For Survey 2, it was in the seepage discharge in the open pit east of the dam.

Survey 1 identified primary and secondary seepage paths under the dam (Figures 7 and 8). The plan and profile views show seepage path widths and depths. The green (medium gray) shading indicates seepage paths. The black lines are interpretations of seepage paths between the two electrodes.

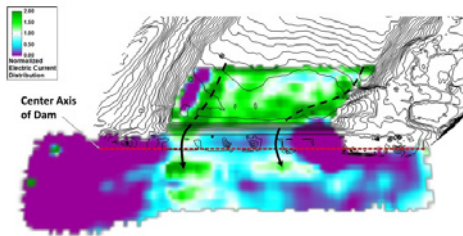


Figure 7 – Two seepage paths under dam

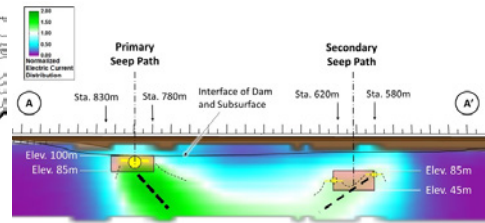


Figure 8 – Seepage path elevations

The results confirmed that there are no other seepage paths of any significance through or under the dam. This provided confidence that piping and internal erosion were not concerns for the dam itself because the identified seepage paths are in the foundation materials under the dam and not in the dam structure itself. So the geotechnical investigations for piping potential could be focused on the foundation materials under the dam and not on the dam structure itself.

A geotechnical investigation was completed by drilling into the seepage path target areas identified by the survey. The drilling confirmed the survey findings. Remedial measures are now being planned that will be significantly less in cost than if the survey had not been completed and seepage paths not found because the investigation was targeted on the areas of concern.

Tailings Dam Study 3

Tailings Dam Study 3 involves a TSF with a tailings dam in a valley. A seepage collection pond is downstream of the tailings dam. A waste rock dump occupies one of the valley sides of the TSF. A 2-kilometer long drainage collection trench is aligned along the toe of this dump (Figure 9).

Seepage from the TSF collects in a collection system and is pumped back to the TSF. Additional contribution to the pumped back water is surface runoff from the collection system catchment area. There was concern that some “surface runoff” could also be seepage from the TSF through the left abutment of the tailings dam, and that there could be seepage from the TSF flowing under the collection system and to the environment.



Figure 9 – Tailings facility and waste rock dump

Water that escapes from the waste rock dump drainage collection trench also enters the TSF. However, over time as the TSF rises, the hydraulic gradient could switch from the TSF to the waste rock dump.

The survey was conducted in two phases: Phase 1 to identify and delineate seepage patterns through, under, and around the tailings dam and seepage collection dam to enable them to be stabilised if necessary, for raising the tailings dam; and Phase 2 to identify any deeper seepage paths that might pass under the waste rock dump drainage collection trench and flow to the TSF.

During Phase 1, a seepage path was unexpectedly found into the TSF under the wing wall part of the tailings dam (Figure 10). The seepage path is broad at first but narrows down. This seepage path conveys drainage into the TSF from the east hillside under the wing wall 5 to 6 meters below the ground surface in what was confirmed to be a buried former drainage channel.



Figure S1 – Survey Coverage and Summary of Detected Seepage and Drainage Paths for Main Dam Area

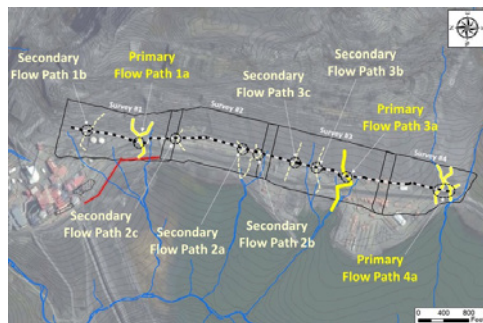


Figure 11 – Plan View of seepage paths

Seepage out of the TSF originates in original drainages under the TSF, converges to a rock under-drain in the original creek channel under the highest part of the dam, and flows through the underdrain to the seepage collection pond (Figure 10). The survey confirmed

that the TSF and seepage pond were performing as designed with no seepage out of the seepage pond.

A third drainage path unrelated to TSF seepage was identified. Originating from the right hillside just downstream of the dam, this drainage conveys water to under the dam's right mitre (Figure 10). Some of this water exits out from under the dam below the mitre. Some drainage mixes with seepage from the TSF. All seepage and drainage were found to be captured in the seepage pond.

No other seepage paths were identified through, under or around the tailings dam and seepage collection pond areas. The survey confirmed the design assumptions and performance expectations, and enabled planning to start for future tailings dam raisings and collection pond relocations to accommodate the increased footprint of an expanded tailings dam.

For the Phase 2 survey, solid lines are primary seepage paths. Light dash lines are secondary seepage paths. Dashed circles show electric current preferentially flowing through and under the trench. Primary seepage paths were found to align with original drainages (Figure 11). Secondary seepage paths are under the trench but are shallower than primary seepage paths.

The survey found that seepage from the waste rock dump was flowing under the dump along the drainage collection trench on the original ground surface. The model identified the depths of the primary seepage paths in the trench (Figure 11 and 12). Figure 13 shows the seepage paths.

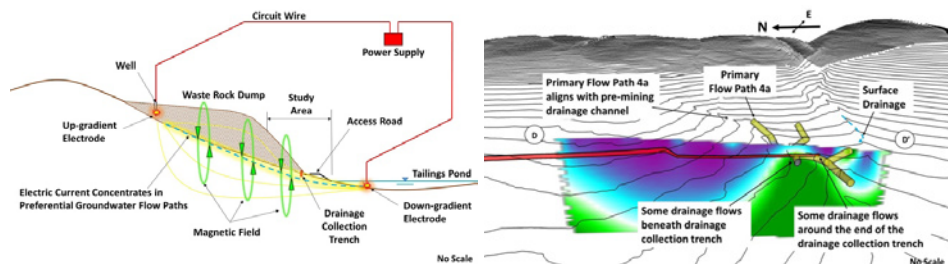


Figure 12 – Plan view of seepage paths

Figure 13 – Cross section of survey layout

Conclusions

The three tailings dam studies show how non-intrusive methods can be used in an observational approach manner to supplement known geological, geotechnical, hydrological and groundwater information to enhance the knowledge of the dam's seepage, stability and integrity conditions..

This knowledge can then be used to cost-effectively support the design of tailings dam stabilizations and future tailings dam raising including for ultimate closure and post-closure, and to provide long-term safety and stability for TSFs and tailings dams.

Acknowledgements

The authors thank Lappeenranta University of Technology for hosting the IMWA 2017 Conference and Tekes for co-funding the conference. The authors also gratefully acknowledge the support of AECOM, Atkins Global and Willowstick Technologies in the preparation of this paper.

References

- Kofoed VO, Jessup ML, Wallace MJ, Qian W (2011) Unique applications of MMR to track preferential groundwater flow paths in dams, mines, environmental sites and leach fields. *International Society of Applied Geophysics, Society of Exploration Geophysicists, The Leading Edge, Special Session: Near Surface Geophysics, ISSN 1070-485X, Vol 30., No.2.*
- Peck RB (1969) Advantages and limitations of the observational method in applied soil mechanics. *Geotechnique*, 19(1): 171-187.
- Williams BC, Riley JA, Montgomery JR, Robinson JA (1996) Hydrologic and geophysical studies at Midnite Mine, Wellpinit, WA: Summary of 1995 field season, U.S. Bureau of Mines Report of Investigations R 19607

Operational water balance model for Siilinjärvi mine

Vesa Kolhinen, Tiia Vento, Juho Jakkila, Markus Huttunen, Marie Korppoo, Bertel Vehviläinen

Finnish Environment Institute (SYKE) Freshwater Centre/Watershed Models, Mechelininkatu 34a, FI-00260 Helsinki, Finland, vesa.kolhinen@ymparisto.fi

Abstract A hydrological forecast model was developed for simulating and forecasting water balance in Yara Siilinjärvi mining area. The purpose of the model was to provide a tool for mining operators for better water management in the mining site. The resulting model is fully operational forecast system, which uses real time meteorological and hydrological data to simulate water balance, water level, discharge, snow and other quantities for each basin in the area. It is currently used by Yara Siilinjärvi mine for operational forecasts.

Key words mine, water balance, modelling, real time simulation, forecast

Introduction

Mining companies face several environmental challenges regarding water management in mining areas: risks caused by excess water are serious and can lead to flooding and dam breaches, as well as spilling substances into downward water ways. Predictive water management is required to forecasts such events and reduce risks at mining site.

In order to address these problems and to provide a tool for mining operators, a hydrological model was developed for simulating and forecasting water balance. The model was developed in Finnish Environment Institute (SYKE) as a TEKES project with collaboration of YARA Siilinjärvi mine, which was used as a pilot area. The model itself is based on the Watershed Simulation and Forecasting System (WSFS), also developed in SYKE. The WSFS consists of a hydrological, runoff and discharge models, and it monitors and forecasts the water levels and discharge of lakes and rivers in real-time. It is the main tool in national flood forecasting, and it has been used for operational water quality modelling as well as climate change research (Vehviläinen 1992, 1994, 2000, Veijalainen 2012). A number of hydrological variables such as precipitation, evaporation, runoff, soil moisture, groundwater storage, and snow pack, etc. are simulated for all catchments in Finland. A wide range of hydrological and meteorological observations are utilized in the operation of the model system.

The hydrological mining site model

Siilinjärvi mining site model is a modified version of the WSFS model. Schematic diagram of the model is shown in Figure 1. All hydrological process models that simulate the water balance, as well as most of the data assimilation routines, are the same as in the nationwide operational model. Implementation of the model to the mining area required a catchment description of the site. That is, sub-basins, reservoirs and discharges in the area had to be determined and modelled. This was established by using elevation data, public maps GIS-data, and reservoir data from Yara and the expertise of hydrologists in SYKE and local

mine personnel. The division into sub-basins was made for the mining area as well as some of the immediate mine surroundings. GIS information consisting of basin areas and locations, outlets, streams, lakes and ponds was derived with the help of a Finnish watershed database available to SYKE. This catchment division is shown in the map in the user interface, shown in Figure 2.

Siilinjärvi site was divided into 28 sub-catchments, most of which contain one lake or pond. The hydrological model describes water balance and inflow in each pond. The water balance of the open mining pit is also included in the model, in order to provide estimates for required pumping capacity in future. The hydrological model uses daily meteorological observations and forecasts to simulate precipitation, evaporation and percolation to the groundwater. The runoff model describes the water flow from the land area into lakes, and the discharge model describes the water flow from one lake to another.

Meteorological data, such as temperature, precipitation and snow depth are available via Finnish Meteorological Institute (FMI) from the meteorological measurement stations located nearby. The Siilinjärvi snow line water equivalent data is also used. On-site snow depth and density measurements conducted during the project by SYKE and Geological Survey of Finland (GTK), were included in the model. Real-time meteorological forecasts are applied to provide daily hydrological forecasts. Furthermore, weather data from the last 50 years is used to produce a long-term climatological forecast. These observations and weather forecasts are received, read and assimilated automatically into the system.

Water level, discharge and pumping data was retrieved from the mine management system by the mine operator about once a month and sent to SYKE in excel format. Automatic and continuous retrieval of measurement, which would provide more accurate real time forecasts, can be included into the system later. However, the continuous measurement data from the in situ devices installed during this project were automatically retrieved and processed into the modelling system.

Model contains a number of free parameters, which were calibrated against the measurements. Moreover, the WSFS also includes a correction model which corrects model inputs (precipitation and temperature) in order to get hydrological quantities (water equivalent of snow, discharge and water level) to better fit the hydrological observations. As temperature and precipitation observations might not be representative for large areas, this method corrects the model state in order to ensure the best possible initial condition for the model on the forecast day.

Results and operation of the system

As a result, a functional WSFS model was obtained for the Siilinjärvi mining area. It works relatively well for the areas where reliable water level and discharge (or pumping) observations are available, as well as for the natural state lakes. However, some difficulties were met when simulating areas where observations are unreliable or not available. As the model can be operated without direct discharge observations using the regulation schedule (as done in

the forecast period), or using a combination of observations and regulation schedule to limit drastic changes in water level, one is still able to obtain sufficiently reasonable results for the areas where reliable observations are missing.

The WSFS mine site model is operated via a web-based interface (Figure 2). It features a clickable map which is used to navigate into different areas and to view their forecasts. All the observations and forecasts are updated automatically, but additional observations can be filled manually via the interface. The simulation is run automatically daily, but can be run also manually, if necessary. Numerical data produced by the system can also be exported into other systems.

Actual operation of the system is controlled using discharge forecasts and regulation schedules. Using the interface operator can set desired values for pumping and discharge from ponds. These discharge forecasts will be then be used for given period of time. Additionally operators can use regulation schedules to specify how much water will be pumped or discharged at certain water levels. The system then automatically adjusts discharges accordingly, and subsequent forecasts will be based on these settings.

Results are presented graphically on the interface web page. Hydrological quantities, such as water level, discharge or pumping, precipitation, evaporation, runoff etc., are all presented as graphs by time for each sub-catchment (in practice for each lake/pond). Example images for water level and pumping of one of the ponds, Vesiallas, are shown in Figure 3. Forecasts for each pond are shown as a coloured band, different colour for each probability fractile. Long term forecast based on historical observations can be used to make probability forecasts for water level and outflows. These results can be used for discharge planning and preparation for various events, such as spring floods.

As the model can be modified for both catchment setup and forecasts, different alternate scenarios can be studied as well. For example, when the mining site is being developed, new reservoirs build and pumping lines installed, their effects to the water balance and discharge can be simulated in the WSFS model. Moreover, weather forecasts can be modified to take account possible climate change scenarios in the future, and to estimate their effect on runoff and discharges. Using different modifications can thus be used to study various, possibly worst case scenarios and addressing possible problems in water management before they appear. This could help minimizing costly risks at the mining site.

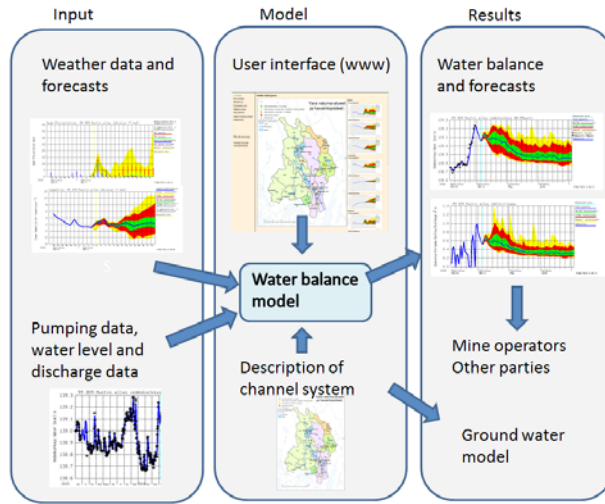


Figure 1 Schematic diagram for the WSFS model. The model consists of the actual hydrological water balance model and a watershed description (lake and channel system), shown in the middle. It uses hydrological observations (water level, discharge, pumping, etc.) as well as weather observations and forecasts as starting and reference points for simulation. Model then produces forecasts for all the lakes and ponds in the area. Additionally, numerical data can be extracted from the WSFS to be used in other applications and by other parties.

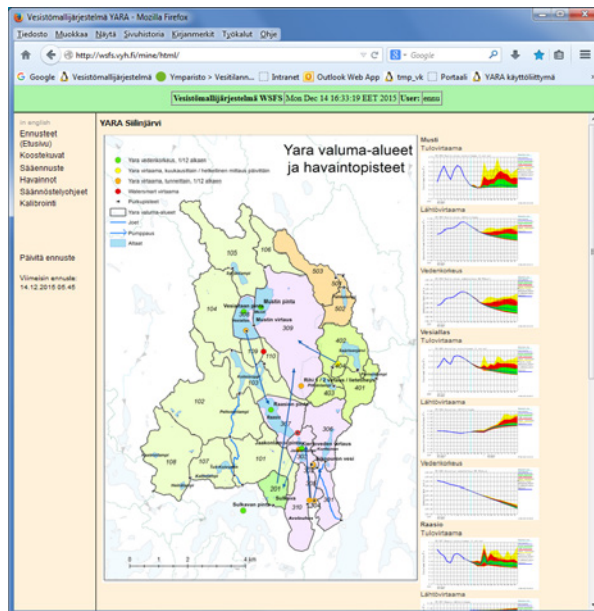


Figure 2 Web interface for WSFS model. Clickable map shows the watershed description in the mining area and in some surrounding area. Clicking the map opens water balance pictures of the area. Some relevant graphs are on the right side of the map. Menu on the left side bar contains entries for entering observations, regulations schedules and discharge forecasts.

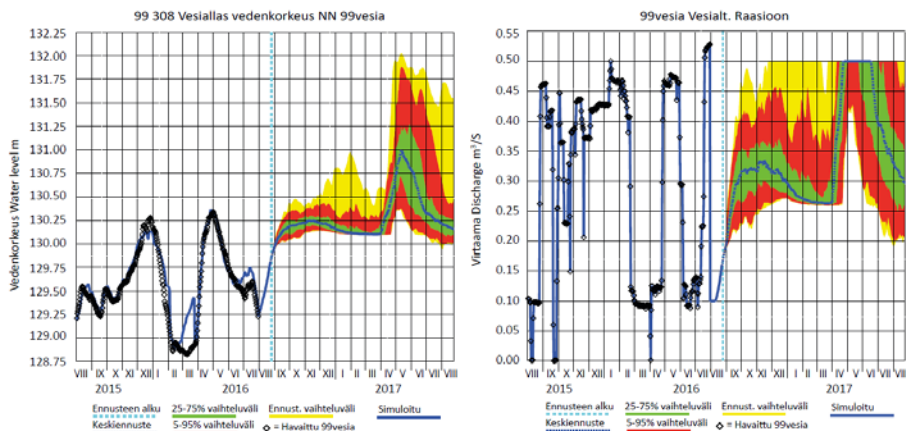


Figure 3 Water level (on the left) and pumping (on the right) of Vesiallas pond are shown here as an example. Vertical dashed blue line shows the simulation date. Green, red and yellow bands on the right of it shows probability fractiles (50, 70, 90, 100 %) of forecasts.

Conclusions

A hydrological forecast model for Yara Siilinjärvi mining site was developed for simulating and forecasting water balance in the area. This model aims to provide a tool for mining operators for better water management in the site. It works relatively well in the areas where discharge and water level observations are reliable, but there some difficulties in the areas where observations might be unreliable. Yara is currently using the system and evaluating its usefulness for further development.

Acknowledgements

This work was done in WaterSmart project, which is a part of the sustainable extractive industry program Green Mining by Tekes. The project was co-funded by Tekes – the Finnish Funding Agency for Technology and Innovation.

References

- Vehviläinen, B. (1992) Snow cover models in operational watershed forecasting. SYKE, Helsinki. Publications of Water and Environment Research Institute 11. 112 p. ISBN 951-47-5712-2.
- Vehviläinen, B. (1994) The watershed simulation and forecasting system in the National Board of Waters and the Environment. SYKE, Helsinki. Publications of the Water and Environment Research Institute 17. 13 p. ISBN 951-47-9749-3.
- Vehviläinen, B. (2000) Hydrological forecasting and real-time monitoring: The Watershed Simulation and Forecasting System (WSFS). John Wiley & Sons Ltd, Chichester. Hydrological and limnological aspects of lake monitoring. 13-20. ISBN 0-471-89988-7.
- Veijalainen, (N. 2012) Estimation of climate change impacts on hydrology and floods in Finland. School of Engineering, Helsinki. Aalto University publication series DOCTORAL DISSERTATIONS 55/2012. 211 p. ISBN (printed) 978-952-60-4613-6 ISBN (pdf) 978-952-60-4614-3.

2 Regional

Assessment of the effects of mine closure activities to waste rock drainage quality at the Hitura Ni-Cu mine, Finland

Teemu Karlsson¹, Päivi Kauppila¹, Marja Lehtonen²

¹*Geological Survey of Finland, P.O. Box 1237, FI-70211 Kuopio, Finland, teemu.karlsson@gtk.fi*

²*Geological Survey of Finland, P.O. Box 96, FI-02151 Espoo, Finland*

Abstract Choosing right management methods is essential for efficient closure and design of mining waste facilities. To assess potential effects of mine closure activities to waste rock drainage quality at the Hitura Ni-Cu mine in Finland, a surface water investigation and filled-in lysimeter tests were performed. According to the results, current environmental effect on the surface water quality caused by the waste rock piles is relatively small, but disruption of the mica schist pile *e.g.* by shaping might cause additional mobilisation of harmful elements, especially Ni. Instead, the mica schist pile could be shaped and covered with the serpentinite waste rock material which has significantly lower element mobility and alkaline drainage.

Key words lysimeter, static tests, waste rock utilisation, element mobility

Introduction

After mining operations, mineral waste material dumps are left behind that may cause detrimental effects on the environment if closure is not done appropriately (Kauppila et al. 2013). Thorough planning, field investigations and characterisation of materials are crucial for the selection of suitable closure methods. Desired closure objectives may not be achieved due to inappropriate closure activities, or the environmental impacts may even get worse as a result of undesired mobilization of potentially harmful elements.

The effects of closure activities on waste rock facilities and possibilities for waste rock utilization were assessed at the Hitura Ni-Cu mine, which is currently facing closure. Two different waste rock piles are situated at the Hitura mine site: a serpentinite pile and a mica schist pile. The planned closure activities would include shaping and landscaping of both piles. In this study, the current environmental effects on surface waters around the mine site caused by the rock piles were investigated through field measurements and water quality analyses. The waste rocks were characterised chemically and mineralogically, and field scale lysimeters were constructed to assess leaching of potentially harmful elements from disturbed weathered rock material, and to study the potential use of serpentinite as a cover material on the mica schist pile.

Study area

Hitura mine is located in Nivala, Finland (fig. 1). The mine operated in several periods during 1970–2013. The main products were Ni and Cu, which were extracted from an ultramafic sulphide deposit. The operations started as open pit mining shifting to underground min-

ing in 1991 (Heikkinen et al. 2002). The last mining company was declared bankruptcy at the end of 2015 and final closure of the site was initiated including plans to shape the waste rock piles.

The Hitura deposit consists mainly of serpentinite and, in lesser amounts, amphiboles and mica schists (Papunen 1970). Waste rocks have been deposited in two separate piles during 1970–1993: the serpentinite pile (2.2 Mm³) and the mica schist pile (3.5 Mm³) with additional 3 Mm³ of overburden of Quaternary sediments (Ahma ympäristö 2013). Mine waters from the Hitura mine site flow through a ditch system to the nearby Kalajoki River (fig. 1), which discharges to the Bothnian Bay of the Baltic Sea around 70 km northwest.

Materials and methods

The current environmental effects on the water quality of the ditches surrounding the waste rock piles were investigated through field measurements and water quality analyses in June 2016. Field measurements were repeated in April 2017. The water samples were taken from the ditches Hituranoja (WS1) and Töllinoja (WS2), upstream of the mica schist waste rock area representing background water quality, from seepage water discharging from the mica schist pile (WS3), and from the ditch of the joined Hituranoja and Töllinoja ditches downstream of the mica schist waste rock pile (WS4) (fig. 1). Representative surface water sampling points could not be found around the serpentinite pile, therefore only field measurements were performed. The field analyses were performed with a portable YSI multiparameter sonde, and included pH and electrical conductivity (EC). Laboratory analyses included total concentrations of dissolved elements with ICP-OES/MS from filtered (0.45 µm), preserved (1 M HNO₃) samples, and anion concentration analyses with ion chromatography from untreated samples.

Field scale lysimeters were applied to investigate longer term leaching of the waste rock materials in natural conditions to simulate the impact of disturbance of the mica schist waste rock pile by earthworks and the usability of serpentinite in covering the mica schist pile. The samples for the lysimeters (1 m³ of serpentinite, LY1, and 2 m³ of mica schist, LY2) were collected from the weathered surface parts of the waste rock piles with an excavator (fig. 1). The grain size distribution of the samples was heterogeneous with the largest rocks up to 10 to 20 cm. Rocks larger than that were removed manually.

The lysimeter test setup consisted of four 1 m³ lysimeters, which were constructed on December 2015 at the premises of the Geological Survey of Finland (GTK) in Kuopio, eastern Finland. One lysimeter was left empty for background water analysis and to monitor potential contamination of the lysimeter containers, one was filled with serpentinite (LY1.1), and two with mica schist (LY2.1 and LY2.2). The filled-in lysimeters contained around 800 L of waste rocks, weighing approximately 1600 kg. The mica schist lysimeter LY2.2 was covered with a 15 cm layer of serpentinite in April 2016 to further evaluate suitability of serpentine as a cover material for mica schist. The cover was placed five months after the construction to ensure equal starting levels for both mica schist lysimeters and applicability of lysimeter LY2.1 as a control lysimeter for the cover material test.

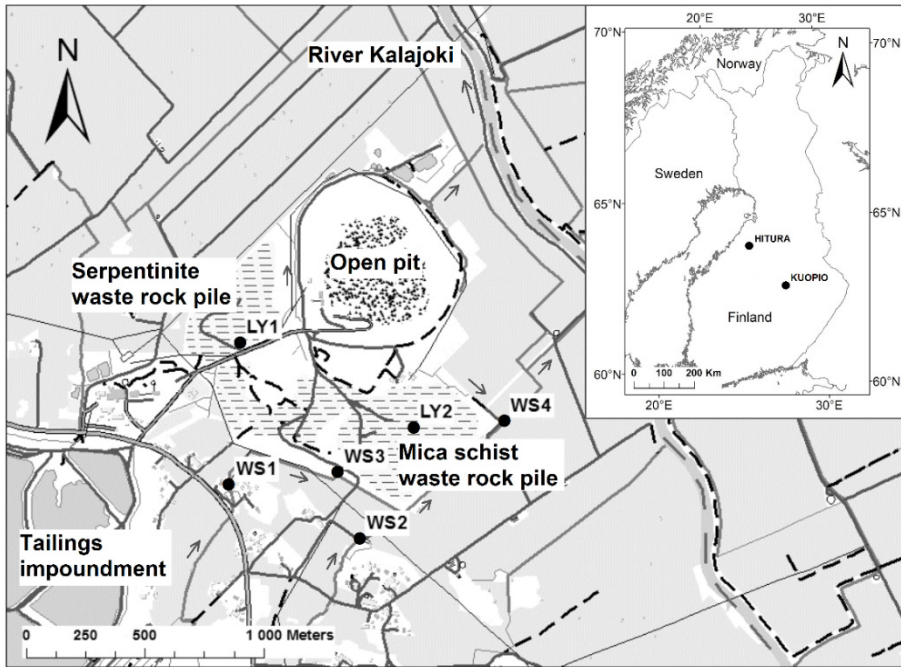


Figure 1 The location and setting of the Hitura mine site and sampling points. WS = water sampling point, LY = sampling point for lysimeter tests. (Basemaps © National Land Survey of Finland.)

During the filling of the lysimeters, 10 L samples were taken from the serpentinite and mica schist for the chemical and mineralogical characterisation. The chemical characterisation included analyses of total element concentrations of pulverised samples with XRF and assessment of acid production potential with modified ABA-test (standard CEN EN 15875:2008). Total sulphur was determined using high temperature combustion method and IR detection (ISO15178, Leco-furnace method). Chemical analyses were performed in the accredited laboratory of Labtium Oy. Mineralogical composition was measured from the ground samples with field-emission scanning electron microscope (FE-SEM, JEOL JSM 7100F Schottky) at the GTK Geolaboratory.

The amount and quality of lysimeter seepage waters were measured periodically. Seepage waters were collected in plastic canisters and analysed for pH, EC, anions and dissolved elements. The pH and EC were measured in the field with a portable YSI-meter, and anions (from untreated samples) and dissolved elements (from filtered (0.45 μm), preserved (1 M HNO_3) samples) were determined in an accredited laboratory by Labtium Oy using ion chromatography and ICP-OES/MS, respectively. Field duplicates, field blanks and laboratory duplicates were used to ensure quality in the sampling and the analysis.

Results and discussion

Surface waters

Surface waters in the ditches around the Hitura mica schist waste rock pile were mainly neutral (fig. 2). In June 2016, the pH value in the water discharging from the waste rock pile area was practically the same (6.8) as in the background measurement points in the Töllinoja and Hituranoja ditches (6.9) suggesting negligible input of acidity from the waste rock pile. This was despite the seepage waters of the pile were acidic with pH around 4. However, the EC of the seepages was around 300–500 mS/m, and an increase in the EC of the Töllinoja ditch (from around 12 mS/m upstream of the pile to around 35 mS/m downstream of the pile) indicated minor input of ARD affected waters into the ditch. Water in the ditch flowing around the serpentinite waste rock pile altered from circumneutral (pH 6.5) to alkaline (pH 7.6–8). The field measurements in April 2017 showed similar pH tendencies in the surface waters as observed in June 2016, but the pH values were overall slightly lower. For instance, the Töllinoja background pH value dropped from 6.8 in June 2016 to 6.1 in April 2017. This might be due to the seasonal water quality changes as the April samples were taken after the snow melt period.

As suggested by the EC, some metal loading occurred from the mica schist pile into the ditches with Ni and Cu as primary metals. The dissolved metal concentrations in the mica schist pile seepage water (WS3) were high, the water containing 4520 µg/L of Ni and 245 µg/L of Cu (fig. 3). However, the Ni concentrations in the Töllinoja ditch increased from 3.3–6.3 µg/L of the background (WS1 and WS2) only to 94 µg/L in the downstream sampling point of the waste rock area (WS4). In addition, increase in the Cu concentration in the Töllinoja ditch was negligible, from 2.1–2.8 to 3.7 µg/L (fig. 3). Obviously, small flow rates of the seepages compared to those of the Töllinoja ditch result in dilution of the metal concentrations.

Despite the dilution, the nickel concentration in the discharge point of the mica schist waste rock area in the Töllinoja ditch (94 µg/L) exceeded the average annual Ni limit value of 20 µg/L set by the European environmental quality standard (EQS) applicable to surface waters (EC 2008). Nevertheless, the effect caused by the ditch water is considered overall insignificant, as the average flow of the Kalajoki River, the receiving water body of the Hitura waste rock discharge, is relatively high, 164 m³/s (Savolainen & Leiviskä 2008), compared to the flow in the Töllinoja ditch, 0.2 m³/s (Heikkinen et al. 2004). In fact, no marked change was observed in the EC of the Kalajoki River water between the sampling points located upstream (EC 4.4 mS/m) and downstream (EC 4.8 mS/m) of the discharge from the waste rock area. In addition, pH remained circumneutral in the Kalajoki river below the discharge point even though a minor change in pH was recorded between the two sampling points (from 7.0 to 6.7).

Lysimeter tests

Mineralogical and chemical characterization of the mica schist and serpentinite used in the lysimeter tests were carried out to assess their environmental properties and ARD potential. Based on the results, the mica schist (LY2) is composed of quartz (24.3%), plagioclase

The serpentinite (LY1) is mostly composed of serpentine (70.0%) and talc (13.7%) and contains only small amount of sulphides (pyrrhotite 0.02% and pentlandite 0.01%) but notable carbonates (calcite content 0.96%). Similar to the mica schist, the primary contaminants in the serpentine are Ni (1009 mg/kg) and Cu (169 mg/kg) (tab. 1). The ABA test and the mineralogy indicated that the serpentinite is not potentially acid producing (NRP = 28.5 and neutralizing minerals >> acid producing minerals) (tab. 1).

Following the characterization, a total mass of the main contaminants in the lysimeters was estimated based on the total Ni and Cu concentrations and the estimated mass of rock material in the lysimeters (1600 kg). The calculations showed that the serpentinite lysimeter (LY1.1) contains less than half the amount of Ni (1.6 kg) and Cu (0.3 kg) than the mica schist lysimeters (LY2.1 and LY2.2; Ni 3.6 kg and Cu 1.2 kg).

Table 1 Ni and Cu concentrations, and parameters for acid production potential calculations of the lysimeter rock materials.

	Ni	Cu	S	AP	NP	NPR
	XRF	XRF	Leco			
	mg/kg	mg/kg	%	kg CaCO ₃ /t	kg CaCO ₃ /t	
LY1 / serpentinite	1009	169	0.14	4.4	124	28.5
LY2 / mica schist	2290	771	2.28	71.1	15.7	0.2

AP = acid production potential, NP = neutralization potential, NPR = neutralization potential ratio

Altogether 9 water samples were collected from the lysimeters during a one-year monitoring period (fig. 4). In accordance with the characterization results, the seepage water from the serpentinite lysimeter (LY1.1) was alkaline (pH around 8.3 on average) with low metal contents (Ni 4–15 µg/L, Cu 0.8–30 µg/L) and EC (53 mS/m), whereas the seepages from the mica schist lysimeters (LY2.1 and LY2.2) were acidic (average pH≈4.5) and contained high amounts of dissolved metals (average EC≈250–240 mS/m), especially Ni (24300–120000 µg/L) and Cu (400–2000 µg/L). In addition, the SO₄ concentrations of the mica schist lysimeter seepages (620–3100 mg/L) were tenfold compared with those of the serpentinite (95–220 mg/L) indicating considerable sulphide oxidation in the mica schist and only minor oxidation in the serpentinite. The leached metal concentrations from the mica gneiss lysimeters were notably higher than observed in the actual seepage water of the waste rock pile. This underlines that disturbance of the pile may result in excess release of ARD from the pile.

The released loads of metals and SO₄ were calculated for the whole observation period based on the amounts and metal concentrations of the seepage waters (fig. 4). The results show that the release of Ni and Cu from the serpentinite with good buffering capacity (lysimeter LY1.1; 0.8 mg of Ni i.e. 0.00005% of the total Ni mass in the lysimeter) is negligible compared to those of the oxidized mica gneiss with low acid buffering capacity (lysimeter LY2.1:

4030 mg of Ni and 74 mg of Cu i.e. 0.1% Ni and 0.006% Cu of the total masses; lysimeter LY2.2 4046 mg of Ni and 60 mg of Cu i.e. 0.1% Ni and 0.005% Cu of the total masses), even though the amounts of Ni and Cu were also high in the serpentinite material. Overall, the loads of the metals and SO_4 from the lysimeters were the highest in the beginning of the lysimeter tests (fig. 4). This is likely due to the mobilization of metals from secondary minerals and weathered mineral surfaces as especially the collected mica schist samples were strongly weathered.

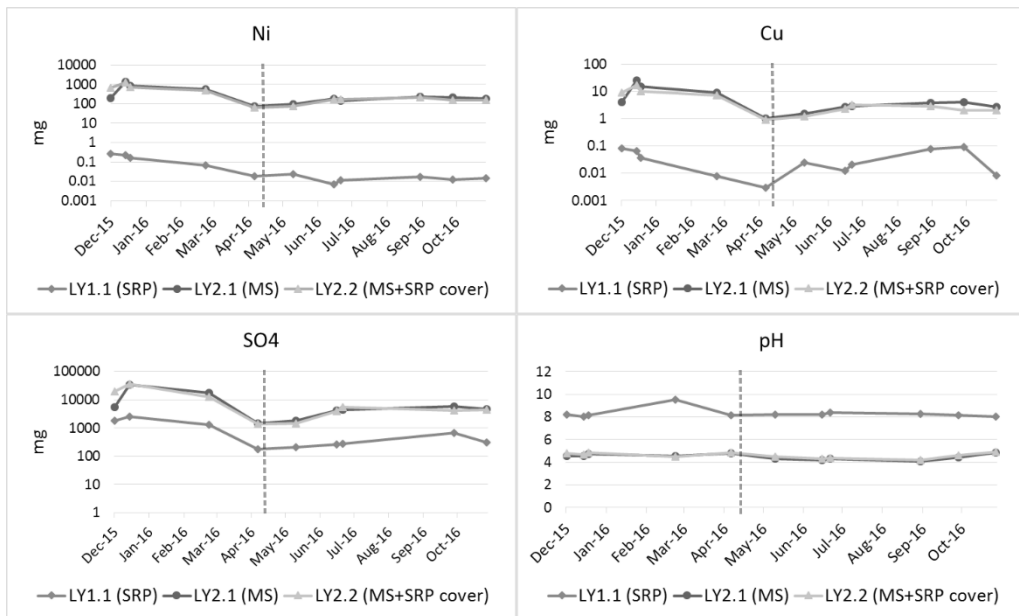


Figure 4 Amounts (mg) of Ni, Cu and SO_4 , and pH leached out of the lysimeters during the observations period. LY1.1 = serpentinite, LY2.1 = mica schist, LY2.2 = mica schist with 15 cm of serpentinite on top. The dashed line represents the date when LY2.2 was covered with a 15 cm layer of serpentinite.

The addition of 15 cm of serpentinite on top of the mica schist lysimeter (LY2.2) five months after the initial set up of the lysimeter tests did not have any significant effect on the seepage water pH or the metal and SO_4 loads during the observation period, despite the alkalinity of the serpentinite (fig. 4). This is most likely because the sulphide oxidation is difficult to cease once started. In addition, the observation period after the placement of the cover was quite short.

Conclusions

Both waste rock piles at the Hitura mine site, the serpentinite and mica schist piles, contain high concentrations of potentially harmful elements, especially Ni and Cu. In addition, the mica schist is potentially acid producing. According to the field investigations, the current environmental effect on the surface water quality caused by the waste rock piles is nevertheless relatively small. Even though the seepages of the mica schist pile are acidic and contain

high Ni, Cu and SO₄, the outflow water from the waste rock area is neutral with low metal contents as a result of e.g. dilution with background stream waters, and the existing impact on the receiving water body, the River Kalajoki, seems to be insignificant.

According to the lysimeter test results, disturbance of the weathered mica schist waste rock pile surface, e.g. by shaping the slopes, is likely to result in excess production of ARD and in degradation of the surface water quality discharging from the mine site. On the other hand, the lysimeters showed that the serpentinite is producing alkaline waters with low input of metals, and could therefore provide a potential cover material for the mica schist to decrease ARD. Monitoring of lysimeters will be continued to evaluate the use of serpentinite as a cover in longer term.

Acknowledgements

This study was conducted as part of the KaiHaMe-project (2015–2018) funded by the European Regional Development Fund (ERDF), GTK and several industrial partners.

References

- Ahma Ympäristö Oy (2013) Belvedere Mining Oy – Hituran avolouhoksen laajennuksen ympäristövaikutusten arviointiohjelma. Belvedere Mining Oy – the environmental impact assessment of the expansion of the open pit of Hitura mine (in Finnish)
- European Council (2008) Directive 2008/105/EC of the European Parliament and of the Council of 16 December 2008 on environmental quality standards in the field of water policy. <http://eur-lex.europa.eu/legal-content/FI/TXT/?uri=celex:32008L0105>
- Heikkinen PM, Korkka-Niemi K, Lahti M, Salonen VP (2002) Groundwater and surface water contamination in the area of the Hitura nickel mine, Western Finland. *Environ Geol* 42:313–329
- Heikkinen PM, Pullinen A, Hatakka T (2004) Hituran kaivoksen sivukivikasojen ja rikastushiekka-alueen ympärysojen pintavesikartoitus, virtaamamittaukset sekä ympärysojen ja kaivoksen vesien laatu toukokuussa 2004. Geological Survey of Finland, archive report. 31 p (in Finnish)
- Papunen H (1970) Sulfide mineralogy of the Kotalahti and Hitura nickel-copper ores, Finland. *Ann Acad Sci Fenn AIII Geologica-Geographica* 109, 74 pp
- Kauppila P, Räisänen ML, Myllyoja S (Eds) (2013) Best Environmental Practices in Metal Ore Mining. Finnish Environment Institute. *The Finnish Environment* 29en/2011, 219 pp, <https://helda.helsinki.fi/handle/10138/40006>
- Savolainen M, Leiviskä P (2008). Kalajoen vesistön tulvantorjunnan toimintasuunnitelma. Pohjois-Pohjanmaan ympäristökeskuksen raportteja 2/2008, 94 pp (in Finnish)

Monitoring of mine water

Michael Drobniowski, Holger Witthaus

*RAG Aktiengesellschaft, Servicebereich Technik- und Logistkdienste, Shamrockring 1,
44623 Herne*

Abstract Observation of mine water level and chemical composition of water is one of the most important tasks today and in a long term view for German hard coal mining. The main aspect is the control and proof of avoiding any damage on public life and nature by former mining activities, as far it is possible by state of the art measures.

A wide range of monitoring measures is realized in a deposit of hardcoal, which was mined out for more than 2 centuries by underground mines in levels up to a depth of more than 1500 metres.

Key words Mine water monitoring, Post-mining water management, hard coal mining

Introduction

This paper gives an overview to the measures of monitoring in the area of active and closed mines. The requirements to the monitoring system are results of knowledge and experience regarding geological parameters, influence of mining activities to the ground, aims of environmental protection in the densely populated areas of mining in Germany, as well as state of the art in technological research.

Scope of monitoring:

The monitoring includes:

- Level of mine water in every local section
- Amount of mine water flow in former mining areas underground
- Pumping activities and quantity of emission to rivers
- Chemistry of mine water at the point of emission
- Chemistry of mine water in the underground
- Industrial loads in mine water
- Observation of deep ground water levels above carboniferous strata package
- Observation of deformation and subsidence of former mining areas
- Observation of seismic activity potentially caused by rising minewater level.

In addition measures are taken for proofing the long term composition of pumping activities. In an exemplary description a view on modern technology of shaft and pipeline monitoring is given.

Monitoring of mine water level

As an example the area of Ruhr district is shown in a map view. The whole area extents over app. 400 km² and currently 11 pump stations and districts of different mine water levels. The districts are combined in departments according to actual mine water levels (fig. 1).

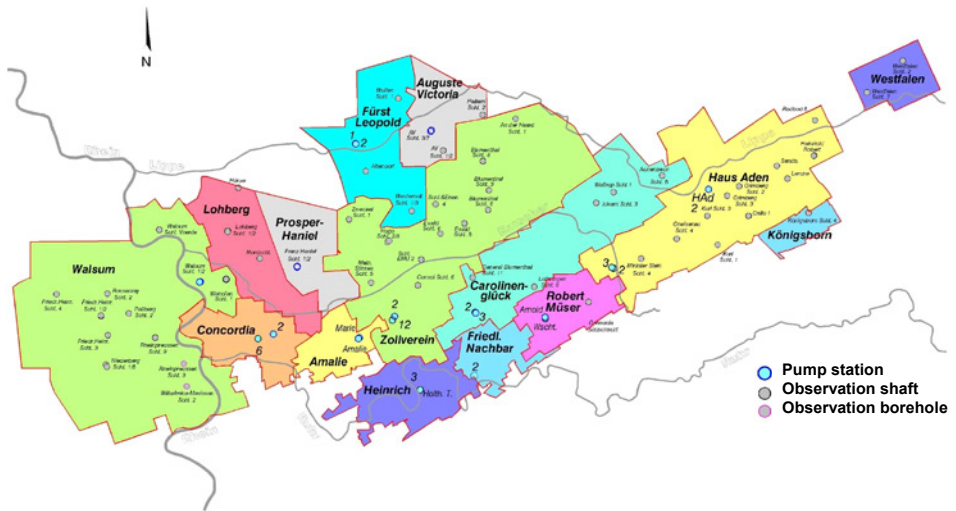


Figure 1: Ruhr area with districts, pump stations and points of water level observation.

In the mining area the mine water level is measured periodically by plumbing in shafts and plumbing pipelines in former shafts. Figure 1 includes the overview of located measurement points in the map view (RAG AG 2014).

The technique of plumbing is applied as mechanical plumbing using a sensor for signal of water level and a rope released by a wind for documenting the length – or stational probes installed below the minewater level and determination the water load above by measurement of pressure (fig. 2) and send that signal to a central observation headquarter (fig. 3).



Figure 2: Example of stational probe for mine water level observation – recovered to surface.

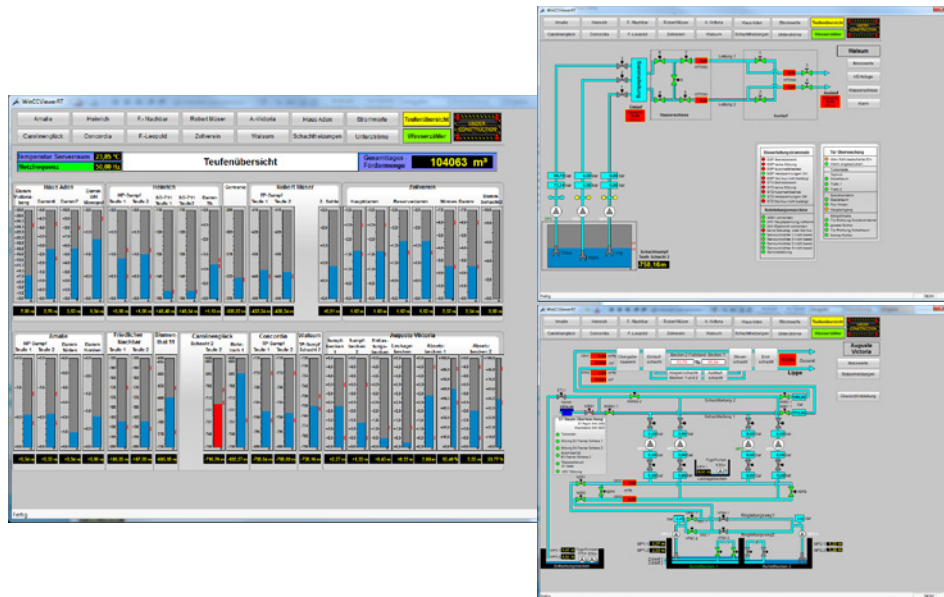


Figure 3: Headquarter of observation – exemplary documentation of water level.

The left side of fig. 3 shows an overview to all pump stations of observation. The red column shows a shaft that is not observed due to installation work. The right part shows a typical well station observation in the upper part, the lower part an underground pump station and structure.

Amount of mine water flow and pumping activities

The final documentation of a closed mine includes all located water inflow points and quantities. In addition pumping activities are reported and documented on a daily bases. By comparing the amounts of lifted water volume to prospected inflow to the water station the basic of risk management are documented.

Results of the forecasted mine water level in each district can be compared to actual measuring results and is analysed for interpreting the function of gateways in the underground and recalibrating of modelling in iterative processing and intense information transfer to experts.

Chemistry of mine water underground and at point of emission

The evaluation of mine water is based on regulations by the mining administrative. Five categories of standard tests are presently used. Usually they are elements of a test every 6 months, additional examination was done every year or every 3 years (according to previous results of testing).

One aim of testing is proofing the influence on water quality of emission and following the legislative restricted limits of water quality. Another aim is to proof the results of predicted

concentrations based on numerical modelling. A permanent recalibration of the parameters of influence is possible and a continuous improvement of modelling takes place. The modelling is described in another report at this conference (Ch. Klinger, DMT) with the background of additional monitoring of industrial loads.

Communication

In addition to specific demands of reporting and documentation an online platform gives information to the public at the RAG website (RAG 2017). This follows the aim of RAG strategy, to be a loyal and transparent partner for public, administration and industry in every way the company can do.

Fig. 4 gives an example as map view to the Ruhr area and a choice of information. The map shows an area of appr. 100 kilometers extension from East to West. The green markings show points of mine water level observation. The purple dots aligned to rows are points of measurement to document ground movement. The blue triangle marks are points of seismic sensing. They are concentrated in the area of still active mining panels. By a click on a point of interest the user can get more information – including history of data development.

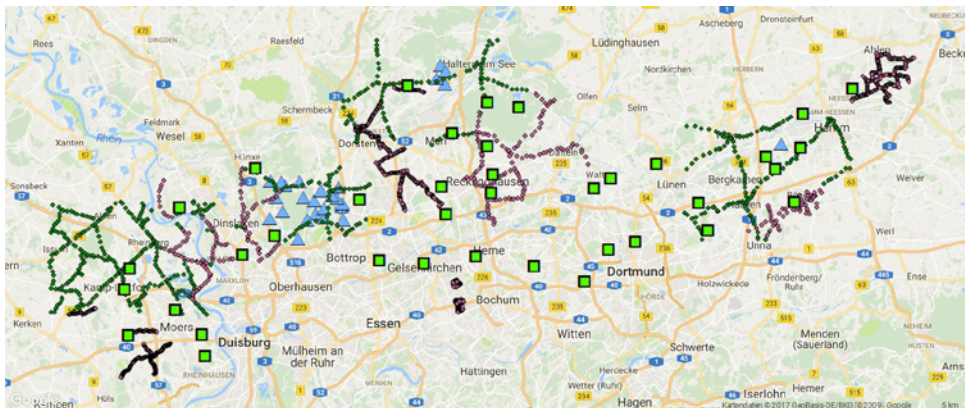


Figure 4: Online information at RAG platform (BID, basic map by ©google) (RAG 2017).

Modern monitoring methods

Modern methods are used in several terms of observation eg. monitoring of the ground movement at surface. European satellite program provides aerial photos and physical data which are analyzed for additional survey.

The latest expansion of the monitoring system is the conception and test run of underground probes especially developed for the environment in closed mines.

Standards of measuring in industry fail in this application, because there is no chance of maintenance or repair. Also the probes have to face the conditions of mine water contact for a long term. Figure 5 shows on the left side the principle construction and sensors of that probe.

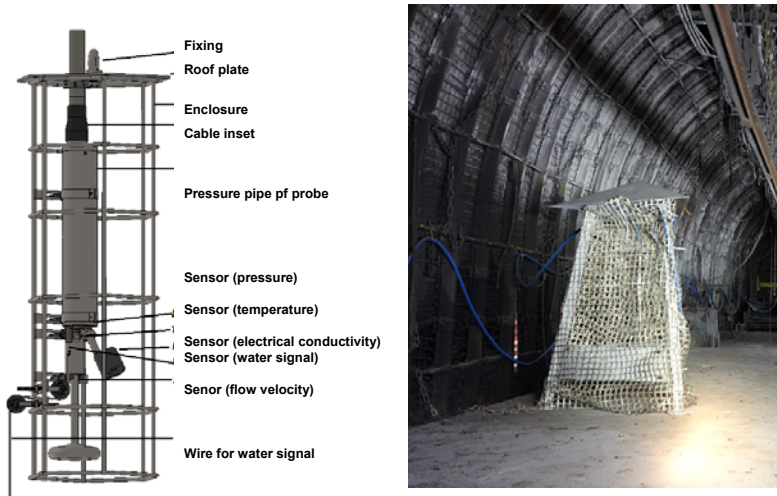


Figure 5: Underground probe for long term observation in closed mines.

On the right side an installed probe, using a specific development of safety construction is figured. The development is done in an ongoing research project with partners from Technical University of Bochum, DMT company and Sea&Sun Technology company (SST). The probe is based on deep sea observation by SST and has to be modified for underground specification.

Current research work is done in cooperation between RAG, DMT company and DLR company for stereophotogrammetric observation of shafts and well-pipelines. The application gives three dimensional models of shaft structure by using a probe. High resolution of this modelling allows observation of deformation, incrustation or damage of the structure. Figure 6 shows a basic instrumentation developed by DMT for laser-scanning probes on the left (a.), the centre picture a model of development (b.) and on the right a graphic example of present documentation by laser scanning (c.) (annual report research RAG 2014).

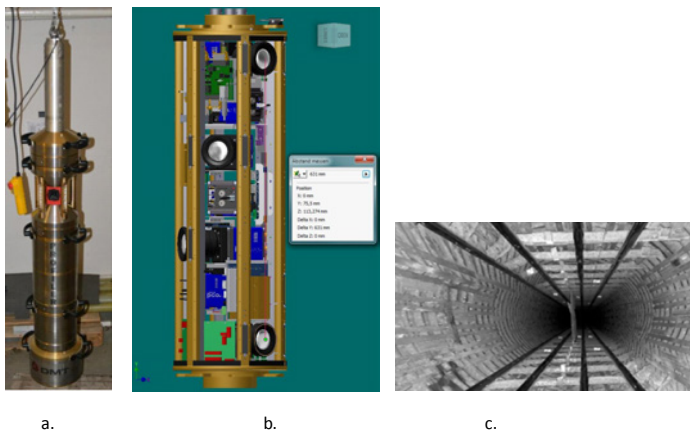


Figure 6: Current model for shaft and well-pipe observation.

Conclusions

RAG fulfils a wide range of monitoring measures. Observation is applied in every way of state of the art technology to prevent any risk from actual and former mining activities. Underground hard coal mining for more than 200 years in Germany includes risks of mine water rising, gas exhausting from abandoned areas, surface deformation and seismic events. Based on third party expertise RAG operates any requested monitoring system as a reliable partner for mining administration and public institutions. In addition RAG communicates any results to the public in an open and transparent way. This work will continue in a long term duration, even if the last hard coal mine in Germany will close in the year 2018. The future work concentrates on optimizing the mine water management by safe and economic concepts and technologies.

References

- RAG AG (2014) Annual report research RAG 2014, not published, RAG Aktiengesellschaft, Herne
- RAG AG (2014) Konzept zur langfristigen Optimierung der Grubenwasserhaltung der RAG Aktiengesellschaft für Nordrhein-Westfalen, Herne
- www.rag-stiftung.de/en/perpetual-obligations/
- RAG AG (2017) Bürgerinformationsdienst (BID) der RAG Aktiengesellschaft, Herne
- <http://www.bid.rag.de/bid/>

Development and installation of an underground measurement technique at the pilot mine “Auguste Victoria” for a mid- to long-term monitoring of the mine water level rise

Steffen Kruse¹, Michael Bendrat¹, Christian Melchers¹, Bernd vom Berg¹, Holger Witthaus²

¹*Technische Hochschule Georg Agricola, Research Institute of Post-Mining, Herner Strasse 45, 44787 Bochum, Germany*

²*RAG Aktiengesellschaft, Servicebereich Technik- und Logistikdienste BT GPK Grubenwasserkonzept, Shamrockring 1, 44623 Herne, Germany*

Abstract Monitoring mine water level rise in a coal mine after its closing is an important issue. Therefore, a measurement technique will be established in the mine to provide direct and continuous recordings of different measured parameters. The development and installation of such an underground measurement data logging system for short- and long-term observation of the mine water level rise at the mine “Auguste Victoria” (Germany, Marl) allows to gain in situ measurement data. This information leads to a better understanding of the mine water level rising process.

Key words IMWA 2017, underground measurement, data logging system, mine water level rise

Introduction

After the activity of German hard coal mining, the mine water level will rise. For a better understanding of the rising process, the concept must include the determination of suitable locations for the installation of the measurement system and the specification of suitable water and air parameters. Therefore, a sturdy and failsafe system must be adjusted to the underground conditions and has to pass a testing period in a laboratory and at surface conditions before it is installed in the underground mine “Auguste Victoria”. With the help of this measurement logging system, data of the mine water level rise can be attained in its spatial and temporal progression. By doing so, the target state can be permanently compared to the actual one. The evaluation of the obtained data has to give evidence of the successive rebound of mine water in existing mine facilities after mine closure and supplemented existing monitoring systems(RAG 2014).

Best practice

System requirements

The monitoring parameters were selected regarding both the recording of the mine water level and the chemical analysis of the mine water. Likewise, there was the plan to measure the methane concentration and the air pressure response in the underground workings during the mine water rise. Where the recording of the mine water level in abandoned mine workings is concerned, measuring the water pressure plays a crucial part. The pressure of the in-situ water column corresponds with the mine water level. Therefore, the exact mounting heights of the pressure transducers have to be documented. Furthermore, the in-

dividual pressure transducers ensure that the hydraulic potential of the mine working is recorded directly, something which allows to determine the flow direction of the mine water. Moreover, the flow speed of the mine water was to be measured. Regarding the recording of the chemical composition, it was required to record the mine water temperature as well as the specific electrical conductivity (Melchers & Dogan 2016).

To develop a suitable monitoring system, product information was evaluated and possible solutions were discussed with renowned mining companies and companies of the chemical and deep sea business. Specific technical concepts had to be developed in order to measure the parameters mentioned above. One key requirement on the monitoring system to be developed was its longevity – the system had to last as long as possible. This requirement was fulfilled by constructing an electrical component design of a most simple structure using as few components as possible. In addition, direct connections were chosen where possible between the actual probe and the evaluation system. This resulted in the parallel connection concept selected, i.e., every single probe is connected by a separate conductor. If one probe fails or the pertinent transmission cable to the surface is damaged, then only one measuring probe stops working. Power to all underground system components is supplied from the surface. These reflections resulted in the system diagram shown in figure (1):

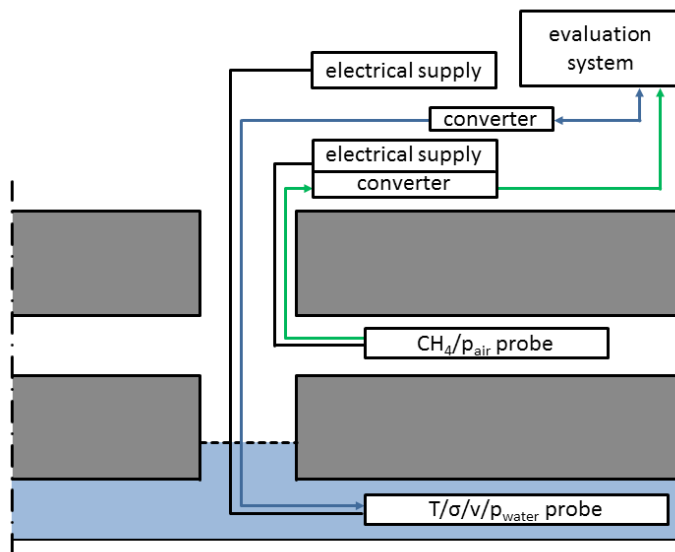


Figure 1 system overview of the entire concept

Other requirements on the system components were due to the extreme environmental conditions underground. Only such components were chosen for installation at the colliery “Auguste Victoria” which – as they would be located under water later – withstand a water pressure of 100bar. Those components include the water sensors, the enclosure of the water probe including its gaskets and the connecting cables and their bushings. They were selected because they are robust and resistant to mine water and mechanical strain. The power

supply and the communication have to overcome a distance of several kilometres. To ensure that the sensors intended for air pressure and methane concentration would be of a long life, they were chosen for use in an environment of high humidity. Moreover, all sensors have to work maintenance-free and all components that are either installed underground or have an interface to underground installations must be of intrinsically safe design and explosion prevented typification checked in an individual detailed expertise by a third party. The following tables (1 and 2) summarise the measuring parameters.

Table 1 *Water measuring parameters*

Parameters	Range	Resolution	Accuracy
temperature [°C]	10–60	0.01	+/- 0.05
water pressure [bar]	0–100	0.003	+/- 0.15
specific electrical conductivity [mS/cm]	0–200	0.004	+/- 0.1
flow rate and direction [m/s]	+/- 3	0.002	+/- 0.03

Table 2 *Air measuring parameters*

Parameters	Range	Resolution	Accuracy
atmospheric pressure [hPa]	0–2000	1	+/- 2
methane concentration [vol.%]	0–100	0.01 to 0.1	+/- 5

Selection and test of system components

The market research undertaken showed that the system components available on the market did not fully meet those requirements. As this system has to be installed at short notice as part of this project, components had to be selected and modified that were principally suitable. Here, the particular challenge was that the measuring components had to be supplied with low electrical power over a very long cable distance. This low electrical energy is one of the requirements of the explosion protection standard. For the air sensors, components were found which met nearly all requirements, so only slight modifications were necessary. The data transmission components, however, were completely newly developed for this system. The electrical power supply could also be established using components which only needed minor modifications. For monitoring the water measuring values a deep-sea probe was modified. As only few experiential tests were available for the mine water use of this probe, and there is no opportunity of a fault analysis with subsequent improvements in case the probe fails later, several test were conducted; these tests tested the probe approximating real conditions in mine water at the surface and underground.

For the first test runs of the system, a not modified probe was used which was equipped with the sensors required, including an inductive conductivity sensor, a temperature sensor, a pressure sensor and an X-Y flowmeter. The first test environment was located at the surface mine water channel at the water treatment plant “Gravenhorst” of the colliery “Ibbenbüren”. This mine water has a high iron content, and the probe remained in the water for c. two

weeks. The next test run was done at another surface mine water channel at the colliery “Ib-benbüren”, i.e. a mine water channel of the water treatment plant “Püßelbüren”. This mine water had a high salt content and again the probe remained in the water for c. two weeks. After the test runs had been completed, the probe was returned to the manufacturer who performed a functionality test on the probe. After it had successfully passed this functionality test, the probe was tested further in underground conditions. The test environment chosen was that of a suitable location at the colliery “Auguste Victoria”. In this case, the probe remained for about six months in the mine water. After this test, the probe was again submitted to a functionality test by the manufacturer and no malfunctions of the sensors or the probe were identified. The middle electrode of the flow sensor was strongly affected by corrosion, but, according to the sensor manufacturer, this would not impair the functionality of the flow sensor. The probe suspension, made of V4A, disintegrated due to corrosion; thus, it became clear that the suspension had to be modified as well for the probe to be developed. Moreover, the examinations showed the response of the entire probe and its sensors and connecting plugs in mine waters. Even the thickness and impact of settlements as well as the impact of corrosion on the probe enclosure, the sensors and the connecting plugs and gaskets could be examined. In addition, where possible, the values measured in the tests were compared with those measured in the laboratory for the pit and thus checked for plausibility. Furthermore, the automatic data recording and processing were examined and optimised for permanent operation. The experience gathered here was utilised in the concept that was implemented later and contributed to an overall improvement of the system.

The system that was finally implemented benefited from the experience and reflections made here. Now, the probe is suspended on a rack that will protect it against broken stone and parts floating in the water. Here, the probe is suspended to move freely within the rack so that any inclination caused by any level convergences can be offset by realigning the probe. The installation and fastening of the cables is largely done at the ceiling of the gallery to avoid possible damage caused by rock fall. For each individual measuring location, the cable path was chosen with due diligence and accuracy by carrying out a number of mine visits.

The rough selection of the locations for recording the mine water level and its rise were done based on the rise concept devised by RAG for the colliery “Auguste Victoria”. Mutual mine visits of all measuring locations helped to determine the exact measuring points. Such measuring points were intended for all main waterways as well as the influent and effluent points in the pit. These points include in particular the overflow from the coal field “Hal-tern” [1W], the influx from the colliery “Brassert” [2W], the influent and effluent points of the colliery “Lippe” [3W], and the main waterway [4W]. The selected locations allow a direct recording of the most important mine waterways and thus essentially of the major waterway. On the other hand, the locations selected also ensure an area measurement of the worked field at the colliery “Auguste Victoria”.

The location of the measuring components for recording the air pressure and the methane content is intended at below sea level in the shaft 3/7 [13L] at the “Auguste Victoria” location

at a depth of 841.6m. By doing so it can be ensured that this measuring point will be flooded at a very late point in time and that the measurement can be carried out for a very long period. The following tables (3 and 4) and plans of the mine workings (2 and 3) provide an overview of the measuring points. All details were determined in close collaboration with RAG.

Table 3 Location of measuring points for the water parameter

No	Operating point	Name	Pressure sensor below sea level [m]	Direction from	to
1W	0205/0205	C 301 / RS6 SO 30	1106.1	AV3	Haltern
2W	0215	C 215 / Q 5 SW 38	991.4	AV1/2	Wulfen
3W	0513/0505	D 440 / DB NW 60	1111.6	AV8	Wulfen
4W	0513	C 513 / Q6 NO 60	1113.1	AV8	Wulfen

Table 4 Location of measuring point for the air parameters

No	Operating point	Name	Below sea level [m]
13L	0131	Tipper loading side, 4 th level, AV3 north	841.6

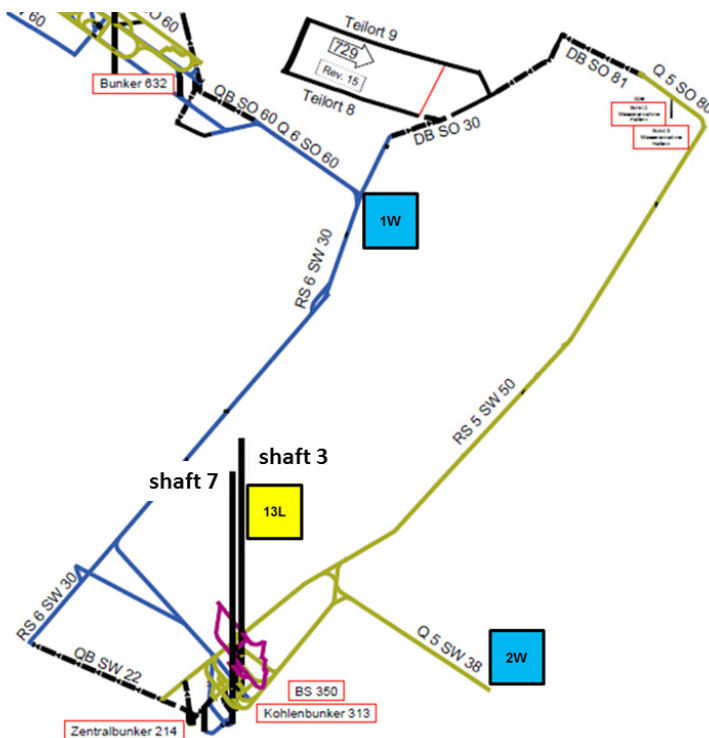


Figure 2 Measuring points in the worked field 20/30



Figure 4 water measuring probe with frame

References

- Melchers C, Dogan T (2016) Study on Mine Water flooding that occurred in Hard-Coal Mining Areas in Germany and Europe. In Kretschmann J, Melchers C (Eds) Done for good. Challenges of Post-Mining. Anthology by the Research Institute of Post-Mining, Bochum: 147–152
- RAG (2014) Konzept zur langfristigen Optimierung der Grubenwasserhaltung der RAG Aktiengesellschaft für Nordrhein-Westfalen. 29 pp

Mass Flow Reduction in Mining Water: Valuation of Measures with due regard to the requirements of the Water Framework Directive

Bernd Bräutigam¹, Norbert Molitor², Birgit Harpke³, Klaus Heise³

¹ *Plejades GmbH – Independent Experts, Beethovenstraße 10A, 09599 Freiberg*

² *Plejades GmbH – Independent Experts, Feldstr. 5, 64347 Griesheim*

³ *Landesanstalt für Altlastenfreistellung Sachsen-Anhalt, Maxim-Gorki-Straße 10, 39108 Magdeburg*

Abstract A case study identified the impact of the Schlüsselstollen, the main drainage tunnel of the abandoned copper slate deposit within the Mansfeld syncline, on the transport of pollutants into the rivers Saale and Elbe with the aim of estimating the impact of potential measures on surface waters and to derive recommendations for action. This was done first for a huge abandoned metal mining area in Germany and the methodology proposed in this case study can be used for valuation of other (abandoned or active) mining sites.

Key words Water Framework Directive, Mine Water, Mine Closure, Mass-flow-reduction

Introduction

Besides other protocols, the Water Framework Directive (WFD 2000) defined the "aim of achieving good ecological potential and good surface water chemical status by the latest" 2015 which was challenging for water bodies draining huge abandoned mining sites. Following an inventory and assessment of the then current state of the flooded mine workings and the drainage system of the Mansfeld syncline, suggestions for technical solutions should have been made to reduce mass flow of metal pollutants, especially of particle-bound potentially toxic metals in the receiving rivers. The following goals were defined for the case study, which was carried out between 2011 and 2013:

- Balancing of discharge and concentration of pollutants based on long-term measurements
- Data evaluation of particle-bound pollutants from the Schlüsselstollen drain water
- Additional analyses on potentially toxic metals for verification of available chemical analyses
- Comparison between the solute load and total load
- Sedimentation tests with suspended solids in sweet and salty water
- Assessment, valuation and derivation of measures for mass flow reduction with due regard
- to the requirements of the Water Framework Directive

Overview about Mine Works and Mine Flooding

For about 800 years copper slate has been mined within the Mansfeld and Sangerhausen synclines south of the Harz Mountains in the middle of Germany. It was in the 16th century when the first drainage tunnels were driven in the Mansfeld syncline and since 1879 the whole Mansfeld copper slate mining area has been drained by the Schlüsselstollen drainage tunnel. This level tunnel is 31.06 km long and one of the longest levels in Europe. It drains into the Saale River via the Schlenze River (see Fig. 1).

After the active mining was closed in 1969 all extraction space was flooded until 1981 and from 1982 until 1992 high saline mine water from the adjacent Sangerhausen mining area was additionally discharged into the mine works via a pipeline and one of the central shafts in the syncline (Bolzeschacht). By the end all the mine water was discharging into the Schlüsselstollen at the so called “overflow point Glückhilfsschacht” (see Fig. 1).

In total within the Mansfeld syncline 44 million m³ of mined space was flooded and about 150 million m³ of natural underground space. Mining was carried out up to a depth of about 1,000 m and the mining galleries have a total length of about 1,000 km. The surface of the flooded water body comprises an area of about 150 km². Between 1915 and 1968 the average inflow into the mine works was about 30 m³/min where 84 % was salty water from the level below the Schlüsselstollen and about 16 % was sweet water from the level above (ARGE GFE 1992).



Figure 1 Course of the drainage tunnel „Schlüsselstollen“ and course of the river Schlenze and Saale in der Mansfelder Mulde. Google Earth

The type and quantity of the ores mined from the copper slate as well as the geological conditions of the deposit determine the type and quantity of pollutants which are discharged together with the mine water into the receiving rivers.

Discharge of the Schlüsselstollen and Mass Flow

Average discharge of the Schlüsselstollen is between 20 and 26 m³/min but can jump up to 50 m³/min in the case of heavy rainfalls.

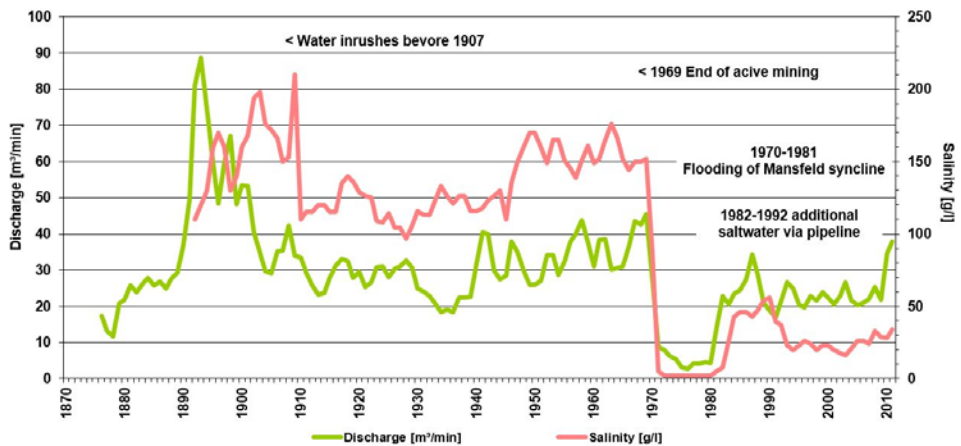


Figure 2 Discharge and average salinity in mine water of the Schlüsselstollen, 1876 – 2011

The flooded mine water table dips slightly from about 81–78 m NN at Eisleben (see Fig. 1) to about 74 m NN at the overflow point. An overview about the development of discharge over the time is shown in Fig. 2.

Annual chemical analysis is available for Na, Ca, chloride and sulphate since 1967 and for some metals (Pb, Cu and Zn) since November 1979. Monthly chemical analysis is available since August 1981 for metals As, Pb, Cd, Cu, and Zn. After termination of the salt water transfer pipeline in 1992 water sampling started for all relevant metals (As, Pb, Cd, Cr, Cu, Ni, Hg and Zn) on quarterly basis. A detailed overview about the distribution of metals in water from different mine adits of the Mansfeld syncline is given in (PLEJADES 2012).

Besides the potentially toxic metals the salt load in the mine water is of major importance for the environment: the annual salt load is about 350,000 t of mainly sodium chloride. Because of the sulfidic origin of the deposit and the high salt concentration potentially toxic metals are transported mainly in dissolved form. Based on a proven methodology (LHW 2012) in years with higher than average discharge (2010, 2011) metal loads of mine water up to 160 t/yr and salt loads up to 600,000 t/yr have been ascertained. Loads for single metals are as follows: 150 t/yr Zn, 3 t/yr Pb, 2.5 t/yr Cu, all other metals (As, Cd, Cr, Ni) about 2 t/yr (PLEJADES 2012). Mercury was also analysed but not detected. Because of an approximate constant concentration of metals and salt in the mine water the mass loads vary accordingly to the discharge of the Schlüsselstollen.

Because of the fact that the discharge of the direct receiving river Schlenze (about 0.1 m³/s) is less than one third of that of Schlüsselstollen the environmental impact on the Schlenze River is tremendous. The annual average environmental quality standards (EQS-AA) for water and sediment are exceeded for Cd, Pb, Zn, Cu, Ni and As and the maximum allowable concentration (EQS-MAC) is exceeded for Cd. In contrast the impact on Saale River is neg-

ligible for some of the metals because of a significantly larger discharge of about 100 m³/s. Consequently in the Saale River an exceedance of the EQS-AA was only measured at two gauge stations for Zn and Cd.

Description of the Mine System: Flooded Mine Works – Drainage Tunnel

Based on the chemical composition of the groundwater (within the flooded mine works) and of the drainage water along the Schlüsselstollen and at its level mouth, the Mansfeld syncline mine system can be characterised as follows (see Fig. 3):

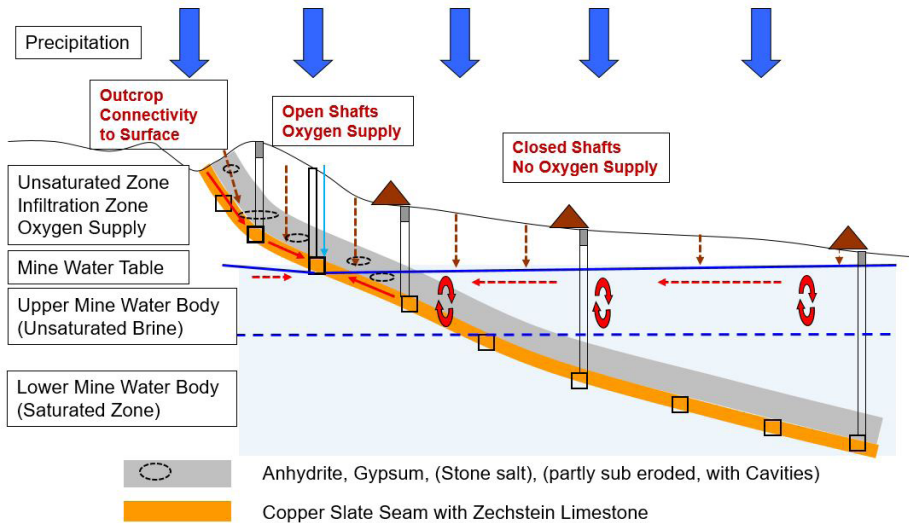


Figure 3 Flooded Mansfeld syncline – schematic view of the flow conditions in the mine system

- **Groundwater recharge:** Zone above the flooded mine works (level of Schlüsselstollen), highly saturated with oxygen and with relatively low primary mobilisation of metals. Interaction with the Upper flooded mine water body.
- **Upper flooded mine water body above -70 m NN:** Zone below the mine water table but above the saturated zone with high concentrations of metals and salt, but not saturated brine. Advective interaction with groundwater recharge and possibility of significant mobilisation of metals.
- **Lower flooded mine water body below -70 m NN:** Zone flooded with saturated brine, therefore negligible convection and interaction with the upper zone; stable density layering.

The main source of metals is the geogenic sulphide ore deposit. The process of oxidation of water-insoluble sulphides into soluble sulphates is supported by atmospheric oxygen which accelerates the mobilisation of metals. In the high saline mine water the metal sulphates are converted into readily soluble metal chlorides. Atmospheric oxygen supply is caused by

groundwater recharge and mine ventilation in a small part of the mine works which is still open for control and maintenance. *The Schlüsselstollen system therefore can be described as a quasi-stable state (with natural fluctuations) with permanent and everlasting mobilisation and emission of geogenic potentially toxic metals.*

Measures of Mass Flow Reduction

According to the Water Framework Directive (WFD 2000) a “good status” had to be achieved by 2015 at the latest. In case the EQSs are exceeded the causes have to be found and measures have to be proposed / realised. In case of point sources (such as mine adits/drainage tunnels) best available techniques (BAT) should be implemented (Article 10, WFD).

Definition of Planes of Action

Generally we can define three planes of action for measures which should be assessed in a first step (PLEJADES 2013):

Plane 1: Measures with direct impact on the source
(Release of pollutants directly from the ore deposit Mansfeld syncline, “up-stream/source”)

Measures at the source

Plane 2: Measures with impact within the subsurface migration path
(Mine works and hydrogeological environment within the Mansfeld syncline, “in-stream”)

Measures within the migration path

Plane 3: Measures with impact outside the mine works and adits
(After discharge off the level mouth, down-stream/end-of-pipe”)

Measures on the protected (natural) resource

Furthermore an additional – fourth plane of action can be defined which is an administrative measure that describes the existing and achievable status.

Plane 4: Toleration of the status achieved so far and of the future status based on reduced environmental quality standards, if necessary with restrictions for water quality and water usage
(Continuation of recent measures which ensure the operational reliability of the drainage system Schlüsselstollen)

Toleration of the (achieved) status quo

Assessment and Valuation of Measures

Before starting the assessment all measures which were theoretically possible have been described for each plane of action (planes 1-3). Then, in a first step, each measure was assessed individually based on the following main criteria:

- Technical feasibility
- Effort
- Approvability
- Time line for implementation
- Achievement of objectives
- Appropriateness

Daily business shows that, de facto, in most cases **approvability** determines feasibility of measures. *Therefore approvability is mandatory for any valuation of appropriate and technically feasible measures.* For a better assessment of the **appropriateness** investment cost and maintenance cost (potentially everlasting cost) had to be examined. Furthermore, for better evaluation of the *achievement of objectives* and finally the *approvability* additional ecological / environmental criteria were used which show the possible impact on environmental sustainability:

- Impairment of overall appearance of the landscape
- Impairment of habitat quality
- Danger of remobilisation of pollutants
- Necessity and possibility of disposal
- Improvement of public good
- Evaluation of sustainability

Based on these results, in a second step, a comparative and qualitative evaluation was made for comparison of the measures. Only three measures remained for further assessment:

- Limited feasible measures with a limited impact: chemical immobilisation
- Feasible measures with low or no impact: reduction of (suspended) solids, direct pipeline to the Saale River
- Accompanied measures with low impact: Acquiescence

All other measures had to be excluded from further assessment because of the following reasons:

- Measures which are not executable and measures which are executable but with substantial risk and/or which can only be realised with excessive cost and limited impact:
 - Removal of the source
 - Inclusion of the source
 - Hydraulic immobilisation
 - Reduction of dissolved pollutants
 - In-situ measures of water treatment
- Disproportionate measures (effective technical measures but with excessive cost):
 - Ex-situ measures of water treatment

To ensure an objective evaluation of the appropriateness of measures the ratio between benefit (impact on reduction of pollutants) and effort (cost) was assessed considering the prorated mass flow from the Schlüsselstollen and the total mass flow in the receiving rivers Schlenze and Saale. It also became obvious that all measures which implicate the closure of the drainage tunnel had to be excluded from further assessment:

- Closure of the Schlüsselstollen would cause the outlet of polluted mine water into other water bodies (via other drainage adits on higher levels) and therefore a significant deterioration of the current situation.
- Furthermore the closure of the Schlüsselstollen would lead to a rise of the groundwater level that would cause uncontrollable water outflows in depressions and lowlands and the weakening of soluble near-surface rocks. This would lead to a hazard or damage of existing infrastructure (roads, buildings) and to possible additional emissions of pollutants.

Deduction of Feasible and Appropriate Measures

As a result of a detailed evaluation (see internet link: PLEJADES 2013) preservation of the status quo (acquiescence) was defined as the only realisable solution. Consequently the following measures were defined for attainment of the best possible status:

- Reduction of oxygen supply to the open mine works (termination of active ventilation and closure of the remaining shafts and adits in the rear part of the mine) and therefore reduction of the potentially toxic metals loads within the framework of mine closure.
- Reduction of particle-bound mass flow using a sediment trap at the level mouth.
- Preservation of the Schlüsselstollen from the overflow point to the level mouth (about 12 km) with active maintenance to ensure everlasting drainage of the Mansfeld syncline.

Conclusions

Preservation of the Schlüsselstollen drainage tunnel in combination with termination of active ventilation and closure of remaining mine openings is the only reasonable measure which ensures a targeted and controlled drainage of the Mansfeld syncline and prevents a deterioration of the current situation. An accompanying monitoring program would help to adjust the environmental quality standards in the Schlenze and Saale Rivers.

References

- WFD (2000) Directive 2000/60/EC of the European Parliament and of the Council of 23 October 2000 establishing a framework for Community action in the field of water policy as amended by Decision 2455/2001/EC and Directives 2008/32/EC, 2008/105/EC and 2009/31/EC.
- ARGE GFE GmbH Halle / HPC-Consult (1992) Studie zu den regionalen Auswirkungen einer Aufgabe des bestehenden hydrogeologischen Niveaus des Schlüsselstollens und weiterer zutage entwässernder Stollensysteme im ehemaligen Kupferschieferbergbau der Mansfelder Mulde, Halle, 59 pp, Appendices
-

- LHW (2012): Data basis/Methodology for mass flow calculations within the framework of the ad-hoc work group Pollutants/Sediment Management of the work group Surface Waters of the FGG Elbe, unpublished doc., (German)
- PLEJADES (2012): Frachtreduzierung Schlüsselstollen, Bericht zum Arbeitspaket A: Ermittlung der Auswirkungen des Schlüsselstollens auf den partikelgebundenen Schadstofftransport in der Saale/Elbe, Magdeburg; Juli 2012 (http://www.fgg-elbe.de/hintergrunddokumente-bp2.html?file=tl_files/Downloads/EG_WRRL/hgi/hgd_bp2/Einzelstudien/Fachbericht_Frachtreduzierung_Schlusselstollen__Teil_A.pdf)
- PLEJADES (2013): Frachtreduzierung Schlüsselstollen, Bericht zum Arbeitspaket B: Bewertung von technisch realisierbaren und verhältnismäßigen Maßnahmen, Magdeburg; April 2013 (http://www.fgg-elbe.de/hintergrunddokumente-bp2.html?file=tl_files/Downloads/EG_WRRL/hgi/hgd_bp2/Einzelstudien/Fachbericht_Frachtreduzierung_Schlusselstollen__Teil_B.pdf)

Passive Mine Water Treatment with a full scale, containerized Vertical Flow Reactor at the abandoned Metsämönttu Mine Site, Finland

Christian Wolkersdorfer^{1,2}, Busisiwe Qonya²

¹*Lappeenranta University of Technology, Laboratory of Green Chemistry, Sammonkatu 12, 50130 Mikkeli, Finland, christian@wolkersdorfer.info*

²*South African Research Chair for Acid Mine Drainage Treatment, Tshwane University of Technology (TUT), Private Bag X680, Pretoria 0001, South Africa*

Abstract This paper describes the first full scale, containerized VFR operating in Finland. Other than previous installations published, the VFR is sized such that all the mine water discharging from the abandoned Metsämönttu mine site can be treated. The design criteria allow treatment of 1 to 35 L/min of circum-neutral mine water. During a 6 weeks small scale experimental VFR operation, the iron removal rate, flow and the on-site parameters were measured regularly. Based on these data, the full scale reactor was constructed and all before mentioned parameters were measured. In addition, a tracer test with NaCl to evaluate the mean residence time in the reactor and an on-site oxidation test with the mine water was conducted.

The experimental reactor removed more than 80 % of the iron in the mine water. The full scale VFR meanwhile removes 95 % of the iron and about 80 % of the arsenic in the mine water. Electrical conductivities ranged between 250 and 1300 $\mu\text{S}/\text{cm}$, pH between 7.0 and 7.9 and the redox-potential between 140 and 360 mV. Inflow total iron concentrations ranged between 6.3 and 10.7 mg/L and the outflow concentrations 0.2 and 10.0 mg/L. The tracer test revealed a mean residence time of 10 ± 1 h, which is substantially below the design criteria of 48 hours. Oxidation of the mine water reached 90 % after 1 h, starting from an initial oxygen saturation of 30 %. No removal of sulphate or a statistically significant decrease of the mine water's mineralisation was observed.

Key words vertical flow reactor, Finland, passive treatment, Metsämönttu, abandoned mine

Introduction

Mine water treatment at abandoned mine sites is often challenging (Wolkersdorfer 2008; Younger et al. 2002). It is therefore important to provide mine water treatment techniques that can operate independently, which is often the case for passive mine water treatment options (Brown et al. 2002; Gusek 2013; Younger 2000). One of these is the vertical flow reactor (VFR) that was first introduced about a decade ago (Sapsford et al. 2006) and has been described and used at various locations (Florence et al. 2016; Yang et al. 2011; Yim et al. 2014) since then.

Simplified, a vertical flow reactor consists of a tank and a coarse substrate at the tank's bottom that allows microorganisms to grow ("schmutzdecke") and iron sludge to settle. It works similar to a slow sand filtration system, in which polluted water is filtered through coarse gravel and a layer of sand above it. Water flows gravity driven vertically downward, at velocities depending on the size of the gravel bed. To remove Fe from circumneutral mine water, VFRs work more effectively under aerobic conditions (Sapsford et al. 2007).

The precipitation of Fe³⁺-ochre on the surface is due to adsorption of Fe²⁺ on the existing ochre particles, which is then followed by the auto-catalytic oxidation forming even more ochre (Barnes 2008). Once the ochre bed is building up, the filtration effect and removal properties for Fe of the VFR increase.

So far, VFRs used in the UK, China and Korea are specifically designed tanks for treating mine water on a chosen mine site. Though the Taff Merthyr pilot scale plant was constructed using pre-manufactured parts for a “commercially available bespoke steel panelled water tank” (Sapsford et al. 2005) and other sites used intermediate bulk containers (Dey et al. 2003), they were not in itself containerized VFRs. The new approach described here is using a modified container which allows easy access and removal of the sludge as well as the gravel bed.

The aim of the project was to show that a containerized VFR can be used at the Metsämonttu mine site and that the mine water can be treated to an environmentally better quality than without the VFR.

Description of mine site

Metsämonttu (“forrest pit”) is an abandoned underground copper-zinc-lead-silver-gold mine in Aijala, situated in the Salo municipality (formerly Kisko) of the Salo sub-region of Southwest Finland (Varsinais-Suomi). Mining in this area dates back to the 17th century, but the Metsämonttu deposit was only discovered in 1945. A first drill hole was started in 1946 and the mine was operated from 1952–1958 and 1964–1974. As rich ore reserves were discovered, Outokumpo Oy started mining in 1951, initially with an open pit exploration but subsequently, a 3 × 4 m shaft I was sunk to a depth of 135 m (Turunen 1953; Varma 1954) and later deepened to 235 m. Based on the production data, shaft II, which is located 280 m south of shaft I, was very likely sunk between 1961 and 1962 and reached a depth of 545 m. Both shafts are connected with each other through the +190 m level. In the vicinity of the Metsämonttu mine, three other abandoned mines are located: the Aijala, Aurums-Aijala and the Hopeamonttu mines, which operated during various times between the 17th and 20th century (Mäkelä 1989; Papunen 1986; Puustinen 2003). Though the ore processed was still high, the mine was finally closed in 1974. Production numbers vary from source to source, but are around 1.1 t Au, 20 t Ag, 45 kt Zn, 7.1 kt Pb, 1.6 kt Cu and 113 kt S (Geological Survey of Finland (GTK) 2016; Nurmi and Rasilainen 2015).

Tectonically and genetically, the mine belongs to the Orijärvi-Aijala area (Aijala subarea *sensu* Eilu) of the Uusimaa Belt and is classified as a Zn-Cu±Au volcanic massive sulphide (VMS) deposit (Eilu et al. 2012; Hanski 2015; Latvalahti 1979). It is characterised by felsic to mafic volcanics and chemical sedimentary sections. Usually, the volcanics are intensely altered with an increase of K, Fe and Mg and a decrease of Na and Ca with gneisses of varying composition and skarn, all of them highly metamorphosed (Eilu et al. 2012). According to Latvalahti (1979), this alteration results in “dolomitization, silicification, sericitization and magnesium-iron metasomatism” of the ore deposit. This nearly vertical deposit has a maximum thickness of 20 m, but mostly it is less than 10 m thick and the ore itself is located

within dolomitic limestones and skarns as well as quartz and cordierite-anthophyllite wall rocks in disseminated or breccia deposits. Typical main ore minerals are pyrrhotite, pyrite, chalcocopyrite, sphalerite and galena with a large number of secondary minerals.



Figure 1 Iron staining at the uncontrolled mine water discharge of the Metsämonttu site (2015-07-02).

No details about the flooding period of the Metsämonttu mine are known and eventually the mine water started to discharge from the abandoned and decommissioned shaft. Using the iron staining and sludge build up as an indicator (fig. 1), it can be assumed the mine water flooded the cellar of the mine building and discharged from there into a northern direction into waste rock and a natural wetland area. Downstream of the mine, no more iron staining can be observed.

Methods and Material

Initially, a commercially available, 100 L tank was used to identify if the iron concentration of the Metsämonttu mine water can be reduced by means of a VFR. The flow was controlled with a valve to range around 1 L/min and the iron concentration as well as the on-site parameters measured regularly for 38 days. Thereafter, a 20 ft container was modified on-site into a VFR and transported to the Metsämonttu site where it was filled with a gravel bed and the inflow and outflow adjusted to take all the water discharging from shaft 1 (fig. 2). Flow was measured with a van Essen CD Diver through a calibrated $\frac{1}{2}$ V-Weir.

Water analyses were conducted daily to monthly and on-site parameters pH, temperature, redox-potential, oxygen concentration and electrical conductivity (EC) measured with HACH probes. Iron concentrations were measured on-site with a Hach photometer and alkalinity and acidity with a Hach digital titrator. Filtered ($0.45 \mu\text{m}$ membrane filters) and unfiltered samples were analysed with ICP-MS and discrete analysers at Ramboll Oy in Lahati. All containers were rinsed three times and the filtered samples acidified with ultra-pure

HNO₃. Samples were kept cool at below 6 °C after sampling in cooler boxes or fridges and transported to the lab as soon as logistics allowed.

The experimental tank was filled with commercially available, white inert granodiorite of 0.5 to 1 cm diameter (purchased from a garden centre), whilst the full scale containerized tank was filled with 32–64 mm mica gneiss.

A NaCl tracer test was conducted with commercially available food salt (Meira Jodioitu Ruokasuola) of 2089.79 g mass. EC was measured every minute with a van Essen CTD diver and the EC–NaCl relationship established with a calibration of the mine water and the food quality salt.

Sludge of the experimental VFR was dried and sent for XRF as well as SEM-EDS analysis at LUT in Lappeenranta.



Figure 2 Picture of the Metsämonttu VFR at the end of the initial filling period (2016-08-08), before the installation of the aeration device.

Results and Discussion

Though the on-site parameters of the Metsämonttu shaft 1 discharge are fluctuating throughout the year, the chemical parameters are relatively constant (tab. 1). From an environmental point of view, the mine water can't be described as polluting, though the iron precipitates leaves an unesthetical staining around the former, uncontrolled point of discharge (fig. 1). Downstream the mine site, natural attenuation reduces the potential contaminants As and Fe to 1.3 µg/L and 92 µg/L, respectively. These values can be explained by the circum-neutral characteristic of the mine water, with a pH between 6.9 and 7.9, caused by the buffering capacity of the carbonate wall rock of the ore deposit. The mine water sometimes has a slight aromatic smell, which is caused by the PAHs Fluorene (5 µg/L) and Pyrene (7

pg/L), which are usually originating from gasoline, diesel fuel, and heating oils (Ibanez et al. 2007; Weiner 2010) used in the underground mine workings. As the mine water is discharging directly from the shaft, the redox-potential and the oxygen saturation are usually low, with average around 150 mV and 5%, respectively.

Table 1 Mine Water Quality of the Metsämonttu mine water discharge between 2015 and 2016.

Parameter (n = 8)	Value
Temperature, °C	7.0 – 11.9
Electrical conductivity, µS/cm	579 – 1288
pH, –	6.9 – 7.9
Redoxpotential, mV (SHE)	100 – 290
Fe _{tot} , mg/L	6.7 – 15.6
As, µg/L	52 – 55
U, µg/L	2.7 – 3.5
SO ₄ ²⁻ , mg/L	230 – 290
HCO ₃ ⁻ , mg/L	180 – 292
O ₂ , mg/L	0.1 – 18.3
Q, L/min	0.6 – 34.6

Mine Water from the shaft discharge was partly diverted into the experimental VFR for 38 days. Inflow and outflow pH ranged between 7.2 and 7.5, inflow E_h between 70 and 90 mV, while outflow E_h ranged from 150 to 300 mV. Inflow Fe_{tot} was between 6 and 11 mg/L, while the outflow Fe_{tot} ranged between 0.4 and 10 mg/L, resulting in a removal rate starting at 11 % and reaching a value as high as 96 % towards the end of these 38 days (fig. 3). This result was promising enough to design a full scale VFR based on a 20 ft open container, which was commissioned on August 5th, 2016. Removal rates for Fe_{tot} increased from about 20 % to above 85 %, but substantially decreased during the winter months of 2016/2017, which might be contributed to reduced microbial activity during that time of the year. Another reason could be that the redoxpotential of the mine water stayed too high or that the partly frozen aeration system was not capable of oxygenating the mine water high enough. In an on-site aeration experiment it could be shown that the oxygen content of the mine water could rise from about 31 % to 90 % within 1 h, but the redoxpotential stayed low between 90 and 100 mV, which is not high enough to oxidize all of the ferrous iron.

In order to identify the mean residence time of the mine water within the VFR, a tracer test with food quality NaCl was conducted. A recovery rate of only 37% was achieved, as the tracer test might have been stopped too early. Based on the tracer test results, the mean residence time in the VFR is 10 h 17 min, which can be considered too low for all the iron oxyhydrate to

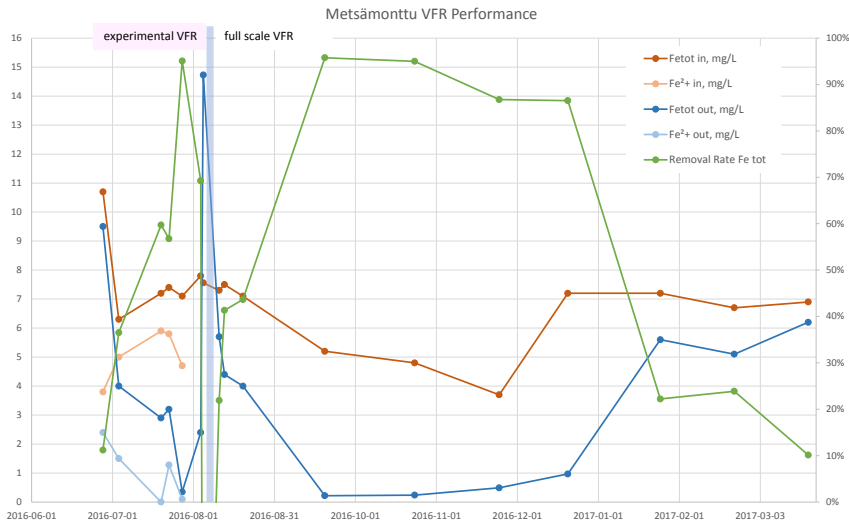


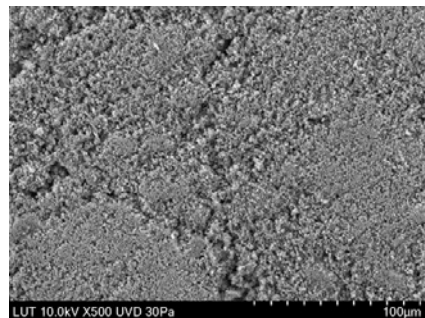
Figure 3 Performance of the experimental and the full scale VFR between June 2016 and March 2017.

settle or react. This might be another cause for the reduction in the removal rate over time. Further investigations will be done during the summer months of 2017.

Besides the Fe, also As was removed in the VFR, which is very likely a result of co-precipitation with the Fe oxyhydrate. Other semi-metals and metals did not show a statistically significant change in concentration. In the SEM EDS analysis, As could not be found, but the results clearly show that the sludge is primarily iron oxyhydrate with some single particles in the sample showing carbonates (tab. 2). XRF analyses only showed amorphous substances.

Table 2 Results of SEM EDS analysis of the sludge in the experimental VFR and related image. Averages from area and single particle analysis.

Element	Average, %	Standard deviation, %	n
C	12.3	14.1	8
O	38.9	6.1	8
Mg	0.4	0.2	5
Al	0.7	0.8	5
Si	5.4	6.8	8
S	4.4	7.7	5
Ca	2.1	0.9	8
Fe	34.3	17.4	8
Na	6.4	–	1
Zn	21.3	–	1



Conclusions

The two experimental and full scale vertical flow reactors proved that it is possible to treat circum neutral mine water with this technique and when using correct design criteria, removal rates of up to 95 % can be achieved. The project also proved that it is possible to containerize a VFR so that it can easily be constructed of-site and transported to the treatment site. It could also be shown that the relatively low mean residence time of the mine water in the reactor seems not to affect the removal rate, which might be due to the fact that the water can be oxidised relatively quickly. No precise explanation can be given for the low removal rates during the winter months, but very likely the design needs to be changed so that the aeration system will not freeze in winter.

Another reason for the decreased performance might be that the gravel used in the containerized VFR is too coarse and that the high initial removal rates are an indication for the first sludge that build up. No removal of sulphate or a statistically significant decrease of the mine water's mineralisation was observed and is neither expected nor needed for the relatively low mineralized water.

Acknowledgements

The authors thank Tekes for funding the FiDiPro Chair at Lappeenranta University of Technology (CW) and Lappeenranta University of Technology Research Foundation Committee for co-financing the research visit through a grant to BQ. We also thank the owners of the Metsämonttu mine site, Martti Antero and Riku Bergroth, for their assistance. Timo Ruskeeniemi identified the rocks used in the containerized VFR and Toni Väkiparta conducted the XRD measurements on the experimental VFR sludge. Special thanks to the stakeholders within the iMineWa project and all colleagues and friends who helped during sampling or preparation of the site.

References

- Barnes A (2008) The rates and mechanisms of Fe(II) oxidation in a passive vertical flow reactor for the treatment of ferruginous mine water. Cardiff University
- Brown M, Barley B, Wood H (2002) *Minewater Treatment – Technology, Application and Policy*. IWA Publishing, London
- Dey M, Sadler PJK, Williams KP (2003) A novel approach to mine water treatment. *Land Contam Reclam* 11(2):253-258. doi:10.2462/09670513.822
- Eilu P, Ahtola T, Äikäs O, Halkoaho T, Heikura P, Hulkki H, Iljina M, Juopperi H, Karinen T, Kärkkäinen N, Konnunaho J, Kontinen A, Kontoniemi O, Korkiakoski E, Korsakova M, Kuivasaari T, Kyläkoski M, Makkonen H, Niiranen T, Nikander J, Nykänen V, Perdahl JA, Pohjolainen E, Räsänen J, Sorjonen-Ward P, Tiainen M, Tontti M, Torppa A, Västi K (2012) Metallogenic Areas in Finland. Special paper – Geological Survey of Finland 53:207-342
- Florence K, Sapsford DJ, Johnson DB, Kay CM, Wolkersdorfer C (2016) Iron mineral accretion from acid mine drainage and its application in passive treatment. *Environ Technol* 37(11):1428-1440. doi:10.1080/09593330.2015.1118558
- Geological Survey of Finland (GTK) (2016) Metsämonttu. In: Mineral Deposit Report. http://tupa.gtk.fi/karttasovellus/mdae/raportti/578_Mets%C3%A4monttu.pdf Accessed 2017-04-14
- Gusek JJ (2013) A Periodic Table of Passive Treatment for Mining Influenced Water – Revisited. In: Brown A, Figueroa L, Wolkersdorfer C (eds) *Reliable Mine Water Technology*. International Mine Water Association, Golden, p 575-580
- Hanski E (2015) Chapter 2 – Synthesis of the Geological Evolution and Metallogeny of Finland. In: Maier WD, Lahtinen R, O'Brien H (eds) *Mineral Deposits of Finland*. Elsevier, p 39-71

- Ibanez JG, Hernandez-Esparza M, Doria-Serrano C, Fregoso-Infante A, Singh MM (2007) *Environmental Chemistry – Fundamentals*. Springer, Heidelberg
- Latvalahti U (1979) Cu-Zn-Pb ores in the Aijala-Orijarvi area, southwest Finland. *Econ Geol* 74(5):1035-1059. doi:10.2113/gsecongeo.74.5.1035
- Mäkelä U (1989) Geological and geochemical environments of Precambrian sulphide deposits in southwestern Finland. *Ann Acad Sci Fenn A 3 Geol Geogr* 151:1-102
- Nurmi PA, Rasilainen K (2015) Chapter 11 – Finland’s Mineral Resources: Opportunities and challenges for future mining. In: Maier WD, Lahtinen R, O’Brien H (eds) *Mineral Deposits of Finland*. Elsevier, p 753-780
- Papunen H (1986) Geology and ore deposits of southwestern Finland. In: Gaál G (ed) 17e *Nordiska Geologmötet 1986 – Excursion guide, excursion C 3 – Metallogeny and ore deposits in South Finland*. vol Guide 16. *Geologian Tutkimuskeskus, Espoo*, p 8-18
- Puustinen K (2003) Suomen kaivosteollisuus ja mineraalisten raaka-aineiden tuotanto vuosina 1530–2001, historiallinen katsaus erityisesti tuotantolukujen valossa, *Geological Survey of Finland, Report M 10.1/2003/3, Espoo*, 578 p
- Sapsford DJ, Barnes A, Dey M, Liang L, Williams KP (2005) A novel method for passive treatment of mine water using a vertical flow accretion system. In: Loredó J, Pendás F (eds) *Mine Water 2005 – Mine Closure*. University of Oviedo, Oviedo, p 389-394
- Sapsford DJ, Barnes A, Dey M, Williams K, Jarvis A, Younger P (2007) *Low Footprint Passive Mine Water Treatment: Field Demonstration and Application*. *Mine Water Environ* 26(4):243-250. doi:10.1007/s10230-007-0012-6
- Sapsford DJ, Barnes A, Dey M, Williams KP, Jarvis A, Younger P, Liang L (2006) Iron and Manganese Removal in a Vertical Flow Reactor for Passive Treatment of Mine Water. Paper presented at the ICARD 2006, St. Louis, 7:1831-1843 [CD-ROM].
- Turunen E (1953) Aijalan ja Metsämöntun kaivokset [The Aijala and Metsämönttu mines]. *Vuoriteollisuus – Bergshanteringen* 11:16-28
- Varma A (1954) The copper-zinc ore deposits of Aijala and Metsämönttu. *Geol Tutkimuslaitos* 55:20-24
- Weiner ER (2010) *Applications of Environmental Aquatic Chemistry – A Practical Guide*, 2 edn. CRC Press, Boca Raton
- Wolkersdorfer C (2008) *Water Management at Abandoned Flooded Underground Mines – Fundamentals, Tracer Tests, Modelling, Water Treatment*. Springer, Heidelberg
- Yang S, Wu P, Zhang R, Dong H (2011) 有氧垂直折流式反应池处理煤矿酸性废水 [Treatment of acid mine drainage using aerobic baffled vertical flow reactor]. *环境工程学报 [Chin J Environ Eng]* 5(4):789-794
- Yim GJ, Cheong YW, Hong JH, Hur W (2014) The role of each compartment in a two-compartment vertical flow reactor for ferruginous mine water treatment. *Water Res* 62(10):11-19. doi:10.1016/j.watres.2014.05.016
- Younger PL (2000) The adoption and adaptation of passive treatment technologies for mine waters in the United Kingdom. *Mine Water Environ* 19(2):84-97. doi:10.1007/BF02687257
- Younger PL, Banwart SA, Hedin RS (2002) *Mine Water – Hydrology, Pollution, Remediation*. Kluwer, Dordrecht

Exploration of Cambrian limestone groundwater runoff zones based on underground tracer tests

Qi Wang¹, Tiantian Wang², Xinyi Wang^{2,3}

¹*School of Rescours and Enviroment, North China University Of Water Resources And Electric Power, Zhengzhou, 450045, China*

²*Institute of Resources and Environment, Henan Polytechnic University, Jiaozuo, 454000, China*

³*Institute of Energy and Chemical Industry of China Pingmei Shenma Group, Pingdingshan 467000, China*

Abstract To detect the occurrence conditions of Cambrian limestone (CL) groundwater runoff zones in Pingdingshan Coalfield No.2 mine and Wuzhai mine, the underground tracer tests of CL are investigated. The results show that groundwater velocity and permeability coefficient of CL aquifers is up to 3.011 m/d and 3.4233 m/d, which proved the existence of groundwater runoff zones. Reverse fault and fault fracture zone on both sides of No.2 mine fault is a key factor affecting the spatial distribution of runoff zone in CL aquifers. The determination of CL runoff zone lays the foundation for controlling water hazard from coal floor.

Key words Cambrian limestone groundwater, Intensive runoff zone, Tracer tests, Permeability coefficient.

Introduction

In the North China Coalfield (NCC), Ordovician or Cambrian limestone (CL) aquifers are the main water disaster threat in the process of overlying coal seam mining. Pingdingshan Coalfield is located in the NCC, the water disaster in the process of 2₁ and 1₅ coal mining is the floor CL aquifers, with large thickness, high temperature, high pressure and uneven karst development. By the influence of complex fault distribution and groundwater flow in coalfield, the runoff zones of the CL aquifers are developed. The runoff zones play an important control role in the CL water pressure, water temperature, and water inflow and water inrush. Therefore, the study on the distribution and water control characteristics of runoff zones will have the vital significance to the prevention and control of coal seam floor limestone water hazard.

Based on the connectivity test and mine geological data of No.2 and Wuzhai mine of the Pingdingshan Coalfield, the distribution characteristics and formation mechanism of the concentrated runoff zones of CL aquifers is analyzed to provide a theoretical basis for the prevention and control of mine floor water disaster.

Background of the research area

The No.2 mine and Wuzhai mine is located in the southwest wing of Likou syncline, the footwall of Guodishan fault (Fig. 1). The stratum trends at 100°-120° and plunge at 10°-30°, while the dip angle is 8°-12°. There are 9 large and medium sized faults exposed in No.2 mine and Wuzhai mine field. Except for No.2 mine reverse fault, the vertical displacement of the other faults is small and short, which have little effect on coal mining. The No.2 mine reverse fault is located in the south centre of No.2 mine and Wuzhai mine. The hanging wall (northern part) rose and the footwall (southern part) dropped, striking at 90°-145°,

plunging at 0° - 55° , with an extent of 5 km. The dip angle is 25° - 50° , with a 5- 40 m vertical displacement, which increased with the decreasing of depth.

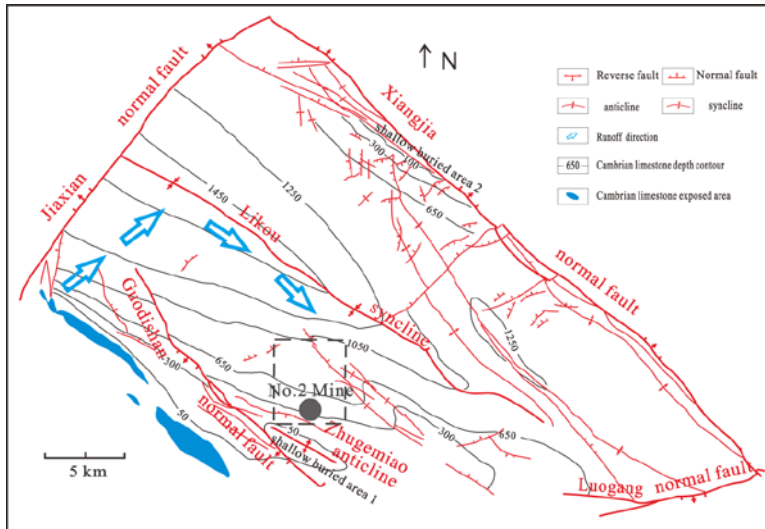


Figure 1 Geological structure and buried depth distribution of the CL in Pingdingshan Coalfield

The thick CL aquifers accept the ground water recharge from overlying Quaternary strata (with thickness of 20 – 50 m) near the Zhugemiao anticline. After that, the groundwater flowed along the direction of rock tendency from shallow to deep or along the fault fractured zone to the north east. Then, the drawdown funnel was formed in No.2 mine and Wuzhai mine, due to the control of draining depressurization.

Arrangement of traces tests

The tracer test is an effective method to detect the water conductivity of faults, the hydraulic connection between different aquifers, the movement state of the limestone groundwater, the direction of the extension of the runoff zone and estimate the groundwater flow velocity. To detect the distribution of runoff zones of the CL aquifers in No.2 mine and Wuzhai mine, 2 tracer tests were carried out in the mine from December 4 to 7, 2013 and March 14 to 15, 2014. The launching point (LP) is located in the fracture zone of No.2 mine main roadway west at an elevation of -86 m. Six receiving points (RP) were set in the underground water outlet in the first experiment, 4 of them are located in No.2 mine, and the other are located in Wuzhai mine (Fig. 2). The target layers are the CL aquifers, and the groundwater samples were collected from the receiving point of the CL aquifers. The launching and receiving data of tracer tests are shown in Tab. 1.

Iodide ion was used as a tracer because this element was undetectable in the CL groundwater prior to testing. The concentration of potassium iodide released at the LP was 250 mg/L, and the iodide ion concentration was 184.028 mg/L. Two hundred and sixty four water samples were collected during the two tests, and water samples were sent to the laboratory to determine the iodide ion content using ICS-1100 ion chromatography system. Tracer

concentrations at RPs as well as travel times from the LP to RPs are presented in Tab. 2. Obviously, the iodide ion was detected in varying degrees from each RP.

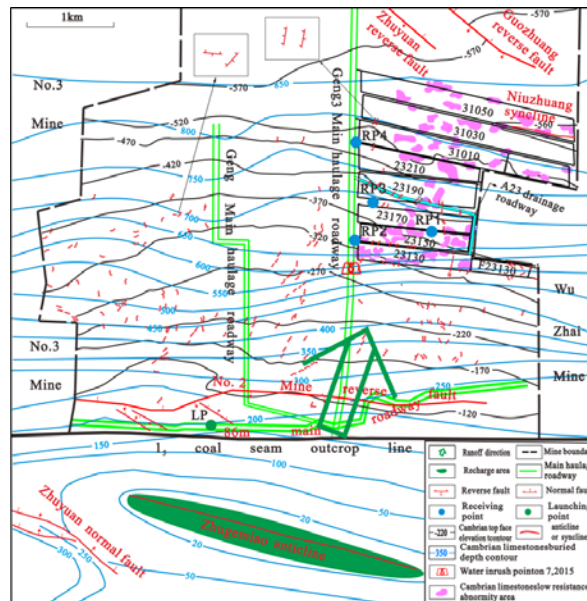


Figure 2 Location of the launching point and receiving points of the tracer tests

Table 1 Location and parameters of the LP and RPs

Test point	Location	Water level elevation of CL (m)	Distance to LP (m)	Water surface slope
LP	-86 m main roadway in No.2 mine	-86	0	
RP1	23170 air alley in No.2 mine	-395	3 162.54	0.0977
RP2	The intersection of 23130 air alley and Geng3 main haulage roadway in No.2 mine	-320	2 548.23	0.0918
RP3	23170 haulage alley in No.2 mine	-400	3 003.81	0.1045
RP4	The intersection of 31010 air alley and Geng3 main haulage roadway in No.2 mine	-500	3 587.75	0.1154
RP5	21020 haulage alley in Wuzhai mine	-400	3 791.79	0.0828
RP6	-320 m main haulage roadway in Wuzhai mine	-330	4 040.57	0.0604

Table 2 Time and traces concentration of the LP and RPs

Test point	The first time		The second time		Note
	Concentration (mg/L)	Time (h)	Concentration (mg/L)	Time (h)	
LP	184.028	0	184.028	0	The first time is 10:30 a.m., February 6, 2013; The second time is 9:30 a.m., March 14, 2014
RP1	0.008	50.00	0.073	18.50	
RP2	0.376	52.00	0.007	16.50	
RP3	0.017	45.50	0.095	17.50	
RP4	0.009	70.83	0.003	22.50	
RP5	0.011	30.50	No samples		
RP6	0.008	16.50	No samples		

Connectivity test of concentrated runoff zone

The CL groundwater velocity, using the distance between the LP and RPs, and the tracer travel time was calculated (Tab. 3). The estimated groundwater velocity is between 1 176 and 5 877 m/d, and its mean value is 3 011 m/d. The velocity value of No.2 mine and Wuzhai mine are respectively 2 656 m/d and 4 430 m/d.

Table 3 Calculated values of groundwater velocity and permeability coefficients

Mine name	Location	The first time		The second time	
		Velocity (m/d)	Permeability coefficient (m/d)	Velocity (m/d)	Permeability coefficient (m/d)
No.2 mine	RP1	1 518	15 537	4102	41 993
	RP2	1 176	12 811	3706	40 376
	RP3	1 584	15 162	4119	39 421
	RP4	1 215	10 534	3826	33 162
Wuzhai mine	RP5	2 983	36 035	–	–
	RP6	5 877	97 304	–	–

According to the hydraulic gradient and groundwater velocity, permeability coefficient of the CL aquifers in No.2 mine and Wuzhai mine could be calculated by using Darcy's law (Tab. 3). The estimated permeability coefficient is between 10 534 and 97 304 m/d, with a mean value of 34 233 m/d. The permeability coefficient of No.2 mine and Wuzhai mine are respectively 26 124m/d and 66 669 m/d.

According to the existing research results, when the permeability coefficient is greater than 50 m/d, it can be defined as the strong permeability aquifer. The permeability coefficient

of the CL in No.2 mine and Wuzhai mine is far greater than 50 m/d, which illustrates the existence of runoff zones in CL aquifers. The field geological survey shows that the visual width of the LP is about 30-60 cm, which extends from north to west. Its extension is very deep and can be heard to contain water flow, which can prove the existence of the runoff zones in CL aquifers.

Genetic analyses of the runoff zones

The 3 middle size normal faults on both sides of the LP, which are parallel to each other, are distributed in the range of 600 m. It strike at north-west and plunge at north-east, with 15 m displacement. The northwestern part pinch out in the southern part of the No.2 mine reversed fault. At these composite zone of fault and thin out site, the strata are fractured and karst landscapes are developed. Therefore, it becomes a fractured zone with strong water permeability. The strike of the LP fracture zone is consistent with the medium normal fault, which could be caused by the medium normal fault. In brief, the fractured zone in the medium normal faults laid the foundation of the concentrated runoff in the CL groundwater, which in the south part of No.2 mine reversed fault.

As can be seen from Fig. 3, the CL aquifers at both sides of No.2 mine reversed fault were not entirely disconnect by the fault, and still maintained a certain continuity, which has no effect on groundwater flow. According to drilling data, in 29 boreholes, with the CL exposed, 50% of them are distributed on both sides of the No.2 mine reverse fault. This illustrates the CL karst landscapes were relatively developed on both sides of the fault. Therefore, the hydraulic connection of the CL aquifers on both sides of fault is close. The exposed information in the tunnel at the north side of No.2 mine reverse fault and the working face illustrated that small faults were well developed in the Geng2 mining area, with zonal distribution (Fig. 3). The average density of faults was 73 strip/km². These small faults mainly strike at NE, with the larger dip angle. This made the CL extremely broken, and also provided a channel for the groundwater flow from southwest to northeast and from shallow to deep.

According to the distribution of faults and fracture zones, the movement mechanism of iodide tracer could be obtained. The tracer injected into the site first flowed westward along the fracture zone. After flowing through the No.2 mine reverse fault, it flowed along the fault zone to the northeast. Then the iodide tracer could be detected when arriving at No. 1, 2, 3, 4, 5, 6 RPs.

The results of the tracer tests and the analysis of the fault fracture zone shows that the CL groundwater runoff zones were developed at both sides of No.2 mine reverse fault. The runoff zones are: from the LP at -86 m main roadway to the working face 23130, 23170 of No.2 mine and working face 21020 of Wuzhai mine. But at the RP4 (elevation of -500 m), the iodide concentration was the lowest of the 2 tracer tests, which illustrated the hydraulic connection between deep groundwater and shallow groundwater of the CL is not close. That means the groundwater runoff zone has not reached the depth of -500 m. Plane and vertical distribution of the CL groundwater runoff zones in No.2 mine and Wuzhai mine could be further determined by geophysical prospecting, hydro-geological boreholes and the exposed condition of tunnel.

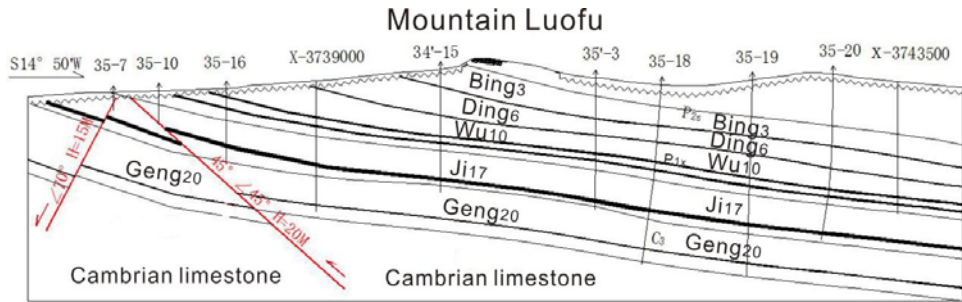


Figure 3 Section map of inverse fault in No.2 Mine of Pingdingshan Coalfield

Conclusions

The groundwater velocity of the CL groundwater in No.2 mine and Wuzhai mine estimated by the tracer test is 3 011 m/d. The permeability coefficient of the aquifers is 34 233 m/d. The above results proved the existence of the CL groundwater runoff zones.

Within No. 2 mine, small faults are well-developed, and have an average density of 73 strip/km². Well-runoff tunnels are developed within these fault zones. Indeed, small faults control the runoff of the CL groundwater.

The runoff zones provide a well channel for the CL groundwater in No.2 mine and Wuzhai mine that flow from southwest to northeast and the flow from shallow to deep plays an important role in the process of disaster prevention in coal mine.

References

- State Administration of Work Safety, State Administration of Coal mine safety (2009) Provisions for prevention and control of water in coal mines. China Coal Industry Publishing House
- Wu Qiang, Zhao Suqi, Sun Wenhao, Cui Fangya, et al. (2013) Classification of the hydrogeological type of coal mine and analysis of its characteristics in China. *Journal of China Coal Society* 38 (6):901-905
- Dong Shuning, Hu Weiyue (2007). Basic characteristics and main controlling factors of coal mine water hazard in China. *Coal Geology & Exploration* 35 (5):34-38
- Jing Guoxun, Li Dehai, Wang Xinyi, et al. (2014) Expert interpretation of coal mine safety regulations. China University of Mining and Technology Press
- Bu Changsen, Zhang Xicheng, Yin Wancai (2001). Inundation in the North-China Type Coalfields and the Status Quo of its Protection. *Geological Review* 47 (7): 405-408
- Zhang Peng, Sun Yajun, Cao Huanju (2012) Study on technology of safety mining above pressurized aquifer in seam floor. *Coal Science and Technology* 39 (9):104-107
- Yin Shangxian, Hu Weiyue, Liu Qisheng, et al. (2008) Risk assessment for water inrush from confined aquifers located under coal seams. *Journal of China University of Mining & Technology* 37(3): 311-315
- Chen Hanqiu, Zhai Yu, Hui Shengli, et al. (2011) Evaluation on water inrush danger from aquifer under seam floor and water inrush prevention and control countermeasures. *Coal Science and Technology* (08): 112-115

- Zhang Jianguo, Wang Luhe, Kang Guofeng, et al. (2012) "2012~2015" planning for coalmine limestone water regional control of China Pingmei Shenma Group, China University of Mining and Technology Press
- Xu Yanchun, Yang Yang (2014) New Progress on Floor Grouting Reinforcement Technology of Water Control in Coal Mining Face. *Coal Science and Technology* 42(1): 98-101
- Han Depin, Li Dan, Cheng Jiulong, et al. (2010) DC method of advanced detecting disastrous water-conducting geological structures along same layer. *Journal of china coal society* 35(4): 635-639
- Su Lin, Liu Xinming, Liu Yi (2011) Application of Prospecting Water-rich Area of Coal with TEM. *Chinese Journal of Engineering Geophysics* 8 (1): 6-9
- Wang Xinyi, Li Shifeng, Xu Guangquan, et al. (2011) *Special Hydrogeology*. China University of Mining and Technology Press
- Qi Wang, Xinyi Wang, Quanlin Hou (2016). Geothermal Water at a Coal Mine: From Risk to Resource. *Mine Water and the Environment* (35)3: 294-301
- Chen Kuikui, Wang Xinyi (2015) Analysis of the factors causing roof water inrush in coal seam mining with thin bedrock. *Chemical Engineering Transactions* 46 (12):679-684
- Qi Wang, Xinyi Wang, Xiaoman Liu, et al. (2015) Evaluation of Hydraulic Characteristics of the Normal Fault Based on Key Data. *The Open Fuels & Energy Science Journal* 8 (1): 265-271
- Renzheng Li, Qi Wang, Xinyi Wang, et al. (2017) Relationship Analysis of the Degree of Fault Complexity and the Water Irruption Rate, Based on Fractal Theory. *Mine Water and the Environment* 36(1):18-23

Similarities in Mine Water Management Challenges in Polar and Desert Climates: Two Case Studies

Houcayne El Idrysy

SRK Consulting (UK) Ltd, 17 Churchill Way, Cardiff, United Kingdom, hidrysy@srk.co.uk

Abstract Water resources availability and management in extreme climates are usually challenging for mining projects. The present paper focuses on two extreme conditions: the desert and the polar (Tundra subtype) climates. Despite the obvious difference between these two extreme conditions, water resources availability and management for mines in both climates show some striking similarities that may seem surprising. Such similarities relate to the following aspects especially:

- Atmospheric precipitation patterns
- Water inflows into mines
- Tailings management
- Water supply and groundwater quality

This paper illustrates the above similarities with two case studies.

Key words Extreme Climate, Permafrost, Desert, Mine Water Management, Water Supply.

Introduction

Water management in polar and dry climates (Belda et al. 2014) entails specific challenges to mining projects. The rainfall scarcity and sharp seasonal fluctuation in these climate conditions make mine water supply difficult and therefore the mine project development requires rigorous measures to minimise the use of water and maximise its recycling to fulfil the water demand. Such stringent requirement has a direct effect on the selection of the appropriate approach to tailings management, as well as the identification of the water supply source.

To illustrate the mine water management challenges and similarities in these two climates, this paper presents a polar climate project in Russia and a dry climate project in the Sahara Desert. To ease reference for the reader, since the project in Russia is in a polar (Tundra subtype) climate with a thick permafrost layer present, the project will be referred to here as the “permafrost” project and the second project will be referred to as the “desert” project.

Discussion

Project location and summary

The locations of the two projects presented in this paper are shown in Figure 1 and photographs of the landscape of each site are presented in Figure 2. This paper is based on the findings of the mine development Feasibility Study (FS) for both projects.

The permafrost project (the Mangazeisky Silver Project) is located some 400 km north of Yakutsk in Russia (Figure 1). It is a combined open pit and underground mining operation with the open pit mining comprising a small open pit of approximately 90m depth and a few narrow trenches up to 30 m deep. Topographic elevations in the project area range from ap-

proximately 1240 m above sea level (masl) at the high ridge near the proposed mine, to 840 masl at the adjacent valley floor (Figure 2). The streams are characterised by steeply dissected valleys. The site catchment belongs to the basin of the Yana River, which flows north into the Laptev Sea. Surface water flow in the area ceases during the winter season due to the freezing temperatures, which cause the formation of ice along the river and stream beds.

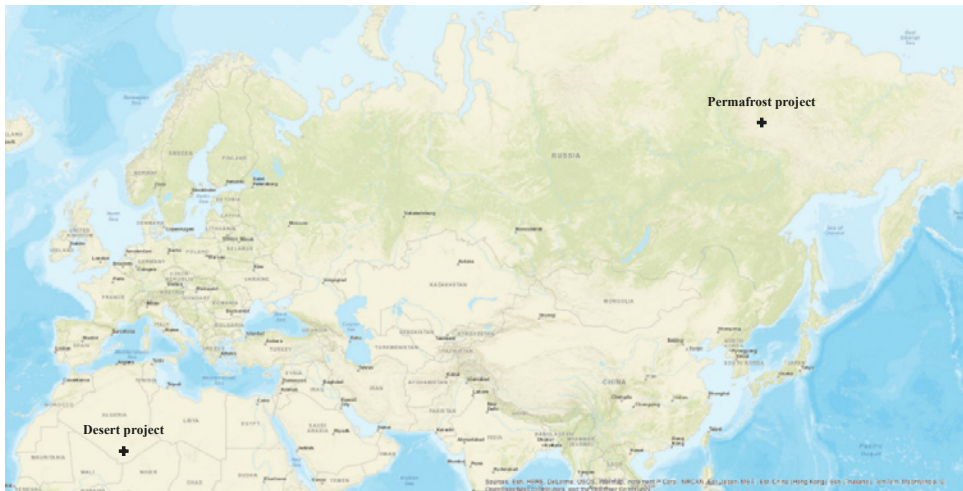


Figure 1 Approximate locations of the two projects

The desert case study is the Nahda Tungsten underground mine Project, located in the barren Tanezrouft region of far southern Algeria, a region that extends along the borders of Niger and Mali, west of the Hoggar mountains. The terrain of the desert project is generally flat and sandy with some rocky outcrops in the north-western part of the concession (Figure 2). The elevation of the permit area varies between 545 and 728 m above mean sea level (masl). Wadis in the local area serve as witness to historic water erosion when the Sahara Desert's climate was wetter. Wind erosion is currently the main driver of the landscape structure and due to the absence of dense vegetation the landscape is more prone to erosion.

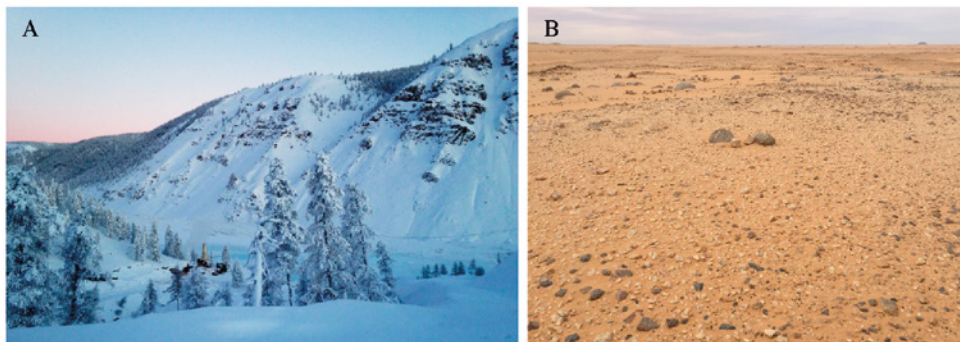


Figure 2 Views of the two sites: (a) the permafrost site in February and (b) the desert site in January. (source: Author's photos from site visits)

Atmospheric precipitation pattern

A global map showing the pattern of average annual precipitation worldwide is presented in Figure 3 (Evans 1996). This map illustrates the striking similarities between the desert and polar Tundra subtype climates with respect to atmospheric precipitation over the year which is very low in both regions.

Accordingly, the desert climate, which occurs in arid areas such as the Sahara, is characterised by high air temperature and low atmospheric precipitation. The permafrost areas, which have a polar type of climate in cold regions such as Siberia and north of Canada and Alaska, also show low atmospheric precipitation but low air temperature. Weather station records show that the amount of rainfall is less than 250 mm per year in both the permafrost and desert areas. The annual average rainfall in the Algerian Desert is generally below 100 mm in the northernmost part. The scarcity of rainfall is aggravated by its irregularity. The presence of slow but constant winds exacerbate the dryness and aridity of the Sahara by causing enhanced rates of evaporation.

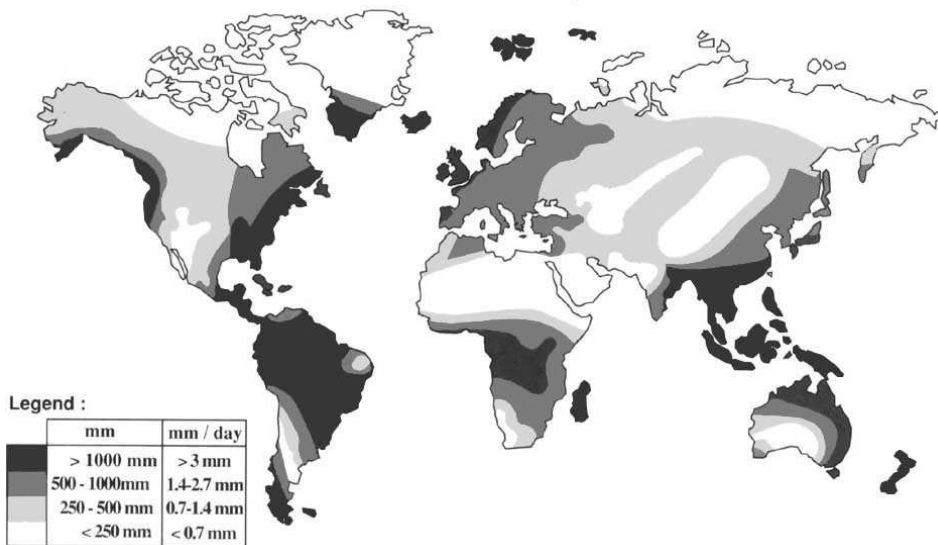


Figure 3 Global map of average annual precipitation
(source: <http://www.fao.org/docrep/w5183e/w5183e01.jpg>).

The nearest weather station precipitation and temperature data from the Global Historical Climatology Network (GHCN) were used in the analysis for both projects. The data were obtained via the U.S National Oceanic and Atmospheric Administration (NOAA) website (NOAA, 2015).

In the permafrost project area the two weather stations of Sebyan-Kuel and Syuryen-Kyuyel, located 45 and 80 km respectively from the project, are the nearest stations with longterm

precipitation records. The average annual precipitation at the Sebyan-Kuel and Syuryen-Kyuyel weather stations is 203 mm and 337 mm, respectively. More than 60% of the precipitation occurs during the warm season. The highest average amount of precipitation occurs in June and July (59 mm and 76 mm, respectively) and the lowest in the winter months, from November to March.

Table 1 Average monthly precipitation for both projects, based on the nearest station data, mm.

Station	Jan	Feb	Mar	Apr	May	Jun	Jul	Aug	Sep	Oct	Nov	Dec	Year
Permafrost Project (Sebyan-Kuel)	3	3	3	8	12	59	39	31	25	13	3	4	203
Desert Project (In Guezzam)	11.4	0.9	2	3	5.2	13.2	15.7	8	20.9	0	0	0	80.3

The climate characterization for the desert project was based on data from the nearest station, In Guezzam, located some 140 km south of the project site. The data consist of a total of 20 years of monthly climate data and 20 years of daily rainfall data. The average monthly and annual precipitation recorded in the nearest weather stations for both projects are presented in Table 1.

The estimated magnitudes of 24h storm events for both project are shown in Table 2. 24h storms are commonly less than 25 mm in the permafrost project area and are not expected to be much higher than 60 mm for events of 50-year return period or more. For the desert project the maximum 24h rainfall recorded over the 20-year monitoring period from 1996 to 2015 was 60 mm. The frequency analysis suggests a maximum 24h rainfall magnitude of around 70 mm for 50-year return period and 90 mm for 100-year return period events.

Table 2 Estimated extreme Event 24-hour Rainfall Storms for both projects

Return Period (year)	Estimated 24-hour Extreme Rainfall Depths (mm)	
	Desert site	Permafrost site
5	22.6	36.24
10	34.5	43.15
20	48.5	49.77
50	70.6	58.34
100	90.4	64.76

Expected water inflows into the mine

Because of the scarcity of atmospheric precipitation (and the presence of an impervious permafrost layer in the case of the polar site) inflows of groundwater and surface water runoff

into mines in these two climate conditions are commonly low and therefore manageable using in-pit sump pumps rather than active dewatering from outside the mine.

Permafrost project

The hydrogeology of the site is characterised by the presence of the following formations:

- An active layer, where the temperature levels during the warm season reaches thawing point;
- The underlying permafrost layer: the permanently frozen ground; and
- Bedrock beneath the permafrost, which has the potential to contain groundwater.

The measured downhole temperature profiles, obtained from full year temperature monitoring, indicate a maximum thawing soil thickness of 1.75 to 2.75 m, reached in late August. Such a thin active layer, which remains frozen for most of the year, has a very limited storage capacity.

Using a geothermal gradient obtained from the temperature monitoring in deep boreholes, the thickness of the permafrost layer was estimated to be between 190m in the river valley to 400m in the top of the hills. Considering the significant thickness of the permafrost in the project area, the sub-permafrost aquifer is located far below the weathered layer, and groundwater flow seems to be mainly driven by geological structures (faults and fracture networks).

Six deep boreholes were drilled to investigate the sub-permafrost aquifer along the river valleys, and airlift and pumping tests carried out to assess the aquifer potential and estimate its hydraulic parameters. The results showed that the aquifer is highly confined, with all boreholes being artesian. The highest pumping rates achieved ranges from 1 L/s to less than 3 L/s (10 m³/h).

Due to the pit and underground mine being located fully in the permafrost layer, groundwater inflow into the mine was estimated to be negligible. The average surface water runoff into the proposed pits over the mine life was estimated to vary between 440 and 1700 m³/day due to rainfall events in the summer time.

Desert project

Hydrogeological investigations in the desert site revealed the existence of a small confined aquifer comprising a fractured horizon in the crystalline bedrock. The recharge area for the aquifer is believed to be the Atakor mountains, which are located more than 250 km north of the site at an altitude of 2000 masl, whereas the approximate elevation of the project area is 500 masl.

Of 44 boreholes drilled at the early stage of exploration on site only 9% were hydraulically productive. The borehole tests indicated a strong anisotropy of the fracture network. The

most productive well, where the static groundwater level was recorded at 52 meters below ground level, produced an average flow rate of 126 m³/day (1.45 L/s). A pilot mine shaft of 6 m² section constructed in the past at the site to a depth of 100 meters showed a static water level of 40m below ground. The shaft was hydraulically tested at a rate varying from 15 to 37 m³/day, inducing a drawdown of 18 m; a level that did not stabilise indicating low aquifer yield and limited storage capacity. The aquifer properties, the low rainfall in the area and the remote location of the recharge zone indicate that aquifer yields and therefore groundwater inflows into the proposed mine will be very low.

Tailings management

Ore processing for the permafrost project is expected to produce some 805,000 tons of tailings over the 8 years Life of Mine (LoM). For the desert project the amount of tailings expected from ore processing over the 6 years of mine life is around 900,000 tons. Due to the difficulties of water supply for ore processing all year round, water conservation in both projects is an important driver in selecting the tailings disposal technology. Based on such criteria, a filtered tailings design was developed for both projects. The similarity of the tailings Feasibility Study design criteria for both projects is illustrated in Table 3 (SRK, 2016 and 2017).

Table 3 Tailings management Feasibility Study design criteria for the two projects

Tailings Management Design Criteria	Permafrost project	Desert Project
Tailings Deposition Type	Filter press dewatered tailings or 'filter cake'.	Filter press dewatered tailings or 'filter cake'.
Tailings Facility Capacity	805,000 tons	900,000 tons
Tailings Facility Design Life	8 years	6 years
Tailings Moisture Content	15%	15%
Tailings Deposited Dry density	1.77 t/m ³	1.4 t/m ³
Tailings Design Storm (considering 100y return period 24h duration)	65 mm	90 mm

Filtered tailings are typically produced in a two-step process using a high-density thickener and vacuum or pressure filters in series. This allows the solids content by mass (w/w) of the tailings material to be raised above 85%. Using this method allows a recovery of up to 95% of the process water in the tailings. Furthermore, filtered tailings material present a lower risk of instability and environmental impact compared to wet tailings, and they are typically transported by trucks or conveyors and deposited in successive lifts to form a dry stack.

Water supply and groundwater quality

Owing to the thickened tailings technique and water recycling, the estimated fresh water demand for the desert and permafrost projects were reduced to around 130 m³/day and 260 m³/day, respectively, including the processing plant and mine camp water requirements.

Due to the precipitation and temperature patterns in both desert and polar climates, water supply must rely on a groundwater resource, which is often ‘fossil’ (paleo) water due to minimal recharge of the aquifers. Over the years such low recharge has led to an increase in salt concentration in groundwater.

The sub-permafrost aquifer is the only potential water source for the permafrost project during the cold period of the year when surface waters are frozen. Using aquifer parameter data obtained from borehole tests, in addition to geological and permafrost information, a groundwater model was developed and scenarios of long term borehole pumping for water supply simulated to assess the availability of the required amount of water in the aquifer for various pumping rates and patterns. The model results indicated the existence of enough water storage to supply the mine for the project life with the required amount of water. Subsequent testing of actual water supply wells, which is still ongoing, is corroborating such findings.

Borehole tests at the desert project suggested very low storage capacity of the small local aquifer. Therefore, water supply is envisaged from another groundwater source some 80 km from the site. In such a location, historic water wells have been operating for a long time and appear to guarantee the water supply for the project. Due to the selected tailings management technique, water recycling is maximised and the water supply needs are reduced to the minimum. Therefore, the small amount of makeup water required for the project over such a distance will be transported to site by track.

pH and salinity of groundwater at both sites are shown in Table 4 (SRK, 2016 and 2017).

Table 4 Summary of groundwater quality

Site	Groundwater quality parameters		Comment
	pH	Salinity (TDS) mg/L	
Permafrost site	7.3-7.5	~2,270	Water can be used for ore processing but needs treatment to become drinkable
Desert site	6.7	2,260-2,550	Water can be used for ore processing but needs treatment to become drinkable

Conclusions

The water management elements in a mining project are linked through the project water balance, which often reflects either a need for additional water supply, water treatment or discharge into the environment. This paper illustrated the striking similarities that can be observed in both the polar (Tundra subtype) and desert climate conditions using two case studies.

Whilst the scarcity of both rainfall and groundwater (and extreme temperature fluctuations) in the permafrost and desert locations result in low and manageable inflows of water

into the mines, this also leads to a shortage in water resources and dictates specific water management measures to be taken to fulfil the mine project needs. Thus, the use of filtered tailings was envisaged in both the presented case studies to maximize process water recovery within the processing plant and reduce makeup water demand. Fossil groundwater remains the main source of water supply for these mine projects, but due to its high salinity such water requires treatment before it can be used as a potable supply.

Acknowledgements

The author would like to thank the Clients of both the Mangazeisky and Nahda projects for allowing this paper to be presented in the IMWA 2017 Conference and colleagues that contributed to either of the FS, namely Samantha Barnes, Lenar Sultanov, and David Cooper.

References

- Belda et al. 2014, Climate classification revisited: from Köppen to Trewartha. CLIMATE RESEARCH (Clim Res). Vol. 59: 1–13, 2014. doi: 10.3354/cr01204.
- Evans, T. E., (1996) The effects of changes in the world hydrological cycle on availability of water resources. <http://www.fao.org/docrep/w5183e/w5183e04.htm>
- NOAA (2015), Global Historical Climatology Network (GHCN) data, from National Climatic Data Center: <https://www.ncdc.noaa.gov/oa/climate/ghcn-daily/>
- SRK Consulting (UK) Ltd (2016) Mangazeisky hydrogeological FS report.
- SRK Consulting (UK) Ltd (2017) Nahdha Project Climate Study and TSF interim report.

Mine Water Hydrodynamics, Stratification and Geochemistry for Mine Closure – The Metsämonttu Zn-Cu-Pb-Au-Ag-Mine, Finland

Christian Wolkersdorfer^{1,2}

¹*Lappeenranta University of Technology, Laboratory of Green Chemistry, Sammonkatu 12, 50130 Mikkeli, Finland, christian@wolkersdorfer.info*

²*South African Research Chair for Acid Mine Drainage Treatment, Tshwane University of Technology (TUT), Private Bag X680, Pretoria 0001, South Africa*

Abstract In the case of the Metsämonttu Zn-Cu-Pb-Au-Ag-mine in Finland, which was closed in the 1970ies, the mine water chemistry, isotopes, flow and the stratification in the mine was measured for a duration of two years. Based on the results, a still ongoing tracer test was initiated. The reason for this investigation was to understand which hydrodynamic and chemical processes are occurring in a closed underground mine and how this knowledge can be used for future mine closures or in-situ remediation options as so far no general conclusions can be reported.

It was found that the mine water shows no substantial vertical stratification but that a horizontal stratification occurs which causes the water in the two shafts to be of different chemical and isotopic signatures. While the electrical conductivity in shaft 2 was low, close to low mineralized ground water, the electrical conductivity in shaft 1 was higher, showing an interaction between the ore deposit and the water. The current results of the tracer test also show that the mine water velocity seems to be very slow as no tracer was found after 3 months of operation of the tracer test.

Key words hydrodynamics, geochemistry, Metsämonttu, abandoned mine

Introduction

In the times of economic down turn, when resources deplete or political decisions require the closure of underground mines, the question arises of how to conduct mine closure. This paper will address this question. In the past, the underground mines were simply allowed to flood by turning the mine pumps off and allowing the groundwater *alias* mine water table within the mine to rise (Wolkersdorfer 2008). Once the inflow and outflow quantity of the mine water equalised or the mine water reached the lowest point of discharge, the mine water either entered the receiving water courses or was directed into a mine water treatment plant (“pump and treat”). Yet, changing environmental standards and social awareness of potential problems relating to polluted or acid mine drainage demands a more thorough planning of the flooding and mine closure process (Stacey et al. 2010a, b). Recent and current examples, where mine flooding resulted or will result in thorough planning are the German hard Coal mines (Coldewey et al. 2014; Rosner 2011), the Witwatersrand gold mines (Coetzee 2016) or the Cape Breton Island hard coal mines (Shea 2009), and in many cases a vertical stratification in the shafts was observed (Wolkersdorfer et al. 2016).

The abandoned Finnish Metsämonttu mine with two shafts was chosen as a case to study mine water chemistry, hydrodynamics and the stratification within the mine water body. For two years, chemical water data was collected, isotope studies conducted and a tracer test initiated. This proceedings paper describes the first results of these investigations. A de-

scription of the mine water treatment experiments is given in another paper of this author in this proceedings volume.

Description of mine site

The following description of the mine site is taken from Wolkersdorfer and Qonya (2017). Metsämonttu (“forrest pit”) is an abandoned underground copper-zinc-lead-silver-gold mine in Aijala, situated in the Salo municipality (formerly Kisko) of the Salo sub-region of Southwest Finland (Varsinais-Suomi). Mining in this area dates back to the 17th century, but the Metsämonttu deposit was only discovered in 1945. A first drill hole was started in 1946 and the mine was operated from 1952–1958 and 1964–1974 (figures differ). As rich ore reserves were discovered, Outokumpu Oy started mining in 1951, initially with an open pit exploration but subsequently, a 3 × 4 m shaft I was sunk to a depth of 135 m (Turunen 1953; Varma 1954) and later deepened to 235 m. Mining was conducted using shrinkage-stoping with longitudinal stopes and partly cut-and-fill stoping (Matikainen and Särkkä 1982; Varma 1954). Based on the production data, shaft II, which is located 280 m south of shaft I, was very likely sunk between 1961 and 1962 and reached a depth of 545 m (fig. 1). Both shafts are connected with each other through the +190 m level. In the vicinity of the Metsämonttu mine, three other abandoned mines are located: the Aijala, Aurums-Aijala and the Hopeamonttu mines, which operated during various times between the 17th and 20th century (Mäkelä 1989; Papunen 1986; Puustinen 2003). Though the amount of ore processed was still high, the mine was finally closed in 1974. Production numbers vary from source to source, but are around 1.1 t Au, 20 t Ag, 45 kt Zn, 7.1 kt Pb, 1.6 kt Cu and 113 kt S from a total of 1.5 Mt of ore mined (Geological Survey of Finland (GTK) 2017; Nurmi and Rasilainen 2015).

Tectonically and genetically, the mine belongs to the Orijärvi-Aijala area (Aijala subarea *sensu* Eilu) of the Uusimaa Belt and is classified as a Zn-Cu±Au volcanic massive sulphide (VMS) deposit (Eilu et al. 2012; Hanski 2015; Latvalahti 1979). It is characterised by felsic to mafic volcanics and chemical sedimentary sections. Usually, the volcanics are intensely altered with an increase of K, Fe and Mg and a decrease of Na and Ca with gneisses of varying composition and skarn, all of them highly metamorphosed (Eilu et al. 2012). According to Latvalahti (1979), this alteration results in “dolomitization, silicification, sericitization and magnesium-iron metasomatism” of the ore deposit. This nearly vertical deposit has a maximum thickness of 20 m, but mostly it is less than 10 m thick and the ore itself is located within dolomitic limestones and skarns as well as quartz and cordierite-anthophyllite wall rocks in disseminated or breccia deposits. Typical main ore minerals are pyrrhotite (18–20 %), pyrite (9–10 %), sphalerite (7 %), chalcopyrite (0.25 %) and galena (0.12 %) with a large number of secondary minerals (Turunen 1953; Varma 1975, Table 1).

On the first visit in 2015, ferrous mine water with a circum-neutral pH was discharging from shaft 1 into the cellar of the abandoned shaft housing and from there into the receiving environment. After about 50 m of surface flow, where substantial ochre deposits have been build up since the mine closure, the mine water seeped into a waste rock pile north of the shaft building. At the point of discharge from the shaft into the cellar, H₂S could be smelled

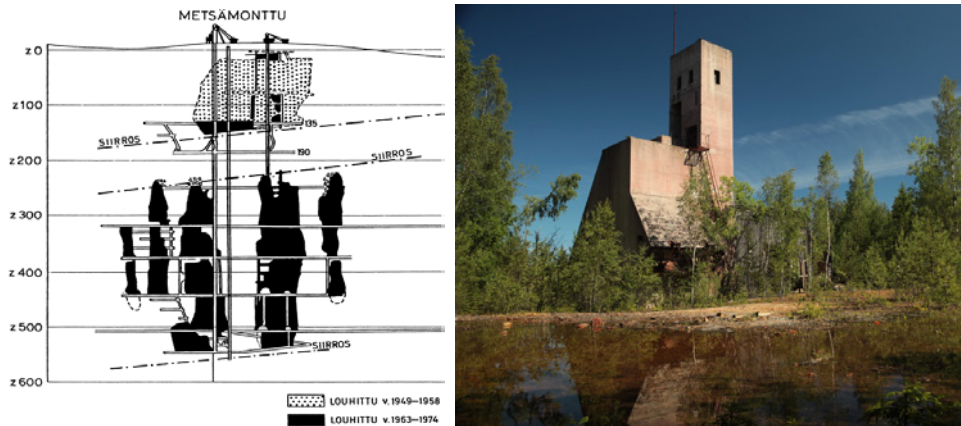


Figure 1 Left: Cross section of the Metsämonttu mine site with shaft 1 on the right and shaft 2 on the left. Indicated are the two mining phases (from Warma 1975). Siirros: fault, louhittu: mined. Right: shaft 1 and part of the flooded open pit lake in the foreground (2015-07-02).

and white filaments, very likely sulfur reducing bacteria, could be observed. In shaft 2, the mine water was standing 11.63 m below shaft bank and a 20 cm (1 m³) thick layer of badly smelling oil, grease and fat was encountered. This was later removed from a specialised company. In both shafts, the mine water has a distinctive aromatic smell of PAHs.

Methods and Material

Mine water samples were taken in filtered, acidified (0.2 µm) and unfiltered aliquots and analysed in the accredited Ramboll Lahti laboratory using ICP-MS and discrete analysers. k_B and k_A were analysed in the field with a Hach digital titrator and on site parameters measured with the relevant Hach electrodes connected to a Hach HQ40D. Stable isotope ratios $\delta^{18}\text{O}$ and $\delta^2\text{H}$ were sampled in 2 mL glass vials with septum screw caps were completely filled with water samples and analyzed at the Institute for Groundwater Management, Technical University of Dresden, Germany by a stable isotope mass spectrometer MAT 253 (Thermo Fisher Co., Bremen, Germany) after pyrolysis in a high temperature pyrolysis device at 1450 °C (HEKAtech Co, Wegberg, Germany). $\delta^{18}\text{O}$ and $\delta^2\text{H}$ ratios were estimated by an average of a fourfold analysis and calibrated by the IAEA-standards VSMOW2 and SLAP2. Temperature and electrical conductivity measurements in the shafts were conducted once using a Heron Conductivity Plus 300 m dipper (the instrument failed to work properly after the first measurements). Depth dependent water samples were taken with a 1 L plastic depth sampler. While shaft one could be sampled up to its maximum depth of 210 m, shaft 2 had an obstacle in a depth of 290 m and could not be sampled to the maximum depth. Flow was measured with the bucket and stopwatch method.

Results and Discussion

Water is discharging from shaft 1 at a flow rate of 0.6 – 34.6 L/min, with an average of 9.3 L/min ($n = 66$). pH values are circumneutral between 6.0 and 7.9 with an average of 7.0 and electrical conductivities range from 209 to 1300 µS/cm with an average of 550 µS/

cm. No water discharges from shaft 2, as the mine water level is 13 m below surface. Based on the production data, the mine has a volume of 500 – 600,000 m³, which would result in an average theoretical flooding time of 100 years. As this is obviously wrong, the mine water make during production and the flooding period must have been higher, but no data is known hitherto, and the first flush period can therefore not be calculated.

All chemical and isotope data show that the mine waters in the two shafts of the Metsämonttu mine are slightly, but statistically significantly different (Tab. 1 and Fig. 3). In general, the mine water in shaft 1 is higher mineralised than that of shaft 2. Isotopic analysis show that the samples in shaft 1 are heavier compared to those of shaft 2, but are not on one of the local meteoric water lines of Finland. Yet, as mine water in shaft 2 is clearly precipitation influenced, this water falls within the range of isotope signature typical for rain water in Finland, as reported by Kortelainen (2007). The difference between these two isotopic compositions could be related to winter or summer isotope signatures in the two shafts, an isotopic fractionation of mine water in shaft 1 or mixing with water showing heavier isotope ratios. Detailed studies to understand these differences are still ongoing. From the depth depended temperature and electrical conductivity measurement in shaft 1, two distinctive water bodies can be identified, whereas the upper one is characterised by lower temperatures and electrical conductivities, compared to the lower water body. As would be expected, the separation occurs at one of the main levels connected to shaft 1 (+83 m level, 80 m below ground). Interestingly, this difference is not mirrored in the chemical composition of the mine water at different depths, which can either be related to a malfunctioning of the dipper or the depth depended samples were not taken in the depth indicated. Though the chemical analysis also show a tendency to higher mineralisation with depth, it is not as obvious as in the dipper measurements.

Some of the most distinct difference between the two shafts is the trace metal concentration. While shaft 2 is generally lower mineralised than shaft 1, there are some, hitherto unexplained differences: Al, Cd, Cu and Zn are higher in shaft 2 than in shaft 1. As the average pH in both shafts is similar, one reason might be the redox potential, which is around 105 mV in shaft 1 and 275 mV in shaft 2. Most metals are less mobile in lower redox conditions than in higher ones, which partly might explain this difference. One of the main reasons for the higher mineralisation in shaft 1 is the fact that the water flows through large parts through backfilled stopes, while the mine water in shaft 2 is predominantly rain or ground water flowing into the shaft. The higher sulfate concentrations in shaft 1 are an indication of pyrite weathering, but the protons are buffered by the prevailing carbonates in the ore body. Only in the lowest part of shaft 2 the shaft is connected with the ore body, but cannot be samples due to obstacles in the shaft.

Interesting is the relatively high As-concentration in the mine water of shaft 1, which is due to the occurrence of elemental As and As minerals in the ore body, as described by Warma (1975). This is an indication that the mine water discharging at shaft 1 either flows through the backfilled stopes or the unmined ore body, whereupon the first option is more unlikely due to the waste rock–cement mixture used for backfilling.

Table 1 Results of the depth dependent chemical analysis in the shafts 1 and 2 between 2015-08-20 and 2016-12-21. $n = 4$. The relative standard deviation for most of the parameters is around 11%. Ion balance from PHREEQC (WATEQ4F database) calculation.

	Shaft 1				Shaft 2			
	15 m	65 m	145 m	210 m	13 m	95 m	220 m	290 m
Ca, mg/L	110	107	110	113	37	37	42	46
Mg, mg/L	9.3	9.3	9.7	9.6	1.6	1.6	2.4	3.6
Na, mg/L	11.7	11.4	12.5	12.5	5.2	5.1	6.9	10.6
K, mg/L	2.2	2.2	2.2	2.3	1.4	1.3	1.3	1.4
Sr, mg/L	0.2	0.2	0.2	0.2	0.0	0.0	0.1	0.1
Li, µg/L	5.0	5.3	5.4	5.0	1.4	1.5	1.7	1.8
NH ₄ , mg/L	0.2	0.2	0.2	0.1	<0.006	<0.006	0.02	0.01
HCO ₃ , mg/L	160	160	160	160	95	95	96	96
SO ₄ , mg/L	198	198	208	215	28	28	53	48
Cl, mg/L	3.1	2.9	3.1	3.2	2.5	2.4	2.7	4.7
F, mg/L	1.5	1.4	1.4	1.4	0.2	0.2	0.2	0.2
Fe, mg/L	7.7	7.7	8.0	8.0	0.6	0.6	1.0	1.3
Mn, mg/L	0.7	0.6	0.7	0.7	0.0	0.0	0.1	0.1
As, µg/L	51.5	51.3	52.0	51.0	1.7	1.7	2.8	3.1
Al, µg/L	<10	<10	<10	<10	118	120	120	115
Ba, µg/L	9.9	9.8	9.9	9.9	8.3	8.1	8.2	8.3
Cd, µg/L	<0.030	<0.030	<0.030	<0.030	0.4	0.4	0.4	0.4
Cu, µg/L	1.4	<1.0	<1.0	<1.0	6.0	6.1	5.9	5.9
Pb, µg/L	1.1	0.9	1.1	2.2	2.8	3.0	3.0	2.8
Si, mg/L	7.7	7.4	7.5	7.4	4.5	4.4	4.6	4.7
U, µg/L	3.2	3.3	3.4	3.4	1.1	1.1	1.3	1.8
Zn, µg/L	8.0	9.3	9.4	12.5	210	208	208	200
Ion balance, %	1.84	0.60	0.83	0.72	1.40	1.31	-1.42	7.95

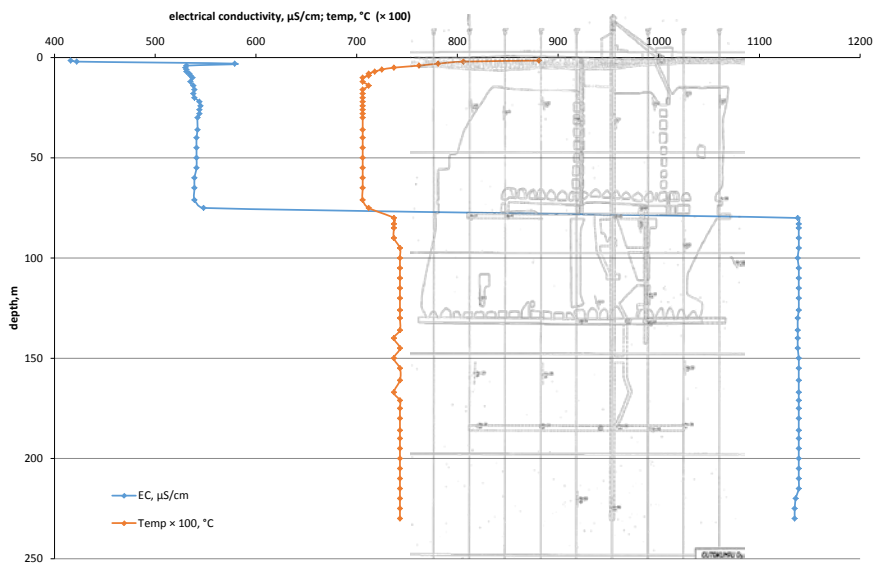


Figure 2 Vertical electrical conductivity (EC) and temperature measurements in the Metsämonttu shaft 1 (2016-08-22). Superimposed is a cross section of shaft 1.

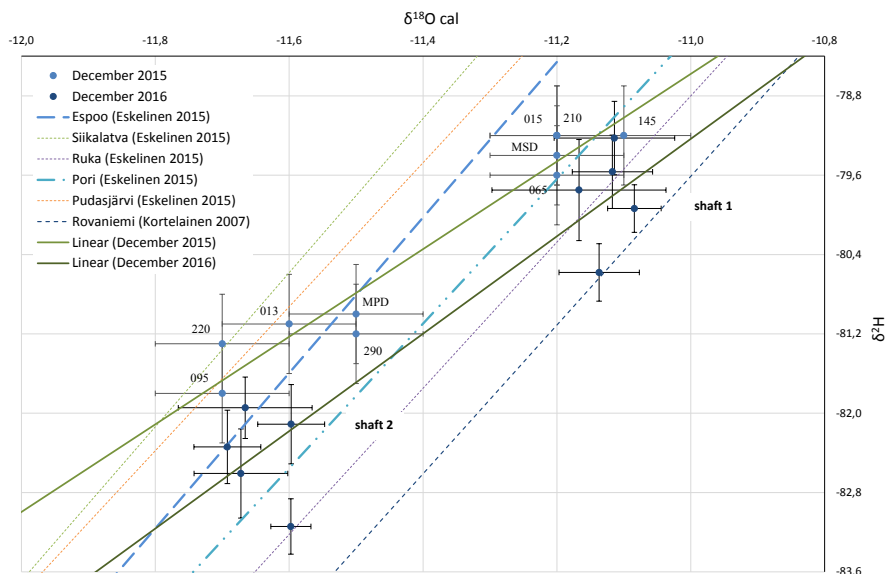


Figure 3 Depth dependent stable isotope compositions in the Metsämonttu mine. LMWL: various local mean water lines from Finland. Left lower cluster from shaft 2, right upper cluster from shaft 1. MPD: Metsämonttu pipe discharge (shaft 1) and MSD: Metsämonttu shaft discharge (shaft 1) Local Meteoric Water lines (LMWL) from Eskelinen et al. (2015) and Kortelainen (2007). Espoo and Pori are the closest to the mine site.

Conclusions

This investigation shows that there is a chance to flood mines such that the discharge of potential pollutants is kept to a minimum. This requires a control of the mine water hydrodynamics to ensure that the surface pollution is minimised. Yet, the results of the investigation do not allow establishing a hypothesis of what causes the stratification to occur at a given position in the shaft. As the two shafts are connected with each other at the +190 m level, it would have been expected that the separation of the two mine water bodies would occur around this depth, but it occurs at the level +83. It is also unknown so far why the stratification measured with the temperature-EC-dipper is not clearly mirrored in the chemical composition of the mine water. What can be concluded is that the mine water discharging at the Metsämonttu mine shows a relatively low mineralisation and that the only constituents of environmental concern are As and Fe, both of which are successfully removed in a passive mine water treatment scheme (Wolkersdorfer and Qonya 2017).

These investigations once again show that natural stratification can occur in abandoned, flooded underground mines. Yet, stratification, as has been shown in other investigations (Wolkersdorfer 2008; Wolkersdorfer et al. 2016), does not occur in all flooded mines. Because stratification can be considered a result of hindered hydrodynamic mixing in a flooded mine, it will be beneficial if mines are technically modified before mine closure to prevent an overall circulation of the water in the to be flooded mine.

Acknowledgements

The authors thank Tekes for funding the FiDiPro Chair at Lappeenranta University of Technology (CW) and Lappeenranta University of Technology Research Foundation Committee for co-financing the research visit through a grant to BQ. We also thank the owners of the Metsämonttu mine site, Martti Antero and Riku Bergroth, for their assistance. Special thanks to the stakeholders within the iMineWa project and all colleagues and friends, especially Maria Mamelkina, who helped during sampling or preparation of the site.

References

- Coetzee H (2016) Management of water levels in the flooded mines of the Witwatersrand, South Africa. In: Drebenstedt C, Paul M (eds) *IMWA 2016 – Mining Meets Water – Conflicts and Solutions*. TU Bergakademie Freiberg, Freiberg, p 630-635
- Coldewey WG, Wesche D, Rudolph T, Melchers C (2014) Methods for Evaluating the Hydraulic Barrier Effects of the Emscher Marl Following Cessation of German Hard-coal Mining. In: Sui W, Sun Y, Wang C (eds) *An Interdisciplinary Response to Mine Water Challenges*. International Mine Water Association, Xuzhou, p 693-698
- Eilu P, Ahtola T, Äikäs O, Halkoaho T, Heikura P, Hulkki H, Iljina M, Juopperi H, Karinen T, Kärkkäinen N, Konnunaho J, Kontinen A, Kontoniemi O, Korkiakoski E, Korsakova M, Kuivasaari T, Kyläkoski M, Makkonen H, Niiranen T, Nikander J, Nykänen V, Perdahl JA, Pohjolainen E, Räsänen J, Sorjonen-Ward P, Tiainen M, Tontti M, Torppa A, Västä K (2012) *Metallogenic Areas in Finland*. Special paper – Geological Survey of Finland 53:207-342
- Eskelinen R, Ronkanen A-K, Rossi P, Isokangas E, Marttila H, Kløve B (2015) A Review of Stable Water Isotope Studies done in Finland. In: https://www.researchgate.net/publication/277580220_A_review_of_stable_water_isotope_studies_done_in_Finland Accessed 2017-05-07
- Geological Survey of Finland (GTK) (2017) *Metsämonttu*. In: Mineral Deposit Report. http://tupa.gtk.fi/karttasovellus/mdae/raportti/578_Mets%C3%A4monttu.pdf Accessed 2017-05-06

- Hanski E (2015) Chapter 2 – Synthesis of the Geological Evolution and Metallogeny of Finland. In: Maier WD, Lahtinen R, O'Brien H (eds) Mineral Deposits of Finland. Elsevier, p 39-71
- Kortelainen N (2007) Isotopic Fingerprints In Surficial Waters – Stable Isotope Methods Applied In Hydrogeological Studies. University of Helsinki
- Latvalahti U (1979) Cu-Zn-Pb ores in the Aijala-Orijarvi area, southwest Finland. *Econ Geol* 74(5):1035-1059. doi:10.2113/gsecongeo.74.5.1035
- Mäkelä U (1989) Geological and geochemical environments of Precambrian sulphide deposits in southwestern Finland. *Ann Acad Sci Fenn A 3 Geol Geogr* 151:1-102
- Matikainen R, Särkkä P (1982) Cut-and-Fill Stopping as Practiced at Outokumpu Oy. In: Hustulid WA (ed) *Underground Mining Methods Handbook*. p 571-584
- Nurmi PA, Rasilainen K (2015) Chapter 11 – Finland's Mineral Resources: Opportunities and challenges for future mining. In: Maier WD, Lahtinen R, O'Brien H (eds) *Mineral Deposits of Finland*. Elsevier, p 753-780
- Papunen H (1986) Geology and ore deposits of southwestern Finland. In: Gaál G (ed) 17e Nordiska Geologmötet 1986 – Excursion guide, excursion C 3 – Metallogeny and ore deposits in South Finland. vol Guide 16. Geologian Tutkimuskeskus, Espoo, p 8-18
- Puustinen K (2003) Suomen kaivosteollisuus ja mineraalisten raaka-aineiden tuotanto vuosina 1530–2001, historiallinen katsaus erityisesti tuotantolukujen valossa, Geological Survey of Finland, Report M 10.1/2003/3, Espoo, 578 p
- Rosner P (2011) Der Grubenwasseranstieg im Aachener und Südlimburger Steinkohlenrevier – Eine hydrogeologisch-bergbauliche Analyse der Wirkungszusammenhänge. unveröff. Diss RWTH Aachen, Aachen
- Shea J (2009) Mine Water Management of Flooded Coal Mines in the Sydney Coal Field, Nova Scotia, Canada. Document Transformation Technologies, Pretoria
- Stacey J, Naude A, Hermanus M, Frankel P (2010a) The socio-economic aspects of mine closure and sustainable development – guideline for the socio-economic aspects of closure – Report 2. *J S Afr Inst Min Metall* 110(7):395-413
- Stacey J, Naude A, Hermanus M, Frankel P (2010b) The socio-economic aspects of mine closure and sustainable development: literature overview and lessons for the socio-economic aspects of closure – Report 1. *J S Afr Inst Min Metall* 110(7):379-394
- Turunen E (1953) Aijalan ja Metsämöntun kaivokset [The Aijala and Metsämönttu mines]. *Vuoriteollisuus – Bergshanteringen* 11:16-28
- Varma A (1954) The copper-zinc ore deposits of Aijala and Metsämönttu. *Geol Tutkimuslaitos* 55:20-24
- Varma A (1975) Outokumpu Oy:n Aijalan ja Metsämöntun kaivosten vaiheita [Outokumpu Ltd: The Aijala and Metsämönttu operations]. *Vuoriteollisuus – Bergshanteringen* 33:94-98
- Wolkersdorfer C (2008) Water Management at Abandoned Flooded Underground Mines – Fundamentals, Tracer Tests, Modelling, Water Treatment. Springer, Heidelberg
- Wolkersdorfer C, Qonya B (2017) Passive Mine Water Treatment with a full scale, containerized Vertical Flow Reactor at the abandoned Metsämönttu Mine Site, Finland. Paper presented at the 13th International Mine Water Association Congress – Mine Water and Circular Economy, Lappeenranta: this issue.
- Wolkersdorfer C, Shongwe L, Schmidt C (2016) Can natural Stratification prevent Pollution by Acid Mine Drainage? Paper presented at the IMWA 2016 – Mining Meets Water – Conflicts and Solutions, Leipzig/Germany:115-121.

Leachate generation and nitrogen release from small-scale rock dumps at the Kiruna iron ore mine

Roger Herbert, Albin Nordström

Department of Earth Sciences, Uppsala University, Villavägen 16, 75236 Uppsala, Sweden Roger.Herbert@geo.uu.se

Abstract Two small-scale waste rock dumps have been constructed in Kiruna, Sweden to investigate the dynamics of leachate generation and nitrogen release over the course of several years. The rock dumps have been constructed of low sulfur rock waste which is not acid generating. The results of the study indicate that, for the two years of this study, water is only discharged intermittently from the rock dumps during snowmelt and during more intense rainfall events. During 2016, concentrations of nitrate and ammonium in the discharge waters ranged up to 46 and 0.14 mg N/L, respectively. The average leachate composition (n = 25) was pH 7.8, alkalinity 55 mg/L HCO_3^- and 1011 mg/L SO_4^{2-} , which is quite similar to the composition of water in the clarification pond at the mine site.

Key words neutral mine drainage, nitrate, ammonium, waste rock, sub-arctic

Introduction

The ultimate source of most of nitrogen cycling at a mine site is the ammonium nitrate – based explosives used in the excavation of the mine. Waste rock, a by-product from the excavation of non-metalliferous rock in mining activities, often contains adsorbed nitrogen compounds (ammonium and nitrate) that are residues from the detonation of the explosives. Once the rock waste is deposited on the ground surface, the percolation of rain and snowmelt through the deposit will leach the nitrogen compounds, potentially impacting local recipients.

All mining activities within the European Union are affected by the Water Framework Directive (WFD), which is locally enforced by legislation within member countries. Since the nitrogen compounds originate from the nitrogen-based explosives used for mining, virtually all mines in Europe will have nitrogen discharges; complying with national environmental regulations will hence be an issue for most actors in the raw material sector using explosives. From the perspective of mining in northern Sweden, the release of ammonium is of primary concern as ammonia has potentially toxic effects on aquatic ecosystems; eutrophication is of secondary importance.

The presence and release of nitrogen compounds from waste rock dumps has received increasing attention over the past 20 years, especially in northern Europe (e.g. Forsberg and Åkerlund 1999, Karlsson and Kauppila 2015, Lindström 2012, Morin and Hutt 2009, VTT 2015, Zaitsev et al. 2008). Bailey et al. (2013) published data from the first large-scale study where the dynamics of nitrogen leaching from waste rock over a period of several years was investigated.

This paper presents the interpretation of two years of monitoring data from small-scale rock dumps. The rock dumps have been constructed with the objective to investigate the dy-

namics of leachate generation and nitrogen release over the course of several years. This is one of the first studies in Scandinavia that studies nitrogen leaching from rock waste above the Arctic circle, and is important for understanding the potential release of nitrogen into nutrient-poor aquatic recipients.

Construction of waste rock dumps

Between July and September 2014, two small waste rock dumps (called hereafter south and north waste rock dump) were constructed at the Kiruna iron ore mine site in northern Sweden. Prior to construction, the ground surface was prepared by filling a pre-existing pond with waste rock. The ground surface was graded so that the elevation decreased by approximately 0.5 meters over the base of the rock deposit (35 meters) and in the direction of the basal drainage outlets (Figure 1). The basal footprint of the rock dumps were 35 m x 35 m. Each rock dump was completely surrounded by a 2 m high berm consisting of waste rock. Each berm was approximately 5 m wide. The basal areas and berms were covered with an impermeable HDPE geomembrane (1.5 mm thick). To enhance drainage to the corner discharge pipes, perforated pipes were installed along two of the sides of both of the waste rock deposits (Figure 1). Drainage water was then led from the corner drainage pipes to two external leachate collection wells which contained V-notch weirs for the quantification of flow.

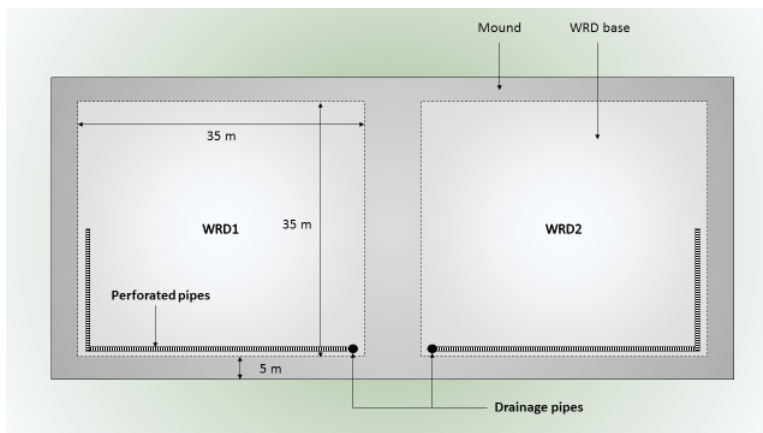


Figure 1 Dimensions of the basal area of waste rock deposit with drainage. Light gray surface is the inner area, while the dark grey borders are the berms. WRD1 = south dump, WRD2 = north dump.

After the installation of the geomembrane and overlying geotextile, the basal areas of the waste rock dumps were carefully covered with approximately 30 cm of fine-grained waste rock (0-30 mm diameter), so as to avoid puncturing the geomembrane with more coarse-grained material. The perforated drainage pipes were placed on top of this material. The dumps were then built up by the alternating deposition of 0-30 mm waste rock and 0-200 mm waste rock.

The two waste rock deposits were built to an approximate height of 8 m over the basal liner, by a combination of end-dumping, push-dumping, and free dumping. Waste rock was un-

loaded using dumpers, either directly at the crests of the waste rock piles (and distributed at the sides by gravity) or at their side and later moved to the crests using a wheel loader. The technique used for construction of the waste rock piles can give rise to structural features that can influence water flow.

Methods

The water level on the upstream sides of the V-notch weirs was measured using pressure transducers that also measured water temperature. Two Campbell Scientific CS451 pressure transducers were connected to a CR1000 data logger in May 2015, and set to store average water levels every 30 minutes. In order to establish a relationship between water level and discharge, the discharge at each weir was manually measured on 27 occasions during May – August 2016 and coupled to a corresponding water level. The measured discharges were used to establish rating curves for both weirs (showing discharge as a function of water depth) by fitting the measured values with the following equation:

$$Q = \left(\frac{8}{15} \right) \cdot \mu \cdot \tan(\alpha) \cdot \sqrt{2g} \cdot h^{5/2}$$

where μ is the weir constant, α is the angle of 90° , g is the gravitational constant, and h is the water depth in the v-notch. However, because of the high variability in measured discharge and water level, it was not possible to accurately fit one distinct rating curve to the measured values. Instead, a stochastic method was applied where 2000 rating curves were constructed by varying the weir constant μ . For each realization, the absolute sum of the residuals between the measured and modeled values was calculated; lower residuals were accredited with better fits and are color-coded accordingly in the resulting rating curves. The rating curve for the north rock dump weir is depicted in Figure 2.

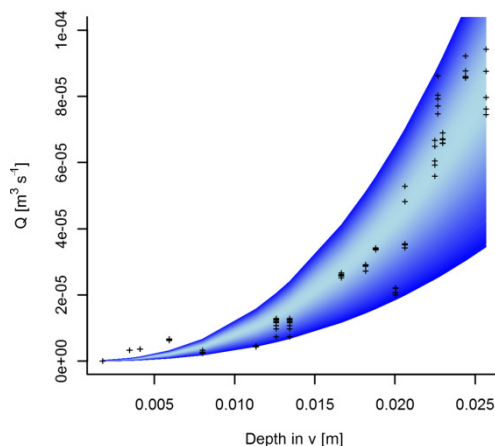


Figure 2 Rating curve for discharge from the north waste rock dump. Lighter blue indicates the lowest absolute sum of residuals, i.e. the best fit to data, while the darker blue is a poorer fit.

When water flow occurred from the waste rock deposits, waste rock leachate was sampled and analyzed once a week for NO_3^- , NO_2^- , NH_4^+ , SO_4^{2-} , Cl^- and pH. Water samples were analyzed by LKAB's accredited water chemistry laboratory.

Results and discussion

Leachate generation

During the period from May 2015 to October 2016, leachate only flowed intermittently from the waste rock dumps (Figure 3). During the first operational year, leachate discharge was very low from both rock dumps; since the rock waste was deposited in a relatively dry state in 2014, most of the infiltrating water during 2015 accumulated in the pore spaces until the field capacity for the material was exceeded. During the second operational year, when water content was significantly greater in the rock dumps (data not shown), peak flows from the dumps were at least an order of magnitude greater (see Figure 3). This is further illustrated in Figure 4 where the cumulative leachate generation is much greater during 2016 than during 2015.

It should be noted that leachate generation is much greater from the south dump compared with the north dump (Figures 3 and 4), even though the discharges should be very similar. During the construction of the rock dumps, the intention was that the basal slope of each dump was to be graded so that basal drainage from the rock dumps would be directed to the vertical drainage pipes (Figure 1). However, because of inadequate grading, it is likely the water along the base of the north rock dump does not flow directly to the drain, but rather to the eastern side of the rock dump. This requires that a large quantity of leachate must accumulate along the base of the north rock dump before it flows to the basal drain.

The total leachate production from the south waste rock dump is in the range 390 – 800 m³ for two hydrological years (cf. Light blue areas on Figure 4). For the Kiruna mine site, the average annual precipitation is 490 mm/year (Kiruna airport, 1961 – 1990). Precipitation falling over an area of 35m x 35m (basal footprint of rock dump) would produce a water volume of 600 m³/year. Considering that most infiltrating water accumulated in the rock dumps during the first year, and that evaporation from the rock dumps is relatively low in the subarctic climate of the region, the measured and calculated leachate production values are in good agreement with each other.

Nitrogen release

The concentrations of dissolved constituents in the rock dump leachate varied over time but did not exhibit any identifiable trend. Average leachate concentrations for the 2016 operational year are shown in Table 1. The leachate concentrations are similar to the concentrations of dissolved constituents in the Kiruna clarification pond (see Nordström and Herbert, 2017, this volume).

Over the two year period reported in this study, 2.4 – 3.2 kg N and 12.3 – 25.3 kg N were leached from the north and south waste rock dumps, respectively; the range of values re-

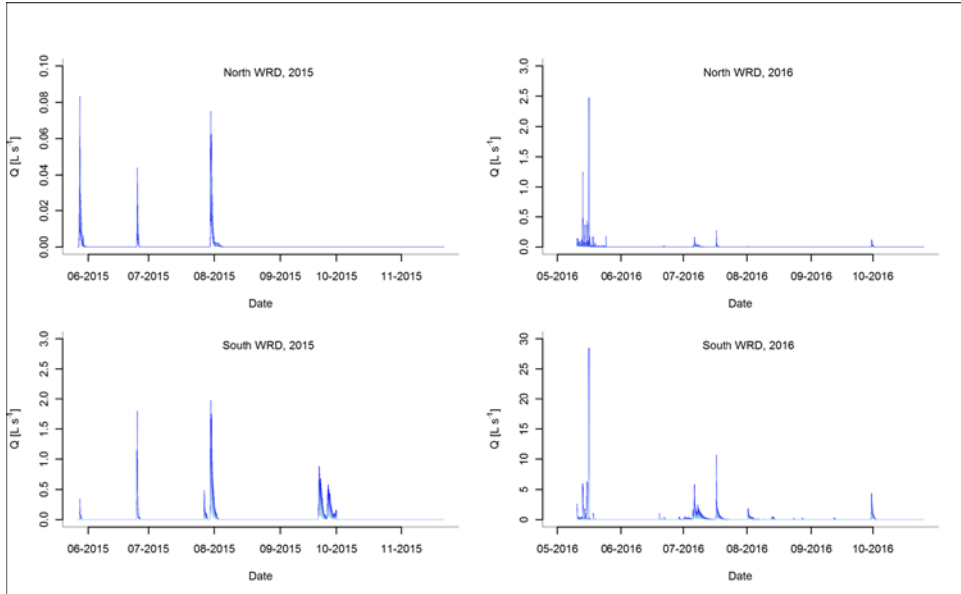


Figure 3 Leachate discharge from north and south waste rock dumps, calculated from rating curves and measured water levels. Note that discharge scales are different for each diagram.

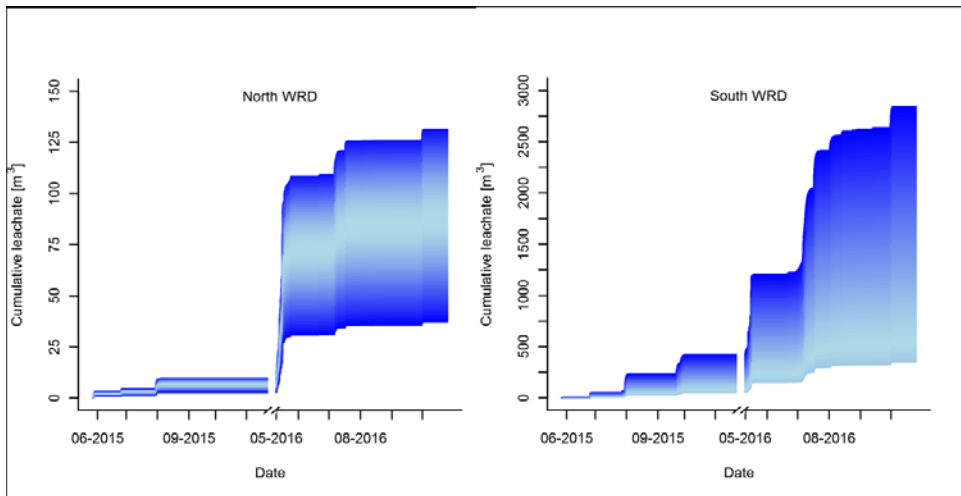


Figure 4 Cumulative leachate generation from north and south waste rock dumps. Color-coding is based on rating curves where lighter blue indicates the lowest absolute sum of residuals, i.e. the best fit to data.

flects the uncertainty in the rating curve for discharges from both deposits. If each rock dump contains ca. 3267 m^3 of material, then these exports correspond to a leaching of $0.74 - 0.98$ and $3.77 - 7.70 \text{ g N/m}^3$ waste rock

In contrast to the results of intermittent sampling during the entire 2016 field season (see above), focused sampling during snowmelt in 2016 identified an apparent cyclicality in both leachate generation and nitrogen concentrations. As shown in Figure 5, leachate generation follows the daily cycles in air temperature, with roughly a 12 hour lag time. Maximum flow rates are measured in the late afternoon / early evening when air temperatures are declining, suggesting that a certain amount of time is needed for snowmelt pulses to propagate to the rock dump drains.

Nitrate concentrations in waste rock leachate also exhibit a cyclical pattern during snowmelt (Figure 5), although the relationship with air temperature is not as apparent as it is for air temperature.

Nitrogen transformations in mining environments

Mine water data from a number of Swedish mines (Lindström 2012, LKAB unpublished data, Nordström and Herbert 2017) generally indicate that >95% of total nitrogen occurs in its most oxidized form, nitrate, in surficial mine drainage. Within an underground mine, a greater proportion of nitrogen may be present as ammonium (LKAB unpublished data), but nitrate is still the predominant nitrogen species. Even though ammonium nitrate explosives contain equal molar amounts of oxidized and reduced nitrogen, the detonation process and oxidizing environment of the mine site favor the occurrence of the more oxidized nitrogen species.

Once released to a surface water environment, either as process water or waste rock leachate, nitrate concentrations will not decrease unless affected by dilution or biological processes (e.g. plant uptake, microbial denitrification). However, denitrification is not expected to be an important process in aerated water. Ammonium concentrations have been shown (Lindström 2012) to decrease in mine waters during warmer periods as the result of nitrification, which is a strongly temperature-dependent microbial process.

Conclusions

The results of this study clearly demonstrate that waste rock is a source of nitrogen in mining environments. Nitrate concentrations as high as 45 mg N/L were detected in waste rock leachate, while ammonium was detected at concentrations < 0.15 mg N/L. In the subarctic climate of the field site, leachate generation is greatest during snowmelt and in connection with intense rainfall events during the summer. Total annual leachate production is comparable with the annual precipitation falling on the rock dump.

Table 1 Average leachate concentrations during 2016 operational year. *n* = 25 samples.

Constituent	Concentration	Constituent	Concentration
pH	7.8	NO ₃ ⁻	32 mg N/L
Alkalinity	55 mg HCO ₃ ⁻ /L	NO ₂ ⁻	0.07 mg N/L
Cl ⁻	33 mg/L	NH ₄ ⁺	0.07 mg N/L
SO ₄ ²⁻	1011 mg/L	F ⁻	0.6 mg/L

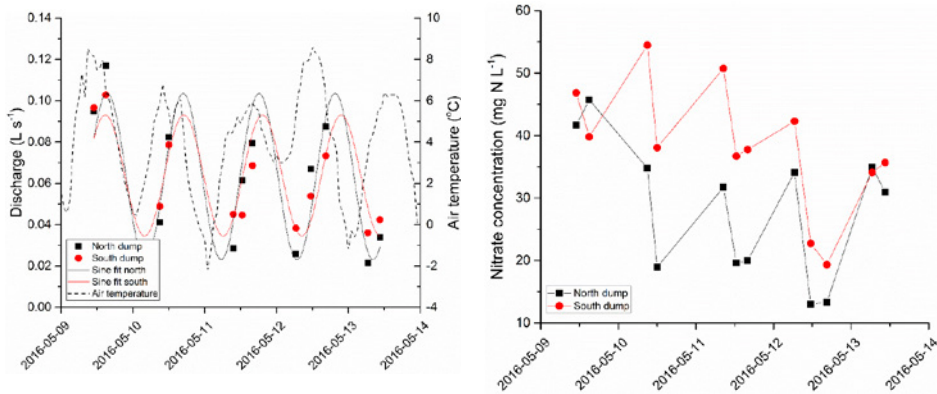


Figure 5 Left: Leachate discharge from north and south rock dump during snowmelt in 2016. Leachate discharge has been fitted with a sine curve to illustrate the cyclicity in discharge, relative to air temperature (right axis). Right: nitrate concentrations during snowmelt.

Acknowledgements

We are grateful to Johan Johansson who coordinated the construction of the waste rock dumps from start to finish and was a key person in the field activities. Many thanks are also extended to Sofia Eckersten who stayed for long hours at the mine site in order to collect water samples. The comments of anonymous reviewers are acknowledged for their input. This project has been funded by VINNOVA grant 2014-01134.

References

- Bailey BL, Smith LJD, Blowes DW, Ptacek CJ, Smith L, Segeo DC (2013) The Diavik waste rock project: Persistence of contaminants from blasting agents in waste rock effluent, *Appl. Geochem.* 36: 256 – 270.
- Forsberg H, Åkerlund H (1999) Nitrogen and explosive residues in LKAB's ore, waste rock, and product flows, MSc thesis, Report 1999:258, Luleå University of Technology (in Swedish).
- Karlsson T, Kauppila T (2015) Release of explosives originated nitrogen from the waste rocks of a dimension stone quarry. Proceedings, 10th International Conference on Acid Rock Drainage and IMWA Annual Conference.
- Lindström L (2012) Nitrogen releases from the mining industry. Swedish industry association of mines, mineral and metal producers. SveMin report (in Swedish). http://www.sveemin.se/?file_download&file=980 (Accessed April 11, 2017).
- Morin KA, Hutt NM (2009) Mine-water leaching of nitrogen species from explosive residues. Proceedings, GeoHalifax2009. 1549 – 1553.
- Nordström A, Herbert R (2017) Field-scale denitrifying woodchip bioreactor treating high nitrate mine water at low temperatures (these proceedings).
- VTT, Technical Research Centre of Finland Ltd (2015) Solutions for control of nitrogen discharges at mines and quarries: Miniman project final report. VTT Technology report 225, Espoo, Finland. 117 p.
- Zaitsev G, Mettänen T, Langwaldt J (2008) Removal of ammonium and nitrate from cold inorganic mine water by fixed-bed biofilm reactors, *Minerals Engin.* 21: 10 – 15.

Evaluation of mine water rebound processes in European Coal Mine Districts to enhance the understanding of hydraulic, hydrochemical and geomechanical processes

Sebastian Westermann¹, Tansel Dogan¹, Bastian Reker¹, Peter Goerke-Mallet¹,
Christian Wolkersdorfer^{2,3}, Christian Melchers¹

¹*University of Applied Sciences TH Georg Agricola, Research Institute of Post-Mining,
Herner Straße 45, 44787 Bochum, Germany*

²*Lappeenranta University of Technology, Laboratory of Green Chemistry, Sammonkatu
12, 50130 Mikkeli, Finland, christian@wolkersdorfer.info*

³*South African Research Chair for Acid Mine Drainage Treatment, Tshwane University
of Technology (TUT), Private Bag X680, Pretoria 0001, South Africa*

Abstract The mine water table has been rising in many hard coal mining areas. Important insights have been gathered concerning the hydrodynamic, hydrochemical and geomechanical changes that accompany a mine water rebound. This contribution provides an overview of a current survey. This survey aims at developing a deeper understanding of the processes which allows to derive generally applicable causal relationships based on it. Such interdependencies are then to be transferred to the Ruhr area in order to contribute to an improved forecast regarding the possible impact a mine water rebound will have on the environment.

Key words mine closure, mine water rebound, hard coal mining, Ruhr area

Introduction

Germany looks back at a long tradition of mining. Currently, approx. 180 Mt/a of lignite are being extracted in open-pit mines and more than 500 Mt/a of minerals are being mined, too (VRB 2016). Coal, salt and ores have been mined for centuries at different depths in underground mining. In 2018, when the last two collieries will close in North-Rhine Westphalia, the hundreds of years of hard coal mining in Germany will be history. The end of the active exploitation of hard coal, however, does not mean the end of the mining operator's responsibilities. In the future, the operator will be responsible for a sustainable and environmentally acceptable mine water management. In Germany, the expressions 'perpetual burdens' or 'perpetual tasks' are two terms that express the scale of this responsibility. Those include the long-term retention of the mine water table at an environmentally acceptable level, poldering measures to regulate the ground water table close to the surface as well as the decontamination of ground water at formerly contaminated colliery sites (e.g. caused by former coking plants). For many years now, concepts have been developed by the mining companies to solve those issues and to continuously enhance those solutions (RAG 2014).

Mine water management in both active and closed mines

Often, as in the Ruhr area, mines are, connected by an underground network of galleries and drifts. Mine water retention does not only mean to keep the mine workings dry where the resources are won, it also means to protect the mine workings at productive mines against a

mine water inrush from closed mines nearby. For that purpose, mines are compiled to form water districts which are hydraulically interconnected.

Depending on its morphological location and the hydrogeological properties of the deposit and its overlying rock, the dewatering of a mine is done by enabling a free drain of mine water via the adits or by actively removing mine water using pumps. Thus, the dewatering in the southern former coalfield of the Ruhr area has been done by draining mine water over the galleries into the river Ruhr and its tributaries (Melchers et al. 2015, 2016), whereas in the central and northern parts of the Ruhr coal mining area, the geomorphological conditions require the mine water to be actively pumped from the shafts.

Mine water rebound in underground mines

Once the exploitation of resources is abandoned and the closure of the mine is completed, the removal of the mine water can be reduced or even finished, provided the (hydro-) geological, mining and ecological circumstances allow for that. The water which continues to flow into the open underground mine workings, but is no longer pumped, results in the mine water table to rise therein and in the overlying rock. The spatio-temporal process of the mine water rebound depends on the geological and hydrogeological properties of the deposit and its overlying rock, the changes of both caused by the mining activities, and finally the geometry of the mine workings. Most of these effects have been extensively studied and described in Wolkersdorfer 1996 and 2006.

This rise in the mine water table can result from the reduction or cessation of the pumping activities and is then called 'passive' or 'internal flooding'. Yet, mine water rebound can also be initiated and even accelerated by the influx of water, which is called 'active' or 'external flooding'. Generally, the course of the mine water rebound can be controlled by means of pumps that either remove the mine water, so to slow down the rising velocity or by pre-setting the height of the mine water table. If no pumps are kept on site and no permanent draining adits are in place, there will be an uncontrolled mine water table rebound up to a level, where the inflow and outflow volumes equalize. In Germany, legal stipulations were implemented more than twenty years ago that prohibit an uncontrolled rise of the mine water table (BBergG 1980).

Example of a mine water rebound

The presented example of a mine water rebound (fig. 1) can be divided into three stages. The first commences after the decommissioning or reduction of the pumping rate; it can be identified by a quick rise of the mine water table ('initial phase'). During the ongoing course, there is a more or less even rise of the mine water table provided the hydrodynamic conditions of the mine workings to be flooded are homogeneous ('intermediate phase'). Changes of the hydrogeological properties, e.g. once the mine water reaches the base of the overlying rock, are reflected by the course of the graph ('heterogeneities'). With the growing decrease of the potential difference between the current and the natural water tables, the speed of the mine water rebound decreases successively, too ('final phase'). The mine water

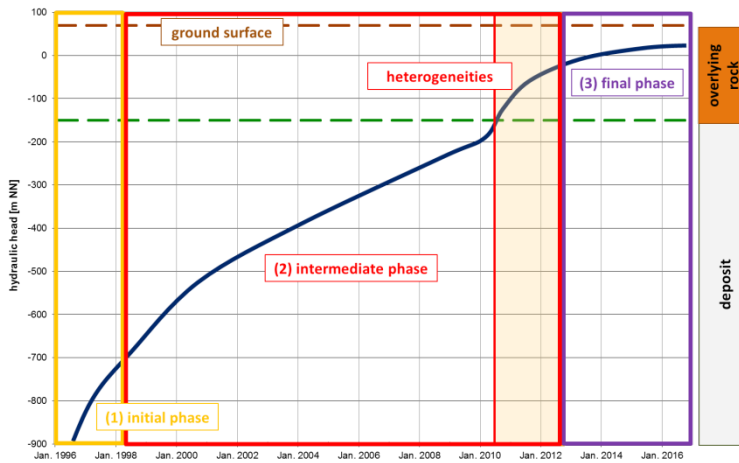


Figure 1 phases of a mine water rebound

table ceases to rise once it has reached equilibrium between inflow and outflow or the level of a dewatering adit.

Potential influence on the environment as part of a large-scale mine water rebound

The rise of mine water table can be accompanied by risks for people, ecology and infrastructure. Especially, if this rise is not controlled as regulating mechanisms have not been established or if this is not noticed as no measuring points have been defined. Figure 2 shows a selection of possible areas and their challenges which mining companies, authorities and scientists will have to tackle after closing a mine but also in respect of the mine water table rise (Kretschmann 2016, Kretschmann & Hegemann 2016).

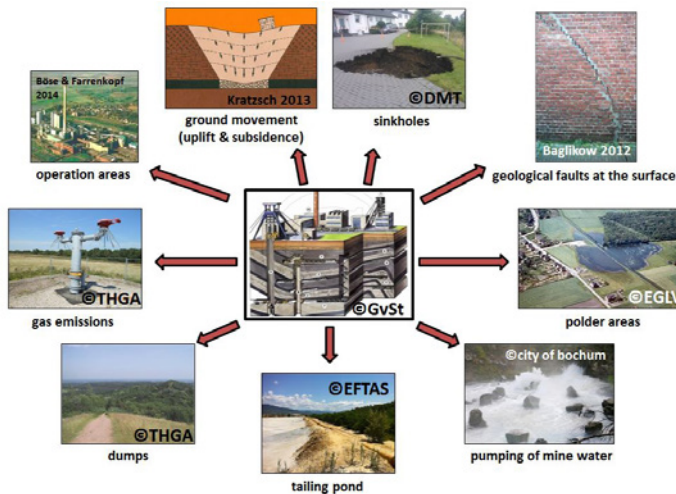


Figure 2 Action fields connected to post-mining

In order to make the potential environmental impact predictable and thus manageable, a deeper understanding of the processes which are occurring is needed. This process understanding has three parts:

- Hydraulics & hydrodynamics,
- Hydrochemistry,
- Geomechanics.

In the following section, the essential foundation of those processes will be outlined; this description is by no means exhaustive.

Hydraulics & hydrodynamics

The speed of the mine water rebound is mainly influenced by the cumulative flows of the deep water and the infiltration water and by the cavity volume that can be used as storage. With the ongoing mine water rebound, the rise velocity decreases successively as the cumulative flows of e.g. deep water are gradually suppressed by the rising mine water. There, the spatial distribution and the temporal development of the cumulative flows might affect the formation of a density layering in the mine workings that is stable over a long period of time (Melchers et al. 2015, Wolkersdorfer 2016).

Looking at finished or highly advanced mine water rebounds, it can be shown that the (hydro-) geological properties of the deposit and its overlying rock have immediate influence on the hydrodynamic processes which are going on underground due to the mine water rebound. For example, observations from the Ruhr area have shown that the rebound speed of the mine water pressure level increases with reaching the base of the low-permeable clay marl rocks of the Emscher formation (Upper Cretaceous), as the cavity volume that can be used for storage decreases (fig. 1).

One effect of a mine water rebound is the migration of gases (including methane). The low dissolution quality of gases in liquids means that gas floating freely in the mine workings and the adjacent rock mass is displaced by the trapped mine water and can discharge at the surface, e.g. at shafts or faults. According to recent insights from the Ruhr basin, the release of gas stops once the seam-bearing layers have been flooded (Melchers 2008).

Hydrochemistry

Due to its genesis, mine water commonly has a higher mineral content than ground water close to the surface. Mine water in hard-coal mining areas often has substantially increased levels of iron and sulphate due to the oxidation process of disulphides (pyrite, marcasite, chalcopyrite). The temporal development of the hydrochemical composition shows in most cases, after the mine water rebound has been completed, an early rise of iron and sulphate concentrations which fall again to their background values (“first flush”) after their maximum values have been reached (usually after decades or centuries) (Younger 1997).

Where the mine water table rises, the higher mineralised mine water can come into contact with drinking water resources used in water management and supply if hydraulically active connections between the mine workings and the overlying strata exist (e.g. via exploration boreholes or inappropriately abandoned shafts); such contact may cause drinking water contamination. Due to the (hydro-)geological properties of the deposit in the central and northern part of the Ruhr basin, where thick and impermeable clay marl rock layers of the Emscher formation exist, a rise of the mine water table into the overlying strata of the Emscher formation is highly unlikely (Hahne & Schmidt 1982, Baltes et al. 1998, Coldewey et al. 2016). Thus, the risk of the drinking water and groundwater reservoirs being negatively influenced by rising mine water has been drastically reduced in areas where thick and hydraulically effective geological barriers are in place (Heitfeld & Rosner 2015).

Geomechanics

The mine water rebound causes an increase in the buoyancy forces and also to a swelling and subsequent increase in volume of clays. In many former mining areas ground heavings caused by those phenomena can be observed. The heaving movements usually occur at large scale and – according to the observations so far – make up a one-digit percentage figure of the subsidence volume (Preuße et al. 2015). In most cases, the ground heavings occur evenly and are not linked to damage-relevant effects. The only damage on structures caused by a mine water rebound known so far was observed in the Erkelenz coalfield in Germany. The reason for this was a flood induced reactivation of a large fault which led to heaving differences of both sides of that fault (Baglikow 2010). Another case was reported by Oberste-Brink (1940), where ground heaving was observed in the Wittener Mulde, Germany.

Study to evaluate the processes of mine water rebound

Currently, a study at the University of Applied Sciences TH Georg Agricola (Research Institute of Post Mining, Germany) is supposed to provide the basis for a deeper understanding of the scientific foundations needed for a sustainable concept to ensure long-term and environmentally acceptable mine water rebound in the hard coal mining areas of North-Rhine Westphalia and Saarland. This evaluation will provide a systematic, uniform and comprehensive analysis of closed and ongoing processes concerning mine water rebound in European hard coal mining areas. This study is based on the initial results published in Melchers & Dogan (2016).

In a first step, coalfields in the following European areas will be examined in detail regarding the experience made with processes of mine water table rises:

- Germany (southern Ruhr area, Saar area, Ibbenbüren, Aachen-Erkelenz, Saxony),
- United Kingdom (East Fife, Northumberland, East Pennines),
- France (Lorraine),
- Netherlands (South Limburg) and
- Poland (Upper Silesia).

In a second step, the evaluation can be applied to other hard coal mining areas (e.g. in Spain) or other types of deposits (e.g. spar or ore). Regarding the hard coal mining areas, the key parameters of (hydro-)geology, mining activities and mine water rebound will be recorded systematically.

The evaluation focuses on the analysis of the spatio-temporal course of the mine water rebound and the related influences and interdependencies on the following: both the quantitative and qualitative changes of the mine water to be drained; the ground movements caused by the processes, and gas migrations close to the ground surface. This overall evaluation intends to identify generally applicable causal relations of mine water rebound, to separate the locally specific conditions and to transfer the insights to other hard coal mining areas where mine water table rises are imminent. This objective applies in particular to the Ruhr area, the Saar hard coal mining and the Ibbenbüren colliery.

Conclusion and outlook

The insights gained and the deeper understanding of the course mine water rebound takes help to develop strategies and measured for long-term mine water management that can be optimised in alignment with sustainable, environmental and economic aspects. Any recommendations for a comprehensive monitoring will be agreed accordingly.

References

- Baglikow V (2010) Schadensrelevante Auswirkungen des Grubenwasseranstiegs im Erkelenzer Steinkohlenrevier. RWTH Aachen publications, Aachen, 121 pp
- Baglikow V (2012) Grubenwasseranstieg in Steinkohlengebieten – Auswirkungen auf die Oberfläche. *Bergbau* 63(1): 16–21
- Baltes B, Fischer-Appelt K, Larue PJ, Javeri V, Thein J, Veerhoff M, Paas N, Justen A, Navarro M, Obermann P, Himmelsbach T, Witthüser K, Harnischmacher S, Zobel J, Schmid GPH, König C, Rosen B, Wendland EC, Müller W, Rüterkamp P, Klinger C, Hewig R (1998) Entwicklung und Anwendung analytischer Methoden zur Eignungsuntersuchung der Verbringung bergbaufremder Rückstände in dauerhaft offene Grubenräume im Festgestein. Final Report. Köln, 126 pp
- Böse C, Farrenkopf, M (2014) Zeche am Strom. Die Geschichte des Bergwerks Walsum. Publication of Deutsches Bergbaumuseum Bochum, Bochum, 514 pp
- BBergG. Bundesberggesetz vom 13. August 1980 (BGBl. I S. 1310), das zuletzt durch Artikel 4 des Gesetzes vom 30. November 2016 (BGBl. I S. 2749) geändert worden ist.
- Coldewey WG, Wesche D, Rudolph T, Melchers C (2016) Methods for Evaluating the Hydraulic Barrier Effects of the Emscher Marl following Cessation of German Hard-Coal Mining. In Sui, Sun & Wang (Eds) *An Interdisciplinary Response to Mine Water Challenges*, Xuzhou: 693–698
- Hahne C, Schmidt R (1982) Die Geologie des Niederrheinisch-Westfälischen Steinkohlengebietes. Verlag Glückauf GmbH, Essen, 106 pp
- Heitfeld M, Rosner, P (2017) Auswirkungen eines Mine water level rises im Ruhrgebiet – bisherige Erfahrungen und Stategien. In Bezirksregierung Arnsberg, Technische Hochschule Georg Agricola (Eds) *NACHBergbauzeit in NRW*, Bochum: 145–157
- Kratzsch H (2011) *Mining Subsidence Engineering*. Springer Verlag Berlin und Heidelberg GmbH & Co. KG, Berlin, 558 pp
- Kretschmann J (2016) The Sustainable Development Strategy of the German Hard Coal Mining Industry. In Kretschmann J, Melchers C (Eds) *Done for good. Challenges of Post-Mining*. Anthology by the Research Institute of Post-Mining, Bochum: 57–68

- Kretschmann J, Hegemann M (2016) New Chances from Old Shafts – Risk Management in Abandoned Mine Sites in Germany. In Kretschmann J, Melchers C (Eds) *Done for good. Challenges of Post-Mining*. Anthology by the Research Institute of Post-Mining, Bochum: 33–46
- Melchers C (2008) Methan im südlichen Münsterland – Genese, Migration, Gefahrenpotenzial. Münster, 154 pp
- Melchers C, Dogan T (2016) Study on Mine Water flooding that occurred in Hard-Coal Mining Areas in Germany and Europe. In Kretschmann J, Melchers C (Eds) *Done for good. Challenges of Post-Mining*. Anthology by the Research Institute of Post-Mining, Bochum: 147–152
- Melchers C., Michel I, Goerke-Mallet P, Welz A (2015) Erste Bestandsaufnahme wasserführender Stollen an der Ruhr. In Meier G et al. (Eds) 15. *Altbergbaukolloquium*, Leoben: 158–168
- Melchers C, Michel I, Hoppe U, Isaac M, Goerke-Mallet P (2016) Methoden zur Ermittlung eines Einzugsgebietes wasserführender Stollen am Beispiel des Franziska Erbstollens in Witten. In Meier G et al. (Eds) 16. *Altbergbaukolloquium*, Goslar: 107–118
- Melchers C, Coldewey WG, Goerke-Mallet P, Wesche D, Henkel L (2015) Dichteschichtungen in Flutungs-wasserkörpern als Beitrag zur Optimierung der langzeitigen Wasserhaltung. In Paul M (Eds) *Sanierte Bergbaustandorte im Spannungsfeld zwischen Nachsorge und Nachnutzung – WISSYM 2015*. Wismut GmbH, Chemnitz: 99–106
- Oberste-Brink K (1940) Die Frage der Hebungen bei Bodenbewegungen infolge Bergbaues [Surface uplift due to ground movements as a result of mining]. *Glückauf* 76(18): 249–256
- Preuße A, Pabst M, Sroka A (2017) Bodenbewegung in Folge des Grubenwasseranstiegs. In Bezirksregierung Arnsberg, Technische Hochschule Georg Agricola (Eds) *NACHBergbauzeit in NRW*, Bochum: 166–174
- RAG (2014) Konzept zur langfristigen Optimierung der Grubenwasserhaltung der RAG Aktiengesellschaft für Nordrhein-Westfalen. 29 pp
- VRB (Vereinigung Rohstoffe und Bergbau e.V.) (2016) Rohstoffland Deutschland. Sichere Rohstoffversorgung für Deutschland und die Rolle des heimischen Bergbaus. Berlin, 24 pp
- Wolkersdorfer C (1996) Hydrogeochemische Verhältnisse im Flutungswasser eines Uranbergwerks – Die Lagerstätte Niederschlema/Alberoda. *Clausthaler Geowissenschaftliche Dissertationen* 50: 1–216
- Wolkersdorfer C (2006) *Water Management at Abandoned Flooded Underground Mines – Fundamentals, Tracer Tests, Modelling, Water Treatment*. Springer Verlag Berlin und Heidelberg GmbH & Co. KG, Heidelberg, 465 pp
- Wolkersdorfer C, Shongwe L, Schmidt C (2016) Can natural Stratification prevent Pollution by Acid Mine Drainage? Paper presented at the IMWA 2016 – Mining Meets Water – Conflicts and Solutions, Leipzig/Germany: 115–121
- Younger PL (1997) The longevity of minewater pollution – a basis for decision making. *Sci Total Environ*, 194–195: 457–466
-

Pit Lake Modelling at the Aitik Mine (Northern Sweden): Importance of Site-Specific Model Inputs and Implications for Closure Planning

¹Alan Martin, ¹Colin Fraser, ¹Donald Dunbar, ²Seth Mueller, ²Nils Eriksson

¹*Lorax Environmental Services Limited, 2289 Burrard St., Vancouver, BC, Canada*

²*Boliden Mineral AB, Boliden Mines, SE-936 81 Boliden, Sweden*

Abstract The large volume of pit lakes and their potential role in mine water management make them a focal point of closure planning. In this paper, the modelling of pit lake physical structure and water quality for the Aitik Pit (Aitik Mine, northern Sweden) is used to illustrate: 1) the importance of developing robust site-specific model inputs for the development of defensible pit lake predictions; and 2) how pit lake water quality predictions can be used to inform and refine mine closure plans.

Key words meromixis, waste rock, tailings, water management, modelling

Introduction

Pit lakes are a common feature of the post-closure landscape at mine sites, where open pits are allowed to fill with various inputs including groundwater, pit wall runoff, precipitation, and surface runoff from the surrounding catchment. Due to the oxidation of exposed sulfide minerals on pit walls, the flushing of soluble metals during pit filling, and in many cases, the input of drainages from waste storage facilities (e.g., tailings and waste rock), many pit lakes are characterized by poor water quality (Gammons and Duhaime 2006). Further, the large volume of pit lakes and their potential role in water management make them a central focus of closure planning. Given the implications for environmental protection, regulatory compliance and potential long-term environmental liability of pit lakes, considerable attention has been given to their characterization, prediction and remediation (Castro and Moore 2000; Martin et al. 2003).

Boliden Mineral AB owns and operates the Aitik open pit copper mine and concentrator 17 km east of Gällivare in northern Sweden. Climate conditions at the site are subarctic in nature, with a mean annual temperature of 0 °C and mean annual precipitation of ~600 mm. Since 1968, the mine has exploited copper-, gold- and silver-bearing ores through the development of the Aitik Pit. During the closure period, the pit will flood to form a pit lake ~1 km wide, 3.5 km long and 525 m deep. Under the final closure configuration, the Aitik Pit will serve as the primary discharge location for mine waters to the receiving environment (Lina River). As part of an integrated closure planning process for the site (Eriksson 2017), the evolution of pit lake physical structure and water quality was modelled to support pit lake management as well as water quality predictions for downstream receptors. In this paper, key pit lake model inputs are described followed by an evaluation of pit lake model results for two closure options for the site. The discussion emphasizes the importance of developing robust model inputs which can then allow for the generation of defensible pit lake water quality predictions and closure plans.

Pit Lake Model Description

Pit lake model simulations were conducted using PitMod, a one-dimensional numerical hydrodynamic model used to predict the spatial and temporal distribution of temperature, density, dissolved oxygen and water quality parameters in lakes (Dunbar 2013). The principal physical processes simulated by PitMod include: 1) heating of the lake surface by incident long- and short-wave solar radiation; 2) sensible heat exchange between the atmosphere and the lake surface; 3) heat loss through black body radiation; 4) wind-driven mixing; 5) convective mixing; 6) ice formation and melting; 7) evaporation; and 8) input of various inflows (direct precipitation, pit wall runoff, surface runoff and groundwater inflow). The biogeochemical component of PitMod incorporates PHREEQC (mineral/gas equilibria, redox reactions) and dissolved oxygen (DO) consumption. A primary strength of PitMod is that it has undergone rigorous verification using empirical data collected from modelled sites in Canada, including the Island Copper Mine and Equity Silver Mine (Crusius et al. 2002; Dunbar and Pieters 2008).

Pit Lake Model Inputs and Scenarios

Inputs to the Aitik Pit during the filling period will include treated effluent (for period of 55 years), Tailings Management Facility (TMF) runoff from the Clarification Pond, TMF seepage, seepage/runoff from the potentially acid forming (PAF) waste rock storage facilities (WRSFs), non-PAF WRSF seepage/runoff, runoff from natural ground, pit wall runoff, groundwater recharge, and direct precipitation to the pit lake surface. Inputs to the Aitik Pit are illustrated conceptually in fig. 1.

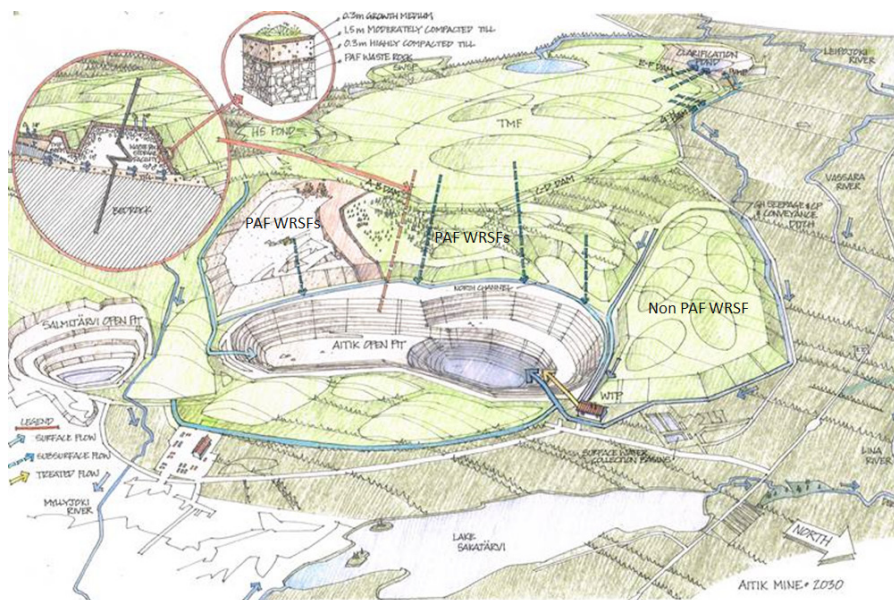


Figure 1 Conceptual figure illustrating the various inputs reporting to the Aitik Pit during the filling period. Illustration shows partially reclaimed Tailings Management Facility (TMF) and Potentially Acid Forming Waste Rock Storage Facilities (PAF WRSFs). WTP = Water Treatment Plant.

Key to the pit lake modelling exercise was the development of defensible flow and water quality values for all inputs. In this regard, extensive studies of the WRSFs, TMF and pit were conducted to support the development of robust flow and chemistry predictions. As part of model input development, site-specific data (flow, seepage water quality, groundwater quality, mineralogy, etc.) were used to the maximum extent possible in the development and calibration of flow and water quality models. Pit lake model inputs that underwent rigorous development included:

- Climate: A synthetic 200-year climate dataset (extending from 2025 to 2225) was used as a common source of input to the models in support of the pit lake, WRSFs and TMF. The dataset was scaled to account for predicted climate change in the region, as described in Fraser et al. (2017);
- TMF and WRSF seepage inflows: Detailed hydrogeochemical modelling for the TMF and WRSFs included water/load balance development, seepage flow modelling, and geochemical modelling (described in Eriksson 2017). The use of site data (flow, seepage water quality, groundwater quality, mineralogy) were maximized to develop and calibrate flow and water quality predictions. For both the TMF and PAF WRSFs, modelling results demonstrate that the quality of seepages is predicted to improve markedly following cover system placement;
- TMF surface runoff: At the beginning of mine closure, surface runoff from the TMF will be diverted to the Aitik Pit for a period of 10 years. A combination of water balance and geochemical modelling was used to generate flow and water quality predictions for this term;
- Pit wall runoff: Pit wall drainage chemistry was based on site water quality data for pit sump samples. The increase in sulfur content with depth on pit wall exposures was used to develop elevation-dependent terms, with pit wall runoff quality improving as the pit lake fills; and
- Groundwater inflows: A function describing the relationship between groundwater inflow and the water level in the pit lake was developed using pit dewatering records.

Two model scenarios for the Aitik Pit were evaluated based on two engineered cover system options for the PAF WRSFs:

- Base Case Scenario: Under the Base Case scenario, the engineered cover system for the PAF WRSF consists of 0.3 m highly compacted till, underlying 1.5 m compacted till, underlying 0.3 m vegetation growth medium (illustrated in fig. 1). This configuration is designed to reduce oxygen ingress into the waste rock, thereby decreasing the potential for sulfide mineral oxidation and acid generation.
- Bentonite Scenario: The merits of this option were evaluated for the same cover configuration as that described for the Base Case, with the addition of 2-5 wt.% bentonite to the compacted till layer. The addition of bentonite can improve material water retention characteristics, increase the degree of saturation, and decrease oxygen ingress, thereby further decreasing the potential for sulfide mineral oxidation.

Both scenarios include a treatment period of 55 years (equivalent to the filling period) that entails lime treatment of recoverable seepages associated with the PAF WRSFs and the TMF. During the treatment period, treated effluents are discharged to the surface of the Aitik pit lake.

Results and Discussion

Water balance model results illustrate the addition of bentonite contributes to a reduction in PAF WRSF seepage to the Aitik Pit as compared to the Base Case. However, the pit filling period (55 years) and average annual discharge (~ 270 L/s) are the same for both scenarios (fig. 2).

The evolution of lake physical structure is not appreciably affected by changes to the water balance that result from the addition of bentonite to the cover systems. Specifically, the Base Case and Bentonite scenarios are characterized by a common evolution in water column density structure, with both showing the development of a permanently stratified (meromictic) water column. In turn, permanent stratification promotes the development of suboxic conditions below a mixed layer that extends seasonally to a depth of ~ 30 m (results for Base Case scenario shown in fig. 3).

Water quality predictions for the bentonite scenario show significantly higher concentrations of trace elements (e.g., Cu and Zn) in lake surface waters at the time of pit overflow as compared to the Base Case (fig. 4). Cu, for example, which represents a parameter of potential concern, shows a mean concentration of 0.5 mg/L at the time over overflow for the Bentonite Scenario (compared to 0.12 mg/L for Base Case). The benefits of bentonite with respect to lake surface water quality are not realized until several decades post filling. Specifically, lower steady-state values for trace elements in pit lake discharges are not observed until Year 80-100 (fig. 4).

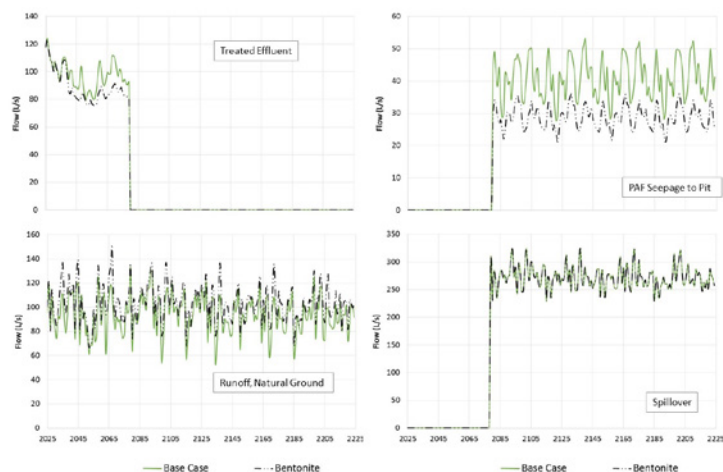


Figure 2 Water balance plots comparing Base Case vs. Bentonite scenarios for treated effluent flow to Aitik Pit (represents treatment of seepage from Potentially Acid Forming (PAF) Waste Rock Storage Facilities for a period of 55 years), untreated seepage from PAF waste rock storage facilities (following treatment period), runoff from natural ground and pit lake spillover (occurs in Year 2080).

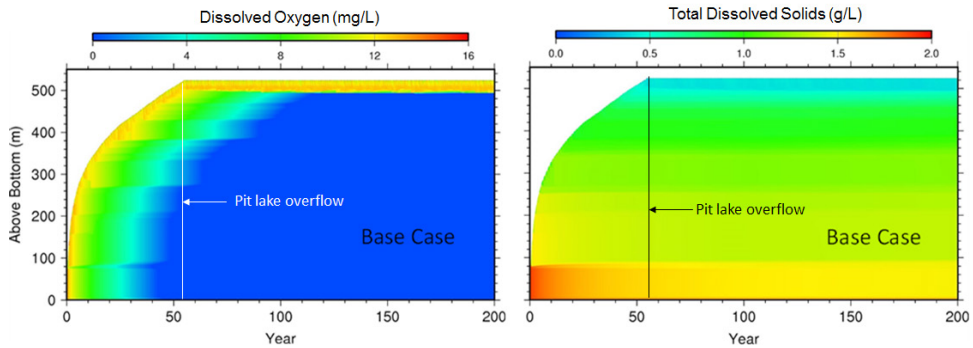


Figure 3 Base case model output showing the vertical and temporal evolution of total dissolved solids and dissolved oxygen for the Aitik pit lake (200 year model period). The evolution of the pit lake surface (as measured from the pit bottom) shows the gradual filling of the pit, with pit lake overflow occurring in year 55.

The higher trace element concentrations at the time of pit lake overflow observed for the Bentonite scenario can be linked to the longer transition period in drainage quality improvements associated with the PAF WRSFs. For a higher net percolation scenario (Base Case Scenario), PAF WRSF seepage quality improvements are realized prior to pit lake overflow, due to the more rapid flushing of soluble oxidation products stored in the WRSFs. Specifically, the rapid improvement in drainage quality for the Base Case allows the bulk of the stored load in the PAF WRSFs to be isolated in the bottom of the stratified pit. For a lower net percolation scenario (Bentonite Scenario), PAF WRSF seepage quality improvements extend over a longer period. This longer transition period allows for a greater proportion of the stored load to mix into the lake surface and be released as overflow, resulting in considerably higher metal concentrations in pit lake discharges.

Following the cessation of treatment after 55 years, water quality conditions for the Bentonite Scenario temporarily worsen in the pit lake surface due to the input of relatively poor quality PAF WRSF seepage to the pit lake surface. This is illustrated for Cu and Zn, both of which show a rebound in concentration upon termination of treatment (fig. 4).

Conclusions and Implications for Closure Management

Overall, the pit lake model results highlight that the water quality of lake surface waters at the time of pit lake overflow is sensitive to the rate of improvement in PAF WRSF seepage chemistry. Under conditions of higher net percolation (Base Case Scenario), PAF WRSF seepage quality improvements are realized early in response to the rapid flushing of stored oxidation products. This allows the bulk of the waste rock load to be stored (and isolated) in the pit bottom. In contrast, under conditions of lower net percolation (Bentonite Scenario), the rate of PAF WRSF seepage quality improvement is slower. This results in the release of stored waste rock loads to the pit lake surface at the time of pit lake overflow, in turn resulting in higher metal concentrations in pit lake discharges.

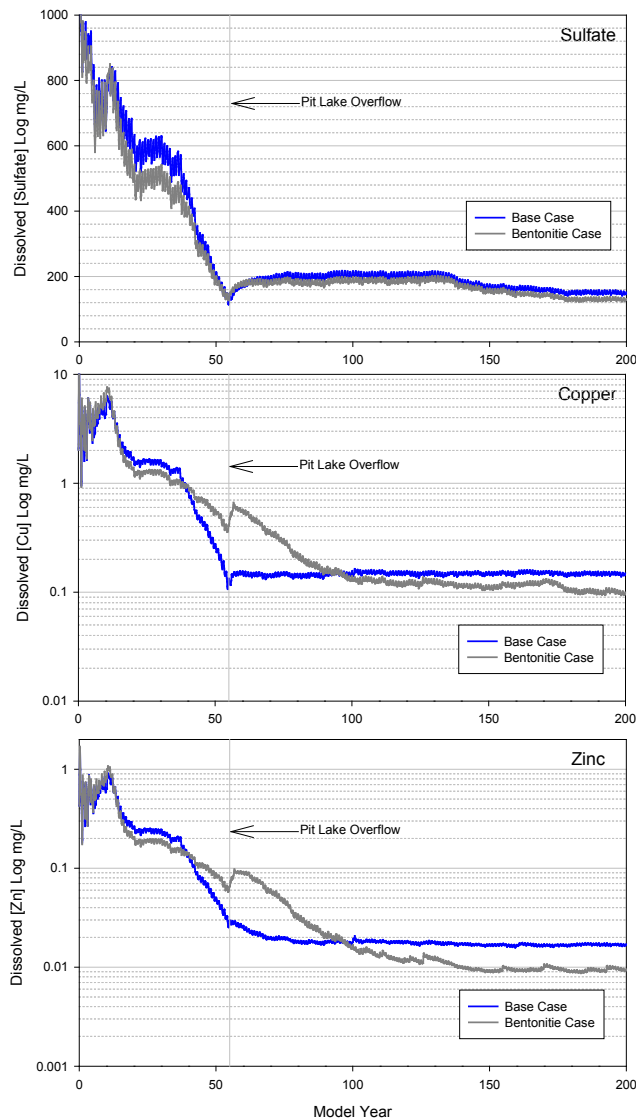


Figure 4 Temporal evolution of dissolved Cu and Zn in surface waters of the Aitik pit lake for Base Case and Bentonite scenarios, both with an assumed treatment period of 55 years. Data represent mean monthly concentrations over the 200 year model period. Timing of pit lake overflow (year 55) is indicated.

The results presented here specifically demonstrate that the benefits of a bentonite cover are limited, and are only realized in the long-term (after 80-100 years). This is perhaps a non-intuitive conclusion, that was only made possible through the development of robust pit lake model inputs. In particular, considerable efforts were required to: 1) quantify the abundance and mineralogy of stored oxidation products, acid-generating minerals and

neutralizing minerals within the WRSFs; 2) predict net percolation into the WRSFs for contrasting engineered cover systems; and 3) predict how seepage quality responds to varying flushing rates.

Acknowledgements

The authors wish to thank two anonymous reviewers who provided comments on the abstract submission.

References

- Castro JM and Moore JN (2000) Pit lakes: their characteristics and the potential for their remediation, *Environ. Geol.* 39: 1254-1260.
- Crusius J, Dunbar D and JJ McNee (2002) Predictions of pit lake water column properties using a coupled mixing and geochemical speciation model. *Transactions for the Society for Mining, Metallurgy and Exploration*, Feb. 26-28, 2001, Denver, Colorado, USA. Vol. 312, p 49-56.
- Dunbar D and Pieters R (2008) Modeling a Physical Mechanism for Removal of Trace Elements from Pit Lake Surface Waters. In: Rapantova N and Hrkal Z (Eds). *Mine Water and the Environment*, June 2 -5, 2006, Ostrava, Czech Republic, p 563-566.
- Dunbar D (2013) Modelling of Pit Lakes. In *Acidic Pit Lakes – The Legacy of Coal and Metal Surface Mines*. In: Geller W, Schultze M, Kleinmann R and Wolkersdorfer C (Eds.), p 186-224, Springer-Verlag Berlin Heidelberg.
- Eriksson N, Mueller S, Forsgren A, Sjöblom A, Martin A, O' Kane M, Eary LE and Aronsson A (2017) Developing closure plans using performance based closure objectives: Aitik Mine (Northern Sweden). 13th Annual Mine Water Association Congress, Rauha-Lappeenranta, Finland, June 25-30, 2017.
- Fraser C, Martin A, Mueller S and Scott J (2017) Incorporating Climate Change Scenarios into Mine Design and Permitting Studies. 13th Annual Mine Water Association Congress, Rauha-Lappeenranta, Finland, June 25-30, 2017.
- Gammons C, and Duaine T (2006) Long Term Changes in the Limnology and Geochemistry of the Berkeley Pit Lake, Butte, Montana. *Mine Water Environ* 25:76-85.
- Martin AJ, Crusius J, McNee JJ, Whittle P, Pieters R, Pedersen TF and Dunbar D (2003) Field-Scale Assessment of Bioremediation Strategies for two Pit Lakes using Limnocorrals. *International Conference on Acid Rock Drainage*, Cairns, Australia, July 2003.

Coal mine flooding in the Lorraine-Saar basin: experience from the French mines

Soazig Corbel, Joël Kaiser, Serge Vicentin

*BRGM (French Geological Survey), DRP/DPSM/UTAM Est, 2 avenue de la Moselle,
57800 Freyming-Merlebach, France, s.corbel@brgm.fr*

Abstract Coal mining in the Lorraine-Saar basin started in the nineteenth century. The coal deposit was mined both in France and in Germany. On the French side, mining ceased in 2004 after 150 years of activity, and as a consequence, the French coal mines got progressively flooded. This study presents the results of the entire monitoring plan for the different mine water reservoirs of the Lorraine coal basin. The actual speed of mine flooding is compared to prediction studies, mine water quality is detailed and content evolution of iron, manganese and suspended solids is discussed for the different mine reservoirs.

Keywords hard coal, mine flooding, water quality, Lorraine-Saar basin

Introduction

Coal mining in the Lorraine-Saar basin started in the nineteenth century. The last French coal was mined in April 2004, and once mining stopped, the water that was infiltrating from groundwater to underground mine workings was no longer pumped out to the surface by the mine operator, Charbonnages de France (CdF). From 2006, mine workings got progressively flooded, creating mine water reservoirs (Figure 1 – Mine workings and mine water reservoirs of the Lorraine-Saar basin.).

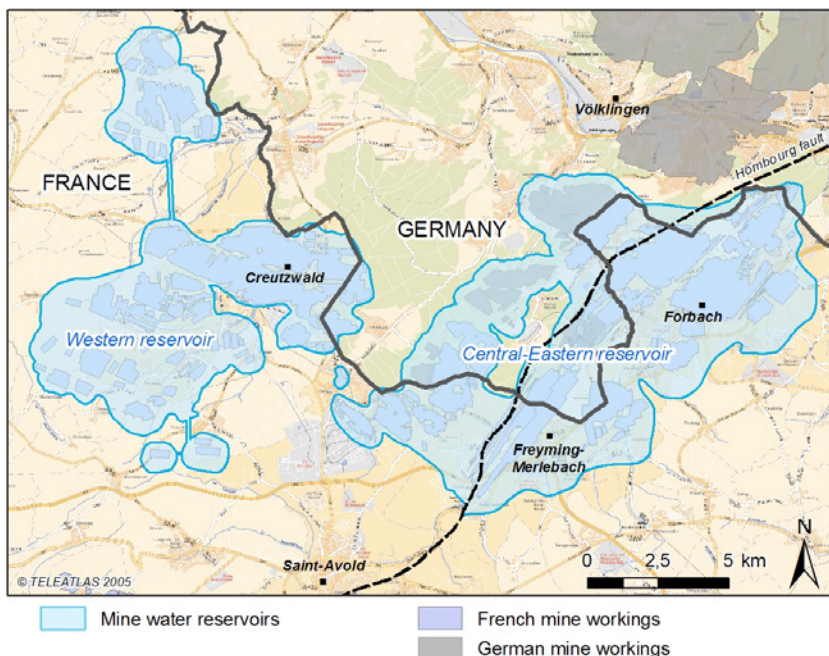


Figure 1 – Mine workings and mine water reservoirs of the Lorraine-Saar basin.

Before its dissolution in 2007, CdF planned and financed remediation operations, including studies to understand mine flooding and its consequences. Following transfer of responsibility for CdF's facilities to the French State in 2008, the Mine Safety and Risk Prevention Department of the French Geological Survey has been managing this remediation activity.

Mine flooding

In 2001, the mine operator CdF started investigating the mechanisms of mine flooding and its consequences. Although coal mines were still operating in the Lorraine basin, planning ahead for post-mining remediation turned out to be necessary.

Mine flooding predictions

Mine flooding assessment was carried out in two phases: volume computation of the residual mining voids and simulation of the mine flooding. The first phase started in 2002 to end in 2005, with a team dedicated only to that task. First, all mine workings maps were digitized, including coal seams and galleries of all exploitation levels for the different exploitation fields. In 2002, CdF used an isolated exploitation field as a case study, to determine coefficient for residual voids depending on the depth of the mine workings and the backfilling methods (Degas 2002). Then from 2003 to 2005, residual mining voids were computed using the residual voids coefficients and the digitized maps, block after block, level after level, for all the mine workings.

The simulation of mine flooding was done in 2006. At that time, CdF was still pumping out water from the underground mine workings. The flow rate of each mine block was assessed and used for the simulation. They were considered equivalent to the flow rates of infiltrating water from the above groundwater. CdF also assessed the state of all galleries linking exploitation fields to each other, concluding that the main galleries were still open. At last, using the residual mining voids, the flow rates of infiltrating water of each block and the connections between each exploitation field, CdF used a simple computation to make mine flooding predictions.

Predictions versus reality

Mine flooding predictions were made for each exploitation field. The example of the Forbach exploitation field, in the Central-Eastern mine water reservoir, is presented Figure 2 – Mine flooding of the Forbach exploitation field.. Two mine flooding scenarios were studied by CdF. The first scenario considered that infiltrations would stay constant until all the mine workings would be flooded, up to the semi-permeable geological layer of the Permian. The second scenario considered that the infiltrations would decrease once the mine flooding reached the last hundred meters of the mine workings.

The mine flooding predictions made all over the Lorraine basin turned out to be pretty accurate, as shown on Figure 2 – Mine flooding of the Forbach exploitation field.. For the Forbach exploitation field, the speed of flooding for the first 500 meters was overestimated by only a month, probably due to an inaccuracy of the residual voids coefficient. Out of the two scenar-

ios studied by CdF, the scenario taking into account a decrease in the infiltrations is the most realistic. However, the speed of flooding for the last 150 meters before reaching the Permian layer was also overestimated, by just over a year. As the shallow mine workings date from early 1900's, the residual mining voids were not easy to assess. The inaccuracy of the prediction of the last 150 meters is most probably due to an inaccurate residual voids computation.

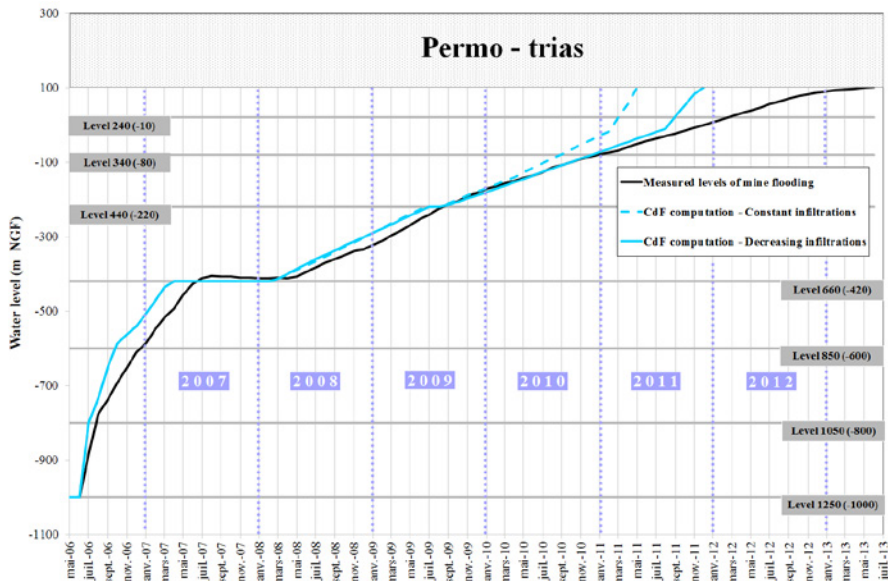


Figure 2 – Mine flooding of the Forbach exploitation field.

Feedback on mine flooding predictions

Although CdF used a straightforward way to predict mine flooding for the coal mines of the Lorraine basin, the predictions were quite accurate. The key of mine flooding predictions is not sophisticated computations, but obviously data gathering. Only staff member of the mine operator were able to properly assess residual mining voids and the conditions of the galleries connecting exploitation fields. However, even with the experience, those miners had trouble assessing old mine workings, and as discussed previously, this inaccuracy immediately lead to an overestimation of the speed of mine flooding.

Mine water quality

To prevent mine water from contaminating the above groundwater once the mine water level has reached the Permian layer, three mine water pumping stations associated to treatment schemes have been built on the Lorraine coal basin. Those pumping stations enable to keep mine flooding under control. They are run by the BRGM as part of their post-mining missions.

Mine water quality monitoring

Water sampling and water analysis are run on the three pumping stations. The pumping stations are installed in old mine shafts, with access to the mine workings. When the coal mines

closed, all the underground mining facilities stayed in place, including machinery, electrical and hydraulic installations. Industrial toxic products such as oils and resins also stayed underground. As a consequence, the water quality is closely monitored, especially regarding dangerous substances. Water analysis for dangerous substances are done every three months.

The dangerous substances analysed are the following: ammonium, cyanide, arsenic, cadmium, chromium, copper, nickel, lead, zinc, phenol index, total hydrocarbons, BTEX (4), HAP (16), formaldehydes, isocyanates, PCBi, COHV.

Mine water quality results

The treatment scheme of La Houve is located in Creutzwald, it treats mine water from the Western mine water reservoir. The treatment scheme has been operating since November 2009. In the first two years, cyanide and a few HAP and BTEX were found in raw mine water at concentrations higher than the environmental quality standards (EQS). Since then, no dangerous substances have been quantified at concentrations higher than the EQS.

The treatment scheme of Simon treats mine water from the Central-Eastern mine water reservoir. The scheme is located in Forbach and has been operating since November 2012. Copper and zinc have been found in raw mine water at concentrations higher than the EQS, since the beginning of pumping. The other substances have not been quantified at concentrations higher than the EQS.

The treatment scheme of Vouters also treats water from the Central-Eastern mine water reservoir, like the treatment scheme of Simon. The scheme is located in Freyming-Merlebach and has been operating since July 2015. Copper and zinc have also been found in raw mine water at concentrations higher than the EQS, since the beginning of pumping. The other substances have not been quantified at concentrations higher than the EQS.

Content evolution of iron and manganese

While pumping stations enable to keep mine flooding under control, treatment schemes enable to lower the raw mine water content in iron, manganese and total suspended solids (TSS), before discharging the treated mine water in local rivers. To be able to design water treatment schemes, predictions of mine water content is compulsory.

Mine water content predictions

Predictions of iron and manganese evolution in the raw mine water were made using the work of Younger (Younger 2000). Predictions were made for the different pumping stations and water treatment schemes using similar hypothesis.

As an example, the main hypothesis for iron evolution were:

- pic concentration of 98 mg/L (\pm 14 mg/L) and stabilization at 5 mg/L (\pm 1,25 mg/L)
- kinetics based on a mine water emergence with a constant flow rate
- 10 % of the volume of the mine reservoir to be leached out by water circulation

Predictions versus reality

Iron and manganese evolution at the pumping station of La Houve are presented Figure 3 – Iron and manganese evolution at the pumping station of La Houve..

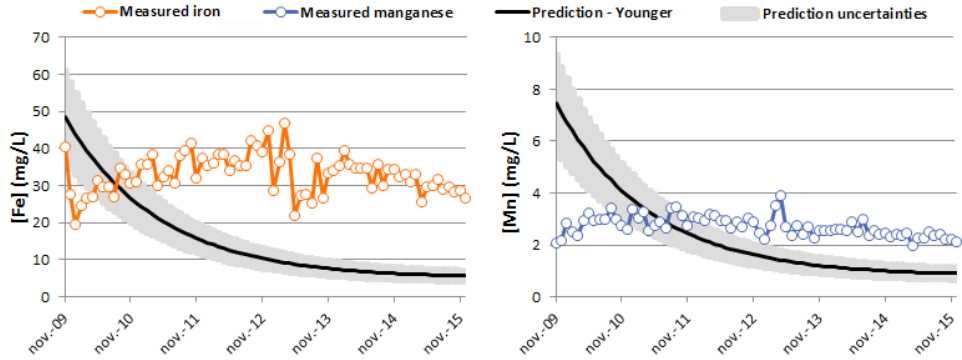


Figure 3 – Iron and manganese evolution at the pumping station of La Houve.

The predictions for iron and manganese evolution at the pumping stations turned out to be wrong. Concentrations were supposed to be high at the start of the emergence, but decreasing quite strongly in a short time. Looking at the real data, it appears that the concentration did not go that high, but they decrease in a much slower way. A major issue regarding these predictions, is that the predictions were used to design the water treatment schemes.

However, predicting iron and manganese evolution is not an easy task. Furthermore, at the time CdF did that study, the pumping stations were not yet an option, and an emergence was supposed to set up instead. Using the work of Zeman (Zeman 2009), predictions were updated to make sure the water treatment scheme had appropriate design.

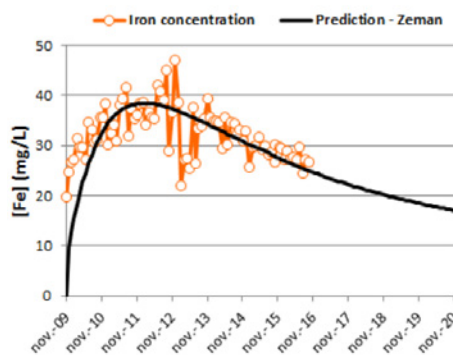


Figure 4 – Updated iron prediction at the pumping station of La Houve.

While the initial study predicted that raw mine water would reach an iron concentration above 10 mg/L by 2013, the new prediction clearly shows that even in 2020, the iron concentration will not have reached the 10 mg/L threshold.

Mine water content predictions feedback

The main issue with the predictions mad using Younger work, was the use of a constant flow rate. Indeed, the mine water pumping stations run at a variable pumping rate, that keeps increasing over the years and will reach its maximum at around 2050. As shown in Figure 4, iron concentration tends to increase with the flow rate. Once the flow rate is stabilized, the iron concentration decreases.

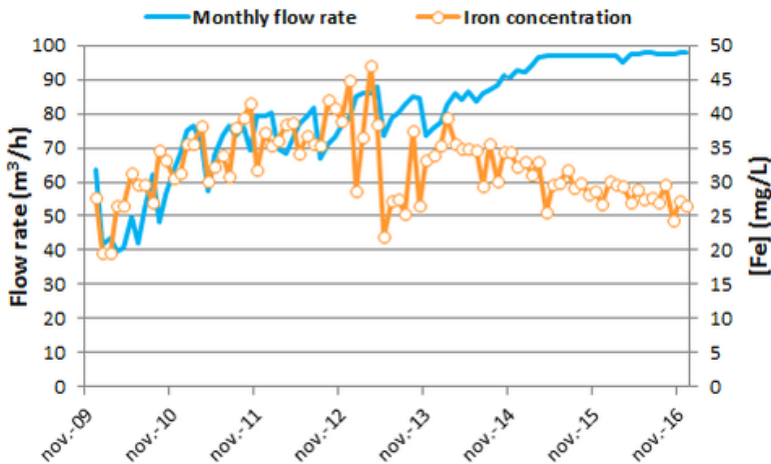


Figure 5 – Correlation between variations in flow rate and iron concentration at La Houve pumping station.

Conclusions

Looking at the example of the French coal mine flooding, it appears that for mine flooding predictions, collecting and computing accurate data is the key element to keep in mind. Regarding the water quality of the two mine water reservoirs of the Lorraine basin, also a few toxic substances were quantified above the EQS at the start of the La Houve treatment scheme, nowadays only copper and zinc are still higher than the EQS in the Central-Eastern mine water reservoir. At last, predicting water quality evolution in terms of iron and manganese is still a difficult task. However, using accurate flow rates increases the chances to get better predictions.

References

- Degas M (2002) Bassin houiller de Lorraine. Détermination du volume des vides miniers résiduels – Cas du bassin de Faulquemont. Houillères du Bassin de Lorraine et Deutsche Steinkohle, reference INERIS-DRS-04-46846/R01
- Younger PL (2000). Predicting temporal changes in total iron concentrations in groundwaters flowing from abandoned deep mines: a first approximation. *Journal of Contaminant Hydrology*, 44(1), pp. 47-69.
- Zeman J, Černík M, and Šupíková I (2009) – Dynamic model of long term geochemical evolution of mine water after mine closure and flooding. Water Institute of Southern Africa & International Mine Water Association: Proceedings. International Mine Water Conference. Pretoria, pp. 828-836.

Sediment And Pore Water Properties Across The Chemocline Of A Mine Water-Impacted Boreal Lake During Winter Stagnation And Autumn Overturn

Tommi Kauppila, Jari Mäkinen, Lauri Solismaa

Geological Survey of Finland, PO Box 1237, 70211 Kuopio, Finland

Abstract Discharge of mine waters into the typically dimictic lakes in the Nordics may cause meromixis in which complete overturns no longer happen. Water column properties were measured from the mining-meromictic Lake Valkjärvi and sediments and pore waters were sampled below, at, and above the chemocline during winter stratification and autumn overturn. Element concentrations were elevated in pore and overlying waters during the overturn. Sediment bulk concentrations showed an opposite behavior. The results demonstrate the importance of the chemocline fluctuation zone on the annual cycle of elements and trace metal concentrations of the sediment compartment.

Introduction

Northern European countries remain a major source of metals with more mines to be opened in the coming years. In countries such as Finland and Sweden, it is often dimictic lakes that receive the effluent waters from the mining operations. In dimictic lakes, thermal stratification is interrupted twice a year by periods of overturn, i.e. mixing of the surface and deeper waters. Mine waters, even those that come from closed mines or that are discharged with strict permit conditions, typically contain high concentrations of electrolytes that increase the density of the waters. In extreme cases, mine waters may cause a condition called meromixis in which complete overturns no longer happen and a permanently stratified monimolimnion forms at the bottom, separated from the overlying mixolimnion by a chemocline.

When mining-induced disrupted annual stratification patterns have started, they may persist even if loading from the mine decreases. This is especially true for meromixis because permanent stratification typically also causes a redox gradient with reducing conditions in the monimolimnion. This redox stratification may contribute to biogeochemical cycling processes at the chemocline (the transitional layer between the upper and deeper water) that work to maintain the permanent stratification. The sediments and their immediate overlying waters also take part in this cycling if processes at the sediment water interface return dissolved constituents into water instead of permanently removing them from circulation.

Lake bottom sediments are a crucial compartment in the lake system, especially regarding the ecological risks of mine waters. This is because harmful concentrations of metals may accumulate in sediments even in cases when concentrations in the water column are not at harmful levels (Väänänen et al. 2016). In the case of metals as hazards, bioavailability is of crucial importance and geochemical conditions play a major role in determining the speciation and bioavailability. In Nordic climates, seasonality modifies these conditions and

in meromictic lakes this is further influenced by the features of the stratification and the migration of the chemocline.

This study examined the chemical properties of the sediment compartment (pore water, immediate overlying water, and bulk sediment) of a mining-impacted meromictic boreal lake. Samples were cored above, at, and below the chemocline at the end of the winter stagnation period (March) and near the end of the open water season during autumn overturn (November) in 2014. Water column properties were measured at both sampling occasions as well. The aim was to study the geochemical properties of the biologically active top layer of the sediments across the chemocline in both winter stagnation and autumn overturn conditions. These data can be useful for the estimation of the ecological risks of metals in the sediments of mining impacted lakes, especially at the zone of seasonal chemocline fluctuation.

Material and methods

Lake Valkeinen is located just south of the closed Kotalahti nickel-copper mine at Oravikoski in Leppävirta, Finland. The mine was in operation between 1959-1987. Waters from the mine site are primarily discharged to a larger lake east of the mine and only a small ditch drains a natural wetland close to the tailings pond towards Lake Valkeinen (Figure 1). Other streams enter the lake from the SE. The lake has a surface area of 19.5 ha and a maximum depth of 16 m.

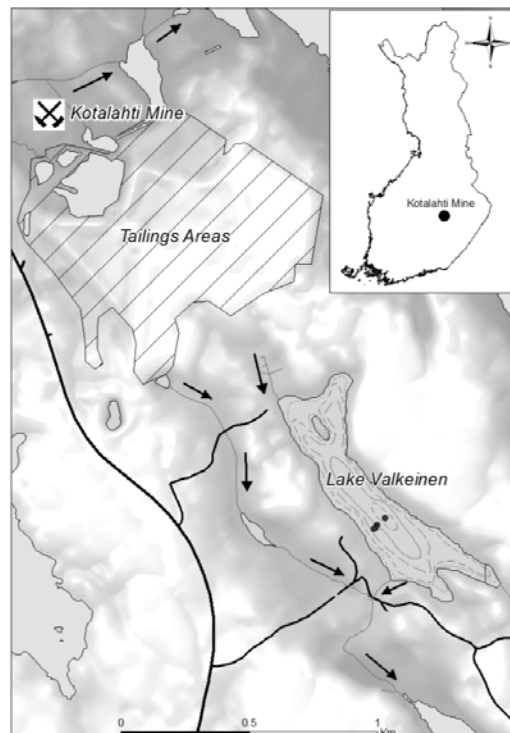


Figure 1. Map of Lake Valkeinen and its location in Finland. Coring sites (8, 10, 14, and 16 m) are marked with dots.

Lake Valkeinen was cored from the ice in late March in 2014 (17.-24.3.2014) and from a boat in early November (3.-6.11.2014). The coring sites form a transect towards the deepest part of the lake: 8 m (above the chemocline), 10 m (near the chemocline), 14 m (below the chemocline), and 16 m (deepest part). The sediments were cored with a Kajak-type corer that closes at the upper end. This preserves the water overlying the sediment during the withdrawal of the corer. A limiter was used to limit the penetration depth of the corer in the sediments to ensure that enough of overlying water was obtained in all cases. Artificial roots ('rhizons') of a nominal pore diameter of 0.2 μm were used to sample both the overlying water and the pore waters (top 5 cm) into pre-vacuumed test tubes. The test tubes for elemental analyses were opened in the field and nitric acid was added for preservation.

The water samples, including water column samples from 2, 10, and 14 m, were analyzed for element concentrations with ICP-AES/MS, major anions with IC (SFS-EN-ISO 10304-1:en), and DOC according to SFS-EN 1484 in the accredited (FINAS T025) testing laboratory of Labtium Ltd. Every tenth sample or at least one in every batch were analyzed as laboratory duplicates and reference materials and field blanks also were analyzed.

The top sediments corresponding to the pore water samples (5 cm) were freeze dried for geochemical analyses with ICP-MS and ICP-AES from microwave-assisted HNO_3 leachates (US EPA 1994). The digestion breaks down sulphides, most salts (e.g., apatite), carbonates, trioctahedral micas, and 2:1 and 1:1 clay minerals but does not appreciably dissolve major silicates. A CN-analyzer was used to determine carbon concentrations. Laboratory duplicates and internal standards were employed for the sediment analyses as well.

Water column properties were measured using a Yellow Springs Instruments XL600 and Professional Plus multiparameter sondes. The variables included depth, temperature, specific conductance (conductivity), pH, reduction potential (ORP), and oxygen. Measurements were also made from the water overlying the sediments in the Kajak corer, and directly from the sediments by pushing the electrodes into the soft sediment. The variables measured from the cores included temperature, pH, ORP, and conductivity. The meters and electrodes were from WTW and Mettler Toledo.

Results

Water column properties

Water column properties show that a monimolimnion devoid of oxygen exists below 10 m also during the autumnal overturn. The mixolimnion remained well aerated (O_2 saturation > 80 %, O_2 11 mg/L) all the way to 9 m where the first small decline was recorded during the overturn. In contrast, O_2 concentration and saturation declined gradually with depth in the mixolimnion during winter stagnation with steeper decline starting at 9 m. There was a decline in O_2 between 2.5 and 3 m during the winter sampling, accompanied with a slight but distinct increase in temperature and a barely detectable drop in pH. The change in temperature at the chemocline was steeper during the overturn with a rapid transition from the stable 3.4 C to the warm (4.7 C) upper part of the monimolimnion. The specific

conductivity of the mixolimnetic water was $460 \mu\text{S}/\text{cm}$ for both autumn and winter down to 6 m. Below this level the conductivity started to gradually increase towards the chemocline during winter stagnation. Conductivity increased to $700 \mu\text{S}/\text{cm}$ in the monimolimnion in both periods with a layer of even more electrolyte rich waters below 14 m (up to $1000 \mu\text{S}/\text{cm}$). Water column pH was higher throughout during the overturn declining from 8.0 at the surface to 7.5 at 9 m and then dropping to 7.0 below the chemocline. There was a layer of higher pH near the lake bottom during both periods and another layer of elevated pH at the rapid decline in ORP at 10.5 m during the winter stagnation. Above this layer, there was a zone of lower pH between 9 and 10 m. Corresponding ORP-pH zoning was not observed during the overturn.

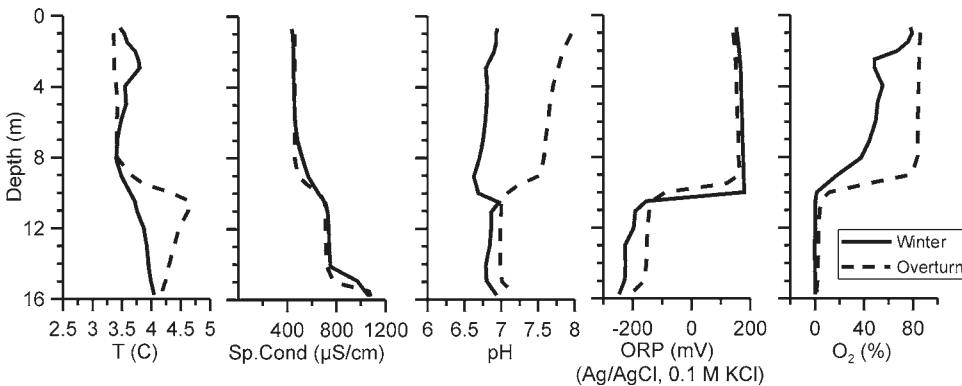


Figure 2. Water column properties at the deepest part of the lake, at the end point of the coring transect. Solid line = winter stagnation, dashed line = autumn overturn.

In accordance with the conductivity results, element concentrations in the water column (results not shown) were higher in the monimolimnion than in the upper part of the mixolimnion during both occasions. Concentrations in the transitional zone were in general between these two extremes. However, Mn, Ni, Co, and Zn concentrations were elevated at the chemocline. Manganese in particular was found at 10 m during the overturn whereas Fe concentrations were conspicuously low in all samples. Similar to most elements, sulfur and SO₄ concentrations increased with depth. Total sulfur and SO₄ molarities coincided at 2 m and 10 m but there was a 2-2.5 mmol/l excess of sulfur at 14 m.

Pore waters and overlying waters

During late winter stagnation, the waters overlying the sediment (10 cm layer) were oxidizing at 8 m (+184 mV using Ag/AgCl, 0.1 M KCl electrode) and turned more reducing at the deeper sites (Table 1). Within the top sediment (at 3 cm), pore waters were reducing at all sites (~ -250 mV). There was a gradual increase in SO₄ concentrations with depth in both the overlying and pore waters. When compared with total S concentrations, SO₄ accounted for most of the sulfur at 8 and 10 m but there was an excess of sulfur (i.e. other species) below the chemocline, especially in the overlying waters at 16 m. In all cases, there was more sulfur in the waters overlying the sediment than in the pore water.

Table 1. Selected properties of pore waters (bottom) and the waters overlying sediments (top). Winter values are on the right, overturn values on the left.

Depth (m)	ORP (mV)	EC ($\mu\text{S}/\text{cm}$)	Al ($\mu\text{g}/\text{L}$)	Fe (mg/L)	Mn ($\mu\text{g}/\text{L}$)	Ni ($\mu\text{g}/\text{L}$)	Zn ($\mu\text{g}/\text{L}$)	S (mg/L)	SO ₄ (mg/L)	DOC (mg/L)	ORP (mV)	EC ($\mu\text{S}/\text{cm}$)	Al ($\mu\text{g}/\text{L}$)	Fe (mg/L)	Mn ($\mu\text{g}/\text{L}$)	Ni ($\mu\text{g}/\text{L}$)	Zn ($\mu\text{g}/\text{L}$)	S (mg/L)	SO ₄ (mg/L)	DOC (mg/L)
8	184	219	8.74	<0.05	20.5	7.99	5.51	82.7	200	5	82	15	<1	0.95	619	7.13	5.28	60.0	180	2.6
10	-10	350	14.6	<0.05	405	10.6	8.46	103	249	3.2	-111	306	12.3	0.52	2780	7.84	16.0	89.0	240	3.1
14	-245	417	37	0.1	2460	5.98	4.86	157	306	5.5	-243	447	32.0	0.07	2030	5.09	1.56	651	400	5.3
16	-208	558	38.8	<0.05	1040	4.47	4.11	380	417	3.5	-364	640	26.0	<0.05	1120	4.60	2.46	808	410	12
8	-220	330	131	7.24	3190	6.72	7.56	71.4	199	9.1	-110	250	28.6	5.26	2980	3.82	7.88	58.0	170	8.1
10	-248	310	170	0.07	3450	3.29	1.45	71.9	207	11	-280	300	35.4	0.08	3060	3.99	10.7	74.6	210	11
14	-290	400	170	<0.05	2230	4.34	4.66	118	243	18	-292	376	53.5	<0.05	1480	3.50	0.59	278	310	12
16	-260	560	154	<0.05	1060	5.53	3.22	161	361	20	-364	640	74.7	<0.05	1180	5.26	0.75	355	330	13

Iron concentrations were again negligible in the pore and overlying waters in the winter with the exception of the pore waters of the shallowest site (7 mg/L). In contrast, Mn concentrations were relatively high in especially the pore waters of the two shallowest sites, declining below the chemocline. In the overlying waters, Mn was all but absent at 8 m and at the highest at 14 m. Here again, Ni and Zn concentrations in the overlying waters were highest at 10 m, accompanied with low pore water concentrations. The highest concentrations of these elements in pore water were found at the shallowest site (8 m). There was more DOC in the pore waters than in the waters overlying the sediment with an increasing trend with depth (from 9 to 20 mg/L).

The autumnal overturn did not result in more oxidizing conditions in either the overlying waters or pore waters at any depth. In fact, overlying water remained more reducing than during the winter at the chemocline (10 m). Similar to the winter stagnation, SO₄ concentrations increased with depth in both the overlying and pore waters with higher concentrations above the sediment than in pore waters. Here again, SO₄ accounted for most of the sulfur at the mixolimnetic sites but the proportion of excess sulfur over SO₄ was higher in both the overlying water (16-21 mmol/l) and pore water (5.5-7.7 mmol/l) than in late winter.

Iron concentrations were very low also during the overturn, with some Fe detected in the shallowest sites. Mn concentrations were highest in the pore waters of the 8 m and 10 m sites while the highest concentrations in the overlying water were measured at 10 m, in line with the water column results. The same was true for Zn and Ni in the overlying waters but, in contrast to winter stagnation, pore water concentrations at the chemocline (10 m) were not conspicuously low. The increasing trend in pore water DOC concentrations with depth was similar to the late winter conditions but this time there was a similar and even more pronounced trend in the overlying water as well. Electrical conductivity increased with depth as in winter and in the water column but the conductivity in the overlying water at 8 m was very low at 15 $\mu\text{S}/\text{cm}$. This general trend was seen in major cations as well.

When the major winter-to-overturn differences in pore waters and overlying waters were examined at different sampling depths, they mostly consisted of cases where concentrations were higher during the overturn. However, there were cases in which concentrations were higher in the winter at the monimolimnetic sites (14 m and 16 m) such as Cr in the overlying water at 16 m, Se in pore water at 14 m and 16 m, and Zn in both water fractions at 14 m and 16 m. In addition, Al concentrations were higher during the winter at all depths. In general, however, concentrations were higher in the autumn and this was especially true for the 10 m coring site which is located close to the chemocline. At this site, especially the concentrations in the waters overlying sediment showed higher element concentrations during the overturn. Concentrations of total sulfur were exceptions to this rule with high autumnal concentrations only in the monimolimnion.

Sediments

As is common for any lake, mining impacted or not, there were trends in sediment element concentrations with depth. These trends stem from the physical and geochemical processes that sort the materials between the shallower and deeper areas of a lake basin. At Lake Valkjärvi as well, elements typical to silicate minerals had higher concentrations in the shallower sediments (Al, Cr, K, Ti, V). In addition, Mn and Pb declined with depth. Elements with higher concentrations deeper in the lake included Co, Fe, S, Ni, and P and also alkaline and alkaline earth metals Ca, Mg, Na, and Sr. As usual, carbon concentrations were higher in the deep water sites, also affecting element concentrations in sediments.

Table 2. Concentrations of selected elements in the sediments (in mg/kg, C in %).
Upper panel = winter, lower panel = overturn.

Depth (m)	Al	As	Ba	Ca	Co	Fe	K	Mg	Mn	Na	Ni	P	Pb	S	Sr	Ti	V	Zn	C
8	17200	15	378	10200	104	48500	2360	7230	2260	317	1120	2250	73	15900	51.6	784	50.9	329	20.4
10	13900	13	234	8870	130	52500	1960	6130	1390	268	979	1930	56	48100	44	623	35.7	187	19.8
14	13500	15	202	11100	216	72100	2130	7400	1230	423	1930	1900	53	71700	55.5	578	31.7	262	21.8
16	13500	16	439	12100	321	103000	1820	7230	2150	347	2050	3620	36	108000	71.7	467	24.9	276	20.3
8	16500	7	241	8820	65	45800	2040	6120	1430	260	560	1580	68	18400	40	709	46	241	19.1
10	13700	7	200	9490	91	45300	2180	6650	1420	313	710	1680	62	42400	43	679	36	181	20.1
14	12200	9	221	11300	265	67900	1800	7060	1130	356	1970	2190	46	70600	51	466	24	251	20.9
16	10100	8	234	11200	230	78600	1740	6990	1150	354	1930	2260	37	84100	53	454	20	256	21.5

Understandably, changes in sediment concentrations were less pronounced than those in the water phases of the sediment realm. In general, concentrations were slightly higher in the winter than in during the overturn (the opposite was true for the waters). The change, although slight, was strongest at the deepest (16 m) and shallowest (8 m) sites. In particular, the concentrations of Fe, Mn, As, and S were higher at 16 m in winter. Fe and S were elevated also at the chemocline zone (10 m) in winter whereas Al and the alkaline and alka-

line earth metal concentrations were lower at that depth. At the shallowest site, above the chemocline fluctuation zone, winter concentrations were higher for e.g. Ba, Ca, Mg, and also Mn, Ni, and Zn.

Discussion

The results show that Lake Valkeinen indeed is meromictic and autumnal overturn is unable to mix the monimolimnion. However, mixing erases the zonation in the mixolimnion seen during winter stagnation with a zone of oxygen consumption, higher temperature, and lower pH at the interface between fresh water from the top at 3 m and the slightly oxygen deficient deeper mixolimnetic water. Mixing also erases the zone of redox reactions at the chemocline with a decline in pH above the redoxcline, presumably due to reprecipitation of the diffused reduced species, and elevated pH immediately below the redoxcline in the reducing monimolimnion. Chemical analyses of the 10 m water column sample suggest that species of Mn, Ni, Co, and Zn play a role here and these same metals also showed high concentrations in the water overlying the sediment at the same depth. Seasonality also affects the monimolimnion, especially the temperature profile, but also the pH and redox conditions to some degree. However, it doesn't erase the layer of high electrolyte content and low ORP at the deepest part of the lake, presumably formed due to reactions at or near the sediment water interface that may also involve redissolution of precipitates settling through the water column. There also was an excess of other, presumably more reduced, sulfur species over SO_4 in the water column, pore waters, and the overlying waters in the monimolimnion, especially during the autumn overturn.

Seasonality had an effect on the element concentrations of the pore waters and the waters overlying the sediments especially at the chemocline. In general, concentrations were higher during the overturn, particularly in the waters overlying the sediments. Major increases at the chemocline compared to winter conditions were seen in Ba, Co, Mn, P, Pb, V, and Zn. In the winter, pore water concentrations of e.g. Zn and Ni were low at 10 m, suggesting binding to sediments may be more efficient. At this time, the ORP values increase rapidly above the chemocline while the O_2 concentrations are low compared to the overturn conditions, suggesting other oxidizing species are present.

In contrast to waters, sediments had slightly higher concentrations of HNO_3 soluble elements in the winter than during the overturn, especially at the deepest and shallowest sites. At the deep, this may be due to precipitation as sulfides because the effect was strongest for Fe, Mn, As, and S. Iron and sulfur also showed higher sediment concentrations at the chemocline in winter.

Conclusions

The results show that seasonality may have an effect on the chemical conditions of the sediment compartment of mining-impacted meromictic lakes. The effect varies with depth and across the chemocline. Furthermore, the response differs between individual elements and also between pore waters and the waters overlying the sediments. Even when the monimolimnion remains stable, conditions change in this reducing, high electrolyte part of the system as well.

Acknowledgements

The study was partly financed by the KaiHali project (Management and restoration of surface water bodies receiving mine waters), financed by the European Regional Development Fund.

References

- US EPA 1994. US EPA 3051. Microwave assisted acid digestion of sediments, sludges, soils and oils.
- Väänänen, K., Kauppila, T., Mäkinen, J., Leppänen, M.T., Lyytikäinen, M. & Akkanen J. 2016. Ecological risk assessment of boreal sediments affected by metal mining: Metal geochemistry, seasonality, and comparison of several risk assessment methods. *Integrated Environmental Assessment and Management* 12: 759-771.

Mine water concept in detail – A case study of closing a German coal mine at Ruhr district

Hagen Frankenhoff, Isabelle Balzer, Dr. Holger Witthaus

*RAG Aktiengesellschaft, Servicebereich Technik- und Logistikdienste,
Shamrockring 1, 44623 Herne, Germany*

Abstract A concept of closing a German hard coal mine includes the decommissioning of underground facilities and addresses all matters of environmental protection in a long term view. Therefore the concept has to describe the decommissioning of production, the separation of mine field infrastructure, the preparation of roadways and the mine water management. The report gives a short overview of the mine layout and geological circumstances, followed by a description of measures for preparation prior to closing including operational aspects and regulatory approvals up to required monitoring measures.

Key words Mine closure, Post-mining water management, hard coal mining

Introduction

RAG Aktiengesellschaft (RAG) is responsible for finishing hard coal mining in Germany up to the year 2018 based on long term contracts and agreements. RAG is following a detailed concept of mine closure for each mine and also considering generic regional aspects. This paper gives an exemplary overview to the closing of an underground hard coal mine in the Ruhr area of Germany. At first some fundamental parameters of the geological and geometrical situation are described. For the description of procedure it is also necessary to mention some important legislative requirements. Based on the regional concept of mine water management the process of mine closure has to fulfil a lot of specific demands. In the following some examples of applied methods and operations regarding mine water management are pointed out.

Basics for closure of a hard coal mine in the Ruhr area

Geological overview

Hard coal deposit of the Ruhr area is located in Carboniferous strata. In the South of the Ruhr district these strata are directly cropping out to the surface. Strata are dipping to the North and the overburden of the Carboniferous is consisting of Tertiary and Quaternary strata.

In total there are approximately 200 seams in Carboniferous rock with a thickness between a few centimeters up to 5 meters. In the northern area of the coal field the seams are located in a depth of approximately 1000 to 1500 meters.

Geometrical and operational parameters of a typical mine

A typical hard coal mine of today consists of several shafts and a large number of roadways in the underground. An area of 20 to 30 square kilometers is covered, more than 130 kilometers of roadways in a depth between 800 meters and 1500 meters describe the scale of a typical mine in numbers.

Legislative basics

Main basics for mining activities in the Ruhr area are formed by a federal legislation and the country codes of North Rhine Westphalia. These laws rule mining in production as well as mine closure. For mine closure additional recommendations of European, federal and local demands are taken into consideration, because danger by post mining risks has to be avoided.

The main challenges of mine closure are:

- prevention of uncontrolled gas emissions,
- control of mine water level with respect to other groundwater levels,
- save of drinking water quality,
- prevention of damage by movement of the ground.

Procedure of closing

Elements of mine water management are applied during production time as well as in time of closure. Important is a continuous observation of mine water quality at any point of inflow in the underground. Due to this demand underground probes are taken and analysed for specific physical and chemical parameters. Table 1 gives a list of parameters that are analysed in standard sampling. The column PP1 describes the standard test range, PP2 minimized simplified tests and PP3 to PP5 additional tests for cases of suspicion.

Table 1 Standard categories of testing procedure for mine water probes (IHS 2007).

	Parameter	PP1	PP2	PP3	PP4	PP5
on-site	colour	x	x			
	clouding	x	x			
	smell	x	x			
	temperature	x	x			
	pH-value	x	x			
	electric conductivity	x	x			
main components	evaporation residue	x				
	total hardness	x				
	Natrium	x	x			
	Calcium	x				
	Magnesium	x				
	Potassium	x				
	Chloride	x	x			
	Sulfate	x	x			
Hydrocarbonate	x					
minor components	Ammonium	x				
	Nitrate	x				
	Nitrite	x				
	Barium	x	x			
	Strontium	x				
	Iron	x	x			
	Manganese	x				
specific extraordinary loads	Radium 226			x		
	Radium 228			x		
	Sulfide					x
	Zinc				x	
	Lead				x	
anthropogenic loads	COD	x	x			
	Phosphor	x				
	Hydrocarbons	x				
	Absorbable organic halogen	x				
	PCB	x	x			
	PCB substitutes	x	x			

Figure 1 gives an exemplary overview to the points of geogenic water inflow to the mine infrastructure at Auguste Victoria mine. The perspective view includes remarks by arrows and a table of water flows for each point. In total the inflow amounts 156 m³ per hour. Different colours indicate different levels of roadway infrastructure. The shafts are marked as AV 3/7, AV 6, AV 8 and AV 9 and WU 1/2 (adjacent mine).

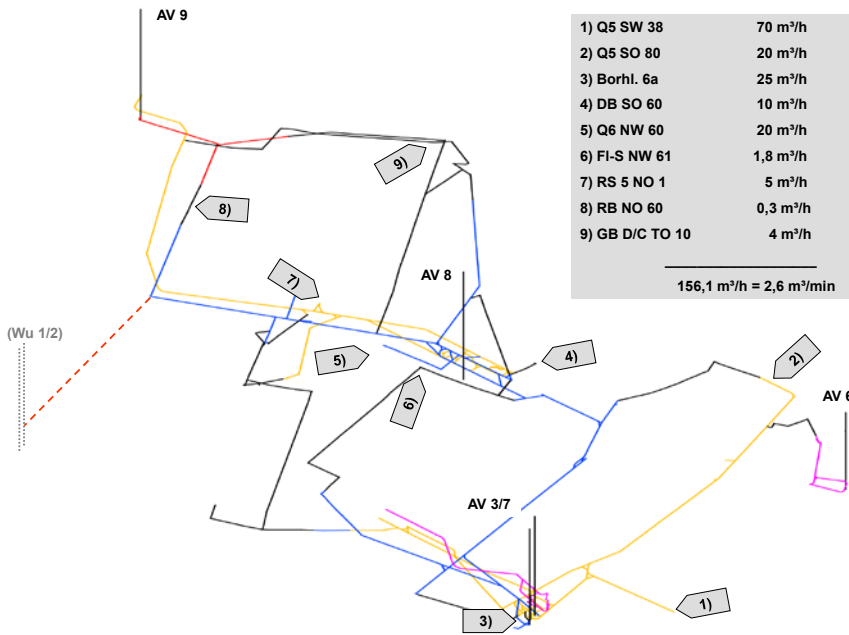


Figure 1 Perspective view on water inflow to Auguste Victoria mine infrastructure

At several places highly mineralized geogenic water flows into the mine. This type of water has often a high content of barium. Different water inflow, mostly from shallow depth, has a different chemical composition and contains a high level of sulfate in most cases.

At the place of conduction of this two different types of water barium sulfate is precipitated. This chemical reaction is having a significant negative influence on the condition of pipelines and pumps. Based on this knowledge RAG uses former mining panels as areas for sedimentation. Therefore this water types are let into these rooms of retention separately. There the salt is precipitated and the clean water is pumped to surface.

After finishing of roadway heading and coal production all required roadways are prepared as water gateways. This includes examination of former workstations for pollutants, installation of a pipeline network and clearing up the roadways. The pipelines are installed to ensure a minimum shape for water conduction even if the roadway support collapses. For achieving a drainage effect, approximately every 100 meters a case filled with gravel covers a point of inlet to the pipes (fig. 2).



Figure 2 Example of pipeline installation underground.

In the first phase of closure the areas of former mining excavations are normally separated, when they are not necessary for infrastructure and ventilation any more. The closure is realized by the installation of concrete structures within the roadway. The structure is dimensioned to prevent mine water inflow as well as gas explosion. The unventilated area behind the concrete wall is characterized by a rising content of methane gas.

A final operating plan, that must have an official statutory approval by the mining authority, is the basis for this procedure.

Connected with this approval commonly specific auxiliary conditions are formulated by the authority, resulting on risks that are recognized and documented in third party expertises. The verification of each process and execution of specific monitoring measures have to be implemented in a final documentation of realization.

Preparation of shafts

Long-term mine water management is aiming on using old shafts as well stations. The regional concept allows minimizing the number of well stations. Because of this concept the underground pumping stations will be substituted by well pumps within the shaft. For this the complete shaft installation has to be recovered and a vertical pipe for each required pump gets installed. A pillar of concrete is filled into the not needed shape of the shaft. The length and static construction of the pillar is depending on specific local parameters for each shaft. The detailed technical planning is aiming on long-term stability, avoiding uncontrolled gas emission and explosion prevention besides economic pumping processing.

Figure 3 shows on the left side a picture of a pumping station in the underground. On the right side figures a scheme of the closed underground roadway system, the pump and pipes for well operation.

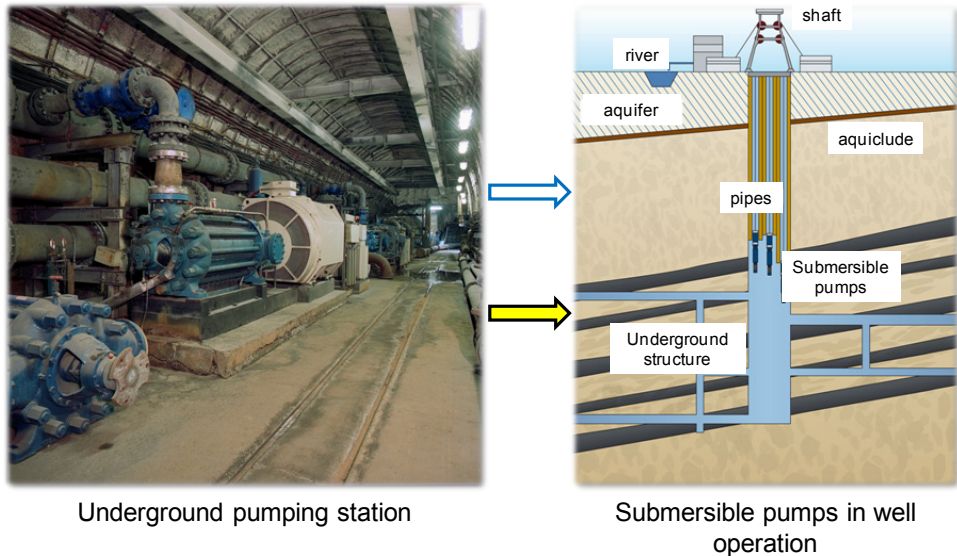


Figure 3 Preparation of shafts for well pumping stations

Operational matters

A mine with a working area of 60 km² cannot be closed in one step. So minimizing of the open underground area is going on stepwise. When an area is prepared for closing and all of the machinery is deconstructed, a barrier dam is constructed in concrete material. This barrier contains pipelines for dewatering measures, must be gastight and also has to be dimensioned to allow explosion protection. If a dam is located in the later water gateway, it must be reopened when the next following underground area is closed.

The preparation for closing starts long before the end of production. Figure 4 shows a perspective view on Auguste Victoria mine 3 years and 2 years before closing. Still active districts in the North (blue circles) are running while other parts of the mine (West and East) are abandoned in that phase (green circles).

Even in that time of closure a roadway was driven to the adjacent mine (grey circle). In the regional concept of mine water management this path is required for underground water flow and finally reduction of well station number.

A monitoring of mine water level is applied to proof the results of predicted rise of water level. The prediction is done by a special software system “Boxmodell” which was designed in cooperation with DMT company. The model gives a prospect on several parts (“Wasser-

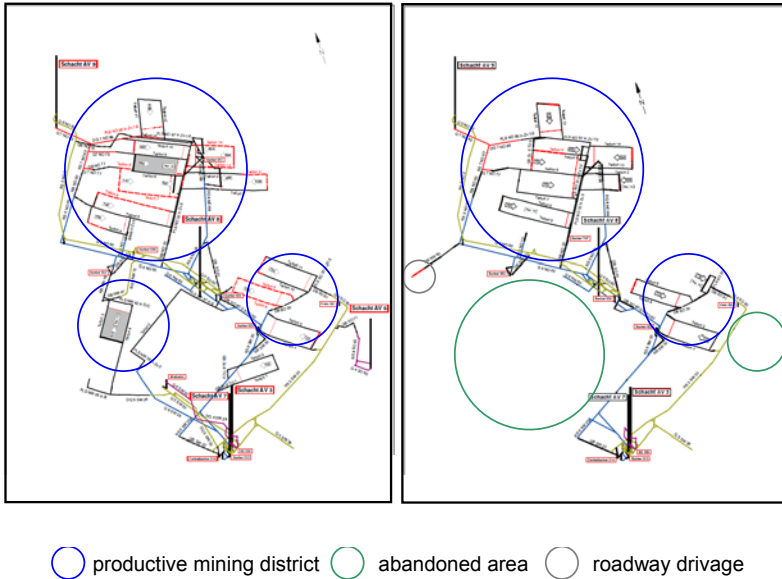


Figure 4 Exemplary comparison of retreating areas in a mine

provinzen”) within a regional model and contains several boxes for simulating the mine water management. The modelling is done with respect to several geometrical, physical and chemical parameters and is recalibrated consequently by monitoring results and water analysis. Figure 5 gives a prospective view on the model of the Ruhr area in total. Each box is vertically subdivided into several plates. Each plate provides an individual set of modelling parameters. Figure 6 shows a comparison of forecast and measured data of water level. The graph shows different points/areas as arrays printing (time series) and dots as results of monitoring.

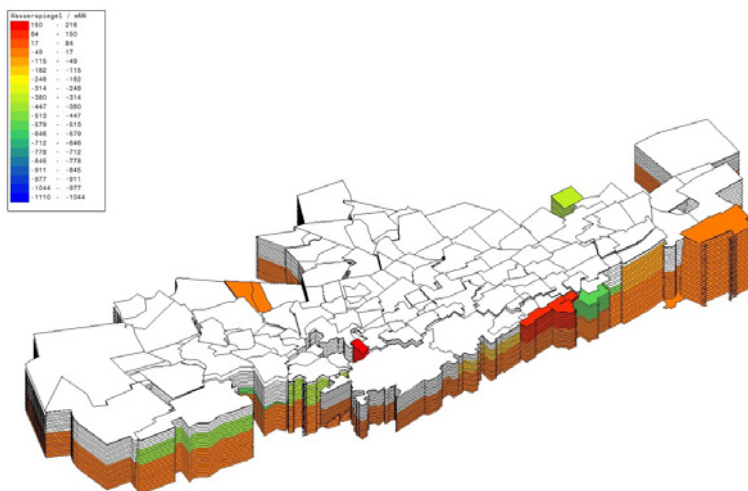


Figure 5 Boxmodel for simulation – example Ruhr area (DMT, Eckart et al.)

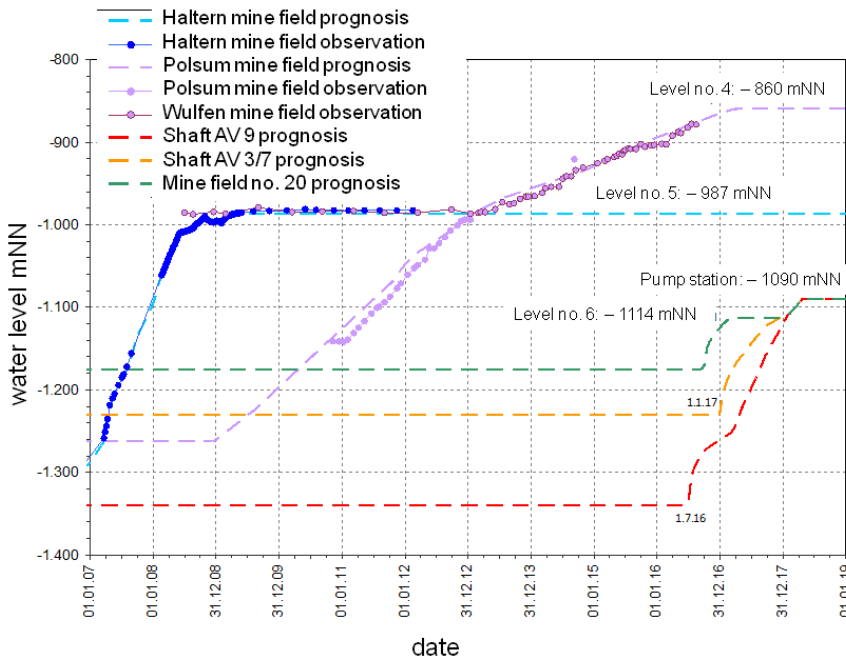


Figure 6 Simulation of exemplary mine water levels and monitoring results (DMT)

Conclusions and outlook

Closing of an underground mine is a long-term project. Beside RAG as the mining company it requires teamwork of water scientists, mining administration, constructors, planning engineers and lawyers for cooperation. Since the year 2007 RAG follows regional conceptions and did close several mines successfully. Underground roadways were used as water gateways to minimize the number of pumping stations. To get optimized results of later activities for pumping all water gateways are prepared carefully with respect to chemical composition of different mine water qualities. The described example gives an overview to a wide spread of measures that are executed for closing and realisation of regional water management. Up to now RAG did proof the success of the work for each mine by results of monitoring.

When the last German hard coal mine will close in 2018 all remaining pumping stations will be optimized for long-term run. This means to prepare additional old shafts for well pumping stations and proof successful realisation of the mine water concept by ongoing monitoring processing. Besides common monitoring from surface also modern underground probes will be used for long-term measurement of in-situ water parameters.

References

- Eckart, M. , Kories, H., Rengers, R. & Unland, W. 2004. Application of a numerical model to facilitate mine water management in large coal fields in Germany. / *Mine Water 2004 – Process, Policy and progress*, Newcastle upon Tyne, vol. 2, 209-218.
- Eckart, M., Klinger, C, Unland, W., Rengers, R., Metz, M., Blachere A.: Prognose der Flutungsauswirkungen im Steinkohlenbergbau – 5. Altbergbaukollquium, 3.-5. November 2005, Technische Hochschule Clausthal, Tagungsband S. 401-415.

Mine Water Management in the Ruhr coalfield

Michael Drobniowski, Isabelle Balzer, Hagen Frankenhoff, Dr. Holger Witthaus

*RAG Aktiengesellschaft, Servicebereich Technik- und Logistikkdienste,
Shamrockring 1, 44623 Herne*

Abstract Today, the RAG Corporation is the last hard coal mining operator in Germany. In the Ruhr coalfield it is operating one active mine and 11 dewatering stations. At the end of 2018 the subsidized hard coal mining is finally ceasing but the mine water management will continue for an unlimited period of time. Therefore the RAG Corporation was obligated to develop a new sustainable mine water management system for the post-mining era to protect the ground surface and drinking water reservoirs.

Key words Mine water management, Post-mining mine water management, hard coal mining

Introduction

In 1968, the RAG Aktiengesellschaft (RAG Corporation) was founded as a consolidation company of the Ruhr mining industry and is nowadays the last hard coal mining company in Germany. Today it is operating two remaining collieries, one in the Ibbenbüren coalfield and one in the Ruhr coalfield. Coal mining in the Saar coalfield ended in 2012, but the mine workings are still open and used for mine water management. In 2016, 104.5 million m³ mine water were pumped in the three coalfields by the RAG Corporation (fig. 1). This paper is focussing on mine water management in the Ruhr coalfield.

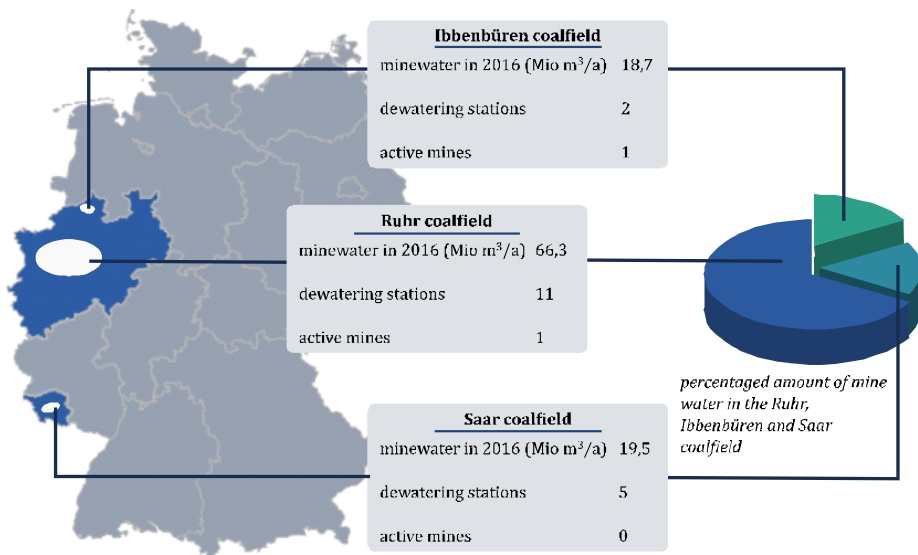


Figure 1 Hard coal mining and mine water management in Germany.

The Ruhr coalfield is located in north-west Germany in the state of North Rhine-Westphalia.

It lies in the catchment of the tributaries Ruhr, Emscher and Lippe of the River Rhine. The occurrence of vast coal deposits has led to the development of one of the largest polycentric metropolitan areas in Europe. The Ruhr area extends over 4,430 km² and consists of several large industrial cities. It is one of the most densely populated mining areas worldwide.

The Ruhr coalfield contains 3,000 m of Upper Carboniferous coal-bearing strata and nearly 300 coal seams with a thickness ranging from <0.5 to 3 m. The carboniferous strata are outcropping in the southern part of the Ruhr area in the valley of the river Ruhr and are dipping towards the north. Due to that geological condition mining in the valley of the Ruhr dates back to medieval times. Following the dip of the carboniferous sequences, and with ongoing industrialization and new technical developments in mine water management, mining activities moved towards the north. In the northern part of the Ruhr Area, within the range of the river Lippe, the cretaceous overburden reaches a thickness of 1000 m (Henningsen and Katzung 2006).

Status Quo

At the time of the foundation of the RAG in 1969, 56 collieries were in operation. 52 collieries were passed to the RAG Corporation and 4 collieries remained independent (Huske 2006). This number declined steadily so that in 2017 only one active colliery remained in the Ruhr coalfield (the colliery Prosper-Haniel located in the city of Bottrop). Due to combined mining, most of the collieries were connected in the underground at several levels by mine workings. If underground pumping stops at one colliery, the rising water will flow to the adjacent mine. Therefore, a network of pumping stations is still active in the whole Ruhr coalfield – even with reduced mining activities. Today and in the past, the main task of the mine water management was to keep the mine dry and guarantee safe working conditions for the last remaining collieries.

In 2016 66.3 million cubic meters of mine water were pumped to the surface by a network of 11 dewatering stations and one active mine in the Ruhr coalfield (fig. 1). Almost half of that water is pumped in the southern part of the coalfield where the carboniferous strata are outcropping and mining activities stopped in the 1960ies. Pumping can here take place at shallow depth and the water is only slightly mineralized. The water is discharged directly into the river Ruhr. Without pumping the water in the southern part of the coalfield would flow northwards following the dip of the strata and reach adjacent mines or dewatering stations. There it would have to be pumped from greater depths and with a higher amount of dissolved minerals.

Going to the north, the cretaceous overburden and consequently the pumping height are gradually increasing. Water is discharged into the rivers Emscher and Lippe (fig. 2).

Today's underground pumping stations at the rivers Ruhr, Emscher and Lippe are consisting of a system with two open shafts for mine ventilation and connecting roadways. Centrifugal pumps are installed in the roadways and are pumping the water to the surface. In the western part of the Ruhr coalfield the pumping station Walsum has already been re-

constructed as a well-operating pumping station. It is using submersible pumps and maintenance works take place from the surface. Mine workings have been closed completely. The pumping station Walsum started working in June 2016 and is discharging directly into the River Rhine.

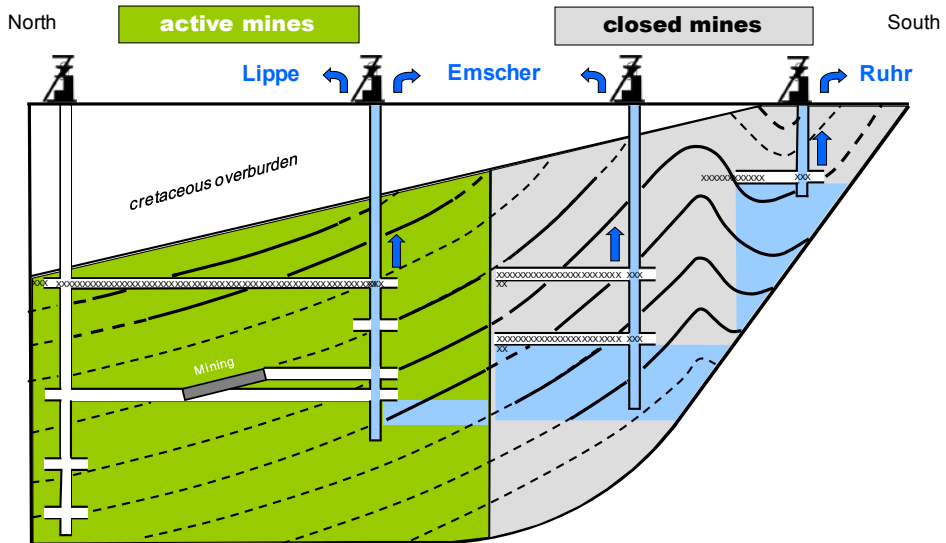


Figure 2 Cross-section of the Ruhr coalfield – mining activities and mine water management

Post-mining mine water management

At the end of 2018, when hard coal mining operations will finally be ceasing in the Ruhr coalfield, the dewatering of the carboniferous strata is no longer necessary with regard to safe working conditions for the miners. Anyway, mine drainage in this densely populated region is regarded as a perpetual obligation resulting from the coal-mining operations. For that reason mine drainage is regarded as a task for an unlimited period of time to maintain the water level at a pre-determined safe level. In the future, the most important objective of mine water management will be the protection of the ground surface and especially of groundwater reservoirs. Nevertheless the RAG Corporation was obligated to develop a new concept to operate mine drainage in a responsible, efficient and cost-effective way in the post-mining era.

Basic options to meet the demands of the post-mining mine water management are the rebound of the water-level to a pre-determined safe level, the reduction of pumping stations and well-operated pumping from the shaft with submersible pumps. The post-mining mine water management is shown in Fig. 3. It is planned to reduce the number of pumping stations to a total number of six: In the south of the coalfield, the dewatering stations discharging into the river Ruhr will remain (Heinrich, Friedlicher Nachbar and Robert Müser). In the east, the only remaining dewatering station will be Haus Aden. The dewatering station Walsum is already reconstructed and will continue dewatering the western part of

the coalfield in the post-mining era. After closing the last mine Prosper-Haniel in 2018, the water management in the central part of the coalfield can be adapted. Therefore the former mine Lohberg will be reconstructed as a dewatering station. Mine water can directly be discharged into the river Rhine. There will be no more discharge of mine water into the river Emscher (RAG AG 2014).

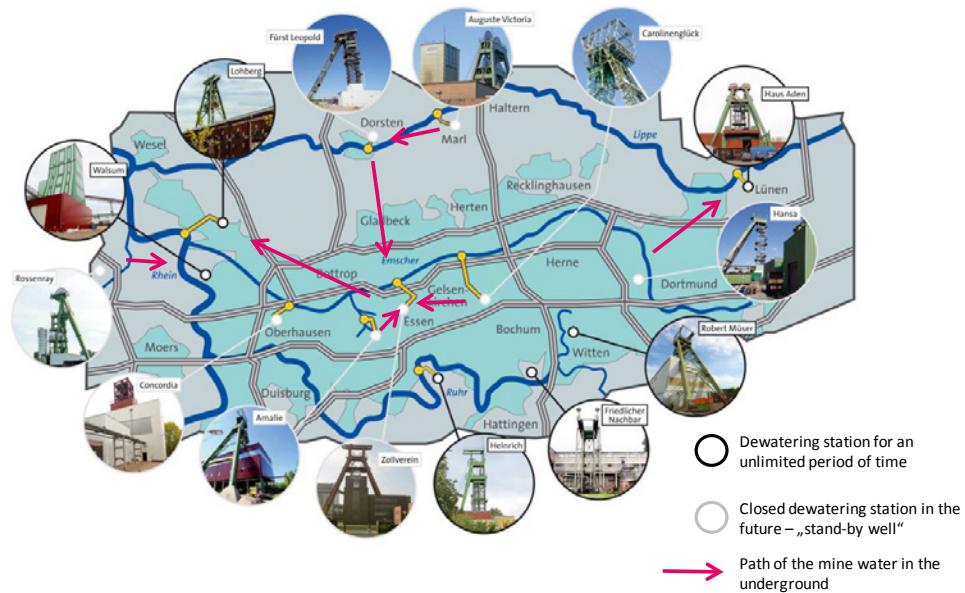


Figure 3 Post-mining mine water management

The connecting mine workings between the different dewatering stations can then be used to transmit the water in the underground to the next active pumping station (fig 3). Indispensable for the underground transmission is the rebound of the mine water – at least to the level of the connecting mine workings. Simultaneously the pumping stations will be reconstructed into well-operating stations: The remaining mine workings of the dewatering station will be closed. With the backfilling of the shaft a system pipes is installed, so that pumping could restart from the shaft with submersible pumps. In case the pumping station is dispensable in the post-mining mine water management, the shafts will be backfilled as a “stand-by well”. This means, that there will be either a pipeline in the backfilling or that the backfilling is realized in a way that allows reopening. Underground blockages or roof falls can stop or limit the underground discharge to the next pumping station. In this case the “stand-by wells” can be activated to access the mine water table. If necessary the rise of the mine water can be controlled by using submersible pumps. To avoid an uncontrolled rebound of the water table, mine water levels in the Carboniferous are constantly monitored. Currently there are nearly 50 monitoring sites in former shafts (RAG AG 2014).

Opportunities of the mine water management concept

Implementing the new mine water management concept is not only an important contribution to meet responsibilities resulting from the coal-mining operations of the RAG Corporation but also an active contribution to environmental protection. The rebound of the mine water level and a reduced pumping height result in a reduced energy use. This implies not only financial benefits but also a reduction of CO₂-emissions. Numerical modelling also predicts the restriction of highly mineralized geogenic water flowing into the carboniferous aquifer with higher water levels. Hence a better water quality will be pumped and discharged into the rivers. With the additional reduction of pumping stations and the concentration of pumping activities discharging directly into the River Rhine, a better water quality in the surface water will be achieved. Especially the river Emscher will completely be free of mine water discharge. Overall 240 km of watercourse will be free of mine water discharge. This would be an important contribution to fulfill the requirements of the Water Framework Directive (RAG AG 2014).

Abandoning the remaining mine workings and using submersible pumps is another important factor of meeting the demands of the post-mining era. The expensive maintenance of the mine workings will be obsolete. In addition less manpower is needed to operate the pumping stations and mine drainage will work in a more cost-effective way (RAG AG 2014).

Financing

In 2007, the German federal state, the coal mining states North Rhine–Westphalia and Saarland, the RAG Corporation and the Union IG BCE (Mining, Chemical and Energy Industrial Union) agreed to discontinue government subsidies for hard coal mining with the end of the year 2018. They agreed to find socially acceptable means of ending hard coal mining, and measures to finance the continuing obligations from the coal mining operations. Beginning in 2019, an annual €220 million will be needed to finance the measures for a permanent management of mine- and groundwater in the former Saar, Ruhr and Ibbenbüren coalfield. Therefore the RAG-Stiftung (“RAG Foundation”) was established in June 2007. To provide the financial means in the future, the RAG-Stiftung is investing its assets in a safe and profitable manner (fig 4). With the beginning of 2019 the foundation will pay for mine water management, polder measures and groundwater purification. The correction of mining-related damage will not be paid by the RAG-Stiftung but directly by the RAG Corporation.

Besides financing the perpetual obligations from mining, the foundation is supporting projects in education, science and culture in the former mining regions. Its aim is to preserve the mining heritage for future generations and help to develop new opportunities for the former industrial regions (www.rag-stiftung.de).

Conclusions

Closely linked to the extraction of hard coal is the management of the mine water. Without any measures to control the inflowing water into the mine, coal extraction is not possible. Therefore mine water management in the hard coal mining districts in Germany has been

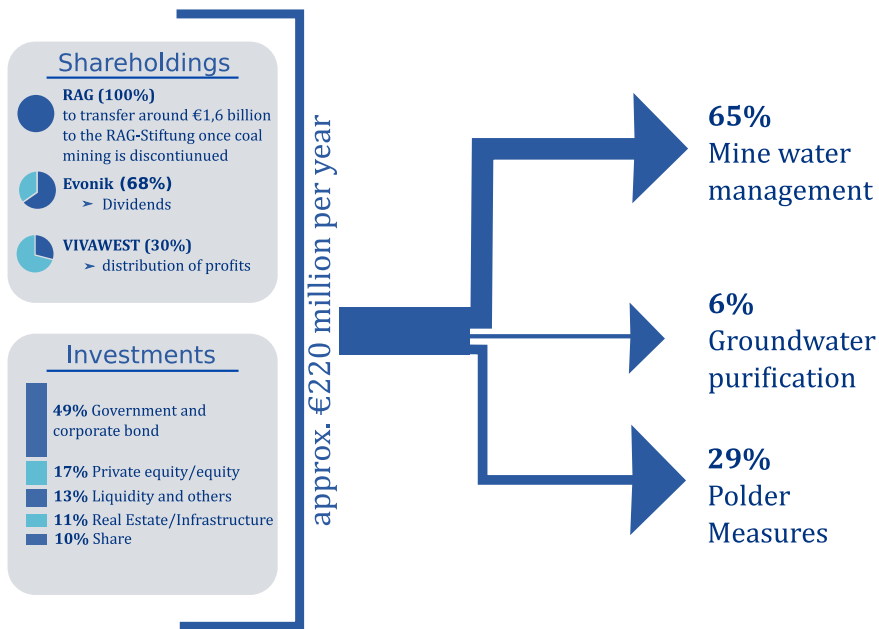


Figure 4 Financing of the perpetual obligations from mining by the RAG-Stiftung (after RAG-Stiftung Infograph "The RAG-Stiftung at a glance")

taking place for more than 250 years. With the closing of the last hard coal mines in Germany in 2018, an important chapter in German industrial history is coming to an end. Nevertheless there are obligations from hard coal mining operations with unlimited duration like the mine water management. The RAG Corporation will take charge of these responsibilities. The development of the post-mining mine water management is an important contribution to fulfill these obligations especially with regard to environmental protection and financing.

References

- Henningsen D, Katzung G (2006) Einführung in die Geologie Deutschlands, Elsevier, München
- Huske, J (2006) Die Steinkohlenzechen an der Ruhr, Dt. Bergbau-Museum, Bochum
- RAG AG (2014) Konzept zur langfristigen Optimierung der Grubenwasserhaltung der RAG Aktiengesellschaft für Nordrhein-Westfalen, Herne www.rag-stiftung.de/en/perpetual-obligations/

Under Ice Treatment and Discharge Of A Tailings Impoundment – A Case Study From The Lupin Mine Nunavut, Canada

Andrea Bowie¹, Arlene Stearman¹, Tom Sharp¹ and Patrick Downey²

¹*SRK Consulting (Canada) Inc., Suite 2200, 1600 West Hastings St., Vancouver, BC, Canada V6E 3X2*

²*Elgin Mining Inc., 750 West Pender St., Vancouver, BC, Canada V6H 2T7*

Abstract Water management and treatment in cold regions faces many challenges, a core one being the limited open water season. In 2015, treatment and discharge of water stored in a tailings impoundment extended into the winter season under complete ice cover. Lime was added to raise the pH (4.7) of poorly buffered water (alkalinity <2.0 mg/L as CaCO₃) into an acceptable range for discharge. In total 2,171,000 m³ were discharged to the environment in 2015 with an average pH of 7.0 (alkalinity 4.4 mg/L as CaCO₃). Under ice water quality remained consistent during discharge and highlights the possibility for extending treatment programs when circumstances warrant it.

Key words Water Treatment, Under Ice, Lime, Neutralization, Adaptive Monitoring

Introduction

The Lupin Mine is located in Nunavut, Canada, 400 km north of Yellowknife, 1,400 km north of Edmonton, at 65° 46' N latitude and 111° 14' W longitude, and approximately 60 km south of the Arctic Circle. The site is accessed by a 1,950 m airstrip, which is Jet aircraft capable, and occasionally the winter road from the diamond mines east of Yellowknife is extended to Lupin. The Lupin Mine has been maintained in a care and maintenance status since 2005. Periodically water that accumulates in the tailings impoundment needs to be discharged. In 2015, treatment and discharge of water stored in a tailings impoundment extended into the winter season. The discharge quality objective was to raise the pH (4.7) of poorly buffered water (alkalinity <2.0 mg/L as CaCO₃) into the permitted pH range of 6.0 to 9.5.

The tailings impoundment is comprised of solids retention cells (Cells 1, 2, 3 and 5) and three liquid polishing ponds (Cell 4, Pond 1 and Pond 2) (Figure 1). All precipitation and runoff falling within the facility ultimately reports to Pond 2 (the Pond) (Figure 2). The Pond is contained by geomembrane lined perimeter dams, Dam 1A and Dam 2. The design allows for the aggradation of permafrost into the dam's core. In order to maintain conservative operating freeboard levels at the perimeter dams, water needs to be treated and discharged every two to four years. The frequency, depends on cumulative runoff and precipitation as well as the amount discharged during the last treatment campaign.

Since the site has been maintained in a care and maintenance status, three treatment campaigns were carried out in 2005, 2009 and 2012. Only the total volume and water quality discharged to the environment was available from the 2005 and 2009 treatment programs. The operational data from the 2012 treatment program was not thoroughly documented, however all compliance data required by the water licence was. All treatment programs were carried out during the open water season, spanning from mid-July to early October.

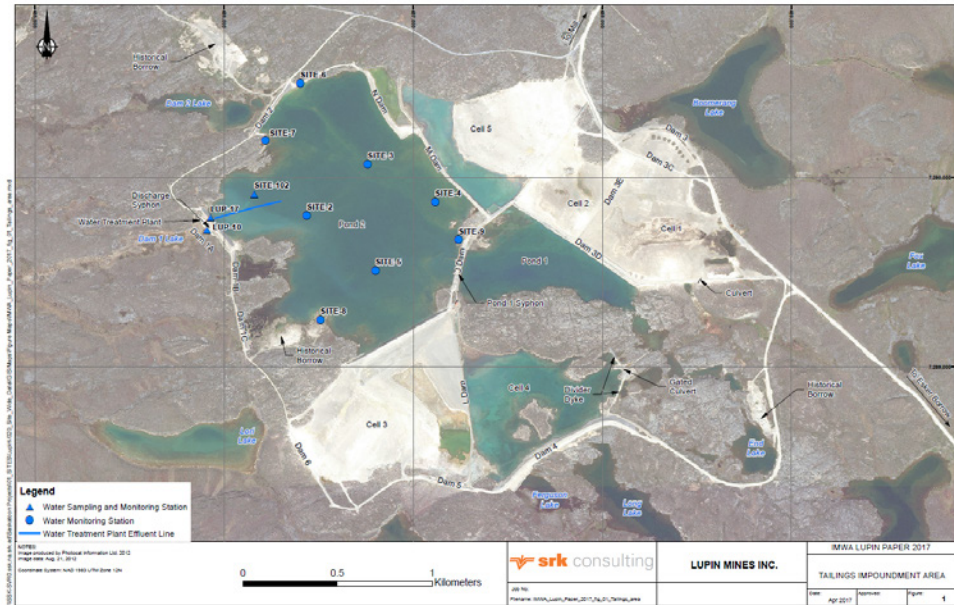


Figure 1 Lupin Mine Tailings Impoundment and Sample Locations

The buffering capacity of the Pond water is very low. Before treatment in 2012 and 2015 water quality data was collected and the alkalinity was <5.0 and <2.0 mg/L as CaCO_3 , respectively. In order to raise the pH of the Pond hydrated lime was added (Pouw 2014). The introduction of OH^- ions into solution consumed acidity (Aubé 2003). Since there was very little alkalinity in solution to buffer the OH^- addition the pH of the solution increased dramatically with small doses of lime (Stumm 1996). The limited buffering capacity means the target pH for treatment can be easily overshot.

Results from the 2012 Treatment Campaign

In total 1,067,000 m^3 of treated water were discharged from Pond 2 in 2012. Five points within the lake were monitored for pH, temperature and conductivity during the treatment program: Site 1 through Site 5 as depicted in Figure 1 (Site 1 is water sampling and monitoring station Site-102). The treatment plant was located on Dam 1A (compliance sample point LUP-10 is downgradient of the siphons on this dam [Figure 1]). The 2012 program was designed to focus on treating water within a Bay area spanning from the sample point LUP-17 out to Site 2 in Figure 1 (Figure 3).

The treatment strategy was to remove water from the Pond, dose it with lime, and pump it back to the Pond and allow the treated water to mix with the untreated portion of pond water. The pond water was pumped to a 22 m^3 tank on Dam 1A. Once full, lime was added to the tank to create a lime slurry of roughly 1 to 10% (by weight). The lime slurry was then pumped back to the Pond via a perforated pipeline within the Bay. This cycle was repeated until the entire Pond was above the target pH. The water was then held in the Pond until it



Figure 2 Lupin Mine Pond 2 of the Tailings Impoundment Area

equilibrated with atmospheric carbon dioxide and mix with the portion of untreated Pond water. The pH decreased into the acceptable range for discharge. Pond water was transferred via two 20” siphons from a depth of 3 m off Dam 1A to Dam Lake, ultimately reporting to Contwoyto Lake.

The main conclusions from the 2012 program was that the Bay could not be treated in isolation, the Bay pH could be easily overshoot, and the lime slurry needed to be dilute (<2% by weight). These findings were discovered during the initial treatment period before discharge. Initially more lime slurry was added to the Bay than required and a portion of the lime particles settled to the bottom. Also since the Pond water was so poorly buffered the pH was initially above the acceptable discharge criteria (pH >9.5). Treatment stopped and the Bay was left to mix with the remaining Pond water and to reach equilibrium with atmospheric carbon dioxide (Figure 3). The pH of the Bay eventually lowered back below 6.5 and treatment started again. pH was challenging to maintain within the range for discharge.

Results from the 2015 Treatment Campaign

For the 2015 treatment program a number of changes were made to use lessons learned by the mine operator in 2012.

- A longer pipeline extended out to Site 2 (500 m). The first 300 m was solid pipe, while the last 200 m had 1 inch holes drilled every 10 m. A plume of treated water spanned 200 m in the outer part of the Bay.
- The lime slurry concentration was maintained between 0.5 and 1% (by weight). Using a lower dosage allowed for greater control when treating the Pond. Especially once an ice layer formed on the Bay and wind assisted mixing and the diffusion of atmospheric carbon dioxide into the Pond was limited.



Figure 3 The Bay area in Pond 2 during the 2012 Treatment Campaign

- The process was changed to a continuous operations. When the treatment tank reached half empty, the intake pump was turned on. Once full, lime was added to the tank. The process was repeated throughout active treatment.
- Five shore sample points were added to the Pond. These locations were introduced to allow for data collection on days when the wind made Pond access by boat unsafe. These locations could still be monitored and provide some direction around the required lime dosage.

Throughout the 2015 treatment program, daily water quality readings were taken from Sites 1 through 9 and LUP-17 for pH, temperature and conductivity. For sites 1 through 5, readings were taken at 1 m, 2 m and 3 m depths on days when there were safe boating conditions. Once discharge commenced, compliance monitoring was conducted at the discharge point (LUP-10). All compliance monitoring and toxicity testing met the Lupin Mine water licence conditions.

The temperature profiles at Sites 1 through 5 remained consistent with increasing depth and decreased from 14.5 to 4°C between August 15 and September 22, respectively. This indicates thermal stratification did not inhibit vertical mixing in the Pond to a depth of 3 m. The Pond was treated from August 18 until October 12. In total 26,000 m³ of water was withdrawn from the impoundment and treated with 73 t of hydrated lime (<1% by weight slurry) and then pumped back into the tailings impoundment to neutralize the untreated portion of water. The Pond pH was indicative of the extent of treatment and used to provide instant

feedback to the treatment program. The pH was a parameter easily monitored in the field through handheld Oakton pH meters calibrated daily before use.

Figure 4 shows the pH recorded at Sites 1 through 5. On September 8 and 9, the wind speed decreased to 1 km/hr and wind mixing was less vigorous. The pH at 3 m for Site 1 and 2 reached 9.1 and 7.5, respectively. Treatment was temporarily shut down. On September 10 the wind picked up again and the pH lowered back down to 6.3 and 5.7 for Site 1 and 2, respectively. Wind mixing also likely increased the rate of carbon dioxide transfer into the pond which also lowered the pH.

The poor buffering capacity of the pond was observed during the September no wind event. No discharge to the environment was occurring at the time, however the sensitivity of the system to active treatment is important for operational control. The adaptive operational approach was implemented. When setting target lime dosages for the day, wind strength and direction as well as the previous pond pH readings were all taken into consideration. The daily operating strategy was discussed with the operators before the start of each shift. Operators were also required to report no wind events to prevent a spike in the Bay pH.

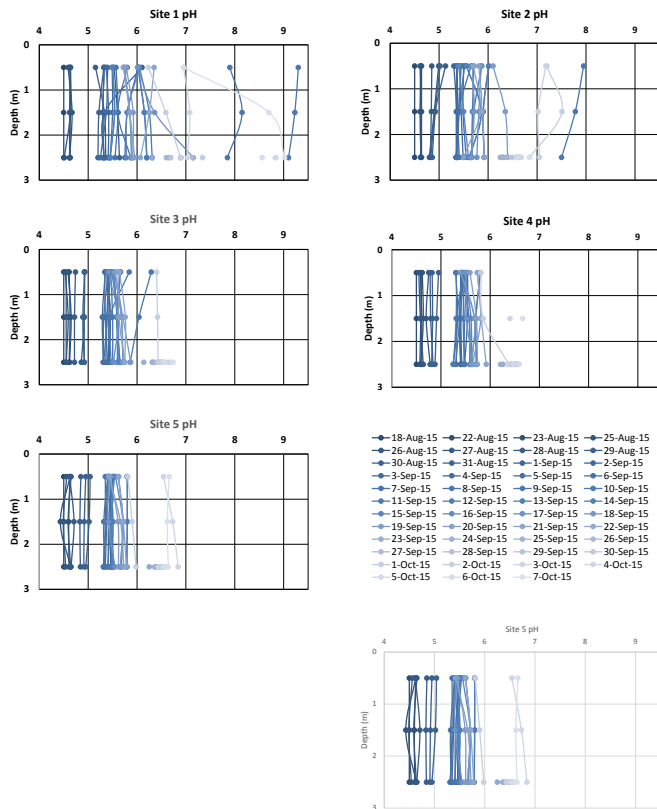


Figure 4 Pond pH Readings throughout the 2015 Treatment Campaign

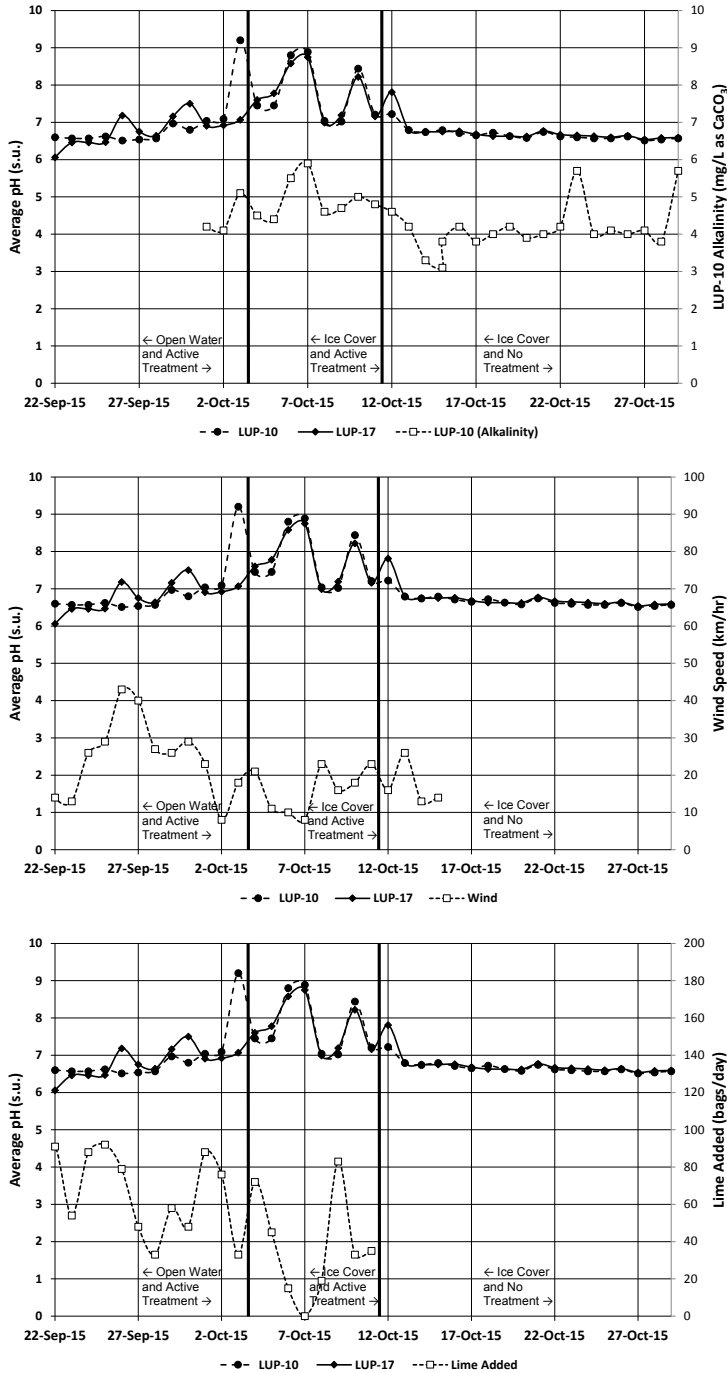


Figure 5 Discharge Alkalinity, Wind Speed and Lime Added with respect to LUP-17 and LUP-10 pH

Discharge to the environment commenced on September 23 and continued until October 29. Three distinct operational conditions occurred during discharge:

- Active treatment and open water
- Active treatment and ice cover
- No treatment and ice cover

During discharge, water quality was monitored at the effluent compliance point (LUP-10). Daily pH, temperature and conductivity readings were recorded in field, and samples were sent to ALS in Yellowknife for additional analysis. Daily alkalinity and pH values recorded at LUP-10 were compared to pH values observed at Sites 1 and 2 (Figure 5). The pH readings were also compared to wind speed to see how wind speed could affect the pH. Additionally, the lime dosage rate was also plotted to see how the dosage was lowered based on observation.

For the open water active treatment period, the water quality observed was largely driven by wind mixing. The average pH and alkalinity were 7.0 and 4.4 mg/L as CaCO₃, respectively. Once ice formation started on the Pond, carbon dioxide diffusion and wind mixing were limited, making lime dosage control more critical. For under ice treatment and discharge, the average discharge pH and alkalinity were 7.8 and 4.9 mg/L as CaCO₃, respectively. Finally for under ice discharge and treatment, the lake chemistry was observed to be fairly consistent. When the Pond water was isolated from the atmosphere, mixing with the untreated water could lower the pH and alkalinity. For under ice discharge without treatment, the average pH and alkalinity steadily dropped to 6.6 and 3.8 mg/L as CaCO₃, respectively.

Conclusions

In total 2,171,000 m³ were discharged to the environment in 2015 with an average pH and alkalinity of 7.0 and 4.4 mg/L as CaCO₃, respectively. The overall treatment program was successful even when extended into the winter. Though winter treatment presents many practical operating issues, especially in an isolated north climate, consistent water quality was maintained throughout under ice discharge.

For similar seasonal treatment programs, there is a possibility to extend the treatment season into the winter. Although this is not a preferred or often planned approach, there are certain circumstances where this could prove beneficial for operations to maintain safe water levels in a tailings impoundment or other holding reservoirs. Once treatment finished, the under ice pond pH and alkalinity decreased suggesting that discharge could not be sustained for long periods without treatment. The treatment program was successful due to the adaptive nature of the monitoring program and constant feedback with the treatment plant operators. Although under ice treatment programs face a number of operational issues, successful execution is possible when extended discharge is required.

Acknowledgements

The authors thank Elgin Mining for the opportunity to publish the work completed at the Lupin Mine during the 2015 treatment program of Pond 2.

References

- Pouw K, Campbell K, Babel L (2014) Study to Identify BATEA for the Management and Control of Effluent Quality from Mines. Mine Environment Neutral Drainage (MEND) Report 3.50.1.
- Stumm W, Morgan J (1996) Dissolved Carbon Dioxide. In Aquatic Chemistry: Chemical Equilibria and Rates in Natural Waters Third Edition. John Wiley & Sons, Inc. Hoboken, New Jersey. pp 171-205.
- Aubé B, Zinck J (2003) Lime treatment of Acid Mine Drainage in Canada. Presented and published at Brazil-Canada Seminar on Mine Rehabilitation. Florianópolis, Brazil, 1-3 December 2003.

Large scale grouting to reconstruct groundwater barrier and its geoenvironmental impact

Wanghua Sui^{1,4}, Binbin Yang^{1,2}, Shitian Zheng³, Rongjie Hu⁴

¹*China University of Mining and Technology, 1 University Rd, Xuzhou, Jiangsu, 221116, China*

²*State Specialized Laboratory for Mine Water Hazards and Prevention, 1 University Rd, Xuzhou, Jiangsu, 221116, China*

³*Xi'an Research Institute of China Coal Technology & Engineering Group, 82.Jinye 1st Road Xi'an Shaanxi, China*

⁴*National Engineering Research Center of Coal Mine Water Hazard Controlling, 157 xichang Rd, Suzhou, Anhui, 234000, China*

Abstract This paper presents an investigation of large scale grouting and its environmental effect on hydrogeological conditions of coal mines. In order to control and mitigate water inrush disasters while mining above or under aquifers, which generally are reinforced by using grouting as an impermeability treatment. The research of the hydrogeological environmental variation can provide theoretical and technical support for the safe mining above or and aquifers and to maximize the economic efficiency of coal production. Based on the water yield and water table of coalmines, the effect of hydrogeological environment have been analyzed in this study.

Key words aquifers, environmental variation, hydrogeology, grouting

Introduction

Grouting applications in many engineering fields, such as foundation and dam reinforcement, groundwater inrush and its prevention and control and sand consolidation, shutdown of abandoned mine, and flooded mine recovery production (Andjelkovic et al. 2013; Kociánová et al. 2016; Li et al. 2016). Groundwater inrush is the most common geological hazard in coal mines in China. In order to prevent and control water inrush disasters when mining above or under aquifers, which generally should be reinforced by using grouting as an impermeability treatment (Xu and Yang 2014). The hydrogeological parameters of aquifers such as permeability coefficient have changed considerably, especially the groundwater seepage field after grouting reconstruction. Hydrogeological characterization of aquifers due to coal mining are important for preventing panels from water inrush, reducing mine drainage and surface water pollution and ensuring mining safety (Xu et al. 2013; Zhang et al. 2006).

The aquifers, coal seam and geological structure and other geological objects are mostly hidden in the ground when mining above or under aquifers. The hydrogeological conditions which are complex to simple will be beneficial to mining, although the structure and function of groundwater environment system have been changed. The research of the hydrogeological environment variation can provide theoretical and technical support for the safe mining above or under aquifers and to maximize the economic efficiency of coal production. Based on the hydrogeological parameters of coalmines in which aquifers have been grouted reconstructions, the negative and positive effect of hydrogeological and groundwater en-

vironment have been analyzed in this study. The characteristics of aquifers with grouting as an impermeability treatment have been obtained. Finally, the effect of hydrogeological environment has been provided for mining and grouting reference.

Grouting for the reinforcement of aquifers

Mining engineering is a typical environmental reconstruction process, the project not only to ensure the safety of mining, but also to ensure that the environment is not destroyed (Zhou et al. 2007). Grouting reinforcement as a method and means to change the hydrogeological condition of rock mass. Grouting reinforcement is an effective method which tries to eliminate the disadvantages of traditional drainage, and strive to promote the realization of safe, efficient and low cost mining. Under certain pressure, the slurry is dehydrated, consolidated or gelled in the void or channel which was originally occupied by water in the grouting purpose layer. The combination of stone body or gel and surrounding rock mass. In this way, the water leakage of the floor rock is blocked, and the strength of the water layer and the water separation performance are improved. The aquifer is changed into an aquiclude, and the water inflow of the panel will be significantly reduced. At the same time, it can protect the precious groundwater resources. The grouting reinforcement of aquifer realized by drilling, and the panel of the borehole is connected with the grouting target layer. When the aquifer is rich in water and the head pressure is high, or the bottom of the coal seam floor is thin, and the aquiclude has a water control structure broken zone. The transformation of the bottom aquifer and aquifuge grouting water control method, by increasing the thickness of water resisting layer which can reduce water inrush coefficient and the water inrush risk, and has significant effect and scale of the project, is currently applied in most coal mines. There are two drilling methods for grouting, drilling underground and ground surface, as shown in Figure 1.

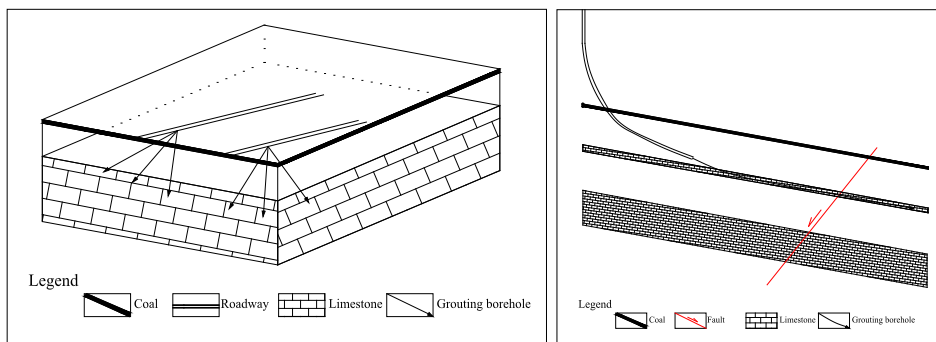


Figure 1 Aquifer grouting reinforcement technique principle

Geological conditions

The Zhuxianzhuang Coalmine is located in the southeast of Suzhou, in Anhui Province in China (Figure 2). Coal measures in the Zhuxianzhuang Coalmine is covered by the Cenozoic, which averages 255m in thickness. The Seam 8 is a productive coal seam which occurred in Shihezi Formation of Permian. The thickness of Seam 8 is between 7.0 and 13.0 m with an

average thickness of 10.03 m. These aquifers and aquiclude in the Cenozoic are formed multi-layer composite structure due to the interactive deposition. The first, second, third, fourth aquifers in the Cenozoic, the fifth aquifers in the Jurassic, karst fractured aquifer in the Carboniferous and Ordovician respectively are mainly aquifers in the coalmine, as shown in Figure 3 .

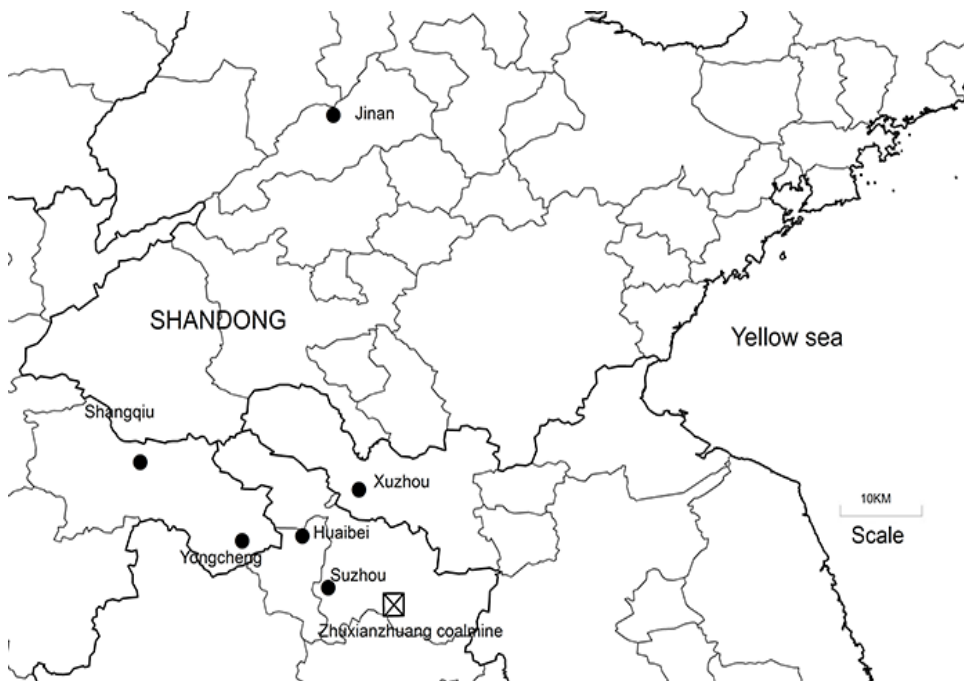


Figure 2 The location of the Zhuxianzhuang Coalmine

There has been hydraulic connection among the fourth, fifth, karst fractured and limestone of the Ordovician aquifers. The water yield property gradually becomes stronger with the increase of conglomerate thickness. There a water inrush has been occurred in the panel of 866-1, and the water source was from the fifth aquifers in the Jurassic. Thus, the overburden failure due to the mining results in the fifth aquifer to be communicated. The fifth aquifers in the Jurassic must be transformed by grouting or dewatering.

Determination of the scheme

The area of coal seam which is covered with the fifth aquifer is 2.8km². 1120 drills needed as the spacing is 50m. The cost of the grouting project is at least \$ 667 million. The cost of this scheme is too high, and it is difficult to exploit under high water pressure. There has been hydraulic connection between the fifth and other aquifers. When the pressure of the aquifer was reduced by dewatering, the fifth aquifer will recharged by the other aquifers, which results in the cost of dewatering is high and a long time need.

Stratigraphic Unit		Columnar legend 100m Scale	Thickness(m)	Remarks
System	Formation			
Quaternary			Average(17.06)	First aquifer
				Aquiclude
			Average(30.98)	Second aquifer
				Aquiclude
			Average(25.97)	Third aquifer
Neogene				Aquiclude
				Fourth aquifer
Jurassic	Sisian Formation		Average(65)	Fifth aquifer
Permian	Shihezi Formation			Aquiclude
				Aquifer
			8	Average(10.03)
	Shanxi Formation			Aquifer
				Aquiclude
				Aquifer
Carboniferous	Taiyuan Formation			Aquifer
Ordovician	Bessii Formation			Aquiclude
	Majagou Formation			Aquifer

Figure 3 The aquifers and aquiclude in the coalmine

Consequently, a curtain wall is needed that will prevent the fifth aquifer recharged by the aquifers outside the wall. Then, the water pressure of the fifth aquifer can be reduced by dewatering inside the wall. The curtain wall has been constructed in the east and north of the field with 3.13 km in length and 40 m in thickness. The drilling footage will be 73,098 m, and 150,000 t cement concrete and 120,000 t fly ash will be consumed.

Geoenvironmental impact

With the large scale grouting performed, the underground water level has been changed inside and outside the wall, as shown in Figure 4. The characteristics of the fifth aquifer with grouting as an impermeability treatment can be obtained. The water level of the fifth aquifer is lower inside than outside of the wall. Because of the pressure of the grouting, the surface has been changed. Figure 5 shows the surface above on the fifth aquifer around the grouting drilled has been uplifted as a result of grouting stress.

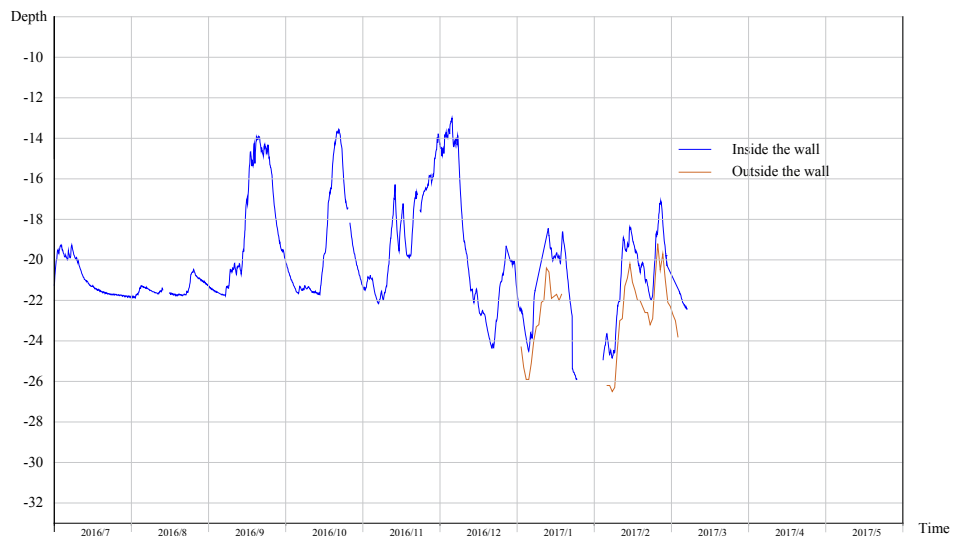


Figure 4 The water level of the fifth aquifer inside and outside the curtain wall

Conclusions

In order to prevent and control water inrush disasters when mining under aquifers, a curtain wall has been constructed by using the grouting as an impermeability treatment. The curtain wall will be constructed in the east and north of the field with 3.13 km in length and 40 m in thickness. The groundwater environment of the coalfield will be reengineered. The influence of mining activities on groundwater environment and surface environment will be reduced. Based on the water yield and water table of coalmines in which aquifers have been grouted reconstructions, the effect of hydrogeological environment has been analyzed in this study. Finally, the effect of hydrogeological environment has been provided for mining and grouting reference.



Figure 5 The surface around the grouting drilled

Acknowledgements

The authors would like to acknowledge financial support from the 973 Program under Grant No. 2013CB227903, and a Project Funded by the Priority Academic Program Development of Jiangsu Higher Education Institutions.

References

- Andjelkovic V, Lazarevic Z, Nedovic V, Stojanovic Z (2013) Application of the pressure grouting in the hydraulic tunnels. *Tunnelling Underground Space Technology*, 37(6), 165-179, doi:10.1016/j.tust.2012.08.012
- Kociánová M, Drochytka R, Černý, V (2016) Technology of remediation of embankment dams by optimal grout. *Procedia Engineering*, 151, 257-264, doi:10.1016/j.proeng.2016.07.370
- Li SC, Liu RT, Zhang QS, Zhang X (2016) Protection against water or mud inrush in tunnels by grouting: A review. *Journal of Rock Mechanics and Geotechnical Engineering*, 8(5), doi:753-766.10.1016/j.jrmge.2016.05.002
- Rafi JY, Stille H (2014) Control of rock jacking considering spread of grout and grouting pressure. *Tunnelling and Underground Space Technology*, 40, 1-15, doi:10.1016/j.tust.2013.09.005
- Rafi JY, Stille H (2015) Applicability of using GIN method, by considering theoretical approach of grouting design. *Geotechnical and Geological Engineering*, 33(6), 1431-1448, doi:10.1007/s10706-015-9910-8
- Xu YC, Yang Y (2014) New progress on floor grouting reinforcement technology of water control in coal mining face. *Coal Science and Technology*, 42(1), 98-101, doi:10.13199/j.cnki.cst.2014.01.023[in Chinese]
- Xu YC, Chen SR, Liu J, Li WM, Wang HZ (2013) Analysis of watery partition and reinforcement effect for reinforcing mining face with floor grouting in jiaozuo coal area. *Coal mining technology*, 2013, 18(3) :110-113, doi:10.13532/j.cnki.cn11-3677/td.2013.03.026 [in Chinese]
- Zhang MQ, Zhang WQ, Sun GQ (2006) Evaluation technique of grouting effect and its Application to engineering. *Chinese Journal of Rock Mechanics and Engineering*, 25(Supp.2), 3909-3918 [in Chinese].

Zhou KP, Gao F, Gu DS (2007) Mining environment regenerating and new thoughts on the development of mining industry. China mining magazine, 16(4), 34-36[in Chinese].

Independent investigation of reclamation at exploration drill holes at the remote Pebble copper prospect, Alaska

Kendra Zamzow¹, Dave Chambers,²

¹*Center for Science in Public Participation, PO Box 1250 Chickaloon, AK 99674 US
kzamzow@csp2.org*

²*Center for Science in Public Participation, 224 North Church Avenue, Bozeman, MT,
59715 US*

Abstract The proposed Pebble mine in Alaska-- a copper, gold, molybdenum prospect – was intensively explored from 2004-2012. No core drilling has occurred since 2012. However, many drill holes have not been fully and properly abandoned and continue to require inspections. In 2016, one week apart, state regulators and a science team (Center for Science in Public Participation, CSP2) investigated over 100 drill sites each, and had different conclusions regarding the success of reclamation.

Key words acid soil, artesian, drill cuttings, mine water, reclamation

Introduction

Most mining projects do not make it past the exploration stage. Drilling began at the Pebble copper-gold-molybdenum prospect in 1988, with intensive exploration 2004 -2012, primarily by the Pebble Limited Partnership (PLP). All drilling was suspended after 2013. There are 1,355 drill holes ranging from piezometers as shallow as 1 foot deep to exploration holes 6,000 feet deep. As scientists unaffiliated with the mining company or State regulators, we investigated the impact of disposal practices, the success of reclamation, and the adequacy of the regulatory method of assessing closure.

Risks to salmon

The development of this world-class copper sulfide deposit poses the risk of releasing acid mine drainage and copper into the environment. Salmon are highly sensitive to copper which, at very low concentrations, affects navigation and predator avoidance (McIntyre et al. 2012). Waters in the area are very low in copper and low in the alkalinity and dissolved organic carbon that could ameliorate impacts of trace elements (PLP 2011; Zamzow 2011; Craven unpublished). Small concentrations of copper that enter salmon habitat could quickly become bioavailable. The deposit sits at the headwaters of three important salmon rivers. Lakes, shallow “kettle ponds”, wetlands, and over 4,000 documented springs are located around the deposit. Salmon have been documented in tributaries throughout the area, including on top of the deposit (Woody and O’Neal 2009).

Drill hole abandonment and waste disposal procedures

Exploration is conducted under a permit (DNR 2014-2016 Multiple Land Use Permit) that requires drill casings to be cut off at ground level, natural vegetation re-established and holes to be plugged

“with bentonite holeplug, a benseal mud...for a minimum of 10 feet within the top 20 feet of the drill hole in competent material. The remainder of the hole will be backfilled to the surface with drill cuttings....Complete filling of the drill holes...is the preferred method...”

In the process of exploratory drilling, water pumped from local ponds and creeks is mixed with drilling muds and circulated downhole to bring “rock flour” drill cuttings to the surface. Drilling muds may contain petroleum distillate, bentonite clay, barite, polyacrylamide and other additives (Wober 2009). Drilling wastewater was discharged directly onto tundra, into kettle ponds, or circulated through drill sumps to settle cuttings before discharge. Drill wastewater sump pits were in partial use at the Pebble site at least as early as 2003, but waste was discharged without sumps through at least 2007 based on review of Alaska Department of Natural Resources (DNR) inspection reports. Drill waste was commonly pumped 500 to 1,000 feet away from the drill site. Records of disposal sites were not kept.

“The practice results in the deposition of finely ground rock, bentonitic clay, and other additive materials being deposited on the tundra. ... Gray coatings of clay were seen in areas where drill fluids have been recently discharged....There is some concern in places where multiple wells are being discharged into topographic depressions.... considerable amounts of clay material being deposited in the depression.” (DNR inspection report July 26-27, 2007)

Regulatory inspections

PLP classifies sites as (1) active, (2) inactive (maintained for future use), or (3) plugged and (A-E) the extent of repair work remaining. A “3E” rating indicates plugged and fully reclaimed. DNR inspected sites at least twice a year 2004-2013 (active drilling) and annually 2014- 2015, apparently targeting sites without a 3E rating. Many sites were inspected only from the air, some inspected only during drilling but not after the hole was abandoned, and no environmental samples were collected.

PLP performed maintenance and revegetation work in fall 2015 and spring 2016. State inspections were July 26-27, 2016 targeting sites rated below 3E and added a selection of random sites. Based on available DNR field reports, over 1,000 sites never had a DNR inspection until 2016.

Methods

Site location and sample site selection

The site is located 200 air miles from Anchorage or ten miles from Nondalton village. There are no roads. The field sampling crew based out of Nondalton and was transported to the site daily by helicopter from August 1 – 5, 2016. Preliminary sites were selected based on a list of PLP’s 1,355 drill holes, with age, depth, and reclamation rating. We chose reference sites (no history of issues) and sites with risk characteristics (e.g. a history of artesian con-

ditions). We included a subset of ponds sampled by the US Geological Survey in 2007-2008 (Fey et al. 2009). Once at a target site, we visited drill holes within walking distance, for a total of 70 opportunistic sites. This optimized our time and introduced some randomness into site selection. In all 101 drill sites were inspected over five days, representing 8% of the total drill holes.

Field methods

Upon arrival at a site, the area was photo-documented. Water pH, temperature, and specific conductance (SC) were measured with a YSI 556 or a YSI 1030 meter at water bodies adjacent to drill sites, in standing water at the base of drill casings, and from the casing at artesian drill holes. Field meters were calibrated each morning and checked each evening in pH buffers (pH 4.01, 7.00, 10.01) and conductivity solution (447 $\mu\text{S}/\text{cm}$). Soil or sediment pH was measured in the field at select sites with a YSI meter after placing soil in a glass beaker and adding distilled water.

Sample collection

Water for general chemistry analysis was collected as grab samples in a 1 liter (1L) HDPE container rinsed three times in site water. Trip and equipment blanks were carried. Duplicate soil samples were collected at four sites and duplicate water samples were collected at three sites. Soil or sediment were collected along a depth of 3-6" and homogenized in a Ziploc[®] bag. At some sites, only the top layer of drill cuttings, evident as fine-grained gray or orange material, was collected. All samples were placed immediately in a cooler containing gel ice, placed in a refrigerator upon return to the field camp, and transported to the laboratory within two to seven days of collection. Samples were analyzed at the University of Alaska in Anchorage. Analyses were performed for pH, SC, fluoride, chloride, sulfate, nitrate, Be, Na, Mg, Al, K, Ca, V, Cr, Mn, Fe, Co, Ni, Cu, Zn, As, Se, Mo, Ag, Cd, Sb, Ba, Tl, Pb, Th, and U. An ion chromatograph (Dionex ICS 5000+) was used to determine anion concentrations. Total metals were determined with an ICP-MS (EPA 200.8, extract method EPA 3050b). No dissolved metals analysis was conducted. For soil and sediment, anions, pH and SC were determined from 1:5 water extracts.

Results

We visited 101 drill holes (Table 1). Many drill sites did not have water on them. Acid drainage water was not observed. Sites with artesian flow, artesian containment (plugs, valves, and bolted plates), or impacted by drill cuttings have current or reasonably foreseeable future environmental impact. Patchy vegetation, while an impact, should resolve over time with the exception of four sites with non-native grasses. "Minor issues" sites had steel drill casings, frequently rusted with no cap, extending from 6 inches to two feet above the ground surface, posing a risk to indigenous hunters on snow machines; snowpoles marked some, but this is not a permanent solution as they require replacement.

Table 1 Drill hole reclamation impact categories. We categorized drill sites based on visual impacts or analytical results. (First column) PLP ranked sites based on their own inspections as 1= active well 2= inactive 3=plugged A-D=sites with past issues or needing frequent inspection. E= fully reclaimed.

PLP site ranking	Fully reclaimed sites	Drill hole cuttings	Drill waste discharge area	Artesian drill holes	Casings with bolts or valves	Vegetation issues	Minor issues
1 A-D	4	1	0	2	1	0	1
2 A-D	0	1	0	2	3	1	0
3 A-D	0	0	0	0	0	0	1
1E	13	4	2	0	2	5	11
2E	3	0	0	1	0	2	6
3E	9	6	1	1	1	13	1
Unknown	0	0	0	1	0	0	2
Total	29	12	3	7	7	21	22

Water samples were all low-neutral pH (pH 5.3 to 7.8). Surface water temperatures (ponds, wetlands) were 11°C – 24°C with specific conductance of 9-109 µS/cm. Artesian sites had lower water temperatures, reflecting groundwater sources, at 6°C – 11°C and higher SC of 97- 289 µS/cm, also generally associated with groundwater. Sediment (n=5) fell within natural wetland pH, between 4.9 and 7.2. Soil pH (n=7) was low-neutral (5.1 to 6.2) except where drill cutting were present.

Vegetation

Non-native species were observed at four sites and spreading downwind; at least one site was intentionally seeded. We consistently observed sites 4 to 13 years old at which natural vegetation had not re-established on reclaimed drill waste pits. Overburden soil covering pits had pH 5.1-6.2 suggesting material was uncontaminated with drill cuttings or sulfides. Failure of re-growth may be due to desiccation of tundra mats placed on overburden or poor reclamation practices.

Artesian drill holes

Artesian upwelling was observed at seven sites; including sites with and without drill casings (Fig. 1). Analytical samples were collected at five artesian sites. Although pH was generally consistent (pH 5.2-7.4), chemistry was not (Table 2). Only two were elevated in copper. Not shown are DDH 4202 and DDH 5330. These open drill stems were wet at the base; both had sediment elevated in copper and molybdenum but only DDH 4202 had elevated metals in water – it is likely both had been leaking at one time, but DDH 5330 is now under control.



Figure 1 Artesian site. Artesian water welled up at a site with two markers (Site DDH 7380/7386) where the casing has been removed. Some casings, like DDH 8410 pictured with a base of cracked cement, had plugs or plates bolted to them, presumably to prevent artesian flow. A similar bolted casing was artesian through a broken ball valve.

Table 2 Artesian water chemistry. Only site DDH 7386 had been inspected before; in 2016 the site we visited had two markers (DDH 7380, DDH 7386). Site DDH 7365 had artesian flow sampled by USGS in 2008; in 2016 flow was contained by a valve, opened to collect sample water. PLP classified site DDH 9475 as “converted to active well”, but it had no casing above ground. Attempts to stop the artesian flow had failed. At site DDH 7382 – the drill casing was capped but grout and artesian water with elevated trace metals was seeping from around the base of the casing into a wetland. *Bold = above Alaska chronic aquatic life criteria*

Site	pH	Sulfate mg/L	Cu µg/L	Na mg/L	Other analytes detected
DDH 7365, artesian contained	7.0	11	15	35	Fe, Mn, Pb
DDH 7365, artesian free-flowing (2008)	6.7	12	3	42	Fe
Artesian, leaking standpipe, no ID	6.9	6	0.7	8	Zn
DDH 7380/7386, artesian flow	na	8	76	13	Al, Ca, Zn, As, Cd and more
DDH 9475, artesian flow	6.9-7.4	700-720	< 2	196	Cl, Ca, Mg, Al, Fe, Mn
DDH 7382, wetland water downhill from leaking casing	5.2	7	215	5	Ba, Al, Fe, Mn, Zn, As, Pb

Drill cuttings

Fine-grained “rock flour” drill cuttings reached the surface in two ways. First, discharged into natural depressions during drilling, they remain on the surface in 2016. Second, post-drilling they appear to have discharged from casings, indicating groundwater pushed cuttings to the surface. Drill cuttings present as fine-grained gray or orange material in depressions, around the base of drill stems and as a trail from the casing downgradient. Cuttings covered and killed vegetation. Visually and chemically these are distinct from locations where vegetation did not re-establish on drill waste pits.

Drill cuttings were universally elevated in copper and molybdenum (Table 3). The pH of drill cuttings was acidic. Soil from depressions and areas in which drill waste had been discharged had pH of 2.7-6.6, depending on the amount of soil collected with the overlying cuttings (data not shown).

Table 3 Drill cuttings chemistry. Baseline is from Fey et al. 2009 and PLP 2011.

Sample description	pH	Sulfate mg/L	Ag mg/kg	As mg/kg	Cu mg/kg	Mo mg/kg
Baseline soil	5-6.0	13-67	<0.2	2-11	9-20	0.4-16
DDH 3129, drill cuttings	3.2	72-546	<5	108-175	422 – 1,650	215-233
DDH 7392, drill cuttings	3.0	109-176	9	13	1,066	334
GH05-60, cuttings with soil	3.5	25-49	<5	14	122	21

Potential impact of drill pits on groundwater

In 2011 an active drilling site (DDH 11540) was sampled at the drill waste pit and in a wetland spring downgradient (Woody et al. 2012). In 2016 we re-sampled the wetland spring. The wetland spring in 2016 had the same pH and conductivity as the 2011 sample, but was elevated in minor and trace elements relative to 2011 (Table 4). We cored drill waste from deep in the pit: a blue-grey material that swelled. Pit waste was elevated in SC (1,150 $\mu\text{S}/\text{cm}$), Cu (475 mg/kg) and Mo (38 mg/kg) relative to background sediment (Cu < 200 mg/kg; Mo < 10 mg/kg). Pit material and water quality changes suggest potential mobilization of Cu and Mo from the pit into the wetland.

Table 4 Wetland spring water, 2011 and 2016. The 2011 data is from Woody et al. 2012. na= not analyzed

	pH	SC $\mu\text{S}/\text{cm}$	Al mg/L	As $\mu\text{g}/\text{L}$	Cu $\mu\text{g}/\text{L}$	Fe mg/L	Mn $\mu\text{g}/\text{L}$	Mo $\mu\text{g}/\text{L}$	Zn $\mu\text{g}/\text{L}$
2011 spring water	6.6	66	0.02	<0.15	0.25	0.09	6	na	2
2016 spring water	6.5	97	0.23	0.7	1.8	7	336	2	4

Discussion

From July 26-27, 2016, State inspectors visited 134 drill sites, requesting PLP perform further work at nine. Although artesian sites were noted by regulators, no samples were collected to understand how the environment was impacted. Discolored water was dismissed as “iron staining” or “anaerobic bacteria activity” with no evidence. They concluded: *“the operator ...addresses maintenance and repair issues ...to industry best management practices..... no violations of any other permits were identified”*. From August 1-5, 2016 we categorized only 29 of 101 drill sites as fully reclaimed to permit standards. Twenty-two sites were inspected by both DNR and CSP2; we both listed 14 with no problems. The remaining eight are artesian or holes with artesian water contained by valves or other means (Table 5).

There are important differences in the interpretation of “reclaimed”. Our interpretation is that sites with drill casings above ground have not met permit conditions. Sites with artesian flow contained by valves or other means may be “stable” but are not fully reclaimed – they will require maintenance.

Interpretation differences influence policy. Our visual observations and analytical chemistry showed discharging drill waste to tundra allows cuttings oxidize and turn acid; this should be stopped. It suggests drill waste pits may leach into groundwater springs; pits may need to be lined. Holes drilled more than ten years ago required replacement of Margo plugs. It is in the best interest of the State of Alaska to understand how frequently these fail and whether sites will need maintenance in perpetuity, and how frequently, drill cuttings have flushed out of abandoned holes. Yet there is no incentive for PLP to provide this information if there are no repercussions for violating permit conditions.

Conclusions

Our investigation determined that often permit conditions were not completely met. Environmental impacts are occurring and will occur in the future. Changes in policies and practices could achieve more effective reclamation and minimize environmental impacts. However, if regulators continue to base their interpretations only on visual inspections, do not recognize disturbances such as non-native vegetation and surface drill cuttings, and rely on mining company assessments to determine sites to inspect, they limit the information they can use to change drilling practices.

Acknowledgements

The authors thank United Tribes of Bristol Bay, Dillingham, Alaska for funding this project. We are deeply appreciative for the accompaniment and knowledge of George Alexie, tribal member of Nondalton.

Table 5 Sites inspected by both DNR and us. The 14 sites with no impact are not shown. Sites with asterisk appear to have had no State inspection until 2016. All sites are ranked as needing

maintenance/inspection.

Drill site	Our assessment	DNR assessment	PLP rank
DDH 5330	Former artesian under control	Artesian repaired with Margo plug 2015. Surface water may be ponded precipitation.	1D
DDH 5332*	No problems	Small artesian flow. Ask PLP for a work plan.	3C
DDH 7365*	Artesian controlled with valve. Standpipe water high in Cu and more	No problems	1C
DDH 7382*	Artesian. Wetland water very high in Cu; many other elements detected.	No problems	2D
DDH 8413	Artesian controlled with bolt or plug.	No problems.	2D
DDH 8423	Artesian controlled with bolt or plug.	No problems. New Margo plug installed 2015.	2D
DDH 9475*	Artesian. Some elements elevated.	Artesian. Fall 2015 re-grouting failed. Ask PLP to continue to investigate a resolution.	1D
GH 06-72*	Artesian. Not sampled.	Minor upwelling. Margo plug is rusty. Sheen is probably bacterial. Change rating to 1B.	1D

References

- Craven A, Maest A, Ryan J, Aiken G, Lipton J, Morris J, Zamzow K (unpublished) Laboratory estimation of Cu-dissolved organic matter complexation and its relevance to fish toxicity in streams draining the Pebble deposit in Alaska
- Fey DL, Granitto M, Giles SA, Smith SM, Eppinger RG, Kelly KD (2009) Geochemical data for samples collected in 2008 near the concealed Pebble porphyry Cu-Au-Mo deposit, southwest Alaska: U.S. Geological Survey Open-File Report 2009-1239, 107 p, <http://pubs.usgs.gov/of/2009/1239>
- McIntyre JK, Baldwin DH, Beauchamp DA, Scholz NL (2012) Low-level copper exposures increase visibility and vulnerability of juvenile coho salmon to cutthroat trout predators. *Ecol Applications* 22 (5): 1460-1471
- PLP (2011) Environmental Baseline Document, Chapter 10 – Trace elements
- Wober G (2009) Case 3AN-09-9173 Exhibit no. 3053 Supreme Court of the State of Alaska
- Woody CA, O'Neal S (2009) Fish surveys in headwater streams of the Nushagak and Kvichak river drainages, Bristol Bay, Alaska, 2008-2009. Nature Conservancy, Anchorage, AK
- Woody CA, Zamzow K, Welker M, O'Neal S (2012) Water quality at Pebble prospect drill rig #6, South Fork Kaktuli River, Bristol Bay, Alaska 22-23 Oct 2011. Nature Conservancy, Anchorage, AK
- Zamzow K (2011) Surface water quality near the Pebble prospect, southwest Alaska, 2009-2010: Nushagak, Kvichak, and Chulitna drainage headwaters. Nature Conservancy, Anchorage, AK

Environmental assessment of closeded coal mine territory using GIS analysis

Nikolai Maksimovich¹, Sergey Pyankov², Elena Khayrulina¹

¹*Institute of Natural Science of Perm State National Research University, 614990, Perm, Genlel st., 4, Russia, khayrulina@psu.ru*

²*Faculty of Geography of Perm State National Research University, 614990, Perm, Bukireva st., 15, Russia*

Abstract Coal mining usually causes complex environmental problems. Reclamation projects for mined land require deep analysis of the spatial distribution of environmental risks. GIS-based assessment was performed to create effective reclamation plans for the area of the abandoned Kizel coal basin (Russia). The GIS-based environmental assessment utilizes a catchment-based approach and methods of mathematical and cartographic modeling using remote sensing data. GIS analysis was used to detect all possible sources of acid waters, visualize the spatial and temporal distribution of pollutants, the areas most threatened by soil degradation, and map the analytical and synthetic criteria characterizing the environmental situation.

Key words abandoned coal mine, GIS analysis, acid mine water, deforestation, flooding

Introduction

GIS technology is viewed as a powerful tool that supports environmental impact assessment and environmental management decision-making in coal mining areas with high anthropogenic pressure in China, USA, and Central Europe (Bian, Lu 2013, Gorokhovich et al. 2003, Naydenova, Roumenina 2009, Yu et al. 2014). GIS technology offers many tools for manipulating spatial data, including environmental monitoring, evaluation and prediction of negative technological environmental impacts, and provides an opportunity for shaping new approaches to the objective analysis of environmental damage, spatial analysis and assessment of environmental pollution, decisions for science-based planning and quantifying efficiency of reclamation activities, etc.

One of the most effective tools for the integrated environment assessment is the development of problem-oriented catchment-scale GIS applications and methods for handling a large amount of heterogeneous spatial data using a mathematical simulation and map-based modeling approach (Pyankov, Kalinin 2013). One of the major advantages of a comprehensive catchment-scale GIS modeling system is the possibility of combining multi-source heterogeneous spatial data for the implementation of the integrated geo-environmental assessment and improvement of environmental monitoring and planning.

The experience of development and implementation of such catchment-scale GIS technologies for environmental assessment and monitoring in areas with high anthropogenic risks is still virtually lacking in Russia. This causes the need for the development of new methods of integrated environmental assessment using a mathematical simulation and map-based modeling approach. The synthetic geo-images produced by modeling can be used to detect

zones threatened by environmental crisis and disaster at regional and local scales (Pyankov, Kalinin 2009). Using such an approach allows us to analyze the wide variety of phenomena and relationships within the geosystem as a whole.

The Kizel coal basin (the Western Urals, Russia) was used as an example to tackle the issues related to the integrated assessment of environmental conditions in areas with high anthropogenic loads (fig. 1).

Mining in the Kizel coal basin had been carried out for more than 200 years. Over 35 million m³ of waste rocks had been accumulated in more than 70 tailingspiles. Mines were closed down in the 1990s, but their closure did not resolve the environmental problems. The cessation of mining led to a gradual restoration of the water table, which in turn posed a serious environmental issue. Twelve disused mine adits started to discharge water to the surface as the water was allowed to rise to its natural position. As a result of discharge, the hydrochemical facies of river water are characterized to be SO₄-Fe-Al, with TDS between 640 and 6,000 mg/L, sulfate concentration between 1,000 and 3,700, iron between 70 and 900, aluminum between 11 and 160 mg/L, and pH of 2.5–2.9 (Maksimovich, Khayulina 2014). Now, the zone of environmental impact exceeds 10 000 km². Rivers play an important role in the long-range transport of pollutants from different sources of surface water pollution.



Figure 1 Location of the Kizel coal basin (a, Russian Federation, b, Perm region)

The national environmental monitoring program adopted for the area of the Kizel coal basin includes collection of water samples from acid mine drainage zones and polluted rivers. Data on land degradation and variations in pollution levels are not available. The results of the national monitoring program did not allow reliable determination of the extent of pollution and identification of secondary pollution sources in order to locate potential areas for land reclamation. The developed GIS is designed to solve the following tasks.

Methods

An integrated environmental assessment of each particular site is carried out using a set of spatial criteria, which can be used to monitor environmental changes and identify areas of environmental concern. These criteria may include pH, sulfate content, heavy metal content, species composition of the surface-water bacterial community, and the area of degraded land. The area of intensive soil pollution with degraded forest was detected from SPOT-6 satellite images in the visible spectrum bands, as well as from high resolution satellite images obtained from open source mapping services.

The visible part of the spectrum are also used to assess the degree of acidic mine water pollution. LANDSAT-8 satellite images are obtained during the summer low water level period, the polluted water is distinguished by brown or orange colours. The ratio of green and red could be used for the identification of contaminated sites of water bodies.

Integrating land survey and remote sensing data allows one to produce synthetic geo-images, which provide objective representation of the environmental conditions and can be used to evaluate the effectiveness of reclamation strategies.

A cartographic and attribute GIS database of the Kizel coal basin consists of the digital elevation models (DEMs) and catchment boundaries delineated from SRTM-90, SRTM-Xband's DEMs. Detailed DEMs were generated for waste rock piles and adjacent areas which will be used for the identification of the direction of drainage from piles and delineation of polluted areas (scale 1:10 000).

The documentation and mapping of data on potential sources of surface water and groundwater contamination (mine drainage, waste rock piles, polluted springs) will help identify variations in the pollutant levels at watersheds.

Results

Both historical data and satellite images are used to compile the inventory of flows and mine drainage from waste rock piles over the entire coal basin area. The determination of hydrographic characteristics on 1:100,000-scale digital topographic maps revealed the exceedance of the maximum contaminant levels streams (tab. 1).

River bottom sediments the chemical composition of which is impacted by the discharge of acid mine water and drainage water is recognized as a permanent secondary source of contamination to river systems. Field studies showed that mining-impacted bottom sediments of rivers contain large amounts of amorphous Fe and Al hydroxides (up to 77 %) and are bright orange in color. They accumulate in stream reaches and are present as rusty coatings on coarse-grained sediments on channel bars. Aqueous extracts have high contents of sulfates and iron oxides and pH of 2.5-4. Common accessory minerals are goethite (до 2 %), lepidocrocite (up to 3 %). Annual variations in river water level lead to the increase in the areal extent of contaminated bottom sediments and also cause harmful effects on coastal ecosystems.

Table 1 Proportion of polluted rivers in the Kizel coal basin

Basin	Length, km		Proportion, %	Total length of rivers in the basin, km		
	Main stream	Polluted portion		Total	Polluted	Polluted by mine drainage waters
Yaiva	303	138	45	4864	417	178
Kos'va	307	103	33	4404	170	40
Us'va (without Yuzh. Vil'va River)	272	93	34	2237	94	-
Yuzhnaya Vil'va	173	35	20	1851	48	10
Chusovaya (without Us'va River)	307	74	13	7823	88	28

LANDSAT images of rare flood events were used to detect and map areas of potential contamination in river floodplains during flooding (fig. 2).

Mathematical and map-based modeling of the river floodplains impacted by mine drainage from the Kizel coal basin combined with the results of field studies was used for the interpretation of remote sensing images and modeling of flood prone areas. The results of interpretation showed that the polluted area is much larger than previously reported.

The total area of the river floodplains where near-stream vegetation could be affected by abandoned mine drainage during a peak flood event was estimated (from a LANDSAT image of 23.05.1998) to be 9642 ha.

The evaluation of environmental damage and development of mitigation measures should be done on the basis of estimating the area of degraded land and forest as a result of soil acidification or increased trace element concentrations. High-resolution satellite imagery and field data are used to detect and map degradation in land areas (fig. 3).

These data will be used to control the progression of changes in environmental conditions as a result of acid mine drainage from waste rock piles, mine waters and contamination caused by polluted flood water.

Conclusions

The proposed method of GIS-based environmental assessment uses mathematical simulation, map-based modeling, and remote sensing data. GIS analysis was used to identify all sources of acid mine drainage, map spatial and temporal distribution of pollutants, analytical and synthetic criteria characteristic of the environmental situation, e.g., soil degradation and deforestation. The results of this project were used to update historical data from the national environmental monitoring program, and delineate areas of bottom sediment contamination which are considered as a secondary source of environmental contamination.

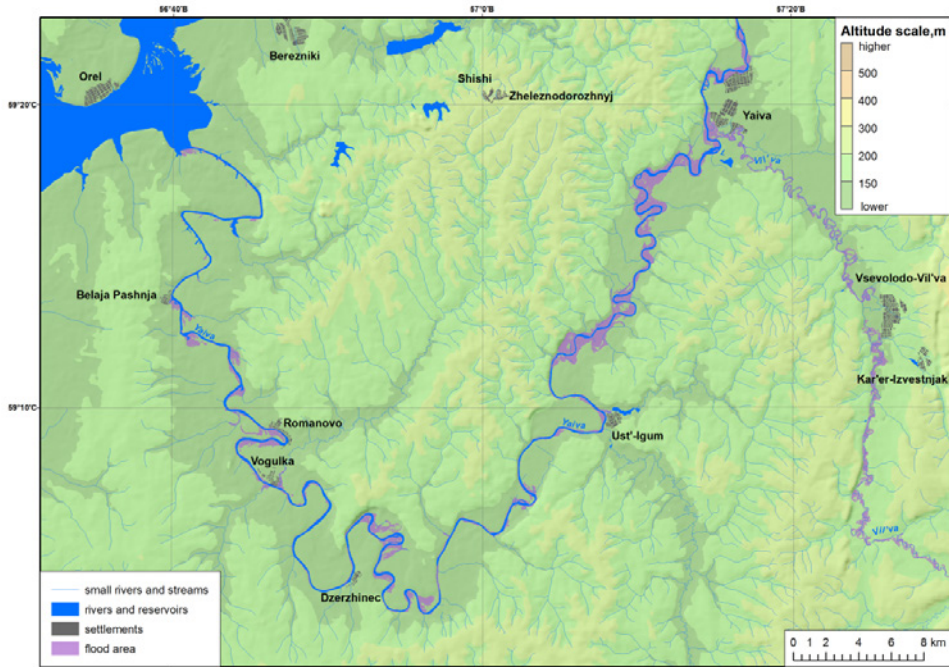


Figure 2 Flood prone areas along the Yaiva and Severnaya Vil'va Rivers

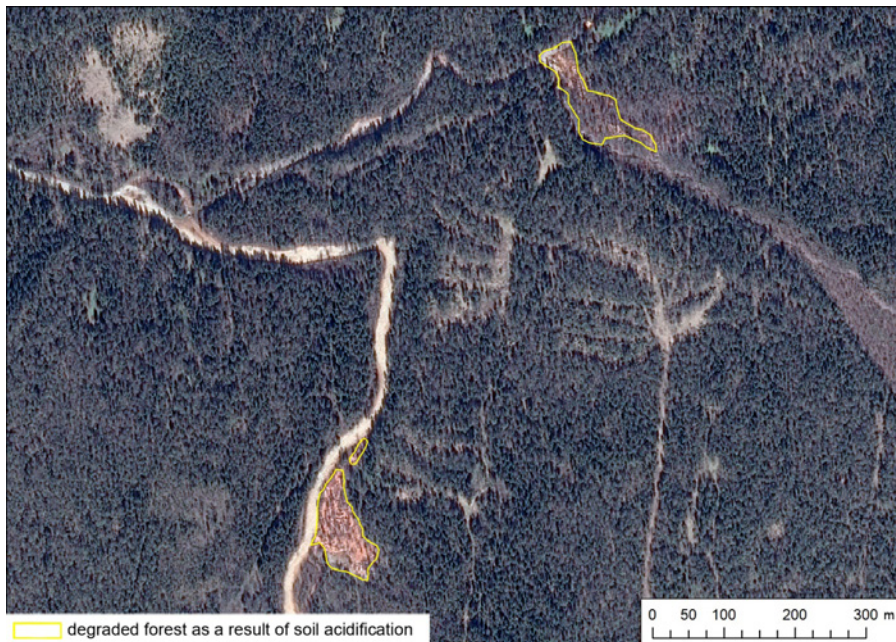


Figure 3 Areas of forest degradation as a result of acid drainage seeping from mine shafts in the Sev. Vil'va River valley

GIS analysis was used to map areas with the highest environmental risks and prioritize reclamation activity. The government can use these results for the implementation of a complex reclamation project within the Kizel coal basin.

Acknowledgements

This study was supported by the Russian Foundation for Basic Research and the Russian Geographical Society (projects no. 17-05-41114 and no. 17-45-590793).

References

- Bian Z, Lu Q (2013) Ecological effect analysis of land use change in coal mining area based on ecosystem service valuing: A case study in Jiawang. *Environmental Earth Sciences* 8:1619 – 1630, doi: 10.1007/s12665-012-1855-0
- Gorokhovich Y, Reid M, Mignone E, Voros A (2003) Prioritizing Abandoned Coal Mine Reclamation Projects Within the Contiguous United States Using Geographic Information System Extrapolation. *Environmental Management* 32(4):527 – 534, doi: 10.1007/s00267-003-3043-1
- Maximovich N, Khayrulina E (2014) Artificial geochemical barriers for environmental improvement in a coal basin region. *Environmental Earth Sciences* 72:1915-1924, doi: 10.1007/s12665-014-3099-7
- Naydenova V, Roumenina E (2009) Monitoring the mining effect at drainage basin level using geoinformation technologies. *Central European Journal of Geosciences* 1:318 – 339, doi: 10.2478/v10085-009-0023-6
- Pyankov SV, Kalinin VG (2009) Methodological aspects of spatial analysis of the river runoff formation by using mathematical cartographical modeling. *Russian Meteorology and Hydrology* 34(1):58-61
- Pyankov SV, Kalinin VG (2013) Development of generalized integral index for estimating complex impact of major factors of winter runoff formation. *Russian Meteorology and Hydrology* 38 (7): 496–502
- Yu XX, Lü WC, Yang X, Zhu YZ, Jiang FW, Huang H, Hang YF (2014) Research on the automatic monitoring system for coal mining subsidence. *Applied Mechanics and Materials* 644–650:1355-1360

Removal of Metals from Mining Wastewaters by Utilization of Natural and Modified Peat as Sorbent Materials

Gogoi, H.¹, Leiviskä, T.¹, Heiderscheidt, E.², Postila, H.² & Tanskanen, J.¹

¹ *University of Oulu, Chemical Process Engineering, P.O. Box 4300, FIN-90014, University of Oulu, Oulu, Finland*

² *University of Oulu, Water Resources and Environmental Engineering, P.O. Box 4300, FIN-90014, University of Oulu, Oulu, Finland*

Abstract This study investigated metal removal efficiency of natural (N peat) and HCl treated peat (HCl peat) using batch sorption tests with real mining wastewaters. FTIR and XPS studies revealed that peat modification did not alter the structure of the sorbent. HCl peat exhibited higher maximum metal uptake capacity (22.4 mg Ni/ g) than N peat (17.9 mg Ni/g). Sorbents removed arsenic most efficiently (80%, dosage 1 g/L). Optimum contact times ranged between 30–60 min. Our study revealed that although HCl peat had better settling properties, N peat displayed overall better purification performance, representing thus the most cost-effective and sustainable option.

Key words Biosorbent, sorption, dosage, contact time

Introduction

Mining wastewater releases metals such as lead (Pb), copper (Cu), nickel (Ni), zinc (Zn), chromium (Cr), cadmium (Ca), mercury (Hg) and manganese (Mn) into the environment. These metals are hazardous as they do not biodegrade and tend to bioaccumulate (Fu & Wang 2011). In an attempt to provide a sustainable alternative to conventional water purification methods, the application of biosorbents was studied. The metal removal efficiency was assessed of natural and modified peat, a cheap and abundantly available biomass in Finland. Peat consists of organic compounds with various active functional groups such as hydroxyl, carboxyl, sulphonic and phenolic groups, which are responsible for the rapid metal cation uptake onto their surface (Bartczak *et al.* in press).

However, little information is available on how such biosorbents behave when introduced into real wastewaters (Keränen *et al.* 2015). Thus, the main objective of this research was to study the viability of using natural (N peat) and modified peat (HCl peat) for metal removal from wastewaters obtained from a mining site in northern Finland. The modification of peat was performed using hydrochloric acid (HCl), aiming at enhancing the wettability and settling properties of N peat since it is quite hydrophobic and exhibits poor settling behavior. Additionally, HCl treatment should desorb metal ions, which are sorbed on N peat, improving its metal sorption capacity. The goal was to evaluate the sorption efficiency of N peat and HCl peat at different contact times and temperatures (23 °C and 5 °C) to simulate the conditions that can be found in different applications.

Materials and Methods

Chemicals and raw materials

Peat obtained from Stora Enso Veitsiluoto pulp mill in Kemi, Finland was dried at 80 °C for 24 h and sieved to 90-250 µm size fraction. The raw mining drainage water tested had the following characteristics: 79.4 µg/L aluminum (Al), 28.6 µg/L arsenic (As), 591 µg/L iron (Fe), 1510 µg/L Mn, 128 µg/L Ni, 180 µg/L antimony (Sb), 3.9 mg/L dissolved organic carbon (DOC), 14000 µg/L total nitrogen, 7800 µg/L NO₃-N, 340 µg/L NO₂-N, 5500 µg/L NH₄-N, 84 mg/L chlorine, 1000 mg/L SO₄. Filtered samples (0.45 µm) of the mining drainage water contained: 9.15 µg/L Al, 16.2 µg/L As, 9.85 µg/L Fe, 1475 µg/L Mn, 129.5 µg/L Ni, 170 µg/L Sb and 3.4 mg/L DOC. The measured electrical conductivity was 2.3 mS/cm.

The dilution of concentrated HCl solution and dissolution of solid nickel nitrate (Ni(NO₃)₂) in ultrapure Milli-Q water were conducted in the creation of stock solutions (HCl 0.2 M and 1000 Ni mg/L). The pH of the Ni(NO₃)₂ solutions was adjusted using 0.1 M HCl and 0.1 M NaOH. Nitric acid (0.5%) (HNO₃, 65%) was used in the preservation of water samples for metal analysis.

HCl modification of peat

Raw peat (15 g) was weighed in a glass beaker to which 250 mL of 0.2 M HCl was added. The mixture was stirred at 25 °C for 2 h and washed with water (about 1000 mL was used in total) to bring the pH to 5. The product (HCl peat) was dried at 60 °C overnight. The same procedure was performed for a second batch using 60 g of peat (1L of HCl was used). The HCl peat gave a yield of 92.1 ± 6.5 %.

Batch Sorption Experiments

Pre-selected sorbent mass was weighed and transferred to polypropylene bottles. A pre-selected volume of water was then added to the bottles, which were then transferred to some rotary shaker equipment (30 rpm/min). The samples were shaken for a pre-determined period at room temperature (23 ± 2 °C) and the sorbents were then separated from solution by centrifugation (4500 rpm for 1.5 min) followed by syringe filtration (0.45 µm). The extracted solutions were sent for metal analysis and their final pH was measured. The maximum sorption capacity curve of the sorbents was obtained using a similar batch sorption procedure where 1 g/L dosage of peat sorbent was shaken with 50 mL of the nickel nitrate solutions (2-75.8 mg/L). The initial pH of the nickel nitrate solutions ranged between 5.6-6.0 and the pH of the mixture was adjusted to 5.8-6.0 after one hour of shaking to avoid a significant pH change. While studying the effect of the dosage, batch tests were conducted at room temperature (23 ± 2 °C) using 1-10 g/L of peat sorbent, 200 mL of mining drainage water (pH_{initial}: 7.6-8.0) and 24 h contact time. The effect of the contact time was studied at two temperatures (23 ± 2 °C and 5 ± 2 °C) using a dosage of 2 g/L and contact times of 15 min, 30 min, 60 min and 24 h.

Analyses

Elemental analysis was performed using inductively coupled plasma mass spectrometry (ICP-MS) according to standardized methods SFS-EN ISO 17294-2:2005. The pH measurements were conducted with a Metrohm 744 pH meter. The electrical conductivity was measured using a VWR Phenomenal PC 5000H and turbidity was determined with a Hach Ratio/XR turbidimeter.

The FTIR spectra of fresh and treated ground sorbents were measured in the 400-4000 cm^{-1} wave number region with a Bruker Vertex V80 vacuum FT-IR spectrometer and using the OPUS program. The XPS spectra were carried out for fresh (as such and ground) and treated (ground, 2 g/L, room T, 24 h, washed with deionized water until neutral pH was attained) sorbents with a Thermo Fisher Scientific ESCALAB 250Xi and using a monochromatic Al K α source (1486.6 eV). The sorbents were mounted on indium foil. The XPS data analyses were performed with Advantage software and the Shirley function was used to subtract the background. The charge correction was performed by setting the binding energy of adventitious carbon to 284.8 eV. The C 1s spectra were fitted using a Shirley background and a Gaussian-Lorentzian sum function.

Results

Characterization of Biomass Sorbents

The FTIR spectra of N peat and HCl peat are presented in Fig. 1a, which shows that both sorbents exhibited similar peaks, indicating no visible changes due to acid treatment. Broad bands at 3421 cm^{-1} and 3529 cm^{-1} were observed in both peat materials, representing the presence of hydroxyl groups and hydrogen bonds, as it has been well established that the spectral range between 3200-3600 cm^{-1} represents these functional groups (Nakanishi 1962; Williams and Fleming 1995). Groups of methoxyl and $-\text{OCH}_3$ (C-H stretching vibrations) can be seen at transmittance bands 2920 cm^{-1} and 2921 cm^{-1} (Herbert 1960). Stretching vibrations of C-H have also presented at 2852 cm^{-1} (Bartczak *et al.* in press). In both N peat and HCl peat, carboxylic groups (COO^-) were present at 1650 cm^{-1} , which presence is supported by Bulgariu *et al.* (2011), where the FTIR spectral range between 1600-1650 cm^{-1} of natural and modified peat proved to be related to carbonyl bonds from carboxylic acids. The stretching vibrations of C-O bonds were exhibited at 1091 cm^{-1} , which according to Bartczak *et al.* (in press) appear in the range of 110-1000 cm^{-1} . Interestingly, the N peat and HCl peat used had nearly identical spectra (Fig. 1a) to their fresh forms, thus it could be inferred that the sorbents were fairly stable.

According to the XPS data, the fresh N peat and HCl peat surface contained mainly carbon and oxygen with small amounts of nitrogen, sulphur and iron. The C 1s spectra of fresh peat products were fitted to three peaks (Fig. 1 b), namely 1) aromatic and aliphatic carbon (C-C, C-H; 284.8-284.9 eV), 2) carbon having a single bond with oxygen and nitrogen (C-O, C-N; 286.2-286.4 eV) and 3) carbon having two bonds with oxygen (O-C-O, C-O; 288.0-288.2 eV). HCl treatment of peat did not significantly affect the element content of the peat

surface or the C 1s spectrum. The N 1s spectrum showed a single peak at 400.0-401.0 eV and the nitrogen in peat was mainly present in amide form. The presence of small amounts of pyridinic nitrogen peaks and quaternary nitrogen is possible with peat material, and they exist at the lower and higher BE side of the amide nitrogen peak (Kelemen *et al.* 2006).

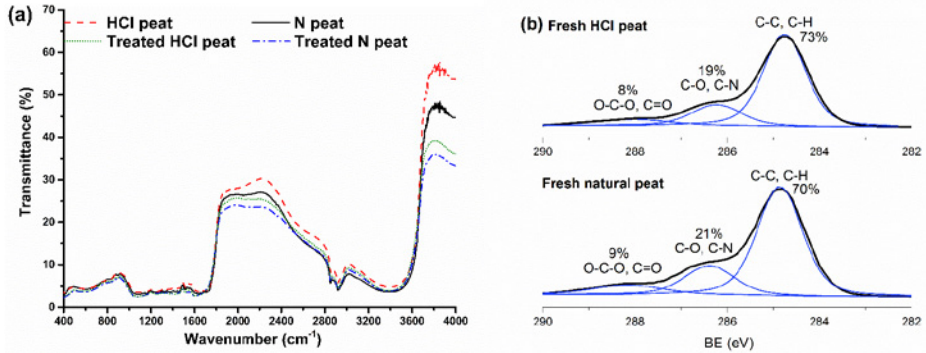


Figure 1. (a) FTIR spectra of fresh and treated N peat and HCl peat samples; (b) XPS spectra of C 1s for fresh HCl-treated and natural peat. Thick solid line: experimental curve; thin solid line (blue): fitting curve.

Maximum Capacity and Effect of Sorbent Dosage

The maximum sorption capacity obtained for N peat was 17.9 mg Ni/g while for HCl peat it was 22.4 mg Ni/g (data not shown). Thus, HCl peat exhibited a higher metal sorption capacity compared to N peat. The metal removal efficiency of the peat sorbents from mining drainage waters at different dosages (1-4 g/L), room temperature and 24 h contact time were evaluated for Al, As, Fe, Mn, Ni and Sb but it was observed that most of the Al and Fe were removed when the mining drainage water was filtered (0.45 μm syringe filters). Hence, removal rates of As, Mn, Ni and Sb were analyzed (Fig. 2). The pH of treated wastewater decreased with an increasing sorbent dosage. The pH decrease was more accentuated in the HCl peat treated samples ($\text{pH}_{24\text{h}} = 4.6\text{-}6.6$) than in the N peat treated samples ($\text{pH}_{24\text{h}} = 6.1\text{-}7.1$).

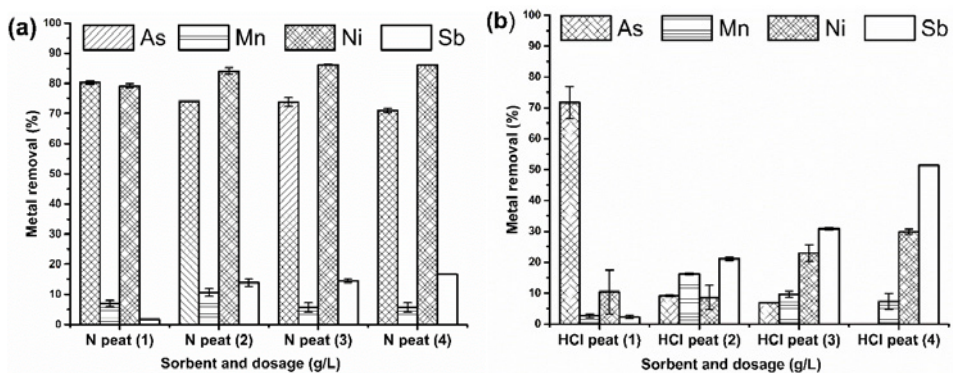


Figure 2. Effect of sorbent dosage (1, 2, 3 or 4 g/L) on metal ion removal % using (a) N peat and (b) HCl peat. 23 ± 2 °C. Error bars represent max and min of experiment replicates.

N peat proved to be a highly efficient sorbent, which achieved >80% Ni removal and >70% As removal at all tested dosages (Fig. 2 a). The optimum dosage for Ni removal was 2 g/L while for As it was 1 g/L. Low removal efficiencies were observed for Mn and Sb at all tested dosages. The sorption performance of HCl peat was significantly lower than that of N peat (Fig. 2 b). Efficient As removal (80%) at 1g/L was achieved; however, higher dosages exhibited lower to negligible removal results. Unlike with N peat, Sb removal increased with an increasing dosage of HCl peat, reaching 50% removal at 4 g/L.

When comparing the surface composition of fresh and used sorbents, only slight changes could be noticed. For instance, a larger amount of iron (≈ 0.16 atomic %) and the appearance of a small amount of calcium (≈ 0.5 atomic %) was observed at the sorbents' surfaces. The presence of As, Mn, Ni and Sb was not detected by XPS.

Effect of Contact Time and Temperature

The effect of contact time on the metal removal efficiency of N peat and HCl peat was tested at room temperature (23 ± 2 °C) and at 5 °C (Fig. 3 and 4). Leaching of Mn into the treated wastewaters occurred, thus Mn is not represented in the figures. The wastewater samples treated with HCl peat exhibited a more significant drop in pH ($\text{pH}_{24\text{h}} = 5.8$) compared to N peat ($\text{pH}_{24\text{h}} = 6.6$).

Regarding the experiments with N peat conducted at 23 ± 2 °C (Fig. 3 a), As and Ni were the only metals effectively removed. Their removal rates increased linearly with contact time. Optimum Ni removal (85%) was achieved after 24 h. For As, the optimum contact time was 60 min resulting in 70% removal, although a slight increase in removal at a higher contact time was observed. In the case of HCl peat (Fig. 3 b), the optimum contact time was 30 min for As and Ni (50% and 55% removal, respectively). Overall, the metal removal efficiency of HCl peat was lower than that of N peat irrespective of the contact times, and the metal being evaluated (%) significantly decreased at 24 h contact time.

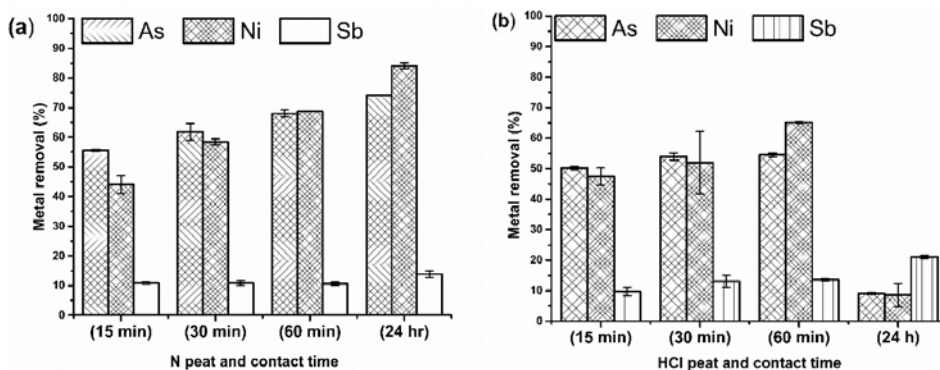


Figure 3. Effect of time (23 ± 2 °C) on metal removal (%) from mining wastewater using (a) N peat and (b) HCl peat. 2 g/L dosage. 232 °C. Error bars represent max and min of experiment replicates.

The effect of contact time at low temperature (5 °C) is shown in Fig. 4. The $\text{pH}_{24\text{h}}$ of wastewater samples treated with HCl peat and N peat was around 6.2 and 6.8, respectively. The experiments at 5 °C had lower metal removal (%) than at room temperature for both sorbents. For N peat, As and Ni removal (%) increased with time; the optimum As (60%) and Ni (50%) removal was achieved at 60 min. However, no significant dependence on contact time was observed for HCl peat; although there was a slight increase in the amount of As removal at 60 min (55%) compared to 30 min contact time (50%).

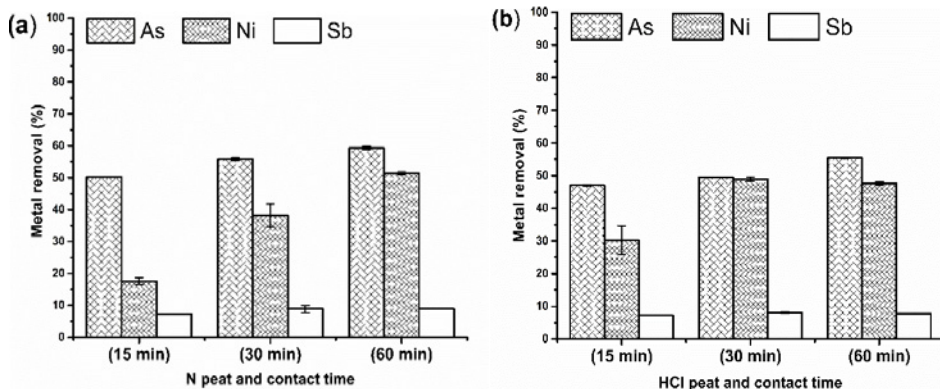


Figure 4. Effect of time (5 °C) on metal removal (%) from mining wastewater using (a) N peat and (b) HCl peat. 2 g/L dosage. 5 ± 2 °C. Error bars represent max and min of experiment replicates.

Discussion

In this study, the metal removal performance of N peat and HCl peat was evaluated for the treatment of mining wastewater at different doses and contact times. Overall, N peat performance was clearly better than that of HCl peat. The aim of treating peat with HCl acid was to enhance the sorbent metal uptake capacity by altering its structure so that the functional groups present were more readily available for adsorbing metal ions. Furthermore, the goal was to improve the settling characteristics of the peat particles. Although not so significant in batch test conditions, enhancing the settling characteristics of peat would be very valuable in real applications. Visual observations pointed to an improved settling ability of HCl peat but its sorption capacity was lower than that of N peat throughout the study. The sorption efficiency of a sorbent for a particular metal depends on several factors such as the affinity of the metal ion towards sorption sites on the sorbent, composition and pH of the wastewater. The main functional groups in the peat responsible for metal uptake are considered to be the phenolic and carboxylic groups (as shown in FTIR results) provided by fulvic and humic acids, which are capable of rapid metal cation uptake in exchange for release of H^+ ions into the solutions (Brown, *et al.* 2000; Holub & Balintova 2014). Acidic treatment of peat contributed to a lower equilibrium pH of the treated wastewater, which can be related to release of hydrogen ions. Thus a straight comparison between the sorbents is difficult due to the different equilibrium pH values of the treated wastewater. Gosset *et al.* (1986) also reported that unsieved and unacidified samples of peat performed better in

copper removal compared to sieved, acid-modified peat samples. However, other studies such as the one reported by Batista *et al.* (2009) found that HCl modification of certain peat species increased their Cr(III) uptake.

The sorption efficiency of peat towards different metals was observed to depend on the metal species present in the treatment solution. N peat and HCl peat exhibited high to moderate As and Ni removal but low Mn and Sb removal capacity. Studies have shown that this difference in metal ion affinity towards peat can be attributed to chemical properties such as the ionic potential, reduction potential and electronegativity of the metal ion among other factors. For example, the research by Liu *et al.* (2008) proved that the reduction potential of metal ions is related to their affinity to be adsorbed on peat. The standard reduction potential (E°) of As(V), Ni, Sb(V) and Mn are 0.560 V, -0.25 V, 0.605 V and -1.185 V respectively, which (except for Sb(V)) are in line with the findings of Liu *et al.* (2008), who stated that the higher the reduction potential, the higher the metal ion removal (%). Since the final pH of treated wastewater was found to be slightly acidic after the sorption experiments, the reduction potential of As and Sb for acidic solutions was considered. Speciation of As and Sb depends on the redox potential and pH; however, the particular oxidation states of As(V) and Sb(V) were assumed to be present in the studied wastewaters based on reports that As was present as arsenate [As(V)] and Sb predominantly existed as antimonite [Sb(V)] under oxidizing aerobic conditions such as in surface waters (Nicomel *et al.* 2015). Throughout our experiments, As and Ni were the most efficiently removed metals, followed by Sb with Mn. This is in agreement with the dependence of metal affinity towards peat on reduction potential. It is worth mentioning that the removal mechanism of metalloids (As and Sb) may be different than metal cations such as Ni, since metalloids are capable of co-precipitating as hydroxides with metals like Fe and Mn present in high concentrations in mining waters, but the extent of this co-precipitation mechanism is still not clear (Palmer *et al.* 2015).

Experiments studying the effect of contact time at 23 ± 2 °C indicated that, once equilibrium had been achieved, the HCl peat sorbent reached saturation and the elongated contact time led to metal desorption into the solution. This is particularly challenging for the treatment of changing water quality i.e., metal concentrations that fluctuate over time. In addition, contact time experiments conducted at 5 °C showed that temperature plays a key role in the sorption behavior of N peat while acid-modified peat was not significantly affected by the change in temperature.

Conclusions

From the batch sorption tests carried out to study the effect of dosage, contact time and temperature on the performance of natural and HCl-modified peat for the treatment of mining wastewaters, the following can be concluded:

1. N peat was a better sorbent than HCl peat. The equilibrium pH of HCl peat was considerably lower than that of N peat, thus the lower pH due to acid treatment coupled with the nature of the wastewater could have led to the lower sorption efficiency of modified peat.

2. Arsenic and nickel were the most efficiently removed metals by both N peat and HCl peat. Removal of Mn and Sb was very low in all sorption experiments except for the 4 g/L dosage of HCl peat, which removed around 50% Sb.
3. The sorbents performed better at 23 ± 2 °C in comparison with 5 ± 2 °C. The removal of As was fairly independent of contact time while Ni removal was highly dependent on contact time.

Acknowledgements

The study has been done as part of project “Development, Evaluation and Optimization of Measures to Reduce the Impact on the Environment from Mining Activities in Northern Regions”, funded from Interreg Nord 2014-2020 program.

References

- Bartczak P, Norman M, Klapiszewski L, Karwańska N, Kawalec M, Baczyńska M, Wykowski M, Jakub Z, Ciesielczyk F, Jesionowski T (in press) Removal of nickel (II) and lead (II) ions from aqueous solutions using peat as low-cost adsorbent: A kinetic and equilibrium study. *Arab. J. Chem.* In press.
- Batista APS, Romão LPC, Arguelho MLPM, Garcia CAB, Alves JPH, Passos EA, Rosa AH (2009) Biosorption of Cr(III) using natura and chemically treated tropical peats. *J. Hazard. Mater.* 163, pp. 517-523.
- Brown PA, Gill SA, Allen SJ (2000) Metal removal from wastewater using peat. *Water Res.* 34 (16), pp. 3907-3916.
- Bulgariu L, Bulgariu D, Macoveanu M (2011) Adsorptive performance of alkaline treated peat for heavy metal removal. *Sep. Sci. Technol.* 46, pp. 1023-1033.
- Fu F, Wang Q (2011) Removal of heavy metal ions from wastewaters: a review. *J. Environ. Manage.* 92, pp. 408-418.
- Gosset T, Trancart J-L & Thévenot DR (1986) Batch metal removal by peat. *Water Res.* 20 (1), pp. 21-26.
- Herbert H (1960) Infrared spectra of lignin and related compounds. II. Conifer lignin and model compounds. *J. Org. Chem.* 25, pp. 405-413.
- Holub M, Balintova M (2014) Removal of inorganic compounds from acidic solutions by sorption. The 9th International Conference “Environmental Engineering”, Selected Papers, Article number: enviro.2014.078.
- Kalmykova Y, Strömvall, Steenari B-M (2008) Adsorption of Cd, Cu, Ni, Pb and Zn on spagnum peat from solutions with low metal concentrations. *J. Hazard. Mater.* 158, pp. 885-891.
- Kelemen SR, Afeworki M, Gorbaty ML, Kwiatek PJ, Sansone M, Walters CC (2006) Thermal transformations of nitrogen and sulfur forms in peat related to coalification. *Energy Fuels.* 20, pp. 635-652.
- Keränen A, Leiviskä T, Zinicovscaia I, Frontasyeva MV, Hormi O, Tanskanen J (2015) Quaternized pine sawdust in the treatment of mining wastewater. *Environ. Tech.* 37, pp. 1-8.
- Nakanishi K (1962) *Infrared Absorption Spectroscopy-Practical*. Nankodo Company Ltd, Tokyo.
- Nicomel NR, Leus K, Folens K, Voort PVD, Laing GD (2015) Technologies for arsenic removal from water: current status and future perspective. *Int. J. Environ. Res. Public Health.* 13(62), pp. 1-24.
- Palmer K, Ronkanen AK, Kløve B (2015) Efficient removal of arsenic, antimony and nickel from mine wastewaters in Northern treatment peatlands and potential risks in their long-term use. *Ecol. Eng.* 75, pp. 350-364.
- Williams DH, Fleming I (1995) *Spectroscopic Methods in Organic Chemistry*, fifth ed. McGraw-Hill. London, ISBN: 0-07-709147-7.

Towards minimum impact copper concentrator – The link between water and tailings

Dr Piia Suvio¹, Tuukka Kotiranta², Janne Kauppi³, Kaj Jansson⁴

¹*Outotec (Canada) Ltd, 1551 Corporate Road, L7L 6M3 Burlington, Canada*

²*Outotec Research Center, Kuparitie 10, PO Box 69, Finland*

³*Outotec (Finland) Oy, Tukkipuutkatu 1, PO Box 29, 53101 Lappeenranta, Finland*

⁴*Outotec (Finland) Oy, Rauhalanpuisto 9, 02230 Espoo, Finland*

Abstract The paper is based on a simulated (HSC-SIM) study that investigated the link between environmental aspects and tailings management during a 15-year mine life. The findings evolve around water balance of a concentrator for different tailings management options and investigate their impact on water use, make-up and seepage from the tailings facilities, as well as changes on recycled water, evaporation, tailings lock-up and rainfall. Filtered tailings method can reduce the fresh water input index in a temperate climate by up to 80% and in arid up to 90% i.e. from 26.7 to 5.8 and from 67.3 to 6.5 kg blue water/kg concentrate produced respectively.

Key words water management, water balance, tailings management, seepage, TSF, HSC-SIM, Outotec

Introduction

Concentrators

Minerals processing concentrators are facing growing challenges with the fresh water availability and quality, which at worst case leads to serious reduction in the recovery of metals within the flotation process. Furthermore, environmental limitations for tailings management and related conventional tailings storage facilities, as well as water consumption and discharge volumes and quality arise a need for more sustainable operations. The continuing trend of lower grades in mineral deposits leads to further water consumption and expanding tailings storage facilities. Climate change in turn in having an impact on the available water supply (IPCC, 2014).

Water Management in Mineral Processing

Water is a commodity that has had an impact on mineral processing for decades. Often used frivolously, modern economic and social pressures are forcing a change to reduce water usage while improving the quality of water and effluents. Some studies Water management and recycling in mineral processing industry has been studied earlier (Joe et al. 1974-1984), as have the energy and water savings in tailings handling (Sellgren 1984). Franks et al, 2011 studied sustainable disposal of mining waste. Studies with full process including tailings and water management and their impact on the operational risk, economics and water savings has been discussed by Jansson et al. 2014 and Kotiranta et al. 2015. Holistic tailings management solutions with related water considerations were outlined by Suvio et al. 2016.

Hoekstra developed the water footprinting concept in 2002 and has been at the forefront of the related research. He acts as a member of the supervisory council of the Water Footprint Network (www.waterfootprintnetwork.org), which has since 2008 provided a leadership in the water footprinting numerous societal activities. This website provides information on footprint and how to calculate it for various different activities. The website also provides information on the impact of human activities on the use of different types of water in the activities ranging from food production to the impact of energy carriers and gives information on how virtual water affects the footprint of different activities (Hoekstra et al. 2011, Mekonnen and Hoekstra 2012, Dallemand JF and Gerbens-Leenes, PW, 2013).

Several studies exist on the analysis of economics, energy and environmental matters relating to different aspects of water, such as the economics and environmental considerations of portable water systems (Fagan et al. 2011, Loubet, et al. 2014, Nair, 2014), but a very a limited number of studies that link waste or material and water or water quality. Some do exist however, like the study carried out by Van Schaik et al. 2010, who applied a very large system optimization model that linked industry and farming wastewater to an industrial water treatment plant, combined with metallurgical processing of residues to maximize resource efficiency.

The study to which this paper is based on follows a similar approach as Van Schaik et al. (2010) in that simulation basis was used to map compounds and total flows with the objective to perform an environmental analysis in order to determine the optimal economic solution, but also considering the environmental impact (Reuter et al, 2015). A comprehensive sustainability indicator framework has been recently developed that combines numerous impacts into one simple result, while comparing it to a benchmark (Rönnlund et al. 2015). This allows combining and evaluation water, energy and materials simultaneously. This paper develops further the concepts presented by Jansson et al. (2014) and Kotiranta et al. (2015).

Water and Tailings Management

Water is used in many processes within mineral processing, but most of the water losses occur within the tailings processing and disposal area. New technologies that can increase the recovery of water are actively being developed, but the key to improving the efficiency of water use and reducing risks lies in closing water loops and increasing the slurry density in the tailings processing. With this shift from conventional tailings technologies towards paste and dry stacking, water efficiency is vastly improved, but it might in turn lead to process water challenges with impurities, reagents and fines being recycled and accumulated within the production processes and needs to be taken into account as a part of the holistic water and tailings management.

In conventional tailings systems, the process waters originate from natural sources and/ or include mine dewatering waters and the amount needed is directly related to the environmental conditions and filterability of the tailings dam, which indicates how much water is lost in this process stage. With these kinds of process conditions it is estimated that a Cu

refinery process located in a temperate zone uses between 0.6–0.9 m³ of water per ton of ore (Jansson et al. 2014; Kotiranta T. et al. 2015).

A shift towards more advanced tailings processing options, such as filtered tailings, not only changes the set-up of the water flows, but also the water quality, when moving away from a conventional tailings dam with a 30–60-day water retention time and bio/chemical reactions taking place, to a dry stack/high density process, where the water is in contact with the solids for only a few hours with the tailings and water being separated in the thickener. The changes on water quality taking place at the conventional dam may be harmful, especially for polymetallic mineral processes. In some cases, metal recovery or selectivity may be negatively impacted without suitable process water treatment.

In the dry stacking model, where the water can be much more effectively captured and reused back in the process, the amount of process make-up water is strongly reduced. The estimated water usage drops to 0.15–0.2 m³ of water per ton of ore in a Cu refinery plant located in a temperate zone (Jansson et al. 2014; Kotiranta T. et al. 2015), equaling up to 80% savings in comparison to conventional tailings processing. The final rate of water savings is dependent on the final layout of the tailings management solution and on the climate zone, in which the mine and the process are located.

Methodology

Study Scope

The calculation outlined in this paper are based on an imaginary 20Mt/a capacity copper concentrator (porphyry Cu) with an estimated 15 year life time of the mine. The process set-up used for the concentrator plant includes 1 SAG mill, 2x Ball mills, 2 lines with 8 flotation cells each, 1 regrinding HIG mill, one concentrate thickener as well as 2 PF concentrate filters with a storage system. Water calculations were carried out for two different climate scenarios of a temperate and semiarid/arid location. In both cases fresh water intake was determined to be about 10 km away from the concentrator with a 25 m static head. The tailings area was also located 10 km away from the concentrator with 25 m static head. No considerations were given to mine water, freezing conditions, dust control (wind), acid mine drainage (AMD) generated water or earth quakes were taken into account. Project scope includes considerations for 4 different tailings processing methods of conventional, thickened, paste and filtered tailings

Approach

The basic water and material balances were calculated for four different tailings processing approaches, including: Case 1: Conventional tailings management, Case 2: Thickened tailings management, Case 3: Paste tailings management and Case 4: Filtered tailings management based on the approach discussed by Reuter et al. (2015). In all mass balance calculation the focus was on fresh water intake in order to estimate blue water footprint in line with the water footprint concept. Furthermore, estimates were carried out for effluent volumes from different tailings processing approaches.

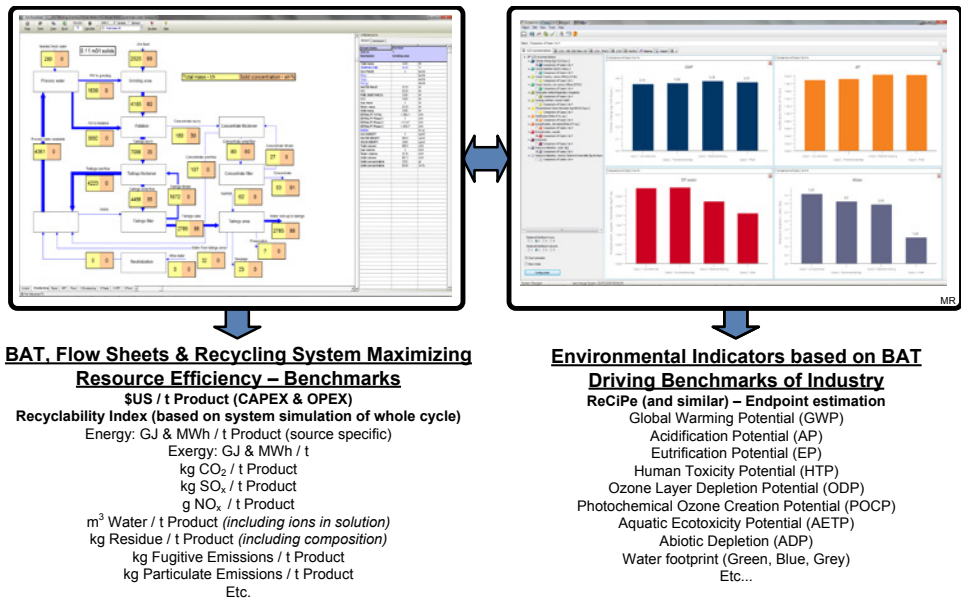


Figure 1 Summary of the methodology: Left the HSC Simulation (www.outotec.com) of the water system for the four cases and right the environmental footprint calculation produced from the simulation results by life cycle assessment tool GaBi (www.thinkstep.com) (Reuter et al, 2015).

In order to carry out the simulation and obtain the average water flows (Figure 1), data for climate conditions and soil seepage capacity were inputted into the Outotec thermodynamic HSC simulation tool, which is steady state simulator, where all the data inputted into the process also exit the process and it is able to carry out calculations to provide a snapshot of a specific situation. HSC-SIM is not able to take into account the normal process variations. The climate conditions for the selected site were gathered from www.WorldClimateGuide.co.uk, whereas the soil seepage capacity was estimated from data collected from mines nearby the imaginary location for this minerals processing site. The results for the flows were used as a basis of the cost calculations discussed by Jansson et al. 2014 and Kotiranta 2015 and also to produce the data used in the environmental footprint software GaBi (www.thinkstep.com) (see Reuter et al. 2015) for details).

Study Outcome

The original idea of the study was to investigate possibilities to decrease the whole operational costs of the minerals processing during the 15-year mine life. The considerations included both CAPEX and OPEX costs together with indirect costs including legal and other official procedures and unpredictable costs such as operational risks (e.g. production losses due to water shortage), regulation/environmental/rehabilitation, reputation and financial risks. It was found out that the combined costs of CAPEX and OPEX with the four studied cases were fairly close to each other.

Further to financial considerations, the study provided several results for different tailings processing options, including water footprint, operational risks, risks related to dam wall and its construction, water requirements, global warming potential (CO₂ impact), environmental impact analysis and considerations for their relation. Following the estimation of the operational risks related to different tailings processing options, a simple risk matrix, with *risk value* in € versus potential *risk level* was set up with the basic operational risks. Figure 2 depicts various scenarios for three solution types of conventional tailings management (black), paste (green) and filtered tailings (blue).

As seen from this evaluation, the highest operational risks are allocated to conventional tailings management, and lowest to the filtered tailings. It can be concluded that switching from conventional tailings to dry stacking technology, it is possible to reduce the operational risks.

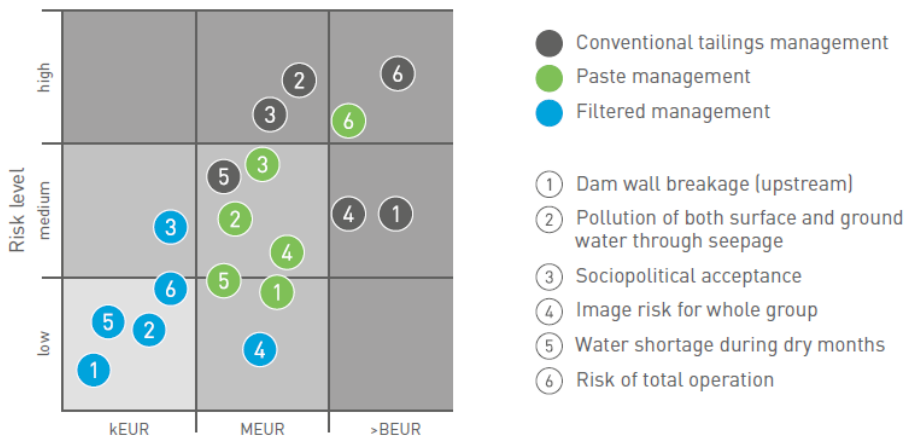


Figure 2 Risk matrix for the assessment of operational risks associated with different tailings management processes

The results of this paper discuss especially the risks related to the water and its relation to tailings processing. Some of the most important considerations here include risks related to the climate conditions and seepages from tailings facilities, which have been considered a water consumer. As previously mentioned, the water related calculations were carried out for two different location scenarios, where the first was located in the temperate zone, where summers are relatively hot and dry and autumns and springs are wet with lots of rain. The average rainfall was 52 mm/month and evaporation is 45 mm/month (from 0 to 144). The second scenario is located in a semiarid to arid zone with average rainfall of 20 mm/month and evaporation 238mm/month (from 84 to 415). For both cases the area for total water collection area is 725 ha.

Results

Fresh-water and seepages

Risks related to climate conditions and seepages create the biggest pressures for water within the concentrator environment as the water is lost with no ability to recover via these ways. For the first location scenario the average rainfall is 52 mm/month and the second 20 mm/month, the evaporation was 45mm/month and 238mm/months respectively. The concentrator of the first scenario is located in a temperate zone, whereas the second is located in an arid climate zone and even the average rainfall at the arid zone is approximately 40% of the rainfall in the temperate zone, the evaporation is more than 450% of the evaporation at the temperate zone.

Figures 3 and 4 show the estimated seepage amount (b) in the two different scenarios for the 4 different tailings management options. In both cases high seepage is related to conventional and thickened tailings management options, whereas with the paste and filtered tailings management options the water is locked inside the tailings by capillary forces and the only accountable and partly recoverable seepage would arise during heavy rain fall conditions. In the arid climate scenario, the seepage is almost non-existing at the paste and filtered tailings management option. What should be noted is that in an arid location fresh water need is dramatically lower for conventional tailings than thickened tailings management during the summer months.

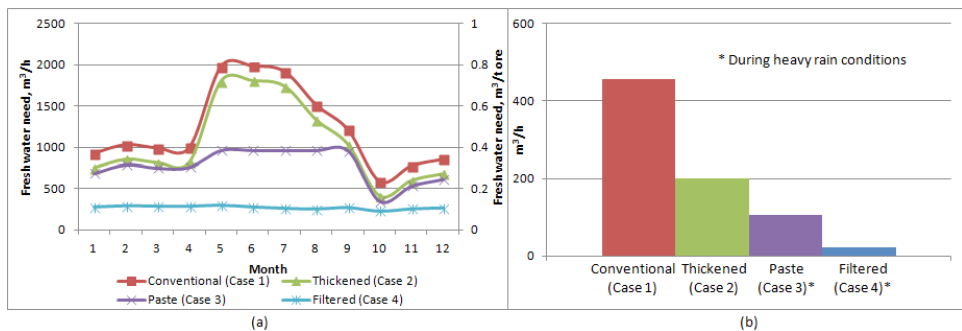


Figure 3: Risk related to seepages from tailings management facilities. Monthly fresh water make-up of the plant (a) and the estimated total seepage from the tailings facilities (b)

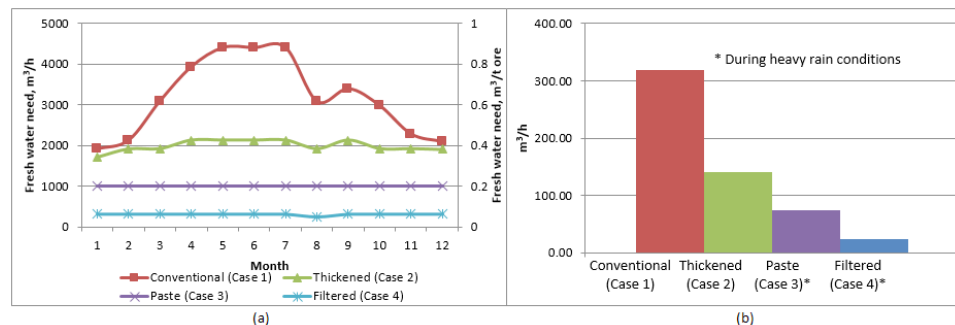


Figure 4 Risk related to seepages from tailings management facilities at an arid region. Monthly fresh water make-up of the plant (a) and the estimated total seepage from the tailings facilities (b)

The climate impact on average fresh water demand was estimated based on Figures 3 and 4. In both scenarios it can be seen that traditional and thickened tailings management processes have the highest water needs. It can also be seen that the filtered tailings management option squeezed the most water from the tailings and therefore has the highest capability from the water conservation and reuse point of view. This showed that the filtered option decreases the water footprint significantly i.e. at the first case from 26.7 to 5.8 kg blue water/kg concentrate produced (or 0.51 to 0.11 kg blue water/kg ore feed) and at the second case from 67.3 to 6.5 kg blue water/kg concentrate produced (or 1.29 to 0.12 kg blue water/kg ore feed). The advanced tailings management options also improved the water quality and toxicity indicators. What is important to note is that the fresh water need for the arid scenario is much higher for the conventional tailings management than for the other tailings management options, whereas for the temperate scenario, both conventional and paste tailings management option has high fresh water need. When drilling down deeper on the different tailings management methods at the arid location (Figure 5-8) and the investigating different water factors, including recycled water, evaporation, tailings lock-up, seepage and rainfall, it can be seen that there are clear differences between the different tailings management options.

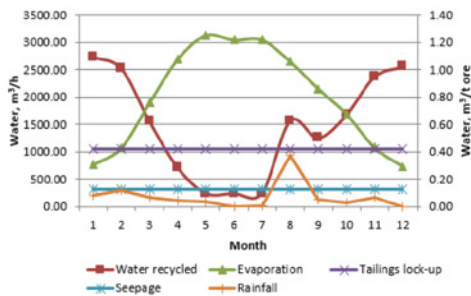


Figure 5 Water in Conventional Tailings Management

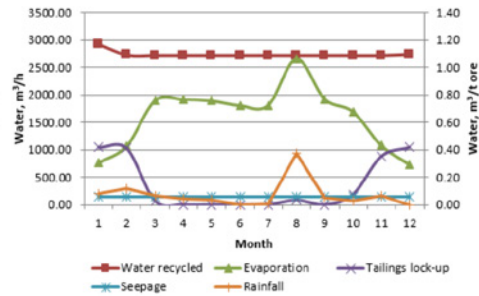


Figure 6 Water in Thickener Tailings Management

As seen in Figure 5 and 6, in the case of conventional and thickened tailings, water evaporation, especially in summer months reaches 2500-3000 m³/h, whereas with paste tailings it's below 2500 m³/h throughout, but generally around 1000 m³/h and with filtered tailings there isn't even enough water present to evaporate more than residual amounts. The amount of the recycled water is also impacted by the tailings management method and whereas for filter, paste and thickened tailings the numbers are fairly stable and approx. 4500, 3500 and 2750 m³/h respectively, for conventional tailings management, the amount of recycled water varies a lot from and in summer months dives under 500 m³/h.

Water Mass Balances

Furthermore, water balance calculations were carried out for all the different tailings management options and these can be seen in Figures 9-12. It should be noted that rainfall, evaporation and seepages are not shown in the water mass balances.

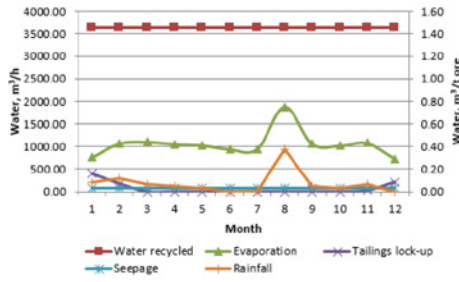


Figure 7 Water in Paste Tailings Management

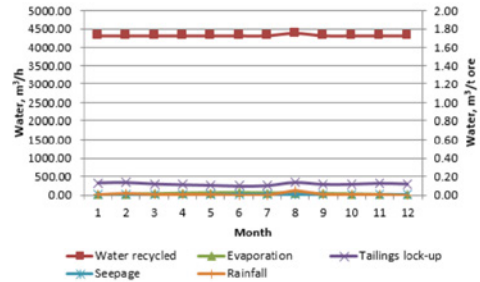


Figure 8 Water in Filtered Tailings Management

Case 1: The simulation results with Conventional tailings management effects on fresh water usage

Conventional option is shown in (Virhe: Viitteen lähde ei löydy). Using the simulation for sensitivity analysis one can estimate that the average fresh water need is around 1.3 m³/t-ore or 3700 m³/h with a typical 15% addition to the calculation due to process flow variations at the conventional tailings balance due to the tailings dam.

Case 2: The simulation results with thickened tailings management effects on fresh water usage

Figure 5b shows the impact of thickened tailings. In an arid climate the thickened tailings processing decreases the fresh water usage significantly to under 2000 m³/h. In the thickened tailings management part of the water is still circulated through tailings area and the rainfall and evaporation in the area will have effect on the plant water balance. This means an average fresh water usage still averages 0.77 m³/t ore.

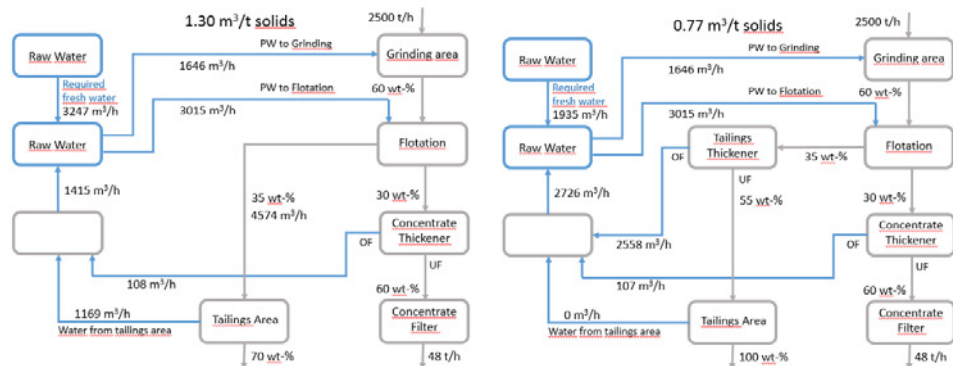


Figure 5 Simplified water balance calculations for conventional tailings (a, on the left) and for thickened tailings management (b, on the right)

Case 3: The simulation results with paste tailings management effects on fresh water usage

As the paste thickener underflow is estimated to be near 70% and the sand lock-in-capability to 30% then a very small or no effluent treatment is needed. The fresh water usage is still in the range of 0.4 m³/h, and the average need around 1000m³/h. If paste backfill options is applied, most of the operational risks are reduced, but water related management considerations remain important.

Case 4: The simulation results with filtered tailings management effects on fresh water usage

This filtered tailings mass balance shows that the big opportunity for lowering the required fresh water amount comes from the removal of wet tailings. In addition this approach also minimize seepage issues and risk through contaminating ground water, evaporation losses are minimized. Furthermore, the rainfall does not impact the dry stacking option in a same ways as in the previous three cases. Under optimal conditions the fresh water usage is estimated to be around 0.13 m³/t ore and the fresh water flow around 310m³/h.

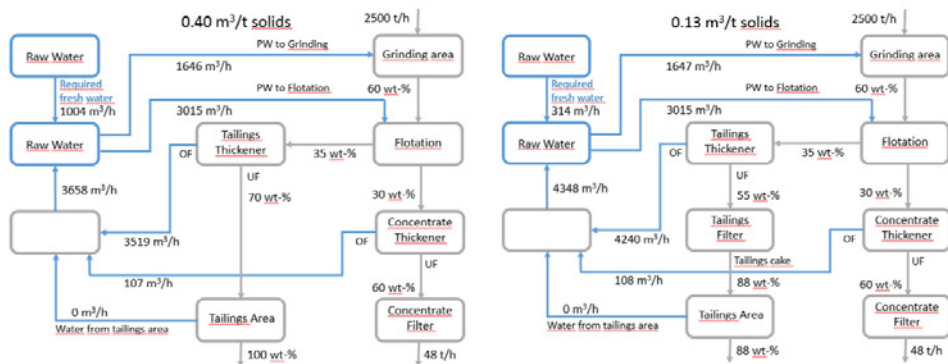


Figure 6 Simplified water balance calculations for paste thickening (a, on the left) and for filtered tailings management (b, on the right)

The above described results represent the situation with the ores that are currently being processed. However, in the future lower grade deposits will increase the capacity of the processing plants and therefore the fresh water requirements, therefore placing extra pressure on the water related considerations and will stress the need for tailings and water related considerations at the concentrator environment.

Conclusions

Water related challenges have ever increasing impact on concentrator operations. Risk related to poor fresh water quality and scarcity, wet tailings dam and new effluent limitations are growing. The choice of tailings management option has a strong impact on the water balances and especially fresh water requirements, water recycling possibilities, seepage from the TSF and evaporation.

The finding of this study include:

- The future of water management includes more closed water loops and smaller consumption volumes to overcome increasing operational risks
- Paste thickening is a very good alternative with low operational risks, especially if a backfill option does exist, but it does not solve the water management issues
- Filtered tailings have the most neutral water balance out of the tailings management options studied with required fresh water input of 0.13m³/ton of ore
- The above described results represent the situation with the ores that are currently being generally processes. However, in the future lower grade deposits will increase the capacity of the processing plants and will increase the fresh water requirements, therefore placing extra pressure on the water related considerations and will stress the need for tailings and water related considerations at the concentrator environment

References

- Dallemand, J.F, Gerbens-Leenes, PW eds. (2013), *Bioenergy and Water*, European Commission, Joint Research Centre, Institute for Energy & Transport, 289p. ISBN 978-92-79-33187-9
- Fagan JE, Reuter MA, Langford KJ (2010), Dynamic performance metrics of integrated urban water systems *Resource Conservation Recycling*, 54: 719-736.
- Franks, D, Boger, D, Côte, C, and Mulligan, D, (2011), Sustainable development principles for the disposal of mining and mineral processing wastes, *Resource Policy* 36(2): 114-122GaBi 6, “Software and System Databases for Life Cycle Engineering”, Stuttgart-Echterdingen, www.thinkstep.com (1992-2014).
- Hoekstra, AY, Chapagain, AK, Aldaya, MM, Mekonnen, MM (2011), *The Water Footprint Assessment Manual Setting the Global Standard*, Earthscan Ltd, London, UK, 203p. ISBN: 978-1-84971-279-8
- IPCC, 2014. *Climate Change 2014 Synthesis Report Summary for Policymakers*, Fifth Assessment Report (AR5). 32p.
- Jansson, K, Kauppi, J, Kotiranta, T, (2014), Towards minimum impact Cu concentrator – A conceptual study, *Materia*: 4, 64-67.Loubet, P, Roux, P, Loiseau, E, Bellon-Maurel, V (2104): Life cycle assessments of urban water systems: A comparative analysis of selected peer-reviewed literature, *Water Research*, 67(12): 187-202.
- Jansson, K, Kauppi, J, Kotiranta, T, (2014), Towards minimum impact Cu concentrator – A conceptual study; 2014 IMPC SUSTAINABILITY SYMPOSIUM, Santiago de Chile
- Joe, E. (1984), Water and solution recycling practice in the Canadian mineral industry, Conference on Mineral Processing and Extractive Metallurgy (IMM and CSM), Kunming, China.
- Joe, E. and Pickett, D: (1974), Water reuse in Canadian ore-concentration plants-present status, problems and progress, *Minerals and the environment*, Proceedings of an international symposium, The institution of Mining and Metallurgy, London.
- Kotiranta, T, Horn, S, Jansson, K and Reuter M (2015), Towards a “Minimum Impact” Copper Concentrator: A Sustainability Assessment, Proceming, 11th International Mineral Processing Conference, Santiago, Chile
- Mekonnen, MM, Hoekstra AY (2012), A Global Assessment of the Water Footprint of Farm Animal Products, *Ecosystems*, 15: 401-415
- Nair, S, George, B, Malano, HM, Arora, M, Nawarathn, B (2014), Water–energy–greenhouse gas nexus of urban water systems: Review of concepts, state-of-art and methods, *Resources, Conservation and Recycling*, 89(8): 1-10.

- Reuter, MA, Van Schaik, A, Gediga, J (2015), Simulation-based design for resource efficiency of metal production and recycling systems, Cases: Copper production and recycling, eWaste (LED Lamps), Nickel pig iron, *International Journal of Life Cycle Assessment*, 20(5): 671-693.
- Rönnlund, I, Reuter, MA, Horn, S, Aho, J, Päällysaho, M, Ylimäki, L, Pursula, T (2015), Sustainability indicator framework implemented in the metallurgical industry: Part 1-A comprehensive view and benchmark, *International Journal of Life Cycle Assessment* (submitted).
- Sellgren, A (1984), Energy and water savings in handling of mine tailings slurries, *The Ninth International Technical Conference on Slurry Transportation, USA*
- Van Schaik, A, Reuter, MA, Van Stokkom, H, Jonk, J, Witter, V (2010): Management of the Web of Water and Web of Materials, *Minerals Engineering*, 23: 157-174.
- Suvio, P, Palmer, J, del Olmo, AG and Kauppi, J (2016) White Paper on Holistic Tailings Management Solutions. Available at <http://www.outotec.com/en/Minerals-processing-newsletter/2016-1-Minerva-Tailings-management/>
- Water Footprint Network (2008-2015): Various reports and literature, www.waterfootprintnetwork.org.

Hydrostratigraphy and 3D Modelling of a Bank Storage Affected Aquifer in a mineral exploration area in Sodankylä, Northern Finland

Susanne Charlotta Åberg¹, Annika Katarina Åberg¹, Kirsti Korkka-Niemi¹, Veli-Pekka Salonen¹

¹ *Department of Geosciences and Geography, PL 64 (Gustaf Hällströmin katu 2a), University of Helsinki, 00014, Helsinki, FINLAND, susanne.berg@helsinki.fi*

Abstract 3D geological modelling and flow modelling were used to investigate groundwater flow patterns near Kersilö, Sodankylä, close to a Cu-Ni-PGE discovery named Sakatti. A MODFLOW-NWT model was generated to simulate the groundwater table. Alternating sorted sediment and till units were observed within the study area, indicating complex aquifer conditions. The hydrological settings were examined to understand the changes driven by the regulation of the River Kitinen. The results of flow modelling indicate groundwater movement towards the river. The artificial rise in the river stage has caused wetting of the mire area near Matarakoski.

Key words groundwater, surface water, modelling, surficial deposits, mire hydrology, mining environment

Introduction

A prominent Cu-Ni-PGE mineralization named Sakatti has been discovered close to the River Kitinen in Sodankylä, Northern Finland (Brownscombe et al. 2015). The deposit is located below the Natura 2000 protected Viiankiaapa mire (fig. 1). In Northern Finland, the sedimentary package is often a complex combination of deposits from alternating glacial and ice-free events, as demonstrated in previous studies (e.g. Hirvas 1991). Therefore, aquifers are usually small and scattered (Lahermo 1973) and inadequately studied. It is vital to understand the hydrostratigraphy of surficial deposits and the surface water–groundwater interactions in order to conduct exploration activities in a sustainable way.

The River Kitinen has been regulated by hydroelectric power plants constructed by Kemijoki Oy since the 1960s (Marttunen et al. 2004). In its pristine state, the river was known to be subject to extensive spring flooding, which affected the hydrology of the Viiankiaapa mire and the local flow patterns of surface and groundwater. The regulation of the river ended the major flooding events and was hypothesised to change the surface and groundwater flow patterns.

The aim of this study was to utilize geological 3D modelling and flow modelling as tools to understand the flow patterns of surface water and groundwater and examine how the regulation of the river has affected the hydrological settings of the study area.

Materials and methods

All available information on surficial deposits (e.g. Gustavsson et al. 1979), stratigraphic sites (Hirvas 1991), groundwater monitoring wells and bedrock topography was collected into a GIS database called the Kersilö database (Åberg et al. 2017) within the area X: 482

000–500 000, Y: 7 500 000–7 480 000 (EUREF-FIN TM35 coordinate system). A 3D model of surficial deposits and the bedrock surface was generated near Sakatti covering an area of 3.0 x 3.5 km (fig. 1). In addition to the Kersilö database, ground penetrating radar (GPR) profiles from two field campaigns in April and August 2015 were used as input data for the 3D modelling (fig. 1) and groundwater table interpretations. The 3D model was generated with Leapfrog Geo®. It consisted of seven sediments units, a peat layer, the River Kitinen, weathered bedrock and bedrock surface (fig. 2, tab. 1).

A simplified version of the 3D model (see tab. 1) was converted into a groundwater flow model. MODFLOW-NWT (Niswonger et al. 2011) was chosen as the modelling code due its suitability for unconfined and highly heterogeneous aquifer conditions. The flow model consisted of eight layers with varying hydraulic conductivity zones defined by the 3D model (see tab. 1). The hydraulic conductivities of the hydrostratigraphic units were then calculated from the geometric means of calculated hydraulic conductivity values based on previous grain-size analyses and slug tests. The flow model was manually calibrated with UCODE_2014 (Hill and Tiedeman 2007) by adjusting the hydraulic conductivities to obtain a better fit between the observed and simulated groundwater table. The yearly variation in the groundwater table was also studied from recordings of the 17 monitoring wells (fig. 1).

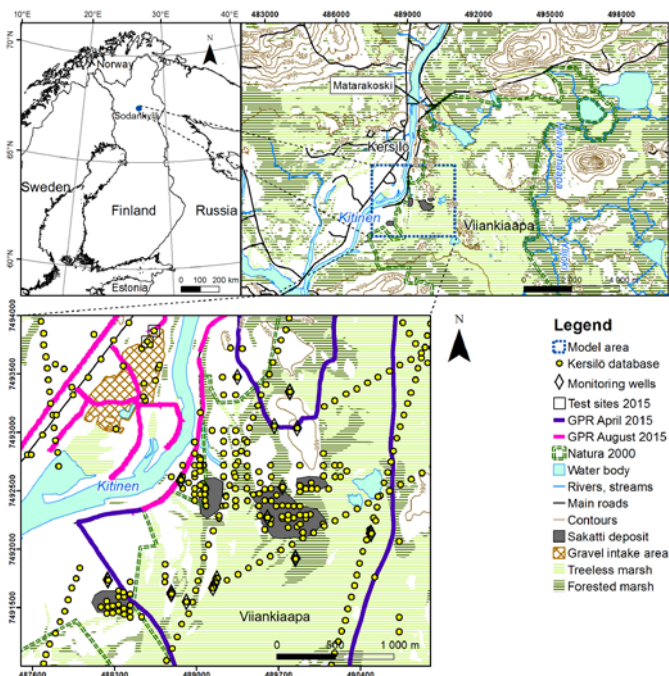


Figure 1 Location of the study area around the River Kitinen in Northern Finland (above). The Kersilö database and ground penetrating radar (GPR) profiles were used as input data for the 3D model (below). The Kersilö database indicates the locations of available surficial deposit and bedrock surface observations. Terrain polygons © National Land Survey of Finland, Sakatti deposit modified after Brownscombe (2015).

The surface water flow direction was estimated in the Viiankiaapa area by using ortho images, a two-metre-resolution LiDAR DEM and existing flow directions from maps. Changes in the hydrological settings of the River Kitinen were examined from different maps and unpublished discharge and river stage data obtained from Kemijoki Oy.

Results

Table 1 The geological units of the 3D model and flow model. The unit of hydraulic conductivities is $m\ s^{-1}$. HK = horizontal hydraulic conductivity. VK = vertical hydraulic conductivity.

Modelled unit	3D model	Flow model	Original HK parameter*	Calibrated HK parameter	VK multiplier α
River Kitinen	x	x	1.0E-01	1.0E-01	1
Peat	x	x	8.5E-06	1.0E-03	0.001
Top deposits	x	x	2.3E-05	2.3E-05	0.1
Upper till	x	x	4.1E-06	4.1E-06	0.1
Middle sorted deposits	x	x	6.9E-04	7.3E-06	0.1
Middle till	x				
Lower sorted deposits	x				
Lower till assemblage	x	x	1.6E-05	1.6E-05	0.1
Lowest sands and gravels	x	x	1.5E-04	1.5E-04	0.1
Weathered bedrock	x				
Bedrock	x	x	9.4E-06	9.4E-06	1

*Geometric mean of the calculated hydraulic conductivities

α The multiplier of vertical hydraulic conductivity that was used in the calibrated model

According to the 3D model, the volume of surficial deposits is 0.096 km³, of which 59% is till, 32% is sorted deposits and 9% is peat. The average thickness of surficial deposits is 9.1 m and the thickness varies from 0 to 41 m. The altitude of the bedrock topography varies between 148–190 m. The aquifer systems are complex and scattered due to alternating sorted and unsorted deposits. The low hydraulic conductivity of till units conceals perched groundwater conditions.

The flow model indicates that groundwater mainly flows towards the River Kitinen (fig. 3). At monitoring wells close to the River Kitinen, higher annual variation in the groundwater table was recorded during 2012–2015, indicating a possible bank storage situation.

Surface water flows towards the River Kitinen on the eastern side of the river and towards the smaller rivers Hiivanahaapa and Ylijoki (fig. 1) on the western side. The construction of

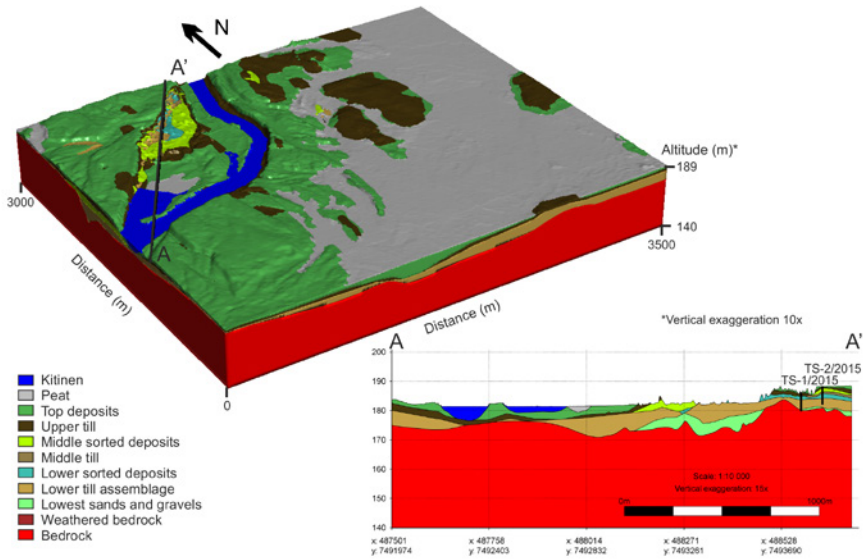


Figure 2 3D model of unconsolidated sediments and bedrock topography near Kersilö village (above) and cross-section A-A' of the 3D model (below). The location of the 3D model is presented in fig. 1. The sediment structure is tentatively based on the interpretation of the test sites TS-1/2015 and TS-2/2015.

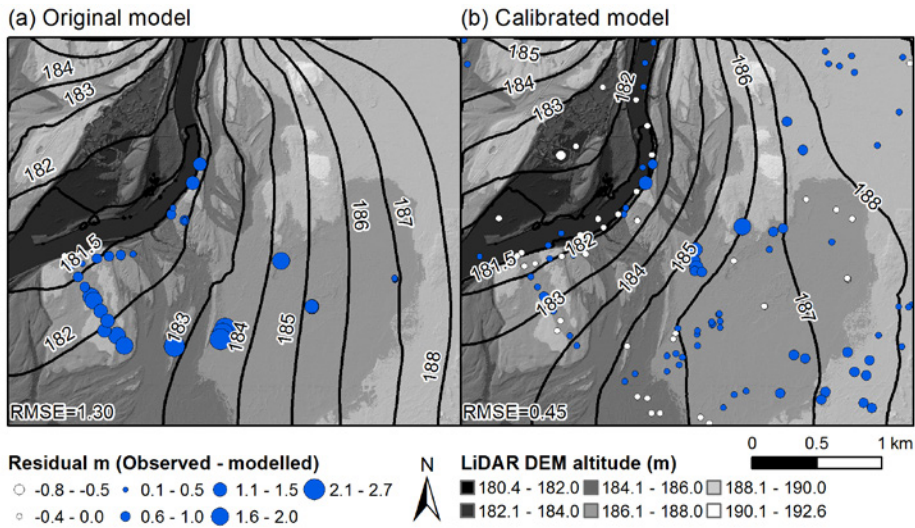


Figure 3 Groundwater flow modelling results with groundwater table observations interpreted from GPR profiles, groundwater monitoring wells and surface water bodies (rivers, flarks etc.). (a) The first version of the model with the original parameters calculated from the geometric means of hydraulic conductivities. (b) Manual calibration of the model with surface water body points included. The surface water points were added to achieve better calibration results in the mire area. LiDAR DEM © National Land Survey of Finland.

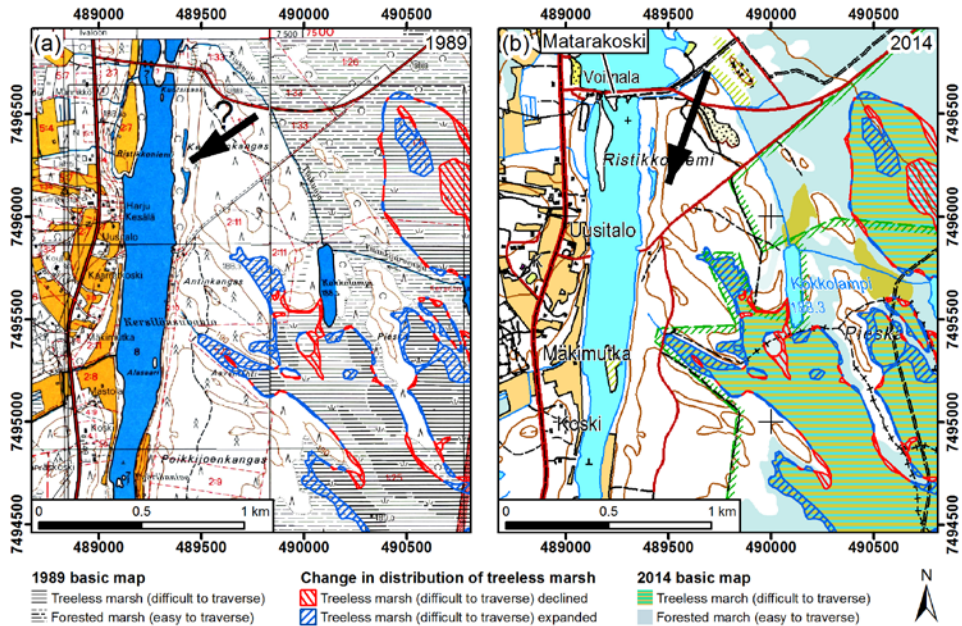


Figure 4 The change in the distribution of treeless marsh in the Kokkolampi area near Matarakoski hydroelectric power plant. (a) The situation in 1989 before the construction of the Matarakoski hydroelectric power plant; (b) the present situation. The treeless marsh area increased near Kokkolampi from 1989 to 2014. The black arrows indicate the estimated groundwater flow directions near Matarakoski. Basic maps (2014, 1989) © National Land Survey of Finland.

the Matarakoski hydroelectric power plant in 1995 has caused a rise of several metres in the river stage in the Matarakoski area and a reduction in flooding of the river. At the same time, the mire area near Kokkolampi has become wetter (fig. 4), which is an indication of a rise in the groundwater table in the area due the elevated river stage.

Discussion

MODFLOW-NWT was suitable for the heterogeneous and unconfined aquifers systems of the study area. The flow model results were highly dependent on the hydraulic conductivities of the sediments and their distributions. Parameter estimation with UCODE_2014 (Hill and Tiedeman 2007) was also tested. However, the manual calibration resulted in a more reliable fit and convergence due to the low sensitivities of most parameters according to sensitivity analysis. The RMSE of the calibrated model was 0.45, indicating a fairly good fit. The poor fit in the south eastern corner (fig. 3) of the model area was due the peat layer modelled in the area being too thin. The observations in the middle of the study area indicate perched groundwater, which would explain the underestimation of the groundwater table. The uncertainties of the groundwater flow model are highly dependent on the uncertainties of the 3D model. Thus, reconstruction of the 3D model, especially the peat unit, and parameter estimation with UCODE_2014 will be carried out. Due to the simplicity of MODFLOW, the

open-source flow-modelling software ParFlow (Kollet and Maxwell 2006) will be used for more detailed modelling of groundwater recharge.

The construction of the Matarakoski power plant has changed the hydrological settings. The rise in the river stage has probably affected the groundwater table, causing the wetting of the mire area near Kokkolampi. Changes in the groundwater flow patterns may also affect the biodiversity of the mire. According to Karplund (1990), the regulation of the river has caused a decline in the distribution of many endangered flood-dependent species in the area.

3D modelling of surficial deposits can be applied to estimate the volume and the distribution of the groundwater reservoirs. In addition, it can be applied into infrastructure planning and evaluation of siting of the mining facilities. Groundwater model may also facilitate how the change in flow patterns affects distribution of groundwater dependent plants.

Conclusions

Groundwater flow modelling and interpretations of surface water flow direction both indicated flow towards the River Kitinen. Groundwater modelling is an effective tool to estimate the continuity of geological units in study areas with scarce data. However, the actual uncertainty of the flow model is difficult to evaluate due to uncertainties in the structure of the 3D model. Further calibration or reconstruction of the flow model is needed to obtain a better fit.

The construction of power plants has considerably changed the hydrological system of the river and the mire area due to reduced flooding. The rise in the river stage has affected the groundwater flow near Matarakoski, changing a possible bank storage situation, as indicated by the yearly groundwater table variations at the monitoring wells. To gain a better understanding of the system, more groundwater observations near the dam are needed.

Acknowledgements

The working group for support: Anne Rautio, Tatu Lahtinen, Jyri Laakso, Enni Suonperä and Emilia Koivisto. The funders for making this study possible: Maa- ja vesitekniiikan tuki ry. and K. H. Renlund Foundation. Data sharing: Mikko Huokuna from the Finnish Environment Institute (river stage data), Juha-Petri Kämäräinen from ELY Centre (flood and discharge data, Kitinen), Juho Päiväniemi from Kemijoki Oy (discharge data of Kemijoki Oy) and Jari Uusikivi from the Finnish Environment Institute (modelled runoff data, discharge data). Maps: Geological Survey of Finland and National Land Survey of Finland. We thank AA Sakatti Mining Oy for material and inspiration for this study.

References

- Brownscombe W, Ihlenfeld C, Coppard J, Hartshorne C, Klatt S, Siikaluoma JK, Herrington RJ (2015) Chapter 3.7 – The Sakatti Cu-Ni-PGE Sulfide Deposit in Northern Finland. In: O'Brien WDM (ed) Mineral Deposits of Finland. Elsevier, pp 211-252. doi:<http://dx.doi.org/10.1016/B978-0-12-410438-9.00009-1>
- Gustavsson N, Noras P, Tanskanen H (1979) Seloste geokemiallisen kartoituksen tutkimusmenetelmistä: Report on geochemical mapping methods. Tutkimusraportti n: o 39. Geologinen tutkimuslaitos, Espoo, 20 p
-

- Hill MC, Tiedeman CR (2007) Effective groundwater model calibration: with analysis of data, sensitivities, predictions, and uncertainty. John Wiley & Sons, 20 p
- Hirvas H (1991) Pleistocene stratigraphy of Finnish Lapland vol 354. Bulletin – Geological Survey of Finland. Geologian Tutkimuskeskus, Espoo, 123 p
- Karplund T (1990) Sodankylän ympäristönhoito-ohjelma. Nordia tiedonantoja, vol Sarja B 1. Pohjois-Suomen maantieteellinen seura r.y., Oulu, 90 p
- Kollet SJ, Maxwell RM (2006) Integrated surface–groundwater flow modeling: A free-surface overland flow boundary condition in a parallel groundwater flow model *Advances in Water Resources* 29:945–958 doi:10.1016/j.advwatres.2005.08.006
- Lahermo P (1973) ground water of Central and West Lapland interpreted on the basis of black and white aerial photographs Geological Survey of Finland, Bulletin 262:5–48
- Marttunen M et al. (2004) Kemijärven säännöstelyn kehittäminen–yhteenveto ja suositukset vol 718. Lapin ympäristökeskus, Suomen ympäristökeskus, pp 236
- Niswonger RG, Panday S, Ibaraki M (2011) MODFLOW-NWT, a Newton formulation for MODFLOW-2005. US Geological Survey Techniques and Methods 6-A37. 44 p
- Åberg AK, Salonen V-P, Korkka-Niemi K, Rautio A, Koivisto E, Åberg SC (2017) GIS-based 3D sedimentary model for visualizing complex glacial deposition in Kersilö, Finnish Lapland *Boreal Environment Research* 22:277–298

Facial and Paleogeografic Understanding of Tertiary Sediments as Basis to Predict their Specific AMD Release

André Simon¹, Jochen Rascher², Nils Hoth¹, Carsten Drebenstedt¹

¹TU Bergakademie Freiberg, Germany, Institute of Mining and Special Civil Engineering, Gustav-Zeuner-Straße 1A, 09599 Freiberg, Germany, andre.simon@tu-freiberg.de

²GEOmontan GmbH Freiberg, Am St. Niclas Schacht 13 – 09599 Freiberg, Germany

Abstract Acid Mine Drainage (AMD) is a known problem for many mining companies. In future overburden, metal sulphides are weathered, such as pyrite and marcasite. In lignite mining, eocene, oligocene and quaternary sediments of different genesis and lithological-geochemical composition are recovered and dumped. The aim of a modern opencast mining is to prevent or at least minimize AMD during the operation by structured excavation and tilting. This is done by mixing acidifying sediments and sediments containing carbonates. Therefore, it is necessary to know the facies formation of the sediment layers or aquifers, which will be the future overburden.

Key words lignite mining, pyrite weathering, AMD, genesis of sediments, facies, buffering carbonates, advanced mining technology, dump structure, geochemistry, glacial till

Introduction

Non-cohesive sediments in lignite mine sites contain partially pyrite (FeS_2), marcasite or other metal sulphides. So lignite mining stimulates sulphide weathering connected with AMD phenomena and massive mobilisation of acidity, sulphate and cation metals after groundwater rise (Figure 1). The weathering of the sulphides is embedded in hydro-geochemical buffering reactions. To reduce the acidification of groundwater around the lignite dumpsites, it is necessary to get knowledge about the sediments by evaluating the acidification and buffer potentials of the overburden units. For sustainable strategic activities, these investigations need to consider the geology, paleogeographic-genesis of sediments, the applied mass management and mining technology.

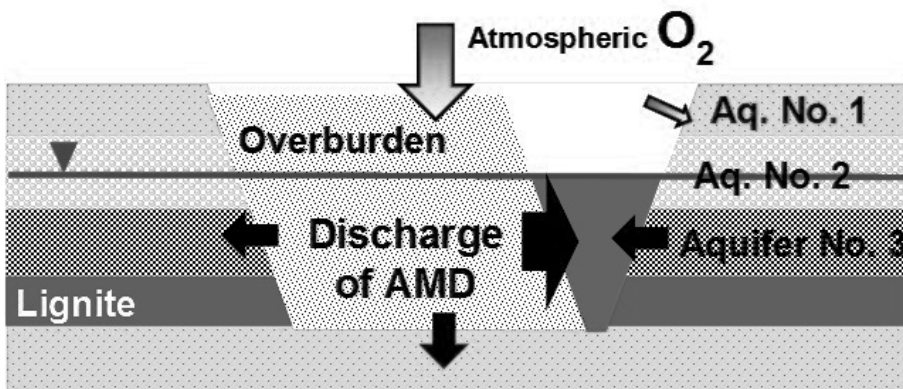


Figure 1 Scheme of discharge of AMD caused by different sediments

The main intention of the research was to identify technological reduction measures to minimise groundwater acidification based on the hydro chemical situation within the mining field considering the mining technology. A complete avoidance of the acidity generated through mining operations is impossible up to now. It is rather a question of minimising the negative effects by applying appropriate technology from the initial mine development to the final reclamation.

Methods

To solve the AMD problem sustainably, a working scheme was created including the three sections of geology, geochemistry and the production technology. Each of these sections were investigated in parallel processing.

In collaboration with colleagues from the company GEOmontan GmbH Freiberg, Germany, a geological model for the Mid-German region was improved by analyses of drillings in the forefront of the mine sites and by evaluated known data. A geological and facial examination of the drilling materials makes it possible to assign the sediments to individual units.

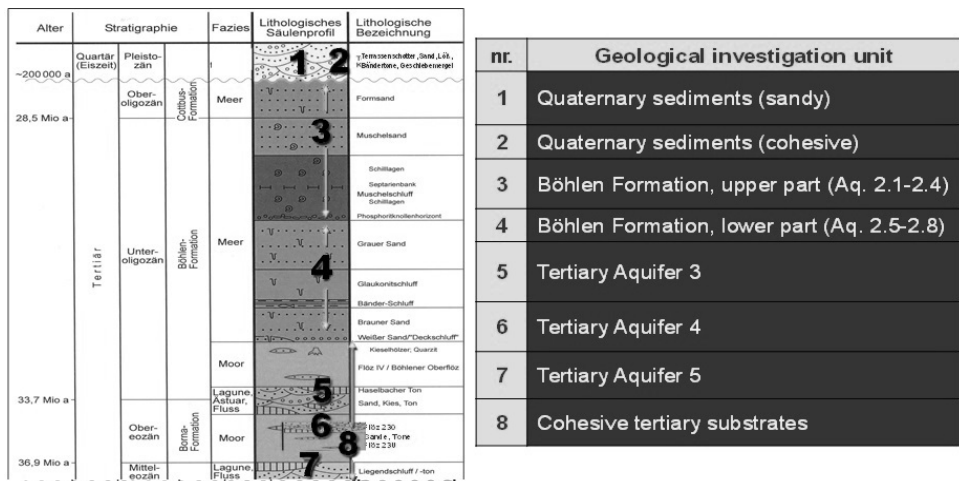


Figure 2 Geological Scheme and investigation units of the future overburden (Simon, 2016A).

The Mid-German geological units above the lignite seam has to be divided into eight geological investigation units (IU), shown in Figure 2. For example, the sandy (IU 1 – aquifer 1) and cohesive quaternary (IU 2) can be defined as summarising geological units. The tertiary sediments are subdivided into the aquifer two (upper/lower part) to five and the cohesive sediments (IU No. 8).

The formation of these sediments is very different. Quaternary and sandy sediments (IU 1) are glacial-fluviatile formed and cohesive sediments (IU 2) are glacially formed. High carbonate contents, more than 1 M%, were measured in cohesive quaternary sediments by carbon-sulfur analysis. The units of aquifer 2 are marine, but the upper part (IU 3) is more

related to tidal flat, the lower part (IU 4) to shallow sea. The Mid-German aquifer 3 (IU 5) is related to estuary formation, mean a deposition of sandy materials in a river delta. Aquifer 4 and 5 (IU 6 & 7) are fluvial sediments, disposals in a river basin. Cohesive tertiary sediments (IU 8) are limnical deposits.

The sequence of sedimentation from fluvial (oldest tertiary sediments) to estuarine to marine (youngest tertiary sediments) is shown in Figure 3. The different geochemical properties of the geological investigation units can be explained by different forms of sedimentation.

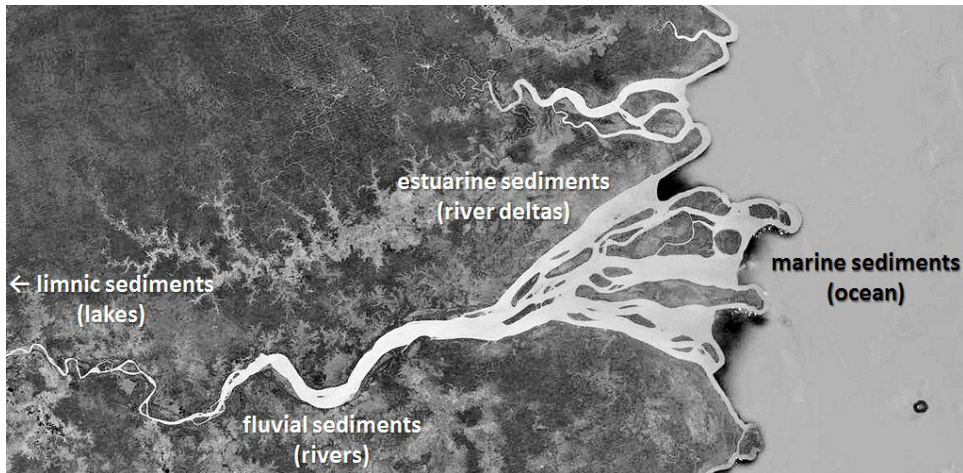


Figure 3 Sedimentation types of tertiary aquifers. (image Landsat / Copernicus via google earth)

To characterize the accessibility and weathering potentials for the major geological units several weathering tests were performed. The different Mid-German sediment materials were stacked in photo bowls, exposed to weathering by atmospheric oxygen, humidificated and stirred in intervals. The investigated sediments were stored at a constant temperature of about 10°C in the refridgerator, the mean soil temperature in the Mid-German area.

The weathered materials were analysed in intervals after approximately 0, 7, 21, 50, 100, 250 and 500 days. The wide spectra of analyses includes pH-value, electric conductivity, iron and sulphate photometry, trace metals concentration (like lead, zinc, cobalt, chromium and hydrolytic acidity (HA)). To determine the hydrolytic acidity, as a measure for the tendency of acidification, 40 g field-moist sediment has to filled in wide neck bottles. It is loaded with 100 mL of a 0.1 molar calcium acetate solution and shaken for 1 hour by overhead shaker. A centrifuge separated solid and liquid fractions before the supernate was titrated with 0.1 M NaOH solution to a pH value of pH 8.2.

Results and Implementation

By superposing the results of the weathering test with the results of the analyses of the hydrolytic acidity and geological and facial examination, it is possible to mark problematic

aquifers and implement suitable technological countermeasures. In Table 1 the sediments and their facial formation are listed, sorted by the shown hydrolytic acidity after a weathering of 250 days.

It could be shown, glacial and glaci-fluviatil sediments are unproblematic. Likewise, the sediments with a marine formation in the tidal flat are not acidifying after 250 days. They have nearly no release of iron and sulphate too. The fluviatile sediments or river sediments have also nearly no acidification potential ($HA < 11$ mmol/kg DM). Estuarine sediments or aquifers formed in a river delta have moderate acidification potential (HA 10-50 mmol/kg DM). Marine sediments formed in shallow basins of the ocean have an acidifying potential of 50 mmol/kg up to 200 mmol/kg DM.

Nevertheless, no rule without exceptions. By the treatment of tertiary sands during the ice age, quaternary sediments can also object acidity potentials. However, this occurs only marginally in erosion channels. In our example, a quaternary aquifer had a hydrolytic acidity of 27 mmol/kg DM.

In summary, the marine sediments (shallow sea) and the estuarine sediments are the main polluter of AMD in the Mid-German lignite mining region. Linking these acidifying and buffering potentials of the quaternary sediments with their thickness ratios an adapted dumping system can be established.

Conclusions

The Mid-German lignite mines are able to prevent AMD by the admixing of quaternary masses with tertiary sediments (main-AMD-polluter) without an addition of external buffers.

Short exposure times of the problematic sediments to atmospheric oxygen, prompt covering of acidic sediments in combination with the dump structure by tilting thin layers of acidic and buffering sediments will minimize AMD. It is possible to save the cost-intensive admixing of buffer materials such as lime or dolomite.

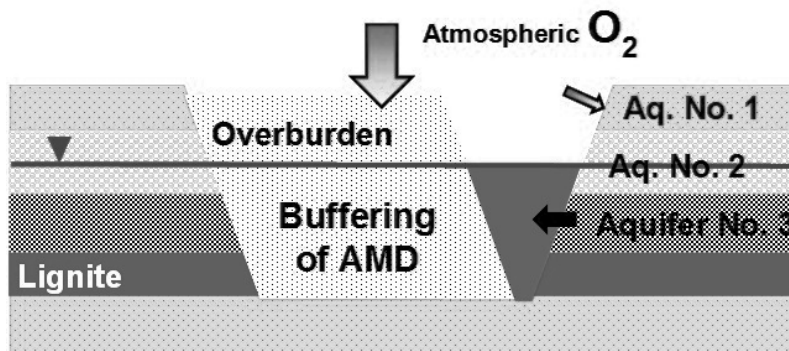


Figure 4 Scheme of buffering of AMD caused by targeted extraction and dumping

Table 1 Sedimentation vs. Hydrolytic Acidity (HA)

facies formation	sediment	HA (250d) mmol/kg
glaci-fluviatil	Aq. 18	0.2
glacial	Glacial Till	0.4
glaci-fluviatil	Aq. 16o	0.4
marine (tidal flat)	Aq. 24	0.7
glacial	Glacial Till	1.0
marine (tidal flat)	Aq. 24	1.5
marine (tidal flat)	Aq. 25	1.6
glaci-fluviatil	Aq. 16o	3.6
glacial	Glacial Till	4.2
glaci-fluviatil	Aq. 16o	7.1
fluviatil	Aq. 5251	7.7
fluviatil (estuary)	Aq. 42	8.6
limnic-fluviatil	Clay	10.3
limnic-fluviatil	Clay	10.9
estuary	Aq. 31	11.4
estuary	Aq. 32	15.6
marine (shallow sea)	Aq. 26/28	22.4
estuary	Aq. 32	23.3
glaci-fluviatil	Aq. 16o	26.6
estuary	Aq. 31	32.8
estuary	Aq. 3231	35.6
estuary	Aq. 32	36.6
estuary	Aq.3	44.0
marine (shallow sea)	Aq. 282	55.2
marine (shallow sea)	Aq. 26	91.3
marine (shallow sea)	Aq. 26	156.3
marine (shallow sea)	Aq. 27	174.3

By superposing the geology, technology and hydrogeochemistry, the opencast mining technology can be adapted and effective countermeasures can be introduced to avoid the discharge of AMD from dumps to aquifers, rivers and residual lakes.

Fortunately, the realization of the technology transition requires no additional major equipment. The implementation in MIBRAG mines can be done with the present excavators, conveyors, conveyor switches and spreaders. Nevertheless, a qualified technological control of mining, transport and deposit is necessary.

Transfer of knowledge

Looking at the geological situation in central German lignite mines, parallels can be drawn to other lignite mining regions. For example, in the lignite mine of Schöningen (HSR GmbH) the same paleographic and hydrochemical linkages exist. The marine sediments from shallow seas show high acidification potential. Figure 5 shows typical AMD discharges from marine – shallow sea – sediments with a pH-level of \approx pH 2, high release of sulphate, iron and other metals.



Figure 5 Picture of the discharge AMD- water from marine sediments, mine Schöningen, Germany 2017

In Schöningen mine after ending active mining AMD is still an issue. In necessary reclamation and recultivation work, targeted mass management must be carried out. This is the only way to prevent further release of acid, iron, sulphate and metals such as cobalt, nickel, zinc, lead and cadmium into the planned residual lake and into groundwater. While supporting the embankment and flattening the edge of the mine, which takes place anyway, it is possible to cover marine sediments from shallow sea by quaternary, glacial or glaci-fluviatile formed sediments. This investment will be amortized by lower follow-up costs.

Acknowledgements

The authors thank the MIBRAG mbH for the research possibility in the mine sites of “Vereinigtes Schleenhain” and Profen. In addition, the authors thank the Helmstedter Revier GmbH for getting access to the mine site of Schöningen.

Gerda Standke, Marlies Grimmer, Elke von Hünefeld-Mugova, and Juliane Günther we thank too. They have contributed to the success with their paleogeographical and geological expertise, patience, charm and laboratory skills.

References

- Simon A, Hoth N, Drebenstedt P, Jolas P. (2016) Strategies to Avoid AMD in Active Lignite Mining. IMWA 2016, Leipzig, Germany,
- Simon A, Hoth N, Drebenstedt P, Jolas P. (2016A) Construction of Dumps in Continuous Mining Considering the Hydro Geo Chemistry to Avoid AMD and geotechnical Failures. 13th ISCSM 2016, Belgrad: p. 537-546
- Simon A (2015) Erarbeitung einer Methodik zur Reduzierung der Sauerwasserbildung durch gezielte Abraumverkipfung unter Beachtung geogener Potentiale. [Development of a methodology for reducing acid water formation through specific overburden tilting under consideration of geogenic potentials] Ph.D.-thesis TU Bergakademie Freiberg
- Sonntag A (2005) Karte der an der Oberfläche anstehenden Bildungen mit Darstellung ausgewählter Geotope und geologischer Objekte [Map of the formations existing at the service, with representations of selected geo-tubs and geological objects], Uckermark District, with brochure, (4) Kleinmachnow/Potsdam.

3 Physical Water Management

Capão Xavier Mine Water Drainage Management (Minas Gerais, Brazil)

Rafael Fernández Rubio^{1,2}, Fabiana Vasconcelos Caldas³, David Lorca Fernández²,
César Grandchamp³, Mauro Lobo de Razende³

¹Madrid School of Mines. Madrid Polytechnic University. Spain

²FRASA Consulting Engineers. Luna 45. 28120 Ciudad Santo Domingo (Madrid). Spain.
rfrubio@gmail.com / proyectos@frasaingenieros.com

³VALE, S.A. Geotecnia Mina e Hidrogeologia Ferrosos Sul. Mina da Mutuca. 34000-000 Nova Lima, MG. Brazil. fabiana.caldas@vale.com / cesar.grandchamp@vale.com / mauro.lobo@vale.com

Abstract The Capão Xavier Mine (Brazil) applies in-advance drainage technology through deep wells, pumping water suitable for human consumption. This water extraction reduces flow in some springs used for public water supply in the city of Belo Horizonte. All decreases are compensated with mine drainage water, improving the water system guaranty. This system optimizes management of water resources, and makes it compatible with the mining operations.

Key words Brazil, iron open pit, dewatering, preventive in advance drainage, water management.

Mine location and operation

The Capão Xavier Mine (CXM) is an open pit iron mine (fig. 1), and the property of VALE Company. The exploited minerals are hematite and lateritic iron ore, locally known as canga; the steriles are itabirite and clays). CXM is located 15 km south of the city of Belo Horizonte, in the State of Minas Gerais (Brazil), in the Iron Quadrangle (Dorr 1969).



Figure 1. Capão Xavier iron mine (Minas Gerais, Brazil).

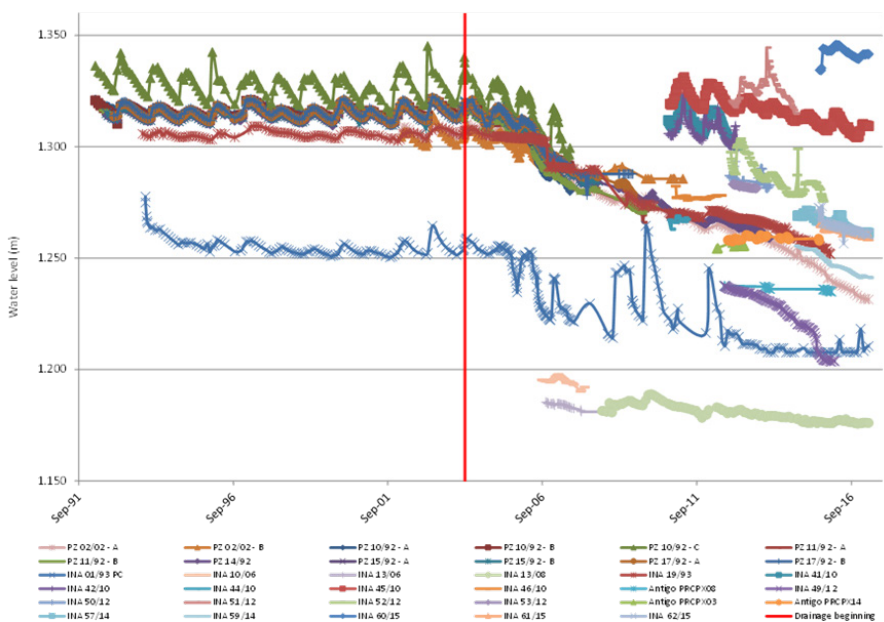
According to the current production plan, at the end of its life, CXM will have extracted 220 million tons of mineral (163 million of concentrated product + 57 million of inert waste); additionally, about 145 million tons of sterile will have been removed. All of the waste rock, as well as most of the sterile mine inert, have being placed at the exhausted Mutuca open pit, thus promoting its morphological and landscape rehabilitation.

Hydrogeological context

CXM is located in the Cauê Formation, integrated by itabirite with hematite, dolomite, and manganese interlayers. This formation is the main aquifer in the Iron Quadrangle because of dissolution of carbonates and silica in the itabirite rocks, forming deposits of iron oxides up to 500 meters deep, with high permeability and strong anisotropy. The under-layer Batatal Formation is integrated by phyllites of low permeability. The overburden consists of the Gandarela Formation, which is composed of limestone, dolomite, dolomitic itabirite, and phyllite with high karstic permeability, with thick packets of ferruginous clay with low permeability. Sub-vertical dikes and sub-horizontal sills of mafic intrusive rock individualize the whole package in hydrogeologically isolated blocks.

The main springs are associated with the Cauê aquifer, with low seasonal variability of flows. There is a record of 24 years of piezometric levels, corresponding to about 50 single, double, and triple piezometers. The records show a clear influence of rainfall, registering rapid rises with the rain, and the most extensive drawdown during the dry periods (Fernandez Rubio et al. 2009). The drain-induced drawdown occurs with varying intensity, depending on distance to the pumping well and the presence or absence of impermeable dikes.

The behavior of piezometric levels in the various observation wells, present seasonal variable oscillations, related to the annual rainfall recharge. At the beginning of each hydrological cycle, usually in October, piezometric levels achieve their minimums, rising rapidly with the onset of rains, until they reaches their maximum values, around March or April, when they begin to decay with the dry season. The amplitude of this seasonal fluctuation



Vertical red line: beginning of drainage (2004).

Figure 2. Temporal evolution of groundwater level in the piezometers inside and around the mine.

varies from point to point, depending on the type of aquifer and hydrogeological conditions, involving parameters such as porosity and hydraulic conductivity, as well as heterogeneity and anisotropy.

In addition to the annual cycles, piezometric levels also feature multi-year variations, whose trends are common to all points of observation installed around the mine (fig. 2). These cycles are characterized according to hydrogeological domains distinguished in the surroundings of the mine.

Hydroclimatology

Rainfall studies were carried out based on rainfall records collected in pluviometric stations installed and monitored by VALE, together with the data of the Morro Velho station, with rainfall records since 1885.

The pluviometry regime presents a rainy season from October to March, collecting on average more than 90% of the annual rainfall, and a “dry” season, from April to September. The historical average annual precipitation (1984/2016) is 1,797 mm, with a minimum of 1,039 mm and a maximum of 2,612 mm (1 to 2.5 ratio between minimum and maximum). The last four hydrological cycles (from 2012/2013) have been below the historical average, producing a substantial water deficit during the last three years. As a result, there is a widespread decline in the aquifer’s water table and in flow from springs.

Hydrological and water management context

Most of the mineral reserves of CXM are located below the water table; therefore, exploitation required an important drainage operation. CXM is located near some springs that have been used to supply the water requirements of the city of Belo Horizonte. Given this proximity, very detailed hydrogeological studies were needed to evaluate the likely effect of mining activity on water resources (Amorim et al. 1999). These studies were developed by the mining companies (MBR, and then VALE), and by the company responsible for the water administration and distribution (COPASA MG), and directed by FRASA Consulting Engineers. The studies included the implementation of a detailed network of hydrological monitoring, with records of flow and water levels for 25 years. They have highlighted the compatibility between mining and the use of dewatering waters to complement the urban supply system.

Based on very detailed and comprehensive monitoring, it has been possible to develop an exceptional database, which has proven very useful for rational water management, with protocols that allow mining to take place without any harm to the use of water resources.

In August 2005, a landmark mine water management plan based on all of the available hydrogeological studies was presented. In June 2006, the dewatering operation yielded a flow of 278 L/s. In August 2006, VALE merged its water drainage pipeline into the Belo Horizonte water supply system, adding the capability of providing 250 L/s. Since February 2008, this mine water drainage has been feeding the COPASA MG pipeline with complete success.

Mine drainage and water management

CXM lies along a hydrographic divide: to the North, Southeast, Southwest, and Northwest, water is being extracted, for Mutuca, Fechos, Catarina, and Barreiro, respectively. Based on hydrogeological studies, it was apparent from the beginning that some of the spring flows and well yields that these areas depended on would be reduced by the drawdown.

In this context, the drained water was used to mitigate the hydrological impact caused by drainage. The pumped water was more than enough to meet the needs of the mining operation and to ensure the public a water supply.

At the end of the life of the mine, it is predicted that the gradual reduction of drainage and the flooding of the open pit will generate a lake, with a maximum depth of 177 m and an average depth of 70 m, capable of holding 55 million cubic meters. The lake will receive water from rain, runoff, and groundwater discharges. This lake, in addition to contributing to biological diversity, will operate as a large reservoir. It will be connected to the water supply system and will help optimize the management of the available water resources, providing water during the dry season. The area adjacent to the mine will be rehabilitated, so that it can be integrated into the Serra do Rola Moça State Park.

With the recovery of the piezometric levels, impacts on spring flows will gradually cease. However, given the water balance, the dimensions of the hydrological basin, the water table evolution, the evaporation rates and the adopted water management, full flooding of the open pit could take many years. Until spring flow is restored to the original status of the hydrogeological systems, the areas' water requirements can be met by using the existing deep wells, in quantities corresponding to the remaining impacts on watershed springs.

In this context, the water management plan is based on using the pumped groundwater and then the lake to compensate for reduced water availability during operation, deactivation, and post-deactivation, against any dewatering influence. A hydrological monitoring program will be maintained, supported by systematic and reliable measurements of the hydrogeological parameters, to predict, identify, and quantify any interference of mine activities on the water management system. Potential impacts and the effectiveness of mitigation measures will be carefully managed, and information on the management of water resources will be provided to the local authorities and to the public.

Moreover, relative to water quality, the studies have shown to everyone's satisfaction that, due to the low mineralization of the groundwater, the positive water balance between precipitation and evaporation, and the absence of soluble salts in the rocks, good water quality is predicted. Having said that, this groundwater must be protected from contamination by organic content and the potential impact of urban sewage.

Current situation

Today the dewatering of CXM is being carried out by deep wells (fig. 3). There has been a gradual flow reduction over time due to reduction of the aquifer-saturated thickness and

lower transmissivity. Total water production has been maintained at values below the maximum permitted discharge (278 L/s).

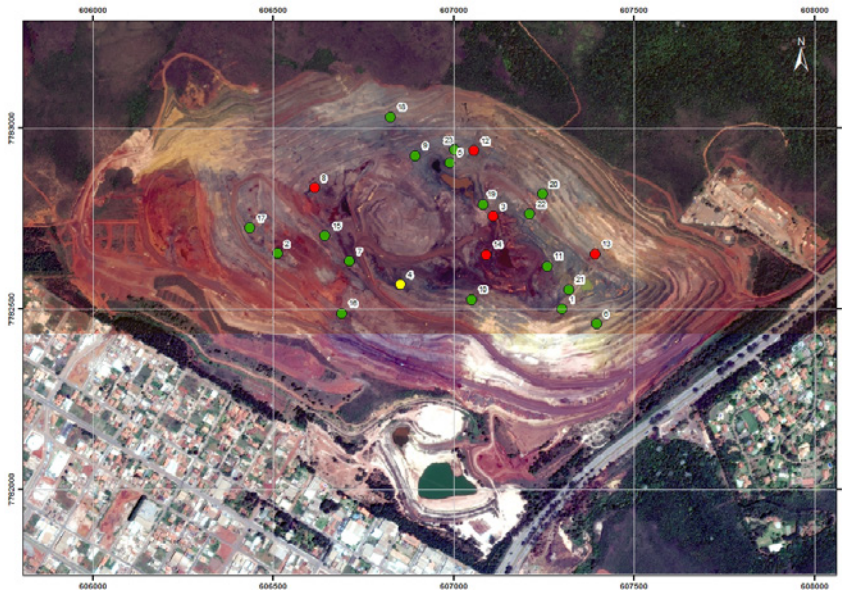


Figure 3. Location of the dewatering wells in Capão Xavier Mine.

Drainage water management

As discussed above, there are four basins surrounding CXM. Urban water supply is administered by COPASA MG. Weekly measurement of flows are maintained, mostly by fixed instruments like level gauge or Parshall (fig. 4).

In general, during the dry season, the entire tributary water is used for urban supply while during the rainy season, spillovers of surpluses are frequent. In recent years, the reduced rainfall has added to the effect of the mine dewatering on flow from some of the springs, but despite this, the flows generally correspond well to the conceptual hydrogeological model forecasts.

Looking at the flow evolution, it is possible to identify a highly variable flow regime, with strong seasonal variation of flow rates. The minimum occurs predominantly in September and October, with a fast increase with the onset of the rainy season. Flow its maximum in January and February, followed by a slow decay until it again reaches the minimum flow.

There is also a less variable flow regime that corresponds fundamentally to the drainage of the deep aquifers. This is related to a micro-fissured aquifer system, without major conduit collectors, in a regime of several years' regulation. The corresponding water points show common multi-year variability. Total discharges are often greater than the total rainfall on

the watershed, which indicates that the hydrogeological basin is greater than the surface watershed runoff. As a general feature, the trend of decreasing flows during the hydrological cycles of low rainfall can be seen very clearly in the last four cycles (fig. 4).

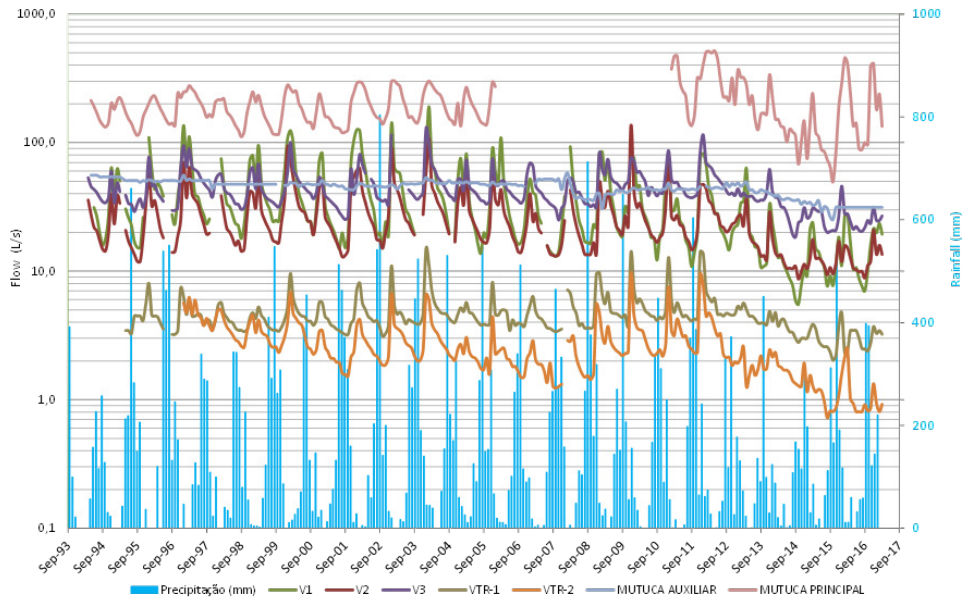


Figure 4. Temporal evolution of rainfall and flows in the Mutuca basin.

Hydrological impacts and mitigation

For the assessment of the impacts on systems of **highly variable flow regime**, the following methodology is applied:

- Calculation of average expected flow rates for the months of August, September and October, based on predefined equations;
- Calculation of the difference between the monthly average flow rates and calculated measures;
- Checking if the difference is within the margin of error of the estimate value by comparing the absolute values with the largest positive and negative differences obtained earlier;
- Characterization and quantification of the impact when the difference is negative and are outside the margin of error for two consecutive months.

On **less variable flow regime** systems, the following methodology is used:

- Comparison of registered flow (monthly average) and the lowest monthly average previously registered;
- Characterization and quantification of the impact when the monthly average flow rate recorded is less than the lowest monthly average previously registered for two consecutive months.

To enable the immediate replacement of the water supply system, a structure was prepared, sized to contribute up to 250 L/s to the COPASA MG pipeline. The terms of commitment between VALE and COPASA MG established that VALE should provide the COPASA MG, a flow rate equivalent to at least 1/3 of the total pumped. If new hydrological impacts are identified in the future, it will be necessary to check to see if the sum of the reductions in flows exceeds the value of preventive replacement (1/3 of the pumped flow). Should this occur, the supply of water would be immediately increased to the pipeline, in order to mitigate the full impact.

Compensation

The lowering of the water level is monitored in order to mitigate the hydrological spring impact, i.e. maintain the availability of water. To achieve this, at least 33% of the pumped water is supplied to the CXM COPASA for urban supply (besides 20% for the Mar Azul Mine). If the impact on watersheds were higher, it would compensate with pumped drainage.

Since February 2008, CXM has delivered substantially more water than this commitment to COPASA, as can be seen in Figure 5. This is how, for example, in the year 2015/2016, the hydrological value impacted by lowering the water level of the mines Capão Xavier, Mar Azul and Tamanduá was 44.77 L/s. According to the agreement with COPASA MG, VALE should have provided 56.96 L/s, while actually it provided 91.69 L/s from the drawdown of the water level in Capão Xavier, significantly over its commitment with COPASA MG.

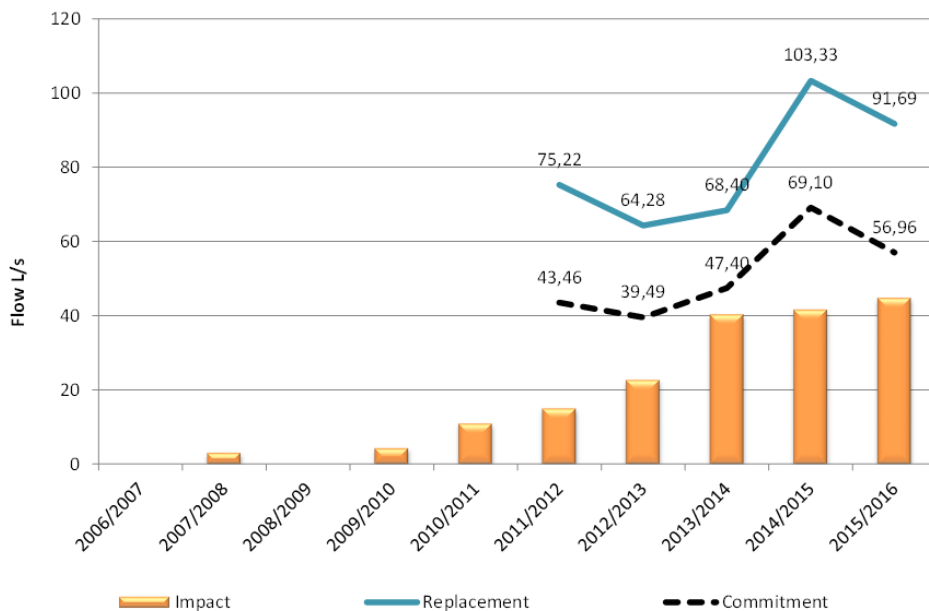


Figure 5. Drawdown-related impacts of mining drainage water level (and the low rainfall in recent years) and compensation.

Related with impact on the wells attending the water supply of Jardim Monte Verde Condominium, VALE is providing 4 L/s of water through a pipe specially built for this purpose, as part of a commitment made over its demand.

In this way, it is maintained and improved the availability of water supply system of RMBH and the third wells affected by the lowering of the water level in the CXM.

References

- Amorim, LQ; Fernandez Rubio, R; Alkmim, FF (1999). The effects of mining Capão Xavier iron ore deposit on the water supply of Belo Horizonte, Minas Gerais, Brazil. *Mine, Water & Environment* 1999 IMWA Congress, proceedings. Seville, Spain. p. 359-366.
- Dorr, JN (1969). Physiographic, stratigraphic and structural development of the Quadrilátero Ferrífero, Minas Gerais, Brazil. United States Geological Survey, Professional Paper, 641-A: 1-110.
- Fernández Rubio, R; Grandchamp, C; Lobo de Rezende, M; Lorca Fernández, D, Bertachini, AC (2009). Dewatering at the Capão Xavier Iron Open Pit Mine. Minas Gerais, Brazil. *International Mine Water Conference*. Pretoria, South Africa.

Effect of operational parameters on the performance of an integrated semi- passive bioprocess.

TS Marais¹, RJ Huddy¹, RP van Hille^{1,2}, STL Harrison¹

¹*Centre for Bioprocess Engineering Research, Department of Chemical Engineering, University of Cape Town, Private Bag X1, Rondebosch, 7701, South Africa*

²*The Moss Group, 13 Bell Crescent, Westlake Business Park, Westlake Drive, Tokai, 7945, South Africa*

Abstract Contamination of South Africa water resources in mining areas by metals and salinity, including acid rock drainage (ARD), is a major risk. Remediating this is important to minimise the impact on the environment and surrounding communities. This paper investigates system performance of an integrated semi-passive bioprocess for simultaneous sulphate reduction and partial sulphide oxidation within a single linear flow channel reactor (LFCR) unit, as a function of the operating conditions of hydraulic residence time (HRT), electron donor and reactor size. The work aims to contribute to the characterisation of a novel integrated bioprocess, from an engineering and microbial ecology perspective.

Key words semi-passive process, biological sulphate reduction, partial sulphide oxidation

Introduction

In South Africa, historical gold and coal mining and related activities have left a legacy of acid rock drainage (ARD) which threatens the public water supply (McCarthy 2011). Impacted water is characterised by high levels of acidity, sulphates and potentially toxic metals with low concentrations of organic material (McCarthy 2011). The potential long-term nature of ARD generation and predicted increases in unmet water demand in South Africa drive the need for economically sustainable treatment operations to address the ARD problem over extended periods of time.

Despite extensive research demonstrating the technical feasibility and potential of biological sulphate reduction (BSR) for ARD treatment, relatively few commercial processes have been developed. The application of these technologies has been limited to niche applications, mainly due to the relatively slow kinetics of sulphate reducers, high cost of electron donor (e.g. ethanol, methanol and volatile fatty acids) and challenges in managing the resulting sulphide product, which is significantly more toxic than sulphate (Rose 2013). Active BSR systems are well described throughout literature. Passive BSR systems are limited to traditional wetlands or packed bed reactors with the drawback of unpredictability in system performance (Zagury et al. 2007). To address the ARD challenges in the context of South Africa, a low-cost technical solution for application in remote areas without highly trained personnel is required to deliver predictable performance. This has led to the development of an integrated semi-passive process based on a linear flow channel reactor (LFCR) which enables simultaneous sulphate reduction and partial sulphide oxidation, with the recovery of a value adding elemental sulphur product (van Hille et al. 2016). In the LFCR, niche en-

vironments are formed, partitioning a distinct aerobic zone at the air liquid interface and an anaerobic zone within the bulk volume of the reactor. The sulphate reducing bacteria (SRB) under anaerobic conditions in the bulk volume reduce sulphate in the presence of a suitable electron donor to sulphide. The sulphide is partially re-oxidised by SOB under oxygen limiting conditions at the air/liquid interface, forming a floating sulphur biofilm.

The effects of various parameters on BSR such as sulphate concentration, temperature, pH, electron donor availability and type, inhibitory effects of metal and sulphide concentration, as well as the use of carrier matrices have been reported with the aim of improving the stability and reliability of these treatments (Elliott et al. 1998; Tsukamoto & Miller. 1999; Moosa et al. 2002; Utgikar et al. 2003; Moosa et al. 2005; Baskaran & Nemati 2006). When introduced as perturbations, the severity of these effects depends on their type, magnitude, duration and frequency. The correct regulation and maintenance of these parameters is therefore essential for optimal process efficiency. Key challenges expected for implementation of the upscaling of integrated process from lab to commercial scale are the selection of a suitable carbon source, the attainment of suitable hydraulic residence time (HRT) and resilience to its fluctuation.

This paper addresses the effect of operating conditions and substrate on the performance of an integrated semi-passive system. Its main objectives are to assess the effect of HRT and reactor volume on system performance and to assess the potential of acetate as alternative carbon source to lactate. It also introduces microbial ecology and community dynamics aspects of the system.

Methodology

Microbial cultures and reactor operation

The SRB mixed microbial community was obtained from Prof. Rose at Rhodes University, and has been maintained at the University of Cape Town (UCT) over an extended period on modified Postagate B medium (van Hille and Mooruth 2013). The sulphide oxidising bacteria (SOB) culture was obtained from van Hille, UCT (van Hille and Mooruth 2013). The reactors were operated at a feed sulphate concentration of 1000 mg/L supplemented with lactate or acetate to maintain a chemical oxygen demand (COD) to sulphate ratio of 0.7. The reactors were run at 30 °C and neutral pH.

Linear Flow Channel Reactor (LFCR)

Two geometrically similar lab-scale Perspex LFCRs (2 L and 8 L), fitted with carbon fibres for biomass retention, were tested. The 8 L reactor simulated the dimensions of the pilot plant under study. The channel reactor was relatively well mixed with limited turbulent mixing. The 2 L LFCR is fully described by van Hille et al. (2016).

Modifications introduced include the reorientation of the carbon microfibers for enhanced biomass retention and the inclusion of a heat exchanger (4 mm ID) for temperature control. Intact colonized carbon microfibers and floating sulphur biofilm were fixed in paraformal-

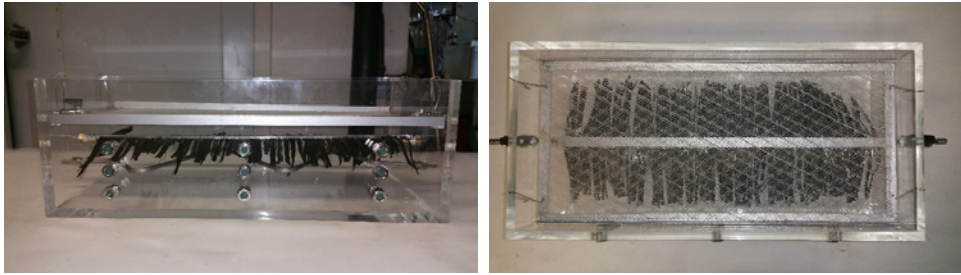


Figure 1: Images illustrating the LFCR design a) side view b) top view of the 8 L LFCR prior to inoculation fitted with strips of carbon microfibers, heat-exchange coil and harvesting mesh plate.

dehyde or glutaraldehyde for fluorescence in situ hybridisation (FISH) and scanning electron microscopy (SEM) analysis, respectively.

Analytical methods

Dissolved sulphide was quantified using the colorimetric N,N-dimethyl-p-phenylenediamine method (APHA 2005). Residual sulphate concentrations were measured using the barium sulphate method (APHA 2005). Volatile fatty acids (VFAs) analysis was conducted to quantify the concentration of lactic, acetic, and propionic acids in the feed and reactor samples. The concentration of each VFA was determined using HPLC on a Waters Breeze 2 HPLC system equipped with a Bio-Rad Aminex HPX-87H column and a UV (210 nm wavelength) detector (van Hille and Mooruth 2013). The pH analysis was conducted on a Cyberscan 2500 micro pH meter. Redox potential was measured using a Metrohm pH lab 827 redox meter.

Floating sulphur biofilm collapse and harvesting

The floating sulphur biofilm (FSB) is not attached to a solid surface, instead develops at the air-liquid interface of the bulk fluid relying on surface tension for support. The biofilm “scaffold” consists of extracellular polymeric substances (EPS). This imparts structural integrity and retains the biomass and elemental sulphur. The FSB was collapsed by physically disrupting the biofilm with a spatula and allowing the fragments to settle on the mesh-plate (termed collapse). Following disruption, the biofilm reformed to cover the entire surface of the reactor within 24 h. The sulphur product could be recovered by removing the mesh-plate and collecting the accumulated biofilm (termed harvesting). The biofilm was dried at 37°C and weighed.

Results and discussion

The reactors were inoculated with an active SRB culture and operated at a 4 day HRT. Fig. 1 illustrates the system performance and operation of the 2 L LFCR fed lactate. Experiment 1 and 2 were operated for 12 and 29 days respectively prior to collapse, evaluating the effect of biofilm collapse on system performance over time. Initially, a thin biofilm formed on the surface of the LFCRs, providing a barrier to oxygen mass transfer and creating the necessary redox and microenvironment partial sulphide oxidation to elemental sulphur.

Sulphate reduction, in the anaerobic bulk fluid, caused the dissolved sulphide concentration to increase steadily, from 50 to 220 mg/L and 260 mg/L for experiment 1 and 2, achieving sulphate conversion efficiencies of 47 and 61% for experiment 1 and 2, respectively (Fig. 1). This confirmed effective biological sulphate reduction and the establishment of an active SRB community.

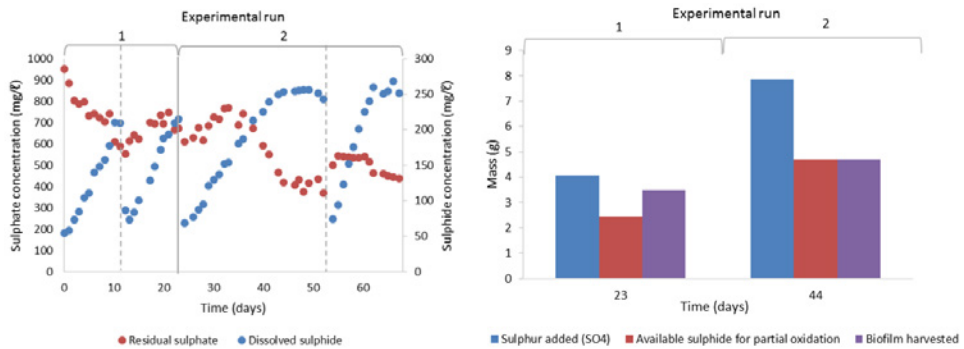
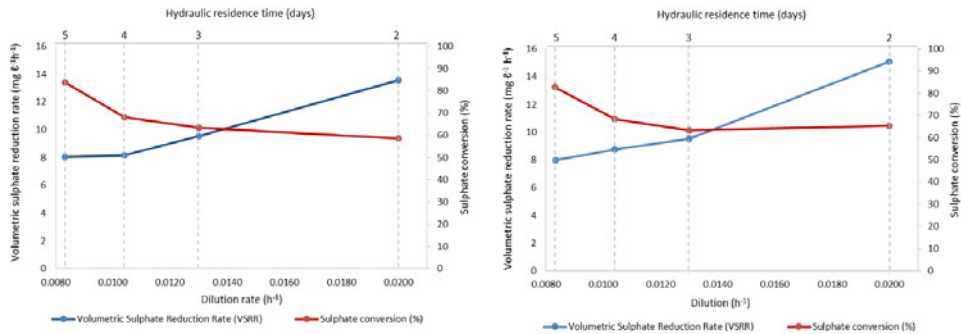


Figure 1: Integrated LFCR performance on lactate a) BSR performance showing residual sulphate and dissolved sulphide concentration as a function of time, vertical lines indicate biofilm collapse (dashed) and harvest (solid), b) partial sulphide oxidation via floating sulphur biofilm showing the total amount of sulphur added in the form of sulphate over the duration of the experiment, sulphur in g in the form of dissolved sulphide available for partial oxidation, and total mass of biofilm recovered.

The system maintained a high sulphide concentration until biofilm collapse or harvesting. Disruption to the biofilm resulted in a rapid decrease in dissolved sulphide concentration, due to re-oxidation following the removal of the barrier to oxygen mass transfer. The re-oxidation was only partial, indicating the complete consumption of oxygen entering the system. The bulk fluid remained anaerobic and sulphate reduction was not affected. As the biofilm reformed, retarding oxygen mass transfer, the sulphide concentration increased again. This cycle could be repeated numerous times.

From Fig. 1b, it was shown that collapsing and harvesting the biofilm more frequently (experiment 1) allowed for higher biofilm recovery than running the system for longer periods of time (experiment 2). As the FSB matures over time, oxygen mass transfer across the biofilm becomes limiting, significantly reducing the rate of sulphide oxidation with concomitant accumulation of dissolved sulphide in the reactor. The time between collapse and harvesting events affects the composition of the biofilm, with the ratio of elemental sulphur to organic material shifting. A study by Mooruth et al. (2013) revealed the proportional relationship of FSB content (sulphur and organic material) as a function of HRT. A decrease in HRT led to an increase in the relative proportion of elemental sulphur while the organic composition decreased. Data in Fig. 1a indicated that longer periods between FSB collapse and harvesting (experiment 2) promoted higher sulphate conversion. This suggests that the integrated system be further optimized to maximize sulphate removal with minimal sacrifice in sulphide oxidation through controlled management of FSB inter-collapsing and harvesting regimes.

Figure 2: Effect of residence time on system performance showing volumetric sulphate reduction rate and sulphate conversion efficiency as a function of dilution rate a) 2L lactate fed LFCR, B) 8L lactate fed LFCR.



The effect of HRT (5 to 2 days) was studied in a 2 L and 8 L LFCR using lactate as a sole carbon source (Fig. 2). A stable FSB and steady state was achieved at each HRT. Negligible difference was observed in system performance in terms of VSRR and sulphate conversion efficiency with LFCR scale. An increase in volumetric sulphate reduction rate (VSRR) (2 L: 8.05 – 13.56 mg L⁻¹ h⁻¹; 8 L: 7.96 – 15.11 mg L⁻¹ h⁻¹) and decrease in sulphate conversion efficiency (2 L: 84 – 59%; 8 L: 83 – 65%) was observed as the HRT was reduced from 5 to 2 days. The highest VSRR output was exhibited under a 2 day HRT at 12.8 and 15.1 mg L⁻¹ h⁻¹ with the highest sulphate conversion efficiency obtained at a 5 day HRT accounting for 84 and 83 % for the 2 L and 8 L LFCR respectively.

The outcome confirms that HRT plays a critical role in the overall microbial activity. At a shorter HRT the system did not allow adequate reaction time to reach high conversion efficiency based on the available bacterial activity; however, it promoted faster VSRRs. The data suggest that the maximum VSRR may be further increased with a lower HRT, albeit at the cost of conversion efficiency. In systems without adequate biomass retention, operating the system below an HRT of 1 day resulted in system failure as a consequence of increased proliferation of fermentative microorganisms, reduced sulphate conversion efficiency and cell washout (Oyokola et al. 2009). Based on the compromise between rate and conversion, the choice of HRT should consider the desired water quality and treatment rate.

Lactate as a sole carbon source was more efficient than acetate (Tab. 1). Maximum sulphate conversion efficiencies obtained in a 2 L LFCR configuration for lactate and acetate were 84 and 62 % at a VSRR of 8.05 and 5.90 mg L⁻¹ h⁻¹ respectively. The lactate was fully utilized through incomplete oxidation to acetate which accumulated; this contributed to relatively high residual COD measured in the effluent (results not shown).

Table 1: The effect of carbon source and linear flow channel reactor (LFCR) configuration on volumetric sulphate reduction rate (VSRR) and sulphate conversion efficiency.

Reactor configuration	Carbon source	Sulphate loading rate (mg L ⁻¹ h ⁻¹)	Volumetric sulphate reduction rate (mg L ⁻¹ h ⁻¹)	Sulphate conversion efficiency (%)
2 L LFCR	Acetate	9.63	5.90	62
2 L LFCR	Lactate	9.63	8.05	84
8 L LFCR*	Lactate	9.63	7.97	83

*Different aspect ratio to simulate pilot plant specifications

Acetate as a sole carbon source showed 73% utilization through complete oxidation with low residual COD in the effluent. The acetate-fed reactor required a long start up period (± 40 days) while both 2 and 8 L lactate-fed LFCRs were stable within ± 20 days. The low VSRR and long start up period with acetate may be attributed to the lower growth rate of complete oxidizers (doubling time 10-16 h) in contrast to incomplete oxidisers (doubling time 3-10 h) (Celis et al. 2013). The lactate-fed SRBs, catalysing incomplete oxidation of the carbon source are more robust, evident during collapse and harvesting of the FSB (Fig. 1a) (Celis et al., 2013). Following perturbation, the lactate system recovered quickly with negligible effect on VSRR. In contrast, the acetate-fed LFCR was more sensitive to biofilm collapse and harvesting, showing decreased VSRR and a longer recovery period. Hence, carbon source selection impacts effluent quality and performance, robustness and cost of ARD treatment.

Conclusion

The research to date has demonstrated the feasibility of the integrated process. Geometry and operating reactor volume showed minimal effect on system performance over the range considered, thus confirming the stability and robustness of the integrated sulphur process on scale up from a 2 L to 8 L LFCR. Scaling up the process to commercial scale has yet to be demonstrated. The findings conclude that 1) the regulation of biofilm collapse and harvesting is critical for establishing high sulphate removal and efficient sulphur recovery; 2) obtaining optimal system operation is characterised by a compromise between VSRR and sulphate removal efficiency; and 3) acetate as a carbon source facilitated complete carbon oxidation resulting in lower residual COD but also a less robust system when exposed to perturbations. Ultimately, this information will be compiled and applied to inform further optimisation of the bioprocess for efficient treatment of contaminated mining wastewater effluents, including a detailed understanding of the response of the microbial community to process perturbations.

Acknowledgments

The authors acknowledge the Water Research Commission (WRC), the Department of Science and Technology (DST), and the National Research Foundation (NRF) of South Africa for funding through the South African Research Chair in Bioprocess Engineering (UID 64778) held by STLH. Dr. Huddy is funded through a DST/NRF research career advancement fellowship (UID 91465). Tynan Marais acknowledges studentship support from the NRF.

References

- APHA (American Public Health Association) (2005) Standard Methods for the Examination of Water and Wastewater, 21st Edition. American Public Health Association, Washington, D.C.
- Baskaran V, Nemati M (2006) Anaerobic reduction of sulfate in immobilized cell bioreactors, using a microbial culture originated from an oil reservoir. *Biochemical Engineering Journal*, 314(2): 148–159.
- Celis LB, Gallegos-Garcia M, Vidriales G, Razo-Flores E (2013) Rapid start-up of a sulfidogenic biofilm reactor: overcoming low acetate consumption. *J Chem Technol Biotechnol* 88: 1672–1679.
- Elliott P, Ragusa S, Catcheside D (1998) Growth of sulfate-reducing bacteria under acidic conditions in an upflow anaerobic bioreactor as a treatment system for acid mine drainage. *Water Research*. 32: 3724-3730.
- Loy, A., Lehner, A., Lee, N., Adamczyk, J., Meier, H., Ernst, J., Schleifer, K.-H., Wagner, M., 2002. Oligonucleotide Microarray for 16S rRNA Gene-Based Detection of All Recognized Lineages of Sulfate-Reducing Prokaryotes in the Environment. *Applied and Environmental Microbiology* 68, 5064–5081. doi:10.1128/AEM.68.10.5064-5081.2002
- McCarthy TS (2011) The impact of acid mine drainage in South Africa. *South African Journal of Science*, 107 (5/6): 1-7.
- Mooruth N (2013) An investigation towards passive treatment solutions for the oxidation of sulphide and subsequent removal of sulphur from acid mine water. PhD thesis, University of Cape Town, South Africa.
- Moosa S, Nemati M, Harrison STL (2002) A kinetic study on anaerobic reduction of sulphate, Part I : Effect of sulphate concentration, *Chemical Engineering Science* 57, 2773–2780.
- Moosa S, Nemati M, Harrison STL (2005) A kinetic study on anaerobic reduction of sulphate, part II: incorporation of temperature effects in the kinetic model. *Chemical Engineering Science* 60(13): 3517–3524.
- Rose P (2013) Long-term sustainability in the management of acid mine drainage wastewaters – development of the Rhodes BioSURE Process, *Water SA* 39(5): 583–592.
- Tsukamoto T, Miller G (1999) Methanol as a carbon source for microbiological treatment of acid mine drainage. *Water Research*, 33(6), 1365–1370.
- Utgikar VP, Tabak HH, Haines JR, Govind R (2003) Quantification of toxic and inhibitory impact of copper and zinc on mixed cultures of sulfate-reducing bacteria. *Biotechnology and Bioengineering*, 82(3), 306–12pp.
- van Hille R, Mooruth N, Marais T, Naidoo N, Moss G, Harrison S, Muhlbauer R (2016) Development of a pilot-scale semi-passive system for the bioremediation of ARD. *Proceedings IMWA* 2016. 957-964.
- Zagury GJ, Kulnieks VI, Neculita CM (2007) Characterization and reactivity assessment of organic substrates for sulphate-reducing bacteria in acid mine drainage treatment. *Chemosphere* 64: 944–954.

Break Free from Your Inertia

Victor Muñoz

SRK Consulting (Canada) Inc., 1066 W Hastings Street, Vancouver, BC, Canada V6E 3X2

Abstract Innovation is the coveted fruit of all consultancies. Unfortunately, innovation most often exists within the world of academia, where theoretical concepts appear to supply simple solutions to complex problems. Meteorological data have increasingly complemented data from ground-based sources to the extent of real-time information. R statistical computing language, provide powerful data access, compilation, analysis, and graphing tools. In addition, the time required to perform typical hydrological analyses is significantly reduced by several orders of magnitude when compared to traditional methods. R can bridge the gap between academia and consultancies—marrying innovation with simplicity, affordability, and practical application—and help improve our understanding of the global environment.

Key words Hydrology, R, tools, spreadsheets, innovation

Introduction

Innovation is the coveted fruit of all consultancies. Yet, it appears restricted to academia, where theoretical concepts are applied to complex problems and appear to provide simple solutions. In reality, these solutions are rarely simple, practical, or affordable. Herein lies the great paradox of innovation.

Information Paradigm – from Spreadsheets to Satellite Information

Over the past 20 years, the complexity of data collection and analysis tools has evolved with the exponential increase of available data.

Most experienced mining consultants graduated when consultancy work was just beginning to become technique-driven and discipline-specific. The fields of water management and hydrology have since seen a significant shift in methodology. For example, hydrology in the 1980s was based mostly on monthly or daily data collected from local meteorological stations; most of the information was compiled as isohyets maps of simplified yearly or monthly tables.

In the 1980's, applying satellite technology in a meteorological context was introduced, but information was scarce and not yet public. During this time, the bulk of hydrologic analyses relied on simple spreadsheet software such as Lotus 1-2-3 and early versions of Microsoft Excel. The growth of the internet in the 1990s, carried the benefits of access to increasing amounts of information. Today, meteorological information from satellite databases can be used to complement data from ground-based sources such that real-time hydrological information is accessible.

The publication of the First Assessment Report by the Intergovernmental Panel on Climate Change (IPCC) in 1990 spurred increased modelling of climate data (IPCC 1990). The amount of information has since increased exponentially. Available data sources include

satellite, ground stations, and projections resulting from climate modelling. Examples of some of these worldwide data sources are listed in Appendix A.

The Problem

Sources such as those listed in Appendix A produce large volumes of data. For these data to be effective in understanding regional and local hydrology, they must be processed efficiently. However, the consultancy environment presents two main challenges to efficient data capture and analysis:

- 1) **Drain on time:** Too much time is spent in data capture and repetitive data processing, instead of on data analysis and problem-solving. The budget is consumed by simple repetitive tasks instead of scientific analysis and potential innovation.
- 2) **Data processing limitations:** The sheer size of spreadsheets become difficult to process, creating computer processing delays and software crashes. This is also an unnecessary drain on budget and resources.

About R—a Possible Solution for Hydrology

Most end users of climate data are not engineers nor work in a mining-related field, but rather work in academia, where time pressures differ from those in the consultancy environment. Script-based programming tools allow consultants to reduce data processing time to a matter of seconds, thus enable hydrological analyses to extend beyond the scope of conventional consultancy work.

The R statistical language is an example of script-based programming. *R* is a free, open-source software environment that was released in 1993. It has since become the standard problem-solving tool for a growing body of researchers in industry, government, and academia who work with large quantities of data. Statistical methods and other functionalities can be modified and combined by the final users, therefore *R* is always pertinent and up-to-date. *R* has built-in access to public information from government institutions, including the United States Geological Survey (USGS 2016), NOAA (NOAA 2016), and Google tools (Gesmann, Castillo and Cheng 2017) and APIs (Google 2017).

R is based on a simple lean environment, and its capacities can be extended through thousands of libraries obtained from CRAN (Comprehensive R Archive Network, one of the most valuable package repositories) (CRAN 2017), as well as from other sites. CRAN's libraries are public and free, and most of them directly reference public papers and specific library manuals. More than 10,300 libraries are available as of April 2017 (CRAN 2017).

Some particular libraries relevant to hydrological analyses are:

- **HydroTSM:** Provides compilation of tools for hydrological data and time series analyses (Zambrano-Bigiarini 2016).
- **EcoHydrology:** Provides sets of hydrology-related tools for engineers and scientists, from snowmelt models to baseflow analyses (Fuka et al. 2014).

- **Evapotranspiration:** Provides methodology to calculate evapotranspiration from Penman-Monteith, Penman, FAO, Morton (Guo and Westra 2016).
- **ncdf4:** Enables reading of netCDF files, the typical format used for climate change or world climate data; this tool can read files containing several gigabytes of information in a few seconds (Pierce 2015).
- **nsRFA:** Provides a collection of statistical tools for predictive (non-supervised) applications of regional analysis methods in hydrology, including L-moments applications (Viglione et al. 2016).
- **caret:** Provides the compilation of several functions (more than 40 packages) to create predictive models. These tools include: artificial neural networking, machine learning, parallel processing, bootstrapping, and resampling (Kuhn 2016).
- **Parallel:** Allows the division of tasks along all the CPU cores available. Simply applying three lines of code can divide a task between multicores (i.e. divide the workload into 8 or 20 cores simultaneously) (R Core Team 2017).

Personal Contribution – Hydro Library

Using this rich programming environment, I created several short scripts that grew in complexity over time to now form a local library. The compilation of these scripts and these saving time increased my productivity and allows me to invest in more complex hydrological problems and obtain more challenging sources. This positive feedback loop started with the curiosity to use new sources and methodologies beyond spreadsheets to improve quality, productivity, and consistency.

Currently, I am already using more than 40 different other public libraries that are the building blocks upon which I base my work necessities. These facilitate data access, compilation, and analysis. These custom-made scripts can be reused and therefore can be applied to different projects, improving hydrologic studies in any region of the world.

Most of the actual hydrological sources presented in Appendix A are impossible to manage and to use with typical spreadsheet tools, because most of these sources work with climate files such as netCDF files (Unidata 2017). netCDF files are the standard for climate information, and are typically used as an output from satellite information, reanalysis or climate change outputs. One netCDF file can contain hourly precipitation information for the entire planet from 1979 to now, and can be as big as 15GB, which is beyond what any spreadsheet can process or even read.

In addition, the time required to perform typical hydrological analyses is greatly reduced. Figure 1 below compares the time frame of data processing for standard spreadsheets and R, at both linear and logarithmic scale. In all cases, the time reduction is higher than 95%, which demonstrates that this is a standard time reduction for R-scripts.

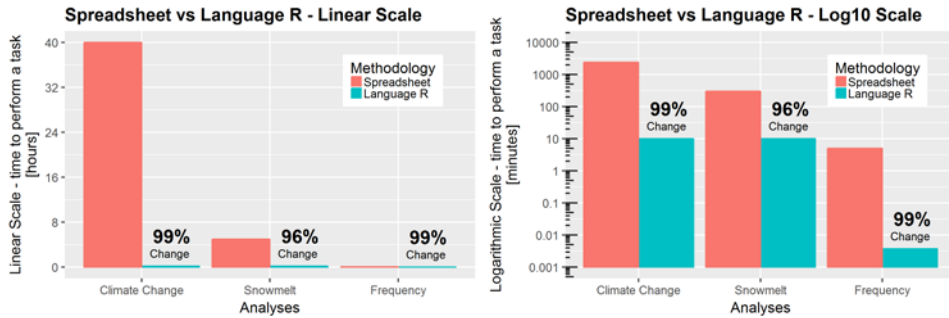


Figure 1: Comparison in processing time between Spreadsheet and R.

The time required for three types of analyses using spreadsheets is compared with time required using R language:

- **Climate change analysis time frame:** The evaluation of climate change data, anywhere on the planet, used to take one week. It now takes only two minutes of processing time with the new methodology. The analysis captures and processes current information (35 GB of information for IPCC Assessment Report AR5), reads historical information from reanalyses (10 GB) and then resolves in one engineer design parameter (Muñoz, Shapka-Felps, and Rykaart 2017).
- **Snowmelt analysis time frame:** Traditional snowmelt models, based on a simplified temperature index, take around of five hours to generate. The EcoHydRology Library (Fuka et al. 2016) presents an energy snowmelt model (Walter et al. 2005) that is typically more representative than the temperature index. It used worldwide meteorological information obtained directly from re-analysis ERA-Interim (ECMWF 2017), and accessing worldwide topographical information from the USGS (USGS 1996), such as slope and topographical aspect. A simple snowmelt model for any place on the planet can be presented in less than 10 minutes.
- **Frequency analysis time frame:** Based on the public nsRFA library (Viglione et al. 2016), the approach reduces the frequency analysis time from five minutes to around one second or less. This methodology includes an L-moment result, which is less sensitive to outliers (Hosking and Wallis 2005).

These few examples present a reduction in processing time that can be invested in broader and deeper analyses (if required) of meteorological parameters, such as correlation matrixes, cluster analyzes, artificial neural network, and Bayesian statistics. Additionally, these parameters are already implemented in dozens of libraries in R (CRAN 2017).

These types of analyses are outside of the scope of any spreadsheet-based analysis and potentially gives the consultancy sector an improved capacity for worldwide meteorological estimations. Overall, this change from spreadsheets to R which is completely free for everybody, brings the consultancy environment more definitive results that up-to-date with worldwide meteorological estimations.

Academia has a proactive advantage, where effective research and study are encouraged and can create innovation. In contrast, the consultancy environment supports the development of practical and familiar tools that lead to simple results. We can learn from academia and integrate new tools, information, and technology into our consultancy work. Breaking off from the inertia of familiar protocols offers new opportunities that can give rise to a more efficient use of information in a fraction of the time needed for traditional methods.

Conclusion

The amount of data available for hydrological analyses has increased dramatically, thanks to the availability of vast public databases and powerful data management tools. It is time to progress beyond limited traditional tools such as spreadsheets that have kept us in a technological comfort zone. Adopting current databases and tools can heal the gap between consultancy and academia—marrying simplicity and innovation—thereby helping to improve our understanding of the global environment.

References

- [CRAN] Comprehensive R Archive Network (2017) Download and install R. The Comprehensive R Archive Network. <https://cran.r-project.org>
- [ECCC] Environment and Climate Change Canada (2017) The Canadian Regional Climate Model. Environment and Climate Change Canada. <http://www.ec.gc.ca/ccmac-ccema/default.asp?lang=en&n=82DDoFCC-1>
- [ECMWF] European Centre for Medium-Range Weather Forecast (2017) Reanalysis ERA-Interim. <http://www.ecmwf.int/en/research/climate-reanalysis/era-interim> ERA-Interim
- Fuka, D.R., Walter, M.T., Archibald, J.A., Steenhuis, T.S. and Easton, Z.M. (2016) R library EcohydRology: A community modelling foundation for Eco-Hydrology. <https://cran.r-project.org/web/packages/EcoHydRology/EcoHydRology.pdf>
- Gesmann, M., Castillo, D. and Cheng, J. (2017) R library googleVis: Interface to Google Charts. <https://cran.r-project.org/web/packages/googleVis/googleVis.pdf>
- Google. Accessed (2017) Google Maps APIs. <https://developers.google.com/maps/>
- Guo, D. and Westra, S. (2016) R library Evapotranspiration: Modelling Actual, Potential and Reference Crop Evapotranspiration. <https://cran.r-project.org/web/packages/Evapotranspiration/Evapotranspiration.pdf>
- [IPCC] Intergovernmental Panel on Climate Change (1990) IPCC first assessment climate change 1990. IPCC.
- Hosking, J.R.M. and Wallis J.R. (2005) Regional Frequency Analysis: An Approach Based on L-moments. Cambridge University Press.
- Kuhn, M. (2016) R library Classification and Regression Training. <https://cran.r-project.org/web/packages/caret/caret.pdf>
- [NASA] National Aeronautics and Space Administration (2017) Prediction of Worldwide Energy Resource. <https://power.larc.nasa.gov/>
- [NOAA] National Oceanic and Atmospheric Administration (2016) R library rnoaa: 'NOAA' Weather Data from R. <https://cran.r-project.org/web/packages/rnoaa/rnoaa.pdf>
- [NOAA] National Oceanic and Atmospheric Administration (2017) National Centers for Environmental Information. <https://gis.ncdc.noaa.gov/maps/ncei>
- Muñoz, V., Shapka-Felps, T. and Rykaart, M. (2017) Integrating Climate Change into Engineering Design. IMWA 2017 – Mine Water & Circular Economy Conference
- Pierce, D. (2015) R library ncd4 Interface to Unidata netCDF (Version 4 or Earlier) Format Data Files. <https://cran.r-project.org/web/packages/ncdf4/ncdf4.pdf>

- R Core Team. (2017) R library parallel Support for Parallel computation in R. <https://stat.ethz.ch/R-manual/R-devel/library/parallel/doc/parallel.pdf>
- Reanalyses.org. (2017) Atmospheric Reanalyses Comparison Table. Advancing Reanalysis. <http://reanalyses.org>
- Unidata (2017) Network Common Data Form (NetCDF). Unidata. <http://www.unidata.ucar.edu/software/netcdf>
- [USGS] U.S. Geological Survey (1996) Global 30 Arc-Second Elevation (GTOPO30). <https://lta.cr.usgs.gov/GTOPO30>
- [USGS] U.S. Geological Survey (2016) R library dataRetrieval: Retrieval Functions for USGS and EPA Hydrologic and Water Quality Data.SGS r info libraries. <https://cran.r-project.org/web/packages/dataRetrieval/dataRetrieval.pdf>
- Viglione, A., Hosking, J.R.M., Laio, F., Miller, A., Gaume, E., Payrastre, O., Salinas, J.L., N’Guyen, C.C. and Halbert, K. (2016) R library nsRFA Non-supervised Regional Frequency Analysis. <https://cran.r-project.org/web/packages/nsRFA/nsRFA.pdf>
- Walter, M.T., Brooks, E.S., McCool, D.K., King, L.G., Molnau, M., and Boll, J. (2005) Process-based snowmelt modeling: does it require more input data than temperature-index modeling? *Journal of Hydrology* 300(1): 65–75, doi:10.1016/j.jhydrol.2004.05.002
- Zambrano-Bigiarini, M. (2016) R library hydroTSM Time series management, analysis and interpolation for hydrological modelling. <https://cran.r-project.org/web/packages/hydroTSM/hydroTSM.pdf>
- Zambrano-Bigiarini, M., Nauditt,A., Birkel, C., Verbist, K. and Ribbe, L. (2017) Temporal and spatial evaluation of satellite-based rainfall estimates across the complex topographical and climatic gradients of Chile. *Hydrol. Earth Syst. Sci.*, 21, 1295–1320, 2017; doi:10.5194/hess-21-1295-2017

Appendix A – Climate Data Sources

Each of the following worldwide meteorological sources provide an understanding of climatic parameters in a given area on the planet such as precipitation, temperature, wind speed, solar radiation, relative humidity, dew point temperature, and evaporation. All of these sources are freely available for everybody:

- **National Climatic Data Center from NOAA (Source: land surface stations):** NOAA databases provide access to worldwide, ground-based meteorological information. Two important databases are the Global Surface Summary of the Day (GSOD), with more than 9,000 stations, and the Global Historical Climatology Network (GHCN), with in excess of 75,000 stations located in more than 180 countries (NOAA 2017). Records span up to data 150 years. The NOAA databases are excellent sources for historical and current meteorological data.
- **Satellite-based rainfall estimates (Source: satellite data):** There are several satellite sources of precipitation data which cover a variety of assumptions, spatial resolutions, and coverage. Most of them cover latitudes between 60° to 50° degrees North and 60° to 50° degrees South, with a variable temporal resolution from 0.04° to 0.25° (~4 to 28 km). As an example of these sources or dataset are: CMORPH, PERSIANN, PERSIANN-CDR, PERSIANN-CCS, TRMM, CHIRPSv2, MSWEPv1.1 and PGFv3. (Zambrano- Bigiarini et al 2017).
- **Reanalysis tools (Source: processed ground and satellite data):** Reanalysis uses a process called data assimilation to combine data from satellites, land surface stations, and numerical models to simulate the earth’s climate. The time step for reanalysis can be as short as eight hours and can be applied to data collected since 1979. Two good examples of reanalysis tools are Modern-Era Retrospective Analysis for Research and Applications (MERRA) (NASA 2017) and ERA-Interim from the European Centre for Medium-Range Weather Forecasts (ECMWF 2017). MERRA and ERA-Interim encompass more than 100

meteorological parameters, including total precipitation, rainfall, snowfall, wind speed, air temperature, and relative humidity.

- **Global climate change models (Source: climatic models):** Global climate change models and scenarios are presented as assessment reports by member meteorological institutes of the Intergovernmental Panel on Climate Change (ECCC 2017). Each model and scenario presents projections of meteorological parameters for the entire planet, typically up to the year 2100. The combination of climate models and scenarios can produce hundreds of projections for any given location on earth. This variation among projections can be incorporated into long-term climate predictions for a given area.

Use of water from the WVII-16 leak in the Wieliczka Salt Mine (Poland)

Kajetan d'Obyrn, Marzena Poleć, Adam Postawa

AGH University of Science and Technology, Faculty of Geology, Geophysics and Environmental Protection, al. Mickiewicza 30, 30-059 Kraków, Poland, dobyrn@agh.edu.pl, polec@agh.edu.pl, postawa@agh.edu.pl

Abstract The Wieliczka Salt Mine (Poland) deals with water hazard every day. The most dangerous groundwater inflow occurred in the Layer 2 chamber (called WVII-16) in December 1972. This continuous inflow comes from sandstones belonging to the Chodenice formation. Water captured from this leakage is considered a brine, with medicinal properties, with low salt concentrations (ca. 60 g/L). This study shows that this leakage has a stable chemical and isotopic composition and its flow has a downward trend. This work presents balneotherapeutic use in case when enclosure of the leak is possible in a stable and controlled way.

Key words Wieliczka Salt Mine, water hazard, use of salt water

Introduction

The Wieliczka Salt Mine is a unique facility in the World, where mining dates back to the 13th century. That means, more than 700 years of an uninterrupted exploitation, which eventually ended in 1994. Currently, mining works in this facility are performed only for securing, or liquidation of excavations. It is one of the most interesting mining facilities in the world, and in 1978 it was listed on the UNESCO World Heritage List. Today it plays the role of a museum, cultural and touristic place, and also balneotherapeutic facility, where an innovative method of treatment with use of salt microclimate is applied. Wieliczka became famous in the 19th century thanks to Dr. Feliks Boczkowski, Boczkowski's activity was continued by Prof. Mieczysław Skulimowski, who worked in Wieliczka Salt Mine as a medical doctor. He used, as a first one, the microclimate of salt excavations for treatment (d'Obyrn, Rajchel, 2015). The aerosol in salt chambers, containing chloride, sodium, magnesium and calcium ions, has beneficial properties in the treatment of respiratory diseases. The microclimate of inactive excavations is characterized by extraordinary bacteriological purity, constant air temperature about 10–12°C, and high humidity of 80–90%. In 2011, the mine has been granted the status of a health resort. Patients come to Wieliczka to treat upper and lower respiratory diseases of nose, sinuses, or bronchus (Obtułowicz, 2002). For treatment purposes, brine from the WVII-16 leak is used from the depth of 250 m.

Geological and hydrogeological setting

Salt deposit in the Wieliczka area is a part of the Miocene salt-forming formation of the Carpathian Foredeep (Fig. 1). The Wieliczka salt deposit extends from west to east, for about 10 km, with the average width about 1.2 km. This deposit has a complex geological structure, due to the Carpathian flysch structure, which has been folded and moved towards the north on the salt-forming formation. The Layer 2 Chamber with the WVII-16 leakage is located in the western zone of the mine.

In the area of Wieliczka there are four Tertiary water-bearing horizons, and one located in Quaternary sediments. The Quaternary aquifer in the mine area is composed of varigrained sands, gravel, and rubble. The water table in this aquifer is unconfined, and only in a few places is confined. Depth of this water table reaches several meters. The youngest aquifer in the Tertiary formations occurs in the Grabowiec Beds. These formations are localized directly above the Chodenice Beds, and these rocks are in contact with the Quaternary formations. The hydraulic conductivity of these layers is high, due to the occurrence of sandy layers in Grabowiec Beds, and ranges from $2.4 \cdot 10^{-5}$ m/s to $8.5 \cdot 10^{-5}$ m/s. These formations are located outside of the area of presented study. Another Tertiary level occurs in the Chodenice Beds. These formations are poorly permeable, and mostly consist of mudstones and clay shales, but also contain fragments of poorly consolidated coarse sandstones with sand lenses, and mudstone. These sandstones represent water preferential flowpaths. The hydraulic conductivity of these formations ranges from $5.8 \cdot 10^{-9}$ m/s to $6.4 \cdot 10^{-6}$ m/s. The evaporate formation is characterized by confined water table and poor permeability of rocks with hydraulic conductivity of $2.5 \cdot 10^{-9}$ to $7.2 \cdot 10^{-6}$ m/s. Within this formation there are two types of aquifers: karst-fissured and porous-fissured. The oldest aquifer (Tertiary) is associated with the Skawina Beds, which consists of sandstones, mudstones, and fissured marly claystones. The Skawina Beds are characterized by a hydraulic conductivity rate of 10^{-7} to 10^{-9} m/s, creating a confined, fissured aquifer (Brudnik et al., 2010).

In this part of the mine, the hydrogeological conditions are formed by sandy series of Chodenice Beds contacting with the deposit from the north. These layers have many cracks and suffosion deformation, and the outcrops of these layers are covered by permeable Quaternary rocks. This results in a continuous supply of atmospheric water. At present, the water hazard at the Wieliczka salt mine is mainly related to the Chodenice Beds. The inflow attributed to these layers constitutes about 85% of the total inflow to the mine, of which about 60% comes from the WVII-16 leakage in the Layer 2 Chamber (Maj, d'Obyrn, 2015).

Area of the Layer 2 Chamber contains layers of evaporate formation bordering at the north with Chodenice Beds. In evaporate formation there are Spiza salts, extracted in the space of the Layer 2 Chamber. The Chodenice Beds are primarily sandy, with concentration of conglomerates, and crumbling rocks. The WVII-16 leakage is located at the clay-gypsum cap boundary, which surrounds salt deposit and salt layers, and is supplied through sandy series of Chodenice Beds by precipitation (Fig. 2).

The leakage of WVII-16

The Layer 2 Chamber was created in the middle of the 20th century, near boundary of the deposit. When exploitation in this mining area ended, this chamber was used as the tank that was used to increase the concentration of the brine by leaching of salt rock surrounding it. As a result of operation of this tank, the pillars of the chamber were dissolved, resulting in hydraulic contact between the sandstone of the sandy series of the Chodenice Beds and the Layer 2 Chamber cavity. At the bottom of this chamber exist poorly permeable, non-dissolving rocks, which limit the contact of brine with water from the outside of the deposit. Leakage in the northern side of the Chamber was confirmed in December 1972. It consisted

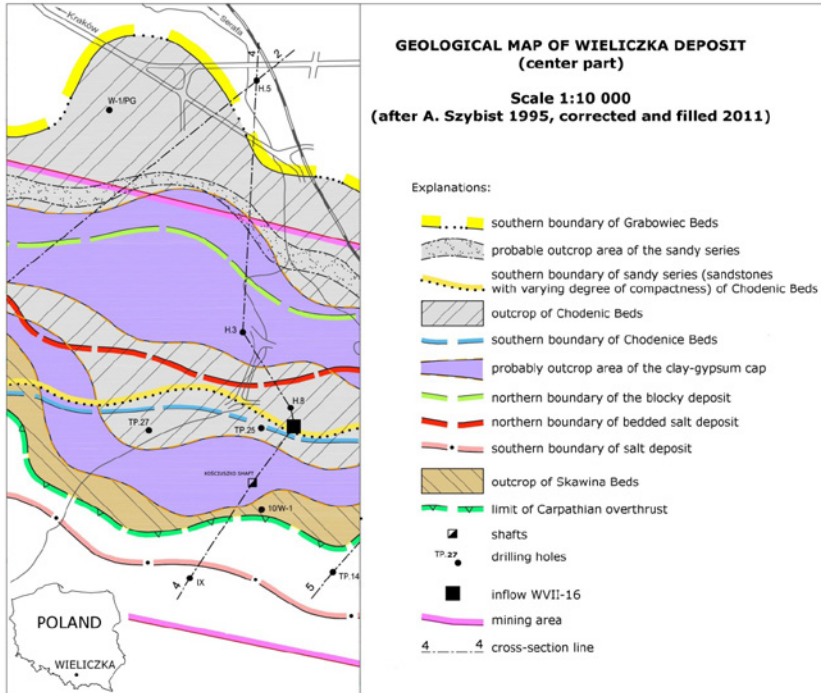


Figure 1 Geological map of the Wieliczka salt deposit (after Szybist, 2011)

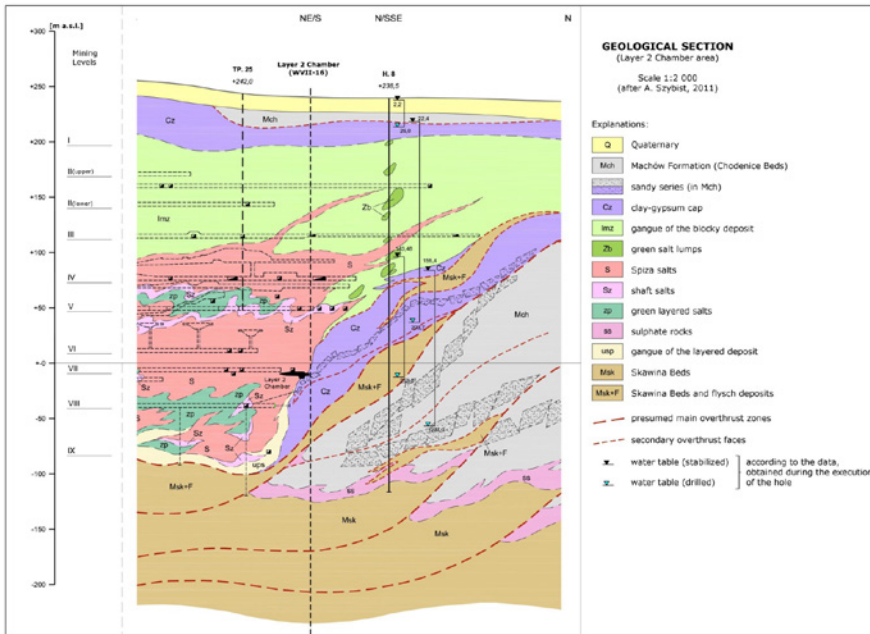


Figure 2 Geological section of the Wieliczka salt deposit in the near of the Layer 2 Chamber (after Szybist, 2011)

of brine with low content of NaCl (about 60 g NaCl/L_ and initial discharge of of 22 m³/h. The WVII-16 leakage was captured in the support pavement in the northern part of the Layer 2 Chamber, which construction was completed in March 1977. This water flows naturally from behind the pavement casing to the metal hopper, from where is piped to tanks on level VIII. Then is pumped to the surface, by the Kościuszko shaft (Witczak et al. 2016).

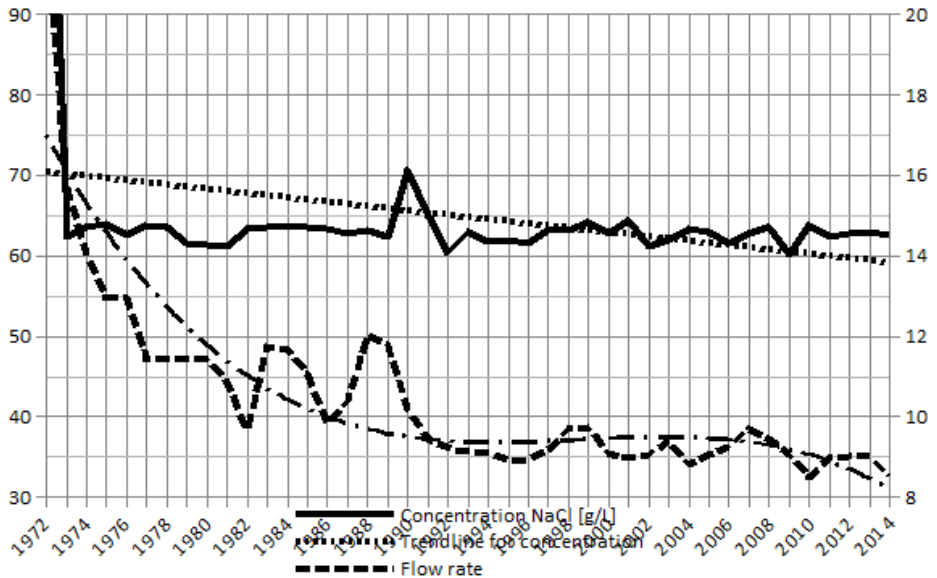


Figure 3 Trends in the leak WVII-16 flow rate and the NaCl concentration in years 1972–2014 (own work).

Balneological characteristics of brines from WVII-16 leak

Changes in flow and Na Cl concentration are shown in the graph (Fig. 3). In the case of the leak discharge an explicit downward trend can be observed, with the average discharge in 2014 of 8.74 m³/h. Decreasing discharge without substantial change in isotopic composition (Fig. 4) may suggest that we are dealing with a large volume and limited supply system, which is slowly draining (Brudnik et al., 2007). In terms of NaCl content in the leak there is no clear trend. Average content of NaCl from 1972–2014 is 64.80 g/L (Witczak et al., 2016). Analysis of chemical composition of waters from this leakage indicate slight variations, qualifying these waters as a Cl-Na brine.

No substantial tritium content was detected in the leak, and low values of $\delta^{18}\text{O}$, indicate origin of this water from a colder climatic period, and possible precipitation during the Pleistocene period. As a result of this leak, the original flow direction (W–E) was reversed and made changes in the pressure pattern. In the future it may increase amount of modern water with lower mineralization in the inflow into the the Layer 2 Chamber (Witczak et al., 2016)

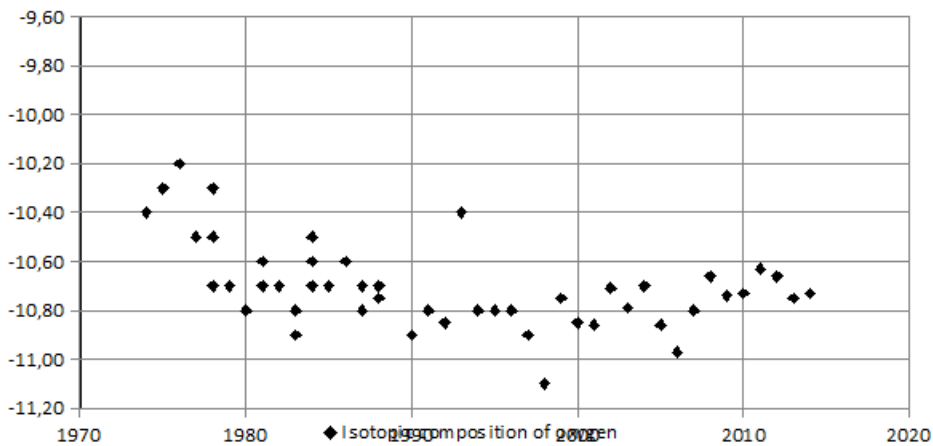


Figure 4 Isotopic composition of oxygen in the leak WVII-16 in the period 1974-2014.

Balneotherapy use of brines from WVII-16 leak

Relatively high inflows to the mine, around 130,000 m³/year, require safe system of collection. Water from the inflows to the Wieliczka Salt Mine is currently used for the production of brewed salt, and partly as a medium for backfilling sand, used to eliminate unnecessary excavations.

The WVII-16 leakage brine was considered a medicinal water in 2013, and has been used in the Graduation Tower at the Wieliczka Salt Mine since 2014 (Fig. 5). The active surface of the graduation tower, where brine flows through the blackthorn twigs to form an aerosol is 3200 m² and brine tanks have capacity of 275 m³ (d'Obyrn, Rajchel, 2015). In the Graduation tower brine flows down from the top of the construction, along the walls covered with blackthorn. As a result of splashing, microscopic droplets of brine are formed. Eventually, brine is accumulated in the tanks at bottom of the construction. Mineral-rich brine droplets in the air form specific microclimate which is regarded as having beneficial health effect, and provides a space for inhalation in the open area.

Conclusions

Current study allows to conclude that the WVII-16 leakage is characterized by a constant and stable isotopic and chemical composition. There is also the clear downward trend in leak capacity.

So far, on the basis of isotopic studies, in the WVII-16 leakage originate from Pleistocene waters have been detected, whose composition was stable. However, it cannot be excluded that in several decades contemporary waters influenced by atmospheric precipitation occur in the leakage. That modern water would come from the outcrop of sandy series of the Chodenice Beds. WVII-16 leakage can be considered as a stable and does not threaten to the safety of the Mine.



Figure 5 Graduation Tower in Wieliczka Salt Mine (photo: K. d'Obyrn)

Acknowledgements

This research was financially supported by the Polish Ministry of Science and Higher Education and AGH University (statutory research no. 11.11.140.797).

References

- Brudnik K, Czop M, Motyka J, d'Obyrn K, Rogoż M, Witczak S, (2010) The complex hydrogeology of the unique Wieliczka salt mine. "Przegląd Geologiczny" Vol. 58, Nr 9(1): 787–796
- Brudnik K, Przybyło J, Winid B, (2007) Wydajność wycieków WVI-32, WVII-16 i WVI-6 jako element oceny sytuacji hydrogeologicznej badanego rejonu złoża soli Wieliczka. *Wiertnictwo Nafta Gaz* t. 24, n. 1 [in Polish]
- d'Obyrn K, Rajchel L, (2015) Balneoterapeutyczne wykorzystanie solanek w uzdrowisku Kopalnia Soli "Wieliczka". "Przegląd Geologiczny" Vol. 63, nr 10/2: 981-984 [in Polish]
- Maj A, d'Obyrn K, (2015) Określenie stanu podporowej tamy przeciwwodnej i jej ruchów na podstawie obserwacji geodezyjnych w komorze Layer w kopalni Wieliczka. "Przegląd Górniczy" Nr 11: 68-79 [in Polish]
- Obtułowicz K, (2002) Aerozole kopalniane. [In:] Ney R. (red.), *Modelowe studium kompleksowego wykorzystania i ochrony surowców balneologicznych Krakowa i okolicy*. PAN IGSMiE [in Polish]
- Witczak S, d'Obyrn K, Duliński M, Rajchel L, (2016) Conditions of medicinal water supply in the Wieliczka Salt Mine. *Biuletyn Państwowego Instytutu Geologicznego* Vol. 466, p. 313–322 [in Polish]

Tailings Water Hydraulics Analyses for Risk Based Design

Simon Lorentz^{1,2}

¹*SRK Consulting, 265 Oxford road, Illovo, Johannesburg, South Africa. SLorentz@srk.co.za*

²*Centre for Water Resources Research, University of KwaZulu-Natal, South Africa*

Abstract Commensurate objectives of optimal water use, as well as of risk based design criteria, require viable estimates of the hydraulic behaviour of impounded materials during deposition and post closure. The HYDRUS-2D soil-water physics model is used to illustrate ranges of hydraulic behaviour in cycloned and spigotting deposition in metal tailings impoundments for a range of deposition criteria. The results summarise criteria leading to optimal water use, impoundment instabilities and unacceptable leaching below the impoundment. These criteria can be applied to optimise water use during tailings deposition as well as satisfy predictions during risk based design.

Key words Tailings hydraulics, Risk based design.

Introduction

Commensurate objectives of optimal water use in cost effective tailings impoundment development, as well as of risk based design criteria require viable estimates of the saturated and unsaturated hydraulic behaviour of impounded materials during deposition and post closure. Common methods of estimating drainage, seepage and phreatic surface development in tailings impoundments consider contributions from the pool and average atmospheric inputs at the tailings surface. However, detailed deposition sequences, rainfall and evaporation fluxes and the hydraulic behaviour of the material are often called for to satisfy risk based design criteria and to optimise water use. In particular, tailings deposition using centrifuge methods to separate coarse fractions (underflow) for deposition in the outer walls and fines (overflow) into the tailings beach, require consideration of water influxes into the outer edges, comprising high hydraulic conductivity underflow material, as well as variable influxes from the pool and tailings beach. While holistic risk based approaches are desired (Rademeyer et al. 2008; Yibas et al. 2012; Barrera et al. 2015), detailed technical analysis allows for optimising water use together with satisfying stability criteria and minimising environmental impacts through seepage. Excessive water deposition with underflow material may result in stability criteria being violated, whereas a reduction in water content deposited with the underflow may require adjustment of drain positioning to optimize water recovery and minimize head build-up on base liner systems. Accurate estimates of the development of positive hydraulic heads within the tailings are critical for stability estimates, drainage design, considerations of base lining methods and leachate predictions.

The HYDRUS-2D soil-water physics model is used to illustrate ranges of hydraulic behaviour in cycloned deposition as well as traditional spigotting in gold, copper and platinum tailings impoundments for a range of deposition criteria, daily atmospheric inputs, drain placement and base liner conditions. The examples are applied to a hillslope deposition, where a 2D analysis is warranted (Garrick et al. 2014).

Methods

In order to simulate the hydraulic performance of a proposed platinum tailings dam, an existing dam was first characterised and the simulated phreatic surface position, fluxes to drains and hydraulic gradients were compared to those observed. Once satisfactory performance of the 2D model is obtained, the proposed design can be evaluated.

The hydraulic properties of the existing tailings dams were measured using in-situ double ring infiltrometer, tension infiltrometer and Guelph permeameter tests on site and supplemented with constant head laboratory tests on undisturbed samples. Gold, Copper and Platinum tailings materials were measured for comparative purposes. The depth of in-situ measurements was only possible to 2.5 m below surface and so the results of piezocone tests were analysed in an attempt to determine hydraulic conductivities in consolidated materials to a depth of 50 m below surface. However, the results were highly variable and were only used as a guide in the modelling.

In the Platinum tailings, in-situ observations of the phreatic surface levels were made through piezometers installed to below the saturated water level. Piezocone observations were interpreted together with the piezometer observations to determine effective vertical hydraulic gradients.

Observation of fluxes from the tailings dam drains were extracted from mine records, although some seepage was observed through the toe walls on occasions.

The simulation modelling included the rainfall and potential evaporation drivers as well as slurry water inputs. In the simulation of the cyclone deposition in the platinum tailings, the slurry inputs were divided between water deposited with the coarse underflow material on the edge and the overflow water deposited on the beach (fig. 1). Intermittent rain and slurry inputs to the surface of a 2D (Šimůnek et al. 2006) section of the tailings dam pose a difficulty in simulating the entire section (Rykaart et al. 2001; Rykaart and Wilson 2003) and so HYDRUS-1D (Šimůnek et al. 2009) simulations of rainfall, potential evaporation and intermittent slurry application were used to derive effective boundary fluxes on the surface. These were applied as variable flux or atmospheric boundary conditions (fig. 1). Drains were simulated by specifying seepage face boundary conditions and the pool was specified as a constant head boundary. Liner systems at the base of the tailings, comprising porous media materials were included by specifying the hydraulic characteristics of the liner materials. However, in order to simulate geomembrane liners, an iterative approach was used. Here, the fluxes through the liner cannot be derived through Darcy physics, so a relationship between the imposed head on the liner and the subsequent flux was derived for various liner qualities (Giroud and Bonaparte 1989; La Touche and Hollie 2012). The head-flux relationship was applied as a variable flux bottom boundary condition in an iterative simulation until the heads dictated by the saturated/unsaturated flow through the tailings and the flux through the liner were in equilibrium.

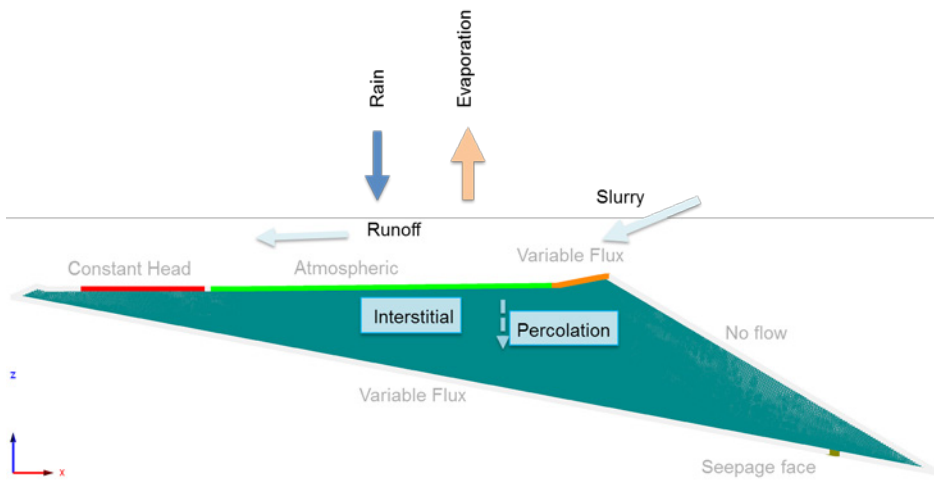


Figure 1 Illustrated processes and boundary conditions of the 2D simulated tailings dam

Results

The results of typical hydraulics conductivity measurements on the tailings surface are presented in tab. 1. No significant differences between the saturated hydraulic conductivities on the surface were found between the edge and pool of the tailings as listed for the gold tailings. However, significant differences of the hydraulic conductivities at small tensions (200 mm) were measured. These decreased from the edge of the tailings to the pool location,

Table 1 Surface Hydraulic Conductivities of Gold, Copper and Platinum Tailings.

Material	Position	Ksat (m/s)	K(200) (m/s)
Gold	Edge	2.6×10^{-6}	6.1×10^{-7}
Gold	Middle	1.9×10^{-6}	1.0×10^{-7}
Gold	Pool	2.8×10^{-6}	6.3×10^{-8}
Copper	Edge	3.9×10^{-6}	3.7×10^{-7}
Platinum	Underflow	7.9×10^{-6}	
Platinum	Overflow Edge	5.6×10^{-6}	
Platinum	Overflow Middle	5.4×10^{-6}	
Platinum	Overflow Pool	5.9×10^{-7}	

Ksat = Saturated hydraulic conductivity

K(200) = Hydraulic conductivity at tension 200 mm

Differences between the platinum underflow material and the overflow material were evi-

dent with depth below the surface (fig. 2). Here, the coarse underflow material is an order of magnitude higher than the overflow material at depth below 1 m.

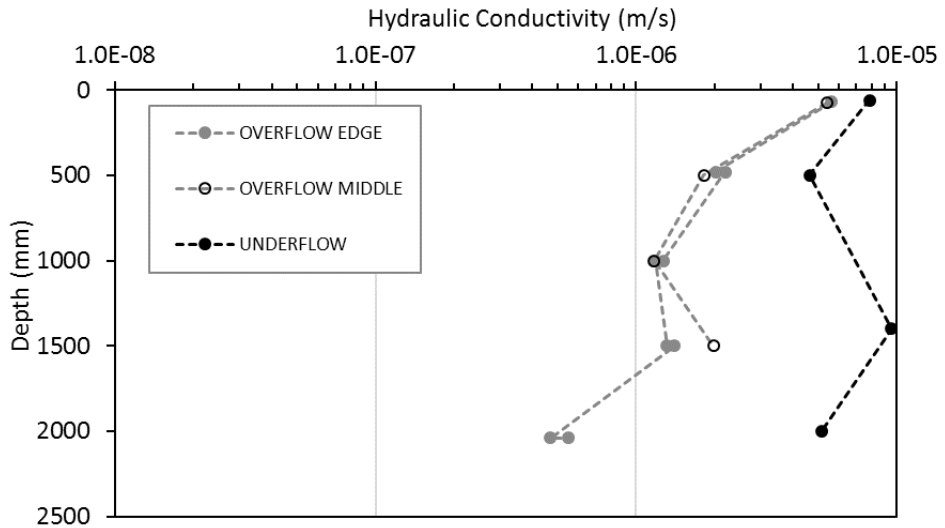


Figure 2 Saturated hydraulic conductivities in the Platinum tailings.

The HYDRUS-2D simulations of the phreatic surface of the existing platinum dam compared favourably to the observed levels. The simulated fluxes from the drains ranged from 120 m³/day to 425 m³/day, whereas observed values ranged between 184 m³/day and 272 m³/day. The higher simulated peak values were considered feasible due to the observed seepage from ungauged sources.

Comparing the simulated vertical gradients with those inferred from piezocone/piezometer observations revealed an under simulation of the vertical gradient. However, with a seepage loss from the base of the dam specified at 3.5 mm/day, the gradient matched. Nevertheless, the interpretive work between piezocone and piezometer observation is continuing in order to improve these comparisons.

With the model performing suitably, illustrative scenarios of the proposed design were performed at a development stage of 100 m. The phreatic surfaces resulting from conventional tailings deposition are illustrated for gold, copper and platinum tailings in fig. 3a. These indicate the drawdown to a blanket drain which results in stable tailings slopes.

However, deposition of large quantities of water with coarse underflow material in cyclone deposition could impose a stability risk (fig. 3b). Slurry water from the underflow moves rapidly through the material until it reached the underflow/overflow interface. Here, the water does not preferentially discharge down the high conductivity underflow material, but is drawn into the overflow tailings along a length of the interface. This results in a raised

phreatic surface unless the water deposited with the underflow is reduced from 25% to 8% of the total slurry water (fig. 3b). The phreatic surface position is worsened if intermediate drains, placed between the toe drain and the blanket drain fail.

The addition of a further drain, 150 m upslope of the blanket drain, alleviates the phreatic surface further (fig. 3c). Seepage losses through a geomembrane liner also lowers the phreatic surface. Here, environmental impacts need to be evaluated and improved liner conditions specified, if required.

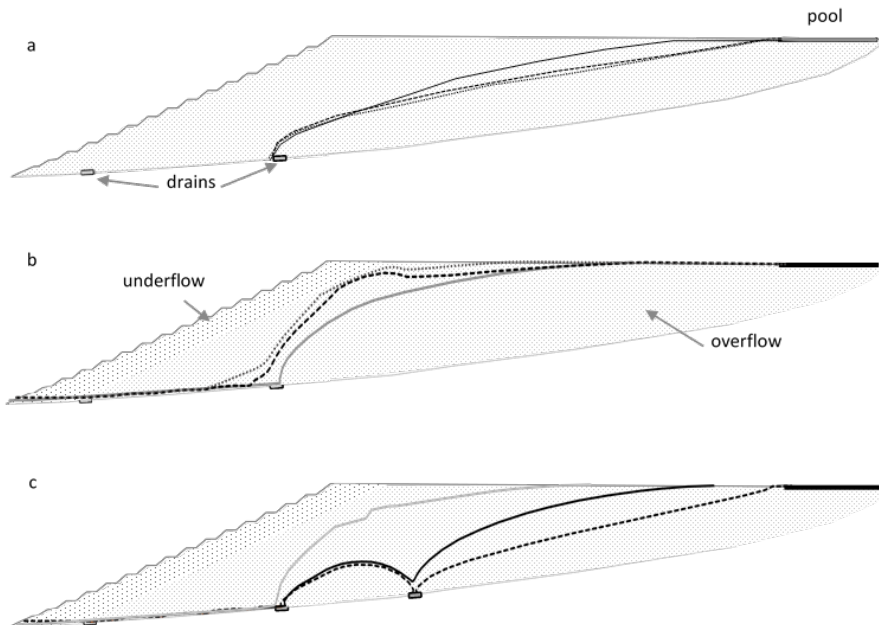


Figure 3 Simulated phreatic surfaces of a) conventional deposition of platinum (solid grey line), gold (dashed line) and gold (dotted line) tailings; b) cyclone deposition of platinum tailings with 8% of the slurry water deposited with the underflow (solid grey line), 25% of the slurry water deposited with the underflow (dashed line) and 25% of the slurry water deposited with the underflow without intermediate drains between the toe drain and the blanket drain and c) cyclone deposition with 15% of the slurry water deposited with the underflow (solid grey line), with a second drain 150m upslope of the blanket drain (solid black line) and with a second drain with seepage from the base (dashed black line).

Conclusions

The results summarise criteria leading to optimal water use, impoundment instabilities and unacceptable leaching below the impoundment. In particular, results of cyclone deposition indicate that reducing the water:solids ratio of underflow deposition on a 100 m high tailings impoundment from 25% to 8% of the total slurry water, improves the stability criteria with drains positioned between 200 m and 350 m from the toe, while effectively capturing percolating water for recirculation and minimizing the pressure head on the base.

These criteria can be applied to optimise water use during tailings deposition as well as satisfy predictions of tailings hydraulic fluxes and pressure distribution during risk based design.

Acknowledgements

The author thanks Lappeenranta University of Technology for hosting the IMWA 2017 Conference and Tekes for co-funding the conference. Thanks are also due to Dr Goitom Adhanom for laboratory analyses at the Centre for Water Resources Research, University of KwaZulu-Natal and to colleagues at SRK Consulting and IMWA reviewers for review of the paper.

References

- Barrera S, Cacciuttolo C, Caldwell J (2015) Reassessment of best available tailings management practices. Proceedings Tailings and Mine Waste 2015, Vancouver, BC, October 26 to 28, 2015.
- Garrick H, Digges La Touche D, Plimmer B, Hybert D (2014) Assessing the Hydraulic Performance of Tailings Management Facilities. In: Hunger E, Brown T, Lucas G (eds) Proceedings of the 17th Extractive Industry Geology Conference. Extractive Industry Geology Conferences Ltd.
- Giroud JP, Bonaparte R (1989) Leakage through Liners Constructed with Geomembranes – Part I. Geomembrane Liners. *Geotextiles and Membranes*, 8:278-67.
- La Touche GD, Hollie G (2012) Hydraulic performance of liners in tailings management and heap leach facilities. – In: McCullough CD, Lund MA, Wyse L: International Mine Water Association Symposium, Bunbury, Australia: 371-378.
- Lorentz SA, Goba P, Pretorius JJ (2001) Hydrological Processes Research: Experiments and Measurements of Soil Hydraulic Characteristics. Water Research Commission Report 744/1/01, Pretoria.
- Pulles W, Yibas B, Lorentz S, Maiyana B (2011) Development of water balances for operational and post-closure situations for gold mine residue deposits to be used as input to pollution prediction studies for such facilities WRC Report No.1460/1/11. Water Research Commission, Pretoria.
- Rademeyer B, Wates JA, Bezuidenhout N, Jones GA, Rust E, Lorentz S, van Deventer P, Pulles W, Hattingh J (2008) A Preliminary Decision Support System for the Sustainable Design, Operation and Closure of Metalliferous Mine Residue Disposal Facilities. Water Research Commission Report: 1551/1/08. WRC Pretoria.
- Rykaart EM, Wilson GW (2003) Methodology for calculating the closure water balance for an acid generating tailings impoundment. 6th International Conference on Acid Rock Drainage. Cairns, QLD, Australia, 12-18 July 2003.
- Rykaart M, Fredlund M, Stianson J (2001) Solving Tailings Impoundment Water Balance Problems with 3-D Seepage Software. *Geotechnical News*, December. GeoSpec. Bi-Tech Publishing. Vancouver, B.C., Canada: 50-54.
- Šimůnek J, Šejna M, Saito H, Sakai M, van Genuchten MTh (2009) The HYDRUS-1D Software Package for Simulating the One-Dimensional Movement of Water, Heat, and Multiple Solutes in Variably-Saturated Media, V4.08, University of Riverside, CA.
- Šimůnek J, van Genuchten MTh, Šejna M (2006) The HYDRUS Software Package for Simulating the Two- and Three-Dimensional Movement of Water, Heat, and Multiple Solutes in Variably-Saturated Media. Technical Manual V1. PC Progress, Prague, Czech Republic.
- Yibas B, Pulles W, Lorentz S, Maiyana B, Nengovhela C (2012) Oxidation process and hydrology of tailings dams from TSFs management- The Witwatersrand experience, South Africa. International Mine Water Association Symposium, Bunbury, Australia, pp 245–255.

Water management in mining – Measuring and demonstrating value-impact of management strategies

Raul Mollehuara Canales^{1, 2}, Maria Sinche Gonzalez¹

¹*Oulu Mining School Faculty, University of Oulu, Linnanmaa Campus, Finland*

²*WATEN-ST Water & Environment Sustainable Technologies, 5095 South Australia, Australia*

Abstract Water quality in mining environments can be widely influenced by external factors and processes making difficult to measure the total impact of water management strategies. Stringent requirements demand best practices more than ever, and managing all aspects of water is critical as expectations of stakeholders and water users are diverse. Mine operators have to demonstrate that their strategies are designed to satisfy those expectations and are not only for compliance. This paper addresses these imperatives in a framework responding to those identified drivers. A case study shows the evolution of water quality in response to driven efforts in managing water quality.

Key words water, quality, mine, management, environment

Introduction

Water quality in mining environments is influenced by activities associated with mineral extraction or mineral processing. Water is the main transport mechanism carrying out pollution within and outside the mine site. Natural and industrial processes distribute widely water constituents into the environment and sometimes in concentrations exceeding regulatory standards. Stringent requirements from the public and regulatory agencies demand best management practices more than ever. Business and organizations formulate their management strategies based on these requirements. For instance, mining companies formulate their environmental management strategies based on the environmental commitments established in their EIA, EIS and Closure plans. Managing all aspects of water is critical and difficult as expectations of a variety of stakeholders and water users can be diverse. Hence, water management strategies should respond to these expectations and align with the regulatory requirements and guidelines for water quality protection.

Methodology

Measuring environmental performance is challenging when the monitoring criteria focus on compliance of inputs and outputs alone. As a result, more than often the functional activity of monitoring becomes a status quo that can prolong the need for the primary design.

Figure 1 Integrated water management framework proposes a framework standing on knowledge management support throughout the life of mine. A review and assurance of the water management strategy and all associated elements are paramount for a successful implementation.

The most practical approach for a mining company to measure water quality variability is to conduct monitoring but demonstrating sustainable performance could become difficult

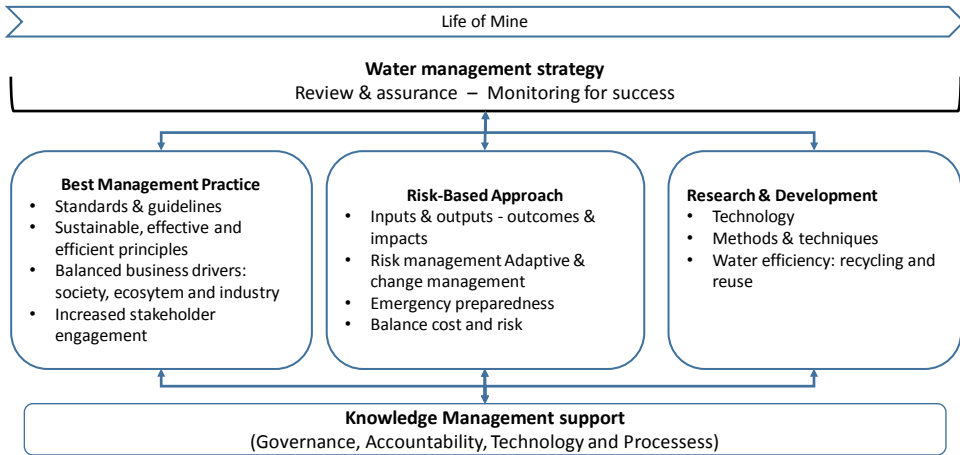


Figure 1 Integrated water management framework

when the monitoring criteria lack clarity. Companies require a better and a quantitative understanding of the performance of their management strategies.

The total impact of management strategies is a function of the combined environmental, social and economic impacts. In this approach, monitoring for success extends beyond tracking changes in the water quality of the effluent downstream and includes tracking changes in the catchment system in response to management strategies over time. Hence, monitoring not only targets defined and agreed water quality parameters, but also seeks to confirm the outcomes and impacts anticipated in management strategies. In this context, the paper presents a monitoring context shifting from inputs and outputs, towards outcomes and impacts (Figure 2 Effectiveness of water quality measurement criteria adopted in monitoring programs).

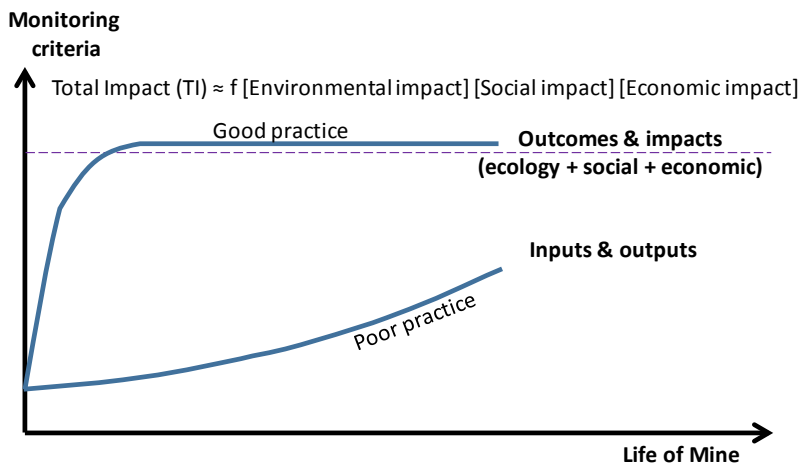


Figure 2 Effectiveness of water quality measurement criteria adopted in monitoring programs

By measuring these outcomes and impacts, businesses and organizations can calibrate their strategies and understand whether these are working or not.

Case study

The former Brukunga mine site is located 50 km east of Adelaide in the Adelaide Hills eastern of the Mount Lofty Ranges (Figure 3 Former Brukunga mine site is located 45 km to the east of the city of Adelaide in South Australia (Source: Geoscience Australia 2017)). The mine operated from the 1950s through to 1970s extracting and processing iron sulphide to source sulphur for the production of sulphuric acid and fertilizer. The site occupies approximately 165 hectares comprising open pits, 8 Million tonnes waste rock and 3.5 million tonnes of tailings. Environmental issues arising from the former operation included low-grade sulfidic ore in waste rock dumps adjacent to the local Dawesley Creek, exposed fresh sulphide mineralization on the quarry floor, tailings storage facility, acid water seepage and pollution of natural drainage. The mine site rapidly became a source of acid drainage with the generation of potential contaminants (Taylor and Cox 2003).

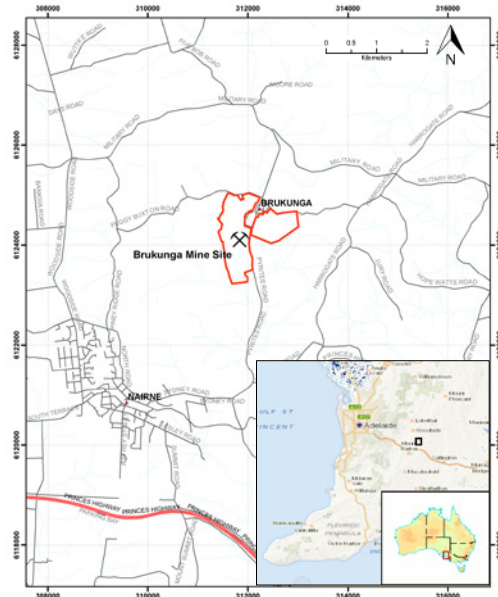


Figure 3 Former Brukunga mine site is located 45 km to the east of the city of Adelaide in South Australia (Source: Geoscience Australia 2017)

Following the cease of operations at the former Brukunga mine site, the water quality was impacted in local the creek along the way for nearly 70 km of flow stream representing almost 43 km in a straight line and affecting farmland, agriculture and ecosystems.

The Brukunga mine affected the socio-ecological system of the local Dawesley Creek including associated terrestrial ecosystems, local families and businesses using these ecosystems. As a result, properties downstream of the mine were advised not to use water from the creek

and were compensated with subsidized water supply. The former mine became a financial and environmental liability to Government (Armstrong and Cox 1977).

In 2001, the Government committed funding to conduct remediation works and to improve water quality in Dawesley Creek. Under the guidance of a team of experts, the site has been subject of extensive research to identify a suitable whole-of-site strategy to remediate the site. The mine site is currently undergoing rehabilitation but water management at the site continues. A water management infrastructure continues to collect, intercept and treat acid and metalliferous drainage (AMD) generated at the site in order to manage water quality in the local creek.

Management strategy and water quality criteria

A whole-of-site remediation strategy outlines the strategic objectives below:

- Improve water quality in Dawesley Creek to a standard as good as possible.
- Substantially limit or avoid the need to intercept and treat acid waters indefinitely.
- Return all or part of the site back to productive uses or for environmental/ ecosystem values.
- Apply leading practice to site management and mine completion.

The strategy establishes the objective for water to meet quality standards in the local creek in agreement with the demand of downstream water users; i.e. irrigation and livestock. A water quality criteria to meet environmental and ecosystem values is monitored following the jurisdiction policy and guidelines for water quality (Table 1) (Stevens and Fullston 2015).

Parameter	EPP 2003 ⁽¹⁾			ANZECC 2000 ⁽²⁾		
	Aquatic ecosystem(a)	Agriculture (b)	Livestock (c)	Freshwater (d)	Irrigation (e)	Livestock (f)
pH	6.5-9	4.5-9		6.5-9	6-9	id
EC (μ S/cm)				100-5000	7000-7500	4000-5970
Sulphate (mg/L)			~1000			~1000
Aluminum (mg/L)	0.01	1	5	0.08	5-20	5
Cadmium (mg/L)	0.002	0.01	0.01	0.0004	0.01-0.05	0.01
Copper (mg/L)	0.01	0.2	0.5	0.0018	0.2-5	0.4-1
Iron (mg/L)	1	1	id	id	0.2-10	
Manganese (mg/L)		2		2.5	0.2-10	
Zinc (mg/L)	0.05	2	20	0.015	2-5	20

Table 1 Water quality standards as requirement for the water quality monitoring criteria

(1) South Australia Environment Protection Authority – Environment Protection (Water Quality) Policy 2003 (SA EPA 2003)

(2) The Australian and New Zealand Environment Conservation Council – Australian and New Zealand Guidelines for Fresh and Marine Water Quality (ANZECC 2000)

id insufficient data

Water quality program

- Pre-diversion (1998-2003). Partial relocation of waste rock dumps, tailings covered with bio-solids, vegetation to reduce infiltration and promote evapotranspiration.
- Post-diversion (2004-2014). A major diversion of clean waters to bypass the mine site and upgrade of the treatment plant.
- Post-diversion extended (2014-2015). Improvements in the diversion system. Increased interception and treatment prior to discharge.

Monitoring of water flows, water quality and riparian ecosystem to measure the effectiveness of the strategies in accordance with the standards of the jurisdiction in Table 1. From 2016 water quality is monitored against ANZECC 2000 guidelines only.

Results

The primary focus of intervention has been to address the water quality in the local creek and the main indicators of water quality are the standards presented in Table 1 and in accordance with the South Australian Environment Protection Authority (SA EPA) and the Australian and New Zealand Environment Conservation Council (ANZECC).

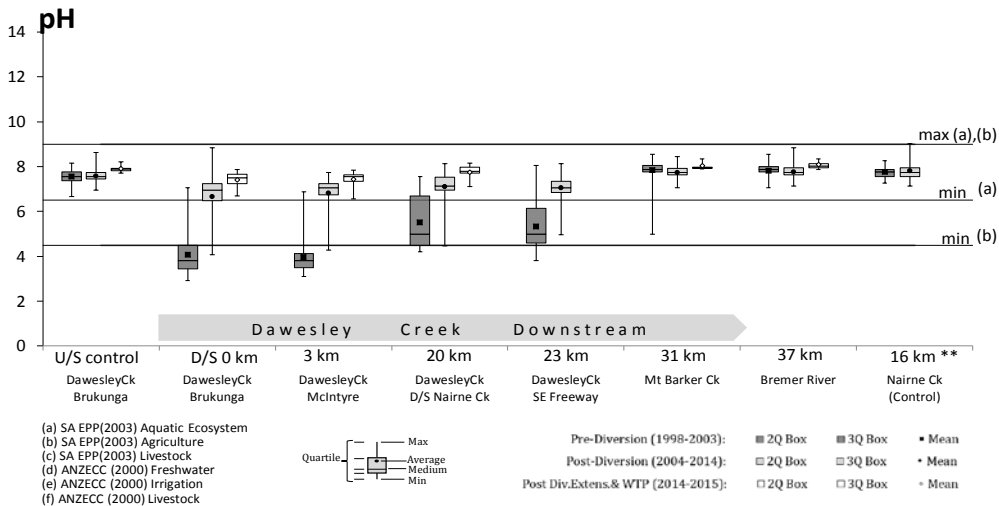


Figure 4 Progressive improvements on pH values as one of the main indicators of water quality (** tributary control 16km downstream, data source: Brukunga water monitoring reports)

The water quality in Dawesley Creek improved progressively after numerous works at different times. Figure 4 Progressive improvements on pH values as one of the main indicators of water quality (** tributary control 16km downstream, data source: Brukunga water monitoring reports) shows the changes in pH readings at different points in Dawesley Creek. The dark grey indicators show the pH levels pre-diversion of Dawesley Creek (1998-2003), the light grey indicators show the average readings post-diversion (2004-2014), and the white indicators represent the current levels since the extension of the Dawesley Creek diversion

and improvements in the treatment plant (June 2014-2015). Other parameters have also shown trending improvements in water quality with moderate volatility (Figure 5). The information derived from the monitoring program shows pH levels are within the range for both agriculture and aquatic ecosystem. Salinity meets the standards for the aquatic ecosystem, agriculture and livestock. Sulphate in relation to water for livestock remains volatile and outside threshold immediate to the mine site but it recovers at 3km downstream. Aluminium in water has improved and is within the threshold for livestock but outside the threshold for agriculture to 20km. Aluminium is a naturally occurring element in Dawesley Creek and does not meet criteria for the aquatic ecosystem to the full length of the creek. Cadmium in water is within the threshold for agriculture and livestock, but above the threshold for the aquatic ecosystem to 20km. Copper is within the threshold for agriculture, livestock and the aquatic ecosystem. Iron is a naturally occurring element in Dawesley Creek and it was always outside threshold for both agriculture and the aquatic ecosystem. It is improving but the condition remains down to 20km. Manganese control has improved and is within the threshold for ag-

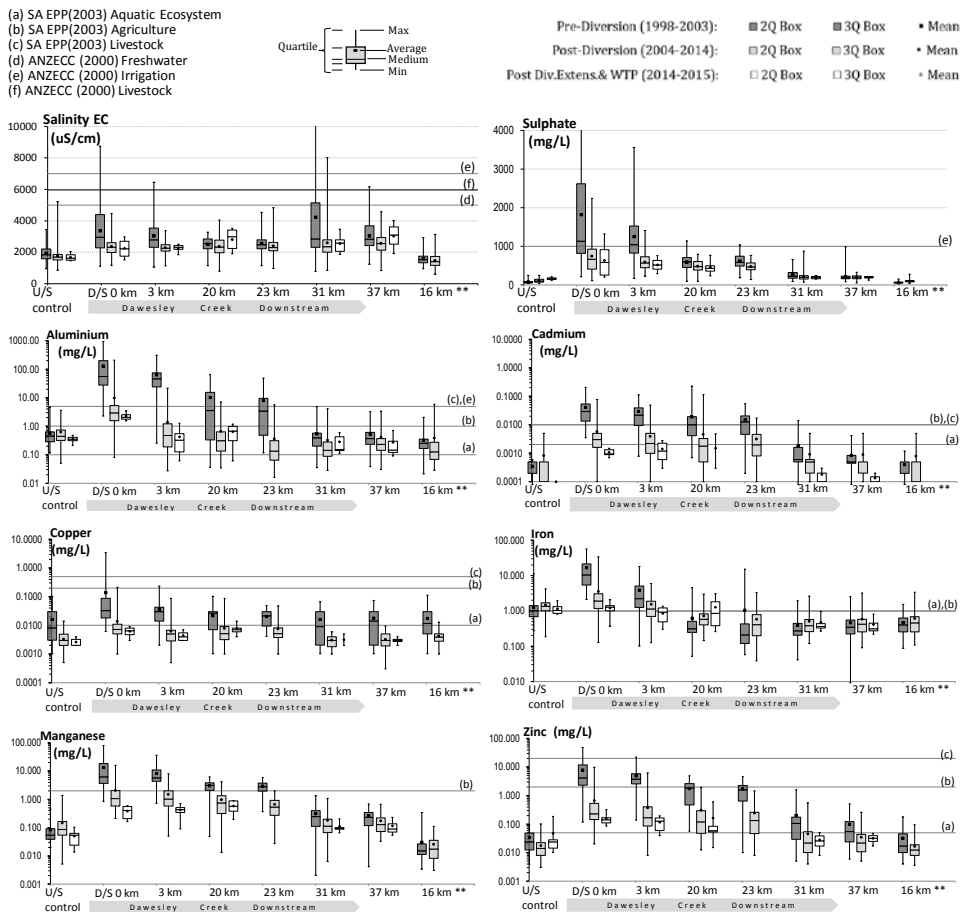


Figure 5 Temporal and spatial variability of water quality in Dawesley creek in response to management strategies (Data source: Brukunga water monitoring reports).

riculture water. There is no threshold for livestock. Zinc is within the threshold for livestock and agriculture but outside the threshold for the aquatic ecosystem to 20km but improving.

Conclusions

A comprehensive water quality program incorporates the needs of other water users.

Monitoring temporal and spatial variations of water quality can allow constructing a representation of the trends and the effectiveness of the management strategies. The complexity in identifying the future conditions of the catchment system arises when the variability in water quality is due to non-point sources and where the strategy has limited control.

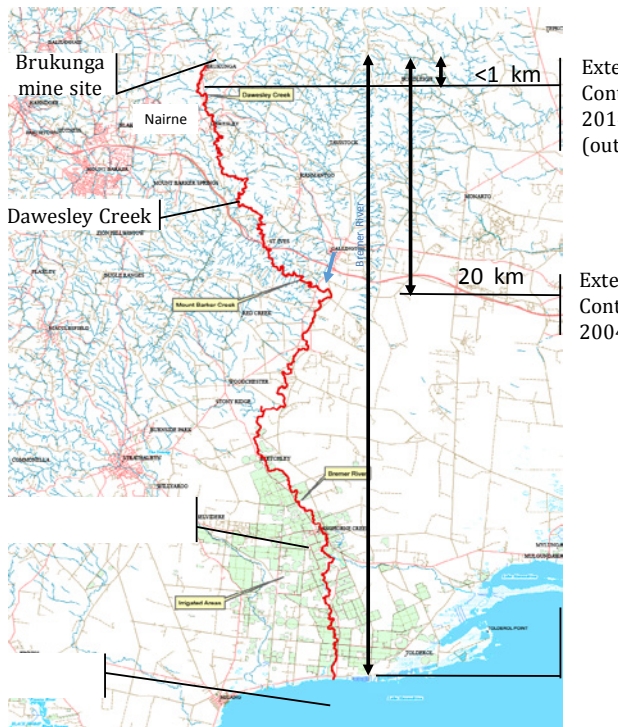


Figure 6 Water quality improvements with reference to agriculture irrigation & livestock quality standards (Mollehuara 2016)

A monitoring program that aims agreed criteria for water quality could demonstrate the improvements as a result of the works conducted in the water quality program (Figure 6 Water quality improvements with reference to agriculture irrigation & livestock quality standards (Mollehuara 2016)).

Acknowledgements

The authors thanks K. H. Renlund Foundation. Also with grateful acknowledgement to the staff at Brukunga mine site – Ross Stevens, Catherine Fullston and Paul Wandner.

References

- ANZECC (2000) ANZECC 2000 Guidelines.
- Armstrong D, Cox R (1977) The Brukunga Pyrite Mine – South Australia A Review of Developments since Closure in 1972. In: 9th International Mine Water Congress. pp 201–207
- Mollehuara R (2016) Former Brukunga Mine Site (SA) Lessons of a long-term remediation strategy. In: Dealing with Derelict Mines 2016. NSW, pp 1–25
- SA EPA (2003) Environment Protection (Water Quality) Policy 2003. 1–35.
- Stevens R, Fullston C (2015) Brukunga Remediation Program Water Monitoring reports.
- Taylor GF, Cox RC (2003) The Brukunga Pyrite Mine – A Field Laboratory for Acid Rock Drainage Studies. In: 6th ICARD. Cairns, pp 93–106

Flooding of the uranium mine at Königstein/Saxony – current status and monitoring conducted

S. Eulenberger, U. Jenk, M. Paul

Wismut GmbH, Jagdschänkenstraße 29, 09117 Chemnitz, Germany

Abstract From 1984 on, at the Königstein site uranium was exclusively mined by in-situ leaching, in response to ever more decreasing ore grades. As a consequence of the applied sulfuric acid leach technology the affected geological formation exhibits a high acid potential, associated with high concentrations of easily soluble contaminants (metals, uranium included) in the mine water. In order to mitigate the environmental impact of the mine along the water pathway, remediation requires a controlled mine flooding scheme. Due to the specific hydro-geological and hydro-chemical conditions, monitoring of the groundwater quality is a key element of water monitoring at the site. The paper describes the approach of hydrochemical groundwater monitoring during mine flooding and presents solutions for representative groundwater monitoring under challenging sampling conditions in monitoring wells with depths down to 350 m below surface. The current status of mine flooding is outlined and selected monitoring results are highlighted.

Key words Uranium mining, mine flooding, Königstein mine, groundwater, monitoring

Introduction

The Königstein uranium mine is situated in an ecologically sensitive and densely populated area in the Elbe Sandstone Mountains, some 20 km southeast of Dresden, close to the Elbe river. It is classified as a typical roll-front sandstone hosted uranium deposit with an extension of about 2.5 km × 10 km (Tonndorf 2000). Workable uranium mineralization is hosted in the so-called 4th aquifer of Cenomanian age, the lowermost of four Cretaceous sandstone aquifers of the Pirna sedimentary basin (Fig. 1). The overlying Turonian 3rd aquifer, however, is classified as the region's most important local drinking water reservoir.

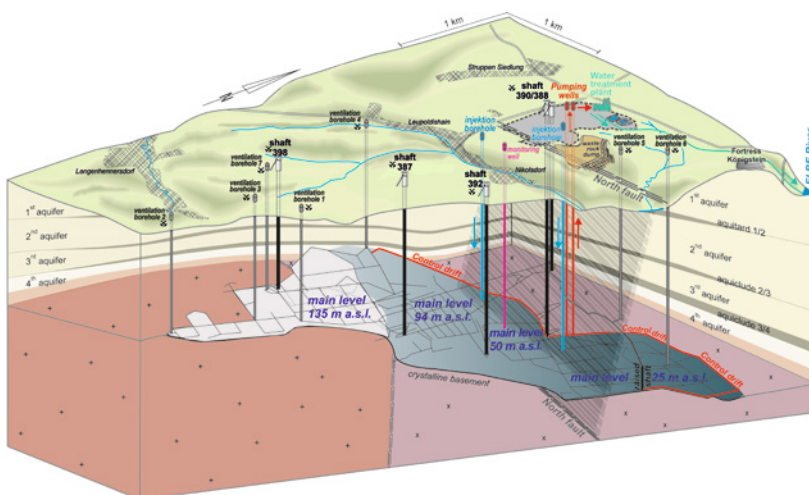


Figure 1 3D geological view of the Königstein mine (Jenk et al. 2014a)

Between 1967 and 1990 the deposit was exploited by SDAG Wismut, first using conventional underground mining methods. Development of the mine site extended over a surface area of approximately 6.5 km² and comprised four main levels (Fig. 1). In response to the ever more decreasing ore grades, from 1984 on uranium was exclusively mined by in-situ block leaching, using sulphuric acid. Production totaled some 18,000 tonnes of uranium. As of 1991, remaining resources were reported to be about 8,500 t U, including those at the unmined sub-deposits of Thürmsdorf and Pirna. In conjunction with the termination of operations by the East German uranium industry in 1990 the Königstein mine was decommissioned. Remediation activities were focused on the safe closure of the underground mine and preparation for flooding. The floodable mine voids comprised a total volume of around 2.8 million m³. Due to the substantial quantities of sulphuric acid applied during production, mine water was strongly acid and contained very high concentrations of sulphate and easily soluble contaminants as metals and radionuclides.

With a view to minimizing environmental impacts, flooding of the Königstein mine is conducted as a controlled process with due regard to the hydraulic and hydrochemical specifics of the site. Basic elements of the controlled flooding include the system of control drifts and associated extraction wells, water injection wells, the flood water treatment unit and a licenced dump for the disposal of radioactive residues from water treatment.

For the purpose of identifying possible environmental impacts at the Königstein rehabilitation site, groundwater, seepage and surface water, discharge of treated process water, air quality and geomechanical aspects are constantly monitored.

Current above-ground groundwater monitoring

Owing to the depth of the mined deposit ranging from 150 m to 300 m below ground and to the site's hydraulic conditions, groundwater monitoring is a key element for the safe implementation of controlled flooding. Monitoring applies to aquifer #4 (Cenomanian sandstone) and in particular to aquifer #3 (Lower Turonian sandstone).

Controlled flooding of mine section I was initiated in January 2001 with open, accessible control drifts. In addition to above ground monitoring, the staged flood water rise with stoppages at the levels of 50, 80 and 110 m a.s.l. (above sea level) was accompanied by detailed underground flood water and groundwater monitoring from the accessible mine voids. This underground monitoring network comprised 31 flood water and 46 groundwater measurement points.

As from August 2009 the control drifts were flooded and hence the underground monitoring system was abandoned. Monitoring of the subsequent flood water rise from 110 m to the level of 140 m a.s.l. was performed exclusively from above ground by means of the groundwater monitoring network deployed in aquifers #3 and #4.

The measuring network for the hydrochemical monitoring of aquifers #3 and #4 comprises a total of 70 monitoring wells and has a surface extension of about 70 km². According to

their importance and the monitoring goal, monitoring wells are divided into three categories and are sampled in different cycles:

- Basic monitoring: Widespread measuring network to monitor the general state of aquifers, sampling in a four-year cycle;
- Trend monitoring: Monitoring of mid-term changes without relevance to decision-making in the short term, sampling in a two-year cycle;
- Proximity monitoring: Monitoring of areas which, if any, are first impacted by flood water encroachment, sampling at least once a year.

Additionally, more intensive monitoring is provided to selected monitoring wells located in the proximity area where flood-induced impacts might be expected to occur at an early stage and which, for that very reason, are of particular relevance for controlling the mine flooding process during the active flooding phases. That pertains to six monitoring wells in aquifer #3 overlying the mine as well as to five monitoring wells in aquifer #4 along the northern rim. These monitoring wells are sampled in aquifer #3 in four to twelve cycles per year and in aquifer #4 biannually. Furthermore the most part of it is equipped with stationary groundwater probes to ensure continuous monitoring of water levels and electric conductivity.

The range of analyses to be performed is adapted to the relevant category of monitoring wells and does not exceed the defined parameters listed below:

- Macro constituents: TDS, filterable materials, Na, K, Mg, Ca, Fe, Fe²⁺/Fe³⁺, Mn, Al, Si, Cl, F, SO₄, NH₄, NO₃, NO₂, PO₄, HCO₃, (CO₃);
- Trace elements: Zn, Cu, Co, Ni, Pb, Cd, As, Ba, Sr, REE (Ce, Dy, Er, Eu, Gd, Ho, La, Lu, Nd, Pr, Sm, Tb, Tm Yb);
- Radionuclides: U-nat., Ra-226, range of naturally occurring radionuclides;
- Organics: TOC, AOX, Hydrocarbons.

Mine water indicators such as uranium, zinc, sulfate, cerium and neodymium in particular serve the goal of early detecting any mine water encroachment. With the aim of assessing flood water impacts on aquifer #3 indication values of these parameters were derived to apply to the 6 monitoring wells located on top of the mine (see Table 1). These indication values are based on maximum concentrations measured so far of the element under consideration plus a safety margin. This approach takes inhomogeneities in element distribution within the aquifer and effects due to changes in hydraulic conditions into consideration.

Table 1 Indication values for flood water impact to 3rd aquifer on top of mine workings

Parameter	Uranium [µg/L]	Zinc [µg/L]	SO ₄ [mg/L]	Cerium [µg/L]	Neodymium [µg/L]
Indication value	100	300	300	20	20

In the event that exceedance of indication values has been reliably established on the basis of repeated sampling countermeasures may be taken as appropriate. Potential countermeasures also involve the lowering of the level to which the flood water has risen. Decision-making on measures to be implemented will have to consider the spatial situation and the extent of the flood water impact. To this effect, a panel has been appointed on which sit representatives of Wismut GmbH and regulators.

Technology for mobile pump sampling of deep monitoring wells

At the beginning of the 1990s, Wismut established a monitoring network of groundwater monitoring wells to monitor groundwater quality at the Königstein site. Both by their design and the materials used these wells fully comply with sampling quality standards. The wells are provided with PVC casings of an inner diameter of at least 5 inches (approximately 125 mm), and each well taps a single aquifer. Owing to the location of the monitored aquifers #3 and #4, the monitoring wells reach down to depths of 350 m and screening lengths amounted to 70 m. In particular during the initial stage of mine flooding with fully developed depression cone, depths to groundwater-levels exceeded the 200 m mark at a large number of monitoring wells.

While commercial equipment is available for representative pump sampling of groundwater monitoring wells down to depths of ca. 80 m (pump type: MP 1, manufactured by Grundfos), monitoring staff had to resort to scoop sampling for deeper aquifers still in the 1990s. However, it is known from experience that data derived from scooped samples and in particular those from unexploited ground are only of limited representativity with regard to the surrounding aquifer. Reasons for this frequently include a diminished flow through from the aquifer as well as alterations of the well water induced by convective flow in the water column.

As a result of intensive development efforts, mobile equipment has become available since the early 2000s which permits representative pump sampling to be performed at all groundwater monitoring wells at the Königstein site. Mounted on trailer and truck the two units MTA200 und MTP350 (see Fig. 2) were tailored to the conditions of the site and are intended for pump sampling from two different depth ranges. The mobile units feature good cross-country mobility and by their sufficiently high and easily adjustable pumping rates they allow to comply with the hydraulic sampling criteria and to provide constant in-situ parameters. Sampling of one groundwater monitoring well is completed within one work shift (Eulenberger & Greif 2016).

Using intensive field tests during the commissioning phase of sampling equipment, adapted pumping conditions for each monitoring well were derived. With regard to optimized sampling conditions at Königstein site, a total delivery of 1.5 times of the well water content was determined for sufficient removal of altered water before taking a representative groundwater sample.



Figure 2 Trailer mounted deep pumping unit MTA-200 (left) and deep pumping unit MTP-350 (right) during sampling operations on deep groundwater monitoring wells at the Königstein site

Using an adjustable motor-driven submersible pump with 3 inches in diameter, the MTA200 provides pump rates of 0.5 – 1.2 m³/h with a maximum delivery head of 160 m. Centerpiece of this system is the combination of a pump cable with suspension rope inside and a nylon riser hose, both reeled onto electronic synchronized winches. This innovative design enables very short set-up/take-down times of merely 15 min and a workable handling by two operators.

Sampling unit MTP350 is suitable for delivery heads up to 320 m and covers pump rates up to 2.5 m³/h, based on a likewise adjustable 4-inches motor-driven submersible pump. Separate logging cable, pump cable and 3/4-inches riser hose (20 mm) which are reeled onto hydraulic driven winches, have to be tied together by purpose-built clamps and cable clips for preventing loops inside the borehole. Therefore set-up/take-down at a 250 m deep monitoring well takes about 45 min each, using three operators. The entire system is mounted on cross country truck with box body divided in lab unit (front) for sample preparation and utility section at the rear part.

Results

Controlled flooding of mine section I was initiated in January 2001 with open control drifts. At that time, flood water was collected in basins below ground by means of an elaborate drainage adits and galleries system and subsequently – separately from uncontaminated groundwater – pumped via main shafts #388/390 to the surface for treatment.

Since control drifts were flooded mine flood water is pumped from the control drift system which acts as a horizontal well. For this purpose, extraction wells A' and B were drilled north of shafts #388/390 and linked by chambers to the northern control drift. With control drifts henceforth flooded, the rise of the flood water level was resumed in April 2011 and lasted until January 2013 when the final level of 139.5 m a.s.l. was reached. At this currently maintained flood water level of maximum 140 m a.s.l., permitted in section I, the total fill volume of mine voids and replenishable pore volume in cretaceous sandstone has been identified amounting to a total of about 7 million m³ of water (Jenk et al. 2014b).

The mine flooding process was reliably surveilled by comprehensive monitoring of groundwater measuring points deployed both underground and above ground. At the same time, a reliable data base was established for an assessment of the flooding process. Data recorded during the final flood water rise from 110 to 140 m a.s.l. (from 04/2011 through to 01/2013) document in particular that the exclusively remained above ground deployed groundwater monitoring network is capable of detecting an impact of the mine flooding on the surrounding groundwater. Custom-built mobile pumping equipment allows representative sampling of the site's deeper-than-average groundwater monitoring wells for reliable monitoring of groundwater quality from above ground.

Down to the present day, the acquired monitoring data allow to safely exclude any impact downstream of aquifers #3 and #4 caused by encroaching flood water. This is exemplified by uranium concentrations recorded during the period of flood water rise from the level of 110 to 140 m a.s.l. and during the current stoppage from groundwater measuring points within the aquifer #3 on top of the mine (see Fig. 3).

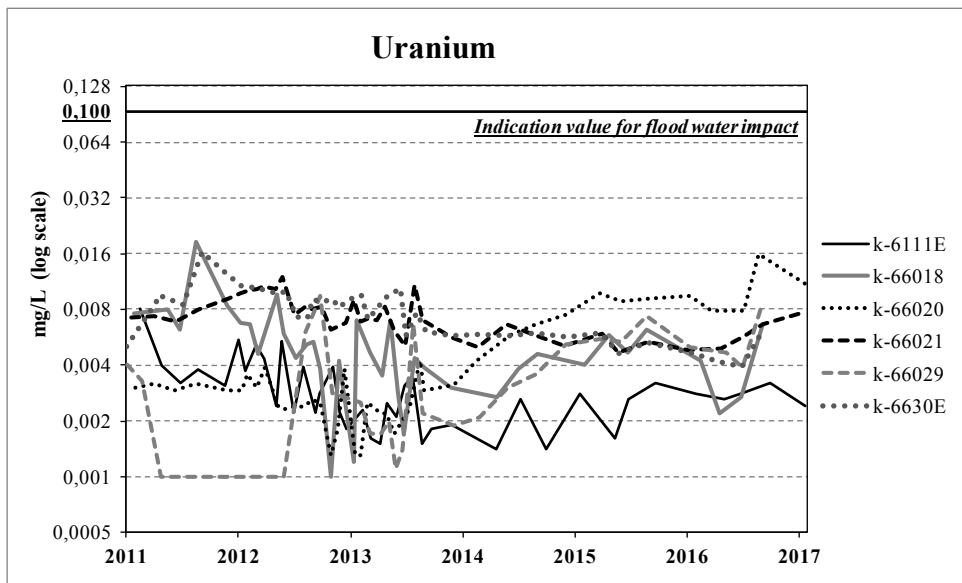


Figure 3 Uranium concentrations in monitoring wells in aquifer #3 on top of the mine since 2011

Outlook

Owing to the natural inflow of groundwater, pumping the flood water via extraction wells is imperative for maintaining the current flood water table of about 139.5 m a.s.l. and can be terminated only if a natural flood level of approximately 200 m a.s.l. is achieved. Flooding of mine section II is aimed at the recovery of these hydraulic conditions which prevailed prior to mine development.

Considering the absence of a sustainable alternative technical solution solely a final flooding would enable a complete and conclusive remediation of the site. Unavoidably linked with limited emissions of pollutants into the surrounding aquifers, the permitting procedure for this flooding step, initiated in December 2011, is still pending. A new approach to push the flooding progress is the definition of an observation and control area for a spatial limited encroachment of the surrounding aquifers #4 and #3. This area is framed by the contour of the existing mining concession and an already granted pollution-rim of the aquifer #4. Currently, technical discussions with respect to potential scenarios and connected risks with the relevant authorities are conducted. As a result, a permit application for a hydraulic test was submitted in March 2017 to obtain basic data for better prediction of the hydrological and geochemical conditions in consequence of a further flooding.

The Königstein site is equipped with a groundwater monitoring system which ensures both the current and future secure monitoring of mine flooding. Depending on regulatory framework conditions yet to be put in concrete terms for the implementation of flooding section II of the Königstein mine, occasional amendments to the existing measuring network might become necessary.

References

- Tonnendorf, H. (2000) Die Uranlagerstätte Königstein. Bergbaumonographie.- Sächsisches Landesamt für Umwelt und Geologie, Sächsisches Oberbergamt (2000) 208 p.
- Jenk, U., Nindel, K., Wedekind, C., Frenzel, M., Uebe, R., Eulenberger, S., Metschies, T., Terra, U., Gross, U. (2014a) Bericht zur Flutung der Grube Königstein, Teilbereich I – 140 m NN, Wismut GmbH, report number WIS K 358 (2014)
- Jenk, U.; Frenzel, M.; Metschies, T.; Paul, M. (2014b): Flooding of the Underground Uranium Leach Operation at Königstein (Germany) – A Multidisciplinary Report. – In: Sui, Wanghua; Sun, Yajun & Wang, Changshen: An Interdisciplinary Response to Mine Water Challenges. – p. 715 – 719; Xuzhou, China (China University of Mining and Technology)
- Eulenberger S., Greif, A. (2016) Erfahrungen bei der Probenahme an tiefen Grundwasserbeschaffenheitsmessstellen, Tagungsunterlagen zum Lehrgang „Repräsentative Grundwasserprobenahme“, 29.09. bis 01.10.2016, Halle, Tagungsband (2016).

Integration of Solid Matter Coupled Contaminant Transport into the 3D Reactive Transport Boxmodel by the Example of PCB in German Hard Coal Mining

Christoph Klinger¹, Michael Eckart¹, Joachim Löchte²

¹*DMT GmbH & Co. KG, Geo Engineering & Exploration, Exploration & Hydrogeology, Am Technologiepark 1, 45307 Essen, Germany, Christoph.Klinger@dm-t-group.com*

²*RAG Aktiengesellschaft, Health, Safety, Environment, Shamrockring 1, 44623 Herne, Joachim.Loechte@rag.de*

Abstract So far, mainly inorganic compounds have been relevant for the evaluation and prognosis of mine water pumped and discharged. In the course of the current closedown of the German hard coal mines, however, substances hazardous to waters must also be taken into account when withdrawing. It was therefore also necessary to consider components from operating leaking fluids in the context of flood predictions. These mostly organic compounds have mobilisation and transport properties completely different from salts. High sorption coefficients lead to high proportions of particle-bound transport. This required a corresponding adjustment of the Boxmodel used in the German coal mining.

Key words Reactive Mass Transport, Modelling, PCB, Mine Flooding, Particle Transport

Introduction

In connection with the withdrawal from still open mine voids and the subsequent flooding, it must be considered that during the mining operation some substances hazardous to waters were used underground. This implies a potential risk within the scope of the flooding, when such substances have leaked and are still present in the mine building. By common classification, the underground generally handled diesel fuel and the used oil are considered to be hazardous to water. This material stock has to be expanded by special additives and various ingredients such as glue, solvents, etc. Substances which can be mobilised therefrom are predominantly mineral oil hydrocarbons.

During active mining but also during and after flooding, such anthropogenic substances can be discharged by means of dissolving and transporting processes with the rising mine water, thus released into the environment. It is important to know the respective chemical properties and relevant mobilisation processes in order to estimate, evaluate, forecast and, if necessary, reduce the discharge of these substances. In the case of particulate bound substances, these properties are completely different from water-soluble compounds. Due to the potential environmental impact of this substance group, the Boxmodel, which is used to describe and forecast mine water rise and water quality (Eckart et al. 2010), has been accordingly enhanced.

Substance relevance and mobility

Mineral oil products which may have leaked into the mining gallery ground are, to a large extent, complex mixtures of mineral oil hydrocarbons with different properties. In particular, diesel oils have relevant water-soluble fractions. Water solubility of these mineral hydrocarbons decreases with increasing molecule length. However, mine water in the German

coal mines show only low contents of water-endangering organic substances. This can be seen, for example, in the low concentrations (almost always <0.1 mg/L) of the widespread and comparatively well water soluble mineral oil hydrocarbons in mine waters from already flooded mineworks, in regular monitoring. This value corresponds with environmental regulations. Such low substance contents can be attributed to the fact that also the mineral oil hydrocarbons which predominantly build up the lubricants are well bound to the fine-grained and organic rich substances contained in the gallery ground and are thus only available to a limited extent for a dissolution processes.

The situation is somewhat different for toxic substances whose detection and environmental limits are significantly lower. In German hard coal mining, fire-retardant PCB/PCDM-containing hydraulic fluids were used at Ruhr, Ibbenbüren and Saar from 1964 until 1989. Leaks, defects, etc., led to loss of liquid, so it can be assumed that also some of the PCB-containing hydraulic fluids remained underground. PCBs are toxic and very persistent. On the other hand, they have the high tendency to adsorption especially on organogenically rich solids (LANUV 2015). This leads to low concentrations dissolved in water. Measurements at various locations show that PCBs are still present in the mine water (LUA 2015). However, the amounts have now declined so far that identification mostly is conducted via separation of the solid particles contained in the mine water. The PCB content of the solid particles is then determined. Normal water analysis cannot detect these low concentrations. Research is currently under way to determine the amount of PCB truly dissolved in such mine water. However, it is apparent that the larger proportion of the PCB discharge is in particulate form.

Due to this strong tendency of PCBs to bind to particle surfaces, mobilisation and transport of this fraction are fundamentally different from real solutes. Classical transport approaches based on solution and precipitation, such as those known e.g. for salts, cannot be applied here. Not the solubility properties of the organics themselves control the transport process, but rather those of the carrier particles as well as various sorption-desorption equilibria.

It is a prerequisite for the mobilisation of such substances that particles containing PCBs enter the mine water. In contrast to soluble substances, the solids are eroded in turbulent water flow and sedimented again at low flow rates. The processes concerning fine particle transport in a mine are complex and strongly dominated by local and variable processes (mining activity, type of lithology, water level, gallery dip, etc.). Erosion processes (turbulence) are a function of the flow velocity and thus of the local site conditions. Particle coupled PCB release can then only take place in not flooded old (see period of PCB use) galleries in which turbulent flow or mining activity takes place (such erosion channels can be seen in the mines at various points after water entry into inclined sections). Once a gallery is flooded, turbulent flow and mining activities are missing. Flow velocities in such sections are in the range of a few meters per minute, so that a sedimentation of suspended matter is much more probable than re-suspension. This means that water level rise / flooding does not lead to a corresponding deterioration in the quality of the mine water. The operating state is rather the most unfavourable boundary condition for the discharge of such substances.

Model-relevant processes

Water-soluble organic pollutants from operating fluids will behave similarly to geogene substances present in the mineworks. These include easily soluble salts and substances present in pore water. Above all, products of pyrite oxidation such as sulphate and iron are mobilised in solute form. Their mobilisation and flushing behaviour is known and is taken into account by the usual prognosis models. Correspondingly, the development of dissolved organic compounds can be modelled. However, sources are significantly smaller compared to geogene substances.

For an understanding of the transport processes of solid particles with organic substances fixed or sorbed to them and their representation in a model, new parameters must be taken into account. The basic approach is not reversible binding to the solid particles. It is then sufficient to describe the transport of these particles. However, it is also possible in principle to take into account sorption-desorption processes for these mobile particles.

This means that flow velocity and grain sizes must be considered for modelling. There is hardly any information on the grain size distribution of particles contained in the mine water. However, it is obvious that in case of abandoned mines only very small particles can remain mobile after the flow from a distant source to the water discharge due to the low flow velocities in a water-filled gallery. The model concept therefore takes into account three particle fractions. These represent fractions of different properties without specific particle size assignments and can contain a differentiated PCB spectrum. Nearly no sedimentation is assigned to a mobile fraction according to colloidal finest particles.

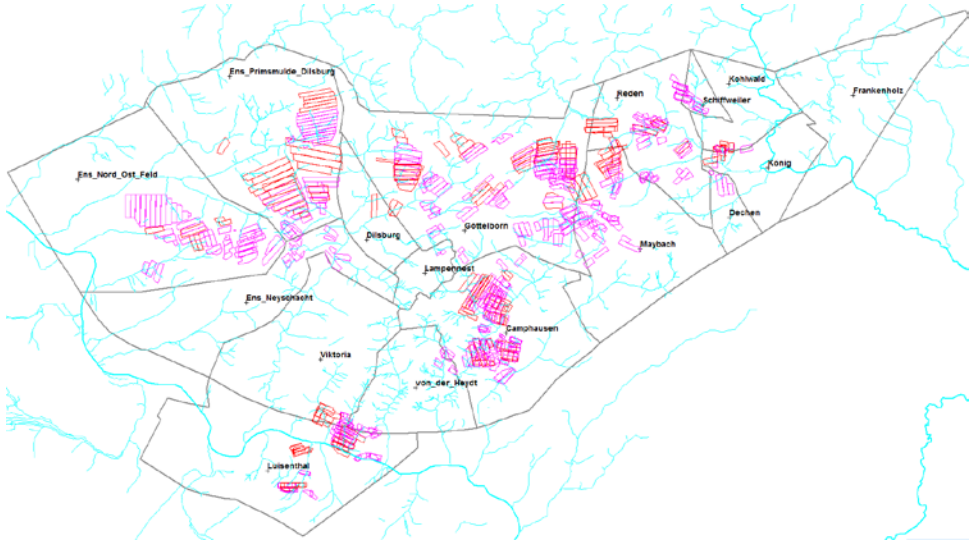


Figure 1 Large-scale distribution of longwall mining sites with PCB- and PCDM-use at the example of the minefields at the Saar/Germany.

The model approach considers, according to the data availability, no concrete sites for the spatial allocation and distribution of the PCB sources. A generalised approach is required, which follows the principle of proportionality: where more has been mined with such operating fluids, the probability is higher that PCBs have been emitted and are available as source. Figure 1 shows this geographical distribution of mining sites in the PCB/PCDM time for the site example Saar Area. Using this method, the potential source of the substance for the individual model boxes (slices) can be described in a level differentiated manner (fig. 2). The ratio of PCB-containing and PCB-free particles can be derived from the respective volume ratio in the respective model slice. This value then represents an average value of the very heterogeneous substance distribution and mobilisation potential in reality. In addition, the processes of particle mobilisation and the spatial conditions of a coal mine have to be considered as a function of water level development. This complex system has been described in its components and interactions and transferred to the Boxmodel.

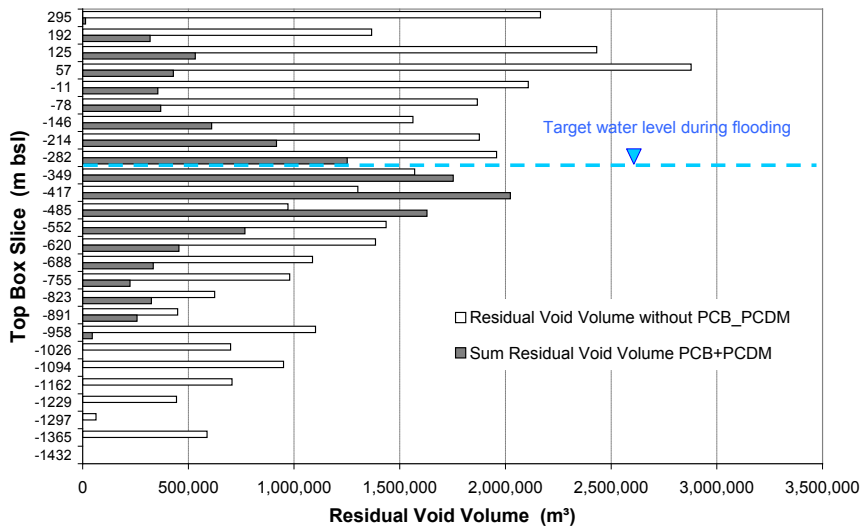


Figure 2 Depth distribution of the residual void volume from mining operations within and outside the period of use of PCB/PCDM-containing operating fluids (water province Duhamel / Ensдорf).

Model tool

The box model program BOX3D is used to calculate the non-stationary three-dimensional flow and reactive mass transport (Klinger et al. 2012). It consists of a freely structured model according to the volume balance method, which can take into account defined random geometries (boxes) and a reactive material transport model directly coupled to it. Both models are solved simultaneously. The mass transport model describes the concentration development in the mine water taking into account the release of substances during flooding (e.g., SO_4 , Fe, trace metals) and the mixture with geological inflows, which often have high salinity. The mass transport model has reaction terms which can take into account the various sorption and desorption processes as well as chemical reactions between and within

phases (dissolution-precipitation reactions). Bacterial processes (e.g., sulphate reduction) can also be calculated as the transport of solid particles, which is quite different from solutes. Based on the calculated flow velocity field, the mass transfer equation (convection equation) is solved in parallel for the liquid phase. Mineral phases were implemented for the solid phase. There may be interactions between the migrants within the liquid, but also between the liquid, gaseous and solid phases.

In the model, the relevant interrelations and substance properties are structured and converted into a calculation concept. This always requires a clear assignment of substance contents to phases, which is not always easy and unambiguous analytically. PCB transport is always particle transport in the current model version due to otherwise missing data and is therefore still considered independent of dissolved substances. A defined PCB content (in μg of congener/kg of suspended matter) is attributed to these particles from the areas which act as the PCB source. The PCB content of this particle is fixed and does not change during transport. When mixing with particle-free mine water, the content of suspended matter (and therefore the PCB concentration in the solid particle phase) is changing but not the transported PCB mass. This PCB load can – by stringent perpetuation of this concept – be reduced only by sedimentation of particles. The sedimentation depends on the type and size of the particles as well as the flow velocity of the mine water on the flow path to the source up to the discharge point. It is assumed that PCBs are predominantly bound to particles which we call “primary” and consist of components (e.g., clay minerals, coal) of the surrounding rock.

The model also takes into account interactions between different particle types. In precipitation reactions, two products are formed: a phase grown on surfaces, which no longer participates in the flow transport process, and fine-grained particulate solids, which are transported with the flowing mine water. PCB-containing solid “primary” particles are subject, in addition to a self-sedimentation, to a co-precipitation with the above-mentioned precipitations (e.g. of BaSO_4). This is because it is known that in the case of mineral growth in the solid phase, other components are also incorporated into the mineral matrix. The sedimentation affects the mineral-specific particles originating from precipitation as well as the “primary” particles:

$$R_{\text{Sedimentation}} = -k_{\text{Sedimentation}} \times c_{\text{Particle}} \quad [\text{mg/L/s}] \quad (\text{for all particle types})$$

$$R_{\text{Coprecipitation}} = (R_{\text{BaSO}_4\text{_directP}} + R_{\text{CaCO}_3\text{_directP}} + R_{\text{FeOH}_3\text{_directP}}) \times k_{\text{Coprecipitation}} \times c_{\text{Particle_primary}}$$

The sedimentation has a clear dependence on the flow velocity. In this respect, empirical correlations to the flow velocity were evaluated and described in terms of the model. In principle, it should be noted that model and measurements have limitations due to the diffuse transitions in the particle sizes. Particles also exist below the pore size of the filters usually used for separating solids. Such colloidal particles can be a few nm in size and thus sediment very slowly. The kinetic approach to the sedimentation calculation in the model takes account of these relationships caused by the grain size distribution and leads to an asymptotic

development of the remaining solids contents. This approach is based on the grain size dependencies between sedimentation and transport as depicted in the Hjulstrøm diagram (Hjulstrøm 1935). The result of this dependence of the sedimentation rate on the velocity of the flow is that with increasing water level of the mine an increasing slowdown of the flow conditions begins, the sedimentation effects increase and thus the particle concentrations decreases significantly.

Results

The model was applicated and calibrated for the water extraction from the Saar mines. In addition to usual macrochemical components and trace metals a focus was the solids content and the PCB concentration in the discharged mine water. Here, too, a forecast for the water level rise up to -320 m bsl was derived. Since PCB transport in the mine water takes place via solid particles, these also represent the essential factor for the calibration of the mass transport model. The contents of the filterable substances measured are very low in the discharges of abandoned mines. Figure 3 shows the development for the pumping station Camphausen (Saar). The detection limit is 2 mg/L and most measurements are below this value. However, after an earlier increase in the water level, an initially clearly increased solids content could be observed. This is due to flooding-related changes in the flow regime with the flush of galleries and possibly overflow situations with turbulent flow and erosion. The values then gradually decrease, similar to the flushing curves of sulphate. It can be assumed that the exchange of the particle laden water and sedimentation processes superimpose in the calming water reservoir. Subsequent changes in the measured values due to iron hydroxide precipitation were taken into account.

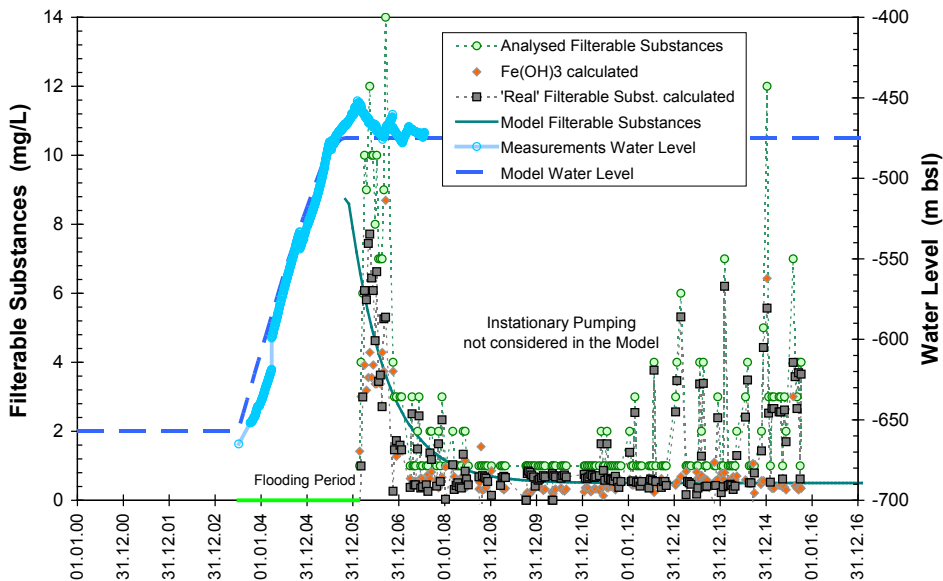


Figure 3 Measured values for particulate solids in mine water Camphausen with evaluations and calibration of the Boxmodel.

The level of the PCB content of the particulate solids in the discharges is a result of the proportion of the PCB potential areas (see fig. 1) and is therefore adjusted during calibration. As a result of the PCB examination method (see above) and the low solids contents described, the analysis results vary widely. The analysis data show PCB sum content (6 resp. 7 congeners) between 10 and several 100 $\mu\text{g}/\text{kg}$ for the separated solid particles at the pump locations (fig. 4). The available measured values were therefore weighted. The outlier values were ignored, and analyses carried out on larger quantities of material were given some priority for the calibration. The control of the balance of particle concentration (mg/L) and its PCB content ($\mu\text{g}/\text{kg}$) results in the fractions-relevant concentrations (ng/L) calculated therefrom.

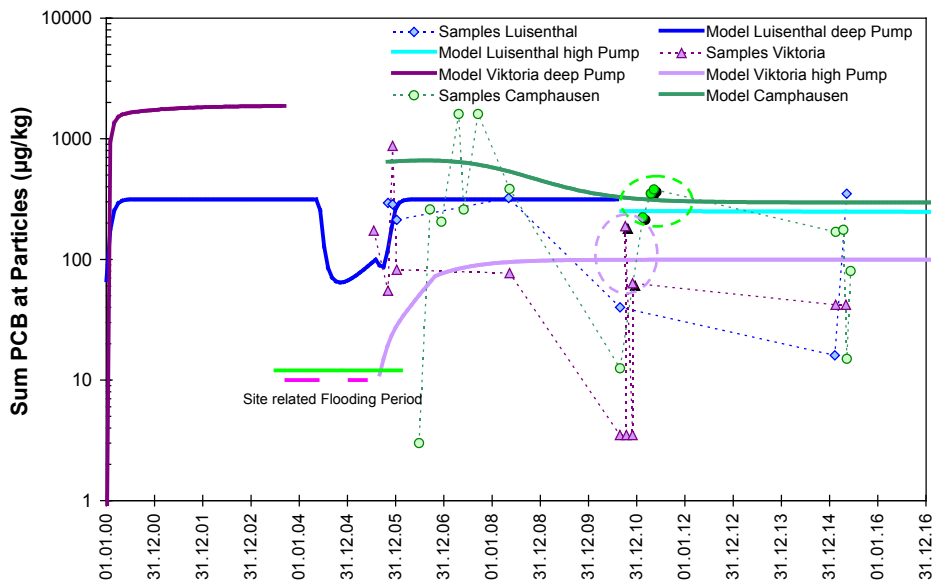


Figure 4 Measured values for the total PCB content of the particulate solid (= filterable substances) with calibration of the Boxmodel for three Saarpumping stations (Luisenthal, Viktoria, Camphausen).

The water rise for the investigation area Saar up to the level -320 m bsl will last approx. 3 years. The model results for the PCB discharge (fig. 5) are mainly a result of the behaviour of the solids contents transported in the water. It is expected that the development shown in Figure 3 will be repeated (mobilisation followed by increased sedimentation resp. reduced erosion). The load of the PCBs attached to these solids follows the same processes. Unlike sulphate (and similar salts), the source of the particle bound substance is not below the water level but above it. Water increase thus reduces the potential release. This will lead to a 75% reduction in PCB loads from the study area according to the model projections.

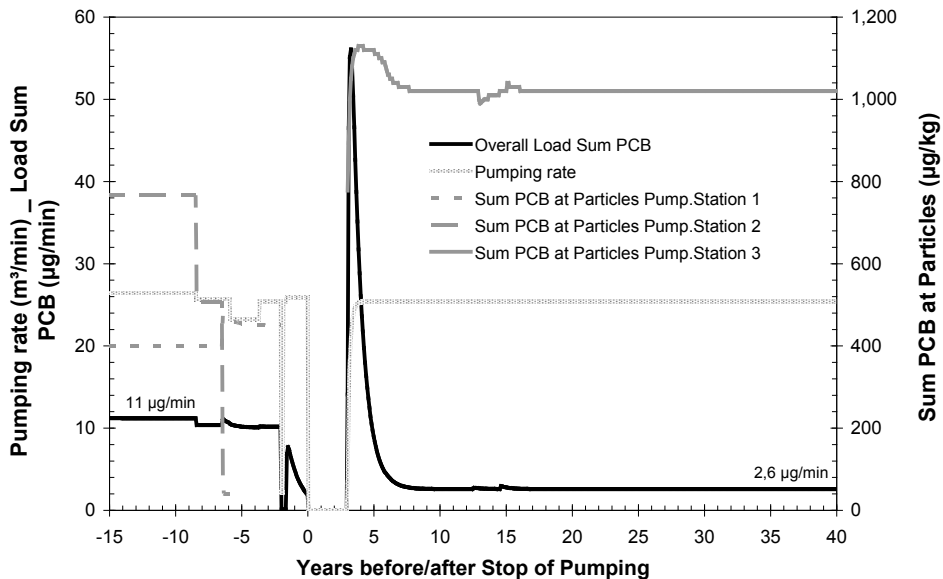


Figure 5 Model prognosis for the development of the PCB load as well as the determining pumping rates and PCB solids content for the total water extraction in the Saar model area.

Conclusions

Basis for the modelling of the PCB output is the modelling of mobilisation and sedimentation of particles in the course of water flow in the mines. As a result, it seems plausible that water level rise reduces the mobilisation potential for PCBs. PCBs are obviously mobilised, as long as the relevant mine cavities are not yet flooded. Flooding of a PCB contamination in a gallery ground prevents turbulent flow and thus detachment of particles from the floor. In order to minimise such particle bound pollutants, therefore, keeping the water level down is the wrong strategy. Water rise with the highest possible water levels, on the other hand, neutralises the PCB source and in addition reduces the amount of water and salt water discharged. Results for this particle-bound transport are also applicable to other higher molecular weight organic compounds because they are also as dominantly bound to fine particles as PCBs. The model concept can also take into account the sorption / desorption processes to which such substances are subject.

References

- Eckart M, Rüterkamp P, Klinger C, Kories H, Gzyl G (2010): Qualitätsentwicklung der Grubenwässer bei der Flutung von Steinkohlen- und Erzbergwerken. Merkel, B.J. & Schipek, M. (eds.): Grubenwässer – Herausforderungen und Lösungen, 61. Berg- und Hüttenmännischer Tag, 123-131, TU BA Freiberg
- Hjulström, F. (1935). Studies of the morphological activity of rivers as illustrated by the River Fyris. Bulletin of the Geological Institute, 25, 221–527. University of Uppsala

- Klinger C, Charmoille A, Bueno J, Gzyl G, Garzon Súcar B (2012): Strategies for follow-up care and utilisation of closing and flooding in European hard coal mining areas. *International Journal of Coal Geology*, 89, Special Issue European Coal Conference 2010, 51 – 61
- LANUV (2015): Belastungen von Oberflächengewässern und von aktiven Grubenwassereinleitungen mit bergbaubürtigen PCB (und PCB-Ersatzstoffen) – Ergebnisse des LANUV-Sondermessprogramms 2015. Landesamt für Natur, Umwelt und Verbraucherschutz NRW, 38 pp
- LUA (2015): Stand der PCB-Belastungen in Saarländischen Fließgewässern (Schwebstoffe und Biota). Landesamt für Umwelt- und Arbeitsschutz des Saarlandes, Geschäftsbereich 2 Wasser, Fachbereich 2.4 Gewässerökologie, Bericht 2.4 – 2015 – 01, 42 pp

Mercury Accumulation and Bio-transportation in Wetlands Biota Affected by Gold Mining - Modelling and Remediation

Ewa M. Cukrowska, Hlanganani Tutu, Luke Chimuka, Odwa Mbanga

Environmental Analytical Chemistry, School of Chemistry, University of the Witwatersrand, Johannesburg, South Africa, E-mail: ewa.cukrowska@wits.ac.za

Abstract Phytoremediation is cost-effective, eco-friendly technology for the removal of metals contaminating aquatic ecosystems. Biogeochemical models for mercury in wetlands were developed by monitoring its accumulation, speciation, methylation and bio-transportation with seasonal changes, emissions, transformations of environmental parameters and biological responses. The lowest bioaccumulation factors were during the wet season indicating lower macrophyte uptake capacity. Translocation factors show mercury accumulation in roots in the wet season; opposite to the dry season. Few plants are proposed for constructed wetlands for mercury phytoremediation. The different uptake and speciation patterns suggest that the most effective wetlands should include few different plant species working together.

Key words mercury, wetlands, bioaccumulation, methylation, phytoremediation

Introduction

Wetlands have several functions that aid in the removal of metals and ameliorate AMD. Sulphates and metals are trapped by wetlands (Perry and Kleinmann 1991). The ability of wetland to act as chemical sinks is due to the presence of plants. Phytoremediation is economically viable biological soil remediation method alternative for the removal of metals contaminating aquatic ecosystems (Padmavathiamma et al. 2007). Biosorption capacity depends on: the metal ion (atomic mass, ionic ray, and valence), environmental conditions (pH, temp. conductivity, contact time, biomass), nature of a biosorbent (Wang and Chen 2009). Many wetlands contain higher concentrations of total and methylmercury and have been shown to be sources and sinks of mercury and most always sources of methylmercury (Guentzel, 2009). Nevertheless, these ecosystems not only respond to direct environmental changes but to the combined or integrated influences of different anthropogenic activities taking place along their watersheds. Indeed, they are permanently at risk. This project was inspired by the paucity of research on mercury and methylmercury in wetland biota growing in semi-arid areas affected by mining and other industrial activities. Unfortunately there are very few long term records of mercury and methylmercury in wetland plants in SA, moreover, no seasonal changes of the mercury loads in affected areas were reported until very recently (Lusilao-Makiese et al. 2014, 2016), thus establishing widespread baselines or current trends is presently difficult. Understanding the bio-transportation and accumulation of mercury in wetland biota is necessary in order to predict the potential impacts and hazards associated with mercury contamination. In addition, it also important to determine how these seasonal changes will affect the Hg speciation in this type of ecosystems.

Materials and Methods

Sampling area

The main wetland area chosen for this study is Germiston in the east of Johannesburg, South Africa (fig.1).

The sampling site is down the slope of the reprocessed tailing footprint (TF). Thus, metals from the tailing footprint are washed to the sampling site via fluvial transportation and erosion. The water from the Natalspruit River flows through the wetland and end up ultimately in the Vaal River which is used as a water source for greater Johannesburg.

Two sampling campaigns were conducted during the wet and late dry seasons. Plants, water and topsoil from where the plants grew were collected from the wetland adjacent to the tailing footprint. The wet and dry seasons sampling was motivated by the need of understanding the seasonal impact on the Hg accumulation, bio-transportation and distribution in wetland in the semiarid area. Sampling points were selected based on data obtained from the wet season sampling.

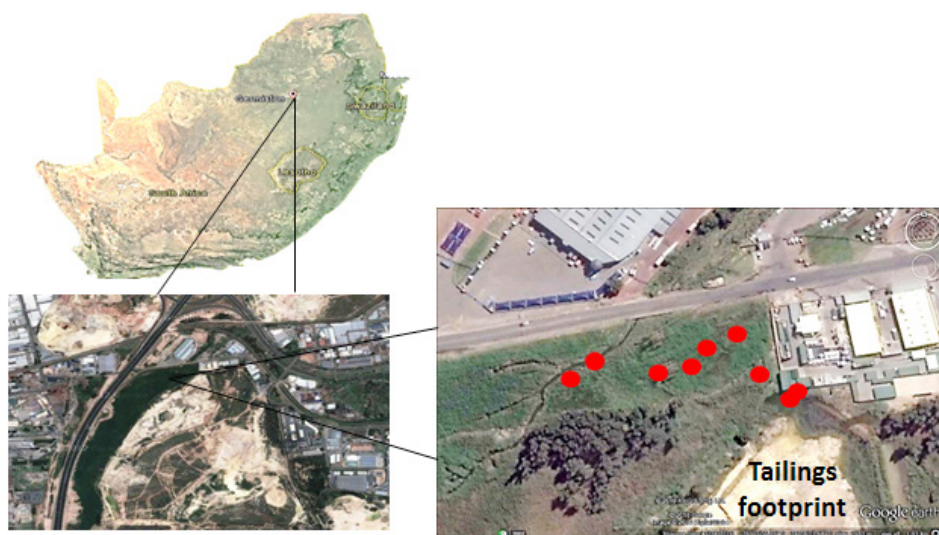


Figure 1 Geographical location of the Germiston sampling site together with points where samples were collected..

Sampling and sample pre-treatment

Waters were collected as duplicate samples into acid-washed and conditioned borosilicate bottles with PTFE-lined caps, according to commonly accepted sampling procedures (USEPA, 2007). Each sample was divided into two parts: the one was filtered under vacuum with 0.45 μm filter papers (Millipore, USA) and used for the determination of anions (Cl^- and SO_4^{2-}) by ion chromatography (IC); the other was acidified with 1% (v/v) HCl suprapure (37%, Sigma Aldrich). The samples were transferred in borosilicate bottles with PTFE-lined caps and stored at 4°C until analysis.

Field parameters such as temperature (T), pH and redox potential (Eh) were measured *in situ* using portable meters (WTW multi-parameter instrument pH/Cond 340i and ORP, Germany). GPS coordinates were taken at each sampling point and were used for mapping. Plant species were randomly collected in triplicates. The entire above ground tissues of the plant material together with the roots and sediments from where the plant grew were collected. Vegetation samples consisted of six different plant species (fig. 2).

To rid the samples of any metals that could be attached to the surface, they were thoroughly rinsed with de-ionized water and kept in polyethylene bags. Later, the plant material was cut into smaller pieces and appropriately sorted out into categories of roots, stem, leaves and seeds. Vegetation samples were then frozen and lyophilized at -40°C for 48 hours. Lyophilized samples were ground into fine homogenous powder using a pestle and a mortar with the aid of liquid nitrogen (Heller and Weber 1998). These were kept in cleaned polystyrene bottles in the dark, to prevent photodegradation (Yu and Yan 2003).

The method employed for plant sample treatment was acquired from an existing sample pre-treatment method developed by the United States Environmental Protection Agency (USEPA 1996).

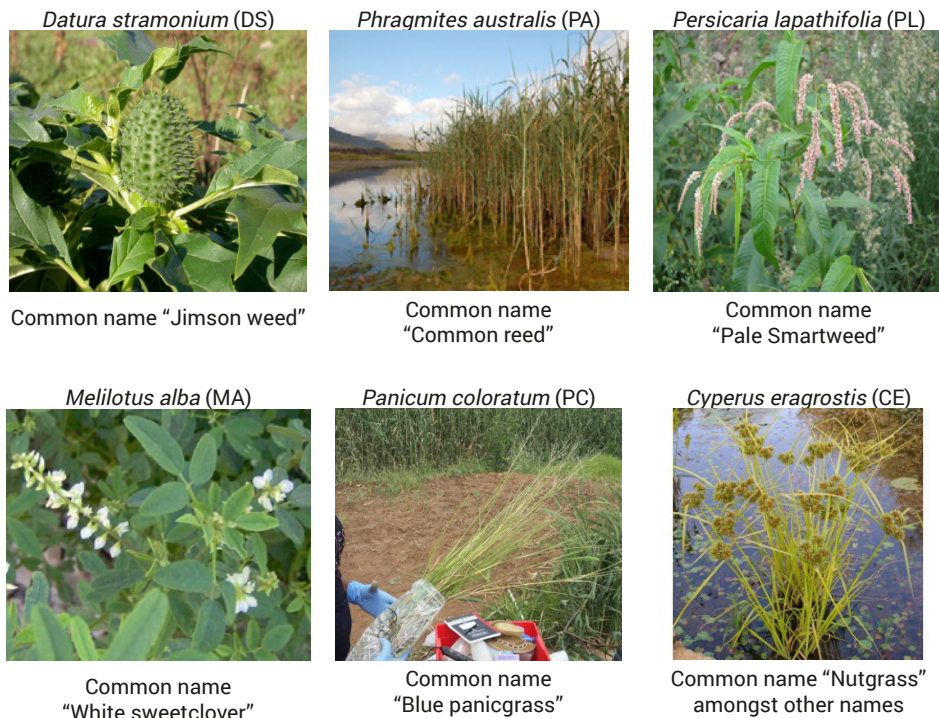


Figure 2 Plant species used in the study

Results and Discussion

Field measurements

Table 1 shows the measured parameters in sediments where plants were collected. In the wet season, pH was slightly acidic to neutral. In dry season the pH of sediments samples ranged from 4.1 to 6.4 and the redox potential from 0.26 to 0.49 V. Sediments samples in dry season are acidic in all studied sites. The lower pH values observed in dry season is an evidence of the acidification of the area through pyrite oxidation.

Table 1 Field measurements for sediments in areas where wetland's plants were collected.

Sample	Temp.	pH	Eh (V)	Temp.	pH	Eh (V)
Wet season			Dry season			
DS	25	7.3	0.42	18	6.0	0.26
PA	23	7.3	0.42	19	4.1	0.38
PL	23	7.3	0.42	20	4.1	0.38
MA	21	7.3	0.42	18	6.0	0.49
PC	25	4.2	0.55	18	6.4	0.38
CE	26	7.3	0.42	18	4.1	0.39

Mercury concentration in sediments and plants

Total Hg and organo mercury concentrations in sediments and plants are shown in figure 3. PA showed the highest mercury concentrations in tissues. In most cases, HgT concentrations in sediments were significantly higher than those in roots in a wet season. However, species such as CE and PC had a higher concentration in roots than in sediments. The highest root concentrations of Hg were observed in CE. CE had also the highest Hg concentration in stem (fig. 3). Generally, during a wet season the mercury levels were descending on the way roots-stem-leaves. The dry seasons patterns differ depends on the individual plant species. Generally MHg concentrations in a dry season are higher.

Bioaccumulation and translocation factors

The lowest BFs were registered for PA during the wet season indicating that Hg is mainly retained by sediments (tab. 2). The plant species with BF higher than 1 were CE and PC indicating a higher macrophyte uptake capacity. This trend was again observed with the behaviour of CE in the dry season. According to the TFs, metals were accumulated fundamentally in roots. TFs were greater than 1 for all mercury species in the dry season (tab.2). Some correlations were found varying according to species and plant tissue.

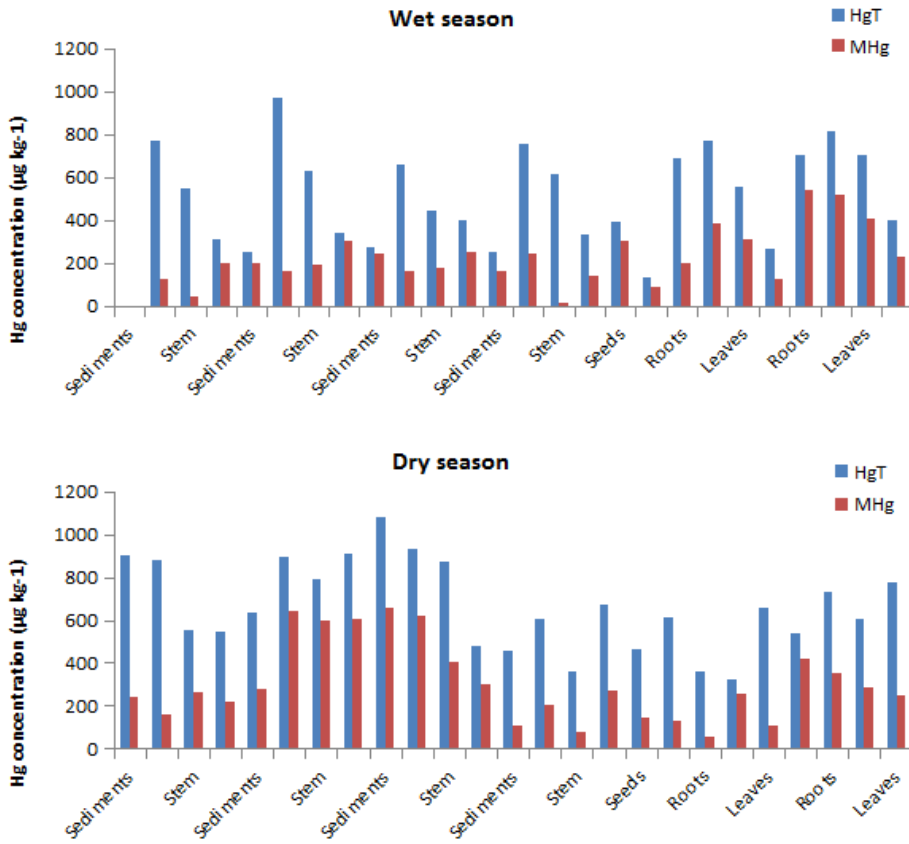


Figure 3 HgT and MHg concentrations ($\mu\text{g kg}^{-1}$ dry weight) in the sediments and plant tissues.

Table 2 Bioaccumulation factor (roots/sediment) and Translocation factor (leaves/roots).

Sample	Wet season		Dry season	
	BF_s	TF_s	BF_s	TF_s
DS	0.81	0.64	1.31	1.11
PA	0.64	0.43	1.42	1.01
PL	0.70	0.45	0.98	0.62
MA	0.66	0.56	0.86	0.51
PC	1.11	0.34	0.58	1.83
CE	1.16	0.49	1.30	1.06

Seasonality of the mercury biogeochemical cycle

In a wet season four from the selected plant species had the lower concentration of HgT in roots compared to sediments. (species: PL, PA, MA and DS). The exclusion of metals from the root tissues has been suggested as a metal tolerance strategy (Weis and Weis 2004); a metal precipitates within the rhizosphere only by formation of insoluble complexes of mercury which results to lower bioavailability, thus reducing the uptake by the roots. This is confirmed by the bioaccumulation factor values calculated for these species were less than 1. A different trend was observed for PC and CE – the concentration of HgT in roots was greater than in sediments and the BF values were greater than 1 showing bioaccumulation of mercury. It could be inferred that these species have the ability to oxidise sediments in the rhizosphere. This leads to remobilisation of metal contaminants increasing their bioavailability.

The TF values of all the plant species in the wet season were less than 1 meaning the Hg was predominantly concentrated in the roots (tab. 2). This indicates limited mobility of mercury once inside the plant. Binding positively charged metal ions to negative charges in the cell walls of the roots, metal phytate formation, and chelation to phytochelatins followed by accumulation in vacuoles have been invoked as mechanisms to reduce metal transport and increase metal tolerance (Chaney 1993).

The levels of MHg concentrations were generally low in the wet season with the exception of CE and PC species. MHg is volatile and can easily evaporate in a hot season reducing its concentration in sediments and plant tissues. In South Africa, most wetlands are river-fed and therefore undergo seasonal changes with flooding in summer and drying out in winter. Due to high temperatures in summer, high evapotranspiration rates may result in loss of volatile methylmercury into the atmosphere. CE and PC had the highest concentration of MHg in the wet season and TF values greater than 1. This is indicative of significant translocation from sediments to roots. Mercury methylation occurs in the rhizosphere where sulfate reducing bacteria are found (Patty et al., 2009). Therefore for CE and PC some of HgT was converted to MHg in the rhizosphere and was translocated to the aerial tissues. Both these species shows similar pattern for THg and MHg with concentration of both forms decreasing from roots to leaves. Species PL, PA and MA shows similar pattern for MHg highest in stems than in roots and leaves. Only DS presented the highest MHg concentration in leaves in the wet season. In general the levels of mercury (HgT and MHg) were higher in the dry season. Mercury total cumulated in sediments serves as a reservoir for production of organomercury in anaerobic conditions. CE and PC had highest concentration of HgT in roots compared to sediments. However the leaves accumulated more HgT for both species in the dry season.

There changes noted in the distribution of HgT and MHg in PC, and DS during the dry season showed the highest MHg in leaves. Surface roughness could be one of the reasons as to why leaves and seeds of DS accumulated more mercury trapping particulates. MA and CE showed the pattern of decreasing MHg from roots to leaves during the dry season. PA

showed the biggest increase of MHg and HgT in all their tissues. The percentage conversion to organomercury was the highest. It also presented significant translocation of HgT from the sediments to the above ground plant tissues; the TF value greater than 1. This behaviour could be attributed to the presence of bacteria in the rhizosphere. The presence of microbial symbionts such as rhizosphere bacteria is one of the factors that can affect the accumulation of metals in wetland plants (Wies and Wies 2004). This was confirmed by a study that the presence of periphyton associated with PA in wetlands enhanced the ability to accumulate and retain metals (Lakatos et al. 1999). This specie is the most common in SA wetlands occupying 60 to 90% (in constructed wetlands) of areas.

Mercury has the ability to be transported over long-range distances in the atmosphere, can also be distributed from the mine tailings by wind, therefore its concentration in the leaves could also be from atmospheric deposition. Mercury can get translocated into the plants' system through foliar absorption. This process is more pronounced in the dry season due to the persistence of mercury particulates on the leaves and the absence of the washing rainfall. Furthermore, evaporation of water from sediments together with the dehydration of plant leaves by transpiration increase the metal concentration.

Conclusions

Wetland plants demonstrated that they can grow in mercury-polluted areas and have the potential to uptake the metal. Metal translocation into leaves appears to be restricted in some wetland plants, this is however not the case with other species such as CE and PC. Translocation factor gives an idea whether a plant can sufficiently take up Hg from the sediments to the aerial tissues. Besides their uptake capacity, plant species investigated developed mechanisms to cope with elevated levels of mercury and this enhances their phytoremediation capacity. CE, PC, PA and MA could be proposed as Hg biomonitors and phytoremediators, being useful species to be utilized in constructed wetlands for the treatment of industrial effluents. The different uptake and speciation patterns suggest that the most effective wetlands (including constructed wetlands) should include few different plant species working together.

Acknowledgements

The authors thank the Water Research Commission, SA for funding this project.

References

- Chaney, R L (1993) Zinc phytotoxicity. In Zinc in soils and plants. Springer Netherlands, (p 135-150)
- Guentzel, JL (2009) Wetland influences on mercury transport and bioaccumulation in South Carolina. *Science of the Total Environment* 407(4):1344-1353
- Heller AA and Weber JH (1998) Seasonal study of speciation of mercury(II) and monomethylmercury in *Spartina alterniflora* from the Great Bay estuary, NH, *Science of the Total Environment* 221:181-188
- Lakatos G, Kiss M and Mészáros I (1999) Heavy metal content of common reed (*Phragmites australis*/Cav./Trin. ex Steudel) and its periphyton in Hungarian shallow standing waters. In: *Biology, Ecology and Management of Aquatic Plants*. ED: Dumont HJ, Kluwer Academic Publishers

- Lusilao-Makiese, J G, Tessier E, Amouroux D, Tutu H, Chimuka L, Weiersbye I, and Cukrowska EM (2014) Seasonal distribution and speciation of mercury in a gold mining area, north-west province, South Africa. *Toxicological & Environmental Chemistry*, 96(3):387-402
- Lusilao-Makiese JG, Tessier E, Amouroux D, Tutu H, Chimuka L, Weiersbye I, Cukrowska EM (2016). Mercury speciation and dispersion from an active gold mine, the West Wits area, South Africa. *Environmental Monitoring and Assessment*, 188: 47-56
- Padmavathiamma Prabha K, and Loretta Y Li (2007) Phytoremediation technology: hyper-accumulation metals in plants. *Water, Air, and Soil Pollution* 184(1-4): 105-126.
- Patty C, Barnett B, Mooney B, Kahn A, Levy S, Liu Y, and Andrews JC (2009) Using X-ray microscopy and Hg L₃ XANES to study Hg binding in the rhizosphere of *Spartina cordgrass*. *Environmental Science & Technology*, 43(19):7397-7402
- Perry A, Kleinmann RL (1991) The use of constructed wetlands in the treatment of acid mine drainage. In: *Natural Resources Forum*, Blackwell Publishing Ltd. (Vol. 15 (3):178-184
- USEPA (1996) Microwave Assisted Acid Digestion of Siliceous and Organically Based Matrices, US Environmental Protection Agency Method 3052, December 1996, 20.
- USEPA (2007) SW-846 Methods, Chapter 3: Inorganic analytes, Rev.4, February 2007, available at www.epa.gov/osw/hazard/testmethods/sw846/pdfs/chap3.pdf.
- Wang J and Chen C (2009) Biosorbents for heavy metals removal and their future. *Biotechnology Advances* 27: 195–226.
- Weis JS, and Weis P (2004) Metal uptake, transport and release by wetland plants: implications for phytoremediation and restoration. *Environment International*, 30(5):685-700
- Yu LP and Yan XP (2003) Factors affecting the stability of inorganic and methylmercury during sample storage, *Trends in Analytical Chemistry* 22:245-253

Utilizing Geophysics As A Delineation Tool for Groundwater Flow Paths And Contaminants Along A Graben

JSDR Zielke-Olivier¹, PD Vermeulen¹

¹*University of the Free State, Institute for Groundwater Studies, 205 Nelson Mandela Drive, Park West, 9301 Bloemfontein, South Africa, josephzielke@gmail.com, vermeulend@ufs.ac.za*

Abstract Seepage from industrial operations into an underlying graben structure resulted in a lowered groundwater quality. A geophysical investigation was conducted across this graben to determine its influence on the pollution distribution and to improve the geohydrological understanding. Geophysical modelling indicated zones of elevated conductivity associated with fault planes, tailings dams, discard dumps and quarries. Additionally, groundwater chemistry obtained at high conductivity zones suggested seepage into both the shallow weathered aquifer and the deeper fractured aquifer underlying the study area. This study demonstrated that applied geophysics in combination with geohydrological data is a useful tool for detecting contaminant groundwater flow paths.

Key words Electrical resistivity tomography, electromagnetics, graben, groundwater contamination

Introduction

Mining and industrial sites with abundant infrastructure and complex operations pose a geohydrological challenge when delineating and managing groundwater contaminants along geological structures. Long term groundwater monitoring revealed an increased salinity within a quarry as well as the shallow weathered and lower fractured aquifer in the vicinity of tailings dams, discard dumps and a variety of industrial operations. In addition, streams within the research area exceeded the electrical conductivity limits granted for a water use license.

The study site was located in the north-eastern section of the Karoo Basin, South Africa, resembling a retro-arc foreland basin. According to Johnson et al. (2006), the area is dominated by lithologies of the Permian Vryheid Formation of the Ecca Group, consisting of upward-coarsening cycles of siltstone, mudstone, immature sandstone and carbonaceous shale. Locally, several faults were identified which together form part of a larger graben structure with a displacement of approximately 22 m (Vermeulen and Dennis 2009). Two aquifer types were classified by Grobbelaar (2001) within the study area: An upper weathered Ecca aquifer with an average yield of 0.6 l/s (King 2003) and a deeper fractured Ecca aquifer with an average yield of 0.2 l/s (King 2003). Although these aquifers are relatively low yielding, bedding planes and secondary structures such as fractures and fissures could contribute to the dispersion of contaminants from mining and industrial activities located on the fault system.

Research was based on a study conducted by Vermeulen and Usher (2009) describing the effects of contaminant migration along a graben structure. Results showed that seepage leaked into the groundwater from an adjacent discard dump and that the graben functioned

as a highly conductive zone. In addition, a northward decreasing salinity in the direction of a bordering stream suggested that the fault zone could act as a barrier for groundwater flow or that dilution took place over a distance. Overall, surface water was identified as the main factor spreading pollutants across the study site. A drainage system was constructed to prevent seepage from the discard dump. However, this did not improve the water quality of the stream and quarry after a decade of existence. Therefore it was recommended to extend the area of investigation to determine the groundwater flow direction along the fault zones as well as to determine the salt load contribution into the system by individual industrial activities.

This study aimed to identify flow paths of possible seepage from industrial operations into a quarry and graben by combining electrical resistivity tomography, electromagnetic methods and hydrochemical data. Furthermore, this research could contribute to a more comprehensive understanding of whether the underlying graben may aid in the distribution of contaminants along fault planes and into adjacent streams.

Methodology

Electrical resistivity tomography (ERT)

The ERT method was employed to detect groundwater occurrences and changes in lithology by measuring the apparent resistivity. The apparent resistivity is obtained as the product of a measured resistance from the ground and a geometric factor for a given electrode array (Reynolds, 2011). This method is based on the fact that different geological units are more or less resistive to an induced electrical current applied. A detailed description on ERT methods is available in Telford et al. (1990).

A Terrameter ABEM SAS 1000 with a Lund Imaging System and a Wenner array was utilized to measure the apparent resistivity of the subsurface. A broad and refined grid with a total of 35 traverses was surveyed across a 12 km section of the fault system using a unit electrode spacing of 5 m and 2.5 m respectively (Fig. 1). The electrode spacing was chosen based on a) the need to record data with a high spatial resolution and b) the physical limitations on the lengths of the electrode arrays posed by the surface infrastructure, quarries and wetlands. However, a decrease in electrode spacing does not only increase the spatial resolution but reduces the maximum depth of investigation that can be obtained (Fourie and Vermeulen 2008). The measured data was inverted with the computer program RES2DINV to generate pseudosections of the transects.

Electromagnetic Method (EM)

A frequency-domain, small-loop system, Geonics EM34-3, was applied to detect pollution plumes and groundwater flow paths within the subsurface. As described by Telford et al. (1990), a transmitter coil generates a transient electromagnetic field in and over the earth's surface and a receiver coil measures the response of the ground to the propagation of the incident alternating electromagnetic waves created. The distance between the transmitter and receiver coil was kept constant at a 40 m inter-coil spacing. A 40 m inter-coil spacing was

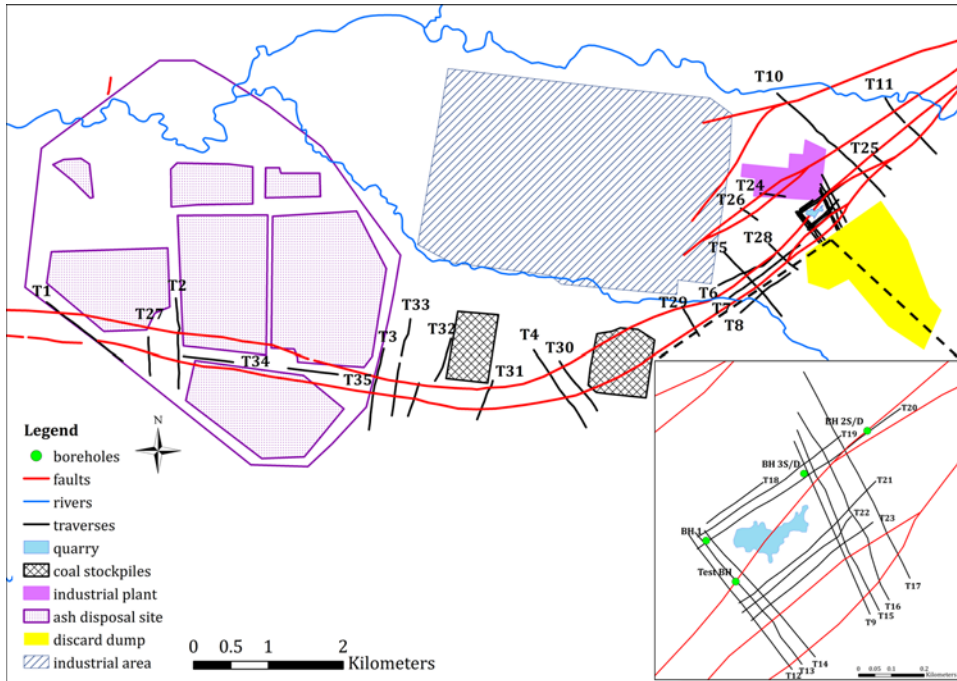


Figure 1 Schematic map of the study area indicating the outlines of the geophysical survey grids.

utilised to allow measurements up to an approximate depth of 60 m. The coils were moved along each transect at regular intervals of 5 m whereby the measured apparent conductivity was recorded (in mS/m). Coordinates of measuring stations were noted in 50 m intervals. Both, the vertical and horizontal dipole modes were employed to detect electromagnetic anomalies at depth and near-surface, respectively (Reynolds, 2011). Only 11 traverses were surveyed with the EM method due to disturbances of surrounding industrial operations and excessive infrastructure. In order to enhance the geohydrological interpretation, the EM profiles were compared to the ERT pseudosections, borehole logs and groundwater chemistry of monitoring wells in close proximity of the surveyed transects.

Results and Discussion

A geophysical investigation conducted across the graben displayed low apparent resistivity values in close proximity to ash tailings dams, discard dumps and mine water dams, insinuating that seepage may drain from these facilities. For example, Fig. 2 showed a broad, low apparent resistivity zone between the fault mapped at station 1100 m and station 1400 m near an ash tailings dam. This could imply that seepage from the ash tailings dam percolates into the shallow weathered aquifer and deeper fractured aquifer. In addition, the pseudo-section of Profile T1 pointed out that a lithology comprising lower apparent resistivity may exist within the graben between the two fault planes at stations 550 m and 1100 m as previously observed by Vermeulen and Usher (2009).

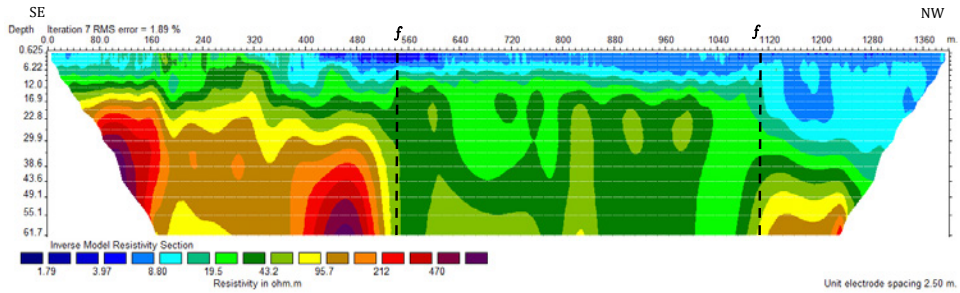


Figure 2 Inverted resistivity model along Profile T1.

A pseudosection of Profile T20 (Fig. 3) was conducted north of the water-filled quarry containing a high salinity. It had raised concerns that seepage from the quarry could contribute to groundwater and surface water pollution in the area and along the underlying fault. Profile T20 showed a shallow zone of elevated apparent conductivity that increased in depth from station 90 m to 700 m. This could imply seepage from the quarry into the shallow weathered and fractured aquifer. High apparent conductivity values below 1.79 Ω m near the surface between stations 320 m to 700 m could indicate that wetlands are affected by drainage from the adjacent quarry. Furthermore, the elevated apparent conductivity between station 90 m and 280 m could represent a potential flow path into the quarry based on the elevation profile of the area. A dolerite sill north of the quarry could form potential flow paths along the contact zone with the country rock.

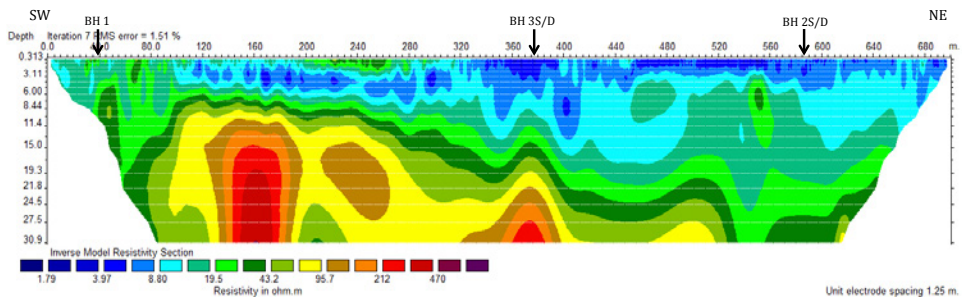


Figure 3 Inverted resistivity model along Profile T20.

Based on the groundwater chemistry of the monitoring boreholes presented in Fig. 1, the shallow and deeper boreholes BH 3S/D located downstream of the water-filled quarry seemed to be influenced by seepage from the quarry. Both, the monitoring boreholes and the quarry contained the same Ca/Mg/SO₄/Cl water type (Fig. 4). This suggests a possible groundwater flow connection between the quarry and the underlying aquifers, and is also supported by the ERT pseudosection. In addition, groundwater samples of the deeper borehole BH 3D and the quarry showed the same electrical conductivity (EC) trend. Shallow borehole BH 2S was drilled into a fault plane and indicated a shift in groundwater type from Ca/Mg/HCO₃ to Ca/Mg/SO₄/Cl during one decade of monitoring. Furthermore, both the quarry and borehole BH 2S showed the same EC trend over time. This could point to a possible link between the quarry and the shallow aquifer by means of the highly conductive

fault plane underlying the quarry. In comparison, the groundwater chemistry of the underlying deeper fractured aquifer obtained from borehole BH 2D did not seem to be affected by seepage from the quarry as the water type remained constant as Ca/Mg/HCO₃ water. The groundwater chemistry of borehole BH 1, located west of the quarry, did not correlate with the hydrochemistry of the quarry and could therefore represent a different aquifer system.

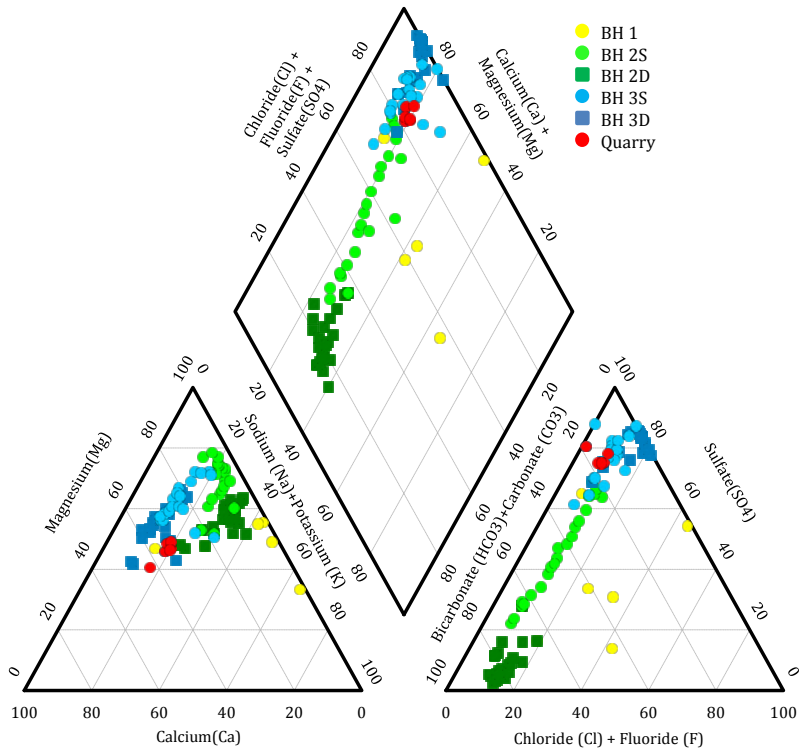


Figure 4 Piper diagram indicating the groundwater chemistry of boreholes along transect T20.

Resistivity Profile T13 was constructed west of the water-filled quarry extending southeast to northwest as indicated in Fig. 5. In the south-eastern section, a more resistive zone was visible near the surface which could constitute a partly weathered dolerite sill based on high apparent resistivity values. A shallow low resistivity zone from station 180 m to 250 m

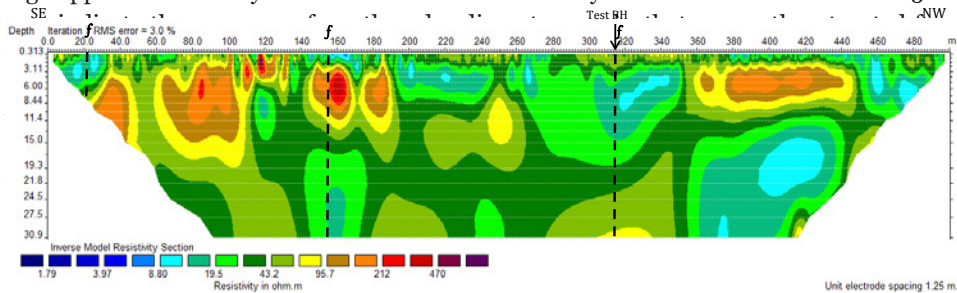


Figure 5 Inverted resistivity model along Profile T13.

An additional pseudosection, Profile T9, was generated east of the water-filled quarry from south-southeast to north-northwest (Fig. 6). A zone of increased apparent resistivity was modelled near the surface to an approximate depth of 20 m from station 0 m to 150 m, possibly indicating the presence of a dolerite sill. A decrease in apparent resistivity below a depth of 20 m could be explained by a change in lithology to less resistive sedimentary rocks of the Karoo Supergroup. Parallel to the quarry between station 240 m and 400 m, a shallow zone of low apparent resistivity was modelled, correlating with a wetland. From station 400 m to 480, the zone of low apparent resistivity increased in depth and corresponds with a mapped fault at station 425 m. This fault plane could have formed a zone of elevated conductivity and might provide groundwater flow paths linked to the quarry. In the northern section of Profile T9, from station 500 m to 560 m, a zone of increased apparent resistivity near the surface could indicate a change in lithology and might represent a dolerite sill.

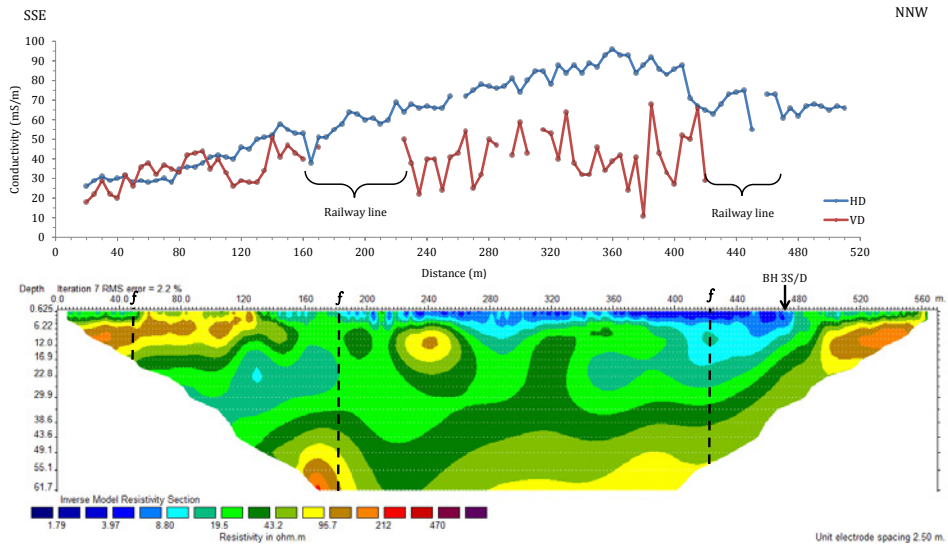


Figure 6 EM profile and inverted resistivity model along Profile T9.

In comparison, the horizontal dipole EM profile along the transverse T9 confirmed an increase in conductivity from station 80 m to station 360 m, most probably resulting from an underlying thicker zone of saturated weathered material. A sudden decrease in conductivity at station 170 m and between station 410 m and 420 m could point to a sudden change in lithology caused by a fault, previously mapped, or could relate to interference generated from the railway line. A general increase in conductivity between station 170 m and 480 m could represent the graben comprising more conductive, less consolidated sedimentary rocks. The vertical dipole EM profile showed a general decrease in conductivity at elevated depth which corresponds with the increased apparent resistivity modelled. However, no specific magnetic anomalies were detected.

Conclusions

A geophysical survey confirmed the presence of previously mapped faults within the graben system. Both ERT and EM methods showed that apparent conductivity values were often elevated near ash tailings dams, water-filled quarries and discard dumps. These zones of elevated conductivity proposed possible seepage of mine water into the underlying aquifers.

Furthermore, ERT pseudosections of a refined grid around a water-filled quarry with high salinity indicated zones of elevated apparent conductivity along the northern fault zone as well as along a backfilled area. High apparent conductivity values were also modelled north of the quarry at the contact zone of a dolerite sill. These findings elucidated that possible flow paths exist west of the quarry via the backfilled zone with a possible elevated transmissivity as well as north and north-east of the quarry along the contact zone with the dolerite sill and the fault zone, respectively. An increase in apparent conductivity from south to north, measured with the horizontal dipole of the EM, could not only indicate a change in lithology near the surface but could also relate to the elevated salinity in the shallow weathered aquifer caused by contaminants. Groundwater monitoring data confirmed an increase in salinity from the quarry downstream towards the boreholes in the northeast.

This study highlighted the complexity in identifying contaminant sources from industrial operations along a graben which may contribute to the elevated salinity in the underlying aquifer systems. Whether the graben provides groundwater flow paths between different pollution sources needs yet to be confirmed with additional measures including drilling of boreholes, aquifer testing and isotope studies. Nevertheless, the geophysical survey was found to be a useful tool in determining high conductivity areas across a large scale structure and will assist the client in managing the water use license enforced by legislations.

Acknowledgements

The authors would like to thank all helping hands who were involved in the extensive field work.

References

- Fourie F, Vermeulen D (2008) Underground Coal Gasification Project: Geophysical Investigations. Unpublished report, IGS2008/02/UCG, Institute for Groundwater Studies, University of the Free State, South Africa 16 pp
- Grobbelaar R (2001) The Long-Term Impact of Intermine Flow from Collieries in the Mpumalanga Coalfields. Unpublished Master Thesis, University of the Free State, South Africa, 136 pp
- Johnson MR, van Vuuren CJ, Visser JNJ, Cole DI, de V Wickens H, Christie ADM, Roberts DL, Brandl G (2006) Sedimentary Rocks of the Karoo Supergroup. In: Johnson MR, Anhaeusser CR, Thomas RJ (Eds), 2006 The Geology of South Africa, Geological Society of South Africa, Johannesburg/Council for Geoscience, Pretoria, p 461-500
- King GM (2003) An Explanation of the 1:500 000 General Hydrogeological Map: Vryheid 2730. Department of Water Affairs and Forestry, Pretoria, 41 pp
- Reynolds JM (2011) An Introduction to Applied and Environmental Geophysics. 2nd ed. Wiley-Blackwell, West Sussex, UK, 696 pp
- Telford WM, Geldart LP, Sheriff RE (1990) Applied Geophysics. 2nd ed. Cambridge University Press, Cambridge, 770 pp

- Vermeulen PD, Dennis I (2009) Numerical Decant Models for Sasol Mining Collieries, Secunda. Unpublished Report No. 2009/25/PDV, Institute for Groundwater Studies, University of the Free State, South Africa, 114 pp
- Vermeulen PD, Usher B (2009) The effect of graben structures on the migration of groundwater contaminants at an industrial site. *Environ Geol* 58:739-749, doi:10.1007/s00254-008-1548-x

Deep mining water control cooperative system based on 3-D directional drilling and controllable grouting techniques

Liu Zaibin^{1,2}, Dong Shuning¹, Wang Wenke², Nan Shenghui¹, Liu Qisheng¹

¹ Xi'an Research Institute Company of China Coal Technology and Engineering Group, Xi'an, Shaanxi Province, 710054

² Chang'an University, Xi'an, Shaanxi Province, 710064

Abstract In order to solve deep mining water hazard prevention and groundwater resource protection problems, 3-D directional drilling and controllable grouting techniques were studied to form the deep mining water control cooperative system. 3-D directional drilling design method was used to improve the effectiveness of horizontal wells in the whole mining area and to reduce unable detecting zone. Artificial grouting foundation and controllable grouting techniques were studied to limit the grouting body scope and to reconstruct the deep Ordovician limestone aquifer. According to an engineering practice, water inrush quantity was reduced effectively during grouting process.

Keywords 3-D directional drilling, grouting, deep mining, mine water control cooperative system

Introduction

With the development of China's coal industry, frequent water inrush disasters led to very serious person casualties and economic losses. In all kinds of water inrush problems, the coal floor water inrush problem as known as mining over confined aquifer water hazard problem in north China coal field has always been a key research hotspot and the research difficulty. Hanxing coal mine area, located in Hebei province, is a typical north China coal field threaten by the basal Ordovician limestone aquifer. When mining activities once revealed areas with conditions of too high basal aquifer pressure, insufficient aquiclude water resistance ability or with existence of water conducting channel, there is a large possibility of water inrush accident (Zhao 2014).

In Hanxing coal mine area, there are 12 coal mines with mining depth more than 800m with 4 coal mines deeper than 1 000 m. For deep mining working faces, hydraulic pressures under coal seam floor are higher than 7.0 MPa, with the highest pressure of 13.2 MPa. During deep coal mining process, water inrushes through coal seam floor are often related to mining activities and accompanied by rock mass stress dynamic phenomena. Deep mining faces a series of problems such as high cost of mine water drainage, water resources waste and highly risk of water inrush. In past twenty years, there were 11 coal seam floor water inrush accidents which flooded 3 mines and 2 mining levels with water flow from 160 m³/h to 24 000 m³/h (Zhao 2015).

There was a terrible shortage of water resources in Hebei province with water resources per capita ownership of 302 m³ which is 13.8 percentage of national average. The water scarcity has seriously affected industrial and agricultural production and also people's everyday life while coal mining activities influence the groundwater environment inevitably. Meantime,

every water inrush accident also causes a large amount of water loss. So the implementation of protective exploitation of water resources which can reduce the influence of coal mining on the groundwater environment has a very important practical significance (Yin 2016).

To solve these problems, deep mining water hazard detection and prevention methods were studied based on 3-D directional drilling and controllable grouting techniques which were applied to a deep coal mine with mining depth from 1 030 m to 1 270 m in north China. Mining and water control cooperative system was established by comprehensive overall planning of mining, drilling, testing and grouting processes. The water control cooperative system is a further development of the regional governance technology. Based on the water control cooperative system, water bursting points were plugged, possible water inrush disasters were prevented, new groundwater problems were controlled immediately and the groundwater resources were protected effectively.

Site description

Mining production situation

The deep mining area of Xingdong coal mine which located in Xingtai Hebei province was studied. The main working bed of Xingdong coal mine is No. 2 coal. The mining overall height, comprehensive longwall coal mining method was used. The mine has multiple working levels and uses vertical shafts including one main and one auxiliary shaft. The deep working level is -980 level. Working faces which are deeper than -980m in Xingdong coal mine belong two working areas distributed beside downhill roadways. The shape of the study area where mining working faces are deeper than -980m is an irregular rectangle with the size of 3.1 km long from north to south and 1 km wide from east to west. The No. 2 coal geological reserves of this area is 11.523 million tons among which 4.7663 million tons coal can be produced.

In the whole study area, No. 2 coal seam floor elevation is from -980 m to -1250 m, the Ordovician limestone hydraulic pressure is +66.84 m, distance from No. 2 coal seam floor to the Ordovician limestone surface is from 85.05 m to 262.5 m with an average of 156.92 m and the water inrush coefficient is from 0.07 MPa/m to 0.098 MPa/m which is bigger than the critical water inrush coefficient of structure development zone.

Formation lithology from No. 2 coal seam floor to the Ordovician limestone surface mainly includes sandstone, mudstone, limestone, alumina, etc. there are ten coal seams and three thin-layer limestone aquifers in this aquiclude layer.

Argillaceous rocks including mudstone, alumina are significant to prevent the Ordovician limestone confined water from inrushing to mining space. Soft and hard rock combination can enhance the Formation water resistance ability. So the key of mine water control cooperative system is to detect hidden water conducting channels to ensure the integrity of the coal seam floor water-resisting layer.

Groundwater inrush cases

Before the mine water control cooperative system was established, there were three Ordovician limestone water inrush accidents as shown in table 1. Two water inrush accidents which are coal seam floor water inrush accidents happened during 2127 working face and 2222 working face mining steps. The No. 15 borehole water inrush accident happened in -980 concentrated supply roadway was caused by a drainage borehole.

Table 1 Ordovician groundwater inrush accidents.

Location	Time	Peak value/m ³ h ⁻¹	Stability value/m ³ h ⁻¹	Observation borehole distance/m	Water levels fall/m
2127 face	4-13-2011	210	142	800	28.662
-980 roadway	5-19-2014	150	92	720	11.98
2222 face	3-1-2015	268	200	724	44.593

Cooperative system establishment

For the deep mining area, existing water bursting points are difficult to govern and new water inrush accidents also still could happen. For the drilling engineering, ground drilling conditions are confined by ground buildings, roads, pipelines, high-voltage power lines, etc. Meantime, this area had a very tight mining schedule. There was no suitable condition for advanced management before mining. Deep Ordovician lime stone has a very low degree and non-uniform karst development, so the detectable and controllable limestone section is very thin.

A series of technologies were studied to solve above difficulties. Flexibility of the ground construction location was improved by reverse and lateral displacements directional drilling techniques. Adaptive capacity to formation conditions was enhanced by long distance bedding countertendency drilling techniques. Mine water control availability was improved by comprehensive test procedures formed by mud displacement, well flushing, pump-in test and grouting test. The water resource was protected during coal mine exploration by the reconstruction of the aquifer system. Deep mine water servosystem was established to control new water inrush accidents and reduce the influence of water inrush. Mining, drilling and grouting processes were orderly planned by the deep mine water control cooperative system to ensure the safety of mine production and to improve the production efficiency.

3-D directional drilling technology

Horizontal Directional drilling

The 3-D directional drilling technology is a development of the horizontal directional drilling. The study of grouting reinforcement techniques on coal floor with multi-branch horizontal well was carried out through ground drilling (Wang 2015, Shen 2016, Chen 2016).

By the control of measuring instrument and geo-steering instrument, and the use of wall materials, horizontal drilling can be achieved in the Ordovician limestone. Horizontal well is the directional well extended to a certain length, its borehole trajectory is nearly level. Horizontal directional branched drilling on ground is drilling technology. Opening vertical holes from the ground, then change it to horizontal well at a certain angle in the target layer. Advantages of horizontal directional drilling technology are sitting flexibility, high efficiency drilling, disadvantages are more invalid footage and large blind area.

3-D directional wells

3-D directional drilling design method was used to improve the effectiveness of horizontal wells in the whole mining area and to reduce unable detecting zone. Inclined straight borehole which can make the inverse displacement and the lateral deflection which can decrease the angle of curvature were designed to adapt the site condition. Each well can be divided to four parts which are straight inclined section, lateral torsional section, uphill climb section, and control function section, as shown in figure1.

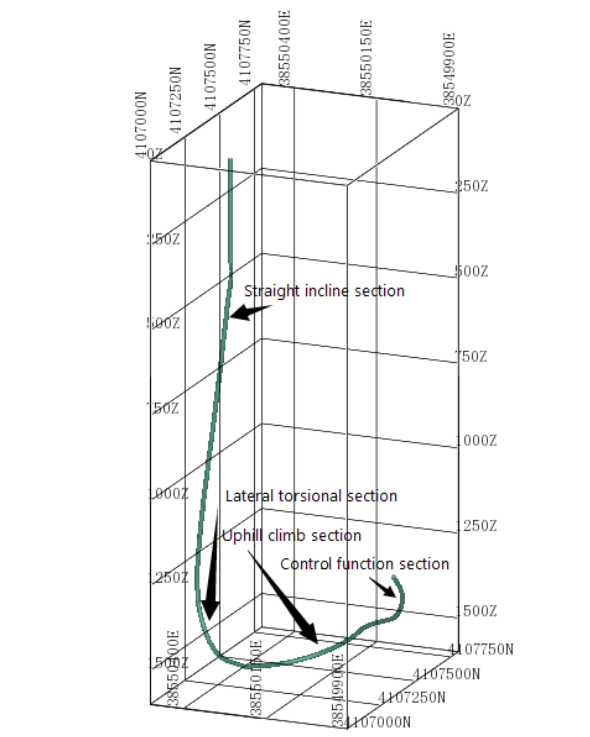


Figure 1 3-D directional well structure.

The study area was controlled by one main well and 22 branch wells which were divided to three different zones, as shown in figure 2. The distribution of branch wells were controlled by working faces distribution and main structures condition.

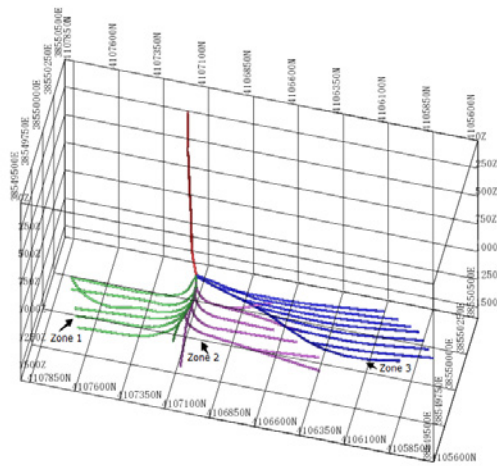


Figure 2 Directional wells distribution.

Controllable grouting technology

Wellhead grouting process

The wellhead grouting process is shown by figure 3. Jet mixing system was used to ensure continuous pulping and grouting. Cement and fly ash are main grouting material. Grouting process includes filling grouting and pressurized grouting stages. In the filling grouting stage, large discharge capacity from 260 L/min to 600 L/min grouting pumps were used. In the high pressure grouting stage, continuous pressurized grouting can increase the diffusion distance and fill tiny cracks.

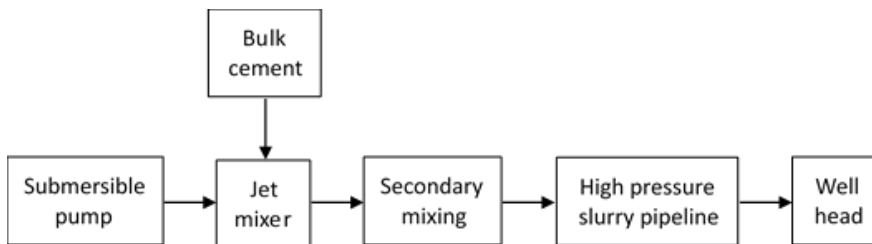


Figure 3 Grouting process flow diagram.

Artificial grouting foundation construction

Artificial grouting foundation and controllable grouting techniques were studied to limit the grouting body scope and to reconstruct the deep Ordovician limestone aquifer. The grouting layer was confined from 80 m to 100 m under the Ordovician surface. During drilling process, encountered structures were analyzed according to mud consumption, pumping and pump-in tests. Different materials including gravel aggregate, sand and fly ash were applied to build artificial foundation.

The grouting body was confined in particular layer to ensure the integrity of the water-resisting layer and can and to block groundwater inrush, as shown in figure 4.

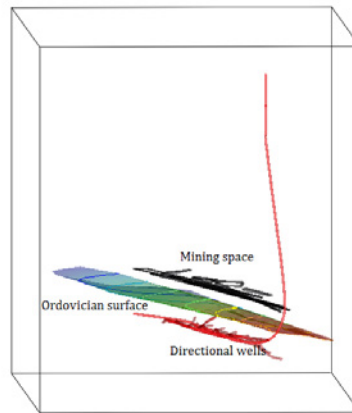


Figure 4 Spatial position relationship.

Mine water control effect

The mining and water control cooperative system was established to accomplish mine water whole process management, to reduce water inrush probability advanced, to reduce current water quantity and to response to new occurrence of water inrush instantly. During the grouting process, water inrush quantity was reduced effectively, as shown in figure 5.

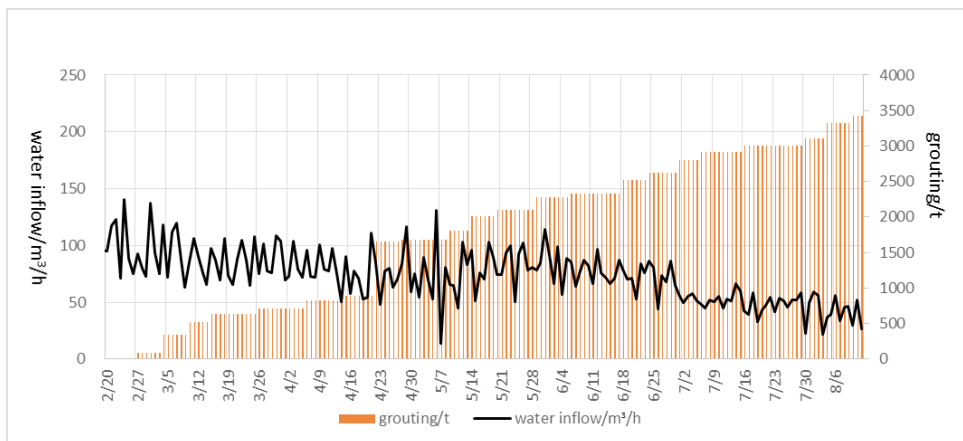


Figure 5 Mine water reduction during grouting process

Conclusions

Deep mine water control engineering practices confirmed that water hazard prevention and groundwater resources protection can be controlled cooperatively during mining process. The 3-D directional drilling technology which is a further development of horizontal direc-

tional drilling technology can detect formation conditions and ensure working faces safety. Controllable grouting technology can reduce grouting quantity, reconstruct the Ordovician aquifer and reduce mine water flow. Multi-source engineering data should be used to analyze hydrogeological information in future.

References

- Chen Lei, Yang Guobin, Zhang Wei. . (2016) Drilling safety technologies for 3D cluster horizontal wells of Junin Block in Orinoco, Venezuela. *Natural Gas Industry* 36(8):100-106. doi:10.3787/j.issn.1000-0976.2016.08.014
- Shen Guobing, Liu Mingguo, Chao Wenxue. (2016) 3D Trajectory control technology for horizontal wells in the fuling shale gas field. *Petroleum Drilling Techniques* 44(2):10-15, doi:10.11911/syztjs.201602002
- Wang Wanqing, Shi Zhongyuan, Fu Qianqian. (2015) Factory drilling technology for Go-7 3D horizontal well group. *Oil Drilling and Production Technology* 37(2):27-31, doi:10.13639/j.odpt.2016.02.008
- Yin Shangxian, Han Yong, Chang Haoyu. (2016) Study on optimal allocation of karst water resources in Hanxing Mining Area. *Coal Science and Technology* 44(8):29-34 doi:10.13199/j.cnki.cst.2016.08.005
- Zhao Qingbiao, Zhang Jiangong, Wang Haiqiao. (2015) Mechanism of coalfield deep mining floor water burst and key technology of regional control in North China. *Journal of North China Institute of Science and Technology* 12(4): 1-7
- Zhao Qingbiao. (2014) Ordovician limestone karst water disaster regional advanced governance technology study and application. *Journal of China Coal Society* 39(6):1112-1117 doi:10.13225/j.cnki.jccs.2014.0475

Tracing mine water inflows, deriving dewatering measures for an open pit and a first trial to adapt the approach for underground mines

David Hagedorn¹, Nils Hoth¹

¹ *Technische Universität Bergakademie Freiberg, Gustav-Zeuner-Straße 1A, 09599 Freiberg, Germany, Nils.Hoth@mabb.tu-freiberg.de, David.Hagedorn@mabb.tu-freiberg.de*

Abstract Within the first part of this paper, an overview is given about the initial approach to trace mine water inflows to their sources, which we presented at IMWA 2016. Recent results of further investigations are described. Furthermore, the procedure for the realization of actual dewatering measures is described. Within the second half of this paper, a trial to adapt our approach for an underground mine is described. Additionally, the later section gives an overview about the results of the adapted approach. In the end it is summarized in which conditions the approach works best.

Key words Dewatering, hard rock open pit, cut and fill, local hydrogeology, flow path interpretation

Introduction and review

Increasing production rates in open pit and underground mines nowadays lead to a deeper and more extensive development of mines. Greater depths may lead to increasing hydraulic heads and significantly increased water inflows. As a consequence, wet mining conditions occur, which in turn lead to a reduced production efficiency and safety risks. To reduce the inflows and their effects, companies have to implement dewatering systems. A good understanding of the local hydrogeology and water flow paths is the basis for the implementation of effective dewatering measures.

At last year's IMWA, we presented our approach to trace water inflows into BOLIDEN's Aitik open pit to derive suitable dewatering measures for the mine. Our approach for the sampling in Aitik was to sample different inflows into the mine, as well as natural and artificial surface waters from ponds, lakes, rivers and ditches in the vicinity of the mine. We evaluated the results of water sample analysis by identifying differences, similarities and connection between the waters. Based on the field parameters pH and Eh value, alkalinity, acidity and electrical conductivity, we grouped the samples. Based on this grouping, we developed different flow path suppositions of how different groups possibly could be interconnected. Following this, we used higher contents of Al, Cu and rare earth elements, which were typical for some waters, as trace elements to verify whether or not our flow path suppositions seemed reasonable. This methodology ruled out the influence of some artificial surface waters on the inflows in the major inflow zone of the pit and relate inflows on the hanging wall to runoff from waste rock dumps and infiltrated waters from the tailings. As a result, costs were saved for planned water management by discarding likely ineffective measures. The following description sums up the example we presented. Figure 1 shows an image of the sampling sites with the major inflow area of the pit.

There was a strong belief that the clarification ponds and a surface ditch (samples represented by the red dots) were leaky and connected to the inflows (represented by samples marked with green dots). **Figure 2** shows that this relation seems very unlikely, as the surface waters have higher contents of Al, Cu and REE, while the inflows show lack of significant concentrations of these elements. Thus, an already planned and probably ineffective sealing of the ditch could be eliminated and costs were saved (Hagedorn et al 2016).

Further research and derived dewatering measures in Aitik

Based on the outcomes of our sample analysis, on site discussions took place with the local experts about the inflow characteristics and possible sources of the major inflows. These discussions lead to a new understanding of the inflow regime. Some of the inflowing waters showed a sulfidic, mouldy smell. Additionally it came up that the area on the surface used to be a bog area in pre-mining conditions and that the material on the waste rock dump on the surface is likely to produce such sulfidic runoffs. Based on these findings, a new conceptual model of the inflows was developed. We assumed that runoffs from the dump infiltrate to the first sedimentary layer, where they mix with the ground waters in this horizon, which are related to the old bog waters. Within the sedimentary layer, the waters infiltrate into an extensively fractured zone, which is related to the ore body. Within this zone, the waters sink down and enter the pit 200 meters below. To verify this supposition, it was decided to drill shallow wells in the area of the fractured zone. The wells were used for short pumping tests and water sampling for chemical analysis. Water levels were usually hit at depths about 80 meters below ground surface.

Pumping test results show that the closer the well is to the fractured zone, the well yield is higher. Historical reports and pumping tests on wells in this area support this outcome. Results of the chemical analysis are still pending, but it seems very likely that the sampled well waters will show similarities in elemental contents and behaviour. Longer pumping tests shall be executed in the near future, and longer term discharge from the wells may lead to visible reduction of the pore pressures at piezometers in the vicinity or even to visibly lower inflows. Based on the results, wells will be selected for continuous dewatering objectives. If the pumping trials are effective, our next aim for Aitik is to reduce the inflows in the hanging wall, which we assume to be related to the tailings and the runoffs from the waste rock dumps.

Adapting our approach for an underground mine

As our investigations lead to new insights in Aitik, BOLIDEN gave us the opportunity to adapt our approach for their underground mine Renström. Renström is located in the Boliden area in the Swedish province Västerbottens län. Renström started production in 1952 and produced 318 000 tons of ore in 2014. Main metals within the ore are zinc, copper, lead, silver and gold. With about 1400 m depth, Renström is the deepest mine in Sweden. Upwards mechanized cut and fill mining with hydraulic backfill is the main mining method applied in Renström. Within wider ore bodies, the technique of drift and fill with cement stabilised backfill is applied. To mine the sill pillars, vertical stoping with hydraulic backfill is applied. During the history of the mine backfill materials have included natural sand, tailings and waste rock. To visualize the conditions a little, **Figure 3** shows a sketch of the lower part of Renström between the level 500 and 1400 m below the ground. (BOLIDEN 2016)



Figure 1 Example for sample relation hypothesis. Red dots represent samples of possible sources and green dots represent samples from inflows, with local coordinates from Hagedorn et al. (2016)

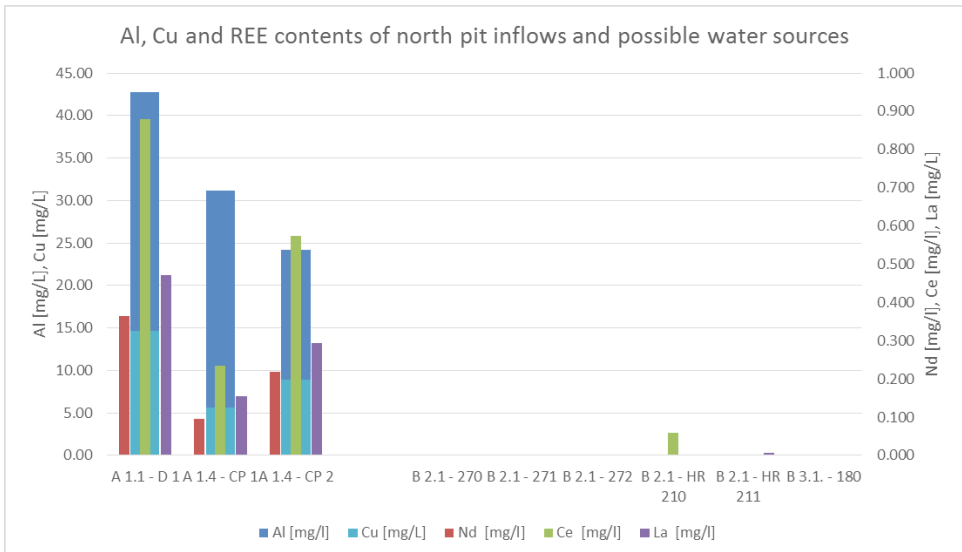


Figure 2 Al, Cu, Nd, Ce, and La contents of sampled sources and inflows, from Hagedorn et al. (2016)

Renström had problems with water inflows in the deeper part of the mine, where water flowed through the fractures of the sill pillars with pressures measured in drainage wells of about 5 bar. It is assumed that water from overlying, mined out areas leaks down through the sill pillars. Some fractured sill pillars have collapsed, which is a serious safety issue. Therefore, the mining had to be paused until the water pressure was reduced. As 20 % of the mine production comes from the sill pillar mining, the pausing has an impact on the production rate. To take suitable measures to avoid the water pressure above and within the sill pillars and to reduce the water inflows to the production area, it is necessary to identify the sources of the inflows. (Isaksson 2016)

As the possible flow regimes in underground mines are usually more complex and sources of inflows cannot be distinguished as sharply as in open pit mines, we had to adjust our sampling approach. We split the potential sources into surface waters, underground waters and other sources. Samples we assumed to be inflows were divided into samples from inflows from backfill drainage and from crosscuts. Of the total 29 samples, we took 6 surface water samples from lakes, a river and water treatment ponds, and the remaining samples were collected in different parts of the mine.

The grouping of samples based on the on-site measured field parameters pH and Eh value, alkalinity, acidity and electrical conductivity resulted in three major groups: natural surface waters, samples with similarities to natural surface waters, stronger mineralized samples with moderate alkalinity and low acidity and other samples. As most of the laboratory sample results showed similar characteristics and these samples could only be divided into two major groups, the development of flow path suppositions also became more challenging. For the flow path supposition development it is furthermore necessary to have a good conceptual understanding of the mine site. Old underground mines like Renström are usually quite complex, achieving a conceptual understanding for such a mine makes it even more ambitious to develop this flow path suppositions.

Unfortunately for our trace analysis, almost all of the waters showed a neutral to slightly alkaline pH values. As a consequence, the waters did not contain any typical Al, Cu, Nd, Ce and La contents, which we used as trace elements for certain Aitik mine waters. Because of these limitations and the big similarities between the sampled waters, the whole interpretation process needed to be based on a wider spectre of parameters and made the analysis more complex.

Results of Additional Water Analysis

Complete analysis with a wide range of elements, a TC/TN-analysis and an analysis of the stable isotopes ($^2\text{H}/^{18}\text{O}$) have been carried out for all samples, and the results were used to derive new insights of the flow regime. As already mentioned, the sampled waters showed many similarities, which unfortunately continued in the additional analyses for the Renström samples.

Nevertheless, the measured parameters gave some useful hints and information. For instance, some samples indicate relations to surface waters, based on their low mineralization

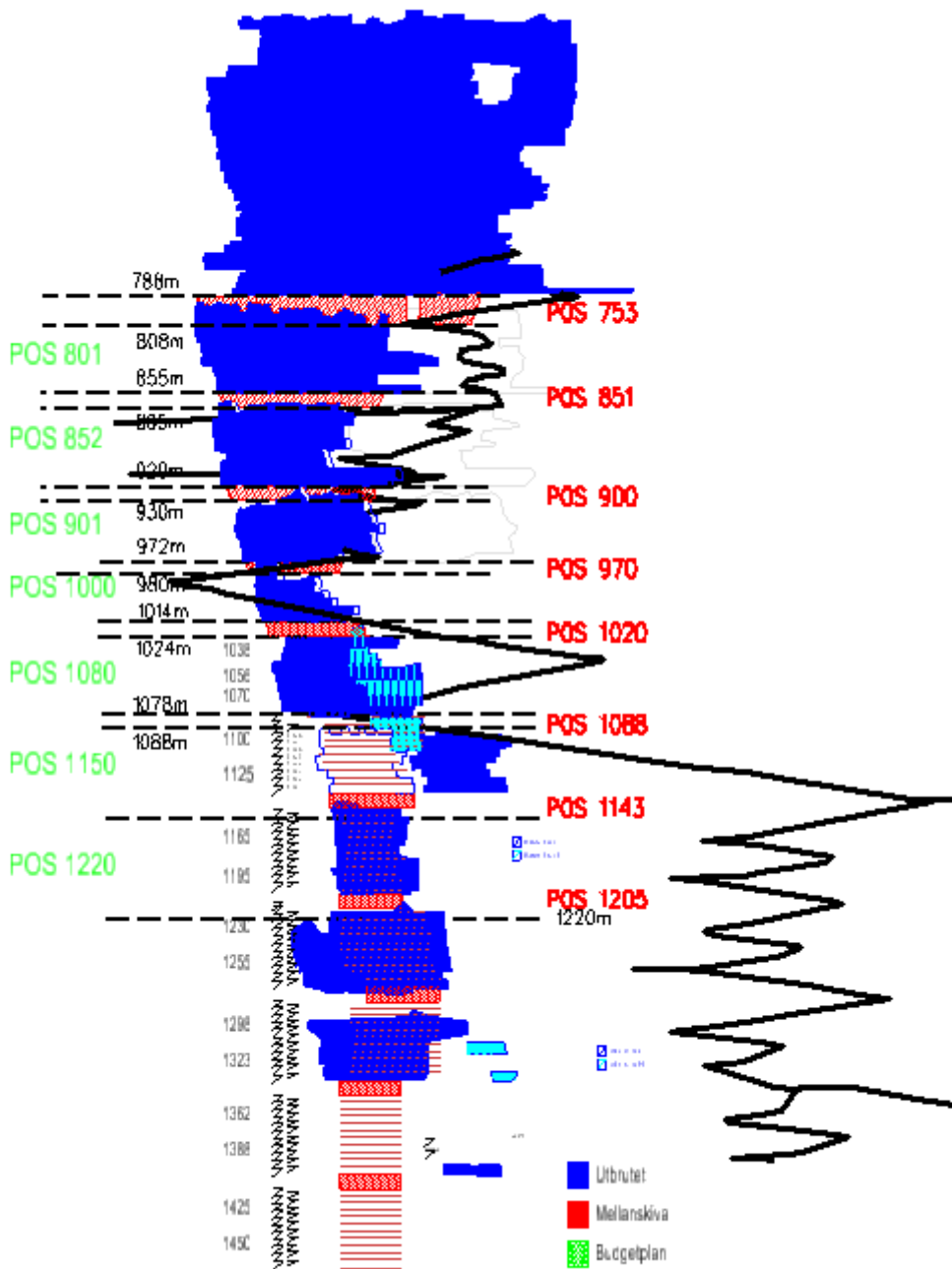


Figure 3 Sketch of the lower part of Renström, blue areas are mined ore, red shaded areas are remaining sill pillars, black line shows the main ramp, from Isaksson (2016)

and their isotope signature. Especially, quite high inflows from exploration wells for a future ore body showed very similar conditions to what we suspect to be near surface ground waters. Unfortunately it is unclear at this moment whether the waters are generated within the future ore body or within the section between well opening and ore body. We suggested further research on the origin of these waters resulting in a significant inflow and the relation to shallow groundwater may have a major influence on the efficiency of the mining of this ore body.

Some samples in the upper part of the Renström mine also show some indications for a relation to shallow groundwater, but they are not as distinct as for the waters from the exploration wells. They may also be connected to the basins of the service waters, which are used for drilling and other mine operations. Further isotopic measurements regarding the local seasonal variations of the isotopic composition in the area may lead to more reliable information.

For the deeper inflows, it gets a little trickier, as the waters are mineralized but very similar. What we can say so far is that the waters in the sumps and pump stations match with the inflowing waters. It is very likely that they are similar, and the waters in the sumps and pump stations represent the inflows as these have to be pumped out of the mine. But we cannot exclude that the basins from sumps and pump stations are connected to the inflows through fractures, as there are no in and output measurements for the basins. Of course, this seems unlikely, but so far we cannot rule it out. If the inflows are not interconnected with the basins they may originate from the waters which were used for the hydraulic backfill or deep groundwater, which enters the backfilled areas through pores or fractures. To derive further information about the origin of the waters in the backfilled areas, further analyses of parameters are necessary. For example, a sample from a deep well could provide information about the characteristics of the deep ground waters. Due to the long history of the mine, there is limited information about where which materials, binders and waters have been applied for the backfill. As these materials influence the water conditions, core logs from the backfilled areas could give further hints about the inflow origins. Furthermore, in and output data of the hydraulic backfill areas and their drainage could provide valuable information about the origin of the waters.

Furthermore, some Renström samples showed surprisingly elevated total inorganic carbon and total nitrogen. We are still looking for the sources. One idea is that it might be connected to the applied explosives.

Conclusions

What we can derive from the results in Aitik is that our approach to trace mine inflows to their sources by comparing their field parameters, elemental contents, isotopic signatures and TC/TN values worked well so far. Nevertheless, the final assessment needs to be based on the outcome of the derived dewatering measures, the results of first trials for the major inflow zone will be available in the near future. Further steps will then be to target other inflow zones.

What we learned from Renström is that our approach is limited, if the sources of waters and inflows are very similar to each other. The best starting situation requires clearly different waters within the investigation area. For example, acidic waters which contain typical REE contents. Nevertheless, we could identify hints for the origins of certain waters, too, but they are not as clear as in Aitik. Therefore, it is necessary to carry out further investigations. In this way, interpretation goes on and is not finalized yet. Further research could lead to a better understanding of the flow regime in Renström.

Another research goal is to increase the understanding of the local hydrogeology and actual flow paths in Aitik and Renström in order to provide further information for decision making for the implementation of further dewatering measures, with the higher aim of reducing the overall water inflows and increase the production efficiency and safety by establishing dryer mining conditions.

References

BOLIDEN (2016) Renström Visitor Presentation. Internal Document

Hagedorn D, Hoth N, Mwagalanyi H (2016) Dewatering challenges in an large scale production hard rock open pit in northern Sweden. Mining Meets Water – Conflicts and Solutions, IMWA 2016, (S. 503). Leipzig.

Isaksson M (2016) Renström water problem description and personal conversations

Tracer Test in Mine Water of the Abandoned Edendale Lead Mine, South Africa

Mokone, M. P.¹, Wolkersdorfer, C.^{1,2}

¹*Tshwane University of Technology (TUT), Private Bag X680, Pretoria 0001, South Africa
MokoneMP@tut.ac.za*

²*Lappeenranta University of Technology, Laboratory of Green Chemistry, Sammonkatu 12, 50130
Mikkeli, Finland*

Abstract Tracer tests are deployed to determine the hydraulic connectivity of flow paths or connections from surface and underground mines. This paper describes a mine water tracer test in a flooded, South African underground lead mine. Sodium chloride was injected as a tracer into one shaft and the electrical conductivity was measured continuously. The EC curve showed multiple peaks and tracer recovery was 17 %. The mine aquifer appears to be fractured and there is poor hydraulic connectivity. It appears that the main hydraulic processes within the flooded mine is subject to advection flow. There was no contamination in the receiving water course as the metal concentrations are within regulated standards; the likelihood of water quality degradation is therefore moderate.

Key words abandoned mine, tracer test, fractured aquifer, mass recovery, Edendale, South Africa

Introduction

In many parts of the world, mining is known as one of the main cause of environmental concerns. Economic and environmental reasons have caused closure of many mines without rehabilitation and has led to alteration of the hydrogeological environment (Banks et al. 1997; Razowska 2001). In South Africa, legislation and guidelines have been adopted to address mine closure and post-mining water management even so abandoned mines remain a liability (Kgari et al. 2016). Silver mining in South Africa started around 1880 when the “Pretoria Silver Belt” was prospected in Pretoria, Gauteng Province. Consequently, the development of mineral mining grew country wide and as a result, many of the smaller mines were abandoned (Kgari et al. 2016; Reeks 2012). When mines are abandoned, the rebound of the water table can lead to contaminated groundwater to flow into underlying aquifers causing degradation to the quality of receiving surface water and groundwater, eventually making it unsuitable for further use (Cidu et al. 2007; Wolkersdorfer 2005; Younger et al. 2005). Environmental problems associated with abandoned mines are controlled by the type of mining employed (underground or surface mining). Approximation of mine water quality draining from surface mines is well developed but such is more or less absent in abandoned flooded underground mines. The flooding of underground mines might cause the supporting structures to collapse and subside causing inaccessibility to the shafts or adits of the mine. This further increases the permeability and porosity and alters the groundwater flow as the underlying aquifer becomes fractured (Booth et al. 1998; Mhlongo and Amponsah-Dacosta 2016; Younger 2000). Hydrodynamics governing the movement and transport of mine water in flooded underground mines is not commonly acknowledged in South Africa. The general focus of most investigations in South Africa has been on contamination treatment and inhibition of water discharge (Kgari et al. 2016). However, planning remediation strategies and the calculation of reactive transport within

the mine depend on the understanding of the volume of flooded mines and hydraulic properties (Wolkersdorfer 2005).

Tracer tests have been employed to trace the hydrodynamic conditions of flooded underground mines and interconnections of groundwater flow. The publications of tracer tests results in abandoned underground mines are not commonly known. Therefore, there is less experience in mine water tracing. Tracers are used depending on site conditions and aims (Wolkersdorfer et al. 2002). Although, in the past, tracer techniques focused on groundwater flow in karstic aquifers, there has been development in previous decades for the use of tracers as a hydrologic investigating tool. Tracers are inferred to as any constituent which by design is introduced into the aquifer to determine flow paths, groundwater velocities, mass flow and contamination transport (Divine and McDonnell 2005). Understanding the hydraulic connection between mine workings, surface and ground water is needed for source determination of water and pollutants at the discharge point as so to support remediation measures (Kgari et al. 2016).

The main objective of the present study was to conduct a tracer test in the mine water of the abandoned Edendale Lead Mine (Tshwane East) with the aim of identifying potential mine water pollution and to characterize the mine water quality, to eventually understand the hydrodynamic processes around the mine. This is important as there are a primary and high school nearby and the mine is located adjacent to the Edendalespruit, where numerous farms and some private residential areas rely on borehole water.

Location and mining history

The abandoned Edendale Lead Mine is a former underground lead and silver mine located in Pretoria East, Silverton on farm Nooitgedagt 333 JR South Africa (Fig. 1). It is situated in the Silverton Formation of the Pretoria Group that forms part of the Transvaal Supergroup. This formation comprises of carbonate mudrocks which are interbedded with sandstones, chert and dolomite. Geologically the host rocks around shafts E12 and E13 comprises of quartzite of the Magaliesberg formation imbedded with limestone and shales (Eriksson et al. 2012). Detailed historic mine plans are not available, but Edendale mine No. 1 is on the north of the R513 and Edendale mine No. 2 is on south of the road. The remaining shafts were numbered by the Council of Geoscience and not according to the historic mine plans. Only three mine shafts remain: shaft 1 at mine 1 and shafts 12 and 13 at mine 2. For the purpose of this study the shafts are referred to as Edendale mineshaft 1, 12 and 13 (E01, E12, E13). Mining operation lasted from 1890 to 1974, producing 6333 t of ore: 4762 t of lead, 1127 t of silver and 105 t of antimony (Glass 2006). When mining began 120 years ago, galena, zinc, sphalerite, chalcopyrite, and cerussite were the main minerals mined. In 1904 mine 1 and mine 2 had shafts which were 41 and 61 m in depth respectively. During this period 11000 t of ore was mined of which 80 % was galena. Furthermore, a shaft in mine 2 was sunk to 212 m in 1905 and 1120 t of lead ore was produced (Reeks 2012). A new shaft was opened in 1921 and in a depth of 17 m connected to the adjacent shaft. This new shaft was sunk 36 m beneath the cerussite vein, which was 46 cm wide and produced first grade galena. Westward of the new shaft, a connecting shaft was also opened and had initially

54 m in depth and later was sunk to 214 m. Annually, the mined vein produced 40 t of ore (Reeks 2012). This increase in depth caused water inflows which required massive pumping allowing the mine to sell million litres of water to other mines monthly. The Edendale Point of Discharge (EPD) discharges water into the Edendalespruit as so a conduits to the Rood-eplaat catchment dam. Currently the measured water level is 1.9 m at E12 which is 6.49 m deep and 2 m at E13 which is 3.45 m deep (Fig. 2). Water volume in the two shaft was calculated using mineshaft breathe and width of 1 m and 1.5m respectively. At present the total volume estimated at E12 is 6.89 m³ and 0.99 m³ at E13 with a flow rate of 0.5 L/min at EPD.

Methods

Water samples were collected at the shafts using a dropper rope, at the point of discharge and upstream as well as downstream of the mining area in the Edendalespruit. Water samples were collected 3 times from various sample localities (Fig.1) in both wet and dry seasons from 2015-03-09 to 2016-10-29. On-site parameters (pH, redox, temperature, electrical conductivity and dissolved oxygen) were measured using Hach instruments at point of sampling. Bicarbonate alkalinity was determined on-site using a Hach digital titrator and mathematically from the difference in the ion balance. Major and minor anion concentrations were determined on non-acidified and acidified water samples by ICP-MS an a discrete analyser at Waterlab Pty (Ltd) as well as major and minor trace element concentrations which were analysed by ICP-MS and ICP-OES. 21 kg of food quality NaCl were dissolved into 75 L of tap water in the lab before the start of the tracer test and the solute was injected into shaft E12 on 2016-09-11. The concentration of sodium chloride was measured by van Essen Diver electrical conductivity probes which were placed at the discharge point and shaft E13. Monitoring measurements were conducted for a period of 4 months at 20 min intervals. Recovery rate was calculated using electrical conductivity measured at EPD equation (1-4) where, t: time; C: concentration; Q: flow; C_m: Mean concentration; Δsalt: difference salt mass; : total mass, F: Factor (0.5295); RR: Recovery Rate

$$1. \quad C = EC \times F$$

$$2. \quad \Delta salt = C_m \times t \times Q$$

$$3. \quad \sum mass = \frac{\Delta salt}{1000}$$

$$4. \quad RR = \frac{\sum mass}{Injected\ mass} \%$$

Results and Discussion

Mine Water

The mine water discharging from the mine and in the mine shafts shows a circumneutral pH of 6.1–7.4, with a redox potential between 90 and 470 mV and oxygen saturation below

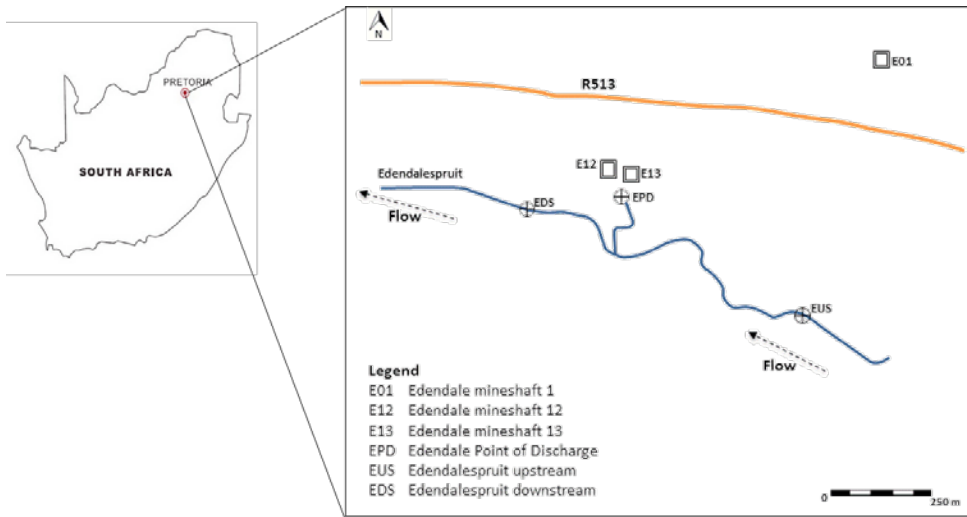


Figure 1 Location of the abandoned Edendale Lead Mine

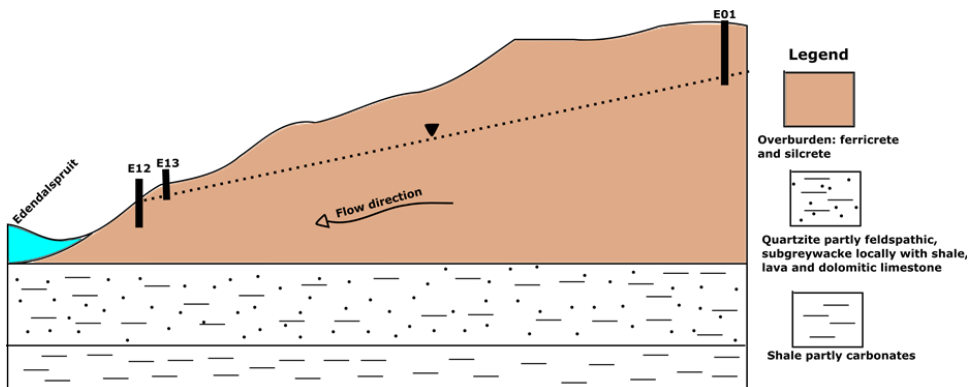


Figure 2 Conceptual model of hydrogeology of the abandoned Edendale Lead Mine

60%, with substantially lower values in the shafts and the point of discharge (Tab. 1). These low oxygen concentrations are a result of bacterial activity and plants in the Edendalespruit stream which consume oxygen. Pb, Ag and Sb were below the detection limits. Moderate silicon concentrations were detected at all sites but slightly higher at shaft E12. Na was found to be slightly higher downstream the mine site, possibly as a result of chemicals formerly used in the ore processing plant. An indication for that could be the higher electrical conductivity downstream this location. SO_4^{2-} -concentration is 239 mg/L downstream and 136 mg/L upstream, with low concentrations within the shafts and the point of discharge. Ca and Mg were slightly high at the discharge point (68 mg/L and 41 mg/L, respectively) but according to EPA (2009), there is no health effect at concentrations below 100 mg/L. Mn concentrations were 1.3 mg/L at EPD and 2.8 mg/L at E13, which is above the secondary contamination limit of 0.05 mg/L primary drinking water standard (EPA 2009). In a Piper

diagram, it can be seen that the mine water of the Edendale Lead Mine is alkaline (Fig. 1). Mine water characterized at EPD are in the HCO_3^- type while E12, E13, EUS and EDS are dominated by the Mg–Ca type, so as in E13 and EUS, the SO_4^{2-} type is introduced and Cl type is also introduced at E13. The samples show relatively more alkaline earth metals than alkali metals. The main rock type found in the study area is limestone and dolomite, which explains the concentrations of Mg, Ca and bicarbonate in most of the samples.

Table 1 On-site parameters and mine water composition (mg/L) from the abandoned Edendale Lead Mine. Pb, As, Ag and Sb were below the detection limit; n: chemical analysis / on-site parameter; \pm is standard deviation of sample population. Average of the pH calculated using the $\{H^+\}$, b.d: below detection limit.

	EUS	E12	E13	EPD	EDS
pH	6.9 \pm 0.4	6.7 \pm 0.1	6.7 \pm 0.2	6.7 \pm 0.4	6.6 \pm 0.7
Redox, mV	328 \pm 123	319 \pm 42	306 \pm 86	224 \pm 65	227 \pm 65
EC, $\mu\text{S}/\text{cm}$	437 \pm 134	603 \pm 15	466 \pm 118	615 \pm 18	670 \pm 84
Temp, $^{\circ}\text{C}$	21.5 \pm 2.5	22.9 \pm 1.3	23.8 \pm 2.0	21.8 \pm 2.1	22.0 \pm 1.5
HCO_3^-	371 \pm 260	406 \pm 16	336 \pm 179	421 \pm 13	399 \pm 165
SO_4^{2-}	55 \pm 70	0.6 \pm 1.2	27 \pm 24	5 \pm 4	102 \pm 121
Cl	5 \pm 1	5 \pm 1	4 \pm 2	5 \pm 1	4 \pm 2
B	0.009 \pm 0.007	0.010 \pm 0.007	0.012 \pm 0.008	0.019 \pm 0.010	0.011 \pm 0.009
Ba	0.050 \pm 0.350	0.131 \pm 0.009	0.110 \pm 0.012	0.086 \pm 0.061	0.079 \pm 0.020
Ca	39 \pm 19	59 \pm 1	42 \pm 16	63 \pm 4	61 \pm 5
Fe	0.028 \pm 2.025	0.129 \pm 0.164	0.029 \pm 0.04	0.058 \pm 0.041	0.027 \pm 0.04
K	3.5 \pm 0.7	3.7 \pm 0.4	3 \pm 1	4.5 \pm 0.6	1.5 \pm 1.7
Mg	32 \pm 16	37 \pm 1	26 \pm 9	40 \pm 2	52 \pm 2
Mn	0.12 \pm 0.15	0.73 \pm 0.04	1.74 \pm 0.80	1.25 \pm 0.36	0.11 \pm 0.11
Na	7 \pm 4	9 \pm 0.4	6 \pm 3	10 \pm 0.6	17 \pm 2
P	0.01 \pm 0.01	0.04 \pm 0.04	b.d.	0.01 \pm 0.1	0.02 \pm 0.01
Si	12 \pm 6	19 \pm 0.2	13 \pm 3	17 \pm 0.1	17 \pm 2
Sr	0.127 \pm 0.070	0.174 \pm 0.270	0.127 \pm 0.030	0.179 \pm 0.020	0.193 \pm 0.030
Ti	0.078 \pm 0.030	0.119 \pm 0.011	0.077 \pm 0.020	0.119 \pm 0.014	0.120 \pm 0.023
Zn	0.09 \pm 0.08	0.06 \pm 0.04	0.39 \pm 0.20	0.02 \pm 0.02	0.23 \pm 0.27
n	3 / 3	3 / 9	3 / 9	3 / 10	3 / 3

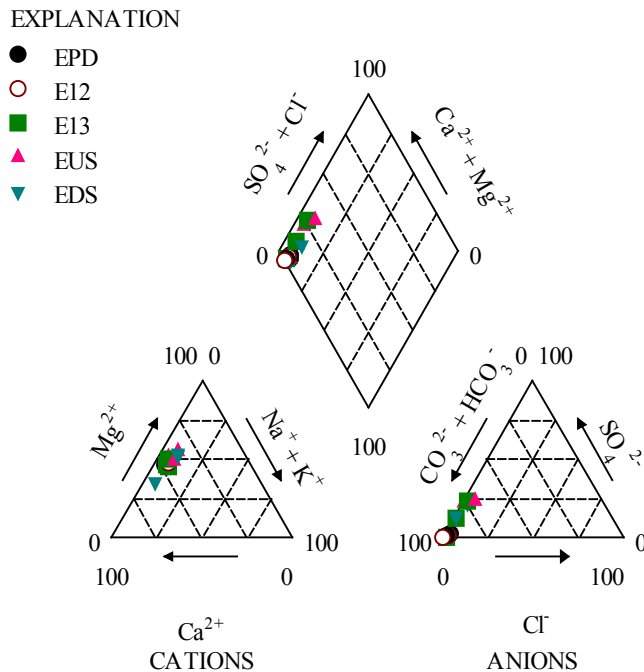


Figure 3: Piper diagram for samples collected at the abandoned Edendale Lead Mine; $n = 15$, averages of three sampling campaigns.

Tracer Test

During the tracer test, the electrical conductivity increased in the wet months (Fig. 4), which can clearly be attributed to the sodium chloride tracer (Wolkersdorfer et al. 2002) being transported by the rain water infiltrating into the subsurface. Only 17.1% of the injected tracer was recovered (Fig. 5). Considering the geological and hydrodynamic setting, the low recovery rate might be caused by a poor hydraulic connectivity between the point of injection and point of discharge or a density driven settlement of the concentrated tracer. The first EC peak occurred in October 2015, second, third and fourth peaks were detected in November, December and January respectively. When there are multiple peaks in the EC measurement it shows that the tracer might be transported via various flow paths so as the dispersion and velocity are not the same (Leibundgut et al. 2011) or the rain events cause the tracer to be flushed out of the mine. No peaks were observed in E13 (Fig. 4). Therefore, it can be assumed that the tracer does not flow into shaft E13. This result shows that the tracer is transported from shaft E12 directly to the point of discharge but not to the adjacent shaft E13.

Conclusions

As has been shown, the mine water at the abandoned Edendale lead mine has a circum-neutral pH. Due to the low concentrations of potentially toxic elements, no negative effects on the population's health will be expected. In the Piper diagram, it can be seen that the mine

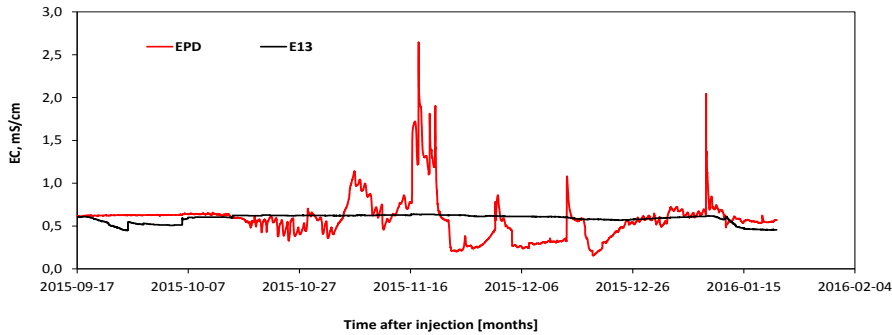


Figure 4 EC measurement in shaft E13 and the discharge point of the abandoned Edendale Lead Mine during the tracer test

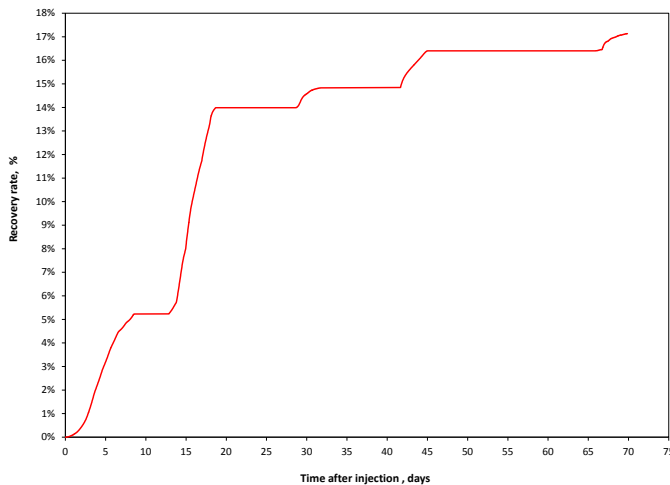


Figure 5 Recovery rate of the Edendale tracer test.

water is of the HCO_3 -Ca-Mg type. The tracer injected into shaft E12 was only detected at EPD which is an indicator that there is no transport to shaft E13. Furthermore, the tracer test proved that the flow is advection based and there is no active hydraulic connection between the two shafts. Because 17% of the injected NaCl was recovered after 4 months of the tracer test, either an obstruction because of an adit collapse, a denser mine water-brine pocket is still in the shaft or there is diffuse flow into the adjacent mine workings or the host rock. Both the EC measurements and the low tracer mass recovery are indicative for this assumption. Overall, the results obtained so far show that there will be no deteriorating contamination of the receiving water courses.

Acknowledgments

We thank Tshwane University of Technology and the NRF for funding this work, which is the result of an MTech research supported by the SARChI Chair on Mine Water Management. In addition, the authors thank the owners of the Edendale Lead Mine for granting access to the site. CW thanks Henk Coetzee for introducing him to this site.

References

- Banks D, Younger PL, Arnesen R, Iversen ER, Banks SB (1997) Mine-water chemistry: the good, the bad and the ugly. *Environ Geol* 32(3):157-174
- Booth C, Spande E, Pattee C, Miller J, Bertsch L (1998) Positive and negative impacts of longwall mine subsidence on a sandstone aquifer. *Environ Geol* 34(2-3):223-233
- Cidu R, Biddau R, Nieddu G (2007) Rebound at Pb-Zn Mines Hosted in Carbonate Aquifers: Influence on the Chemistry of Ground Water. *Mine Water Environ* 26(2):88-101. doi:10.1007/s10230-007-0155-5
- Divine CD, McDonnell JJ (2005) The future of applied tracers in hydrogeology. *Hydrogeol J* 13:255-258
- EPA (2009) Ground Water and Drinking Water National Primary Drinking Water Regulation-Inorganic Chemicals.
- Eriksson PG, Bartman R, Catuneanu O, Mazumder R, Lenhardt N (2012) A case study of microbial mat-related features in coastal epeiric sandstones from the Paleoproterozoic Pretoria Group (Transvaal Supergroup, Kaapvaal craton, South Africa); The effect of preservation (reflecting sequence stratigraphic models) on the relationship between mat features and inferred paleoenvironment. *Sedimentary Geology* 263:67-75
- Glass J (2006) The environmental impact of the abandoned Edendale lead mine near Tshwane, South Africa. Minor Dissertation, University of Johannesburg
- Kgari T, Van Wyk Y, Coetzee H, Dippenaar M (2016) Mine Water approach using Tracers in South African abandoned Coal Mines. IMWA 2016 – Mining Meets Water – Conflicts and Solutions, proceedings:410-416
- Leibundgut C, Maloszewski P, Külls C (2011) Tracers in hydrology. John Wiley & Sons
- Mhlongo SE, Amponsah-Dacosta F (2016) A review of problems and solutions of abandoned mines in South Africa. *Int J Min Reclam Env* 30(4):279-294
- Razowska L (2001) Changes of groundwater chemistry caused by flooding of iron mines (Czestochowa, Southern Poland). *J Hydrol* 244:17-32
- Reeks GW (2012) A history of silver mining in the greater Pretoria region, 1885-1999.
- Wolkersdorfer C (2005) Mine water tracer tests as a basis for remediation strategies. *Chem Erde Geochem* 65:64-74
- Wolkersdorfer C, Feldtner N, Trebušak I (2002) Mine water tracing—a tool for assessing flow paths in flooded underground mines. *Mine Water Environ* 21(1):7-14
- Younger PL (2000) Nature and practical implications of heterogeneities in the geochemistry of zinc-rich, alkaline mine waters in an underground F–Pb mine in the UK. *Appl Geochem* 15(9):1383-1397. doi:10.1016/S0883-2927(00)00010-X
- Younger PL, Coulton RH, Froggatt EC (2005) The contribution of science to risk-based decision-making: lessons from the development of full-scale treatment measures for acidic mine waters at Wheal Jane, UK. *Sci Total Environ* 338(1–2):137-154. doi:10.1016/j.scitotenv.2004.09.014

Storage of arsenic-rich gold mine tailings as future resources

Dave Craw, Gemma Kerr, Kirstine Malloch, Christine McLachlan

Geology Department, University of Otago, Dunedin 9010, New Zealand

Abstract Arsenic-bearing gold mine tailings in New Zealand have been stored at mine sites for up to 100 years. Primary arsenopyrite remains largely unaffected by oxidation in water-saturated tailings on a time scale of years to decades. Tailings that have been roasted to release encapsulated gold contain ferric iron oxide and ferric arsenate minerals that are stable on a time scale of decades. Waters leaving these tailings storage sites have low dissolved As (<0.1 mg/L). Arsenolite, As_2O_3 , is a highly soluble intermediate oxidation product of arsenopyrite during roasting and under surficial conditions, and can contribute to localised elevated dissolved As concentrations. However, under most conditions, dissolved As is adsorbed by iron oxyhydroxides. Long-term storage of As-bearing gold mine tailings can be managed to limit As discharges, and is desirable to retain potential resources that can be more efficiently reprocessed in the future.

Key words arsenic, arsenopyrite, hematite, scorodite, tailings, decant water, circumneutral

Introduction

Gold extraction from ore is never 100% efficient, so some Au remains in most mine wastes. Most residual gold typically remains in tailings that have been excavated, crushed, ground, and commonly concentrated during processing. These tailings represent potential resources from which the residual gold may be extracted at some time in the future when better processing techniques have been developed. In the meantime, the tailings need to be stored in an environmentally benign manner so that any discharging waters have low contents of potentially toxic dissolved load. Dissolved arsenic is the most significant potential discharge issue around such tailings storage sites.

Historic and modern mine sites in New Zealand provide insights into the key mineralogical and geochemical features of orogenic gold deposits in mine tailings from several ore processing techniques. Arsenopyrite (FeAsS) is the principal As-bearing mineral, which contains significant encapsulated gold. Many mines have created sulphide concentrates during gold extraction, and tailings are rich in arsenopyrite. Some mines have oxidised sulphides during processing, and residues contain As-rich oxide minerals including arsenolite ($\text{As}^{\text{I}}_2\text{O}_3$), and a range of oxidised Fe^{III} -bearing minerals with high arsenate contents including scorodite ($\text{FeAs}^{\text{V}}\text{O}_4 \cdot 2\text{H}_2\text{O}$).

Methods

Data for this study were collected at the active Macraes gold mine in southern New Zealand, where routine water quality monitoring is carried out for processing and environmental purposes. Mineralogical studies were carried out on sulphide concentrate tailings to augment the water monitoring programme. Mineralogical characteristics of historic mine tailings were determined by scanning electron microscopy (SEM) with energy dispersive

analytical capability. Associated water runoff was analysed by Hill-Laboratories, Hamilton, New Zealand. Details of methods are contained in the appended references.

Macraes gold mine

The Macraes gold mine is a world-class orogenic deposit that has been in operation since 1990 (MacKenzie and Craw 2016). Gold is encapsulated in pyrite and arsenopyrite, and processing involves production of a sulphide concentrate via flotation of crushed and ground ore, and gold is extracted by carbon-in-pulp cyanidation. When the mine first opened, the sulphide concentrate was reground to 15 μm and fed directly to the cyanide system, after which the residues were accumulated in a dedicated concentrate tailings impoundment (Fig. 1a,b). However, after 1993 the sulphide-rich residue was remixed with silicate tailings and discharged into a nearby larger impoundment, leaving the concentrate impoundment unused from that time. Low gold recoveries from some ore types caused the introduction in 1999 of a pressure oxidation autoclave to decompose the sulphides in the concentrate at 225°C before passing the oxidised material to cyanidation. The success of this change in process prompted reprocessing of the sulphides stored in the dedicated concentrate tailings impoundment (Fig. 1a,b).

Monitoring of the full 13-year life of the As-rich concentrate tailings impoundment at the Macraes mine provides an example of the geochemical and mineralogical changes that occurred in arsenopyrite-rich tailings during storage. Low permeability of the tailings ensured that most tailings remained water-saturated and arsenopyrite was essentially unaltered (Fig. 1b).

Tailings waters accumulated on the surface of the impoundment in a decant pond (Fig. 1a). Dissolved As concentrations in these decant pond were high and variable over time as processing activities occasionally provided new water inputs, and were commonly tens to hundreds of mg/L (Fig. 2a). The pH was initially high (Fig. 2b) because the waters were derived directly from the cyanidation plant that operates at pH 10-5-11. However, the pH dropped over time (Fig. 2b) as the impoundment was mostly inactive, and waters interacted with rock calcite in the tailings. Tailings waters percolated through the tailings and the retaining dam (constructed of waste rock), and were collected at a sump at the toe of the dam (Fig. 1a). These waters remained below 1 mg/L dissolved As, and the pH was consistently circumneutral, between 6 and 7 (Fig. 2c).

Only minor oxidation of sulphides occurred in the upper metre of the tailings during the 13 years of storage. This caused localised acidification on the centimetre scale (down to pH 3-4), and minor formation of arsenate mineral encrustations (Craw et al. 2002). The resultant acid reacted with abundant calcite in the tailings, resulting in moderate to high levels of dissolved sulphate and bicarbonate in the decant pond (Fig. 2d). The tailings were excavated (Fig. 3) and successfully and economically reprocessed for residual gold when the pressure-oxidation system was added to the processing plant.

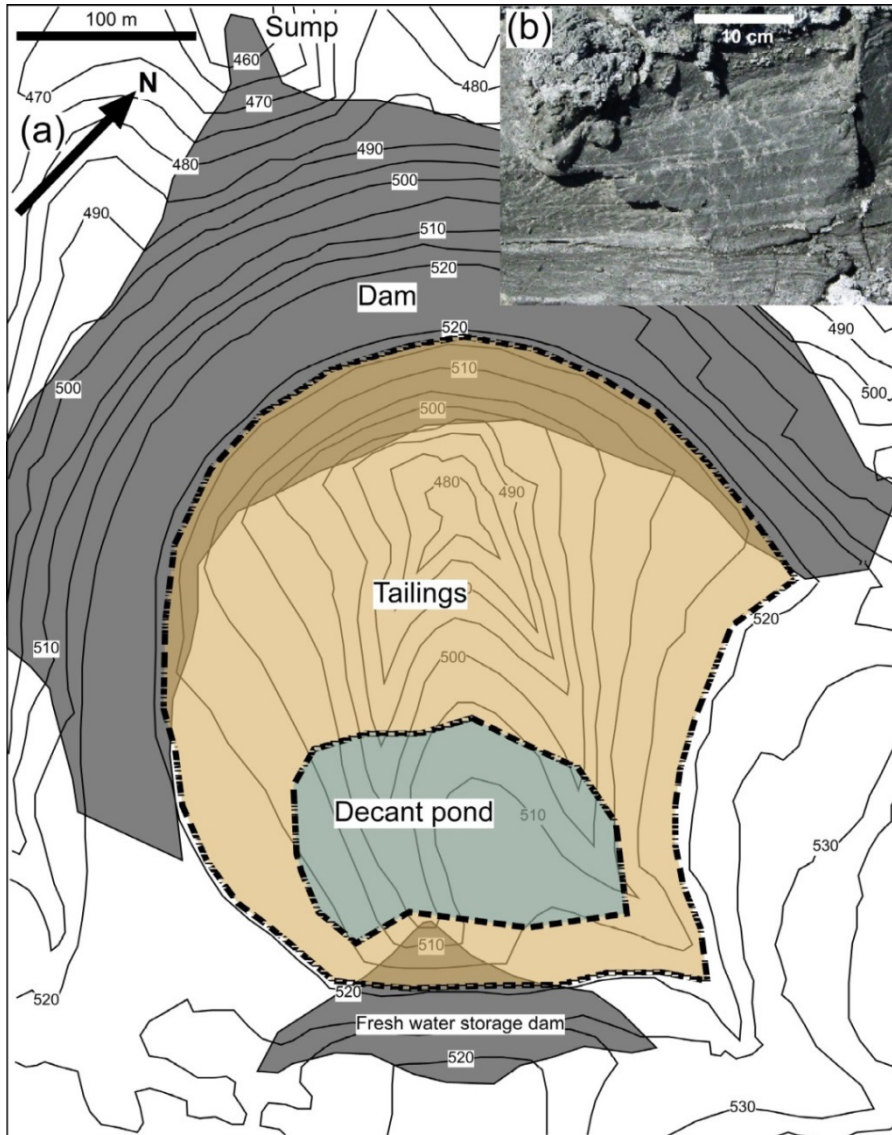


Figure 1 (a). Map of the concentrate tailings impoundment at Macraes mine, with contours on basement and dams to show the volume of tailings. (b) Photograph of tailings after storage for 10 years, observed during excavation for reprocessing. Grey colour and preservation of initial depositional bedding confirms the lack of oxidation.

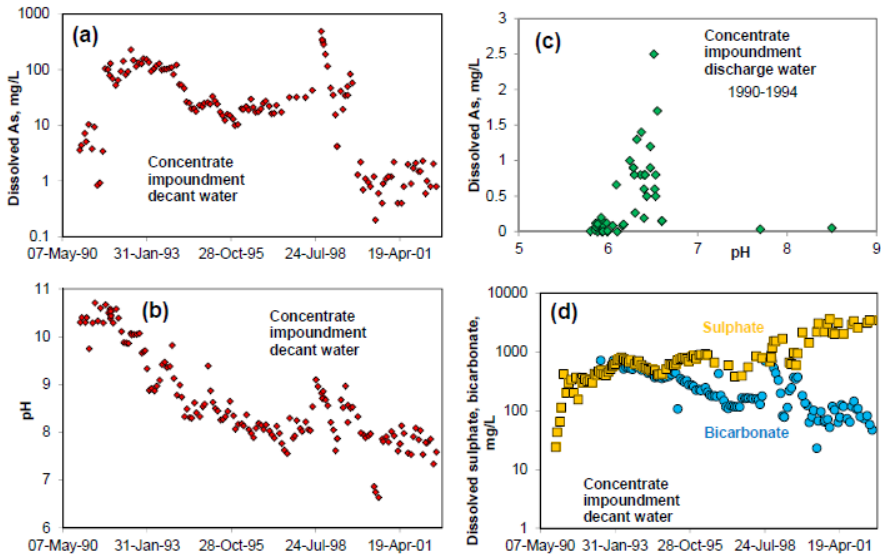


Figure 2 Geochemistry of waters in the Macraes concentrate tailings impoundment. (a) Time series for dissolved As in the decant pond. (b) Time series for pH in the decant pond. (c) Dissolved As and pH in discharge waters collected at the sump at dam toe. (d) Time series for dissolved sulphate and alkalinity in decant pond waters.

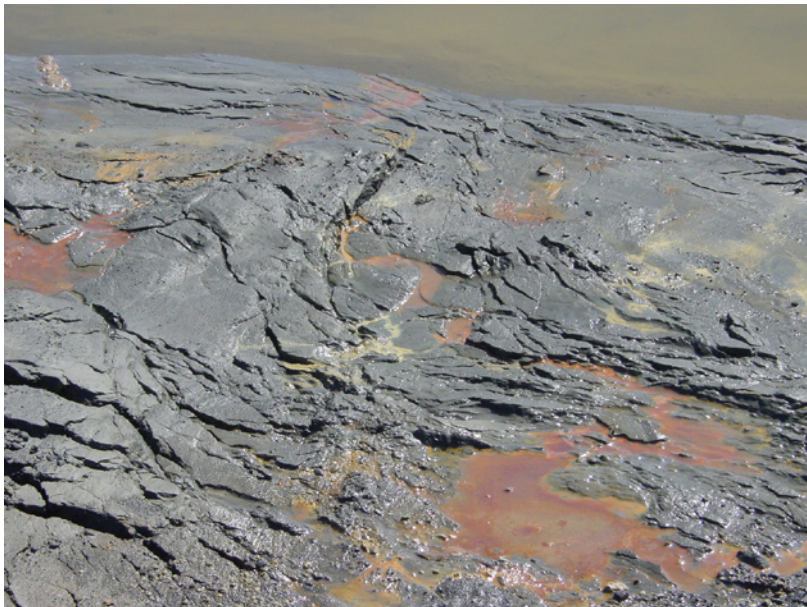
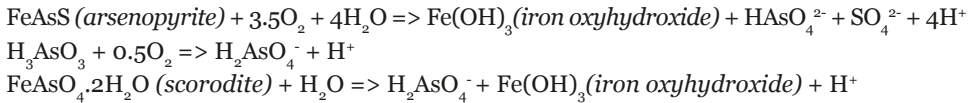


Figure 3 Photograph (view is 2 metres across) of Macraes mine concentrate tailings during reprocessing. Localised oxidation and acidification of tailings waters (to pH 4-5) occurred, with associated neutralisation by rock calcite in tailings to yield precipitates of gypsum (white) and iron oxyhydroxide (brown). Some jarosite formation (yellow) occurred as well.

Oxidation mineralogy

Oxidation of iron in pyrite and arsenopyrite in the surficial environment form iron oxyhydroxide under most conditions (Fig. 4a). Arsenic oxidation initially yields dissolved H_3AsO_3 , and this can precipitate arsenolite under evaporative conditions (Fig. 4a). Further oxidation produces dissolved H_2AsO_4^- and/or HAsO_4^{2-} , which can precipitate as amorphous or crystalline scorodite with iron oxyhydroxide, or jarosite under acid oxidised conditions (Fig. 4a). Oxidation and dissolution of arsenic during these processes can cause some acidification of associated waters at mine sites (e.g., Haffert and Craw 2008):



During the reprocessing activity at Macraes, minor oxidation and localised acidification of tailings waters occurred, but this was almost immediately neutralised by calcite, with precipitation of iron oxyhydroxides (Fig. 3). The iron oxyhydroxide precipitates formed from the Macraes mine tailings waters, especially in the vicinity of discharge waters in and near collection sumps, have high surface area, and this readily adsorbs abundant dissolved As (Roddick-Lanzilotta et al. 2002). This adsorption is at least partially responsible for the lowered dissolved As in waters that emanated from the toe of the concentrate tailings dam (Fig. 1a, 2c).

Oxidation of the sulphides at elevated temperatures involves similar mineralogy and reactions, at accelerated rates (Fig. 4b). The principal iron minerals produced in this process are hematite or amorphous iron oxyhydroxide. Arsenolite is an intermediate oxidation product of arsenate, and the ultimate product is iron arsenate (variably hydrated at high temperatures). Jarosite is also a common product of this oxidation process if the system becomes acidified (Fig. 4b), where potassium is typically derived from muscovite in the ore feed. The pressure oxidation process at the modern Macraes mine yields an acidified product consisting mainly of hematite, As-poor jarosite and iron arsenate, with a range of minor compounds (Craw 2006; Kerr et al. 2015).

Historic mine tailings

The tailings from the pressure oxidation system at Macraes mine are recombined and severely diluted with the silicate rich flotation tailings, so observations on their evolution over time are more difficult than for the older concentrate tailings described above. In order to examine the long-term stability of this type of material, we have focussed on historic tailings at sites in southern New Zealand in which sulphide concentrates were made and roasted, and the resultant tailings were left abandoned for up to 100 years (McLachlan et al. 2016; Malloch et al. 2017). These tailings still contain minor amounts of gold, but the dispersed nature of their current sites and the small volumes involved mean that they are unlikely to be economic for gold extraction in the foreseeable future. However, they provide a useful window into mineralogical and geochemical processes that have occurred on a time scale of decades.

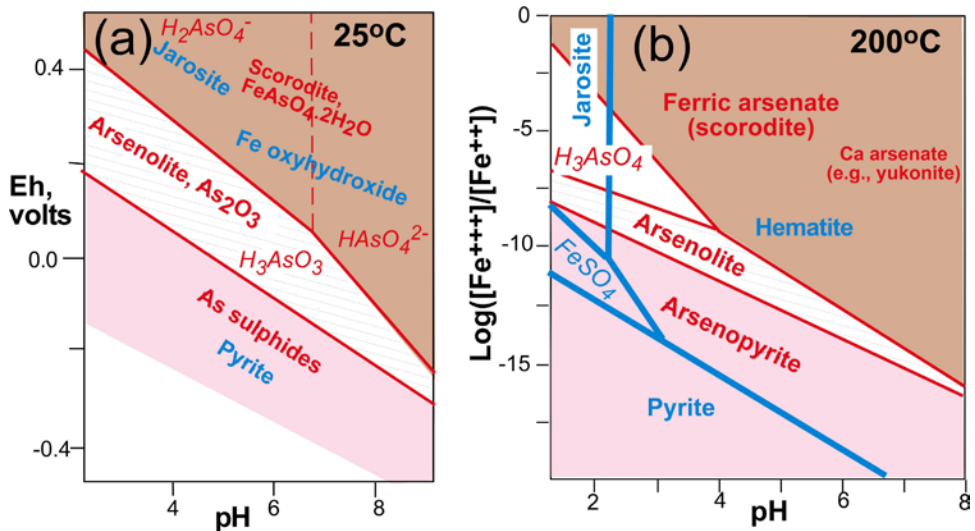


Figure 4 Mineral stability diagrams for oxidation of pyrite and arsenopyrite (summarised from Craw 2006; Haffert and Craw 2008). (a) Surficial environment. (b) Roasting of sulphide concentrate.

More primitive oxidation processes than pressure oxidation were used at these sites, dominated by Edwards roasters. Waters within these tailings typically have low to moderate dissolved As at circumneutral pH (Fig. 5a). Some scorodite and minor yukonite (Ca-Fe³⁺ arsenate; Fig. 5b) were formed in the roaster and discharged to tailings. However, ferric iron compounds such as hematite (±maghemite) were the principal products of the roasting process at the historic sites, and these formed distinctly red tailings deposits. The iron minerals are largely pseudomorphous after the original sulphide grains, and are variably porous as a result of expulsion of sulphur from their structures. The iron compounds contain variable amounts of arsenic, either encapsulated or as solid solution, up to 5 wt% (Fig. 5c). Despite the long periods of subsequent storage, these As-bearing iron compounds are relatively inert in the environment and have provided effective long-term As sequestration. Although dissolved As can be as high as 1 mg/L in tailings waters, waters leaving these sites are more dilute, with dissolved As <0.01 mg/L (Fig. 5a). Laboratory leaching experiments on this material over up to 6 months show that only low levels of dissolved As (~0.1 mg/L) can be extracted from the tailings (Fig. 5a).

Arsenolite was an intermediate oxidation product during the historic roasting process, and this was saved as a separate byproduct at times (Haffert and Craw 2008). Arsenolite locally formed a minor component of the hematite-rich tailings as well. Arsenolite is highly soluble and is the most environmentally undesirable residual mineral, resulting from locally extremely elevated levels (~100 mg/L) of dissolved As (Fig. 5a).

Some residues of unroasted sulphide concentrates occur at the studied historic mine sites. These sulphides have been largely oxidised to iron oxyhydroxides and scorodite (Druzicka

and Craw 2015; Malloch et al. 2017), but some relict sulphide grains have been preserved (Fig. 5d). These sulphides are inevitably armoured and encapsulated in the secondary mineral products, which limits their rates of further decomposition. Further, the abundant iron oxyhydroxide material present in these tailings has adsorbed at least some of the As mobilised from the sulphides. Consequently, the waters leaving these sites have low dissolved As.

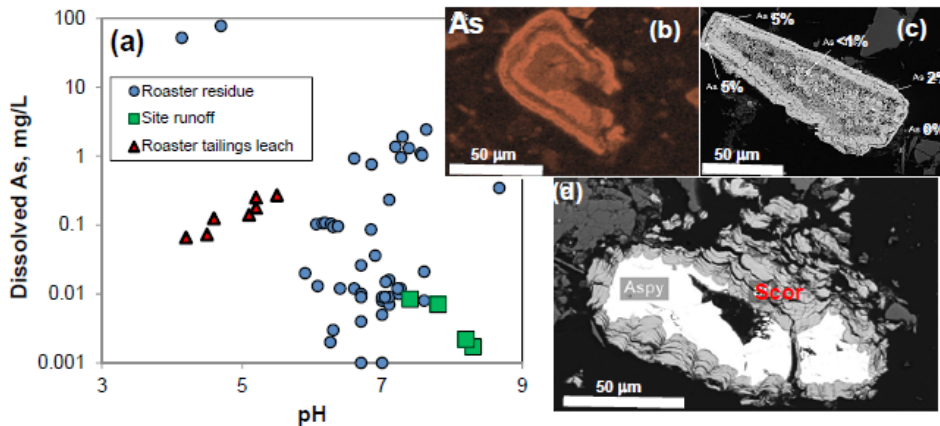


Figure 5 Arsenic mobility in 70-100 year old tailings. (a) Dissolved As vs pH for waters emanating from tailings residues from two historic mine sites. (b) SEM map showing zoned As distribution in a yukonite (Ca-Fe arsenate) bearing particle in roasted sulphide ore tailings. (c) SEM backscatter image of zoned hematite particle showing As compositions. (d) SEM backscatter image of a relict arsenopyrite particle (white) armoured by Fe-As-rich alteration layers (Scor), in unroasted sulphide concentrate tailings.

Conclusions

Gold mine tailings are potential resources for the future, and they should be managed as such. This management should involve prediction and monitoring of the mobility of accompanying arsenic in the tailings waters. The levels of dissolved As can be predicted from the mineralogy of the tailings and the nature of the water flow pathways around a tailings repository. Short-term (13 years) storage of arsenopyrite-bearing tailings at the Macraes mine allowed subsequent successful reprocessing of those tailings for the remaining gold when processing technology was improved. There were some locally elevated dissolved As concentrations and minor acidification within the tailings repository, but discharging waters remained with circumneutral pH and low dissolved As. Historic mine tailings that had involved roasting of sulphides to release encapsulated gold contain As-bearing hematite. This material has remained largely inert for up to 100 years, and discharging waters from these sites have very low dissolved As contents. However, arsenolite is an intermediate oxidation product of arsenopyrite during roasting, and this mineral has higher solubility and can yield extremely high dissolved As concentrations. Dissolved As is strongly attenuated by adsorption to high surface area iron oxyhydroxides that form during roasting and under surficial conditions. Hence despite the abundance of As-bearing minerals in gold mine tailings, most associated waters have low dissolved As.

Acknowledgements

This research was funded by NZ Ministry for Business, Innovation and Employment via CRL Energy Ltd. Additional funding was provided by University of Otago. SEM images were obtained at the Otago Centre for Electron Microscopy. Logistical support was kindly provided by OceanaGold Ltd and NZ Department of Conservation, and we particularly appreciate help from Debbie Clarke, Barry Mathieson, and Jim Staton. Discussions with James Pope and Dave Trumm were helpful in formulating ideas for this paper.

References

- Craw D (2006) Pressure-oxidation autoclave as an analogue for acid-sulphate alteration in epithermal systems. *Mineralium Deposita* 41: 357-368.
- Craw D, MacKenzie D (2016) Macraes gold deposit, New Zealand. SpringerBriefs in World Mineral Deposits. ISBN 978-3-319-35158-2, Berlin, 130 pp.
- Craw D, Koons PO, Chappell DA (2002) Arsenic distribution during formation and capping of an oxidized sulphidic minesoil, Macraes mine, New Zealand. *Journal of Geochemical Exploration* 76: 13-29.
- Druzicka J, Craw D (2015) Metalloid attenuation from runoff waters at an historic orogenic gold mine, New Zealand. *Mine Water and Environment* 34: 417-429.
- Haffert L, Craw D (2008) Mineralogical controls on environmental mobility of arsenic from historic mine processing residues, New Zealand. *Applied Geochemistry* 23: 1467-1483.
- Kerr G, Druzicka J, Lilly K, Craw D (2015) Jarosite solid solution associated with arsenic-rich mine waters, Macraes mine, New Zealand. *Mine Water and Environment* 34: 363-374.
- McLachlan C, Craw D (2016) Characterisation of tailings at Prohibition Mine Site, Waiuta, Westland. Proceedings of the 49th Australasian Institute of Mining and Metallurgy (AusIMM) New Zealand Branch Annual Conference, pp. 259-268.
- Malloch K, Craw D, Trumm D (2017). Arsenic mineralogy and distribution at the historic Alexander gold mine, Reefton Goldfield, New Zealand. *New Zealand Journal of Geology and Geophysics* 60 (in press).
- Roddick-Lanzilotta AJ, McQuillan AJ, Craw D (2002) Infrared spectroscopic characterisation of arsenate(V) ion adsorption from mine waters, Macraes Mine, New Zealand. *Applied Geochemistry* 17: 445-454.

Integrating Climate Change into Water Management Design

Victor Muñoz¹, Tia Shapka-Fels¹, Maritz Rykaart¹

¹*SRK Consulting (Canada) Inc., 1066 W Hastings Street, Vancouver, BC, Canada V6E 3X2*

Abstract This paper presents a combination of methods to meet the challenge of incorporating global climate change models into predictions of meteorological events and trends using publicly available data to determine meteorological design values. A purpose-built script was developed with the statistical language R to compile changes in multiple climate variables for a given longitude, latitude, and time period. Input information includes global climate change (GCC) models from Intergovernmental Panel on Climate Change Assessment Reports 1–5. The available GCC models were weighted equally during statistical evaluation of the overall cumulative results. Results were then compared to trends in historical data obtained from reanalysis climatic models. This overall procedure combines analysis of GCC models and historical data to define design values of the percentage change expected to use for civil structures and water management.

Key words Climate Change, GCC, applied engineering, hydrology, water management

Introduction

The lack of consistent processes to integrate global climate change (GCC) into engineering design acts as a barrier in the ability to address the effects of GCC on infrastructure (CSA 2012). Thus, the expectation exists within the engineering community and local governmental entities that GCC must be actively incorporated into engineering design.

This paper describes a method that uses computer programming to analyze GCC models and historical data in parallel. The results are then statistically compared to produce a single GCC design value. The method can help guide engineers during design of climate-dependent infrastructure and can be applied to any location in the world and for many climate variables. For example, in northern latitudes, tailings and waste rock freezing is used to control acidic runoff from facilities, and frozen core dams are often used to contain tailings and contaminated water. Projects in warmer climates with submerged tailings can be affected by an increase in temperature and thus evaporation. Globally, projects are dependent on water balances and predictions of mean annual precipitation.

The proposed method involves: (1) collating and evaluating baseline climate data, (2) querying available GCC prediction models, and (3) forecasting climate trends. Results are then graphically summarized. Baseline reanalysis data were sourced from ERA-Interim, produced by the European Centre for Medium-Range Weather Forecast (ECMWF), whereas GCC models from five Intergovernmental Panel on Climate Change (IPCC) Assessment Reports (ARs) were accessed through Environment and Climate Change Canada (ECCC) (2016). The entire procedure was accomplished using a purpose-built script developed with R software (Comprehensive R Archive Network 2016). The change in the mean air temperature of Yellowknife, Canada, was used to illustrate the procedure and analytical results.

Many GCC software packages are available through research institutions (e.g. the Pacific Climate Impacts Consortium). In some cases, GCC modelling provides highly detailed climate predictions, but these are usually only applied to specific regions. As well, most GCC modelling methods do not compare historical trends against available models. The major difference between the procedure described here and other GCC tools and sources is trend analysis of historical data. For example, ClimateWNA (described by Wang et al. 2012), ClimateBC, ClimateNA, and the Statistically Downscaled Climate Scenarios offered by the Pacific Climate Impacts Consortium (2016) produce detailed downscaled climate predictions based on a subset of available GCC models. They can only be applied for regions within North America. Although downscaling climate data allows for higher climate resolution, a trade-off exists between the geographical range of applicability and the increase in the time needed to produce results. In addition, increased performance and accuracy are not guaranteed with increasing resolution (Charron 2014).

Conceptual Methodology

The proposed methodology produces a conservative value (larger magnitude of GCC) when comparing historical trends and GCC models. For projects where historical trends show GCC is occurring more rapidly than predicted by GCC models, the historical trend is projected. For locations where GCC is predicted to exceed historical trend forecasting, the results from R are consistent with other GCC models.

Script Deployment

Assessment Reports

Design elements of a given project include the location, infrastructure risk associated with GCC, and climate variables deemed important for analysis. It is necessary to identify the GCC models available for each important climate variable. The five chosen IPCC AR models and scenarios contain monthly GCC modelling predictions for any location in the world:

- First Assessment Report (FAR) (IPCC 1990)
- Second Assessment Report (SAR) (IPCC 1995)
- Third Assessment Report (TAR) (IPCC 2001)
- Fourth Assessment Report (AR4) (IPCC 2007)
- Fifth Assessment Report (AR5) (IPCC 2014)

The GCC models and scenarios presented in AR1 to AR5 assume application of radiative forces (energy fluxes) through different anthropogenic sources that result in discharge of varying concentrations of atmospheric greenhouse gases. These radiative forces are not constant through time because they depend on global anthropogenic behavior, such as environmental policies, population growth, economic growth, energy sources, land use, and hydrocarbon usage. Each GCC model presented in the ARs represents these radiative forces differently and thus each presents a different GCC scenario, underscored by its own model assumptions and boundary conditions. The maximum projection time frame considered in this method is to the year 2100.

None of the GCC models are inherently superior or inferior. Likewise, the newer generation of ARs are not necessarily more reliable than older versions. Instead, they represent more detailed consideration of global anthropogenic forces. Typically, the user must apply professional judgment when choosing the most suitable model or generation of models for design, which is invariably biased. The proposed method aims to eliminate this bias by weighting the available models equally (Flato et al. 2013).

The AR1–AR4 data cover the years 1960–2100 for a variety of climate variables. The AR5 data cover the years 1900–2100 in NetCDF format (Unidata 2016) and provide temperature and total precipitation, but include fewer other meteorological variables in comparison. Significant data gaps exist in the ARs, depending on the report, scenario evaluated, and assessed variable.

Although the meteorological variables in AR1 to AR5 were used for most analyses, some GCC design values were calculated for other key variables through application of empirical models (e.g. extreme storm events and snowpack thickness using snowmelt energy models) (Walter et al. 2005).

Reanalysis: ERA-Interim

To best represent the historical trends, a reanalysis approach was used because the availability and timespan of records tend to be more consistent than regional meteorological stations. Reanalysis spans several decades and covers the entire planet. Publicly available reanalysis data from ERA-Interim (ECMWF 2016) comprise six-hour time interval data from 1979 to 2016, based on a 0.75° latitude by 0.75° longitude grid. If necessary, data from regional meteorological stations can be compared with the reanalysis data to validate the reanalysis data for a specific site, especially for projects in mountainous terrain.

The reanalysis models generally use 3D-variational (3DVar) and 4D-variational (4DVar) methods for data assimilation of the measured meteorological information when compared with short-term forecast information. 4DVar assimilation is more representative of the measured values because forecast information is corrected within the respective time step. ERA-Interim is one of few available and up-to-date reanalysis models with 4DVar data assimilation for a small grid size (Reanalyses.org 2016). These characteristics support the use of ERA-Interim for historical meteorological information.

Data Retrieval and Use of R

Data from AR1 to AR4 were downloaded from ECCC source files for a given site based on longitude and latitude. Data retrieval is automated within the R script, and data retrieval and analysis can be completed within minutes. The script is coded to be applicable to all projects, with few inputs and standardized outputs. AR5 information and ERA-Interim reanalysis databases were downloaded prior to use of the script. R software then facilitated presentation of the results in publication-quality figures.

Baseline Analysis

Using every model available in the five ARs, the GCC was projected with respect to a set baseline conditions over a time interval of 30 years, which is generally accepted as a statistically significant period (Baddour and Kontongomde 2007). The baseline and projected periods are defined as follows:

- The baseline period (1976–2005) coincides with that adopted for AR5 by ECCC. This is the estimation of the climate data based on the GCC models.
- Three projection periods, 2011–2040, 2041–2070, and 2071–2100, represent the future when GCC models are applied.

The projected change in a given climate variable for each time period can be automatically calculated using R script. Results can be presented in the form of a cumulative probabilistic curve. For the purpose of this method, only the overall cumulative probabilistic curve associated with data from all the available ARs combined is needed because all GCC models are equally weighted (IPCC 2014).

Trend Analysis

Historical reanalysis data from ERA-Interim were assessed by (1) identifying the trend and (2) estimating the statistical significance of the trend. Five trend analysis methods were used:

- Ordinary least square (Maidment 1992)
- Quantile regression (Koenker 1978)
- Mann-Kendall and Theil Sen (Mann 1945; Sen 1968)
- Zhang (Zhang et al. 2000)
- Yue and Pilon (Yue et al. 2002)

The outcome of the trend analysis is a figure illustrating the different trends and the statistical significance of each regression method. Significant trends ($p\text{-value} < 0.05$) are displayed on the cumulative probabilistic curve (Figure 1).

Design Value Determination

Following completion of the baseline and trend analyses, a design recommendation is presented for the identified meteorological variable and time period. This design value is shown on the cumulative probabilistic curve (Figure 1), depending on which analysis outcome is deemed to be more representative of the location based on a simple calculation. If the previous trend analysis showed no historical statistical significance, then the design variable would be the percent change associated with 50% cumulative probability based on the GCC models. However, if there were statistically significant historical trends, then the design variable would be calculated based on the following equation:

$$\text{Climate Change Design Value} = \text{Max.} \left(\begin{array}{l} 50\% \text{ Cumulative Probability,} \\ \text{Mean}\{ \text{Regression}_{p\text{-value} < 0.05} \} \end{array} \right)$$

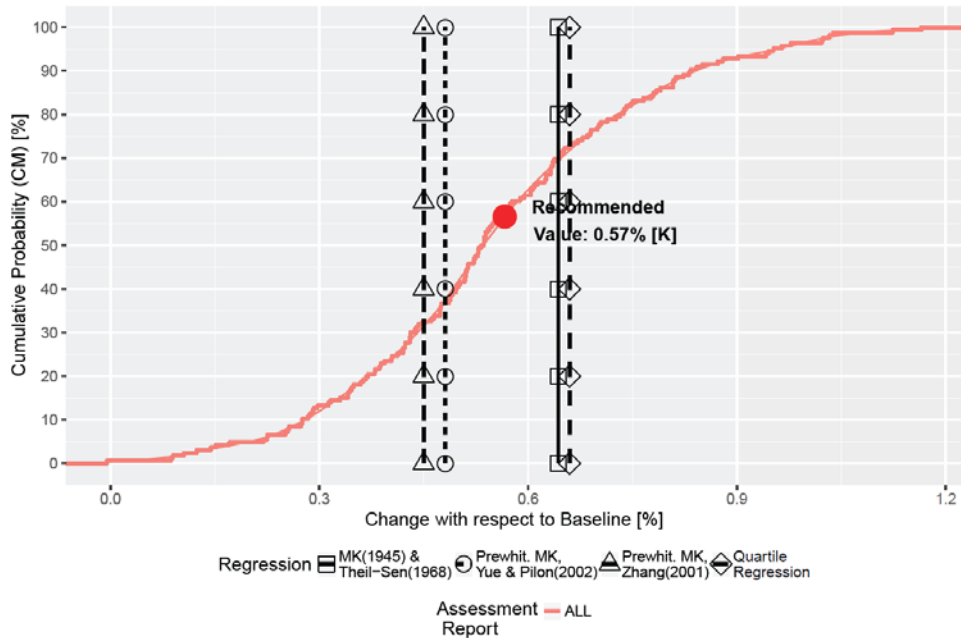


Figure 1 Summary of baseline and trend analyses, including the cumulative probabilistic curve based on climate change models, and statistically significant historical trends. The design value represents the change in air temperature expected for 2011 to 2040 for Yellowknife, Canada.

Discussion

The proposed method facilitates incorporation of GCC into engineering design in a practical way and is to be applied in addition to normal engineering best practices that are already implemented during engineering design. Such practices include the consideration of site-specific and engineering investigations, design codes, and the use of safety factors, risk management, and professional judgment.

GCC models inherently contain several assumptions, and there is no clear way to assess the accuracy of a given model. The proposed procedure statistically analyzes all climate predictions included in the IPCC ARs and identifies trends in historical data to produce the most representative GCC design variable for a given location and time period. The method eliminates the bias introduced by selecting a single model and compares GCC models with historical data.

The limitations of this procedure are inherent in GCC analysis. The source data are publicly available, and the software and methods that use these data share flaws associated with the data. Another limitation is the maximum time horizon over which the GCC models are projected. ECCC provides data access for models up to the year 2100. There are few GCC projections beyond 2100, and the uncertainty and variability in these models tends to be high (IPCC 2014). Therefore, it is considered appropriate to limit the use of models projecting beyond the year 2100 in engineering applications.

References

- Baddour, O. and Kontongomde, H. 2007. The role of climatological normals in a changing climate. World Meteorological Organization.
- [CSA] Canadian Standards Association. 2010. Technical Guide-Infrastructure in permafrost: a guideline for climate change adaptation. CSA Special Publication Plus: 4011-10.
- [CSA] Canadian Standards Association. 2012. National survey of Canada's infrastructure engineers about climate change. Ottawa: Engineers Canada and CSA Group.
- Charron, I. 2014. A guidebook on climate scenarios: Using climate information to guide adaptation research and decisions. Ouranos,
- The Comprehensive R Archive Network. Accessed May 24 2016. Download and install R. The Comprehensive R Archive Network. <https://cran.r-project.org>
- [ECCC] Environment and Climate Change Canada. Accessed May 18 2016. The Canadian Regional Climate Model. Environment and Climate Change Canada. <http://www.ec.gc.ca/ccmac-cccma/default.asp?lang=en&n=82DD0FCC-1>
- [ECMRWF] European Centre for Medium-Range Weather Forecast. Accessed May 18 2016. ERA-Interim. ECMRWF. <http://www.ecmwf.int/en/research/climate-reanalysis/era-interim>
- Flato, G., Marotzke, J., Abiodun, B., Braconnot, P., Chou, S.C., Collins, W., and Cox, P. 2013. Evaluation of climate models. In: Climate change 2013: the physical science basis. Contribution of Working Group I to the Fifth Assessment Report of the Intergovernmental Panel on Climate Change: 741–866. Cambridge University Press.
- [IPCC] Intergovernmental Panel on Climate Change. 1990. IPCC first assessment climate change 1990. IPCC.
- [IPCC] Intergovernmental Panel on Climate Change. 1995. IPCC second assessment climate change 1995. IPCC.
- [IPCC] Intergovernmental Panel on Climate Change. 2001. Climate change 2001: synthesis report. A Contribution of Working Groups I, II, and III to the Third Assessment Report of the Intergovernmental Panel on Climate Change. Cambridge University Press.
- [IPCC] Intergovernmental Panel on Climate Change. 2007. Climate change 2007: synthesis report. Contribution of Working Groups I, II and III to the Fourth Assessment Report of the Intergovernmental Panel on Climate Change. IPCC.
- [IPCC] Intergovernmental Panel on Climate Change. 2014. Climate change 2014: synthesis report. Contribution of Working Groups I, II and III to the Fifth Assessment Report of the Intergovernmental Panel on Climate Change. IPCC.
- Koenker, R.W., and Bassett Jr G.W. 1978. Regression quantiles. *Econometrica: Journal of the Econometric Society* 46(1): 33–50, doi:10.2307/1913643
- Maidment, D.R. 1992. Handbook of hydrology. McGraw-Hill Inc.
- Mann, H.B. 1945. Nonparametric tests against trend. *Econometrica: Journal of the Econometric Society* 13: 245–259, doi:10.2307/1907187
- Pacific Climate Impacts Consortium. Accessed May 18 2016. Statistically Downscaled Climate Scenarios. Pacific Climate Impacts Consortium. <https://www.pacificclimate.org/data/statistically-downscaled-climate-scenarios>
- Reanalyses.org. Accessed May 24 2016. Atmospheric Reanalyses Comparison Table. Advancing Reanalysis. <http://reanalyses.org>
- Sen, P.K. 1968. Estimates of the regression coefficient based on Kendall's tau. *Journal of the American Statistical Association* 63(324): 1379–1389, doi:10.1080/01621459.1968.10480934
- Unidata. Accessed May 19 2016. Network Common Data Form (NetCDF). Unidata. <http://www.unidata.ucar.edu/software/netcdf>
- Walter, M.T., Brooks, E.S., McCool, D.K., King, L.G., Molnau, M., and Boll, J. 2005. Process-based snowmelt modeling: does it require more input data than temperature-index modeling? *Journal of Hydrology* 300(1): 65–75, doi:10.1016/j.jhydrol.2004.05.002
-

- Wang, T., Hamann, A., Spittlehouse, D.L., and Murdock, T.Q. 2012. ClimateWNA-high-resolution spatial climate data for western North America. *Journal of Applied Meteorology and Climatology* 51(1):16–29, doi:10.1175/JAMC-D-11-043.1
- Yue, S., Pilon, P., Phinney, B., and Cavadias, G. 2002. The influence of autocorrelation on the ability to detect trend in hydrological series. *Hydrological Processes* 16(9): 1807–1829, doi:10.1002/hyp.1095
- Zhang, X., Vincent, L.A., Hogg, W.D., and Niitsoo, A. 2000. Temperature and precipitation trends in Canada during the 20th century. *Atmosphere-Ocean* 38(3): 395–429, doi:10.1080/07055900.2000.9649654

Assessing Flood Hydrology in Data Scarce Tropical regions: a Congo (ROC) case study

David R.A. Carruth^{1,2}, Francis P. Smith¹

¹*SRK Consulting (UK) Limited, Churchill House, 17 Churchill Way, Cardiff CF10 2HH, United Kingdom*

²*Hawkes Bay Regional Council, 159 Dalton Street, Napier 4110, New Zealand*

Abstract A robust hydrological assessment can be a challenging task in regions where a lack of data, of sufficient quality, is available to fully validate analysis. This level of uncertainty is heightened in studies of flood hydrology for tropical regions, where spatio-temporal variation in rainfall can be significant and the associated timing of flooding can be challenging to determine.

The Tchivouba catchment, situated within the Republic of Congo, was used as a basis for the study of flood hydrology in the tropics, and the methods presented in this paper aim at reducing uncertainty in instances of data scarcity in similar settings.

Introduction

The focus for this study was to provide a robust assessment of the flood hydrology for a proposed mine development, situated in the Republic of Congo (RoC). The location of the progressive open pit would require significant river engineering works, with construction of multiple dams and river diversions proposed to enable progression of the pit and safeguard the mine operatives. A detailed study of both the regional and local climate and hydrology was therefore commissioned to ensure production of the most efficient, reliable and cost effective engineering design solutions for surface water systems.

Estimation of flood flows is challenging in many parts of the African continent, but particularly so in the RoC where hydro-meteorological data is so scarce that development of suitably robust statistical methods to estimate flood flows has not been possible. For example, use of statistical methods, such as regional analysis or flood frequency curve development, is not possible given the lack of data to feed into the analysis. Regional analysis is conventionally done through either 'pooling' data from catchments with similar hydrological characteristics to make predictions such as that in the Flood Estimation Handbook (CEH 1999) or fitting regression lines to the large sets of data (McKerchar and Pearson 1989), to develop a relationship for prediction of flood flow in each region within the country of study. Where data is only available for a limited number of catchments, often at a regional scale, (catchment sizes in excess of 500 km²), with insufficient temporal resolution in the frequency of measurements, combined with records often of insufficient length (<20 years), development of such regional relationships, or even a single site flood frequency curve, is extremely challenging.

In the absence of these alternate, more data reliant and statistically robust methods, hydrologists working within industry often resort to making flood predictions using simplified event based rainfall-runoff models. The tendency within a consultancy environment in the mining industry, is to adopt the simplest and most efficient method that produces

the most conservative flood discharge. Using methods such as the Rational or SCS Runoff Curve Number (CN) method, this allows for uncertainties associated with a lack of data and incorporates an allowance for risk within the engineering design.

Though the methods themselves are robust when applied correctly, some only produce a single flood peak, making them unsuitable for input to design of flood control structures (dams) and their 'lumped' nature means they fail to properly account for the variable physical characteristics of a particular catchment (soils, vegetation cover, topography) and result in more uncertain flood predictions. A subsequent result is often excessive over designed solutions for surface water infrastructure.

Adequately representing the spatial and temporal variation of rainfall within a model presents additional challenges to a hydrologist working in data scarce regions of the world. It is often common practise to use a hyetograph developed elsewhere that shares similar meteorological conditions to the study catchment, such as the SCS dimensionless distributions. The problem with these solutions is that these are now significantly outdated, were developed using averaged data from very large regions in the United States of America (USA) that have regionally different ratios between short duration and long duration rainfall values, and are no longer recommended for use in the USA by the NRCS, let alone elsewhere. Where sufficient site-specific data is available, nested storm patterns can be generated to produce a hypothetical storm, however temporal resolution issues often hinder the development of reliable statistics.

This study applied a bottom up approach, with the baseline hydro-meteorological monitoring network reviewed and improved, to establish a stronger representation of rainfall-runoff response in the area. A detailed review of climatic influences, both at a regional and local scale was performed, with remotely sensed TRMM data used to support the analysis. A hydrological model was built utilising the HEC-HMS platform and the ModClark transform and SCS-CN loss methodologies, requiring the development of design hyetographs, using a time-distribution method, which allowed determination of the most adequate shape for the hyetograph. Further refinement of the model resulted from validation of simulated outputs in response to measured events, utilising a stage monitoring device installed during the study period. Model outputs were used directly as inputs to a 1D-hydraulic model, which considering the semi-braided planform typology presented multiple challenges. This paper aims to emphasize that selection of the most appropriate methods of analysis and modelling, taking into account project specific constraints, is critical to understanding flood hydrology. This must be underpinned by a local scale baseline monitoring network with adequate spatial coverage and temporal resolution, quality controlled data and a clear understanding of the regional and global scale factors which impact local conditions.

It should be understood that the aim of this paper is not to critique or pass judgement on the work of others, nor is it to present a perfect methodology for industry based hydrologist to follow. Rather it presents one solution that may be useful in some instances and outlines the

approach taken to understand the unique climate and hydrological setting of the study area and the methods applied to overcome the uncertainty in flood flow estimation associated with limited data.

Case Study Location and Background

The 113 km² Tchivouba catchment within the Republic of Congo was used as a basis for the study of flood hydrology in tropical regions. Located in the south-west of the ROC within the coastal plain, a narrow strip of land between the Mayombe Mountains and the Atlantic coast, the Tchivouba is a tributary of the Loémé river, which drains approximately 3,199 km² into the Lakes of Cayo and Louafouleba before discharging into the Atlantic Ocean, see Figure 1.

In broad terms, the climate in the RoC is strongly influenced by the movement of the Inter-Tropical Convergence Zone (ITCZ). The warm 'pseudo'-monsoon flux of south-westerly moist air from the Atlantic produces a large zone of convective clouds. The behaviour of the ITCZ from year to year is deemed the primary factor in precipitation variability across the region in which the Tchivouba Catchment is situated. However, a paucity of high quality long-term climate datasets of sufficient spatio-temporal resolution prevent deeper understanding and quantification of rainfall variability (Todd & Washington 2004; Washington et al. 2013, Nicholson and Grist 2003).

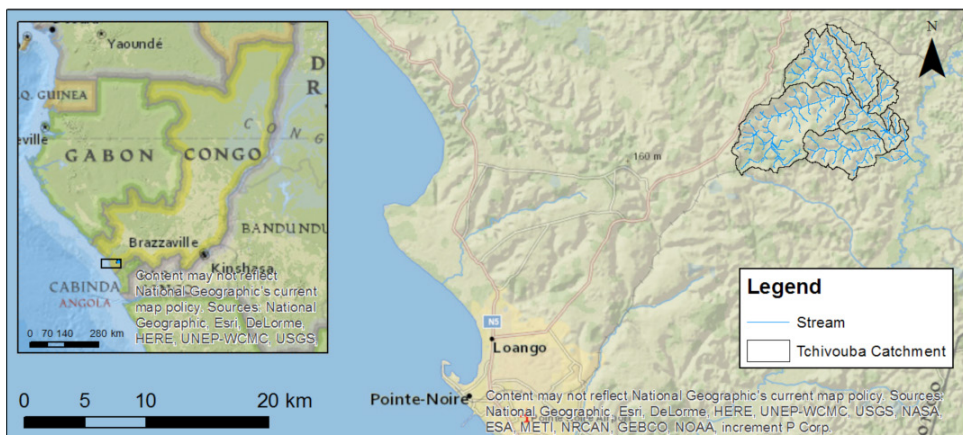


Figure 1: Project location

Methods

A detailed climate and catchment characterisation study was completed, to determine both the quantity and spatial variability of rainfall falling within the Tchivouba catchment, and the catchment characteristics that influence the interception, storage, losses and propagation of storm runoff response throughout the catchment.

Long-term regional rainfall data was collected to support site-specific short-term rainfall records collected at four project rain gauges installed within the catchment. High-resolution satellite-based precipitation estimates derived from the Tropical Rainfall Measuring

Mission (TRMM) precipitation radar were utilized, demonstrating the significant spatial variability in rainfall resulting from the large-scale convection system influenced by the movement of the Inter-Tropical Convergence Zone. A long-term synthetic rainfall time-series was developed for the catchment, based on regression analysis between the local stations and the regional climate station records and design storm rainfall depths calculated utilising the annual maxima method with the Gumbel extreme value distribution and the Cunnane plotting position formula. Individual storm events measured within the project area were analysed and dimensionless mass curves developed following the Huff (1967) methodology, to determine the temporal distribution of each design storm event defined for use within the model.

To better understand the natural runoff regime within the project area, a hydrometric station was installed within the upper reaches of the catchment where well-defined channels and in-bank flow was evident. Downstream, the project was inundated wetland, resulting in difficulties accurately obtaining hydrometric measurements of the runoff hydrograph in these areas. Although limited, this upstream location provided a validation point for subsequent modelling, and considering water management infrastructure for the mine would be located at sub-catchment outlets in the form of diversion channels and attenuation dams prior to the low-lying floodplain, allowed for some degree of confidence in subsequent design flood flows.

Detailed catchment topography, vegetation and land use mapping had been obtained through a LiDAR survey within the lower floodplain regions of the catchment. These were supplemented in the outer reaches by satellite imagery and digital elevation data obtained via the Shuttle Radar Topography Mission (SRTM). A regional soil map and field investigations using infiltration tests and soil definition were used to define the soils and shallow subsurface conditions in the area.

To determine design flood response at various locations throughout the project area, a detailed rainfall-runoff model was required that would provide the flexibility to characterize and define the variable rainfall-runoff relationship throughout the catchment. Utilising site specific data, an improvement on lumped, catch all methods such as the Rational Method was sought, to better simulate the spatial variability in runoff response within the local area using a method more appropriate for the catchment size and location. A HEC-HMS model was constructed, utilising a gridded SCS-Curve Number (CN) loss methodology and Mod-Clark transformation to provide a quasi-distributed rainfall-runoff model. By discretizing the catchment domain into a uniform grid, a linear quasi-distributed transformation method was utilised that has the ability to account for spatial variations in rainfall and losses using the grid. Rainfall excess was determined for each grid cell and routed through a linear reservoir accounting for catchment storage effects. The runoff travel time for each grid cell was calculated and scaled to overall catchment time of concentration based on the travel time to the catchment outlet. The SCS curve number loss method was then utilised and spatial variation within the catchment included within the grid. By utilising a relatively fine

grid resolution, this method used a discharge-weighted approach to determining the overall runoff from the catchment as opposed to a weighted CN, providing a more accurate representation of runoff response, particularly considering the considerable spatial variation in topography, land use and sub-surface saturation. The gridded CN were calculated using a land cover and soil map for the catchment alongside a table relating land use to curve numbers for each hydrologic soil group in the catchment area using reference hydrological soil-cover complexes.

An initial abstraction ratio, (the initial rainfall amount in mm that is retained before runoff commences), plays an important role in the calculated runoff depth, the hydrograph peak and the temporal distribution of runoff. It is for the most part dependent on climatic conditions and arguably the most ambiguous of the parameters defined within the modelling process, investigated in many studies (Jiang 2001; Hawkins et al. 2002 and Mishra and Singh 2004) with determined values ranging between 0.01 and 0.3. Due to the obvious ambiguity, a sensitivity analysis was performed to provide the best understanding of sub-catchment response to variations in this parameter.

The boundary of the modeled area was defined as the outline of the entire Tchivouba catchment; which incorporates all contributing streams and rivers upstream from the final outlet into the River Loémé in the SE part of the project area. The catchment has been split into a number of sub-catchments, each defined in relation to specific junctions within the main Tchivouba network that represent the confluences of incoming tributaries. These channels are all slow moving owing to the fact they are densely vegetated and have shallow channel slopes. The relatively shallow cross-sectional channel profiles of these watercourses, together with debris deposited within them, results in regular 'out of bank' flow.

An unsteady state 1D hydraulic model was constructed using HEC-RAS to incorporate approximately 9.4km of the Tchivouva river, from its confluence with the Loeme River to a point 1.5 km upstream of the proposed open pit. Cross-sectional information was obtained directly from LiDAR survey information, with site access and the swamp conditions of the lower regions preventing the collection of detailed in-channel geometries. Given the shallow nature of the flood plain channels, this approach was determined to at least provide a conservative approach to flood line determination, with cross sectional topography at worst underestimating the conveyance potential of the channel due to the LiDAR reflectance from the water surface. A sensitivity analysis was performed to assess the sensitivity of the model to changes in key input parameters. The results indicate the model is not particularly sensitive to change in input parameters. However, there was clearly a need to identify roughness values for the model which are representative of those in reality as high values of n , mean higher predicted water levels, albeit minor ones in this study. Land-use and vegetation mapping, aerial photography, assessment of obstruction and in channel sampling allowed representative n -values to be incorporated into the model.

Results and Discussion

Utilising detailed rainfall analysis, design rainfall depths and design hyetographs were developed that adequately represented the local magnitude and temporal distribution of design storm rainfall, see Figure 2. The derived design hyetograph, developed from analysing all the significant storms in the available monitoring record, has a temporal distribution typical of a convective storm, with the majority of rainfall falling in the second quartile. A clear understanding of the large scale processes driving the localized rainfall distribution, coupled with an understanding of what convective storm hyetographs should look like in terms of the cumulative mass distribution in time, provided confidence that the hyetograph developed for input to the model, which subsequently strongly influences the rainfall-runoff relationship within it, would be representative of the study catchment.

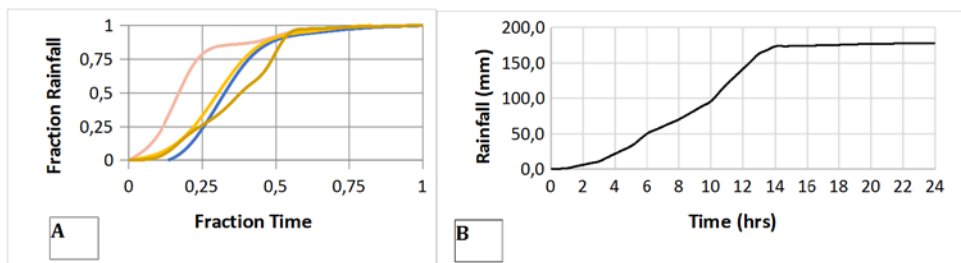


Figure 2: Nested storm analysis (A) and subsequent 100 year 24-hour design hyetograph (B).

Utilising the measured flow data available within the upper catchment, the model was refined in a simple calibration to increase confidence in the selection of an appropriate Initial Abstraction ratio (IaR). Individual storm events were modelled and IaR adjusted to produce the best fit between the measured and simulated hydrograph, see examples in Figure 3. An IaR of 0.165 was defined for use in the model.

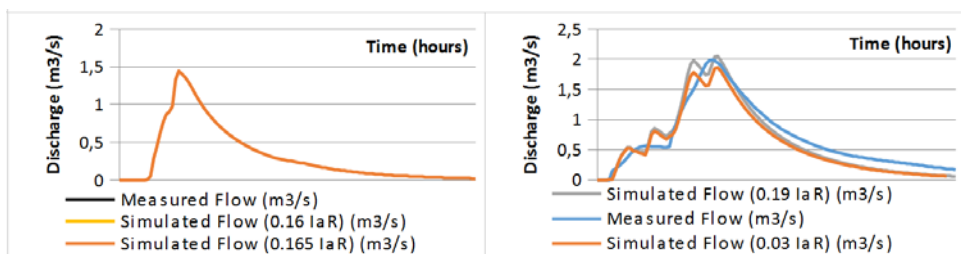


Figure 3: Sample of 'calibration' runs – two individual storm events in this example.

The ModClark model was then utilised to simulate the rainfall loss and runoff response across the Tchivouba catchment, with Figure 4 demonstrating the runoff hydrograph within the Upper Tchivouba sub-catchment for the 1 in 10 and 1 in 100 design storm. This achieved a key aim for the study, which was to use more detailed methods of assessing the hydrology, than those in previous studies of watercourses in this catchment in order to arrive at more

representative flood flow estimates. These improved estimates then provide appropriately conservative engineering design inputs and ultimately result in the most cost effective and sustainable design solutions for water management infrastructure.

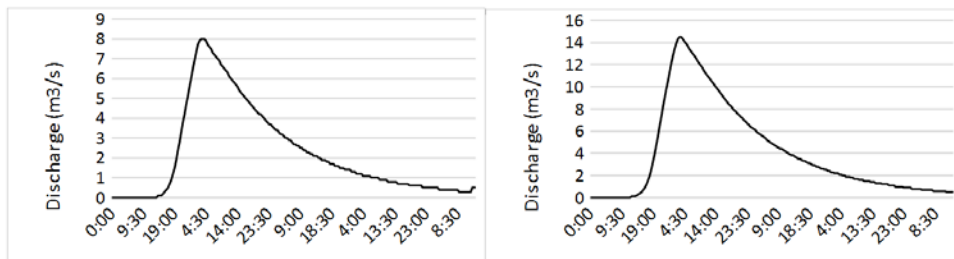


Figure 4: 24 hour design storm runoff hydrograph; 1 in 10 year (A), 1 in 100 year (B).

Confidence that the lower estimates provided by the ModCLARK model were representative of the catchment in flood conditions was provided by the model calibration process. Model outputs matched well with the time to peak and magnitude for the observed storm events selected for the calibration process.

The model hydrographs were utilised in a 1D HEC-RAS model to simulate the expected flood levels within the catchment and future mine area, to highlight the at risk areas and inform future design and mitigation measures.

The length of record available for both stage and flow within the lower catchment only allowed development of a preliminary rating curve, and one which is particularly sparse at the upper end, so full calibration of the hydraulic model outputs was not possible.

Conclusions

In order to reduce uncertainty in flood predictions, this study utilised high resolution TRMM data in unison with a network of rain gauges to increase understanding of the spatial distribution of rainfall across the Tchivouba catchment and allow development of a representative design rainfall hyetograph for input to hydrological modelling.

The choice of a quasi-distributed hydrological model allowed better representation of catchment response to rainfall events, reducing the uncertainties associated with use of lumped models with little parameterisation, used in prior studies of the project area.

Uncertainty in predictions was also reduced in the modelling process through event based calibration of the hydrological model, and through detailed sensitivity analysis of both the hydrological and hydraulic models to changes in key parameters. Installation of an automatic stage monitoring device in a suitable reach within the catchment allowed development of a preliminary rating curve for model calibration. Prior to this, no reliable continuous measurements of river stage and discharge had been collected.

Whilst every effort was made to isolate the uncertainty within the hydrological model, using observed data to calibrate the rate of initial abstraction, the number of observed events from which calibration was performed was limited, both in terms of total number and in terms of the magnitude of events. Further improvement could be made in future as more extensive climate and surface water records are collated, allowing for updated flood predictions. These datasets would refine the outputs of the hydrological model and produce a better rating curve with which to calibrate hydraulic models.

In conclusion, this study has advanced knowledge of the hydrological and hydraulic flood behaviour of the project, through extension to the baseline monitoring network, data collection and quality assurance, appropriate choice of modelling software and model calibration and sensitivity analysis. By its very nature flood prediction is uncertain, but by applying each of these steps even when under significant constraints, the authors have found during the course of this study that these can be significantly reduced.

Acknowledgements

The authors thank Cominco Resources Limited for giving us the opportunity to conduct this study and present this paper using their data. Also for their collaboration in what has been a challenging and highly rewarding study to have worked on.

References

- Hawkins RH, Jiang R, Woodward DE, Hjelmfelt AT, Van Mullem JA (2002) "Runoff Curve Number Method: Examination of the Initial Abstraction Ratio". Proceedings of the Second Federal Interagency Hydrologic Modeling Conference, Las Vegas, Nevada. U.S. Geological Survey
- Jiang R (2001) Investigation of runoff curve number initial abstraction ratio. MS thesis, Watershed Management, University of Arizona, Tucson, AZ. 120 pp.
- Huff FA (1967) Time distribution of rainfall in heavy storms, *Water Resources Research*, 3, 1007-1019.
- Institute of Hydrology (1999) Flood estimation handbook. (reprinted in 2008 by Centre for Ecology and Hydrology).
- McKerchar AL, Pearson CP (1989) Flood Estimation – A Revised Design Procedure, *Transactions IPENZ*, 16(2/CE), 59-65.
- Mishra SK, Singh VP (2004) Long-term hydrological simulation based on the Soil Conservation Service curve 21 number. *Hydrological Processes* 18: 1291-1313.
- Nicholson SE, Grist JP (2003) The Seasonal Evolution of the Atmospheric Circulation over West Africa and Equatorial Africa. *Journal of Climate*, 16, 1013 – 1030.
- Todd MC, Washington R (2004) Climate Variability in Central Equatorial Africa: Influence from the Atlantic Sector. *Geophys. Res. Lett.*, 31, 4pp.
- Washington R, James R, Pearce H, Pokanm WM, Moufouma-Okia W (2013) Congo Basin Rainfall Climatology: can we believe the Climate Models? *Phil Trans R Soc B* 368: 20120296.

Incorporating Climate Change Scenarios into Mine Design and Permitting Studies

Colin Fraser¹, Alan Martin¹, Seth Mueller² and James Scott³

Lorax Environmental Services Ltd., Canada¹; Boliden AB, Sweden²; Goldcorp, Canada³

Abstract This paper summarizes recent experience building climate change scenario data into mine design and permitting studies in Canada and Sweden. For a proposed mine in Yukon Territory, Canada, and an existing mine in northern Sweden, this paper: 1) summarizes recent climate trends and future climate change scenario data for the two mine sites; 2) summarizes steps taken to create long-term, daily- climate datasets that account for a changing climate; and, 3) by drawing on water model results from the two sites, highlight mine-water-climate issues and general management considerations for locations likely to experience warmer and wetter climate regimes.

Key words Climate change, water balance studies, cold regions

Introduction

Recently completed studies at Coffee Gold and Aitik Mines required long-term and forward looking climate records be assembled to drive various mine-site and receiving stream water models. For the Coffee Gold Project, climate data were assembled spanning the period 2018 to 2100 inclusive (i.e., Construction 2018-2020, Operations 2021-2032, Closure 2033-42 and Post-closure 2043-2100), with assembled data used to drive the following models: a heap leach facility (HLF) water balance model (WBM), a permafrost thaw model, a MODFLOW groundwater model and a site-wide water balance and water quality model. For the Aitik Mine, climate data were assembled for a 200-yr closure timeline (i.e., 2025 to 2225) and then used as input to several assessment models: e.g., water balance and geochemical models configured for the Aitik tailings storage facility (TSF) and waste rock storage facilities (WRSF), a hydro-dynamic pit lake water quality model, as well as a recipient water quality model that was configured using GoldSim.

The Coffee Gold Mine (62° 53' N, 139° 22' W) is a proposed gold development in west-central Yukon, approximately 125 km south of Dawson, YT, Canada. Major infrastructure related to mining and processing at the Project includes: an upgraded road; a primary waste rock storage facility; several open pits; water diversion structures and storage ponds; haul roads; primary and secondary crushing facilities; a heap leach facility; a gold refinery; and an accommodation complex. Proposed infrastructure will be situated at high elevation (~1,250 m asl), where local climate conditions are as follows: average annual temperature (T) is -2.6 °C and average annual precipitation (P) is estimated to be 485 mm (65% rain, 35% snow). At the time of paper preparation, Goldcorp was preparing an environmental assessment application, with intentions to embark on more detailed permitting studies thereafter.

Boliden AB is overseeing an expansion at the Aitik Mine that will increase mining and processing capacity from 36 to 45 million tonnes per year (Mt/y). Accordingly, the Aitik Mine Closure Plan was recently updated and technical assessments were conducted in support of

the undertaking. The Aitik Mine (67° 04' N, 22° 55' E) is situated near Gällivare, Sweden, and shows a subarctic climate that is characterized by long, cold winters and short mild summers. Recent climate data indicate annual P and evapotranspiration (ET) are 607 mm and 309 mm respectively for the mine site, with a mean annual T of 0.0 °C.

Data Sources

Coffee Gold Mine

Baseline climate and hydrology data collected at the Coffee Gold Mine (2011 to present), including outputs from 11 continuously recording hydrometric stations, an automated weather station and several snow courses established at multiple elevations, were available. Additionally, monitoring data from measurement networks operated by Federal and State/Territorial agencies in the YT (Environment Canada, Yukon Snow Survey Network) and Alaska (National Oceanic and Atmosphere Administration (NOAA), SNOTEL network operated by the Natural Resources Conservation Service (NRCS)) were used to frame the climate context of the baseline period in terms of broader long-term pattern/trend and range of variability. Finally, monthly climate change scenario data (2001 to 2100, CMIP3/AR4 – A2 Scenario, 2 km grid) for grid points covering the Coffee Gold Mine site (Scenario Network for Alaska and Arctic Planning) were used in this study.

Aitik Mine

Baseline data (i.e., T, P, relative humidity, solar radiation, wind speed) collected at the Aitik mine site weather station (2010 to present), were available and incorporated into the study. Historical T and P data collected at locations adjacent (i.e., Gällivare and Malberget, Sweden; within 15 km) and at further distance (Jokkmokk, Abisko, Lainio, Sweden; within 100 km) from the Aitik mine were also utilized. Furthermore, a suite of climate change scenario results provided by the Rossby Centre (SMHI 2014), including downscaled, daily- climate data (T, P, RH, radiation, wind), were available via the CORDEX (COordinated Regional climate Downscaling EXperiment) data portal.

Climate Trends and the Instrumental Record

Baseline data were limited in their temporal extent (i.e., <5 years) and thus reliable patterns and trends were not readily discernible within this time frame. However, through a comparative process of daily, monthly, seasonal and annual climate metrics, conditions at nearest regional climate stations (e.g., McQuesten, YT – 125 km away; Gällivare, SWE – 15 km) were confirmed to be robust proxies for the mine sites. Instrumental records for McQuesten and Gällivare confirm the following climate patterns and trends for the past three decades: 1) air temperatures have increased steadily at Coffee Gold, though the overall P signature for the region is mixed and exhibits little change over the past thirty years; and 2) recent climate measurements near the Aitik mine show increasing trends for both T and P.

Climate data from nearest regional stations were also compared to other proximal regional stations, but with much longer records. Several suitable stations were identified (e.g., Mayo, YT – 85-year climate record; Jokkmokk, SWE – situated south of Aitik and shows ~150-year

climate record). The results of this comparison confirmed the short-term (decadal) T and P signatures describe for McQuesten and Gällivare, but also characterized recent trends against a longer (century scale) observational timeline. Using anomaly plot format (Equation 1), positive anomalies (indicative of warmer and wetter than average conditions) and negative anomalies (indicative of cooler and drier than average conditions) were generated (Figure 1).

Anomaly (T, P) = (Observation – Mean)/Standard Deviation (**Equation 1**)

Overall, temperature anomaly plots for Mayo and Jokkmokk show strong evidence for recent warming (i.e., since the 1990s), as well, both records show a pronounced warm period which occurred in the 1930s and 1940s. The precipitation anomaly plots (Figure 1, lower plots) generally show wetter than average conditions since the 1970s at Mayo, whereas results for Jokkmokk show wetter conditions over the past 70 years (compared to the long-term average), as well as evidence for more recent P increases (since the 1990s).

Motivating Factors for Climate Change Scenario Selection

The following were motivating factors for the selection of climate change scenarios and usage of modelled future climate datasets:

- Best Practices – Several directional documents (e.g., IPCC 2013 and Comer 2007) summarize recommendations and best practices for the assembly and integration of climate change scenario data for purposes of impact modelling. As per best practices, climate change scenario data available for Coffee Gold and Aitik were ensembles, or averages, of results from multiple climate models (e.g., CMIP5/AR5, 9 model average for RCPs – Aitik Mine).

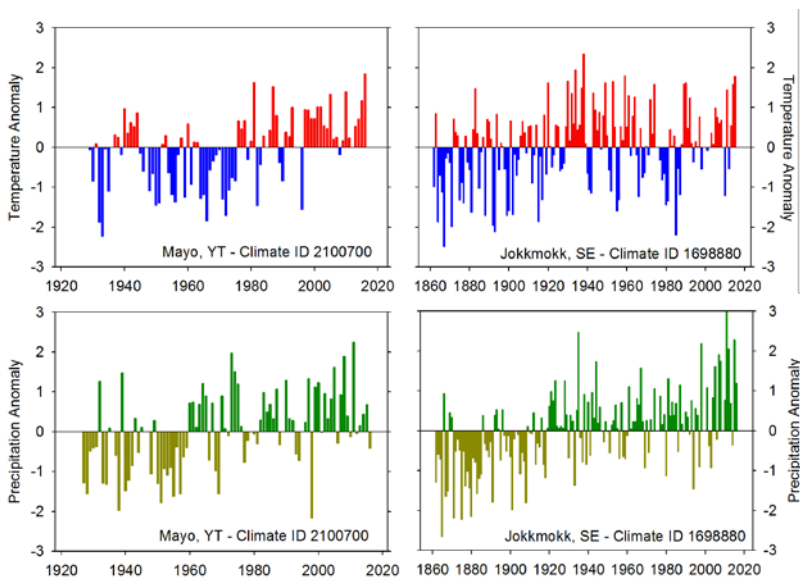


Figure 1 Air temperature and precipitation anomaly plots for long-term monitoring stations near the Coffee Gold mine (left) and Aitik mine (right).

- **Historic and Recent Climate Trends** – Patterns and trends returned by recent- and long-term monitoring data were considerations in the selection of preferential climate change scenarios. In the case of Coffee Gold, the A2 (worst case) scenario was selected in part because future T and P trends closely match trends in the instrumental record for the past 50 years.
- **Consultation and Engagement** – It is often common practice to select climate change scenario(s) in collaboration with others (e.g., between technical leads, regulatory agencies and possibly with a broader stakeholder groups). For Coffee Gold, discussions with a First Nations technical team and guidance provided by an independent climate research centre (Pacific Climate Impacts Consortium) influenced the scenario selection process.
- **Continuity** – e.g., Phase 1 pit lake modelling studies at Aitik mine incorporated climate change scenario data for the A1B (middle scenario, SRES). When the pit lake model was recently updated, there were practical benefits (e.g., prior regulatory acceptance) to re-index the study to a middle climate change scenario (i.e., RCP4.5).
- **Practical Purposes** – For both Projects, the breadth and extent of climate change integration to the various technical assessments was balanced with project budget, scope, schedule and modelling objectives.

Future Climate Trends

At annual frequency (2000-2100), monthly climate change scenario data and predicted trends are summarized for the two mine sites in Figure 2. Plots for Coffee Gold are based on the A2 SRES emission scenario (worst case), noting that predicted changes shown below equate closely to RCP8.5 outputs which are now published but unavailable when the study was completed. By comparison, the data shown for Aitik Mine are based on RCP4.5 (middle scenario) for the 2000 to 2100 time-period.

Overall patterns and trends for the two mine sites show several similarities: 1) T and P data are indicative that future climate will be warmer and wetter at both stations, with increases being roughly 3 °C (T) and +25% (P) for each site by 2100; 2) T increases are apparent at both stations for all seasons, but the predicted T increase is greatest for winter (Dec, Jan, Feb; e.g., approximately 5 °C by 2100 for Coffee Gold); 3) plots for both Coffee Gold and Aitik Mines confirm predicted increases in seasonal precipitation by 2100, noting that P magnitude and increasing trends are greater for summer (Jun, Jul, Aug) and autumn (Sep, Oct, Nov) compared to winter (Dec, Jan, Feb) and spring (Mar, Apr, May).

Climate Datasets as Inputs to Mine Site Impact Models

Coffee Gold Mine

To generate a long-term climate record for the Coffee Gold Mine, daily climate data (i.e., T and P) from the mine site and a nearby regional station (McQuesten, YT) were assembled

to create monthly predictive relationships based on periods of overlapping data. Next, the regional station (predictor) and monthly predictive relationships (e.g., for T and P) were utilized to compute a 28-year, daily- synthetic climate record representative of the mine site. To span the full Project life (i.e., 2018 to 2100), the Coffee Gold climate record was looped three times to create an 84-year, daily- climate record.

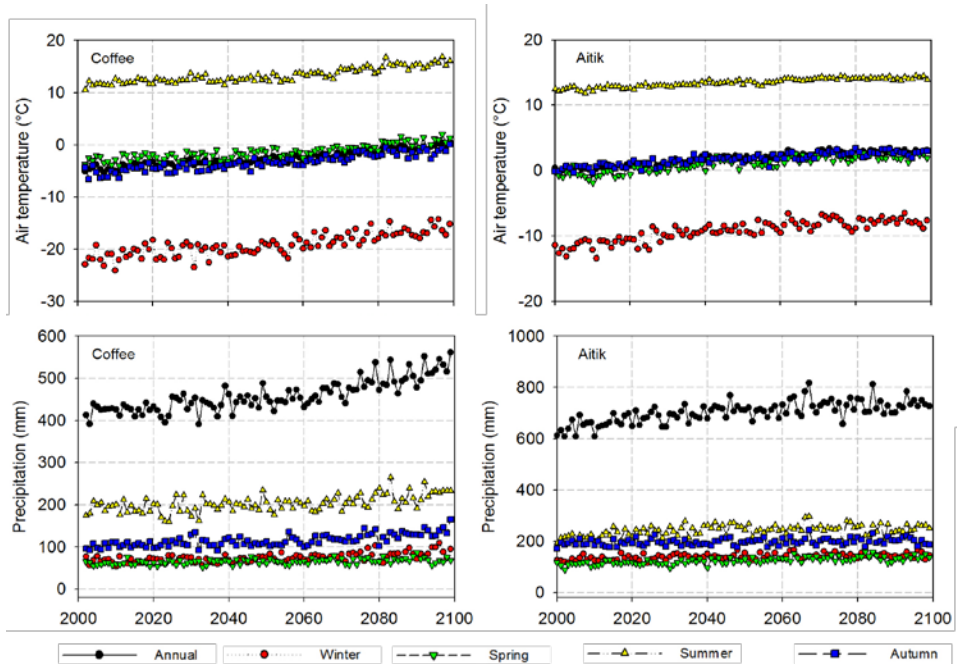


Figure 2 Climate change scenario data for the Coffee Gold Mine (left) and Aitik Mine (right). Predictions are shown for T and P to year 2100.

To represent a plausible future condition, climate change scenario data were downloaded from the Scenario Network for Alaska and Arctic Planning. Monthly T and P predictions (2001 to 2100, CMIP3/AR4 – A2 Scenario, 2 km resolution) for grid points covering the mine site extent were downloaded, averaged and then used to scale the 84-year daily climate record. The resultant time series (T and P shown) is shown in Figure 3 to illustrate the range of variability and trends with time (i.e., increasing T and P) that are inherent in the synthetic dataset.

Aitik Mine

For the Aitik Closure Plan, down-scaled, daily- and monthly future climate data for grid cell locations nearest to the mine site were available for download from the CORDEX data portal. Predicted air temperature and precipitation data for the four nearest grid cells to the mine site were downloaded and inspected to confirm consistency between points for RCP4.5. Once satisfied as to their consistency, daily climate data for the closest grid cell to the Aitik mine were downloaded for RCP4.5, EC-EARTH for key water balance variables:

e.g., wind speed; air temperature, precipitation, atmospheric pressure, specific humidity, energy balance terms and potential evaporation (computed using modified Penman-Monteith formulation). The downloaded climate data were used directly to represent the 2025 to 2100 timeframe. To extend the climate record to the year 2225, the data for the period 2065 to 2100 were repeated to cover the period from 2100 to 2225.

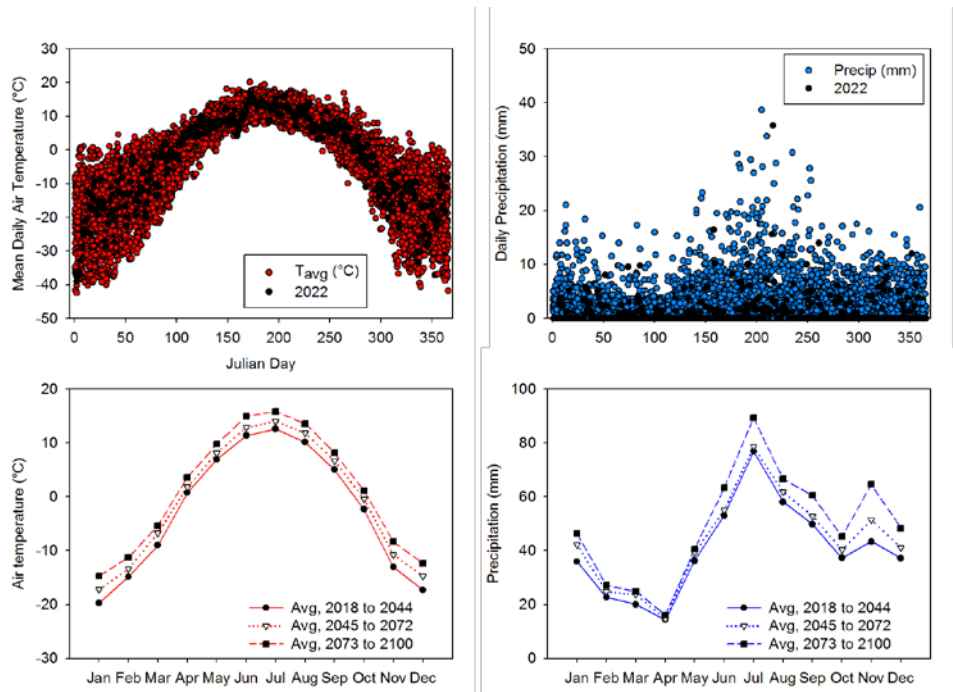


Figure 3 Time series data from the Coffee Gold Mine water balance model. In the upper portion of the figure, daily time series data (2018-2100; year 2022) are shown for T and P . In the lower two panels, monthly average T and P trends are shown for three time periods.

Management Considerations

Adopting Climate Change as Base Case – For both Coffee Gold and Aitik Mines, climate change was adopted as Base Case, rather than considering future climate change as a sensitivity analysis or a *posteriori* evaluation. In both Yukon Territory and Sweden, climate change scenario data are readily available to end-users and are easy to incorporate into mine impact models.

Expectations of Regulators, Stakeholders – Building climate change into mine site evaluations as Base Case can build trust with regulators and stakeholders. The Yukon Government for example, regularly reports on past, present and future climate trends and a general expectation for environmental assessment applications is a comprehensive consideration of climate change. Outright omission of climate change from a water modelling assessment would be potentially viewed as a notable regulatory submission gap.

Warmer and Wetter Climate Future – Assessments at Coffee Gold and Aitik indicate that warmer and wetter climate conditions will impart changes on the behaviour of mine facilities and adjacent receiving streams, compared to model outputs based on stationary (i.e., no trends) assumptions for climate conditions.

- For the Aitik Pit Lake model, warmer and wetter conditions returned a shorter fill time (by ~15 years) owing mainly to increased amounts of contact water (WRSF) and natural runoff generated by contributing areas adjacent to the pit. Higher rates of precipitation to the pit lake surface (with time and owing to a wetter future) also expedite filling, but potential gains are offset by enhanced rates of lake evaporation under future warmer conditions.
- For the Coffee Gold Project, the long-term rate of seepage from the reclaimed HLF following drain-down and closure is predicted to increase in magnitude through the Post-closure phase (2043-2100) of the Project. Further, assumed increases in precipitation to 2100 return increased production of contact water (e.g., pit wall runoff that reports to filling and spilling pit lakes; seepage that reports from the toe of the main WRSF proposed for the Project).
- Receiving stream assessments conducted for the two mine sites confirm the following runoff/streamflow changes under a warmer and wetter future climate regime: 1) progressive and earlier onset of freshet, later occurrence of autumn freeze up, and a longer ice-free season; 2) shifts with time to the proportions of P realized as rain vs. snowfall; 3) increases in baseflow conditions and likelihood of mid-winter melt events; and, 4) progressive increases in receiving environment flows with time.

Populating Models, Range of Variability and Future Trends – For northern environments that are predicted to be warmer and wetter in the future, there is clear value (i.e., regulatory acceptance; risk management for proponent) in demonstrating that closure plans and associated mitigations remain robust when tested against a broad range of climate conditions. While guided by single emission scenario (Coffee Gold) or RCP scenario (Aitik), daily climate inputs, that account for the full range of variability per parameter, were assembled and used to drive an array of mine impact models.

Conclusions

To drive hydrological and/or geochemical models, technical evaluations undertaken for the Coffee Gold Project and Aitik Mine required assembly of long-duration and forward looking climate datasets. Instrumental records at stations adjacent, or near, the two mine sites show evidence of increasing trends in air temperature and precipitation. Furthermore, downscaled climate change scenario indicate future climate will be warmer and wetter at both stations, with increases being roughly 3 °C (T) and +25% (P) for each site by 2100.

To ensure consistency with respect to the climate data used by the various modelling teams, a common climate dataset was assembled for each project that specifically accounted for

predictions of climate change for the local region. For the Aitik mine, closure plan assessments drew upon readily available and high-quality information generated by the SMHI and the Rossby Centre, including modelled daily climate data and runoff data specific to the site. In contrast, necessary climate inputs for the Coffee Gold Mine were synthetically generated by combining baseline, regional and downscaled climate change scenario data. The climate-water issues were unique to each mine site; however, robust management responses and defensible plans were successfully defined for Coffee Gold and Aitik Mines while considering climate change as Base Case.

Acknowledgements

The authors thank two anonymous reviewers who provided comments on an earlier draft of this paper. Baseline hydro-meteorology data for the Coffee Gold Mine was provided by Ken Nordin, Laberge Environmental Services – Whitehorse, YT.

References

- Fenech A, Comer C, Gough B (2007) Selecting a global climate model for understanding future projections of climate change. In: Fenech, A MacLellan J (Eds), *Linking climate models to policy and decision-making*, Toronto, Ontario: Environment Canada, 252 pp
- IPCC (2013) *Climate Change 2013: The Physical Science Basis*. In: Stocker TF, Qin D, Plattner GK, Tignor M, Allen SK, Boschung J, Nauels A, Xia Y, Bex V, Midgley PM (Eds), *Contribution of Working Group I to the Fifth Assessment Report of the Intergovernmental Panel on Climate Change*, Cambridge University Press, United Kingdom and New York, NY, USA, 1535 pp
- SMHI (2014) *CORDEX scenarios for Europe from the Rossby Centre regional climate model RCA4*. Report Meteorology and Climatology No. 116, Swedish Meteorological and Hydrological Institute, SE 601 76 Norrköping, Sweden, 84 pp

Integrated removal of inorganic contaminants from Acid Mine Drainage using BOF Slag, Lime, Soda ash and Reverse Osmosis (RO): Implication for the Production of Drinking Water

Vhahangwele Masindi^{1,2}, Muhammad Suhail Osman¹

¹Council for Scientific and Industrial Research (CSIR), Built Environment (BE), Hydraulic Infrastructure Engineering (HIE), P.O Box 395, Pretoria, 0001, South Africa, Tel: +2712 841 4107, Fax: +27128414847, VMasindi@csir.co.za,, MOsman@csir.co.za

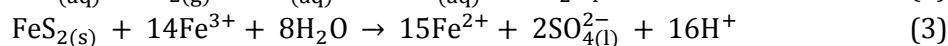
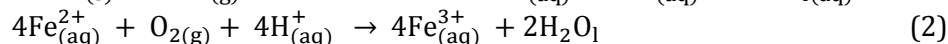
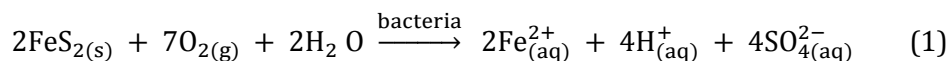
²Department of Environmental Sciences, School of Agriculture and Environmental Sciences, University of South Africa (UNISA), P. O. Box 392, Florida, 1710, South Africa, masindivhahangwele@gmail.com

Abstract This study evaluated the interaction of acid mine drainage (AMD) with Basic Oxygen Furnace (BOF) slag. The reaction proved that $\text{pH} \geq 10$, and 99% metals removal and 75% sulphate removal were achieved. Sulphate concentration was reduced from 18000 to 4000 mg/L hence requiring another purification technology. Hardness was reduced using lime and soda ash. Reverse Osmosis (RO) was used to further clean the water to drinking standard. A single pass two element RO system was simulated in Reverse Osmosis System Analysis (ROSA). The produced water complied with the South African National Standard (SANS) 241 Drinking Water Specifications.

Key words Acid mine drainage; Basic Oxygen Furnace (BOF) slag; inorganic contaminants; neutralization

Introduction

Sulphides bearing mineral exposed during mining activities are prone to react with water and oxygen during rainfall and underground leakages hence leading to the formation of acid mine drainage. In most instances, the formation of AMD can be represented by the following chemical equations (1 – 4) (Masindi 2016; Masindi et al. 2015c):



Due to the nature of a host rock, the resultant mine effluents is rich in Sulphate, Fe, Al, Mn and traces of other constituents (Clyde et al. 2016). For the interest of the public and environmental protection, this mine water need to be treated prior discharge (Pozo-Antonio et al. 2014). South Africa has advanced significantly in terms of mine water treatment (Masindi 2016). Mainly they rely on the use of raw limestone and lime for mine water treatment (Bologo et al. 2012; Maree et al. 2013), this technology has been successfully proven and it is commonly used in mining industries. The only limitation of limestone is partial removal

of contaminants from mine effluents and the limitation of reaching $\text{pH} \leq 7$ (Masindi et al. 2015a). Lime is very effective but cost factor limit its application because it is generated from calcination of limestone (Maree et al. 2013). Moreover, the generated sludge contains hazardous materials that can degrade the environment and pose serious health risk to aquatic and terrestrial organisms (Masindi et al. 2015c). To minimise the use of virgin materials for mine water treatment and to foster the process of sustainable development, several waste material had to be applied to remediate mine water. Masindi (2016) successfully used cryptocrystalline magnesite tailings for mine water treatment. Name and Sheridan (2014) used metallurgical slags for mine water treatment but they did not explore the chemistry thereof. Another study also explored the application of BOF slag for mine water treatment (Lee et al. 2016). This study, therefore, attempt to explore the chemistry of BOF slag and the resultant products and processed water after interacting with AMD. BOF slag is rich in Fe and Ca hence making it much easier to recover magnetite and gypsum (Belhadj et al. 2012). Geochemical model will be employed to point out the mineral phases that are likely to form during the interaction of BOF slag and AMD.

Materials and methods

Materials

BOF slag was collected from a Steel industry in South Africa. Field AMD samples were collected from a coal mine in Mpumalanga Province, South Africa. BOF slag samples were milled to a fine powder using a Retsch RS 200 vibratory ball mill for 15 minutes at 800 rpm. Thereafter, it was passed through a $32 \mu\text{m}$ particle size sieve to get the desired size. The samples were kept in a zip-lock plastic bag until utilization for AMD treatment.

Characterisation of aqueous samples

pH, Total Dissolved Solids (TDS) and Electrical Conductivity (EC) were monitored using CRISON MM40 portable pH/EC/TDS/Temperature multimeter probe. Aqueous samples were analysed using ICP-MS (7500ce, Agilent, Alpharetta, GA, USA). The accuracy of the analysis was monitored by analysis of National Institute of Standards and Technology (NIST) water standards.

Mineralogical, elemental and microstructural properties

Mineralogical composition of BOF slag and resulting solid residues was determined using XRD. Elemental composition was determined using XRF, the Thermo Fisher ARL-9400 XP+ Sequential XRF with WinXRF software. Morphology was determined using HR-SEM (JOEL JSM – 7500F, Hitachi, Tokyo, Japan). Crystallography and micrographs of cryptocrystalline magnesite were also ascertained using HR-TEM (JEM – 2100 electron microscope, Angus Crescent, Netherland).

Interacting BOF slag and AMD

Coal AMD samples were treated at optimized conditions in order to assess the effectiveness of BOF slag. This is a succession study from a study that focused on the chemistry of AMD post contacting the BOF slag. The resultant solid residue after treatment of field AMD was

characterized in an attempt to gain an insight as to the fate of chemical species. Name and Sheridan (2014) reported that the optimum conditions for remediation of acid mine drainage using BOF slag is 60 min of shaking time and 100g/1 L S/L ratios. Jafaripour et al. (2015) reported that 15 mins was enough for the removal of heavy metals from acid mine drainage using BOS sludge. For the purpose of this study 60 mins and 100g/1 L S/L ratios will be used to determine the efficiency of BOF slag for high sulphate and Fe-rich coal mine water.

ROSA membrane analysis

Permeate Flux reported by ROSA is calculated based on ACTIVE membrane area. Reverse Osmosis System Analysis for FILMTEC™ Membranes, ROSA version 9.1 Configuration with DB U399339_359.

Proposed AMD treatment network

The schematic presentation of the BOF, lime, soda ash and RO treatment is shown in fig. 1.

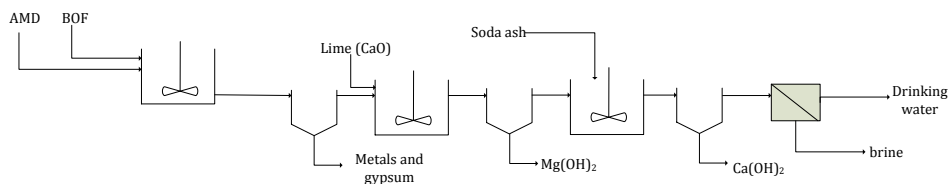


Figure 1 Schematic presentation of the proposed treatment process

Results and discussion

Production of drinking water using BOF slag and Reverse Osmosis system

The chemical profile of raw coal AMD, BOF reacted-AMD, lime and soda ash softened water, and DWS/SANS standards is shown in tab. 1.

The initial pH of acid mine drainage was 7.5 prior treatment hence indicating that there was potential neutralisation of mine water by natural processes (tab. 2). After contacting the BOF slag with AMD at 100g/1L solid to liquid ratio the pH increase to 13, thereafter, the introduction of lime and soda ash showed no difference in the residual pH. An increase in pH was directly proportional to alkalinity which increased from 20 to 1995 after contacting the BOF slag. It was insignificantly increased to 2004 and 2090 after adding lime and soda ash respectively. Total dissolved solids (TDS) and Electrical Conductivity (EC) were also directly proportional; this may be attributed to dissolution of neutralizing agents thus releasing elements to water. Thereafter, the introduction of lime and soda ash did not have impacts on the TDS and EC hence that some elements were being removed in each stage approach. Lime was added to remove sulphate and soda ash was added to remove the Ca. The total hardness was observed to be high in the Gold mine water (>1500), after contacting the BOF slag, it was observed to have increased hence indicating possible dissolution of Ca and Mg species and mineral phases. The levels of metal species were observed to have decreased after contacting all the neutralising

agents. The reduction of Fe and other chemical species may also be described by the potential formation of magnetite. Sulphate was also observed to have decreased after contacting the BOF slag hence indicating the possibility of gypsum recovery. Similar results were obtained by Masindi et al. (2015). All the parameters complied with SANS 241 water quality guidelines except for sulphate, cobalt, and sodium. Alkalinity, EC, and TDS were also above the prescribed limits. After using the ROSA software for cleaning up the water from BOF slag, Lime and soda ash, the resultant water quality water meeting the prescribed limits as recommended by the SANS 241 water quality guidelines (tab. 2).

Table 1 Chemical profile of raw coal AMD, BOF reacted-AMD and DWS/SANS standards

Parameters	AMD	BOF	Lime	Na ₂ CO ₃	Units	SANS standards
Alkalinity CaCO ₃ as Mg/L	<5.0	11	2004	2090	mg/L	≤120
pH (25°C)	2	8	13	13	-	≥5 to ≤9.7
Electrical Conductivity (EC)	960	470	800	920	mS/cm	≤170
Total Dissolved solids (TDS)	36000	13000	4300	4600	mg/L	≤1200
Total Hardness	3131	5080	3200	<0.5	mg/L	-
Aluminium	500	<0.70	<0.5	<0.5	µg/L	≤300
Iron	6000	<0.80	<0.5	<0.5	µg/L	≤300
Manganese	125	20	<0.5	<0.5	µg/L	≤100
Sodium	30	50	200	2000	mg/L	≤200
Potassium	2	10	20	20	mg/L	≤20
Calcium	500	800	1300	<0.5	mg/L	≤300
Magnesium	480	700	<0.5	<0.5	mg/L	≤400
Cobalt	25	<0.35	40	30	µg/L	≤0.2
Copper	1.5	<0.40	<0.5	<0.5	µg/L	≤2000
Lead	5	<0.10	<0.5	<0.5	µg/L	≤10
Nickel	30	<0.40	<0.5	<0.5	µg/L	≤70
Zinc	200	<0.60	<0.5	<0.5	µg/L	≤5
Cadmium	10	<0.20	<0.5	<0.5	µg/L	≤3
Silicon	30	1.5	0.1	0.3	mg/L	≤6
Sulphate	18000	4570	2000	2000	mg/L	≤500

Table 2 Chemical profile of RO cleaned water and DWS/SANS 241 water quality standards

Name	Pass Streams (mg/L as Ion)					SANS standards
	Feed	Adjusted Feed	Concentrate Stage 1	Permeate		
				Stage 1	Total	
NH4+ + NH3	0.00	0.00	0.00	0.00	0.00	≤ 1.5
K	9.50	9.50	13.33	0.57	0.57	≤20
Na	54.00	54.00	75.82	3.09	3.09	≤200
Mg	723.00	723.00	1029.92	6.87	6.87	≤400
Ca	844.01	844.01	1202.39	7.77	7.77	≤300
Sr	0.00	0.00	0.00	0.00	0.00	≤6
Ba	0.00	0.00	0.00	0.00	0.00	≤0.5
CO3	0.64	0.64	1.56	0.00	0.00	≤-
HCO3	427.03	427.03	603.79	11.71	11.71	≤-
NO3	0.00	0.00	0.00	0.00	0.00	≤1
Cl	69.23	69.34	97.32	4.04	4.04	≤5
F	0.00	0.00	0.00	0.00	0.00	≤1.5
SO4	4569.98	4569.98	6512.11	38.38	38.38	≤500
SiO2	1.50	1.50	2.12	0.05	0.05	≤6
Boron	0.00	0.00	0.00	0.00	0.00	≤2.4
CO2	70.30	70.30	70.75	70.21	70.19	≤-
TDS	6698.90	6699.01	9538.38	72.47	72.47	≤1200
pH	6.70	6.70	6.80	5.42	5.42	≤5 to 9.7

Elemental composition of raw BOF slag and the resultant residues

The elemental composition of raw BOF slag and AMD-reacted BOF slag is reported in tab. 3.

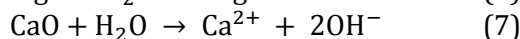
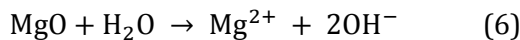
Table 3 Elemental composition of raw BOF slag and AMD-reacted BOF slag

Elements	Raw BOF slag	AMD-Reacted BOF slag
SiO ₂	13.52	11.28
TiO ₂	0.35	0.28
Al ₂ O ₃	7.78	7.59
Fe ₂ O ₃ (t)	25.81	28.55
MnO	4.37	3.60
MgO	7.16	5.91
CaO	38.41	29.69
Na ₂ O	0.33	0.20
K ₂ O	0.04	0.03
P ₂ O ₅	1.198	0.963
CoO	<0.001	0.002
Cr ₂ O ₃	0.168	0.111
CuO	<0.001	0.003
NiO	0.007	0.014
PbO	0.017	0.017
SO ₃	0.608	9.69
V ₂ O ₅	0.128	0.102
BaO	0.019	0.015
ZnO	0.005	0.037
LOI	-0.19	1.97
Total	99.70	100.04
H ₂ O	0.54	7.13

The XRF results revealed that the raw BOF slag consist of Ca, Fe, Si, Al, Mg and Mn as major components. Ca was available at elevated concentration as compared to the rest. After contacting the AMD, the level of alkali and earth alkali metals went down hence indicating dissolution of base cations. Base metals lead to an increase in pH hence precipitating the metals as hydroxide as indicated in the equation below (equation 5).



The dissolution of base cations from BOF slag may be represented by the following equations (Masindi et al. 2015d):



This may lead to an increase in the pH of the aqueous system with the subsequent precipitation of chemical species. An increase in pH of the product water may be due to dissolution of traces of silicates as shown by XRD and XRF and the release of Mg, Ca and Na as revealed by XRF and EDS may also contribute to an increase in pH. Silicate will react with acidity in AMD through ion exchange and partial dissolution hence leading to an increase in pH (Masindi et al. 2015b).



After reacting BOF slag with AMD, the content of S and Fe went up hence indicating possible attenuation of these chemical species from water. This could better be explained by the water quality.

Conclusions

This study further validated that BOF slag can be used for the treatment of very acidic, and metalliferous mine water with a literature breaking sulphate concentration. Reaction of BOF slag and coal mine water led to an increase in pH (≥ 10) and a significant reduction in inorganic species concentrations. Attenuation of sulphate, Al, Mn, Fe and other chemical species was observed to be optimum at 60 min of agitation at S: L ratio of 1 g: 100 mL. Under these conditions, the pH achieved was ≥ 10 , which is suitable enough for metal removal. From This study has further verified that BOF slag has the potential of neutralizing the acidity and attenuating toxic chemical species from coal mine water. The residual alkaline earth metals and sulphate were removed using reverse osmosis (RO) as simulated by ROSA simulation software and the produced water meet the drinking water quality. As such, this study proved that the coupling of RO process to BOF slag and different softeners will produce water of drinking standard.

Acknowledgements

The authors wish to express their sincere gratitude to the Council for Scientific and Industrial research (CSIR), Tshwane University of Technology for providing lab space to execute this research work. The authors would also like to thank National Research Foundation (NRF) for sponsoring this project.

References

- Belhadj E, Diliberto C, Lecomte A (2012) Characterization and activation of Basic Oxygen Furnace slag. *Cem Concr Compos* 34:34-40, doi:10.1016/j.cemconcomp.2011.08.012
- Bologo V, Maree JP, Carlsson F (2012) Application of magnesium hydroxide and barium hydroxide for the removal of metals and sulphate from mine water. *Water SA* 38:23-28
- Clyde EJ, Champagne P, Jamieson HE, Gorman C, Sourial J (2016) The use of a passive treatment system for the mitigation of acid mine drainage at the Williams Brothers Mine (California): pilot-scale study. *Journal of Cleaner Production* 130:116-125, doi:10.1016/j.jclepro.2016.03.145
- Jafaripour A, Rowson NA, Ghataora GS (2015) Utilisation of residue gas sludge (BOS sludge) for removal of heavy metals from acid mine drainage (AMD). *Int J Miner Process* 144:90-96, doi:10.1016/j.minpro.2015.10.002
- Lee W-C, Lee S-W, Yun S-T, Lee P-K, Hwang YS, Kim S-O (2016) A novel method of utilizing permeable reactive kiddle (PRK) for the remediation of acid mine drainage. *J Hazard Mater* 301:332-341, doi:10.1016/j.jhazmat.2015.09.009
- Maree JP, Mujuru M, Bologo V, Daniels N, Mpholoane D (2013) Neutralisation treatment of AMD at affordable cost. *Water SA* 39:245-250
- Masindi V (2016) A novel technology for neutralizing acidity and attenuating toxic chemical species from acid mine drainage using cryptocrystalline magnesite tailings. *Journal of Water Process Engineering* 10:67-77, doi:10.1016/j.jwpe.2016.02.002
- Masindi V, Gitari MW, Tutu H, De Beer M (2015a) Passive remediation of acid mine drainage using cryptocrystalline magnesite: A batch experimental and geochemical modelling approach. *Water SA* 41:677-682, doi:10.4314/wsa.v41i5.10
- Masindi V, Gitari MW, Tutu H, DeBeer M (2015b) Efficiency of ball milled South African bentonite clay for remediation of acid mine drainage. *Journal of Water Process Engineering* 8:227-240, doi:10.1016/j.jwpe.2015.11.001
- Masindi V, Gitari MW, Tutu H, DeBeer M (2015c) Synthesis of cryptocrystalline magnesite-bentonite clay composite and its application for neutralization and attenuation of inorganic contaminants in acidic and metalliferous mine drainage. *Journal of Water Process Engineering*, doi:10.1016/j.jwpe.2015.11.007
- Masindi V, Gitari MW, Tutu H, DeBeer M (2015d) Synthesis of cryptocrystalline magnesite-bentonite clay composite and its application for neutralization and attenuation of inorganic contaminants in acidic and metalliferous mine drainage. *Journal of Water Process Engineering*, doi:10.1016/j.jwpe.2015.11.007
- Name T, Sheridan C (2014) Remediation of acid mine drainage using metallurgical slags. *Miner Eng* 64:15-22, doi:10.1016/j.mineng.2014.03.024
- Pozo-Antonio S, Puente-Luna I, Lagüela-López S, Veiga-Ríos M (2014) Techniques to correct and prevent acid mine drainage: A review. *DYNA (Colombia)* 81:73-80

Aquifer ReInjection Scheme for Excess Mine Water: Design Methodology and Outcomes

Grace Yungwirth¹, Ed Austin², Martin Preene³, Flann Corcoran¹, Joanna Birch¹

¹*Golder Associates (UK) Ltd., Suite 9.10, 20 Eastbourne Terrace, London, W2 6LG, UK,
Gyungwirth@golder.com, fcorcoran@golder.com, jbirch@golder.com*

²*Golder Associates (UK) Ltd., Sirius Building, The Clocktower, South Gyle Crescent,
Edinburgh, EH12 9LB, UK, eaustin@golder.com*

³*Preene Groundwater Consulting, 18 Berry Lane, Horbury, Wakefield, West Yorkshire,
WF4 5HD, UK, mp@preene.com*

Abstract Groundwater reinjection systems represent a potential technique in mine water management to: (1) reduce the need for surface discharge or other management processes for excess mine water; and (2) reduce stress on local groundwater resources caused by net abstraction of groundwater. Reinjection systems, through managed aquifer recharge, can help achieve a more sustainable development whereby clean water is returned to the local catchment.

This case study illustrates a method for quantifying requirements for reinjection arrays as part of a mine water management system, where aquifer characteristics including groundwater depth, permeability and lateral extent will vary.

Key words Mine Water, ReInjection, groundwater, sustainability, managed aquifer recharge

Introduction

The controlled reinjection (RI) of water to an aquifer, or managed aquifer recharge, can provide an opportunity for improvements to sustainability in mine operations by reducing the discharge to surface of groundwater arising from dewatering, thus minimising the wastage of finite water resources. Such schemes are not without their challenges, however. The choice of land available for RI at mine properties is often limited, with uncertain and variable characteristics and properties related to topography, groundwater depth, expected RI well performance, and receiving aquifer permeability.

Such RI schemes commonly make use of multiple RI well arrays within the mine property. A successful scheme will require site-specific data to inform the design to achieve the water management objectives. Site-specific challenges must be addressed in the design of the RI testing programme which will feed into the design calculations. This paper presents a case study based on a mine in Europe to demonstrate the challenges associated with the design, testing and assessment of a RI scheme.

Reinjection Scheme Concept

The objective of a groundwater RI scheme is to route excess clean water sourced from mine water sources to a RI wellfield so that it can be injected and returned to the local aquifer system. Appropriate mine water sources are typically clean groundwater sourced from dewatering activities. Dirty mine water, or “contact water”, would be managed by a separate system and is not considered in this discussion.

RI Test Design Considerations

Key factors in the design of a hydrogeologic test programme for a RI system include:

1. A hydrogeology test methodology tailored and adapted to site conditions;
2. Availability of adequate monitoring locations (water levels and climate records);
3. Careful control of the water delivery system to ensure consistent inflow rates;
4. Avoidance of air intrusion within injected water; and
5. Sufficiently long RI test duration.

1. Hydrogeology Test Methodology Tailored and Adapted to Site Conditions

Factors to consider when designing an appropriate hydrogeology test programme include:

- (a) Using all testor monitoring locations to characterise heterogeneous aquifers;
- (b) Considering use of conventional testing techniques (e.g. packer or pumping tests), which may be more practical to undertake than injection testing to supplement the aquifer test dataset;
- (c) Allowing for site topography and access in the layout of the test array; and
- (d) Allowing for access to a water supply to feed the test array during RI testing. This includes routing of supply piping, sourcing water from pumping wells distant enough not to affect the RI test results, and sourcing water of similar quality to that to be used in the permanent RI system.

2. Availability of Adequate Monitoring Locations (Water Levels and Climate Records)

Installation of monitoring wells is a cost to the project and may not be considered of high value to an operator trying to minimise drilling costs. However, monitoring at the RI wells alone may not be sufficient to determine aquifer performance, particularly in space-limited or bounded environments. Monitoring locations separate to the RI wells can be incorporated into the permanent performance monitoring system of the RI wellfield, thereby limiting project cost. Adequate pre- and post-test monitoring data should also be collected along with seasonal and test-specific rainfall records to understand both the unsaturated depth to groundwater and the effect of rain events on the natural and induced groundwater table.

3. Careful Control of Water Delivery System to Ensure Consistent Inflow Rates

Feeding the RI wells by gravity may present challenges in maintaining a constant and controlled flow rate during the test period, particularly in locations of varying topography. Upstream control of hydraulic head on the feed pipeline may be required. In the current case study, this challenge was addressed by using a header tank placed near to the RI test wells. This acted as a buffer to short-term changes in flow rates from the water source, as well as mechanism for more discrete control of the driving heads.

4. Avoidance of Air Intrusion Within Injected Water

Entrained air within the RI well feed water can promote well clogging by leading to air entrainment in the RI well pack or precipitation of dissolved minerals causing well clogging

(Pyne, 1994). Both have the effect of reducing well efficiency. This can be mitigated by fitting valves and outlets that allow flushing of the feed lines and headworks of air prior to introduction of the water to the RI test well. Sealed headworks, if used, require additional care to control air within the system. Drop tubes should be installed within the RI wells to minimise turbulent flow causing air entrainment when the water is injected.

5. Sufficiently Long RI Test Duration

Test duration should ideally be sufficient to (a) observe the effects of any hydraulic boundaries, (b) observe superposition effects from adjacent RI wells, and (c) assess changes in well performance over time. Often it is not possible to run long term tests during preliminary design phases, however, they should be planned to run for as long as practicable. Access to water supply to feed the injection wells may factor into the test duration planning. Longer term assessment can continue during commissioning of the RI arrays which can lead to design revisions during construction.

Case Study – Reinjection System Testing and Design for Mine Water Management

This paper examines the process of developing a clean water RI scheme on a mine site in Europe. The practical challenges associated with the RI test site included the following:

- The aquifer to be dewatered and reinjected into is a fractured rock aquifer which had not previously been characterised in detail;
- Expected aquifer anisotropy and heterogeneity;
- Space-limiting topography within mine property, causing challenges for well placement and limited access to test locations;
- Placement of wells is limited laterally necessitating linear array layouts;
- Limited thickness of unsaturated zone at some locations, resulting in constraints on water level rise during reinjection; and
- Challenging logistics for water delivery to the RI test sites requiring a complex network of piping.

The testing programme was designed to address these challenges as discussed below.

RI Test Array Construction and Hydrogeology Testing

A series of RI wells were constructed to test the RI area. These wells were expected to be utilised for both testing and as part of the site permanent RI system. Wells were drilled at 300 mm diameter to a depth of either 150 to 300 m below ground level, dependant on geology, and completed with filter packs and 200 mm diameter well screens. To observe groundwater level response, monitoring wells were constructed near to the RI wells to equivalent depths. Where possible, the RI wells were located in pairs to form array locations. Typically the test arrays were constructed along a valley side road as indicated in Figure 1.

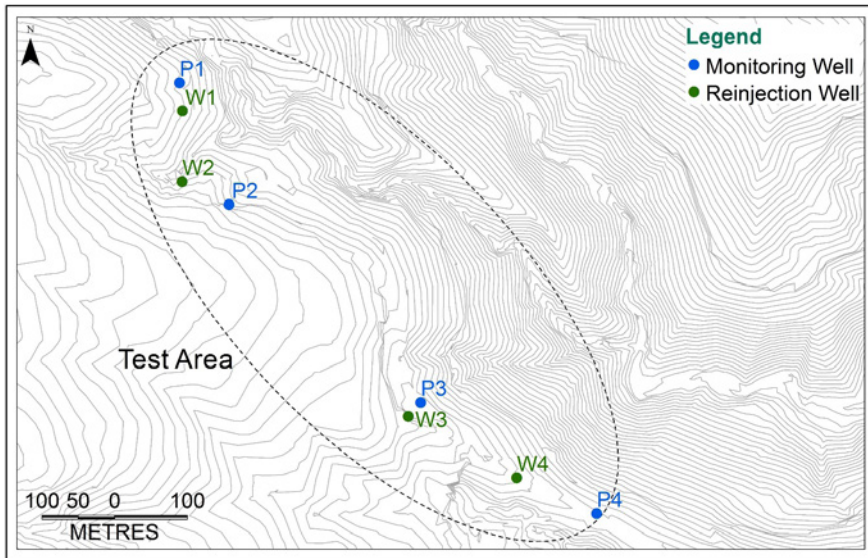


Figure 1: Plan view of typical layout of reinjection test arrays.

As the area had not yet been hydrogeologically characterised, a series of hydrogeologic tests were undertaken in both the RI wells and monitoring wells. A summary of the testing performed is presented in Table 1. Water for the testing activities was sourced from groundwater abstraction wells distant to the test array transmitted by 100 mm diameter pipe.

Typical results from the RI testing are presented in the Analysis and Evaluation Section below.

Analysis and Evaluation

A summary of results from all tests conducted is as follows:

- Packer Tests: estimated bulk K of 10^{-6} m/s to 10^{-8} m/s;
- Well performance: specific capacity of up to 7.5 m³/hr/m for abstraction and 4.5 m³/hr/m for injection; and
- Aquifer analyses: estimated T of up to 400 m²/d.

Typical results from the RI testing are presented in Figure 2 and Figure 3.

In several of the tests the results suggested the presence of hydraulic barrier boundary conditions. Some tests also showed incomplete recovery of groundwater levels with recovery to levels significantly higher than pre-test conditions, suggesting the filling of storage in a bounded aquifer. Both of these observations are potentially problematic for an RI system as groundwater levels could rise more quickly than anticipated or the volume of water which can be injected could be limited by the filling of bounded aquifer storage. RI well performance could also be impacted by weather conditions. Heavy rainfall events during the test

period were shown to influence shallow groundwater levels. Higher groundwater levels reduce both the available injection head and the thickness of the unsaturated zone, which can make injection wells less effective.

Table 1 Hydrogeologic Test Phases Conducted

Hydrogeology Test Type	Test Description	Analysis and Evaluation
Monitoring Well Testing		
In-situ packer tests	Falling head and constant rate tests during construction	Analysed to obtain aquifer parameters – Transmissivity (T) & Hydraulic Conductivity (K)
Reinjection Well Testing		
Step Tests	To assess capacities and sustainable pumping rates for subsequent tests	Analysed to obtain aquifer parameters – T & K Well performance assessment
Constant Rate Pumping Tests with Recovery	Minimum of 24 hours pumping from RI wells.	Analysed to obtain aquifer parameters – T & K, to assess boundary conditions, and well performance
Injection Step Tests	To assess capacities and sustainable injection rates for subsequent tests	Analysed to obtain aquifer parameters – T & K Well performance assessment
Constant Rate Injection Test with Recovery	Continuous and constant gravity-fed injection of pumped groundwater into RI wells for minimum of 48 hours	Analysed to obtain aquifer parameters – T & K, to assess boundary conditions, and well performance

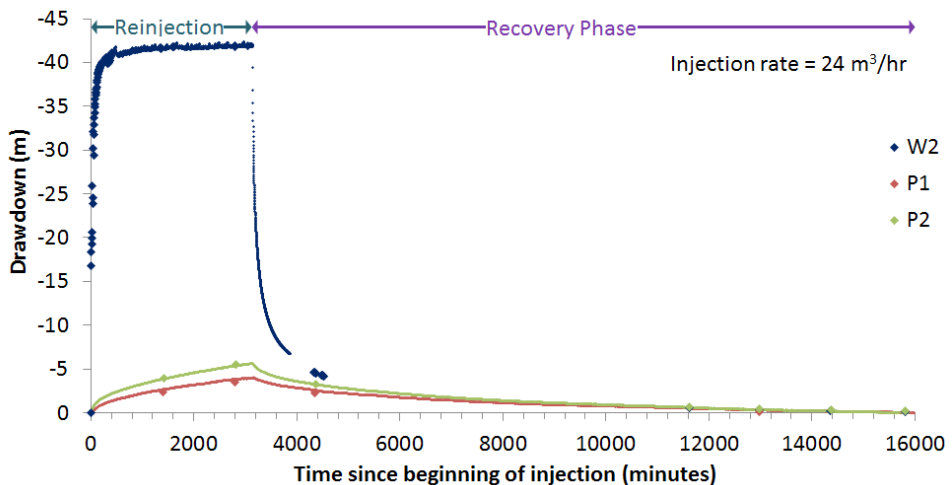


Figure 2: Typical Reinjection Test with Recovery Phase – negative drawdown indicates water level rise.

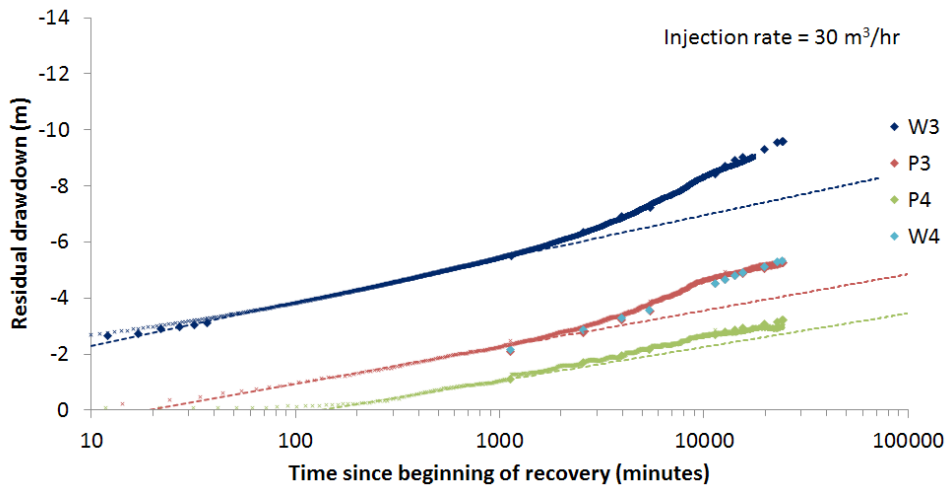


Figure 3: Typical Plot of ReInjection Test Recovery Phase as residual drawdown versus time (log scale) – negative drawdown indicates water level rise.

RI testing suggests that long-term RI may be possible for clean water disposal at the project site. RI into an individual RI well is likely to affect the performance of nearby RI wells in an array of multiple RI wells. Longer duration RI trials were recommended to further investigate the presence of barrier boundary conditions and well performance.

Design Calculations and Key Performance Factors

Design calculations for the array of multiple RI wells proposed for the full scheme were based on the principle of superposition of drawdown (Preene *et al.* 2016), using best-case (where the rise in groundwater levels resulting from a given injection rate was relatively low) and worst-case (where the rise in groundwater levels resulting from the same injection rate was higher) responses to RI extrapolated from field test data from individual wells. Specific drawdown curves from RI data were extrapolated to two years of injection to support the development of these scenarios. Using this method, various RI well array layouts were considered for the short- and long-term phases of mine operation, which had differing water management requirements. A highest permissible groundwater level was applied in the design as a constraint on injection rates and well spacing. The highest permissible groundwater level was typically set to avoid water levels close to the RI wells rising to within 10 m of ground level.

The method identified the likely number of RI wells and well spacing required to enable RI at the desired rate in various phases of the mine operation under best- and worst-case scenarios. In the course of the design an understanding was developed of the optimal balance between RI well numbers and spacing.

Several performance factors proved to be key to the design calculation and should be assessed during the testing phase. These are summarised in Table 2.

Table 2: *Reinjection Scheme Key Performance Factors*

Aquifer Characteristics	Wellfield Design Criteria
<ul style="list-style-type: none"> • Pre-injection depth to groundwater table • Hydraulic conductivity and anisotropy • Aquifer lateral extent • Presence and location of hydraulic boundary conditions • Aquifer response to weather events 	<ul style="list-style-type: none"> • Well efficiency and rate of decrease over time • Potential range of suitable well spacing • Potential well interaction/ superposition effects

Ongoing monitoring and assessment on commissioning should be used to refine the system design and for maintenance and operational control.

Conclusions

Reinjection wellfields can be used to limit the amount of groundwater to be managed by other means within the mine water management plan. This paper has discussed design of a testing programme to determine design parameters for a Reinjection array. The case study discussed demonstrates the successful testing and assessment of a reinjection scheme in a complex and anisotropic aquifer dominated by discrete features. Design of the reinjection system based on this test work must consider key performance factors including aquifer characteristics and wellfield performance criteria. System design calculations should consider available land constraints and incorporate best- and worst-case scenarios for well and aquifer conditions.

References

- Preene, M. Roberts, T.O.L. and Powrie, W. (2016). *Groundwater Control – Design and Practice*, 2nd Edition. Construction Industry Research and Information Association, CIRIA Report C750, London.
- Pyne, R D G (1994). *Groundwater Recharge and Wells: A Guide to Aquifer Storage Recovery*. Lewis Publishers, Boca Raton.

Important Characteristics of Membranes for Reliable Water and Wastewater Processes for Discharge and Re-use

Pete O'Connell, *Pall Water, Cortland, NY, USA*

Tim Lilley, Pall Corporation, Portsmouth, UK

Abstract Treatment of raw water for operations and wastewater poses many challenges. Raw water often contains constituents such as particulates, organics and minerals that can make it unsuitable for potable, process re-use or discharge. Mine wastewater from operations and domestic applications can contain contaminants that require ever more stringent removal standards. A previous IMWA paper (Lilley, 2013) addressed ways operators can use membrane technology to economically treat wastewater for discharge or process re-use. This paper addresses low pressure membrane characteristics and how the various materials, manufacturing techniques and chemical compatibilities play a role in the performance, longevity, and ultimate selection.

Key words microfiltration, membrane, water treatment

Introduction

The use of low pressure membranes has gained acceptance as an economical and robust method to treat raw and wastewater sources. The demand for higher quality incoming water and stricter discharge regulations are driving the trend toward membranes. This is true whether the low pressure membranes are used as pre or post treatment to other processes. Membranes provide excellent removal of coagulated or precipitated solids, as well as protecting high pressure, semi-permeable membranes such as Nano-Filtration (NF) or Reverse Osmosis (RO) products. The material and manufacturing process greatly affects the suitability of various membranes for these uses.

Low pressure hollow fiber membranes have been on the market for well over 25 years and improvements have been made in composition and manufacturing, resulting in increased durability, chemical compatibility and porosity. Knowledge of the various types of products on the market, their strengths and advantages, and their field experience is vital in applying membranes correctly.

Membrane characteristics

Low Pressure (LP) membranes separate suspended particulate matter from water. High pressure membranes (NF, RO) separate dissolved solids from water (Lorch, 1981). LP membranes are usually configured as small, polymeric hollow fibers, potted together to form modules, which are assembled on racks to accommodate the required flows. They can be operated pressurized or as submerged under partial vacuum. Flow paths can be inside-out or outside-in. The choice of operating modes should be fully evaluated as several factors will affect the economics and effectiveness.

Hollow Fiber membranes are generally classified as Microfiltration (MF) or Ultrafiltration (UF). While the exact definitions of these terms are somewhat vague and the ranges overlap,

MF for water treatment is usually in the 0.05 – 1.0 micron range while UF is typically measured in Molecular Weight Cut Off (MWCO) and the pores range from about 50 to 150 kilo Dalton (kD) when used in the water industry. Table 1 shows the approximate relationship between these numbers and ranges.

Table 1 Comparative pore size measurements and membrane classification

Particle Size (Microns)	10^{-4}	10^{-3}	10^{-2}	10^{-1}	10^0	10^1	10^2	10^3
Approx. Molecular Wt. (Dalton)	100	200	20,000	100,000	500,000	~	~	~
Membrane Classification			UF		MF			

Membrane materials

Hollow Fiber membranes can be manufactured from a number of materials, but most used to treat water are polymeric in nature; manufactured from a host of plastics but most commonly the following:

- Polyvinylidene Fluoride (PVDF)
- Polysulfone (PS)
- Polyacrlonitrile (PAN)
- Polyethersulfone (PES)
- Polyvinyl Chloride (PVC)
- Polypropylene (PP)

There are some ceramic based membranes on the market that can have niche applications and are being introduced to the general water treatment market, but the high initial cost has limited their desirability and acceptance.

One membrane in the market is constructed of polysulfone (PS), often used in the biopharmaceutical industry as they are tolerant of higher temperatures and can be heat sterilized. PS membranes are typically used for very fine particulate filtration, with some reaching the 6,000 MWCO range which can remove organics and long chain hydrocarbons. These membranes are typically not specified for wastewater applications due to durability limitations. PS membranes in the range of 6 – 30 kD are often intended for ultrapure water applications.

Membranes composed of polyethersulfone (PES) are more common in potable and wastewater applications, but a chlorine restriction of 200,000 ppm-hr may limit effectiveness on difficult feed sources where extensive cleaning is required.

PVDF polymeric membranes have become the material of choice in the US and other regions for drinking and waste water markets due to their high tolerance for cleaning chemicals and oxidizers used extensively in those applications. Mining is no exception as the use

of a variety of coagulants, oxidants and cleaning chemicals are necessary for optimal operation. An installation in the tar sands in Alberta Canada recovered the condensate from stripping operations and the PVDF membranes had to be cleaned with a commercial degreaser. Despite this harsh use, the membranes had a useful life of more than 6 years. Figure 1 shows the molecular structure of PVDF. This fluorocarbon compound, if optimally processed into hollow fibers, makes a product especially resistant to high and low pH chemicals.

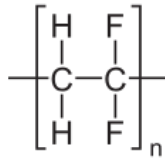


Figure 1 Molecular Structure of Polyvinylidene Fluoride

Hollow Fiber membrane manufacturing

Since PVDF is rapidly becoming the preferred membrane, it is important to understand the available manufacturing techniques. These can be responsible for major differences in membrane performance and life.

Most PVDF, UF membranes are produced by the Non-solvent Induced Phase Separation (NIPS) method. Here the PVDF-solvent solution, as it leaves the fiber producing equipment, is immersed in a non-solvent, usually water, where the solvent is exchanged for the non-solvent, leaving the water in the solidifying fiber and the solvent in the bath (Lloyd, 1990).

MF fibers can be produced by this process, but using a Thermally Induced Phase Separation (TIPS) method produces a membrane with higher porosity, strength, and chemical resistance. This is due to the high crystalline PVDF resulting from this method. In this process, semi-crystalline PVDF is solidified by removing the thermal energy from the solution. Table 2 compares these methods. Generally speaking, it is more common to produce MF membranes using the TIPS method.

Table 2 Effects of Membrane Spinning Methods on the Physical and Chemical Strength of PVDF Membranes

Membrane Type	Pore Size	Spinning Method	Characteristics
Ultrafiltration Membrane	<0.01 – 0.01 micron	Non-solvent Induced Phase Separation (NIPS)	Generally, both physical and chemical strength is weak
Microfiltration Membrane	0.05 – 1.0 micron	NIPS	Physical and chemical strength weak
Microfiltration Membrane	0.05 – 1.0 micron	Thermally Induced Phase Separation (TIPS)	Physical and chemical strength is strong

Structure of PVDF membranes

The TIPS process results in a membrane that can be operated at a higher flow per unit area (flux), a very symmetrical structure, and superior chemical resistance. The bonds of the plastic structure are very solid, producing a long lasting membrane. Even on raw surface water the TIPS membranes have been proven to last up to 15 years in service, compared to an average life of 5-7 years for some NIPS fibers.

Chemical Tolerance of PVDF membranes

Figure 2 shows the results of testing by Asahi of NIPS and TIPS fibers (Liu, 2007). A chemical compatibility soak was performed that showed the TIPS fibers could withstand a high pH solution proven to be very successful process cleaning product in remove organics from the fibers, including certain fats, oils and greases, often found in municipal and mining waste waters. The elongation retention is a measurement fiber ductility as compared to new.

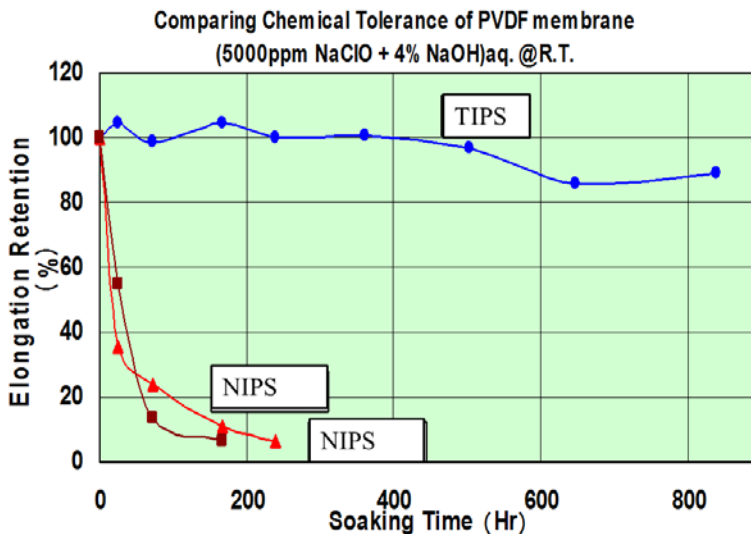


Figure 2 Chemical tolerance of differing manufacturing methods of PVDF membranes

Ultra or Micro Filtration?

The differences in pore sizes for the two categories of Hollow Fiber filtration was presented in Table 1 above. The choice of UF or MF for mine process, drinking and waste water depends on many factors, including regulations (much of Europe for instance, require UF for drinking water treatment), particulate size of the contaminants to be removed and the need for aggressive cleaning of the membrane to remove particles and other foulants that are being removed from the stream.

Removal ratings however are very similar between the two membranes, so unless the elimination of virus or similar sized particles is necessary, a TIPS Microfiltration membrane is usually the better choice due to the robust nature product due to the material and manu-

facturing process. If coagulation is used before the MF, additional fine particles, including viruses can be removed. The coagulated solids can be settled out or removed directly by the membranes. A settleable floc is not necessary if membranes are employed. Table 3 shows the removal performance of MF and UF for drinking water pathogens and other solids.

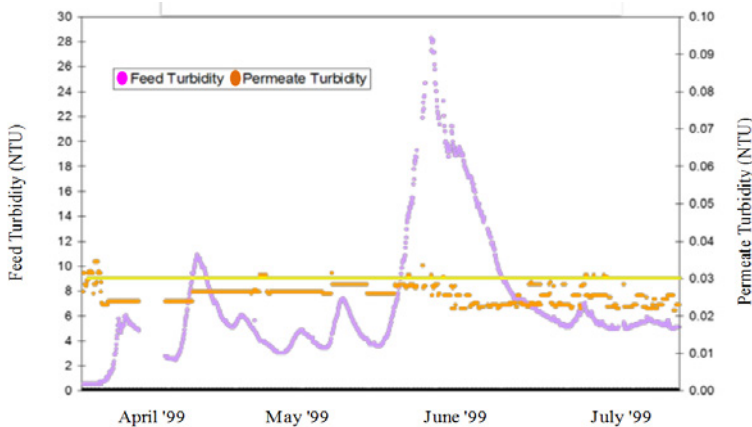
Table 3 Contaminant Removal by MF and UF

Particle or Microbe	MF	UF
Giardia Cysts	4.5-7 log	5-7 log
Cryptosporidium	4.5-7 log	5-7 log
MS-2 Virus	0.5-3.0 log	4.5-6 log
Particle Counts		
<2 micron	<10/ml	<10/ml
2-5 micron	<10/ml	<10/ml
5-15 micron	<1/ml	<1/ml
Filtrate Turbidity Average	0.01-0.03 NTU	0.01-0.03 NTU

NTU – Nephelometric Turbidity Units

In comparison with conventional granular media or pressurized sand filtration, membranes provide a greater level of consistency and a much lower levels of turbidity in the filtrate. Due to the nature of the membrane pore distribution, this improved quality is independent of the level of particulates in the inlet water. Figure 3 shows an installation on surface water in the US State of Washington that had very “flashy” raw water turbidities, yet the filtrate turbidity was consistently less than 0.03 NTU

Figure 3 Filtrate turbidity in relationship to Feed – MF



Hollow Fiber membrane applications

Most mining water applications are related to the treatment of waste generated by the mining operation or produced water that is a by-product of the excavation. Some treat-

ment involves improving the water quality prior to high pressure water filtration for feed to boilers and other equipment. In either of these or other mine applications, the addition of chemicals to oxidize or precipitate metals, organics or particulates is often employed. It is worth repeating that the tolerance of the membrane to these chemicals, either completely reacted by the contaminant, or accidentally overdosed is of vital importance to the success of the process and the life of the membrane. A typical “membrane solution” to a conventional coagulation system to remove metals, organics or fine particles is shown in Figure 4.

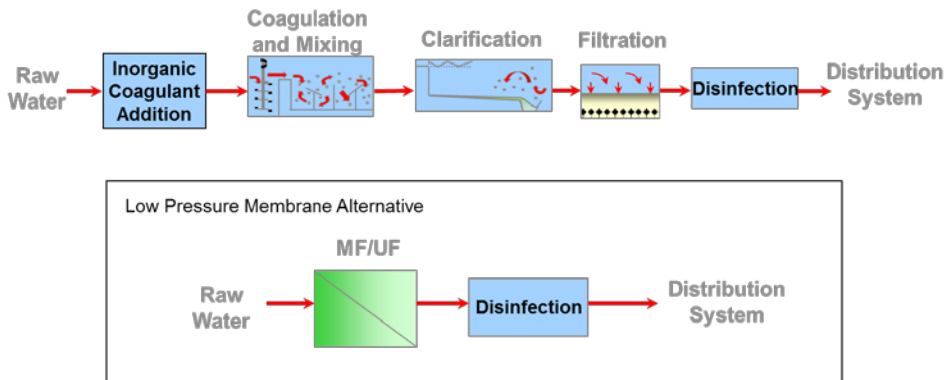


Figure 4 Membrane versus conventional process treatment

Membrane systems advantages over convention treatment

Figure 4 above illustrates one of the ways membranes can replace conventional treatment. The choice of membranes over conventional treatment provide the following additional benefits:

- Membranes provide a higher level of protection. Membranes provide an absolute barrier compared to conventional processes in water treatment do not. If the membrane integral, particles greater than the pore size are removed.
- Hollow fiber microfiltration produces a consistent effluent (typically 0.03-0.05 NTU) regardless of influent turbidity.
- Membranes have a higher recovery, up to 98% for MF. Less waste means less cost.
- Smaller footprint than conventional, often eliminating clarifiers. At least 10% to 20% savings
- Less sludge disposal issues if coagulation can be eliminated
- Can reduce chemical use.
- Integrity Testable
- Remote operation

Conclusions

Mine water operations can greatly benefit from employing low pressure membranes in their overall treatment scheme. Whether it is pre-filtration for Reverse Osmosis or coagu-

lating and removing contaminants to achieve regulatory compliance, membranes provide an attractive option. But only if a full understanding of their characteristics, strengths and weakness is understood. A superior membrane allows the use of a wide range of chemical pre-treatments to allow the membrane to remove the substance of concern. Tolerance to a wide range of cleaning regimes is required to obtain the best value and longest life of the membranes.

PVDF, microfiltration membranes, manufactured by the TIPS method provide the best option on the market today. They are available in a number of configurations from very small packaged systems to mobile units that can be moved from site to site, to systems for very large volumes or flows.

References

- Liu, C (2007) Mechanical and Chemical Stabilities of Polymeric Membranes, AWWA Water Quality Technology Conference, November 4 – 8, (2007), Charlotte, NC, USA
- Lorch, W (1981) Handbook of Water Purification, McGraw-Hill, London,
- Lloyd, D (1990) Journal of Membrane Science vol 52, Issue 3, p. 239-261
- Lilley, T (2013): Optimising mine pit dewatering treatment techniques to meet production deadlines. In: Brown, A.; Figueroa, L. & Wolkersdorfer, Ch.(Eds): Reliable Mine Water Technology (Vol I) p. 649 – 655; Denver, Colorado, USA (pubs) (ISBN 978-0-615-79385-6).

Coal mine pitlakes in South Africa

Andrew Johnstone¹, Lizel Kennedy²

¹*GCS (Pty) Ltd, 63 Wessel Road, Rivonia, Johannesburg, South Africa, 2128,
andrewj@gcs-sa.biz*

²*University of the Free State, 205 Nelson Mandela Dr, Park West, Bloemfontein, 9301,
kennedylizel@yahoo.co.za*

Abstract It is estimated that there are over 110 coal mine pitlakes in South Africa associated with active, closed and abandoned mines. The final pitlake water quality impacts on the long term mine closure options. Pitlakes evolution has been studied globally and are used as a mine closure option worldwide. Despite there being numerous coal mine pitlakes in South Africa there has been very little research to determine if pitlakes are a viable mine closure option. This paper discusses the preliminary results of a South African Water Research Commission (WRC) funded investigation of four different coal mine pitlakes from various coal basins in South Africa. The paper describes field investigations of the pitlakes, involving profiling and sampling. Chemical algal and bacteriological analysis for the profiling has confirmed that stratification does occur in the pitlakes. Additional work will be undertaken to quantify the pitlake water balances especially in pitlakes that are hydraulically connected to old mine workings. The research found that the sustainability of the pit lakes is a function of the previous mining method and the relative size of the pitlake in comparison to the disturbed area. The research will result in the development of a manual for optimization of South African coal mine pit lakes to ensure that they are a sustainable environmental option for closure.

Key words Pitlake, water quality, stratification,

Introduction

Coal mining in South Africa commenced in the mid 1800's and is still the primary source of energy for the country, with coal fired power stations producing more than 90% of the country's electricity demand. Coal mining will continue to supply the growing energy demands and export, leaving behind old coal mines waste, alterations to the landscape and in the case of open cast mining, pitlakes. There are well over 110 pitlakes in South Africa most being in the Mpumalanga and Natal Coal fields, where the majority of the historical mining occurred.

Pitlakes are typically formed when groundwater levels rebound in the final void of an open cast coal mine. Historically, the final voids in South African opencast mines were not back-filled in an attempt to manage the water in the mines. This has led to the historical mining landscape being littered with pitlakes of various sizes and depths. In general, pit lakes are perceived to be associated with poor water quality water and pose a risk of overflowing and discharging contaminated water into surrounding water resources. In some cases, pitlakes were found to have relatively good water quality in conditions of low pyrite and high carbonate availability and large inputs of organic or inorganic nutrients prevail.

Little work has been done on characteristics of coal mine pitlakes in South Africa and their impact on the surrounding groundwater and surface water systems, and this study attempts to address the shortfall. Historical and ongoing mining in the coal fields of Mpumalanga,

Natal and the Waterberg has created a number of coal mine pit lakes which range in age, depth and area. This project funded by the South African Water Research Commission investigates and compares four existing pitlakes in the Mpumalanga, Natal and Waterberg coal fields that have different geological, geochemical and hydrogeological characteristics and thus, are expected to display different pit lake behaviour and water quality evolution.

The water quality in pit lakes is governed by three major controls which includes limnological and geochemical processes as well as the geology which all contribute to the hydro-geochemical characteristics of a pit lake. Of particular importance in this study was the investigation of limnological controls in the pit lakes and their impact on water quality and in-situ water chemistry over time. The limnological controls are grouped into processes which physically separate the water column into two or more horizontal layers due to chemical and/or temperature gradients, called stratification, and processes that vertically homogenise the water column by mixing. (Bowell, 2002).

The physical limnology of pit lakes can therefore be described by two conceptual models namely holomictic pit lakes and meromictic pit lakes. Holomictic pit lakes consists of two distinct layers – an upper oxygenised layer and a lower, oxygen depleted layer- separated by a transition layer characterised by steep thermal gradients, called the thermocline.

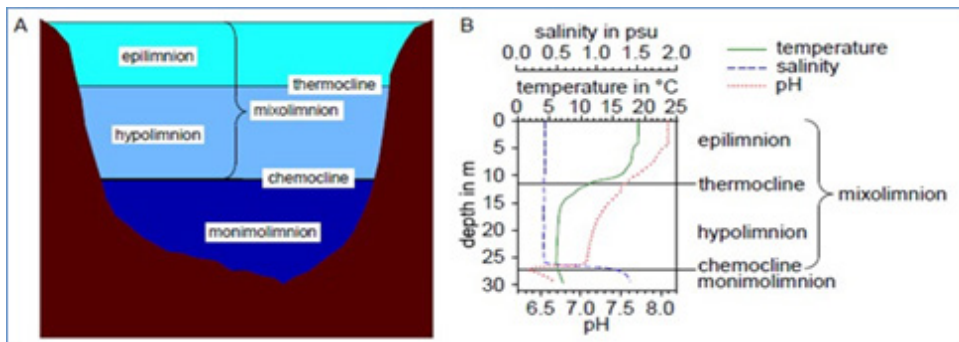


Figure 1 Typical limnology of a Meromictic pitlake (Schultze et al. 2016)

A Meromictic pit lakes comprise a third, chemically inactive layer at the bottom of the pit lake. When overturn occurs, this lowest layer does not participate in the mixing event and can be considered as a mechanism to concentrate contaminants at the bottom of the pit lake (Schultze et al. 2016).

In general, pit lakes are geologically young, artificial and geochemically complex systems which reflect permanent modifications to hydrologic systems and usually display poor water quality affected by poor quality leachate and in some cases acid mine drainage. The final lake surface levels represent the greatest risk of pitlake closure to stakeholders due to potential overflow and discharge of poor quality water to regional surface water bodies and groundwater resources.

In South Africa, there are a number of typical pit lakes which can be classed into three types according to the mining method and the final pit lake which will in turn determine its hydrological behaviour and chemical evolution. These are:

- Terminal pit lakes which are a result of a single excavation,
- Pit lakes associated with the final void of opencast operations that has partially been backfilled and rehabilitated,
- Pit lakes as a result of both underground and open cast operations where the open and underground mining operation are hydraulically connected.

Terminal pit lakes act as a hydrological sink and the only outflow from these pit lakes is by means of evaporation with the consequence of evapo-concentration of chemical components in the lake. Pit lakes associated with final voids of opencast operations where concurrent rehabilitation took place receive water which interacts with opencast spoils prior to entering the pit lake and this may cause an increase in the total dissolved solids in the lake, depending on chemical characterisation of backfill material. If the water level in the pit lake fluctuates to above the water table, water may move from the pit lake into the surrounding groundwater table and this process may reverse in South Africa where evaporation exceeds rainfall by a factor of 2. Pit lakes which resulted from underground operations and open cast mining of the shallow coal (<40m) receive water from the underground mines which may impact the overall water quality and chemistry profile of these pit lakes.

Study Areas

The study area selected are in the different coalfields of South Africa, namely Waterberg Pitlake A and Pitlake B&C in the Mpumalanga coalfields and Pitlake D.

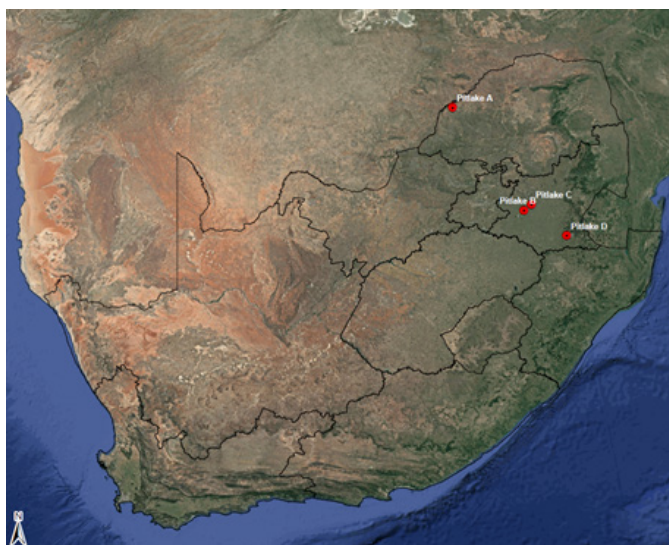


Figure 2: Map of South Africa with positions of pitlakes

Table 1: Age, size, depth and volume of each pit lake with their respective coal fields.

Pit lake	Coal Field	Age (years)	Max (m)
A	Waterberg	6	60
B	Highveld	20	20
C	Witbank	26	3
D	Natal	10	10

Pitlake A

Pit lake A is situated in the Waterberg coal field of South Africa. The area is characterised by an arid climate with high evapotranspiration of 2000 mm/a and annual average rainfall of 400 mm. Due to high temperatures in the summer months, significant evapo-concentration is expected. The pit lake formed in a void left by a single bulk excavation of coal to a depth of 96 m. Geologically, the area consists of Karoo Supergroup successions with the coal-bearing horizons consisting of the Upper and Middle Ecca group where 11 coal zones are present. Mining activities ceased in 2010 where after groundwater levels rebound to equilibrium levels and displayed stable conditions for at least six years. The pit is not connected to other mining operations and therefore acts as a stand-alone pitlake which receives water from limited surface run-off from the Greater Limpopo River Catchment area and groundwater inflow from the surrounding aquifer. At the time of investigation, the depth of the pit lake was 68 m.

**Figure 3:** Pitlake A**Figure 4:** Aerial image of Pitlake A

Pit Lake B

Pit lake B is located in the Mpumalanga. The opencast operation has been partially back-filled and rehabilitated, leaving a pit lake with a maximum depth of 20 m. The geology of the area consists of sandstones interbedded with siltstone, grit and mudstones which forms part of the Ecca group of the Karoo Super group. Although coal seam No 1 to 5 present at this colliery, coal is mainly extracted from coal seam No.4, which varies in thickness of 4.8 to 70 m (Hancox and Gotz 2014). The climate is temperate with a mean annual rainfall of approximately 711 mm and average evaporation of 1730 mm.



Figure 5: Pitlake B



Figure 6: Arial Image of Pitlake B

Pitlake C

Pit lake C is situated in Mpumalanga coal field. The opencast operations ended in 1991 after which the groundwater level was left to rebound to equilibrium levels. The roll-over mining method was employed where coal was extracted from the Vryheid formation of the Ecca Group of the main Karoo basin. The area consists of alternating sandstones and shales with coal seam No. 1 to 5 present (Hancox and Gotz 2014). The majority of this opencast operation has been backfilled and rehabilitated leaving a relatively narrow and elongated pit lake with a maximum depth of 3 m.

The climate is temperate with an average annual rainfall of 670 mm/a and potential evaporation of 1600 mm.



Figure 7: Pitlake C



Figure8: Arial Image of Pit Lake C

Pitlake D

Pit lake D is situated in the Natal coal field, where coal is extracted from the Alfred, Gus and Dundas seams. The mining operation comprised of an underground and opencast activities which commenced in 1997 and ceased in 2007. The opencast area is hydraulically connected to the underground mine and both are connected to the pitlake. The maximum depth is 10 m. The area receives high rainfall, mostly in the form of heavy thunderstorms. Mean annual rainfall is 700mm and potential evaporation of 1 700 mm.



Figure 9: Pitlake D



Figure 10: Plan view of Pit Lake D indicating the underground portion and rehabilitated opencast area.

Methodology

The field investigation involved four different study areas related to the respective conceptual models of pit lake types. The aim of the investigation was to determine the water quality and chemical signature of the pit lakes as well as possible stratification brought about by steep thermal or chemical gradients. The method of investigation comprised of multiparameter depth profiles with an YSI EXO (Yellow Springs Instruments) profiler and water sampling with a submersible pump connected to a 12 V energy source. Sampling depths were derived from the water quality profiles, whereby the position of the thermocline was used to distinguish the thickness of the epilimnion and hypolimnion to ensure sampling of both layers. Profiling and sampling were performed at the same position in the pit lake, typically the deepest point in the pit lake. Lateral homogeneity of the pit lake water quality was assumed. Chemistry, bacteriological and algal samples were sent for analysis. Unfortunately, at the time of this paper laboratory analysis was only received for Pit Lake A and D.

Results: Water Quality

Pit Lake A

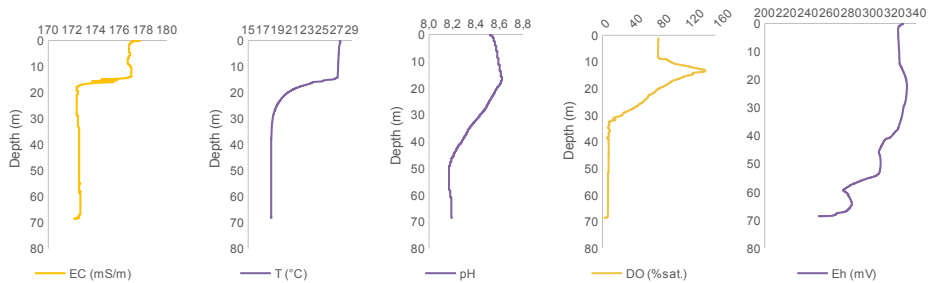


Figure 11: Water column profiles for Pit Lake A (Jan 2017).

Pit Lake B

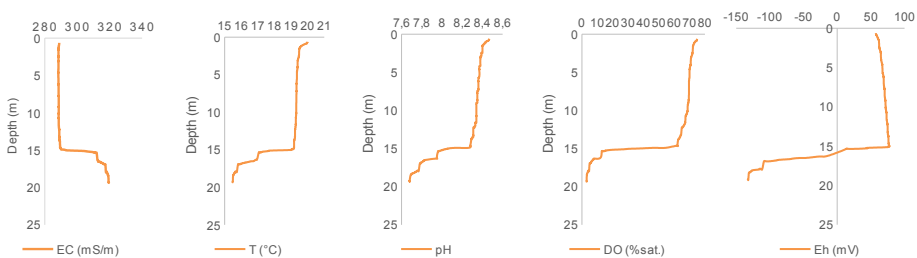


Figure 12: Water column profiles of Pit lake B (April 2017).

Pit Lake C

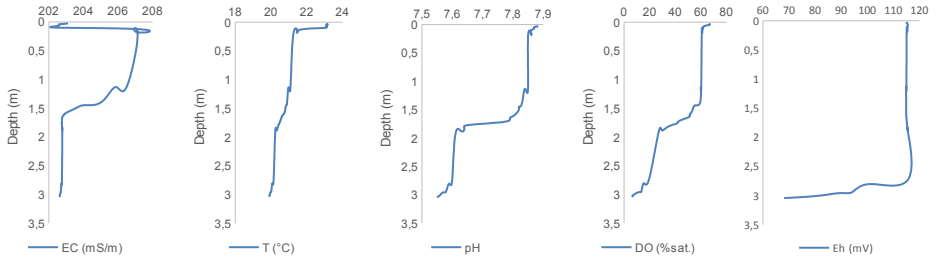


Figure 13: Water column profiles of Pit lake D (March 2017.)

Pit Lake D

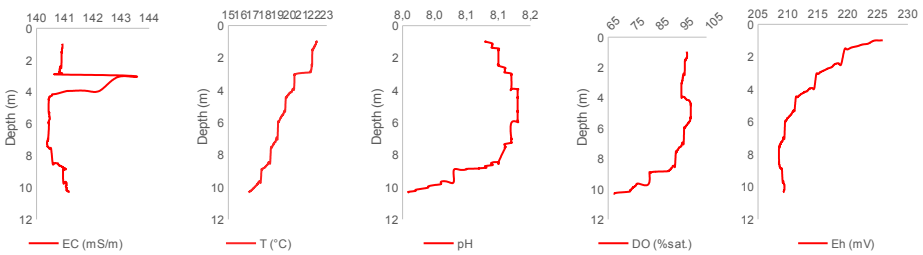


Figure 14: Water column profiles of Pit lake D (November 2016.)

Water Quality Pitlakes A & D

At this stage only the water quality of pitlakes A and D is available which involves the inorganic chemistry, bacteriologic and algal analysis.

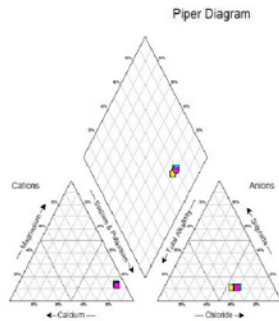


Figure 15: Water chemistry of Pitlake A.

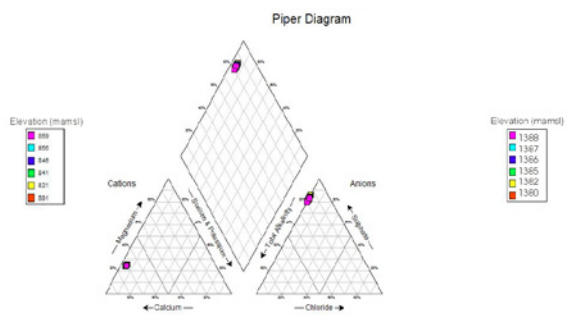


Figure 16: Water chemistry of Pitlake D.

Pitlake A is a single bulk sample and not adjacent to any other workings. As a result the pit-lake water balance comprises rainfall and groundwater inflow and the losses comprise only of evaporation. The electrical conductivity ranges from 176 on surface to 172 mS/cm at 60 m. The water is a sodium chloride water with Na of 260 mg/L and Cl 348 mg/L, with SO4 concentrations of 108mg/L. The surrounding aquifer water quality is also sodium chloride

in nature with Na 200mg/L, Cl 295mg/L and surprisingly low SO₄ of less than 10mg/L . The metal content is very low due to the relatively alkaline pH

Pitlake D is linked to both opencast and underground workings. The EC is 133 mS/m and the water is largely a calcium carbonate in character with Ca 240mg/L, SO₄ 600, and very low Cl 2mg/L and Na 16mg/L .The metal content is very low due to the relatively alkaline pH

Discussion

The water quality in the four pitlakes investigated are markedly different with variations in the stratification and in the overall pit water quality. All samples were taken in the summer months.

Table 2: Pitlake Water Quality

	EC mS/m	T C	pH	DO %Sat	Eh Mv	Depth of Thermocline	Depth of Pit Lake
Pit A	176	27	8,5	80	325	13,93	68,55
Pit B	290	20	8,5	80	80	14,91	19,25
Pit C	200	23	7,9	70	125	1	3
Pit D	141	23	8,1	100	230	2,85	10,1

Electrical Conductivity: The EC varied from 176 to 290 mS/cm (TDS 1126 to 1856 mg/L) and in general the poorer water quality on surface except in the case of Pitlake B. Pit Lake B is an opencast operation and the reasons for the lower poorer quality is not clear.

Temperature: In all cases the top of the pit lakes was warmer than the lower portions of the pitlake. This can be expected as the sampling was undertaken in the summer months. The thermoclines varied between 13.93 below surface for the deep pitlakes to 1 m for the very shallow lakes.

pH: In all cases the pH of the pitlakes were alkaline on surface and did not vary significantly with depth indicating that the pitlakes are alkaline and as a result did not show a major influences of acid mine drainage if either of the lakes.

Dissolved Oxygen: Dissolved oxygen as expected decreased with depth. This is typical of a pitlake and as a result will impact on the biota with a general increase in the algal, invertebrate and vertebrate species in the upper levels of the pitlakes.

Eh: the redox potential of all the pit lakes is positive except the lower portion of pitlake B which is negative

Bacteriological Analysis: Water samples analysed were taken from all pitlakes for microbial diversity. Result have only been received from pitlake D. The analysis involved using

denaturing gradient gel electrophoresis (DGGE) fingerprinting method. Initial identification of possible micro-organisms present through sequence analysis elucidates possible environmental condition(s). The DGGE fingerprinting revealed possible diverse bacterial population in the samples. PDP6-2M (Pit Lake D profile 6 at 2m) and PDP6-3.5M have similar DGGE fingerprinting with possible dominant phylotypes. Samples PDP3-2M, PDP3-6M, and PDP3-14M also possess similar DGGE fingerprinting. However, sequence analyses will reveal the identity of bacteria present in the samples.

Algal Sampling

Only results have been received for Pitlake A. The planktonic chlorophyll algal concentration was determined by lowering a secchi disc (0.2 m diameter) and subsequently obtaining the secchi depth. Sampling was performed to a maximum depth of three times the secchi depth. The secchi depth was determined as 7 m in Pitlake A and samples were collected at 0.5 m, 1 m, 7 m and 20 m.

- Sample 1.2- 0.5 m depth = 3 µg/L
- Sample 1.3- 1m depth = 6 µg/L
- Sample 1.8- 7 m depth = 3 µg/L
- Sample 1.7- 20 m depth = <1 µg/L

According to the results given, it can be seen that the pit lake is mainly oligotrophic with the highest concentration of chlorophyll-a occurring at approximately 1 m below the surface of the water.

Water Balance

In all the pitlakes investigated there is negative water balance when comparing rainfall and evaporation. There is not a major change in the pitlake levels between seasons due to other sources of recharge to the pitlake. In the case of pitlake A the inflow of groundwater from the surrounding aquifer plays a significant role in maintaining the pitlake level. In the other pitlake B, C & D which are connected historical mine workings here is additional flow from the old mine workings into the pitlake. Additional work will be undertaken to quantify the pitlake water balance.

Conclusion

The Project is still in its infancy and a lot of the data must still be analysed. There are however some interesting results from the four pitlakes. Additional work will involve chemical bacteriological and algal analysis. All pitlakes water balances will be modelled to determine sources and sinks.

References

Bowell RJ (2002) the hydrogeochemical dynamics of mine pit lakes. In: *Mine Water Hydrogeology and Geochemistry*, YOUNGER PL AND ROBINS NS, 198, Geological Society, London, Special Publications, p 159-185.

- Geller W, Schultze M, Kleinmann R and Wolkersdorfer C (eds) (2013) *Acidic Pit Lakes: The Legacy of Coal and Metal Surface Mines*. Springer-Verlag Berlin Heidelberg, Germany. P 525.
- Hancox PJ and GÖTZ AE (2014) A Review article: South Africa's Coal fields – A 2014 perspective. *International Journal of Coal Geology* 132, p 170-254.
- Schultze M, Castendyk D, Wendt-Potthoff K, Sánchez-España J and Bohrer B (2016) On the relevance of meromixis in pit lakes – an update *Proceedings IMWA 2016, Freiberg/Germany | Drebenstedt, Carsten, Paul, Michael (eds.) | Mining Meets Water – Conflicts and Solutions*.

Use of Geothermal Heat of Mine Waters in Upper Silesian Coal Basin, Southern Poland – Possibilities and Impediments

Ewa Janson¹, Grzegorz Gzyl¹, Marcin Głodniok¹, Małgorzata Markowska¹

¹*Central Mining Institute, Gwarków Square 1, Katowice, Poland*
ejanson@gig.eu, ggzyl@gig.eu, mglodniok@gig.eu, mmarkowska@gig.eu

Abstract In Upper Silesian Coal Basin, Poland where mining activity and energy production is based on hard coal, alternative sources of energy are largely underdeveloped. Complicated geological structure of USCB as well as interconnections of active and abandoned mines are the main reason that mine closure is associated with continuous dewatering. The process results in discharge of c.a. 80 million m³/year of mine water from pumping systems in abandoned mines. Mine waters are very limitedly used for geothermal purposes, although there is huge potential for that. Paper presents possibilities and problems of implementation nonconventional mine water heat extraction in polish conditions.

Key words Geothermal heat, mine water, mine closure

Introduction

The investigations described in current paper are being carried out in the frame of an international project under the EU Research Fund For Coal and Steel, named: “Low Carbon Afterlife: Sustainable Use of Flooded Coal Mine Voids as a Thermal Energy Source – a Baseline Activity for Minimising Post-Closure Environmental Risks” (Acronym: LoCAL). The LoCAL Project aimed at providing bespoke tools for investigating flow and heat transfer in flooded mine workings. New tools for quantifying and modelling heat transfer in networks of flooded mine workings have been under development in frame of the project as well as overcoming the hydrochemical barriers to effective heat transfer from raw and treated mine waters (ochre clogging phenomenon which affects a lot of mine water heating and cooling systems). The LoCAL project not only have covered technical and engineering issues, but also provided economic and management models for efficient energy extraction and distribution. Technical, legal, managerial and cost-benefit analyses of various types of heat pump systems have been carried out. Project activities have been simultaneously undertaken in mining areas by research organizations in partnership with industrial enterprises in the UK (by University of Glasgow in partnership with Alkane Energy Ltd.), in Spain (by University of Oviedo, with HUNOSA as the industrial partner) as well as in Poland (Central Mining Institute, in partnership with Armada Development).

This paper presents general overview of limitations and the potential in use of mine waters for geothermal heat extraction in USCB, Poland. International cooperation within the project LoCAL gave the opportunity to provide wider technical, technological and engineering overview for geothermal use of mine waters in USCB. Research investigations, pilot and monitoring activities in Polish site – abandoned coal mine Szombierki in Bytom (Northern part of USCB) are now completed.

LoCAL project outcomes revealed very stable temperatures of mine waters pumped in Szombierki system ranging from 23.2 to 28.0°C, and remarkable stability in the characteristics of the main hydrothermal reservoirs. Monitoring campaign was conducted to assess chemical and isotopic composition of mine water in Szombierki mine and results revealed promising technological capacity for geothermal purpose.

Experience gained during the project in relation to pilot action pointed out the obstacles and capabilities of its implementation in polish conditions, especially for future operators and end – users of still nonconventional source of geothermal energy – water from abandoned coal mines.

Use of mine waters for geothermal purpose

The potential of the use of water from underground mines for geothermal purpose was first investigated back in the 1970s. Water in the Springhill coal mines with a temperature of 18°C was used for geothermal energy production in Nova Scotia, Canada (Jessop 1995) and numerous sites all over the world: Park Hills, USA; Follida, Norway; Shettleston, UK; and Ochil View, UK (Wolkersdorfer 2008). In USCB, Poland pumped mine water temperatures range from 11.3 to 29.2°C, generally increasing with depth. Given that many of these waters are pumped in urban areas (where there is a demand for space-heating and cooling) and given that several of the former colliery sites are ripe for redevelopment, the mine waters have a high potential for ground source heating and cooling via the use of heat pumps (Banks et al. 2004; Gudek 2006; Karwasiecka 2001; Małolepszy et al. 2005; Solik-Heliasz and Małolepszy 2001;). The viability of this has been demonstrated at a small scale with coal mine water in Scotland (Burnside et al. 2016) and at a large (district heating) scale at Heerlen, Netherlands (Demollin-Schneiders 2008).

The usual method to exploit geothermal energy contained within mine water is heat pumps in conjunction with either open or closed loops (Hall et al. 2011). Heat pumps can be used to provide both space heating and cooling. In the winter, energy is taken from the water and in the summer, energy transferred into the water (Małolepszy, 2003). If the mine water is used only for heating, it may cause the temperature of the water to slowly decrease, resulting in a diminished heating capacity. The amount of energy recovered will depend primarily on the size and number of heat pumps that are installed. These in turn will be based on the temperature and flow of water from or back into the mine (Hall, et al. 2011) of abandoned coal mine workings with recent practical advances in overcoming the perceived environmental risk obstacles to heat-pump exploitation of mine water, to interrogate and document full-scale working examples of newly-developed mine water heat pump pilot systems in three European countries.

The concept of mine water use as a heat source is fully in line with the EU's environmental policy objectives. Such activity refer to the EU climate and energy package (especially in context of CO₂ reduction), in polish energy package 3x20% means 20% reduction of CO₂, 20% lower energy consumption and 20% increase of the use of renewable sources of energy (Ryżyński and Majer 2015). These legal requirements should be taken as priority in plan-

ning and implementation of geothermal installation with use of mine waters. As experiences gained during the LoCAL project revealed – many obstacles occurred in this process.

Project area in USCB, Poland

In USCB Poland since 1989, 34 of the 65 hard coal mines in Upper Silesia have been abandoned and the remaining collieries have been forced to adopt a free-market approach. In 2014 restructuring process of Polish mining industry has been reached second phase and 5 hard coal mines are going to be closed down due to economic and technical problems (depletion of coal deposits etc). In the Bytom Syncline (northern part of USCB) intensive underground exploitation of coal and Zn-Pb ore since the 19th century has changed the local groundwater flow and chemistry regime. After mine abandonment, dewatering is continued to protect hydrologically connected low-lying coal deposits and active mines from water inundation.

The study area is located in the Bytom Syncline (Figure 1), in the northern part of the Upper Silesian Coal Basin in Poland. Records of coal mining in Bytom Syncline date back to the 16th Century, with initial shallow workings of coal mines and Zn-Pb ore mines. The area of mining exploitation (active and abandoned) and dewatering fields covers c. 60 km² and has an average altitude of 270 – 295 m asl., with a maximum depth of mining exploitation of c. 900 m bgl (-630 m asl.). Active exploitation of coal is conducted in three mining fields (Bobrek, Centrum and Piekary), and dewatering of abandoned mines is continued in Powstańców Śl – Bytom I, Szombierki (coal mines) and Bolko – (Zn-Pb mine) (Janson et al. 2016)

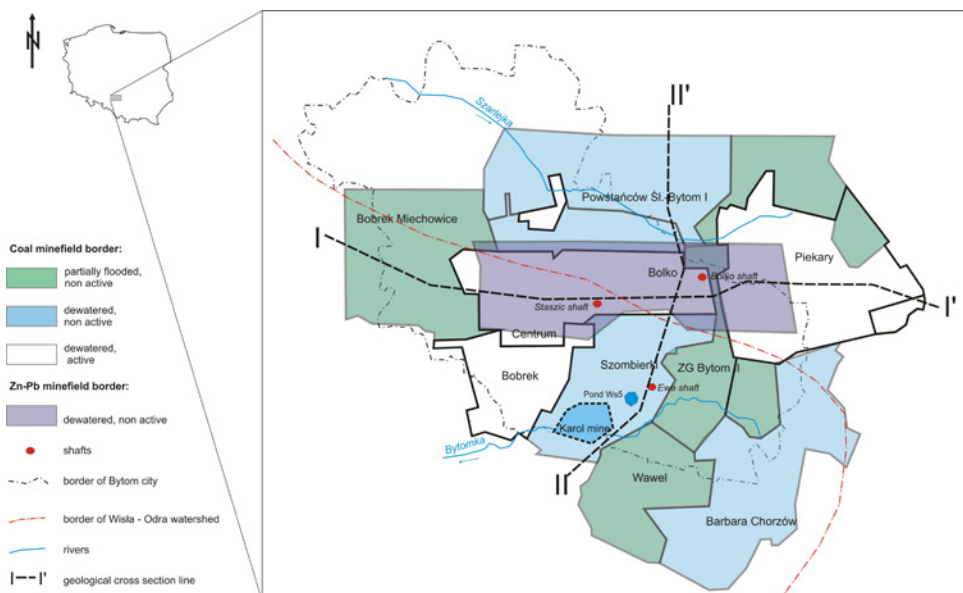


Figure 1 Location of Szombierki mine field in Bytom Syncline (Janson et al. 2016).

During LoCAL activities monitoring campaign was conducted and first results were published (Janson et al. 2016). Its outcomes revealed very stable temperatures of mine waters pumped in Szombierki system ranging from 23.2 to 28.0°C, and remarkable stability in the characteristics of the main hydrothermal reservoirs. It seems to be huge potential for heat exchange, taking into consideration chemistry of pumped water (very low concentration of total iron and probable less problems with ochre precipitation observed in other project's sites described by Athresh et al. 2016) as well as very stable temperature on the discharge point at the surface – 24.2 to 25.0°C.

Pilot site is located in Bytom on post mining area where polish project partner – Armada Development, continues its activity after land reclamation as golf course club and housing development (figure 2). The proximity of mine water discharge from abandoned but still dewatered Szombierki mine (to protect interconnected active mines, like Bobrek coal mine in Bytom city centre against water hazard) was an argument for using renewable energy as the main source for heating and cooling at the planned residential area. Szombierki mine is now included in Polish Mine Restructuring Company, with one of department (CZOK) which is responsible for dewatering abandoned hard coal mines in Upper Silesia. Szombierki is one of CZOK's 15 pumping stations with continuous dewatering. Polish Mine Restructuring Company is the owner of technical infrastructure and shaft “Ewa” (source of water for future installation).



Figure 2 Location of golf course of Armada Development and surface reservoir of mine water (fot. E. Janson).

During the project activities in relation to pilot installation in Armada the main problem occurred when the permission for use of water generally resulted in delay of construction works. In June 2015 it was possible to obtain the preliminary permission from Central Mine Dewatering Department (CZOK – owner of mine water) for uptake of heat from mine wa-

ters with the note that final legal and financial terms for future water use will be designed. Armada Development got also an acceptance from CZOK of construction project for pilot site. After a lengthy period of seeking to resolve minewater ownership and access the matter was resolved in February 2016, when finally Armada received permission for use the water for free. Collection and transfer pipeline was installed and the 9KW compacted heat pump system was constructed during the second half of 2016. Final installation of the heating systems in the buildings utilising fan coil units was carried out in early 2017 with the system now being operational (figure 3).



Figure 3 Pilot installation of heat pump in Armada Development (fot. M. Glodniok).

Unfortunately, the pumping of mine water at the Szombierki site by the mine operators (CZOK) may be terminated in the next few years. The pumping is currently carried out to protect working mines and the pumping regime may be rationalised at other sites leading to non-availability of the pumped mine water in future. While the main activity of CZOK is to protect active coal mines against water hazard, this point emphasises the need to establish the long-term certainty of continued pumping in evaluating project development. After closure all coal mines in Bytom basin probably the necessity of dewatering abandoned mines would determine possibility of mine water use for heat exchange. Understanding the ownership and rights to utilise the mine water is shown to be a key aspect to be established prior to proceeding in developing a mine water heating and cooling project.

Impacts from social acceptance for geothermal energy projects may occur on the local, regional or national level. There are two main ways of understanding of social impact of geothermal heat of mine waters. First: impact of the geothermal project on the society – it can

have both positive and negative impact leading to changes to people's way of life, culture, community structure, stability, services and facilities. Second way of understanding it the impact of society, especially of social awareness and people's level of participation in decision-making processes on realization of any geothermal project.

Conclusions

Positive reception of planned use of geothermal heat of mine water is based on mostly on people's awareness of possible improved standard of living while maintaining relatively low heating costs and of positive impact on environment. In order to ensure this, it is necessary to perform earlier research on lack of possible negative impact on landscape and recreational areas and lack of negative impact on water quality (especially on water for such uses as drinking or irrigation) and widely spread their results among potentially interested people, and above all among decision-makers. LoCAL project revealed that different interests of stakeholders, local community and end-users in general result that the probability of project development is dubious. When developing projects, there are social – connected crucial aspects, such as involvement of stakeholders into economic and environmental benefits from first moment, including information and general understanding of potential in geothermal heat form mine water discharged into tributaries as waste water.

Taking into consideration research tools and experiences gained during the project, it seems like the important issue here is the availability of geothermal heat from mine waters that can be used for beneficial use as well as good planning and understanding of all stakeholders (industrial and otherwise). This is a good post-closure opportunity to mitigate impacts on environment.

Acknowledgements

Field research, sampling, construction of pilot installation and research analysis were carried out within the frame of research project: Low-Carbon After-Life (LoCAL) Sustainable Use of Flooded Coal Mine Voids as a Thermal Energy Source – a Baseline Activity for Minimising Post-Closure Environmental Risks, co-financed by Research Fund for Coal and Steel, July 2014 – July 2017.

References

- Athresh AP, Al-Habaibeh A and Parker K, 2016. The design and evaluation of an open loop ground source heat pump operating in an ochre-rich coal mine water environment. *International Journal of Coal Geology*, Volume 164, p 69–76
 - Banks D, Skarphagen H, Wiltshire R, Jessop C (2004) Heat pumps as a tool for energy recovery from mining wastes. In: Gieré R, Stille P (eds) *Energy, Waste and the Environment: a Geochemical Perspective*. Geological Society (London) Special Publ 236: 499-513
 - Burnside NM, Banks D, Boyce AJ, Athresh A, 2016. Hydrochemistry and stable isotopes as tools for understanding the sustainability of minewater geothermal energy production from a 'standing column' heat pump system: Markham Colliery, Bolsover, Derbyshire, UK. *International Journal of Coal Geology*, 165, 223-230.
 - Demollin-Schneiders E (2008) Mijnwaterproject Heerlen: lessons learned, things to do. Proc, Conf Minewater '08, Aachen (Germany) and Heerlen (Netherlands),
 - Gudek P (2006) Simulation of dewatering deep coal mines in Poland and feasibility of recovering geothermal energy. MSc Diss, School of Earth and Environment, Univ of Leeds, UK
-

- Hall A, Scott JA, Shang H, Jessop A (1995) Geothermal energy from old mines at Springhill, Nova Scotia, Canada. In: Proceedings world geothermal congress, 1995, p 463–8
- Janson E, Boyce AJ, Burnside N, Gzyl G (2016) Preliminary investigation on temperature, chemistry and isotopes of mine water pumped in Bytom geological basin (USCB Poland) as a potential geothermal energy source, *International Journal of Coal Geology* 164 (2016) 104–114
- Karwasiecka M (2001) The geothermal field of the Upper Silesian Coal Basin. Proc, Conf on Geothermal Energy in Underground Mines, Ustroń, Poland, p 41-49
- Małolepszy Z (2003) Low temperature, man-made geothermal reservoirs in abandoned workings of underground mines. In: 28th workshop on geothermal reservoir engineering. 2003
- Małolepszy Z, Demollin-Schneiders E, Bowers D (2005) Potential use of geothermal mine waters in Europe. Proc., World Geothermal Congress, Antalya, Turkey, 3pp
- Ryżyński G, Majer E (2015) Low temperature geothermal energy –geological information and legal preceeding *Geological Review*, 63 p 1388-1396
- Solik-Heliasz E, Małolepszy Z (2001) Possibilities of utilization of geothermal energy from mine waters in the Upper Silesian Coal Basin. Proc, Conf Geothermal energy in underground mines, Ustroń, Poland
- Wolkersdorfer Ch (2008) Water management at abandoned flooded underground mines: fundamentals, tracer tests, modelling, water treatment. Heidelberg: Springer p 465

Dewatering Impacts of a South African Underground Coal Mine

P.J.H. Lourens¹, P.D. Vermeulen²

¹*University of the Free State, Institute for Groundwater Studies, 205 Nelson Mandela Drive, Bloemfontein 9300, South Africa, lourenspjh@ufs.ac.za*

²*University of the Free State, Faculty of Natural and Agricultural Sciences, 205 Nelson Mandela Drive, Bloemfontein 9300, South Africa, vermeulend@ufs.ac.za*

Abstract The University of the Free State investigated the possible dewatering of boreholes situated on the farm properties in the vicinity of an underground coal mine. The investigation consisted of a hydrocensus phase, pumping tests and groundwater sample collection in underground mine workings phase. It was concluded that the boreholes on the farm properties not situated directly above the underground mine workings, are not affected by the dewatering activities. To determine the origin of the water flowing down the ventilation shaft, a detailed study of a possible geological structure to the west of the shaft is recommended.

Key Words Dewatering, hydrocensus, pumping test, geological structure

Introduction

The Institute for Groundwater Studies at the University of the Free State investigated the possible dewatering of boreholes situated on the farm properties in the vicinity of an underground coal mine. An investigation was required as the land owners complained that there is a reduction in the yield of their boreholes supplying domestic and livestock water to their properties as a result of the underground mining activities.

Methods

The investigation consisted of three phases. Phase one was a hydrocensus on the farm properties gathering boreholes geographical position, boreholes water level depth, equipment (pumps) installed in the boreholes and collection of water samples (where possible) for inorganic quality analysis. Phase two consisted of borehole yield determination by conducting pumping tests on the boreholes identified in the hydrocensus phase. Phase three included a visit to the underground mine workings, where water samples were collected at different groundwater inflow locations (especially water flowing in at a ventilation shaft).

Groundwater sample collection was done according the guidelines set out in the Groundwater Sampling Manual (2nd Edition) that was published by the Water Research Commission in 2007. The pumping tests were performed according to the guidelines set out in the Manual on Pumping Test Analysis in Fractured-Rock Aquifers that was published by the Water Research Commission in 2002.

All the data was converted into a format that is compatible with the FC and WISH software packages. The FC software package is used to analyse pumping test data and the WISH

software package is used to graphically represent the data gathered. Monthly groundwater monitoring data of the underground mine was also incorporated for interpretation purposes.

Topography and Hydrological Regime

The study area is drained by a non-perennial stream and its tributaries with flow in a northerly direction (Figure 1). The topography ranges between 1450 and 1511 metres above main sea-level (mamsl). The annual rainfall is approximately 660 mm per annum, and mostly received in the summer season (Weatherbase 2017).

Hydrogeological Regime

The local groundwater regime of the study area comprises of the following hydro-stratigraphic subdivisions:

- The **shallow weathered groundwater regime** associated with Quaternary deposits of the Karoo Supergroup i.e. alluvium, colluvium and weathered Karoo rocks.
- The **intermediate groundwater regime** associated with hard fractured Karoo rocks i.e. sandstone and dolerite of the Karoo Supergroup.
- The **deep groundwater regime associated** with pre-Karoo rocks i.e. karst aquifer comprised of dolomitic rocks of the Transvaal Supergroup.
- The **unnatural groundwater regime** (mine groundwater regime) – is still being developed (mine voids) as a result of mining.

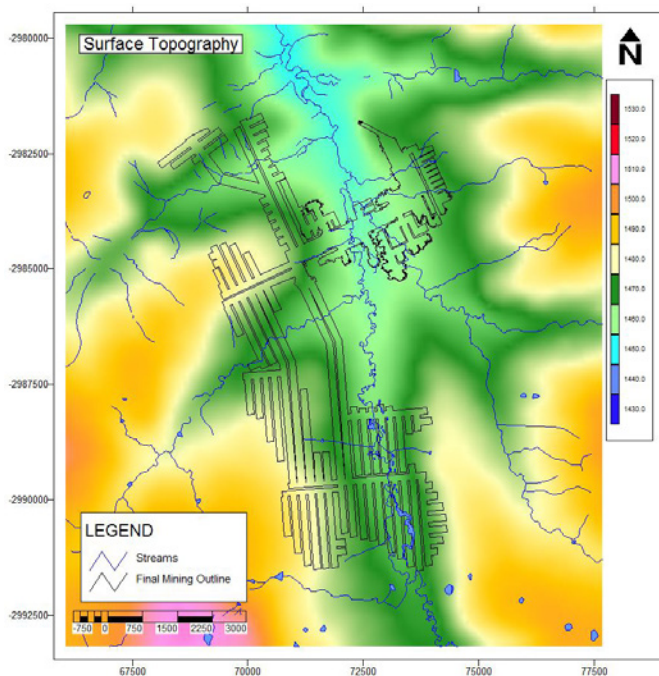


Figure 1 Surface topography and drainage streams of the study area.

Proportional Water Level Distribution

A total of fifty two boreholes were identified on the surrounding farm properties (Figure 2). The total depth of these boreholes ranges between 30 and 90 metres. Therefore it can be assumed that these boreholes only intersects the shallow weathered and intermediate groundwater regimes. Thus, the farmers only utilises groundwater from these two hydro-geological regimes.

The water levels of the hydrocensus boreholes ranges between 2.58 and 46.18 mbgl, with most water levels shallower than 10 mbgl (Figure 2). The water levels of the boreholes monitoring the shallow weathered and intermediate groundwater regimes ranges between 2.15 and 66.74 mbgl (Figure 3), which are very similar to that of the hydrocensus boreholes. An interesting observation, is that the deep water levels (>50 mbgl) are all situated along the contact zones of dolerite and the surrounding host rock (Figure 4). This may also be a geological structure related to the Vredefort Meteorite Impact Structure.

Water Level Trends

Figure 5 and Figure 6 illustrates the water level depth time graphs for the boreholes monitoring the shallow weathered, intermediate and deep groundwater regimes. The water levels in boreholes MK004, MK009, MK011, MK022 and MK025 remained sideways over time. MK022 is equipped with a submersible pump which supplies water on a daily basis to the adjacent dairy farm, from there the erratic behaviour.

The water levels in MK001, MK002, MK008, MK010, MK012, MK023, MK024 and MK026 indicate a declining trend since 2008. The rate of water level decline in MK001, MK002 and MK010 started to increase in 2008 until September 2012, after which it flattened out again. The decline in water level is probably the intermediate groundwater regime that drains into the underground mine workings as a result of mine dewatering activities. This is especially the case for MK001 and MK002 which is situated directly above the underground mine workings.

The declining water level trends for the deep boreholes MK012, MK023, MK024 and MK026 may be associated with the response to goafing which occurred in 2008. Most of the water levels of the boreholes that indicated a rapid decline seems to be at a stabilizing level. An interesting observation is that the water levels of the monitoring boreholes that is not situated directly above the underground mine workings (0.3 km to 1.2 km from the nearest underground mine operations), does not seem to be affected by the dewatering activities.

Hydrochemistry

The chemical character of the boreholes situated along the possible geological structure identified in the west are similar to the chemical character as the water that flows down the ventilation shaft (Figure 7). This strengthens the hypothesis that the water flowing down the ventilation shaft originates from this structure or structures. The chemical character of the water in the eastern section of the underground workings is similar to the chemical character of the monitoring boreholes above the eastern section. Thus implies that the water in the eastern section originates from the overlying aquifer.

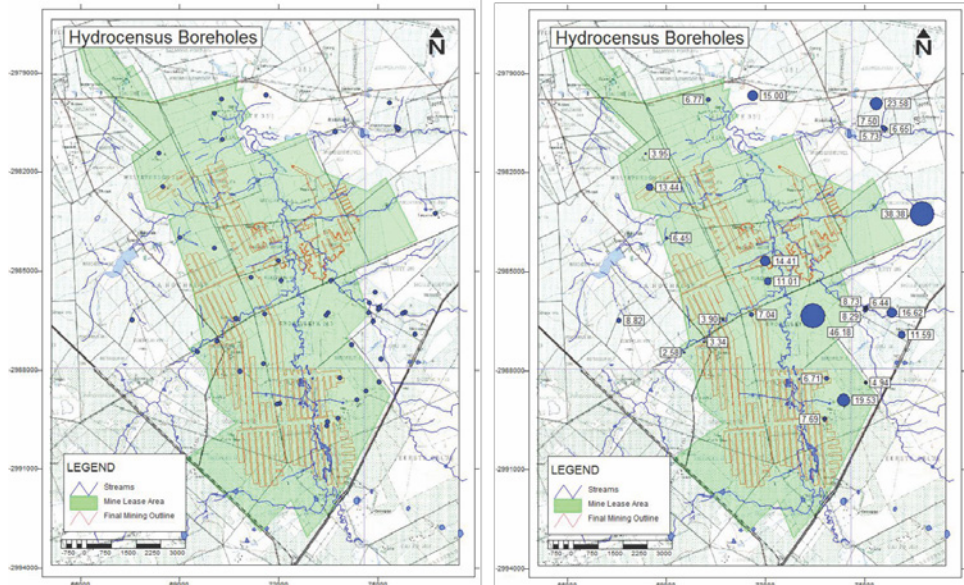


Figure 2 Hydrocensus boreholes (blue circles) location (left) and proportional water levels distribution (right) maps.

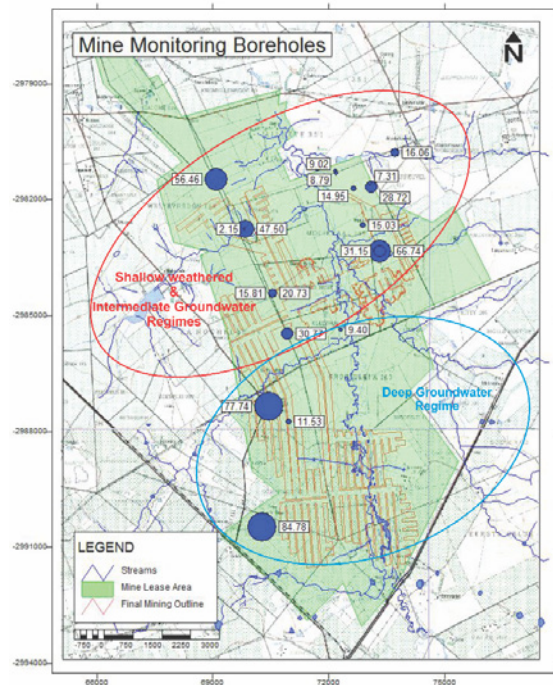


Figure 3 Proportional water level distribution map of the boreholes monitoring the shallow weathered, intermediate and deep groundwater regimes.

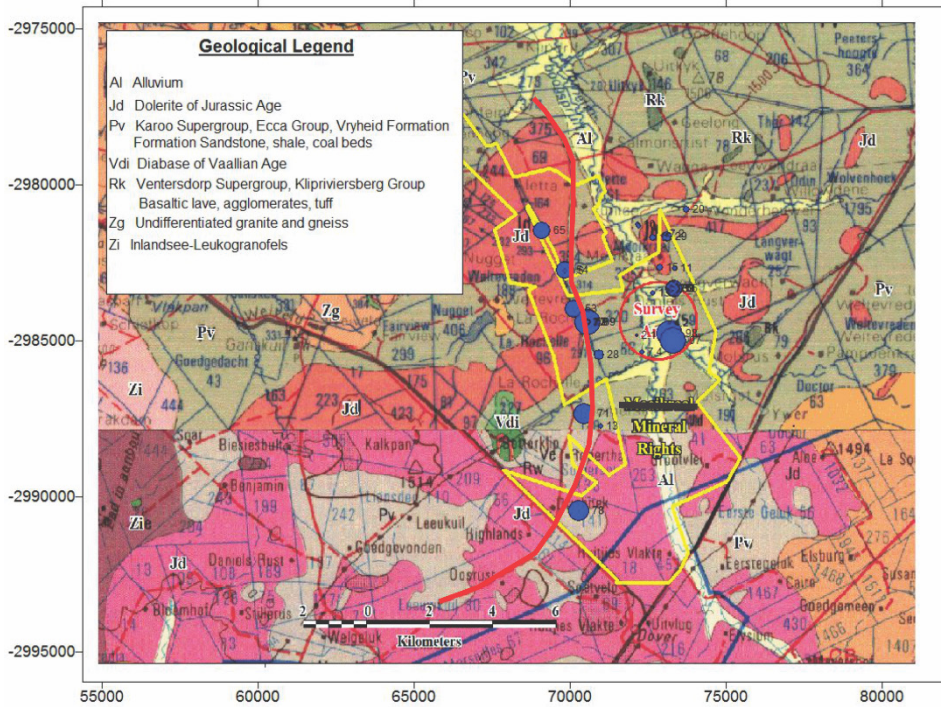


Figure 4 Proportional water level distribution map superimposed over the geological map. Red Line – Contact between dolerite and host rock, also possible Vredefort Meteorite Impact Structure.

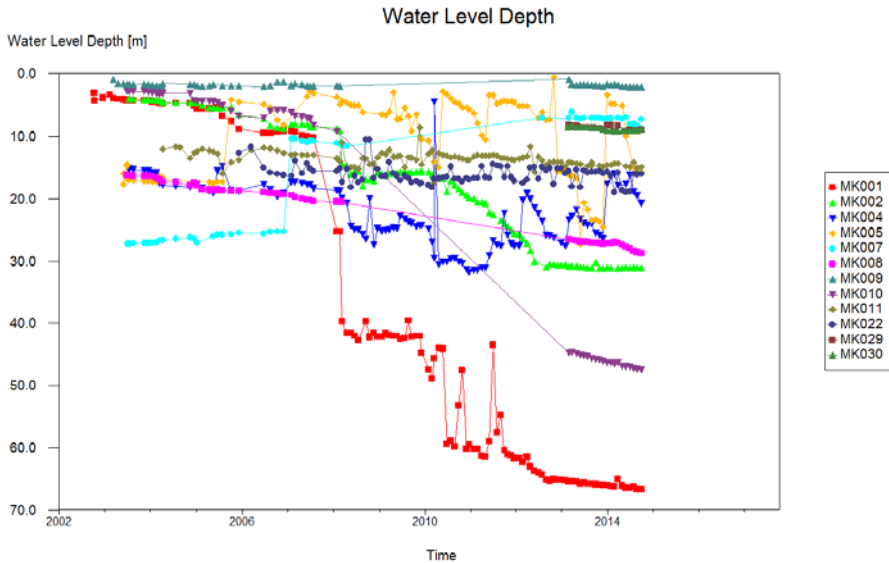


Figure 5 Water level time graph of the boreholes monitoring the shallow weathered and intermediate groundwater regimes.

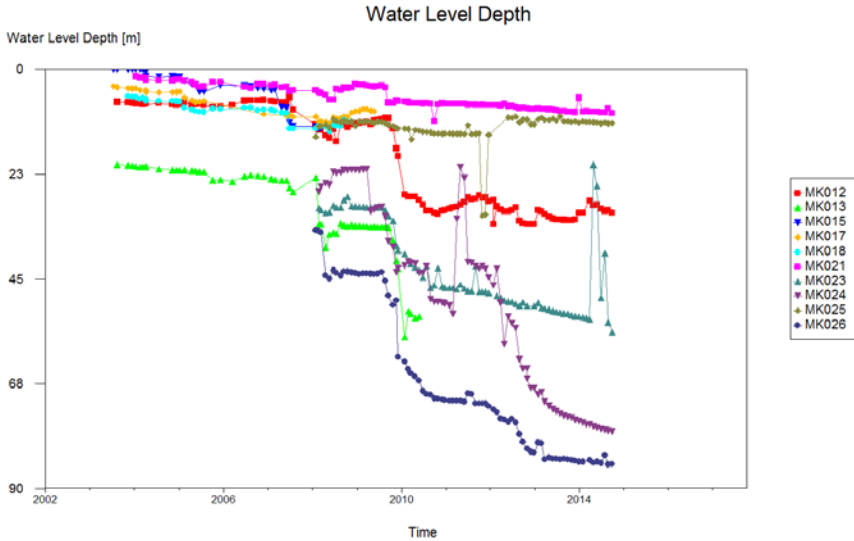


Figure 6 Water level time graph of the boreholes monitoring the deep groundwater regime.

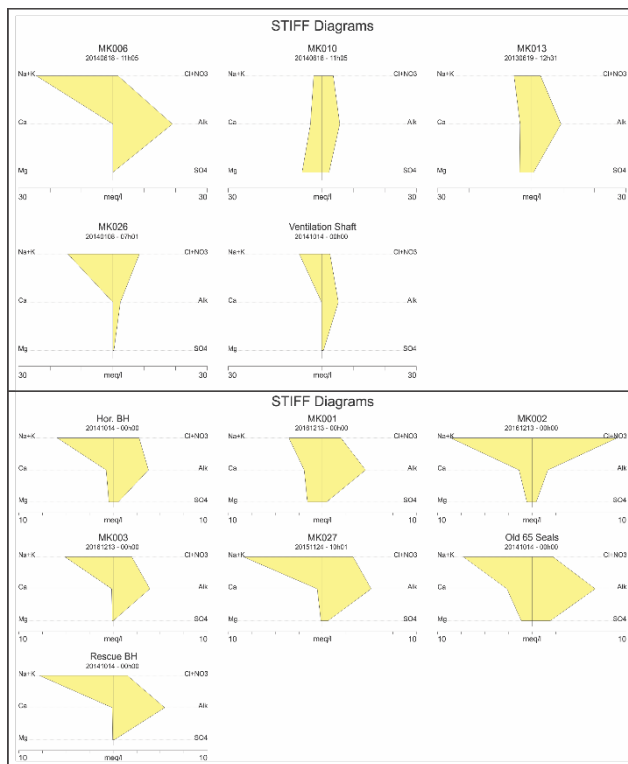


Figure 7 Stiff diagrams of the ventilation shaft vs that of the boreholes situated on the possible geological structure (top) and stiff diagrams of the eastern section vs that of the overlying aquifer (bottom).

Borehole Yields

Pumping tests was performed on nine boreholes. The transmissivity of the boreholes and their sustainable yield varies (Table). The yields of these boreholes are typical yields associated with the Karoo formations i.e. between 0.5 and 1.5 L/s. Two boreholes situated towards the south (GV2; GV23) have yields less than 0.1 L/s, which can be classified as being unproductive (uneconomical).

The borehole with the highest transmissivity (272.3 m²/d) is situated directly above the mine out area. The higher yielding boreholes obviously have higher transmissivities, ranging between 12.5 and 272.3 m²/d. According to the pump test data, the average transmissivity of the shallow weathered aquifer and intermediate aquifer is approximately 71 m²/d.

Table 1 Transmissivity and sustainable yield of boreholes pump tested.

SiteName	Transmissivity (m ² /d)	Sustainable Yield (L/s for 24hr abstraction duration)
GV21	0.8	0.01
GV23	1.9	0.01
GV25	67.8	1.5
GV26	118.6	3.5
GV27	23.1	0.9
LR2	272.3	2.0
LR5	83.2	1.0
MR1	12.5	0.4
WH2	16.8	0.6

Conclusions

The boreholes of the farm properties intersects the shallow weathered and intermediated groundwater regimes. Thus, the farmers only utilises groundwater from these two hydro-geological regimes. The water levels of the hydrocensus boreholes are very similar to that monitoring the shallow weathered and intermediate groundwater regime.

The water levels of the monitoring boreholes not situated directly above the underground mine workings, does not seem to be affected by the dewatering activities. Therefore, it can be concluded that the boreholes on the farm properties not situated directly above the underground mine workings, are not affected by the dewatering activities.

The deep water levels (>50 mbgl) are all situated along the contact zones of dolerite and the surrounding host rock. This may also be a geological structure related to the Vredefort Meteorite Impact Structure. Considering the similar chemical character of these boreholes to that of the water flowing down the ventilation shaft, the hypothesis that the water originates

from these structure or structures are strengthened. The aquifer overlying the underground mine workings in the eastern section drains into mine workings due to dewatering activities. The sustainable yields determined are very similar to that expected of Karoo formations in South Africa, i.e. between 0.5 and 1.5L/s. According to the pumping test data, the average transmissivity of the shallow weathered and intermediate groundwater regimes is approximately 66 m²/d.

The possible dewatering structure or structures identified in the west should be further investigated. This is to test the hypothesis that the water flowing down the ventilation shaft originates from these structure of structures.

References

- Van Tonder GJ, Bardenhagen I, Riemann K, Van Bosch J, Dzanga P, Xu Y (2002) Manual on pumping test analysis in fractured-rock aquifers. Water Research Commission (WRC) of South Africa, Report No 1116/1/02, ISBN No 1 86845 861 X. Pretoria
- Weatherbase (2016) Sasolburg, South Africa [Online] Available at: <http://www.weatherbase.com/weather/weather-summary.php3?s=605018&cityname=Sasolburg%2C+Orange+Free+State%2C+south+Africa&units=> [Accessed 15 September 2016]
- Weaver JMC, Cavé L, Talma AS (2007) Groundwater Sampling (2nd Ed). Water Research Commission (WRC) of South Africa, Report No. TT 303/07, ISBN No 978-1-77005-545-2. Pretoria

Hydrochemical and isotope geochemical evaluation of density stratification in mine water bodies of the Ruhr coalfield

Laura Henkel¹, Christian Melchers¹

¹*Technische Hochschule Georg Agricola, Research Institute of Post-Mining, Herner Straße 45, 44787 Bochum, Germany*

Abstract After mining activities in the Ruhr coalfield ceased, mine water rises in the mine excavations. In flooded shafts distinct stratification patterns between differently mineralised and stagnant water bodies have been observed at a variety of locations. The influx of more brine-type water from the surrounding rock mass and the mine workings on the one hand and the infiltration of less mineralised meteoric waters on the other hand causes substantial density differences in the mine water column. Temporal stability of stratification was proven by continuous, depth-based geophysical measurements in combination with hydrochemical and isotope geochemical investigations on levelled samples.

Key words IMWA 2017, stable isotopes, stratification, hard coal mining, Ruhr coalfield

Introduction

By the end of 2018, the last remaining active coal mine in Germany's largest hard-coal mining area, the Ruhr District, will be closed. The phase of post-mining will be taking over active mining operations with its major aim to manage the complex tasks around mine closures. Risk assessment and monitoring is a key perspective of the research associated with post-mining and will be conducted in close collaboration with the mining authorities and companies. With a maximum population density of 2,800 people per km², the Ruhr District is the largest urban agglomeration in Germany and one of the most densely populated coal mining areas worldwide. Early coal mining activities date back to the 12th century. Since then, a total of about 10 billion tonnes of coal has been produced (Melchers 2015a). As the coal-bearing Upper Carboniferous strata is gently dipping to the north the extensive underground mining process reached a maximum depth of 1,500 m below the surface in the northern part of the mined Ruhr coal deposit. As a consequence, numerous shafts and boreholes were drilled to enable mining of deep coal seams during the active production phase. Some of these shafts were used to install submersible pumps for mine water drainage in order to retain the groundwater at a certain level. Currently, there are 11 mine water management facilities which are pumping more than 60 million m³ water per year (GVST 2015). Moreover, the existing drainage system must be maintained for the future to prevent urban and rural areas from being flooded or impacted by mine water due to subsidence associated with the extensive mining operations. Therefore, adjusted water management measures will continue in perpetuity after coal mining has ceased. Within the decommissioning area abandoned mine shafts are filled with water to varying degrees and hence provide an excellent possibility to monitor the water quality trend with depth. Depending on the geology and tectonics of the surrounding strata and the shaft lining mine cavities are pathways for heat and material flows between the ground-water reservoir, other geological strata and the atmosphere. Monitoring measures reveal stratification of mine water bodies at some of the

investigated sites. Those are characterised by substantial changes in electrical conductivity (EC) as a measure of electrolyte (dissolved ionisable constituents) inventory/total dissolved solids (TDS) and/or temperature both affecting density as a major controlling factor to separate off homogenous bodies of water. Individual water bodies typically have constant levels of temperature, EC, and hence, density throughout the water column and can be regarded as “fully mixed” or equilibrated. Geophysical measurements and depth-differentiated sampling in flooded abandoned mine shafts, monitoring wells and boreholes located in the Ruhr District are carried out as part of on-going investigations to evaluate stratification patterns in mine water bodies. Understanding the development of the chemical composition and possible density layering of rising mine water in disused collieries plays a key role in any risk assessment process affecting environmental impact. In the following contribution one site that has been investigated throughout this study is presented as an example.

Methods

Down-hole measurements are conducted using a multi-parameter probe which not only measures pressure, temperature and EC of the fluid but also pH, reduction-oxidation (i.e. redox potential) and dissolved oxygen. With a diameter of up to 45 mm, a length of 1.5 m and a system of measurement cables up to 1.000 m in length the probe records a continuous profile of the borehole fluid properties with depth. The probe’s specifications are presented in Table 1.

Table 1 Technical specifications of the used multi-parameter probe

Parameter	Range	Accuracy	Resolution
Pressure	0..1000 dbar	0.05 % F.S.	0.0015 % F.S.
Temperature	1..+50 °C	0.005 °C	0.001 °C
EC			
<i>Salt water</i>	0..70 mS/cm	0.007 mS/cm	1.1 mS/cm
<i>Fresh water</i>	0..7000 µS/cm	5 µS/cm	0.1 µS/cm
Oxygen	0..50 ppm	1.1 ppm	1.1 ppm
pH	0..14 pH	0.01 pH	0.001 pH
Redox	+/- 1000 mV	1 mV	0.1 mV

Since the conductivity in an electrolyte solution is essentially dependent on the concentration of electrolytes, the measured EC is a useful indicator of TDS. The results are commonly used to determine the mixing of fresh/meteoric and saline water, i.e. brine. In order to obtain comparable results, the measured values must be referenced to a uniform reference temperature, because EC is dependent on temperature (Langguth and Voigt 2003). All the measuring devices used in this study are configured to automatically process the temperature compensation so that all values specified in this text are referring to a temperature of 25 °C. According to the response times of the sensors the sampling rate is adjusted to 1 metre per

minute. During the first measurement downhole the water column is directly logged in order to reduce the possibility of water disturbances from induced currents by the measuring device. Following a preliminary assessment of the log the levels of depth sampling are determined. Depth samples are collected with a 1.0 L capacity water sampler one day later, allowing time for the borehole chemistry to equilibrate. Directly after sample collection on-the-spot parameters such as pH and EC are measured directly with a multi-parameter portable meter (WTW ProfiLine Multi 3320) in the field. All water samples are transferred into containers and, if necessary, treated and condensed for major ion and stable isotope analysis according to DIN 38402-13. Isotope analysis includes measurements of stable isotope ratios of hydrogen, oxygen, dissolved inorganic carbon (DIC) and sulphur.

Study area

The Ruhr District, named after the river Ruhr, covers parts of the Federal State of North-Rhine Westphalia (NRW). The Ruhr metropolitan region is the largest urban agglomeration and simultaneously the largest hard coal mining region in Germany. In the beginning of mining activities, the extraction of hard coal was concentrated in the south, where the coal seams crop out directly at the surface (Pfläging 1999). The coal-bearing Carboniferous strata was extensively folded during the Variscan orogeny and reshaped by syn- to post-Variscan break tectonics. North to the river Ruhr, the thickness of the overburden rock increases continuously, and the Carboniferous rocks are unconformably overlain by massive post-Variscan deposits of Late Cretaceous to Quaternary age. According to its extensive distribution, the Upper Cretaceous strata with thicknesses of up to 900 m (Hilden et al. 1995) comprise the most important overburden unit. In the stratigraphical sequence, massive, fissured and local karstified limestones of Cenomanian and Turonian age are overlain by a up to 800 m thick unit called the “Emscher Mergel”, Coniacian to lower Santonian clay marlstones (Fig. 1). Beneath the topmost water-impermeable 1 to 2 m, which have been weathered to a clayey silt or silty clay, the clayey marlstone can be fractured and water-bearing to a depth of some 30 to 50 m. Fracturing becomes less common towards the bottom of the zone and finally closes up completely, creating an aquiclude. The Emscher Mergel acts as a major regional seal/aquiclude and separates the deeper groundwater storey of the Cenomanian and Turonian from the upper groundwater storey of the Quaternary and the fractured zone (Melchers et al. 2014).

Case Study

Located in the north-western part of the Ruhr District shaft Hermann 1 and shaft Hermann 2 are not influenced by current dewatering measures. They are 1072 m (Hermann 1) and 950 m (Hermann 2) deep, are around 80 m apart and have not been backfilled yet. After evaluation of the available documentation the shafts have already been flooded in 1929. Current water levels are about -230 m NHN¹. Borehole data reveal total cap rock thicknesses of 800 m. The sequence comprises the Emscher Mergel up to a depth of 600 m followed by Cenomanian and Turonian strata down to a depth of 800 m, which unconformably overlies the bedrock of coal seam-bearing Upper Carboniferous strata. Cenomanian and Turonian beds mainly con-

¹ NHN: “Normalhöhennull” (“standard elevation zero”) is a standard reference level, the equivalent of sea level, used in Germany to measure height.

sist of fractured limestone and are commonly known as a regional aquifer. Two horizontal working levels for coal mining were built in 850 m and 950 m depth respectively.

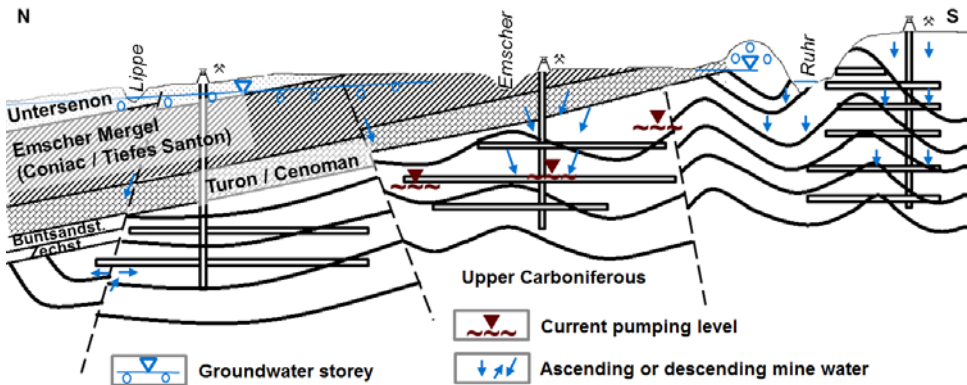


Figure 1: Schematic section through the Ruhr coalfield (greatly exaggerated) after Hahne and Schmidt (1982)

Results

Figure 2 shows the trend of temperature and EC in the investigated water columns in shaft Hermann 1 and shaft Hermann 2. The dashed line specifies the calculated geothermal gradient of $3.7\text{ }^{\circ}\text{C}/100\text{ m}$ after Leonhardt (1983). Additionally, the hydrochemical data indicating the mol% of major ions is presented to the right of the graph in pie charts respectively for the depth from which the samples were collected. Here, all ions which exceed 1 mol% of the total solution content are listed. Up to a depth of 850 m EC and temperature indicate constant values averaging around $9,000\text{ }\mu\text{S}/\text{cm}$ and $30\text{ }^{\circ}\text{C}$. Below 850 m a 1.3 m thick boundary layer follows in which the values increase sharply to an average of $146,000\text{ }\mu\text{S}/\text{cm}$ and $41\text{ }^{\circ}\text{C}$ respectively. A brief look at the log provides clear evidence that the temperature distribution within the entire water body does not correlate with the geothermal gradient. Hydrochemically all samples are Na-Cl type fluids with Na^+ concentration being directly proportional to that of Cl^- . All samples of the upper layer still contain traceable concentrations of bicarbonate (HCO_3^-) and sulphate (SO_4^{2-}) ions. First investigations of stable sulphur isotope data within both shafts reflect the stratification pattern displayed in the geophysical log. The determined $\delta^{34}\text{S}$ value for the deeper water body in shaft Hermann 1 is 10.0 ‰ lower compared to the upper water body. All water samples taken from the upper water body show similar values accounting for the homogeneity of the water body between the water surface and 850 m. No stable sulphur isotope value for the dissolved sulphate could be determined for the deeper water body of shaft Hermann 1 due to the low sulphate concentration.

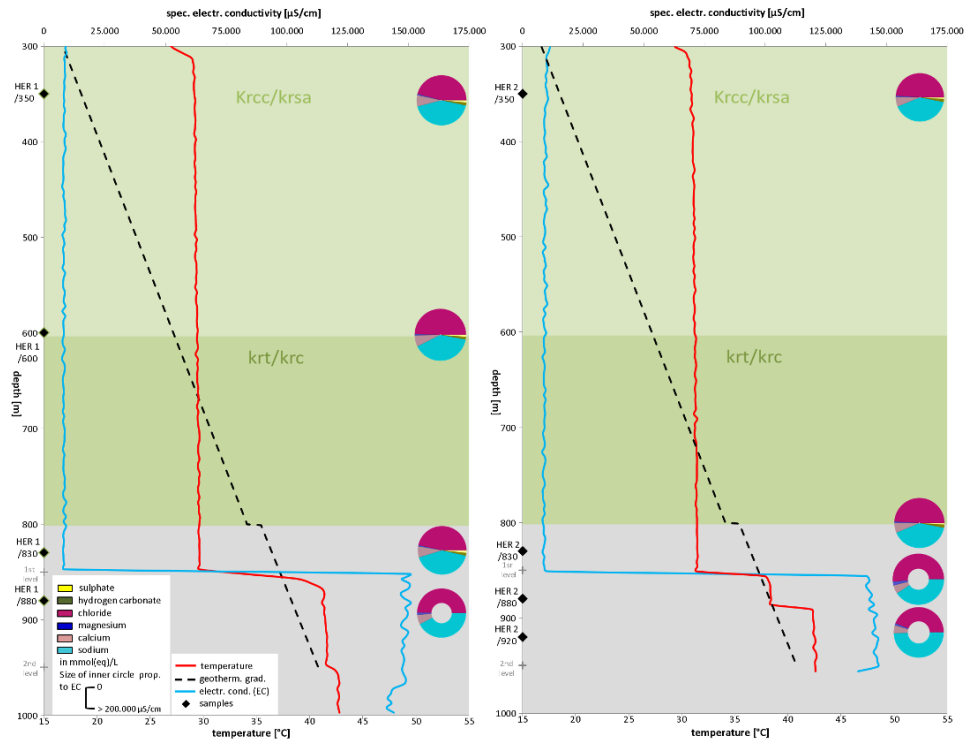


Figure 2 Water quality trend of shaft Hermann 1 (left) and shaft Hermann 2 (right). Depth is indicated in metres below ground surface. Colours indicate lithology (light green: Emscher Mergel, dark green: Cenomanian/Turonian, grey: Carboniferous).

Discussion

The formation of density stratification has been identified both in shafts that have already been flooded as well as in shafts that are still undergoing this process. It is obviously not related to the chemical composition of the different fluids, as stratifications are acquired between different water types, such as Na-HCO₃⁻ and Na-Cl type fluids, and also between individual Na-Cl type water bodies of different TDS (as it is the case in shaft Hermann 1 and 2). The thickness of homogeneous water bodies can vary from just a few metres to as much as several hundred metres. However, the boundary layer is very distinctive with usually no more than a few decimetres in depth. According to present knowledge the formation of boundary layers is largely based on water inflow from the surrounding rock and on rock-specific properties such as thermal conductivity and fracturing. However, the shaft lining can also play a role here, as this provides the route for water inflow at the individual horizon levels.

Repeated geophysical measurements in shaft Hermann 1 and 2 reveal the formation of stable density stratification. In the water columns of both shafts a sharp boundary layer is located at a depth of 850 m. It is apparent from the documents that the two shafts are con-

nected via the 1st level (850 m-level) in approximately this depth. All hydrochemical and stable isotope data which have been evaluated so far point to an active hydraulic communication over the mine workings and possibly the surrounding rock. Previous studies dealing with this subject considered a temperature-dependent density-driven flow as a reason for this phenomenon (e.g. Gebhart et al. 1988, Melchers 2015, Wolkersdorfer 1996).

The triggering force for this movement is seen in the geothermal gradient. Theoretically, in an underground water column this gradient warms up the deeper-lying mine water and induces convective transport related current phenomena (Berthold 2009). These prevent the mixing of inflows of a different solute composition, which leads to the formation of a further convection cell. Flow velocity measurements in combination with numerical simulations conducted by Kories et al. (2004) revealed numerous circular currents being responsible for the homogeneous conditions within the water body of shaft Hermann 1. In their model current velocities appear to be high in regions of homogeneity and low near the boundary layer. The authors further demonstrated that a continuous fresh water recharge is crucial for a stable stratification. In available records dealing with the Hermann coal mine relatively high quantities of water flowing in from the side-walls during the active production phase are documented. In combination with high underground temperatures and sales problems at the coal market the costs for the drainage forced the early closure of the mine. Latest camera inspections of the upper shaft lining above the water surface in course of on-going monitoring measures point to steady inflow of near-surface water through the brick walls. As a result, the observed conditions plead for a continuous water recharge.

In geochemical terms, the mine water generally equates to a mixture of ground water and soil leachate that has been geochemically altered by the various processes taking place in and around the mine workings. As a result, processes such as gas dissolution and release, evaporation and condensation can alter the solute concentrations within the water column. According to the results of the hydrochemical analysis combined with the regional hydrogeology, the upper water body is subject to exchange reactions with water from the upper as well as with water from the lower groundwater aquifer. Pursuant to the assumption that water exchange between the two water bodies is minimal across the boundary layer, flow of the brine type lower water body in both shafts points to an interaction with the deep formation water of the Carboniferous strata. In order to specify origin and flow path of the water and to assess the associated physicochemical processes affecting the water bodies such as water-rock-interactions, stable isotope geochemical investigations have been performed on all collected samples. The significant difference of 10 ‰ in the stable sulphur isotope data of shaft Hermann 2 indicates an additional sulphur source mixed with the sulphate inventory of meteoric water in the lower water body. We assume that this secondary source with a depleted ^{34}S value stems most likely from organic sulphur in the hard coal. Alternatively, alteration by sulphate reducing bacteria cannot be ruled out. In the future the data has to be interpreted in terms of stable isotope distribution patterns under consideration of calculations concerning the mass balance and equilibrium or kinetic isotope effects. The density differences along with distinct stable sulphur and oxygen isotope signatures of the dissolved

sulphate as well as stable carbon isotopes of the DIC help to understand mass flow across the stratification boundary and addresses microbial processes in a first attempt. Stratification patterns in old mine workings play a crucial role in post-mining management regarding disposal and treatment of contaminated waters and need to be monitored. Hence, it can act as a barrier for contaminated mine waters and lower the potential risk of mine water mixing with groundwater reservoirs.

References

- Berthold S (2009) Geophysikalischer Nachweis freier Konvektion in Grundwassermessstellen und Bohrungen, DGFZ, 230 pp
- DIN 38402-13:1985-12: German Standard methods for the examination of water, waste water and Sludge, general Information (group A), sampling from aquifers (A13)
- Gebhart B, Jaluria Y, Mahajan RL, Sammakia B (1988) Buoyancy-induced flows and transport. Hemisphere Publ. Corp, 1001 pp
- GVST (2015) Gesamtverband Steinkohle e.V. Jahresbericht 2015 – Verantwortlich handeln. Perspektiven schaffen, Herne, Germany, 86 pp
- Hahne C, Schmidt R (1982) Die Geologie des Niederrheinisch-Westfälischen Steinkohlengebietes: Einführung in das Steinkohlengebirge und seine Montangeologie. Verlag Glückauf, Essen, 106 pp
- Hilden HD, Drozdowski G, Hiß G, Lehmann F, Michel G, Skupin K, Staude H, Thiermann A, Dahm-Ahrens H (1995) Geologie im Münsterland. Krefeld, 195 pp
- Kories H, Rüterkamp P, Sippel M. (Eds) (2004) Field and numerical studies of water stratification in flooded shafts. In: Jarvis AP, Dudgeon BA, Younger PL (Eds.), Mine Water 2004, Proceedings, International Mine Water Association Symposium, vol. 1. University of Newcastle, Newcastle upon Tyne, p 149–159
- Langguth HR, Voigt R (2003) Hydrogeologische Methoden. Springer, Berlin Heidelberg, 1005 pp
- Leonhardt J (1983) Die Gebirgstemperaturen im Ruhr-Revier. Das Markscheidewesen 90 (2): 218–229.
- Melchers C, Coldewey WG, Wesche D (2014) Ausbildung von Dichteschichtungen in Schächten des Steinkohlenbergbaus im Ruhrrevier. In Meier G et al. (Eds) 14. Altbergbaukolloquium, Gelsenkirchen, p 156–162
- Melchers C, Goerke-Mallet P, Henkel L, Hegemann M (2015a) Experiences with mine closure in the European coal mining industry: An overview of the situation in Germany and adjacent regions. In Fourie AB, Tibbett M, Sawatsky L, van Zyl D (eds), Proceedings of Mine Closure Conference 2015, Vancouver, Canada, p 711–724
- Melchers C, Coldewey WG, Goerke-Mallet P, Wesche D, Henkel L (2015b) Dichteschichtungen in Flutungs-wasserkörpern als Beitrag zur Optimierung der langzeitigen Wasserhaltung. In Paul M (Eds) Sanierte Bergbaustandorte im Spannungsfeld zwischen Nachsorge und Nachnutzung – WISSYM 2015. Wismut GmbH, Chemnitz, p 99–106
- Pfläging K (1999) Steins Reise durch den Kohlenbergbau an der Ruhr, Der junge Freiherr vom Stein als Bergdirektor in der Grafschaft Mark. Schriftenreihe des Heimat- und Geschichtsvereins Sprockhövel eV. Geiger Press, Vol 7, 255 pp
- Wolkersdorfer C (1996) Hydrogeochemische Verhältnisse im Flutungswasser eines Uranbergwerks – Die Lagerstätte Niederschlema/Alberoda. Clausthaler Geowissenschaftliche Dissertationen 50:1–216.

Biophysical closure criteria without reference sites: Evaluating river diversions around mines

Melanie L. Blanchette¹, Mark A. Lund¹

¹*Mine Water and Environment Research Centre (Miwer.org), ECU Centre for Ecosystem Management, School of Science, Edith Cowan University, Perth, Western Australia AUSTRALIA 6027, m.blanchette@ecu.edu.au.*

Abstract The use of ‘reference’ sites to rehabilitate mined lands often creates unrealistic targets, resulting in environmentally underperforming sites. Previously, we proposed a more achievable approach to mine closure by comparing the bio-physical characteristics of rehabilitated sites to overall ecosystem variability (i.e., the ‘system variability’ approach), rather than specific target reference sites. We tested this model by evaluating the bio-physical state of river diversions around two mined areas in Australia’s Hunter Valley. The model clearly identifies how diversion sites differ from non-diverted sections of river, providing a practical example of model application.

Key words Hunter Valley, multivariate, ordination, aquatic macrophytes, water quality, riparian

Introduction

The use of ‘reference sites’ is accepted by regulators as rehabilitation targets in areas disturbed by mining activities. A ‘reference site’ is broadly perceived as having desirable conditions, processes, and/or taxa with which to compare impacted sites. Generally, reference sites co-occur with disturbed sites, yet are unimpacted and retain “naturalness” of the biota (Stoddard et al. 2006). However, this approach is flawed, often creating impossible or unrealistic targets for miners seeking to close rehabilitated lands. For example, many systems are so heavily modified that co-occurring unimpacted sites do not exist (Chessman and Royal 2004). In the instance where reference sites are nominated, a judgement call must be made as to the ‘desirable’ traits of a reference site (Stoddard et al. 2006). Determination is then required as to how similar impacted sites have to be to reference sites in order to meet rehabilitation objectives. Natural seasonal variability can also confound efforts to define and compare reference sites (sensu Blanchette et al. 2016). Essentially, reference sites are a human construct, resulting in restoration targets where changing ideals and natural variability ensure the goalposts are constantly shifting.

River condition assessment programs that capture the natural variability of the system can provide alternatives to reference sites and clarify rehabilitation goals (see Blanchette et al. 2016 for examples). Our model compares the biophysical criteria in rehabilitated sites to the overall spatial and temporal bio-physical variability of the local environment (hereafter referred to as ‘system variability’), rather than specific reference sites. We used riverine environments in the Hunter Valley, New South Wales, Australia to develop and test the model but the system variability approach can also be applied to terrestrial ecosystems.

The system variability approach to closure uses established analytical techniques (multivariate ordination) and current monitoring approaches. It has many advantages over the use

of reference sites, in that the criteria are likely to be more ecologically relevant by reflecting natural variability and existing land impacts, as well as having clear endpoints. Essentially, our approach is an extension of commonly used ecological assessment methods that have been applied to facilitate closure. Current ecological assessment techniques focus on using multivariate approaches to highlight *differences* in communities (i.e., demonstrating the impact of mining); we are simply suggesting that where there is *no significant difference* between the rehabilitated area and other parts of the ecosystem, closure has been achieved. Therefore, the purpose of this research is to test the model developed in Blanchette et al. (2016).

Methods

Catchment description and hydrology – The Hunter Catchment (21,500 km²) is located in New South Wales, south eastern Australia. The Hunter River has been highly modified since European settlement for industry, agriculture, flood mitigation and domestic use. Hunter Catchment waterways are seasonal, tending to flow more during the ‘wet season’ in response to rainfall (November–April) and less during the ‘dry season’ (May–October), although flooding can occur at any time. The overall flow regime of the Upper Hunter River consists of long periods of seasonally-responsive low flows punctuated by rare high-magnitude flood events (see Hoyle et al. 2007).

This research focusses on The Goulburn River (Figure 1) and Bowman’s Creek (Figure 2), two waterways within the Hunter Catchment. Both rivers have been modified by coal mining activities, resulting in complex hydrological conditions where anthropogenic effects interact with the natural seasonal flows.

The Goulburn River contains a trapezoidal diversion currently undergoing terrestrial rehabilitation. Downstream of the diversion the discharge of operational groundwater transformed the naturally seasonally-flowing river into a continuously flowing system. Artificially increasing base flow stability and reducing flow variability (i.e., drying periods) promotes excessive growth of certain aquatic macrophyte species (Bunn and Arthington 2002), which was observed throughout the Goulburn River study area (see Fig. 3A).

The diversion in Bowman’s Creek was operational in 2012 and designed to mimic ‘natural’ river characteristics (morphology, in-stream aquatic habitats). The hydrology of Bowman’s Creek appears to be largely unregulated and similar to the overall flow regime of the Upper Hunter River (station GS 210130; NSW Office of Water; May 1994–April 2017). Similar to the Goulburn River, however, excessive growth of reeds and other aquatic macrophytes occurred within the diversions (Fig. 3B), indicating that even subtle changes in the natural flow regime by artificial diversions, which may undetectable by gauging stations, have an ecological effect.

Data collection – The overall experimental design was 32 sites at two rivers (Bowman’s Creek; 12 sites, Goulburn River; 20 sites) repeatedly sampled during a hydro-period (May–December 2016). Sites (50 m fixed longitudinal transects) were selected based on

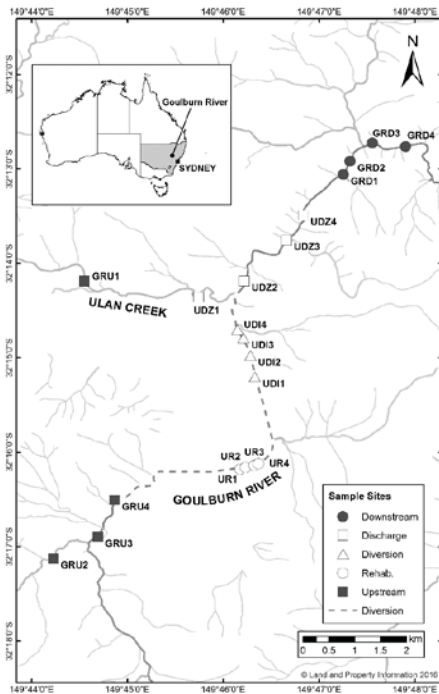


Figure 1 Goulburn River, New South Wales, Australia. Sites numbered upstream (1) to downstream (4) and grouped according to river section. Dashed lines are constructed river diversions and solid lines are natural water courses.

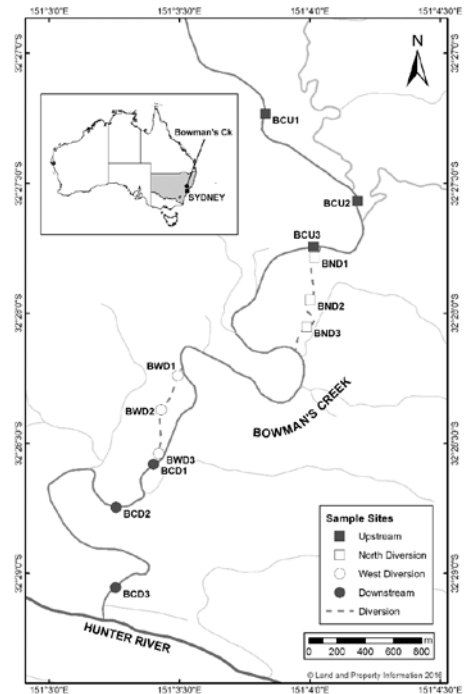


Figure 2 Bowman's Creek, New South Wales, Australia. Sites and lines arranged as per Figure 1. (n.b., river currently flows through constructed diversions rather than co-occurring natural stretches of Bowman's Creek).



Figure 3 Study sites on the Goulburn River (Fig. 3A; 'rehab' site UR2, and Bowman's Creek (Fig. 3B; 'diversion' site BND1). See Figures 1 and 2 for map and site references.

accessibility and representativeness of the biophysical variables of each river. Bowman's Creek was sampled twice: once during the nominal 'late wet/early dry' season (May 2016) and once during the nominal 'late dry/early wet' season (December 2016). The Goulburn was sampled three times (May, September, December 2016).

In situ water quality measurements of turbidity (NTU), pH, conductivity (mS/cm), temperature (°C) and oxidation-reduction potential (ORP; mV) were collected with a Hydrolab Quanta at a 10-cm depth once at each site. *In situ* soil measurements of pH and ORP (mV) at a 1 cm depth were collected at five points along the 50 m transect encompassing all in-stream habitats, where present (i.e., hydrological features, aquatic macrophytes, sediment variability). Flow (m/s) was measured 5–7 cm below the water surface using a digital flow meter at five points along transects, accounting for all in-stream hydraulic habitats. Water was collected and analysed for metals and nutrients (Appendix 1) at the Edith Cowan University Analytical Chemical Laboratory.

Percent cover of the wetted transect by periphyton/filamentous algae, aquatic plants, terrestrial leaf litter, bare sediments, iron flocculent, blanketing supra-benthic silt, or bacterial-algal mat was quantified using an index as per Blanchette and Pearson (2012), and sediment composition was determined using a modified Phi scale index as per Blanchette and Pearson (2012). Riparian condition was quantified on both left and right banks with a modified ‘tropical rapid appraisal of riparian condition’ method (sensu Blanchette and Pearson 2012; Dixon et al. 2006) developed specifically for intermittently-flowing rivers disturbed by mining.

Data analysis – Data were analysed as described in Blanchette et al. (2016), and rivers were analysed separately. Briefly, principal components analysis (PCA) in PRIMER (Clarke and Gorley 2006) was used to visually portray similarity among sites based on multiple variables as a physical distance, allowing variability tracking over time and determination of influential variables (Ramette 2007). Permutational MANOVA (PERMANOVA; also in PRIMER) with a Euclidean distance (9999 permutations) was used as a hypothesis test to ascertain whether biophysical variables between and among sites were significantly different ($p < 0.05$; H_0 = no significant difference) (Clarke and Gorley 2006). Data were analysed in three separate components: *in situ* continuous data, *in situ* indices, and water quality analyses (Appendix A). Variables were individually transformed where appropriate and all data was normalised prior to analysis.

Results & Discussion – Rivers

Goulburn River – Across all sites, time was a significant ($F_2 = 6.31$, $p < 0.001$) factor structuring *in situ* continuous data (see Appendix 1). Within individual times (May, September and December 2016), *in situ* continuous data from ‘rehab.’ and ‘diversion’ sites were consistently significantly different ($p < 0.05$) from the rest of the catchment. PCA for *in situ* continuous data indicated that the rehab and diversion sites tracked together through time yet remained distinct from the rest of the study sites due to a higher percent cover of rushes, turbidity, and benthic shade, as well as lower soil ORP and pH levels, slower (but more persistent) velocities, lower water ORP readings and less canopy cover and fringing bank vegetation (Figure 4). Rush-covered sites were associated with lower soil ORP due to organic matter turnover in a thick benthic root mat. Low levels of ORP are associated with anoxic (and even methanogenic) conditions (Boulton et al. 2014), indicating that the microbial activity of these sites – fundamental to ecosystem processes – likely differs from the rest of the catchment. Excessive aquatic plant growth was likely due to changes in the natural flow regime and increased light levels due to a loss of canopy.

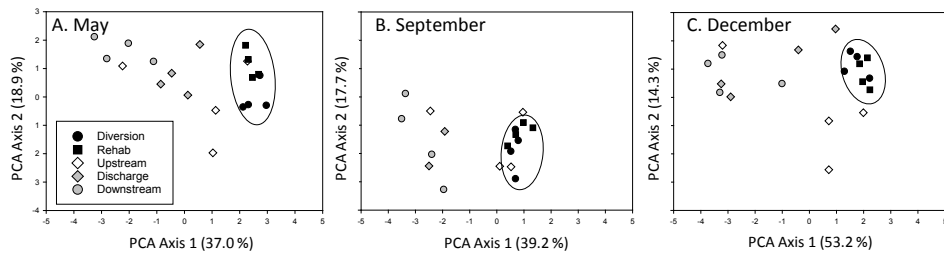


Figure 4 Principal components analysis (PCA) plots of *in situ* continuous data (see Appendix 1) from the Goulburn River. Plots depict temporal shifts in the data at the river scale. Diversion and rehab sites were significantly different to the rest of the river, despite tracking similarly over time.

Similar to the *in situ* continuous data, time was significant ($F_2 = 1.88$, $p = 0.04$) on *in situ* indices (Appendix 1) across all sites. However, unlike the continuous data, the *in situ* indices were only different across all sites in May and September ($p < 0.01$). At the river scale there was a significant spatial effect ($F_4 = 6.76$, $p < 0.001$), with pairwise analyses indicating that, with the exception of the discharge and upstream sites ($p = 0.06$), *in situ* indices between all sites were significantly different ($p < 0.05$). PCA for *in situ* indices indicated little temporal variability across all sites, with rehab and diversion sites clustering together across all times (not shown). The rehab and diversion sites separated from the rest of the catchment due to the presence of blanketing iron flocculent. Downstream sites (located in a national park) had higher levels of leaf litter, filamentous algae, canopy cover and canopy health, more understory, and bare benthic sediments.

Across all sites in the Goulburn River, there was a significant effect of time ($F_2 = 13.10$, $p < 0.001$) on water quality (Appendix 1), and pairwise analysis indicated that water qualities at all times were significantly different from each other ($p < 0.001$). Within individual times, water quality data from downstream and discharge sites were significantly different ($p < 0.05$) from the rest of the river, particularly in May and December. PCA for water quality data in the Goulburn demonstrated that the discharge and downstream sites tracked together through time, remaining distinct from the rest of the study sites (data not shown), and were associated with SO_4 , K, S, Ca, and Mg (commonly associated with groundwater discharge). Upstream sites were associated with phosphorous (total P, PO_4), likely due to surface run off from agriculture and clearing (Schoumans et al. 2014), and the diversion/rehab sites were rich in iron (due to groundwater incursion), nitrogen, and carbon (likely due to decomposition of reeds). The strongest relationships between sites and water quality variables occurred in May, when sites were shallower and less hydrologically connected. This is a classic phenomenon in Australian rivers, where sites evolve into unique ‘mesocosms’ along a drying river (Blanchette and Pearson 2013; Sheldon 2005).

Bowman’s Creek – Across all sites, time was significant ($F_1 = 3.58$, $p < 0.01$) in structuring *in situ* continuous data (Appendix 1). Within times (May and December), pairwise analysis indicated that sites were not significantly different ($p > 0.05$). However, across both times, site was a significant factor ($F_3 = 3.91$, $p < 0.001$), and PCA showed separation between di-

version and non-diversion sites (data not shown). This seemingly incongruous result highlights the issue of scale, a concept underpinning ecological monitoring and rehabilitation (Lindenmayer and Likens 2010). Diversion sites had a higher cover of rushes, and non-diversion had more trailing bank vegetation, greater canopy cover, and were deeper. Rushes were outcompeting trailing bank vegetation in the diversion. Trailing bank vegetation is an important structural component of river ecosystems, with invertebrate communities changing in response to vegetation growth and concurrent effects on localised flow regime (Armitage et al. 2001). Rushes were also altering benthic characteristics by forming layers of silt over gravel and cobble. Aquatic macroinvertebrates are particularly reliant on benthic composition as it forms a significant aspect of their ‘habitat templet’ (Townsend and Hildrew 1994). Increased growth of rushes has also resulted in sites becoming shallower; pools that serve as dry-season refugia for aquatic taxa (Dudgeon et al. 2006) are at risk of disappearing.

Time was not a significant factor structuring *in situ* indices (Appendix 1) in Bowman’s Creek at the river scale ($F_1 = 1.90$, $p = 0.06$), although site was significant ($F_3 = 4.46$, $p < 0.01$). Pairwise analysis for site groups indicated that the diversion sites were significantly different ($p < 0.01$) to the rest of the river. The North and West diversion sites were not significantly different to each other ($p = 0.184$). PCA showed separation between diversion and non-diversion sites (Figure 5), and diversion sites had a higher cover of true aquatic plants (submerged, floating, and emergent), whereas non-diversion sites had greater canopy health and higher covers of in-stream and bankside leaf litter.

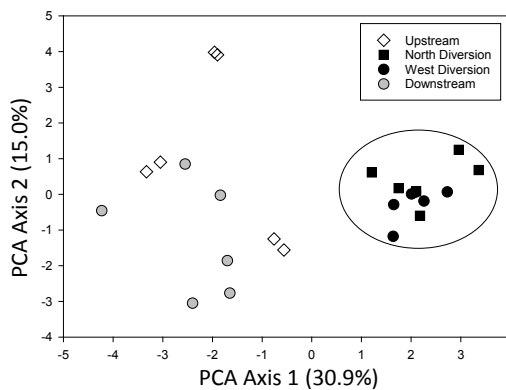


Figure 5 Principal components analysis of *in situ* indices (see Appendix 1) in Bowman’s Creek during May and December 2016. North and West diversion sites were significantly different from upstream and downstream sites ($p < 0.05$), but not significantly different from each other.

Water quality parameters (Appendix 1) in Bowman’s creek varied over time ($F_1 = 9.28$, $p < 0.001$), but not space (*a priori* site groups; $F_3 = 1.24$, $p = 0.21$). PCA showed separation between water quality parameters in May and December (data not shown), with May data driven by higher levels of Mn, Zn and Ca, and December sites characterised by nutrients (total N, total P, and DOC).

Discussion – Applying the ‘system variability’ model to mine closure

Developing the system variability model first involves measuring a suite of meaningful variables that account for seasonality and spatial scale. Next, determination of influential environmental variables and deciding which are influenced by mining (as opposed to other land uses). Finally, weighing up the cost/benefit of altering the variables to achieve rehabilitation. This method is in opposition to the reference site approach, which can force practitioners to choose generic key indicators *before* they begin collecting data. For example, in the Goulburn, reed growth and iron appear to be separating diversion sites from the rest of the river. With that knowledge, the company can decide whether they want to rehabilitate flow regimes and increase canopy cover, and/or correct groundwater inflows. The system variability model can assist this process by tracking progress over time; even if a site isn't fully rehabilitated, tracking towards the rest of the river could be viewed as progress and fulfilment of closure requirements.

Although regulators are used to the ‘reference idea’ for rehabilitation, ordination is routinely used in government and consulting to ‘prove’ that a site was impacted by mining. We are using this method in the opposite way: to determine if a site matches the rest of the system, and what variables need to be manipulated for rehabilitation.

This research has demonstrated that rehabilitation programs have to consider within- and among-site variability, not just absolute similarity. Two sites will never share identical ideal characteristics; a more reasonable goal would be to achieve rehabilitated sites that share characteristics of the area in which they exist, and behave in a similar fashion over time. Ignoring variability does not serve to rehabilitate mined landscapes, and productive outcomes are likely to be achieved in collaborations between scientists and industry managers (*sensu* Blanchette and Lund 2016).

APPENDIX A – Grouped variables for data analysis (units as per methods section).

- *In situ* continuous: turbidity, pH, conductivity, temperature, water ORP, velocity, sample depth, percent of site covered by rushes, percent canopy cover, percent of bank with trailing vegetation, soil pH, soil ORP.
- *In situ* indices: periphyton/filamentous algae, aquatic plants, leaf litter, bare sediments, iron flocculent, sediment composition, canopy cover, canopy health, understory cover, organic litter on bankside, exposed soil on bankside, grass cover on banks, dominant bankside sediment, undercutting, gullyng, damage from animals.
- Water quality variables: B, Al, Cr, Mn, Fe, Co, Ni, Cu, Zn, As, Se, Cd, Hg, Pb, U, Ca, K, Na, Mg, S, NH₄, NO_x, Total N, PO₄, Total P, Cl⁻, SO₄, Total C, DOC.

Acknowledgements

Australian Coal Association Research Program (ACARP), ECU School of Science. Mr. Jonathon Boeyen constructed site maps with GIS data provided by the Australian state governments of WA and NSW.

References

- Armitage P, Lattmann K, Kneebone N, Harris I (2001) Bank profile and structure as determinants of macroinvertebrate assemblages—seasonal changes and management *Regulated Rivers: Research & Management* 17:543-556
- Blanchette M, Pearson R (2013) Dynamics of habitats and macroinvertebrate assemblages in rivers of the Australian dry tropics *Freshwater Biology*
- Blanchette ML, Lund MA (2016) Pit lakes are a global legacy of mining: an integrated approach to achieving sustainable ecosystems and value for communities *Current Opinion in Environmental Sustainability* 23:28-34
- Blanchette ML, Lund MA, Stoney R, Short D, Harkin C Bio-physical closure criteria without reference sites: realistic targets in modified rivers. In: Drebenstedt C, Paul M (eds) *International Mine Water Association: Mining Meets Water – Conflicts and Solutions*, Leipzig, Germany, 2016. pp 586-592
- Blanchette ML, Pearson RG (2012) Macroinvertebrate assemblages in rivers of the Australian dry tropics are highly variable *Freshwater Science* 31:865-881 doi:10.1899/11-068.1
- Boulton A, Brock M, Robson B, Ryder D, Chambers J, Davis J (2014) *Australian freshwater ecology: processes and management*. John Wiley & Sons,
- Bunn SE, Arthington AH (2002) Basic principles and ecological consequences of altered flow regimes for aquatic biodiversity *Environmental management* 30:492-507
- Chessman BC, Royal MJ (2004) Bioassessment without reference sites: use of environmental filters to predict natural assemblages of river macroinvertebrates *Journal of the North American Benthological Society* 23:599-615
- Clarke K, Gorley R (2006) *User manual/tutorial PRIMER-E Ltd*, Plymouth
- Dixon I, Douglas M, Dowe J, Burrows D (2006) *Tropical Rapid Appraisal of Riparian Condition*. Land & Water Australia,
- Dudgeon D et al. (2006) Freshwater biodiversity: importance, threats, status and conservation challenges *Biological reviews* 81:163-182
- Hoyle J, Brierley G, Brooks A, Fryirs K (2007) Sediment organisation along the upper Hunter River, Australia: a multivariate statistical approach *Developments in Earth Surface Processes* 11:409-441
- Lindenmayer DB, Likens GE (2010) The science and application of ecological monitoring *Biological conservation* 143:1317-1328
- Ramette A (2007) Multivariate analyses in microbial ecology *FEMS Microbiology Ecology* 62:142-160
- Schoumans O et al. (2014) Mitigation options to reduce phosphorus losses from the agricultural sector and improve surface water quality: a review *Science of the Total Environment* 468:1255-1266
- Sheldon F (2005) Incorporating Natural Variability into the Assessment of Ecological Health in Australian Dryland Rivers *Hydrobiologia* 552:45-56 doi:10.1007/s10750-005-1504-7
- Stoddard JL, Larsen DP, Hawkins CP, Johnson RK, Norris RH (2006) Setting expectations for the ecological condition of streams: the concept of reference condition *Ecological Applications* 16:1267-1276
- Townsend CR, Hildrew AG (1994) Species traits in relation to a habitat templet for river systems *Freshwater Biology* 31:265-275

Water in Mining – Challenges for Reuse

Sílvia C.A. França¹, Lucas S. Andrade¹, Pamela E.V. Loayza², Bruna C. Trampus¹

¹Center for Mineral Technology, CETEM, Av. Pedro Calmon, 900 Cidade Universitária, Rio de Janeiro-RJ, Brazil sfranca@cetem.gov.br

²Pontifical Catholic University of Rio de Janeiro, PUC-Rio, R. Marquês de São Vicente, 225 – Gávea, Rio de Janeiro – RJ, Brazil

Abstract The use of tailings dewatering operations, such as particle aggregation, thickening and filtration, can reduce freshwater consumption in many mineral processing plants. This paper evaluates dewatering of two mineral tailings, from nickel and bauxite-alumina plants, aiming to improve the water recovery and reuse. Results show that natural polymers (humic acid and chitosan) are efficient to aggregate and settle red mud particles, with turbidity reduction of up to 95%. For nickel tailings, high molecular weight polymers are more efficient. The insertion of filtration allowed an extra water recovery up to 65%. Furthermore, it can make suitable dry stacking of tailings.

Key words Tailings dewatering, particle aggregation, filtration, red mud, nickel tailings, water reuse

Introduction

Mining activity demands large volumes of water and, consequently, generates significant amounts of tailings, which must be disposed of in an environmentally sustainable way, with reasonable cost. Mineral tailings are mostly discharged as concentrated pulps or slurries, so dewatering plays an important role in the final characteristics of the tailings produced (Mudd 2008). The use of thickeners near the ore processing plant allows the partial recovery and recirculation of process water and chemicals at relatively low costs, also helping to reduce new water abstraction, which enables lower operating costs and environmental impact.

Water scarcity, due to environmental issues as well as competition among various uses (e.g., drinking, farming, recreation, etc.) is one of the factors that stimulates the application of new technologies for the disposal of mining tailings (Wang et al. 2014). A distribution of mineral tailings disposal systems is shown in Figure 1 (Davies 2011), where it can be seen that conventional dewatering (thickening and filtration) is still the dominant method.

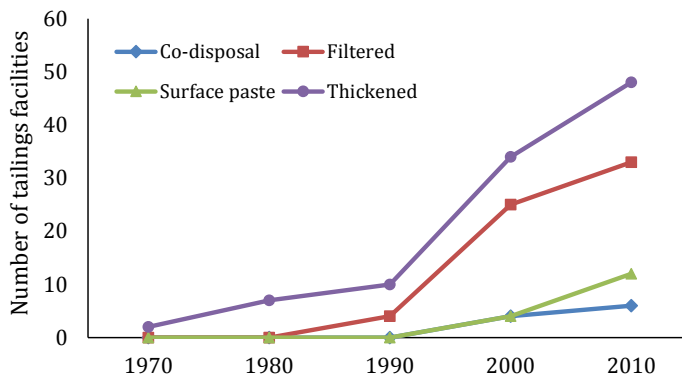


Figure 1 Tailings disposal systems in the mining industry (Davies 2011)

The efficiency of solid-liquid separation plants is directly related to the auxiliary chemicals used for particle aggregation (coagulation and flocculation). In the case of solid-liquid separation for recovery of industrial water, pulps or tailings containing clay minerals are more difficult to process because of the lamellar structure of a large part of the silicate minerals present, causing a need for flocculation. Parsapour et al. (2014) report that the increase in molecular weight of flocculant polymers reduces the density of the flocs due to the increase in the amount of water entrapped in the floc structure, whereas polymers with relatively smaller molecular weight can produce flocs of greater density, because they imprison less water in their structure.

Two tailings streams were considered in this study, from nickel and bauxite operations, due to the importance of both minerals to Brazilian mineral production and the challenges faced by these industrial plants regarding tailings disposal and water reuse.

Nickel tailings can contain 40-50% water along with residual Ni (0.3%) left over from the beneficiation process. The processing this material involves regrinding, desliming and metal recovery by column flotation. As a consequence, the new tailings generated by this reprocessing are even finer and can contain chemicals, requiring efficient dewatering for disposal and water reuse.

Disposal of red mud, a residue from bauxite refineries produced in the Bayer process, is a major challenge to the aluminum industry, due to its high toxicity and alkalinity. It is the world's leading industrial waste by volume and its generation is increasing by approximately 120 Mt/year (Kobya et al. 2014). This residue is filtrated before disposal, but small particles still remain in the filtrate, along with dissolved compounds, giving the effluent a reddish color due to the high iron oxide content and causticity ($10 < \text{pH} < 12$), so these particles need to be removed. Due to their surface properties and size, they will not settle naturally, making it necessary to aggregate them to improve solid-liquid separation. Therefore, the use of alternative reagents (coagulants and flocculants) that can promote aggregation into a highly alkaline medium can reduce the cost and improve efficiency, especially regarding water recycling to the processing plant (Aldi 2009).

Methods

Two tailings samples were studied: a red mud sample, with very fine particles ($d_{50} = 5.7 \mu\text{m}$, $P_{80} = 17 \mu\text{m}$) and a nickel tailing, with particle size $d_{50} = 12 \mu\text{m}$, $P_{80} = 30 \mu\text{m}$. Two groups of flocculant polymers were studied: natural polymers (Sigma-Aldrich) with low molecular weight, chitosan ($2.32 \times 10^5 \text{ g}\cdot\text{mol}^{-1}$) and humic acid HA ($2.31 \times 10^4 \text{ g}\cdot\text{mol}^{-1}$), as reported by Loayza et al. (2015). The second group was composed by three commercial flocculant polymers – polyacrylamides (BASF) identified in this paper as Z7565 (cationic polymer), and R10 and R90 (anionic polymers), with molecular weights ranging from $7.27 \times 10^6 \text{ g}\cdot\text{mol}^{-1}$ for R10 to $1.84 \times 10^7 \text{ g}\cdot\text{mol}^{-1}$ for R90 (Andrade 2016).

The zeta potential measurements were carried out with a DT 1200 spectrometer (Dispersion Technology™) to determine surface charges for both tailings particles as well as for the polymer solutions. The tailings pulps were prepared with 10% solids (by weight) with

the addition of an indifferent electrolyte, KNO_3 0.01 and 0.001 M. The zeta potentials were measured in the pH range of 2.0 to 12.5, adjusted with KOH and HNO_3 dilute solutions.

Flocculant polymers were prepared based on specific methods, as described by Loayza et al. (2015) and Gadelha & França (2015). Flocculation and sedimentation tests were performed in a jar testing device (Nova Ética™). For red mud suspensions, 1.0% solids slurries were prepared using deionized (Milli-Q® system) and tap water to evaluate the influence of ions present in the water. The slurries were prepared in a beaker with 2.0 L capacity at room temperature and stirred for 3 minutes at 190 rpm (rapid mixing). Then chitosan (30 g/t) was added and stirred at the same rotation for 1.2 minutes, followed by HA (10 g/t), maintaining the system under stirring for an additional 1.2 minutes. The stirring speed was reduced to 95 rpm (slow mixing) to promote floc growth, for 1 minute. After stirring, the slurry was allowed to stand at room temperature for a 1-hour sedimentation period.

Nickel tailings slurries were prepared with solids concentrations of 10, 15, 18 and 23% (w/v). Flocculant polymers Z7565, R10 and R90 were used in solutions of 0.5 g/L (Andrade 2016), for dosages of 40, 60, 80, 100 and 200 g/t. For flocculation and sedimentation tests, the nickel tailings slurries were stirred for 3 minutes at 300 rpm; after which the flocculant polymer was added and mixed for 1 minute at 300 rpm, and then at 150 rpm for 2 additional minutes. The slurry was left standing for sedimentation for 1 hour.

After sedimentation, small aliquots of the supernatant liquid were retrieved for determination of turbidity in a portable Hach™ 2100P turbidimeter. With this result, it was possible to calculate the solids removal efficiency of the different polymers used, regarding the solid-liquid aggregation/sedimentation and in relation to Brazilian environmental legislation, which requires turbidity values of 100 NTU for water reuse and 40 NTU for discharge.

Aiming for higher efficiencies on water recovery, filtration tests were run in a Filtratest™ unit, manufactured by Bokela, with a filtration area of 19.63 cm². A polypropylene fabric with multifilament yarns and air permeability of 1.5-5 m³/min/m² was used, under pressure drop of 2 bar. After the experiment, the filter cake was dried in an oven at 100±5 °C to constant weight for moisture content measurement. In this step, only slurries with 10, 15 and 23% solids concentration (w/v) were filtered, because low concentration slurries did not provide enough solids in the underflow to form cake.

Results and Discussion

Red mud treatment: zeta potential curves for the red mud sample and natural polymers are shown in the Figure 2.

The red mud particles and chitosan had similar surface charges in the entire pH range studied. For the HA, the surface charges were the opposite to those of the red mud in the 3<pH<6 range. Considering that the natural pH of red mud tailings is around 10.5-12, the largest difference between zeta potential of red mud particles and polymers, at this pH range, was observed for chitosan.

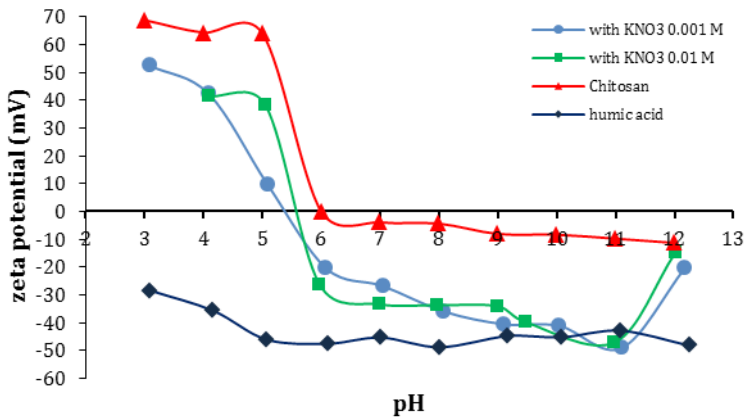


Figure 2 Surface charge of red mud (with KNO₃) and natural polymers (chitosan and humic acid)

The unflocculated red mud slurry presented average turbidity range of 500-550 NTU. At this pH, the flocculation efficiency was low for both types of water and flocculant, with high values of turbidity (up to 300 NTU), even after treatment (flocculation and sedimentation), as can be observed in Figure 3. These results might be due to the poor adsorption of polymers on the red mud particles' surfaces. Therefore, for pH in the range of 7 to 8, the flocculation of particles was efficient and produced supernatants with turbidity of 10 NTU, with chitosan as flocculant, corroborating the findings of Yang et al. (2014). The co-flocculation effect could be noticed also at pH 7-8 with the use of chitosan and HA, resulting in supernatants with less than 5 NTU, equivalent to 99% turbidity removal, allowing immediate water reuse.

Since the natural pH of red mud from refineries is around 10.5-12, another important aspect to highlight is that at pH near the isoelectric point (pH~12), the adsorption was efficient, especially in the presence of both chitosan and HA. A turbidity value around 33 NTU was attained, showing the potential of using a combination of these polymers, at natural red mud pH, for wastewater treatment and water reuse, improving the process in economic and environmental terms.

The zeta potential curves of the nickel tailings are shown in Figure 4. As can be noticed, nickel tailing show negative surface charge in most of the pH range, including the natural pH 6.5. An isoelectric point was observed around pH 10.5 and up to this value, charges were positive. In the range 6.5<pH<8.5 the surface charge reached values below -30 mV, corresponding to an unstable region, making aggregation more difficult (Loayza et al. 2015). In this case, high molecular weight polymers can be more efficient for particle aggregation.

Despite the highly negative surface charges in this tailings sample, Deniz (2014) reported that an advantage exists of using high molecular weight anionic polyacrylamide – in contrast to cationic polymers – to flocculate negatively charged particles, because the primer can produce flocs with increased settling rate and a distinct sediment structure. Considering the

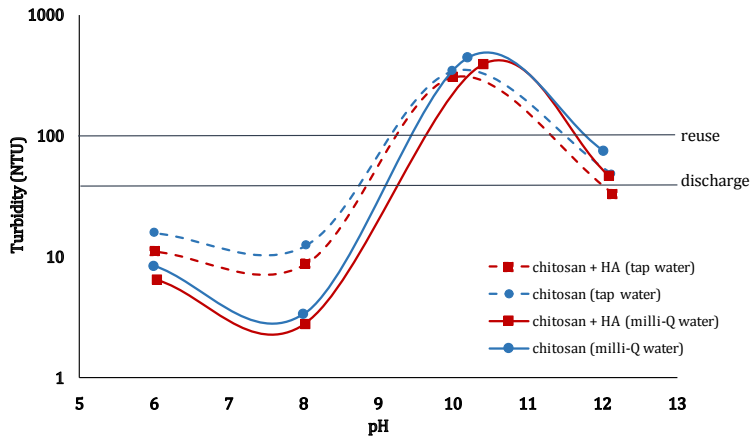


Figure 3 Turbidity removal of flocculated red mud

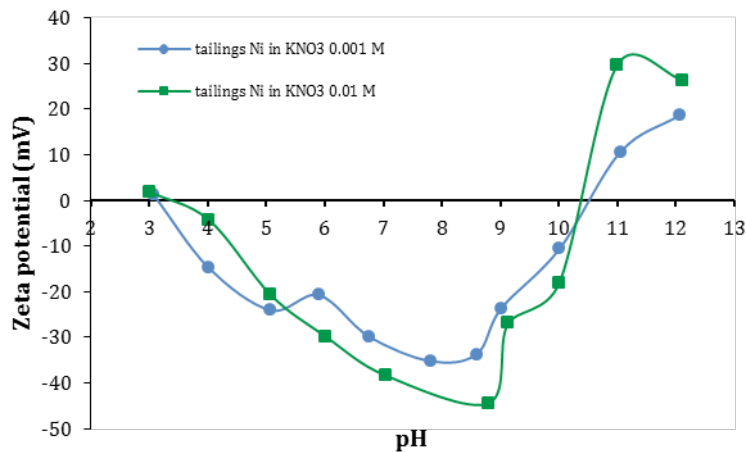


Figure 4 Surface charge of Ni tailings

presence of clay minerals (kaolinite) in the nickel tailings sample, the anionic polymers can also avoid the re-stabilization of clay particles by excessive polymer adsorption driven by strong electrostatic attraction.

The significant increase of the settling rate due to the use of flocculant polymers is depicted in the sedimentation curves (Figure 5). In addition, Table 1 shows the results for residual turbidity after nickel tailings treatment. Based on the results presented in Table 1, it can be seen that the Z7565 and R10 flocculant polymers promoted efficient solid-liquid separation, with high sedimentation rates and turbidity values below 40 NTU in the overflow. Regarding the settling velocity, the results show the importance of using flocculant polymers to

improve settling rates and enable faster reuse of process water. The flocculant polymer R10 (100 g/t) promoted an increase of 21% in floc diameter in relation to polymer Z7565, and 54% in relation to polymer R90.

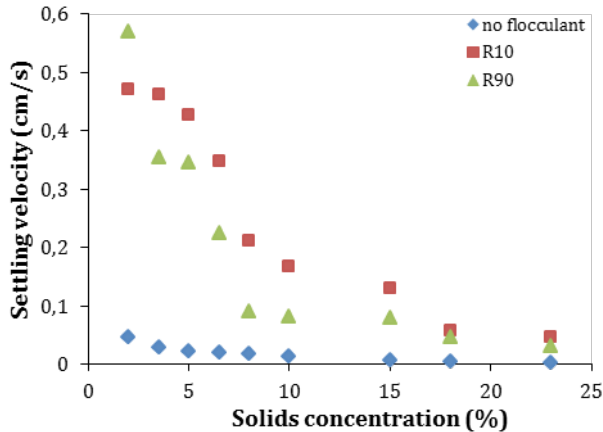


Figure 5 Settling velocity for natural and flocculated nickel tailings

Table 1 Residual turbidity of thickened nickel tailings flocculated with different polymers

Slurry characteristic	Polymer dosage (g/t)	Solids concentration (%)			
		10	15	18	23
Natural	No polymer	43432	44160	63872	80000
	40	108	226	332	266
	60	44.5	113	203	81.7
R10	80	42.1	64.4	201	303
	100	6.11	10.2	4.04	5.33
	200	3.43	3.12	4.77	6.38
	40	187	202	181	311
R90	60	79.4	155	225	262
	80	108	113	238	296
	100	6.00	36.0	7.65	14.8
	200	2.39	1.93	3.75	6.44
Z7965	60	68.3	123	241	324
	100	5.87	13.3	7.03	5.84
	200	1.78	4.62	2.40	2.45

After thickening, tailings (underflow) are usually pumped into tailings ponds where the particulate matter will settle, with slow rates of water release and solids compaction. To improve the dewatering process and water recovery and hasten water reuse, part of the underflow was submitted to a filtration step instead of pumping the slurry to the tailings pond. The results of water recovery due to filtration are presented in Figure 6.

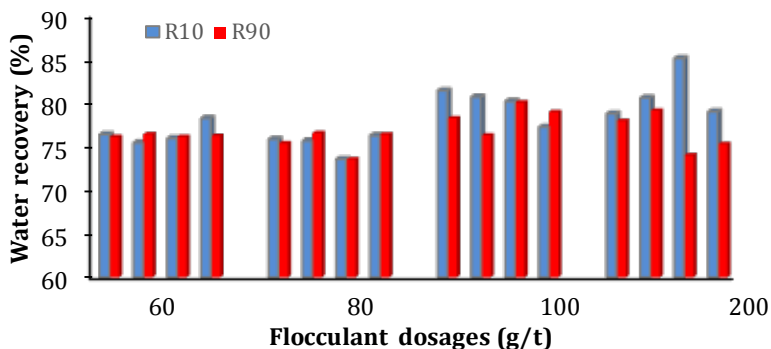


Figure 6 Water recovery by pressure filtration for different flocculant dosages

The results show that it possible to proceed with the immediate reuse 68-85% of process water, thus improving the dewatering plant with the filtration operation. Besides the water recovery, filters can produce cakes with 10 to 15% moisture, allowing dry stacking of the low moisture tailings, as also reported by Davies (2011). Flocculant polymers with higher molecular weight (R90) can entrap more water in the floc structure and reduce the water recovery by filtration. Parsapour et al. (2014) observed the same dewatering behavior. Polymer R10 performed better in water release under extra shear and pressure drop.

Conclusions

Natural polymers such as chitosan and humic acid can be used for red mud tailings treatment, to remove color and suspended particles, reaching turbidity reduction of up to 95% and satisfying the limits of Brazilian environmental legislation for water reuse or discharge. For nickel tailings, the use of high molecular weight polymers improved dewatering operations by increasing settling velocity up to 60%, allowing faster water reuse. The insertion of a filtration step for dewatering of thickened material allowed the production of low moisture cake, suitable for dry stacking, besides an extra 65% water recovery.

Acknowledgements

We thank the mining companies Votorantim and Alunorte for supplying the tailings samples for this study, and CETEM for the research grant in the Technical Internship Program (undergraduate student Lucas S. Andrade).

References

- Aldi J (2009) Achieving excellence in liquid effluent treatment at Alunorte. *Light Metals* 2009, 21-24
- Andrade LS (2016) Desaguamento de polpas minerais floculadas (Dewatering of flocculated slurries). Trabalho de conclusão de curso (Undergraduate final project), EQ/UFRJ, Rio de Janeiro, 52p
- Davies M (2011) Filtered dry stacked tailings – the fundamentals. In: *Proceedings Tailings and Mine Waste 2011*, Vancouver-BC, Canada
- Deniz V (2013) Use of co-polymer flocculants for eliminate of the environmental effects of wastewater of a coal washer and design of thickener for supplies of fresh water. *Energy Sources, Part A: Recovery, Utilization, and Environmental Effects* 35(22):2132-2140
- Gadelha TS, França SCA (2015) Polymer assessment for dewatering and filtration of nickel ore tailings. In: 2015 Enviromine 4th International Seminar on Environmental Issues in Mining, Gecamin, Lima-Peru, 15ENV_C05
- Kobyta M, Oncel MS, Demirbas E, Şık E, Akyol A, Ince M (2014) The application of electrocoagulation process for treatment of the red mud dam wastewater from Bayer's process. *Journal of Environmental Chemical Engineering* 2:2211–2220, doi.org/10.1016/j.jece.2014.09.008
- Loayza PEV, França SCA, Brocchi, EA (2015) The use of natural polymers (chitosan and humic acid) in the red mud wastewater treatment. In: 2015 Enviromine 4th International Seminar on Environmental Issues in Mining, Gecamin, Lima-Peru, 15ENV_C07
- Mudd GM (2008) Sustainability reporting and water resources: a preliminary assessment of embodied water and sustainable mining. *Mine Water Environ* 27:136-144, doi:10.1007/s10230-008-0037-5
- Parsapour G, Arghavani E, Banisi S, Mousavi S. (2014) Improving performance of the Gol-E-Gohar iron ore concentration plant thickener. *Proceedings of IMPC 2014 (Dewatering section)*, Gecamin Publications, Santiago, Chile.
- Wang C, Harbottle D, Liu Q, Xu Z (2014). Current state of fine mineral tailings treatment: A critical review on theory and practice. *Minerals Engineering* 58: 113–131, doi:10.1016/j.mineng.2014.01.018
- Yang Z, Li H, Yan H, Wu H, Yang H, Wu Q, Li H, Li A, Cheng R (2014) Evaluation of a novel chitosan-based flocculant with high flocculation performance, low toxicity and good floc properties. *Journal of Hazardous Materials* 276: 480–488, doi:10.1016/j.jhazmat.2014.05.061

Low-Cost Biological Treatment of Metal- and Sulphate-Contaminated Mine Waters

John William Neale¹, Heinrich Hagspühl Muller¹, Mariekie Gericke¹
and Ritva Mühlbauer²

¹*Mintek, Private Bag X3015, Randburg, 2125, South Africa,*

JohnN@mintek.co.za, HeinrichM@mintek.co.za, MariekieG@mintek.co.za

²*Anglo American Thermal Coal, 44 Main Street, Marshalltown, Johannesburg, South Africa,*
ritva.muhlbauer@angloamerican.com

Abstract This paper describes the development of a passive biological sulphate reduction (BSR) process. Laboratory-scale test work was performed on a mine-impacted water from a South African coal mine. The substrate mix comprised wood chips, wood shavings, hay, lucerne and cow manure. Over 90 % sulphate removal was achieved, the pH level was raised to above 7, and metals were precipitated. Operating parameters were optimised to increase process kinetics.

The results were used to design a pilot plant which will be operated at the coal mine, treating several hundred litres of water per day.

Keywords passive treatment, biological sulphate reduction, mine waters, pilot plant

Introduction

The threat to the South African environment from acid mine drainage and mine-impacted waters is well documented (NSTF/SAASTA 2011; Turton 2013). Effluents from the gold- and coal-mining industries can severely impact upon the quality of water supplies, and affect all major industries across the value chain. These acidic and metal-contaminated waters are typically treated by lime neutralisation, which removes the metals and increases the pH levels, but the discharge sulphate level remains high (Lorax Environmental 2003). Biological treatment using sulphate-reducing bacteria offers an alternative to conventional technologies for the localised treatment of effluents from the mining and metallurgical industries. The process has several advantages: both sulphate and metals are reduced to low levels, and less solid waste is produced compared to chemical precipitation. Passive processes have relatively low capital costs, and operating costs can be substantially reduced by using inexpensive carbon and energy sources. Numerous BSR plants have operated worldwide, focused primarily on increasing the pH levels and precipitating the metals (Watzlaf *et al.* 2004; Doshi 2006; Jamil and Clarke 2013). In South Africa, however, stringent regulations enforce lower sulphate discharge limits of 200600 mg/L (Arnold *et al.*, 2016), for which BSR is ideally suited.

The main objectives of the test work programme were to:

- Identify a suitable low-cost substrate and electron donor to be used in the process.
- Determine the maximum extent of sulphate removal during passive biological treatment of the mine water.
- Evaluate the effect of key operating parameters on the rate and extent of sulphate reduction, including temperature, pH level, sulphate loading, metal concentrations and hydraulic residence time (HRT).

Methods

Water Samples

Two water samples from a South African coal mine, located near eMalahleni (formerly Witbank) in Mpumalanga Province, South Africa, were utilised in the test work programme. The water samples contained trace quantities of several base metals, over 3000 mg/L of sulphate, and appreciable quantities of magnesium, calcium and manganese. The alkalinity of the water sample was 516 mg/L, and the pH level was 7.26.

Equipment

The test work was conducted in a series of three water-jacketed columns, each 1 m tall and 0.3 m wide, giving an internal volume of just over 70 L, as shown in fig. 1 and fig. 2. Each column was supported on a stand, which housed a conical section with a single outlet. A perforated plate, placed between the column and the conical section, acted as a support for the substrate.



Figure 1 Multi-stage column system

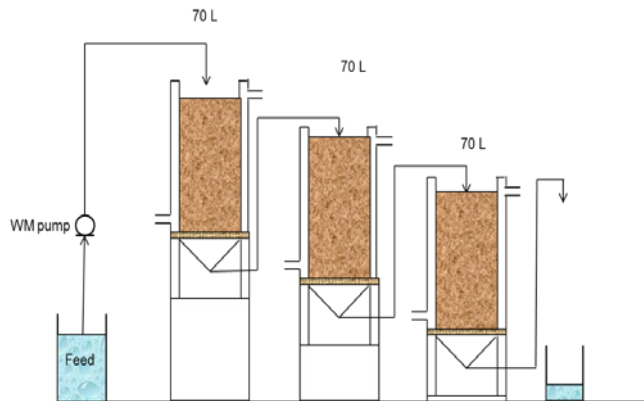


Figure 2 Schematic diagram of the three-stage column setup

The water jackets of the columns were connected to a heating and chilling unit, which was fitted with a pump that circulated water through the jackets. Measurement of the temperature in the columns was used to control the flow rate of water through the water jackets, allowing the column temperatures to be maintained at 20 °C, eliminating temperature fluctuations caused by daily and seasonal variations in the ambient condition.

All of the columns were packed with a mixture of the following quantities of organic substrates (measured by volume), which were mixed together and blended before being loaded into the columns:

- 20 % cow manure
- 20 % hay
- 20 % wood shavings and saw dust
- 40 % wood chips

A layer of silica pebbles was spread over the top of the distribution plate, to prevent blockages of the holes in the distribution plate caused by fines migrating downwards.

Inoculation, Start-up and Operation

The cow manure that formed 20 % of the substrate was the main source of sulphate reducing bacteria (SRB) and cellulose degraders. In addition, a 10 L quantity of product liquor from an existing BSR process was added to the substrate mixture during its blending, in order to supplement the inoculum with an active culture and reduce the start-up time.

The blended substrate mixture was firmly hand-packed into the columns. The columns were slowly filled by pumping mine water into the bottom of the column. In this way, air bubbles in the substrate were forced out as the water level slowly rose through the column.

The mine water feed was stored in a 10 L tank, from where it was pumped to the top of the first-stage column. The feed flow rate was adjusted to target a particular HRT. The water percolated in a downward-flowing flooded mode through the substrate bed, and exited through a flexible tube attached to the bottom of the column. The flexible tube was routed up the outside of the column to near the top edge. A T-piece was fitted to the top of the tube to assist with fluid level adjustment inside the column, and to direct the flow to the next column. The product from the third-stage column was collected over a 24-hour period, and the volume was measured and logged daily.

Daily measurements were made of the pH levels, redox potentials (vs Ag|AgCl), electrical conductivity and sulphate concentrations in each column. Routine sulphate concentrations were measured using the barium chloride gravimetric method (Jeffery *et al.* 1989). Once steady-state operation was achieved, liquor samples were collected from each column and submitted for metal analysis by inductively coupled plasma optical emission spectrometry (ICP-OES), sulphate determination using liquid ion chromatography (IC), sodium and potassium analysis by atomic absorption spectroscopy (AAS), while ammonium and phosphate were measured by colorimetric techniques.

Process Chemistry

The simplified process chemistry of the biological sulphate reduction process is as follows:



Results

The HRT in each column was initially set at 7 days. At the outset, cow manure was the preferred substrate, but it was found to have a clay-like structure, which was not porous enough to allow good contact between the fluid and the substrate. When the cow manure was mixed with lucerne straw, the performance of the columns improved. It was determined that regular addition of the faster-reacting components of the substrate (cow manure and lucerne straw) was required to maintain the performance levels. In the latter stages of the test, “kraal” manure and lucerne pellets were evaluated as an alternative to cow manure. (“Kraal” is the Afrikaans word describing an enclosure for cattle or other livestock. Kraal manure consists of organic material comprised of the residues of plants that are digested by cattle and then composted.) The results reported here are for the last 200 days of the test work programme, where the objective was to reduce the HRT by regular addition of substrate (kraal manure and lucerne). On day 315, 10 L of substrate was removed from the first-stage column and replaced with 5 L of kraal manure and 5 L of lucerne pellets. Thereafter, regular substrate replenishment was undertaken, as summarised in tab. 1, which also shows the impact that this had on the extent of sulphate reduction achieved in the first-stage column.

Table 1 Schedule for the addition of fast-reacting substrate

Day	Kraal manure added (L)	Lucerne pellets added (L)	First-stage sulphate reduction (%)
315	5	5	45.6
350, 364, 378	1	0	68.5, 54.2, 55.8
388, 395, 406	1	1	59.1, 49.3, 46.7
417, 431, 438	1	1	72.7, 96.1, 96.5
446, 452, 461	1	1	92.8, 95.9, 92.7
474	1	1	95.1

On day 465, the mine water feed to the plant changed slightly, as the original sample was depleted. The new feed was similar to the first one, with almost exactly the same sulphate concentration.

The routine measurements of the pH levels, redox potentials, conductivities, sulphate concentrations, sulphate removal levels and sulphate reduction rates are shown in fig. 3.

The pH levels ranged between 7.0 and 7.5, and the redox potentials remained below around 320 mV (vs Ag|AgCl), even after the HRT in each stage was reduced from 7 to 4 days.

Each addition of fresh substrate resulted in an immediate increase in the conductivity of the solution, indicating the release of ions from the substrate. By day 406, after several substrate replenishments, the conductivity in Column 1 increased from 5 to about 7 mS/cm,

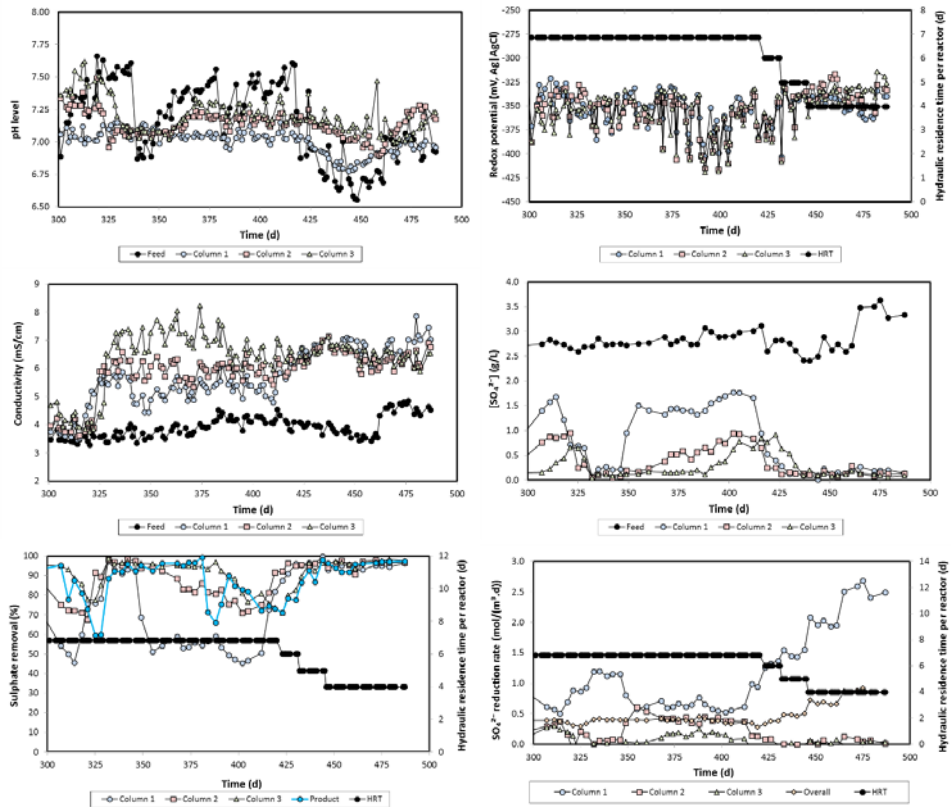


Figure 3 Performance of the biological sulphate removal reactor system

and the sulphate concentration decreased to around 500 mg/L. Towards the end of the run, the performance improved further, with the concentration in the final effluent being maintained below 150 mg/L, even after the single-stage HRT was reduced to 4 days.

With routine substrate replenishment, the sulphate removal level in Column 1 increased from around 50 % on day 412 to over 95 % by day 430. This made it possible to reduce the HRT in each column from 7 to 4 days. Even after this was done, the sulphate removal level remained above 95 %. It is anticipated that further reductions in the HRT will be possible, allowing the sulphate removal load to be spread over the three columns. Further optimisation of the quantity and frequency of the addition of fresh substrate will also be investigated. Towards the end of the experiment, the volumetric rate of sulphate reduction in Column 1 increased to over 2.5 mol/(m³.d) as the HRT was reduced to 4 days. The overall sulphate reduction rate increased to around 0.9 mol/(m³.d) by day 465, with very little contribution from Columns 2 and 3.

On day 486, water samples were removed from the columns and chemically analysed. The results are summarised in tab. 2.

Table 2 Measured chemical compositions in the biological sulphate reduction plant on day 486

Element/ compound	Feed (mg/L)	Column 1 (mg/L)	Column 2 (mg/L)	Column 3 (mg/L)
SO ₂	3340	140	130	90
S ²⁻	9	802	360	200
NH	5	709	858	697
Be	<0.02	<0.02	<0.02	<0.02
HCO	106	7802	7676	7260
Na	258	195	209	241
Mg	537	514	447	399
Al	4.7	3.7	3.0	2.2
Si	5.2	23	27	29
PO ₃	<0.01	<0.01	0.1	0.1
Cl	<0.01	0.35	0.34	0.34
K	172	456	531	548
Ca	587	475	544	400
Cr	0.07	0.09	0.18	0.33
Mn	36	2.0	3.4	2.5
Fe	0.49	1.16	0.95	1.56
Co	0.06	<0.02	<0.02	<0.02
Ni	0.07	0.09	0.06	0.16
Cu	<0.02	0.03	0.04	0.02
Zn	<0.02	0.02	0.02	0.02
As, Mo, Ag, Cd	<0.02	<0.02	<0.02	<0.02
Pb	<0.02	0.1	<0.02	<0.02
Alkalinity	87	6395	6292	5951
pH level	6.93	6.97	7.20	7.23

The sulphate concentration in the final effluent was 90 mg/L, indicating a sulphate removal level of over 97 %. The residual sulphide, ammonium, bicarbonate, sodium, magnesium, potassium and calcium concentrations were relatively high, and manganese was not completely removed. In a separate experiment (data not shown), it has been shown that sulphide and manganese can be removed using a two-stage process comprising an oxidation pond and a pebble-bed pond. Significant reductions in the ammonium, bicarbonate, phosphate and calcium levels, and minor reductions in the magnesium and potassium levels, can also be achieved.

The fitness for use of the treated effluent produced (after the polishing process to remove residual metals) is currently being evaluated. Use of the water for crop irrigation (for both food and energy crops) is being considered.

Pilot Plant Design and Construction

A pilot plant will be installed at a South African coal mine in Mpumalanga Province, South Africa. Although the treatment process is intended to be “passive”, safety is a paramount requirement, requiring some “active” aspects to be incorporated into the design. The pilot plant was designed conservatively, with a HRT per stage of 6 days, at a feed rate of 245 L/d, giving a plant comprising three reactors with an active volume of around 7 m³ each.

To ensure safe operation of the pilot plant, a gas scrubber was incorporated into the design to capture and eliminate any gaseous hydrogen sulphide (H_2S) emissions from the BSR reactors. To assist in the capture of the H_2S emissions, closed vessels with a vent were specified in the design.

Manufacturing of the BSR plant has been completed (fig. 4), and the plant will be installed at the mine site shortly. An inoculum for the pilot plant has been prepared at Mintek. A total of around 4000 L is available, which will be transported to the site once the plant has been installed. The support materials and substrate have been blended, and will be transported to the mine site in 1 m^3 bulk bags.



Figure 4 Biological sulphate reduction pilot plant, showing the reactors (left) and the gas scrubber (right)

Conclusions

The passive BSR process is a low-cost, low-maintenance niche technology, envisaged to find application in the coal- and gold-mining industries. It is aimed at treating relatively low volumes of mine waters emanating from existing processes, and especially after mine closure, to produce effluents with sulphate concentrations that are within the limits specified by regulations for discharge or re-use.

The results described here have demonstrated very high sulphate removal levels. A pilot plant has been designed and will be operated at a local coal mine site to demonstrate the process. Further work will be conducted to optimise the process parameters and to polish the effluent from the biological process, and attention will also be given to the treatment and disposal of the spent substrate materials.

Acknowledgements

This paper is published with the permission of Mintek. The work reported in this publication was conducted within the framework of the ACQUEAU-labelled project called MIWARE (Mine water as a resource). Mintek's contribution to the project is funded jointly by Mintek and the South African Department of Science and Technology (DST), overseen by the Water Research Commission (WRC).

References

- Arnold M, Gericke M, Mühlbauer R (2016) Technologies for sulphate removal with valorisation options. IMWA2016 Annual Conference: Mining meets water – conflicts and solutions, Leipzig, 4 pp
- Doshi SM (2006) Bioremediation of acid mine drainage using sulfate-reducing bacteria. US Environmental Protection Agency, Washington, D.C., 65 pp
- Jamil IM, Clarke WP (2013) Bioremediation for acid mine drainage: organic solid waste as carbon sources for sulfate-reducing bacteria: a review. *J Mech Eng Sci* 5:569–581, doi:10.15282/jmes.5.2013.3.0054
- Jeffery GH, Bassett J, Mendham J, Denney RC (1989) Vogel's textbook of quantitative chemical analysis – 5th ed. Longman Scientific & Technical, Harlow, Essex, p 490–493
- Lorax Environmental (2003) Treatment of sulphate in mine effluents. International Network of Acid Prevention, London, 129 pp
- NSTF/SAASTA (2011) Proceedings of a critical thinkers' forum on acid mine drainage: possible solutions. National Science and Technology Forum and South African Agency for Science and Technology Advancement, 49 pp
- Turton A (2013) SAWEF Paradigm Shifter No. 1 – Debunking persistent myths about AMD in the quest for a sustainable solution. South African Water, Energy and Food Forum, 38 pp
- Watzlaf GR, Schroeder KT, Kleinmann RLP, Kairies CL, Nairn RW (2004) The passive treatment of coal mine drainage. U.S. Department of Energy, National Energy Technology Laboratory, Pittsburgh, Pennsylvania, 72 pp

Managed Aquifer Recharge Integration Potentiality In Arid Climate Conditions In The Jordan Rift Valley

Marwan Ghanem

Birzeit University, P.O.Box 14, Ramallah – Palestine, mghanem@birzeit.edu

Abstract The Jordan Rift Valley (JRV) catchments are places of extreme water scarcity and continuing overexploitation of the Plio-Pleistocene aquifer system. The groundwater basin is overexploited and there exists a threat of groundwater quality deterioration and salinization. Tens of research projects have been conducted in the Eastern Basin catchments that drain into the JRV with the overall conclusion that integration of surface water and groundwater management into full-scale IWRM approaches are needed. Implementation processes by decision makers are hampered by the complexity of the water system and the political tensions in the region. Wastewater reuse and desalination will increase the amount of usable water, but do not affect the overall water balance. Managed Aquifer Recharge (MAR) projects would be beneficial to enhance productive water availability of the region. Dams and reservoirs that have been installed at the outlet of major wadis provide additional groundwater recharge but are characterised by high evaporation losses and progressive silting. Therefore, alternatives need to be evaluated. Due to fast hydraulic reactions and short residence times of contaminants in the aquifer system, karstic aquifers prevailing in the area are particularly vulnerable to contamination. For careful site selection for MAR schemes in the JRV, a site selection study is recommended that integrates existing knowledge with additional data collection and model calculations. At this point, major targets for MAR schemes are the alluvial aquifer system, as well as the Upper Carbonate Aquifers system, which is hydraulically connected with the alluvial aquifer in many locations.

Keywords MAR of carbonate and alluvial aquifer, Jordan Rift Valley

Introduction

Water resources in the Jordan Rift valley are scarce in nature. The increasing population growth in the Jordan Rift Valley has put more pressure on the existing limited resources in the region. The steep gradient of the Jordan Valley produces a shadow effect, which reduces the quantity of the rainfall in the Jordan Rift valley (Arad & Michaeli, 1967). This basin is of great tectonic complexity and the major movement is eastwards with a southerly component near the river Jordan (Guttman, 1995). The aquifer system in the study area includes the sub-aquifers of Quaternary and Neogene formations (Ghanem, 1999). This covers the formations of Jenin sub series (Eocene), Beida & Lisan (Neogene & Pleistocene) as well as alluvium. The Pleistocene sub-aquifer consists of unconsolidated sand, gravel, cobbles, and boulders of different sizes separated by impermeable layers of saline lacustrine marl deposits (Rofe and Raffetey, 1965). The Eocene deposits are composed of limestone, dolomite, chert, gravel with sand and clay filling the intersect ices and forming alluvial fans. The groundwater occurring in the alluvial fans differs quantitatively and qualitatively according to its location within the fan. Fresh water occurs around the apex of the fan, whereas saline water occurs at the fringes. Very steep deep faults in the Jordan Rift valley may cause deep circulation of the groundwater bringing it into contact with salty formations which appears as brackish springs near the Jordan river. Integrated Water resources management includes all water resources of the Lower Jordan River, namely ground water, waste water, saline water, and flood water.

These issues are explored with a series of test sites along the Jordan valley. Test sites are planned for infiltration of reclaimed wastewater, infiltration of water from flash floods, infiltration of urban surface runoff and irrigation of agricultural area with treated sewage. The test sites are embedded into several water balance studies and finally, a numerical groundwater flow model will be needed for the entire Lower Jordan Valley for verifications. The investigation area covers the Lower Jordan River Valley and reaches down to the northern part of the Dead Sea. It comprises an area of about 2000 km². The dominating tectonic element of the Jordan River Valley is the Dead Sea Transform (DST) a segment of the East African – Red Sea Rift System. At the northern shores of the Dead Sea the valley floor is at ca. -400 m below sea level whereas the surrounding highlands reach on average 800 m above sea level.

Materials and Methods

Water resources status in the Lower Jordan River Basin (LJRB): closed basin

The study area constitutes parts of a closed river basin with a pronounced water deficit. A progressive closure of the basin means in this case that almost no water is left to be mobilized and used while demand, notably in urban areas, keeps increasing (Venot, Molle et al., 2006). Figure 1 lists the key elements in the anthropogenic modified water cycle of the LJRB. The final sinks of water in the LJRB are evaporation and water exports, there is no surplus water running to the open sea. The area is characterised by severe water scarcity. Figure 2 shows the Schematic Hydrogeological Profile of the Lower Jordan Valley. Aquifers are seriously overexploited and groundwater levels have been dropping during the last decades. As a result, the surface area of the sea has already shrunk by one-third, springs around the sea are drying up and sinkholes (areas of severe land subsidence) are forming, threatening historical sites and infrastructure.

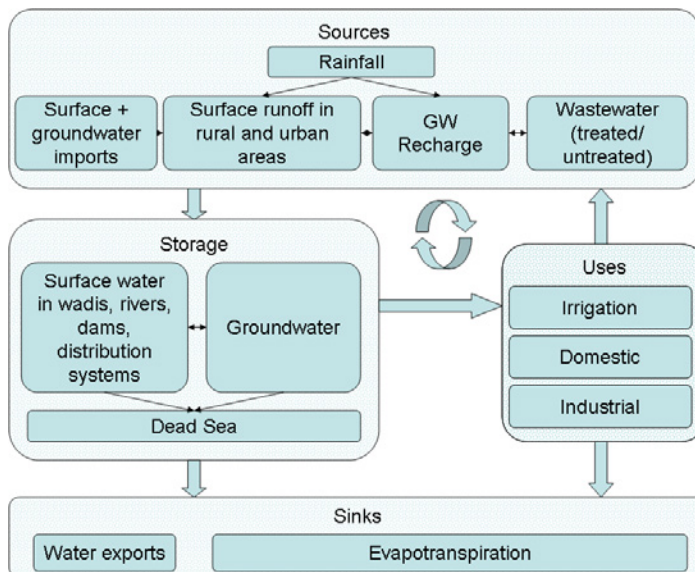


Figure 1 Key elements of the water cycle in a closed river basin: the case of the lower Jordan River.

Water quality of surface water is deteriorating due both due to reduction in natural flow volumes but also due to the many known and unknown releases of sewage into surface water. The situation is pronounced at the Lower Jordan River, whose waters were also historically more saline than the waters north of the Tiberias lake and of lower quality (Nissenbaum, 1969 in Farber et al., 2005). While flows of untreated wastewater in the wadis obviously constitute a pollution hazard, they still provide an augmentation of the Lower Jordan River base flow.

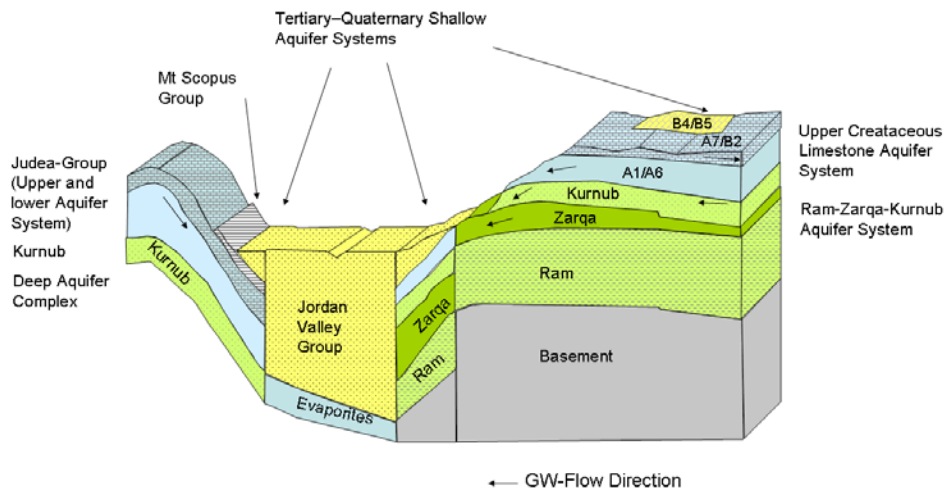


Figure 2 Schematic Hydrogeological Profile of the Lower Jordan Valley. Assembled from various sources (Salameh and Udluft, 1985; USGS, 1998; The Hashemite Kingdom of Jordan, 2004).

Water resources status in the Lower Jordan River Basin (LJRB): Groundwater

As groundwater is the major source of drinking water in the Lower Jordan River basin, hydrogeological aspects exert a dominant influence on the water management. Especially on the west bank, groundwater is the most important source of fresh water supply in the area. The tectonically and sedimentologically complex setting in the LJRB produces a large number of local and regional aquifers. While major lithostratigraphic units were mapped in the region, hydrodynamic connections between aquifers and the borders of subsurface drainage basins are still a research topic. The various local aquifers may be grouped into three major aquifer systems:

- (i) Tertiary-Quaternary Shallow Aquifer System: Alluvial aquifers are present at the floor of the Jordan Valley and the fans of the incoming wadis, where the alluvium is in contact with the aquifers of Upper Cretaceous age (Ailjun series). The alluvial aquifer extends from the northern shore of the Dead Sea in the south to the downstream part of the Yarmouk River in the north. The thickness of the alluvium in the Jordan Valley varies from zero along the eastern boundary to about 750 m in the deepest part of the basin near the Jordan River. An average thickness of

400 m may be reasonable for the purpose of hydrological considerations (The Hashemite Kingdom of Jordan, 2004). On the western side of the Jordan Valley, the term Shallow Aquifer Hydraulic Complex is used. It comprises Pleistocene sedimentary and alluvial deposits of the Quaternary age which receive localized annual recharge from wadi flows. The extent to which this aquifer is recharged from lower aquifers has not been determined and may be a function of faulting and fracturing.

- (ii) Upper Cretaceous Limestone Aquifer System is known as the Judea Group and is subdivided into an upper and a lower aquifer system. In terms of extracted volumes, this is the most important aquifer system in the region. It receives the major part of the groundwater recharge in the area, occurring mainly in the high mountain regions on both sides.
- (iii) Kurnub Group of Lower Cretaceous age consists mainly of sandstone. For the movement of groundwater the intergranular porosity of the sandstones is of minor importance, because most of the intergranular space is filled with siliceous cement.

Results and Discussions

Managed aquifer recharge (MAR) encompasses a whole suite of internationally used terms such as rainwater harvesting or artificial recharge. MAR describes intentional storage and treatment of water in aquifers. The term 'artificial recharge' has also been used to describe this, but adverse connotations of 'artificial', in a society where community participation in water resources management is becoming more prevalent, suggested that it was time for a new name. Managed recharge is intentional as opposed to the effects of land clearing, irrigation, and installing water mains where recharge increases are incidental (Gale, 2005). Figure 3 shows the basic types for MAR but the actual implementation of schemes is varying widely with different concepts in many cultures. Typical goals of managed aquifer recharge perceived in the region are (i) maintain and increase the natural groundwater as an economic resource. (ii) avoid further salinization and salt water intrusion (iii) decrease losses due to evaporation (iv) create a seasonal water storage (v) provide treatment and storage for reclaimed wastewater for subsequent reuse). Table 1 illustrates the methodologies for Managed Aquifer Recharge and their applications in the Jower Jordan River Basin.

While there is more than a millennium of experiences of using rainwater and surface runoff in rural areas by various forms of rainwater harvesting, the use of treated wastewater is young in comparison. Nowadays intentional replenishment of aquifers by highly treated reclaimed waters is increasingly being practised in developed countries with the full support of communities, and health and environment regulators, for aquifers that are under stress through imbalances between rates of extraction and natural recharge (Dillon, Toze et al., 2004; Dillon and Jimenez in press). With strong population growth in many urban centres and reduction of agricultural water demand by use of innovative irrigation technologies, the need to set up more sustainable urban water systems becomes obvious.

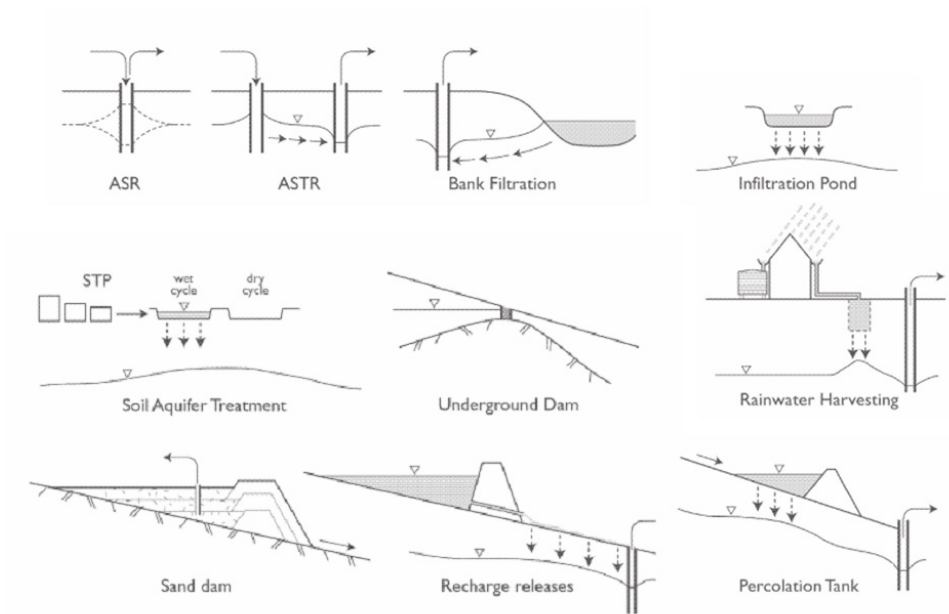


Figure 3 Schematic of types of management of aquifer recharge (Dillon, 2005). Abbreviations: ASR=Aquifer Storage & Recovery, ASTR=Aquifer, Storage, Transfer & Recovery, STP = Sewage Treatment Plant.

Table 1 Methodologies for Managed Aquifer Recharge (Gale, 2005) and their applications in the Lower Jordan River Basin.

General methodologies for MAR	
Spreading methods	Infiltration ponds and basins Soil Aquifer Treatment Controlled flooding Incidental recharge from irrigation
In-channel modifications	Percolation ponds behind check-dams, gabions, etc. Sand storage dams Subsurface dams Leaky dams and recharge releases
Well, shaft and borehole recharge	Open wells and shafts Aquifer storage and recovery (ASR) Aquifer storage, treatment and recovery (ASTR)
Induced bank filtration	Bank filtration Inter-/dune filtration
Rainwater harvesting	Field bunds, agricultural ponds Roof-top rainwater harvesting

Rainwater collection and storage schemes are traditionally carried out in Jordan and continued especially in rural villages. One of the techniques involves the filling of excavations close to wadi beds with a clay liner at the bottom, coarse rocks in the middle and a cover at the top. Due to the ongoing, unfavourable political situation in Palestine, there has been little scope for the construction of artificial recharge sites in the last decades. Current systems centre on rainwater harvesting, looking back upon long tradition and experience. Within the local context, managed aquifer recharge examples are grouped under the section “non conventional technologies”. Popular methods are (i) covered, underground reservoirs (locally called wells or cisterns) or (ii) pools made from earth or steel, covered with black plastic sheets to prevent algae growth (Carlo, 2007). The cisterns supply an estimated 6.6 mcm per year within the West Bank. Cisterns serve an essential purpose, meeting water needs left unfulfilled by the devastated infrastructure. In most cases, cisterns collect water from rooftops during the rainy season, which is then stored in subsurface containers, usually ranging in size from 60-100 cubic meters. A large percentage of water collected in cisterns is used for domestic purposes. Tankers are also used to fill cisterns, especially in the summer months when the cisterns dry up due to the lack of rainfall (Shehabadeen, 2007).

While these systems are effective in storing rainwater and securing the water supply during dry times, they are not recharging the groundwater directly. A direct recharge, however, is achieved through the numerous retaining walls on the agricultural fields. The retaining walls hinder surface runoff and enforce downward infiltration of water.

Incidental recharge occurs from a significant number of cesspits, but is associated with high nutrient and contaminant loads.

Conclusion

In general, the overexploitation of all aquifers in the region calls for recharge enhancement. Even without a recovery of the injected water close to the recharge site, a major environmental benefit will be achieved. Aquifers with high transmissivities are available close to the surface and successful examples are already implemented in the region. Mixing of injected water with saline groundwater bodies has proved to be low in international case studies. Beyond the hydrogeological constraints also the source of recharge water, the proximity to this source, the quality of the source and the availability of the source water has to be evaluated. Within the LJRB, both surface runoff and wastewater are available as sources. While significant amount of wastewater is produced in the urban areas, it is as far as possible used for irrigation following treatment. However, only a between 50% and 80% of the population are already served by sewerage systems. The alluvial fan aquifers at the inlets of the wadis to the Jordan valley offer a good potential for MAR due to their hydraulic conductivity, the gentle gradients and the long retention time. A major concern for the alluvial aquifers in the Jordan Valley is the mixing of the recharged water with saline groundwater. However, international studies have demonstrated that the mixing can be very low due to the slow groundwater movement and that efficient recovery is possible (Pavelic, Dillon et al., 2006). The Upper Cretaceous limestone aquifer system offers ample storage space but its use must be planned carefully due to the many fast discharge options via springs. Planning for MAR

must take the local circumstances into account, such as the strong seasonality of rainfall, and high intensity peak rain events which require large reservoirs to provide temporal storage for runoff during flash floods. High technology options like ASR require significant experience in set-up and maintenance, especially with regard to the prevention of clogging and may not be suitable at this point. Furthermore, surface runoff from urban areas may be strongly polluted as no effective source control measures are currently in place. This review showed that a considerable potential in the lower Jordan River basin for managed aquifer recharge exists. However, MAR is not yet identified as a major goal in the national water master planning. Currently the main focus is on water demand management, water supply management and institutional reforms (Taha and Magiera, 2006). Considering the currently limited depth of this review of MAR activities in the Lower Jordan River basin, it is essential to increase the coverage by incorporating more of the locally available grey literature. In order to unlock the potential for MAR in the region, a series of background and feasibility studies on the following topics are recommended:

- Increase of groundwater recharge from reservoir structures by removal/disturbance of low permeability reservoir sediments.
- Artificial recharge from open reservoirs into alluvial fan aquifers
- Use of urban surface runoff for groundwater recharge
- Holistic urban water balances and construction of sustainable water systems in the fast growing urban areas
- Quantification of the impact of MAR in terms of evaporation prevention
- Cost-benefit analysis of MAR within the IWRM framework under the consideration that all the recharged water volumes (irrespective of the recovery possibilities on spot) are effectively adding up to the total water availability in the Jordan River basin.

References

- Arad A and Michaeli A (1967) Hydrogeological investigation in the western catchment of the Dead Sea, Israeli journal of earth sciences, vol.16, pp. 181 – 196.
- Carlo A (2007) Socio economic impacts of using water harvesting techniques & water supply systems in Ein Quina Village, Palestine Hydrological Group: 60.
- Dillon P (2005) "Future management of aquifer recharge." *Hydrogeology Journal*(13): 313- 316.
- Dillon PS, Toze et al. (2004) Conjunctive Use Of Urban Surface Water And Groundwater For Improved Urban Water Security. IAH Congress Zacatecas 2004, Zacatecas, Mexico.
- Farber EA Vengosh, et al. (2005) "Management scenarios for the Jordan River salinity crisis." *Applied Geochemistry*(20): 2138-2153.
- Gale I (2005) Strategies for Managed Aquifer Recharge (MAR) in semi-arid areas. Paris, France, Unesco-IHP.
- Ghanem M (1999) Hydrogeology and Hydrochemistry of Faria drainage basin, Freiburger Heft, ISBN.
- Guttman Y (1995) The hydrology of the eastern basin and possibilities for the development of water resources from the pharaoh stream to the Judean desert, Tahal, Tel Aviv, 01/95/105.
- Pavelic PP Dillon et al. (2006) "Hydraulic evaluation of aquifer storage and recovery (ASR) with urban stormwater in a brackish limestone aquifer." *Hydrogeology Journal*(14):1544-555.
- Rofe and Raffetey Consulting Eng (1965) West Bank Hydrology: Nablus district Water Resources Survey, Geological and Hydrological report, 120pp.
- Salameh E and P Udluft (1985) "The hydrodynamic pattern of the central part of Jordan." *Jahrbuch C, Hannover*.(38): 39-53.

- Shehabadeen A (2007) Health Impact of Groundwater Pollutant. Ramallah, Palestinian Hydrology Group: 42.
- Taha S and Magiera P (2006) Water management in Jordan under scarce conditions. International Conference on Water Governance in the MENA Region Volume, 12.
- The Hashemite Kingdom of Jordan (2004) Digital Water Master Plan. Amman, Jordan, Ministry of Water and Irrigation.
- USGS (1998) Overview of Middle East Water Resources – Water Resources of Palestinian, Jordanian and Israeli Interest: 44.
- Venot JP et al. (2006) Dealing with Closed Basins: The case of the Lower Jordan River Basin. World Water Week 2006, Stockholm.

Mine Water – valued resource or missed opportunity?

Tim Saxby¹

¹*Jacobs Australia Pty Ltd, South Brisbane, Queensland, Australia, Tim.Saxby@jacobs.com*

Abstract For mining operations in Australia, water is an essential element that affects operational viability. Too little constrains production; too much can prevent access to orebodies and require release. Achieving a balance is difficult, particularly in open cut mining operations.

Climatic extremes present two key challenges, being:

- Sourcing water during periods of deficit.
- Managing mine water during periods of excess.

Water supports a range of economic and community benefits, but are we realising maximum value across a mines' lifecycle? Why are these opportunities being missed – Is it attitudinal, water quality, availability, regulatory or pure economics that is limiting us?

Keywords mining, economics, agriculture, regulation, climate

Introduction

The Australian climate is typified by climatic extremes. For eastern Australia, this is predominately driven by the long term cycles as a result of the movement of warm water across the Pacific Ocean between the Americas and Asia / Australia, known as La Nina and El Nino. Water is a key input for agriculture and mining operations to support production. Climatic variability presents challenges to mining operations which can affect their viability. Within the Bowen Basin, mining and agriculture rely on the same water sources.

Mining operations also generate and release excess volumes of Mine Affected Water (MAW) to the environment. MAW occurs as a result of rainfall and runoff within disturbed catchments, or as a result of aquifer dewatering in advance of mining. MAW is typically stored in disused pits until it is able to be reused or release.

Mines are located adjacent to agriculture. There is potential for greater economic and community benefits as a result of better water management and use, particularly within the context of a highly variable climate. This paper explores these benefits, as well as the barriers to them.

Geographical and Climatic Context

The Bowen Basin, located within Central Queensland in Australia, produces approximately 160 Million Tonnes Per Annum (MTPa) of coking and 58 MTPa of thermal coal. Annual rainfall varies depending on distance from the coast, however is typically 600-800mm per annum. Evaporation is far greater, being 2,000-2,500mm per annum. Rainfall varies depending on the La Nina / El Nino cycle which drives the climatic extremes. Recent examples are the 2001-07 drought (El Nino) which was broken by successive years of above average to highest on record rainfall, resulting in flooding from 2007 to 2011.

Nearly all of the mines within the Bowen Basin are within the Fitzroy River catchment, comprised of the Isaac and Connors Rivers in the north, the Nogoa-McKenzie to the central-west, and the Dawson River in the south, and draw water from this system. Additional supply is sourced from the Burdekin River and associated tributaries and pumped to mines within the Bowen Basin. The Nogoa-McKenzie River has a maximum annual water allocation of 255,000 ML/a (DNRM, 2015), whilst the Burdekin (below Burdekin Falls Dam) has an annual maximum allocation of 235,000 ML/a (DNRM, 2011).

Agriculture is the predominant land use, with irrigated cropping being of similar extents to mining. Carrol (*eWater CRC, 2004*) summarised the catchment landuse as comprising:

- Grazing: >13 million ha (130,000 km²).
- Dryland cropping: approximately 0.8 to 1 million ha (10,000 km²)
- Irrigated cropping: 45,000 ha (450 km²).
- Open cut coal mining: > 50,000 ha (500 km²).

Towns and communities are scattered throughout the Basin. These towns, the agricultural users and mining compete for land and water.

Water Sources, Quality Requirements, and Regulation

Mining

Mines utilise diverse water sources which typically include at least two of the following:

- Surface water runoff from disturbed catchments within the mines – known as MAW,
- Groundwater from dewatering and aquifer depressurisation – also known as MAW, and
- Raw water sourced from water supply borefields, dams and weirs, and delivered to site via pipelines – known as raw water.

Mining operations use water that is generated onsite for coal processing, dust suppression and other mining related activities. Each site is however reliant on raw water from ‘clean’ sources that have not been contaminated. This is due to operational requirements to support mining activities and for potable uses. Under current legislation and drinking water standards (Queensland Water Supply and Security Act (2011) and the Australian Drinking Water Guidelines (2015)), MAW cannot be used as a source for potable due to potential health risks.

The quality of MAW is dependent on the contributing catchments and associated geochemistry. The quality of groundwater varies depending on aquifer conditions. Water quality varies depending on the catchment, the time it has been stored for, and changes in quality due to evaporation. Typically, MAW ranges from a pH of 6.0 up to 9.0, and Electrical Conductivity (EC) of 4,000 to 15,000 uS/cm.

To comply with their Environmental Authorities (EA)’s (which govern the mining operations and the permissible activities), mines are required to retain all MAW and store and/

or reuse this water. The ability to discharge MAW from each mine is dependent on their respective EA, but most mines have conditions and performance criteria which permit the release of MAW and excess water generated from rainfall events receiving waters. These releases are permitted only when receiving waters have sufficient streamflow to dilute the water being released, with upstream and downstream monitoring.

Most EA's have an end of pipe maximum water quality limit of 10,000 $\mu\text{S}/\text{cm}$ EC and pH of 8.5 for releases from the mines. The volume that is released is dependent on streamflow, and downstream water quality limits range up to 2,000 $\mu\text{S}/\text{cm}$ EC. The current release arrangements have been in place since 2012 following the 2011 flood event. This provides a workable framework for mining operations to achieve release and reduce their MAW inventories.

MAW is typically reused unless its EC exceeds suitable limits. This varies between coal mining operations, but once the water quality exceeds release limits of 10,000 $\mu\text{S}/\text{cm}$, it is unable to be used due to impacts on coal processing, mining fleet and on the composition of the coal product.

Releases are monitored by the Queensland Department of Environment and Heritage Protection (DEHP). Mines are required to notify DEHP immediately once releases occur, with current release data being published online during the period of release. Totals of historic releases are however not publicly available. Based on observations of recent events for FY16, release volumes have been estimated to total 4,100 ML for 23 of the total of 51 recorded releases. The observed quality varies from 500 $\mu\text{S}/\text{cm}$ up to 10,500 $\mu\text{S}/\text{cm}$. The location of the releases are principally from mines within the Isaac and McKenzie – tributaries of the Fitzroy River.

Agriculture

Board acre cropping of pulses, grains and cotton typically rely on rainfall and are supplemented by irrigation. Water is sourced either from groundwater aquifers under licence or large irrigation schemes, such as Fairbairn Dam on the Nogoia River and its associated downstream weirs. Within this irrigated scheme, crops including cotton, peanuts, chickpea, and corn are grown, with horticulture producing citrus, table grapes, and melons. Water from dams and weirs is typically low in salts (EC at or below 200 $\mu\text{S}/\text{cm}$) and which is ideal for supporting agriculture.

Interrelated legislation defines the suitability of various sources and its quality for cropping. Regulations permit the use of high EC water, however use of high EC and specifically mine affected water is restricted to pasture and tree crops. This is a human health requirement, and prevents the use of mine affected water for horticulture.

Within Queensland, water produced as part of coal seam gas (CSG) operations is of a similar quality. The Coal Seam Gas Water Management Policy (DEHP, 2012) with supporting

legislation and referenced Acts requires proponents to achieve beneficial reuse of this water or reinjection of the water. This was implemented to mitigate the open storage of CSG water and evaporation in lieu of use for beneficial purposes. A key difference for CSG water is that it is regarded as a waste first and foremost. The Policy does permit use of CSG water for drinking water purposes, however the potential risks and impacts must be understood and sufficient treatment barriers implemented. Beneficial reuse, such as agriculture, is encouraged.

Whilst not specifically applied to coal mines and reuse of water from coal mining operations, it could be assumed that this or similar legislation would be applied to mining as the source and quality of the water is similar.

Communities

Numerous communities rely on water sourced from surface water sources or from groundwater. Major towns (>1,000 persons – Emerald, Blackwater, Middlemount, Moranbah, Moura, Dysart) rely on the same surface water sources that supply mines.

Under the Water Supply Security and Health Act (2011) MAW cannot be used as a water source.

Even if the water were appropriately treated, community attitudes regarding where water is sourced from may limit its use due to perceived quality and health risks.

Indirect reuse of MAW does currently occur when discharges from mines occur during major streamflow events. However, there is a high level of dilution, with the relative volume of the controlled MAW discharges being far less than the diffuse sources from agricultural operations, which comprises the majority of the landuse and therefore streamflow within the Fitzroy River. Tension exists between mines and agriculture regarding the source of pollution within the Fitzroy River, which is ultimately affecting the health of the Great Barrier Reef.

Demands and the impact of Climatic Variability

Water Demands

Limited data is available for raw demands associated with coal production for individual mine sites, as this information has historically been regarded as ‘commercial in confidence’, and difficult to source in a consolidated manner. Evans (2003) suggested that ‘approximately 200L of fresh water (raw water) can be consumed for every tonne of coal produced, although that can vary both upwards and downwards according to operating practice and circumstances’.

The demand for raw water does not necessarily account for the total water demand onsite. For the purposes of comparison, a raw water demand of 200 L/tonne has been adopted. In Financial Year (FY) 2014-2015, the Bowen Basin produced 218.62 MT of coking and ther-

mal coal. This translates to a raw water demand of approximately 43,723 ML/annum. When compared to the total allocations of 247,000 ML/annum (Nogoa-McKenzie River – Fitzroy River System), and the 235,000 ML/annum (Burdekin River), mine demands are relatively small, representing less than 10% of both sources' maximum available allocations.

The mines and townships hold 'high priority' water allocations, which are higher cost but also more reliable. During periods of extended drought, lower priority allocations (which are typically held by agricultural users) are reduced. This means the value of water increases, but also the extent of land under cropping decreases, impacting farming operations.

For agriculture, water demands vary depending on the prevailing seasonal conditions. Broadacre crops are heavily reliant on rainfall and are supplemented with irrigation (e.g. wheat, sorghum, cotton) whilst horticultural crops such as citrus are highly irrigation dependent. Accounting for typical seasonal rainfall of 200mm, only high intensity crops require additional water to support growth. Wheat is successfully grown as a broadacre crop relying only on rainfall. A lack of rainfall leads to smaller yields, but crop success.

The typical water demand and yield for specific crops is summarised Table 1 below.

Table 1 *Crop Water Demands (Total and Seasonal) vs Yield*

Crop Type	Total Water Demand (Typical)	Seasonal Water Demand	Yield	Data Source
Wheat	3 ML/ha	<1 ML/ha	4.5 t/ha	Dept Agriculture and Fisheries Qld (2012)
Cotton	5.4 ML/ha	3.4 ML/ha	1.9 bales/ha	Australian Cotton (2012)
Citrus (Oranges)	5-8 ML/ha	3-5 ML/ha	40-50 t/ha	Growcom (2001)

Using the FY16 release volumes of 4,100 ML for 23 release events (ignoring quality and storage limitations) and adopting the Seasonal Water Demand, an additional 18,450 tonnes of wheat, 2,291 bales of cotton, or approximately 41,000 tonnes of citrus could have been produced.

There are limitations on the use of MAW, particularly for citrus. EC levels of 400-700µS/cm in sandy and loam soil represent the limiting quality parameter for citrus. Similar limitations for wheat and cotton are likely to occur.

Climatic Extremes and Variability

Climatic extremes are dependent on the La Nina / El Nino cycle. The most recent climatic extremes were the 2001-07 drought (El Nino) which was broken by record successive years of above average to highest on record rainfall, resulting in flooding from 2007 to 2011 (La Nina).

Since 2011, the prevailing climate has been neutral, with neither strong La Nina or El Nino events occurring. This doesn't mean that climatic extremes and variability haven't occurred.

By comparing the recent historic rainfall with historic median, the 10% dry and 90% wet suggests that from 2012 to 2014, annual rainfall was close to average, with 2015 being drier than average and approaching 10% dry. Recent historic data is presented in Table 2.

Table 2 Moranbah: Historic Rainfall (2012 to 2016)

Year	2012	2013	2014	2015	2016
Rainfall (mm)	426	590.4	549	459	1036
Median (mm)	607	10% Dry (mm)	375	90% Wet (mm)	883

Further interrogation of recent historic climate suggests a highly variable climate, with intense rainfall events and extended periods of dry weather, including unseasonal rainfall. The monthly rainfall vs recorded monthly historic median and percentiles is presented in Figure 1.

As shown in Figure 1 the recorded rainfall has been below median for most of 2015, approaching or being at the 10% Dry recorded levels (i.e. very dry). In 2016, there were major rainfall events in January and December, and unseasonal rainfall in June-July. The intervening periods were generally well below median.

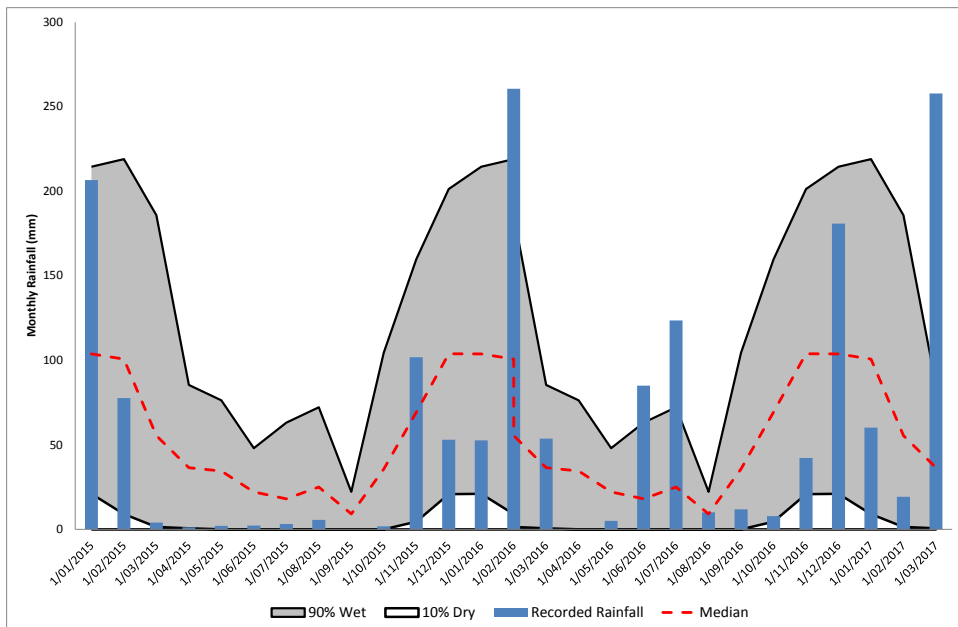


Figure 1 Moranbah: Historic Rainfall by month vs Median and Percentiles (2015-2017)

The variability of climate could be regarded as typical, however the rapid changes between wet and dry, and scale of rainfall events, including seasonality, creates challenges for man-

aging water on mine sites, and capturing MAW for other purposes. The recent climate is considered to be representative of the challenges faced by mining operations, and the potential opportunities.

Challenges and Opportunities

There are a range of challenges and opportunities associated with climatic variability.

- **Water Quality:** From a physico-chemical perspective, and ignoring regulatory issues, the ability to use water from mines depends on the ability to collect and store MAW, and maintain its quality to ensure its suitability and availability for reuse. This is difficult, as most MAW catchments feature spoil or tailings; and the storages themselves are invariably disused mine pits with direct aquifer connections. The water chemistry within these disused pits is also not well understood.
- **Cost – Capital and Operational:** the irrigation schemes within the Fitzroy and Burdekin Rivers were established using Commonwealth and State funds to establish viable agricultural industries. Water from these schemes have a relatively low operational cost. The capital has largely been sunk into these schemes, and the low cost of water enables margin creation from the crop being grown. Extensive irrigation infrastructure would be needed to enable agricultural use of MAW. Whilst not expected to be completely cost prohibitive, when other sources of water are low cost, high cost water will not be used.
- **Regulatory Environment:** the regulatory environment is reasonably advanced for the use of MAW for other purposes, but MAW use is limited to within mines, or for release to the environment. Within Queensland, there are currently no mines that sell or give away MAW to third parties for use as a disposal method. This is due to current EA's restricting mines from transferring water off lease, even if this is to another mine. Changes to these arrangements require renegotiation of the EA's, which could expose mines to stricter operating conditions. This means the mines are unwilling to explore beneficial reuse schemes due to the potential regulatory consequences. As demonstrated within the CSG industry, developing water reuse schemes is possible when necessary to meet regulatory requirements. However as mines can release water without amending their EA's, it is unlikely that schemes would be developed.
- **Attitudinal:** the primary focus of mining operations is to produce coal as cost efficiently as possible. Creating and storing water is not be regarded as 'core business', amending an EA could be high risk, and as there is no business or regulatory imperative, this would not typically be undertaken. Even where individual corporations have identified economic or social values and potential benefits from using the water, decisions are conservatively made so as not to risk impacting core business of mining.

- **Community:** the attitudes of the local community are important to the acceptance of MAW for alternative uses. There have been issues associated with the use of highly treated wastewater as an indirect potable resource. MAW does not carry the same perception, however it is regarded as ‘dirty’ or contaminated. Therefore, whilst it could be perfectly suitable in some instances, community concern would likely limit its use to non-food crop purposes.

Conclusion

Whilst there are a range of limitations and challenges to the use of MAW, there is no single reason rather a combination of issues. The use of MAW is not a necessity for agriculture; other sources of water are cheap and readily available; and the regulatory environment presents its own challenges. Therefore, it is not likely that the use of MAW will occur in the near future.

Despite the current constraints for offsite beneficial reuse of MAW there are opportunities. These are:

- **Preventing water becoming MAW in the first place:** by reducing contributing catchments via diversion or rehabilitation (subject to regulatory approval), less volume would require storage prior to release. This in turn would lead to greater freshwater runoff that could be extracted downstream by other users.
- **Reducing raw water demands by maximising MAW use:** allocations that are currently held could be reduced or eliminated and made available for agriculture if MAW use was maximised in a sustainable manner. This would require consideration of long term availability and risk. If this occurred, more high security water would become available for other uses such as agriculture and other high value customers.

The ability to achieve these improvements depends on how well mining operations understand their water requirements and how it varies with climate within an ever changing disturbance footprint, and the associated risk to operations.

Of the potential causes of missed economic and community benefits across a mines’ lifecycle, it is considered that the attitudes of mines and the community are the root cause. Water isn’t valued highly enough as a commodity to change attitudes which would in turn change regulations and drive economics. The CSG industry in Queensland demonstrates how regulations can drive actions, and how beneficial reuse schemes can achieve benefits, but strong drivers do not currently exist.

Post-mining the ability to use voids needs further consideration, recognising the intent of closure is to achieve a stable landform that requires no further ongoing management or maintenance, with stormwater runoff at a suitable quality resulting in no legacy issues. There is potential to realise community and economic benefits – it is a matter of valuing the resource appropriately and creating the right opportunities for use.

Acknowledgements

The author thanks Fiona Stark for providing critical comments and review inputs to this paper.

References

- Australian Bureau of Meteorology (2017) Climate Data Online. Bureau of Meteorology.
- Water Planning (North) Department of Environment and Resource Management (DERM) (2010), Burdekin Basin Resource Operations Plan December 2009 Amended October 2010 Revision 2.
- Water Policy—Department of Natural Resource and Mines (2015) Fitzroy Basin Resource Operations Plan September 2014 Amended September 2015. State of Queensland.
- Carrol C (2002) Fitzroy River – Catchment Characteristics. eWater Cooperative Research Centre for Catchment Hydrology.
- Evans R, Roe P and Roy R (2003) Water Use and Sustainable Development in Coal Mining – A Case Study from Central Queensland. Sustainable Minerals Institute, UQ and BMA Coal.
- Growcom (2001). Water for Profit Benchmark – Irrigating Citrus. Growcom, Department of Primary Industries and the National Centre for Engineering in Agriculture
- Cotton Australia (2007). Water use efficiency in the Cotton Industry. Cotton Australia Pty Ltd.
- Department of Agriculture and Fisheries (2012) Wheat – Planting Information. Department of Agriculture and Fisheries, State of Queensland.
- Department of Environment and Heritage Protection Government (2012) Coal Seam Gas Water Management Policy. Department of Environment and Heritage Protection

Integrating water balance modelling in the economic feasibility analysis of metals mining

Jyrki Savolainen, Mikael Collan, Pasi Luukka

*Lappeenranta University of Technology, School of Business and Management,
Skinnarilankatu 34, 53851 Lappeenranta, Finland, savoljyr@gmail.com; mikael.collan;
pasi.luukka@lut.fi*

Abstract Realization of mine water management related risks can, e.g., cause temporary shut-downs of mining operations leading to decreased economic returns of metal mining operations. In this paper, a techno-economic system model for metal mines is applied to study this issue. The usability of the model is illustrated with a numerical simulation to analyze the effect of including the additional (unlimited) water storage capacity on the mine profitability and on mine value. The illustrated method allows modeling of water management investments within mining investments, while traditional analyses tend to present water balance modeling and mining profitability as separate issues.

Key words Water balance, Profitability, System dynamic modelling, Simulation, Risk management

Introduction

It is well-known that the feasibility of metal mines may be compromised by inadequate water management policies (ICMM 2012). In the investment decision making process these issues are typically treated as minor matters, which have to be dealt with in order to maintain acceptance of metals mining from the community and the environmental points of view. This is contrary to what we know about the cost of water management in mining, it has been observed that water infrastructure may account for up to ten percent of CAPEX in the mining industry (Fleming 2016). The unremarkable role of water management in profitability analysis may partially be due to the lack of proper techno-economic models for metals mining.

Brown (2010) states that an appropriate mine water evaluation (model) should reflect the full range of possible outcomes of water management. According to Gao et al. (2014) the currently applied engineering models, OPSIM and GoldSim, are not suitable for evaluating long-term water management strategies under a range of climate scenarios. In this paper, we present a novel approach that is different from the purely engineering oriented models found in the literature so far and that combines the technical and economic effects of investments to mine water management to mine profitability, and that is very useful in understanding the size of the added value generated by investments into mine water management.

Metal mining investments are large, irreversible investments with long economic lifetimes. Their profitability is conditioned by several project (geological and technical) and market uncertainties (see discussion in, e.g., Botin et al. 2013; Kenzap & Kazakidis 2013; Park & Nelson 2013). This paper focuses on the water management related uncertainties. Technical analysis of a metal mining project is supplemented with an economic feasibility calcu-

lation. Surveys of Bartrop & White (1995); Bhappu & Guzman (1995), and Smith (2002) suggest that mining companies typically apply discounted cash-flow (DCF) based methods, such as the Net Present Value (NPV), or Internal Rate of Return (IRR) to value metal mining projects. For a review of valuation methods we point the interested reader to refer to, e.g., Eves (2013) and Lawrence (2002). The traditional DCF-based methods assume that a metal mining operation is run from the start of the mine, without cessation, until the end of life of mine. In reality, however, metal prices may vary even tens of percent per year, which in turn typically leads to temporary mine closings and re-openings. It has been suggested by Brennan & Schwartz (1985a; 1985b) that a metal could be valued analogically to financial option. In other words, a metal is only mined, when the return of metal sales exceeds the costs of production – and if profitability is not reached, then the mine should be temporarily closed.

Besides the option for temporary closing, metal mining operations usually include also other *real options*. These range from options found in production planning to the option of permanent abandonment of the project. A real option (RO) refers to a possibility, but not an obligation to implement these actions, to steer the profitability of an investment. One of these real options is the option to include water management (investment) in a mine. Reviews of real options in metal mining industry are provided by, e.g., Savolainen (2016b) and Newman et al. (2010).

Trigeorgis (1993) suggest that the value of a real option can be determined by comparing the value of project value with a RO (“expanded NPV”) and without it (“Passive NPV”) as follows:

$$\text{Value of Real Options} = \text{Expanded NPV} - \text{Passive NPV} \quad (1)$$

This simple valuation logic underlies the valuation that is used here in evaluating the difference in value emanating from (optional) investments in to water balance management. The rest of the paper is organized as follows. Next section introduces the models applied and it is followed by the case example description with simulations. The paper ends with discussion and conclusions.

The model used

In this paper, we run a Monte Carlo analysis on a generic system dynamic feasibility model of metal mining investments, introduced in Savolainen et al. (2017). The model imitates the structure of a real world metal mining investment and consists of several sub-models presenting different aspects of a mining investment. The simulations conducted use a time step of one month. A high level illustrative presentation of the model is visible in fig. 1.

A simple water balance model is created to study the profitability effect of investing in effective water management (see fig. 2), and linked to the production calculation part of the existing techno-economic metal mine profitability analysis model.

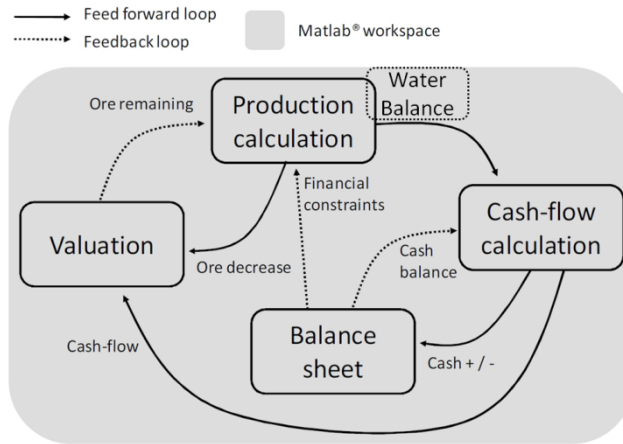


Figure 1 A schematic diagram of a system dynamic feasibility model for metal mining investments. The water balance model is connected to the production calculation and marked with a dashed line

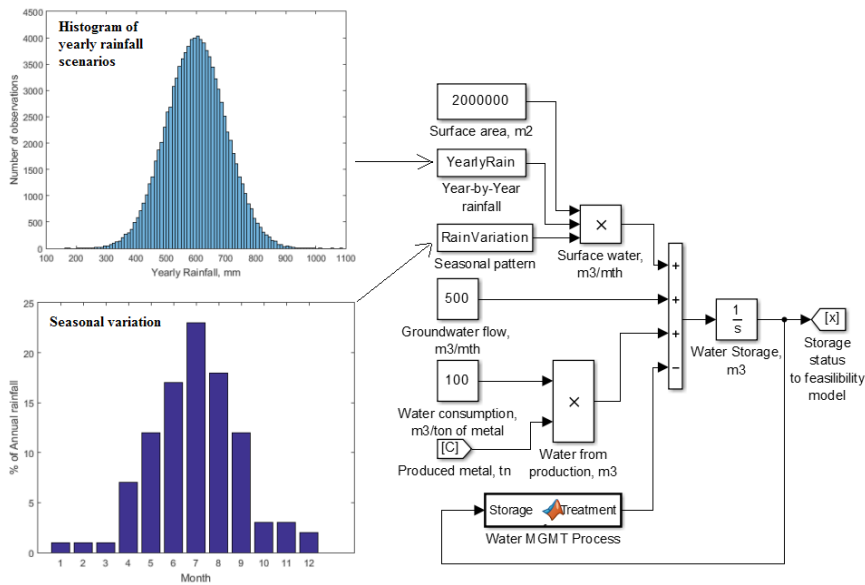


Figure 2 A system dynamic water balance model with randomized yearly rain and seasonal variation is linked into an economic feasibility model

Brown (2010) suggests that some of the major difficulties in mine water evaluations are related to mine inflow predictions and mine dewatering. In the illustrative case (fig. 2) the water balance is dependent on the uncertain yearly precipitation in the mining area, which creates an additional load to the water storage. The evaporation is assumed to be insignificant. The groundwater flow (mine dewatering) is assumed to be fixed. The amount of produced metal is left as a binary control variable, which can be adjusted to steer the overall water balance.

Illustrative case and simulation results

In this paper we are interested in a metal mining project that is under development that would be operating in a high rainfall area. The yearly rainfall is assumed to be normally distributed with a mean value of 600mm and a standard deviation of 150mm. The detailed process description of the water management is not of importance in this paper: it is simply assumed that the final treatment of all waters originating from the mining operation / mining area is done in a centralized purification process, with a fixed capacity. Other key parameters of the project are listed in tab. 1.

Table 1 List of key variables in the feasibility analysis of the illustrative case example. Modified from Savolainen et al. 2016

Variable	Unit	Pessimistic	Most Likely	Optimistic	Volatility, %
Reserve size	Tons	72 000	140 000	210 000	-
Metal yield	Tons/month	1 000	1 200	1 400	-
Production ramp	Tons/month	50	100	200	-
Unit cost	EUR/ton	4 000	3 500	3 000	-
Fixed cost	EUR/month	3 000 000	2 500 000	2 000 000	-
Construction time	Months	36	24	12	-
Construction cost	EUR	80 000 000	60 000 000	40 000 000	-
Unit price	EUR/ton	14 000	16 000	18 000	5
Exchange rate	USD/EUR		1,1 (fixed)		-

The project management is facing a decision on the extent to which additional water storage capacity investments are made. It is assumed that in order to regulate the water feed to the water treatment process during periods of high water levels the metal production has to be temporarily stopped. Additional unlimited water storage capacity, above the base case of 1Mm³ is the option to be considered for the purposes of this research. Unlimited capacity is studied, because the idea is to understand the “limits” of the needed storage capacity for better adjusting water storage investment size and the profitability effect of such a capacity on the project (how much the closures caused by the 1Mm³ vs. unlimited water storage with no closures affect the project value). Fig. 3 presents an illustration of 100 simulated developments of the mine’s water balance. The individual simulation runs in fig. 3 (left) are dependent on the realization of uncertainties presented in tab. 1.

The right hand side of fig. 3 shows that the average water storage levels are somewhere close to 2 Mm³ and indicate that that might be a reasonable size for the initial water storage investment (rather than the planned 1 Mm³). However, the left hand side of fig. 3 shows that many of the simulated storage levels remain under the initial design of 1 Mm³, indicating that there is a realistic possibility to consider that the construction of any extra storage capacity could be postponed.

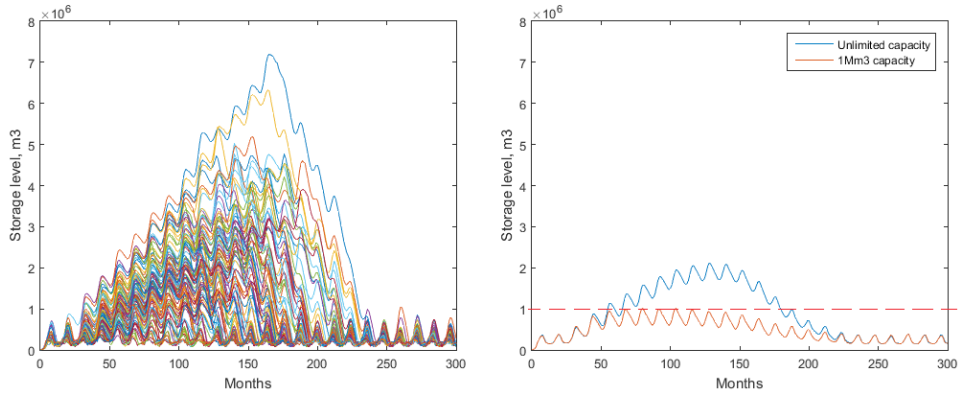


Figure 3 LEFT: example of 100 simulations of water storage level. RIGHT: average water storage level with and without and with storage constraint

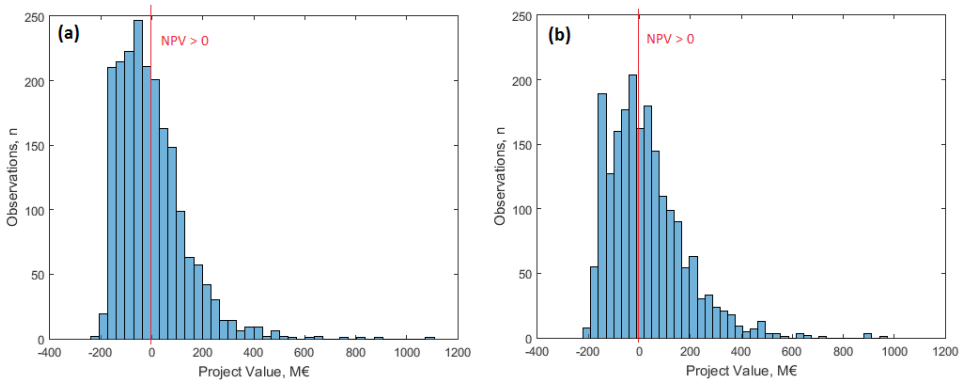


Figure 4 Histogram of results from 2000 rounds Monte Carlo. Simulated project value (a) with a water storage constraint of 1 Mm³ (b) without storage constraint

To investigate the economic effect of the water management issue, a 2000 round Monte Carlo simulation is run with the model, while assuming a water storage capacity of 1 Mm³ and another one assuming no capacity restriction in the water storage. The resulting NPVs are compared in order to determine the value effect. Resulting histograms of these Monte Carlo simulation runs are presented in fig. 3. Tab. 2 summarizes the obtained results.

Table 2 Project NPV comparison. (*) = real option value of additional water storage capacity

Value	No storage constraint „Expanded NPV“	Storage constraint „Passive NPV“	Difference
NPV, mean (M€)	24,47	-1,38	25,85 (*)
NPV > 0, probability (%)	50,8	42,9	7,9

Tab. 2 shows that the NPV of metal mine increases by 25.85 M€ without the water storage constraint, which equals the real option value of Eq. 1. To create a *theoretically* viable operation with NPV=0, the maximum amount that could be spent in the initial design to de-bottleneck the water management constraints is 24.47M€ (25.85M€ – 1.38M€). For example, if the water management constraint could be dealt in the initial design with, say, 10% of most likely initial cost estimate of 60M€, then the expected project value would be ~18.47M€ (24.47M€-6.00M€).

This numerical example illustrates how we can derive better information on the effect and “parameters” of water management investments via a techno-economic model that includes the ability to analyze the economic effects of water management investments.

Discussion and conclusions

This paper has demonstrated the importance of water balance to the overall feasibility of a metal mine by using an illustrative numerical example of a mine operating in a high rainfall area. The illustration has shown that the proposed methodology can be used in gaining a better understanding of the needed water management capacity and of the profitability effects of water management capacity. The used model is generic and it can also be used to model water shortages present in the (semi-)arid areas.

The timing and the cost of water storage investment was left outside the scope of this research. As the building time of extra water capacity is likely to be less than a year, a trigger value for the start of construction could, e.g., be set in the model, which depends on the current water storage level and its rate of change. Furthermore, the construction could be phased in the model to further reduce the risk of over investment. These topics remain issues for further study.

References

- Bartrop S, White A (1995) Spade work – how miners value resources. JASSA 7–13.
- Bhappu RR, Guzman J (1995) Mineral Investment Decision Making: Study of Practices. Eng. Min. J. July:36–38.
- Botin J, Del Castillo MF, Guzman R (2013) A real options application to manage risk related intrinsic variables of a mine plan: a case study on Chuquicamata Underground Mine Project. J South African Inst Min Metall 113:583–592.
- Brennan M, Schwartz E (1985a) A New Approach to Evaluating Natural Resource Investments. Midl Corp Financ J 3:42–47.
- Brennan M, Schwartz E (1985b) Evaluating Natural Resource Investments. J Bus 58:135–157.
- Brown A (2010) Reliable mine water technology. Mine Water Environ 29:85–91. doi: 10.1007/s10230-010-0111-7
- Eves C (2013) The valuation of long life mines: Current issues and methodologies. In: 19th Annual Pacific-Rim Real Estate Society Conference Melbourne Australia, 13-16 January 2013. pp 1–17
- Fleming H (2016) Water Management in the Mining industry. The CEO Water Mandate Stockholm Multi-Stakeholder Working Sessions, Stockholm, Sweden, p 24
- Gao L, Barrett D, Chen Y, et al. (2014) A systems model combining process-based simulation and multi-objective optimisation for strategic management of mine water. Environ Model Softw 60:250–264. doi: 10.1016/j.envsoft.2014.06.020

- ICMM (2012) *Water management in mining: a selection of case studies*. London, U.K.
- Kenzap SA, Kazakidis VN (2013) Operating risk assessment for underground metal mining systems : overview and discussion. *Int J Min Miner Eng* 4:175–200. doi: 10.1504/IJMME.2013.053167
- Lawrence RD (2002) Valuation of mineral properties without mineral resources: A review of market-based approaches. *CIM Bull* 95:7.
- Newman AM, Rubio E, Caro R, et al. (2010) A Review of Operations Research in Mine Planning. *Interfaces (Providence)* 40:222–245. doi: 10.1287/inte.1090.0492
- Park HM, Nelson MG (2013) Mining project evaluation process for investment decisions: Risk variables in mining projects – part one. *Min Eng* 65:18–21.
- Savolainen J (2016) Real options in metal mining project valuation : Review of literature. *Resour Policy* 50:49–65. doi: 10.1016/j.resourpol.2016.08.007
- Savolainen J, Collan M, Luukka P (2017) Analyzing operational real options in metal mining investments with a system dynamic model. *Eng Econ* 62:54–72. doi: 10.1080/0013791X.2016.1167988
- Savolainen J, Collan M, Luukka P (2016) Combining system dynamic modeling and the Datar-Mathews – method for analyzing metal mine investments. *Acta Univ Palacki Olomuc Fac Rerum Nat Math* 55:95–110.
- Smith LD (2002) Discounted Cash Flow Analysis Methodology and Discount Rates. *CIM Bull* 95:101–108.
- Trigeorgis L (1993) The Nature of Option Interactions and the Valuation of Investments with Multiple Real Options. *J Financ Quant Anal* 28:1–20.

4 Modelling

Simulation of Mine Water Rebound in the Ostrava Basin – Part of the Upper Silesian Coal Basin

Nad'a Rapantova¹, David Grycz², Pavel Malucha², Vladimir Mandrla²

¹VSB – Technical University of Ostrava, Czech Republic; ²Green Gas DPB, a.s.

Abstract

Because of the gradual decline of mining in the Czech part of the Upper Silesian Coal Basin, mine closure in the active part of basin and the termination of mine water pumping from abandoned mines is planned. Until now the mine water is maintained at specified level at already abandoned Ostrava Basin to prevent overflow from abandoned to active mines. Therefore, the need arises to predict groundwater rebound to the original conditions, unaffected by mining.

For this purpose, the construction of the mathematical model of mine flooding has begun. For the model construction the DHI FEFLOW software is utilized. Due to the complexity of the rock environment at the site and the need of incorporation as much mine workings as possible into the model, the size of the model is beyond what is typically done in FEFLOW. The model covers an area of 15.7×12.7 km with vertical extent of 1200 m. The total number of elements in the finite element mesh is more than 26 million. Vertical discretization of the model domain was done into 300 layers. The principal hydraulic properties of the rock environment (hydraulic conductivity and unsaturated-flow porosity), are determined with a set of more than 36 million data points. Furthermore, a complex net of 1D line discrete features representing the mining shafts and galleries has been imported into the model. The mine water quality evolution is not considered in this task, even so, the size and complexity of the model is currently on the limit of conventional desktop computer performance.

Hydraulic properties and boundary conditions are being calibrated based on the observation of the first part of mine water rebound to the level -380 m b.s.l. This is a level on which the mine water is maintained by pumping from one central shaft in the abandoned partial basin. The mine water level is observed on one additional shaft proving water level difference in order of tens of meters (throttled interconnections between partial basins – mine pools).

The present state of simulation and experience from solving this demanding task – distributed modelling of mine water rebound will be presented.

Waste Disposal In The Open Pits: The Hydrogeological Aspects And The Influence On the Environment (The South Urals, Russia)

Petr Rybnikov, Liudmila Rybnikova

The Institute of mining, Ural branch of the Russian Academy of Sciences, Ekaterinburg, Russia ribnikoff@yandex.ru, luserib@mail.ru

Abstract The activities of the mining and processing industries lead to the formation of a mining landscape. Reclamation of mined-out space is an effective way of solving environmental problems in the mining areas. It is advisable to use wastes from the mining and processing industries to bring the disturbed areas of land to satisfy the development condition. Hydrodynamic and hydrochemical history of the object, sampling and laboratory study of the interaction of filling mixes with quarry water, hydrogeomigration modeling were used to substantiate the technology of waste disposal in the exhausted Vostochniy quarry of the Magnetic Mountain (Chelyabinsk region, Russia).

Key words waste disposal, open pit, filling mixture, remediation, hydrogeological forecast, pollution prediction.

Introduction

The purpose of the work is to justify the expediency and ecological safety of reclamation of the Vostochniy quarry of the Magnetic Mountain (Chelyabinsk region, Russia) using slag processing products as stowing materials. For such a substantiation, it is necessary to evaluate the hydrogeoeological consequences of the disposal of waste in the developed space.

For OJSC “Magnitogorsk Iron and Steel Works” the solution of a number of interrelated problems is extremely urgent: reclamation of worked quarries and waste disposal of own-made wastes during the formation of filling mixes. Their solution will allow us to approach the issue of the restoration of territories that have been disturbed by years of mining activity. Magnitogorsk iron ore deposit is located in the South Urals, 12 km from the center of Magnitogorsk. Distance to the nearest water bodies: 5 km to the west towards the Magnitogorsk reservoir on the river Urals, 5 km to the east to the river Suhaya (left-bank tributary of the Ural River) and sludge storage on it. The Magnitogorsk deposit is located mainly in the limestone (marble) of the Magnetic Mountain.

The Magnitogorsk iron ore deposit has been worked out since 1747. The deposit “The Magnetic Mountain” was worked by two quarries: Zapadnyy, 105 m deep, in the period 1929 – 1994; Vostochniy, depth of 130 m, from 1946 to 2006. The total area of the worked out space of the Vostochniy pit is 163 hectares, the length of 1945 m, the width of 1015 m, the height of the ledges is 10 m. To date, the deposit has been worked out, 538 million tons of ore were mined.

During the development of the Zapadnyy and Vostochniy quarries of the deposit, drainage was carried out by deep dewatering wells in combination with sump pumping. Frac-

ture-karst waters, associated with Paleozoic rocks, have the greatest influence on the water cut of open pits.

Formation of the chemical composition of the underground waters of the deposit is associated with the mineralogical composition of the ore zone and the presence of sulphides in the composition of magnetite ores. Under natural conditions, they did not exert a significant influence due to poor solubility. In the process of strip mining with dewatering, the oxidation of sulfides begins, the groundwater acquires a sulphate composition (the sulfate ion content is up to 1.5 g/dm³), the mineralization rises to 2.2 g/dm³.

Testing and chemical analysis

It is planned to use filling mixes based on slag processing products with the addition of some types of waste as a material for filling the quarry. The share of metallurgical slag in the volume of industrial waste of the plant without waste of ore-dressing production is about 80%. The basis of metallurgical slags is composed of oxides of CaO, SiO₂, MgO, and FeO. Sulfur in slags is in the form of sulfides or sulphates Ca²⁺, Mn²⁺ and Fe²⁺.

The composition of the waters formed during the storage of filling mixtures is determined by the influence of environmental factors: water composition, temperature (Lottermoser 2010; Mironenko and Rumynin 1999). The active behavior of the filling material in the water can have a negative effect on the quality of underground and surface water.

To assess the environmental hazard of wastes that will be used for filling mixtures during reclamation of the Vostochniy quarry, laboratory experiments were conducted: 10 samples of slags were selected and one sample from a mixture of basic metallurgical wastes was additionally prepared. The results of the investigation of the interaction of slag materials with a quarry (11 samples) and distilled water (11 samples) make it possible to evaluate, by analysis of aqueous extracts, the time variation in pH and the degree of leaching of the components. We performed advanced laboratory studies of main and micro – component composition of water samples using methods of mass spectrometry with inductively coupled plasma ICP-MS.

The change in the hydrogen index occurs in the first 7 days, it increases from 7 to 10 – 12 units, in the future it does not change (experiments were conducted for 21 days). Ten-fold dilution with water reduced the pH by only one unit. Table 1 shows the results of the analysis of the micro-component composition of quarry waters and aqueous extracts. Comparing them with the indicators of the waters of the Zapadny quarry (re-cultivated at the present time) allows us to conclude that in the course of the reclamation of the Vostochniy quarry its water can be enriched with a number of components, including an increase in the content of sodium, aluminum, calcium, copper, zinc, strontium, mercury, lead, but this process will not lead to a noticeable contamination of the hydrosphere. The composition of water will change from sulphate magnesium-calcium to chloride potassium-sodium-calcium.

Table 1 Composition of water extracts and quarry waters, mg/dm³ (including ICP-MS results)

Index	Water extracts		Quarry			Russian MAC/ MPC (for fishery purposes rivers and ponds)
	Q*	D**	Vostochniy	Podotvalniy	Zapadniy	
pH	11.0	11.0	7.9	7.9	12.0	—
B ⁺	0.04	0.03	0.19	0.63	0.03	0.10
Na ⁺	147	98	45	112	180	120
Mg ²⁺	0	0	79	88	< d. e.	40
Al ³⁺	0.42	2.55	0.10	0.03	0.07	0.04
Si ²⁺	4.2	2.5	2.9	8.6	0.6	—
K ⁺	48	36	3	2	84	—
Ca ²⁺	234	217	354	267	389	180
Mn ²⁺	0.016	0.005	0.013	0.235	4.0 10 ⁻⁴	0.01
Fe _{общ}	0.10	0.04	0.24	0.21	< n. o.	0.10
Cu ²⁺	0.014	0.016	0.006	0.001	0.001	0.001
Zn ²⁺	0.10	0.129	0.03	< d. e.	< d. e.	0.01
Br ⁺	0.162	0.099	0.051	0.360	0.466	1.35
Sr ²⁺	2.31	1.70	0.69	1.38	2.08	0.40
Ba ²⁺	0.18	0.63	0.01	0.02	0.84	—
Hg ²⁺	2.3 10⁻⁴	1.4 10⁻⁴	< d. e.	< d. e.	< d. e.	1.0 10 ⁻⁵
Pb ²⁺	4.7 10 ⁻³	4.3 10 ⁻³	9.4 10 ⁻⁴	1.7 10 ⁻⁴	6.8 10 ⁻⁵	6.0 10 ⁻³
SO ₄ ²⁻	579	118	1156	984	318	100

*Interaction of filling material and quarry water; **Interaction of filling material and distilled water; d. e. — chemical determination error; bold are values greater than Russian MAC/MPC (for fishery purposes rivers and ponds)

Mathematic modeling

A number of forecasting tasks were solved for the hydrogeological justification possibility of reclamation of the Vostochniy quarry. The purpose of their solution was: assessment of the necessary flow rate of the drainage to ensure storage in a dry state; forecast of groundwater levels with a change in the ratio of drainage from the Zapadniy and Vostochniy quarries; an estimation of probability of flooding of territories in case of complete cessation of a drainage; the forecast of distribution of polluting substances to the discharging zones in the process of reclamation of the Vostochniy quarry and after its completion.

Mathematical modeling was used to predict changes in the hydrodynamic and geomigration situation: Modflow and MT3D included in the PMwin package (Chiang and Kinzelbach 2001). The outer contour of the model is adopted in accordance with the natural boundaries of the formation of groundwater flows, based on the assumption of the coincidence of the boundaries of formation of surface and underground runoff (treated as one watershed). In the west and east, the boundaries correspond to regional drains; In the south and north, the boundaries are drawn in accordance with local watersheds (impermeable boundary).

The internal boundary conditions are the drainage systems of quarries, to simulate the discharge of groundwater into the sump in the corresponding blocks, a third-kind boundary condition (drain) was specified. The depth of the drain corresponds to the marks of the bottom of the quarry. Surface water bodies and streams are schematized as a boundary condition of the third kind, taking into account the filtration resistance of the bed (river hydraulic conductance). The mean annual value of infiltration intensity (recharge) was taken as equivalent to a regional module of underground runoff (about 50 mm/year). At the metallurgical site, the infiltration rate increases to 100 mm / year due to leaks from water-bearing communications.

Changes in the filtration properties (hydraulic conductivity) of the fissured-karst (fracture-karst) aquifer are associated with lithological differences and geomorphological position: the highest values of the order of 1 m/day (transmissivity about 100-150 m²/day) are inherent in the Ural and Sukhaya river valleys, they decrease to 0.1-0.05 m/day (transmissivity about 10-30 m²/day) by the watershed (Lukner and Shestakov 1976).

The solution of transient migration tasks was carried out for the conservative component, (for example, the chlorine ion). Its content in the water of the Zapadniy quarry is 350 – 400 mg/dm³ with a background value of 100 mg/dm³. As the main process, which regulates mass transfer, advection (convection) was considered.

The simulation was carried out in two stages. For calibrating the model, a number of inverse tasks were solved at the first one: the hydraulic conductivity, storage coefficients, and recharge conditions were refined; the sensitivity of the model was checked. The criterion of consistency of the model is the coincidence of the model and actual levels of groundwater, as well as the balance components of the watershed. For the calibration of parameters, the following stages of territory development provided with monitoring information were considered: 1 – natural (undisturbed) conditions (steady state); 2 – situation at the end of excavation at quarries (steady state); 3 – period from 1991 to 2013 (transient).

The main task of the second stage of modeling: justification of the operating mode of the drainage system, allowing to ensure the storage of the filling mixture above the groundwater level in dry form.

At this stage, the forecast tasks are solved, three scenarios are considered:

- 1) drainage is carried out from both quarries: from the Vostochniy – to ensure the possibility of storing filling mixes in a dry state, the drainage from the Zapadny one remains at the level that has developed to date;
- 2) there is no drainage from both quarries: the filling of the Vostochniy quarry continues; Drainage from the Zapadny quarry is terminated and its filling begins;
- 3) drainage is performed only from the Vostochniy quarry – to ensure the possibility of storing filling mixes in it in a dry state.

The results of solving the forecast tasks show that the first scenario is the safest: there is no flooding of the adjacent territories, the potential pollution does not extend to regional drains and is localized in the immediate vicinity of quarries.

The second scenario is the worst (fig 1): there is flooding of the territory, after 5 years, pollution from both the Zapadny and Vostochniy quarries reaches regional drains. In the center of the industrial site of the metallurgical plant, the groundwater level will rise by 2 to 4 meters, and the concentration of the conservative polluting component will increase by 1.5 to 2 times. In Figure 1, the position of the front of pollution from the Zapadny and Vostochniy quarries with complete cessation of the water outflow in 50 years is shown.

The third scenario is intermediate in degree of danger: to the east into the valley of the river Suhaya pollution does not extend, the rise in the level in the center of the industrial site will be about 2 m, and the concentration of the conservative polluting component may increase by 1.5 times.

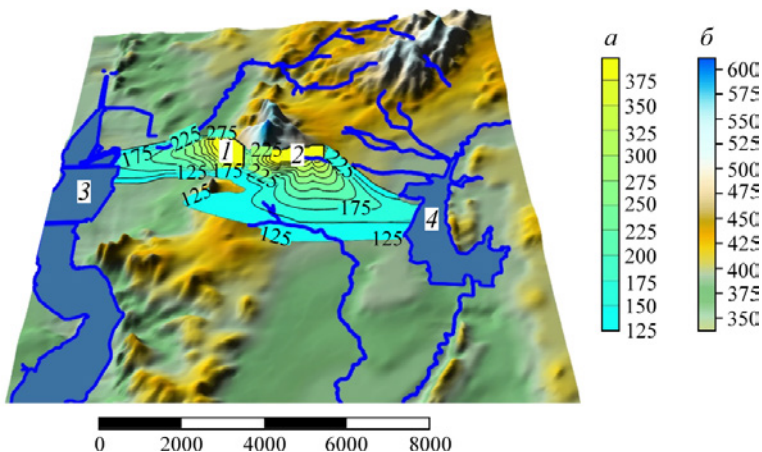


Figure 1 Forecast concentration of the conservative component in groundwater 50 years after the complete cessation of the drainage (the second scenario): 1 – Zapadny quarry; 2 – Vostochniy quarry; 3 – Magnitogorsk reservoir; 4 – sludge storage; a – concentration scale, mg/dm³; b – relief altitude scale, absolute marks, m

Recommendations for reclamation

The safe filling of the Vostochniy quarry with filling mixtures is possible when drainage of both quarries is working: this will ensure the preservation of the groundwater level on the marks excluding the influence on the residential and industrial zone during the work. In the process of reclamation (about 10 years), the depth of the water level in the area of the Eastern pit is determined by the reclamation technology. In accordance with this technology, it should be possible to store the filling mixture in a dry state. Backfill with filling mixtures will be done in layers of 2 m with the preliminary formation of an impermeable waterproofing screen (from clay or geomembrane). As the developed space is filled, the depth of drainage and the discharge of the drainage can decrease after the increase in the mark of the bottom of the reclamation space.

From the perspective of mass transfer, the reclamation process is divided into three stages. At the initial stage, the groundwater level should be maintained below the bottom of the quarry, groundwater pollution occurs in the immediate vicinity of the quarry. At the second stage, water drainage can be reduced (approximately 2 times compared with the initial stage), the direction of movement of groundwater and the development of the pollution area will change significantly. At this stage, it is necessary to provide for the expansion of the monitoring network to provide information on the extent of flooding of the territory, processes and intensity of groundwater pollution. At the third stage (after filling the worked out space to about the level of the earth's surface), drainage can be stopped, but only on condition that monitoring results do not record flooding of territories and groundwater contamination.

Conclusion

If the technical requirements are met, the use of mining and processing waste to reclamation of quarries is a potentially environmental friendly technology.

The main requirement for the reclamation of the Vostchoni quarry is the control over the position of the groundwater level in the process of reclamation. There should be chosen such a flow rate of drainage that each new layer of the filling mixture is in the dried state until it is covered with a waterproof layer.

After filling the waste space with filling materials, drainage can be terminated, provided that monitoring results show no flooding of territories and groundwater contamination.

Reclamation of the Eastern quarry of the Magnetic Mountain with the use of filling mixes will lead to the improvement of the ecological situation, which is especially important for the area of the metallurgical plant, where a huge volume of metallurgical wastes is accumulated.

References

- Chiang WH and Kinzelbach W (2001) 3D-Groundwater Modeling with PMWIN. First edition. Springer-Verlag Berlin Heidelberg New York. 346 pp
- Lottermoser BG (2010) Mine Wastes. Characterization, Treatment and Environmental Impacts. Springer-Verlag Berlin Heidelberg. 335 p
- Lukner LK, Shestakov VM (1976) Modeling of geofiltration. Moscow: Nedra. 407 p (in Russian)
- Mironenko VA, Rumynin VG (1999) Problems of hydrogeoecology. T 3 (Book 1). Applied research. Moscow: Izd-vo GGU. 1999. 312 p (in Russian)
-

Novel Approach to Acid Pit Lake Treatment and Management

Jacob Croall¹; Peter White¹; Briony Coleman², Julia Schmidt², Steve Skidmore²

¹*Newmont Metallurgical Services, 10101 E Dry Creek Rd. Englewood CO, 80112*

²*Lone Tree Mine, 29100 Lone Tree Mine Rd, Valmy, NV 89438*

Abstract The onset of acidic pit lake conditions at Newmont's Lone Tree mine was rapid, and deteriorated to a problematic whole-lake chemistry. Complex geochemical predictions had been unsuccessful, and the acid load and geologic sources and transport mechanisms were unable to be quantified; this challenged remediation attempts, which ultimately exacerbated water quality issues. The paper relates to the successful quantification of acidity ingress, leading to compliant water quality through targeted treatment of surface water, and the development of a long term management plan in-line with company values and economic considerations relating to potential treatment design.

Introduction

Newmont Mining Corporation's Lone Tree Mine is located in Humboldt County, Nevada, approximately four miles northwest of the town of Valmy. Lone Tree Mine initiated production in 1991 with an open pit mine and has utilized various ore beneficiation methods that include heap leach, flotation and autoclave milling operations. The pre-mining groundwater elevation was approximately 50 feet below original topography. Active dewatering of the open pit area was required to facilitate mining and ceased in November 2006 at which time the open pit final depth of 3,570 ft. began filling with groundwater. Pit lake filling predictions anticipate the lake will achieve a maximum depth of 865 ft after 100 years, reaching 90% of its final depth in 2026 and 90% of its final volume in 2046 (ITASCA 2010). At its maximum depth the Lone Tree pit lake is a hydraulic sink and will not contribute to surface or ground water.

The pit consists of two zones separated by a saddle. Figure 1 presents a schematic cross-section of the Lone Tree pit prior to filling. The main sub-pit Section 11 is deepest in the south, with a final base elevation of 3,570 ft. Sub-pit 13 was back-filled with sulphide waste, encapsulated with oxide material to the north to create a 400-600ft buffer zone, and a 40ft vertical buffer zone.

There are four main lithological units that are of significance to the assessment of water quality in the pit lake.

Valmy Formation – A large percentage of the eastern portion of the pit shell. Mineralization occurs in breccias that have been partially cemented. Pyrite is present in fractures in the quartzite and coarser grained than the reduced Havallah Formation.

Wayne Zone – A large normal fault that is steeply dipping. Geologic units are downfaulted in excess of 1,000 ft. and this unit occurs from the surface to the bottom of the pit on the hanging and foot wall sides.

Alluvium – Limited alluvial deposits are net neutralising and only present in upper benches of the pit surface. This unit contributes minor groundwater flow compared to the bedrock units.

Havallah Formation – The sequence is made up of sandy limestones and conglomerate that has been decalcified.

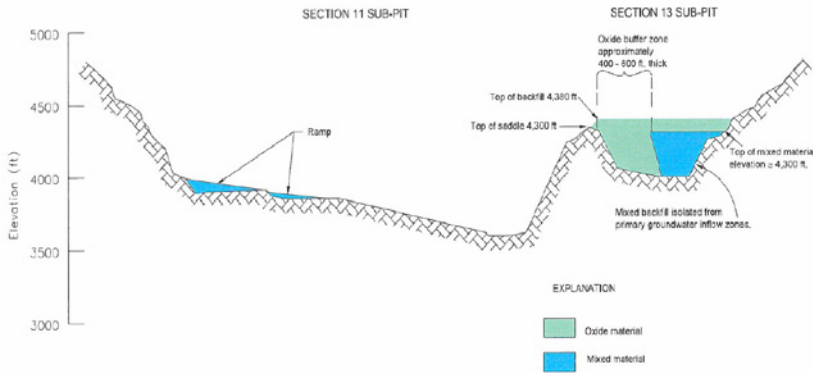


Figure 1 Cross-sectional schematic of Lone Tree pit and sub Section 13 backfill.

The waste rock is shown by major unit lithology in Figure 2, indicating the area of exposed material at the surface of the pit shell. The rock types that were classified as net acid generating, net acid neutralizing, and those as uncertain are shown. The data used to generate the classifications is presented in Table 1 and 2, from two independent geochemical classification activities.

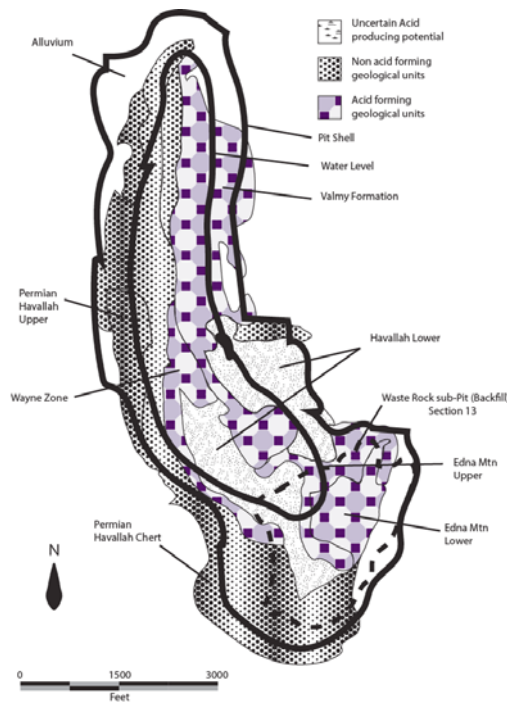


Figure 2 Map of major geological formations within Lone Tree pit lake

Table 1 Summary of Geochemical testing data performed for Newmont in 1995.

Geologic Unit	Kinetic Tests					Static Tests	
	Av NCV	Av ANP	AvAGP	HCT 20 wk	#HCT	Static Tests	# Static tests
	(% CO ₂)	(% CO ₂)	(% CO ₂)	pH	#	Av. NCV	#
Battle Mtn	-0.81	0.33	1.14	2.3	3	-1.24	23
Edna Mtn lower	-1.45	0.24	1.69	2.5	7	-0.87	30
Valmy	-1.66	0.27	1.93	2.4	4	-1.55	26
Havallah Lower Reduced	-5.67	1.17	7.20	6.2	2	0.16	50
Havallah Lower Oxide	-1.14	0.76	1.89	2.5	2	0.53	48
Havallah Chert	2.45	2.56	0.10	6.7	2	-3.8	7
Wayne Zone	-4.86	0.56	5.43	1.9	3		

Table 2 Summary of Geochemical testing data performed for Newmont in 2010.

Geologic Unit	AGP ppt CaCO ₃	ANP ppt CaCO ₃	Paste pH pH	HCT 20 wks pH
Havallah Chert	0.6	27.3	7.89	7.5
Alluvium	<0.3	210	7.76	8.1
Havallah Upper	<0.3	49	8.04	8.0
Havallah Lower	7.3	62.9	7.13	7.5
Edna Mountain Upper	31.9	33	6.09	3.2
Edna Mountain Lower	178	7.2	3.19	2.0
Valmy	38.4	<0.3	2.52	2.1

The geochemical characterization testwork undertaken represented the dominant material types of the Lone Tree pit lithology, and demonstrated a high propensity for net acid generation with rapid onset in the Valmy, Wayne Zone and Edna Mountain Formations, with some uncertainty around the Havallah formation. Based upon Figure 2 these lithology's have comprised up to 50% of the exposed wall rock during lake filling to date, and are expected to be approximately 30-35% of the wall rock exposed above the final pit lake elevation.

In 1994, these results (207 static tests and 24 20 week kinetic humidity cells) were used to estimate pit lake water quality using MINTEQA2. The resulting model predicted circum-neutral (pH 8.7) water quality with elevated TDS, antimony, fluoride, and nickel. A revision of the model in 1996 predicted a higher pH of 9.1. The rapid onset of acidic conditions in the pit lake suggests the modelling technique was incongruous.

Pit Lake Chemistry development

Upon cessation of dewatering operations at the Lone Tree Mine, the pH of the initial pit lake was circum-neutral in December 2006; the pit lake pH decreased in late 2007 declining to 3 to 3.5 by early 2008. Pit lake treatment in the form of alkalinity additions was initiated in 2008 to increase pH and reduce metal concentrations (Fig. 3). Beginning in 2011 the lake began to thermally stratify in the summer months. Treatment via caustic, followed by lime additions was conducted seasonally during summer and fall months. Alkalinity additions during stratification failed to improve the surface pH conditions, resulting in low pH (~3) in surface water (epilimnion), and high pH in the deeper water (hypolimnion). With the onset of lake mixing in the fall, high pH conditions were observed in the entire lake column (Fig. 3).

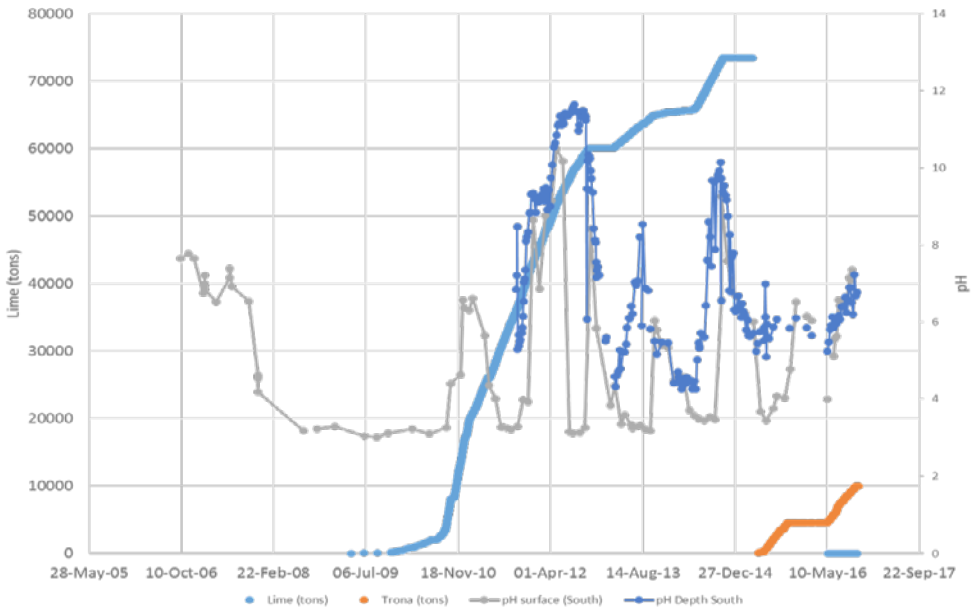


Figure 3 Lime and Trona addition, south surface and depth pH.

No relationship between surface pH and lime addition was evident (Fig. 3), and whole lake swings of pH from 3-10 were occurring with the onset and breakdown of stratification. It became evident that the lime was not dissolving in the surface waters, and there was no way to determine acid ingress or the utilization/efficiency of lime addition.

Once the initial assessment of lake neutrality was deemed to be incorrect, the site now had to re-evaluate and predict the likely lake condition for the future and hence the best way to maintain desirable pH conditions in the surface of the lake, all without any reliable data on the source and magnitude of acidity entering.

In 2014, Newmont Metallurgical Services was enlisted to determine a means to quantify the acidity ingress in order to evaluate the most effective and economically viable methods to

control and maintain pit lake water quality. It was determined that lime solubility had prevented the efficient delivery of alkalinity, and that almost all of the alkalinity dosed in this manner was not utilized in the epilimnion prior to traversing to depth. Therefore a more soluble product would be desired.

Trona

Trona (sodium sesqui-carbonate) was selected as the sole source of alkalinity addition as maximum dissolution rates in the surface waters can be achieved. The rationale is to measure the alkalinity / acidity weekly as normal part of the monitory activity, and determine acidity ingress according to the following equation (Eqn. 1);

$$\text{Acidity ingress} = \frac{\text{Alkalinity added} - \text{Acidity change}}{\text{Time interval}}$$

Equation 1 Acidity ingress calculation

This calculation can be performed for each time frame between surface acidity measurements in summer months, during which time either no alkalinity source is dosed, or a soluble source is used. Incomplete dissolution of an alkalinity source leads to unusable results. *Alkalinity added* is derived from trona addition and epilimnion volume, and is in the units of (negative) grams of calcium carbonate per cubic meter of epilimnion. *Acidity change* is derived from the averaged measured values for acidity in surface water and is in the units of grams of calcium carbonate per cubic meter of epilimnion. *Acidity ingress* is then all acidity coming into the surface of the lake and is in the units of (negative) grams calcium carbonate per cubic meter of epilimnion for a given *Time interval* in days. Typically, the units of acidity are converted to grams sulfuric acid per day.

Results

After two years of data with trona as the sole alkalinity source, we have measured an average daily acid ingress of approximately 17 tonnes of sulfuric acid equivalent (Tab. 3).

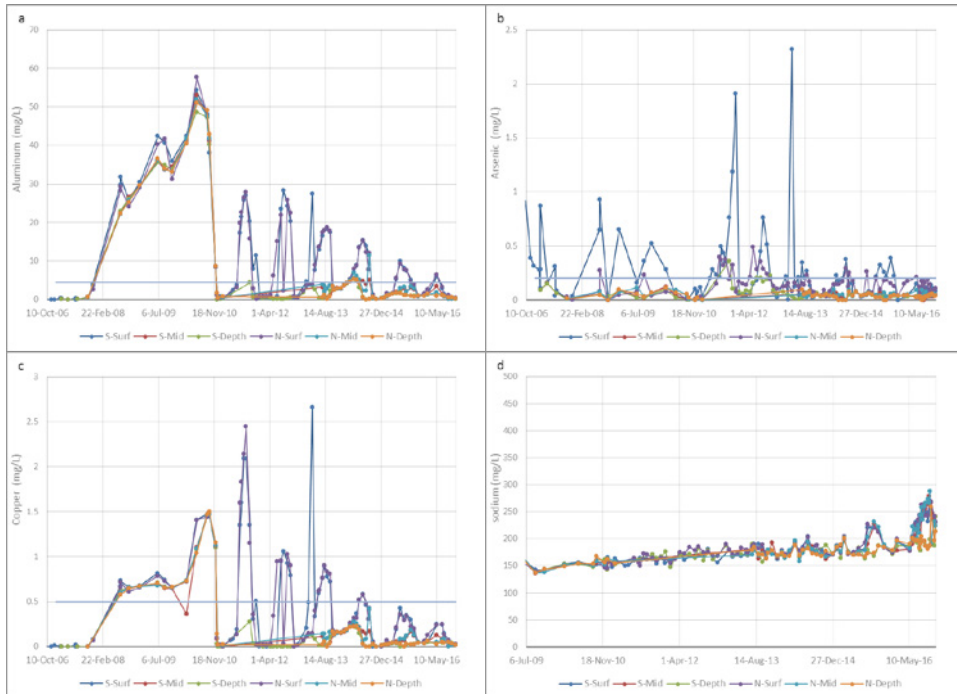
Table 3 Summary of acidity ingress in (-) gCaCO₃/m³ and tonnes H₂SO₄ / day

Species	units	Year	June	July	August	September	Average
H ₂ SO ₄	tonnes / day	2015	16.1	15.2	16.3	21.4	17.3
		2016	11.9	32.2	22.9	2.0	17.2

Lake amendment attempts have demonstrated a measurable improvement to water quality in the pit lake (Fig. 4a-d), and the extension to trona has not only yielded an understanding of acidity ingress, it has achieved the desired water quality.

Discussion

The calculated acidity ingress at Lone Tree is remarkably consistent for the time period measured, and provides a basis for the neutralization requirements in the near term. Further assessment of the acidity ingress (using trona) is required to develop long term trends, which will validate source terms and pathways and develop long term predictions required



Figures 4 a, b, c, d Concentration of aluminium, arsenic, copper, and sodium, respectively, for each sampling point and depth.

for capital investment purposes. Put simply; it is equally undesirable to over or under expend capital to solve this problem.

Trona *may* be the long term solution for this application, however sodium is the balancing ion within the trona molecule, and is conservative in a closed basin system such as Lone Tree. Continued addition of sodium will result in proportional total dissolved solids (TDS) increase, and is determined to be 6–8 mg/L per year (Na), which is acceptable on a short / medium term basis given the 2000 mg/L Na limit (Fig. 4d), and is largely dependent on the long term acidity ingress trend. The nature of sodium as compared to calcium in this case achieves two further benefits, making a longer term trial desirable; 1. Sodium concentration in the epilimnion allows for tracking of alkalinity distribution and, 2. Sodium concentration in the hypolimnion during stratification allows for the assessment of trona neutralisation efficiency, and can correct the acidity ingress calculation.

In addition to TDS, ultimately trona may not be an economic alkalinity source. Delivered, trona is about \$180/t, or in terms of alkalinity, \$280/t as CaCO_3 . Quicklime (CaO) is about \$130/t, or in terms of alkalinity, \$75/t as CaCO_3 . For this application, the economic and sustainable alkalinity source is most likely CaO . Both require capital investment for dosing and distribution; to overcome the solubility and distribution challenges already experienced. Further to the empirical calculation and trend analysis for acidity at Lone Tree, reinterpre-

tation of the geochemical model based on the empirically derived acidity data as calibration, may yet yield a useful tool for the assessment of sources and pathways of acidity, and provide confidence in the water quality prediction long term. This recalibration, lessons learned and reassessment of the geochemical modelling approach, is likely to be useful for the wider industry. We intend to monitor and evaluate long term options over the next 5-7 years.

Summary

Geochemical modelling predicted neutral pit lake chemistry, instead acid conditions developed less than one year after pit filling began. Ad-hoc neutralization was attempted using caustic followed by quicklime, to some effect on overall lake chemistry. Lime dissolution and thermal lake stratification complicated reagent utilization assessments, and continued neutral conditions were not obtained. Sodium sesquicarbonate (trona) was used successfully over two stratification seasons, and acid ingress was quantified as 17 tonnes H_2SO_4 per day. The calibrated ingress is now being used to reassess the original model assumptions to better understand acidity source terms and potential long term trends to meet process design requirements for a water treatment system, and to inform other geochemical models.

References

(ITASCA 2010). 2010 update of numerical groundwater flow modeling for Newmont Mining corporation's lone tree mine Humboldt County, Nevada

This paper is solely based on internal reports of Newmont USA Limited's operation. This includes the geological data, history of the mine and chemical developments. As these reports are not available to the public, no references have been provided.

Control of the remediation of anoxic AMD groundwater by sulphate reduction in a subsoil reactor

Ralph Schöpke¹, Volker Preuß¹, Lena Zahn², Konrad Thürmer^{1,2}, Manja Walko³,
Oliver Totsche⁴

1 Brandenburg University of Technology Cottbus-Senftenberg, Chair of Water Technology and Urban Hydraulic Engineering, schoepke@b-tu.de, preuss@b-tu.de

2 Institut für Wasserwirtschaft, Siedlungswasserbau und Ökologie GmbH (IWSÖ GmbH), lena.zahn@iwsoe.de, konrad.thuermer@iwsoe.de

3 Research Institute for Post-Mining Landscapes (FIB e.V.), m.walko@fib-ev.de

4 Lausitzer und Mitteldeutsche Bergbau-Verwaltungsgesellschaft mbH, Germany, Oliver.Totsche@lmbv.de

Abstract Groundwater containing high amounts of products of pyrite weathering in consequence of lignite surface mining flows into receiving waters for a number of years. Iron hydroxides causing turbidity and silting will strongly affect surface waters for many decades. In addition to liming acidic surface waters and the conventional treating of mine waters, microbial sulphate reduction of the inflowing anoxic acid mine drainage (AMD) groundwater is tested for long-term remediation. During a pilot project at Lusatia / Germany glycerol as a carbon source and nutrient solutions of N and P are infiltrated in an anoxic AMD groundwater stream by lances (Hildmann et al. 2016). Planning and operation were carried out based on the model as proposed below.

Introduction

Lignite surface mining in Lusatia, Eastern Germany caused pyrite weathering due to lowering of the groundwater level. Owing to the post-mining rebound of groundwater level, iron- and sulphate-rich groundwater enters the surrounding environment for a number of years. A possible solution to remediate the groundwater and to protect receiving water courses is the use of sulphate reduction in-situ in the aquifer.

The oxidation of pyrite and other sulphides generates the acidity of acid mine drainage (AMD). Using the sum parameter of acid capacity ($K_{S_{4,3}}$) and the concentrations of iron, aluminium and manganese the neutralization potential (NP) is defined by equation 1.

$$NP \approx K_{S_{4,3}} - 3c_{Al^{3+}} - 2c_{Fe^{2+}} - 2c_{Mn^{2+}} \quad (1)$$

Reactions that produce AMD and their inversion as a result of remediation can be presented as vectors in an acidity/sulphate concentration plane, wherein acidity is represented by negative neutralisation potential ($-NP$) (Schöpke et al. 2016, Fig. 3). A statistical linear relationship between the acidity and the sulphate concentration is frequently observed in AMD contaminated groundwaters. Ferrous iron generates the majority of acidity. Due to aeration and oxidation, AMD forms acidic lakes. Alternatively, in buffered rivers iron hydroxides cause a brown turbidity.

Acid surface waters, e.g. lakes, can be neutralised by liming. During this process, the neutralisation potential increases and achieves positive values, whereas the concentration of

sulphate remains constant. Anoxic AMD groundwater flows can be treated by microbial sulphate reduction. As a result, acidity and sulphate concentration decrease at a stoichiometric ratio and iron sulphide precipitates. In case of lack of iron, toxic hydrogen sulphide will be formed. As the reaction progresses, precipitation of calcite may occur.

Our concept for remediation

Sulphate reduction in the aquifer – that is our concept for remediation of AMD groundwater. Analogous to microbial types of passive AMD treatment it is based on natural processes to neutralize acidity due to precipitation of iron sulphide. Constructed wetland processes require large areas to treat moderately acidic AMD. However, we don't have large areas and therefore make use of the great volume of the aquifer. The concept has been developed to treat stagnant and flowing groundwater bodies that may endanger receiving water courses. Emanating from hot spots, acidity can reach up to concentrations of $\text{NP} \approx -20 \text{ mmol/L}$ (1000 mg/L CaCO_3 or $\approx 500 \text{ mg/L Fe}$).

To enrich the groundwater with substrate it is extracted and re-infiltrated after mixing with glycerol and nutrients (nitrogen N, phosphorus P) if necessary as shown in Fig. 1. The infiltration of the substrate-enriched groundwater happens periodically. Between two cycles of infiltration, the groundwater flows freely. Both water bodies mix in the downstream via hydrodynamic dispersion effects. A mixed culture of autochthonous sulphate-reducing microorganisms multiplies in the downstream and the subsoil reactor develops.

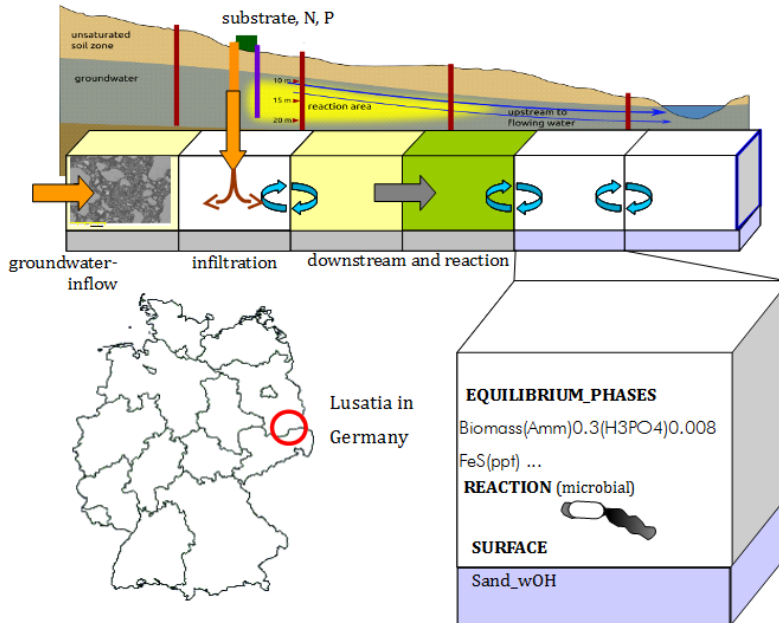
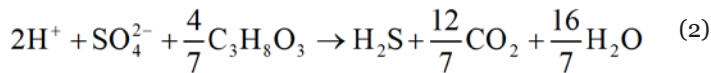


Figure 1 Scheme and nomenclature (phreeqc) of the mixed cell model (above and right side) and position of the study area in Lusatia, Germany (left side)

The pilot projects were prepared by laboratory experiments, field tests (Tab. 2) and modeling with phreeqc (Parkhurst & Appelo 2006). This article concentrates on geo- and biochemical problems.

Biochemical reactions

Sulphate can be reduced to hydrogen sulphide by easily degradable organic substances, Eq.(2). In Lusatia, methanol and glycerol are accepted as substrates. Together, hydrogen sulphide and ferrous iron precipitate as iron sulphide, Eq.(3). The pH value and the available concentration of iron determine the concentration of remaining hydrogen sulphide.



Taking the expected conversion of ferrous iron and possibly concentrations of oxygen and ferric iron, the need for substrate is calculated according to Eq.(4) using the stoichiometric coefficients $n(i)$ given in Tab. 1.

Table 1 Stoichiometric coefficients $v(i)$ of substrates used for sulphate reduction

Substrate	M g/mol	Stoichiometric coefficients $n(i)$			
		$n(\text{O}_2)$	$n(\text{Fe}(3))$	$n(\text{Fe}(2))$	
Carbohydrate	$\{\text{CH}_2\text{O}\}$	30	1.00	2.25	2.00
Methanol	CH_3OH	32	0.67	1.50	1.33
Glycerol	$\text{C}_3\text{H}_8\text{O}_3$	92	3.5	0.64	0.57
Ethanol	$\text{C}_2\text{H}_5\text{OH}$	46	3.00	0.75	0.67
Acetic acid	CH_3COOH	60	2.00	1.13	1.00
calculated BOD	O_2	32	1.00	2.25	2.00

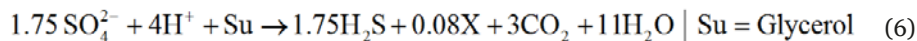
Alternatively, the biochemical oxygen demand (BOD) can also be specified for mixtures.

$$c_{\text{Substrat}} = v_{\text{O}_2} \cdot \Delta c_{\text{O}_2} + v_{\text{Fe}(3)} \cdot \Delta c_{\text{Fe}(3)} + v_{\text{Fe}(2)} \cdot \Delta c_{\text{Fe}(2)} \quad (4)$$

The growth kinetics of microbial biomass in the form of substrate consumption is determined by growth rate (μ_o), concentration of Biomass (c_{Biomass}), pH value, temperature (Temp) as well as monod- and inhibition terms ($f_i(i)$) as described in Schöpke et al. (2011) and in Eq. (5).

$$\frac{\partial c_{\text{Su}}}{\partial t} = \mu_o \cdot c_{\text{Biomass}} \cdot f(\text{Temp}) \cdot f(\text{pH}) \cdot f_{\text{Su}}(c_{\text{Su}}) \cdot f_{\text{SO}_4}(c_{\text{SO}_4}) \cdot f_{\text{N}}(c_{\text{N}}) \cdot f_{\text{P}}(c_{\text{P}}) \cdot f_{\text{I}}(c_{\text{I}}) \quad (5)$$

Eq. 6 describes the yield of biomass. To characterize with phreeqc the consumption of nutrients and substrate the intermediate product X was defined.



This intermediate product X condenses to the phase Biomass. The composition of the phase Biomass corresponds to the expression in Eq. (7) but can slightly differ.



The kinetic of the lysis of Biomass is defined as first-order reaction. At its decay, the phase Biomass releases again the bound nutrients and the substrate. All kinetic constants researched by Schöpke et al. (2011) were adapted to the considered processes. The Monod-constants used in the terms $f_i(i)$ only had to be changed slightly. During the model adjustment, the reaction mechanisms as well as the formation of intermediate products can still be altered. In the considered aquifers, methanogenesis can be neglected.

Pore systems

In the pore system of the aquifer, different biochemical reactions take place. The stationary solid matrix consists of quartz sand, clay minerals and organic particles. Pore solution flows through the interstices. Pseudoparticles consisting of fine grains were sometimes found in aquifers in the area of mine dumps. Their inner pore system is only accessible by diffusion. Pleistocene aquifers contain predominantly quartz particles with traces of clay and lignite. The stationary surface area of the pore system will be defined as pore gel. Surface phases, mineral phases, bacteria and extracellular substances will mainly form the pore gel. Solid humic substances can be mobilised at increasing pH value. The thermodynamics of the pore gel may differ from that of the pore solution and the process constants can slightly deviate from the macroscopically known constants. The geochemical software phreeqc can calculate all processes in the system of pore gel and pore solution. For this purpose, the tabulated values of thermodynamic constants were adjusted to test results.

Transport model

All processes of pore solution and pore gel were included in every cell of the *mixed cell* transport problem. The flow path between the infiltration and each measuring point (25 m, 30 m, 100 m, 200 m) will be described as flow tube, which takes into account the filtration processes. The flow tube consists of 1 m long *mixed cells*. The *rates* and *kinetics blocks* are adapted to the described biochemistry of sulphate reduction.

Application of sulphate reduction in subsoil reactors

Tab. 2 gives an overview of the initial conditions at individual test sites in Lusatia/Germany. The results concerning lake RL 111 documented Preuß (2004), in the case of Senftenberger See Koch et al. (2006) and in the case of Skadodamm Schöpke et al. (2011). Experiences with sulphate reduction in acidic lake water (No. 0) will not be discussed in this article. The pilot project at the location Ruhlmühle is still running (Hildmann et al. 2016).

Table 2 Locations of application and some of the characteristics of the respective test sides

No.	location	year	aquifer	particularities
0	lake RL 111	2001-2004	lake	pH < 3.5, aerob
1	Senftenberger See	2002-2003	tertiary	Mobilisation of humic substances
2	Skadodamm	2008-2010	dump	pH > 4.8, Al < 0.2 mg/L
3	Ruhlmühle	2014-2017	quaternary	pH < 4.1, Al > 10 mg/L

At the location Ruhlmühle in the north of Saxony (Germany, No. 3), a groundwater stream of $Q = 200\text{--}300\text{ m}^3/\text{d}$ is treated by microbial sulphate reduction (Fig. 1). The groundwater is extracted by three wells and re-infiltrated intermittently after mixing with glycerol and nutrients. The infiltration line consists of 30 lances and has a width of about 100 m. Along a flow length of 300 m the subsoil reactor develops. The flowtime is 300 to 500 days. To infiltrate substrate-enriched groundwater into the entire flow cross-section the lances are arranged in three horizons.

Taking into account more than five specially selected measuring points, the model was adapted to the changes of groundwater quality. By this, the longitudinal profiles of the concentrations of iron and sulphide after 900 days of treatment in Fig. 2 were calculated. The precipitation front of iron sulphide (FeS) is located at approximately 145 m of flow path. At this point, however, already 500 m water column flowed through the subsoil reactor. The arrow in Fig. 2 indicates the retarded migrating iron front. Precipitated iron is supplied by desorption from the solid matrix. The lost iron will be exchanged for aluminium, calcium and other dissolved cations (competing adsorption). That is why the front of the iron removal migrates more slowly than the infiltration front.

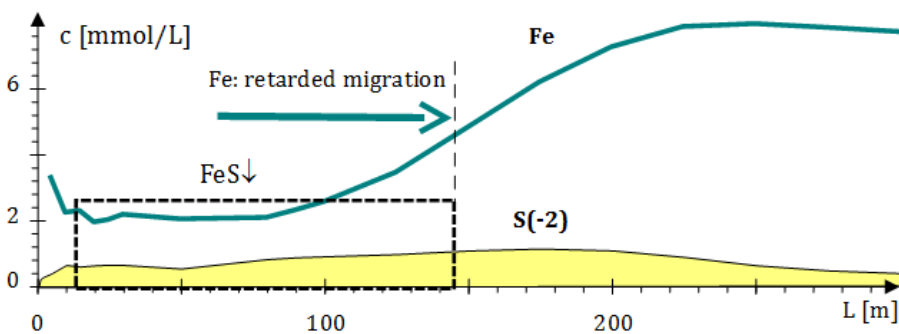


Figure 2 Modeled longitudinal sections of iron (Fe) and sulphide (S(-2)) concentrations after 900 days of treatment based on monitoring data at the location Ruhlmühle (No. 3).

Fig. 3 demonstrates the development of the acidity (-NP) and of the sulphate concentration (SO_4) due to the treatment at the measuring points after 20 and 30 m of flow path as described in Schöpke et al. (2016). The change of groundwater quality over 900 days of

treatment (dark blue) can be explained as a combination of the theoretical vector of sulphate reduction (black) and the vector of a slight buffering by the aquifer matrix (light blue). According to Eq. 1, the acidity correlates with the remaining concentration of iron (brown, dashed).

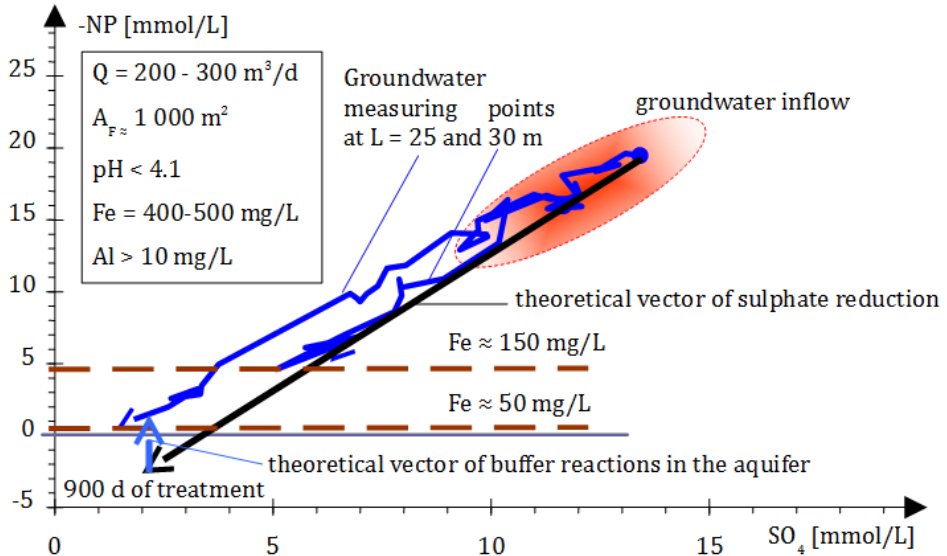


Figure 3 Effects of microbial sulphate reduction in the aquifer at the location Ruhlmühle shown in the acidity/sulphate concentration plane as well as treatment parameters and the original groundwater quality.

After 900 days of treatment, the residual concentration of iron approaches 50 mg/L. As mentioned, the remaining concentration of hydrogen sulphide depends on the iron concentration and the pH value. Close to the infiltration point, the success of the remediation with low sulfide residues is already achieved. At the location No. 2 (Tab. 2, Skadodamm), on a width of 20 m a groundwater stream of only 13 m³/d and with a higher pH value was treated. After the period of adaptation, the sulphate reduction already took place in the first ten meters. Several developed concentration fronts migrate at different speeds through the aquifer because of competing adsorption as just described. Due to substrate overdose during the phase of infiltration at this location hydrogen sulphide was formed. The hydrogen sulphide migrated with the groundwater stream and on its further flow path caught up with the retarded migrating ferrous iron. At the location No. 1 (Tab. 2, Senftenberger See) the mobilisation of humic substances in the groundwater was observed as consequence of increasing pH value. This process can also be described by means of the proposed model (phreeqc).

Conclusions

Microbial sulphate reduction allows long-term treatment of AMD sources and migration pathways. Tab. 3 shows the specific reduction of acidity and other performance parameters

of individual sulphate reducing reactors. Skousen et al. (2017) specify for a vertically flowed through wetland a specific reduction of acidity of maximal 35 g/(m²·d). Regarding their performance, subsoil reactors are comparable to constructed wetlands. However, a larger reaction space is available.

Table 3 Performance parameters of differently working sulphate reducing reactors

Reactor	DNP mol/(m ² ·d)	Dacidity g/(m ² ·d)	flow length L m	running time d
vertically flowed wetland	0.7	max. 35	» 0.5 – 2	no information
Skadodamm (No. 2)	0.45	23	9	360
Ruhlmühle (No. 3)	1.8	90	25 – 30	> 850

So far in case of subsoil sulphate reduction, the test times were not sufficient to indicate long-term concentrations of hydrogen sulphide and residual substrate. Obstructions by reaction products and gas bubbles were observed in no event. The basics of the preparation and assessment of these treatment methods were developed. An important element is geochemical modeling. The model can describe the biochemistry, the competing sorption on the aquifer matrix and the mobilisation of humic substances on the flow path. Important input parameters are the pH value as well as the concentrations of iron, aluminium, sulphate and nutrients. The site-typical conditions have to be explored accurately. Adapted simulations (phreeqc) can also describe the different velocities of migration and effects of mobilisation of humic substances at increasing pH values.

So far, the strict German and European environmental legislation result in the use of pure chemicals as substrates and therefore cause high costs. Alternative substrates should be selected on the following conditions:

- Prohibition of deterioration.
- Criteria for the assessment of good chemical status.
- No danger of eutrophication in adjacent waters.
- The treated groundwater has to be suitable for drinking water treatment.

Depending on the geochemical conditions, the treatment measures require several years of adaption of the autochthonous microorganisms. By means of a model-supported process control, complete substrate consumption can be aimed at and the residual concentration of hydrogen sulfide can be minimized. Unanswered questions of detail have to be clarified by monitoring and modeling during future applications. The proposed principles of sulphate reducing reactors can be adapted to technical systems (end of pipe).

Acknowledgements

The authors thank LMBV for project leading and cooperation. Financial support from LMBV and BMBF is gratefully acknowledged.

References

- Hildmann C, Schöpke R, Walko M, Mazur K (2016) Microbial Iron Retention in the Groundwater upstream to a River. In: Drebenstedt C, Paul M. (Hg.) Mining Meets Water – Conflicts and Solutions.; IMWA Leipzig, Proceedings, IMWA 2016 in Leipzig, Germany, July 11-15
- Koch R, Schöpke R, Mangold S, Regel R, Striemann A (2006): Entwicklung und Erprobung eines Verfahrens zur Untergrundsäuerung von Kippengrundwässern. Schriftenreihe Siedlungswasserwirtschaft und Umwelt, Bd.11, <https://www-docs.b-tu.de/fg-wassertechnik/public/Publikationen/Schriftenreihe/Heft11.pdf>
- Parkhurst DL, Appelo CAJ (2006): User's guide to phreeqc (version 2) – a computer program for speciation, batch-reaction, one-dimensional transport and inverse geochemical calculations. Water-Resources Investigations Report , S. 99-4259
- Preuß V (2004) Entwicklung eines biochemischen Verfahrens zur Aufbereitung sulfathaltiger Wässer am Beispiel der Entsäuerung schwefelsaurer Tagebaurestseen. Schriftenreihe Siedlungswasserwirtschaft und Umwelt, Bd. 9, https://www-docs.b-tu.de/fg-wassertechnik/public/Publikationen/Schriftenreihe/Heft_9.pdf
- Schöpke R, Preuß V, Zahn L, Thürmer K (2016) Modelling the changes in water quality of AMD along the flow path. In: Drebenstedt C, Paul M (Hg.) Mining Meets Water – Conflicts and Solutions. IMWA Leipzig, Proceedings, IMWA 2016 in Leipzig, Germany, July 11-15
- Schöpke R, Gast M, Walko M, Regel R, Koch R, Thürmer K (2011) Wissenschaftliche Auswertung von Sanierungsversuchen zur Untergrundsulfatreduktion im ehemaligen Lausitzer Bergbaurevier, Schriftenreihe Siedlungswasserwirtschaft und Umwelt Bd.21, <https://www-docs.b-tu.de/fg-wassertechnik/public/Publikationen/Schriftenreihe/Heft21.pdf>
- Skousen J, Zipper CE, Rose R, Ziemkiewicz PF, Nairn R, McDonald LM, Kleinmann R.L (2017) Review of Passive Systems for Acid Mine Drainage Treatment. Mine Water and the Environment, Volume 36, Number 1, pp. 133-153

Finely Discretized Numerical Flow Model of Complex Multiple Open Pit Mine For Reliable Inflow and Pore Pressure Simulations – An African Perspective

Brendon Bredenkamp¹ Eric Levay² Alkie Marais³ Arjan van 't Zelfde⁴

¹*GCS Water and Environmental Consultants (Pty) Ltd, 63 Wessel Road, Woodmead, Johannesburg, Gauteng, RSA, brendon@gcs-sa.biz*

²*Vale Mozambique, Vila Carbomoc, Casa 20, Tete, Mozambique, eric.levay@vale.com*

³*GCS Water and Environmental Consultants (Pty) Ltd, 63 Wessel Road, Woodmead, Johannesburg, Gauteng, RSA, alkie@gcs-sa.biz*

⁴*GCS Water and Environmental Consultants (Pty) Ltd, 63 Wessel Road, Woodmead, Johannesburg, Gauteng, RSA, arjanv@gcs-sa.biz*

Abstract Flow modelling has become one of the best prediction tools to quantify groundwater inflows and pore pressure distribution in open pit mines. Accurate discretization of the geological features, multiple hydrogeostratigraphic zones and detailed open pit geometries into numerical models are essential when assessing these aspects.

This paper presents a case study of Moatize Mine where multiple open pits are operated simultaneously in a complex hydrogeological environment. Fine model discretization allowed for a realistic distribution of input transmissivity and specific storage throughout the model domain. Simulated pore pressures and groundwater inflows were used to guide slope and mine water infrastructure design.

Key words fine discretization, groundwater inflow, numerical flow model, open pit

Introduction

The Vale SA Moatize Mine is located near the town of Moatize, approximately 16km north-east of the Provincial capital Tete, in north-western Mozambique. There are at least eleven potentially economic coal deposits in the Vale project area, of which six will be mined. Mining operations started in 2010 and will reach an annual production of 18 million tons in 2017.

Given the potential depth of the open pits (maximum depth of 290m below surface) groundwater was required to be managed as part of the mining process. Vale SA thus identified the need for a numerical flow model that could be used as management tool across the Vale mining area to quantify groundwater inflows and pore pressure distribution within the open pits.

Methodology

A comprehensive hydrogeological investigation was completed during the Bankable Feasibility Study (BFS) of the mine in 2006. This study entailed the siting and drilling of 131 hydrogeological test boreholes used for aquifer testing. A combination of hydrogeological drilling, aquifer testing as well as geological models was used to conceptualise the numerical model domain. The data was pre-processed for incorporation and translation into the numerical model.

The main purpose of model was to construct a calibrated steady state and transient model capable of simulating predictive scenario for groundwater influx and pore pressure estimation. Groundwater Modeling System (Aquaveo LLC 2017) a pre- and post-processing package for MODFLOW and MODFLOW-NWT (Niswonger et al. 2011) was used for the process. The modelling process involved the following steps:

- Construction and setup of the model;
- Conceptual model translation into the numerical discretization;
- Model calibration/verification; and
- Scenario Modelling.

Conceptual Hydrogeological Model

The project area is located in the Moatize-Minjova coal basin that has an asymmetrical synclinal structure, bordered by faults, with several inclined blocks (as can be seen in Figure 1). Coal formations in the basin, occur in a graben structure. Karoo Supergroup sediments were deposited unconformably onto the Proterozoic crystalline basement in subsiding grabens or half graben. Basement gabbro and anorthosite form the high lying ridges and hills surrounding the various mining sections. Post Karoo (early Jurassic) dolerite intrusion took place in both the Karoo sediment and the basement rock.

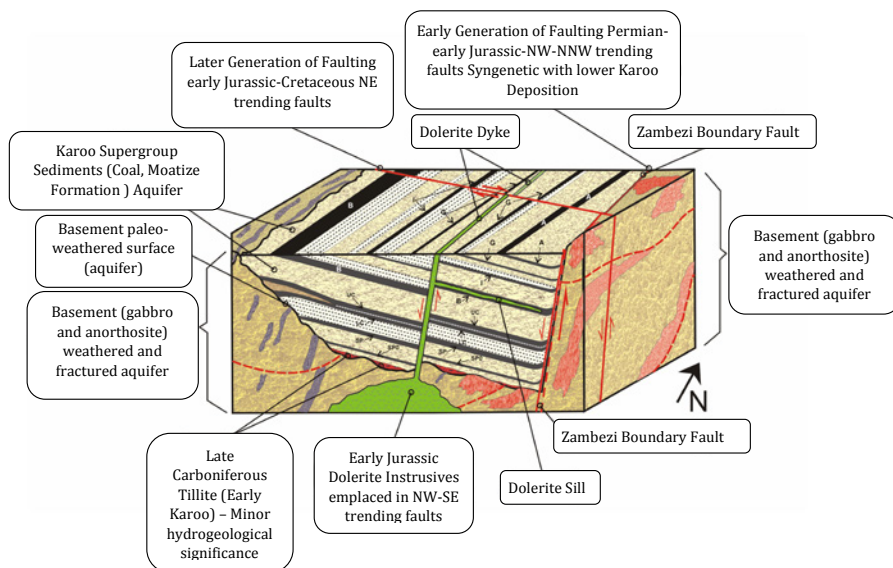


Figure 1: Schematic block diagram of Karoo sediments deposited in a half graben structure (after Rio Doce Mozambique 2006)

A summary of the hydrogeological conceptualisation is discussed below:

- Average depth of weathering in the Karoo Supergroup aquifer ranges between 15 and 20 m. Water strikes are associated with minor fracturing, most likely bed-

ding planes fractures on the contact with the major coal seams. Transmissivity values of Karoo sediments vary between 0.05 and 1.5 m²/d. and storativity, mostly between 0.001 and 0.00001.

- Groundwater occurrence may be enhanced along faults and dyke contact zones within the Karoo strata and/or within the underlying Basement rocks. Higher yielding boreholes are generally associated with NE-SW trending structures.
- NW-SE trending Zambezi Boundary Fault and dolerite dykes are potential flow barriers
- Groundwater levels are typical between 5 and 15 metres deep (range between artesian and 50 m below surface).
- Borehole yields were generally lower 1 l/s in areas where smaller weathered pockets and minor fracturing occur. An enhancement of groundwater occurs along faulting, with recorded yields from 3 to 15 l/s. A large number of these higher yielding structures have a NE – SW trend. The basement rock aquifer also have a low transmissivity in the order of 0.5 m²/d, however faulting is associated with transmissivities up to 3 orders higher. Basement aquifer seems to be less developed with depth. Preferred basement aquifer zone is 25 to 60 m deep.
- Parts of the paleo-weathered surface offers better aquifer properties compared to areas investigated where the basement is exposed to surface with shallow weathering. Some of the highest borehole blowout yields identified during the BFS study were recorded where faulting occurs in the basement below the Karoo Supergroup units.
- Based on Chloride (Cl) Method calculations and previous studies, an average recharge value of 2.6 mm/annum was used (0.4% of mean annual precipitation) over the model domain.

Model discretization

Modelling focussed on the six mining sections in the current long term mine plan. The model area was discretized by a 689 x 1000 grid in the x and y direction and consisted of 33 layers (8m layer thickness). A total of 4782747 active cells were found in the model grid. Grid refinement of 25 m x 25 m x 8 m cells around the mining areas was applied with coarser grid cell sizes of 200 m x 200 m x 8 m away from the mining areas.

River boundary conditions were applied to the Revubue and Zambezi rivers at the north-western and southwestern boundaries of the model domain. No-flow boundary conditions were applied to topographical catchment boundaries along parts of the north-western and eastern ends of the model domain.

For the area outside the concession coal resources only the four upper model layers were activated as the hydraulic conductivity in these areas decrease rapidly with depth in the presence of the basement rocks. For the mining areas the basement paleo-weathered aquifer was chosen as the bottom hydrostratigraphic unit of the model.

The hydrostratigraphic units were then translated into the 3D discretisation using a grid overlay function, whereby each cell of the model is assigned a hydrogeological parameters based on the intersecting hydrostratigraphic unit (as seen in Figure 2). The Moatize Formation solid was created by using the depth to weathering as the top and the Souza Pinto coal seam as the bottom. For the three major coal seams the top of seam and bottom of seam was used and included all the partings associated with each seam. Cells that should not contribute to groundwater flow (deep unfractured rock) were made inactive by assigning an 'inactive' hydrostratigraphic unit.

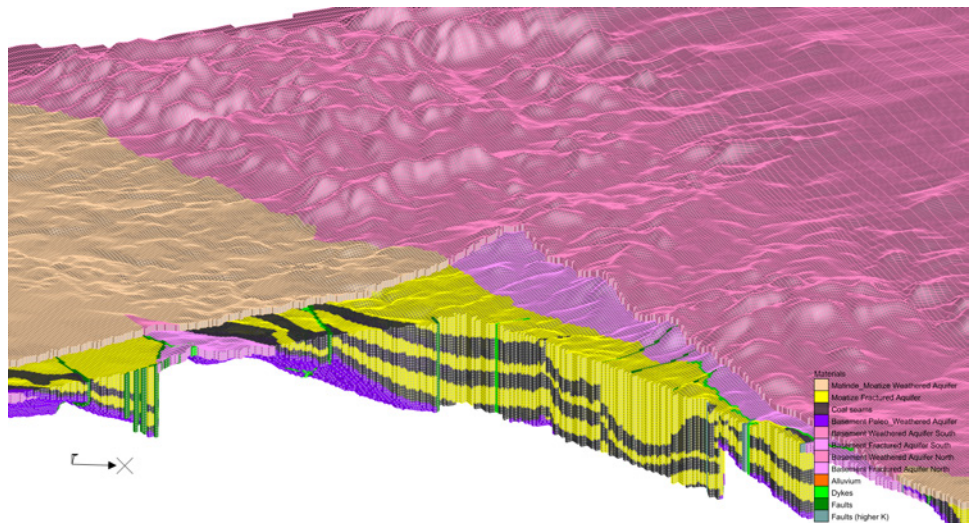


Figure 2: 3D Oblique view of model illustrating the translation of the hydrostratigraphic units into the discretization

Model Calibration and Sensitivity Analysis

Initial estimates of the hydraulic conductivity for the different geological units were obtained from the aquifer test data collected as part of the hydrogeological field program. These hydraulic conductivity values were assigned to the hydrostratigraphic units in the model area. Performance measurements were evaluated during the calibration of the model as:

- **Model convergence:** Model convergence was obtained during calibration and a maximum change in heads between iterations was set to 1.0×10^{-5} m.
- **Water Balance:** The mass balance for entire model achieved a water balance error of less than 0.0001%.
- **Quantitative measures:** The difference in measured compared to calculated head was less than 5 m for 124 observation boreholes. Steady-state calibration was regarded as sufficient at mean error (ME) = -0.33 m, mean absolute error (MAE) = 2.75 m, root mean square error (RMSE) = 3.41 m and normalised root mean square error (NRMSE) = 3.3%.

A sensitivity analysis of the model found recharge and hydraulic conductivity of the weathered aquifer to be sensitive to change. Groundwater inflows into one of the deeper operational pits was used to verify the model and the model's ability to perform predictive scenarios. An estimated inflow of $\sim 400 \text{ m}^3/\text{d}$ was simulated for the beginning of 2016, this volume correlated to the inflow flux measured by the mine.

Fine discretization thus allowed for a more realistic representation of the geological model in the numerical model grid. A refined distribution of transmissivity and specific storage/specific yield throughout the model domain was achieved.

This finely discretized numerical model with a large number of cells pushed the boundaries of the graphic user interface and computer processing abilities. Nevertheless the model run time was acceptable and the model was able to perform predictive simulations for the open pits based on the transient life of mine plans.

Simulated groundwater inflows

Scenario modelling using the calibrated transient model was conducted to assess the pit groundwater inflows and drawdown extents for existing and proposed open pit mining. Latest available pit shells and schedules were incorporated into the model. Annual pit shells with yearly intervals were provided for the period 2016 – 2026, after which the interval increased to 5 yearly. Simulated groundwater inflows volumes (Figure 3) were extracted for all six mining areas with the cumulative volume reaching $\pm 7000 \text{ m}^3/\text{day}$ in 2040.

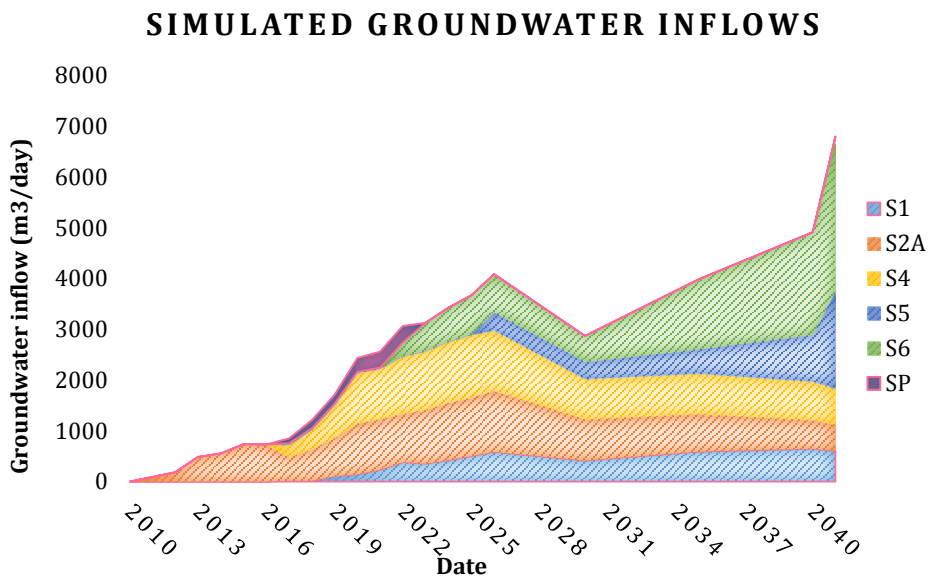


Figure 3: Simulated groundwater inflows of the six open pits which was used in the mine water balance to assist with long term water management and planning

Mine water management

Moatize Mine has a water deficit and is located in an areas with unreliable rainfall (MAP: 642mm), where severe dry spells could occur. Evaporation generally exceeds the average rainfall. Groundwater inflows therefore played an important role in augmenting the water supply especially related to dust suppression and beneficiation plant demand. Simulated groundwater inflow volumes was also used to guide water infrastructure design and to assist in the planning of future water availability for the mine complex.

Mining occurs in a hydrogeological environment with generally a low to average permeability as a result simulated groundwater inflows into the pits was be regarded as manageable without the need for active dewatering systems such as abstraction boreholes (based on the present mine scheduling). Mine scheduling and design could thus allow for upfront planning, sizing and construction of dewatering sumps at least two benches below the mining level with the assistance of modelling results. Simulated groundwater inflow volumes was used to spec appropriately sized sump pumps and infrastructure required to abstract the passive groundwater inflow into each pit. This information was also required as input into external mining service provider contracts as they were often required to provide turnkey mining operations and thus operate the dewatering system.

A finely discretized flow model allowed the mine to assess the changes in drawdown around the open pits as the pit geometry changed, thus providing an early warning system for any potential impact on community supply boreholes.

Three dimensional pore water pressures was extracted from the model based on the transient pit shell schedules. These pore water pressures provided valuable input into the geomechanical models and was used in the slope design process (a cross section from the model can be seen in Figure 4). Flow modelling also allowed for the testing of different pit shells whereby the results could be fed back into the geomechanical investigation.

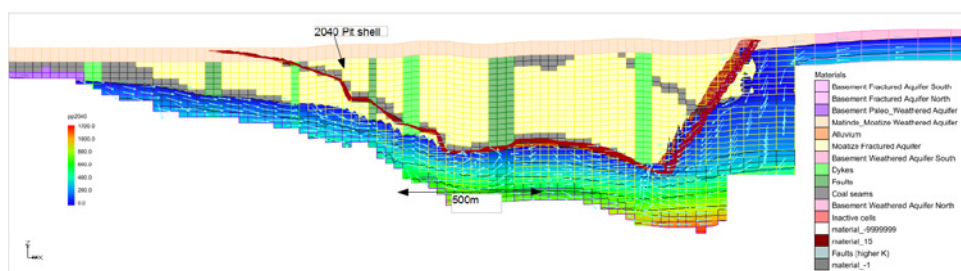


Figure 4: Model Cross Section depicting a 2040 open pit shell with associated simulated pore water pressures (kPa) and flow vectors. The deeper sections of the high wall appear to be saturated. These profiles were used by the geotechnical engineers during the slope design.

Conclusions

A realistic aquifer depressurisation and flux for each mining step could be simulated as the open pit geometry could accurately be included in the finely discretized model. Simulation

results were more realistic than previous simpler numerical models developed for the mine. The numerical model is thus used as an active groundwater management tool that is updated periodically with the latest pit shells and groundwater monitoring data to continuously assess the changes and potential impacts on the hydrogeological environment.

A finely discretized flow model provided inputs to various stakeholders and departments at the mine such mine planning, water utilities, geotechnical and environmental, by reliably estimating transient groundwater inflows and pore pressures for the different open pits.

Acknowledgements

The authors thank Vale SA Mozambique for approving the submission of this work and paper for presentation at the 2017 IMWA conference in Lappeenranta, Finland.

References

- Aquaveo LLC (2017) Groundwater Modeling System (GMS), version 10.2.4.
- Niswonger, R.G., Panday, S, and Ibaraki, M (2011) MODFLOW-NWT, A Newton formulation for MODFLOW-2005: U.S. Geological Survey Techniques and Methods 6–A37, 44 p
- Rio Doce Moçambique, (2006). Moatize Coal Project – Feasibility Study Level: Geological Exploration Report. Final Version.

3-dimensional geologic and groundwater flow modelling for coal mining areas as decision support tool

- Iterative interaction workflow to establish a reliable groundwater model -

Wieland Philipp ¹, Friedemann Brückner ², Michael Rüger ³, Holger Mansel ²

¹*Lausitzer und Mitteldeutsche Bergbau-Verwaltungsgesellschaft mbH, Walter-Köhn-Straße 2, 04356 Leipzig, Germany, wieland.philipp@lmbv.de*

²*Ingenieurbüro für Grundwasser GmbH, Nonnenstr. 9, 04229 Leipzig, Germany, f.brueckner@ibgw-leipzig.de; h.mansel@ibgw-leipzig.de*

³*HPC AG, Am Stadtweg 8, 06217 Merseburg, Germany, michael.rueger@hpc.ag*

Abstract This paper describes the modelling workflow to develop a reliable geological model and a reliable hydrogeological model which were used within a cause study of a landslide in an open pit lignite mine. It is shown that interdisciplinary collaboration between field geologists, geological modellers and groundwater modellers is highly important to set up a consistent groundwater model. Thereby, the iterative interaction of the involved nature scientists and engineers is a crucial requirement to face difficulties and uncertainties in the practical modelling workflow. As shown in this paper the classic “in sequence” modelling workflow may lead to a misunderstanding of the hydrological processes and a misunderstanding of the geological setting.

Key words geological modelling, hydrogeological modelling, lignite mining, groundwater pressure

Introduction

Remediation of large disused lignite mine areas and establishing structural stability are very complex and long-term projects. In several areas landslides with expansions of partly over 1 km² occurred unexpectedly although the embankments were declared as stable. One of the most dramatic landslides took place in the former lignite mine of Nachterstedt in 2009 (Fig. 1). About 4.5 million cubic metre dump slope slid into the half flooded open pit lake (Katzenbach, 2013). Thereby, three houses collapsed into the pit lake and three people lost their lives. As a consequence, several hectares of mine dumping areas were locked for public use to re-evaluate these areas and to restabilize them if necessary. In the course of the re-evaluation, but also by public and juridical demand as well as for future and exemplary assessment of other areas, the causes of the landslide had to be found.

As groundwater is one of the forcing parameters to provoke landslides (Förster, 1997), reliable geological and hydrogeological models are fundamental elements in the cause study to answer geological, geotechnical and hydrogeological questions.

Therefore, a groundwater model is an appropriate tool to understand subsurface flow processes and to predict the response of changes within these processes. The basic information of a groundwater model is the knowledge of the subsurface system. Hence, the geological model has always been recognized as a very important element in groundwater modelling (Anderson & Woessner, 1992). The accuracy of the model and the reliability of the predicted

future scenarios are dominated by the geological certainty (Carrera & Neuman, 1986, Harar et al. 2003, Troldborg, 2004, Eaton, 2006, Poeter & Anderson, 2005).

This paper discusses the development of a geological structure model starting with the basic information such as borehole data and on base of the geological model the establishment of a groundwater model. It indicates the significance of the iterative interactions between the field geologists (basic information/borehole data), the geological modellers (geological structure model) and the groundwater modeller (groundwater flow model) to face difficulties and uncertainties during the modelling workflow and to provide a consistent geological model and hydrogeological model in the cause study of the mentioned landslide. It is exemplarily shown, that this iterative modelling workflow should be considered instead of the classic “in sequence” modelling workflow especially in complex geological and hydrogeological settings with high requirements on the models.



Figure 1 Aerial view of the 2009 landslide Nachterstedt

Study area

The lignite mine area is located nearby the village of Nachterstedt in Central Germany. Since the 19th century the area was extensively used by lignite mining both open pit and underground mining. Thus, the area is characterized by mining dumps and remaining open pits.

The geological setting is dominated by a complicated geological structure (Fig. 2) which mainly can be distinguished by an anticlinal salt dome of the Upper Permian salt. Thick estuarine tertiary sediments were deposited at the transverse basin. The syngenetic subsidence of the paralic basin of deposition led to a small scale variety in the lithological conditions

in horizontal but also lateral direction. In Quaternary the study area was shaped by salt tectonics and quaternary meltwater channels, which eroded the tertiary sediments partly.

Likewise, the hydrogeological dynamics can be characterized by intense lateral and vertical variations of the groundwater level (Fig. 2). The artificial mining dump aquifer, which is an unconfined aquifer, is an extreme heterogeneous mixture of clay, silt, sand, gravel and lignite components. The natural aquifers are spatially limited with large variations in thickness and permeability. There is a connection to very permeable quaternary gravel outside the lignite basin. Thus, the groundwater flows from the quaternary gravel with its high water yield through the tertiary alternating layers and through the heterogeneous mining dump with its minor water yield into the remaining open pit. As a consequence the groundwater is flowing both in radial and ascending direction into the rising open pit lake. Depth-dependent groundwater pressure differences result partially in artesian conditions in the vicinity of the open pit lake.

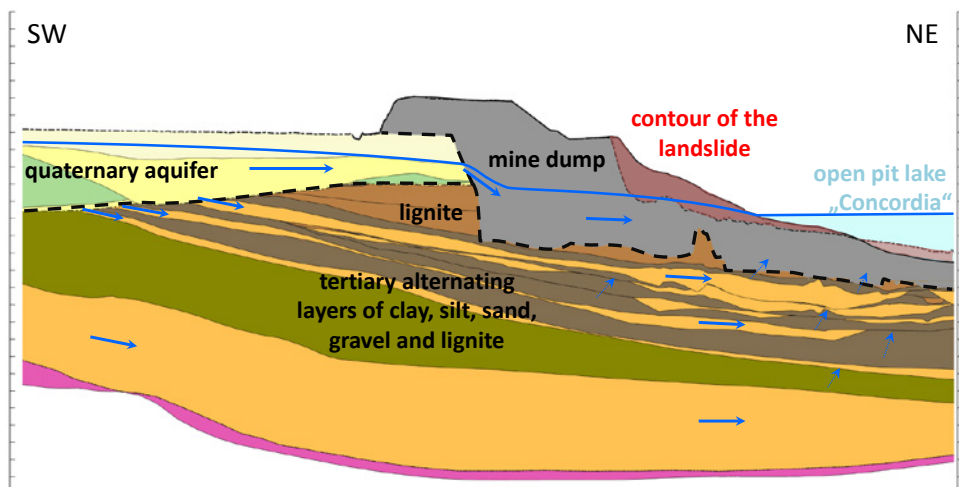


Figure 2 Cross section to show the complex geological and hydrogeological situation.

Geological and groundwater modelling workflow

A 3-dimensional geological structure model was used to provide basic information for the cause study of the landslide. The model includes both the natural conditions of the geological structure as well as the artificial structure like mine dumps. In detail, the geological structure model was used to:

- create a database of all historical information
- create a 3-dimensional image of the complex geological conditions which helps to gain knowledge of the subsurface system
- provide the basic input data for all following model applications in the fields of hydrogeology, geotechnical engineering and remediation strategy
- provide a decision support tool for further investigations and remediation planning

About 3,900 historical soil profiles were digitalized and integrated in a borehole database. With the help of the database all soil profiles were subjected to a first stratigraphic classification. Further data input to the model was obtained by geological maps and geological cross sections from former exploration phases. On the basis of the soil profiles, the knowledge of the geological processes and the other mentioned information, a first version of the geological model could be established (Fig. 3 - “a”) with the help of the SURPAC modelling software (boundary surface model).

Altogether 39 boundary surfaces were created for the respective stratigraphic formations. With the help of a spatial review of the borehole data in the model a plausibility check of the stratigraphic classification of the soil profiles was carried out. If necessary, single layers of the soil profiles were reclassified (Fig. 3 - “b”). Though, the exchange between the geological modeller and the field geologist is essential.

The established 3-dimensional geological structure model provided a geometrical basis for the hydrogeological flow model (Fig. 3 - “c”).

The groundwater flow has been simulated with the large-scale groundwater flow model “Nachterstedt” based on the simulation software PCGEOFIM (Blankenburg et al. 2016). PCGEOFIM is a finite volume groundwater flow simulation software which is specifically designed for mining and post-mining areas. It provides particular features to be appropriate for the mining-specific conditions like time-dependent changes of geological structure and subsurface parameters – all combined in one model run.

The basis of a reliable groundwater model is the geological structure model which considers all layers in respect of relevant hydrogeological processes. The quality of the groundwater model depends strongly on the knowledge of the geology (Anderson & Woessner, 1992). Thus, the layers of the built up 3-dimensional geological structure model were transferred into the structure of the groundwater model (Fig. 3 - “c”). In the end, 26 relevant hydrogeological layers were transferred as not all 39 stratigraphic layers had to be considered for the groundwater model.

Furthermore, the knowledge and implementation of boundary conditions is necessary for groundwater modelling. Boundary conditions like drainage wells, mining pit lakes with its changing water levels as well as other relevant hydraulic parameters like regional precipitation and evapotranspiration were taken into account. By considering the mentioned data the model can be calibrated.

By comparing existing measurement data with the calculation results while the model calibration process, the past trends as well as the actual state should be simulated with the smallest possible deviation. Through specific changes of the permeability parameters or the boundary conditions the simulation results can be adapted in order to obtain a minimum deviation between the calculated and the measured water levels or flow rates by trial and er-

ror. Thus, the basis of a successful model calibration is a sufficient number of representative groundwater observation wells in all relevant hydrogeological layers (Fig. 3 - “e”). After the successful completion of the model calibration, the model can be used to predict changes or future behaviour in groundwater dynamics as well to “backcast” past situations.

It is important to ensure that all the qualified groundwater observation wells are representative of the hydrogeological layer they were assigned to by the field geologist. Therefore, again the iterative form of modelling was applied. Based on the hydrogeological calculation results, the stratigraphic classifications were revised and adapted in some cases, e.g. if certain measured groundwater levels do not fit into the general image of the groundwater dynamics and no hydrogeological explanation of the divergent water levels can be found (Fig. 3 - “f”).

During the calibration procedure of the groundwater model and “backcast” calculations for the cause study of the landslide of Nachterstedt discrepancies appeared between the understanding of the hydrological processes and the geological structure. A rising head test indicated that certain hydrogeological layers below the slid area showed not the expected groundwater dynamics according to the constructed geological model. The rising head test was accomplished by switching off the drainage wells which were installed in the confined aquifers. A steep rising water level was observed through a tight monitoring system of groundwater observation wells and piezometers successfully installed below the lake surface. An even groundwater flow direction was expected in the aquifer for the steady state, since the aquifer was initially awaited as almost homogeneous and uniformly distributed. By analysing the data that was collected during the pumping test, a narrow defined pressure anomaly with noticeable artesian water levels could be detected, which only could be explained by a specification of the geological structure model. Finally, intensive discussions between the geologists and hydrogeologists revealed, that excessive fluctuations in thickness and permeability within the aquifer with extreme spatial variations of the parameter values be present. Therefore, the geological model had to be revised by reclassification of the original borehole data regarding the recent hydrogeological results (Fig. 3 - “d”).

During the whole workflow process, all this iterative interaction steps “a” to “f” have to be proceeded in close coordination with the engineers and natural scientists – not necessarily to establish a perfectly calibrated model but to simulate realistic possible running processes within the field of geology and hydrogeology. Thus, it is crucial that every single adjustment of the models has to be intensively discussed with all involved geologist and modellers.

Conclusion

In applied but also in scientific groundwater modelling, often the geological model is taken as a given and unchangeable component as a consequence of an already existing geological model. Hence, e.g. the calibration and the resolution of the groundwater model are frequently called into question and need to be revised if necessary during the entire modelling workflow. But once the geological model is not sufficiently precise to challenge the issues which should be answered by the groundwater model, the results of the groundwater model

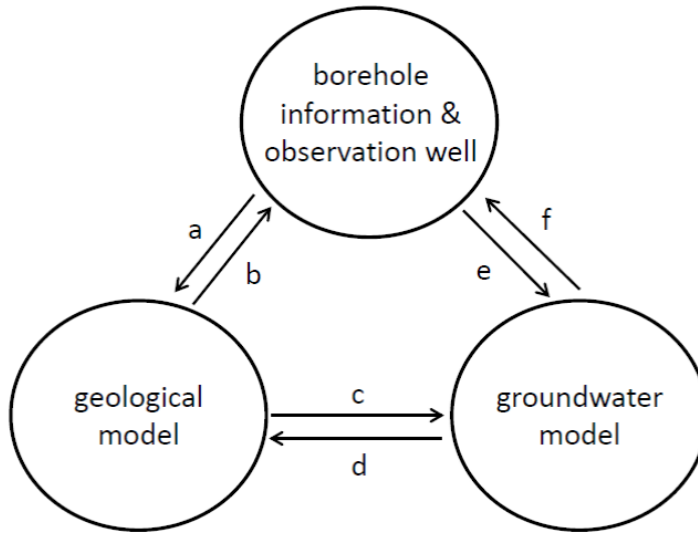


Figure 3 Flow chart with the iterative interactions during the modelling workflow, explanation of the letters in the text

cannot be reliable. As shown in this paper the classic “in sequence” modelling workflow – basic geological information to a geological structure model to a groundwater model – may lead to a misunderstanding of the hydrological processes and a misunderstanding of the geological setting. Hence, continues discussions between the involved field geologist, geological and groundwater modeller are helping to improve the understanding of the subsurface processes. Furthermore, the iterative interaction steps as shown in Fig. 3 can verify the results of the basic information like classification of stratification, the geological model and also the groundwater model. This leads to a solid understanding of the running processes and thereby to the establishment of a suitable model concept.

References

- Anderson, M. P. and Woessner W. W.: Applied groundwater modelling simulating flow and advective transport. San Diego, CA:Academic Press; 1992.
- Blankenburg, R.; Sames, D. and Boy, S.: PCGEOFIM Anwenderdokumentation, Ingenieurbüro für Grundwasser GmbH, Leipzig 2016.
- Carrera, J. and Neuman, S. P.: Estimation of aquifers parameters under transient and steady state conditions: 1. Maximum likelihood method incorporating prior information, Water Resources Research, Volume 22, 199–210, 1986.
- Eaton, T.: On the importance of geological heterogeneity for flow simulation, Sedimentary Geology, 184, 187–201, 2006.
- Förster, W.: Bodenmechanik, Teubner Verlag, 1997.
- Harrar, W. G., Sonnenborg, T. O., and Henriksen, H. J.: Capture zone, travel time and solute transport predictions using inverse modelling and different geological models, Hydrogeology 30 Journal, 11, 536–548, 2003.
- Katzenbach, R.: Abschlussbericht Ursachenforschung, Böschungsbewegung in Nachterstedt am 18.07.2009, Darmstadt 2013.

- Poeter, E. M. and Anderson, D.: Multimodel ranking and inference in ground water modelling, *Groundwater*, 43(4), 597–605, 2005.
- Troldborg, L.: The influence of conceptual geological models on the simulation of flow and transport in Quaternary aquifer systems, PhD thesis, Geological Survey of Denmark and Greenland, Report 2004/107, 2004.

Quantitative Evaluation Mining Impact on Unconsolidated Aquifers In Western China's Inner Mongolia-Shaanxi mine Region

Chunhu Zhao^{1,2}, Weiyue HU^{1,2}, Dewu JIN^{1,2}

¹Xi'an Research Institute of China Coal Technology & Engineering Group Corp Xi'an, 710054, Shaanxi, People's Republic of China

²Shaanxi Key Laboratory of Prevention and Control Technology for Coal Mine Water Hazard, Xi'an, 710077, Shaanxi, People's Republic of China

Abstract The degree of quantitative research about the groundwater disturbance caused by coal mining is insufficient. In this paper, it is concluded that the spatial scale of deformation and destruction caused by mining is the main factor to control the loss of groundwater, and presents numerical method to deal with the fractured zones into a drainage boundary, the parameter partition for the bending zone, and the resubdivision for the surface subsidence area. Finally, in the case of coal mine, the simulation results shown that the loss of groundwater resources is about $1.90 \times 10^4 \text{ m}^3/\text{d}$ due to the mining disturbance.

Keywords Groundwater; loose aquifer; quantitative evaluation; numerical simulation; fractured zone

Introduction

The western region of China is the main base for the exploitation of coal resources. Groundwater is the main water resources which has the extremely important ecological function in this area^[1,2], under the influence of large-scale and high intensity of coal resources exploitation, it is inevitable to cause the destruction to the groundwater, which aggravate the water resources shortage and the destruction of the ecological environment in the region, this problem has become more and more concerned by the China government and society. In developed countries, because of the difference of national basic energy structure, there are few researches on the dynamic disturbance of groundwater caused by coal mining, which mainly focuses on the problem of mine water pollution risk assessment and closure of mine reclamation^[3,4]. Chinese scholars had used different methods to study the problem of groundwater dynamic response, but has not formed a recognized, more systematic evaluation method, these are mainly macro analysis, the evaluation of the quantitative degree is obviously insufficient.

In recent years, the numerical method has been developed rapidly in the evaluation, prediction and management of water resources. which greatly improves the quantitative analysis of groundwater resources evaluation^[5], such as some scholars put mine water inflow as the discharge of pumping wells by artificially given a certain amount of pumping water, or to increase the parameter of surrounding rock permeability by multiplied certain proportion coefficient (such as 1.2 and 1.5 times etc.)^[6-10], but the amount of pumping water or coefficients are given with strong subjectivity, ignored the groundwater response mechanism from coal mining disturbance. In this paper, the author combines the study of overburden failure with the simulation of groundwater system, the mechanism of mining influence on groundwater is analyzed. presents numerical methods to deal with the factor of deforma-

tion and destruction caused by mining in the groundwater numerical model, To establish a computer numerical evaluation model for the disturbance of groundwater system with high degree of quantification.

Disturbance mechanism of coal mining on groundwater

Damage and deformation of surrounding rock under the influence of mining disturbance

The mining scholars and groundwater research scholars have a more consistent understanding for the damage and deformation caused by coal mining, it is considered that the overlying strata in the coal seam mining is divided into the caving zone, fracture zone and curved zone from mined coal seam to surface (fig.1), this is the classical theory of “covering rock zoning”^[1]. at the same time, the surface subsidence area is formed on the ground surface, Thus, the typical mining overburden disturbance can be summed up as “three zones and one area “. because the fracture zone directly connected with caving zone , and has strong hydraulic conductivity, so the two zones are collectively referred to as the “water conducted fractured zone”, hereinafter referred to as fractured zone H_f .

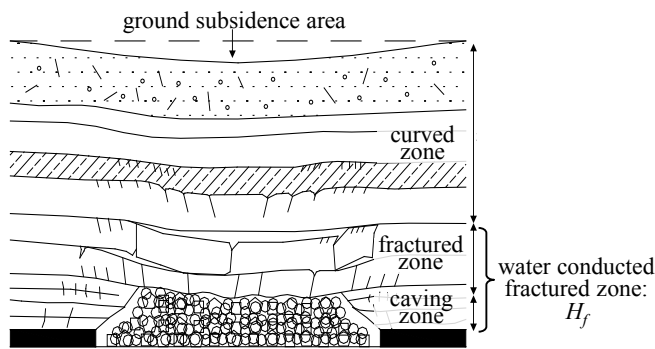


Figure 1 the diagram of three zones and one area

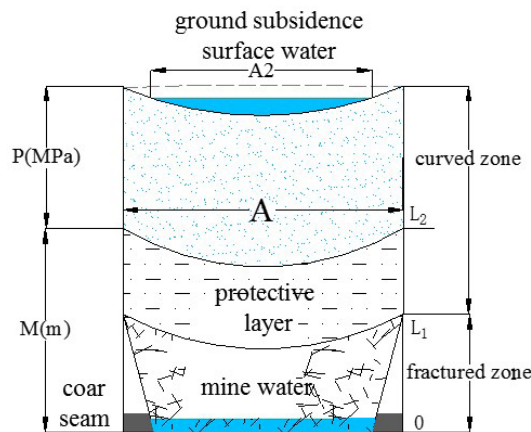


Figure2 the disturbance of groundwater system

The influence mechanism of “three zones and one area” on groundwater

In general, the amount of groundwater resources loss caused by coal mining is mainly composed of three parts, The amount of leakage from the overlying aquifer to the mining space is Q_1 , and the leakage of water supply in the lateral aquifer is Q_2 , which is caused by the water loss caused by surface subsidence water Q_3 :

(1) the leakage amount of groundwater (Q_1)

In order to facilitate the analytical method, the water conducted fractured zone is defined as a trapezoidal. As shown in fig.2, the plane area of fractured zone is A (m^2); the fractured zone height is L_1 (m); the thickness between the loose aquifers and the coal seam is M (m); the permeability coefficient K (m/d); the water pressure at the plate of loose aquifer is p (MPa); u is the actual flow rate of groundwater in the protective layer; R for groundwater bulk density (N/m^3), take the roof of the coal seam as the “o” datum, according to the classical groundwater dynamic analysis method^[12]:

the water head values at the top (L_1 height) of the fractured zone is:

$$H_1 = L_1 + P / r + u^2 / 2g$$

Because of large mine water drainage, the fractured zone is directly connected with the atmosphere, so the pore water pressure is atmospheric pressure at the top (L_1 height) of the fractured zone, $P = 0$, then:

$$H_1 = L_1 + u^2 / 2g$$

The water level value at the top of the protective layer is H_2 (on L_2 height):

$$H_2 = L_2 + P / r + u^2 / 2g$$

According to Darcy’s law, the amount of water leakage (Q_1) can be expressed as:

$$\begin{aligned} Q_1 &= K * A \frac{(M - L_1 + P / r)}{M - L_1} \\ &= K * A \left(1 + \frac{P}{(M - L_1) * r} \right) \end{aligned} \quad (\text{Equation 1})$$

When fracture zone extends directly to the loose aquifers or even surface, the protection layer thickness is zero, the leakage forms do not obey the Darcy’s law, the groundwater will directly along the conducted fractured zone into the stope, eventually leading to the aquifers to be drained at the top of the mined spacer.

(2) lateral drainage (Q_2)

In general, the loss of groundwater resources in the aquifer is dominated by lateral drainage Q_2 . According to the “Large diameter well method” based on the steady flow analysis:

$$Q_2 = 1.366K \frac{(2H - S)S}{\lg R_0 - \lg r_0} \quad (\text{Equation2})$$

In the formula 2, permeability coefficient K , m/d; water head height H , m; groundwater drawdown S due to mine drainage, the radius of influence R_0 , m; the radius of reference for mining space r_0 , m;

The aquifer is assumed to be homogeneous and infinite, the natural water level approximate horizontal, R_0 can be calculated using the following formula $R_0 = r_0 + R$, Where F is the scope of the excavation area, m^2 . From the formula 4 we can see that the water flowing fractured aquifer area revealed F is larger, the greater the amount of underground water leakage.

(3) the loss amount of groundwater invalid evaporation (Q_3)

When the depth of the mining coal seam is larger, the mining fractured zone can not break through the protective layer which below the loose aquifer, and the depth of ground subsidence is greater than the depth of the groundwater, the surface water will be formed in the ground subsidence. so the groundwater is converted into surface water, which causes the groundwater from phreatic evaporation to surface water evaporation, which increases the amount of evaporation, it is a form of the loss of groundwater resources. the phreatic evaporation capability parameter is E_1 , the water surface evaporation capability parameter is E_2 , and the area of surface water is A_2 (M_2), the amount of groundwater invalid evaporation:

$$Q_3 = (E_2 - E_1) * A_2 \quad (\text{Equation 3})$$

Quantitative evaluation method of mining disturbance of groundwater

The numerical treatment technology for the "fractured zone"

When fracture zone extend to a certain height, the groundwater from the fractured aquifer along the fractured zone cracks into the mining space, result in the aquifer lateral recharge is cut off at the top of the mining space. The groundwater has formed a "discharge strips" along the contact zone between the fractured aquifer and fractured zone (fig.3). Similarly, groundwater along the fractured zone cracks into the mining space, constitute a relatively stable supply for mine water. Finally, the aquifer groundwater level which cut by the fracture is reduced to the bottom plate of the aquifer.

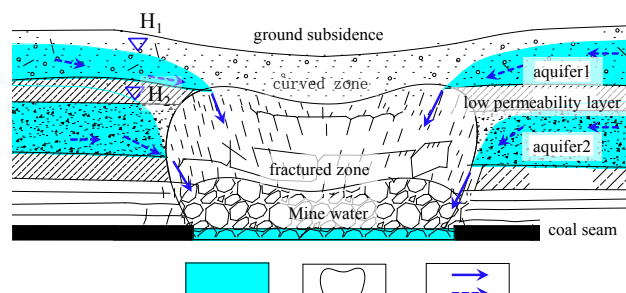


Figure 3 the relationship between groundwater and water flowing fractured zone

In the Visual MODFLOW model, the contact zone or discharge strips between the aquifer and fractured zone are treated as the “drainage” boundary to realize the numerical treatment of the vertical leakage Q_1 and the lateral discharge Q_2 .

In the model the drainage (Drain) boundary is calculated as:

$$\begin{cases} Q_{1,2} = C_D (H - H_D) & H > H_D \\ Q_{1,2} = 0 & H \leq H_D \end{cases} \text{ (Equation 4)}$$

which C_D —Cell permeability parameter, m^2/d ; H —water head, m ; H_D —Elevation of drainage or elevation of aquifer floor, m .

Numerical treatment technology for “curved zone”

Generally, the fractured zone will be extend to the surface when the shallow seam is mined, and the overlying strata can not form the “curved zone”. However, the curved zone is formed between the fracture zone and the ground surface when the deep buried coal seam is mined. According to previous research results^[13,14], although the “curved zone” rock layer is not formed the fractured cracks with the high conductivity, because of the change of the in-situ stress state, the rock is deformed, which leads to the change of the permeability of the overburden in the different section of the curved zone.

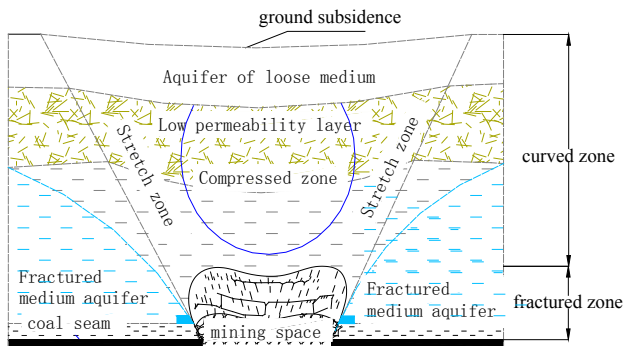


Figure 4 the bending zone

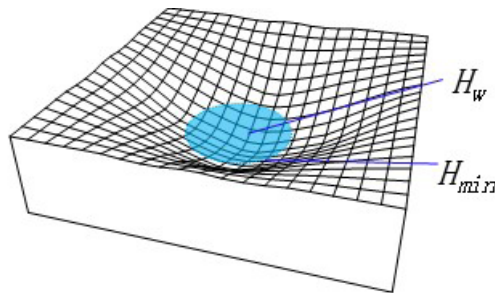


Figure 5 the ground subsidence

As shown in fig.4, Because the rock stratum of the curved belt is still continuous medium, and groundwater movement still obey the Darcy flow, So the parameters of the permeability can be partitioned according to the changing tendency of the rock stratum permeability before and after mining, Re assignment of the permeability coefficient in the partition, this is the numerical processing technology for the “curved zone” in the groundwater model.

Numerical treatment technology for “ground subsidence”

On the one hand, ground subsidence reduces the depth of the groundwater level, the lower the depth of groundwater level, the greater the amount of water evaporation. On the other hand, when the ground surface subsidence is greater than the depth of groundwater, the groundwater evaporation is converted into water surface evaporation, thus increasing the loss of groundwater resources. As shown in fig.5, ground elevation of groundwater model is re divided according to the predicted results of the ground subsidence or the measured results.

Note that, we should try to run the model after re changing the ground elevation, in order to analyze the relationship between the elevation value H_{min} at the lowest point of the ground subsidence and the elevation value H_w of groundwater level, When $H_{min} < H_w$, the groundwater is exposed on the surface, so the water evaporation coefficient should be modified to the surface evaporation coefficient in the groundwater area; When the $H_{min} \geq H_w$, groundwater is not exposed to the surface, so the groundwater discharge is still the phreatic evaporation, the groundwater evaporation will increase because of groundwater depth reduction.

Case study

This paper takes the Bulianta mine as the case which located in west China, the mining coal seam is No.1⁻² and 2⁻² of the Jurassic, and coal seam buried less than 150m, the surface is completely covered with the quaternary loose sand medium, and overlying bedrock thickness in less than 80m. loose layer thickness in 15 ~ 30m. as shown in fig.6 and fig.8a, in natural conditions before the coal mining, the loose aquifer groundwater mainly receive precipitation infiltration recharge, and exposed to surface in valley cutting zone, thus forming a perennial or seasonal rivers, such as BuLian river, Huojitu river and so on, those surface water is groundwater discharge zones.

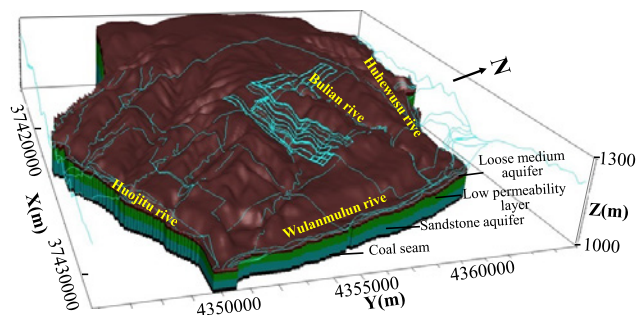


Figure 6 Sketch map of study area

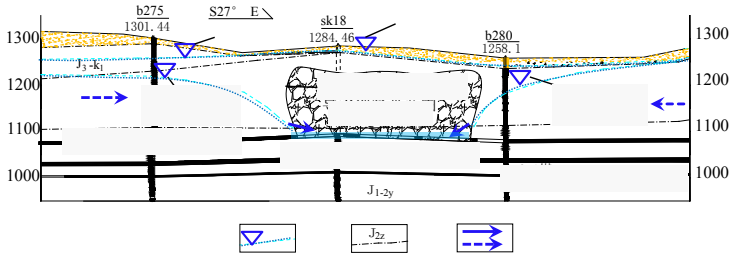


Figure 7 Groundwater level contour (2006 measured: m)

The Bulianta coal mine large-scale development of coal resources began in 2002, the actual output reached 35 million tons/year in 2012, as shown in fig.8b, due to the disturbance of coal mining, the fractured zone will extend to the surface when the shallow seam is mined, and the overlying strata can not form the “curved zone”.

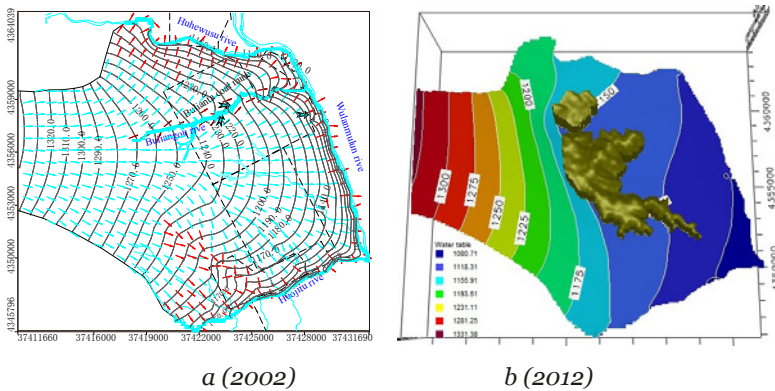


Figure 8 Groundwater level contour (2012 calculated: m)

In 2012, with the increase of mining area, the damaged aquifer area increased, a huge water level drop funnel is formed with the mining sector as the center. as shown in fig.8b, the water level dropped by about 30m, The aquifer is directly drained at the top of the mined area (yellow area). the amount of groundwater discharge to the mining space (the amount of groundwater leakage) is reached $1.9 \times 10^4 \text{ m}^3/\text{d}$ (tab. 1).

Table 1 Comparison of calculation results

Computing method	water ($\times 10^4 \text{ m}^3/\text{d}$)	problem
Quantitative numerical analysis	1.9	reasonable: the total loss of groundwater into the mining space
Mine measured drainage	0.852	too small: does not include the amount of accumulating water in mine and reuse water for coal mining
Large diameter well analytical calculation	4.4	too large: Large diameter well method assumes that the conditions for the four catchment, infinite aquifer, homogeneous, does not conform to the actual hydrogeological conditions

Summary

(1) The spatial scale of the formation of “the fracture zone and the curved zone “ is the main factor to control the loss of groundwater: the larger area of fractured zone by coal mining disturbance, the higher the fracture zone, the stronger the permeability of the curved zone layer, and the greater the amount of groundwater seepage.

(2) Put forward the numerical processing technology for “fracture zone and curved zone ”in the groundwater model :the fracture zone can be simplified as a kind of drainage boundary condition, Re assignment of the permeability coefficient in the curved zone, and re divided the ground elevation in ground subsidence.

(3) The case simulation results shown that groundwater level decline more than 30m (2012), the loss of groundwater resources is about $1.90 \times 10^4 \text{m}^3/\text{d}$ due to the mining disturbance.

Acknowledgements

This paper is supported by the Chinese 13th Five-Year key research and development program (2016YFC0501102), and China Coal Technology& Engineering Group Co., Ltd. Technology Innovation Fund (2013ZD002-02).

Reference

- Wang S. Study On Coal Mining for protecting Ecological Water Level in the Ecological Fragile Mining Area[J]. Metal Mine, 2009.
- Wang S M, Huang Q X, Fan L M, et al. Study on overburden aquiclude and water protection mining regionization in the ecological fragile mining area[J]. Journal of China Coal Society, 2010, 35(1):7-14.
- Lines G C, Morrissey D J. Hydrology of the Ferron sandstone aquifer and effects of proposed surface-coal mining in Castle Valley, Utah[R]. Geological Survey, Reston, VA(USA), 1983.
- Booth C J. Strat-Movement Concepts and the Hydrogeological Impact of Underground Coal Mining[J]. Groundwater, 1986, 24(4):507-515.
- Lin X Y. Historical Change and Prospect of Discipline Development of “Groundwater Science and Engineering”[J]. Journal of Jilin University, 2007, 37(2):209-215.
- Zhang F, Liu W. A Numerical Simulation on the Influence of Underground Water Flow Regime Caused by Coal Mining – A Case Study in Daliuta, Shenfu Mining Area. Journal of Safety & Environment, 2002.
- Liu Huaizhong. Quantitative evaluation of groundwater system disturbance in mining area [D]. China University of Mining and Technology. 2011.12.
- Li Yang. Study on the movement law of overlying strata in shallow coal seam mining and its influence on groundwater [D]. China University of Mining and Technology (Beijing), 2012.
- Li Ying. The hydrological and ecological effects caused by groundwater resources and coal mining in the coal distribution area of Northern Shaanxi Province [D]. Chang’an University, 2008.
- Wu Xijun. Study on river runoff change and ecological base flow in coal mining area [D]. Xi’an University of technology, 2013.
- QIAN Minggao, SHI Pingwu, XU Jialin. Mining pressure and strata control[M]. Xuzhou: China University of Mining and Technology Press, 2010:98-101. (in Chinese)
- Xue Yuqun, Zhu Xueyu. Groundwater dynamics [M]. Geological Publishing House, 1979
- Sui Wanghua, the engineering geology of the soil deformation of mining subsidence [M]. China University of Mining and Technology press, 1999.
- Li Tao. Study on the structure variation and water resources of the large-scale mining of coal in the coal of Northern Shaanxi [D]. Xuzhou: China University of Mining and Technology, 2012.
-

Reproduction of a Complex Tracer Test through Explicit Simulation of a Heterogeneous Aquifer using Bayesian Markov Chain Monte Carlo

John Mayer¹, Ray Yost²

¹*SRK Consulting (Canada) Inc., Vancouver, BC, Canada, Email: jmayer@srk.com*

²*TECK Resources Ltd., Sparwood, BC, Canada*

Abstract Simulation of tracer response curves in waste rock systems can be difficult using conventional numerical techniques, due to the presence of local heterogeneities. Instead, alternative methods are required that can explicitly handle the inhomogeneous nature of flow. Such an approach is presented herein that couples sequential Gaussian simulation with Bayesian inference using a Markov Chain. Results show that complex tracer behaviour can be reproduced using simple, spatially conditioned, Markov Chains. Additionally, external conditioning routines are found to be more efficient in controlling Markov state transition compared to random resampling or collocated cokriging.

Key words Tracer Test, Geostatistics, Bayesian, Waste Rock, Markov Chain

Introduction

The basic conceptual model for backfill into a previously mined out open pit is that of a relatively homogeneous, coarse-grained, granular media with some degree of anisotropy in hydraulic conductivity due to the mechanics of the backfill process. While this model is a reasonable starting point, flow behaviour in real world systems is often more complex due to the variability in dump emplacement.

Much like depositional facies in a sedimentary environment, backfilled pits display particle segregation resulting in interbedded layers forming along the angle of repose. The degree of segregation is a direct result of the style of dump emplacement, which is affected by such factors as lift height, initial gradation, and placement technique (BCMWRPRC 1991). Generally, the greater the lift height, the more segregation occurs with larger particles displaying longer run-outs. The end result is a fining upward sedimentary sequence, which can have a relatively simple or highly complex spatial distribution.

Characterization of the hydraulic behaviour of such backfilled systems often occurs through multi-stage field programs. Early stage testing may involve slug and/or pump testing, which while providing larger-scale equivalent hydraulic properties, is often unable to deconvolute the intricacies of highly heterogeneous flow systems. This is where subsequent stage tracer testing can be useful, as it can confirm the presence of and help delineate heterogeneities in the backfill.

Recent bromide tracer testing in such a backfilled dump has shown the heterogeneous nature of such systems, with tracer behaviour displaying a highly complex plume distribution (Figure 1). Reproduction of such behaviour proved difficult using conventional numerical modelling techniques, which were unable to reproduce the plume using simple conceptual model setups. Instead, a coupled Bayesian inference and geostatistical approach was ap-

plied (Irving and Singha 2010; Mariethoz et al. 2010). This involved construction of a random series of heterogeneous hydraulic conductivity (K) and porosity (n) fields, which were assessed based on their conditional probability of reproducing the measured bromide concentration curves.

Field Observations

Tracer testing was conducted using a dipole configuration, whereby water extracted from the pumping well was directly reinjected into the injection well forming a continuous loop (Figure 1). Water was cycled at a constant rate of 546 m³/day. During the first 22 days of the test, bromide tracer was added to the reinjected water at an average concentration of 34.7 mg/L. This was followed by passive cycling and monitoring for an additional 87 days (i.e. water from the pumping well was re-injected without any bromide added). Bromide concentration curves were monitored at the pumping well (PW) and four waterloo sampling ports (WP1-4).

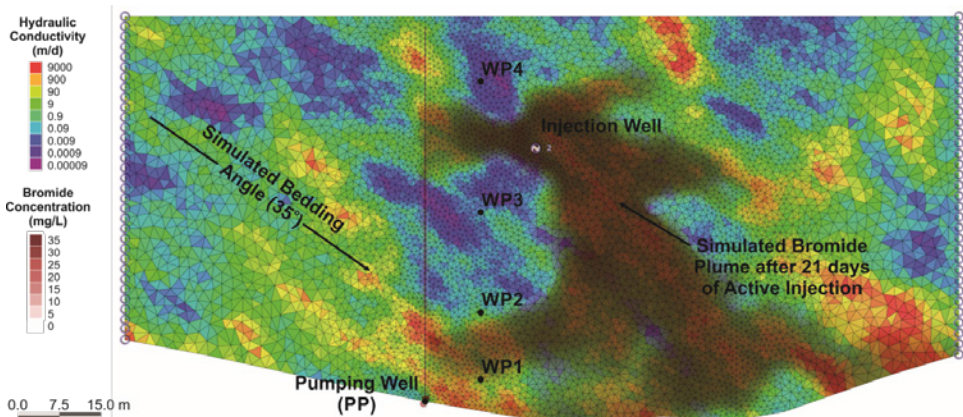


Figure 1 Two-dimensional groundwater flow setup in FEFLOW. Simulated bromide plume and random K field are presented for the highest probability model generated using the external conditioning approach.

Results of the tracer test showed appreciable amounts of tracer only in the deepest part of the flow system (PP and WP4), while the upper most zones nearest the injection horizon displayed minimal (WP2) to no response (WP3 and WP4). This odd response behaviour was unexpected, and suggested that the dump emplacement is far more heterogeneous than pre-test homogeneous models suggested.

Methodology

Numerical Groundwater Simulation Model

Numerical groundwater modelling has been completed using the modelling software FEFLOW (DHI 2016). A two-dimensional planar model was setup through the current back-filled pit (Figure 1). Groundwater flow behaviour was modelled assuming saturated, steady-state conditions; while transport modelling was conducted under transient conditions. Left

and right edges of the model were set as constant head boundaries. The top and bottom boundaries were simulated using no-flow (zero-flux) conditions. Dipole pumping was simulated using two coupled constant flux boundaries with the rate adjusted to match the measured head observed in the injection well. Active tracer injection was simulated using a constant concentration boundary set to an average value of 34.7 mg/L for the first 21.5 days. This was followed by linking of the pumping and injection well concentrations to simulate passive dipole cycling for the remaining 87.5 days.

Geostatistical Simulation

Random generation of the heterogeneous hydraulic conductivity and porosity fields were conducted using sequential Gaussian simulation (SGS; Deutsch and Journel 1998). The approach works by sequentially generating random variates within a set of grid nodes based on Gaussian deviations from a stationary mean. Heterogeneity is imposed through the conditioning of local probability distributions using simple kriging routines, with the heterogeneous structure defined by vario- and/or correlograms. The sequential generation sequence is randomized between trials using a random walk. The end result is a random realization of a continuous variable which matches the underlying spatial structure of said variable.

Bayesian Markov Chain Monte Carlo

Estimation of the *in-situ* heterogeneity structure was conducted using Bayesian inference, with FEFLOW models assessed based on their conditional probability of reproducing the measured bromide behaviour. Specifically, models were assessed using Bayes' Theorem:

$$P(x|\theta) = \frac{P(\theta \vee x)P(x)}{P(\theta)} \quad \text{Equation 1}$$

where:

- $P(x \vee \theta)$ is the posterior distribution or conditional probability that the model state (i.e. heterogeneous random field) is representative of the tracer response behaviour.
- $P(\theta \vee x)$ is the conditional probability that the model matches the observed tracer behaviour given the simulated model state (i.e. random field).
- $P(x)$ is the prior probability, or one's belief before conducting the modelling that the simulated heterogeneous structure is representative of the *in-situ* conditions.
- $P(\theta)$ is a normalization constant related to the modelling errors.

In practice, the direct solution of Bayes' Theorem is often difficult, owing to the calculation of $P(\theta)$ which requires prior knowledge of model errors. Instead, it is often easier to approximate the equation using a Monte Carlo solution, such as Markov Chain Monte Carlo (MCMC). The approach works by setting up a Markov chain, which has an equilibrium distribution that matches the desired posterior distribution ($P(x|\theta)$). One method of setting

up such a chain is the Metropolis algorithm (Metropolis et al. 1956). The approach involves a five step procedure:

1. Initialize a random heterogeneous state (x_{old}).
2. Randomly generate a new state (x_{new}) from the old state (x_{old}) based on a symmetric, transitional jump function (typically a Gaussian distribution).
3. Calculate the acceptance ratio (α):

$$\alpha = \min \left[1, \frac{L(\theta | x_{new}) P(x_{new})}{L(\theta | x_{old}) P(x_{old})} \right] \quad \text{Equation 2}$$

4. Randomly select a uniform value (u) between 0 and 1:
 - a. If $u \leq \alpha$ move to the new state ($x_{old} = x_{new}$), else
 - b. If $u > \alpha$ remain in the current state ($x_{old} = x_{old}$)
5. Restart the algorithm at step 2.

In order to limit the impact of the random starting position, an initial N states are discarded at the start of the sequence (known as the burn-in period), while the algorithm converges on the high probability space. Once the burn-in period is complete, samples are saved every N steps, with interstitial steps discarded to limit autocorrelation effects. The process is repeated until the desired sample size is reached.

Misfit Function

Definition of a misfit function is required in order to assess the conditional likelihood that the current model state (i.e. random field) is representative of the *in-situ* groundwater conditions. This was conducted by assuming independent, normally distributed data errors, resulting in the conditional likelihood being defined by (Mosegaard and Tarantola 2005):

$$L(\theta \vee x) = \exp \left(\frac{-\sum (\theta_{mod} - \theta_{obs})^2}{\sigma^2} \right) \quad \text{Equation 3}$$

where θ_{mod} and θ_{obs} are the calculated and measured response curves, and σ^2 is the standard deviation in the data errors.

Combined Model Structures

The above methodology was incorporated into FEFLOW using IFM programming (Figure 2). Transition between Markov states was controlled using three separate algorithms. These include:

1. **Random resampling:** during each iteration of the Markov chain a random

subset of the model elements were regenerated using the SGS code (Irving and Singha 2010).

2. Collocated cokriging: the new state was cokriged from the previous state, with

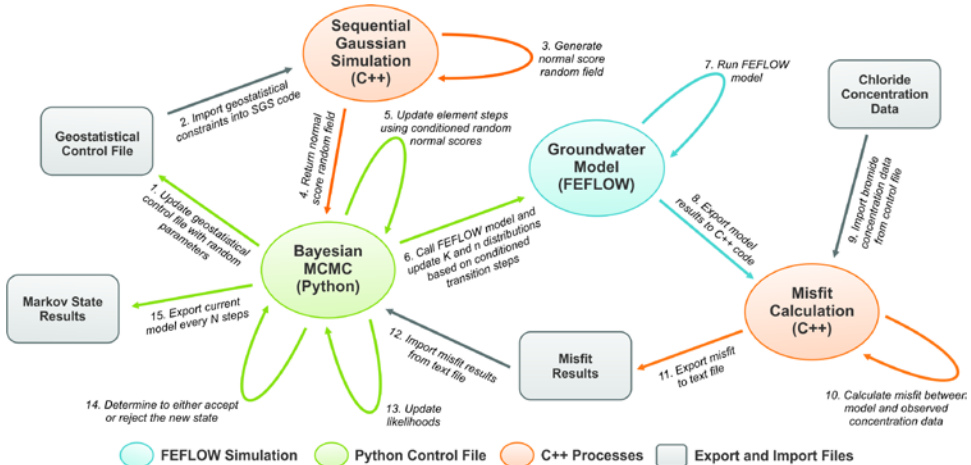


Figure 2 Overview of model structure using external conditioning approach.

the transition controlled using a correlation coefficient (Xu et al. 1992).

3. **External conditioning:** each element was treated using a unique set of variables (K, n), with transition between the states controlled using individual Gaussian jump functions. Spatial conditioning is imposed by conditioning the Gaussian jumps based on the jumps of nearby neighbours using SGS.

In a well constrained Markov chain the jump size should be optimized to ensure efficiency in the model solution. A chain with a jump that is too small will mix poorly, and be inefficient at converging on the high probability space; while too large of a jump will have a poor acceptance rate again resulting in poor mixing and convergence. Roberts et al. (1997) showed that for single-variate Gaussian solutions the target acceptance rate should be 50% to optimize chain convergence towards high probability space. This drops to 23% for N -dimensional Gaussian distributions.

Prior Information

Before initiating the Markov Chain process, the SGS generator needed to be setup to allow for construction of Markov states. This was done by reviewing field data, published literature, and best engineering judgement, in order to define the input parameters.

Backfill sedimentary sequencing was simulated using three key parameters: bedding angle, anisotropy factor, and spatial continuity. The bedding angle was set to the angle of repose (35°). Due to the relatively unknown nature of the anisotropy factor and spatial continuity, uniform priors were assumed, which varied between 1^x to 3^x and 2 to 20 m respectively.

Prior porosity information was available from downhole nuclear magnetic resonance (NMR) testing in the observation well. Results of the NMR analysis indicate a mobile water fraction (effective porosity) of 0.276, with a standard deviation of 0.08.

Large-scale hydraulic conductivity estimates were available from a prior pump test conducted in the injection well. Estimates of the hydraulic conductivity indicate a mean value of 436 m/d. Small-scale variability in the conductivity was estimated from NMR results, which suggest a log-transformed standard deviation between 0.35 to 1.71 orders of magnitude. A vertical trend in the hydraulic conductivity was simulated to reproduce grain size segregation associated with dump emplacement. The trend was assigned based on a uniform distribution between one and three orders of magnitude across the saturated thickness.

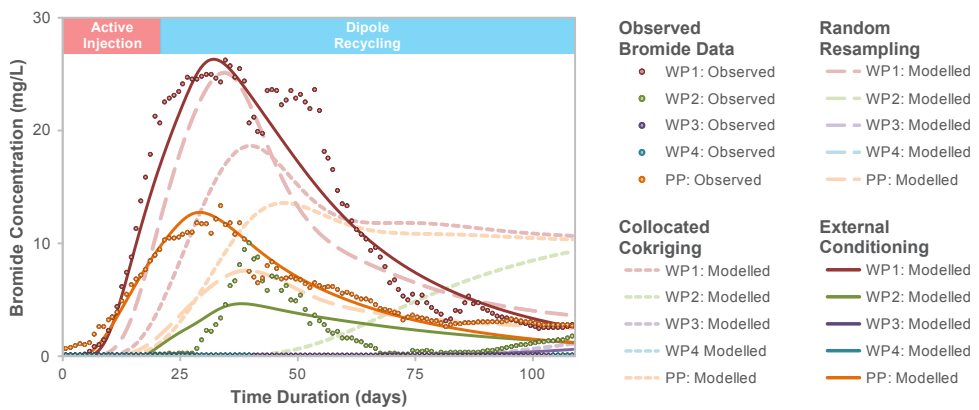


Figure 3 Comparison of highest probability models with observational data.

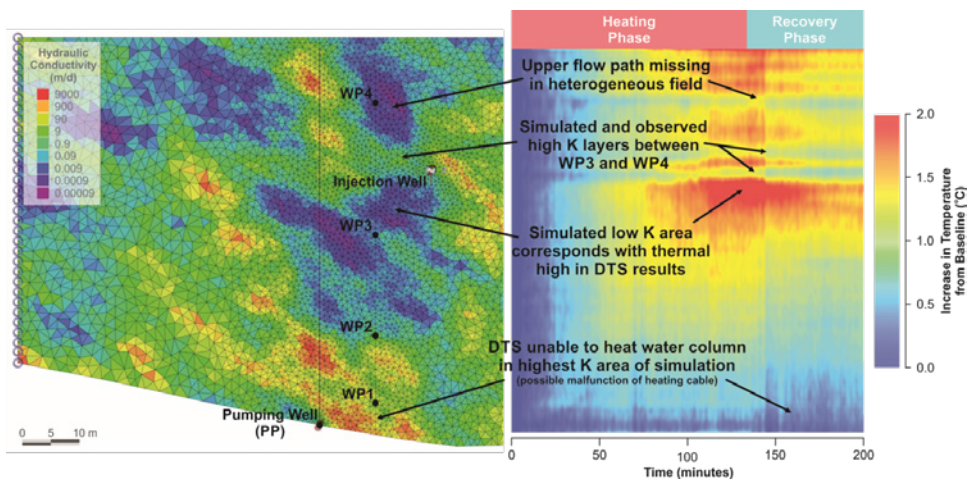


Figure 4 Comparison of highest probability random field, generated using external conditioning method, with distributed temperature sensing (DTS) results.

Stochastic Results and DiscussionThe three tested Markov transition algorithms showed varying degrees of success in converging on the high probability space. Initial results using the random resampling approach showed promise during the initial burn-in period, with acceptance rates near 30%; however rates soon dropped below 2% as the model misfit approached $14,000 \text{ (mg/L)}^2$ (Figure 3). The percentage of the model resampled was varied between 90 and 99%, but acceptance rates did not improve significantly, likely due to the small number of elements resampled during each iteration.

Collocated cokriging routines were found to have improved convergence compared to random resampling, with models converging on a higher probability space after an initial 24 hour run ($4,000 \text{ mg/L}^2$; Figure 3). The improved convergence was likely associated with the complete resampling of all elements between Markov states. Correlation coefficients were varied between 0.8 and 0.999, with improved acceptance rates (40%) found when using higher correlation coefficients (0.999). Convergence was found to flat-line near a misfit of $4,000 \text{ mg/L}^2$ with minimal model improvement during subsequent runs.

The final attempted transition algorithm, external conditioning, was found to be the most efficient at convergence on the high probability space. Model misfits were found to drop from an initial starting value $26,000 \text{ mg/L}^2$ to a minimum of $1,700 \text{ mg/L}^2$ after less than 12 hours, or 3,000 model runs. Subsequent simulations showed further convergence with a minimum value of $1,000 \text{ mg/L}^2$ after 25,000 trials (Figure 1, Figure 3). Acceptance rates remained high even in higher probability space, with rates near 27%. Gaussian jumps were set to 1.3% and 13% of the standard deviation in the K and n parameters, respectively.

As a validation step, random fields generated using the external conditioning algorithm were compared to distributed temperature sensing (DTS) field results. DTS tests allow for flow-path characterization by heating a well column and then monitoring the recovery to baseline (Banks et al. 2014). Areas of higher hydraulic conductivity are more difficult to heat and recover quicker compared to lower conductivity zones. A visual comparison between the DTS and Bayesian-MCMC results indicate a reasonable agreement between the two independent methods (Figure 4).

Conclusions and Future Work

Heterogeneity is an intrinsic property of waste rock systems; however, such attributes are typically overlooked when systems are modelled using larger-scale equivalent porous media properties. While this is often appropriate for calibration of models to pump tests, it can fail to recognise the nuances of waste rock deposition. Bromide response behaviour presented herein has shown that local-scale flow dynamics can be heavily influenced by this depositional history. Early results have shown that the coupling of Bayesian-MCMC approaches with geostatistical routines can provide an effective approach to simulate such heterogeneity. Additionally, the approach was found to have improved convergence when Markov state transition was controlled by external conditioning routines, as opposed to random resampling or collocated cokriging. Research remains on-going with additional model runs being conducted to further explore the probability space.

Acknowledgements

This research was supported by SRK Consulting (Canada) Ltd. and Teck Resources Ltd. The authors would like to thank Victor Munoz, Marko Adzic, Jennifer Mayer, and Aaron Fultz for their reviews of the abstract and/or manuscript. In addition, we thank Dan Mackie, Chris Kennedy, Daryl Hockley, Lee Barbour, and Marek Novak for their support throughout the project.

References

- Banks EW, Shanafield MA, Cook PG (2014) Induced temperature gradients to examine groundwater flowpaths in open boreholes. *Ground Water* 52:943-949
- British Columbia Mine Waste Rock Pile Research Committee, BCMWRPRC (1991) Mined rock and overburden piles: investigation and design manual. Interim Guidelines. 128 pp
- Deutsch CV, Journé AG (1998) GSLIB: geostatistical software library and user's guide. Oxford University Press, New York, USA. 384 p.W
- DHI-WASY GmbH (2016) FEFLOW: finite-element simulation systems for subsurface flow and transport processes. Version 7.0 (Update 9). 64-bit. Software. Berlin, Germany.
- Irving J, Singha K (2010) Stochastic inversion of tracer test and electrical geophysical data to estimate hydraulic conductivities. *Water Resour Res* 46:W11514 doi:10.1029/2009WR008340
- Mariethoz G, Renard P, Caers J (2010) Bayesian inverse problem and optimization with iterative spatial resampling. *Water Resources Research*. 46:W11530
- Metropolis N, Rosenbluth AW, Rosenbluth MN, Teller AH, Teller E (1953) Equation of state calculations by fast computing machines. *J Chem Phys* 21:1087-1092
- Mosegaard K, Tarantola A (2005) Monte Carlo sampling of solutions to inverse problems. *J Geophys Res* 100(B7):12431-12447 doi:10.1029/94JB03097
- Roberts GO, Gelman A, Gilks WR (1997) Weak convergence and optimal scaling of random walk Metropolis algorithms. *Ann Appl Probab* 7:110-120
- Xu W, Tran TT, Srivastava RM, Journé AG (1992) Integrating seismic data in reservoir modelling: the collocated cokriging alternative. *SPE Annu Tech Conf Exhib*. Washington, DC, USA 833-842

Kittilä Gold Mine dewatering assessment: benefits of a new approach

Päivi Picken¹, Tuomo Karvonen², Eero Heikkinen³, Tiina Vaittinen³, Ville-Matti Seppä³, Jaakko Saukkoriipi⁴,

¹*Pöyry Finland Oy, Koskikatu 27 B, 96100 Rovaniemi, Finland, paivi.picken@poyry.com*

²*Waterhope, Munkkiniemen Puistotie 20 A 6, 00330, Helsinki, Finland*

³*Pöyry Finland Oy, Jaakonkatu 3, 01620, Vantaa, Finland*

⁴*Pöyry Finland Oy, Elektriikkatie 13, 90590, Oulu, Finland*

Abstract Water inflows into Kittilä Gold Mine underground workings were predicted over a selected time period, as the mine expands to deeper regimes. A new approach enabled effective studying of large regional datasets and complex underground workings, which are constantly changing. Posiva Flow Log was used for hydraulic testing. Generalizations of soil and bedrock were carried out. RQD-values (rock quality designation) were worked into a RQD-voxel model using geostatistics. Dependency between K-values and RQD values was determined, simplification of the underground space was carried out and a numerical groundwater model generated (continuous time-lapse simulation). Inflow during past mining was used for calibration.

Key words mine dewatering, hydrogeology, modelling

Introduction

Agnico Eagle Finland Oy Kittilä Gold Mine is located in Finnish Lapland, Kittilä municipality. Mining operations started in 2008 with two open pits Suurikuusikko and Roura. Underground operations started 2010. Since November 2012 mining has taken place only underground. Currently Kittilä Gold Mine production rate is 1.6 Mt/year and underground operations are gradually reaching deeper. A hydrogeological study was carried out 2015-2016 to support the mine operations and permitting. The objective of the study was to define the inflow quantities to the underground workings during 2014-2035. Primary focus was set for the time period 2016-2020. As a part of the survey inflow qualities in the different parts of the mine were assessed, as well as mass balances of certain water quality variables. This paper focuses to the inflow quantities, to the methodology behind the results, the benefits of the approach and uncertainties.

Methods

Background data, case conceptualization and model definition

Several data sources were used for conceptualization and defining the extent of the hydrogeological model. Initial available data included water courses and catchment areas, elevation model, climatic and hydrological data. Modeling volume was large enough to include the complete catchment area, so the source of water was net precipitation and recharge from soil layers to bedrock. Lateral recharge was neglected. Some prior hydraulic conductivity data was available, concerning one part of the study area. Soil cover, types and thickness were generalised. Bedrock was generalized into four main categories: mafic volcanic tuff, mafic graphitic tuff, tholeiitic basalt and shear zone (Figure 1), which was mainly containing

the ore. Other data included ground water monitoring data and dewatering rates which were used in calibration using groundwater table, and geometry of the planned underground workings for the years 2014 – 2035. Leakage records from drilling were also available. Stress field was not used in modelling. Data sources included Geological Survey of Finland, Finnish Meteorological Institute, Finnish Environment Institute, National Land Survey of Finland and Agnico Eagle.

Processing of rock fracturing data

Rock fracturing was used for hydraulic characterization of rocks. Rock Quality Designation (RQD) available from drill core logging was processed with inverse distance squared method to a voxel model and extrapolated to cover areas without data, using depth position and lithological and deformation models. The volume of the model covers $8 \times 13 \times 1,3$ km with cell size 40 m x 40 m in horizontal direction, and in vertical direction increasing from 1.0 to 10 m at the top 20 m, then being 40 m below depth of 20 m.

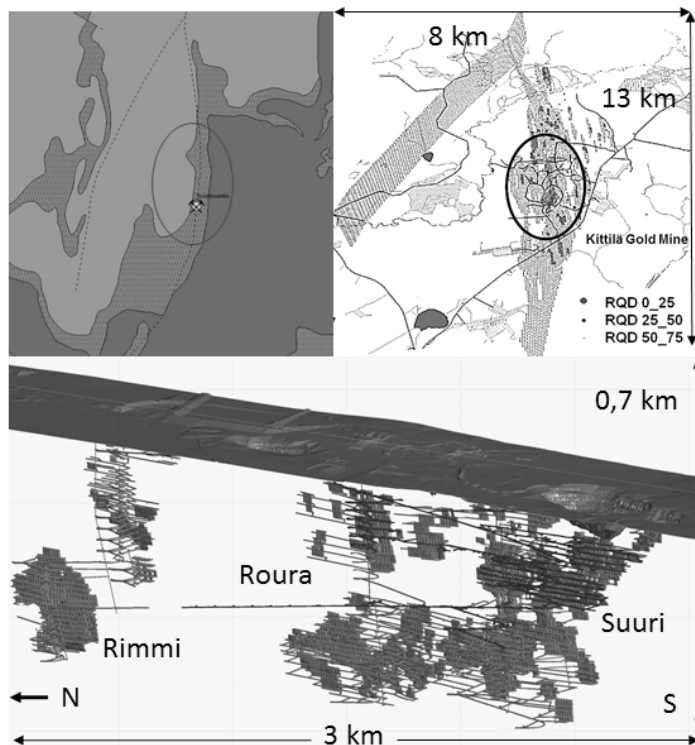


Figure 1. Modelling area and volume of Kittilä Gold Mine together with regional geology. Upper on the left: Tholeiitic basalt (dark grey), mafic volcanite (light grey) and graphitic volcanite (medium grey), regional shear zones with dash lines, and mine area with a circle. Upper on the right: RQD values 0-75 % (grey voxels) modelled at borehole covered volumes, and generalised from deterministic regional shear zone model elsewhere. RQD values 75 – 100 % excluded. Below: mine geometry on a side view from the West.

Composite files from core RQD data (5 m cells) were generated inside bedrock domains and calculated to voxel model at four stages within each bedrock domain, increasing the search distance at 50m, 100m, 200m and 500m to fill empty blocks. Search ellipsoid directions were based on geostatistical investigation and on the mine staff knowledge and experience of the site. Fracturing is more typically encountered in the upper part of the bedrock and in deeper parts of the site in the major shear or fault zones. Layer thickness of the more intensely fractured surficial rock was also based on the drill core data, and was defined for each bedrock category separately, studying the median of composites as function of depth (Figure 2).

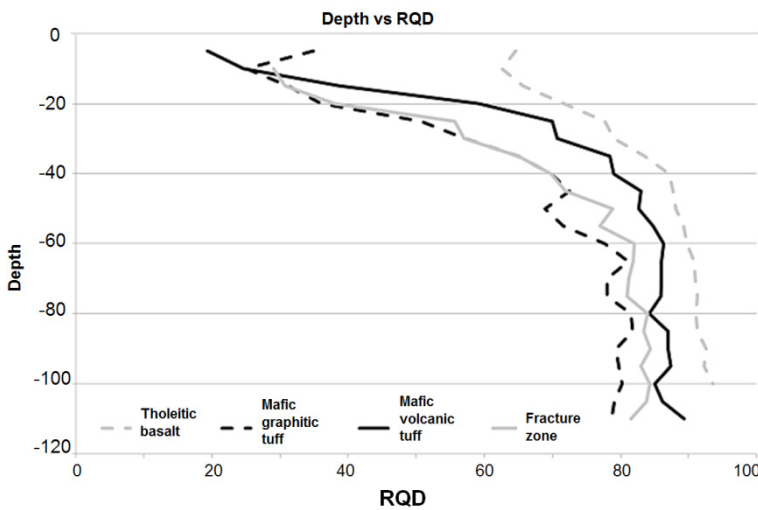


Figure 2. Median RQD in lithology classes and shear zone vs. depth.

A generalised dependency was derived between measured hydraulic conductivity from boreholes and the RQD from the same boreholes and depth levels. The model was transferred to numerical hydrological modelling. Hydrological model area was defined based on catchment areas, the elevation model, water courses, and geometry of the shear zones. Preliminary modelling was carried out to test suitability of the chosen model extent and available data sets – and to support planning of field investigations. Preliminary and final modelling used the same approach. The model is described later in this paper.

Field investigations

New rock hydraulic conductivity data was produced during the project, covering the ore and the shear zone – and surrounding host rocks. New borehole studies included four deep holes from the ground surface, three deep characterisation holes from the research tunnel and six underground production holes. For these holes, PFL (Posiva Flow Log) measurements were carried out, including fracture transmissivity, hydraulic head, flow direction and water electrical conductivity. The method is quick to apply, and is providing well covering information along boreholes on fracture specific transmissivities, which was converted

for modelling to larger scale hydraulic conductivity (K-values of depth intervals and lithological and deformation domains). Measurement took place in natural status and under pumping (using achievable constant drawdown in each borehole, for example 10 m). The measurement procedure was adjusted to gain efficiency so that largest transmissivities ($T > 10^{-8} \text{ m}^2/\text{s}$) could be detected and generalised in five meter blocks to average hydraulic conductivities (K-values, m/s) by summarizing fracture transmissivities and dividing the sum with the length of the assessed interval. Field investigations included also measurements of electrical conductivity of groundwater. Borehole measurements from ground level provided information about the hydraulic head and its variation which made it possible to assess the mine dewatering impact on the hydraulic head in the mine surroundings, as the measurements are showing which fractures are currently connected to the underground workings. Monitoring programme was designed for gathering up information of both seasonal and spatial variation of hydraulic head. Shut-off interference testing was carried out between five underground production holes sealed with packers at collar and equipped with logger installations for hydraulic head measurement. Zones having highest transmissivity were assumed to be associated with the changes in hydraulic head. Suggested installation of permanent vibrating wire piezometers was replaced with these shut-off tests and subsequent temporary monitoring due to mine production related time and site availability limitations. During the course of time the monitoring and progress of dewatering will indicate possible effects of stress field or discharging the aquifer, and modelling can be revised accordingly. A structural geology logging was carried out for the measured boreholes. Drill cores were assessed with Q'-method, where Q' is calculated with Equation 1 (Barton 2014):

$$Q' = \frac{RQD}{J_n} \cdot \frac{J_r}{J_a} \quad (\text{Equation 1}),$$

where J_n is joint set number, J_r is joint roughness number and J_a is joint alteration number. Special attention was paid to such fracture zones were investigated where Q' -values were typically small (< 0.1). Necessarily Q' does not correlate with hydraulic conductivity, as an open individual fracture (like a fault core zone) may alone cause a high hydraulic conductivity. A leakage survey was carried out in the tunnels by Agnico Eagle staff. Stopes were classified to leakage groups including 1) dry stopes ($< 10\%$ of wall/sealing was moist), 2) dripping stopes ($10\text{-}50\%$ of wall/sealing was moist), and largely dripping stopes ($10\text{-}50\%$ of wall/sealing was moist) and leakages with flow ($> 5 \text{ l/min}$).

Modelling approach

A new method was adopted for predicting the underground leakage. The key challenges in this type of work are the complicated underground geometry and its changes over time. New tunnels and stopes are opened every year and former workings will be closed after ore extraction. From this perspective, finite volume modelling method was chosen instead of finite element or finite difference method. The cell size was kept unchanged around the open underground workings, using same cell size everywhere and accounting the flow proportional to the total volume of open underground space for each cell, allowing flexible modelling of constantly developing underground workings. The method consisted of three sub-models:

1. Predicting the entire rock volume K-values ($\log(K)$), based on voxelized RQD and lithological model
2. Simplification of the complex geometry of the underground mine
3. Predicting the leakage amounts at twice a year steps based on the results from the sub-models 1 and 2

In the sub-model 1 the average K-values and the average RQD value were compared and their site specific large scale interdependence was assessed. Information on fractures intersecting the boreholes, their orientation, or length and connectivity distribution was not available. Based on the interdependence the RQD voxel model was used in the hydrogeological numerical modelling as the hydraulic conductivity information source. Interdependency of RQD and $\log(K)$ was assumed to be linear (Equation 2):

$$\log(K) = A \cdot RQD + B \quad (\text{Equation 2})$$

Above 500 m depth the modeling volume was divided into three regions with different coefficients A and B, and below 500 m constant values were applied. A vertical anisotropy was introduced for the depths below 500 m, based on interpretation of depth and $\log(K)$ relation. Because of the fractured zone, a horizontal anisotropy was included in the model. The degree of anisotropy (2.1) was defined in the calibration context.

In the sub-model 2, effective tunnel length L_{eff} and radius R_{eff} were calculated using average tunnel cross section, the average radius derived from average cross section width (3.1 m in this case) and information about tunnel lengths opened each year. Effective tunnel lengths opened each year are presented in Figure 3.

The third sub-model predicted the leakages in each cell. A modification of a function for equilibrium stage for a long tunnel was used. Initial equation for calculating the leakage quantity to tunnel q ($\text{m}^3/\text{s}/\text{m}$) can be presented in following format, Equation 3 (Goodman et al. 1965, Gustafson 1986, Sievänen 2001):

$$q = \frac{2 \pi K H}{\ln \left(\frac{2H}{R} \right)} + f_{\text{skin}} \quad (\text{Equation 3})$$

where K is hydraulic conductivity (m/s), H is hydraulic head (m), R is tunnel radius (m) and f_{skin} is an empirical coefficient allowing taking into consideration not fully radial flow. Cell specific leakage $Q_{(i,j,k)}$ (m^3/s) was calculated according to following function, Equation 4:

$$Q_{(i,j,k)} = \frac{2 \pi K_{\text{eff}} L_{\text{eff}} (H_a - H_n)}{\ln \left(\frac{H_a - H_n}{R_{\text{eff}}} \right)} + f_{\text{skin}} \quad (\text{Equation 4})$$

L_{eff} and R_{eff} were calculated as explained above. K_{eff} was calculated as the geometric average of current node's and the surrounding nodes' K-values. H_a is hydraulic head around the leaking node as computed by the model and H_n is estimated hydraulic head in the leak-

ing node. The hydrogeological modelling was carried out using numerical solution of the Richards equation (Eymard, 1999, Tracy, 2007, Karvonen 2008, Warsta 2011), which allows calculating simultaneously flows in both soil and bedrock. Moreover, computation of transport of substances was included in the model, taking into account density differences of groundwater.

Model calibration

Modelling was carried out for the period 2008 – 2035, calibrating the model using monitoring and dewatering data from 2008 – 2015. A snow accumulation and melting model was generated to support hydrogeological model calibration in addition to precipitation and evaporation.

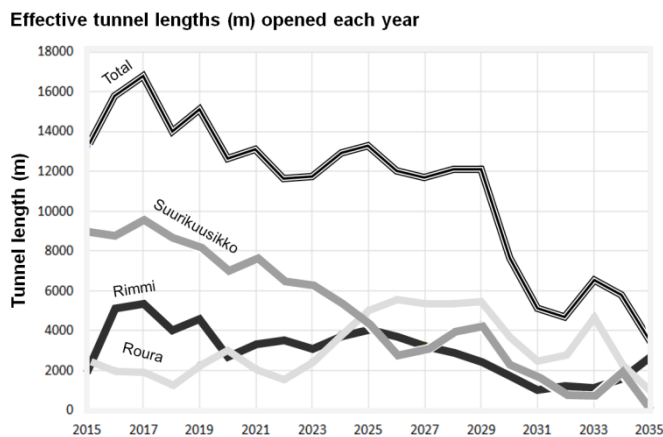


Figure 3 Effective tunnel lengths opened each year: total, Suurikuusikko, Roura and Rimmi.

Final model

Two alternatives were calculated for water leakages, where Alternative 1 was the primary (actual) alternative. Alternative 2 served partially a purpose rather similar to sensitivity analysis, with 50 % higher hydraulic conductivity in bedrock and differing treatment in stope backfills. Mass balance of certain elements and compounds were calculated as transport model for the Alternative 1. The transport model results did not include impacts of any chemical reactions like sulphide oxidation or attenuation. They simply present the water qualities from the rock transported to the underground workings. Outside the scope of this paper, it should be mentioned, that long term impacts of sulphide oxidation and other chemical processes were assessed in a separate geochemistry study and the results were used to support final conclusions and recommendations.

Results

According to the model, dewatering quantity pumped out of the underground workings in 2016 was estimated to be 4.22 M m³/year (482 m³/h). The actual quantity was confirmed to be 4.02 M m³/year at the end of the year 2016. In 2020 the quantity is forecasted to reach

4.77 Mm³/year (545 m³/h). The summary of the water development according to the short term prediction is presented in the Figure 4 below.

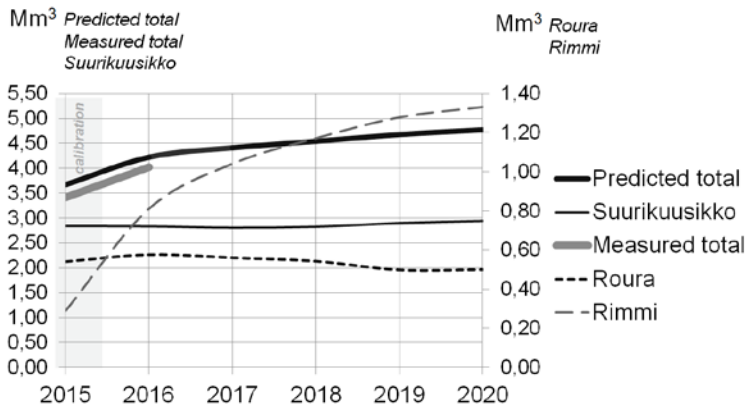


Figure 4. Water amounts to be pumped, Alternative 1. Horizontal axis: time (year). Left vertical axis: predicted total inflows, measured total inflows and Suurikuusikko predicted inflow (million m³/year). Right vertical axis: Roura and Rimmi predicted inflows (million m³/year).

Horizontal and vertical Darcy flow velocities were extracted from the model. Horizontal flow velocities (maximum year) at far ends of the model were extremely low, confirming the model area extent is adequate. Also modelled depth was large enough based on small vertical flow velocities at bottom of the model. Some up-coning of higher density groundwater can take place from the deeper regimes due to density gradient. The most important uncertainties were related to the amount and representativeness of measurement data and to interdependence between RQD and log (K), especially deeper down. There were also uncertainties concerning the hydraulic conductivities at the contact of the stope backfill and bedrock, and the mathematical treatment of flow at mechanic failure in Suurikuusikko open pit floor. Changes above the ground, which might take place over time, were not included to the model inputs. Settings for the horizontal and vertical anisotropy were based on a small number of measurements. Other identified uncertainties were related for example to a specific monitoring points unexplained groundwater table variations, and reliability of measured pumping volumes. There were substantially larger uncertainties related to the long term prediction. Two different underground dewatering water streams were preliminary proposed, though water management design is still an ongoing work. A simplified spread-sheet style calculation basis was generated for calculating water quantities and qualities from the different depths and spatial parts of the mine, when applying different water quality criteria.

Conclusions

Two different time frames were applied for the utilisation of the results. For the short term, years 2016-2020, uncertainties were smaller as the measured data was considered rather well representative. Results of the short term prediction are currently being used for plan-

ning and permitting the next phases of the operations. This far, after a short period, modelled and measured inflows are rather well in the same order of magnitude. In the deeper regime, no open tunnel workings exist and information was gathered from few boreholes. Therefore the long term forecast (2014-2035) has a higher degree of uncertainty and those results are taken as indicative. Concerning long-term forecasting, it should be also noted, that the model was based on 2014 mine planning status and these plans are updated. This study provided an effective and flexible approach to forecast development of inflows to an underground mine over a long time period, though quantity and representativeness of input data steer the reliability of the results. In the used approach, water quantity impacts of opening new underground workings and backfilling them can be assessed in a flexible and rather detailed way. This approach also “recycles” effectively data collected for other purposes. PFL measurements and their interpretations provide information of hydraulic transmissivity variation in rock mass to be used as input in numerical hydrologic modelling. This allows rather detailed dewatering design, taking into consideration different regimes within the mine and gradual changes over time.

Acknowledgements

The authors thank the rest of the project team for their valuable input and Agnico Eagle Finland Oy and Kittilä Gold Mine staff (Andre Wageningen, Pasi Kreivi, Jukka Välimaa and Leena Rajavuori) for co-operation and on-site support during the study.

References

- Barton N, Grimstad E (2014) Forty years with the Q-system in Norway and abroad. *Fjellsprengningsteknikk*, NFF, Oslo, 25 pp
- Eymard R, Gutnic M, Hilhorst D (1999) The finite volume method for Richards equation. *Comput Geosci* 3(3–4):259–294
- Goodman RE, Moya DG, van Schalkwyk A, Javandel I (1965) Ground water inflows during tunnel driving. *Engineering Geology* 2:39–56
- Gustafsson G (1986) Hydrogeological pre-investigations in rock (In Swedish). Swedish Rock Engineering Research Foundation, Report BeFo 84:1/86, 125 pp
- Karvonen T (2008) Surface and near-surface hydrological model of Olkiluoto Island. Posiva Working Report 2008-17, 88 pp
- Sievänen U (2001) Leakage and groutability. Posiva Working Report 06/2001, 82 pp
- Tracy FT (2007) Three-dimensional analytical solutions of Richards’ equation for a box-shaped soil sample with piecewise-constant head boundary conditions on the top. *Journal of Hydrology* 336: 391– 400
- Warsta L (2011) Modelling water flow and soil erosion in clayey, subsurface drained agricultural fields. Aalto University publication series, Doctoral Dissertations 82/2011. Aalto Print, Helsinki, 211 pp

The Application of Discrete Fracture Network Models to Mine Groundwater Studies

Gareth Digges La Touche¹, Mark Cottrell²

¹*Golder Associates (UK) Ltd, Attenborough House, Browns Lane Business Park, Stanton on the Wolds, Nottinghamshire, NG12 5BL, United Kingdom, gdltouche@golder.com*

²*Golder Associates (UK) Ltd, Attenborough House, Browns Lane Business Park, Stanton on the Wolds, Nottinghamshire, NG12 5BL, United Kingdom, mcottrell@golder.com*

Abstract Discrete Fracture Network (DFN) modelling represents an alternative approach to the more usual continuum Representative Elementary Volume (REV) methods for modelling groundwater flow in fractured rocks. The basis of DFN modelling is the cognisance that at every scale, groundwater flow in fractured rocks is dominated by a limited number of discrete pathways formed by fracture connectivity. In this paper we present examples of the use of DFN models to mine groundwater studies. Specifically we will consider the use DFN models for the estimation and prediction of groundwater inflow to underground workings and for the evaluation of heterogeneity.

Key words modelling, DFN, FracMan, discrete fracture network, groundwater

Introduction

Many mine groundwater studies involve the construction of models of groundwater flow, and contaminant transport, to test our conceptual understanding of the hydrogeological regime of a mine site. These range from simple analytical models in a spreadsheet, through analytical element models to numerical finite difference and finite element models. As many of the groundwater systems in which mining occurs are dominated by fracture flow reliance is placed on the concept of the representative elementary volume (REV). The REV is taken as that volume of rock at which flow can be simulated as if it were an equivalent porous media and the influence of individual fracture pathways no longer dominates. The discrete fracture network (DFN) approach provides a paradigm for describing rock fractures (and other discrete features such as faults, breccia layers, and dikes) in a systematic and statistically reproducible manner. Fractures, and faults, are represented as discrete surfaces in three-dimensions. The geometrical properties of intensity, orientation, shape and size for the fractures are described deterministically for known features, and stochastically using observed data from borehole core logging, surface mapping, geophysics and remote sensing (e.g. lineaments) correlated to fracture location and geometry. On top of the geometrical description, the transient hydraulic properties of the fractures/faults are derived using calibration to and simulation of in situ measurements and tests.

Groundwater inflow is an important issue for mining, as aside from the potential for flooding, a knowledge of the inflow rates is important for mitigating groundwater and surface water impacts in terms of both flow and chemistry. Having adequate estimates of mine discharge rates is vital for ensuring that the design of pumping and water treatment infrastructure is fit for purpose (Doe, 2014). We describe in this paper the application of the DFN method to a number of mine water studies: where the conventional REV approach is not

appropriate due to scale; but permit the use of the DFN method to derive hydraulic properties; and the evaluation of heterogeneity.

The Discrete Fracture Network Method

The properties of individual, or discrete, fractures or similar features are explicitly described in a Discrete Fracture Network (DFN) model in order to allow the analysis of fluid flow (Dershowitz and Doe, 1988; Dershowitz and Miller, 1995; Dershowitz et al., 2011; Cottrell 2012). This approach is based on the principles of fluid flow in fractured media. A typical DFN model is shown at Figure 1. A DFN model of a dynamic system must include a representation of the existing natural fractures comprising not only the geometric and hydrological properties but also the geological and geomechanical properties of the three dimensional natural fracture network.

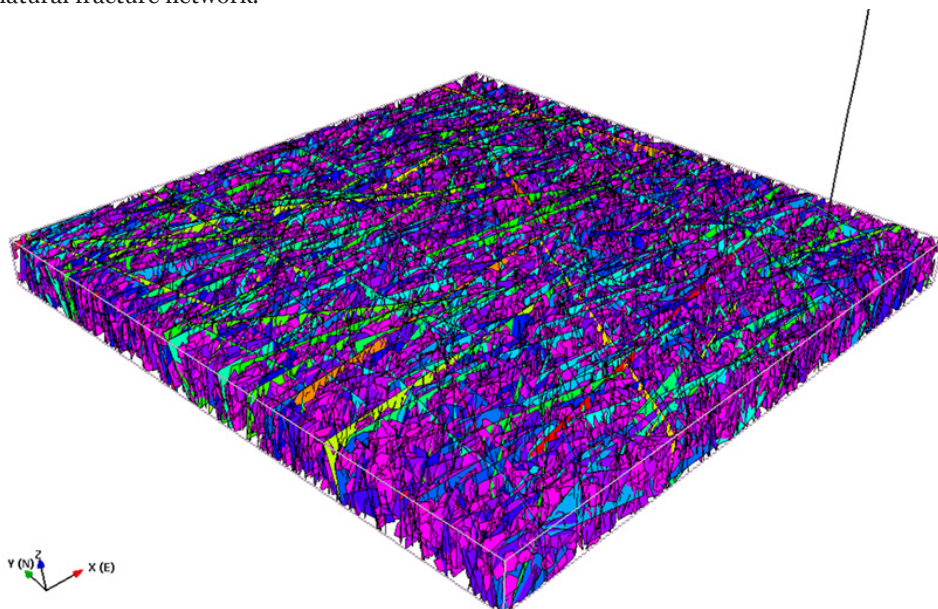


Figure 1 Typical DFN model

An example of the components of a DFN model, is presented at Figure 2. The geological data that describes the natural fracture network in terms of fracture orientation, intensity, and size is presented at Figure 2(a) to (c). Two significant fault structures, Figure 2(d), derived from geophysical data, are included in the full model (Figure 2(e)).

Fracture size is often a function of the mechanical stratigraphy and structural terminations. Fracture intensity may be stated either as a one-dimensional intensity (P10 -fractures/meter, along a specific sampling line), volumetric intensity (P32 – fracture area/volume) or as a fracture porosity (P33 – m³/m³). Volumetric intensity (P32) is most frequently used as it is not influenced by sampling bias due to the sampling direction, as with P10, or by aperture, as with P33.

The construction of a spatial model that describes how fractures are distributed in within the rock mass, and the inter-relationship between fractures, stratigraphy, lithology, and structure is the key to DFN modelling. Fracture orientations can be described using a number of statistical approaches, most typically a hemispherical probability distribution, such as Fisher or Elliptical Fisher, is used. Alternatively, fracture orientations can be linked to local geological factors, such as structural dip, structural position (e.g. on the axis of a fold rather than the fold limbs), Gaussian curvature, stress field, or seismic attributes. Typically, it is found that the key static fracture descriptors of orientation, size, intensity, and shape can be efficiently and effectively described using specific combinations of such attributes derived from multivariate regression analysis. The size of a fracture is stated as the fracture area and shape, often expressed as an “equivalent radius” of a circular-disk shaped fracture of equivalent area.

For hydraulic purposes in the DFN method each fracture is treated as a semi-confined aquifer – thus the hydraulic properties of fractures are transmissivity (kH) and storativity (S), which can be derived from generic or site specific correlations to available transient data (i.e. well test response), or if no such data is available then to fracture size, mechanical (apparent) aperture and transmissivity as well as sometimes to wireline geophysical data and other attributes.

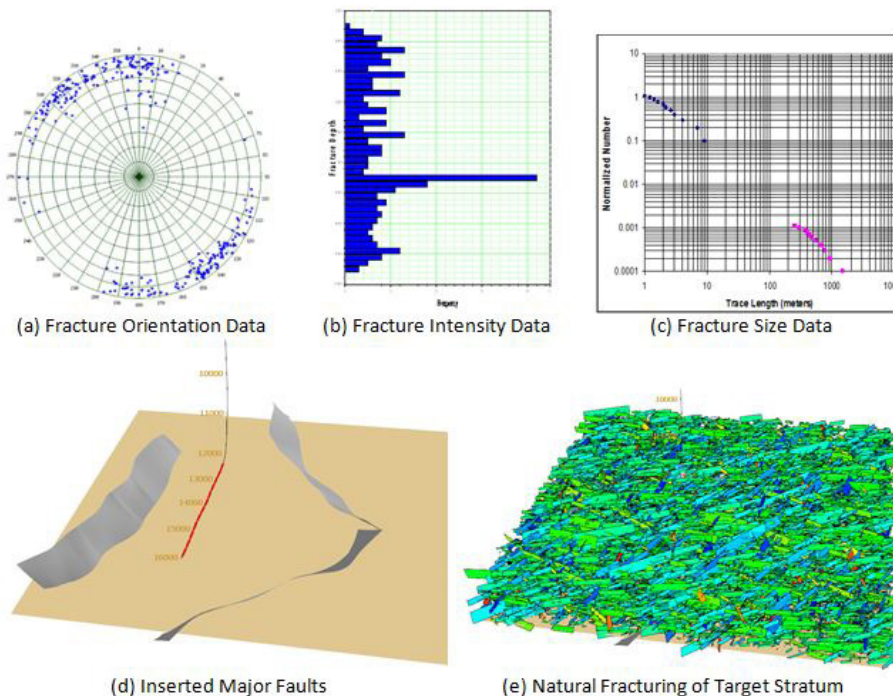


Figure 2 Example of data for DFN model development including mapped major structures (d) and a stochastic representation of the natural fracture distribution (e)

Mine Water Inflow

A DFN model was developed using Golder Associates' FracMan™ software to represent discrete inflows to an underground hardrock mine in North America. The model and approach are described in detail by Doe (2014) and summarised here. The purpose of the model was to enable an assessment of inflows to a planned extension to the mine. Both deterministic and stochastic features were included within the model. Deterministic features included water-bearing faults and veins whose locations are known. The remaining water-bearing fractures were treated stochastically, using probability functions to describe the main geometric and hydraulic properties of the fractures, including fracture intensity, size and orientation. Fracture orientation data was derived from oriented cores, mapping of faults in the mine and from the orientations of the known, major features such as faults (deterministic features). Fracture intensity was derived mainly from a survey of seepage points by mine staff. Fracture sizes were assumed to follow power-law distributions based on an analysis of trace maps of the deterministic features. The fracture transmissivity values were derived from a limited number of packer tests and a database of flow data from grout holes. Multiple realisations of statistically identical DFN fracture model were undertaken to provide a method for assessing potential model uncertainty.

The resultant model (Figure 3) was used to assess firstly the impact of an Aperture Controlled Grouting (ACG) programme, which can be successfully used to reduce groundwater inflow to the mine, and to enable an assessment of inflows to the mine during future development (Figure 4). This allows for effective planning of the management of mine inflows as development proceeds. As with all models, the results are non-unique and other realisations of a fracture network or a porous continuum could produce these same results. The DFN approach does however have the significant advantage of being able to incorporate and honoring the significant controlling geological features (Doe, 2014).

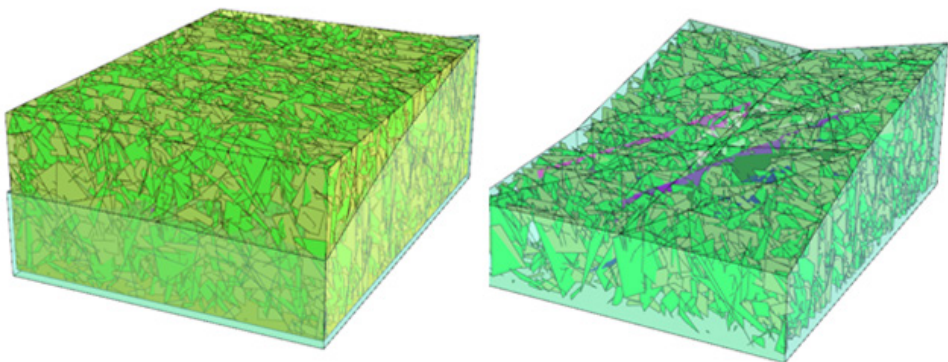
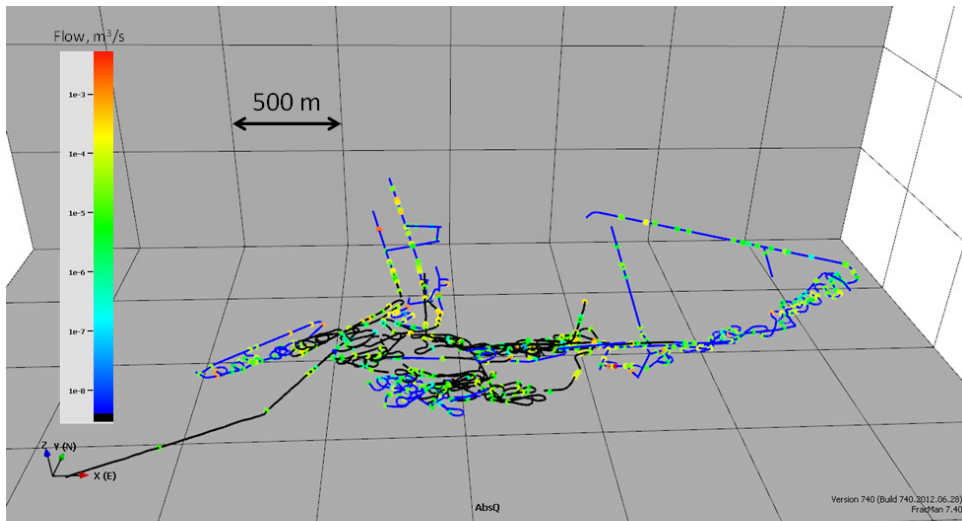


Figure 3 DFN model of the mine area



Black: existing tunnels; Blue: new development

Figure 4 Simulated and Measured Seepage into existing a future development areas

Derivation of Hydraulic Properties

In order to understand the impact of mine closure on the groundwater regime and on discharges from an operational underground polymetallic mine in the southern Caucasus region it was necessary to develop a hydrogeological model of the mine and its environs. The hydrogeological understanding of the mine is currently very limited and is based primarily on studies completed in the 1970s by hydrogeologists of the former Soviet Union. These studies were focused on collecting baseline geological information for the area rather than hydrogeological characterisation. Hence with the exception of some sparse groundwater level and chemistry data there is no hydrogeological data available with the exception of current estimates of discharge from the mine and flows in adjacent rivers. The underground workings sit beneath an area of land covering approximately 400 Hectares, and is accessed by more than 10 individual adits and 3 shafts. The geology comprises Middle Jurassic-age volcanogenic and sedimentary formations. The ore is hosted within metasomatised porphyritic andesite (flows, tuffs and pyroclastics) and volcanogenic conglomerates that are unconformably overlain by a sedimentary sequence of limestone, marls and volcanoclastic sandstone.

A DFN model was constructed (Figure 5) using the FracMan code to represent that fracture networks in the volcanic bedrock hosting the ore body based on fracture data (frequency, orientation and length) recorded in the Soviet mapping and more recent structural geology reports. The objective of the model was to characterise the possible range of hydraulic conductivity generated as a result of the observed fracture density and assumed fracture transmissivity. Reasonable estimates of fracture aperture were made based on field observations and correlations between fracture size and aperture (Dershowitz et al. 2003). Based

on these datasets an upscaled equivalent porous medium (EPM) hydraulic conductivity dataset was calculated using a variation on the method of Oda et al. (1984) where isolated fractures are not included in the calculation. Whilst there is uncertainty in the results it does provide a basis for initial modelling that can be benchmarked against recorded mine discharges and river flows.

The results supported anecdotal information that: the permeability of the volcanic rock matrix is generally low; that inflows are largely restricted to identified fracture corridors; and that inflow to the mine is limited by bedrock permeability rather than the rate of recharge of precipitation to groundwater.

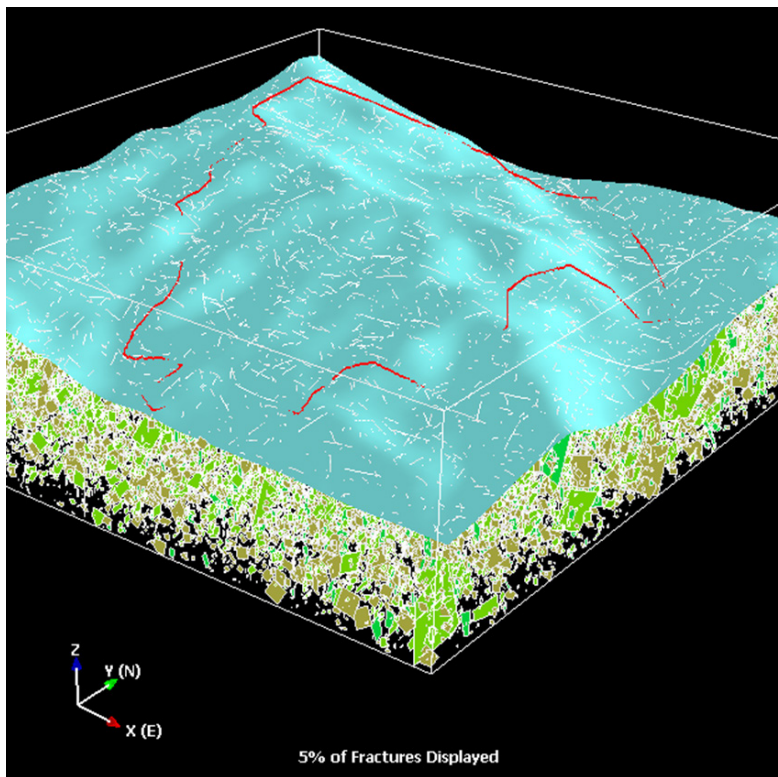


Figure 5 DFN model of the volcanic bedrock in area around the mine

Heterogeneity

An area of uncertainty that often arises is the degree of heterogeneity in fractured strata, be they volcanic or metamorphic “basement” strata or limestones or fractured sandstones. The DFN method may be used to refine estimates of heterogeneity by considering the distribution of fractures (number of fracture sets, frequency, orientation etc.). An example of the use of this approach is as follows. A large dataset of hydraulic conductivity data was available for a fractured limestone aquifer, together with data regarding fracture characteristics from

outcrop mapping, core logging and wireline geophysics (Figure 6). This data was used to update previously synthesised data published by Jones et al. (1999). The objective was to characterise the range of hydraulic conductivity within the area of interest including any variation with depth. An equivalent porous medium (EPM) continuum grid developed for the purpose of a distributed finite difference based flow models of groundwater movement in the area, was imported and for each cell an upscaled hydraulic conductivity (K) was calculated using the method of Oda. The resultant conductivity values (K_x , K_y and K_z) were then exported back to MODFLOW. The resultant hydraulic conductivity matrix confirmed the local dominance of vertical hydraulic connectivity as indicated based on geochemical evidence and the presence of zone of enhanced horizontal hydraulic conductivity, consistent with mapped geological structures.

A similar approach may be used to identify enhancements in hydraulic conductivity around pit walls due to blasting over break and interaction with existing geological structures. This can provide important direction to pit dewatering and in particular pit slope pore pressure management by allowing appropriate targeting of pit slope depressurisation wells.

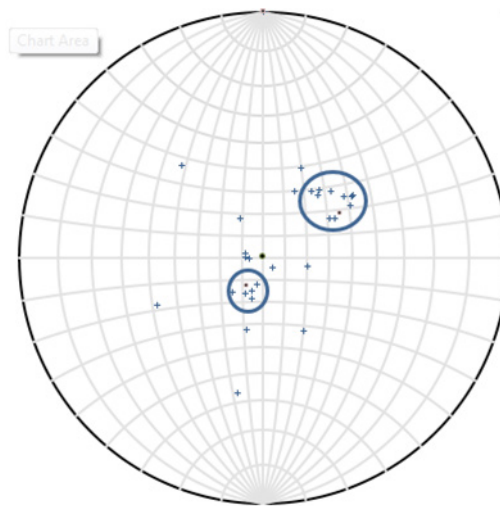


Figure 6 Fracture azimuth and dip for a fractured limestone aquifer

Conclusions

The examples above illustrate the application of the DFN to mine water studies and the associated benefits to hydrogeological characterisation both when detailed information is available to characterise and predict discrete inflows to mines, and to situations where data is sparse but existing geological and structural data sets may be used to build a hydrogeological understanding of a mine site. The examples illustrate the benefit of collecting data to characterise existing natural fractures as part of routine geological and hydrogeological studies.

References

- Cottrell M (2012) A Discrete Fracture Network Approach for Enhancing Development of Fractured Reservoirs. Society of Petroleum Engineers YP Event, The Geological Society, London, United Kingdom, 8 March 2012
- Dershowitz WS and Doe TW (1988) Practical Applications of Discrete Fracture Approaches in Hydrology, Mining, and Petroleum Extraction. Proceedings, International Conference on Fluid Flow in Fractured Rocks, Atlanta. Georgia State University, Atlanta. 381-396.
- Dershowitz WS, Doe TW, Uchida M and Hermanson J (2003) Correlations between Fracture Size, Transmissivity, and Aperture. P. Culligan, H. Einstein, and A. Whittle, ed. Soil Rock America, 2003. Proceedings of the 12th Panamerican Conference on Soil Mechanics and Geotechnical Engineering, 887-891
- Dershowitz WS and Miller I (1995) Dual Porosity Fracture Flow and Transport, Geophysical Research Letters: 11, 1441-1444
- Digges La Touche G, and Cottrell M, 2012, "Application of discrete fracture network modelling to environmental risk management for unconventional oil and gas projects", Conference Poster PESGB London
- Doe TW (2014) Discrete Fracture Network Simulation of Groundwater Inflow to an Underground Mine. International Discrete Fracture Network Engineering Conference, Washington, 2014
- Oda M, Suzuki K. and Maeshibu T (1984) Elastic compliance for rock-like materials with random cracks. Soils and Foundations: 24(3), 27-40
- Jones MA, Pringle AB, Fulton IM, O'Neill S, (1999) Discrete fracture network modelling applied to groundwater resource exploitation in southwest Ireland. In MacCaffrey KJW, Lonergan L and Wilkinson JJ (eds) Fractures, Fluid Flow and Mineralization. Geological Society, London, Special Publication: 155, 83-103

Posiva Flow Log (PFL), Tool for detection of groundwater flows in bedrock

Jere Komulainen

Pöyry Finland Oy, Jaakonkatu 3, 01620 Vantaa, Finland, jere.komulainen@poyry.com

Abstract Groundwater flow in borehole is conventionally measured with inline spinner or thermal pulse flow loggers that measure water flow along a borehole. This is fast way to find the most flowing fractures but measurement accuracy depends on total flow below measurement depth. If total flow along a borehole is very large it is very difficult to detect smaller flow changes that indicate flowing fractures. Posiva flow log tool avoids the deterioration of measurement accuracy by introducing a flow guide that bypasses flow along a borehole and measures only the flow coming from a certain borehole depth interval, associated with fractures.

Key words Posiva flow log, groundwater flow, borehole, hydrology, flow measurement

Introduction

Posiva flow log (PFL) tool has been developed by Pöyry for hydrogeological investigations in design and construction of repository of high-level spent nuclear fuel. The development of the tool started 30 years ago and first measurements were conducted in early 90s. The device has been used mostly in investigations for Posiva and SKB, the nuclear waste management companies in Finland and Sweden, and hundreds of boreholes have been measured during more than 20 years. In recent years couple of measurement campaigns have been conducted also for mining companies. Posiva Oy is the owner of the PFL measurement tools but Pöyry conducts the PFL measurements.

The measurement technique of PFL tool is unique and it combines accuracy and resolution of double packer hydraulic testing and measurement speed of inline spinner or thermal pulse flow logger. The idea of the PFL measurement is different than the basic double packer hydraulic measurement. In double packer measurement the measurement section is isolated by inflatable packers and pressure in the measurement section is changed in order to obtain flow changes. The isolation by inflatable packers is a slow process and the pressure change after packer inflation takes some time too. With PFL tool the isolation of measurement section is done with flexible rubber discs (*Figure 1*) that maintain the isolation of measurement sector even during movement of the tool and therefore no time is needed for isolating the measurement section after moving the probe to a new location. Apart of lacking requirement for inflatable packers, the measurement is speeded up by using constant drawdown created by borehole pumping to create pressure changes to obtain flow values in different pressures. With PFL measurements two different pressure conditions are obtained with two individual measurement runs. During both of the measurement runs the pressure (drawdown) is kept steady. Usually the first measurement run is conducted in natural (non-pumped) conditions and another one while water level is kept lower by pumping continuously. This way pressure conditions are steady during flow measurements and there is no need to wait for pressure changes in all measurement locations.



Figure 1 PFL tool with measurement section setup. Yellow disks are used to isolate measurement section from rest of the borehole.

PFL Method

The PFL tool measures water flow, pressure, electrical conductivity (EC) and temperature of the borehole water and single point resistance of borehole wall. All these, except single point resistance, are measured in every measurement location when probe is at standstill. The measurement time at each station is 45 seconds. Resistance is measured also during moving the probe between measurement stations. As the measurement time is so short the entire measurement speed depends on number of measurement points and speed that the probe is moved. The speed of movement cannot be very fast but about 5cm/s speed can be obtained. The flow sensor in the probe is very small and that is the component which has required most development. The flow sensor is a plastic tube with three thermistors inside. All of the thermistors measure temperature and the one in the middle also has a heating function. The determination of flow rate through the flow sensor is based on giving a heat pulse with the central thermistor and monitoring the cooling of the thermistor. The faster the temperature drops after the heat pulse the larger is the flow rate. Using different heating powers flow rates of 30 – 300 000 ml/h can be determined. The temperature of water is recorded also before the heat pulse.

High precision pressure measurement is needed to record the exact pressure conditions in which flow rates are obtained. Especially the pressure difference between the two measurement runs has to be determined with high accuracy. The pressure sensor fitted into PFL probes works in pressure range from 1 bar to 150 bar.

Electrical conductivity of water is measured with a commercial sensor which has been modified to endure high pressure and fitted to the PFL probe. The electrical conductivity can be measured from borehole water or from flow channel before the fracture water mixes with the borehole water. EC readings are calibrated with laboratory reference liquids (KCl) to a high accuracy.

Single point resistance is measured between single point electrode between rubber disks (*Figure 1*) and body of the probe. Borehole features visible in the resistivity data are fractures that allow water flow over the rubber disks and changes in electrical conductivity of borehole wall rock. The resistance is recorded while the probe is moved to next flow measurement point and therefore depth resolution of the resistance data is about 1/cm. The single point resistance anomalies can be used for depth matching between different measurement runs, and it also reveals position of a flowing fracture because fractures typically are seen as low resistance anomaly along logging profile in the rock mass.

The boreholes can be up to 1500 m long and diameter in range from 56 mm up to 200 mm. The most typically measured borehole diameter is 76 mm (NQ). The quality of drilling af-

fects the quality of measurement results as smooth borehole wall ensures that the rubber disks isolate the measurement section well. Therefore diamond (core) rotary drilled boreholes are preferred as the quality of borehole wall is better than in boreholes made with other drilling techniques.

Finding water flowing fractures in a borehole is probably the most important task for the PFL tool. While a borehole is pumped and sufficient drawdown has been created all water-flowing fractures should be visible to PFL probe. Usually all flowing fracture locations can be found with one measurement run under pumped conditions. The PFL probe measures the flow that comes from the measurement section and therefore the total flow along a borehole doesn't affect the ability to detect flowing fractures along a borehole. The inline spinner flow logger on the contrary measures the flow along a borehole and therefore as the flow rate increases in upper part of a borehole the measurement accuracy deteriorates. The *Figure 2* illustrates the difference of fracture flow determination using PFL probe when flow is measured from measurement section and when flow along a borehole is measured. Red line represents the PFL measurement with 2 m section length and green line represents the measurement of flow along a borehole (measured with PFL probe by removing lower rubber disks and blocking bypass tube). Two fractures are detected from the flow along a borehole flow but no more. The flow along the borehole changes between depths of 10 – 50 m by 2 litres per minute but the exact depth of the change is difficult to be said. In this case fractures above depth of 52 m cannot be detected based on flow along the borehole measurement (spinner or thermal pulse) even though there are fractures with total flow of more than 1 l/min. The PFL tool can differentiate between each of the fractures, provide their exact position in borehole length and fracture specific transmissivity. Minimum duration of the PFL measurement in 1000 m long borehole using 5 m long section and 1 m measurement interval is about two days.

Using other borehole logging and core logging data, like acoustic or optical televiewer images and borehole geophysical data, it is possible to associate the flow data into borehole conditions, faults, as well as fracture orientations and aperture. Associating the flow data to fractures, and for example to fracture network analysis or numerical hydraulic modelling, is requiring depth matching to core data, which is enabled by dense station interval, good position accuracy and depth reference data provided by single point resistance logging.

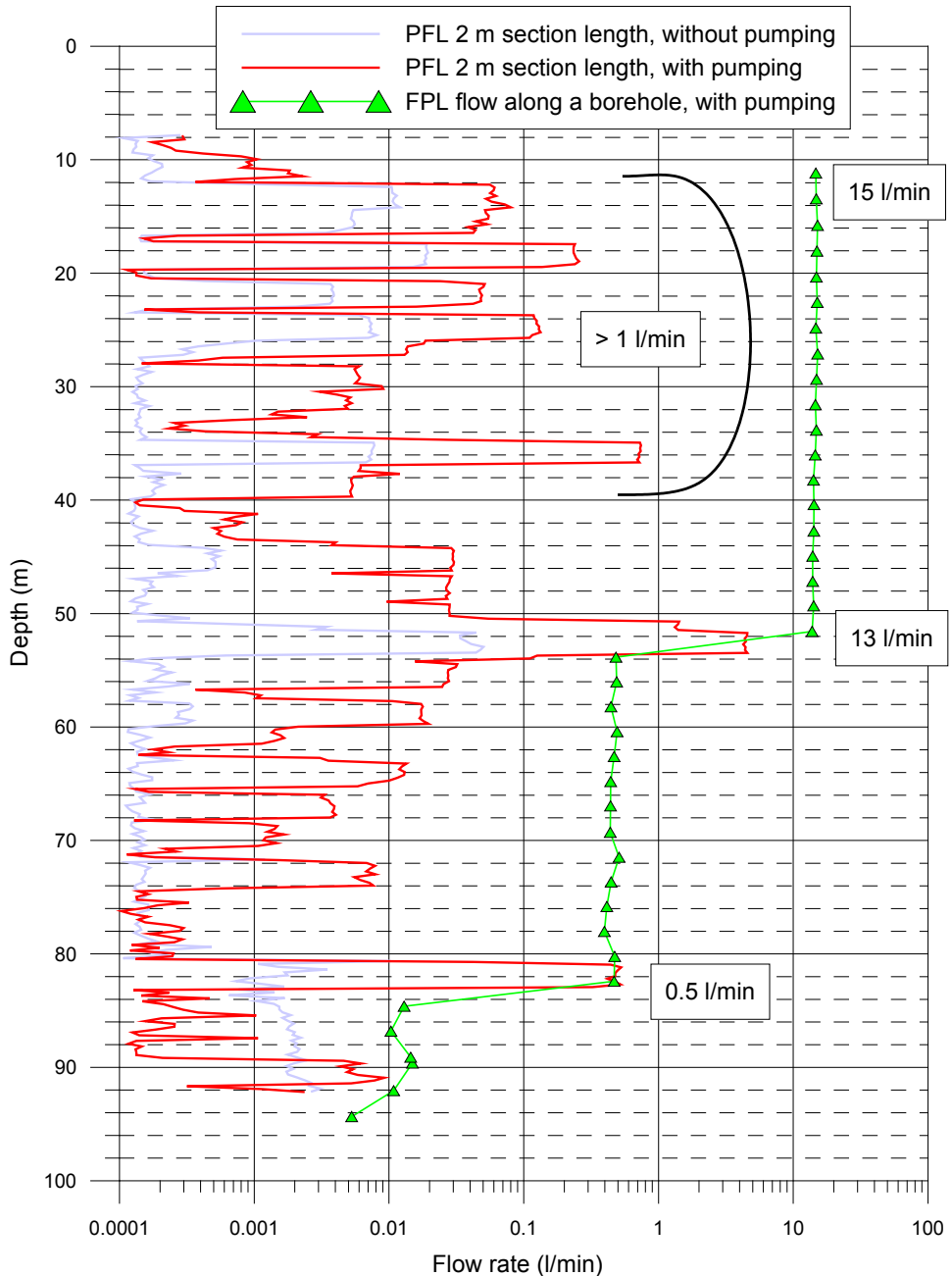


Figure 2 Comparison of flow logging results obtained with PFL tool using flow guide to measure flow from measurement section and flow along a borehole. Each rectangular shaped level has width of sector length (here 2 m) and has eight flow records (here at 0.25 m spacing).

Length of the measurement section can be from 0.5 m to 10 m and measurement interval is usually about $1/5$ of the measurement section length. The reason for measuring flow more frequently than once at a certain borehole section is that not all flow measurements are successful and because interleaved measurements improve flow interpretation in regards to both flow rate and fracture location. Bad borehole sections might cause rubber disk leakages at one measurement point but the flow rate at the depth can still be determined based on previous and next measurement points. The measurement interval determines how accurately flowing fractures can be located in a borehole.

Transmissivity of borehole section can be estimated based on single measurement run in pumped conditions with an assumption that fracture flows are zero in natural (unpumped) conditions. In reality not all flow rates are zero in natural condition but usually so small that they can be neglected in order to get estimate of transmissivity. However in some cases pressure conditions in the surrounding bedrock are affected by hydraulic sinks (hydraulic connections to lower pressure potential) like underground tunnel or a valley nearby. In these cases fracture flows might be directed out of a borehole even during pumping of a borehole. In these cases transmissivity cannot be estimated based on one measurement as flow rate into bedrock in unpumped conditions is larger than during pumping and it cannot be estimated. Using minimum two drawdown levels, it is possible to define structure or fracture specific hydraulic head even in case of topographic differences (valleys and hills) and in case of tunnels and underground workings (openings). Usually the other pressure condition is natural conditions without pumping of measured borehole. When flow rate in unpumped conditions has been measured the transmissivity can be estimated based on flow and pressure differences between the two measurements taking into account certain assumed flow geometry (Marsily 1986).

Water sample collection

To obtain information from electrical conductivity of groundwater in the fractures rather than in the open borehole, the PFL probe can be stopped at a fracture location for longer time to measure electrical conductivity of water. At a constant drawdown the EC of groundwater gradually changes to level representative for the fracture. Continuing monitoring several minutes until the EC reading would be stabilised onto a low or high level compared to surrounding borehole, the fracture EC value (and time series) can be stored, and this data further used in groundwater salinity interpretation.

In addition to measuring ground water flows from fractures the water coming from fractures can be collected into a container. The water sample collecting process is similar with normal PFL flow logging but when a target fracture has been reached the probe is stopped on the fracture. While the probe is on the fracture and ground water flow coming from the fracture is measured also the electrical conductivity of water is measured. After the flow and EC values are stable valves of the sample container are opened. The measurement of flow and EC are on all the time during water sample collection and when the water contained has been filled with fracture specific water the valves are closed. Selection of a fracture from which sample is taken is based on preceding PFL measurements, and the sampling is a

separate downhole run for each specimen. Container is retrieved after each sampling, and brought to laboratory for more precise analysis.

The basic procedure of collecting a water sample from a water flowing fracture is described above but what are the factors that should be considered when choosing where to take water samples. It is clear that the more the borehole is pumped the larger are the fracture flows and the faster the sample collection is. But how do we make sure the water coming from a fracture really is originally from the same fracture? Estimations of representativeness of fracture specific water can be made based on fracture flow rates in natural conditions.

Example case for selecting fractures for water sampling is presented in *Figure 3*. In this case most of the fracture flows are large and taking water sample looks easy. But what if the borehole has stayed as it is several months after it was drilled. Is it possible that some of the fractures had had flow into the bedrock? This can be cleared up by measuring the fracture flows in unpumped conditions (gray line in *Figure 3*). In this case the fracture at depth of 65 m seems to have flow into the bedrock (triangle pointing up means flow direction from bedrock into a borehole and triangle pointing down flow into bedrock). The flow is not large, only 0.1 l/min, but over time large quantities of water can flow into the fracture. In this case 0.15 l/min flow continuing one month accumulates to total of 6500 litres of water. All this water is originated from other fractures in the borehole. When water sample collection is started flow rates in unpumped and pumped conditions should be known in order to estimate how long pumping period is needed before representative water sample can be taken. In this case it would take more than 4 days to get same amount of water out from the fracture than entered the fracture during a month in natural conditions.

The water sample container maintain the water pressure when brought up therefore possible dissolved gases stay inside the container and can be analysed in a laboratory. The container has been rated up to pressure of 150 bar so it can be used to collect samples from depth between 0 – 1500 m.

Measurement sites

Most of the PFL measurements have been conducted for nuclear waste management companies in Finland and Sweden which means the measurement tools pass the high quality requirements (Ludvigson et al. 2002). In mining industry requirements are a bit different but still high quality results and cost effective measurements are expected. The flow measurement accuracy (ml/h) of PFL tool is always the same so lowering the accuracy requirements doesn't speed up the measurement. But lowering the accuracy in which flowing fractures are localized does speed up the measurement because less flow measurements have to be done per borehole. In 1000 m long borehole 10 000 individual flow measurements are needed to obtain 0.1 m accuracy in fracture localization. While localizing fractures with the accuracy of 1 m requires only 1000 individual flow measurements and actual flow measurement time is 1/10 of the measurement time. Time for moving the probe in the borehole remains the same therefore the entire measurement duration is not reduced according to the same ratio.

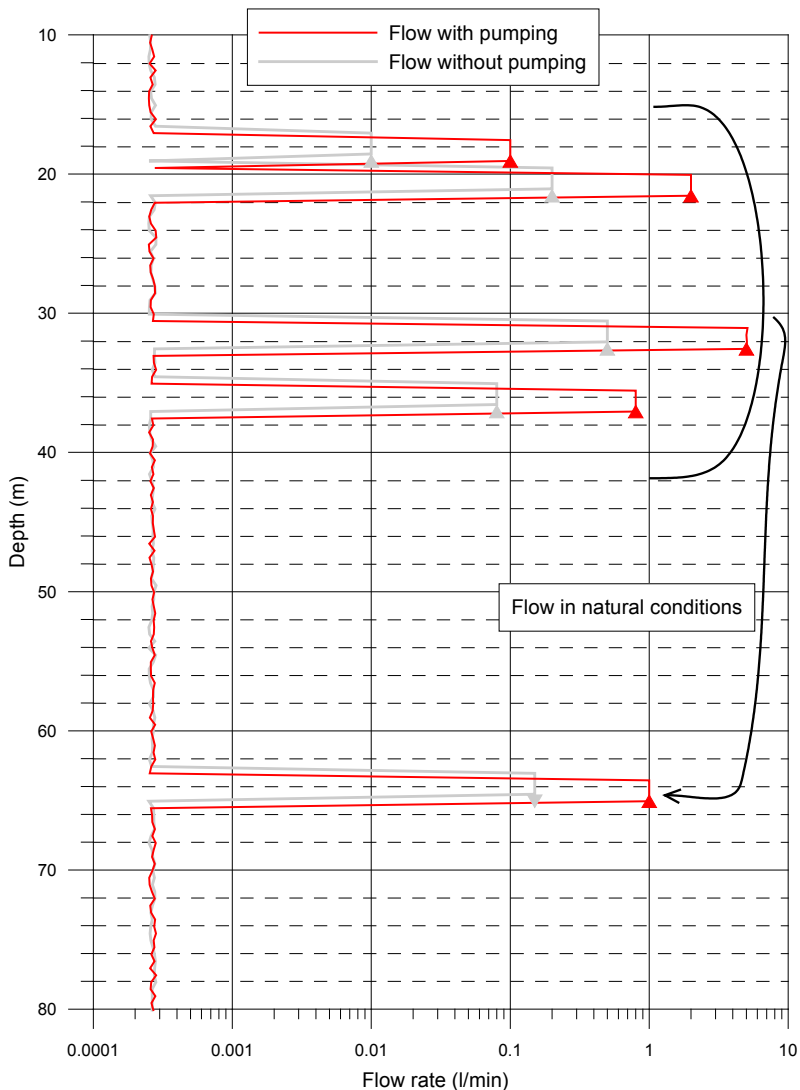


Figure 3 Example of flow conditions in natural conditions. Water from fractures at the upper part of the borehole flow into fracture lower in the borehole.

The PFL equipment is packed in to a trailer which can be taken into different kind of sites. Two examples of measurement sites are presented in *Figure 4*. At Suhanko in Ranua (Gold Fields Arctic Platinum Oy) several boreholes were measured under pumped conditions in 2013. The measurement sites were not accessible with van and trailer so the measurement trailer was lifted on forestry tractor and transported with it. At Nussir mountain in Norway (Nussir ASA) the measurement site located up on a mountain and a bulldozer was used to pull the measurement trailer to the measurement site. Also at Nussir only one measurement run per borehole was conducted in 2016.



Figure 4 Examples of measurement locations. On the left Suhanko (Gold Fields Arctic Platinum Oy) and on the right Nussir mountain (Nussir ASA)

Conclusions

Posiva flow log method is a fast measurement technique to investigate hydraulic conditions in bedrock around a core drilled borehole. The measurement accuracy is high enough for investigations related to high level spent nuclear fuel repository building but the measurement setup can be modified to meet lower accuracy requirements and higher cost efficiency requirements of mining industry. Results have been applied for groundwater management in feasibility assessment stage, and during mining operation.

Water sample collector can be attached to the PFL probe. With the water sampling configuration the measurement is conducted similarly as without water sampler but water sample can be taken at wanted depth and lifted out of a borehole.

Acknowledgements

The author thanks Posiva Oy for cooperation and leasing the measurement equipment for Pöyry to be used in projects that has been conducted for mining companies.

References

- Marsily, G. 1986. Quantitative hydrology, Groundwater Hydrology for Engineers. Academic Press, Inc. London.
- Ludvigson, J-E., Hansson, K. and Rouhiainen, P. 2002. Methodology study of Posiva difference flow meter in borehole KLX02 at Laxemar. SKB Rapport R-01-52.

Hydrogeological investigation of the Witbank, Ermelo and Highveld Coalfields: Implications for the subsurface transport and attenuation of acid mine drainage

Emmanuel Sakala^{1,2}, Francois Fourie², Modreck Gomo², Henk Coetzee¹

¹*Council for Geoscience, Private Bag X112, Pretoria, 0001, South Africa, esakala@geoscience.org.za*

²*Institute of Groundwater Studies, University of the Free State, PO Box 339, Bloemfontein, 9300, South Africa*

Abstract A hydrogeological investigation on coalfield scale was done using available regional data and spatially spaced monitoring boreholes in order to understand the movement of Acid Mine Drainage (AMD) within the soil, vadose zone and aquifers and predict future impacts of surface coal mining activities for planners and regulators. A data-driven GIS artificial neural network was built using hydrogeological and geochemical parameters to produce AMD transport and attenuation factors for the Witbank, Ermelo and Highveld Coalfields. The transport and attenuation factors produced demarcate the coalfields in terms of the expected rates of transport and attenuation of AMD in the subsurface.

Key words Acid mine drainage, vadose zone, soil, transport, attenuation, artificial neural network

Introduction

Mining in South Africa, particularly coal mining, has been the cornerstone for economic development and has contributed significantly to the industrial development of the country. The call to decrease the world's dependence on coal as an energy source is reasonable, since lowering its use would reduce greenhouse gas emissions and environmental impacts associated with coal mining. Considering the benefits of coal mining to the South African economy and the recent global developments focused on the mitigation of environmental problems associated with coal production and use (carbon capture and storage, clean coal technologies and best practice environmental management options for mining and coal waste disposal), it is expected that coal will remain a major component of the South African energy mix for many years.

This paper focuses on coalfield-scale hydrogeological studies on the movement of acid mine drainage within the soil, vadose zone and aquifers. Hydrogeology is useful in understanding the natural subsurface movement and attenuation of Acid Mine Drainage (AMD) and for the future prediction of impacts due to the introduction of AMD on surface by future coal mining activities. The generation of AMD begins with the diffusion of oxygen into moist or wet reactive waste rock, tailings dumps or ore bodies. Sulphide minerals such as pyrite and pyrrhotite found in host rock are then oxidised to form an acidic solution with elevated sulphate concentrations and iron hydroxides. The low pH environment remobilise toxic heavy minerals in solution which can migrate both to the surface and to groundwater resources (Bell 2001).

The study area covers the Highveld, Ermelo and Witbank Coalfields located in the Mpumalanga Province of South Africa, covering an area ~ 23 315 km² (fig. 1). The area receives an

average long-term rainfall of between 600 to 1100 mm (SAWS 2016). Geological information used in this study is based on the 1:250 000 geological maps published by the Council for Geoscience (fig. 1). The study area consist eight major lithological domains namely; the Basement Complex, Witwatersrand Supergroup, Transvaal Supergroup, Bushveld Complex, Dwaarsfontein Complex, Waterberg Group, Karoo Supergroup and Tertiary–Quaternary alluvial deposits. Du Toit and Sonnekus (2014) used geology to classify aquifers within the study area into four types (intergranular, fractured, intergranular-fractured and karst). The intergranular-fractured aquifer type is the most dominant type found within the Witbank, Ermelo and Highveld Coalfields and is very shallow, ranging between depths of 5 m and 20 m, making it susceptible to pollution due to coal mining (Hodgson and Krantz 1998). This high susceptibility to pollution necessitates an understanding of the processes that controls the movement and attenuation of AMD, as well as delineating spatially areas where these processes can occur.

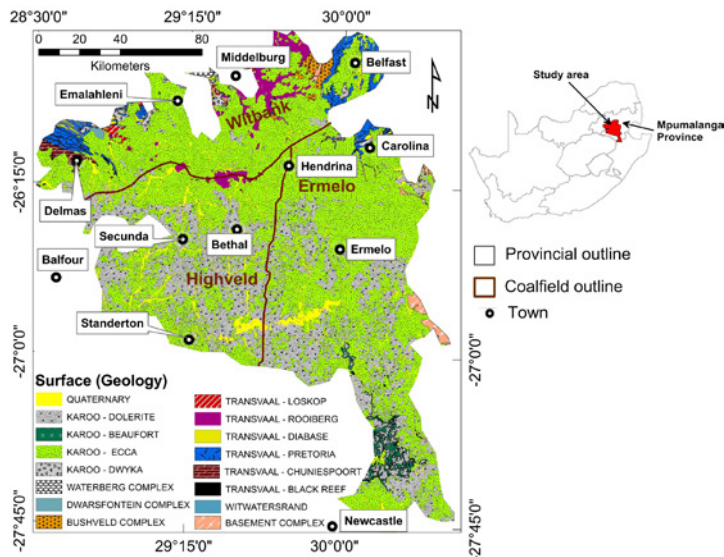


Figure 1 Geological setting of the study area (CGS 2017).

The aquifer system itself plays a role in transport and attenuation of AMD through processes such as dilution and other physical and chemical processes where its hydraulic conductivity controls the ease with which pollution migrate through it (Aller et al. 1987). Values for hydraulic conductivity for the various aquifers in the study area were extracted from Barnard (2000) with the fractured and intergranular-fractured types in the order of 10^{-11} , karst 10^{-4} and intergranular sandy aquifer in the order of 10^{-2} m/s.

Materials and Methods

Factors that affect AMD transport and attenuation in soil, vadose zone and aquifer were investigated in this paper. Data relating to the selected factors (soil clay content, soil thickness, preferential pathways (faults, fractures), vadose zone permeability and aquifer hy-

draulic conductivity) which are readily available at coalfield-scale from various government agencies was used. This paper deals only with AMD from surface sources (tailing dumps, waste-rock discard dumps) where soils control the initial transport of AMD pollution but does not deal with underground and opencast pits sources. Aquifers underlying soils with physical, chemical and biological properties that promote the sorption of pollutants are considered less vulnerable to pollution (Mongwe and Fey 2004). The permeability and infiltration rates of soils are affected by various processes like roots, soil fauna, soil types and degree of compaction related to land-use. In this paper, only the soil clay percentage was used as clay plays a vital role in pollution sorption processes. Soils with high clay content have small pore spaces that reduce permeability and infiltration rates (Mongwe and Fey 2004) which in turn increase the residence time for adsorption of pollution. Of particular importance for water quality of percolation seepage into the subsurface and groundwater is the cation exchange capacity as well as the buffer capacity and pH of the soil. According to soil studies by Lambooy (1984), there is strong positive correlation between clay content and cation exchange capacity for South African soils. For the study area, soil pH and buffering capacity could not be obtained that covers the entire coalfields, hence only clay content was used. Soil data covering the study area at a scale of 1:250 000 was obtained from the Agricultural Research Council Institute for Soil, Climate and Water (ARC-ISCW 2015).

The vadose zone is the unsaturated zone between the surface and the water table which controls the residence time available for the subsurface to interact with the water and pollution. The larger the thickness and the lower permeability of the vadose zone, the higher the possibility of natural attenuation of the pollutants. The vadose zone thickness is referred to as the depth to water table in this paper which was generated from monitoring boreholes from the South African Department of Water and Sanitation (NGA 2015). On a regional scale, zones of weakness within the subsurface include regional faults and fractures which can offer easy passage of pollutants. Information on these geological features was extracted from geological maps and geophysical interpretation maps published by Council for Geoscience on a scale of 1:250 000 (CGS 2017). Reactivity of rocks with AMD is another parameter considered as different rocks react differently in AMD environment. Various laboratory studies (column leach test, XRD and XRF) and kinetic simulations conducted on different types of rocks, revealed that rocks containing carbonate minerals (dolomites) buffer the acidity better than rocks without these minerals, such as silicate rocks (Lapakko 1994).

In selecting the parameters to be used for modelling, spatial association between the available map layers and boreholes with sulphate concentration (> 200 mg/L) was done. This was done based on the assumption that only those parameters which are spatially associated with high sulphate boreholes are somewhat related to AMD transport and attenuation. Spatial association test involves measuring the degree to which things are similarly arranged in space (Carranza 2002). The distance distribution method by Bonham-Carter (1994) was used for the spatial association test. In the method, cumulative frequency distribution curve for each input layer (soil clay content, distance to preferential pathways, aquifer hydraulic conductivity values, depth to water table and AMD-rock reactivity relative value) at every map

location (E) is plotted against the layer value and on the same graph cumulative frequency distribution curve for every high sulphate borehole (O) plotted against the layer value. The difference between these two values at each layer value shows the spatial association where a positive difference ($O > E$) shows positive spatial association, negative difference ($O < E$) shows negative spatial association and no difference ($O = E$) shows independent or no association. According to Carranza (2002), only those layers with an overall positive association are statistically spatially related and negative and/or independent spatial association layers should not be used for modelling geospatial data. Of the six layers tested; soil clay content (fig. 2a), preferential pathways (fig. 2c), vadose zone permeability (fig. 2d), aquifer hydraulic conductivity (fig. 2e), depth to water table (fig. 2f) and AMD-rock reactivity (fig. 2g) show positive difference meaning there is a good positive spatial association with location of boreholes with high sulphate values. The difference curve for soil thickness is negative showing negative spatial association between soil thickness and high sulphate in groundwater (fig. 2b). Based on the spatial association tests, only these parameters that show positive spatial association (clay content, vadose zone permeability, preferential pathways, aquifer hydraulic conductivity, depth to water table and AMD-rock reactivity) were selected for modelling (fig. 3). The transport factor is a term referring to a map product generated by combining selected surface and subsurface properties that controls the movement of AMD. The attenuation factor is a term referring to a map product generated by combining selected surface and subsurface properties that attenuate AMD from reaching the groundwater.

Artificial Neural Networks

Artificial neural networks (ANNs) belong to the data-driven branch of artificial intelligence which is inspired by the biological neural system whereby the computer is trained to do the functions which at the moment humans do best like learning (Shigidi and Garcia 2005).

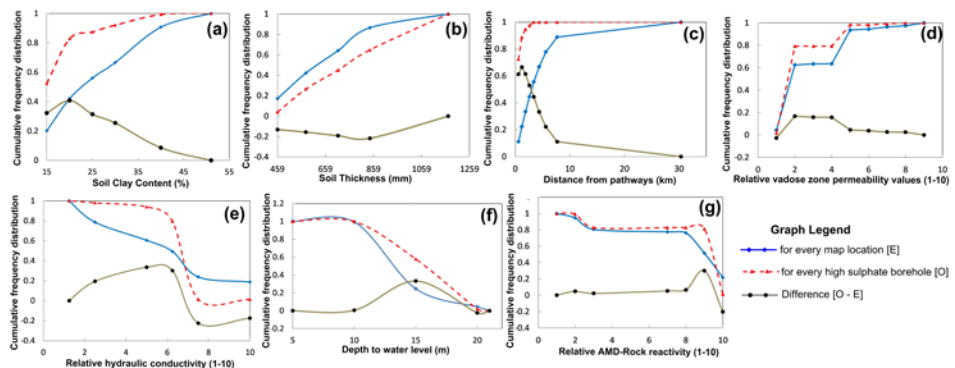


Figure 2 Distance distribution curves for (a) soil clay content (b) soil thickness (c) distance from pathways (d) Vadose zone permeability (e) aquifer hydraulic conductivity (f) depth to water level (g) AMD-Rock reactivity.

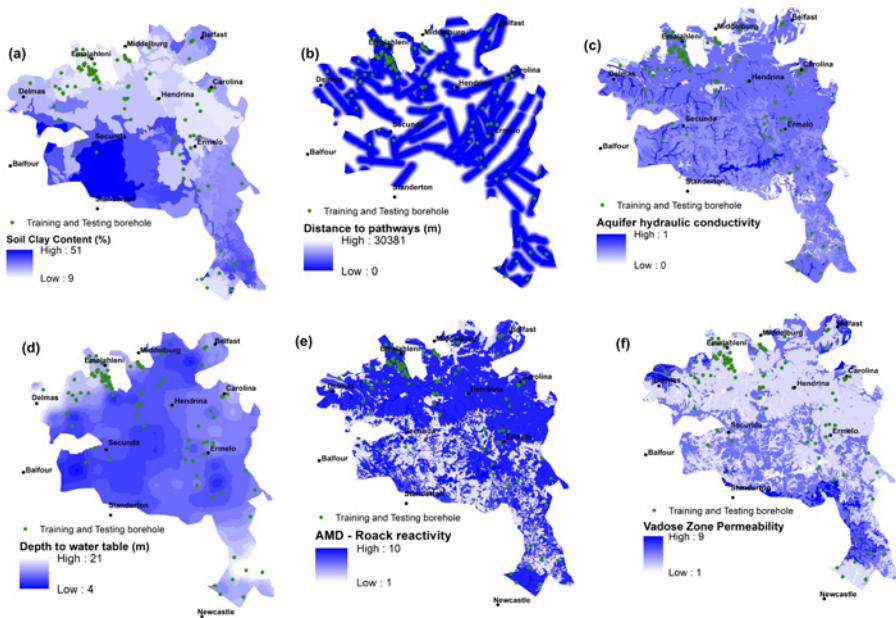


Figure 3 Modelling input parameters (a) soil clay content (b) distance from pathways (c) aquifer hydraulic conductivity (d) depth to water level (e) AMD-Rock reactivity (f) Vadose zone permeability.

The ANNs are trained to extract the general relationship between the input layers and given outputs by giving them a set of examples from which to learn from and store these relationships. After which, the trained ANN is given a set of input layers from which it produces an output based on the stored relationships. The ANNs are made up of input layers that are fed into hidden layers and ultimately connected to the output layer which produces an output response (fig. 4). During training, data is fed into the input layer which communicates to one or more 'hidden layers' where the actual processing is done via a system of weighted 'connections'. ANNs contain some form of 'learning algorithm' which modifies the weights of the connections according to the input patterns that it is presented with (Shigidi and Garcia 2005). In a sense, ANNs learn by example like a child learns to recognize dogs from examples of dogs. In this paper, the learning rule used was the most commonly used learning algorithm; the backpropagation algorithm which basically means that learning is done by backward propagation of the error generated when the training output value is compared with the example output. This process is done repeatedly by modifying the weights until the error is very minimum, thus the ANN would be termed 'trained' and ready for prediction of a correct output from a given a set of new input data. The efficiency in training is dependent on the number of hidden layers. For the study area, the number of hidden layers was estimated using a method by Shigidi and Garcia (2005) and seven hidden layers were found to optimum for both transport and attenuation factors (fig. 4). In the paper, parameters which are spatially associated with high sulphate concentration boreholes (soil clay content, preferential pathways, aquifer hydraulic conductivity) were used as ANN inputs

for the transport factor, while the depth to water table, vadose zone permeability and AMD-rock reactivity were used as ANN inputs for the attenuation factor (fig. 4). In both cases the sulphate concentration in groundwater was used as a training output parameter.

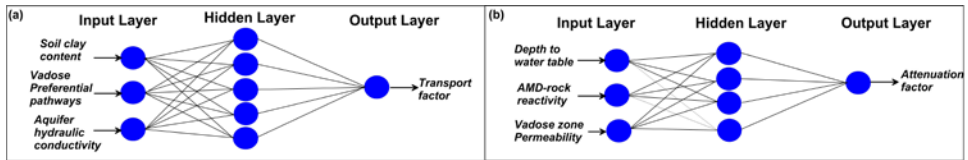


Figure 4 Architecture of the ANN used for a) transport factor and b) attenuation factor.

Results and discussions

The 130 groundwater samples from boreholes scattered throughout the study area were partitioned into 75 % for training and 25 % for testing of the ANN systems. The ANN was trained using sulphate concentration values in groundwater where areas with high sulphate values above 200 mg/l the target quality for drinking water (DWAf 1996) were used as polluted sites and low sulphate values below 200 mg/l as non-polluted training sites. After training, the ANN was used to predict values of the set of boreholes not used in training (testing boreholes). The difference between the predicted and the actual values of the testing samples is the testing error which is used to evaluate the accuracy of the training process and to determine the optimum number of iterations (epochs). The minimum training error of 0.0049 and 0.0034 was archived after 100 epochs for transport and attenuation factors (fig. 5a and 5b). The trained ANNs were then used to generate the transport and attenuation factors for the study area (fig. 5c and 5d).

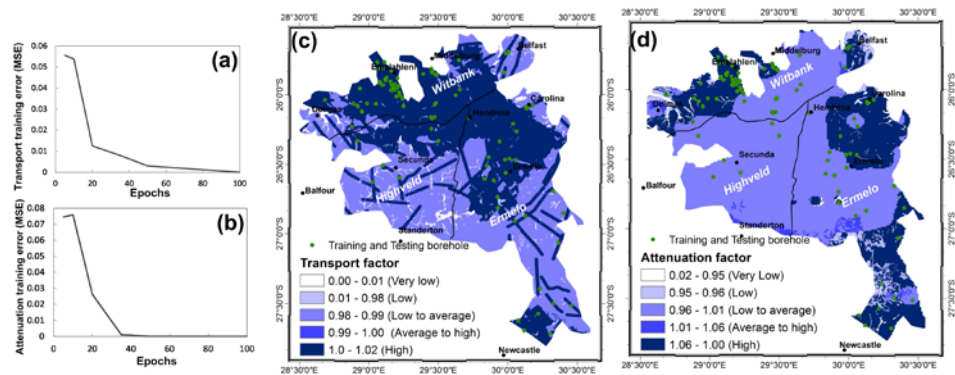


Figure 5 Training graphs for (a) transport factor (b) attenuation factor and modelling results showing the (a) transport factor and (b) attenuation factor.

The transport factor model shows that area between Emalahleni and Ermelo is marked by high transport factor values due to soils with low clay content, high density of pathways coupled with aquifers with higher hydraulic conductivity. Aquifer systems within the high transport factor zones are more susceptible to AMD pollution due to ease of AMD migration. The Delmas, Ermelo, Carolina areas, as well as the southern areas, are marked by high

attenuation factor values due the presence of a thicker vadose zone, higher vadose zone permeability values and rocks with higher AMD-rock reactivity. This means that these parameters together reduce the likelihood of AMD from reach the groundwater, thus to say there is good AMD retention. In general the aquifer systems found in areas with high transport and low attenuation factors are more susceptible to pollution. The transport and attenuation models were validated using dataset which was not used in the modelling process i.e. pH data. Acid mine drainage is associated with high sulphate concentrations and low pH. Data from boreholes within the study area was used to produce a scatter plot of sulphate and pH. The results show a strong negative correlation; hence pH which is a sensitive indicator for AMD was used for model validation fig. 6a). The spatial association test was used to check if the generated models are spatially correlated with boreholes with pH values lower than 5. The spatial associated test reveals a very strong spatial association between pH and both transport and attenuation factors (fig. 6b and 6c).

Conclusion and recommendations

The ANNs were successfully used to produce the transport and attenuation factors for the Witbank, Ermelo and Highveld Coalfields using parameters which show positive spatial association with high sulphate in groundwater. The transport and attenuation factors demarcated areas in terms of the transport and attenuation of AMD in the subsurface. Further field verification is recommended over areas demarcated as high transport and low attenuation factors.

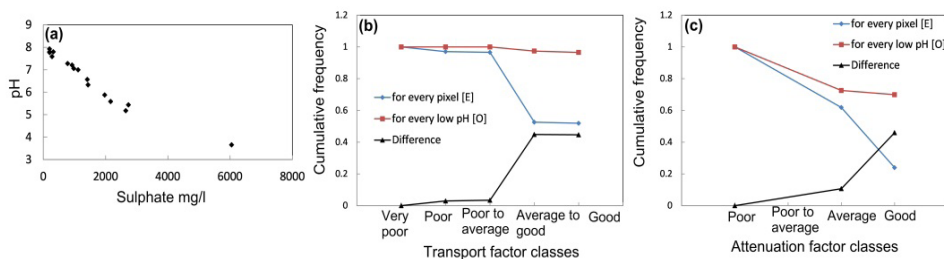


Figure 6 (a) Sulphate – pH relationship, validation results for (b) transport and (b) attenuation factors.

The results can be used to help policy and decision makers to make scientifically informed decisions for future land use planning of the coalfields. The datasets used in this study are readily available from various governmental agencies making the approach cost-effective in evaluating the AMD coalfield-scale subsurface transport and attenuation. The approach developed in this paper can be tested on other coalfields with similar or different hydrogeological settings to determine its robustness. The approach only considers the AMD pollution at a regional scale and cannot be used for a local point sale analysis where a specific site assessment is recommended.

References

- Aller L, Bennet T, Lehr JH, Petty RJ and Hackett G (1987) DRASTIC: A standardized system for evaluating groundwater pollution potential using hydrogeologic settings. U.S. EPA Agricultural Research Council – Institute for Soil, Climate and Water (ARC–ISCW) (2015) Soils of South Africa 1:250 000 scale. Pretoria
- Barnard HC (2000) An explanation of the 1:500000 general Hydrogeological map: Johannesburg 2526
- Bonham-Carter GF (1994) Geographic Information Systems for Geoscientists, Modelling with GIS. Pergamon, Ontario, 398 pp
- Bell FG, Bullock SET, Halbich TFJ and Lindsay P (2001) Environmental impacts associated with an abandoned mine, Witbank coalfield, South Africa. *International Journal of Coal Geology*, 45, 195–216
- Carranza EJM (2002) Geologically-constrained mineral potential mapping: Examples from the Philippines. PhD Thesis. ITC
- Council for Geoscience (CGS)(2017) South African geology database 1:250 000 scale. Pretoria
- Du Toit WH, and Sonnekus CJ (2014) An explanation of the 1:500k hydrogeological map. Nelspruit 2530
- Hodgson FDI and Krantz RM (1998) Groundwater quality deterioration in the Olifants River Catchment above the Loskop Dam with investigations in Witbank Dam Sub-Catchment. WRC# 291/1/98, 272
- Lambooy AM (1984) Relationship between cation exchange capacity, clay content and water retention of Highveld soils. *South African Journal of Plant and Soil*, 1, 33-38
- Lapakko KA (1994) Comparison of Duluth Complex rock dissolution in the laboratory and field. Proceedings of the International Land Reclamation and Mine Drainage Conference and Third International Conference on the Abatement of Acid Mine Drainage, Pittsburgh, PA, 419-428
- Mongwe HG and Fey MV (2004) The buffering capacity of soil materials for various contaminant types and the relationship between soil morphology, chemical properties and buffering capacity: A literature review. WRC report # TT 303/07
- National Groundwater Archive (NGA) (2015) South African national groundwater borehole database, South African Department of Water and Sanitation
- Shigidi A and Garcia LA (2005) Parameter estimation in groundwater hydrology using artificial neural networks. *Journal of computing in civil engineering*, 31, 281-289
- South African Weather Service (SAWS) (2016) Historical Rain Maps, <<http://www.weathersa.co.za/climate/historical-rain-maps>> Accessed: 23 March 2016
- Department of Water Affairs and Forestry (DWAF) (1996) SA Water Quality Guidelines: Domestic Use, 2

Study on Evolution of Mining-induced Crack of Rock Mass Considering Hydromechanical Coupling Effects Based on Stabilized Nano CT Scan

Feng, Feisheng; Du, Wenfeng; Peng, Suping; Xing, Zhen-guo

State Key Laboratory of Coal Resources and Safe Mining, China University of Mining and Technology, Beijing, 100011

Abstract Rocks have different fracture development mechanisms under different circumstances with or without pressure, and under different triaxial confining pressure functions. It is important to research the influence between the development process of internal crack and external factors including different tectonic stress, different water pressure, different pressure rate and so on, realize the randomness and Non-random of crack development, and research the specific development mechanism of crack under a single impact factor.

Key words stabilized Nano CT scan, Mining-induced Crack, Hydromechanical Coupling Effects, maximum major stress

Introduction

In most rock engineering projects, crustal rocks stay in geological environments with fully coupled stress, flow, temperature, and chemical fields for long. In mining and slope engineering projects, the coupling between flow and stress fields is the primary factor controlling the behavior of rock masses. For example, stress field variations can change fractures in a rock mass, such as deformation and growth of pores and fractures, and thereby alter rock permeability and the state of water flow through the rock mass. Meanwhile, changes in fractures can drive the water within them to in turn affect their evolution (Zhang Youtian et al. 2005). The interaction between a rock mass and the water flow in it is referred to as flow-stress coupling.

Rock damage and failure resulting from artificially induced variations in tectonic stress can lead to flow field changes, which have been found as a major cause of engineering accidents and geohazards in practice (Zhu Zhende et al. 2005). Research on development of rock fractures can offer insights into floor rock deformation, damage, and failure as well as geological environments featuring macroscopic coupling. From the perspectives of stress-flow field coupling and engineering practice, the mechanism responsible for fracture development should differ depending on whether there is hydraulic pressure and on the level of confining pressure. Therefore, studying the process of fracture development under varying tectonic stresses, hydraulic pressures and compression rates to determine if fracture development is stochastic or not and the specific mechanism of fracture under the influence of each single factor is of great significance.

Lomize's classical cubic law (Lomize G1951) which deals with the process of water flow in a single fracture, provides a theoretical basis for research on fracture flow. Louis and other scholars (Louis, C et al. 1975) have revised the cubic law through a lot of experiments to

Assume that the distribution pattern and level of abutment pressure at the coal face are constant, and the face's position relative to the x-axis remains unchanged, which means that the abutment pressure and the x-axis, moves horizontally along the y-axis as the face advances. Let y denote the distance traveled by the face along the y-axis. The coordinates of M in the new coordinate system are $(m-y, n)$. Eq. (1) can be rewritten as follows:

$$\left. \begin{aligned} \sigma_x &= -\frac{2}{\pi} \int_{y_1}^{y_2} \frac{p(\xi)m^3 d\xi}{\left[m^2 + (n-\xi)^2\right]^2} \\ \sigma_y &= -\frac{2}{\pi} \int_{y_1}^{y_2} \frac{p(\xi)m(n-\xi)^2 d\xi}{\left[m^2 + (n-\xi)^2\right]^2} \\ \tau_{xy} &= -\frac{2}{\pi} \int_{y_1}^{y_2} \frac{p(\xi)m^2(n-\xi) d\xi}{\left[m^2 + (n-\xi)^2\right]^2} \end{aligned} \right\} \quad (1)$$

The results of calculation can be used to determine the three stress components (XXX) resulting from the abutment pressure increment at M $(x, 100)$ as the face moved forward from 140 m behind M to 260 m in front of it. The horizontal line containing point M, given by $y=100$, was used as the survey line. Eight points were selected from the line, including M1 (40, 100), M2 (35, 100), M3 (30, 100), M4 (25, 100), M5 (20, 100), M6 (15, 100), M7 (10, 100), and M8 (5, 100). The pattern of variation in vertical stress was then derived by substituting the coordinates of these points into Eq. (1) Eq. (1).

According to the results, the stress concentration factors at depths of 5 m, 10 m, 15 m, 20 m, 25 m, 30 m, 35 m, and 40 m in the floor were 2.2, 1.93, 1.73, 1.57, 1.45, 1.35, 1.27, and 1.22, respectively, indicating that the stress concentration factor in the floor decreased with increasing depth. The ratios of vertical stress values at these points to the initial stress were 0.05, 0.1, 0.17, 0.2, 0.24, 0.29, 0.33, and 0.37, respectively, suggesting that the degree of stress relief in the floor decreased with increasing depth of burial.

Permeability of fractured floor rocks

Transient measurement of rock permeability was carried out using the testing system. It is called Electro-Hydraulic Serve controlled Rock Mechanics Testing System, purchased by China University of Mining and Technology from the U.S. instrument manufacturer MTS. The equipment is an advanced rock mechanics testing system for laboratory use. Equipped with three independent closed-loop servo control systems (axial compression, confining pressure, and pore water pressure), it can perform uniaxial (compression) test, pseudo triaxial (compression) test, true triaxial test, pore water pressure measurement, and penetration test. Besides, it can apply loading with different waveforms and at different rates. The vertical compressions on rock and coal samples under test were imposed by the MTS815.02 Electro-Hydraulic Serve controlled Testing System. The displacement and loading rate were kept constant during loading. The sys-

tem was also responsible for collecting real-time data about the vertical loads and deformation experienced by the samples. Fig. 2-4 illustrates how the permeability coefficients of sandstone and mudstone varied with triaxial compression under different confining pressures.



Fig. 2 Figure of Assembling Penetrating Equipment

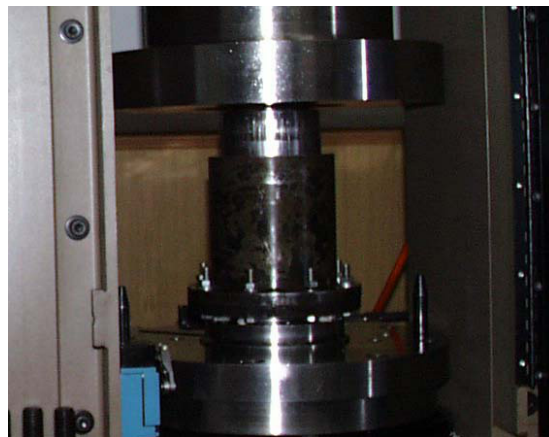


Fig. 3 Penetrating Equipment Is Working

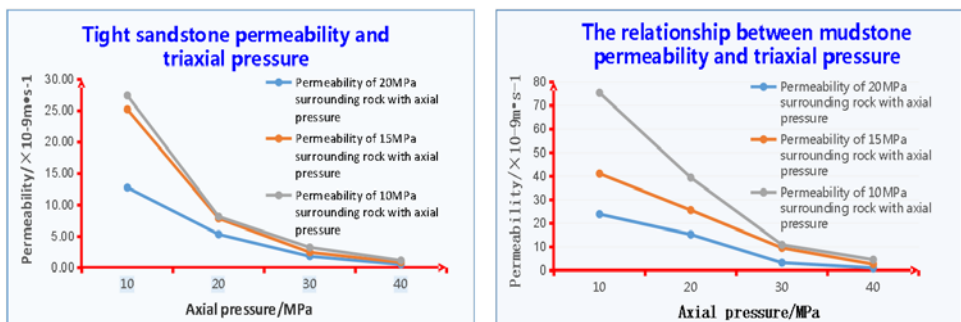


Fig. 4 Relationship between permeability and triaxial compression for sandstone and mudstone

Microscopic analysis of permeability of fractured floor rocks using CT scanning

A micro/nano CT scanning test was carried out using nanoVoxel-3502E (Fig. 5), a test system produced by Sanying Precision Motion Control (Tianjin) Technology co., LTD. It has a resolution of $0.5 \mu\text{m}$ and allows for nondestructive testing. 3D representations of the samples' interior structures were achieved with this system.

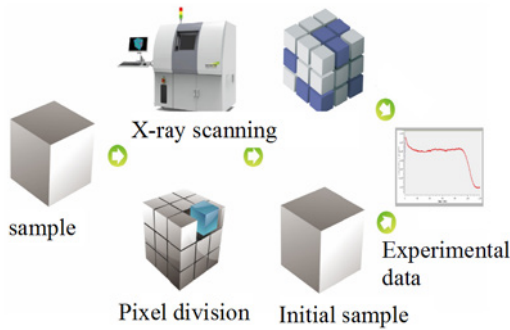


Fig. 5 Schematic of the test system



Fig. 6 Picture of samples

This section studies the samples taken from the floor strata in a coal mine operated by God Warburg Hiller Energy Corporation based on local geological conditions, with a focus on calculation of the samples' porosities and pore volumes and radii, frequency statistics, and extraction of 3D data such as the numbers of pores and throats, pore-to-throat ratio, and areal porosity. Pores in these samples were quantitatively analyzed using the ball-and-stick theory (Fig. 7).

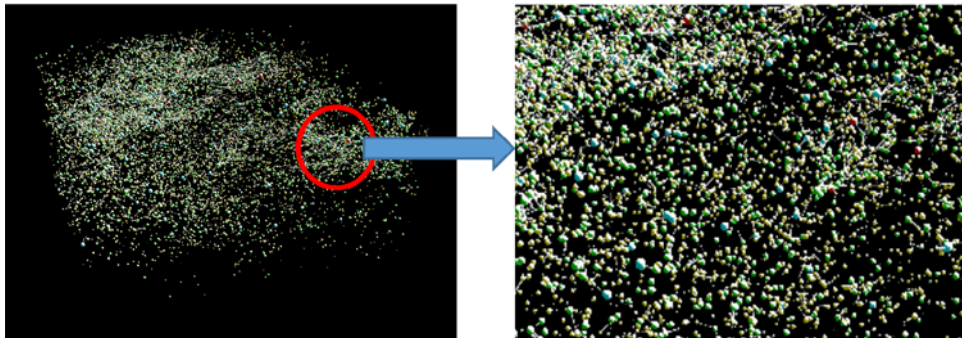


Fig. 7 Schematic of the ball-and-stick

In order to study the mechanism of fracture development on a microscopic scale, we planned to first calculate theoretical hydraulic stress, investigate permeability variation with hydraulic stress by rock mechanics testing, and then compare the results with the microscopic permeability under different stress conditions obtained from real-time scanning. However, due to the extra high precision of the instrument, we encountered many difficulties in improving the instrument. The compression equipment was damaged by excess pressure and is now under repair. The research team is currently trying to develop a real-time Nano-CT scan-

ning test scheme that applies to water-rock coupling conditions and can offer resolutions required for industrial CT scanning. Main results achieved are presented to demonstrate our research progress.

The test scheme encompasses the following steps: micro/nano-scale scanning of the sandstone and mudstone samples, soaking the samples in water for four hours, taking them out for scanning again, soaking the sandstone samples in water for 2 hours and scanning them again. It intends to investigate the influence of water on fractures.

Result analysis: Statistics on pores in mudstone before and after soaking.

Table 1 Statistics on pores in mudstone before and after soaking

Pore volume interval μm^3	Number of pores		Total pore volume μm^3	
	Before soaking	After soaking	Before soaking	After soaking
0– 2.00×10^4		3876	5.60×10^7	5.40×10^7
2.00×10^4 – 5.00×10^4	3620	3455	1.28×10^8	1.22×10^8
5.00×10^4 – 1.00×10^5	3953	3290	2.89×10^8	2.42×10^8
1.00×10^5 – 5.00×10^5	6629	6522	1.51×10^9	1.50×10^9
5.00×10^5 – 1.00×10^6	1585	1541	1.11×10^9	1.09×10^9
1.00×10^6 – 5.00×10^6	1605	1616	3.26×10^9	3.24×10^9
5.00×10^6 – 1.00×10^7	168	167	1.16×10^9	1.16×10^9
1.00×10^7 – 5.00×10^7	80	87	1.47×10^9	1.55×10^9
more than 5.00×10^7	7	10	7.72×10^8	1.20×10^9

Table 2 Statistics on pores in tight sandstone before and after soaking

Quantitative analysis of pore size		Porosity	Total number of pores	Maximum equivalent diameter/ μm	Average equivalent diameter/ μm	Maximum pore volume/ μm^3	Average pore volume/ μm^3
4h	1.010%	55503	1054.2	87.9	6.13×10^8	9.44×10^5	
6h	0.713%	35109	923.35	94.58	4.12×10^8	1.05×10^6	

The analysis reveals that the mudstone's porosity increased with the duration of soaking.

The numbers of small pores, ranging between 0– $1.00 \times 10^6 \mu\text{m}^3$ in volume, decreased after 4 hours of soaking. The numbers of large pores, ranging from 1.00×10^6 to $5.00 \times 10^7 \mu\text{m}^3$ in

volume, did not change or increased as the duration of soaking increased. Fractures in the mudstone gradually disappeared during soaking.

The statistics on the sandstone's porosity before and after soaking are presented below. As shown in the figure, after soaking, small pores in the sandstone decreased in both number and total volume, while large pores increased in both number and total volume.

Based on the data from the scanning test, a numerical model was constructed to simulate the flow through it. The permeability coefficient predicted by the model was $15.3 \times 10^{-9} \text{ m} \cdot \text{s}^{-1}$.

Conclusions

The three-dimensional rock stress at a selected position was theoretically calculated. Rock permeability values under different 3D stresses were measured by rock mechanics testing and the patterns of permeability variation with stress were analyzed. After that, micro/nano CT scanning was performed on the rock samples to examine the statistical regularity in pore and throat data and their relationships with the flow through the rocks.

(1) A semi-infinite elastic mechanical model for determining stress distribution in a mine floor was created by additional stress calculation. Triaxial compressions at different locations in the floor were theoretically obtained. The results show that the degree of stress relief decreased as the burial depth increased.

(2) A rock mechanics test was performed on the rock samples using MTS815.02 Electro-Hydraulic Serve controlled Rock Mechanics Testing System. The test results reveal the pattern of permeability variation with and the ratio of confining pressure to axial compression.

(3) 3D representations of test samples' interior structures were realized by micro/nano CT scanning. Quantitative analysis and space inversion of pores within the samples were performed using the ball-and-stick theory.

Acknowledgements

Financial supports from the State Key Research Development Program of China (2016YFC0501100) and Natural Science Funds Project (Grant No.51604007) are greatly appreciated.

References

- Zhang Youtian (2005) Rock Hydraulic Engineering and Engineering. China Water Conservancy and Hydropower Press, Beijing,482pp
- Zheng Shaohe,Yao Hailin,Ge Xiurun (2004) Coupling analysis on seepage and damage in fractured rock mass. Chinese Journal of Rock Mechanics and Engineering 09:1413-1418.
- WANG Xi-liang,PENG Su-ping,ZHENG Shi-shu (2004) Controlling and predicting water inrush with high pressure in deep mining.Journal of Liaoning Technical University 06:758-760.
- Zhu Zhende,Sun Jun (1999) Coupled Analysis Model of Seepage Field and Damage Field in Fractured Rock Mass and Its Engineering Application. journal of yangtze river scientific research institute 05:22-27.
-

- YANG Tianhong, TANG Chun-an, TAN Zhihong, ZHU Wancheng, FENG Qiyan (2007) State of The Art of Inrush Models in Rock Mass Failure and Developing Trend for Prediction and Forecast of Groundwater Inrush. *Chinese Journal of Rock Mechanics and Engineering* 02: 268-277.
- Lomize, G (1951) Flow in fractured rocks. Gosenergoizdat, Moscow, 1951, 127.
- Louis, C (1975) Rock hydraulics: Report. BRGM, ORLEANS, FRANCE, NO. 74 SGN 035 AME, 1974 *International Journal of Rock Mechanics and Mining Sciences & Geomechanics Abstracts* 12(2): 59.
- Jones Jr, F. A laboratory study of the effects of confining pressure on fracture flow and storage capacity in carbonate rocks[J]. *Journal of Petroleum Technology* 27(1): 21-27.
- GAO Yubing, LIU Shiqi, LYU Bin, LI Kunqi (2016) Mechanism study of floor water inrush around mining field based on micro-crack extension *Journal of Mining & Safety Engineering* 04:624-629.
- Wang Yong – hong, Shen Wen (1996) Prevention and Control of Water Hazards in Coal Mines in China[M]. Beijing: Coal Industry Press. 366pp
- Chen Zhanqing, Yu Bangyong (2015) Advances in seepage mechanics of mining rock mass[J]. *Journal of Southwest Petroleum University (Natural Science Edition)* 03:69-76.
- Purcell W R (1949) Capillary pressures—Their measurement using mercury and the calculation of permeability therefrom. *Journal of Petroleum Technology* 1(2):39-48.
- Thomeer J H M (1960) Introduction of a pore geometrical factor defined by the capillary pressure curve. *Journal of Petroleum Technology* 12(3):73-77.
- Oda, M., Katsube, T., Takemura, T (2002) Microcrack evolution and brittle failure of Inada granite in triaxial compression tests at 140 MPa. *Journal of Geophysical Research* 107(B10).

Downstream geochemistry and proposed treatment – Bellvue Mine AMD, New Zealand

Dave Trumm¹, James Pope², Rae West³, Paul Weber⁴

¹*CRL Energy, 97 Nazareth Avenue, Middleton, Christchurch 8540, d.trumm@crl.co.nz*

²*CRL Energy, 97 Nazareth Avenue, Middleton, Christchurch 8540, j.pope@crl.co.nz*

³*Taranaki Regional Council, 47 Cloten Road, Private Bag 713, Stratford 4352, rae.west@trc.govt.nz*

⁴*O'Kane Consultants (NZ) Ltd, PO Box 8257, Christchurch 8440, pweber@okc-sk.com*

Abstract Geochemical modelling can predict how treatment of one AMD feeding into a complicated system with multiple AMD sources may change the downstream chemistry and, hence, the potential for an aquatic ecosystem to recover. Current chemistry and flow rates for two AMDs and the receiving streams were correlated with precipitation to identify changes in acid loads and resulting effects on streams during and between precipitation events. Geochemical modelling was then used to predict resulting acid load in streams during and between precipitation events if only one of the AMD sources was treated.

Key words Acid mine drainage, modelling, passive treatment, mussel shells, diversion well, Bellvue Mine

Introduction

Many countries have abandoned mines programmes for assessment and remediation of acid mine drainage (AMD), however, no such programme exists for New Zealand. As part of a research grant focused on understanding and managing environmental impacts of mining in New Zealand, the Centre for Minerals Environmental Research (CMER) is planning remediation of AMD at the abandoned underground Bellvue Coal Mine, West Coast, New Zealand. This project contains methodologies that could be applied to abandoned AMD sites throughout New Zealand.

Previous work found that the Bellvue AMD, and several additional AMD sources downstream, discharge into the nearby Cannel Creek, resulting in significant impact (Trumm and Cavanagh 2006). Approximately 62% of the impact to the creek was found to be caused by the Bellvue AMD, 33% of the impact from the abandoned James Mine AMD (located 550m downstream of the Bellvue Mine) and the remaining 5% from the abandoned Jubilee Mine AMD (located 10m downstream of the Bellvue Mine).

Small-scale remediation trials were completed to identify a suitable remediation technique for the AMD (West 2014); based on this work, an up-flow mussel shell reactor has been selected as the remediation solution. Prior to installation of the system, a geochemical conceptual model was developed to understand the current conditions in Cannel Creek from the two major AMD sources, the Bellvue Mine AMD and the James Mine AMD, to predict how treatment of the Bellvue AMD will change the conditions downstream in Cannel Creek and to ensure treatment will achieve suitable water quality targets. The conceptual model is presented in this work.

Methods

Flow rates were measured in Cannel Creek and James Creek (a tributary to Cannel Creek 150m downstream of the James Mine) using a SonTek FlowTracker. Flow rates were measured in the two AMD sites using a bucket and stopwatch method. An Intech WT-HR 1m datalogger was installed in the Bellvue Mine adit and recorded water height every 30 minutes; these data were correlated with measured flow rates from the AMDs to expand flow rate data. Precipitation data were obtained from the NIWA climatic station Greymouth Aero; these data were correlated with measured flow rates in the streams to expand flow rate data across the timeframe of the datalogger data from the mine pool. Field measurements were collected from the two AMD sources, Cannel Creek and James Creek, using a portable YSI 556 multi-probe system. Samples were collected for laboratory analyses and analysed for major chemical parameters, including pH, acidity, alkalinity, sulphate and metals using APHA methods (APHA 2005).

Geochemical modelling was completed on mixed solutions using PHREEQC (version 2) (Appelo and Parkhurst 1999). In all cases, the model was first run to determine the saturation index of Al-bearing minerals and Fe-bearing minerals. If Gibbsite or Schwertmannite were found to be above saturation, the model was then run again, specifying that these minerals would be at equilibrium with the final solution. In these cases, the resulting pH and metal concentrations were always lower. It is likely that true values lie somewhere between these two extremes for each case.

Results

Bellvue AMD flow rates range between 0.041 L/s and 30.3 L/s with an average of 0.93 L/s. The data is characterised by low base level flows with short duration spikes where flow rates first increase rapidly and then decline back to base level at a somewhat slower rate. Ninety-two percent of the flow rates are less than 2 L/s, with 47% below 0.5 L/s. Flow rates from the James Mine AMD range from 0 L/s to 6.0 L/s with an average of 0.14 L/s and there is a linear correlation between the two AMDs. Flow rates were less than 0.40 L/s 95% of the time and less than 0.06 L/s 50% of the time. Flow rates for Cannel Creek range from 2.7 L/s to a maximum of 3,831 L/s with an average of 50 L/s. Flow rates are characterised by a baseline level with short duration, high flow rates during storm events. Eighty percent of the flow rates are less than 50 L/s, 17% range from 50 to 300 L/s, and 3% are greater than 300 L/s. James Creek shows flow rates 20% to 50% of that measured in Cannel Creek.

The flow rate in Cannel Creek, upstream of Bellvue Mine, does correlate to the flow rate of the AMD, suggesting that high flow rates during storm events are not synchronised between the two. During storm events, the flow rate in Cannel Creek peaks approximately 24 hours after maximum precipitation and the flow rate in the AMD peaks an additional 24 hours later. While the AMD flow rate peaks, the flow rate in Cannel Creek has already begun to decline, and can reach baseline levels while the AMD flow rate is still elevated. The relationship of flow rates in Cannel Creek and James Creek to the James Mine AMD shows the same pattern.

The Bellvue Mine AMD has a pH of 2.28-3.01, 69 mg/L Fe, 39 mg/L Al, 0.76 mg/L Mn, 0.32 mg/L Zn and 0.15 mg/L Ni. Water quality does not dilute significantly with increase in flow rate, resulting in an increase in acid load with increase in flow rates (from 6.9 to 918 kg/d). The James Mine AMD has a pH of 2.41-2.80, 148 mg/L Fe, 200 mg/L Al, 6.5 mg/L Mn, 1.21 mg/L Zn and 0.56 mg/L Ni. Similar to the Bellvue Mine AMD, water quality does not dilute significantly with increase in flow rates, and acid load increases with increased flow rate (from 0 to 899 kg/d). A comparison of the acid loads to Cannel Creek from the two AMD sources across the range of flow rates shows that the Bellvue AMD contributes relatively more acidity at low flow than at high flow. At 0.10 L/s, the Bellvue AMD contributes 90% of the sum of the two acid loads. At a flow rate of 1.2 L/s, Bellvue contributes 60% and at a flow rate of 2 L/s, the contribution from Bellvue is only 58%. Since flow rates are less than 1.4 L/s 77% of the time, then the relative contribution to Cannel Creek from Bellvue is mostly 60 to 90% and from the James Mine is mostly 10 to 40%.

Upstream of the AMDs, Cannel Creek has a pH of 4.60-7.28, 0.29 mg/L Fe, 0.14 mg/L Al, and an alkalinity of 3.0-25 mg/L. Downstream of the Bellvue Mine AMD, Cannel Creek has a pH 2.76-4.30, 6.49 mg/L Fe, 5.91 mg/L Al, and 83.4 mg/L acidity. Downstream of the James Mine AMD, Cannel Creek has a pH of 3.11-3.75, 3.3 mg/L Fe, 4.3 mg/L Al, and 42 mg/L acidity. Water quality dilutes with increase in flow rate, however there is some scatter in the data due to the asynchronous flow rates between Cannel Creek and the AMDs during storm events resulting in variable acid load reporting to Cannel Creek. James Creek has a pH of 7.06-7.14, 0.27 mg/L Fe, 0.131 mg/L Al, and 25 mg/L alkalinity. Downstream of the confluence with James Creek, the water chemistry in Cannel Creek improves to a pH of 3.25-4.32, 2.1 mg/L Fe, 3.3 mg/L Al, and 26.4 mg/L acidity.

The asynchronous pattern of the flow regimes in Cannel Creek and the Bellvue AMD during precipitation events has been analysed to determine relative flow rates to be used for geochemical modelling of current stream chemistry and predicted chemistry post treatment of the Bellvue Mine AMD. Data show that for approximately 49% of the time, there has been no precipitation in the previous 24 hours and both Cannel Creek and the AMD are at base flow conditions. The modelled flow rates for this category are 2.7 L/s for Cannel Creek and 0.5 L/s for the AMD. For the remaining 51% of the time, Cannel Creek and the AMD are influenced by precipitation events. These precipitation events have been placed into five categories as follows:

- (a) Start of Precipitation: Cannel Creek is at moderate flow; AMD is at base flow
- (b) Middle Precipitation-1: Cannel Creek is at high flow; AMD is at moderate flow
- (c) Middle Precipitation-2: Cannel Creek is at high flow; AMD is at high flow
- (d) End Precipitation-1: Cannel Creek is at moderate flow; AMD is at moderate flow
- (e) End Precipitation-2: Cannel Creek is at base flow; AMD is at moderate flow

The results of the modelling predict a current pH of 2.95-4.76 in Cannel Creek downstream of the Bellvue AMD, depending on relative flow rates of the stream and the AMD and de-

pending on if Fe and Al minerals are at equilibrium with the water (tab. 1). The lowest pH and highest metal concentrations occur at the very end of precipitation events, when Cannel Creek is near base flow conditions and the AMD is still at moderate flow (“e” category). The next lowest pH occurs during low flow conditions between precipitation events (“No Precipitation” category). The next lowest pH condition also occurs near the end of precipitation events when moderate flow in Cannel Creek is influenced by moderate flow from the AMD (“d” category). The other three modelled conditions, during the start and middle of precipitation events when the flow rate of Cannel Creek is substantially greater than that of the AMD, show relatively high pH in the stream and dilution of metal concentrations reporting from the AMD.

Modelling was completed again for all six flow categories assuming up to 1 L/s of the Bellvue AMD was treated and then discharged to the stream (tab. 2). For the categories where the AMD flow rate was greater than 1 L/s (all flow conditions with the exception of “No Precipitation” and “a” category), the modelling included mixing of the untreated AMD with the treated AMD prior to mixing with Cannel Creek. The results show that overall, 88-91% of the time the pH in Cannel Creek is greater than 5 and 9-12% of the time it is less than 5. The lowest pH is predicted when both Cannel Creek and the AMD are at high flow conditions (“c” category). During this stage, the pH is predicted to be 4.19-4.28. The effects of a typical storm event in the area lasts for approximately three days, from start of precipitation to end of precipitation and return of flow rates to near base level conditions. Once treatment of the Bellvue AMD commences, the category with the lowest resulting pH in Cannel Creek (“c” category) is predicted to last for approximately 13 hours during each storm event and is expected to occur 9% of the time.

Modelling predicts a current pH of 2.87-4.25 in Cannel Creek downstream of the James Mine AMD, depending on relative flow rates of the stream and the AMD and depending on if Fe and Al minerals are at equilibrium with the water (tab. 3). When comparing precipitation categories, the pattern of the severity of impact on pH to Cannel Creek is identical to that from the Bellvue Mine AMD. The lowest pH and highest metal concentrations occur at the very end of precipitation events.

Once treatment of up to 1 L/s of the Bellvue AMD begins, modelling predicts that overall, 49% of the time the pH in Cannel Creek downstream of the James Mine AMD is greater than 5, 29% of the time the pH is between 4 and 5, and 22% of the time the pH is between 3 and 4 (tab. 4). The lowest pH is predicted for the “e” category. During this stage, 1 L/s of Bellvue AMD is being treated but 0.5 L/s is not being treated and 0.25 L/s of James Mine AMD is discharging to Cannel Creek, and the resulting pH is 3.30-3.47. During a typical storm event, this category is predicted to last for approximately four hours and is expected to occur only 3% of the time.

Modelling predicts a current pH of 2.98-6.49 in Cannel Creek downstream of James Creek, depending on relative flow rates of the two streams and the two AMDs and depending on if

Fe and Al minerals are at equilibrium with the water (tab. 5). When comparing precipitation categories, the pattern of the severity of impact on pH to Cannel Creek is identical to that from the Bellvue Mine AMD and James Mine AMD. The lowest pH and highest metal concentrations occur at the very end of precipitation events.

Once treatment of up to 1 L/s of the Bellvue AMD begins, the results show that overall, 78% of the time the pH in Cannel Creek downstream of the tributary is greater than 6, 19% of the time the pH is between 4 and 6 (as high as 5.29), and 3% of the time the pH is between 3 and 4 (tab. 6). The lowest pH is predicted for the “e” category, when Cannel Creek and James Creek have returned to near base-flow flow rates and both the Bellvue Mine AMD and James Mine AMD are still flowing at moderate flow rates.

Table 1 Modelling results for Cannel Creek below Bellvue AMD under current conditions.

Frequency	Condition	Cannel Creek flow (L/s)	Bellvue AMD flow (L/s)	Cannel Creek (just above and just below Bellvue Mine)									
				pH		Fe		Al		Alkalinity			
				Upstream	Downstream	Upstream	Downstream	Upstream	Downstream	Upstream	Downstream		
49%	no precipitation start	base flow	2.7	base flow	0.5	6.09	3.25	0.30	12.7	0.09	6.64	12.76	0
							3.06		2.16		6.64		
18%	precipitation middle	moderate flow	25	base flow	0.75	5.29	4.31	0.25	2.58	0.14	1.37	9.12	0
							4.11		0.067		1.37		
11%	precipitation-1 middle	high flow	100	moderate flow	1.5	5.12	4.76	0.33	0.81	0.23	0.56	3.94	0
							4.45		0.04		0.27		
9%	precipitation-2 middle	high flow	100	high flow	5	5.12	3.96	0.33	1.71	0.23	1.42	3.94	0
							3.86		0.11		1.42		
10%	precipitation-1 end	moderate flow	25	moderate flow	1.5	5.29	3.92	0.25	3.12	0.14	2.11	9.12	0
							3.77		0.15		2.11		
3%	precipitation-2 end	base flow	3.5	moderate flow	1.5	6.09	3.09	0.30	14.6	0.09	9.97	12.76	0
							2.95		4.86		9.97		

Table 2 Modelling results for Cannel Creek below Bellvue AMD assuming 1 L/s treatment of Bellvue AMD.

Frequency	Condition	Cannel Creek flow (L/s)	Bellvue AMD flow (L/s)	Cannel Creek (just above and just below Bellvue Mine)									
				pH		Fe		Al		Alkalinity			
				Upstream	Downstream	Upstream	Downstream	Upstream	Downstream	Upstream	Downstream		
49%	no precipitation start	base flow	2.7	base flow	0.5	6.09	6.04	0.3	0.89	0.09	0.16	12.76	43
							6.03		0.002		0.0004		41
18%	precipitation middle	moderate flow	25	base flow	0.75	5.29	5.46	0.25	0.36	0.14	0.15	9.12	15
							5.44		0.006		0.002		14
11%	precipitation-1 middle	high flow	100	moderate flow	1.5	5.12	5.09	0.33	0.33	0.23	0.28	3.94	4
							4.95		0.01		0.01		2
9%	precipitation-2 middle	high flow	100	high flow	5	5.12	4.28	0.33	1.02	0.23	1.18	3.94	0
							4.19		0.05		1.18		0
10%	precipitation-1 end	moderate flow	25	moderate flow	1.5	5.29	5.25	0.25	0.24	0.14	0.43	9.12	8
							5.14		0.01		0.01		6
3%	precipitation-2 end	base flow	3.5	moderate flow	1.5	6.09	5.63	0.3	0.22	0.09	1.53	12.76	8
							4.83		0.01		0.09		0

Table 3 Modelling results for Cannel Creek below James Mine AMD under current conditions.

Frequency	Condition	Cannel Creek flow upstream of James Mine	James Mine AMD flow (L/s)	Cannel Creek (just above and just below James Mine)									
				pH		Fe		Al		Alkalinity			
				Upstream	Downstream	Upstream	Downstream	Upstream	Downstream	Upstream	Downstream		
49%	no precipitation start	base flow	3.2	base flow	0.06	3.06	3.02	2.16	5.1	6.64	10.5	0.00	0
							3.00		3.38		10.5		
18%	precipitation middle	moderate flow	25.8	base flow	0.1	4.11	3.94	0.07	0.66	1.37	2.20	0.00	0
							3.90		0.10		2.20		
11%	precipitation-1 middle	high flow	102	moderate flow	0.25	4.45	4.25	0.04	0.34	0.27	0.70	0.00	0
							4.22		0.06		0.70		
9%	precipitation-2 middle	high flow	105	high flow	0.95	3.86	3.65	0.11	1.59	1.42	3.39	0.00	0
							3.60		0.24		3.39		
10%	precipitation-1 end	moderate flow	26.5	moderate flow	0.25	3.77	3.60	0.15	1.63	2.11	4.08	0.00	0
							3.55		0.28		4.08		
3%	precipitation-2 end	base flow	5	moderate flow	0.25	2.95	2.90	4.86	12.0	9.97	19.5	0.00	0
							2.87		9.47		19.5		

Table 4 Modelling results for Cannel Creek below James Mine assuming 1 L/s treatment of Bellvue AMD.

Frequency	Condition	Cannel Creek flow upstream of James Mine	James Mine AMD flow (L/s)	Cannel Creek (just above and just below James Mine)									
				pH		Fe		Al		Alkalinity			
				Upstream	Downstream	Upstream	Downstream	Upstream	Downstream	Upstream	Downstream		
49%	no precipitation	base flow	3.2	base flow	0.06	6.04	5.59	2.97	0.16	4.01	42.63	29	
							4.99	0.010	0.030	5			
18%	start precipitation	moderate flow	25.8	base flow	0.1	5.46	4.32	0.36	0.15	0.80	14.82	0	
							4.25	0.047	0.80	0			
11%	middle precipitation-1	high flow	102	moderate flow	0.25	5.09	4.45	0.33	0.28	0.41	3.91	0	
							4.40	0.04	0.41	0			
9%	precipitation-2 middle	high flow	105	high flow	0.95	4.28	3.81	1.02	1.18	3.19	0.00	0	
							3.74	0.15	3.19	0			
10%	end precipitation-1	moderate flow	26.5	moderate flow	0.25	5.25	3.98	0.24	0.43	2.02	8.38	0	
							3.89	0.10	2.02	0			
3%	end precipitation-2	base flow	5	moderate flow	0.25	5.63	3.47	0.22	1.53	10.1	8.02	0	
							3.30	0.98	10.1	0			

Table 5 Modelling results for Cannel Creek below James Creek under current conditions.

Frequency	Condition	Cannel Creek flow downstream of	James Creek flow (L/s)	Cannel Creek (just above and just below James Creek)									
				pH		Fe		Al		Alkalinity			
				Upstream	Downstream	Upstream	Downstream	Upstream	Downstream	Upstream	Downstream		
49%	no precipitation	base flow	3.26	base flow	1.35	3.00	3.21	2.5	10.48	7.5	0.00	0	
							3.19	1.24	7.5	0			
18%	start precipitation	moderate flow	25.9	base flow	12.5	3.9	5.30	0.16	2.20	1.52	0.00	0	
							4.40	0.04	0.51	0			
11%	middle precipitation-1	high flow	102	moderate flow	50	4.22	6.49	0.06	0.70	0.08	0.00	5	
							6.45	0.001	0.0004	0			
9%	precipitation-2 middle	high flow	106	high flow	50	3.6	4.42	0.24	3.39	2.35	0.00	0	
							4.23	0.05	2.12	0			
10%	end precipitation-1	moderate flow	26.8	moderate flow	12.5	3.55	4.24	0.28	4.08	2.83	0.00	0	
							4.19	0.05	2.78	0			
3%	end precipitation-2	base flow	5.25	moderate flow	1.75	2.87	3.02	9.47	19.53	14.7	0.00	0	
							2.98	4.59	14.7	0			

Table 6 Modelling results for Cannel Creek below James Creek assuming 1 L/s treatment of Bellvue AMD.

Frequency	Condition	Cannel Creek flow downstream of	James Creek flow (L/s)	Cannel Creek (just above and just below James Creek)									
				pH		Fe		Al		Alkalinity			
				Upstream	Downstream	Upstream	Downstream	Upstream	Downstream	Upstream	Downstream		
49%	no precipitation	base flow	3.26	base flow	1.35	4.99	6.86	0.09	0.06	4.73	7		
							6.88	0.001	0.001	6			
18%	start precipitation	moderate flow	25.9	base flow	12.5	4.25	6.13	0.12	0.80	0.58	0.00	6	
							6.03	0.002	0.0004	3			
11%	middle precipitation-1	high flow	102	moderate flow	50	4.4	6.41	0.04	0.41	0.32	0.00	7	
							6.43	0.001	0.0004	5			
9%	precipitation-2 middle	high flow	106	high flow	50	3.74	4.85	0.15	3.19	2.22	0.00	1	
							4.27	0.04	1.54	0			
10%	end precipitation-1	moderate flow	26.8	moderate flow	12.5	3.89	5.29	0.15	2.02	1.42	0.00	3	
							4.44	0.03	0.54	0			
3%	end precipitation-2	base flow	5.25	moderate flow	1.75	3.3	3.53	0.80	10.13	7.6	0.00	0	
							3.51	0.36	7.6	0			

Discussion

This work shows that the greatest impact to Cannel Creek from the Bellvue Mine AMD and the James Mine AMD occur at the tail end of storm events, when the flow rates in Cannel Creek have returned to near base level but the flow rates in the AMD are still elevated due to the lag in response time to precipitation. This situation may be common for abandoned underground mines that are near the surface and affected by rainfall (through fracturing, etc.), which discharge AMD to surface water streams and may even occur with large overburden dumps. Dilution of the acidity from the AMD by Cannel Creek occurs to some extent during high flow events, however, this is tempered by the increased acid load in the AMD with increased flow.

Once the Bellvue AMD is being treated, the flow conditions which will have the greatest impact on Cannel Creek will no longer be at the tail end of storm events, but rather, will be

during the highest flow events, when a relatively smaller proportion of the AMD is being treated and stream dilution is not adequate. Downstream however, the greatest impact to Cannel Creek from the James Mine AMD will continue to be during the post-storm event periods, even under the Bellvue AMD treatment scenario. This is because no treatment will be undertaken at the James Mine and the post-storm event scenario involves the least dilution effects of the AMD by Cannel Creek. Likewise, recovery of Cannel Creek after the junction with James Creek will be least during these post-storm events. Fortunately, these post-storm event periods only occur three percent of the time and last for approximately four hours each time.

Ideally, pH levels above 4.5 and metal concentrations below 1 mg/L are necessary for the ecology in the stream to recover (Cavanagh et al. 2010). For approximately 49% of the time this condition will be met for the entire Cannel Creek from Bellvue Mine to the junction with the Nine Mile Creek (1.6km). For the other 51% of the time, the section from James Mine to James Creek (150m) will not meet this condition. For approximately 9% of the time the section between Bellvue Mine and the James Mine (550m) will also not meet this condition, and for approximately 3% of the time the section from James Creek to the Nine Mile Creek (890m) will not meet this condition. It is possible that once the ecology has recovered adequately, it can withstand these short duration pulses of acidic water during precipitation events.

The results of this analysis suggest that contingencies for treatment during Bellvue Mine AMD high flow events should be considered to avoid any pH drop in the stream during these events. Likewise, if additional alkalinity can be added to Cannel Creek during post-storm event periods, there would be less of a drop in pH downstream of the James Mine AMD.

Conclusion

The abandoned Bellvue Mine and James Mine both discharge AMD to nearby Cannel Creek. The Bellvue AMD has a pH of 2.28-3.01 and 69 mg/L Fe, 39 mg/L Al, 0.76 mg/L Mn, 0.32 mg/L Zn, and 0.15 mg/L Ni. The James Mine AMD has a much lower flow rate than the Bellvue Mine AMD and has a pH of 2.41-2.80 and 148 mg/L Fe, 200 mg/L Al, 6.5 mg/L Mn, 1.21 mg/L Zn and 0.56 mg/L Ni. Between 60% and 90% of the hydrogen ion acidity contribution from these two sources is from the Bellvue Mine AMD. The water quality in Cannel Creek degrades from near-neutral pH with low metal concentrations to an acidic stream with high metal concentrations. Both AMD sites show a delayed response to precipitation events, resulting in an asynchronous flow rate pattern with Cannel Creek. The greatest impact to Cannel Creek occurs during post-storm event periods, when the AMD flow rates are still elevated but Cannel Creek is returning to base level.

Once planned treatment is installed at the Bellvue Mine, it is expected that the entire length of Cannel Creek from Bellvue to the Nine Mile Creek (1.6km) will be restored to a pH above 5 during low-flow conditions between precipitation events (40% of the time), which should allow the aquatic ecosystem to recover. However, during precipitation events, various sections of Cannel Creek may not meet a minimum recommended pH of 4.5 for a healthy eco-

system. For 9% of the time, the section from the Bellvue Mine to the James Creek tributary (700m) may not meet this condition and for 3% of the time the section from James Creek to the Nine Mile Creek (890m) may not meet this condition. During all stages of precipitation events (51% of the time), the short section between the James Mine and James Creek (150m) is expected to have a pH below 4.5. It is possible, however, that once recovered, the aquatic ecosystem can withstand these short duration pulses of acidic water during precipitation events. As a result of this work, contingencies for treatment during high flow events will be considered.

Acknowledgements

This research was financed by the Ministry for Business, Innovation and Employment, Contract CRL1202 and the Coal Association of New Zealand. We acknowledge the support of Minerals West Coast, the West Coast Regional Council, Solid Energy New Zealand, and the Department of Conservation. Access to the mine sites was provided by MBD Contracting and Solid Energy New Zealand.

References

- APHA (2005) Standard methods for the examination of water and wastewater, American Public Health Association, Washington, DC, 21st edition.
- Appelo CAJ, Parkhurst DL (1999) User Guide to PHREEQC (V.2) A computer program for speciation, batch-reaction, one-dimensional transport, and inverse geochemical calculations. Denver, CO, http://wwwwbrr.cr.usgs.gov/projects/GWC_coupled/phreeqc.
- Cavanagh JE, Pope J, Harding JS, Trumm D, Craw D, Rait R, Greig H, Niyogi D, Buxton R, Champeau O, Clemens A (2010) A framework for predicting and managing water quality impacts of mining on streams: a user's guide. Landcare Research New Zealand Limited, 2010.
- Trumm D, Cavanagh J (2006) Investigation of remediation of acid-mine-impacted waters at Cannel Creek. Landcare Research Contract Report LC0506/169.
- West R (2014) Trialling small-scale passive systems for treatment of acid mine drainage: A case study from Bellvue Mine, West Coast, New Zealand. Unpublished Masters Thesis, Department of Geological Sciences, University of Canterbury, Christchurch, New Zealand.

Restoration measures of an AMD polluted watershed based on mixing and geochemical models

Carlos Ruiz Cánovas, Francisco Macías, Manuel Olías, Rafael Pérez López

University of Huelva, Department of Earth Sciences, Campus El Carmen, Avenida 3 de Marzo s/n, 21007 Huelva, Spain, carlos.ruiz@dgeo.uhu.es

Abstract This work studies the implementation of a simple mixing and geochemical model to assess the adoption of remediation measures in a highly AMD impacted watershed in SW Spain. The model provides a good snapshot of the impact of potential passive treatment plants on the water quality amelioration of this basin. The implementation of these plants in selected sites would reduce notably the level of metals in the watershed (e.g. from 92 to 99% of Fe and Cu). However, this is a preliminary approach and a more detailed study of each mine site is required to obtain a cost-effective restoration of this watershed.

Key words metal pollution, PHREEQC, Fe precipitation, predictive tools

Introduction

The Directive 2000/60/EC of the European Parliament, so-called Water Framework Directive (WFD), established a communitarian frame of action in the scope of water policy, whose main objective was to achieve a good ecological and chemical quality of all European waters by 2015. The WFD allows the deadline prolongation in cases of technical difficulty, when improvements within the timescale would be economically unsustainable and if natural conditions do not foster the timely improvement. This is the case of the Sancho Reservoir (58 Mm³ of storage capacity), located in the Meca River basin, within the Iberian Pyrite Belt (IPB, SW Spain), which is an extreme case of acid mine drainage (AMD) pollution worldwide. The reservoir water quality has suffered a progressive worsening especially since 2007 due to increasing AMD pressure, yielding low pH values (around 3.5) and high levels of sulfate and metals (Cánovas et al. 2016). The WFD fosters the development of new approaches to assess the impacts of restoration measures on the water quality. This assessment has been previously performed by mass balance approach and reactive transport models (e.g. Kimball et al. 2002 and 2009; Runkel et al. 2007). However the methodology employed in these studies may be expensive, complex and time consuming (i.e. tracer injection tests, synoptic samplings, reactive transport modelling). This work studies the implementation of a mixing and geochemical model to assess the adoption of environmental and cost-effective remediation measures.

Methods

Site description

The Meca River basin has an area of 315 km² and partially drains the mining district of Thar-sis (Fig. 1A), one of the largest of the IPB comprising 16 massive sulfide lenses with original reserves of around 133 million tons (Cánovas et al. 2016). The intense mining activities developed especially from the mid-nineteenth century to the late twentieth have left an exten-

sive area of flooded open-pits, galleries, shafts and mining wastes (Fig. 1) that release metals and acidity to the watershed. Prado Vicioso (PV, Fig. 1B) is an underground mine exploited mainly during the 20th century whose acidic leachates together with those arising from surrounding spoil heaps constitute the source of the Meca River. Afterwards, the Meca River collects the drainages from Esperanza deposit (Fig. 1B). The mineral exploitation in this deposit has led to the formation of an open pit, partially filled with mine wastes. The leachates originated from this pit and several waste dumps located to the east are collected in a small dam that subsequently discharges the contaminated water by overflow (sampling point CE, Fig. 1B). Spoil heaps located to the south and southeast of this open pit also release an acidic leachate (sampling point SH, Fig. 1B). Downstream of the Tharsis complex, the Meca River receives the drainages from La Lapilla (sampling point LAP, Fig. 1B). This mine is surrounded by spoil heaps, low grade ore stockpiles and wastes from cyanide heap leaching whose exposure to atmospheric conditions leads to the generation of an acidic drainage.

To the west, there are two AMD-affected streams reaching the Meca River; Tía Sebastiana Creek and Dehesa Boyal Stream which join the Meca River downstream (sampling points DB and TS; Fig. 1A and B). Both water courses are affected by acidic drainages from spoil heaps and underground galleries that worsen irreversibly the water quality. As a result, the Meca River is deeply contaminated by AMD, transporting huge amounts of contaminants to the Sancho Reservoir which has suffered a progressive acidification in the last years (Cánovas et al. 2016).

Sampling and analytical methods

All AMD-sources from the Tharsis and La Lapilla mines were sampled under different hydrologic conditions in order to study the variability of AMD composition. In addition, different non-affected streams (n=4) were also sampled to establish the background chemical composition of freshwaters in the catchment.

Electrical conductivity (EC), pH and oxidation-reduction potential (ORP) were measured *in situ* for all samples using a Crison MM 40+ portable meter. Samples were filtrated through 0.2 µm filter and acidified to pH < 2 immediately after collection, and finally stored at 4°C until analysis. The chemical analysis were undertaken at the Central Research Services of Huelva University using inductively coupled plasma optical emission spectroscopy (ICP-AES; JY ULTIMA 2) on a Jobin Yvon spectrometer to determine major elements and inductively coupled plasma mass emission spectroscopy (ICP-MS; Agilent 7700) for trace elements. Detection limits were 0.2 mg/L for S, 0.1 mg/L for Na, 0.05 for Fe, K, Mg and Si, 0.02 mg/L for Al, Ca and P, and 1 µg/L for trace elements.

Conceptual design of the mixing and geochemical model

An integrated mixing and geochemical model is proposed to predict the water chemistry under two different scenarios; 1) baseline conditions and 2) after restoration measures. The modeling of baseline conditions is only performed for validation purposes by comparing modeled to measured values of different parameters. The mixing model was initiated using

the MIX code (Carrera et al. 2004) to estimate the mixing ratios of each AMD source and the receiving water. The variables must satisfy some conditions to be suitable in mixing models; exhibit a conservative behavior and their values must be significantly different in the extreme components.

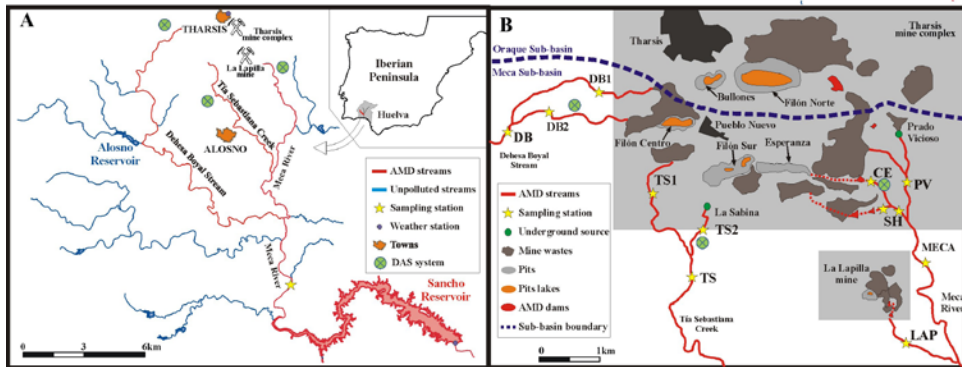


Figure 1 A) Location map of the watershed showing the streams affected by AMD and B) detailed map of main AMD sources in the watershed.

The geochemical model applied to the Odiel River was initiated using the “MIX” data block of the PHREEQC code (Parkhurst and Appelo, 1999), from mixing fractions previously obtained by the MIX code. The model is subsequently improved by applying some geochemical constraints using the “EQUILIBRIUM PHASES” data block, which allows phase assemblages to react with an aqueous solution. These geochemical constraints are based on a previous analysis of the saturation state of main minerals commonly found in AMD environments relative to water samples. In this way, some mineral phases found oversaturated in water were forced to reach equilibrium; i.e. schwertmannite and jarosite for Fe minerals; basaluminite and alunite for Al minerals and gypsum. Equilibrated waters are subsequently mixed with downstream inputs, and so on. Modelled values are compared with those measured in real conditions for validation purposes.

The second step is to perform a mixing model including restoration measures in selected sites. Due to the high acidity and metal content of AMD in the IPB, the restoration measure selected is a passive treatment technology known as Dispersed Alkaline Substrate (DAS), which comprises an inert wood shavings matrix to supply high porosity and reduce the clogging problems, mixed with a fine-grained alkaline reagent to increase the substrate reactivity which induces an increase of water pH after dissolution (Macías et al. 2012; Ayora et al. 2013). As a result of the implementation of DAS technology, an acidic (pH 2-3) and metal-rich drainage (more than 300 mg/L of Fe and Zn and around 100 mg/L of Al) is converted in a near-neutral outflow (pH 7 and alkalinity 250 mg/L of CaCO_3) depleted of metals.

Results and discussion

As can be seen in Figure 2, a good agreement is observed between modelled and measured concentrations of sulfate, Fe and Al ($R^2 = 0.99$). In the case of pH, an acceptable agreement

is observed between modelled and measured values ($R^2 = 0.67$), with a group of samples displaying slightly lower modelled values than measured. This is attributed to the equilibrium condition imposed to waters with respect to Fe oxyhydroxysulfates. The precipitation of these minerals causes the release of protons, giving rise to such differences. Nevertheless, an acceptable validation can be considered according to the simplicity of the model.

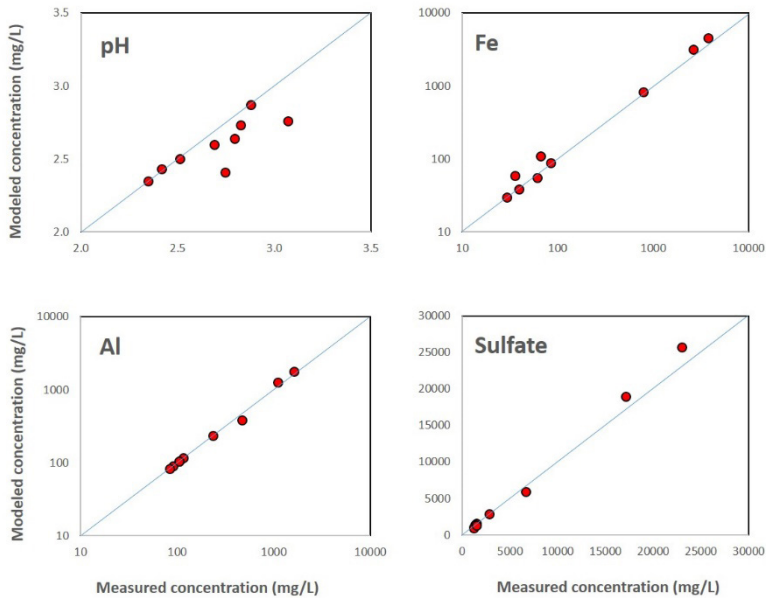


Figure 2 Validation of the model by comparison of modeled and measured values of selected parameters.

Once validated, a second model was performed including the implementation of DAS treatment plants in selected sites. The criteria followed to decide the plant locations were the total contribution of each source and the length of the water course potentially restorable. Table 1 shows the average composition of AMD sources studied and their contribution to the total load released to the Meca River. As can be seen, AMD coming from Corta Esperanza (Fig. 1) is the main contributor of Fe (93%), Zn (90%), acidity (78%), sulfate, Al, Cu and Mn (around 70%). The highest flows are generated from mine galleries and spoils heaps located in the drainage basins of Tia Sebastiana Creek and Dehesa Boyal (TS and DB2; Fig. 1) with average values of 9.2 and 5.5 L/s. Both drainages also constitute around 12% of Al, between 10 and 17% of Cu, 8.6 and 11% of sulfate and 2.2 and 3.5% of total Fe. The pollutant load delivered by the rest of AMD inputs is considerably lower (Table 1).

Taking into account these data, the implementation of a DAS treatment plant in each of these sources (CE, TS and DB2; Fig. 1B) was simulated. The implementation of a DAS treatment plant in the vicinity of Corta Esperanza (CE, Fig. 1) to treat their highly metal-rich effluents (Table 1) causes the removal of around 99% and 97% of total Fe and Zn, respectively, at the end of the river reach (downstream of PV and SH, Fig. 1). Lower removal is

observed for Al (94%), Mn (91%) and Cu (90%) due to the contribution of non-treated effluents downstream of Corta Esperanza (PV and SH, Fig. 1). The lowest removal rate is achieved for sulfate (32%, Fig. 3) due to only a minor fraction of this pollutant is retained in DAS systems by geochemical reactions, i.e. schwertmannite, basaluminite and gypsum precipitation (Macías et al. 2012). Despite the notable removal of pollutants this river reach would not acquire pH values close to neutrality (from pH 2.4 to 3.9; Fig. 3).

Table 1 Average values ($n=3$) of main AMD sources in the study area and contribution to the total load in the watershed.

Sample	Flow L/s	pH	Acidity mg/L CaCO ₃	Al	Cu	Fe mg/L	Mn	Sulfate	Zn
DB1	1.8	3.1	476	38	2.4	112	21	1171	10
DB2	5.5	2.6	2841	351	44	197	59	7822	33
PV	0.4	2.8	1729	255	13	20	46	3116	44
SH	0.7	2.3	2451	283	68	122	33	6405	13
CE	2.7	2.2	30229	2289	259	5576	273	61044	786
TS	9.2	2.6	857	93	18	56	10	1325	6.3
LAP	0.5	2.9	197	54	2.4	15	13	1194	13
<i>Total contribution</i>									
DB1			1.2%	0.90%	0.50%	0.66%	3.4%	1.6%	0.79%
DB2			7.3%	11%	10%	2.2%	16%	8.6%	4.1%
PV			4.5%	2.7%	1.0%	0.13%	3.5%	2.2%	1.8%
SH			6.3%	2.6%	4.8%	0.50%	2.2%	2.1%	0.46%
CE			78%	71%	67%	93%	65%	74%	90%
TS			2.2%	12%	17%	3.5%	9.2%	11%	2.8%
LAP			0.5%	0.70%	0.23%	0.09%	1.4%	1.1%	0.57%

In the case of the effluents reaching the Dehesa Boyal stream (DB1 and DB2), the implementation of a DAS treatment plant in the vicinity of the spoils DB2 (Fig. 1) would remove around 96% and 94% of total Cu and Fe carried by this stream. Lower values were observed for Al (92%), Mn (84%) and Zn (83%; Figure 3). As in the case of the upper reach of the Meca River, only a reduction of 31% in sulfate transport was achieved with the settling of the passive treatment. Notwithstanding, a notable increase in pH values (from 3.9 to 5.7, Fig. 3) would be achieved in this stream after applying restoration measures.

The implementation of a DAS treatment plant in Tia Sebastiana creek to treat the acidic effluents from La Sabina gallery (TS2, Fig. 1) would remove around 92% and 85% of the total Fe and Cu, respectively, carried by the creek. On the contrary, minor amounts of Al (50%), Zn (40%) and Mn (21%) would be removed due to these elements are preferentially delivered by spoil heaps deposited in the vicinity of Filón Centro (TS1, Fig. 1). As a result, pH values would increase from 2.6 to 5.1 in this creek after the implementation of the treatment system (Fig. 3).

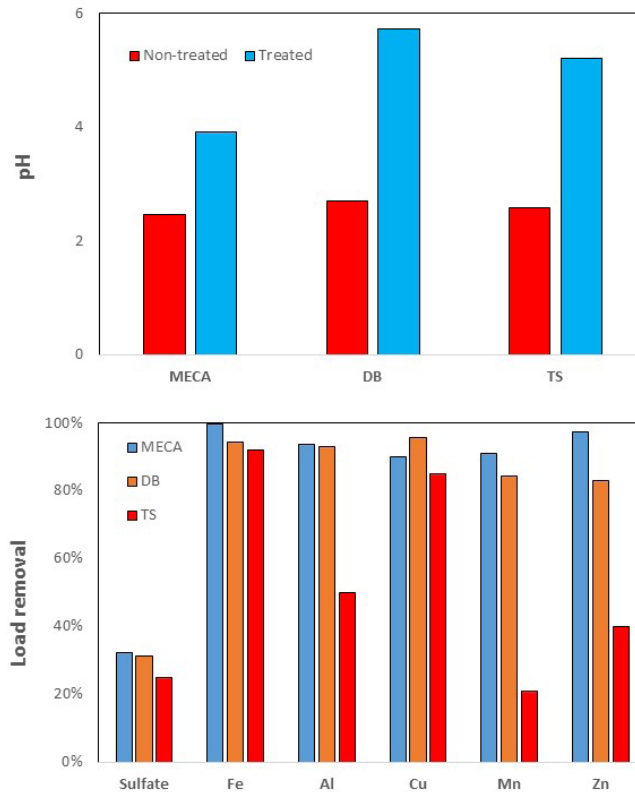


Figure 3 Modelled results of the impact of DAS treatment plants implementation in selected sites of the study area.

Conclusions

This study assesses the potential impact of the implementation of passive treatment plants in selected sites of the Meca River Basin (SW Spain), an extreme case of acid mine drainage (AMD) pollution worldwide. The increasing AMD pollution in this basin during the last years has caused the pollution of main water bodies, especially the Sancho Reservoir which has suffered a progressive acidification since 2007. Once validated a preliminary geochemical model of the starting situation, another model was performed to check the possible implementation of treatment plants in selected sites depending on the pollutant load and the length of the water course potentially restorable. AMD coming from Corta Esperanza is the main contributor of Fe (93%), Zn (90%), acidity (78%), sulfate, Al, Cu and Mn (around 70%) while the highest flows are generated from spoils heaps located in the drainage basins of Tia Sebastiana Creek and Dehesa Boyal (average values of 9.2 and 5.5 L/s).

The implementation of treatment plants in Meca headwaters and Dehesa Boyal would reduce the metal level in both catchments between 83% and 99%, respectively. In the case of the treatment plant located in the basin of Tia Sebastiana creek to treat the AMD arising

from La Sabina gallery, it will be really effective only for Fe (92%) and Cu (85%) due to this plant would not treat the effluents generated from spoil heaps deposited close to Filon Centro, with high values of Al, Mn and Zn. The settlement of these treatment plants would cause a significant increase in pH values (up to 5.7), although this prediction may have a higher uncertainty than in the case of sulfate and metals due to its poorer validation ($r^2 = 0.67$). This study proposes a simple tool to predict the impact of restoration measures in watersheds affected by derelict mines. However, more detailed and site-specific studies are required in order to achieve a cost-effective restoration of the watershed.

Acknowledgements

This work was supported by the Spanish Ministry of Economic and Competitiveness through the project SCYRE (CGL2016-78783-C2-1-R) and the European projects LIFE-ETAD (LIFE12 ENV/ES/000250) and EraMin: Extraction of Rare Earth Elements from Acid Mine Drainage.

References

- Ayora C, Caraballo MA, Macías F, Rötting TS, Carrera J, Nieto JM (2013) Acid mine drainage in the Iberian Pyrite Belt: 2. Lessons learned from recent passive remediation experiences. *Environ Sci Pollut Res* 20:7837–7853. doi:10.1007/s11356-013-1479-2.
- Cánovas CR, Olias M, Macías F, Torres E, San Miguel EG, Galván L, Ayora C, Nieto JM (2016) Water acidification trends in a reservoir of the Iberian Pyrite Belt (SW Spain). *Sci Total Environ* 541: 400–411. <http://dx.doi.org/10.1016/j.scitotenv.2015.09.070>.
- Carrera J, Vázquez-Suñé E, Castillo O, Sánchez-Vila X (2004) A methodology to compute mixing ratios with uncertain end-members. *Water Resour. Res.*, 40: W12101, <http://dx.doi.org/10.1029/2003WR002263>.
- Kimball BA, Runkel RL, Walton-Day K, Bencala, KE (2002) Assessment of metal loads in watersheds affected by acid mine drainage by using tracer injection synoptic sampling: Cement Creek, Colorado, USA. *Appl. Geochem.* 2002, 17, 1183–1207.
- Kimball BA, Runkel RL, Walton-Day K. (2010) An approach to quantify sources, seasonal change, and biogeochemical processes affecting metal loading in streams: Facilitating decisions for remediation of mine drainage. *Appl. Geochem.* 25: 728–740, DOI 10.1016/j.apgeochem.2010.02.005.
- Macías F, Caraballo MA, Nieto JM, Rötting TS, Ayora C (2012a) Natural pretreatment and passive remediation of highly polluted acid mine drainage. *J Environ Manag* 104:93–100. doi:10.1016/j.jenvman.2012.03.027.
- Parkhurst DL, Appelo CAJ (1999) User's guide to PHREEQC (version 2) a computer program for speciation, batch reaction, one-dimensional transport, and inverse geochemical calculations. USGS Water-Resources Investigations Report 99–4259. Denver, p 312.
- Runkel RL, Kimball BA, Walton-Day K, Verplanck PL (2007) A simulation-based approach for estimating pre-mining water quality: Red Mountain Creek, Colorado. *Appl. Geochem.* 22:1899–1918; DOI 10.1016/j.apgeochem.2007.03.054.

Gas Flux Rates and the Linkage with Predicting AMD Loads in Waste Rock Dumps, and Designing Practical Engineering Solutions – Field Based Case Studies in Three Distinct Climates

Steven Pearce¹, Mitchell Barteaux²

¹*Sr. Geo-Environmental Scientist, O’Kane Consultants, Unit 14, St Asaph Business Park, St Asaph, Wales, UK LL17 0LJ spearce@okc-sk.com*

²*Geoscientist, O’Kane Consultants, Fredericton, NB, Canada mbarteaux@okc-sk.com*

Abstract Oxygen flux into waste rock dumps (WRD), as well as the role oxygen plays in the development of acid and metalliferous drainage (AMD) is a critical area of research with respect to management of reactive waste at mining sites. The ability to practically manage gas flux (if at all) is however highly site-specific. O’Kane Consultants (OKC) has completed detailed assessments of gas flux rates as part of WRD investigations and AMD management engineering projects, at sites in three different climatic regions. The extensive data set collected has allowed the improvement of oxygen flux conceptual models to calculate oxygen ingress rates.

Key words Gas flux, Load predictions, cover design, AMD management, WRD instrumentation

Introduction – Gas Flux in WRD

The minimisation of oxygen ingress is widely acknowledged as a key waste management strategy employed at mine sites around the world to address the process of oxidation of reactive materials that may produce negative outcomes. These strategies are adopted to mitigate risks such as spontaneous combustion, toxic gas production, and acid and metalliferous drainage (AMD). In general the movement of air (and thus oxygen) within, and into WRDs occurs by:

- Diffusion through the near surface WRD material, or through engineered cover systems employed as a remediation measure;
- Advection due to density gradients as developed by temperature differences between atmosphere and internal WRD conditions commonly as a result of pyrite oxidation (Lu 2011);
- Dissolved oxygen contained in infiltrating water such as rainfall or snowmelt; and
- Convection cells within WRDs developed due to vertical temperature gradients, which transport air throughout the WRD pore-space due to differences in density (hot air is less dense than old air).

Given the primary role that oxygen plays in the oxidation of reactive minerals like sulfides, reducing their interaction would be an obvious advantage in the successful operation and closure of a WRD in terms of limiting risks such as AMD. It is somewhat surprising then to note in this regard that commonly the focus of AMD management, assessment and management studies are focused primarily on the liquid phase geochemical aspects. For example

a number of key issues can be identified with using industry standard static and kinetic testing procedures for predictions of geochemical evolution of waste materials containing sulfides in the field. In the main there is significant uncertainty with how to apply scale up factors for the extrapolation of laboratory data to the field because the test methods are not linked in any way to the dynamic process of oxygen and water flux in the field.

In this regard it is therefore important to recognise that independent of any geochemical assessment that may be carried out, that site-specific factors that directly influence the dynamic process of gas/water flux are considered. These factors include material characteristics (geochemical and geotechnical), geometry and climate. These factors can be investigated early in mine development it is vital that a good understanding is gained of them to recognize what is achievable in WRD closure, specifically with regards to potential AMD controls and oxygen ingress management.

The following paper reviews three case studies located in three different climate zones, and provides monitoring data to support the conceptual model of oxygen flux in those regions. Specifically, the climate zones include (Peel 2007):

- tropical rainforest– Northern Sumatra, Indonesia;
- arid hot desert – Pilbara, Australia; and
- humid alpine – British Columbia, Canada.

Tropical Rainforest Climate

The Tropical Rainforest site reviewed in this paper is characterized by high rainfall with an annual average of approximately 4,426 mm based on a 35 year climate database. Daily rain events are common, usually occurring in the afternoon, and temperatures are hot and humid. As part of AMD mitigation the site mining teams have employed a progressive waste rock management strategy which aims to mitigate the AMD risks of a WRD by selectively placing finer-grained material at the outer edge of the waste facility as construction progresses. The encapsulation method is a viable option for AMD risk management at this site due to the presence of sufficient volumes of low risk (respect to AMD) material that has suitable texture (i.e. finer grain size fractions), and high rainfall. These contributing factors mean that there is greater probability for the material to remain tension-saturated, thereby reducing the airflow capacity into the waste mass. In addition because of the high rainfall volumes it was understood that net percolation was going to be challenging to manage in the long term, therefore an approach to manage oxygen ingress was determined to be the optimal strategy in AMD management.

Specialised instrumentation has been installed by OKC through 2014 and 2016 to monitor the performance of the WRD. Specifically, the performance of the fine-grained encapsulation layers has been assessed against engineering design objectives such as: decrease of oxygen ingress to acceptable levels and limiting AMD. Instrumentation utilised to date includes oxygen sensors, volumetric water content / electrical conductivity sensors, matric potential and pore-water pressure (Pearce 2014).

Figure 1 presents select temperature and near-surface oxygen data from the WRD at the study site. Internal WRD temperatures (i.e. below 10m depth) are noted very stable and comparable to, but slightly lower than ambient temperature, with lower temperatures being recorded with greater depth. Near-surface (0.5m depth) temperatures however show daily fluctuations, likely reflecting diurnal ambient air variations. The internal temperature profile results in a very low relative differential temperature values between internal and ambient conditions of up to approximately 2°C difference). These conditions result in low temperature gradients to promote advective airflow.

The near-surface oxygen monitoring data shows that concentrations of oxygen at 0.5 m depth are low, and are likely reflecting low oxygen diffusion coefficients through the near-surface layer. Based on the temperature data there is little to no evidence of exothermic activity within the waste which would be present if significant sulfide oxidation were occurring. This provides strong evidence (along with the oxygen data) that limited advective or convective air flow forcing air into or out of the landform. The low oxygen ingress conditions can be attributed to the high moisture retention characteristics of the encapsulation material which results in low air permeability functions for the waste material. The volumetric water content and suction state data collected from the site shows that the encapsulation layer has a high degree of saturation and very low suction, supporting this interpretation.

Drilling results through the main body of the landform showed near neutral pH conditions throughout the depth profile, supporting the interpretation that the encapsulation method is efficient in maintaining oxygen concentrations within the WRD low, and inhibiting the oxidation of PAF.

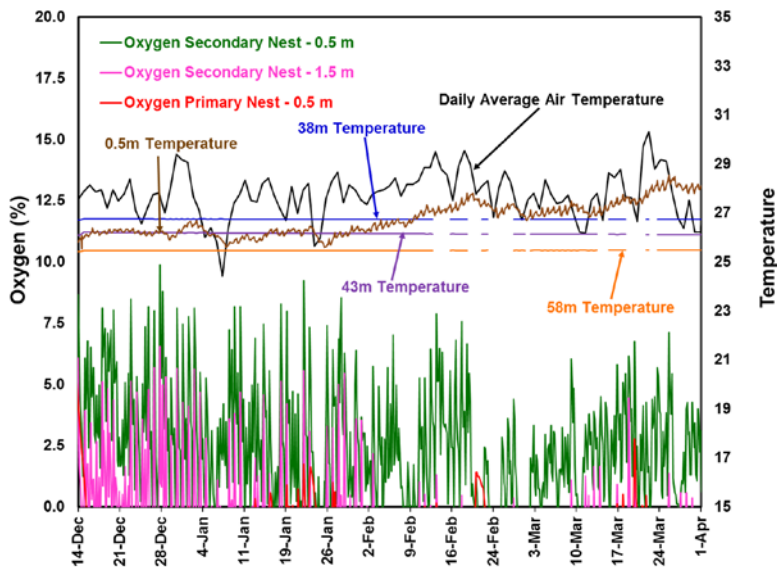


Figure 1 Temperature and oxygen concentration at the tropical rainforest case study location.

Arid Hot Desert Climate

Based on the Köppen-Geiger system (Peel 2007), this study site is classified as an arid hot desert (BWh), and is located in the Pilbara, Western Australia (WA). Almost 75% of the rainfall occurs during summer (October to March, inclusive) and the site experiences hot to very hot summers (with atmospheric temperatures up to 50°C) and warm to cool winters (near zero degrees). The long-term annual average rainfall for the area as quoted by the Australian Bureau of Meteorology is 320 mm. The WRD studied at the site is constructed with high tip heads (40 m), which has resulted in significant material segregation as a result of gravity sorting (Wilson 2011) with PAF material located throughout the WRD profile. As a result of the material sorting, the development of coarse rubble zones at the base of the tip heads have developed, acting as potential pathways for air entry into the landform (Pearce 2014). OKC had the opportunity to complete the installation of over 150 instruments in various waste rock dump landforms in the Pilbara, WA during 2013-2015. The instruments were installed to depths of up to 100 m as part of a long-term monitoring and assessment program. Instruments were installed using the sonic drilling technique and include galvanic oxygen probes, soil matric potential sensors, temperature sensors, and vibrating wire piezometers. The use of sonic drilling allowed the structure of the dumps to be assessed in detail during drilling and in turn the targeting of instrument placement in specific zones.

Figure 2 presents oxygen data and differential temperatures between various depths within one of the WRD profiles and ambient conditions (i.e. WRD temperature minus ambient temperature). Positive differential temperatures indicate when the internal temperature is higher than atmospheric, and negative temperatures demonstrate occurrences where internal temperatures are less than atmospheric. As illustrated, during summer months (September – March) there are instances where the entire WRD profile temperature is lower than ambient conditions, and during winter months (April – October) internal temperature becomes higher than ambient temperature. These variations in temperature differential on a seasonal basis result in dynamic oxygen flux conditions where gradients can change direction. During the winter when ambient temperatures fall below internal WRD temperatures, the result is a strong upwards gas flux forcing mechanism, where oxygen rich air enters the WRD through the basal rubble zones, and depleted less dense air moves towards the top of the WRD. In summer, when temperature gradients are low, or negative, there is potential for cooler oxygen depleted air to exit the toe of the landform, drawing in oxygen-rich air near the surface.

Sulfidic material along with organic carbon content is present within the profile which explains why oxygen concentrations are depleted at depth, however concentrations remain above 10% through the entire profile which is a strong indicator that significant oxygen flux is occurring to maintain oxygen supply through the waste profile. The data indicates that sulfide and carbon oxidation reactions are likely not limited by oxygen supply at this site.

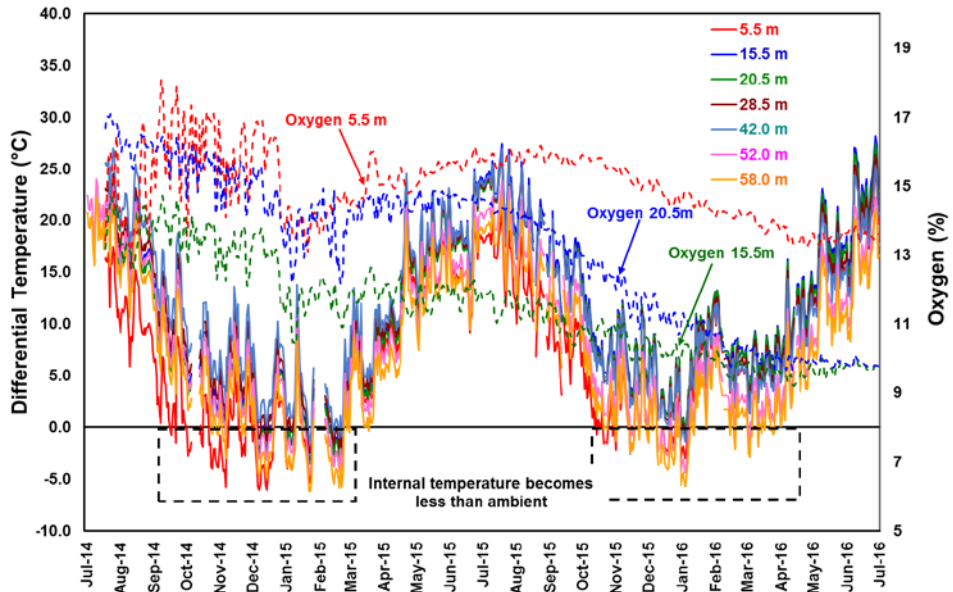


Figure 2 Temperature and oxygen concentration at the arid hot desert case study location.

Humid Alpine Climate

The Equity Silver mine is classified as humid alpine (Patterson 1987) and is used as the case study in this section. The study site is located near Houston, in the central interior of British Columbia, Canada. Information about the site was made available from publically accessible data, primarily as a result of the paper by Morin (2010). A significant amount of data has been collected from the site relating to AMD management, and is explored in said paper, where 23 years of WRD monitoring has taken place (1986-2009).

The Equity site receives approximately 660 mm of precipitation annually in the form of rainfall and snow. Daily average temperature remains below 12°C in summer, with winter daily average temperature falling to as low as -8.4°C for January (Environment Canada 2017).

The Equity WRD has a cover system, which was installed in 1991 and consists of compacted and non-compacted till, including a capillary break layer. The waste rock is relatively coarse in nature lacking appreciable clay or silt sized particles (O’Kane 1998). Based on the material type, it can be assumed that there is little water-holding capacity within the waste, and that airflow is not limited by internal saturated layers. Field data collected from cover system monitoring work (O’Kane 1998) shows that the cover system itself is maintaining low matric suction and a high degree of saturation, therefore minimizing the oxygen diffusion coefficient across the cover system and into the waste rock.

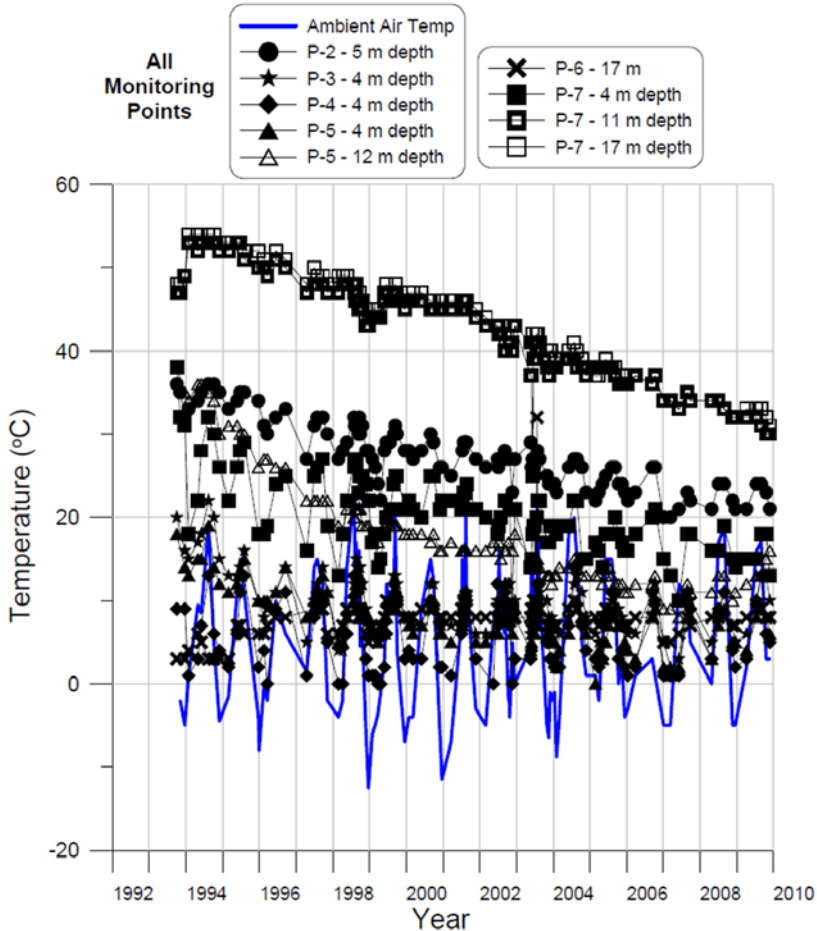


Figure 3 Temperature data with depth at the Equity Silver site (from Morin 2010).

Figure 3 shows the temperature data from the internal waste at the site which displays an overall cooling trend over time, however, it is clear that temperatures at a number of monitoring depths are well above the ambient air temperature. This data indicates significant oxygen ingress is/has occurring to support sulfide oxidation to maintain the elevated temperatures (as a result of exothermic reactions). The temperature differential remains constantly positive year round resulting in conditions that promote advective oxygen flux through the WRD. The data indicates that sulfide oxidation is occurring at an appreciable rate irrespective of the presence of the cover system. Temperature differentials between the WRD and the environment were similar at the humid alpine climate and arid hot desert climate, in that there is a seasonal aspect to the magnitude of the difference. A key difference however is that the humid alpine environment may have temperature gradients that remain positive (and high) throughout the entire year regardless of season, which is not seen at the other environment.

Discussion

Based on the data presented it is clear that although the key processes governing oxygen flux are remain constant across climatic zones, strategies to limit ingress must be tailored to meet site specific factors of which climate is a major factor. It has been demonstrated for example that strategies implemented in tropical climates which utilize highly engineered WRD's that employ fine grained material within cover layers to promote tension saturated conditions can be successful in limiting oxygen flux. However, for climates such as a hot arid dessert which lacks the sufficient rainfall to allow development of tension saturated layers, this would not be a viable option. For areas such as this, it is clear that the key focus would be on waste placement technique, such as limiting the amount of segregation during placement, or the use of advective barriers (such as toe bunds), which cut off the inflow of air through coarse rubble zones. These techniques can provide additional risk reduction by reducing the potential flux of air when high temperature gradients exist.

In climates such as the humid alpine environment WRDs that contain reactive sulfides typically can attain very high internal/external temperature differentials. At these locations a combination of waste placement strategies and cover systems can be used to limit oxygen flux and ingress. Specifically, engineered cover systems, which utilize the enhanced store-and release-concept to maintain a layer at tension saturation as a result of a capillary break has been shown to significantly reduce the diffusion of air into the landform into the longterm (Ayres 2012). In these locations however cover systems may only be effective in limiting diffusive flux, or advective flux in certain times of the year, therefore waste placement techniques such as compacting waste in small lifts or the creation of advective barriers (such as toe bunds) may be employed to reduce bulk advective flux year round.

References

- Australian Bureau of Meteorology (2017) www.bom.gov.au
- Ayres BK, Lanteigne L, O'Kane MA, Meiers G (2012) Whistle mine backfill pit dry cover case study – performance based on six years of field monitoring data. In Proceedings of the 9th international conference of acid rock drainage (ICARD), Ottawa Ontario, Canada, May20-26.
- Environment Canada (2017) www.climate.weather.gc.ca
- Harries J (1997) Acid mine drainage in Australia: Its extent and potential future liability, Supervising Scientist Report 125, Supervising Scientist, Canberra, 94 p.
- Lu N (2001) An analytical assessment on the impact of covers on the onset of air convection in mine wastes. Numerical and Analytical Methods in Geomechanics. August 1999, pp 347–364.
- Morin KA, Hutt NM, Aziz ML (2010) Twenty-three years of monitoring minesite-drainage chemistry, during mining and after closure: The Equity Silver minesite, British Columbia, Canada. http://www.mdag.com/case_studies/cs35.html
- Patterson RJ (1987) Environmental and reclamation measures at Equity Silver Mines Ltd. In Acid mine drainage seminar-workshop, Halifax NS, pp457-477.
- Pearce SR, Barteaux M (2014) Instrumentation of waste rock dumps as part of integrated closure monitoring and assessment, in Mine Closure 2014 Proceedings of the Ninth International Conference on Mine Closure, A.B. Fourie and M. Tibbett (eds), Australian Centre for Geomechanics: Johannesburg
- Pearce SR (2014) Beyond The PAF Cell, in Proceedings of the Eighth Australian Workshop on Acid and Metalliferous Drainage (Eds H Miller and L Preuss), pp 97-110.
-

- Peel MC, Finlayson BL, McMahon TA (2007) Updated world map of the Koppen-Geiger climate classification. *Hydrology and Earth System Sciences*, 11, 1633-1644, 2007
- O’Kane MA, Ayres B (2012) Cover systems that utilise the moisture store-and-release concept – do they work and how can we improve their design and performance?. In *Proceedings of Mine Closure 2012*, Eds A.B. Fourie and M. Tibbett, Australian Centre for Geomatics: Brisbane, pp 401-417.
- O’Kane MA, Wilson GW, Barbour SL (1998) Instrumentation and monitoring of an engineered soil cover system for mine waste rock. In *Canadian Geotechnical Journal* J35: 828-846.
- Wilson GW (2011), Rock dump hydrology: an overview of full-scale excavations and scale-up experiments conducted during the last two decades, in *Proceedings of the Seventh Australian Workshop on Acid and Metalliferous Drainage*, ed L.C. Bell and B. Braddock, Darwin, Northern Territory. pp.307-322

Environmental Attributes and Resource Potential of Mill Tailings from Diverse Mineral Deposit Types

Robert R. Seal, II¹, Nadine M. Piatak¹

¹*U.S. Geological Survey, 954 National Center, Reston, VA 20192, USA, rseal@usgs.gov, npiatak@usgs.gov*

Abstract A suite of over 80 samples of mill tailings from more than 20 different mineral deposit types was geochemically analyzed to evaluate: 1. potential environmental risks to both humans and aquatic ecosystems associated with accidental release of tailings or their leachates; and 2. their resource potential for byproduct critical elements. Dissolved concentrations of metals such as Cd, Co, Cu, Ni, Pb, and Zn were highest in leachates with low pH, whereas concentrations of oxyanions such as As were more complex. Tailings from numerous deposit types show significant enrichment in byproduct critical elements such as In, Ga, and Te relative to average crustal abundances.

Key words tailings, leachate chemistry, byproduct, critical minerals, environmental risk

Introduction

Sustainable mine development requires the identification of environmental risks and planning for the maximization of resource recovery at the earliest stages of mine development – even at the exploration stage. Studies have shown that the geology of various mineral deposit types influences the environmental attributes of those deposits (Plumlee 1999; Seal & Hammarstrom 2003). Mineral-deposit classification provides important information about a deposit's mineralogy, acid-generating potential, acid-neutralizing potential, ore commodities, and trace element associations – all of which define its environmental risks and resource potential. Waste rock compositions may vary from deposit to deposit because of differences in the local geology where a deposit has formed. However, the ore and the mill tailings resulting from its processing should have clear links to the ore deposit model. The fine grain size typical of mill tailings provides more reactive surfaces for weathering and makes downstream transport easier in the event of an unanticipated tailings release. From the resource perspective, the recovery of byproduct commodities is commonly highly inefficient. These byproduct elements can partition into a variety of waste stream components, with mill tailings likely being one of the volumetrically most important.

A suite of over 80 mill tailings samples from more than 20 mineral deposit types was assembled to evaluate environmental risks related to mill tailings and to evaluate their byproduct resource potential on the basis of mineral deposit type (tab. 1). Samples were obtained from active, inactive, and abandoned mines, and from material used for metallurgical testing at proposed mines. These samples and leachates derived from them were characterized by standard geochemical methods. Environmental risks associated with the mill tailings can be evaluated by comparing the bulk geochemistry of the solids to either sediment guidelines for the protection of aquatic organisms or soil guidelines for the protection of human health, and the geochemistry of the leachates to surface water guidelines for the protection of aquatic organisms or drinking water guidelines for the protection of human health.

Methods

Mill tailings samples were characterized using standard bulk geochemical techniques such as wavelength dispersive X-ray fluorescence (XRF) spectroscopy on fused disks, inductively coupled plasma–atomic emission spectroscopy (ICP-AES) and inductively coupled plasma-mass spectrometry (ICP-MS) preceded by a multiple acid digestion, and acid-base accounting. Leachates from mill tailings samples were generated using the USEPA Method 1312 (Synthetic Precipitation Leaching Procedure). USEPA Method 1312 reacts a 1:20 solid to solution mixture for 18 hours with end over end agitation. The solution is a dilute mixture of sulfuric and nitric acids adjusted to pH 5.0. The resulting leachates are characterized using standard procedures for water samples including measurement of unstable parameters (pH, specific conductance, dissolved oxygen, ORP, alkalinity), and filtration (0.45 μm) for chemical analysis using ICP-AES, ICP-MS, and ion chromatography.

Potential environmental risks related to mill tailings and leachates can be evaluated by comparing their geochemical compositions to relevant guidelines for aquatic ecosystem health and human health. For aquatic ecosystem health, surface-water guidelines are found in USEPA (2006) and sediment quality guidelines are found in MacDonald et al. (2000). For human health, drinking water guidelines are found in USEPA (2009) and soil quality guidelines are found in USEPA (2016). Concentrations of trace elements can be compared to the average crustal abundance of those elements to identify samples that show enrichment (Rudnick & Gao 2003).

Results and Discussion

Environmental Risks

The samples span a range of net neutralization potentials (NNP) from -700 to 500 kg CaCO_3/t , paste pH values from 3 to 8.5, and leachate pH values from 2.4 to 10.5. The specific conductance of leachates spanned a wide range from 0.025 to 4.1 mS/cm. In general, the higher specific conductance values were found at lower pH and the lower specific conductance values were found at higher pH.

A comparison of dissolved Cu and As in leachates as a function of pH (fig. 1) and in solids (fig. 2) illustrates many of the salient features of this data set. Copper solubilizes as a cationic species and is highly toxic to aquatic organisms; in contrast, it is an essential micro-nutrient for humans. Arsenic typically solubilizes as an oxyanion. It is a carcinogen toxic to humans and to a lesser extent to aquatic organisms.

Dissolved Cu concentrations in leachates generally correlate inversely with pH; the highest concentrations are found at low pH (fig. 1A). The deposit types exhibiting low leachate pH are those types in which pyrite or pyrrhotite are important constituents of the mill tailings and the acid-neutralizing potential is minimal. These deposit types include volcanic-associated massive sulfide deposits and mesothermal low-sulfidation base metal-rich veins. Leachate from magmatic mafic Ni-Cu-platinum group metal (PGM) deposits vary from low to high pH because of the range of acid-generating potential due to this grouping including

Table 1 Mineral deposit classifications and samples included in study

Deposit Type	Graph category	Number of deposits	Number of samples
Orogenic Au	Au	4	7
Low-sulfidation epithermal Au	Au	1	1
Intrusion-related Au	Au	1	1
Porphyry Cu	Porphyry Cu	1	3
Volcanic-associated massive sulfide	VMS	7	24
Sedimentary-exhalative Zn-Pb-Ag	Sedex	1	1
Mississippi Valley-type Pb-Zn	MVT	1	7
Mesothermal Cu-Zn-Pb-Ag	Mesothermal	1	12
Carbonate replacement Zn-Pb-Ag	Mesothermal	1	4
Simple Sb vein	Sb	2	2
Magmatic Ni-Cu-PGM massive sulfide	Mafic	4	4
Magmatic Cu-Ni-PGM disseminated sulfide	Mafic	1	1
Magmatic reef PGM	Mafic	1	1
Banded iron formation	BIF	3	3
Iron oxide Cu-Au	REE	1	1
Alkaline intrusion REE	REE	1	4
Carbonatite REE	REE	1	1
Sandstone U	U	1	1
Pegmatitic U	U	1	1
Conglomeritic U	U	1	1
Unconformity U	U	2	2
Metasomatitic U	U	1	2

massive sulfide deposits, disseminated sulfide deposits, and sulfide-poor PGM “reef” deposits. Deposit types with leachates that cluster at higher near-neutral to alkaline pH values, such as most orogenic Au deposits and REE deposits, banded Fe formations, and a variety of U deposit types, generally have tailings with low acid-generating potential and high acid-neutralizing potential. The leachates accordingly have low dissolved Cu concentrations. The low concentrations of Cu reflect a combination of the low solubility of Cu at high pH and low endowment of Cu in these mill tailings (fig. 2A). In general, the leaching of Cu from tailings from volcanic-associated massive sulfide deposits, mesothermal base metal vein deposits, and magmatic Ni-Cu massive sulfide deposits poses the greatest potential

risks for aquatic organisms, but only under limited circumstances are likely to be a concern for human health (fig. 1A). In contrast, for deposit types with mill tailings not likely to generate low-pH leachates, concerns for aquatic ecosystem health due to Cu would appear to be minimal and concerns for human health should be essentially non-existent (fig. 1A). The other base metals (Cd, Co, Ni, Pb, Zn) show similar solubility trends in leachates. However, conclusions about their potential toxicity to humans and aquatic organisms will vary on an element and concentration basis.

Dissolved As concentrations in leachates display a “U”-shaped solubility patterns as a function of pH (fig. 1B). Oxyanions, such as As, generally have higher solubility at high pH and absorb onto hydrated ferric oxides at lower pH. The increased solubility at low pH presumably reflects the higher solubility of Fe under these conditions and thus the lack of a substrate for sorption. Leachates from tailings from simple Sb vein deposits pose significant potential risks to both aquatic organisms and humans regardless of leachate pH. Arsenic is a common minor element in these deposits that is not separated from the crushed ore during processing. Some leachates from mill tailings from mesothermal veins, orogenic Au deposits, volcanic-associated massive sulfide deposits, U deposits and banded Fe formations may pose potential human health risks. Other elements that tend to dissolve as oxyanion species (Cr, Sb, Se, Mo, U, V) show similar solubility trends, but their potential toxicity to humans and aquatic organisms will vary on an element by element basis.

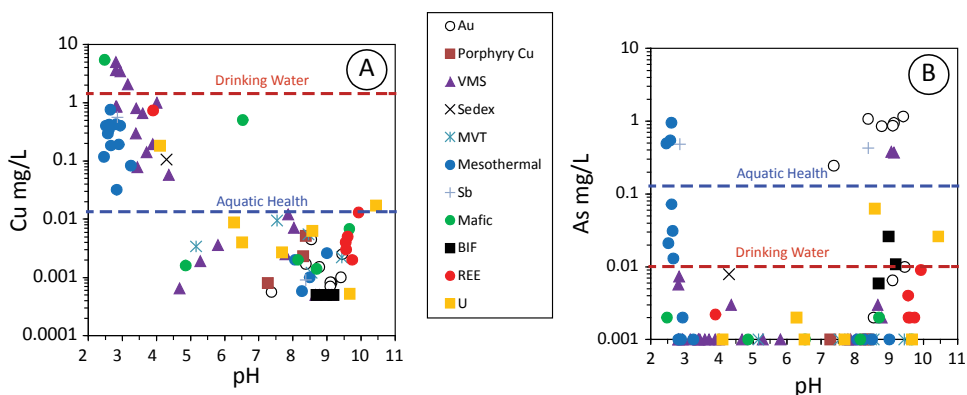


Figure 1 Variations of dissolved Cu (A) or As (B) with pH for various deposit groups. Dashed lines represent human drinking water guidelines (red) and acute aquatic ecosystems guidelines (blue). The acute aquatic guideline for Cu assumes a water hardness of 100 mg/L CaCO₃. See table 1 for an explanation of the legend.

Potential pathways of impacts from Cu and As to aquatic organisms from mill tailings can be identified from considering leachate and bulk solid geochemical compositions together (fig. 2). Some deposit types, such as a volcanic-associated massive sulfide deposits, pose potential risks from both the leaching of trace elements from tailings and the accidental release of tailings to surface water settings. In contrast, tailings from mesothermal vein deposits primarily appear to be a greater concern from the leaching of trace elements from tailings. Most Au deposit types, REE deposit types, banded Fe formations, and U deposit types have

limited potential to impact aquatic organisms from leachate or tailings releases with respect to Cu. In contrast, leachates from tailings from most deposit types have limited potential to affect aquatic organisms from As with the exception of some orogenic Au deposits and mesothermal veins, but accidental release of tailings from these two deposit types pose risks of universal concern related to As. The knowledge gained from this analysis should be beneficial to environmental risk assessments of proposed mines, active mines, and abandoned or inactive mines.

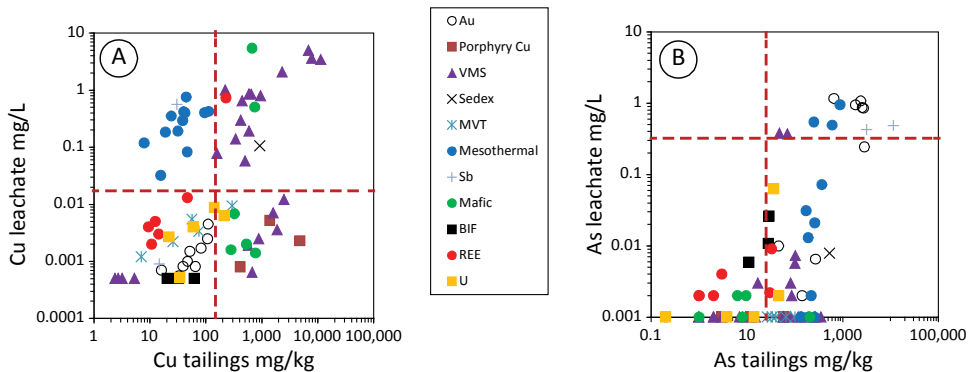


Figure 2 Variations of Cu (A) or As (B) in bulk mill tailings and leachates from mill tailings for various deposit groups. Dashed lines represent guidelines for aquatic ecosystem health. Horizontal lines are for acute toxicity in surface water; vertical lines are probable effect concentrations for sediment. See table 1 for an explanation of the legend.

Resource Potential

The geochemical data set assembled is useful for identifying mill tailings from deposit types for which byproduct commodities, such as technologically critical elements, are anomalously enriched. The variations in the bulk concentrations of Ga, In, and Te compared with the concentrations of elements that are the major commodities extracted, such as Cu, Sn, and Zn, illustrate the value of these data. The concept of an “ore grade” for byproduct commodities is meaningless because their recovery alone does not determine the viability of a mining project. Instead, their anomalous concentrations are best considered relative to the average crustal abundances of these elements (Rudnick & Gao 2003). Maximum concentrations of Ga (58.9 mg/kg), In (20.5 mg/kg), and Te (5.6 mg/kg) were high relative to average crustal abundances for these elements (fig. 3); these maximum concentrations exceed average crustal values for these elements by factors of 3 for Ga, 130 for In, and 5,700 for Te (fig. 3). In fact, maximum concentrations of Cu (11,400 mg/kg), Sn (54.2 mg/kg), Zn (8,740 mg/kg) are also high relative to average crustal abundances. The significant enrichments of Cu, Sn, and Zn presumably reflect inefficient recovery or lack of recovery of these commodities at individual mines. The higher concentrations of Cu are from deposit types for which Cu would have been a primary commodity (porphyry Cu deposits and volcanic-associated massive sulfide deposits), indicating inefficient recovery (fig. 3A). Likewise, the high Zn concentrations were found in tailings from deposits commonly mined for Zn, such as volcanic-associated massive sulfide deposits, sedimentary-exhalative deposits, mesothermal vein deposits, and Mississippi Valley-type deposits (fig. 3B).

Significant byproduct critical elements may be available for recovery at existing mines or by processing mill tailings at inactive or abandoned mines on a deposit type basis. For example, In shows the greatest enrichment in tailings from volcanic-associated massive sulfide deposits and mesothermal vein deposits (fig. 3A,C). Its concentration shows moderate correlations with Cu and Sn concentrations, which implies that it may substitute into Cu or Sn minerals. Gallium is only locally enriched in tailings from some U deposits, porphyry Cu deposits, and volcanic-associated massive sulfide deposits (fig. 3B), and does not appear to correlate with other elements. Tellurium reaches its highest concentrations in tailings from porphyry Cu deposits and orogenic Au deposits, and lacks significant correlations with other elements, such as Cu (fig. 3D). Because of the low crustal abundance of Te (0.001 mg/kg), tailings from most deposits are nominally enriched in Te. Banded Fe formations and most U deposit types tend to be depleted in these byproduct critical elements relative to average crustal abundances. The identification of specific critical elements with specific deposit types may enhance resource recovery at active mines or during remediation of abandoned mines.

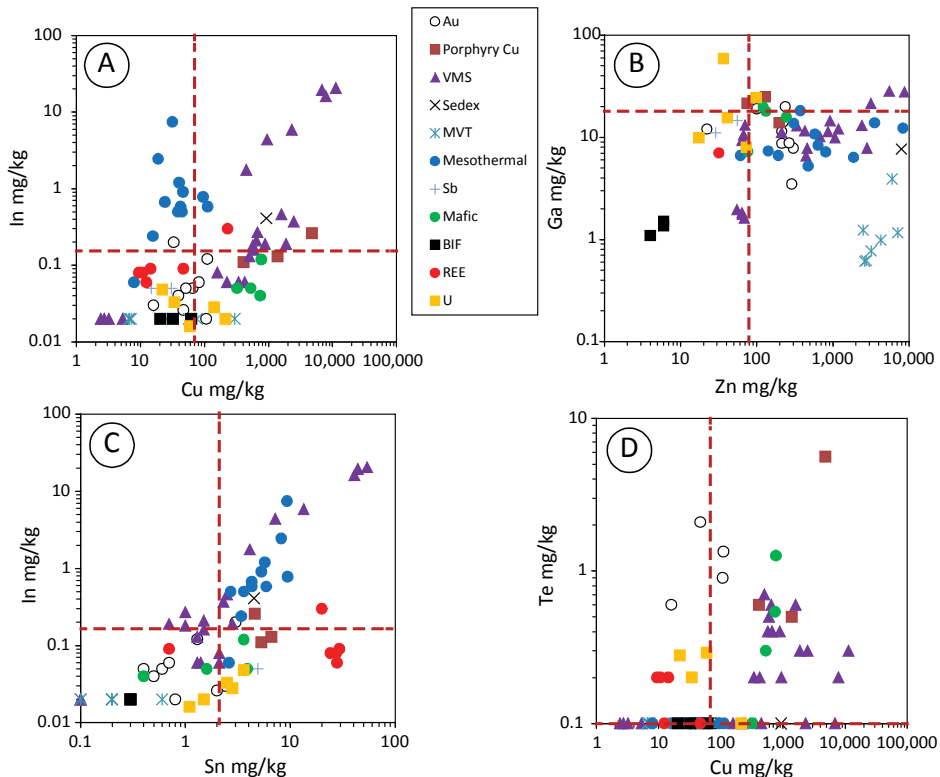


Figure 3 Variations of byproduct critical elements with other trace elements in mill tailings. A. In vs. Cu; B. Ga vs. Zn; C. In vs. Sn; and D. Te vs. Cu. Dashed lines represent the average crustal abundance of these elements. See table 1 for an explanation of the legend.

Conclusions

Insights gained from the geochemistry of mill tailings and their leachates on a deposit type by deposit type basis can be used to anticipate potential environmental risks related to the development of these deposit types, even at the earliest stages of potential mine development – the exploration stage. The knowledge gained from this analysis should be beneficial to environmental assessments of proposed mines, active mines, and abandoned or inactive mines. Tailings from numerous deposit types show significant enrichment in byproduct critical elements such as In, Ga, and Te relative to average crustal abundances, suggesting that increased demand for these critical elements could potentially be met by recovering them at existing mines or by re-mining tailings at abandoned mines.

Acknowledgements

The authors thank Jane Hammarstrom and Harvey Belkin for thoughtful and constructive reviews.

References

- MacDonald DD, Ingersoll CG, Berger TA (2000) Development and evaluation of consensus-based sediment quality guidelines for freshwater ecosystems. *Arch Environ Contam Toxicol* 39:20–31
- Plumlee GS (1999) The environmental geology of mineral deposits. In: Plumlee GS, Logsdon MJ (eds), *The environmental geochemistry of mineral deposits, Part A. Processes, techniques, and health issues*. *Rev Econ Geol* 6A:71–116
- Rudnick RL, Gao S (2003) Composition of the continental crust. *Treatise Geochem* 3.01:1–64
- Seal RR II, Hammarstrom JM (2003) Geoenvironmental models of mineral deposits: examples from massive sulfide and gold deposits: *Environmental Aspects of Mine Wastes*, J.L. Jambor, D.W. Blowes, and A.I.M. Ritchie (eds.), *Mineral Assoc Canada Short Course Series* 31:11–50
- US Environmental Protection Agency (USEPA) (2006) National recommended water quality criteria: accessed April 13, 2017, <https://www.epa.gov/wqc/national-recommended-water-quality-criteria-aquatic-life-criteria-table>
- US Environmental Protection Agency (USEPA) (2009) National Primary Drinking Water Regulations: EPA 816–F–09–004, accessed July 9, 2009, at <http://www.epa.gov/safewater/consumer/pdf/mcl.pdf>
- US Environmental Protection Agency (USEPA) (2016) Regional Screening Levels (RSL) for Chemical Contaminants at Superfund Sites, RSL Table Update May 2016: accessed April 13, 2017, <http://www.epa.gov/region09/superfund/prg/>

Progressive Management of AMD Risk During Construction of an Integrated Waste Storage Landform – A Case Study at Martabe Gold Mine, Indonesia

Steven Pearce¹, Mitchell Barteaux², Ken Grohs³, Janjan Hertrijana³, Henny Purnamasari³, Matthew Orr³, Candra Nugraha³

¹*Sr. Geo-Environmental Scientist, O’Kane Consultants, Unit 14, St Asaph Business Park, St Asaph, Wales, UK LL17 0LJ spearce@okc-sk.com*

²*Geoscientist, O’Kane Consultants, Fredericton, NB, Canada, mbarteaux@okc-sk.com*

³*Agincourt Resources, Martabe Mine, Sumatra, Indonesia*

Abstract Progressive encapsulation methods to mitigate the risk of acid mine drainage (AMD) offer significant advantages (such as a higher safety factor in design) compared to the more commonly implemented “final cover” closure strategies, which are typically vulnerable to single failure modes or events. This paper provides a case study of a progressive encapsulation strategy for the mitigation of acid mine drainage risk being implemented by PT Agincourt Resources at the Martabe Gold Mine, Sumatra, Indonesia, as part of ongoing construction of an integrated waste rock and tailings storage facility (TSF). Data provided includes that collected from an installed instrumentation network.

Key words Integrated waste storage facility, oxygen ingress rates, sealing layer, progressive rehabilitation

Introduction – Progressive Management in Context

Acid mine drainage (AMD) is arguably the most significant liability that mining companies retain post closure with global AMD management costs estimated at approximately \$US 1.5 billion per annum (Harries 1997). These liabilities have resulted in part due to the fact that impacts from AMD may only become apparent at later stages of mine development, and that in many cases planning decisions are made during operational periods without fully addressing the nature of the risk related to AMD with respect to long term storage of waste.

The consequence of these and other factors, such as cost, has seen the proliferation of final cover systems to manage AMD risk, rather than progressive solutions that can be implemented during waste dump construction. Best practice would suggest that AMD prevention is better than mitigation, however many of the most commonly adopted strategies such as implementation of a final cover system do not meet this test, particularly when implemented in response to emerging AMD issues later in the LOM (Pearce 2014).

Progressive management solutions such as focusing on waste placement design concepts, use of internal encapsulation layers, and/or co disposal of waste have been implemented as alternative to end-of life-solutions, however the practice is still not wide spread. Reasons for the practice not being widespread are varied and in many cases site specific, but in general progressive management solutions are typically 1) More expensive than a “containment cell”, 2) Not fully compatible with the mine schedule, 3) Too complicated to build as a result of logistical constraints (such as materials availability).

This paper attempts to demonstrate how progressive management strategies can be successfully achieved during the construction of an integrated waste rock storage facility (WRSF) and TSF given an understanding of integrated mine operations and closure planning.

Martabe Mine Setting

The Martabe gold and silver mine in the Province of North Sumatra is operated by Agincourt Resources. The mine is situated approximately 3 kilometres north of the township of Batangtoru and approximately 40 km south of the port of Sibolga. The mining operations include two open pits, an integrated tailings storage facility (TSF) and an active valley-fill type waste rock storage facility (WRSF) located south of the main tailings impoundment. The primary WRSF area is integrated into and being developed as the main downstream containment structure of the TSF. The WRSF will include all mine waste, including potentially acid forming (PAF) waste rock, from the open pits. There are currently two active pits, and over time additional pits are expected to be brought on line as exploration and resource development activities are progressed. The complex mineralogy of the site requires detailed waste rock modelling and scheduling as the basis for WRSF design and waste management.

Waste Rock Management and Characterisation

A detailed waste rock management plan has been developed by OKC and Agincourt Resources technical teams (mine geology, exploration, mine planning, TSF) for the Martabe mine. The plan provides technical guidance for specific aspects of waste rock management during the development and operational phases, and an overall framework for the management of waste materials during the construction of the TSF.

Agincourt Resources have developed a significant materials characterisation database through geochemical characterisation of the waste rock at the Martabe mine site. Several sources of geochemical data was available to develop the risk-based waste rock classification process flow methodology for operational use in characterising blocks of waste rock.

Waste classification and subsequent modelling into discrete class system in the reserve model and schedule have been designed to take into account the broad characteristics of the deposit and translate this into a means of identifying material based on predicted AMD risk, potential utility for use in construction (soft materials are more amenable to compaction for example), and potential acidity buffering potential (presence of carbonates such as calcite).

The waste classification system and generation of waste schedules for the site are important as materials need to be identified that can be preferentially used in the construction of the sealing layers over the LOM. Bulk waste and internal waste are identified in the model which is an important aspect of waste scheduling as during mining operations grade control drilling is carried out. This activity results in ongoing updates to the model in which internal waste may be re-classified as ore, or may be present in to small volumes to separate out.

Waste Rock Schedule

The waste placement of materials within the TSF embankment is carried out according to a design specification. A detailed mine waste schedule has been developed for the site, which is based on the waste classification system and identifies the sources of materials over LOM to ensure that the build plan can meet the design specification. It is therefore important that the mine schedule and LOM build plan reference each other to ensure the successful management of waste requiring management as it exits the pit. Scheduling is important to be carried out over LOM because design specification indicates that construction of sealing layers require a source of low risk (with respect to AMD) finer textured lower risk materials, and criteria for compaction is based on particle sizing.

The Progressive Encapsulation Method and Oxygen Ingress Assessment

The conceptual model for assessing AMD risk assumes that oxygen availability to PAF waste rock within the WRSF is predominately restricted to a gas transport regime dominated by diffusion rather than advection. This results from a combination of the site's high rainfall and associated infiltration rates, and the placement of fine textured waste on the embankment outer slopes during each embankment raise. This scenario of waste placement and climate is favorable to create and maintain an "engineered tension saturated layer" across the surface of the embankment which limits oxygen ingress and thus AMD production and release.

Figure 1 shows the engineering concept, with PAF material being progressively encapsulated during construction on a lift by lift basis, where lifts constructed as part of the embankment raise are 10m in height, and waste is placed in 1m thick compacted layers.

OKC completed a detailed modelling study of convective and advective airflow within the WRSF LOM design using numerical modeling tools coupled within the GeoStudio (GeoSlope International, 2012) software suite: TEMP/W, AIR/W, and SEEP/W (Pearce 2016). Surface infiltration seepage rates were calculated using VADOSE/W. The objective of the numerical modelling program was to develop guidelines for waste placement. It was anticipated that an easy-to-measure metric (such as in-place dry density) would be required in the field to guide materials placement.

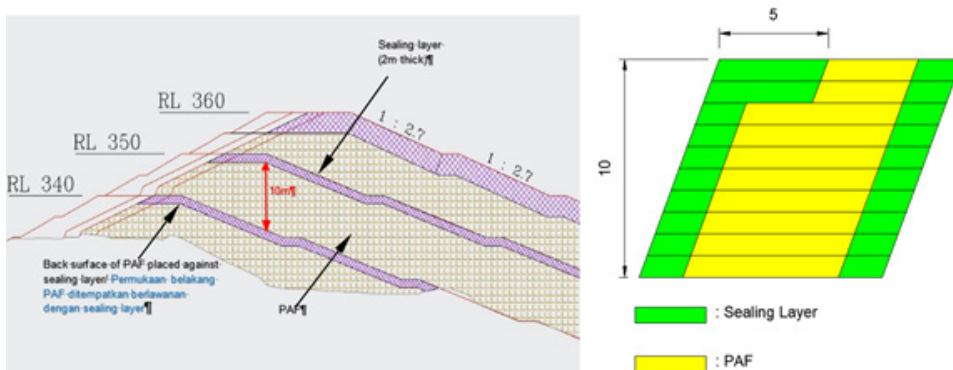


Figure 1 PEM design used as basis for modelling assessment

Density dependent convective airflow is a well-documented process, and has been observed in waste rock piles (Lu 2001). Convective airflow is initiated when a temperature induced density gradient exists between air within waste rock piles and ambient conditions. The presence of a convective cycle is heavily influenced by *in situ* moisture conditions, air temperature within matrix of stored waste rock (as a result of exothermic reactions like sulfide oxidation), ambient air temperature, and material characteristics such as texture and structure (Ball and Schjønning 2002). Key conclusions from the airflow modelling work were

- 1) Advective airflow rates are substantially lower than diffusion rates as a result of the WRSF “wetting up”. As long as the material maintains sufficient saturation advection will not be a significant source of oxygen for oxidation processes.

- 2) Oxygen ingress due to thermal convection cells is anticipated to be low, even with elevated internal WRSF temperature and low degree of saturation conditions (worst case scenario).

- 3) The placement of high grade sulfide sulfur near the outlying slopes of the landform should be minimised.

- 4) Oxygen ingress was shown to be substantially decreased by the presence of the sealing layers. Oxygen ingress varied greatly for the material depending on the texture of the material, its water retention characteristics (determined by k_{sat} , porosity, and air entry value) and the assumed in-place dry density.

- 5) With increased as placed waste density a decrease in oxygen ingress results. However, the result is not simply a result of increased density. Additional compactive effort produces increased density leading to decreased porosity, increased air entry value and water retention, and a decreased k_{sat} . All of these factors lead to an increase in the degree of saturation of the encapsulation system materials and decreased oxygen ingress rates.

Waste placement engineering design

Results from the numerical modelling program were used to inform waste material placement guidelines encompassing the range of potential waste and operational cover system materials for the interior of the WRSF. Material envelopes were developed based on particle size, and included the geotechnical specifications required for the as-constructed sealing layer to reach the specific targets for oxygen ingress (Table 1).

Table 1 Sealing layer material placement guidelines.

Specification Envelope	% Passing #4 Sieve	% Passing #200 Sieve	Minimum Placed Dry Density (kg/m ³)	Maximum permissible k_{sat} (cm/s)
1	92%	65%	1,500	1x10 ⁻⁴
2	82%	50%	1,675	7x10 ⁻⁵
3	72%	38%	1,775	3x10 ⁻⁵
4	55%	25%	1,800	2x10 ⁻⁵
5	40%	12%	1,825	1x10 ⁻⁵

WRSF Concept Validation

PT Agincourt initiated a program to validate the WRSF engineering design concept in 2015, with the objective of confirming that sulfide oxidation within the WRSF embankment is being reduced due to the implementation of the sealing layer concept. Validation work to date has consisted of OKC designing and installing monitoring systems (Figure 2) within the sealing layer profile at two locations (2015 and 2016 installations) to monitor temperature gradients, oxygen concentration, pore-water pressure, volumetric water content, and matric potential. Additional installations are planned for throughout the WRSF construction to capture spatial variability in material properties and evolution. In addition to the collection of *in situ* monitoring data, detailed material sampling and testing is completed during installation and as part of regular construction QA/QC procedures to develop an understanding of geotechnical characteristics across the facility, and ensure that construction specifications are being adhered to.

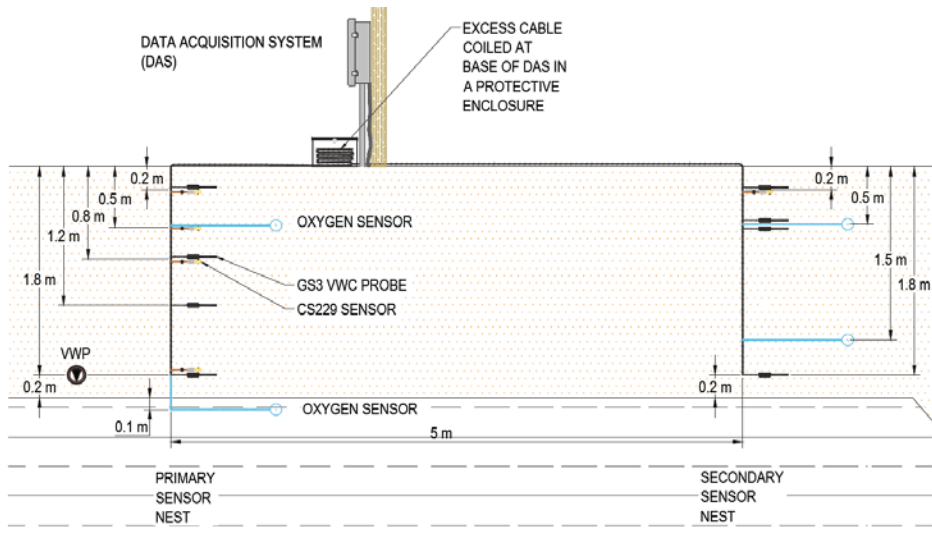


Figure 2 Martabe WRSF sealing layer monitoring system.

Preliminary monitoring data indicates that the the sealing layer is performing in line with the conceptual model and as per modelling predictions. Oxygen concentrations within and below the sealing layer are reduced to near zero, and VWC and suction data are indicative of material that is maintaining a high degree of saturation. Following the placement of additional lifts of material above the WRSF1 station, the observed performance is positive in that oxygen remains low, and moisture conditions are reflecting high water content.

Figure 3 shows the oxygen concentration within the WRSF sealing layer. Oxygen concentration remains at or near zero percent following initial spikes after installation at WRSF1. While oxygen at WRSF2 has slightly higher concentrations at shallow depths, below 0.5m concentrations are minimal. It is noted that material texture and geochemical composition

has resulted in the different response between monitoring locations. In addition additional material was placed as a result of embankment raises over the WRSF1 location in September 2016, while WRSF2 has yet to have material placed above it.

Figure 4 shows the calculated degree saturation at the WRSF2 monitoring location. Saturation calculations are based on material geotechnical testing (porosity) and VWC from *in situ* monitoring. Calculated saturations are high in that they remain above approximately 80%.

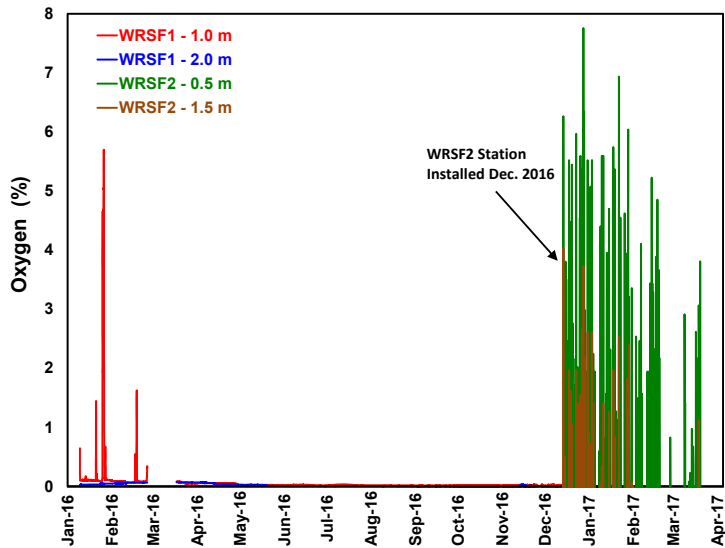


Figure 3 Oxygen concentration within the WRSF sealing layer.

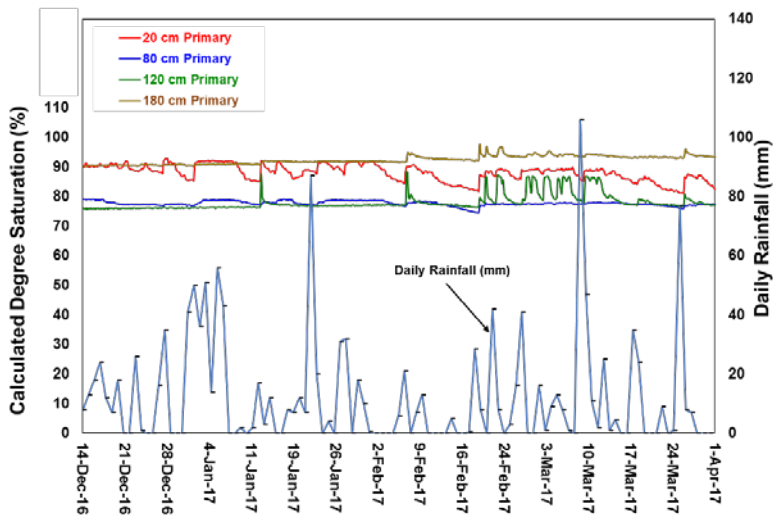


Figure 4 Calculated degree saturation at the WRSF2 monitoring location.

Material characteristics and monitoring data collected during the 2016 monitoring period, were utilised to develop estimates of a range of air permeability (k_{air}) for the field for the various material envelopes at the Martabe site under a range of dry density values (Fig. 5), which is an important facet in understanding the potential air permeability.

In situ dry density significantly affects the achieved field k_{air} , as illustrated in Figure 5. The estimates in k_{air} shows that material can have up to an order of magnitude decrease with increases in compaction effort.

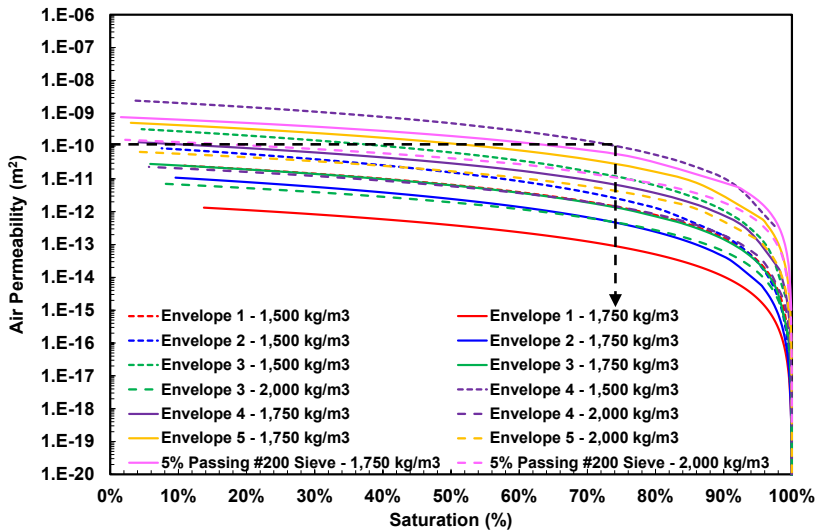


Figure 6 Air permeability of Martabe material under various levels of compaction.

In general, the data shows that if saturation levels are maintained above 75% this would ensure that the air permeability is lower than $1 \times 10^{-10} \text{ m}^2$ (limiting the dominant oxygen ingress mechanism to diffusion) irrespective of the Envelope that the material falls into. These calculations indicate there is some inherent flexibility in the construction of the WRSF sealing layers given that if sufficient fine grained material is not available, oxygen ingress targets can still be achieved through application of increased compaction effort.

Discussion and Conclusion

The placing of sealing layers as part of a progressive closure strategy to mitigate AMD risk has been successfully implemented at the Martabe Gold Mine to date. Conditions supporting this outcome include the site's climate and, the nature of the waste rock from the pit. However successful implementation of this strategy has required detailed waste characterisation studies, complex numerical modelling to identify effective seal specifications and detailed mine planning, and control of construction to defined standards. It is notable that to date the strategy has proven to be compatible with the mine plan, logistically feasible and cost effective. The strategy has been validated to date by detailed *in situ* monitoring studies, with close alignment between modelled and measured performance.

References

- Ball BC, Schjønning P (2002) *Methods of Soils Analysis Part 4* (pp. 1141 – 1158). Madison, Al: Soil Science Society of America.
- Harries J (1997) *Acid mine drainage in Australia: Its extent and potential future liability*, Supervising Scientist Report 125, Supervising Scientist, Canberra, 94 p.
- Lu N (2001) *An analytical assessment on the impact of covers on the onset of air convection in mine wastes. Numerical and Analytical Methods in Geomechanics*. August 1999, pp 347–364.
- Pearce, SR, Orr M, Grohs K, Pearce, J (2016) *Progressive Mine Closure: Martabe as a Case Study*. In *Proceedings of Mine Closure 2016*, Eds. AB Fourie and M Tibbett Perth, Australia. March 15-17 2016, p. 619 -635.
- Pearce SR, Barteaux M (2014) *Instrumentation of waste rock dumps as part of integrated closure monitoring and assessment*, in *Mine Closure 2014 Proceedings of the Ninth International Conference on Mine Closure*, A.B. Fourie and M. Tibbett (eds), Australian Centre for Geomechanics: Brisbane, Australia
- Pearce SR (2014) *Beyond The PAF Cell*, in *Proceedings of the Eighth Australian Workshop on Acid and Metalliferous Drainage* (Eds H Miller and L Preuss), pp 97-110.

Development of a tool for efficient three dimensional reactive multicomponent transport modelling independent from the geohydraulic model system

Wilfried Uhlmann¹, Thomas Claus¹, Kai Zimmermann¹, Thomas Koch²

¹ *Institut für Wasser und Boden Dr. Uhlmann, Dresden, Germany, info@iwb-dresden.de*

² *Lausitz Energie Bergbau AG, Cottbus, Germany, thomas2.koch@leag.de*

Abstract The groundwater in the Lusatian lignite mining district is extensively and sustainably affected by pyrite weathering. The geohydraulics at active mining sites and reclamation sites have been simulated for decades with user specific and well calibrated two- and three-dimensional regional groundwater flow models. Existing modelling software, which offers hydrogeochemical calculations in addition to geohydraulic calculations, requires the migration of existing regional groundwater flow models. This is costly and partially impossible due to special inner and outer boundary conditions. This paper shows the development of a reactive multicomponent transport model using PHREEQC and an existing geohydraulic groundwater flow model.

Key words geohydraulic modelling, hydrogeochemical modelling, groundwater, reactive multicomponent transport modelling, PHREEQC

Introduction

The groundwater in the Lusatian lignite mining district is extensively and sustainably affected by pyrite weathering. The processes of groundwater lowering at active mining sites as well as groundwater rising at reclamation sites have been simulated for decades with user specific and well calibrated two- and three-dimensional regional groundwater flow models. Increasingly, hydrochemical questions, such as the acidification of post-mining lakes, the inflow of iron-rich groundwater into watercourses and the discharge of contaminated water from dumps and piles are becoming more important. Reactive multicomponent transport modelling with hydrogeochemical functionality is the favoured tool to answer these questions. The use of modelling software, which offers hydrogeochemical calculations in addition to geohydraulic calculations, e.g. PHAST, requires the migration of the whole regional groundwater model including its inner and outer boundary conditions. The structures and limitations of the models are often incongruent or specific boundary conditions are not transferable. In the case of user-specific models, this transition is sometimes impossible because special boundary conditions are not transferable.

How can an existing regional groundwater model be used for reactive (hydrogeochemically based) multicomponent transport modelling? And is it possible to optimise these models for a large number of model cells and long-time predictions?

Initial situation

For decades, geohydraulic modelling has been an important planning tool in the Lusatian lignite mining area. In post mining rehabilitation for example, geohydraulic modelling plays a major role in the flooding of pit lakes and their interaction with watercourses. Geohydrau-

lic modelling also provides a significant input for the long-term water resource planning and the management of mining-influenced river catchment areas.

There are several geohydraulic regional models in the Lusatian lignite mining district. The spatial extents of these models are mainly determined by the organizational units of the post mining (former open-cast mining sites or redevelopment areas) and the mining companies (active open-cast mines or production areas). The models are developed and operated by the companies themselves or on their behalf. The composition, the further development and the continuous adaptation of these models to changing boundary conditions and questions require a high personnel and financial effort. Therefore these models are also an economic investment and new developments would cost a lot of time and resources.

With the rise of the groundwater table in the Lusatian lignite mining area, hydrochemical questions play an increasingly important role in the planning proceedings of the mining and post mining companies. For example, predictions on the development of the water quality in pit lakes, the discharge of contaminants from dump sites and the contaminant inputs into watercourses are necessary. The required models are usually developed and applied separately for the specific issues. The hydrogeochemical model system PHREEQC is predominantly used. The PHREEQC model system is a highly flexible tool for hydrogeochemical calculations (Parkhurst et al. 2013).

In the Lusatian lignite mining district, PHREEQC is frequently used for hydrogeochemical modelling to predict the water quality in watercourses and lakes. The necessary water balances for the PHREEQC modelling are derived from hydraulic models for rivers, from water management models for catchment areas and from groundwater flow models. For the groundwater itself, hydrogeochemical modelling has so far only been carried out at a very low level of abstraction, for example by one-dimensional models or conceptual multibox models.

There are numerous models (e.g. OpenGeoSys, Hydrogeochem, TOUGH, PHT3D, PHAST), which combine geohydraulics with hydrogeochemistry. These models have the disadvantage that the geohydraulic part would have to be completely rebuilt and adapted for the respective questions of lignite mining. This would require a complex migration of the whole regional groundwater flow model including its specific inner and outer boundary conditions into the new model. The model structures and limitations of the respective models are often not identical. In the case of models developed for very specific questions in lignite mining, this transition is even impossible because their special boundary conditions are not transferable. A further disadvantage of the abovementioned models is that they often handle only a specific part of the hydrogeochemistry. This raises the question, how existing regional groundwater models could be used for reactive multicomponent transport modelling with the entire functionality and high flexibility of PHREEQC?

Methodological approach

For the coupling of a geohydraulic model with a hydrogeochemical model to a reactive multicomponent transport model the following basic methodological principles were defined:

- The coupling of the geohydraulics and the water quality is done offline. A feedback of hydro- and geochemical processes on the groundwater flow (e.g. density driven effects, buoyancy) are excluded. In the large spatial scales in which the model is to be applied, these effects are mostly negligible.
- The multicomponent transport model uses the model geometry of the geohydraulic model and the steady state or transient water balance calculated by it. Therefore the geohydraulic model must work according to the finite difference method (FDV) or the finite volume method (FVV) in order to maintain the water and mass balance in each model element. The geohydraulic model must provide the flow rates and the water level for each model cell in each time step.
- The full functionality of PHREEQC has to be available in every model cell to represent the hydrogeochemical processes. Therefore it must be possible to formulate and execute a specific PHREEQC script for each model cell.

By adopting the geometry and the water balance of the geohydraulic model, the complete congruence of the models with regard to geohydraulics is ensured and the construction of the multicomponent transport model is thereby simplified and accelerated. Using an appropriate pre-processor, the necessary structures of the multicomponent transport model are generated from the geometry and the water balance of the geohydraulic model. In this way changes in the geohydraulic model are automatically reproduced by the multicomponent transport model.

The solute transport is calculated by an explicit method. However, this method requires a time step limitation according to the Courant-Friedrichs-Lewy criteria. The calculation time step is then dependent on the spatial model discretization and the flow velocity.

The incorporation of PHREEQC into the multicomponent transport model is carried out using a template approach. The problem-specific PHREEQC scripts written by the user can be stored in the model and freely assigned to the model cells. For the calculation, the scripts are then supplemented with the water balance data and executed.

Technical implementation

The development of a corresponding software solution was necessary for the technical implementation of the above described methodological approach. The programming language C# was used for this.

First, a pre-processor was developed that imports the model geometry and the water balance of the geohydraulic model and forms the model structure of the multicomponent transport model (Figure 2). An Application Programming Interface (API) was implemented in the pre-processor to adapt to data structures of various geohydraulic models. Currently, the model geometry and water balance of the geohydraulic model PCGEOFIM® (Sames et.al. 2010) can be imported. This geohydraulic model is widely used in the Lusatian lignite mining district.

In the second step, the initial and boundary conditions for the quality of the groundwater, the geochemical declarations (phase models and kinetics) and the user defined PHREEQC scripts required for the calculation are imported by the pre-processor and assigned to the model cells by grid files (Figure 1, Figure 2).

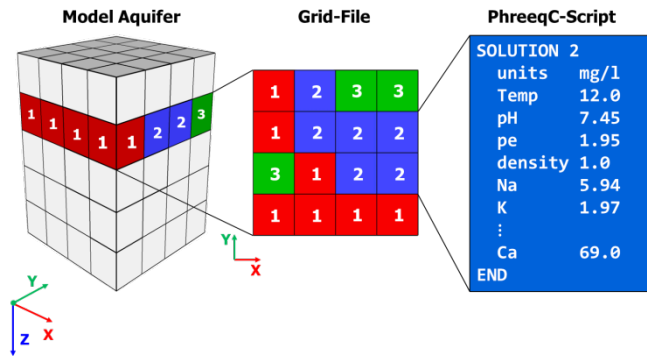


Figure 1: Assignment of PHREEQC scripts and the initial and boundary conditions to the cells of the multicomponent transport model using grid files

The methodological approach for the multicomponent transport model is to calculate the water quality in each model cell with PHREEQC. However, the PHREEQC scripts can only be executed sequentially and single threaded. For models with several ten thousand model cells and long-term predictions of more than a hundred years this results in an immense calculation effort and thus a long calculation time. The calculation speed can be increased only within narrow limits by using powerful computer hardware. In order to carry out the model calculations in an acceptable time and at reasonable costs, an approach to parallelize the PHREEQC calculations has been developed.

For parallelization, the multicomponent transport model is split into segments at each time step. These segments are then distributed and calculated in a computer cluster (Figure 2). The computer cluster is set-up according to a client-server concept and can consist of one or more calculation servers connected via a network. Depending on the performance of the hardware, several PHREEQC instances can be used for the calculations on each calculation server. When the calculations for a time step have been completed, the results for the individual model segments are transferred from the calculation servers to a management client and reassembled to a complete model (Figure 2). The system developed for parallelization is very flexible due to the client-server concept and can be adapted to different structures. For example, the via a computer network connected office computers in a company or a university can be used for the calculations.

The computing speed achieved by the parallelization of the calculations cannot be increased infinitely. When the size of the computer cluster increases, the effort for cluster management, disassembling and reassembling of the model as well as sending and re-

ceiving data increases correspondingly (Amdahl, 1967). At a certain size of the cluster, the administrative expense exceeds the increase in computing speed. The optimum size of the computer cluster depends on the calculation tasks to be performed and cannot be reliably determined in advance. Therefore tuned benchmark tests are necessary for each problem.

The results of each time step are stored by the model and are available for analysis during the model runtime. The results of each time step can also be used as initial values for a new calculation. Thereby it is possible to calculate long-term predictions in shorter subsections. A postprocessor was also developed to evaluate the model results. The results can be displayed and evaluated as maps or videos, or for single points as time series.

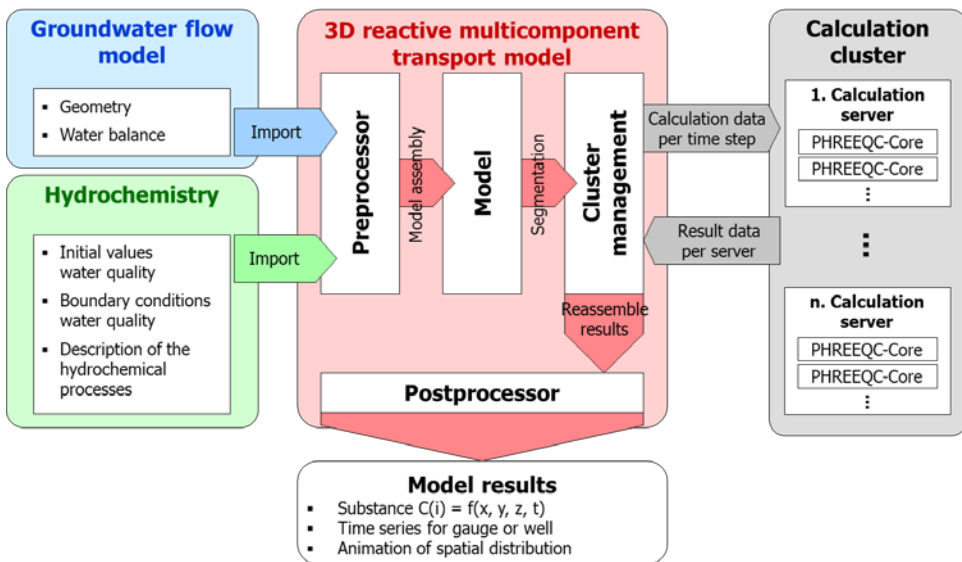


Figure 2: Structural scheme of the reactive multicomponent transport model

Model test

A first test of the developed multicomponent transport model was carried out on a real problem. The question was, when and in what amount the discharge of contaminants from an opencast mine dump reaches a drinking water well gallery located north of the opencast mine.

The multicomponent transport model was constructed for an approx. 11x13 km subarea of an existing geohydraulic model. The model geometry and the steady state groundwater balance were imported unchanged from the geohydraulic model. The horizontal model discretization is 100x100 meters. In the vertical, the model is divided into seven aquifers. The tested multicomponent transport model consists of a total of 104,000 active model cells.

The conceptual geochemical model incorporates a set of 20 relevant chemical components (e.g. pH-value, alkalinity, anorganic carbon, sulphate, iron, calcium, magnesium). The model includes homogeneous and heterogeneous equilibrium reactions, such as complex formation and acid-base reactions as well as cation exchange, surface complexation, mineral solution and mineral precipitation. In addition, homogeneous and heterogeneous kinetic reactions are included, of which sulphate reduction is particularly important in this specific model application.

With the model test, the solute transport from the opencast dump was examined. For the results presentation, the parameter sulphate was chosen as an example. Sulphate concentrations of 1,400 and 200 mg/l were assumed for the groundwater in the dump of the opencast mine and for the groundwater in aquifers beside the opencast mine respectively. The exfiltration of the watercourses was assumed with 400 mg/l, the exfiltration of the lakes with 600 mg/l and the groundwater recharge with 0 mg/l sulphate.

From the model geometry and the steady state water balance, a calculation time step of 18 hours was determined taking the Courant-Friedrich-Lewy criterion into account. For a prediction of 100 years, the calculation of 48.700 time steps was therefore required. For the calculation, ten normal office computers with a total of 60 processor cores were connected via gigabit network. With this hardware configuration, the model calculation took about 20 days.

Figure 3 shows the predicted distribution of the sulphate concentration in the model aquifers along a vertical north-south section through the model at the beginning of simulation, after 50 years and after 100 years. In this illustration, it is clear that the sulphate discharge from the opencast dump in the direction of the well gallery occurs mainly in the upper three aquifers. In the lower aquifers, the solute spread is restricted by geological dislocations with low hydraulic conductivity. In addition, the dilution of the sulphate concentration in the dump by the groundwater recharge can be recognized.

Figure 4 shows the distribution of the sulphate concentration in the 3rd model aquifer at the start of simulation, after 50 years and after 100 years. In the illustration, the dilution of the sulphate concentration in the open pit dump, as well as the discharge of sulphate from the dump towards the drinking water well gallery are clearly visible. After approximately 80 years, the sulphate concentration in the well gallery begins to increase and the sulphate concentration has approximately doubled after about 100 years.

With the model test, the usability and the manageability of the developed reactive multi-component transport model have been proven. In addition, optimization potential for a further increase in terms of calculation speed was discerned. In further model tests more functions will be checked and the prognosis capabilities of the model system will be extended.

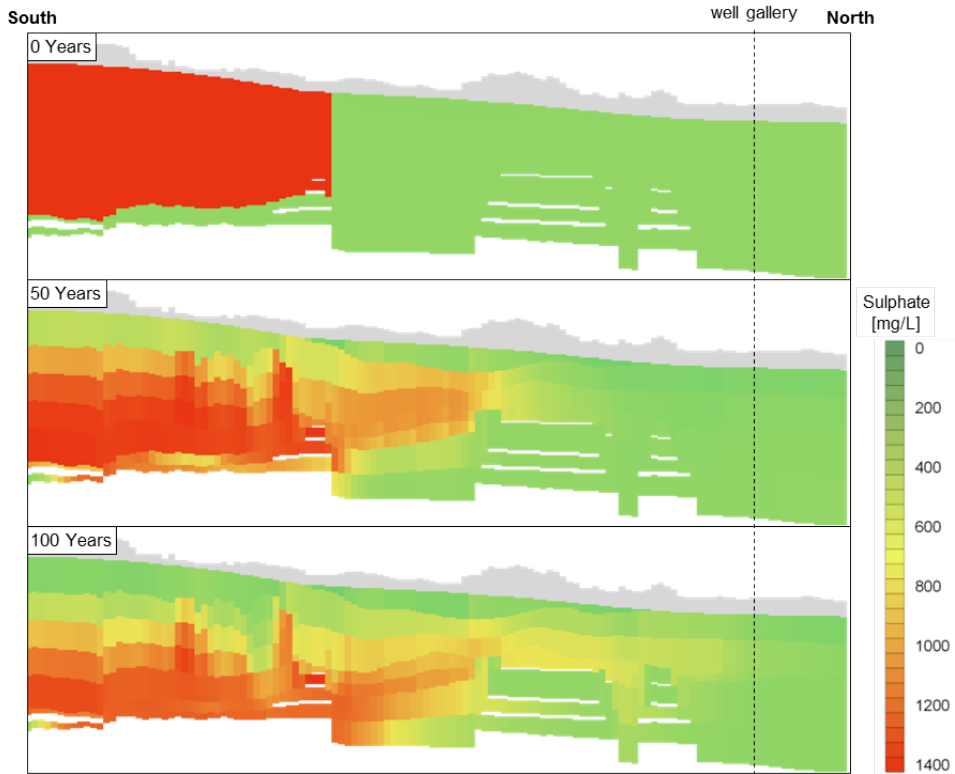


Figure 3: Distribution of the sulphate concentration in a vertical south-north section through the multicomponent transport model at the start of simulation (top), after 50 years (middle) and after 100 years (bottom)

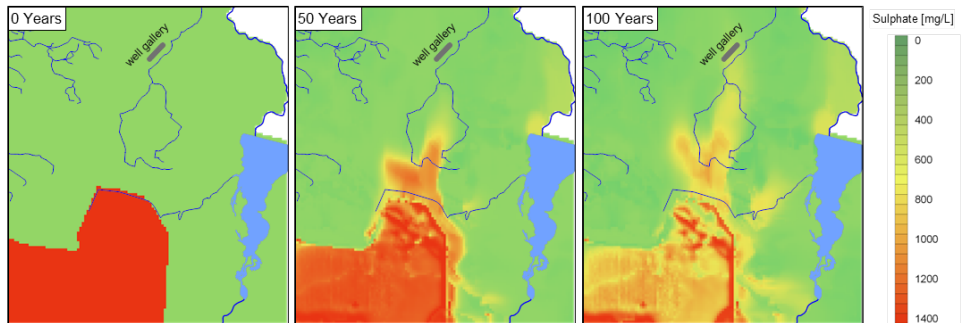


Figure 4: Distribution of the sulphate concentration in the 3rd aquifer of the multicomponent transport model at the start of simulation (left), after 50 years (middle) and after 100 years (right)

Conclusions

With the first successful test of the reactive multicomponent transport model as an offline coupling of the geohydraulic model PCGEOFIM® with PHREEQC on the basis of a real

problem, the practical feasibility of the developed model concept could be demonstrated. It has been shown that three-dimensional hydrogeochemical modelling with the full functionality of PHREEQC based on an existing geohydraulic model is possible in large areas for long prognosis periods with an acceptable calculation time.

Acknowledgements

We would like to thank LEAG (Lausitz Energie Bergbau AG) for the interesting task and the support at the model development.

References

- Amdahl, Gene M.: Validity of the single processor approach to achieving large scale computing capabilities. In: AFIPS Conference Proceedings. Band 30, 1967, S. 483–485, IBM Sunnyvale, California
- Parkhurst, D.L and C.A.J. Appelo: Description of Input and Examples for PHREEQC Version 3—A Computer Program for Speciation, Batch-Reaction, One-Dimensional Transport, and Inverse Geochemical Calculations. US Geological Survey, USA, Denver, Colorado 2013
- Sames, D., Blankenburg, R., Brückner, F., Müller, M.: PCGEOFIM – User manual. Part Model theory (physical and mathematical basics), 2010. Part Geofim-database, 2016.

A model-based study on the discharge of iron-rich groundwater into the Lusatian post-mining lake Lohsa, Germany

Wilfried Uhlmann¹, Kai Zimmermann¹, Sebastian Mix¹, Thomas Claus¹, Oliver Totsche²

¹*Institut für Wasser und Boden Dr. Uhlmann, Dresden, Germany, Wilfried.Uhlmann@iwb-dresden.de*

²*Lausitzer und Mitteldeutsche Bergbau-Verwaltungsgesellschaft mbH, Germany, Oliver.Totsche@lmbv.de*

Abstract As a result of the groundwater rise in the post-mining landscapes of the Lusatian lignite mining district, contaminated groundwater is entering the water courses. To prevent the groundwater contamination of the river Spree between the weir Ruhlmühle and the village Spreewitz, the preferred solution is to capture the iron-rich groundwater with a near river drainage system and discharge it into the nearby reservoir Lohsa II, a former pit lake.

The paper shows the examination of the hydrochemical and ecological consequences on the reservoir Lohsa II using a two-dimensional limnophysical model based on CE-QUAL-W2 4.0.

Key words pit lakes, ferrous und ferric iron, ochre sediments, limnophysical modelling

Introduction

As a result of the groundwater rise in parts of the Lusatian lignite mining district, contaminated groundwater is entering the watercourses. In many cases the groundwater is iron rich and potentially acidic. In the watercourse, the dissolved iron(II) oxidizes, precipitates as iron(III) hydroxide, deposits as an iron sediment on the river bed and inflicts thereby serious damage at the rivers ecology.

To reduce the iron burden of the rivers in the Lusatian lignite mining district a number of measures are examined, planned or already implemented by the Lausitzer und Mitteldeutsche Bergbau-Verwaltungsgesellschaft mbH (LMBV), the company responsible for the rehabilitation of the post mining landscape. To prevent the groundwater contamination of the river Spree between the weir Ruhlmühle and der village Spreewitz, the capture of the groundwater with a near river drainage system and the discharge of the captured groundwater into the nearby reservoir Lohsa II is preferred (Figure 1, Benthaus et al. 2015). In the reservoir, the groundwater can be treated with an existing ship-bound in-lake procedure. Therefore the costs for the water treatment can be reduced and the management of the iron sediment can be solved economically and ecologically. The iron sediment remains in the reservoir, which is covered by German water laws.

Basics

The reservoir Lohsa II originated between 1997 and 2013 in the former lignite open cast mine Lohsa and is divided into five deep basins: Nordostmarkscheide, Westmarkscheide, Drehpunkt Kolpen, Teilfeld 1/2 and Nordmarkscheide. The basins are connected by shallow areas. In the middle of the lake, an island has formed from the inner dump of the mine. On the high-

est water level of +116.4 m NHN, the lake has an area of about 10.8 km² and a sea volume of about 97.4 million m³. About 60.5 million m³ are available for water management (Figure 1).

Together with the reservoirs Dreiweibern and Burghammer, also former pit lakes, the reservoir Lohsa II forms the reservoir system Lohsa II. The reservoir system is located in the bypass of the river Spree. The inlet from the river Spree is located in the east and the outlet to the reservoir Burghammer is located in the north (Figure 1).

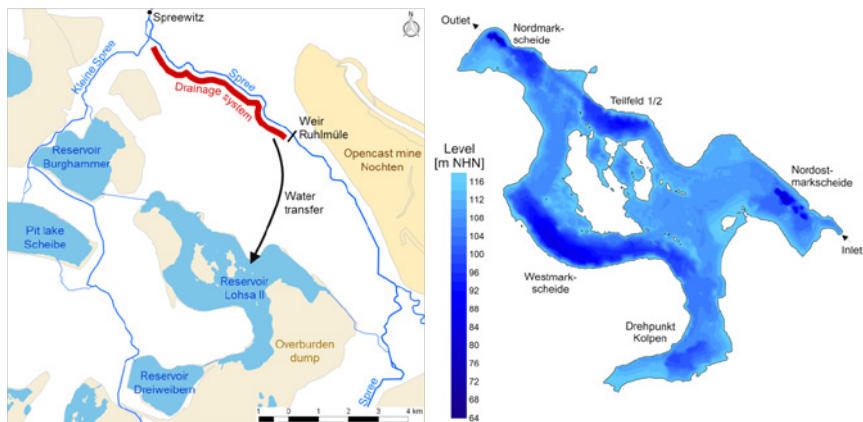


Figure 1: Overview of the Lohsa II reservoir system (left) and the bathymetry of the pit lake Lohsa II (right)

The reservoir Lohsa II is exposed to acidification. In December 2015 the reservoir was neutralized with calcium hydroxide by a ship-bound in-lake treatment (Geller et al. 2013). As a result, the pH-value could be raised to pH = 7 at present and the total iron concentration could be reduced to around 0.3 mg/l. Model-based predictions for the water quality in Lohsa II show that an annual follow-up treatment is necessary to prevent the reacidification of the reservoir.

The amount of groundwater to be captured with the drainage system at the river Spree was provisionally estimated with 0.4 m³/s (Figure 1). The groundwater is anaerobic and characterized by high iron concentrations up to 280 mg/L, a high acidity of approx. 10 mmol/l and a consistent temperature of around +12 °C.

Problem definition

It is expected that the discharge of the collected iron-rich groundwater into the reservoir Lohsa II will result in an increase of the iron concentration and a rapid reacidification. In order to minimize the hydrochemical and ecological consequences for the reservoir Lohsa II, the limnological, hydrochemical and procedural boundary conditions of the discharge have to be clarified. For this purpose, a model-based investigation was carried out on the following questions:

- What is the impact of the groundwater inflow on the reservoir's hydrochemistry, in particular the iron(II) and iron(III) hydroxide concentrations, as well as on the costs of the in-lake water treatment?

- How does the iron rich groundwater spread out in the reservoir and what external factors influence the spread?
- At which site and in what depth does the inflow of the groundwater have to take place in order to minimize adverse effects on the lake? Is the discharge into the shallow basin near the inlet (Nordostmarkscheide) more favourable than the discharge into the central and deep basin (Westrandschlauch)?
- Where in the reservoir does the iron(III) hydroxide deposits? What is the thickness of the iron sediment layer after a certain time? How much storage volume for the iron sediments is available in the reservoir and how long can the process be carried out?

Model selection

The spatial spread of the groundwater in the reservoir was investigated with the two-dimensional model CE-QUAL-W2 4.0, which was used before in similar investigations (Uhlmann et al. 2016). Model version 4.0 incorporates the oxidation of ferrous iron(II) to ferric iron(I-III) hydroxide and the sedimentation of ferric hydroxide as kinetic reactions of different complexity (Cole et al. 2016). The temperature dependence of the ferrous iron oxidation had to be supplemented in the source code of the model.

Model assembly

In CE-QUAL-W2, the reservoir Lohsa II is divided into segments whose positions and boundaries are derived from the bathymetry of the reservoir. The model reproduces the sequence of the deep basins and shallow areas. The main stream runs from the inlet through the deep western basin to the outlet and is represented by a single segment branch (Figure 1). The other basins as well as the “lagoon” in the island area are represented by separate branches. The reservoir was vertical discretized with 0.2 meter in the range of the water level fluctuations and with 0.5 meter in the remaining range.

Model calibration

The thermal stratification behaviour and the oxygen distribution were calibrated on measured temperature and oxygen profiles (Figure 2). For the calibration of the thermal stratification behaviour, the parameters for the wind and radiation influence as well as the ice cover of the lake were used. The oxygen distribution in the lake was calibrated via the oxygen consumption of the sediment. The parameters for the reaction kinetics of iron oxidation and iron sedimentation were derived from measurement data and laboratory tests.

Model application

Different sites and depth for the groundwater inflow were considered as variants (Table 1). The eastern shallow basin at the inlet from the Spree, and therefore the furthest from the outlet (Var.1), as well as the central and deepest basin (Var.2 to 4), are alternatives for the discharge of the iron rich groundwater. A basic variant without a groundwater inflow was used as basis for the evaluation. It is assumed in any case, that concurrently to the discharge of the iron-rich groundwater, the reservoir Lohsa II has to be neutralized. The acid-base state thus is determined by the carbonate balance.

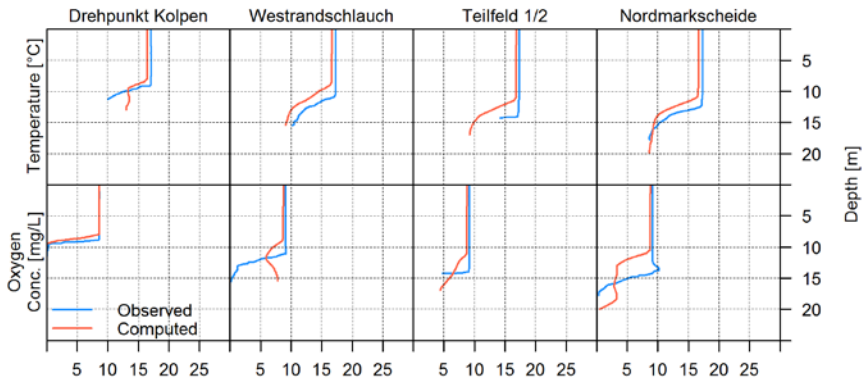


Figure 2: Observed and computed temperature and oxygen profiles in the reservoir Lohsa II

Table 1: Investigated variants for the inflow of the iron rich groundwater into the reservoir Lohsa II

Variant	Inflow site...	Inflow in depth...	Additive
0	---	---	
1	eastern basin	near surface (epilimnion)	calcium hydroxide
2	central basin	near surface (epilimnion)	calcium hydroxide
3	central basin	deep water (metalimnion)	calcium hydroxide
4	central basin	deep water (hypolimnion)	calcium hydroxide, oxygen

Model results

Thermal stratification behaviour and oxygen distribution

The thermal stratification behaviour of the lake is not significantly affected by the groundwater discharge in any variant. A stable dimictic layering behaviour is maintained in all investigated variants (Figure 3). At a near surface inflow (Var.1 and 2), the influence on the stratification behaviour is superimposed by atmospheric processes. An inflow in the deep (Var.3 and 4) leads only locally to a slight increase in the water temperature of the hypolimnion.

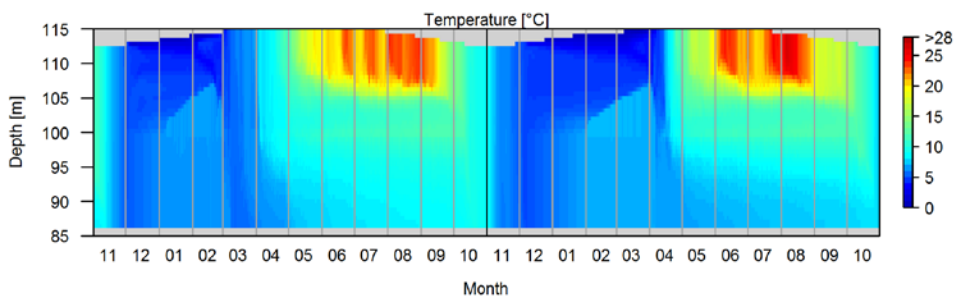


Figure 3: Modelled temperature distribution in the central basin with a groundwater inflow in the metalimnion (Var. 3) in the model years 2002 and 2003

At a near surface discharge of the groundwater (Var.1 and 2), there is always enough oxygen available for the oxidation of the ferrous iron. If the groundwater is discharged in the deep (Var.3 and 4), the available oxygen in the meta- and hypolimnion is completely consumed during the stagnation periods (Figure 4). This can be avoided with additional deep water aeration (Var.4).

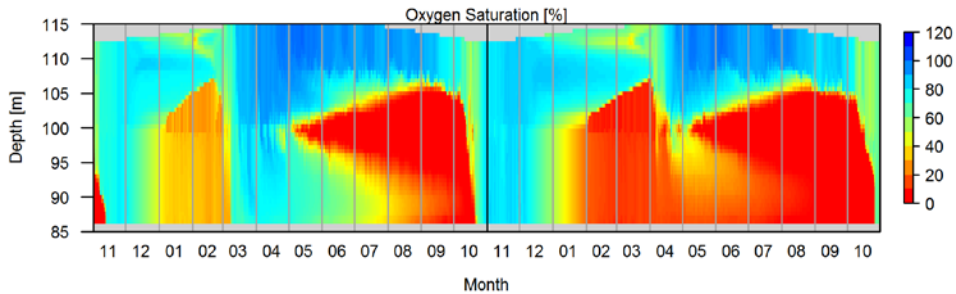


Figure 4: Modelled distribution of the oxygen saturation in the central basin with a groundwater inflow in the metalimnion (Var. 3) in the model years 2002 and 2003

Spatial and temporal distribution patterns of the iron load in the reservoir

In the epilimnion, the iron(II) concentration does not rise above 1 mg/l in any variant. In case of a groundwater discharge in the deep (Var.3 and 4), the iron(II) concentration in the meta- and hypolimnion rises up to 20 mg/l during the summer stagnation period. The oxidation of the iron(II) enriched in the hypolimnion starts again with the autumn circulation period, when the hypolimnion is intermixed into the entire water body (mixolimnion).

At a groundwater inflow near the surface (Var.1 and 2), the iron(III) hydroxide concentration is increased during the summer stagnation period to 15 mg/l in the epilimnion and up to 20 mg/l in the hypolimnion of the deep basins. During the spring and autumn circulation, the iron(III) hydroxide concentration in the whole water body drops to around 10 mg/l.

If the groundwater is discharged in the meta- or hypolimnion (Var.3 and 4), a nearly permanent iron(III) hydroxide concentration of more than 20 mg/l is established there (Figure 5). When the hypolimnion is intermixed into the entire water body during the circulation periods (mixolimnion), the iron(III) hydroxide concentration at the surface of the reservoir spontaneously increases (Figure 5). Such events have already been observed empirically on several pit lakes in the area where the iron input originates from nearby mining dumps. During the summer and winter stagnation periods, the iron(III) hydroxide concentration in the epilimnion is invariably below 2 mg/l. In regard to the iron distribution in the reservoir, a groundwater discharge in the deep in combination with an additional aeration is advantageous.

Temporal iron load at the outlet of the reservoir

Of particular interest were the iron concentration and their temporal variability at the outlet of the reservoir Lohsa II. If the groundwater is discharged near the surface in the eastern ba-

sin (Var.1), the iron(III) hydroxide concentration at the outlet increases only for a few days over 2 mg/l. At a near-surface inflow in the central basin (Var.2), the iron(III) hydroxide concentration at the outlet is over 2 mg/l throughout the year because of the short distance between the inflow site and the outlet. In case of a groundwater inflow in the meta- or hypolimnion (Var.3 and 4), the iron(III) hydroxide concentration at the outlet increases only during the circulation periods above 2 mg/l.

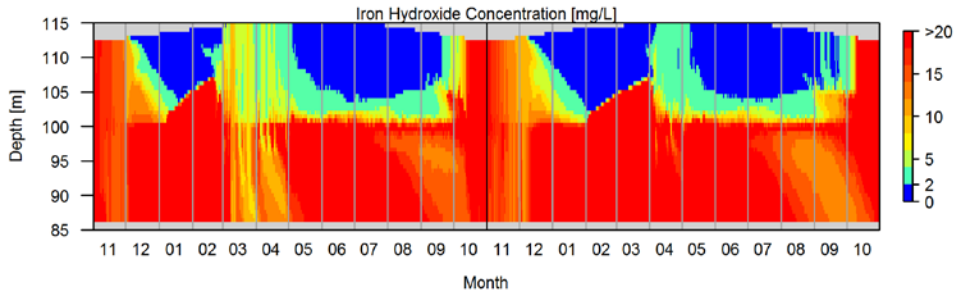


Figure 5: Modelled iron(III) hydroxide distribution in the central basin with a groundwater inflow in the metalimnion (Var. 3) in the model years 2002 and 2003

Spatial distribution of iron sediments

Due to the precipitation of the iron(III) hydroxide, an iron-rich sediment deposit is formed. From experience, the sediment load can be assumed to have an iron content of 400,000 ppm and a dry residue of 5% by mass after medium-term consolidation. When the groundwater is discharged near the surface (Var.1 and 2), the iron(III) hydroxide is distributed over the whole lake, so that the iron rich sediments are deposited nearly everywhere in the reservoir. After 20 years, a sediment thickness of around 1 meter is expected almost in the entire lake (Figure 6, left). When the groundwater is discharged in the meta- or hypolimnion of the deep central basin (Var.3 and 4), the spreading of the iron(III) hydroxide is strongly restricted and the iron sediments are mostly deposited in the deep water areas. After 20 years a sediment thickness of approx. 2.2 meter is expected in the central basin. In the rest of the reservoir the sediment thickness is significantly smaller (Figure 6, right). The extrapolation of the calculations shows that the Lohsa II reservoir can be used for at least 50 years for the discharge of the iron-rich groundwater without losing its basic limnological properties as a dimictic lake.

Conclusions

The model results show that the discharge of the iron-rich groundwater into the pit lake Lohsa II is a technically feasible option for the treatment of the groundwater and the storage of the resulting iron sediments. However, due to the hydrochemical properties and the considerable amount of the groundwater inflow, a supplementary water treatment (neutralization, aeration of the hypolimnion) is necessary.

A groundwater inflow near the surface offers the advantage of a sufficient oxygen supply for the iron oxidation. It is however disadvantageous that the iron(III) hydroxide produced

during the oxidation spreads over the entire surface of the lake and also sediments in the ecologically important littoral zones.

When the groundwater is discharged into the reservoirs meta- or hypolimnion, the spread of the iron(III) hydroxide is strongly restricted. However, the limited oxygen supply in the deep water is consumed entirely by the ferrous iron oxidation. This leads to a corresponding oxygen deficiency in the stagnation period and subsequently to an increase of the fish-toxic iron(II) concentration. This disadvantage can be remedied by an aeration of the deep water. The selection of the inflow site is determined by the available storage volume for the iron sediments. The storage volume in the central sub-basin is much larger than in the other basins of the reservoir. The disadvantage of temporarily increased iron(III) hydroxide concentrations at the outlet of the reservoir must be taken into account.

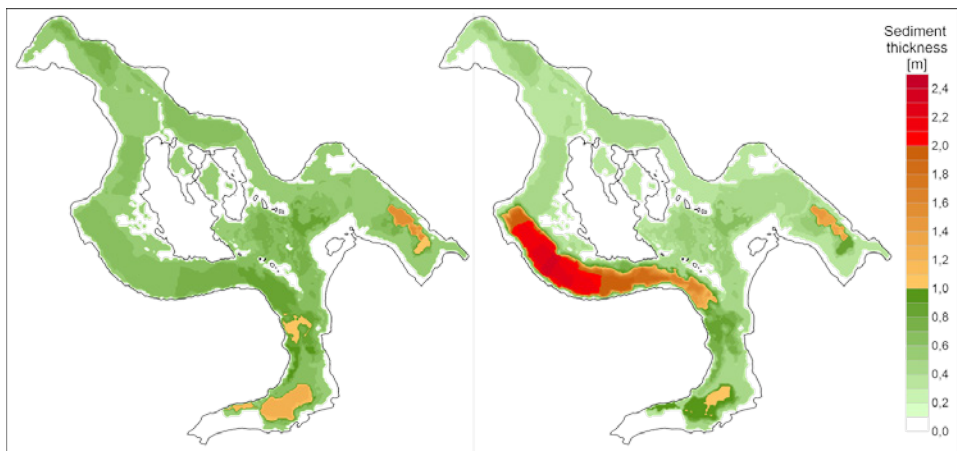


Figure 6: Projected thickness of the iron sediments in the reservoir Lohsa II after 20 years with a groundwater inflow near the surface (Var. 2, left) and in the metalimnion (Var. 3, right) of the central basin

Acknowledgements

We thank the company LMBV for the possibility to attend this investigation and to present the main results.

References

- Cole TM, Wells SA (2016) A Two-Dimensional, Laterally Averaged, Hydrodynamic and Water Quality Model, Version 4.0 User Manual. Portland State University
- Benthaus FC, Uhlmann W, Totsche O (2015) Investigation and strategy on iron removal from water courses in mining induced areas. In: Brown A et al. (Eds.), 2015 10th International Conference on Acid Rock Drainage & IMWA Annual Conference, Santiago, p 1068-1078
- Uhlmann W, Zimmermann K, Mix S, Nixdorf B, Totsche O (2016) Causes of a distinct metalimnic oxygen gradient in the pit lake Senftenberger See in summer 2013 as a case study. In: Drebenstedt et al. (Eds.) Mining Meets Water – Conflicts and Solutions IMWA 2016 in Leipzig, p 261-268
- Geller W, Schultze M, Kleinmann R, Wolkersdorfer C (2012) Acidic Pit Lakes. Springer Science & Business Media, ISBN 3642293840, p 233

Appropriate Catchment Management can Improve the Profitability of a Mine: A Case Study from Dallol, Ethiopia

Malcolm Anderson¹, Tomas C. Goode²

¹*Technical Director, MWH now part of Stantec, Buckingham Court Kingsmead Business Park, Frederick Place London Road, High Wycombe, HP11 1JU UK, malcolm.anderson@mwhglobal.com*

²*Supervising Hydrogeologist, MWH, now part of Stantec, 1620 W. Fountainhead Parkway, Suite 202, Tempe, AZ 85282, USA, tomas.goode@stantec.com*

Abstract How do you secure a fresh water supply for a new mine where groundwater consists of brine located in “the hottest place on earth”, in one of the most remote desert regions of the world, with very little pre-existing information? Catchment management principles provided the solution. YARA and the Ethiopian Government have invested substantial cost, effort, and time into investigation of the Sustainable Yield, Deployable Output, and environmental and local water supply needs in the Dallol region, which has allowed the design of a water supply for the proposed mine with a water quantity and quality that is likely to be both reliable and resilient and to save costs during the LoM (Life of Mine).

Key words catchment water management, groundwater investigations, mining costs

Introduction

Mine water supply has been considered historically as an engineering problem that can be developed as a component of the mine extraction and processing design after completion of the mineral exploration phase. This approach engenders mine profitability at the earliest opportunity, but due principally to the time required to investigate and understand the mine water supply catchments, will always leave substantial latent risks from the uncertainty in the reliability and resilience of the long-term water supply and the impact of the mine on the catchment. In order to address availability, use, management and sustainability of mine water resources, the mining industry has recently developed guidelines to promote implementation of catchment-based water management principles in new mines (ICMM 2017), which is especially relevant in desert regions (Anderson, 2015), or jurisdictions where these guidelines are not enforced, or are not already engendered in national law. However it is important to note that uncertainty in water supply reliability and resilience is also a substantial latent risk that often results in expensive legacy issues as mining progresses. These include moving costly wellfields or river dams built in the wrong place, and/or continuously investing in expensive additional treatment as water quality progressively deteriorates.

YARA Dallol (YARA) are currently developing a potash mine in the Danakil Rift in NE Ethiopia near the Mt. Dallol volcano (Figure 1). The study area is defined by surface water catchments that drain from the Lelegehedi/Ayshet Graben down to the centre of the Danakil Rift, and specifically the area bounded by the Regali River to the north, the Saba River to the south as far as Lake Assale, and the centre of the Danakil Rift. YARA have applied catchment management principles in the development of their proposed mine from the outset of their involvement in 2011, (well before the ICMM publication). This process required

four years of investigation, so upfront costs were reduced by undertaking the catchment management investigations alongside the mineral extraction pilot testing program, and by partnership with the Government of Ethiopia, (who paid for and undertook the early water resources exploration).

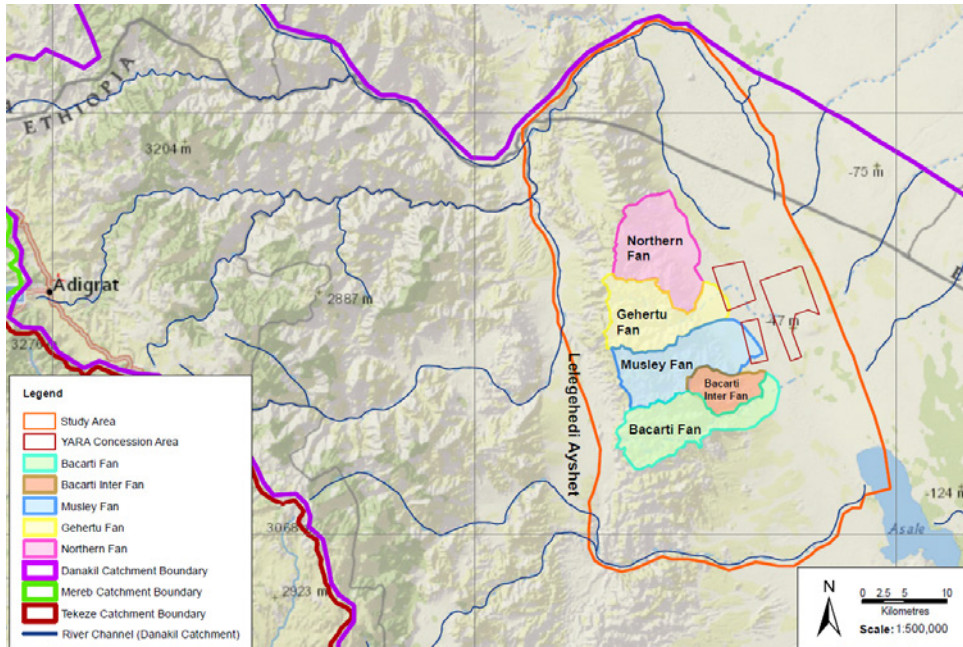


Figure 1: Yara-Dallol study area in the Danakil Depression, Ethiopia

The Sustainable Yield is usually defined as the rate at which water may be removed from the groundwater hydrologic system without removal of water from storage over the medium term. In groundwater systems this is roughly equal to the combined average annual inflows and is often conflated with the sustainable water supply. However, the mine process requires a resilient supply with a reliable quality (in this case of fresh to brackish water), whereas the potash resources are associated with brines. The fresh and brackish water in the area of accessible groundwater floats on the brines and also interacts hydrodynamically with them, placing severe restrictions on the water quality that can be obtained. Thus in the Dallol environment, the deployable output (DO), which is the reliable flow rate at a particular required quality that can be delivered by a single well, or combined wellfield, will always be lower than the aquifer Sustainable Yield. This is due to the water quality mixing that occurs naturally in the system, and in response to the imposed pumping. Thus the imperative of a resilient and reliable water supply requires that the DO be a substantial percentage lower than the aquifer Sustainable Yield and by corollary, at least at a global level, will also be protective of catchment management principles. Thus both aquifer quantities need to be defined in a catchment management study. It is also useful to define three kinds of DO as follows:

- The minimum DO (MinDO) which is the DO that can be delivered during a design drought to provide the resilience required by the design specification.
- The mean DO (MDO) which is the DO available in average rainfall years. It is often the value used to define individual well and combined wellfield extraction licence quantities.
- The peak DO (PDO) which defines the capacity and reliability of the water supply system. It will always be 10 to 20% greater than the MDO to allow for individual pumps and wells to be temporarily switched off for maintenance whilst maintaining mine demand.

Historical Investigations

Mining of the substantial halite salt deposits in the Dallol area of the Danakil depression stretches back to antiquity, and artisanal mining operations continue to cut and transport halite by camel train to the salt market in Makelle to the present day. Commercial mining of potash salts began during the First World War, but ceased once the war ended due to competition from other sources, although it was intermittently restarted on a number of occasions in 1925-1929, 1951-1953, and most notably from 1960 to 1969 by the Ralph Parsons Company. Good regional geological information is available from this last period. This includes descriptions of magnetic and gravity geophysical surveys, lithology, stratigraphy, estimated thicknesses of the main geological units, and the general geological structure, (Holwerda & Hutchinson, 1968 and Bannert et al 1970), and a geology sketch map prepared by Brinckmann & Kursten (1970), that provides the detailed distribution of geological units in the study area. Despite this map being provisional, it is still the most reliable representation currently available. Furthermore the paper by Bannert et al (1969), was produced by the same group of authors as Brinckmann & Kursten (1970), and is effectively a memoir to the map. On the other hand very little groundwater data survives from these early operations. Further, the water supply wells in the Musley fan constructed by the Ralph Parsons Company in the late 1960s have nearly all since collapsed with only approximate locations and summary details of their well depth, groundwater depth and the water quality obtained.

Due to the rudimentary historical data available, four phases of groundwater investigations, undertaken over four years, were necessary to obtain the conceptual groundwater model (CGM). This defines the detailed understanding of the groundwater flow system, including reliable quantities for the annual water balance, Sustainable Yield, and DO available from each wellfield option. The CGM also defines the hydraulic properties of all the key hydraulic units, the groundwater potential gradients, the inflows from direct rainfall and runoff recharge and from regional through-flow, the locations of outflow from springs and predominantly soil evaporation, the locations and control of saltwater and brine density interfaces on groundwater flow and quality, and the modulation of the groundwater density by groundwater temperature (geothermal processes) and soil evaporation (saltwater to brine concentration processes). These steps were as follows:

- i) Phase I: Regional water survey, groundwater exploration and drilling program to determine well yields and water quality of key formations. Commencement of baseline surface water, groundwater level and water quality monitoring.
- ii) Phase II: Drilling of pilot wells, monitoring wells and piezometers and short duration well testing of pilot wells. Preliminary CGM development, targeted water en-

vironment surveys (socio-economic, vegetation, wildlife), and continued baseline monitoring.

- iii) Phase III: Drilling of pilot wells in target aquifers, and short duration testing of pilot wells. Continued surface water and groundwater level and water quality monitoring.
- iv) Phase IV: Drilling of final monitoring well network and long duration testing of pilot wells in potential wellfields. Continued water monitoring program.

Hydrological, Geological and Geophysical Surveys

One of the first steps in the catchment investigation included a spatially extensive transient electro-magnetic (TEM) geophysical survey undertaken in two phases with multiple survey lines parallel to the rift margin and along the target wadis. The TEM method was effective at delineating the fresh water thickness and the depth of the saltwater interface along each survey line. Above this interface, measured resistivity distinguished the major rock units, the water quality in these units, and the depth of the vadose zone. Results of the TEM survey indicated significant differences in freshwater and saline water thicknesses between different alluvial fans. In turn, this provided insight into the freshwater flow system, and the effect of density controls, which result in relatively light freshwater floating as a lens on top of the denser saline water.

An extensive inspection of the geological units at key locations throughout the study area was undertaken in Phase II to identify the geological distribution and succession. This survey confirmed the geology was mostly consistent with the sketch map and stratigraphy of Brinckmann & Kursten (1970). Precambrian massive sandstones, greenstones, volcanics and intrusives form the basement of the system and outcrop in the hills bordering the western margin of the rift. Jurassic limestone, (and locally Jurassic sandstone below), lie unconformably on the Precambrian. The Jurassic units are the best bedrock aquifers in the area, and the locations of the Jurassic inliers and down-faulted blocks control the groundwater flow system, by draining the flow in the Precambrian and redistributing the flow along the Rift margin. The proto-rift sediments of the Neogene Danakil Formation overlie the Jurassic units, and consist of marls, clays, silty sandstones, conglomerates, volcanics and intrusives that together form a confining layer of the Jurassic rocks below. Finally the Quaternary sediments of the current rift comprising sands and gravels in alluvial fans along the rift boundary, transition through sands into the silts and clays, and finally the halite in the centre of the rift playa, as indicated in Figure 2.

An extensive inspection of surface water features was also undertaken in Phase II throughout the study area at the same time as the geological survey. The water features survey, in conjunction with the TEM data, and the monitoring well and piezometer data, defined the key hydraulic features of the system and indicated the preliminary CGM: infiltration in the sands and gravels of the wadis and fans from flood run-off, groundwater through-flow within the bedrock, approximate flow directions, locations of saltwater interfaces, the water quality transition from deep fresh groundwater in the bedrock, to thick fresh water sequences in the alluvial fans, to very shallow brine groundwater in the playa. Soil evapora-

tion from shallow groundwater in both the silt/clay and halite playa sections was identified as the dominant outflow from the system. The surveys also indicated the likely presence of a salt karst flow system within the silt/clay and halite playa, the brackish hot water upwelling along the rift boundary (regional geothermal water), and the superimposed hot brine convection in the volcano geothermal system beneath Mt Dallol. The preliminary CGM is provided in section and plan view in Figures 2 and 3.

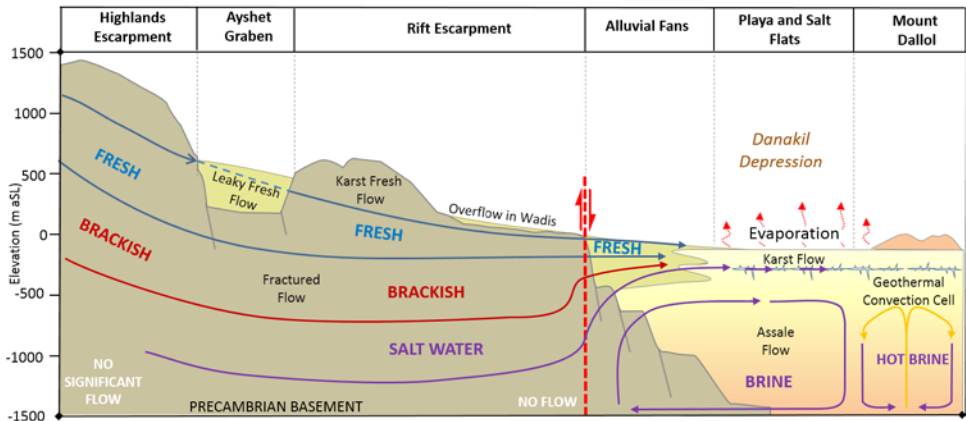


Figure 2: Provisional CGM cartoon section of the Rift Valley in the vicinity of Dallol

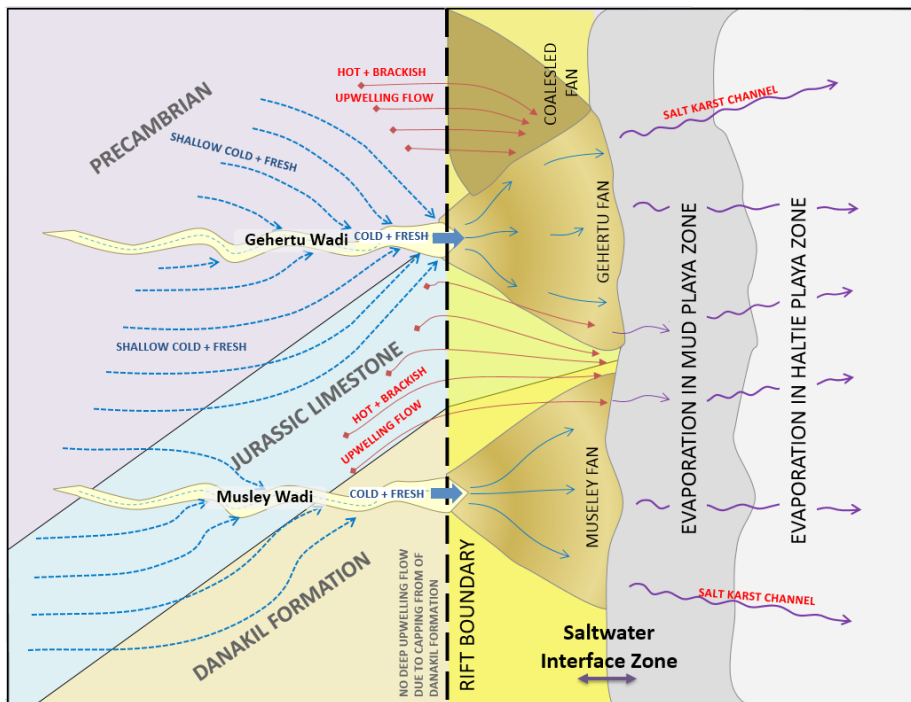


Figure 3: Provisional cartoon map of groundwater flow

Well Construction and Monitoring

An extensive pilot well, monitoring well and piezometer drilling program was developed in phases over the four-year time frame to validate the geology, hydrogeology and preliminary groundwater conceptual model. Hydraulic parameters (transmissivity, storativity, hydraulic conductivity, barrier boundaries, etc) of all key groundwater units were determined initially from short duration (1 to 6 day) tests of the pilot wells, which were then subsequently used as monitoring wells. Groundwater level monitoring (of up to three years) in each monitoring well provided dip and data logger measurements of the daily and seasonal groundwater fluctuations related to precipitation, flooding, and dry season and drought events. This data provided an essential baseline of the typical seasonal behavior of the regional aquifer system.

Water Balance and Sustainable Yield Estimates

The bedrock through-flows to the groundwater system (see Figure 2) are difficult to determine as the depth and thickness of groundwater flow in the rift escarpment bedrock was too deep (expensive) to prove from drilling. Similarly the fresh water through-flow through alluvial fans can't be calculated reliably as fresh water groundwater heads and gradients are affected significantly by their buoyancy on the brines below. However as groundwater inflow will equal groundwater outflow from the system during an average year, measurement of the soil evaporation outflows in the playa initially provided the only method of estimating total outflows and thus the total inflows and Sustainable Yield of the groundwater system. Innovative use of porous cup lysimeters determined the rate of soil evaporation at more than 9 locations across the silt/clay and halite playa. Rates of capillary rise at various locations, times, and depths below ground surface in the playa flats provided estimates of vertical groundwater flow moving out of the system by way of evaporation. Combined lysimeter measurements of soil evaporation rates fed into the CGM. However the rate of evaporation was found to be very sensitive to groundwater depth; doubling for every 10 cm reduction in depth, and although the playa is extremely flat, the potential error in the depth measurement was likely to be at least 10 cm. As a result, an alternative method was required to provide more reliable Sustainable Yield estimates.

Consequently a large number of monitoring wells were drilled during Phase IV in the bedrock in the western rift boundary above the fans, and most importantly above the saltwater interface zone. Thus groundwater elevations determined from well dip data, were largely unaffected by density and buoyancy effects, and were used to construct a flow net to identify groundwater flow directions and gradients, (as well as inflow, up-flow, recharge and discharge zones). The transmissivity and hydraulic conductivity data calculated from the packer, injection, and aquifer tests, along with aquifer thicknesses derived from the drilling and well construction program, and the groundwater gradients from the flow net, were used to calculate aquifer flux rates using the Darcy equation. As the monitoring wells were predominantly located outside the zone affected by saltwater density and buoyancy effects, the Darcy calculations provide the most accurate estimate of the aquifer Sustainable Yield. They also compared favourably with the lysimeter evaporation estimates, providing validation

of these earlier estimates. Overall, both estimates confirmed that flood run-off provides an important augmentation, but only a minor contribution, to the groundwater balance, which is instead dominated by bedrock through-flow.

Well and Wellfield Deployable Output

The MinDO, MDO and PDO of individual wells (and combined wellfields) has been estimated from a numerical groundwater model predicated on the CGM, and calibrated against the water balance and large groundwater data set. The calibrated numerical model demonstrates its accuracy by how closely the steady state and transient model results match the observed conditions of groundwater elevation and water quality. Analytical methods (e.g. Schmorak & Mercado, 1969), were also used to validate and augment the numerical model results to determine the constraints on DO from saltwater upconing and saltwater intrusion.

Pumping tests of pilot wells determined the individual well PDO and validate the numerical model MDO and MinDO estimates. Initial tests of the order of several days established well production capacity (PDO) and water quality parameters in early phases. In phases 3 and 4, measurement of water quality against pumping rate and well depth demonstrated that the water quality was strongly influenced by well design in most of the aquifers. Tests of 2 to 3 months duration in the final phase provided insight into the sustainability, water quality, and MDO available from each location of the aquifer system tested. Water quality degradation was significant within one of the alluvial fan sites, where electrical conductivity (EC) during early tests was initially below 2000 $\mu\text{S}/\text{cm}$, but increased to 7,800 $\mu\text{S}/\text{cm}$ without stabilising during the two month test. However, production rates were comparable in a second well location, where only minor changes in water quality occurred (from 1,900 to 1,970 $\mu\text{S}/\text{cm}$).

Discussion

The value of implementing the catchment management approach from the outset of the project can't be easily understated. The commitment to the thorough investigation of the groundwater and surface water systems had strong benefits in multiple spheres including the hydrological, environmental, engineering, water resources management and regulatory aspects of the water supply project. Desert hydrology is highly variable, and it is widely recognised that data periods of less than 5 years are wholly unreliable due to the large variations in precipitation each year. So it would have been impossible to define the design drought duration (a key element of a reliable and resilient engineering system) from say just 2 years of data. Even with the catchment management commitment, the 5 year rule of thumb will only have just have been achieved in the key data sets by the time the mine approval has been obtained and a construction start has been scheduled.

Secondly it is interesting to speculate what the outcome would have been if the 1969 Ralph Parsons' wellfield had merely been replaced after minimal investigation. The long duration test results clearly indicated that progressive and severe water quality degradation would have occurred over the first one to say 5 years. Over time the data from the catchment water balance and flow net (determined from the catchment management method), indicated that

the water quality was likely to trend towards brine and become prohibitive, requiring a completely new water supply. Furthermore as the salination process is slow, mine construction would likely have been completed by the time a new water supply became an imperative. It is thus almost certain that wellfield development in the wrong location would ultimately have resulted in the requirement for a very expensive remote new water supply, the costs of which would substantially impact the bottom line, whilst the worst case scenario would cause termination of mine production.

More importantly, the other long duration test undertaken to date, indicates that stable and good quality water can be obtained from other aquifer locations. However without the knowledge gained from the 4 years of detailed groundwater investigation, allowing the development of a detailed flow net, it would have been impossible to infer the causes of the good and poor wellfield locations. Thus the commitment to detailed investigation provided a clear decision path to reliably select the proposed wellfields. Furthermore if there is insufficient data to define the fresh water MinDO and MDO reliably, then even in the right location, a wellfield water supply will be unreliable and prone to underperform the design. Thus in summary, a commitment to proper engineering investigation over a period of 4 to 5 years (and by corollary the catchment management approach) is the only way to derive a reliable and cost effective engineering design. This is especially the case in aquifers sensitive to water quality or in locations of highly variable rainfall.

In the environmental sphere, the greater accuracy of the CGM from the commitment to the catchment management methodology allows the impacts of the proposed wellfields to be determined with greater reliability. It thus allows the definition of the most suitable mitigation strategies and the avoidance of approaches that do not work.

In the governmental and permitting sphere, YARA worked closely with the Ministry of Water, Irrigation and Energy, the Department of Water Resources (DWR) and the Water Works Design and Supervision and Enterprise (WWDSE), the government engineering consultancy. During Phase I the works were directed by WWDSE and funded by the MWIE. From Phase II onwards, the investigations were funded by YARA, but the works for each campaign were submitted to the government in advance for approval and authorisation. Furthermore as the works were completed, YARA provided all the data and reports to the DWR and WWDSE for review, consultation, and agreement of next steps through workshops and consultation.

This collaborative approach was perhaps the greatest value of the catchment management approach. From the outset, it was agreed that the Ethiopian Government would own all the data and well infrastructure from the catchment management investigations located outside the YARA mineral concessions. This approach provided the critical data to allow the government entities to exercise regulatory oversight of the investigations, to retain the sole right to licence and control the extraction of any water supplies, whilst at the same time, providing the infrastructure required to monitor and manage any future wellfield devel-

opments. On the other hand, the funding of the investigation costs by YARA from Phase II onwards ensured that the programme was not held up whilst limited cash resources were procured by the government. The reduction in delays was therefore a substantial cost benefit to YARA. However perhaps the greatest value, was the development of trust between the various entities of the Government of Ethiopia and YARA that allowed the catchment management works to progress efficiently and without delays.

In other words in every sphere, it is possible to show the catchment management approach has saved costs in the short term, but should save substantial costs in the medium and longer term.

Conclusions

This brief case study shows that the catchment based water management approach provides cost savings for mine operations when implemented before mine construction. It not only enhances the bottom line in the medium to long-term, but also provides a “licence to operate” by identifying the resource reserve required to protect the water needs of the environment, wildlife and other water users. This study was undertaken in the Rift Valley of NE Ethiopia in a remote, largely undefined and challenging physical environment, so the approach is likely to be transferable anywhere. Key to the investigation was quantification of the Sustainable Yield of the groundwater system as well as the PDO, MDO and MinDO of alternative wellfields and individual wells. This approach has allowed the logical redevelopment of water supplies used by past operations to be recognised as an expensive mistake that needed to be avoided. Finally, early implementation of these investigations, in parallel with the mine process pilot stage (i.e. immediately following exploration) has proven largely successful. However start of water exploration during the mineral exploration phase would have been the best approach as this would have maximised the length of data beyond the minimum of five years required to complete the catchment investigations.

References

- Anderson MD (2015), The strategic advantages of mine water supplies from deep aquifers in the desert regions of the Middle East and North Africa, Proc. 2nd Int. Conf. Mine Water Solutions, Vancouver.
- Bannert, D. et al. (1970) In German, Zur Geologie der Danakil-Senke, Geologische Rundschau, 02, 409-443.
- Brinckmann, J and Kursten, M (1970) Geological Sketchmap of the Danakil Depression. Bundesanstalt für Bodenforschung, Hannover.
- Holwerda, J and Hutchinson, R (1968) Potash-bearing Evaporites in the Danakil Area, Ethiopia. Econ Geol. 63, 124-150
- ICMM (2017) A practical guide to catchment-based water management for the mining and metals industry, www.icmm.com/guide-to-catchment-based-water-management.
- Schmorak S and Mercado A (1969) Upconing of Fresh Water-Seawater Interface below Pumping Wells, Field Study, Wat. Resour. Res. 5, 1290-1311.
- WWDSE (2014) Musley and Adjacent Fan Areas Groundwater Potential Evaluation, Dallol Area Groundwater Potential Assessment Project, Final Report (Annex I and II).
-

Geochemical Processes in a Column: Modeling Humidity Cell Test Results

Ann S. Maest¹ and D. Kirk Nordstrom²

¹*Buka Environmental, 941 8th Street, Boulder, CO 80302, USA. 303-324-6948,
aamaest@gmail.com*

²*U.S. Geological Survey, 3215 Marine Street, Boulder, CO 80303, USA. 303-541-3037,
dkn@usgs.gov*

Abstract Humidity cell tests (HCTs) are used to evaluate the potential for mined materials to leach constituents during operation and closure with an emphasis on sulfide oxidation. Our work evaluates the ion balance of the leachate results, emphasizes secondary mineral weathering and the “early flush” of solutes, and uses two types of geochemical modeling approaches to help understand reactions occurring throughout the tests. Secondary salt dissolution lasted for up to ~60 weeks and overlapped with peak sulfide oxidation. In all tests, sulfide oxidation dominated over a limited time that was rarely apparent at the end or the beginning of the test. Unlike early flush behavior in the laboratory, secondary salt dissolution in the field repeats continually and is linked to precipitation events. Early flush and maximum sulfide oxidation results from HCTs should be retained and used in environmental models and facility design.

Key words humidity cell tests, geochemical modeling, secondary minerals

Introduction

Humidity cell tests (HCTs) are long-term (weeks to years) laboratory leach tests conducted on mined materials (drill core, mine wastes, or wall rock) under oxidizing conditions for estimating the leachate quality of mining materials and wastes. The most common method used is ASTM D5744-13 (ASTM 2013). The purpose of this study is to examine humidity cell leachate chemistry in terms of the underlying geochemical processes and to apply geochemical modeling to HCT results from three U.S. mining projects to determine how this approach might address questions including whether pyrite (or other sulfide) oxidation rates can be distinguished from rates of other processes, such as secondary mineral dissolution and precipitation, and how HCT data could be used for improved predictions. Metal sulfate salts commonly form as efflorescent crusts on sulfide deposits and mine wastes (Nordstrom 1982; Nordstrom and Alpers 1999; Jambor et al. 2000) during periods of evaporation. These salts are rarely considered in mine waste characterization studies, and their effect on water quality can be important when interpreting HCT results.

The HCT results selected for this study are from one active mine and two proposed mining projects in the United States. The geologic settings span a range of rock and mineralization types including a granodioritic intrusion (Pebble Project in Alaska), a metamorphosed sedimentary and volcanic deposit (Buckhorn Mine in Washington State), and a mafic intrusion (PolyMet Project in Minnesota). Samples from each project were selected based on their neutralizing potential (to examine the onset of acidic leachate), the length of the test (one year or longer), the completeness of geochemical analyses on the leachate, and the availability of electronic data. Results from a Pebble Project field test pile are also presented.

Methods

Data sources used for the HCT results were: Pebble, PLP (2011); Buckhorn, Washington State Department of Ecology (2005); and PolyMet, SRK Consulting (2007). The following methods and approaches were used:

- Geochemical modeling using WATEQ4F for aqueous speciation and saturation indices
- Evaluation and correction of charge imbalances
- Calculation of oxidation and dissolution rates
- Inverse modeling of early flush HCT results using PHREEQC
- Comparison and evaluation of field results for two sites.

If the speciated charge imbalances (CIs) in WATEQ4F (Ball and Nordstrom 1991; with database updates) were greater than ± 20 to 25% (Nordstrom et al. 2009), the direction of the CI (positive or negative for the CI) and the conductivity imbalance (δK_{25} ; comparing measured and WATEQ4F-calculated conductivity values, also positive or negative) were examined to determine if cations or anions needed to be adjusted, and in which direction, using the protocols established by McCleskey et al. (2011), and the program was re-run until charge imbalances met the criteria. Using adjusted ORP values (corrected for Eh, available for all samples), Fe aqueous species and saturation indices were calculated in WATEQ4F. Uncertainties in Eh values could affect Fe speciation and saturation index results.

Maximum Fe sulfide oxidation rates were obtained from the change in dissolved SO_4 concentrations over the time that both Fe and SO_4 concentrations were increasing most rapidly. Mineralogic information, as available, and measured molar concentrations of Fe, Cu, and SO_4 were used to infer the most likely sulfide minerals responsible for the observed changes in concentration. Early flush, maximum, and “steady state” SO_4 release rates were calculated using measured HCT concentrations, sample volume, and solid sample mass.

The inverse modeling routine of PHREEQC (Parkhurst and Appelo 2013) was used to estimate the moles of dissolved minerals needed to produce the observed solute concentrations in early-flush HCT samples. Measured major and minor solute concentrations, including metals if present in concentrations $\geq 10^{-5}$ m, were evaluated. Uncertainty was set at 1.0, and the WATEQ4F thermodynamic database was used because it has hydrated sulfate salts. Possible sulfate, chloride, oxide, and carbonate minerals dissolving were selected in the inverse modeling program based on the available phases in PHREEQC and known field occurrences from the literature; choices also needed to be consistent with the solution chemistry, and the SI values from WATEQ4F were used as a guide.

Pebble Limited Partnership initiated a series of field barrel HCTs in 2007 using composited Pre-Tertiary Pebble West Zone core materials from intrusive and mudstone units (see PLP 2011, Appendices 11J and 11C). The HCTs were also run on the same composited Pre-Tertiary Pebble Zone West intrusive and mudstone materials following unmodified ASTM protocols.

Results and Discussion

A subset of the results from each site and method are presented. Typical HCT SO_4 trends in partially weathered, sulfide-bearing samples subjected to a regular leaching sequence show initially elevated SO_4 concentrations (early flush – Ca, Cu, Ni, and other metal concentrations may also be elevated (Price 2009; Jambor et al. 2000)), rapidly decreasing concentrations, later increases in SO_4 concentrations, and then a leveling off of concentrations. In samples that produce acidic drainage, pH values typically start in the neutral range and drop to values below approximately 6, when Fe and SO_4 concentrations increase. Redox potentials often increase as soluble Fe and low pH values create enough Fe(II) and Fe(III) to be electroactive with respect to redox electrodes.

Charge and conductivity imbalances: The CI and the δK_{25} exceeded $\pm 25\%$ in one HCT sample for each of the three sites. These samples should have been re-run and were rejected for our evaluation of salt dissolution and inverse modeling. Using the McCleskey et al. (2011) approach, cations, CI, and δK_{25} were too high for the Pebble and Buckhorn samples, whereas anions, CI, and δK_{25} were too high for the rejected Polymet sample. The results indicate that analytical measurements for HCT leachate samples should be evaluated more carefully.

Oxidation-reduction reactions and rates: Figure 1 shows the changes in Fe speciation, dissolved Cu concentrations, pH, Eh, and ferrihydrite SI over the course of the test for one of the Pebble samples. Sulfate concentrations are shown only for the period when Fe and SO_4 concentrations were increasing most rapidly. After the pH dropped below 4 (about week 60), ferrihydrite was consistently undersaturated. In general, Eh values do not become meaningful until pH values drop below about 4 (Nordstrom 2011). The Fe(III) concentrations and pH were inversely correlated for the most part, and when pH values dropped below 3 for the first time (about week 100), Fe(III) concentrations rose in response to the oxidative dissolution of Fe sulfide. The Fe(II) concentrations remained low as the Eh rose and Fe(II) was converted to Fe(III). Dissolved Cu concentrations were elevated in the early-flush sample and later peaked around 120 weeks, and Fe concentrations peaked around week 150. Measuring Eh in samples with pH values < 4 can improve interpretation of Fe behavior and improve charge balances by adjusting the distribution of Fe(II) and Fe(III). For all samples, Fe concentrations quickly dropped after they peaked, suggesting that Fe oxyhydroxides could be at least partially coating the available sulfide minerals and limiting further dissolution.

Depending on where in the HCT results the reaction or release rates are derived, the time to acid production and other variables can vary widely (Table 1). Maximum SO_4 release rates were 2 to 3 times higher than steady-state rates, and sulfate release rates were even higher during early flush conditions. Similar trends in SO_4 release rates were seen by Lapakko and Trujillo (2015). The maximum sulfide oxidation rate for the Buckhorn sample was about 25 times faster than for the Pebble sample. Iron sulfide in the PolyMet sample took the longest time to oxidize, and maximum sulfide oxidation rate for the Buckhorn sample was about 6.5 times faster than for the PolyMet sample (Table 1). In general, laboratory rates

for single-sulfide mineral experiments are faster than those in the HCTs examined, as expected. However, the maximum Fe sulfide oxidation rate for the Buckhorn sample, in which pyrrhotite is the likely dissolving phase, is similar to that found for pyrrhotite by Nicholson and Sharer (1994). Sulfide mineral oxidation rates are strongly dependent on the presence of Fe-oxidizing bacteria, which are not monitored in HCTs. Because of the lack of information on microbial activity in the HCTs, one should look for these rapid increases in Fe and SO_4 concentrations that indicate pyrite or pyrrhotite oxidation and assume that would be a worse-case scenario for application of laboratory rates to field conditions.

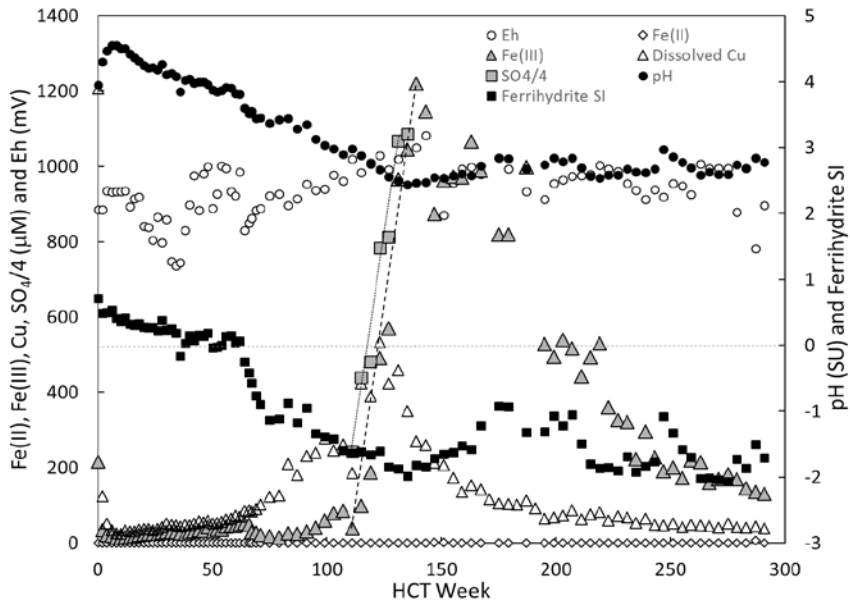


Figure 1. Dissolved Fe species, ferrihydrate saturation index (SI), SO_4 (only during rapid increase), dissolved Cu, and Eh for Pebble sample 3069-0927-0947. Horizontal dashed line is $\text{SI}=0$, and the near-vertical dashed and solid lines represent the data used to calculate Fe sulfide dissolution rates.

Table 1. Sulfate release rates and conditions during early flush, maximum Fe sulfide oxidation, and “steady-state” conditions¹ for the Pebble, Buckhorn, and PolyMet project HCTs

Mine or Project, Location (USA)	Units	Maximum Early Flush	Maximum Fe Sulfide Oxidation	Mean Steady-state
Pebble Project, Alaska	$\text{mg}_{\text{SO}_4} \text{ kg}_{\text{material}}^{-1} \text{ wk}^{-1}$	513	206	68.7
Buckhorn Mine, Washington	$\text{mg}_{\text{SO}_4} \text{ kg}_{\text{material}}^{-1} \text{ wk}^{-1}$	201	429	168
PolyMet Project, Minnesota	$\text{mg}_{\text{SO}_4} \text{ kg}_{\text{material}}^{-1} \text{ wk}^{-1}$	32.0	62.9	36.3

¹ last five weeks of HCT with Fe and SO_4 data, or weeks with most stable release rates

Pebble: granodiorite 2.44%S; Buckhorn: magnetite skarn 1.91%S; PolyMet: anorthositic troctolite 1.83%S

Salt dissolution and inverse modeling: Elevated early-flush HCT results are typically ignored when interpreting the results (Price, 2009). In the field, however, sulfide oxidation weathering products can be present intermittently and repeatedly from year to year and have a strong effect on mine drainage quality. Inverse modeling using PHREEQC with the WATEQ4F database identified gypsum as the dominant dissolving phase for the Pebble and the Buckhorn early-flush samples, with melanterite also identified for the Pebble sample. For the Buckhorn sample, epsomite, halite, and dolomite were possible dissolving phases. For the PolyMet sample, halite, calcite, and epsomite were more important than gypsum. The results suggest that sulfate, chloride, and carbonate salts can explain a substantial portion of the observed solute concentrations in the early flush samples.

The major common cations and anions and the Ca:SO₄ molar ratio for the PolyMet sample during the first 60 weeks of testing are shown in Figure 2. The PolyMet sample was less controlled by gypsum dissolution early in the test, but Ca and SO₄ concentrations tracked each other starting in week 6 and remained linked throughout the remaining approximately 50 weeks of testing. Results suggest that gypsum solubility can mask sulfide dissolution and oxidation because of the elevated SO₄ concentrations, as noted by Price (2009) and others, and testing was needed for at least one year. More frequent analysis especially in the first several weeks of the test would help distinguish sulfate salt dissolution from rapid SO₄ increases that signal sulfide oxidation.

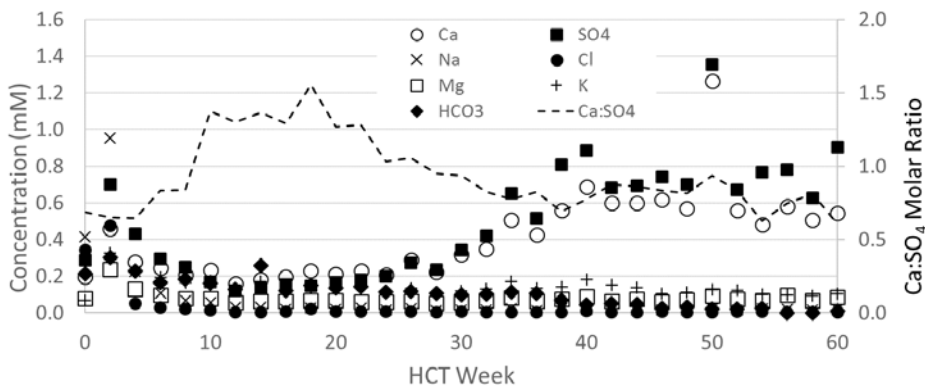


Figure 2. Major ions for the first 60 weeks of HCT testing for PolyMet Project sample 26027(616-626)

Field barrel and HCT comparisons – Pebble Project, Alaska, USA: The Pebble Project field barrels and their related HCTs were as identical in composition and particle size as compositing and sub-sampling allow. The Pebble barrel tests followed ASTM protocols, and were sampled only six to 11 times over a two-year period, mostly in fall and winter (Sept. 2007 to Oct. 2009), and the volume of leachate collected was not noted. Therefore, the effects of snowmelt and rain events on leachate characteristics cannot be fully evaluated. For the intrusive rock samples (Figure 3.a), pH values in most field barrel leachate samples were substantially lower than those early in the HCTs; HCT results never dropped below 6.85, but field values were as low as 5.2. Mudstone samples (Figure 3.b) had HCT pH values

that were eventually substantially lower than barrel-test values after day 600, suggesting that the HCTs could have accelerated weathering and acid generation – possibly because of the lower temperatures in the field in Alaska.

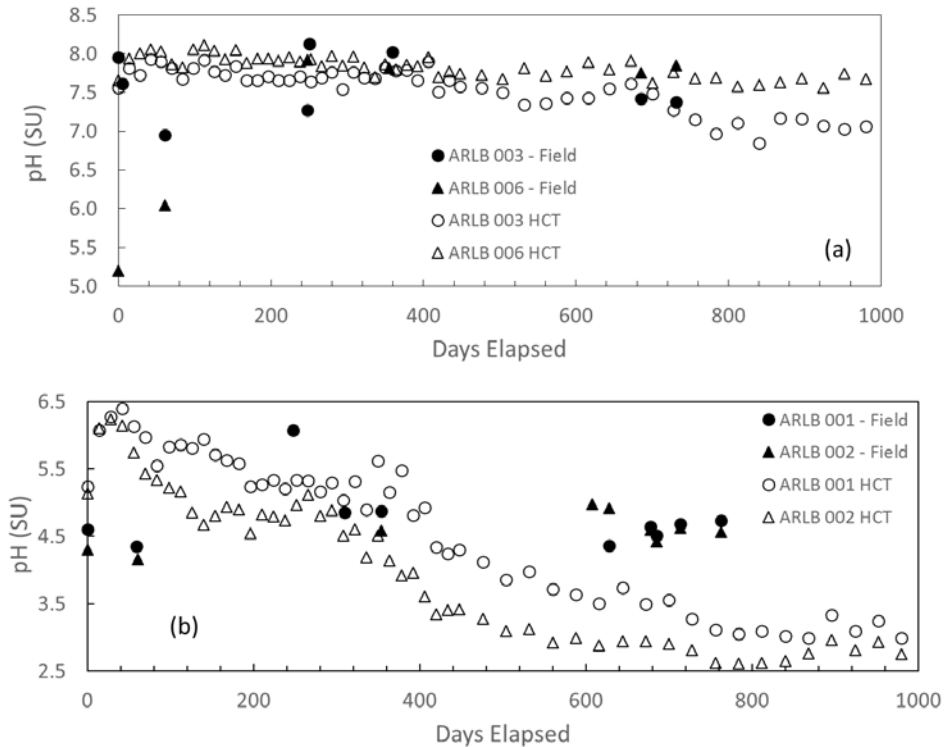


Figure 3. Changes in pH over time for Pebble field barrel vs matched HCTs for Pebble West Zone Pre-Tertiary (mineralized) (a) intrusive rocks (003 and 006), and (b) mudstones (001 and 002). Data source: PLP, 2011, Appendix 11J (field barrel) and 11C (HCTs).

Summary and Conclusions

Early-flush HCT concentrations are ignored in predictions of field pH and solution chemistry. Dissolution and flushing of acidic, metal-rich salts from field tests and waste piles can occur seasonally or after rain or snowmelt events and have a strong effect on leachate and receiving stream chemistry. Early flush and maximum sulfide oxidation results from HCTs should be retained and used in environmental models and facility design. Improved guidance is needed for more consistent interpretation of the results of HCTs that relies on identifying the geochemical processes, the mineralogy, including secondary mineralogy and mineral coatings, the available surface area for reactions, and the influence of hydrologic processes on leachate concentrations in runoff, streams, and groundwater before mining begins. Linked field and laboratory tests should be conducted far more commonly than they are, and reactions involving secondary minerals should be identified and evaluated in the laboratory and the field.

References

- ASTM (2013) Standard Test Method for Laboratory Weathering of Solid Materials Using a Humidity Cell. D 5744-13. West Conshohocken, PA: ASTM International.
- Ball, J.W., Nordstrom, D.K. (1991) User's Manual for WATEQ4F, with Revised Thermodynamic Database and Test Cases for Calculating Speciation of Major, Trace, and Redox Elements in Natural Waters. US Geol. Surv. Open-File Rep. 91-183.
- Jambor, J.L., Nordstrom, D.K., Alpers, C.N. (2000) Metal-sulfate salts from sulfide mineral oxidation. In: Alpers, C.N., Jambor, J.L., and Nordstrom, D.K., (Eds.), *Reviews in Mineralogy and Geochemistry*, Vol., 40, Sulfate Minerals – Crystallography, Geochemistry, and Environmental Significance, P.H. Ribbe, Series Ed., Mineralogical Society of America, Washington, D.C., 303-350.
- Lapakko, K., Trujillo, E. (2015) Pyrite oxidation rates from laboratory tests on waste rock. 10th ICARD/IMWA Annual meeting, Santiago, Chile, April 20-25. 14pp.
- McCleskey, R.B., Nordstrom, D.K., Ryan, J.N. (2011) Electrical conductivity method for natural waters. *Appl. Geochem.* 26, S227-S229.
- Nicholson, R.V., Scharer, J.M. (1994) Laboratory studies of pyrrhotite oxidation kinetics, In: Alpers, C.N., Blowes, D.W. (Eds.), *Environmental Geochemistry of Sulfide Oxidation*, Am. Chem. Soc. Symp. Series 550, Amer. Chem. Soc., Washington D.C., 14-30.
- Nordstrom, D.K. (1982) Aqueous pyrite oxidation and the consequent formation of secondary iron minerals, In: Kittrick, J. A., Fanning, D. S., and Hossner, L. R. (Eds.), *Acid Sulfate Weathering*, Soil Sci. Soc. Am., Madison, WI, 3756.
- Nordstrom, D.K. (2009) Acid rock drainage and climate change. *J. Geochem. Explor.* 100, 97-104.
- Nordstrom, D.K. (2011) Hydrogeochemical processes governing the origin, transport and fate of major and trace elements from mine wastes and mineralized rock to surface waters. *Appl. Geochem.* 26, 1777-1791.
- Nordstrom, D.K., Alpers, C.N. (1999) Geochemistry of acid mine waters. In: G.S. Plumlee and M.J. Logsdon (Eds.), *The Environmental Geochemistry of Mineral Deposits. Part A: Processes, Techniques, and Health Issues*. Rev. Econ. Geol. 6A, Soc. Econ. Geol., Littleton, Colorado, 133-160.
- Parkhurst, D.L., Appelo, C.A.J. (2013) Description of input and examples for PHREEQC version 3: a computer program for speciation, batch-reaction, one-dimensional transport, and inverse geochemical calculations. *Techniques and Methods* 6-A43.
- PLP (Pebble Limited Partnership) (2011) Pebble Project Environmental Baseline Document 2004 through 2008 (with updates in 2010). Chapter 11 and appendices. *Geochemical Characterization, Bristol Bay Drainages*. Prepared by SRK Consulting, Inc. for Pebble Limited Partnership.
- Price, W.A. (2009) Prediction manual for drainage chemistry from sulphidic geologic materials. MEND Report 1.20.1. 579 pp. Report prepared by CANMET, Natural Resources Canada.
- SRK Consulting (2007) RS53/RS42 – Waste Rock Characteristics/Waste Water Quality Modeling – Waste Rock and Lean Ore – NorthMet Project – DRAFT. February/Draft 01, March 9, 2007.
- Washington State Department of Ecology (2005) Buckhorn Mountain Supplemental Draft Environmental Impact Statement: Geochemistry, Surface Water, and Groundwater Quality Discipline Report. October 26. Prepared by URS Corporation.

Financial Modelling for Mine Discharge Treatment Options

Ingrid Dennis¹, Rainier Dennis¹

¹*Centre for Water Sciences and Management, North-West University (NWU), Private Bag X6001, Noordbrug 2520, South Africa, rainier.dennis@nwu.ac.za*

Abstract South Africa is faced with the legacy of environmental impacts due to gold mining which have taken place over 120 years. With the depletion of gold ores, considerable changes to the surface and subsurface water flow pathways have occurred. The generation of acid mine drainage as a result of the oxidation of pyrite and other metal sulphides has led to acidic mine water, elevated levels of sulphate and other toxic metals. This paper discusses the development of financial model for selecting the best treatment option in the East Rand Basin considering the results of an integrated model.

Key words Financial modelling, mine discharge, source apportionment, treatment options

Introduction

South Africa is faced with the legacy of environmental impacts due to gold mining activities which have taken place over 120 years in the Witwatersrand gold mining region. Over time, as economically exploitable gold ores have been depleted and progressive cessation of mining operations have taken place. Gold mining over this period has caused considerable changes to the surface and subsurface water flow pathways. This is due to the influence of historical surface operations, shallow sub-surface mining and deep underground mine excavations. The generation of acid mine drainage as a result of the oxidation of pyrite and other metal sulphides associated with the gold ores has led to acidic mine water, elevated levels of sulphate, and elevated concentrations of mobile toxic metals.

The management of the acid mine drainage poses a major challenge and the Department of Water Affairs (South Africa) conducted a thorough investigation in 2013 into various treatment technology options, their associated costs, risks and maturity levels of each technology (DWA 2013).

In 2011, the Council for Geoscience (South Africa) initiated the East Rand Basin Source Apportionment Study. The mine hydrology, hydrogeology and surface hydrology of the area were modelled by means of a surface run-off model, a regional groundwater model and a mine flooding model. All three the aforementioned models were inter-connected to account for the total water balance and produce an aggregated system response in terms of mass and transport modelling, geochemical speciation and kinetic modelling. A graphic representation of the model framework is shown in Figure 1.

This paper focuses on combining the results of the aforementioned studies to develop a financial model for selecting the best treatment option in the East Rand Basin whilst considering the integrated model results and predicted source-term of the mine discharge.

Study Area

The study area is located in the Gauteng Province of South Africa and covers the East Rand area. In mining terms the area is referred to as the East Rand Basin. Mining in the Eastern Rand portion of the Witwatersrand Goldfields started in approximately 1888 with the Nigel Mines and in 1892 the Van Ryn Estates. The mine lease areas in the basin cover approximately 768 km². It is important to note that the East Rand Basin is geographically, hydrologically and hydrogeologically different from the other Witwatersrand mined basins (Scott, 1995).

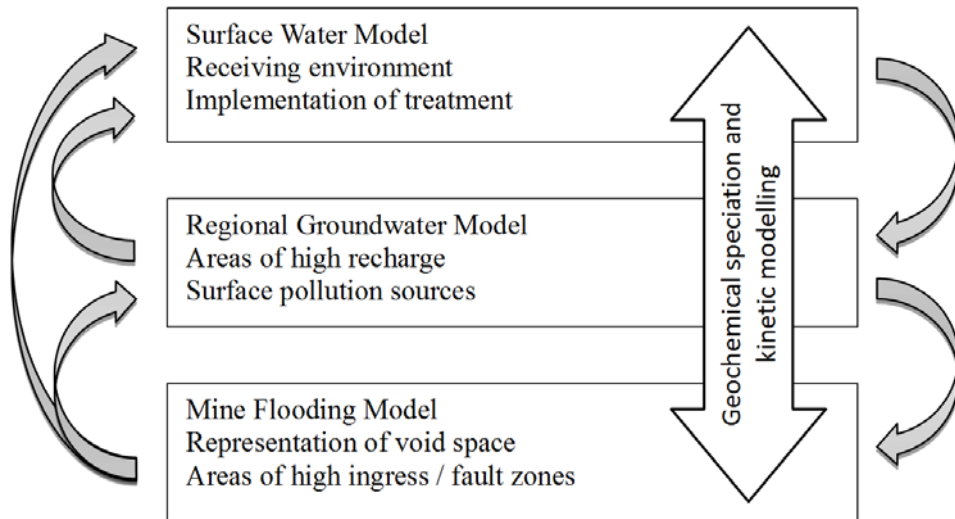


Figure 1 Integrated model concept for source apportionment study.

Methodology

DWA (2013) conducted a thorough investigation into various treatment technology options, their associated costs, risks and maturity levels of each technology. The study found that pre-treatment through the High Density Sludge (HDS) process followed by a conventional multistage Reverse Osmosis (RO) would be the most suitable option. To quote DWA (2013): *“The only solution that can be implemented with a low risk is the HDS process followed by conventional multistage RO. The product water by this process train is also the most versatile in terms of re-use options and is most likely to be accepted by the public or industry should it be considered for potable use or re-use. This process train should be analysed in detail, as it is able to address all associated risks, and costs can be assigned to the elimination of the risks.”*

To perform financial modelling on various treatment scenarios, the cost of treatment is required for a specific plant configuration. The preferred treatment technology under consideration, is the HDS pre-treatment followed by conventional multistage RO. The HDS has a pre-neutralisation stage (pH 5.5-6.0) making use of a 10% limestone slurry and a neutralisation stage where CaO is slaked and dosed as 10% milk-of-lime slurry into the neutralisation reactor (pH 9). This process train however generates waste product that is

stored on a Sludge Storage Facility (SSF) and this should also be taken into account from a financial point of view.

The treatment plant conceptual model is shown in Figure 2. The abstraction volume is assumed to be the capacity of the treatment plant in question. Provision is made in the model to have treated water distributed to water users. All water not distributed to water users are returned to the river for dilution purposes to comply with the desired state of the environment downstream.

Surface water chemistry in South Africa is generally dominated by 3 factors: chemical weathering, chloride salinisation, and sulphate contamination (Huizenga 2011). For the purpose of this study SO_4^{2-} was considered as a conservative tracer in the system. The SO_4^{2-} tracer selection was further motivated by the use of SO_4^{2-} in the field as a tracer next to Tailings Storage Facilities (TSFs), hence the same constituent is used in the financial modelling. A function describing the RO feed SO_4^{2-} versus the RO Permeate SO_4^{2-} was formulated from literature values as a treating function for the proposed plant to illustrate the application of the model based on a dynamic source-term. It is well known that membrane technology is unpredictable in behaviour as it relates to complex water types. It is therefore recommended that pilot studies be conducted with the proposed solution to determine a more accurate treatment function for the model.

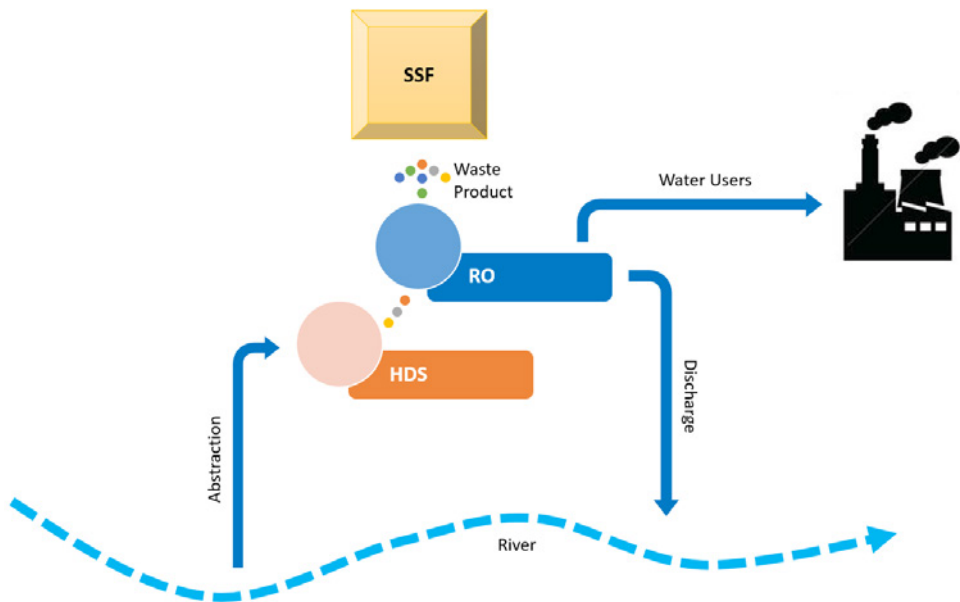


Figure 2 Conceptual model of treatment plant.

The DWA (2013) study calculated the CAPEX and OPEX for each of the proposed plant sub-components described in the conceptual model (fig. 2). These cost estimates were conducted for the Western, Central and Eastern basins, with the advantage that each of the

forementioned basins had a different design capacity, feed water composition and the water compositions were reported on the 95th, 75th and 50th percentiles. Analysing the CAPEX and OPEX data, various relationships could be established to formulate the sub-component costs in terms of the required variables. As an example, an excerpt of these relationships for the sub-components are presented in Figure 3 (SSF, electricity and chemical cost relationships omitted). It should be noted that the CAPEX and OPEX data obtained from DWA (2013) is expressed in terms of 2013 Rand values, but the relationships presented in Figure 3 is expressed in 2016 Rand values (2013 values adjusted with a 6.5% inflation rate).

The integrated model already solves for flows and concentrations at various points in an equivalent network, but cannot connect directly to the proposed financial model. In addition to the aforementioned restriction, the integrated numerical model is computationally expensive and requires extended computational time (in the order of a week depending on the scenario), which is not ideal for considering various financial scenarios by decision makers. Hence the selection of base case scenarios based on annual average responses that describe the physical mass-transport network (fig. 4).

The mass-transport network operates on the principal of the conservation of mass as illustrated in Figure 5 (Louck and Van Beek 2005). Note the modelled system represents the steady state solution for the selected base case scenarios and a decay factor k of 0 was assumed, resulting in conservative mass transport. The symbols C_i and V_i denote the concentration and volume respectively for segments $i = 1, 2, 3, \dots, j$ of the system (fig. 5).

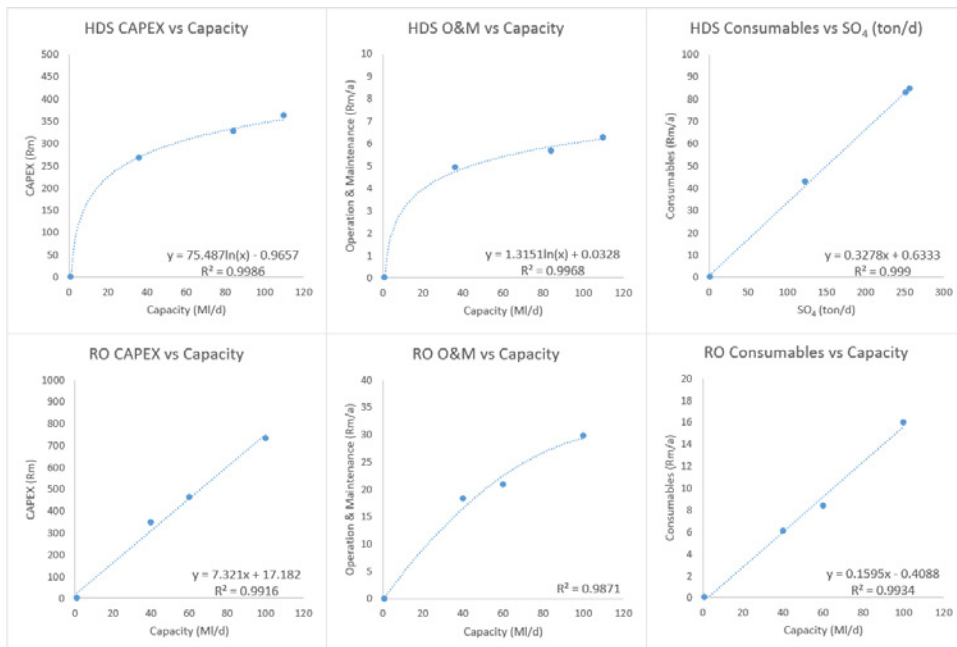


Figure 3 Example CAPEX and OPEX relationships.

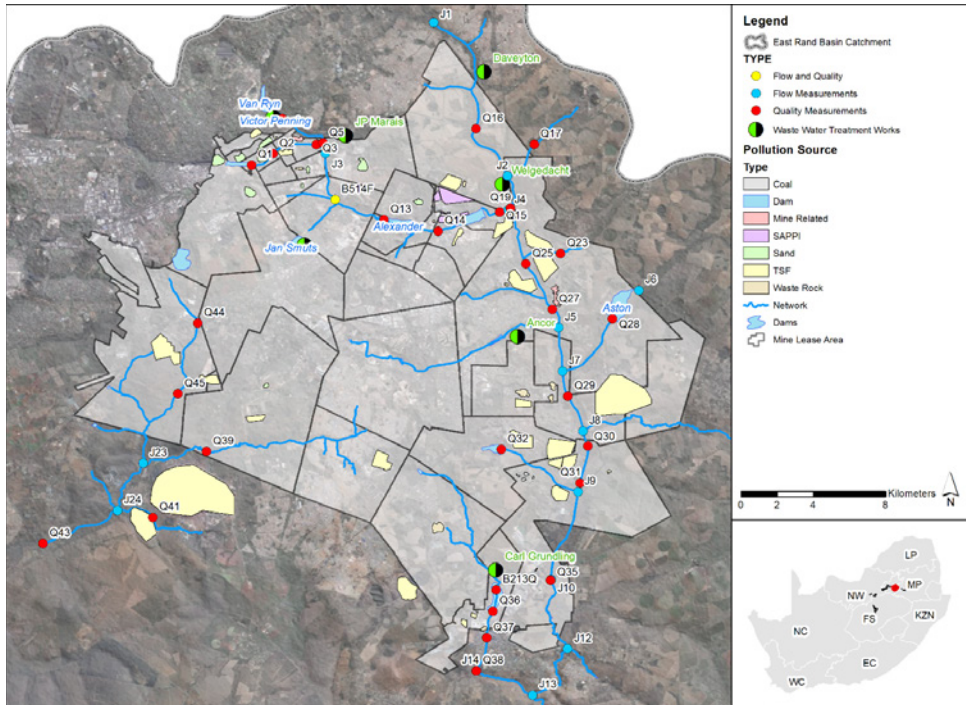


Figure 4 Physical mass-transport network.

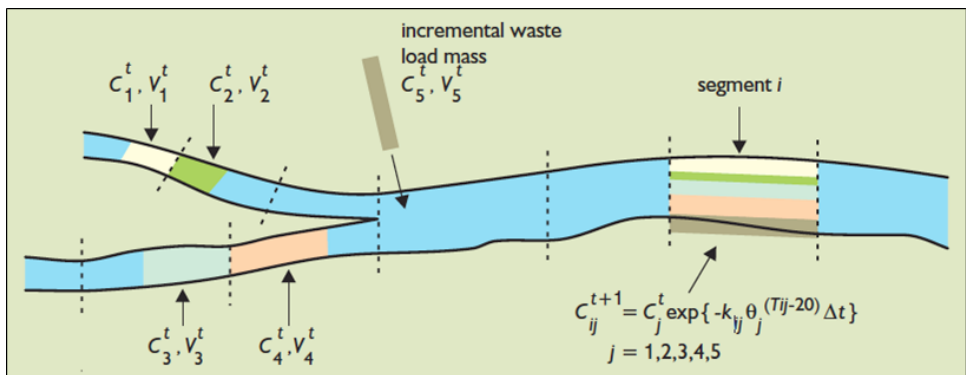


Figure 5 Water quality modelling approach (Loucks and Van Beek 2005).

Results

For the purpose of this paper two scenarios are compared based on the desired state of the environment. Each of the following scenarios consider no water sold as well as the maximum amount of water sold without jeopardising the desired state of the environment:

1. Pumping takes place at Grootvlei No.3 Shaft to maintain the Environmental Critical Level (ECL) and pumped water must be treated and discharged in the Blesbokspruit.

2. No pumping takes place in the system and mine discharge takes place at Nigel No.3 Shaft.

Each of the above scenario has a SO_4^{2-} source-term and predicted discharge rate associated with it as shown in Figure 6.

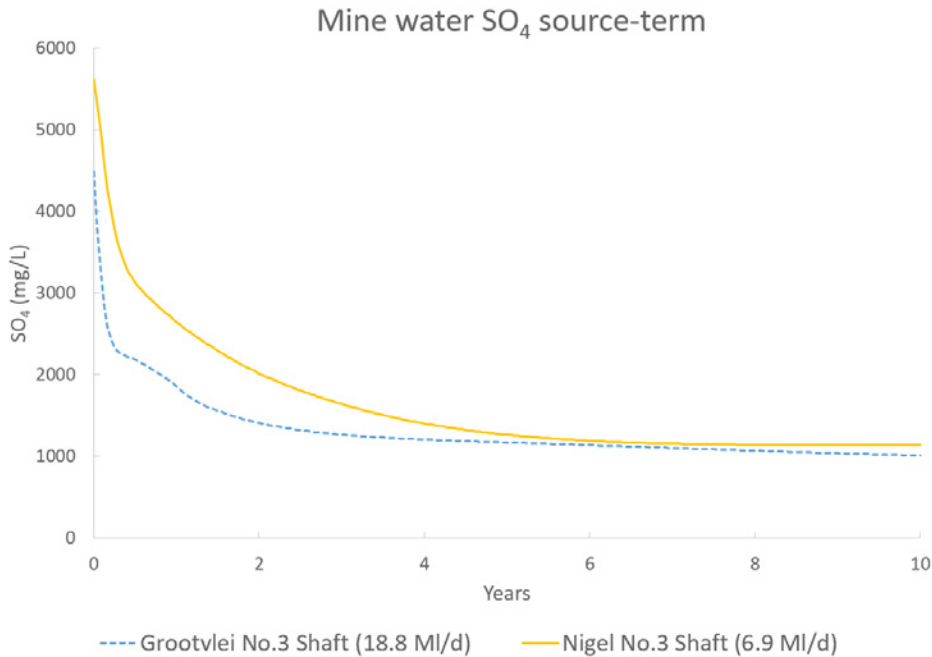


Figure 6 Water quality modelling approach (Loucks and Van Beek 2005).

The following inputs were selected for all the scenarios for comparison purposes: general inflation of 6.5%, electricity inflation of 7.5% and an electricity cost of R1.00/kW. The financial modelling resulted in a CAPEX of R1988 million for Scenario 1 and R587 million for Scenario 2. The OPEX expressed in Present Value (PV) per year is shown in Figure 7. A significant reduction in OPEX is achieved in Scenario 1 by selling 18.8 MI/d treated water at cost. No water is available to sell in Scenario 2 to allow for maximum dilution required to meet the desired environmental state.

Conclusions

Using the base case scenarios obtained from the integrated model and the application of the developed financial model that accounts for a dynamic source-term, various scenarios can be tested to obtain the most cost effective solution. The developed financial model is not area specific but rather technology specific and the same approach can be applied in other areas, but economic indicators must be taken into consideration.

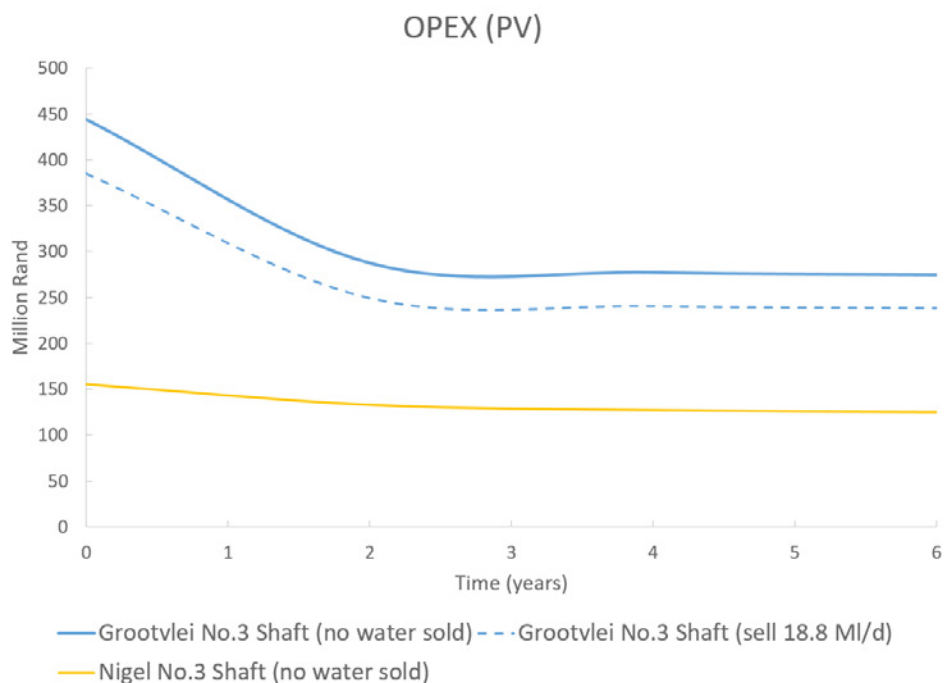


Figure 7 Water quality modelling approach (Loucks and Van Beek 2005).

Acknowledgements

The authors thank the Council for Geoscience, South Africa for making this study possible, in particular Henk Coetzee and Ugo Nzotte. The authors also acknowledge the modelling contribution by Michael Eckart and Christoph Klinger from DMT.

References

- DWA (2013) Feasibility Study for a Long-Term Solution to address the Acid Mine Drainage associated with the East, Central and West Rand underground mining basins. Assessment of the Water Quantity and Quality of the Witwatersrand Mine Voids. DWA Report No.: P RSA 000/00/16512/2
- Huizenga JM (2011) Characterization of the inorganic chemistry of surface waters in South Africa. Water SA Vol. 37 No. 3 July 2011
- Loucks DP, Van Beek E (2005) Water Resources Systems Planning and Management – An Introduction to Methods, Models and Applications. ISBN 92-3-103998-9
- Scott R (1995) Flooding of Central and East Rand gold Mines: an investigation into controls over the inflow rate, water quality and the predicted impacts of flooded mine, Water Research Commission, WRC Report no 486/1/95, South Africa

Spring Flow Estimation After Mine Flooding in a Dolomitic Compartment

Rainier Dennis, Ingrid Dennis

Centre for Water Sciences and Management, North-West University (NWU), Private Bag X6001, Noordbrug 2520, South Africa, rainier.dennis@nwu.ac.za

Abstract Dewatering of a dolomitic compartment, delineated by dykes, is conducted to mine the gold bearing reefs below and reduce mine water ingress. A spring associated with the compartment ceased to flow due to dewatering taking place. Previous studies indicated flow across the dyke boundaries, is mainly due to the presence of grykes that transverse these boundaries. The question of when spring flow will be restored and what volume can be expected, normally requires a detailed numerical model. By making use of the Saturated Volume Fluctuation (SVF) method, a first order estimate of the predicted spring flow and restoration time is calculated.

Key words Spring flow recovery, mine flooding, dolomitic compartment, Saturated Volume Fluctuation

Introduction

The Gemsbokfontein West compartment is situated in the Western Basin of the South African gold mining basins. Mining takes place well below the overlying dolomitic aquifer and dewatering of this aquifer is required to reduce water ingress to the mine workings. Currently dewatering is still taking place at 77 Ml/d from two shafts within the compartment which has led to the cessation of the spring.

The question of when spring flow will be restored and what volume can be expected, generally requires a detailed numerical model accounting for the various boundary conditions e.g. dykes which are considered no flow boundaries and geological faults which are considered high transmissive zones. Since estimates of inflows from adjacent compartments exist from previous studies together with the leakage from the water courses into which the discharged water is pumped, the Saturated Volume Fluctuation (SVF) method was used to provide a first estimate of when spring flow will resume and what typical flow values will be expected.

Study Area

The mining area is characterized by dolomitic compartments formed by dykes compartmentalising the dolomite (fig. 1). Since dewatering operations commenced, the Gemsbokfontein Eye/Spring stopped flowing and this spring is situated in the low-lying area next to a dyke. A distinct drop in water level is observed across the area over time due to the dewatering that is taking place within the compartment.

Water contained in the shallow upper aquifer is attributed to infiltrating rainfall, recharging through weathered material, consequently being delayed by the low permeability of underlying dolomitic material. Although the low permeability of underlying unweathered material delays the infiltration of rainfall, a proportion of the water contained in the upper

aquifer still migrates through to eventually recharge the lower aquifer. A significant portion of the groundwater levels were found to lie within the shallow weathered aquifer. The largest volume of water stored in the main dolomitic aquifer occurs in the first 100 m below the water level. The effective base-depth of this aquifer ranges between 150 m and 200 m below the surface. The underlying dolomites have an approximated thickness of 900 m to 1100 m, however it is unlikely that large amounts of groundwater flow occur below this depth, except along intersecting structural conduits leading to underground mine workings (SRK Consulting 2013).

The conceptual model of the dolomite aquifer consists of a weathered zone with the presence of grykes (highly weathered dolomite) with an average thickness of 5m and a tight dolomite zone below with some fracturing.

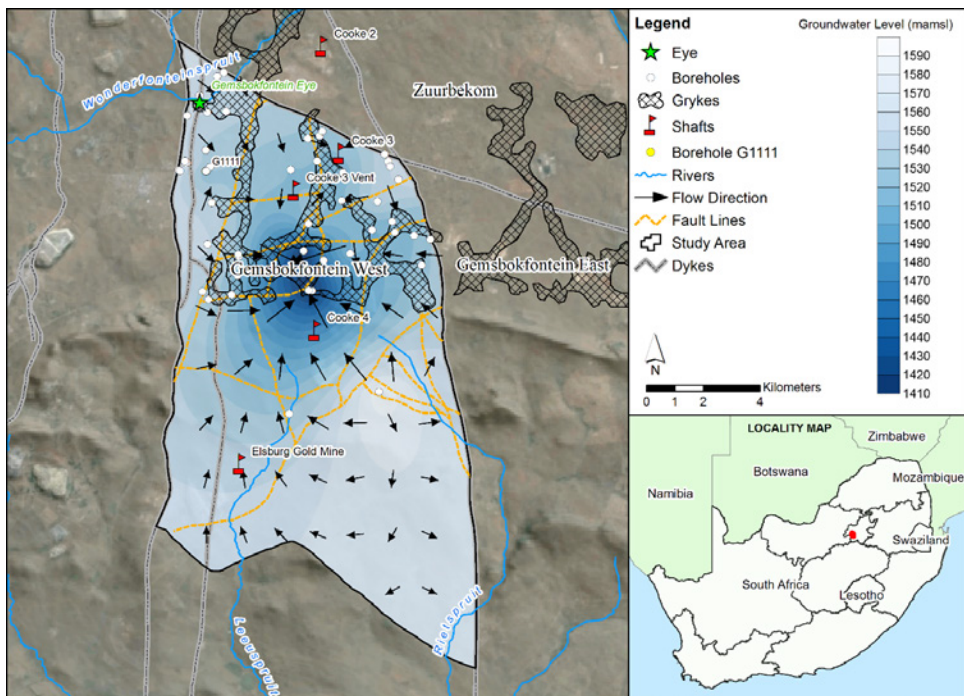


Figure 1 Study area.

MODFLOW Model

The MODFLOW model domain is larger than the dolomitic compartment in question and includes the following dolomitic compartments (fig. 1): Gemsbokfontein West, Gemsbokfontein East and Zuurbekom. A North-South cross-section of the model domain is presented in (fig. 2) to show the dipping of the dolomite layer and the relative thickness.

The MODFLOW model consists of the following three layers and their associated transmissivities: Transvaal ($15 \text{ m}^2/\text{d}$), weathered dolomite ($50 \text{ m}^2/\text{d}$) and deep lying dolomite (20

m²/d). The occurrence of Grykes within the weathered dolomites were assigned a transmissivity of 500 m²/d. Geological lineaments and fault zones were assigned a transmissivity of 100 m²/d and dykes cutting through the study area were considered impermeable.

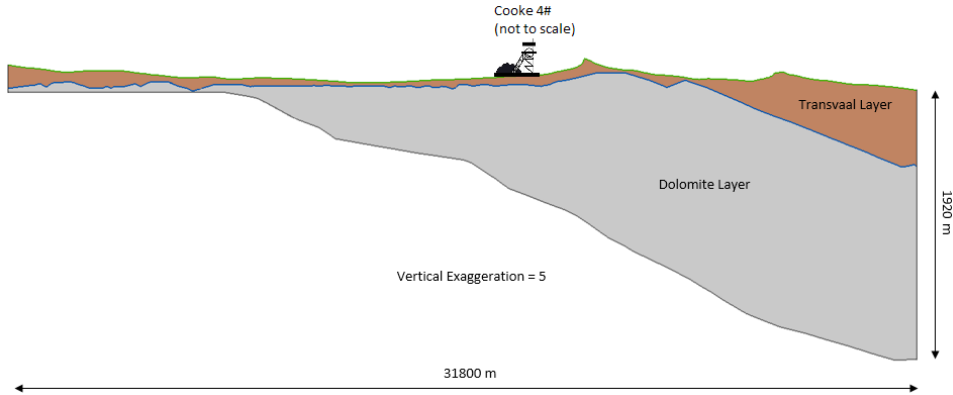


Figure 2 Model domain cross-section.

Methodology

The system in question is modelled making use of the SVF method (Van Tonder and Xu 2000) and then results are compared to that of an existing numerical model (set up using the MODFLOW code) for the same compartment.

The SVF method is based on a general groundwater balance, where the change in storage is expressed as a change in groundwater level and all inflows and outflows are translated to a change in head through the use of the aquifer area and specific yield (eq. 1).

$$h_t = h_{t-1} + \frac{R_t}{S_y} + \frac{Q_i - Q_{out}}{AS_y} \quad (1)$$

where,

t	=	Current time step [T]	S_y	=	Specific Yield
h_t	=	Head in current time step [L]	A	=	Aquifer surface area [L ²]
h_{t-1}	=	Head in previous time step [L]	Q_{in}	=	Sum of all groundwater inflows [L ³]
R_t	=	Recharge in current time step [L]	Q_{out}	=	Sum of all groundwater outflows [L ³]

The fact that specific yield is used, assumes unconfined aquifer conditions. The head values are expressed in meters above mean sea level according to the sign convention used in Equation 1.

The SVF model considers an enclosed area where inflows and outflows are explicitly specified. Inflows from neighbouring compartments and stream losses will vary with a change in head and therefore it is required to make use of a conductance term to properly account for

these head dependent inflows into the system. The conductance term (eq. 3) for the various inflows is formulated in terms of Darcy's law (eq. 2).

$$Q = kiA = k \frac{\Delta H}{L} A = C \Delta H \quad (2)$$

$$C = \frac{k}{L} A \quad (3)$$

where,

Q = Flow (L^3/T)

L = Length of flow (L)

k = Hydraulic conductivity (L/T)

ΔH = Head loss (L)

i = Hydraulic gradient (L/L)

C = Conductance (L^2/T)

A = Cross sectional area of flow (L^2)

By substituting Equation 2 into Equation 1 the general form of the equation applied to the specified problem is presented in Equation 4.

$$h_t = h_{t-1} + \frac{R_t}{S_y} + \frac{\left[\sum_{i=1}^n C_i \Delta H_{i,t} + Q_{i,t} \right] - \left[\sum_{j=1}^m C_j \Delta H_{j,t} + Q_{out,t} \right]}{A S_y} \quad (4)$$

where,

t = Current time step index

C_i = Conductance of inflow term i

n = Total number of inflow terms

C_j = Conductance of outflow term j

i = Inflow term index

ΔH_i = Change in head of inflow term i

m = Total number of outflow terms

ΔH_j = Change in head of outflow term j

j = Outflow term index

Q_{in} = Sum of all non-head dependent inflows

k = Specific Yield layer index

Q_{out} = Sum of all non-head dependent outflows

Model Calibration

Model calibration is achieved by making use of existing known inflows to estimate conductance values where applicable and calibrating the model response to observed measurements by changing recharge and specific yield to obtain the best fit. The known inflows and outflows to the system are summarised in Table 1. It should be noted that the stream losses are considered an inflow to the aquifer system.

Table 1 Summary of known inflows and outflows.

Inflows	MI/d	Outflows	MI/d
Zuurbekom Compartment	9	Cooke 4 Pumping	68
Gemsbok East Compartment	6	Cooke 3 Pumping	9
Leeuspruit Stream Loss	7.5	Gemsbokfontein Eye	0
Rietspruit Stream Loss	5		

The position of the observation borehole G1111 (fig. 1) was chosen to be in close proximity to the spring in question, but also outside the major cone of depression that exists around the shafts. The average drop in water level from historic to current water levels (2016) is estimated at 27m (fig. 2). Making use of the aforementioned drop in water level and current inflows to the system, conductance values for each of the inflows are estimated and the results are presented in Table 2.

Table 2 Summary of known inflows and outflows.

Source	Conductance (m ² /d)
Zuurbekom Compartment	315
Gemsbok East Compartment	210
Leeuspruit Stream Loss	260
Rietspruit Stream Loss	175

The model parameters that were used to obtain the best fit as shown in Figure 3 is presented in Table 3. The effective recharge percentage corresponds well to the 7.5% estimated by Enslin and Kriel (1968) and the 6.7% estimated by the Groundwater Resources Assessment Phase II Project (WRC 2005).

Table 3 SVF fitting parameters.

Parameter	Value
Study Area (km ²)	161
Specific Yield	0.0043
Effective Recharge (%)	7.1
Dolomite Storage (MI/d)	23

The assumptions associated with the SVF model can be summarised as follows:

- All inflows are connected to the mine void via a network of faults within the study area.
- All dykes are considered impermeable and inflows from adjacent compartments are head dependent and therefore controlled via a conductance term.
- All leakage from rivers is also head dependent and controlled via a conductance term.

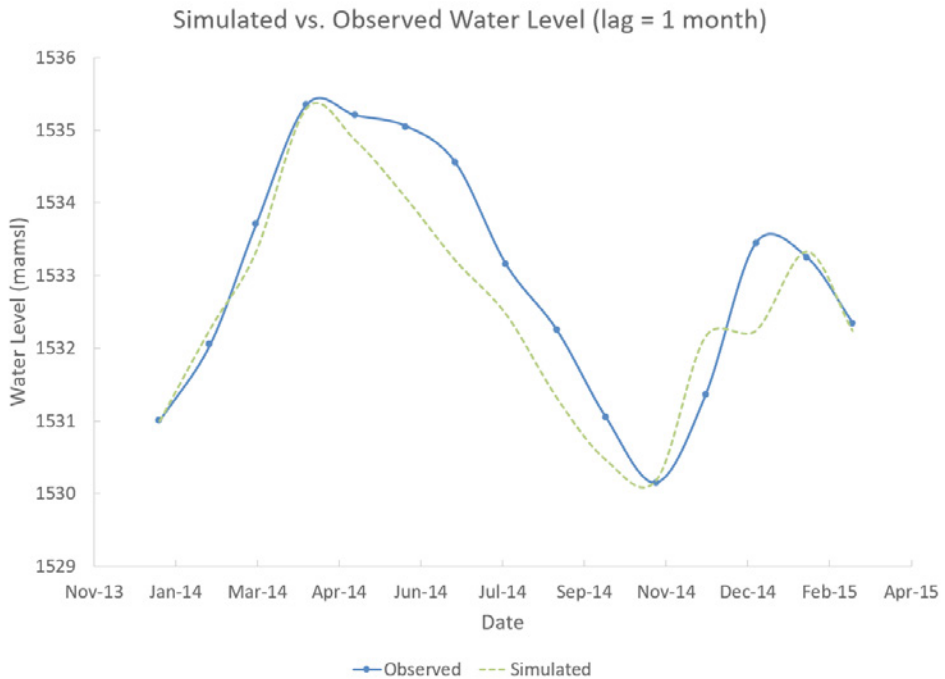


Figure 3 Modelled versus observed groundwater levels.

Results

The proposed SVF model was used for predictive modelling and a historic rainfall sequence was used to drive the simulation as shown in Figure 4. The model predicts that spring flow will commence approximately 9 years after rewatering of the dolomites takes place when the total mine void has flooded. The average predicted spring flow, once fully restored, is estimated at ± 12 Ml/d. Wolmerans (1984) reported a historic spring flow of 9.2 Ml/d. Usher and Scott (2001), Swart et al. (2003) and Dill et al. (2007) all reported historic spring flow of 8.6 Ml/d for the Gemsbokfontein spring prior to mining.

A comparison of the existing numerical model for the study area and the proposed SVF model is shown in Figure 5. Both models predict the start of spring flow within a year of each other. The SVF model seems to reach steady state after 15 years compared to the numerical model which only reaches steady state after approximately 35 years. The steady state spring flow predictions are roughly within 1 Ml/d of each other. The difference in model behaviour is contributed to the fact that the numerical model explicitly accounts for transmissivities of fault lines that cut through the compartment leading to a higher outflow component and a reduced spring flow in the case of the numerical model. This would also explain the longer time period that is required to reach steady state.

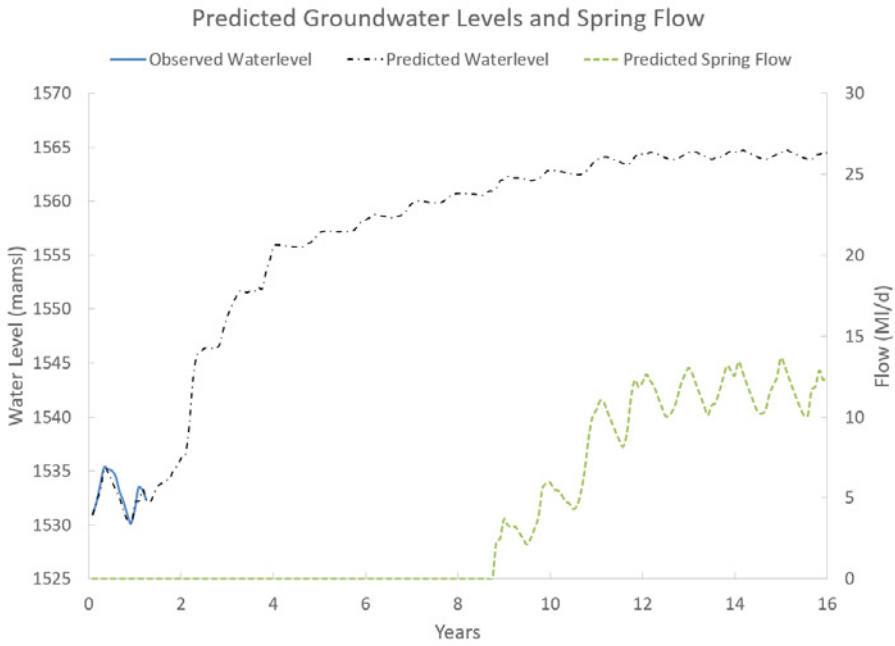


Figure 4 Predicted groundwater levels and spring flow.

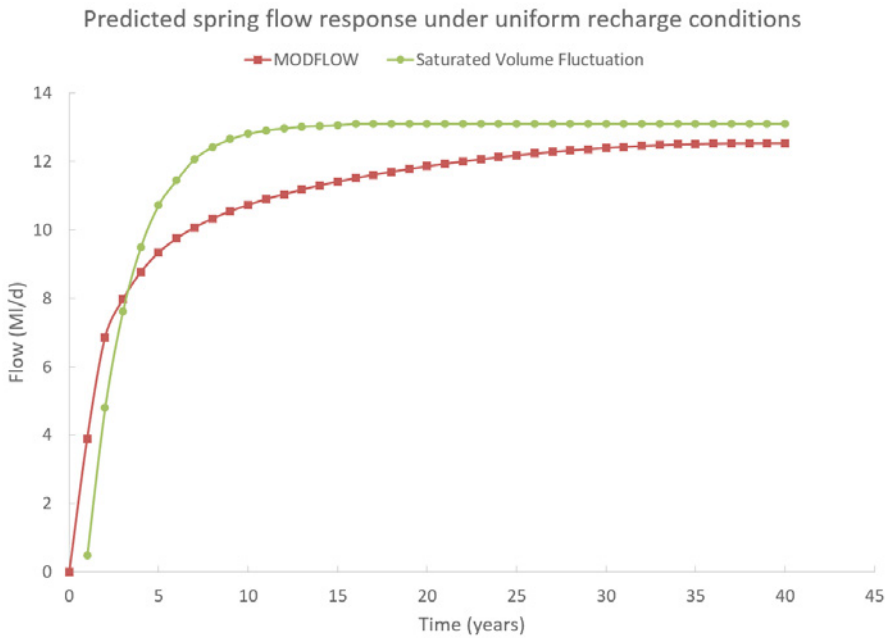


Figure 5 Predicted spring flow comparison with MODFLOW scenario.

Conclusions

Applying the SVF solution to spring flow predictions within a dolomitic compartment is a quick and effective way to obtain first order estimates of when spring flow will commence and typical volumes that can be expected, before embarking on a detailed numerical model capable of more detailed scenarios e.g. quality prognosis. The predictions from an existing numerical model of the study area and that of the proposed SVF model compare well considering the simplicity of the SVF model and the associated limitations and assumptions. However, the time to reach steady state differs as highly transmissive faults are not accounted for in the SVF model.

References

- Dill S, Boer RH, Boshoff HJJ, James AR, Stobart BI (2007) An assessment of the impacts on groundwater quality associated with the backfilling of dolomitic cavities with goldmine tailings. Pretoria, South Africa
- Enslin JF, Kriel JP (1968) The assessment and possible use of dolomitic groundwater resources of the Far West Rand, Transvaal, Republic of South Africa. International conference proceedings, Water for Peace, Washington DC, May 1967, Volume 2
- SRK Consulting (2013) Independent technical report: Gold One Cooke Four Underground operation. Gauteng, South Africa
- Swart CJU, Stoch EJ, Van Jaarsveld CF, Brink ABA (2003) The future of the dolomitic springs after mine closure on the Far West Rand, Gauteng, South Africa
- Usher BH, Scott R (2001) Post mining impacts of gold mining on the West Rand and West Wits Line. In Hodgson FDI, Usher BH, Scott R, Zeelie S, Crywagen L, de Necker (2001) Prediction techniques and preventative measures relating to the post-operational impact of underground mines on the quality of groundwater resources. Water Research Commission, Pretoria
- Van Tonder GJ, Xu Y (2000) A guide for the estimation of groundwater recharge in South Africa. *Water SA* 27(3):341-343
- Wolmerans JF (1984) Ontwikkeling van dolomite gebied aan die verre Wes-Rand: Gebeure in perspektief. University of Pretoria, Pretoria, South Africa
- WRC (2005) Water Resources of South Africa, 2005 Study – Database. WRC Report No TT/380/08, Water Research Commission, Pretoria, South Africa

Comparison of thermodynamic equilibrium and kinetic approach in the predictive evaluation of waste rock seepage quality in Northern Finland.

J. Declercq¹, J. Charles¹, R. Bowell¹, R. Warrender¹ and A. Barnes².

¹ SRK Consulting (UK) Limited, Cardiff, CF10 2HH, Wales, UK, jcharles@srk.co.uk, jdeclercq@srk.co.uk, rbowell@srk.co.uk, rwarrender@srk.co.uk

² Geochemic Limited, Abergavenny, NP7 5JZ, Wales, UK, abarnes@geochemic.co.uk

Abstract Accurate predictions of long-term mine water quality are critical for the assessment of potential project impacts. Ideally these should be undertaken during the early stages of planning and development to inform project design and ensure that appropriate engineered controls are established to minimise environmental impacts. The prediction of future contact water quality from waste materials at the Hannukainen Iron-Oxide-Copper-Gold mine was originally assessed using industry-standard thermodynamic equilibrium calculations of scaled HCT release rates. To address the thermodynamic equilibrium challenges, kinetic modelling methods have also been applied allowing for non-equilibrium calculations as the basis for metal release rate.

Key words PHREEQC, Predictive Numerical Calculations, Modelling, Waste Rock Dump, Source Terms

Introduction

The prediction of source term water quality from mine waste disposal facilities forms the initial step for assessing the effects on water quality in waterbodies adjacent to the facilities. This study aims to compare and contrast two numerical predictive calculation methods (thermodynamic equilibrium and kinetic) using the USGS geochemical code PHREEQC v3.3.5-10806 (Parkhurst & Appelo 1999, 2013). The two modelling approaches have been applied to source term predictions for a conceptual waste rock dump (WRD) at the Hannukainen Iron Oxide Copper Gold (IOCG) Project, located in the Kolari area of Northern Finland. The ore at Hannukainen is hosted in diopside skarn and quartz-albite rocks associated with magnetite, chalcopyrite, pyrite and pyrrhotite.

The widely used thermodynamic equilibrium modelling approach utilises geochemical characterisation data from static and kinetic tests. These laboratory data are scaled to field conditions using the planned physical characteristics of the facility (i.e. waste tonnages, surface area, height, grain size, etc.) coupled with climate data, to develop mass balanced predictions of leachate chemistry as a function of time. This scaled and mass balanced leachate chemistry is then equilibrated using PHREEQC and thermodynamically favoured phases are allowed to precipitate, on the basis of the available mineralogical information, kinetic considerations and the professional experience of the user.

The thermodynamic equilibrium approach presents several challenges due to the reliance on scaled humidity cell data which are not representative of a natural system. These challenges can be partially alleviated through the use of a kinetic modelling approach, which

allows the dissolution and precipitation of mineral phases likely to be present within the modelled facility on the basis of reactivity equations for each mineral. This study has utilised these two approaches to define the source term for only the potentially acid generating (PAG) portion of waste rock from the Hannukainen project.

Geochemical Characterisation Testwork Methods

Samples representative of future waste rock were collected from exploration drillcore and characterised in order to assist in the development of source term leachates that could be used as inputs for the geochemical models. A total of 49 samples were collected for static geochemical characterisation testing, which included Acid Base Accounting (ABA) using the modified Sobek method (Sobek et al. 1978), Net Acid Generation (NAG) tests and whole rock analysis by multi-acid digest followed by ICP-OES/ICP-MS analysis. As part of the static testwork program 10 of the samples were submitted for environmental mineralogical assessment; comprising Optical Microscopy (OM); Scanning Electron Microscopy (SEM) and X-Ray Diffraction (XRD). The static testwork was carried out in order to characterise the acid generating potential of the samples and to determine the range of reactivity of the waste rock material generated from the Hannukainen open pit operations.

Static test results were used to select samples for kinetic humidity cell testing (HCT), to represent the range in leaching characteristics anticipated for the waste material. HCTs were carried out according to the standard ASTM D5744-96 methodology (ASTM 1996) which is used for the assessment of long-term rates of acid generation and metal mobilisation. Eight samples of moderate to high sulfur waste rock materials (one skarn, one schist, three amphibolite and three diorite) were subjected to 170 weeks of HC testing. Weekly effluents were collected and analysed for a range of laboratory parameters in addition to major and trace element chemistry.

Conceptual Model Methodology

The results of the static and kinetic testwork were coupled with information from the mine plan and water balance to develop numerical predictions of future seepage and runoff water quality associated with the mine facilities. The general modelling approach estimated source term water quality under steady-state conditions after 5 and 10 years into life of mine (LOM). Conceptual geochemical models were developed from a review of background and site-specific data in addition to experience with other similar projects (see fig. 1). According to the geology and mine plan, three broad material type classifications are to be exposed during mine life: Potentially Acid Generating (PAG) waste rock (>0.1% sulfur); Non Acid Generating (NAG) waste rock material ($\leq 0.1\%$ sulfur); and NAG overburden (OB).

It is intended that these materials will be segregated during mining and disposed in individual PAG, NAG and overburden cells within the WRD. Quantitative Numerical Predictions (QNP) have been carried out using the thermodynamic equilibrium and kinetic approach in order to predict the source term seepage characteristics for LOM at 5 and 10 years from the PAG cell in the East WRD only.

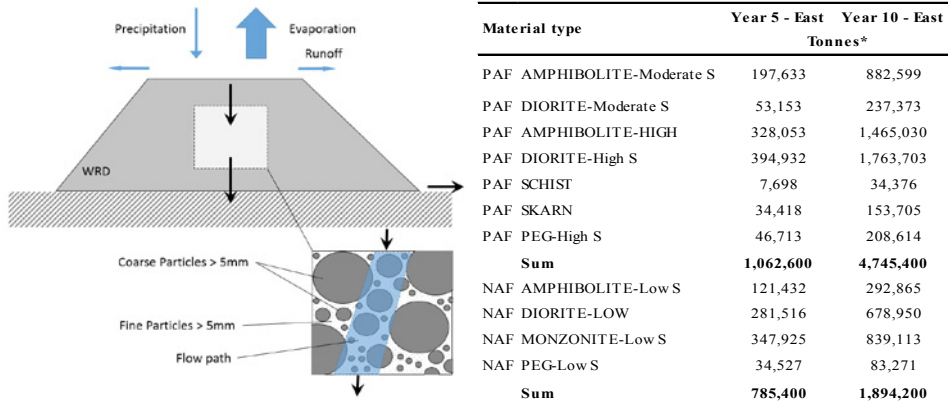


Figure 1: Conceptual model of the Hannukainen WRD

Thermodynamic Equilibrium Model Methodology

The thermodynamic equilibrium approach for the Hannukainen WRD incorporates aspects of both mass balance calculations from scaled laboratory data and thermodynamic equilibration using PHREEQC. The overall approach can be summarised as follows:

- Geochemically characterise the waste rock types and associated tonnages and proportions that will report to the WRD. Characterise the overall leach behaviour as a release rate that is representative of an equivalent kinetic cell of representative WRD composition.
- Evaluate the local climate data (e.g. rainfall and evaporation rates) and WRD design (footprint, cover, tonnage, likely particle size distribution (PSD)) to predict seepage rates.
- Apply a scaling factor to the laboratory-derived solute leach rates to predict the rate of solute release from the overall waste rock facility (Kempton 2012). Divide the solute release rate by the WRD seepage flow rate to calculate the seepage composition as follows:

$$WRD\ Seepage\ water\ quality\ \frac{mg}{L} = \frac{\sum\ Solute\ release\ rate\ \left(\frac{mg}{kg}\ / week\right) \times\ Reactive\ mass\ of\ material \in\ WRD\ (kg)}{Total\ infiltration\ rate\ into\ WRD\ \left(\frac{L}{week}\right)}$$

- Evaluate mineral saturation indices for the predicted solute composition within a geochemical software package, identifying likely solubility controls on solution composition. Allow feasible and kinetically viable mineral precipitation to occur, thereby determining the final WRD seepage quality. A modified version of the Minteq.v4 thermodynamic database supplied with version v3.3.5.10806 of PHREEQC (released June 3rd, 2013) was used. The Minteq.v4 database was selected for this study because it includes a comprehensive range of elements and solid phases for

consideration in water quality predictions as well as key sorption reactions for iron oxyhydroxides. The database was modified to include sorption data for manganese species from the PHREEQC database together with corrections for weak strong site adsorption of anions to hydrous ferric oxide and adsorption data for uranium (VI) to ferrihydrite (Waite et al. 1994).

- Compare the predicted water compositions with those observed from on-site sampling, and determine if site conditions indicate additional controls on water quality and solute concentration.

The predicted rate of solute release from the waste rock mass (R_{field}) is calculated from the laboratory leach rates multiplied by a cumulative scaling factor, derived as the product of several individual scaling factors. The relationship between R_{field} and the laboratory rates can be represented by the following scaling factors (based on work taken from Kempton, 2012):

$$R_{\text{field}} = R_{\text{lab}} \times SF_{\text{moist}} \times SF_{\text{size}} \times SF_{\text{contact}} \times SF_{\text{temp}} \times SF_{\text{O}_2}$$

R_{field} calculated field leaching rate; R_{lab} laboratory determined leach rates; SF_{moist} reduced oxidation due to low moisture; SF_{size} reactivity reduction due to HCT vs field PSD; SF_{contact} reduction due to unflushed mass (retained solutes); SF_{temp} rate relationship for temperature using Arrhenius equation; and SF_{O_2} reactive mass reduction due to O_2 diffusion limits.

SF_{moist} was neglected in the calculations due to the continuous presence of water in the WRD. SF_{contact} describes the proportion of material within the WRD that will be wetted, thus mobilising solutes. This wetting effect is dependent on channelling and development of flow paths within unsaturated waste rock (Birkholzer and Tsang, 1997), which in turn depends on PSD and infiltration rates. Temperature within the PAG material is assumed to be the same as in the laboratory testwork and therefore SF_{temp} is 1. Oxygen ingress has been calculated using the Bennett et al. (2000) equation and shows that oxygen is fully available throughout the WRD therefore SF_{O_2} is neglected.

Kinetic Model Methodology

Site-specific geochemical and mineralogical characterisation data were coupled with literature reaction rates to define kinetic predictive calculations (fig. 2) and determine a realistic reactivity for the mineral phases within the Hannukainen WRD. Mineral precipitation rates were generated directly from the corresponding dissolution rate equations. The majority of these rates were obtained from work carried out by the CarbFix Project no.28348. Within PHREEQC, the rate equations for the different minerals were defined within the RATE data block and integrated over time using the implicit CVODE method (Cohen and Hindmarsh 1996) which can resolve the integration of widely varying rate equations.

All parameters in the rate equations (example of pyrite in tab. 1) are calculated/defined by PHREEQC except the surface area (S_A) in m^2/kg and the mass of the different mineral phases (from SRK 2013). Mineral mass and surface area were defined for each reactive mineral phase and were calculated on the basis of the surface area of a volume of material contacted

by the infiltrating water. This surface area is proportionated to each the primary minerals. Any eventual secondary kinetic phases are defined here with an initial mass and surface area of zero. Fast-reacting secondary minerals such as amorphous silica, gibbsite and gypsum are defined at equilibrium. The system was allowed to react for 10 years.

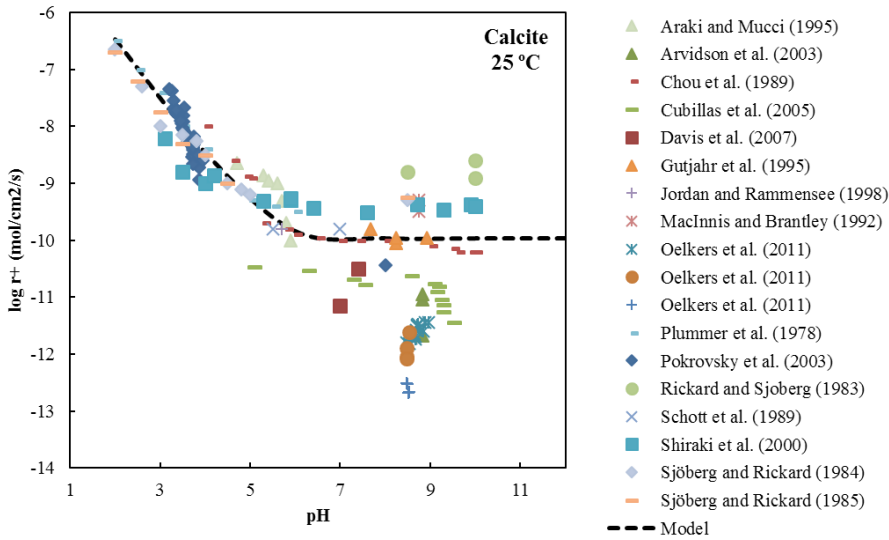


Figure 2: Measured and predicted calcite dissolution rate at 25 °C

Table 1: Rate equations for pyrite based on Palandri and Kharaka (2004)

Equation	Equation No.
$r_{+,a} = A_a \times e^{\frac{-E_a}{RT}} \times a_{Fe^{2+}}^n \times S_A$	(Pyr_1)
$r_{+,b} = A_b \times e^{\frac{-E_b}{RT}} \times a_{O_2}^n \times S_A$	(Pyr_2)
$r_i = r_{+,a} + r_{+,b}$	(Pyr_3)
$r = r_i \times \left(1 - \frac{IAP}{K} / \sigma \right)$	(Pyr_4)

It can be expected that the total mineral mass is unlikely to be available for weathering reactions due to partial exposure of minerals and grain size effects (i.e., surface area factors) and potential encapsulation of minerals by non-reactive phases (Kelemen et al. 2011). Determining the reactive surface area of specific minerals within a waste rock dump is challenging, but can be inferred from the PSD of the waste rock (Cepuritis et al. 2017). The surface area in the system was calculated from PSD measurements carried out on trial pits and the use of the GRAIN 3.0 software.

The dissolution of the different mineralogical phases releases solutes consistent with their stoichiometric proportions as defined by their mineralogical formula. This implies that most major elements e.g. Ca, Si, S, will be controlled by the mineral dissolution or oxidation. However, trace elements such as Hg and As are present as replacements within the mineralogical structure. In the absence of direct chemistry measurement of the different mineralogical phases it has been assumed that most trace elements are controlled by the oxidation of pyrite.

Results and Discussion

Using the thermodynamic equilibrium approach the PAG dump was predicted to generate acidic leachates with a high sulphate load. Metals content is predicted to contain elevated aluminium, cobalt chromium, copper, iron, manganese, mercury, nickel, lead and zinc.

The unscaled kinetic model shows a good agreement with average HCT (pH shown in fig. 3). Consistent with the thermodynamic equilibrium predictions (SRK 2013), calcite disappears within the first year, however the pH remains neutral which supports the hypothesis of silicate buffering, provided by albite, hornblende and kaolinite dissolution. However, this buffering has a limited capacity that is reached by the ongoing generation of acidity by sulfide oxidation. It is predicted that between 3 to 4 years that the pH will turn acid (fig. 3), the onset of this phenomenon can be seen in the HCT data.

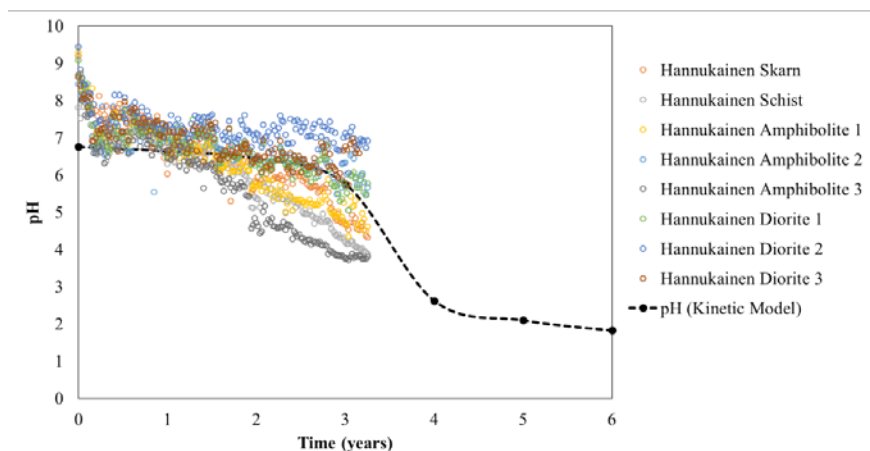


Figure 3: Predicted pH variability with time from kinetic modelling approach compared to weekly HCT pH

The primary advantages of a kinetic modelling approach over the more traditionally-used thermodynamic equilibrium approach are as follows:

- It accounts for minerals with sluggish reaction kinetics, e.g. silicates, allowing their potential neutralisation capacity to be considered within the prediction, as well as addressing the challenge of reactive minerals in sub-arctic conditions;
- It considers both oxidation and dissolution mechanisms and also the precipitation and dissolution of carbonates (depending on the local conditions); and
- It is not limited by equilibrium defined reactions or phases.

The challenges associated with the kinetic predictive numerical calculation approach are generally associated with the fact that chemical kinetic calculations require different input data than chemical equilibrium calculations as follows:

- The surface area of the WRD and the different mineralogical phases must be adequately defined, through the calculation of the surface area from PSD.
- Determination of the reactive surface area (i.e. the proportion of a given mineral phase that will be available for reaction (Jeschke and Dreybrodt 2002)) suffers from the same challenges as the calculation of the reactive mass in the thermodynamic equilibrium method. However, detailed mineralogical assessment can provide insight into the correct proportions of the minerals per lithology as well as potential encapsulation or potential armouring of the phases.
- Trace elements are typically measured by multi element assay, but that analytical technique does not link the elements and their mineralogical host (such as As present in the pyrite structure). This could be overcome by completing a detailed, quantitative mineralogical analysis as part of the geochemical characterisation study. This would allow the mineralogical composition to be determined, and allow the host minerals for various major and trace elements to be identified.
- Dissolution and precipitation rates are defined based the results of laboratory testwork, in which mineral phases dissolve or precipitate in far from equilibrium conditions. As such, the degree to which such rates are representative of field rates are debatable. The rates used in this study are consistent with the dissolution and precipitation rates found in the literature. In addition to the reproduction of HCT results, quantifying the performance of kinetic modelling would require the modelling of kinetic field tests such as field cribs as a validation step.

Conclusions

This study compares thermodynamic equilibrium and kinetic modelling methods for the prediction of source term water quality from a mine waste rock dump at a proposed IOCG deposit in northern Finland. Using an approach based on the definition of kinetic equations for the reactivity of the material allows the decoupling of the calculations from laboratory HCT results as the basis for defining metal release rates. Kinetic equations are based on rate equations from the literature, using mineralogical, temperature, PSD and reactive surface area parameters to calculate seepage chemistry while laboratory and field testwork results

are used to validate the approach. This approach accounts for minerals with sluggish reaction kinetics, e.g. silicates, allowing their potential neutralisation capacity to be considered within the prediction, as well as addressing the challenge of reactive minerals in sub-arctic conditions.

References

- ASTM. (2013). Standard test method for laboratory weathering of solid material using a humidity cell, ASTM D 5744-13e1.
- Bennett, JW, Comarmond, MJ and Jeffery, JJ (2000). Comparison of oxidation rates of sulfidic mine wastes measured in the laboratory and field. Australian Centre for Mining and Environmental Research, Brisbane.
- Birkholzer, J and Tsang, C-F (1997). Solute channelling in unsaturated heterogeneous porous media. *Water Res. Research* 33, pp.2221-2238.
- Cepuritisa, R, Garboczic, EJ, Ferraris, CF, Jacobsena, S and Sørensen, BE. (2017). Measurement of particle size distribution and specific surface area for crushed concrete aggregate fines. *Advanced Powder Technology* Volume 28, Issue 3, March 2017, pp.706–720
- Cohen, SD and Hindmarsh, AD (1996). Cvode, A Stiff/Nonstiff Ode Solver in C. *Computers in Physics* 10(2). August 1996.
- Jeschke, AA and Dreybrodt, W (2002). Dissolution rates of minerals and their relation to surface morphology. *Geochimica et Cosmochimica Acta*, Vol. 66, No. 17, pp. 3055–3062
- Kelemen, PB, Matter, J, Streit, EE, Rudge, JF, Curry, WB, and Blusztajn, J. (2011). Rates and mechanisms of mineral carbonation in peridotite: natural processes and recipes for enhanced, in situ CO₂ capture and storage. *Annual Review of Earth and Planetary Sciences* 39, pp.545-576.
- Kempton, H. (2012). A Review of Scale Factors for Estimating Waste Rock Weathering from Laboratory Tests. ICARD 2012.
- Martin, V, Aubertin, M, Bussiere, B and Chapuis, RP. (2004). Evaluation of unsaturated flow in mine waste rock. *Proceedings of 57th Canadian Geotechnical Conference / 5th Joint CGS/IAH-CNC Conference. Session 7D. pp.14-21.*
- Palandri, JL and Kharaka, YK. (2004). A compilation of rate parameters of water-mineral interaction kinetics for application to geochemical modelling.
- Parkhurst, DL and Appelo, CAJ. (1999). User's guide to PHREEQC (version 2)-A computer program for speciation, batch-reaction, one-dimensional transport, and inverse geochemical calculations: U.S. Geological Survey Water-Resources Investigations Report 99-4259, p. 312.
- Parkhurst, DL and Appelo, CAJ. (2013). Description of input and examples for PHREEQC version 3—A computer program for speciation, batch-reaction, one-dimensional transport, and inverse geochemical calculations: U.S. Geological Survey Techniques and Methods, book 6, chap. A43, 497 p., available only at <http://pubs.usgs.gov/tm/06/a43>.
- Sobek, AA, Schuller, WA, Freeman, JR and Smith RM. (1978). Field and Laboratory Methods Applicable to Overburdens and Minesoils. Report EPA-600/2-78-054, US National Technical Information Report. PB-280495.
- SRK Consulting (UK) Limited. (2013). Hydrological Impact Assessment Report for the Hannukainen Iron Ore-Copper-Gold Project, Phase 2. UK4970. Prepared for Northlands Mines OY.

How geochemical modelling helps understanding processes in mine water treatment plants – examples from former uranium mining sites in Germany

Anne Weber¹, Andrea Kassahun²

¹ *GFI Grundwasser-Consulting-Institut GmbH Dresden, Meraner Straße 10, 01217 Dresden, Germany, aweber@gfi-dresden.de*

² *Wismut GmbH, Jagdschänkenstraße 29, 09117 Chemnitz, Germany*

Abstract Mine waters from former uranium mining sites in Germany contain high concentrations of metal(loids). They are treated by lime precipitation and adsorption technologies. In this work well-defined lab scale experiments were modelled to elucidate reaction networks and their susceptibility to varying water composition. Both treatment technologies involve mineral precipitation-dissolution, gas exchange, surface complexation at ferrihydrite. It was shown that the formation of alkaline earth uranyl carbonate complexes and the precipitation of liebigite-group minerals determine uranium retention in WISMUT's mine water treatment operations. Sensitivity towards sludge composition and stability of arsenic sorption even at reducing conditions were derived from scenario simulations.

Key words: mine water treatment, geochemical modelling, uranium, arsenic

Introduction

In the course of remediation of the former Eastern German uranium mining sites, WISMUT GmbH operates six water treatment plants (WTPs). More than 25 Mm³ of tailings management facility seepage and mine waters are treated annually to remove site specific contaminants (e.g. uranium, radium, arsenic, iron, manganese). Modified lime precipitation is the prevailing technology, immobilizing contaminants by lime addition and induced precipitation of ferrihydrite Fe(OH)₃.

Evolving changes in mine water composition will influence the efficiency of water treatment with respect to the specific contaminants and require adjustments in the treatment technologies. For that purpose different strategies are pursued, e.g. implementation of treatment trains into geochemical models in order to use them as a prognosis tool and search for alternative treatment technologies. For both approaches lab experiments were conducted by WISMUT GmbH under purposefully defined conditions. These experiments allowed for building geochemical models comprising all system relevant processes with proper parameterization. This paper focusses on modelling the processes in selected lab tests.

Methods

Conduction of lime precipitation batch tests

Three precipitation batch tests FV₁, FV₂, FV₃ were conducted representing conditions in the lime precipitation train of the WTP Ronneburg. Per batch test 1 L of inflow water from the WTP was used and the pH was elevated until 9.6 during five stirring steps lasting 20 min each. Increase of pH was achieved by gas exchange with the atmosphere of the carbonate

oversaturated water and lime water addition in steps three to five. Flocculant (Kemira Superfloc® A110) was added before the final 3 h settling period. Experiments FV2 and FV3 were supplemented with 20 mL high density sludge (HDS) before pH rise corresponding to the WTP treatment. Starting solution of FV3 was enriched with 275 mg/L NaHCO₃ to reflect future increase of carbonate concentrations in the Ronneburg mine water.

Water samples were taken from the starting solution and from the experiments before and after settling of precipitates. They were analysed for pH, pe, O₂, Fe²⁺, anions (IC), elements (ICP-OES, ICP-MS). Composition and metal binding of the precipitating sludge was analysed by sequential extraction procedure according to Graupner et al. (2007). Main reactive minerals in the HDS were derived by analysing the results of sequential extraction resulting in a composition of 39 % ferrihydrite, 14 % calcite, 14 % CaO, 5 % magnesite, ca. 1% MgSO₄, CaSO₄, FeCO₃, MnCO₃. Assessment of saturation indices in HDS pore water additionally indicated the presence of swartzite/bayleyite or calciumuranate (UO₄Ca), uranophane (Ca[UO₂]₂[SiO₃OH]₂:5H₂O).

Conduction of FerroSorp® sorption column test

In a lab scale column test 5 mL bed volume of FerroSorp® Plus (HeGo Biotec GmbH) were fed with in average 6.6 mL/h (maximum 12.5 mL/h) seepage water from the tailings management facility (TMF) Helmsdorf (Kassahun et al. 2016) over a period of 280 days. To optimize surface complexation of target contaminants the pH in the seepage solution was adjusted to 6.0 by 0.5 M HCl. Inflow solution was stored in gas tight bags (Tesseraux) to prevent any degassing, precipitation and pH change during the experiment. . Outflow was collected in Erlenmeyer flasks

Samples were taken from each inflow stock solution and at every weekday from the outflow (mixed sample). Samples were analysed for pH, anions (IC), elements (ICP-OES, ICP-MS). Mineralogical analysis of a similar FerroSorp® AW material from Schöpke (2016) declared a composition of 18 % calcite, 5 % goethite, 2 % hematite and 72 % amorphous phases. The latter was attributed to ferrihydrite according to FerroSorp® Plus product information sheet. The effective porosity (0.4) of the filter bed was calculated from measured water volume in the bed. Total porosity (0.8) was taken from Schöpke (2016).

Simulation software and thermodynamic data base

Geochemical simulations were performed with the chemical reaction code PHREEQC (version 3) by Parkhurst & Appelo (2013). As thermodynamic data base (TDB) ThermoChimie (Giffaut et al. 2014) from the French National Radioactive Waste Management Agency was used (version 9bo). It comprises self-consistent data for a still growing number of elements.

In order to fit for conditions in the experiments, ThermoChimie had to be supplemented. Aqueous zinc species and phases as well as molybdenum phases were implemented from the Wateq4F data base. Uranium phases from Minteq.v4 and LLNL data bases (PHREEQC distribution) were supplemented if not already contained. All further included aqueous spe-

cies and phases are summarized in tab. 1 and 2. Focus was set on the implication of uranyl-calcium/magnesium-carbonato-species which were presumed to possibly determine uranium speciation in the WTPs from previous studies (Lietsch et al. 2015).

Data for surface complexation onto ferrihydrite were taken from the Wateq4F data base (PHREEQC distribution), which base on the model of Dzombak & Morel (1990). Surface complexation data further added to the ThermoChimie TDB are summarized tab. 1. Data for uranyl surface complexation were replaced by the more comprehensive data in Waite et al. (1994).

Table 1 Equilibrium constants of aqueous and surface complexes added to the ThermoChimie data set. *Hfo_s*, *Hfo_w*: strong and weak binding sites onto ferrihydrite according to Dzombak & Morel (1990). a: Data base file distributed with PHREEQC.

Reaction	log(k)	Source
$Mg^{2+} + 3 CO_3^{2-} + UO_2^{2+} = MgUO_2(CO_3)_3^{2-}$	26.11	Lietsch et al. (2015)
$6 MoO_4^{2-} + Al^{3+} + 6 H^+ = AlMo_6O_{21}^{3-} + 3 H_2O$	54.99	Minteq.v4 ^a
$3 H_3(AsO_3) + 6 HS^- + 5 H^+ = As_3S_4(HS)_2^- + 9 H_2O$	72.31	Wateq4F ^a
$H_3(AsO_3) + 2 HS^- + H^+ = AsS(OH)(HS)^- + 2 H_2O$	18.04	Wateq4F ^a
$2 Hfo_wOH + UO_2^{2+} = (Hfo_wO)_2UO_2 + 2 H^+$	-6.28	Waite et al. (1994)
$2 Hfo_sOH + UO_2^{2+} = (Hfo_sO)_2UO_2 + 2 H^+$	-2.57	Waite et al. (1994)
$2 Hfo_wOH + UO_2^{2+} + CO_3^{2-} = (Hfo_wO)_2UO_2CO_3^{2-} + 2 H^+$	-0.42	Waite et al. (1994)
$2 Hfo_sOH + UO_2^{2+} + CO_3^{2-} = (Hfo_sO)_2UO_2CO_3^{2-} + 2 H^+$	3.67	Waite et al. (1994)
$Hfo_wOH + Co^{2+} = Hfo_wOCO^+ + H^+$	-3.01	Minteq.v4 ^a
$Hfo_sOH + Co^{2+} = Hfo_sOCO^+ + H^+$	-0.46	Minteq.v4 ^a
$Hfo_wOMo(OH)_3 = Hfo_wOH + 2 H^+ + MoO_4^{2-} + H_2O$	17.96	Gustafsson (2003)
$Hfo_wOMoO_3^- + H_2O = Hfo_wOH + H^+ + MoO_4^{2-}$	9.50	Dzombak & Morel (1990)
$Hfo_wOHMoO_4^{2-} = Hfo_wOH + MoO_4^{2-}$	2.40	Dzombak & Morel (1990)
$(Hfo_wOH)_3(Hfo_wO)Ra^+ + H^+ = 4 Hfo_wOH + Ra^{2+}$	4.45	Sajih et al. (2014)
$(Hfo_wOH)_2(Hfo_wO)_2Ra^{4+} + H^+ = 4 Hfo_wOH + Ra^{2+} + 2 H^+$	-22.20	Sajih et al. (2014)

Except for speciation calculations the data base was used in a modified version with decoupled redox species for uranium (+3, +4, +5, +6) and iron (+2, +3). All relevant reactions were assumed to be equilibrium reactions at any time of the experiments and temperature was set 20 °C (average lab temperature).

Table 2 Equilibrium constants of phases added to the ThermoChimie data set. Thermodynamic data taken from Alwan and Williams (1980) and Gorman-Lewis et al. (2008) for grimselite.

Phase	Reaction	log(k)
Andersonite	$Na_2CaUO_2(CO_3)_3 \cdot 6 H_2O = 2 Na^+ + Ca^{2+} + UO_2^{2+} + 3 CO_3^{2-} + 6 H_2O$	-37.5
Bayleyite	$Mg_2UO_2(CO_3)_3 \cdot 18 H_2O = 2 Mg^{2+} + UO_2^{2+} + 3 CO_3^{2-} + 18 H_2O$	-36.40
Liebigite	$Ca_2UO_2(CO_3)_3 \cdot 10 H_2O = 2 Ca^{2+} + UO_2^{2+} + 3 CO_3^{2-} + 10 H_2O$	-37.20
Swartzite	$CaMgUO_2(CO_3)_3 \cdot 12 H_2O = Ca^{2+} + Mg^{2+} + UO_2^{2+} + 3 CO_3^{2-} + 12 H_2O$	-37.92
Grimselite	$NaK_3UO_2(CO_3)_3 \cdot H_2O = Na^+ + 3 K^+ + UO_2^{2+} + 3 CO_3^{2-} + H_2O$	-37.1

Modelling metal(loid) immobilisation in lime precipitation batch tests

To reproduce metal(loid) retention in the precipitation batch tests, the following processes were implemented in PHREEQC models:

- equilibrium with HDS reactive phases and oxygen, carbon dioxide in the atmosphere,
- complete oxidation of ferrous to ferric iron and precipitation of ferrihydrite,
- addition of lime water as $\text{Ca}(\text{OH})_2$ and precipitation of calcite,
- precipitation of gypsum, carbonates, oxides to model matrix elements,
- surface complexation at ferrihydrite from HDS and at precipitated ferrihydrite,
- precipitation of uranium and cobalt carbonate phases.

Analysed dissolved concentrations of start solutions and after settling of precipitates are shown in fig. 1 together with the modelled concentrations in the supernatant water. Not shown are pH-values which increased from 6.6...7.0 to 9.3 during the experiment and could be reproduced by the model adequately. Generally, modelled concentrations were in good agreement with measured ones, except for manganese. Its, however, low concentrations of 0.1...0.2 mg/L were underestimated by the model.

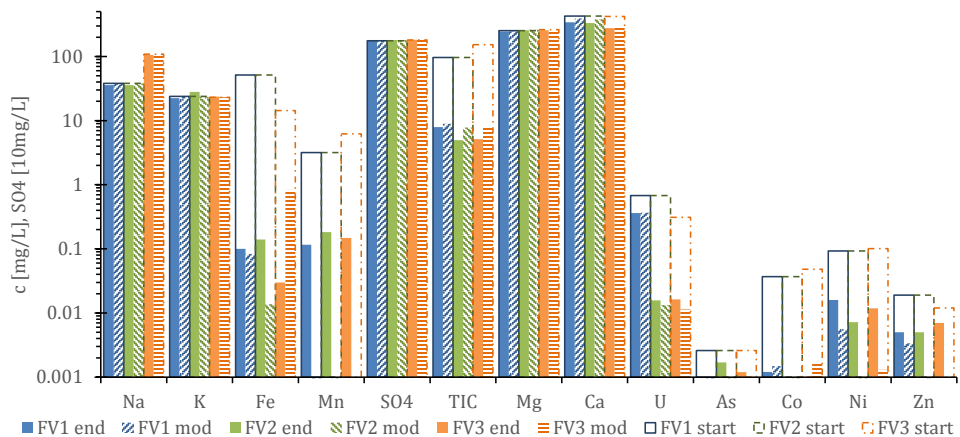


Figure 1 Dissolved concentrations for pH, matrix elements and contaminants in three precipitation batch tests: measured starting and end concentrations and modelled end concentrations (mod).

Measured concentrations of uranium, arsenic, cobalt, zinc, nickel, cadmium could be reproduced applying the surface complexation model without any modification. For uranium and cobalt only additional mineral precipitation reflected measured concentrations. Phases were carefully selected by their saturation index in the solution. Minerals from the liebigite group (swartzite and bayleyite) could match uranium concentrations in the experiments final supernatant best, which coincided with speciation modelling results for the HDS pore water. By addition of spaeocobaltite (CoCO_3) precipitation, supernatant cobalt concentrations could be described well.

In fig. 2 the mass balance of metal(loid)s in the models of the three experiments show the importance of surface complexation at $\text{Fe}(\text{OH})_3$ for metal(loid) treatment in the WTP. In FV1 (no HDS added), immobilisation is lower, especially for uranium, according to the measurements. On the other hand, increase of TIC in the initial solution (FV3) does not significantly change the original (FV2) metal(loid) immobilisation. Scenario calculations with changed initial surface site composition (data not shown), however, identified surface site composition being a sensitive parameter with respect to whether uranium and cobalt are sorbed or not.

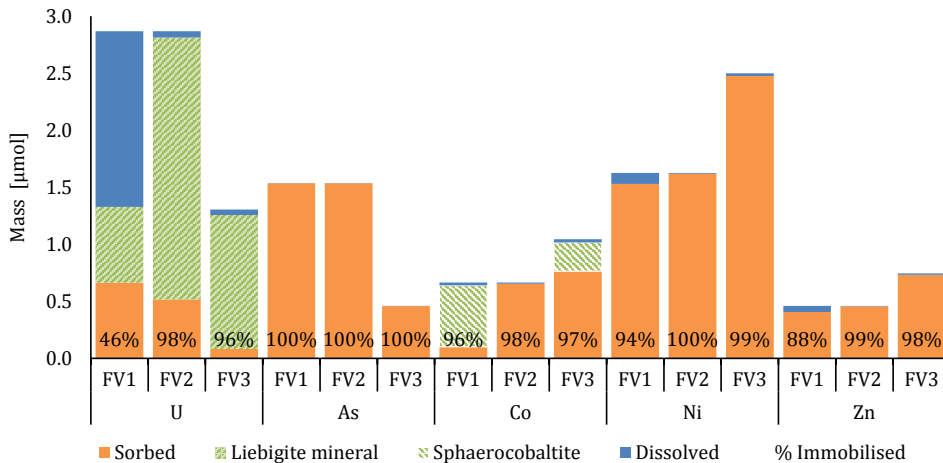


Figure 2 Modelled metal(loid)s mass balances and percentage of immobilisation in precipitation batch tests.

Modelling metal(loid) immobilisation in FerroSorp® sorption columns

Before modelling the FerroSorp® column experiments, possible mineral precipitation or dissolution reactions within the columns were identified by equilibrium calculations of feed and outflow solutions. Thereby, transition of mineral equilibria within the columns was indicated for CaCO_3 -phases, phosphates (e.g. anapaite, chloroapatite), liebigite like minerals (tab. 2), ferrihydrite and magnesite. EDX analysis of the FerroSorp® material before and after the experiment further revealed significant changes in its main composition with an increase of Fe, P and a decrease of Ca content (data not shown).

Modelling the column experiments in PHREEQC was done by first taking into account milieu determining processes and subsequently adapting less sensitive settings to reflect immobilisation of trace elements, in detail:

- one dimensional transport of inflow solution with measured varying composition and flow rate through a porous medium,
- degassing of CO_2 and kinetic dissolution of calcite to reflect pH of ~ 7 within the FerroSorp® bed,

- equilibrium with and surface complexation at ferrihydrite $\text{Fe}(\text{OH})_3$,
- precipitation of liebigite and chloroapatite.

Fig. 3 shows measured and modelled concentrations of four selected elements. Concentration of molybdenum appeared to be sensitive with respect to pH, which is determined by TIC. This was used to adapt pH in the model to 6.8...7.1 within the FerroSorp® bed (no direct pH measurement in the adsorber bed was preformed).

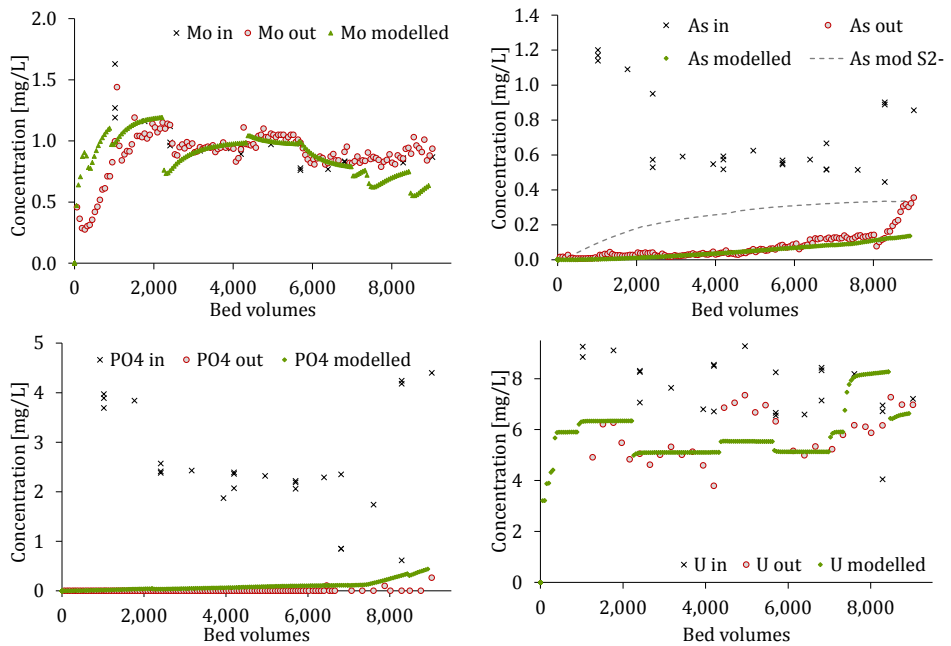


Figure 3 Measured and modelled concentration of target contaminants in a FerroSorp® column test with seepage water from the tailings management facility Helmsdorf. As mod S2-: Additional results from scenario run with 0.5 mg/L S2-in feed solution.

Arsenic immobilisation strongly depends on pH and was only slightly influenced by its redox speciation confirming comparable sorption of the charge neutral arsenite complex (H_3AsO_3) and negatively charged arsenates ($\text{H}(\text{AsO}_4)^{2-}$, $\text{H}_2(\text{AsO}_4)^{-}$) onto ferrihydrite (Jain et al. 1999). Nevertheless, scenario calculations revealed a strong inhibiting effect of dissolved sulphide (fig. 3), which coincides with observations of high arsenic concentrations during periods of microbial sulphate reduction in parallel experiments.

Comparable to the modelling of the lime precipitation tests, uranium effluent concentrations could only be reproduced by the model allowing precipitation of liebigite. Likewise, for phosphate modelled and analysed concentrations match when chloroapatite precipitation is allowed. Surface complexation of uranium only negligibly contributes to its retardation. Liebigite precipitation keeps uranium concentrations at about 5 mg/L according to calcium

availability and pH. However, the newly planned Helmsdorf mine water treatment plant uses ion exchange for uranium retention prior to FerroSorp® adsorption and interactions of uranium with FerroSorp® are secondarily in that case.

Conclusions

Lime induced ferric iron precipitation and sorption at granulated ferric iron hydroxide are current treatment technologies for mine waters from former uranium mining sites in Eastern Germany. Geochemical modelling of lab experiments simulating treatment processes was shown to identify underlying reactions and thus constitutes a useful tool to optimize treatment technologies. Mineral dissolution-precipitation, gas exchange and surface complexation according to Dzombak & Morel well described the behaviour of arsenic, uranium, zinc, nickel, cobalt, molybdenum and other water constituents in water treatment operations. Due to the competitive character of sorption processes, the complete implementation of the reaction network was essential for correct model simulations. This applied especially for the complete carbonate and phosphate reactions.

At site specific conditions uranium forms aquatic alkaline earth carbonate complexes and is marginally subject to surface complexation. Measured uranium concentrations in the experiments could only be modelled by incorporation of minerals from the liebigite-group. Further investigations need to focus on mineralogical detection of these uranium minerals.

Modelling of lime precipitation revealed that the composition of the recirculated sludge was a sensitive parameter for metal(loid) immobilisation. For sorption at granulated ferric hydroxide, the stability of the immobilization process even at reducing conditions for As-III was shown. However sulphate reducing conditions should be avoided as formation of As-S-complexes hinders sorption of arsenic to granulated ferric hydroxide.

Acknowledgements

This work is part of WISMUT GmbH R&D activities on water treatment technologies. Special thanks to Dr. Jan Laubrich for request and support, Birgit Zöbisch and Yvonne Schlesinger for experimental work.

References

- Alwan K, Williams PA (1980) The Aqueous Chemistry of Uranium Minerals. Part 2. Minerals of the Liebigite Group. *Mineral Mag* 43:665–667. doi: 10.1180/minmag.1980.043.329.17
- Dzombak DA, Morel FMM (1990) Surface Complexation Modeling: Hydrus Ferric Oxide. New York, John Wiley, ISBN: 978-0-471-63731-8
- Giffaut E, Grivé M, Blanc P, et al. (2014) Andra thermodynamic database for performance assessment: ThermoChimie. *Appl Geochemistry* 49:225–236. doi: 10.1016/j.apgeochem.2014.05.007
- Gorman-Lewis D, Burns PC, Fein JB (2008) Review of uranyl mineral solubility measurements. *J Chem Thermodyn* 40:335–352. doi: 10.1016/j.jct.2007.12.004
- Graupner T, Kassahun A, Rammlmair D, et al. (2007) Formation of sequences of cemented layers and hardpans within sulfide-bearing mine tailings (mine district Freiberg, Germany). *Appl Geochemistry* 22:2486–2508. doi: 10.1016/j.apgeochem.2007.07.002
- Gustafsson JP (2003) Modelling molybdate and tungstate adsorption to ferrihydrite. *Chem Geol* 200:105–115. doi: 10.1016/S0009-2541(03)00161-X

- Jain A, Raven KP, Loeppert RH (1999) Arsenite and Arsenate Adsorption on Ferrihydrite: Surface Charge Reduction and Net OH- Release Stoichiometry. *Environ. Sci. Technol.* 33:1179–1184
- Kassahun A, Wendler C, Paul M (2016) Ion Exchange for Uranium Removal from TMF Seepage Water. Conference Paper, Int. Bergbausymposium WISSYM 2015, Bad Schlema, 31.08.2015, p 177–182
- Lietsch C, Hoth N, Kassahun A (2015): Investigation of Phenomena in Uranium Mine Water using Hydrogeochemical Modeling – a case study. In: Merkel, BJ, Arab, A (eds): Uranium – Past and Future Challenges, Proceedings of the 7th UMH Conference, Springer, 717–724
- Parkhurst DL, Appelo CAJ (2013) Description of Input and Examples for PHREEQC Version 3 – A Computer Program for Speciation, Batch-Reaction, One-Dimensional Transport, and Inverse Geochemical Calculations. *US Geol Surv Tech Methods*, B 6, chapter A43, 497 pp
- Sajih M, Bryan ND, Livens FR, et al. (2014) Adsorption of radium and barium on goethite and ferrihydrite: A kinetic and surface complexation modelling study. *Geochim Cosmochim Acta* 146:150–163
- Schöpke R (2016) Entwicklung von Bemessungsansätzen für den Einsatz von Adsorptionsfiltern auf der Basis von granuliertem Eisenhydroxid. *ASIM-Mitteilung* 161:85–91
- Waite TD, Davis JA, Payne TE, et al. (1994) Uranium (VI) adsorption to ferrihydrite: Application of a surface complexation. *Geochim Cosmochim Acta* 58:5465–5478

The need for improved representation of groundwater-surface water interaction and recharge in cold temperate – subarctic regions

Alastair Black

SRK Consulting (UK) Ltd, Churchill House, Cardiff CF10 2HH, ablack@srk.co.uk

Abstract Groundwater models are commonly calibrated exclusively to groundwater level data and their predictive capability can be let-down by underdeveloped capabilities in recharge and would benefit from calibration to surface water flow – particularly in areas with seasonal frozen conditions and snowmelt.

Here, we present the Surface-Water-Accounting-Model (SWAcMOD). Designed to work in conjunction with existing groundwater modelling software, SWAcMOD gives the ability to produce detailed recharge, surface-water flows and evapotranspiration inputs for spatially distributed and transient groundwater models.

SWAcMOD enhances groundwater models' capabilities with respect to surface-water interaction with groundwater systems and through the combined approach, groundwater models can additionally be calibrated to gauged river flows further constraining mine water balances.

Key words recharge, surface water, water balance, modelling, MODFLOW

Introduction

Groundwater modelling software benefits from continued development and the two primary 'industry standard' toolsets; MODFLOW-USG, Panday (2013), and FeFlow are comprehensive packages for the representation of saturated zone mine hydrogeology. However, saturated zone models are typically calibrated exclusively to observed groundwater level data and their predictive capability are frequently let down by underdeveloped capabilities in recharge, coupled surface water flow simulation and unsaturated zone processes.

Groundwater models are expected to represent observed groundwater level fluctuation and additionally, in many areas, groundwater interaction with surface water systems and wetlands. The representation of groundwater level trends and seasonal fluctuation relies upon the appropriate magnitude and timing of recharge inputs to the groundwater model, which typically are highly variable spatially. Within groundwater modelling studies in the mining industry the use of basic estimates of recharge directly from rainfall records is not uncommon due to the uncertainty in the parameterisation of processes which delay, attenuate and partition rainfall between groundwater recharge, surface flow and actual evapotranspiration. These basic methods are particularly unsuitable in cold climates with soil-frost and snowpack generation-melt conditions resulting in the model's inability to represent observed responses and to compensate the recharge magnitude deficiencies through erroneous calibration of aquifer properties.

Representation of coupled groundwater and surface water flow systems is common in water resources modelling as regulation of abstraction is typically dependant on river flow thresh-

olds or wetland saturation under the European Water Framework Directive. The program RRRR, Heathcote (2004) is a prime example of MODFLOW preprocessing software which enables more holistic water balance simulation. Good practice of mass conservative, routed and coupled surface systems from this sector can be developed into mining modelling more routinely.

Calculation of time-series recharge to groundwater and groundwater-surface water interaction is well documented and a plethora of 1D and basic 2D modelled examples exist in the literature. It is however challenging to scale the collective surface and subsurface processes applied in these studies to fully spatially distributed and time variant models and this is considered a major reason why overly simplified methodologies are commonly applied. Reasons for the limited number of mining studies with comprehensive handling of recharge and surface water interaction include:

1. The detailed datasets required to parameterise the key surface and subsurface processes have not been available.
2. Input file formats of the most commonly applied groundwater simulation packages (MODFLOW and FeFlow) are bespoke and require purpose built tools for their generation.
3. Difficult to produce and time consuming topological routing networks of surface water drainage need to be built into the model to provide mass conservative river flows.
4. Processes like the calculation of rapid runoff require daily, or sub-daily, transient calculation and the runtime for distributed simulations can be prohibitive.
5. There are several tools in existence however these are closed source or written in programming languages with a reducing user base which results in poor accessibility and limits the adaptation of the tool for the specific needs of new studies.

The Surface Water Accounting Model (SWAcMOD) program is presented herein. In an effort to overcome the above challenges to comprehensively represent the surface and near surface systems in mining groundwater models:

1. Newly available satellite datasets are presented to assist in the parameterisation of the model, alongside more conventional datasets.
 2. The program directly produces the bespoke input files for the industry standard groundwater modelling tool MODFLOW, including the new Unstructured Mesh versions.
 3. Topologically routed river networks can be simulated.
 4. The modelling package is designed to take advantage of increasingly parallel computing architectures.
 5. SWAcMOD is released under the GNU GPLv3 open source licence and written in the Python language to maximise accessibility.
-

Overview

SWAcMOD comprises a workflow of sequential processes derived from existing studies referenced in the literature. Processes can be optionally enabled or disabled depending on the needs of the site being modelled. The program is of modular design permitting additional processes to be added or adapted within the existing workflow.

The workflow constitutes a 1D model from ground surface down through the soil zone and unsaturated zones. The 1D model requires, as a minimum, rainfall and potential evapotranspiration (PE), with potentially additionally temperature and solar flux time series data alongside parameters controlling how water is partitioned through each process. Fig. 1 summarises the 1D workflow.

Represented processes include:

- Canopy / vegetation interception and evaporation.
- Temperature dependant precipitation as snowfall or rainfall.
- Snowpack development and melt.
- Partitioning of rainfall/melt water as rapid runoff.
- Soil Moisture Accounting and actual evapotranspiration (AE) calculation.
- Additional shallow ponding and impervious zone enhancements to the Soil Moisture Accounting.
- Urban water main or canal leakage.
- Interflow and combined near surface lateral flow processes.
- Attenuation of recharge as passes through the unsaturated zone.
- Surface flow time of concentration attenuation.
- Surface water abstractions and discharges.
- Bypass mechanisms of rejected recharge, macropore recharge and runoff recharge.

The 1D workflow is duplicated for each and every groundwater model cell, however the spatially variable parameters controlling each property can be spatially implemented either by zones of identically parameterised cells or via specification of unique values per cell. By this system the 2D parameterisation of the model can be readily setup. Fig. 2 is an example of zonal input of model properties in SWAcMOD at the scale of the MODFLOW-USG groundwater model mesh. Each of the hexagonal cells hosts a 1D workflow as presented in Fig. 1.

Of particular importance in cold climates recharge is the facility to represent most processes optionally using time variant parameterisation which permits frozen conditions and seasonal removal of connections to be imposed. This functionality is additionally used for Soil Moisture Accounting though the FAO 56 methodology permitting changing vegetation or crop rotation.

Fig. 3 is an example catchment summary for a model located in the centre of Finnish Lapland. Processes enabled in this model include snowfall-pack and melt, rapid runoff, Soil Moisture Deficit and AE accounting via an adapted form of the FAO56 methodology, Allen (1998), interflow, macropore bypass recharge (rapid recharge), secondary recharge from runoff (important for representation of observed increased melt recharge as approach surface water courses), surface water attenuation and groundwater recharge lag and attenuation. All processes down to the interflow store have time variant properties to permit soil freeze.

Uncertain model properties have been constrained through calibration to river flow gauging prior to dam construction, measured snow thickness (green dots in Fig. 3), Sentinel Satellite derived snow cover spatial distributions over time and Sentinel Satellite derived AE inference. In addition, several properties, for example rapid runoff characteristics and vegetation rooting depths, have been estimated based on experience from past studies and reference material respectively.

The bottom three plots represent time series inputs for MODFLOW-USG and are the primary outputs for the model. These are the 'surface component of total river flow' (all excluding baseflow), 'Unutilised PE' (the input to control riparian evapotranspiration) and 'recharge to the saturated zone'. These three outputs are spatially distributed however this plot summarises the average daily time series values for this aggregated catchment area.

All units in Fig. 3 are millimetres, the temporal resolution is daily.

Solution to the problem of spatial parameterisation

The primary source of time series input data derives from meteorological stations providing high quality data at a specific locality. River flow gauging additionally provides good constraint on uncertain parameters at catchment scale. In particular, constraining the parameters and processes which influence the rate of recession from high flow events and, separately, the periods where rivers are dominantly groundwater baseflow derived can assist in the estimation of annual recharge magnitude. Beyond this however spatial parameterisation can be highly uncertain and a model's predictive capabilities are not improved through imposition of heterogeneity that cannot be backed up by observed data or conceptual relationships.

A major new source of data has become available in 2016 and 2017 to assist in the spatial parameterisation of surface processes. The Sentinel 2 satellites are part of the European Space Agency's Copernicus Programme and are primarily intended for application in the management of forestry and agriculture, assisting in prediction of crop yields. These data can additionally inform on areas of wet ground, snow cover, general landuse and vegetation efficiency to evapotranspire water. These multi-band data are freely available for all land-masses at a resolution of between 10 and 60m in x-y depending on the band combinations desired with new data for any given location becoming available every 5 days since March 2017 (ESA, 2017).

From recent application in Finnish Lapland it has been our experience that around 60% of the flybys are not adequate for use due to cloud cover. However, a single good dataset each month has been sufficient to observe the evolution of snowpack and melt, and the development of the otherwise highly uncertain vegetation evapotranspiration characteristics, both over space and time. Combined with conventional meteorological and monitoring datasets the uncertainty of processes controlling recharge to groundwater can be greatly reduced. Fig. s 4 through 9 denote Sentinel data for March (dominated by snow melt), August (peak period for vegetation evapotranspiration), and October (as the end of the warm season prior to freezing conditions). The purple and pink in the NDVI and Vegetation index data readily show water, snow and ice cover. The intensity index is an analogue for evapotranspiration.

Solution to the problem of time consuming file formatting and complex river topology

If the surface water processes are enabled, SWAcMOD assists in the generation of topologically sorted routing networks. The inputs to this process are topography and, optionally, user defined river locations.

The output of the overall process is formatted into MODFLOW-USG compliant ASCII files permitting MODFLOW to be run directly. The files currently generated include Recharge (RCH), Stream Flow Routing (SFR) and Evapotranspiration (EVT).

Solution to the problem of run-times and accessibility

Proprietary and closed source modelling packages are anticipated to be the primary barrier to accessibility and adaptability of similar programs, limiting use and applicability to unique study areas. A primary goal of the SWAcMOD program is to facilitate improved representation of water balances, recharge and groundwater – surface water interaction in groundwater modelling and, as such, the program is issued under the open source GNU GPLv3 licence.

The SWAcMod library is written in Python which is arguably one of the most readable and easy-to-use languages. Its built-in, high-level data types (e.g. dictionaries) and dynamic typing (i.e. no need to declare the types of arguments and variables) allow Python code to be on average 3-5 times shorter than analogous Java code, and 5-10 times shorter than C++ or FORTRAN code.

Python has been selected for this program as it is one of the most common programming languages, relatively easy to learn and has a growing user base, particularly in academia and amongst new graduates. Fortran is considered to be used for most scientific codes in the mining industry historically however its user base is declining, this language is rarely taught in universities.

The downside for Python is that it typically runs slower than programs written in low-level implementation languages like C++ or Java, and this is particularly limiting in scientific and numerical computing. In order to mitigate this drawback, we have implemented the

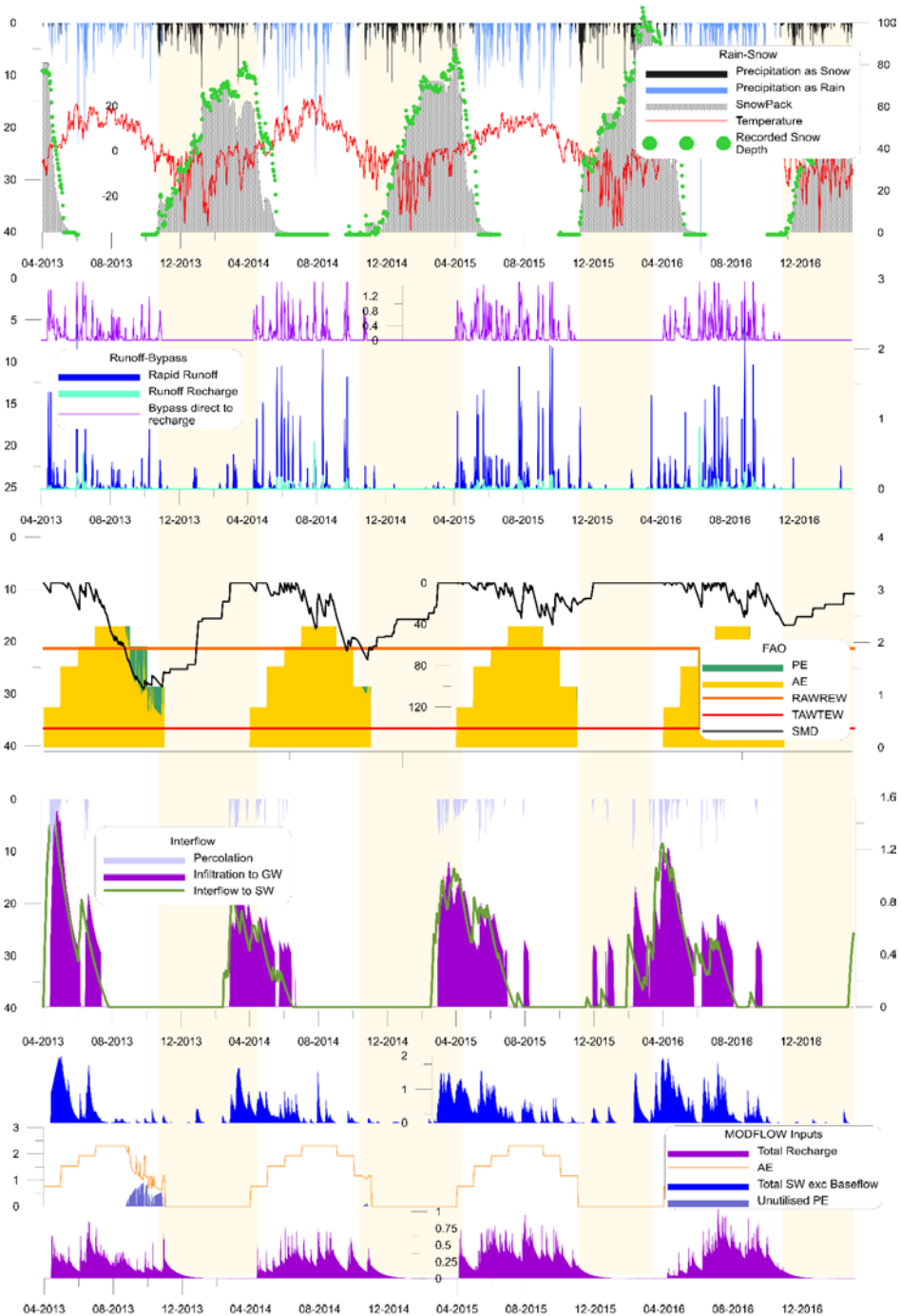


Figure 3 Break down of the outputs from SWaMOD processes for a catchment in central Finnish Lapland.

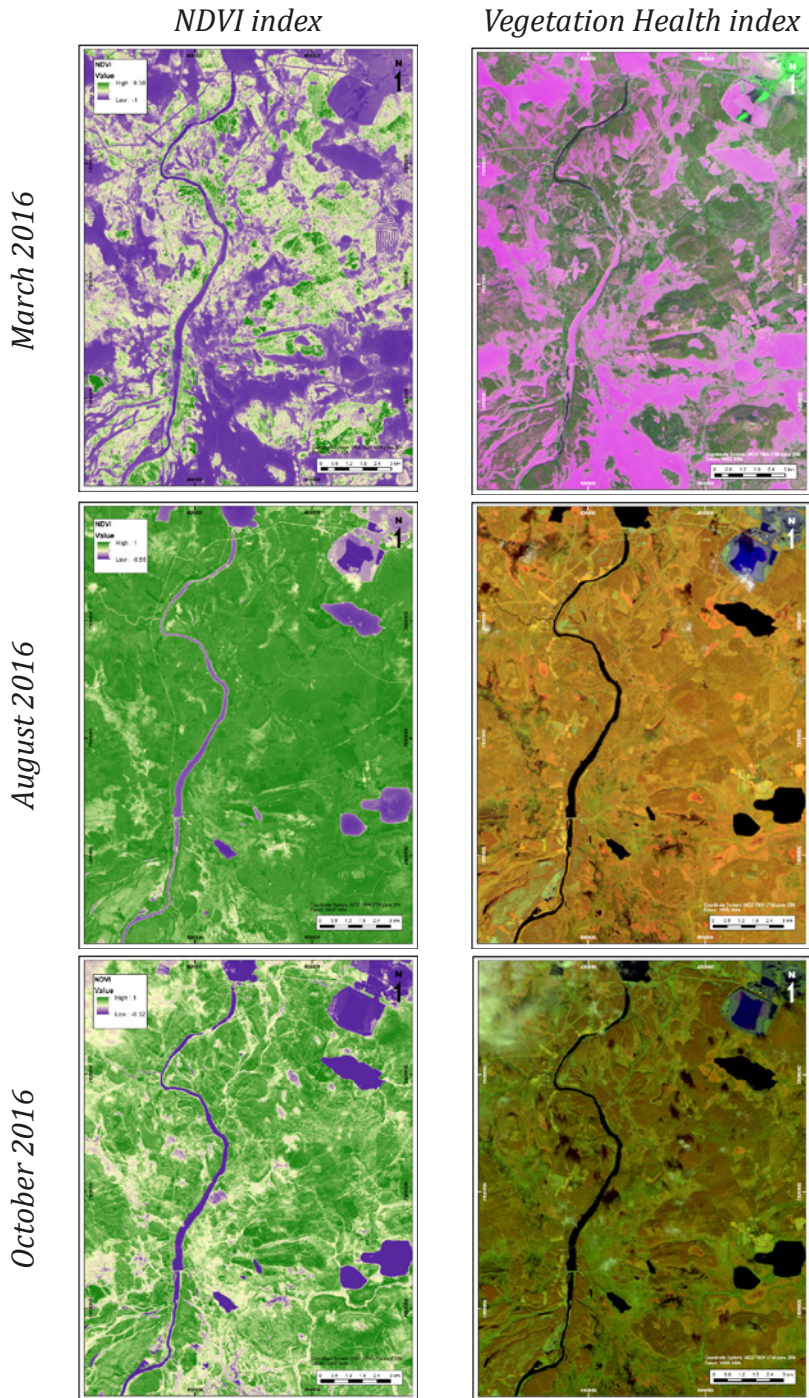


Figure 4 through 9 NDVI and Vegetation Health Index band combinations from Sentinel 2 data.

following 3 strategies: *parallelization*, *vectorization with NumPy* and *use of Cython*. Their combined effect is a 25-fold/core speedup of model time, bringing it down to a few milliseconds per node.

Conclusions

Surface Water Accounting Model (SWAcMOD) has been developed to be an open, accessible, adaptable and fast tool to enable better representation of time variant and spatially heterogeneous recharge, actual evapotranspiration and river flows. Alongside a groundwater modelling package like MODFLOW-USG this integrates catchment water balances. SWAcMOD is designed to work in sequence with MODFLOW and is compatible with the newest Unstructured Grid versions. The processes included within the SWAcMOD program are not new and are based on peer reviewed methods. However, the holistic framework to pull the processes together, rapidly parameterise, generate river topology and methods to invoke parallelisation – reducing runtimes – are considered a new development for the water community. In addition, barriers to robust representation of recharge in particular are considered to result from data scarcity in many mining studies. The SWAcMOD program has been designed to make use of newly available high resolution and free satellite datasets which help to constrain several spatially and temporally variable processes. This, in combination with conventional ground station based data, is a significant improvement in what has been openly available in recent years.

References

- Allen (1998) Crop evapotranspiration – Guidelines for computing crop water requirements – FAO Irrigation and drainage paper 56
- ESA (2017) <https://earth.esa.int/web/sentinel/user-guides/sentinel-2-msi/resolutions/spatial>
- Heathcote (2004) Rainfall routing to runoff and recharge for regional groundwater resource models. *Quarterly Journal of Engineering Geology and Hydrogeology*, 37, 113-130
- Panday et al. (2013), MODFLOW–USG version 1: An unstructured grid version of MODFLOW for simulating groundwater flow and tightly coupled processes using a control volume finite-difference formulation: U.S. Geological Survey Techniques and Methods, book 6, chap. A45

Fractional and sequential recovery of inorganic contaminants from acid mine drainage using cryptocrystalline magnesite

Vhangwele Masindi^{1,2,3}; John G. Ndiritu¹

¹*School of Civil and Environmental Engineering, University of the Witwatersrand, Private Bag 3, WITS 2050, South Africa, john.ndiritu@wits.ac.za*

²*Council for Scientific and Industrial Research (CSIR), Built Environment (BE), Hydraulic Infrastructure Engineering (HIE), P.O Box 395, Pretoria, 0001, South Africa, Tel: +2712 841 4107, Fax: +27128414847, VMasindi@csir.co.za, masindivhangwele@gmail.com*

³*Department of Environmental Sciences, School of Agriculture and Environmental Sciences, University of South Africa (UNISA), P. O. Box 392, Florida, 1710, South Africa*

Abstract This study evaluated the fractional and sequential recovery of inorganic contaminants from acid mine drainage (AMD) using cryptocrystalline magnesite. Batch experimental approach was used to fulfil the goals of this study. The obtained results revealed that $\geq 99.9\%$ of metals were recovered. Experimental and Geochemical modelling revealed that Fe was recovered at $\text{pH} \geq 3.5$, Al at $\text{pH} \geq 4.5$, Mn at $\text{pH} \geq 9$, Cu at $\text{pH} \geq 7$, Zn at $\text{pH} \geq 8$, Pb at $\text{pH} \geq 8$ and Ni at $\text{pH} \geq 9$. This study successfully proved that metal species can be fractionally and sequentially recovered from acid mine drainage using cryptocrystalline magnesite.

Key words Acid mine drainage, cryptocrystalline magnesite, neutralisation, recovery, precipitation

Introduction

Availability of Fe, Al, Mn and sulphate in acid mine drainage at elevated levels makes a valuable source of recoverable minerals. The genesis of these major metals and anions in acid mine drainage is as a result of hydro-geochemical weathering of pyrite and other sulphide bearing lithologies. The presence of toxic chemical species in AMD has raised environmental concerns at regional, national and international scientific communities (Masindi et al. 2017). The resultant water is very acidic hence dissolving the metals in the surrounding rocks. As a result, AMD has $\text{pH} \leq 2$, high dissolved metals and electrical conductivity (Masindi 2016). Chemical species leached to the surrounding aqueous solution include Al, Fe, Mn and SO_4^{2-} , and traces of Cu, Zn, Pb, and Ni. Toxicity and epidemiological studies reported that these metals are hazardous to terrestrial and aquatic organisms on exposure (Masindi et al. 2015), as such, they require treatment prior release to the environment and different end-users.

Passive and active technologies have been developed to treat AMD but downstream products limit their applications. Research studies have been in a quest to come-up with pragmatic and prudent technologies that can be employed for the recovery of valuable minerals (Seo et al. 2017a). The recovery of elements from acid mine drainage will generate some revenues that will aid in off-setting the running cost of the treatment process through commercialisation of the recovered resources (Masindi et al. 2015; Seo et al. 2017a).

Numerous methods have been developed and adopted for the recovery of metals from acid mine drainage and they include: neutralisation, adsorption, filtration, solvent extraction and electro dialysis (Seo et al. 2017a; Simate and Ndlovu 2014). Precipitation has been a commonly used method for metals recovery (Seo et al. 2017a). Precipitators commonly used are sodium hydroxide, sodium carbonate and lime (Seo et al. 2017a). Using these precipitators, metals will be recovered as hydroxides (Masindi et al. 2017). The use of cryptocrystalline magnesite for fractional and sequential recovery of metals from acid mine drainage has never been explored, as such, this is the first study in design and execution to explore the efficiency and feasibility of using cryptocrystalline magnesite to fractionally and sequentially recover potentially toxic metals from acid mine drainage. PHREEQC geochemical model was also employed to complement the experimental results.

Materials and Methods

Materials

Raw magnesite rock was collected from the Folovhodwe Magnesite Mine in Limpopo Province, South Africa. Field AMD samples were collected from a coal mine in Mpumalanga province, South Africa. Before the experiments, magnesite samples were milled to a fine powder for 15 minutes at 800 rpm using a Retsch RS 200 vibratory ball mill and passed through a 32 μm particle size sieve. The samples were kept in a zip-lock plastic bag until utilization for sensitivity study and the recovery of metals.

Characterization

Aqueous samples were analysed using ICP-MS (7500ce, Agilent, Alpharetta, GA, USA). The accuracy of the analysis was monitored by analysis of National Institute of Standards and Technology (NIST) water standards. Three replicate measurements were made on each sample and results are reported as mean average. Morphological properties were examined using Scanning Electron Microscopy (SEM) (JEOL JSM – 840, Hitachi, Tokyo, Japan). PHREEQC geochemical model was used to model the precipitation of chemical species from acid mine drainage.

Results and discussions

Morphology by Scanning Electron Microscopy (SEM)

The morphological properties of raw cryptocrystalline magnesite and AMD-reacted magnesite are shown in fig. 1.

Cryptocrystalline magnesite was observed to contain octagonal sheet and leafy-like structures on its surface (Fig. 1A). This is an indication that the material is heterogeneous. After contacting acid mine drainage (AMD), there was a transformation on the morphological properties of the recovered sludge hence indicating a possible dissolution and a subsequent deposition of chemical species. The sheet and leafy-like structures were observed on the surface of a secondary residue. The morphology was similar throughout the surface hence denoting that the recovered material is homogeneous.

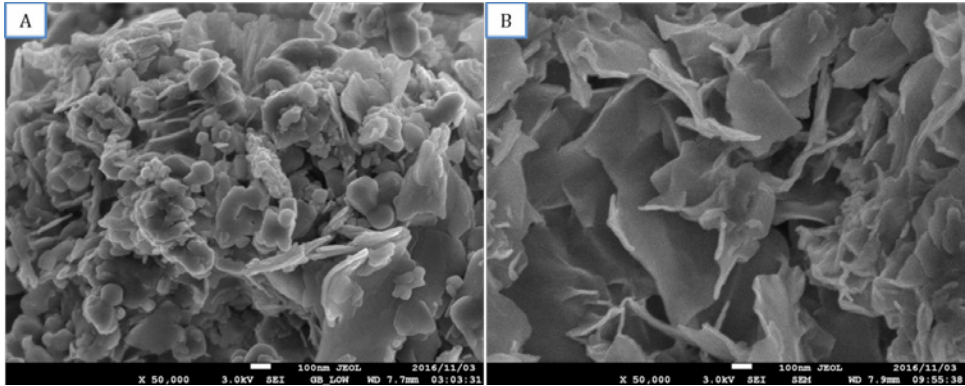


Figure 1 Morphological property of raw magnesite and AMD-reacted magnesite

Effect of pH on the removal of ions

An increase in pH and variation in percentage removal of chemical species during interaction of magnesite with AMD is shown in fig. 2.

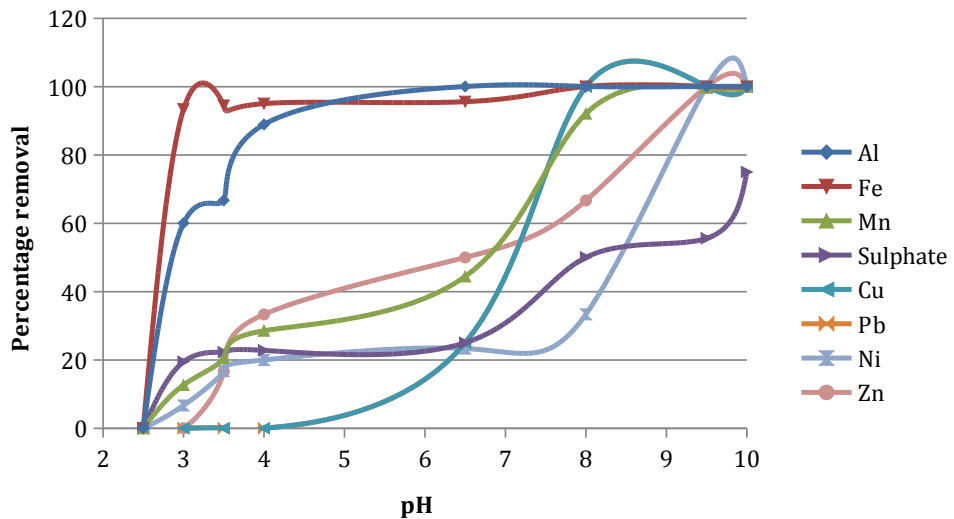


Figure 2 Variation of pH and heavy metals concentration with adsorbent dosage (Conditions: 100 mL solution, 250 rpm shaking speed, <math><32\ \mu\text{m}</math> particle size, 60 min reaction, 26 °C temperature).

As shown in fig. 2, the chemical species removal efficiencies were directly proportional to the pH of the supernatant solution. As the pH was increasing, the metal removal efficiency was also observed to increase, however, this was anticipated. An increase in pH may be attributed to dissolution of CaO and MgO from the magnesite matrices hence leading to an increase in pH. Similar results were reported by Masindi et al. (2015). Furthermore, Figure 2 points out that the chemical species were totally removed from the aqueous solution

($\geq 99.9\%$) with Fe-species removed at $\text{pH} > \approx 4$, Al-species removed at $\text{pH} > \approx 6$ and Mn species removed at $\text{pH} > \approx 9$. The result of this study are consistent with the results obtained by Wei and Viadero Jr (2007). This is an indication of optimum pH suitable for the recovery of this chemical species. Trace elements were observed to precipitate at varying pH regimes with Cu at $\text{pH} \geq 7$, Zn at $\text{pH} \geq 8$, Pb at $\text{pH} \geq 8$, and Ni at $\text{pH} \geq 9$. Similar results were reported by Park et al. (2013). Close to 100% removal efficiency was achieved for all the metals at a given pH gradient except for sulphate. Cu, Ni, Pb and Zn are insignificant due to minute concentration, as such; there is no metal recovery potential for those species.

Geochemical modelling of chemical species removal with varying pH gradients

The PHREEQC modelled Variation in percentage removal of chemical species in AMD is shown in fig. 3.

As shown in fig. 3, the PHREEQC geochemical model simulations indicated that the Fe(III) was removed at $\text{pH} \geq 3.5$. This is due to the fact that AMD was oxidised already on decant and the addition of magnesite increased the pH to > 10 hence making the Fe(III) to precipitate. Fe(II) was observed to precipitate at $\text{pH} > 8.5$. Similar results were reported by Petrilakova et al. (2014). Mn was simulated to precipitate at $\text{pH} 9.5$. Zn was predicted to precipitate at $\text{pH} 10$, Cu was predicted to precipitate at $\text{pH} 8$. These results were consistent to the studies by Petrilakova et al. (2014) and Seo et al. (2017b). Ni and Pb were observed to precipitate at $\text{pH} 8$. Sulphate was observed to precipitate from $\text{pH} 4$ to $\text{pH} 12$. A similar study was reported by Masindi et al. (2016).

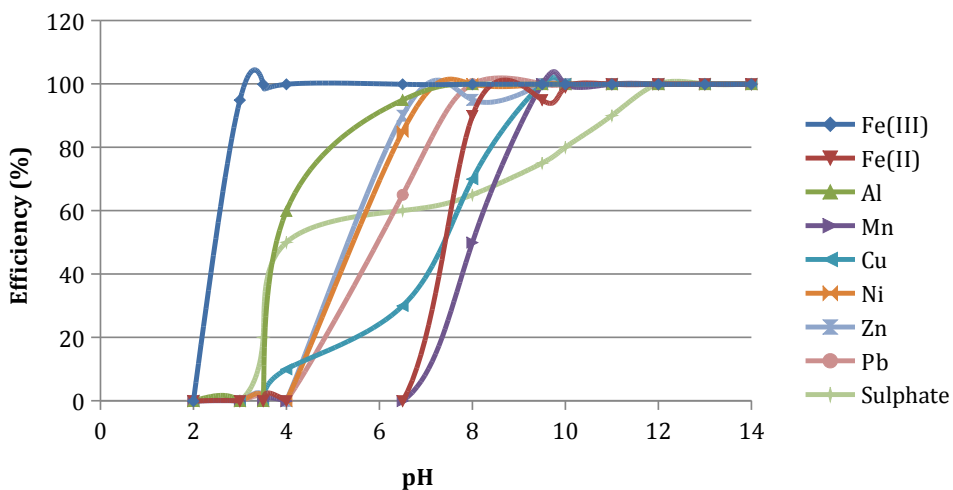


Figure 3 Variations of chemical species concentration with the pH using PHREEQC geochemical modelling.

Sensitivity analysis of cryptocrystalline magnesite to AMD ratios

Sensitivity of acid mine drainage to certain dosages of cryptocrystalline magnesite is shown in fig. 4.

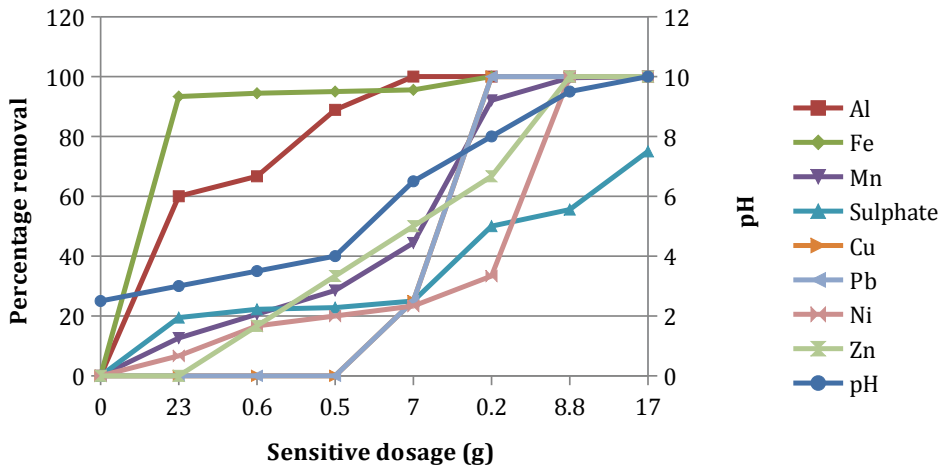


Figure 4 Sensitivity test and ions removal efficiency for AMD and calcine cryptocrystalline magnesite.

The chemical species concentration in AMD water before and after contacting varying dosages of calcined cryptocrystalline magnesite as shown in fig. 4, this will assist in showing the dosage requirement for different mine drainages and their respective pH. The initial pH required 23 g of calcined cryptocrystalline magnesite to increase the pH from 2 to ≈ 3 . This may be attributed to neutralisation of free acidity in an aqueous system. Similar results were reported by Bologo et al. (2012). After that, the dose requirement was significantly reduces. pH was also observed to increase with an increase in dosage. This may be due to addition of extra alkalinity when adding more of calcined cryptocrystalline magnesite. The pH trend is directly related to the metal removal trend as predicted by PHREEQC geochemical modelling.

AMD is characterised of Fe(II) and Fe(III), this makes it the best candidate for the recovery of magnetite. At $\text{pH} > 3$, most of Fe(III) were removed and $\text{pH} > 8$, most of Fe(II) are removed. This can be seen by the pH trend and Fe removal trend as shown in fig. 2. The results corroborate what has been reported in literature (Akinwekomi et al. 2017; Wei and Viadero Jr 2007). Al was optimally removed at $\text{pH} > 6.5$. Similar results were reported by Hedrich and Johnson (2014), Seo et al. (2017a), and Akinwekomi et al. (2017). Cu and Pb were observed to precipitate at $\text{pH} \geq 7.5$. This was similar to the studies conducted by Park et al. (2013), Oh et al. (2016) and Masindi et al. (2016). Ni and Zn precipitated at $\text{pH} \geq \approx 9$. This indicates that this technology can be applied to water with any pH gradient and recover valuable minerals that have commercial value.

Saturation index using PHREEQC geochemical modelling

The saturation indices (SI) of different selected potentially toxic metals at varying final pH are shown in fig. 5.

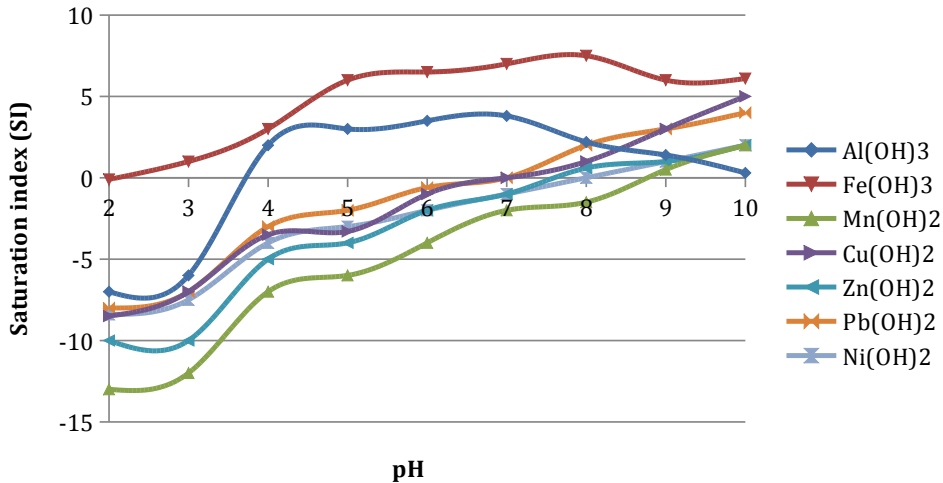


Figure 5 Saturation indices (SI) of different selected potentially toxic metals at varying final pH

As shown in fig. 5, PHREEQC geochemical model was used to complement experimental results and to point out species that are more likely to precipitate during the interaction of magnesite with acid mine drainage. The anticipated sludge were hematite, diaspore, bronchitite, hydrozincite and nickel carbonate. Zn and Ni were expected to precipitate together hence seeking more metallurgical processes for the recovery. This results were also anticipated in a number of published studies such as Masindi et al. (2017) and Park et al. (2013). The obtained results revealed that Fe was recovered at $\text{pH} \geq 3.5$, Al at $\text{pH} \geq 4.5$, Cu at $\text{pH} \geq 7$, Zn at $\text{pH} \geq 8$, Pb at $\text{pH} \geq 8$, Mn at $\text{pH} \geq 9$, and Ni at $\text{pH} \geq 9$. This has proven that metal species in acid mine drainage can be fractionally recovered at varying pH gradients in a sequential manner. The PHREEQC geochemical model results were consistent to the experimental results hence commending and attesting that the obtained results were valid and reputable. This was also confirmed by SEM-EDS.

Conclusions and recommendations

In this study, the recovery efficiency of potentially toxic metals from acid mine drainage by magnesite at varying dosages and pH gradients were successfully evaluated at 60 mins of equilibration. Magnesite increased the pH of acid mine drainage from pH 2 -10 with an increase in dosage. The removal sequence was observed to be pH 3.5 for Fe, pH 4.5 for Al, pH 7 for Cu, pH 8 for Zn, pH 8 for Pb, pH 9 for Mn and Ni. The sequence can be as follow: Fe > Al > Cu > Zn > Pb > Mn > Ni in order. Close to 100% metals removal efficiency was achieved. Further research work is underway to determine the purity of recovered potentially toxic metals.

Acknowledgements

The authors thank would like to thank National Research Foundation (NRF), University of the Witwatersrand and the Council for scientific and industrial research for sponsoring this project.

References

- Akinwekomi V, Maree JP, Zvinowanda C, Masindi V (2017) Synthesis of magnetite from iron-rich mine water using sodium carbonate. *Journal of Environmental Chemical Engineering*, doi:10.1016/j.jece.2017.05.025
- Bologo V, Maree JP, Carlsson F (2012) Application of magnesium hydroxide and barium hydroxide for the removal of metals and sulphate from mine water. *Water SA* 38:23-28
- Hedrich S, Johnson DB (2014) Remediation and Selective Recovery of Metals from Acidic Mine Waters Using Novel Modular Bioreactors. *Environ Sci Technol* 48:12206-12212, doi:10.1021/es5030367
- Masindi V (2016) A novel technology for neutralizing acidity and attenuating toxic chemical species from acid mine drainage using cryptocrystalline magnesite tailings. *Journal of Water Process Engineering* 10:67-77, doi:10.1016/j.jwpe.2016.02.002
- Masindi V, Gitari MW, Tutu H, De Beer M (2015) Passive remediation of acid mine drainage using cryptocrystalline magnesite: A batch experimental and geochemical modelling approach. *Water SA* 41:677-682, doi:10.4314/wsa.v41i5.10
- Masindi V, Gitari MW, Tutu H, De Beer M (2016) Fate of inorganic contaminants post treatment of acid mine drainage by cryptocrystalline magnesite: Complimenting experimental results with a geochemical model. *Journal of Environmental Chemical Engineering* 4:4846-4856, doi:10.1016/j.jece.2016.03.020
- Masindi V, Gitari MW, Tutu H, DeBeer M (2017) Synthesis of cryptocrystalline magnesite–bentonite clay composite and its application for neutralization and attenuation of inorganic contaminants in acidic and metalliferous mine drainage. *Journal of Water Process Engineering* 15:2-17, doi:10.1016/j.jwpe.2015.11.007
- Oh C, Han Y-S, Park JH, Bok S, Cheong Y, Yim G, Ji S (2016) Field application of selective precipitation for recovering Cu and Zn in drainage discharged from an operating mine. *Sci Total Environ* 557–558:212-220, doi:10.1016/j.scitotenv.2016.02.209
- Park SM, Yoo JC, Ji SW, Yang JS, Baek K (2013) Selective recovery of Cu, Zn, and Ni from acid mine drainage. *Environ Geochem Health* 35:735-743
- Petrilakova A, Balintova M, Holub M (2014) Precipitation of heavy metals from acid mine drainage and their geochemical modeling vol 9. doi:10.2478/sspjce-2014-0009
- Seo EY, Cheong YW, Yim GJ, Min KW, Geroni JN (2017a) Recovery of Fe, Al and Mn in acid coal mine drainage by sequential selective precipitation with control of pH. *CATENA* 148, Part 1:11-16, doi:10.1016/j.catena.2016.07.022
- Seo EY, Cheong YW, Yim GJ, Min KW, Geroni JN (2017b) Recovery of Fe, Al and Mn in acid coal mine drainage by sequential selective precipitation with control of pH. *CATENA* 148:11-16, doi:10.1016/j.catena.2016.07.022
- Simate GS, Ndlovu S (2014) Acid mine drainage: Challenges and opportunities. *Journal of Environmental Chemical Engineering* 2:1785-1803, doi:10.1016/j.jece.2014.07.021
- Wei X, Viadero Jr RC (2007) Synthesis of magnetite nanoparticles with ferric iron recovered from acid mine drainage: Implications for environmental engineering. *Colloids Surf Physicochem Eng Aspects* 294:280-286, doi:10.1016/j.colsurfa.2006.07.060

Risk assessment of acidic drainage from waste rock piles using stochastic multicomponent reactive transport modeling

Daniele Pedretti^{1,2}, Roger D. Beckie², K. Ulrich Mayer²

¹*Geological Survey of Finland (GTK), Espoo, Finland*

²*Earth Ocean and Atmospheric Sciences, University of British Columbia, Vancouver (BC) Canada*

Abstract A recently developed risk-assessment framework based on stochastic reactive transport modeling allows evaluating the probability of acidic drainage from mineralogically heterogeneous waste-rock piles (WRPs) over 100s of years. The approach is based on multicomponent reactive transport solved through a computationally efficient streamtube-like formulation. Here, the framework is applied to evaluate the implication of mineral mixing (i.e. blending) and heterogeneity on the neutralizing potential ratio (*NPR*) within WRPs. The results cast doubt on the reliability of *NPR* = 4 as a universal indicator to ensure that acidic drainage is not released from such piles. Blending can strongly mitigate the risk of acidic drainage.

Key words acid rock drainage, reactive transport, blending, uncertainty analysis

Introduction

Correct management of mine waste requires long-term predictions of environmental loadings from sulfide-rich by-products such as waste rocks. These materials can produce acidic drainage when exposed to weathering and in some cases waters with high acidity (pH < 3-4). Elevated concentrations of sulfate and other dissolved metals have also been observed in mine drainage. These aspects increase the water treatment requirements, in many cases for prolonged periods.

Assessing the environmental loadings from waste rock piles requires predicting if (and when) the piles will actually generate polluted drainage, and how much. This task is subject to substantial uncertainty. A main reason for poor predictive capabilities is the complexity in providing accurate quantitative estimates of the probability that infiltrating rainwater in contact with the host rocks will turn acidic over time.

Mineralogical heterogeneity plays a major role in this sense. The geochemical response of the pile depends on a large number of nonlinearly coupled factors occurring at a range of scales (e.g. Lorca et al. 2016; Pedretti et al. 2015). The amount and reactivity of minerals that can contribute to generate acidity (e.g. sulfides) and that of minerals that buffer the acidity, (e.g. carbonates) is necessary information, which is; however, impossible to characterize at each location within a WRP. Consequently, averaging the geochemical behavior of the pile is complicated and intrinsically uncertain.

Stochastic models provide a useful tool when making predictions under uncertainty for a variety of environmental applications (e.g. Pedretti et al. 2012), including mining contexts

(e.g. Eriksson and Destouni, 1997; Malmström et al. 2008). However, stochastic reactive transport models of waste rock weathering are quite challenging, due to the computational intensity required to solve for nonlinearly coupled, large-scale simulations (e.g. Fala et al. 2013). A recently developed risk assessment framework based on streamtube-based modeling and multicomponent reactive transport has been proposed to circumvent some of these challenges and allows studying the likelihood (L) of acidic drainage from mineralogically heterogeneous waste rock piles.

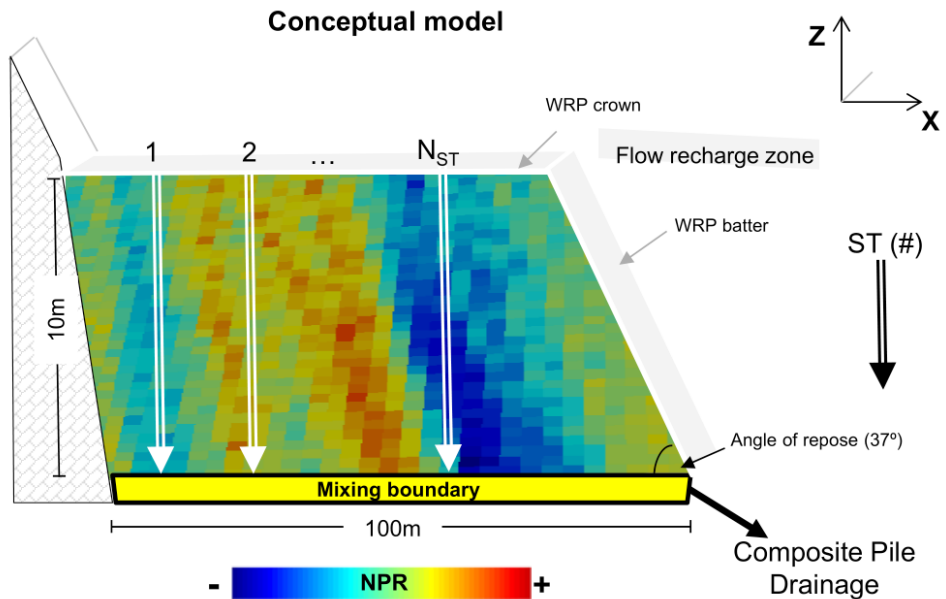


Figure 1 Conceptual model identifying the discretization of a mineralogically heterogeneous WRP into a sequence of streamtubes (STs) and the location of the mixing boundary (after Pedretti et al. 2017).

Pedretti et al. (2017) applied this method, focusing particularly on the impact of mineralogical heterogeneity on the effective neutralizing capacity of the piles. The mineralogical variability was idealized by a spatial variability of abundance of calcite and pyrite, described through geostatistical tools.

Experimental methods based on field and laboratory observations have been suggested to predict the risk for ARD release. For instance, indicators such as the Neutralizing Potential Ratio (NPR) have been proposed to estimate how likely the waste rock drainage will be buffered. When using this method, it is widely accepted that a waste rock with $NPR = 4$ or higher would likely generate neutral pH drainage (e.g. Price, 2009). Approaches such as layering and blending of waste rock have been proposed in the past (e.g. Miller et al. 2003); however, their actual effectiveness to reduce the occurrence of acidic drainage has been questioned. Reactive transport models have been used to calculate the geochemical response of the piles to weathering using a process-based approach. (e.g. Mayer et al. 2002).

The purpose of this work is using the stochastic framework and to extend it to the analysis of scenarios that account for different geostatistics describing the mineralogical variability of waste rock piles. We formulate additional scenarios and by explicitly solving for random realizations within multiple Monte-Carlo simulations. Through this approach, we provide new insights about the impact of heterogeneity on the assessment of environmental risk from waste rock piles. In particular, we focus on the use of geostatistics to evaluate the impact of mineralogical mixing or blending as an effective solution to increase the effective pH-buffering capacity of a WRP.

Methodology

The stochastic framework is formulated according to the approach described in detail in Pedretti et al. (2017). Briefly, the approach describes a multidimensional (2D or 3D) system of any geometry, which is discretized into a number of streamtubes (STs). A ST can be seen as an individual 1D flow path, which is recharged by infiltrating rainfall at one boundary and releases drainage at the other boundary. The collection or bundle of STs forms the entire flow field within the pile. A conceptualization of this approach is depicted in Figure 1.

Each ST is in turn discretized into a number blocks, each of which is hydraulically and geochemically parameterized. Hydraulic properties and geochemical properties such as concentration of geochemical components and solids are defined for each block. A key property relevant for this discussion is the volumetric fraction of a mineral (φ). A heterogeneous distribution of physical and geochemical properties can be assigned by varying these properties in the blocks.

In the context of stochastic modeling, a heterogeneous distribution of these properties can be derived from a multidimensional geostatistical model. For instance, a stochastic distribution can be used to represent a random variability of mineral content (φ) initially present during the construction stage of the waste pile. A useful model to generate stochastic modeling is a Sequential Indicator Simulation (SIS), in which categories of simulated properties are varied according to spatial correlation functions, or equivalently a variogram model. A well-known model is for instance the directional exponential covariance function

$$C(\theta) = \sigma^2 \exp\left(-\frac{d}{r_\theta}\right)$$

where r is the distance between two points, θ is the angle of the anisotropic covariance ellipsoid, a is the range of the correlation along that direction, and σ^2 is the variance of the studied property. The ratio between r_θ and the dimension of the domain along θ provides a measure of the continuity of the mineralogical content along θ .

Each ST forming the WRPs is parameterized according to the corresponding map of properties obtained from the geostatistical model. Each ST is then solved individually as a 1D reactive transport model, which describes unsaturated flow and concentration of compo-

nents within the domain, according to a set of boundary conditions and the specific reaction network.

The solution of each ST provides the concentration of components and discharge rates at the base of each ST. Discharge from streamtubes tend to mix in areas of converging flow. This could occur for instance a stream or at the base of a WRP. Risk assessment of drainage quality from WRPs is not as important for discharge from individual streamtubes within the pile, but is more relevant to assess the overall composition of mixed drainage resulting from merging multiple STs. To facilitate this assessment, mixing of drainage from individual streamtubes must be included in the analysis.

Application

We applied the stochastic framework to analyze the role of mineralogical heterogeneity on the effective neutralizing capacity of WRPs. The problem is defined as in Pedretti et al. (2017), who already addressed a similar problem. We focused on pyrite and calcite as the two primary minerals controlling the distribution of the neutralizing potential ratio (*NPR*) within the pile. The goal of the application is to evaluate if the mean *NPR* value calculated by simple averaging over the entire content of pyrite and calcite minerals within a pile is a sufficiently accurate metric to predict if the total pile drainage will become acidic or remain circumneutral.

Pedretti et al. (2017) concluded that a bulk $NPR = 4$ (a value traditionally considered “safe” for practical applications at mining sites) can sometimes be insufficient to ensure that drainage does not become acidic. Pedretti et al. (2017) adopted a defined r_θ , which corresponded approximately to the vertical extension of the domain (L). In this sense, their simulations mimicked poorly mixed mineralogical conditions within the piles. We extend in this paper the work by Pedretti et al. (2017) by adding new scenarios, which simulate the effects of distribution of minerals with a shorter r_θ , representing conditions of increased mineralogical mixing within the pile.

In Figure 2 we report examples of resulting pyrite $100\text{m} \times 10\text{m}$ 2D maps, discretized into cells of 1m^2 and resulting from the use of different r_θ . Similar fields can be derived for calcite. On average, the two distributions have the same mean amount (i.e. φ) of pyrite. On top, the ratio $r_\theta/L \approx 1$ results in continuity of the individual mineral property along the vertical direction. At the bottom, we adopted a ratio $r_\theta/L \approx 0.3$, which results in more mixed mineralogical conditions within the piles. Readers more familiar with terms more traditionally adopted in the mining industry can find an analogy between “non-blended” (case with $r_\theta/L \approx 1$) and more “blended” (case with $r_\theta/L \approx 0.3$) scenarios. We use these applied terms in the discussion below for clarity.

Following Pedretti et al. (2017), we assumed vertical flow, fully controlled by the recharge rates, and lateral hydraulic homogeneity. No effect of preferential flow is simulated, an aspect which is left open for future developments. Each column of the 2D mineralogical map shown in Figure 2 represents one ST. The resulting mixing of water from the various STs

is calculated by taking the concentrations of components from all STs at the bottom of the pile, and mix them at sequential time intervals. High gas permeability is assumed in the simulations, leading to conditions in equilibrium with the atmosphere.

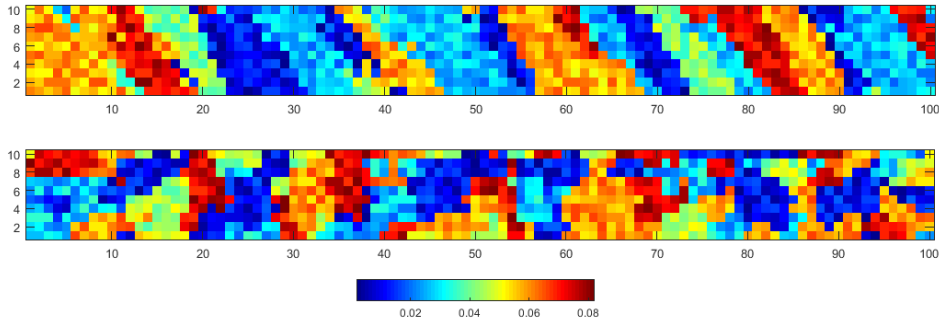


Figure 2 Examples of individual realizations of geostatistical pyrite maps. The mineral distribution in the blended scenario is characterized by short correlation lengths of mineral maps, resulting in more mineralogical mixing than within the non-blended piles.

To directly compare with Pedretti et al. (2017), and using the same r_{θ}/L ratios defined above, we studied the likelihood that a WRP will generate acidic conditions from piles characteristic by two different mean NPR values ($NPR = 2$ and $NPR = 4$). The results are reported in Figure 3, which shows the cumulative density functions obtained for each scenario from an ensemble of 100 equally probable stochastic simulations, all characterized by the same mean NPR and other statistics characterizing their mineralogical properties.

The results highlight the importance of mineralogical mixing on the expected behavior of a pile. In the case of poor mineralogical mixing (i.e. piles not blended) (Figure 3-left), the piles are expected to generate acidity. The likelihood that a $pH < 4$ occurs 50 years after the pile construction, for instance, is approximately 90% for $NPR = 2$ and above 75% for $NPR = 4$. This issue, already highlighted by Pedretti et al. (2017) cast doubts on the universality of the use of the NPR indicator to predict the resulting pH of pile drainage.

In the case of increased mineralogical mixing (i.e. piles blended) (Figure 3-right), we observed that in case of $NPR = 2$ the probability that a pile generates acidic pH remains quite high, and comparable with the non-blended scenario. However, for $NPR = 4$, mixing has a much stronger and positive impact on the results. Indeed, we found that the probability of generating acidic pH becomes virtually negligible ($< 5\%$), suggesting that the combination of mineralogical mixing and $NPR = 4$ can be more optimal to minimize low acidity drainage conditions from waste rock piles.

Conclusion

A recently developed efficient stochastic modeling tool allows generating process-based Monte Carlo simulations for risk assessment in heterogeneous waste rock piles. Risk is defined here as the likelihood of a pile to generate acidic drainage under uncertainty.

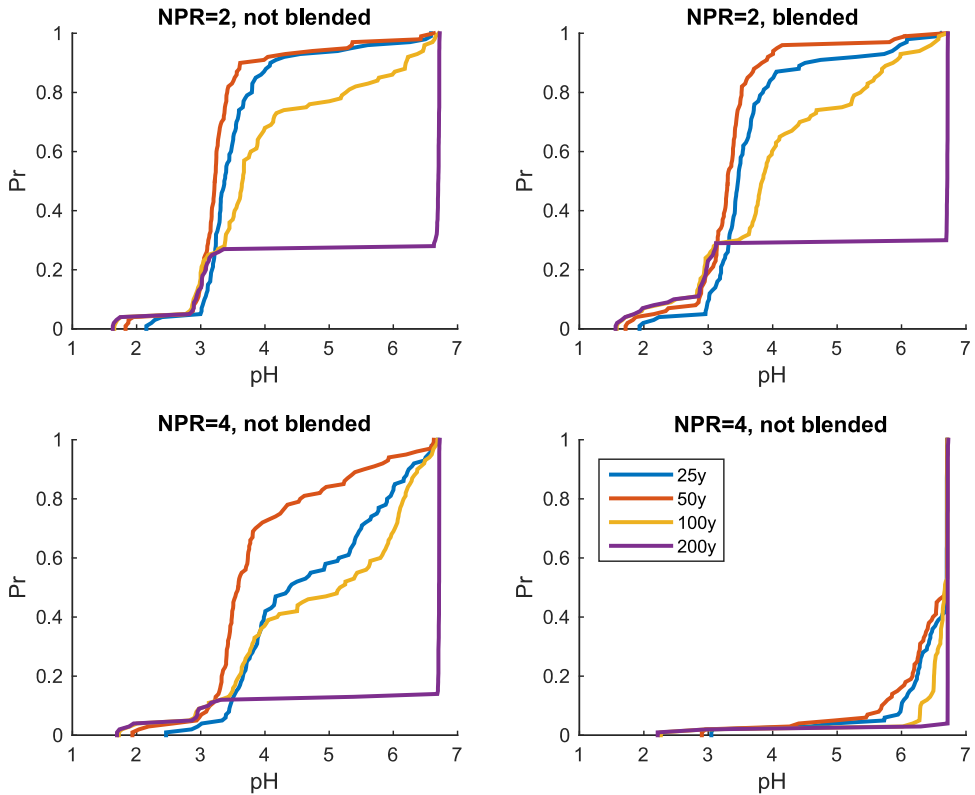


Figure 3 Cumulative probability of resulting pH from waste rock piles characterized by different bulk *NPR* ratios and correlation lengths. “Not blended” refer to waste rocks in which mineral correlation is shorter than in the “blended” waste rocks, where the correlation is continuous over the vertical scale of the pile.

We focused on the *NPR* metric and evaluated how mineralogical heterogeneity is a relevant source of uncertainty to ensure the validity of *NPR* values traditionally considered “safe” from operational perspectives in waste rocks. A recent analysis by Pedretti et al. (2017) focusing on similar problems provides a useful conceptual model and analysis to be tested and compared.

Our analysis reveals that the spatial characteristic of mineralogical heterogeneity can play a major role when defining the actual validity of a specific *NPR* value. In particular, we found that mineralogical mixing (similar to waste rock “blending”) is critical to ensure that *NPR* =4 works as a proper universal metric to ensure no acidic drainage exfiltrating waste rocks. For the conditions simulated in this analysis, when rocks are not blended, the likelihood of drainage with $\text{pH} < 4$ is above 75%, while becoming virtually negligible (<5%) when rocks are blended. On the other hand, *NPR* =2 is insensitive to blending, and always generate high likelihood of acidic leaching.

Development of this study will target different waste rock conditions and more complex scenarios, which include the implication of additional primary and secondary minerals, variable gas and temperature conditions, and hydraulic heterogeneity.

References

- Eriksson N, Destouni G (1997) Combined effects of dissolution kinetics, secondary mineral precipitation, and preferential flow on copper leaching from mining waste rock. *Water Resour. Res.* 33, 471–483. doi: 10.1016/S0022-1694(96)03209-X
- Fala O, Molson J, Aubertin, M, Dawood, I, Bussi re, B, Chapuis RP (2013) A numerical modelling approach to assess long-term unsaturated flow and geochemical transport in a waste rock pile. *Int. J. Min. Reclam. Environ.* 27, 38–55. doi: 10.1080/17480930.2011.644473
- Lorca, ME, Mayer, KU, Pedretti, D, Smith, L, and Beckie, RD (2016) Spatial and Temporal Fluctuations of Pore-Gas Composition in Sulfidic Mine Waste Rock. *Vadose Zone Journal* 15(10) , doi:10.2136/vzj2016.05.0039
- Malmstr m ME, Berglund, S, and Jarsjo, J (2008) Combined effects of spatially variable flow and mineralogy on the attenuation of acid mine drainage in groundwater. *Appl. Geochem.* 23, 1419–1436. doi: 10.1016/j.apgeochem.2007.12.029
- Mayer KU, Frind, EO, and Blowes, DW (2002) Multicomponent reactive transport modeling in variably saturated porous media using a generalized formulation for kinetically controlled reactions. *Water Resour. Res.* 38, 13–1–13–21. doi: 10.1029/2001WR000862
- Miller SD, Smart, RS, Andrina, J, Richards, D (2003) Evaluation of Limestone Covers and Blends for Long Term ARD Control at the Grasberg Mine, Papua Province, Indonesia. In *Proceedings of Sixth International Conference on Acid Rock Drainage (ICARD)*., (Cairns, Queensland, Australia: The Australasian Institute of Mining and Metallurgy, Australia).
- Pedretti D, Barahona-Palomo, M, Bolster, D, Fern ndez-Garcia, D, Sanchez-Vila, X, and Tartakovsky, DM (2012) Probabilistic analysis of maintenance and operation of artificial recharge ponds. *Advances in Water Resources* 36, 23–35 doi:10.1016/j.advwatres.2011.07.008
- Pedretti, D, Lassin, A, and Beckie, RD (2015) Analysis of the potential impact of capillarity on long-term geochemical processes in sulphidic waste-rock dumps. *Applied Geochemistry* 62, 75–83. doi: 10.1016/j.apgeochem.2015.03.017
- Pedretti, D, Mayer, KU, and Beckie, RD (2017) Stochastic multicomponent reactive transport analysis of low quality drainage release from waste rock piles: Controls of the spatial distribution of acid generating and neutralizing minerals. *Journal of Contaminant Hydrology* 201, 30–38 doi: 10.1016/j.jconhyd.2017.04.004
- Price WA (2009) Prediction manual for drainage chemistry from sulphidic geologic materials. MEND report.

Requirements for numerical hydrogeological model implementation for predicting the environmental impact of the mine closure based on the example of the Zn/Pb mines in the Olkusz area

Ewa Kret, Mariusz Czop, Dorota Pietrucin

AGH University of Science and Technology, Department of Hydrogeology and Engineering Geology, A. Mickiewicza 30 Av., 30-059 Krakow, Poland, 1 ekret@agh.edu.pl

Abstract Numerical modelling is the only reliable tool to solve such complex problems as mine closure. This paper presents the requirements for the use of numerical modelling for prediction of aquatic environment changes in the area of the liquidates mines based on the example of Zn/Pb ores mines in the Olkusz region (southern Poland). Author's indicate a set of data that should be prepared to create a reliable numerical model which can be easily applied to simulate mine closure and its impact on the aquatic system, especially rebound of the groundwater table and reactivation of the wetland areas.

Key words mine closure, hydrogeological modelling, environmental impact assessment, Olkusz region

Introduction

Mining is often a highly complex long-term industrial operation, with respect to both technological and planning aspects. The mining industry uses several environmental management tools (e.g. life cycle assessment, multi-criteria decision analysis, etc.) during mine development, operation and closure periods (e.g. Duruncan et al. 2006; Reid et al. 2009; Roussat et al. 2009). However, due to uncertainties associated with the liquidation phase it is crucial to adopt solid management practices for environmental impact assessment. It requires a proper preparation to predict all potential hazards related to the whole process of mine closure and reclamation. It is especially significant not only to the mine owners (as the mine closure plan and its environmental impact is usually considered and included within the pre-feasibility, feasibility and design phases) but also to the local community and the mine surrounding area investors, which could directly be impacted by the mine closure process.

Characterisation and prediction of aquatic system changes in relation to mine closure process and requirements associated with that was based on the example of Zn/Pb ore mines in Olkusz region. The mine liquidation process at this area is planned to start at 2020-22 and its regional character and complex structure associated with land development makes the site an interesting example. The site is located in Southern Poland and it's a part of the Biała Przemsza river basin (tributary of the Vistula river). The main constituents of the geological structure are represented by Triassic formations (sediments of the Lower and Middle Buntsandstein, Rot Formation and Muschelkalk). Underlying the Triassic are Permian and Devonian rock, which build an anticline and elevated tectonic block. On the South from Bukowno city occurs Carboniferous sandstones. The Triassic overburden consist of limestone of the Upper Jurassic, as well as Middle Jurassic marl (East part of the site). However,

Quaternary material covers the entire area by a layer of varying thickness from a few to a few dozen meters in the Biała Przemsza valley. The Triassic aquifer plays dominating role in the hydrogeological conditions and it is in hydraulic contact with Quaternary aquifer (fig. 1).

The underground mine closure, including Zn/Pb ore mines, is directly related to hydrogeological consequences such as: (i) *rebound of the groundwater table* and (ii) *flooding of the depression cone and underground mine workings*, due to the discontinuation of mine dewatering process. The artificially created hydrogeological conditions due to mine operation will slowly develop to their “natural” state from before mine drainage. Such situation, although from a hydrological conditions point of view is a natural and inevitable occurrence, may also generate a number of adverse phenomena. As a result of even several decades of mine drainage activity, there can changes of the developed state occur and they are associated with observed effects such as:

- *disturbance of water regime* – decrease or disappearance of river flow and slow recovery of natural flow, which can take even decades as the underground mine operation – mine dewatering process and depression cone as it direct consequence has usually a regional scale;
- *reactivation of natural wetlands* – in case of Zn/Pb ore mines there is no mining induced subsidence so restoration of bayous and flooding zones occurs naturally;
- *groundwater quality changes* – in case of Zn/Pb ore mines a contamination of groundwater in sulphates and potentially toxic metals can occur as a result of sulphide minerals oxidation to soluble sulphate;

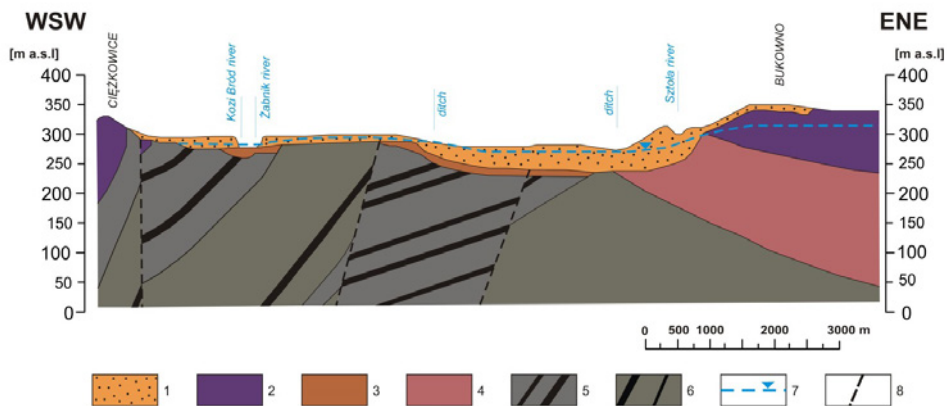


Figure 1 Schematic hydrogeological cross-section of the studied area (Southern part)

1,2 – permeable Quaternary (1) and Triassic (2) deposits;; 3,4 – impermeable Quaternary-Carboniferous (3) and Permian (4) deposits; 5,6 – permeable (5) and impermeable (6) Carboniferous deposits; 7 – Triassic-Quaternary groundwater level; 8 – faults

Methodology for predicting changes of aquatic system related to liquidation based on the on the Olkusz region example

To characterise and describe mine closure there could be two methods: analytical and numerical considered. In case of the Zn/Pb ore mines liquidation in Olkusz region due to its complicated nature and regional impact of the mining operation process (its depression cone up to 600km²) analytical methods are not accurate to properly predict all aquatic system changes and consequences resulted from mine closure process. Numerical methods are more reliable and allows to consider all important parameters and scenarios. However, to apply numerical modelling for mine closure impact on aquatic system and predict its consequences there have to be some special requirements met. The proposed methodology, applied for Zn/Pb ore mines closure in Olkusz region, includes:

- *obtaining a full site description*, assessed through the collection and synthesis of existing data of mining inflow, geological, geo-chemical, hydrogeological characterization of the mine and the surrounding area, including field investigations (rivers and streams flow measurements along with identification of potential water escapes into the rock mass) as well as historical data;
- *data verification and management* using some novel software tools, eg. Hydro Geo-Analyst that integrates a complete suite of analysis; within the HGA data can be quickly analysed, integrated and easily visualised;
- *numerical model development* which requires special emphasis on a structure discretization, which should reflect all important geological layers, both permeable and impermeable (multilayer model). Conceptualization of hydrogeological conditions and proper generalization of the top and bottom of each model layer important for groundwater flow is a key stage of the numerical model development; to predict a restoration of bayous and flooding zones it is a good fit of site topography and geology of Quaternary deposits required to obtain to get reliable results; usually within the numerical model development a site topography is not relevant, as the active cells are located below groundwater table and thus a first model layer is inactive; the model cell size should reflect the scale of the modelled problem – usually between 100–200 m, as the mining operation impact scale typically has regional character;
- *model calibration* – where a requirement is to refer to three types of data: (i) hydraulic head and (ii) surface waters flow measurement and also (iii) to the mine inflow;
- *mine closure scenario simulation* – which requires conducting simulations on transient model as the mine closure process can take dozens of years to reach “natural conditions” and it should be assessed how groundwater table restoration vary in time;

It has to be remembered that mine closure process should be supported not only by numerical modelling and its simulations but also by the wider social, economic, physical and biological contexts within which a mine is located. This will ensure that the broader environment, including its inherent risks and opportunities, influences mine closure, as opposed to merely investigating how the closed mine will impact on the environment and on the surrounding communities. Therefore, it is important for local community and mine's own-

ers to cooperate, especially with the data availability, as it is a common purpose to predict and assess environmental risk from the mine closure, especially that the whole process can take dozens of years.

Results of numerical modelling of Zn/Pb ore mine closure impact on the aquatic system in the Olkusz area

Applying a developed procedure based on the example of Olkusz region (southern Poland), a numerical multilayer model using a Visual MODFLOW, was developed. The modelled area covering 490 km² was divided into 80 rows and 98 columns (oriented in the N-S direction) with the finite-difference grid size 250×250m and with the active area about 250 km². A model structure consists of 6 layers with varying thickness to fully capture the complexity of the hydrogeological conditions at the site (fig. 2, fig. 3). Top and bottom of each model layer is a result of the geological interpolation of approx. 4000 borehole data using kriging method.

According to the proposed methodology the model calibration was based not only on the size of the mine inflow but also mapped to actual groundwater level contours and measured flow values of the rivers (fig. 4). Obtained results indicate good and accurate fit to real data of mine water inflow to the Zn/Pb ore mines in Olkusz region which equals 250-270 m³/min. (Motyka et al. 2016) and results obtained on the model are around 255 m³/min. (4.26m³/s) (tab. 1).

Table 1 Modelled area budget for mining operation and mining closure scenarios

Balance items	mining operation scenario*		mining closure scenario*	
	Input (+)	Output (-)	Input (+)	Output (-)
1. Effective infiltration/Recharge	4.348	0	1.128	0
2. Input/Output (constant-head boundary)	4.611	4.704	2.912	4.038
3. Inflow/outflow to the Zn/Pb ore mines:				
Pomorzany	0.0	3.397	0.0	0.0
Olkusz	0.0	0.764	0.0	0.0
Bolesław	0.005	0.099	0.0	0.0
Total	8.964	8.964	4.041	4.038
Divergence in balance [%]		0.0		0.09

*units in m³/s

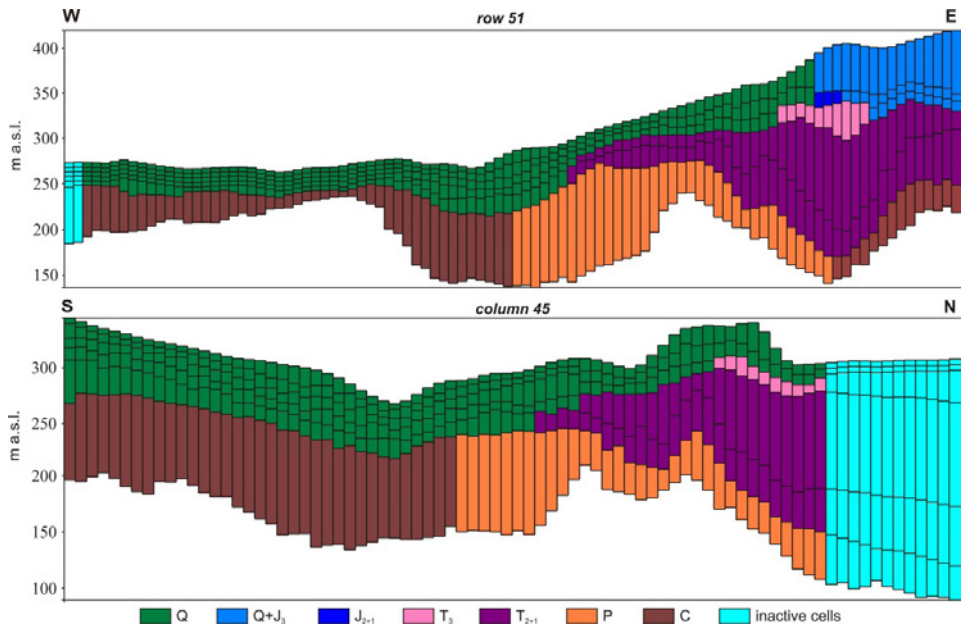


Figure 2 Numerical model of Olkusz region row/column cross-section

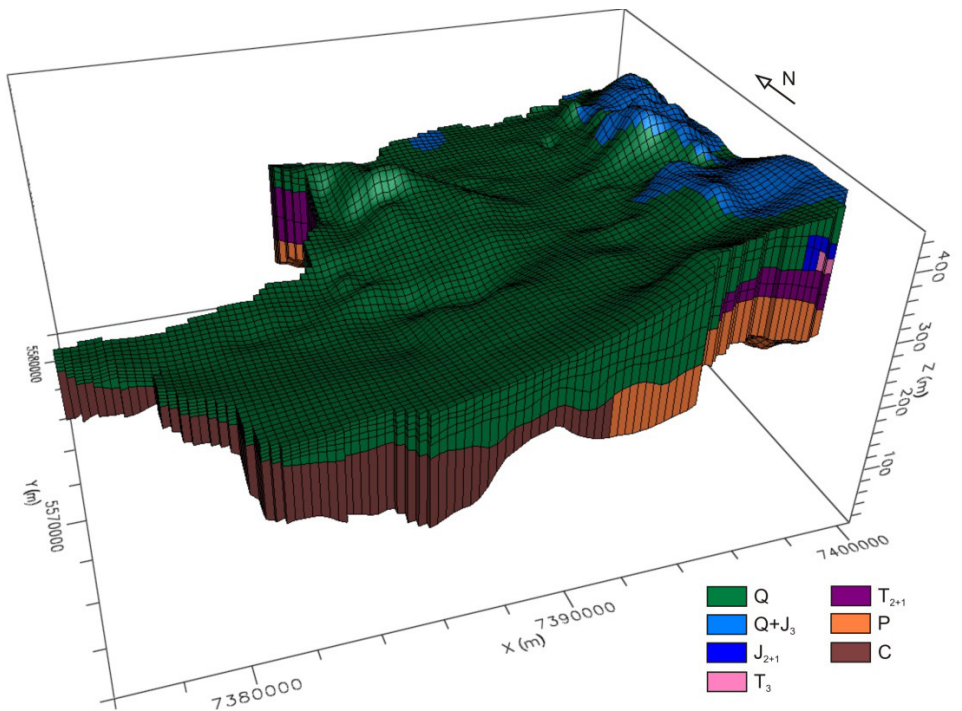


Figure 3 3D structure of numerical model of Olkusz region

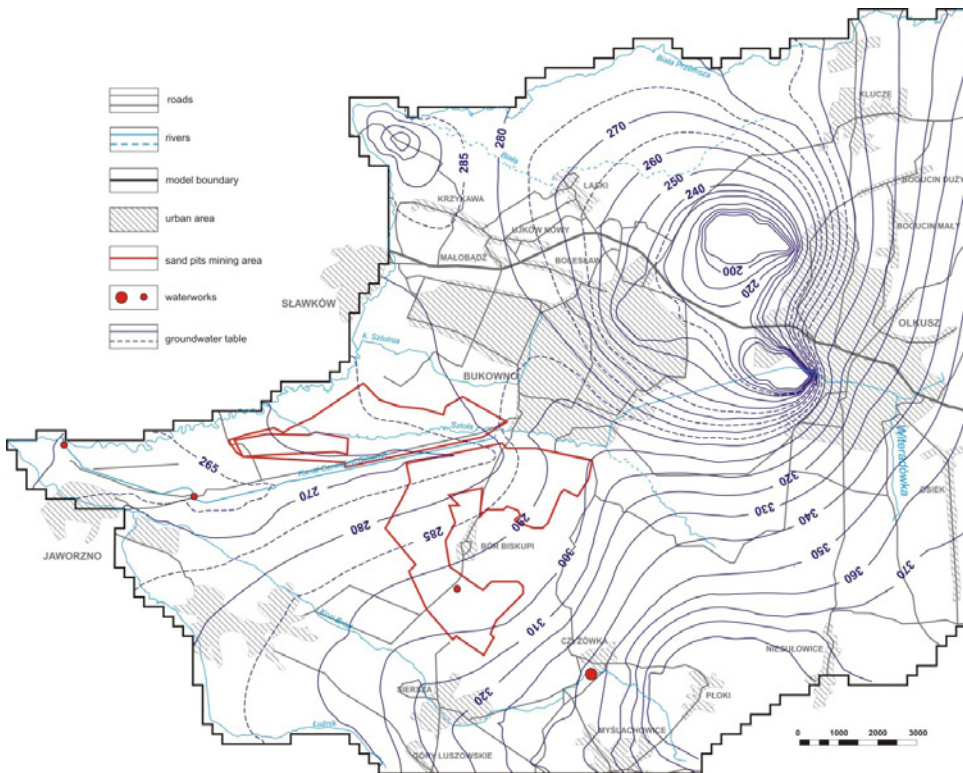


Figure 4 Map of Quaternary-Triassic multi-aquifer groundwater table obtained on the model – mining operation scenario (as of 06.2016)

Hydrogeological model allowed for prediction of the Olkusz mine liquidation impact on the aquatic system, especially at the area of surrounding sand pits, Jaworzno and Silesia waterworks' and changes of the surface waters regime including bayous and flooding zones formation. The new groundwater table for mine closure final scenario (after 100 years) is presented on fig. 5. The calculated total time of complete reconstruction of groundwater level to natural conditions is approx. 90–110 years but the first effects of Zn/Pb ore mines closure would be visible after approx. 25 years.

Conclusions

Prognosis of mine closure process is a very difficult task regarding to its considerable complexity and mathematical description. In most cases, this type of activity is based on a computer simulation performed for numerical modelling of hydrogeological conditions. Therefore, there have to be special requirements achieved to create reliable and accurate model of the site for future scenario development. Taking into account all of them (such as data compilation, model discretization: grid size an multilayer character, its regional scale, transient condition of the mine closure process, and a proper calibration) a numerical model of Zn/Pb ore mines liquidation in Olkusz region was developed as an example of area where a numerical modelling is the best tool to predict mine closure foreseen to start at year 2020-22.

Created model allowed for mine closure impact assessment on aquatic system, especially at the area of surrounding sand pits, Jaworzno and Silesia waterworks' and changes of the surface waters regime including bayous and flooding zones formation. The model can be easily implemented for future use related to new waterworks' location or prediction a new Zn/Pb mine impact in the Zawiercie area.

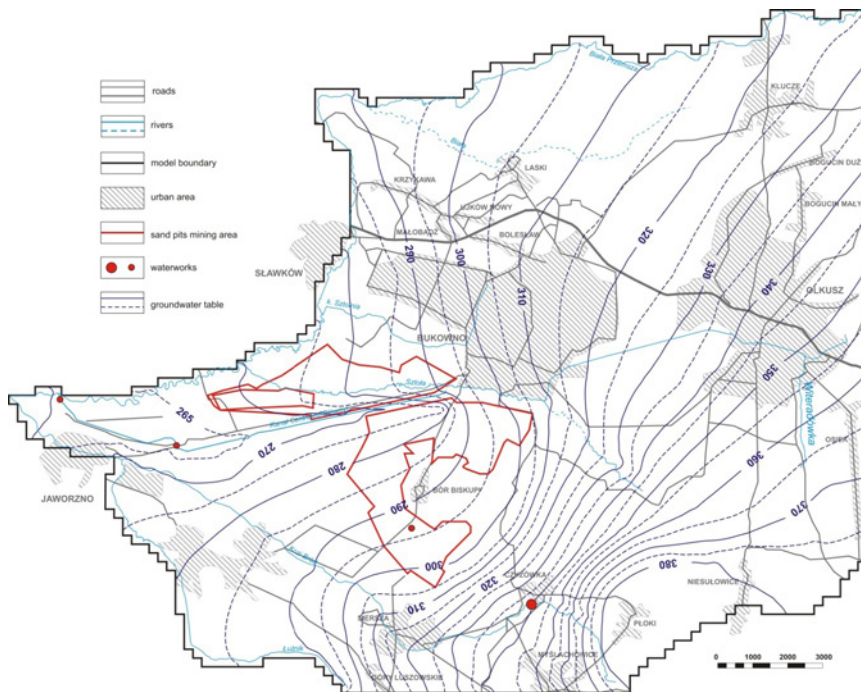


Figure 5 Map of Quaternary-Triassic multi-aquifer groundwater table obtained on the model – mining closure final stage scenario (after 100 years)

Acknowledgements

This paper was financially supported by research programme no. 11.11.140.969 for the Department of Hydrogeology and Engineering Geology at the Faculty of Geology, Geophysics and Environmental Protection of the AGH University of Science and Technology.

References

- Duruncan S, Korre A, Munoz-Melendez G (2006) Mining life cycle modelling: a cradle-to-get gate approach to environmental management in the minerals industry. *J. Clean. Prod.* 14(12–13):1057–1070, doi:10.1016/j.jclepro.2004.12.021
- Motyka J, Adamczyk Z, Juško K (2016) The historical view of the water inflows to the Olkusz zinc and lead mines (SW Poland). *Przegląd Górniczy*. 72 (6): 49–58.
- Reid C, Becaert V, Aubertin M, Rosenbaum RK, Deschenes L (2009) Life cycle assessment of mine tailing management in Canada. *J. Clean. Prod.* 17(4):471–479, doi:10.1016/j.jclepro.2008.08.014
- Roussat N, Dujet C, Mehu J (2009) Choosing a sustainable demolition waste management strategy using multicriteria decision analysis. *Waste Manag.* 29(1):12–20, doi:10.1016/j.wasman.2008.04.010

A misty forest of tall, thin trees with a green undergrowth. The trees are tall and thin, with a light brown bark. The ground is covered in green moss and small plants. The background is hazy and misty, creating a soft, ethereal atmosphere. The lighting is warm and golden, suggesting a sunrise or sunset. The overall scene is peaceful and serene.

These proceedings of the 13th International Mine Water Association Congress in Lappeenranta, Finland, contain 176 oral and poster presentations about mine water related issues. More than 600 authors from 37 nations present papers covering all relevant mine water aspects. Their themes include Finnish Mine Water Issues, Arctic Environment, Mine Closure, Mine Flooding, Mine Water and Exploration, Pit Lakes, Hydrogeology, Geochemistry, Metals & Semi-Metals, Circular Economy & Valorisation, Active & Passive Treatment as well as Case Studies. Currently, these proceedings volume can be considered the most comprehensive compilation of leading, worldwide mine water research and development.

Lappeenranta
University of Technology
Research Reports

ISSN-L 2243-3376
ISSN 2243-3376